INFORMATION TO USERS

This manuscript has been reproduced from the microfilm master. UMI films the text directly from the original or copy submitted. Thus, some thesis and dissertation copies are in typewriter face, while others may be from any type of computer printer.

The quality of this reproduction is dependent upon the quality of the copy submitted. Broken or indistinct print, colored or poor quality illustrations and photographs, print bleedthrough, substandard margins, and improper alignment can adversely affect reproduction.

In the unlikely event that the author did not send UMI a complete manuscript and there are missing pages, these will be noted. Also, if unauthorized copyright material had to be removed, a note will indicate the deletion.

Oversize materials (e.g., maps, drawings, charts) are reproduced by sectioning the original, beginning at the upper left-hand corner and continuing from left to right in equal sections with small overlaps. Each original is also photographed in one exposure and is included in reduced form at the back of the book.

Photographs included in the original manuscript have been reproduced xerographically in this copy. Higher quality 6" x 9" black and white photographic prints are available for any photographs or illustrations appearing in this copy for an additional charge. Contact UMI directly to order.

UMI®

Bell & Howell Information and Learning
300 North Zeeb Road, Ann Arbor, MI 48106-1346 USA
800-521-0600

Reproduced with permission of the copyright owner. Further reproduction prohibited without permission.

Reproduced with permission of the copyright owner. Further reproduction prohibited without permission.

NOTE TO USERS

Page(s) missing in number only; text follows.
Microfilmed as received.

247

This reproduction is the best copy available.

UMI

Reproduced with permission of the copyright owner. Further reproduction prohibited without permission.

Reproduced with permission of the copyright owner. Further reproduction prohibited without permission.

NOMOLOGICAL MECHANISMS OF ANTHROPOID NASOMAXILLARY DIVERSITY

by

James M. McMahon

VOLUME I

A dissertation submitted to the Graduate Faculty in Anthropology in partial fulfillment of the requirement for the degree of Doctor of Philosophy, The City University of New York

1999

Reproduced with permission of the copyright owner. Further reproduction prohibited without permission.

UMI Number: 9946199

Copyright 1999 by
McMahon, James Michael

All rights reserved.

UMI Microform 9946199
Copyright 1999, by UMI Company. All rights reserved.

This microform edition is protected against unauthorized
copying under Title 17, United States Code.

UMI
300 North Zeeb Road
Ann Arbor, MI 48103

Reproduced with permission of the copyright owner. Further reproduction prohibited without permission.

© 1999

JAMES M. McMAHON

All Rights Reserved

Reproduced with permission of the copyright owner. Further reproduction prohibited without permission.

This manuscript has been read and accepted for the Graduate Faculty in Anthropology in satisfaction of the dissertation requirement for the degree of Doctor of Philosophy.

5/21-99

Date

Prof. Timothy Bromage
Chair of Examining Committee

May 21, 1999

Date

Prof. Louise D. Lennihan
Executive Officer

Supervisory Committee:

Prof. Frederick Szalay

Prof. Leslie Marcus

External Reader:

Prof. Donald Enlow

THE CITY UNIVERSITY OF NEW YORK

Reproduced with permission of the copyright owner. Further reproduction prohibited without permission.

Abstract

NOMOLOGICAL MECHANISMS OF
ANTHROPOID NASOMAXILLARY DIVERSITY

by

James M. McMahon

Advisor: Professor Timothy Bromage

The primary objectives of this thesis were (1) to formulate an integrated theoretical, operational and analytical approach to the study of craniofacial diversity, and (2) test specific hypotheses regarding the evolutionary and developmental mechanisms responsible for nasomaxillary diversity among extant anthropoid primates.

Craniofacial diversity derives from variation of underlying genetic and cellular activities during development (proximate causal mechanisms). Nomological distal causal mechanisms (NDCMs) are law-based processes that determine which proximate mechanisms are expressed and which are repressed. Three NDCMs were explored: neo-Darwinian selection, physiological acclimation and biological constraints.

Morphometric 3D landmark data were collected from 300 adult female specimens representing 37 species of extant anthropoids, and from infant specimens representing a subset of 27 species. Methods were developed to deal with the problems of phylogenetic effects and scale adjustment in cross-taxonomic comparative analyses. A multi-level covariance structure analytic technique was devised to test specific hypotheses regarding the affects of growth constraints, body size, brain form, olfaction, locomotion, and mastication on nasomaxillary form. The analysis permitted an examination of the

Reproduced with permission of the copyright owner. Further reproduction prohibited without permission.

independent effects of selection, acclimation and constraints on nasomaxillary form and form variation.

It was found that much of the diversity in the anteroposterior dimension of the nasomaxillary complex (e.g., anterior facial length, maxillary arch length, facial prognathism, nasal bone length, etc.) among anthropoids can be accounted for through an integrated growth process involving both structural and functional components. Brain growth and form interact with the chondrocranium (specifically the spheno-ethmoidal complex), which in turn determines the vector of facial growth.. The extent of facial growth acts to maintain the orientation of occlusal plane within functional limits required for proper mastication. Forces generated during mastication also appear to influence nasomaxillary form, via both selectional and acclimational mechanisms. These results support the hypotheses of Weidenreich, Enlow, Hylander, and others. Neither olfaction nor locomotion appear to substantially affect nasomaxillary form among anthropoids.

The results indicate the primary importance of structural and functional growth constraints and the relationship between brain growth and chondrocranial development in the evolution of anthropoid nasomaxillary diversity.

Reproduced with permission of the copyright owner. Further reproduction prohibited without permission.

Preface

This study examines the nomological (i.e., law-based) mechanisms responsible for the diversity of nasomaxillary morphology among extant Higher Primates, within the context of an integrated ontological and epistemological framework. Some readers will regard this work as basic research in anthropoid craniofacial biology, others will find a thesis on the integration of empirical and theoretical biology, and still others will see a text on methods in comparative (functional) morphology. My overwhelming preoccupation with process, pattern *and* procedure in this work was not originally intended, but arose from what I perceived to be substantial deficiencies in the integration of theory and method in contemporary comparative morphology. To be sure, the comparative morphologist's task is a daunting one, requiring a working knowledge of evolutionary theory, systematics, developmental biology, paleontology, behavioral ecology, biomechanics, morphometrics, research design, data analysis, and more. And yet, there are no textbooks on comparative morphology: each individual researcher is obliged to forge his or her own path when integrating and applying these disciplines in their work.

Perhaps the rapid pace of progress in each of these fields has made it difficult for methodologists to keep up. For example, recent advances in data analysis techniques, particularly covariance structural modeling and hierarchical analysis, have proved to be a double-edged sword, permitting more refined modeling of biological and phylogenetic systems while at the same time exposing new problems and invalidating some of the traditional methods of comparative analysis. One step forward, two steps back. Whatever the reasons, we have not yet adequately delineated which particular combinations of operational, methodological, and analytical procedures (and their attendant assumptions and consequences) are compatible with current conceptual, theoretical and empirical knowledge. In short, comparative evolutionary morphology is currently in a state of methodological flux. The present work is not an attempt to bring order to this "anarchy," but pursues the more modest objective of examining in detail the main procedural issues relevant to basic comparative research, within the context of a cohesive conceptual, theoretical and empirical framework.

This concern with theoretical, operational and analytical integration occupies about one-half of the dissertation. The other half is devoted to the application of a new set of integrated procedures to an understanding of the nomological processes responsible for anthropoid craniofacial morphology. Such knowledge has wide utility in evolutionary biology. For example, in paleobiology, inferences made about the biological roles, and the ecological and evolutionary significance of certain traits in fossil specimens depend on empirically-based knowledge of the causal mechanisms responsible for the corresponding traits in living forms. Likewise, in taxonomy and historical analysis trait phenotypes are too often interpreted without any notion of the myriad of processes that conspired to give rise to them. More basic research is needed on the developmental and evolutionary mechanisms underlying organic form and form variation.

Several themes run the course of this work. Important among them is the view that cross-taxonomic comparative research is not, as sometimes portrayed, the second choice poorer cousin to experimental designs or to studies that examine a few specimens in greater detail. Each of these approaches has its own strengths and weaknesses and the choice of which one, or combination, to use depends upon the nature of the biological problem and research setting. They are complimentary, not alternative, approaches.

James McMahon
New York, 1999

Reproduced with permission of the copyright owner. Further reproduction prohibited without permission.

Acknowledgments

Wilson Mizner, the great American playwright, once wrote: "If you steal from one author, it's plagiarism; if you steal from many, it's research." Dissertation research goes beyond the mere pilfering and integration of ideas, however, and requires the appropriation of many peoples' time, money, and cooperation; and in some case the reorganization of lives. I am indebted to those who have provided academic, financial, and emotional support over the course of my graduate work.

I entered the CUNY Doctoral Program at about the same time that Dr. Timothy Bromage joined the Hunter College and CUNY Graduate Faculty in Anthropology, and his work immediately spurred my interest in craniofacial growth and development. He had barely stepped off the plane from London when I cajoled him into being my advisor. The choice was a good one. For nearly a decade, Tim has meted out sound advise, financial support and the facilities and resources needed to complete my studies (not to mention a steady stream of eclectic music piped through to the histology lab).

Dr. Les Marcus, Queens College, Biology Department, and the American Museum of Natural History, has also played a pivotal role in my graduate career, dissertation work, and professional life in general. Les taught me advanced statistics, morphometrics, and SAS programming. He provided the means for me to attend several advanced statistics workshops and seminars—Il Ciocco, Italy and Leeds, England—and has introduced me to many influential figures in the field of biometry (James Rohlf, Fred Bookstein, K. Mardia, Ian Dryden, and Dennis Slice to name a few). His mentoring has been essential to my professional growth.

I am also grateful to Dr. Fred Szalay, Hunter College and CUNY Graduate Faculty, for his insistence that I receive a well-rounded education in the fundamentals of mammalogy and evolutionary morphology, and for emphasizing the importance of basic comparative research (he insisted we "do our barnacles" before moving on to more complex problems). Fred has also prescribed a steady diet of fascinating and insightful books, which I might not otherwise have read (E.S. Russell's *Form and Function*, and *Foundations of Biophilosophy* by Mahner and Bunge, are two examples).

Thanks also to Dr. Eric Delson, Lehman College, CUNY, and the American Museum of Natural History, who was my first contact in the CUNY program and who acted as my advisor early on. Eric has been a constant supporter, finding me teaching positions, and sponsoring my work at the AMNH.

Several others have gone out of their way to provide encouragement and support. Dr. Chris Meiklejohn, University of Winnipeg, first got me interested in biological anthropology, partly due to his seemingly boundless knowledge of the subject matter and partly due to his infectious enthusiasm for the field, not to mention his good humor and perpetual smile. Drs. Marc Eichen and Nancy Larkin, formerly at the Academic Computing Service, Hunter College, hired me as a SAS coordinator and statistical consultant, a position I held for seven years, and my only year-round source of income during this period. I am deeply grateful to both of them for their many years of support and kindness. Dr. Ezra Shahn, Biology Department, Hunter College, gave me the opportunity to extend my knowledge of astronomy, physics, biochemistry and geology by employing me to teach the laboratory components of the *Foundations of Science* program. Ezra also gave me the opportunity to contribute to the development of the course curriculum and to help organize and participate in two international conferences on science education (New York, 1990;

Reproduced with permission of the copyright owner. Further reproduction prohibited without permission.

New Orleans, 1991). In June 1997, Dr. Stephanie Tortu, Principal Investigator, National Development and Research Institutes, New York, took the chance of hiring me as a Principal Research Associate at the Institute of AIDS Research, NDRI, even though I had not yet completed my Ph.D. and had no formal training or experience in the field of epidemiology. Stephanie allowed me to work flexible hours while completing my thesis, and she has displayed a remarkable blend of patience and encouragement while I grappled with learning a new discipline.

Many other colleagues, peers, and friends lent a helping hand since I came to New York. The late Ian Carmichael, along with Colleen McCann, Patrick Gannon, Beth Strasser, David Dean and Robert Costello "showed me the ropes" when I first enrolled in the CUNY program and my acclimation to New York and to CUNY would have been much more traumatic without their kind help and advise. More recently, Sylvia Atsalis, Doug Broadfield, Linda Brown, Elena Cunningham, Wendy Dirks, Steve Frost, Haviva Goldman, Katy Gonder, Katerina Harvati, Sam Marquez, Reiko Matsuda, Kieran McNulty, Warren Pardi, Eric Sargis and Johanna Warshaw have been my CUNY support network in the "trenches".

I am especially grateful to Warren Pardi for helping me design and build a craniophor, a rather complex devise used to hold a skull and radiographic film in proper orientation for x-ray exposure. Warren gave up his time and his workshop in Long Island for three consecutive weekends in the summer of 1994, and donated all the materials and his considerable skills to get the job done. Special thanks also to Haviva Goldman, who has helped me on innumerable occasions with so many favors I lost count. Also, if it were not for Haviva I would certainly not own a very nice pair of dress shoes (worn only once, to MacDonald's).

I owe a great deal of thanks to Terry Vulcano (CUNY Grad Center) and Ellen DeRiso (Hunter College and CUNY Grad Center) for their administrative help over the years. Without their assistance I would likely still be tangled up in the bureaucratic web of several large institutions.

Thanks to I. Dryden, P. O'Higgins, A. Boyde, C. Dean, J. Rohlf, F. Bookstein, W. Greaves, A. Taylor, and D. Enlow for their advise and discussions relating to my thesis topic. It is my pleasure to thank Prof. Donald Enlow for acting as the outside reader of my dissertation.

The artistic hand of Elizabeth McMahon rendered the illustrations in Chapter 5.

I would also like to acknowledge the exceptional libraries of the American Museum of Natural History, Mt. Sinai Medical School, and the City University of New York Interlibrary system. Using these three resources I was able to locate every single published article or chapter, no matter how obscure, I needed for my dissertation research.

I came into contact with many service representatives over the course of my work. Some were moderately helpful, some not at all, and a few went out of their way to provide assistance. The entire staff at Ewen-Parker X-ray Corporation, Elmsford, NY, deserve special mention for treating my small study with the concern and professionalism normally reserved for multi-million dollar projects. Thanks also to Nancy Chen at Kodak Inc., for supplying me with free test film and advice.

The following people granted me permission to study the primate specimens in their care, and provided assistance in this regard: Dr. Ian Tattersall and Gary Sawyer, Department of Anthropology (AMNH), Dr. Ross MacPhee and the staff of the Department of

Reproduced with permission of the copyright owner. Further reproduction prohibited without permission.

Mammalogy (AMNH), and Dr. Eric Delson, Department of Vertebrate Paleontology (AMNH) and Lehman College (CUNY).

Lastly, but foremost, I would like to express my most heartfelt thanks to my family back in Canada, my grandmother Kay, my mother Doris, father Harold, and my brother Jack and his family Sheryl, Michelle and Michael, and to my friends Dale and Karen for their love and support. The years of separation have not been easy. My sincerest appreciation also extends to my wife's family, father Rogelio, who passed away several years ago, mother Guadalupe, and AieSing, Gina, Jo-Jo, Baby and LA, who made me feel apart of their family from the very beginning. To my friends, the Bambico family, Fred, Bing, and Fredrick, who have been full partners in this journey, my deepest thanks.

I am intensely grateful to my mother for her unwavering love and support for all these years, and for enduring the absence of her son. She instilled in me the belief that I could do it.

Words cannot express the debt of gratitude I owe my wife Beth for her love, friendship, and yes, patience. She endured every hardship and reveled in every success, all the while providing a life outside of my work that sustained and enriched me. She rescued me from my 'throw-everything-in-a-wok' cooking style, and proved that the Roger rabbits of the world really can find a Jessica now and then. Thanks also to my daughter Athena, who grew up much too quickly, and has had to be more self-sufficient than should be expected. I have no reason to delay those driving lessons any longer.

I am proud to dedicate this doctoral dissertation to the three strongest and most extraordinary people I know: my grandmother Kay, my mother Doris, and my wife Beth.

Reproduced with permission of the copyright owner. Further reproduction prohibited without permission.

TABLE OF CONTENTS

VOLUME I

Copyright ii
Approval page iii
Abstract iv
Preface vi
Acknowledgements vii
Table of Contents x
List of Tables and Illustrations xii
Reference Glossary xx
Special Symbols xxiii

Part I Theoretical and Conceptual Framework

Chapter 1 Introduction and Overview 3
Chapter 2 Nomological Morphogenetic Theory 12

Part II Operational Framework

Chapter 3 Research Design 51
Chapter 4 Sample 65
Chapter 5 Data Collection Techniques 100

Part III Analytical Framework

Chapter 6 Phylogenetic Effects: Methods 129
Chapter 7 Phylogenetic Effects: Application 180
Chapter 8 Data Analysis Techniques and Assumptions 198

Part IV Nomological Hypotheses Testing (Constraints)

Chapter 9 Structural Growth Constraints 249
Chapter 10 Body Size Scaling 307
Chapter 11 Brain Form 344

(continued next page)

Reproduced with permission of the copyright owner. Further reproduction prohibited without permission.

VOLUME II

Part V Nomological Hypotheses Testing (Adaptations)

Chapter 12 Olfaction 410
Chapter 13 Locomotion 456
Chapter 14 Mastication 509

Part VI Synthesis and Conclusions

Chapter 15 Nomological Models of Anthropoid Nasomaxillary Diversity ... 601
Chapter 16 Conclusions and Applications 652

Part VII Appendices & Bibliography

Appendix A List and description of anatomical landmarks 681
Appendix B List and description of variables 684
Appendix C SAS/IML programs for constructing unified configurations 692
Appendix D SAS/IML programs to calculate variables from configurations 702
Appendix E Specimen raw variable data 741
Appendix F List of superimposition deviations 777

Bibliography 781

Reproduced with permission of the copyright owner. Further reproduction prohibited without permission.

LISTS OF TABLES AND ILLUSTRATIONS

Box No.	Content Type and Title	Page No.
Box 2.1	*Table*: Classification of sources of control stimuli	15
Box 2.2	*Table*: Skull tissue classification	17
Box 2.3	*Table*: Source of control stimuli by tissue classification	17
Box 2.4	*Table*: List of experimental craniofacial growth studies	32-35
Box 2.5	*Diagram*: Canine size distribution and plot with maxillary length	45
Box 4.1	*Table*: Formulae for determining sample sizes for various analyses	69
Box 4.2	*Table*: Classification of species included in study	75
Box 4.3	*Table*: Test for sample taxonomic proportions	76
Box 4.4	*Table*: Procrustes ANOVA tests of among-subspecies differences	78
Box 4.5	*Diagram*: Photos of *Alouatta palliata* [AMNH #18935]	81
Box 4.6	*Diagram*: Photos of *Ateles geoffroyi* [AMNH #177664]	81
Box 4.7	*Diagram*: Photos of *Lagothrix lagothricha* [AMNH #73555]	82
Box 4.8	*Diagram*: Photos of *Brachyteles arachnoides* [AMNH #80405]	82
Box 4.9	*Diagram*: Photos of *Chiropotes satanas* [AMNH #94120]	83
Box 4.10	*Diagram*: Photos of *Callicebus cupreus* [AMNH #75899]	83
Box 4.11	*Diagram*: Photos of *Pithecia pithecia* [AMNH #]	84
Box 4.12	*Diagram*: Photos of *Pithecia monachus* [AMNH #]	84
Box 4.13	*Diagram*: Photos of *Cebus apella* [AMNH #133631]	85
Box 4.14	*Diagram*: Photos of *Cebus capucinus* [AMNH #137993]	85
Box 4.15	*Diagram*: Photos of *Saimiri sciureus* [AMNH #64096]	86
Box 4.16	*Diagram*: Photos of *Aotus trivirgatus* [AMNH #78587]	86
Box 4.17	*Diagram*: Photos of *Saguinus oedipus* [AMNH #32702]	87
Box 4.18	*Diagram*: Photos of *Callithrix pygmaea* [AMNH #74369]	88
Box 4.19	*Diagram*: Photos of *Callimico goeldii* [AMNH #98367]	88
Box 4.20	*Diagram*: Photos of *Chlorocebus aethiops* [AMNH #80789]	89
Box 4.21	*Diagram*: Photos of *Cercopithecus neglectus* [AMNH #52414]	89
Box 4.22	*Diagram*: Photos of *Cercopithecus mitis* [AMNH #52363]	90
Box 4.23	*Diagram*: Photos of *Cercopithecus ascanius* [AMNH #55027]	90
Box 4.24	*Diagram*: Photos of *Macaca nemestraina* [AMNH #57111]	91
Box 4.25	*Diagram*: Photos of *Macaca fascicularis* [AMNH #102764]	91
Box 4.26	*Diagram*: Photos of *Macaca mulatta* [AMNH #60038]	92
Box 4.27	*Diagram*: Photos of *Papio hamadryas* [AMNH #52668]	92
Box 4.28	*Diagram*: Photos of *Lophocebus albigena* [AMNH #52613]	93
Box 4.29	*Diagram*: Photos of *Procolobus guereza* [AMNH #52238]	93
Box 4.30	*Diagram*: Photos of *Procolobus badius* [AMNH #52267]	94
Box 4.31	*Diagram*: Photos of *Nasalis larvatus* [AMNH #103465]	94
Box 4.32	*Diagram*: Photos of *Presbytis melalophos* [AMNH #102886]	95

Reproduced with permission of the copyright owner. Further reproduction prohibited without permission.

Box 4.33 *Diagram*: Photos of *Semnopithecus entellus* [AMNH #15004] ---------- 95
Box 4.34 *Diagram*: Photos of *Semnopithecus cristata* [AMNH #18935] ---------- 96
Box 4.35 *Diagram*: Photos of *Pongo pygmaeus* [AMNH #200898] ---------- 96
Box 4.36 *Diagram*: Photos of *Hylobates lar* [AMNH #54659] ---------- 97
Box 4.37 *Diagram*: Photos of *Hylobates syndactylus* [AMNH #102195] ---------- 97
Box 4.38 *Diagram*: Photos of *Gorilla gorilla* [AMNH #201472] ---------- 98
Box 4.39 *Diagram*: Photos of *Homo sapiens* ---------- 98
Box 4.40 *Diagram*: Photos of *Pan paniscus* [AMNH #86857] ---------- 99
Box 4.41 *Diagram*: Photos of *Pan troglodytes* [AMNH #] ---------- 99
Box 5.1 *Diagram:* Positive contact lateral cephalograph of *Cebus capucinus* ------ 103
Box 5.2 *Text*: Steps used to produce unified 3D landmark configurations ---------- 106
Box 5.3A *Diagram*: Radiographs illustrating landmarks, variables and planes ------- 107
Box 5.3B *Diagram*: Radiographs illustrating landmarks, variables and planes ------- 108
Box 5.3C *Diagram*: Radiographs illustrating landmarks, variables and planes ------- 109
Box 5.3D *Diagram*: Radiographs illustrating landmarks, variables and planes ------- 110
Box 5.4 *Table*: Descriptive statistics of repeated decimeter measurements --------- 117
Box 5.5 *Table*: Scale-dependent inaccuracy of Polhemus 3DRAW ---------- 118
Box 5.6 *Table*: Scale-dependent inaccuracy of Summagraphics digitizer ---------- 118
Box 5.7 *Table*: Field distortions of Polhemus 3DRAW digitizer ---------- 119
Box 5.8 *Table*: Field distortions of Summagraphics digitizer ---------- 120
Box 5.9 *Table*: Summary of standard deviation for morphometric data ---------- 124
Box 5.10 *Table*: Selected statistics for repeated measures ---------- 126
Box 6.1 *Diagram*: Scatter plot of two traits in 177 catarrhines ---------- 131
Box 6.2 *Diagram*: Same as Box 6.1 with distinct markers ---------- 132
Box 6.3 *Diagram*: Multi-level simulated phylogeny ---------- 135
Box 6.4 *Table*: Model parameters used for each trait in simulations ---------- 135
Box 6.5 *Diagram*: Single-level simulated phylogeny ---------- 136
Box 6.6 *Diagram*: Distribution of Y_1 trait over 400 simulated phylogenies --------- 138
Box 6.7 *Table*: Parameter estimates and Type I error for simulations ---------- 139
Box 6.8 *Diagram*: Histograms of *p*-values for simulated phylogenies ---------- 140
Box 6.9 *Table*: Results of phylogenetic autoregression with example data ---------- 153
Box 6.10 *Diagram*: Time-standardized ACP phenogram ---------- 154
Box 6.11 *Diagram*: Time-unstandardized ACP phenogram ---------- 156
Box 6.12 *Diagram*: Comparison of time-standardized and unstandardized ACP ---- 158
Box 6.13 *Diagram/Table*: Comparison different W matrices in autoregression ------ 166
Box 6.14 *Table*: Type I errors for various nonindependence methods ---------- 171
Box 6.15 *Table:* Type II errors for various nonindependence methods ---------- 176
Box 6.16 *Table*: R-square values for various autoregression methods ---------- 177
Box 7.1 *Diagram*: Working anthropoid phylogeny ---------- 189
Box 7.2 *Matrix*: W matrix of interspecies relationships ---------- 190-191
Box 7.3 *Diagram*: Regression of two traits using log raw data ---------- 196

Reproduced with permission of the copyright owner. Further reproduction prohibited without permission.

Box 7.4 *Diagram*: Regression using log transformed autoregression residuals ----- 196
Box 8.1 *Diagram*: Phenogram showing distribution of maxillary arch length ------203
Box 8.2 *Diagram*: ACP transformation of phenogram in Box 8.1 ----------204
Box 8.3 *Table*: Relationship between scientific and statistical outcomes----------212
Box 8.4 *Diagram*: Path diagram illustrating causal hypothesis ----------215
Box 8.5 *Diagram*: Path diagram of multi-level analysis ----------216
Box 8.6 *Table*: True univariate outliers for raw and log data---------- 225-226
Box 8.7 *Diagram*: Frequency distribution for ACFLGT [YV79] ----------231
Box 8.8 *Table*: Results of Shapiro-Wilk tests of normality ---------- 232-233
Box 8.9 *Table*: Effects of autoregression on data normality ----------234
Box 8.10 *Table*: Effects of log transformation on data normality ----------235
Box 8.11 *Diagram*: Box plots and histograms of variables in various scales --- 237-242
Box 9.1 *Table*: PCA eigenvalues for nasomaxillary variables----------252
Box 9.2 *Diagram:* PCA scree plot for nasomaxillary variables ----------253
Box 9.3 *Table*: PCA component loadings for nasomaxillary variables----------255
Box 9.4 *Diagram*: Plot of first two principal components ----------256
Box 9.5 *Diagram*: Plot of second and third principal components----------258
Box 9.6 *Table*: Summary of PCA results ----------259
Box 9.7 *Matrix*: Scatter plot matrix of nasomaxillary residuals on size-------- 262-263
Box 9.8 *Table*: List of infant specimens used on ontogenetic analysis ----------265
Box 9.9 *Diagram*: Superimpositions of infant and adult facial profiles-------- 269-270
Box 9.10 *Diagram*: Line chart comparing facial growth patterns ----------271
Box 9.11 *Diagram*: Factor plot depicting patterns of facial growth----------272
Box 9.12 *Diagram*: Bimaxillary superimpositions of infant and adult ---------- 274-276
Box 9.13 *Diagram*: Vectors of maxillary growth for anthropoids----------276
Box 9.14 *Diagram*: Biorbitale superimpositions of infant and adult---------- 279-281
Box 9.15 *Matrix*: Correlation matrix of nasomaxillary growth variables ----------282
Box 9.16 *Matrix*: Scatter plot matrix of nasomaxillary growth variables ----------283
Box 9.17 *Diagram*: Model of anterior facial elongation ----------287
Box 9.18 *Diagram*: Model of maxillary arch elongation ----------289
Box 9.19 *Diagram*: Model of facial rotation ----------294
Box 9.20 *Diagram*: Scatter plots for maxillary length-to-breadth growth----------299
Box 9.21 *Diagram*: Mean anthropoid configuration showing selected points --------303
Box 10.1 *Diagram*: Bivariate plots depicting isometry and allometry----------311
Box 10.2 *Diagram*: Allometric plots with non-zero intercept ----------313
Box 10.3 *Diagram*: Triangles showing spurious allometry ----------314
Box 10.4 *Table*: Numerical examples of spurious allometry----------315
Box 10.5 *Diagram*: Allometric equations and plots under varying conditions -------318
Box 10.6 *Diagram:* Regression of general size on centroid size ----------323
Box 10.7 *Diagram*: Regression of dry cranial weight on centriod size ----------324
Box 10.8 *Diagram*: Model showing effects of causal agents on shape ----------326

Reproduced with permission of the copyright owner. Further reproduction prohibited without permission.

Box 10.9 *Table*: Numerical examples of effects of causal agents on shape ----------331
Box 10.10 *Diagram*: Scatter plots of centroid size on nasomaxillary variables-- 337-340
Box 10.11 *Table:* Proportion of nasomaxillary variance accounted for by size--------342
Box 11.1 *Diagram:* Brain and facial growth vectors in relation to body size---------348
Box 11.2 *Table*: Hypotheses regarding brain form and cranial morphology----------358
Box 11.3 *Table*: Endocranial volume measures for anthropoid sample ----------361
Box 11.4 *Diagram*: Plot of endocranial volume against brain weight ----------361
Box 11.5 *Diagram*: Lateral radiographs showing brass-filled olfactory recess-------364
Box 11.6 *Table*: Definitions of orbital terms ----------367
Box 11.7 *Table:* Statistical predictions regarding brain and cranial variables--------369
Box 11.8 *Diagram*: Plot of endocranial volume against centroid size ----------372
Box 11.9 *Diagram*: Plot in Box 11.8 without *Homo* ----------372
Box 11.10 *Diagram:* Plot in Box 11.8 with catarrhines except *Homo* ----------373
Box 11.11 *Diagram*: Plot in Box 11.8 with platyrrhines ----------373
Box 11.12 *Table*: PCA eigenvalues for endocranial and nasomaxillary variables-----374
Box 11.13 *Table*: PCA loadings for endocranial and nasomaxillary variables---------375
Box 11.14 *Diagram*: PCA plot of first two principal component loadings ----------375
Box 11.15 *Table:* ML regression: ΔS_L_Y84 | ΔL_Y41 ----------378
Box 11.16 *Table*: ML regression: ΔL_Y81 | ΔS_L_Y84 ----------378
Box 11.17 *Table*: ML regression: ΔL_Y74 | ΔL_Y79 ----------379
Box 11.18 *Table*: ML regression: ΔL_Y74 | ΔS_L_Y84 ----------379
Box 11.19 *Table*: ML regression: ΔL_Y74 | ΔL_Y81 ----------380
Box 11.20 *Table:* ML regression: ΔL_Y74 | ΔL_Y70 ----------380
Box 11.21 *Table*: ML regression: ΔL_Y74 | ΔL_Y78 ----------381
Box 11.22 *Table*: ML regression: ΔL_Y30 | ΔL_Y74 ----------381
Box 11.23 *Table*: ML regression: ΔL_Y31 | ΔL_Y74 ----------382
Box 11.24 *Table*: ML regression: ΔL_Y30 | ΔL_Y70 ----------382
Box 11.25 *Table*: ML regression: ΔL_Y30 | ΔS_L_Y84 ----------383
Box 11.26 *Table*: ML regression: ΔL_Y30 | ΔL_Y81 ----------383
Box 11.27 *Table*: ML regression: ΔL_Y46 | ΔL_Y79 ----------384
Box 11.28 *Table:* ML regression: ΔL_Y46 | ΔL_Y81 ----------384
Box 11.29 *Table:* ML regression: ΔL_Y46 | ΔL_Y70 ----------385
Box 11.30 *Table*: ML regression: ΔS_L_Y49 | ΔL_Y78 ----------385
Box 11.31 *Table*: ML regression: ΔL_Y45 | ΔL_Y78 ----------386
Box 11.32 *Table*: ML regression: ΔL_Y70 | ΔS_L_Y84 ----------386
Box 11.33 *Table*: ML regression: ΔL_Y70 | ΔL_Y81 ----------387
Box 11.34 *Table*: ML regression: ΔL_Y70 | ΔL_Y78 ----------387
Box 11.35 *Table*: ML regression: ΔS_L_Y14 | ΔS_L_Y84 ----------388
Box 11.36 *Table*: ML regression: ΔS_L_Y14 | ΔL_Y70 ----------388
Box 11.37 *Table*: ML regression: ΔS_L_Y14 | ΔL_Y74 ----------389
Box 11.38 *Table*: ML regression: ΔS_L_Y14 | ΔL_Y78 ----------389

Reproduced with permission of the copyright owner. Further reproduction prohibited without permission.

Box 11.39 *Table*: Partial regression: ΔL_Y74 | ΔS_L_Y84 | ΔL_Y81 ---- 390
Box 11.40 *Table*: Partial regression: ΔL_Y74 | ΔL_Y70 | ΔS_L_Y84 ---- 390
Box 11.41 *Table*: Partial regression: ΔL_Y30 | ΔL_Y70 | ΔL_Y74 ---- 391
Box 11.42 *Diagram*: Scatter plots of endocranial and nasomaxillary variables ---- 392
Box 11.43 *Table*: Descriptive statistics for midfacial cribriform angle ---- 394
Box 11.44 *Diagram*: Schematic model of angular invariance ---- 400
Box 11.45 *Table*: Test of angular invariance for selected variables ---- 401
Box 12.1 *Diagram:* Paths comparing alternative olfactory hypotheses ---- 415
Box 12.2 *Table*: Hypotheses regarding olfaction and craniofacial morphology ---- 416
Box 12.3 *Diagram*: Scatter plot of brain size against foramen magnum size ---- 419
Box 12.4 *Table*: Olfactory bulbs size correlations ---- 420
Box 12.5 *Diagram:* Scatter plot of cribriform plate area and olfactory bulb size ---- 422
Box 12.6 *Diagram*: Scatter plot of olfactory cavity volume and olfactory size ---- 422
Box 12.7 *Table*: Ranking of sample olfactory acuity ---- 424
Box 12.8 *Table:* Mean olfactory acuity scores ---- 426
Box 12.9 *Table*: Statistical predictions regarding olfactory and cranial variables ---- 427
Box 12.10 *Diagram*: Scatter plot endocranial volume against cribriform plate area ---- 429
Box 12.11 *Diagram*: Scatter plot centroid size against cribriform plate area ---- 430
Box 12.12 *Diagram*: Scatter plot endocranial volume against cribriform plate area ---- 430
Box 12.13 *Table*: PCA eigenvalues for olfactory and nasomaxillary variables ---- 431
Box 12.14 *Table*: PCA components loadings for first two principal components ---- 432
Box 12.15 *Diagram*: Plot of first two principal component loadings ---- 432
Box 12.16 *Table*: Means for olfactory acuity by dietary preference ---- 435
Box 12.17 *Table*: ML regression: ΔS_L_Y49 | ΔS_L_Y44 ---- 437
Box 12.18 *Table*: ML regression: ΔS_L_Y1 | ΔS_L_Y44 ---- 438
Box 12.19 *Table*: ML regression: ΔS_L_Y4 | ΔS_L_Y44 ---- 439
Box 12.20 *Table*: ML regression: ΔS_L_Y5 | ΔS_L_Y44 ---- 439
Box 12.21 *Table*: ML regression: ΔS_L_Y6 | ΔS_L_Y44 ---- 440
Box 12.22 *Table*: ML regression: ΔS_L_Y7 | ΔS_L_Y44 ---- 440
Box 12.23 *Table*: ML regression: ΔS_L_Y8 | ΔS_L_Y44 ---- 441
Box 12.24 *Table*: ML regression: ΔS_L_Y14 | ΔS_L_Y44 ---- 441
Box 12.25 *Table*: ML regression: ΔS_L_Y16 | ΔS_L_Y44 ---- 442
Box 12.26 *Table*: ML regression: ΔS_L_Y17 | ΔS_L_Y44 ---- 443
Box 12.27 *Table*: ML regression: ΔS_L_Y18 | ΔS_L_Y44 ---- 443
Box 12.28 *Table*: ML regression: ΔS_L_Y22 | ΔS_L_Y44 ---- 444
Box 12.29 *Table*: ML regression: ΔS_L_Y26 | ΔS_L_Y44 ---- 444
Box 12.30 *Table*: ML regression: ΔL_Y30 | ΔS_L_Y44 ---- 445
Box 12.31 *Table*: ML regression: ΔL_Y33 | ΔS_L_Y44 ---- 445
Box 12.32 *Table*: ML regression: ΔL_Y35 | ΔS_L_Y44 ---- 446
Box 12.33 *Table*: ML regression: ΔL_Y45 | ΔS_L_Y44 ---- 446
Box 12.34 *Table*: ML regression: ΔS_L_Y34 | ΔS_L_Y49 ---- 447

Reproduced with permission of the copyright owner. Further reproduction prohibited without permission.

Box 12.35 *Table*: ML regression: ΔS_L_Y49 | ΔL_Y45 ----------447
Box 12.36 *Table*: ML regression: ΔS_L_Y49 | ΔS_L_Y17 ----------447
Box 12.37 *Table*: ML regression: ΔS_L_Y49 | ΔL_Y30 ----------448
Box 12.38 *Table*: ML regression: ΔS_L_Y49 | ΔL_Y35 ----------448
Box 12.39 *Table*: ML regression: ΔL_Y45 | ΔS_L_Y34 ----------448
Box 12.40 *Diagram*: Scatter plots of cribriform plate against nasomaxilla ----------449
Box 13.1 *Diagram*: Path diagrams comparing alternative hypothoses----------468
Box 13.2 *Table*: Hypotheses regarding locomotion and cranial morphology--- 469-470
Box 13.3 *Table*: Locomotor behavior of anthropoid species ----------473
Box 13.4 *Table*: Statistical predictions regarding locomotion ----------474
Box 13.5 *Diagram*: Scatter plot of condylar index against foramen mag. Slope -----476
Box 13.6 *Table*: Species mean condylar index and FM slope----------479
Box 13.7 *SAS Output*: Multiple regression condylar index on locomotion----------482
Box 13.8 *SAS Output*: Multiple regression FM slope on locomotion ----------483
Box 13.9 *SAS Output*: Multiple regression cranial base angle on locomotion --------484
Box 13.10 *Diagram*: Scatter plot of centroid size against FM slope----------485
Box 13.11 *Diagram*: Scatter plot of centroid size against condylar index ----------486
Box 13.12 *Table*: PCA eigenvalues for locomotor and nasomaxillary variables ------487
Box 13.13 *Table*: PCA components loadings for first two principal components -----488
Box 13.14 *Diagram*: Plot of first two principal component loadings----------489
Box 13.15 *Table*: Regression results from hypotheses statements ----------491
Box 13.16 *Table*: Regression results from hypotheses statements ----------492
Box 13.17 *Table*: ML regression: ΔS_L_Y14 | ΔL_Y70 ----------493
Box 13.18 *Table*: ML regression: ΔL_Y30 | ΔL_Y70 ----------494
Box 13.19 *Table*: ML regression: ΔL_Y32 | ΔL_Y70 ----------495
Box 13.20 *Table*: ML regression: ΔL_Y46 | ΔL_Y70 ----------496
Box 13.21 *Table*: ML regression: ΔL_Y69 | ΔL_Y70 ----------497
Box 13.22 *Table*: ML regression: ΔL_Y70 | ΔS_L_Y84 ----------498
Box 13.23 *Table*: Partial regression: ΔL_Y69 | ΔL_Y70 | ΔS_L_Y84----------498
Box 13.24 *Table*: Multiple regression: ΔL_Y69 | ΔL_Y70 | ΔL_Y81 | ΔS_L_Y84----499
Box 13.25 *Diagram*: Scatter plots of condylar index against cranial variables --------500
Box 13.26 *Diagram*: Scatter plots of CBA against cranial variables ---------- 501-502
Box 13.27 *Diagram*: Path diagram of brain size and cranial traits----------507
Box 14.1 *Diagram*: Path diagrams showing masticatory effects on skull form-------513
Box 14.2 *Table*: Classification of research methods in cranial morphology ----------515
Box 14.3 *Table*: Hypotheses of masticatory effects ---------- 527-528
Box 14.4 *Table*: Dietary properties of anthropoid sample ----------531
Box 14.5 *Diagram*: Depictions of Greaves' triangle of support model ---------- 541-542
Box 14.6 *Table*: Species mean bite force magnitudes----------544
Box 14.7 *Table*: Predicted associations between masticatory and cranial variables -547
Box 14.8 *SAS Output*: Multiple regression of diet on centroid size ----------550

Reproduced with permission of the copyright owner. Further reproduction prohibited without permission.

Box 14.9 *Diagram:* Mean centroid sizes by dietary categories ----------550
Box 14.10 *Diagram*: Skull photos showing mechanical constraints on form ----------553
Box 14.11 *Diagram*: Scatter plots of centroid size on masticatory variables----- 555-557
Box 14.12 *Table*: Predicted associations deduced from hypotheses----------559
Box 14.13 *SAS Output*: Multiple regression results for masticatory variables --- 561-562
Box 14.14 *SAS Output*: Tukey's test for differences among means ----------564
Box 14.15 *Table*: Regression tests relating to hypotheses statements----------568
Box 14.16 *Table*: Multi-level regression tests of hypotheses---------- 578-585
Box 14.17 *Table*: ML regression: ΔS_L_Y4 I ΔS_L_Y57----------586
Box 14.18 *Table*: ML regression: ΔS_L_Y6 I ΔS_L_Y57----------586
Box 14.19 *Table*: ML regression: ΔS_L_Y12 I ΔS_L_Y57 ----------587
Box 14.20 *Table*: ML regression: ΔS_L_Y12 I ΔS_L_Y58 ----------588
Box 14.21 *Table*: ML regression: ΔS_L_Y17 I ΔS_L_Y57 ----------589
Box 14.22 *Table*: ML regression: ΔL_Y13 I ΔS_L_Y57 ----------590
Box 14.23 *Table*: ML regression: ΔS_L_Y14 I ΔL_Y59 ----------591
Box 14.24 *Table*: ML regression: ΔS_L_Y23 I ΔL_Y59 ----------592
Box 14.25 *Table*: ML regression: ΔS_L_Y24 I ΔS_L_Y51 ----------593
Box 14.26 *Table*: ML regression: ΔL_Y30 I ΔL_Y59 ----------593
Box 14.27 *Table*: ML regression: ΔL_Y33 I ΔS_L_Y58 ----------594
Box 14.28 *Table*: ML regression: ΔL_Y33 I ΔS_L_Y57 ----------595
Box 14.29 *Table*: ML regression: ΔL_Y35 I ΔS_L_Y57 ----------596
Box 14.30 *Table*: ML regression: ΔS_L_Y34 I ΔS_L_Y49 ----------596
Box 14.31 *Table*: PCA eigenvalues for masticatory and nasomaxillary variables-----597
Box 14.32 *Table*: PCA components loadings for first two principal components -----598
Box 14.33 *Diagram*: Plot of first two principal component loadings----------598
Box 15.1 *SAS Output*: Model I CSA estimation equations ---------- 603-606
Box 15.2 *Table*: Model I fit indices----------607
Box 15.3 *SAS Output*: Model I condition index collinearity diagnostic --------- 609-611
Box 15.4 *Table*: Model I Lagrange and Wald respecification indices ----------612
Box 15.5 *Table*: Model I to Model II respecification details---------- 613-614
Box 15.6 *SAS Output*: Model II CSA estimation equations ---------- 615-617
Box 15.7 *SAS Output*: Model II condition index collinearity diagnostic -------- 617-619
Box 15.8 *Table*: Model II test for curvilinearity ----------620
Box 15.9 *Table*: Model II test for influential outliers ----------622
Box 15.10 *Table*: Model II fit indices----------623
Box 15.11 *Table*: Model II R-squared ----------624
Box 15.12 *Table*: Model II ANSCOVA table---------- 627-628
Box 15.13 *Diagram*: Path Submodel A----------630
Box 15.14 *Diagram*: Frequency distributions: anterior facial length----------633
Box 15.15 *Diagram*: Selected facial profile configurations ----------637
Box 15.16 *Diagram*: Path Submodel B----------648

Reproduced with permission of the copyright owner. Further reproduction prohibited without permission.

Box 16.1 *Diagram*: Scatter plot of maxillary arch length against centroid size ------674
Box 16.2 *Diagram*: Scatter plot of maxillary arch length against brain size ----------674
Box 16.3 *Diagram*: Residual-by-predicted plot Model II----------675
Box 16.4 *Diagram*: Residual-by-predicted plot Model II, subsample ----------675

Reproduced with permission of the copyright owner. Further reproduction prohibited without permission.

Reference Glossary

ACP (see Ancestrally Centered Phylogeny)

Ancestrally centered phylogeny (ACP): Term given by author to the technique used to transform a multi-level phylogeny into a single-level phylogeny, thereby attempting to restore statistical independence to a set of cross-taxonomic data. It is shown that all valid GLM-based nonindependence techniques (including phylogenetic autoregression, nested ANOVA, and independent contrasts) reduce to the ACP model (also see time-standardized ACP, time-unstandardized ACP). (see Chapters 6-8)

Angular invariance (or geometric invariance): The maintenance of a constant angle formed by two planes or lines (anatomically defined) due to a biological constraint operating throughout ontogeny and/or phylogeny. (see Chapter 11)

Autoregression/ACP procedure: Application of the ACP method in which phylogenetic autoregression is used to estimate the ancestral morphotypes of the last shared ancestors (LSAs) of a set of extent species (also see Ancetrally Centered Phylogeny, phylogenetic autoregression; LSA) (see Chapters 6-8)

Centroid size: Measure used to quantify the scale of each specimen in a sample. Defined operationally as the square root of the sum of the squared distances between the center of a configuration of landmarks and each point in the same configuration. (see Chapter 10)

CRIBS: Measure of olfactory aquity defined as: [log(Δcribriform plate area)$^{0.5}$ - log(Δendocranial volume)$^{0.33}$], using data obtained in this study (also see LOBES) (see Chapter 12)

CSA (covariance structure analysis) see CSM

CSM (covariance structure modeling) [=CSA, SEM]: A multiple regression analytical technique that attempts to assess the fit between a theory-implied model (covariance structure matrix) and a set of empirical relationships (sample covariance matrix). The technique allows the researcher to specify a phenomenological model composed of a series of causal pathways among operationalized variables, and test these pathways for association, taking into account all other pathways in the model. (see Chapter 8)

DCA (distal causal agent): An organic property, function or biological role whose change can potentially effect changes in other organic properties through distal causal mechanisms; proposed DCAs of nasomaxillary morphology include geometric size, brain form, olfaction, locomotion and mastication. (see Chapters 1-3)

Reproduced with permission of the copyright owner. Further reproduction prohibited without permission.

DCM (distal causal mechanism): One of several processes or mechanisms by which DCAs act to effect change in organic properties; DCMs determine the population distribution, propogation or expression of organic properties and thier underlying developmental (proximate) programs; DCMs include selection, acclimation and biological constraints.(see Chapters 1-3)

Delta-transformed data: Data that have been transformed using the ACP procedure. This procedure transforms data from static to dynamic (i.e., the data are transformed from quantity values to values representing a *change* in quantity).(also see Ancestrally Centered Phylogeny) (see Chapters 6-15)

LOBES: Measure of olfactory aquity defined as: [log(bulbus olfactorius)$^{.33}$ - log(cranial volume)$^{.33}$, from data reported in Stephan *et al.*, 1981 (also see CRIBS) (see Chapter 12)

LSA (Last shared ancestor): Term used in association with the ACP method to designate the ancestor of a given focal species that is the last immediate shared ancestor between the focal species and the species in the study sample to which it is most closely related (also see Ancestrally Centered Phylogeny) (see Chapters 6-8)

MBF (maximum bit force): Estimate of the maximum bite force magnitude that a given specimen could generated at a given tooth based on a modified version of Greaves' (1978) three-dimensional model of masticatory function. (see Chapter 14)

Mosimann isometric residual: A method of size adjustment that scales the variates of Y to a common geometric size. Operationally defined as the residual term from a regression of log(Y) on log(X) with the regression slope set to 1.0, where X is centroid size and Y a metric variable. (can also be calculated as log(Y)-log(X)). (see Chapter 10)

MRV (maximum resultant vector): Resultant masticatory force vector through skull at which the magnitude of masticatory muscle force is at its maximum. (see Chapter 15)

Multi-level dataset: In the context of the current study, this refers to the morphometric dataset composed of three analytical levels. (1) M-level data: species mean values, (2) Q-level data: pooled-within species values, and (3) V-level data: individual level values. The three levels are related such that V = M + Q. The multi-level dataset subjected to analyses in the current study was also delta-transformed (see Chapters 6 & 7), log transformed (Chapter 8), and scale standardized (Chapter 10).

Multi-level phylogeny: A phylogenetic tree (hypothetical, mathematical or real) in which descendents are related through a nested inclusive heirarchy of common ancestors. [also see single-level phylogeny] (see Chapter 6)

Reproduced with permission of the copyright owner. Further reproduction prohibited without permission.

Phylogenetic autoregression: Regression-based technique in which a relatedness weight (W) matrix is used to control for "phylogenetic effect" in a cross-taxonomic dataset, thereby attempting to restore statistical independence to one or more sets of measurements. (see Chapter 6)

SBMM (smallest biologically meaningful measurement): The value of the smallest quantity deemed to be biologically meaningful, within the context of a given research domain. The SBMM is important for establishing the effect size and power of statistical test of significance, and in determining the allowable degree of measurement error. [also see SSDM] (see Chapter 4)

SEM (structural equation modeling) see CSM

Single-level phylogeny: A phylogenetic tree (hypothetical, mathematical or real) in which all descendents share one, and only one, immediate common ancestor. [also see multi-level phylogeny] (see Chapter 6)

Size-related quantity: A property of an organism that is associated with but not identidal to geometric size. Weight and surface-area-to-volume ratio are examples of size-related quantities. (see Chapter 10)

Spurious allometry: In the context of explanatory research, an instance in which a morphometric size variable appears to have an allometric effect on another morphometric variable (when in fact it does not) due to model misspecification (i.e., when relevant variables are omitted from the model). (see Chapter 10)

SSDM (smallest statistically detectable measurement): The value of the minimum quantity that can be detected through measurement (i.e., measurement resolution); or the effect size (see Cohen, 1988) that is detectable through analysis (i.e., analytical resolution). Optimally, SSDM should be smaller than SBMM so that the researcher is able to detect, through measurement and analysis, the smallest biologically meaningful quantity. [also see SBMM] (see Chapter 4)

Structural growth constraint: Instance in which changes to one property of an organism during ontogeny induce or constrain changes in another property through their mutual structural integration. (see Chapter 9)

Time-standardized ACP: Variant of ACP method that transforms data into units of *rates* of change from a specified set of ancestors to a specified set of descendents (also see: Ancestrally Centered Phylogeny; time-unstandardized ACP) (see Chapter 6)

Time-unstandardized ACP: Variant of ACP method that transform data into units of *absolute* change from a specified set of ancestors to a specified set of descendents (also see: Ancestrally Centered Phylogeny; time-standardized ACP) (see Chapter 6)

Reproduced with permission of the copyright owner. Further reproduction prohibited without permission.

Special Symbols

▲ Symbol used to represent specimens or species of platyrrhine primates on scatter plots

\+ Symbol used to represent specimens or species of cercopithecoids on scatter plots

■ Symbol used to represent specimens or species of hominoids on scatter plots

Δ Label prefix used to signify that a given variable has been delta-transformed

L_ Label prefix used to signify that a given variable has been log transformed

S_ Label prefix used to signify that a given variable has been size-standardized on cranial centroid size using the Mosimann log-log isometric residual method

B_ Label prefix used to signify that a given variable has been size-standardized on cube root endocranial volume using Mosimann log-log isometric residual method

V Variable symbol signifying that the variable is constructed as a V-level data component (see Multi-level dataset; see Chapter 8)

M Variable symbol signifying that the variable is constructed as an M-level data component (see Multi-level dataset; see Chapter 8)

Q Variable symbol signifying that the variable is constructed as a Q-level data component (see Multi-level dataset; see Chapter 8)

Reproduced with permission of the copyright owner. Further reproduction prohibited without permission.

VOLUME I

Reproduced with permission of the copyright owner. Further reproduction prohibited without permission.

PART I

Theoretical and Conceptual Framework

Reproduced with permission of the copyright owner. Further reproduction prohibited without permission.

Chapter 1. Introduction and Overview

Broadly speaking, this work is about organic diversity—the processes responsible for organic diversity, and the methods used to discover how these processes operate. More specifically, using the methods of comparative biology, I attempt to quantify the effects of a series of causal agents (i.e., changes in body size, brain form, olfaction, locomotion, and mastication) on (the diversity of) nasomaxillary form among extant anthropoid primates. An understanding of the factors responsible for *nasomaxillary* variation is of particular importance since this region figures so prominently in tests of competing paleobiological and systematic hypotheses.

Comparative analysis of nasomaxillary characters such as facial prognathism, dental arch shape, palatal depth, facial height and breadth, and nasal aperture shape have provided important contributions to evolutionary primatology (e.g., Le Gros Clark, 1959; Albrecht, 1978; Wood, 1991). The earliest post-Darwinian attempts to explain variation of primate nasomaxillary form were concerned with form-function adaptations and macroevolutionary "trends" (e.g., Smith, 1912). These adaptational explanations generally fall into one of three main categories: (1) olfaction, (2) locomotion, and (3) mastication.

Best known of the evolutionary scenarios that purport to explain nasomaxillary diversity in terms of olfactory acuity is the "arboreal theory" of Sir Grafton Elliot Smith (1912) and Frederick Wood Jones (1916). Smith (1912) argued that the sense of smell, so vital in a terrestrial habitat, is relegated to a secondary role in an arboreal setting. With the evolution of arboreal mammals,

Reproduced with permission of the copyright owner. Further reproduction prohibited without permission.

such as primates, the olfactory apparatus diminished in size resulting in an overall reduction of the snout. Cartmill (1972, 1974), in his classic critique of the arboreal theory, questioned whether arboreality per se was sufficient to initiate olfactory reduction, but he did not question the proposed causal link between (changes in) olfactory acuity and nasomaxillary form.

Other studies have sought a correspondence between head posture and craniofacial morphology (Bolk, 1909; Weidenreich 1924; DuBrul 1950, 1962). As early as 1896, T. H. Huxley showed in a comparison of modern humans and other mammalian crania that the orientation of the foramen magnum was correlated with several features of facial form. Experimental studies involving rats (e.g. Moss, 1961) also appear to confirmed a link between locomotor behavior and nasomaxillary form in mammals. Moss (1961) found that rats experimentally forced into an orthograde posture experienced a forward migration of the nasomaxillary complex relative to the rest of the cranium. He concluded that "...head carriage plays some role in the mutual adjustment of the facial and neural parts of the head" (p. 305).

A considerable literature has accumulated on the ecological and biological roles of diet and mastication in the production of nasomaxillary variation. The properties of food items consumed by anthropoids and other mammals impose specific requirements on the biomechanics of the masticatory apparatus (Ahlgren 1966; Hiiemae & Crompton 1971; Luschei & Goodwin 1974; Herring, 1976). Masticatory explanations of nasomaxillary form assume that craniofacial morphology will reflect adaptations that establish maximum mechanical efficiency to cope with these requirements. Numerous studies indicate, for example, that

Reproduced with permission of the copyright owner. Further reproduction prohibited without permission.

relative orthognathy, pronounced facial height, and a reduced anterior dentition coincide with masticatory functions associated with a diet of tough or hard-object foods (e.g., Jolly, 1970; Kinzey, 1974; Roberts & Tattersall, 1974; DuBrul, 1977; Sakka, 1984).

An alternative to these adaptational hypotheses is the view that anthropoid nasomaxillary variation arises from allometric scaling to body size. There have been surprisingly few studies on the effects of body size on craniofacial form (Cochard, 1985; Emerson & Bramble, 1993). Shea (1983), following Giles (1956), found that much of the observed variation of nasomaxillary form in African apes could be explained almost entirely by allometric scaling. That is, the proportions of facial length, height and width "...observed in gorillas are what would be predicted if the ontogenetic allometries of chimpanzees were extended to larger sizes" (Shea, 1983:39). Other workers have likewise asserted that body size allometry can account for much of the observed variation in craniofacial morphology of various mammalian taxa (e.g., Freedman, 1962; Fooden, 1969; Albrecht, 1978; Radinsky, 1981; Cochard, 1985).

Another hypothesized source of nasomaxillary variation is the growth and form of the brain. Weidenreich (1941), exploring earlier observations by Studer (1901), contended that mammalian brain size is negatively allometrically related to body size. He further demonstrated that the relatively larger brains of smaller mammals were correlated with a suite of nasomaxillary characteristics, including an orthognathic face, a reduced or missing olfactory recess, reduced maxillary length and height, an occlusal plane that is rotated up anteriorly relative to the Frankfort Horizontal, and a reduced masticatory apparatus. Weidenreich concluded that the

Reproduced with permission of the copyright owner. Further reproduction prohibited without permission.

relative size of the brain was the primary factor determining craniofacial form among mammals.

Three decades later, Enlow and colleagues (e.g., Enlow, 1975) confirmed many of Weidenreich's original observations, and attempted to explain them in terms of developmental and evolutionary constraints. In a comparative sample of mammals Enlow and McNamara (1973) noticed that specimens with relatively large brains, particularly those with expanded frontal lobes, had a marked horizontal orientation of the olfactory bulbs and underlying cribriform plate, and a correspondingly vertical (orthognathic) facial profile. According to Enlow and McNamara (1973), as the frontal lobes expand the cribriform plate is pushed into a more horizontal position. Since the cribriform plate and facial plane maintain an invariant perpendicular angular relationship (due to the intimate connection between the olfactory apparatus, the cribriform plate, the ethmoid, and the entire nasomaxillary complex), a more horizontal cribriform plate translates into a more vertical (orthognathic) facial profile. In this way, the form of the brain and the corresponding orientation of the olfactory bulbs determine the growth trajectory of the face. "The downward rotation of the olfactory bulbs and the whole anterior cranial floor by the enlarged frontal lobes of the cerebrum has caused a corresponding downward rotation of the nasomaxillary complex" (Enlow, 1990:167).

The present study attempts to quantify and qualify the causal effects of changes in body size (Shea, 1983), the size and form of the brain (Weidenreich, 1941) and the concomitant orientation of the olfactory bulbs (Enlow & McNamara, 1973), olfactory acuity (Smith, 1912), head posture (Adams & Moore, 1975), and

Reproduced with permission of the copyright owner. Further reproduction prohibited without permission.

the magnitude and distribution of masticatory forces (Kinzey, 1974; Hylander, 1975) on (the diversity of) anthropoid nasomaxillary form.

By focusing on these five causal agents, I have intentionally limited the study to an analysis involving a class of developmental and evolutionary processes that I refer to as *distal nomological causal mechanisms*. The term *nomological* is defined as relating to or expressing basic laws or rules governing the behavior of physical entities. Nomological processes are by definition regular, repetitive and predictable. By contrast, *chance* processes are characterized by random, idiosyncratic and contingent events, and are not generally predictable (Bock, 1988; Mahner & Bunge, 1997). A good example comes from cosmology, where nomological processes such as nuclear fusion, electromagnetism, and gravitation, can help explain much of the structure of the universe (e.g., the existence of stellar objects and the formation of galaxies). But it is also hypothesized that chance processes, such as random disproportionalities in the distribution of matter in the moments following the Big Bang, played a crucial role in shaping the universe. Likewise, both nomological and chance processes operate at the organic level in the production of biological diversity.

It is often convenient to further divide nomological processes into two types depending upon the causal mechanism involved: proximate or ultimate. In biology, proximate causal mechanisms are those operating at the cellular and subcellular levels (e.g., protein translation in response to an external morphogen), and they are the most immediate causes of organic form. Ultimate causal mechanisms, which operate on both the organismic and superorganismic levels, constitute the evolutionary forces that determine the historical origins and propagation of

Reproduced with permission of the copyright owner. Further reproduction prohibited without permission.

genotypes (Goldsmith, 1991:7). The concept of ultimate causation has recently come under attack by Mahner and Bunge (1997, see p. 40), and in its place I employ the concept of distal causation, which includes mechanisms that determine the patterns of proximate expression of organic form and form variation. I distinguish three main types of *distal nomological causal mechanisms*: Darwinian selection, physiological acclimation, and biological constraint (see Chapter 2). In addition to quantifying the effects of the five causal agents on nasomaxillary form, I also attempt to delineate the distal nomological mechanisms through which they operate to produce morphological variation. For example, if mastication is shown to affect nasomaxillary form, does this causal agent operate via selection, acclimation, biological constraint, or some combination of these mechanisms?

By focusing exclusively on distal nomological processes in this study, I will not be able to provide a complete explanation for anthropoid nasomaxillary diversity. Diversity resulting from chance historical events (i.e., "fully random events and processes" in the ontology of Mahner and Bunge, 1997:42) will be left unexplained. Moreover, it will be shown that nomological and chance processes are so interconnected that it is not entirely possible to isolate nomological mechanisms without specifying some aspects of chance processes (e.g., the contingent historical events affecting a given phylogenetic branching pattern). My objective is therefore to formulate and test a limited model that specifies the contributions of and relationships among the five stipulated causal agents, operating via distal nomological mechanisms, that can account for some proportion of the total variation of nasomaxillary form among anthropoids.

To accomplish this objective I have integrated, in a novel way, a set of

Reproduced with permission of the copyright owner. Further reproduction prohibited without permission.

conceptual, operational and analytical procedures within the context of a comparative research design. At its core, this methodology attempts to emulate an experimental design in which the effects of certain "treatments" or "conditions" (i.e., body size, brain form, olfaction, locomotion, and mastication) and their associated causal mechanisms (i.e., selection, acclimation and constraint) are isolated using a multi-level covariance structural modeling approach.

The study involves morphometric analyses of 300 adult and 24 infant female anthropoid specimens representing 37 species. Biological landmarks were digitized in 3D directly from dry skulls and in 2D from lateral radiographs of the same specimens. The 3D and 2D landmark configurations where then "snapped" together to produce a unified 3D configuration for each specimen consisting of both ectocranial (3D) and midline endocranial (2D) landmarks. This is the first study, to my knowledge, that such a technique has been used. The advantage of collecting data in the form of 3D landmark configurations is that many different kinds of measurements can be calculated from the 3D coordinates, including linear distances, estimated areas and volumes, ratios, angles, and measurements involving constructed points. Coordinate data also permitted 3D static modeling of the skull, and it was therefore possible to calculate maximum potential bite force estimates for each specimen based on a 3D model of its masticatory system.

The significance of this research is four-fold. First, morphometric data on a substantial sample of anthropoid primates is provided (Appendix E). Because the raw data consist of landmark coordinates, many anatomical measurements, in addition to the ones reported here, can easily be extracted from the coordinate matrices using standard algorithms. Second, an integrated conceptual, operational

Reproduced with permission of the copyright owner. Further reproduction prohibited without permission.

and analytical framework is advanced that was designed to increase the power of causal inference in comparative morphological research. Third, this research contributes a series of new hypotheses formulated to explain specific nasomaxillary traits among extant anthropoid primates. These hypotheses will require additional testing, and it is hoped that such tests may shed further light on current issues in the area of primate craniofacial biology. Finally, the findings of this study benefit the fields of primate systematics and paleobiology. An understanding of the underlying causal agents and mechanisms affecting the form (or, more correctly, the change of form) of specific characters is necessary for tests of phylogenetic hypotheses. For example, the causal factors responsible for variation of palatal depth (so often used as a character in tests of hominine phylogeny) is not fully understood, and thus the usefulness of this character in a phylogenetic analysis remains largely unknown. The substantive results obtained in this research will aid in the assessment of the taxonomic value of this and other nasomaxillary characters. Moreover, the greater our understanding of the causes leading to craniofacial variation among extant forms, the better our ability to interpret the paleobiology of extinct species. At the heart of this approach is the ability to predict unknown properties of fossil forms from established nomological causal relationships between known properties of extant forms[1]. Its application is whimsically illustrated by the following anecdote involving the legendary French paleontologist Georges Cuvier. Apparently, one night a group of students bent upon a practical joke broke into Cuvier's rooms, and one student, dressed in a devil's costume of horns, tail, and hoofed feet, approached his bed and declared "Cuvier, I have come to eat you!" Cuvier reportedly woke up,

[1] This approach is also the corner-stone of modern forensic science.

Reproduced with permission of the copyright owner. Further reproduction prohibited without permission.

gave him a single glance, and retorted, "All animals with horns and hooves are herbivorous. You won't eat me," and promptly went back to sleep (Fadiman, 1985).

Reproduced with permission of the copyright owner. Further reproduction prohibited without permission.

Chapter 2. Nomological Morphogenetic Theory

Introduction

In any scientific investigation, the nature of the questions asked and the subsequent methods applied to their resolution depend upon the underlying theoretical framework (*cf.* Sober, 1988; Szalay & Bock, 1991). In evolutionary morphology, when the goal is to explain morphological diversity in terms of nomological mechanisms, methodological procedures and hypotheses formulations must conform to a specified morphogenetic evolutionary model (i.e., a set of theoretical and conceptual parameters relating to the dual processes of ontogeny and phylogeny).

A sundry of morphogenetic models have been advanced (e.g., van Limborgh, 1982; Enlow, 1990; Alberch, 1990; Atchley & Hall, 1991) that integrate knowledge from several converging fields in an attempt to explain morphological diversity. At the heart of this emerging synthesis is an attempt to resolve the relationship between (1) the processes governing the morphological development of a single organism from zygote to death, and (2) the processes responsible for the observed patterns of morphological diversity among organisms and among taxa.

Among vertebrates, organisms go through the same basic stages and processes of development: cleavage, gastrulation, neurulation, cell interaction, migration and differentiation, and organogenesis. Morphological diversity arises from the origin and sorting of variations in these developmental processes. It follows that a consideration of both development and evolution is essential in the study of organic diversity. This argument, first stated by Darwin, has been a

Reproduced with permission of the copyright owner. Further reproduction prohibited without permission.

recurrent theme (and the subject of much debate) in modern morphology (e.g., Haeckel, 1866; Roux, 1881; Thomson, 1988).

The use of developmental data by comparative osteologists, most particularly paleontologists, has increased dramatically over the past twenty years, and it has now become common practice for morphologists to consider in some detail the embryonic history of the tissues with which their calipers come into contact. While it may be true that "...one does not need to know much about the particularities of a system of gene regulation or of pattern formation to make [the claim that] certain evolutionary transformations are more likely than others" (Alberch, 1990:15), it is evident that such data are essential to formulate models of morphology that guide research, and bestow added explanatory power (*cf.* Björk, 1972).

Closely related to the processes of ontogeny and phylogeny are the mechanisms of proximate and distal causation. Although distal causal mechanisms are the primary focus of this research, the two are so tightly connected that it is not possible to comprehend one without reference to the other.

In this chapter I briefly review several important concepts that are vital to current morphological theory, while examining the available evidence to formulate a morphogenetic model that will provide the theoretical framework used throughout this work. I divide the discussion along lines of proximate versus distal mechanisms of morphological diversity.

Proximate Causal Mechanisms of Morphological Diversity

Cellular Control of Development

A common conceptual thread running through the various models of morphological

Reproduced with permission of the copyright owner. Further reproduction prohibited without permission.

diversity is the postulate that *inter-individual variation of organic form obtains from variation of underlying genetic and cellular activities of tissues during development* (de Beer, 1958a; Davidson, 1976). These cellular activities are regulated by chemical signals (morphogens) and other stimuli that originate from a variety of sources (Varrela, 1991). With regard to pre-skeletal and skeletal tissues, van Limborgh (1982) and Atchley and Hall (1991) distinguish three main nonrandom sources of cell-regulating signals: (1) intrinsic genetic, (2) epigenetic, and (3) environmental.

Intrinsic genetic control occurs when a cell lineage's own gene products stimulate and further direct its genetic and cellular activities (autocrinal stimulation). In this event, no paracellular or extracellular information is required for the production of tissue structure and form. Cells under intrinsic genetic control are said to be self-differentiating and self-organizing. Epigenetic control occurs when another cell lineage's gene products provide the stimulus for regulating the genetic activities of the target cells (paracrinal stimulation). In this case, paracellular signals instruct target cell activities in the development of form. Embryonic induction and hormonal regulation of cellular activities are examples of epigenetic control stimuli. Environmental control occurs when the source of the stimulus regulating genetic and cellular activity of the target cells is non-genetic (extracellular stimulation). Cellular response to an electromagnetic field, a mechanical load, or an ingested substance are examples involving environmental control stimuli. It is important to note that in the case of environmental effects, although the control stimulus is non-genetic, the *nature* of the cellular *response* to these stimuli is under genetic regulation and thus subject to evolutionary processes

Reproduced with permission of the copyright owner. Further reproduction prohibited without permission.

(what Sara, 1996, has referred to as a 'sensitive' cell system). The three sources of control stimuli are not mutually exclusive: any given target cell could, in principle, be receiving simultaneous or sequential signals from any combination of sources.

Box 2.1. Classification of source of control stimuli regulating cellular activity in ontogenesis by origin and type of stimulus and associated response. Source: van Limborgh, 1982; Atchley & Hall, 1991.

Source of control stimuli	Type of stimulus	Response by Target Cell
Intrinsic genetic	Autocrinal	Genetic
Epigenetic	Paracrinal	Genetic
Environmental	Extra-cellular	Genetic

This three-way ontology allows us to clarify some of the earlier confusion over the mechanisms of morphogenetic control. For example, Bailey (1985) has contended that over 100 "genetic factors" are involved in the production of morphological variation of the rat mandible, but according to Johnson (1986) only a few "genes" are responsible for morphological variation of this structure (also see Grüneberg, 1975). Atchley (1993) has pointed out that the two statements are not necessarily contradictory, since each author is referring to different categories of control signals. Johnson is referring only to intrinsic genetic factors, whereas Bailey has pooled together intrinsic genetic and epigenetic controls.

Chronological and Regional Variation of Control Stimuli

Research on the development of connective tissue, both past and present, make it abundantly clear that the various cellular control signals do not operate uniformly throughout ontogeny or over the diverse regions of an organism. Murray (1936; reprint 1985) was of the opinion that skeletal development can best be understood in the context of two distinct stages of formation. He argued that the initial processes of pre-skeletal tissue formation (morphogenesis) are regulated by intrinsic genetic

Reproduced with permission of the copyright owner. Further reproduction prohibited without permission.

factors, whereas environmental (including mechanical) factors are mostly responsible for osteogenic growth and remodeling of bone (skeletogenesis).

Scott (1954) subsequently advanced the view that different elements of the skeleton vary with respect to cellular control depending on the mechanism of skeletogenesis. For example, he argued that the development of the desmocranium (the bones of the cranium formed by intramembranous ossification) may be regulated, as Murray suggested, by extrinsic mechanical forces, but the ontogeny of the chondrocranium (cranial bones formed by endochondral ossification) is driven chiefly by intrinsic genetic stimuli.

The skulls of most adult vertebrates are composed of a variety of tissue types and subtypes classified on the basis of numerous properties (see Beresford, 1993, for a recent classification). In addition to classifying bones as either chondrocranial or desmocranial, a second informative criterion for classification involves embryonic tissue derivation: bones derived from visceral (branchial) arch mesenchyme (i.e., the viscerocranium) are distinguished from those derived from mesodermal mesenchyme (i.e., the neurocranium). Box 2.2 lists some of the bones of the vertebrate skull classified by both tissue type and derivation. Box 2.3 relates the source of control stimuli, as proposed by Murray (1936) and Scott (1954), to each of the morpho-skeletal classes listed in Box 2.2. The following sections examine the chronological and regional variation of cellular control of vertebrate skull development.

Reproduced with permission of the copyright owner. Further reproduction prohibited without permission.

Box 2.2 Vertebrate skull precursor tissues and bones classified by tissue type and derivation.

	Morphogenesis	Skeletogenesis	
	Mesenchyme	Desmocranium	Chondrocranium
Viscerocranium	Neural crest derived mesenchyme (Branchial Arches)	Maxilla Premaxilla Zygomatics Vomer Palatines Lacrimals Inf. Nasal Conchae Mandible	Meckel's cartilage Alisphenoid Malleus Incus Stapes Hyoid Ethmoid
Neurocranium	Mesoderm-derived mesenchyme	Occipital (upper part) Temporals (squamous part) Parietals Frontal	Occipital (lower parts) Temporals (petromastoid part) Sphenoid (medial parts)

Box 2.3 Source of control stimuli for the various classes of skeletal tissues.

	Morphogenesis	Skeletogenesis	
	Mesenchyme (Pre-chondro & pre-desmo)	Desmocranium	Chondrocranium
Viscerocranium	Intrinsic (Murray) Epigenetic (current evidence)	Environmental (Murray) Environmental (Scott) Mostly environmental,	Environmental (Murray) Intrinsic (Scott) Intrinsic, Epigenetic & Environmental (current evidence)
Neurocranium	Intrinsic (Murray) Epigenetic & Environmental (current evidence)	some epigenetic (current evidence)	

Morphogenesis

Morphogenesis is the stage of embryonic development characterized by "...the processes that organize the differentiated cells into tissues and organs... [in the] creation of form and structure" (Gilbert, 1988:4). The cellular activities involved in the formation of these new hierarchical levels of organization include "...cell

Reproduced with permission of the copyright owner. Further reproduction prohibited without permission.

movement, migration, changes in shape of individual cells and particularly the differential adhesiveness of their surfaces and content" (Williams & Warwick, 1980:86).

Although morphologically diverse, all vertebrate skulls follow the same general pattern of morphogenesis (de Beer, 1937, reprint 1985; Thorogood, 1993). Elements of the skull develop from embryonic mesenchyme (Hertwig, 1881, cited in Williams & Warwick, 1980) derived either from intraembryonic mesoderm or from the neural crest (see Hall & Hörstadius, 1988). During morphogenesis, mesoderm-derived and crest-derived cells undergo a complex choreography of migrational and translational movement during which important inductive interactions take place with other embryonic tissues (Hall, 1978). Cells derived from the neural crest migrate and differentiate to form branchial arch mesenchyme which will later develop into the skeletal elements of the viscerocranium. Mesoderm-derived mesenchyme, which aggregates dorsal to the branchial arches, provides the material from which the neurocranium later develops. A few skeletal elements (the frontal and otic components of birds, for example) are of mixed composition having developed from mesenchyme at the interface between the two tissue derivatives (Noden, 1978).

Once mesenchymal cells are in position they condense and form models of the bones they will later become. The appearance of these condensations are the first sign of the developing skeleton.[3] Atchley and Hall (1991) contend that the

[3] One recent hypothesis, known as the "Flypaper Model," holds that neural crest cells have a special relationship with Type II collagenous matrix, which "trap" migrating crest cells and channels them into a specified pattern of condensation formation (*cf.* Thorogood, 1988, for an in depth review).

Reproduced with permission of the copyright owner. Further reproduction prohibited without permission.

initial properties of these mesenchymal condensations, as determined by cellular migration, division and death during morphogenesis, are "...a primary determinant of morphological form as expressed in the adult organism" (p. 106). Morphological diversity arises from variation of these cellular activities during morphogenesis, which are, in turn, controlled by intrinsic genetic, epigenetic and environmental signals. A wide variety of signaling proteins have recently been identified, including bone morphogenetic proteins (BMPs) and other members of the transforming growth factor-beta (TGF-beta) superfamily, TGF-alpha inducers, and the so-called steroid/thyroid/retinoic acid superfamily of mediating proteins, such as growth hormone (GH) (Reddi & Cunningham, 1993; Pirinen, 1995; Johnston & Bronsky, 1995; Huang *et al.*, 1996)

Morphogenesis of the Viscerocranium

Methods of distinguishing the effects of intrinsic genetic, epigenetic and environmental control of morphogenesis have traditionally relied upon embryonic ablation and grafting experiments. In these methods, the cellular activities of tissue after removal or change of any potential paracellular or extracellular control stimuli are compared with unaltered homologous tissue. If the morphogenesis of cells that have been grafted to a new location is altered from normal it is reasoned that epigenetic or environmental stimuli must be involved in regulating cellular activity (instructive signaling), beyond simply providing the necessary conditions for continued development (permissive signaling). If morphogenesis of the grafted cells proceeds unchanged, then no epigenetic or environmental stimuli operating at the *local level* could be involved in instructive signaling of cellular activity.

Reproduced with permission of the copyright owner. Further reproduction prohibited without permission.

Hans Spemann, the renowned German embryologist and Nobel laureate, demonstrated both of these cases in his pioneering grafting experiments on salamander embryos. In 1918, Spemann found that ectodermal cells of the kind that normally develop into epidermal tissue, when surgically transplanted, developed into neural plate tissue, normal for cells of the *new* location. This experiment showed that epigenetic inductive signals from surrounding cells influenced the morphogenesis of the ectodermal cells. Six years later, Spemann and Mangold (1924) demonstrated the reverse case—the dorsal lip of the early gastrula of amphibians when grafted to a different location in another embryo nonetheless developed as it would have in its normal location (into notochord and mesodermal tissues).[4] This experiment showed that morphogenesis of the dorsal lip region is not determined by epigenetic inductive signals from surrounding cells, but rather is self-differentiating through intrinsic genetic control (*cf.* Spemann, 1938).

Similar experiments have been conducted on the embryonic viscerocranium of amphibians, birds and mammals. In some studies, various pre-skeletal tissues underwent normal morphogenesis subsequent to *in vivo* or *in vitro* transplantation. This has been demonstrated for mesenchymal primordia of the mouse and rat mandible (Baker, 1941; Manson, 1968; Glasstone, 1971) and for Meckel's cartilage in rats (Richman & Diewert, 1988). These results appear to indicate that morphogenesis of first branchial arch mesenchyme (in rodents and perhaps other mammals) is under intrinsic genetic control, as predicted by Murray (1936).

---

[4] This famous experiment, which formed the basis of Hilde Mangold's doctoral thesis, is one of the few doctoral theses in biology to have directly led to the awarding of the Nobel Prize. Tragically, Hilde Mangold died when her gasoline heater exploded, just weeks before the publication of the 1924 paper. She was only 26 years old at the time (Hamberger, 1984).

Reproduced with permission of the copyright owner. Further reproduction prohibited without permission.

However, Felts (1961) and Herring (1993) have questioned the "normality" of development of these transplanted tissues. Herring points to the absence of "...quantification of the morphology of the transplants," and further contends that "...experimental embryologists are notoriously tolerant of aberrant anatomical details as long as the specimen is alive and recognizable" (p. 157). Furthermore, inductive interactions of the instructive kind may have occurred before or during neural crest migration and mesenchyme differentiation *prior to* transplantation in these experiments; therefore, premigratory epigenetic control of morphogenesis cannot be ruled out.

Numerous studies have shown that isolated *premigratory* neural crest cells, from amphibian and avian embryos, lack the ability to form endochondral or membranous bone *in vitro*, but when allowed to interact with ectodermal epithelia, these cells will differentiate normally into primary cartilage and osteogenic bone (Tyler & Hall, 1977; Hall, 1978; Bee & Thorogood, 1980; for a review see Hall, 1982; Thorogood, 1993). Hall (1980) has evinced that in order for chondroblasts of Meckel's cartilage to differentiate from ectomesenchyme, inductive interactions are required between neural crest cells and several other tissues, including cranial ectoderm (chicks), pharyngeal endoderm (amphibians), and mandibular-arch epithelium (mice). These experiments demonstrate that epigenetic interactions are required for normal cellular activity (including later osteogenesis), but give no hint as to whether premigratory induction of the neural crest actually *instructs* morphogenesis along a given developmental pathway, or simply *permits* further growth and development by establishing vital conditions.

Reproduced with permission of the copyright owner. Further reproduction prohibited without permission.

To resolve this problem, Noden (1983), building upon prior work by Wagner (1949), grafted first arch crest primordia (i.e., *premigratory* neural crest cells) from a quail embryo to the second or third arch location in a chick embryo. The transplanted neural crest cells developed first arch skeletal morphology (i.e., mandibular form) in the second and third arch sites. From these results Noden (1983) concluded that "...the patterns in which skeletal and connective tissues will form... result from programming that occurs before the crest population begins to disperse" (p. 310). However, experiments by Chibon (1966, 1970) with salamander embryos showed that premigratory crest cells grafted to new crest locations resulted in development normal to the new region. "La migration des cellules surnuméraires et leurs localisations finales sont identiques à celles des cellules de la même région de la crête neurale, dans les conditions normales. La régionalisation de la crête neurale est donc maintenue"[5] (Chibon, 1970:479). Currently, it is not possible to tell whether these conflicting findings are due to taxonomic variation of cellular control or simply differences in the method or timing of the grafting techniques.

Yet for the majority of vertebrates studied so-far, evidence indicates that permissive epigenetic interactions involving neural crest-derived mesenchyme are critical during the early stages of morphogenesis, but that at some point, intrinsic signals take over cellular control (Murphy & Bartlett, 1993). Langille and Hall (1993) state that "...in general, with increasing time and as the neural crest cells become more restricted, they acquire greater control of both their own differentiation and morphogenesis and that of adjacent tissues" (p. 102).

---

[5] "The migration of these supernumary cells and their final locations are indentical to those of the cells of the same region of the neural crest, under normal conditions. The regionalization of the neural crest cells is thus maintained." [translation mine]

Reproduced with permission of the copyright owner. Further reproduction prohibited without permission.

It is of interest to note, in this context, that research on the molecular biology of vertebrate skull morphogenesis has revealed several genes containing homeobox sequences that are expressed in the neural crest cells of the developing viscerocranium (e.g., the *dlx* gene, Ellies *et al.*, 1997; the *sonic hedgehog* gene, Helms *et al.*, 1997; also see Hill, *et al.*, 1989), but that no comparable sequences have been found for the neurocranium (Langille & Hall, 1993). Thorogood (1993) considers this as further support for the view that while the development of the neurocranium is directed by epigenetic and environmental stimuli, morphogenesis of the viscerocranium is under primarily intrinsic genetic control (i.e., "...specified in certain crest cells before migration by means of a combinatorial code of expression of homeobox-containing genes..." p.144). Another phylogenetically ancient gene—the 'Slug' gene—has recently been implicated in the regulation of crest cell migration and pluripotentiality (LeDouarin *et al.*, 1994).

Both Noden (1982, 1983) and Thorogood (1993) warn, however, that such intrinsic specification does not occur at the level of the individual cell. This has been established in experiments in which neural crest tissue grafts which have been rotated 180° so that their anteroposterior polarity is reversed prior to grafting nonetheless develop with normal anatomical polarity (Noden, 1983). The precise basis of such self-organization of cell populations is as yet unknown.

Morphogenesis of the Neurocranium

Comparatively little is known of the cellular control of presumptive neurocranial mesemchymal cells during morphogenesis. As with the viscerocranium, epigenetic signals appear to have a permissive rather than instructive inductive influence on

Reproduced with permission of the copyright owner. Further reproduction prohibited without permission.

these cells. Most informative is the embryologically derived disorder known as *duplicatas anterior* in which the affected organism develops two brains each surrounded by a neurocranium. In 1902, Spemann was able to artificially produce *duplicatas anterior* in the newt *Triton*. He showed that the second neurocranium would never have arisen had it not been for the artificially induced embryological development of the second brain (de Beer, 1937). In later experiments, Spemann and Mangold (1924) demonstrated that differentiation of the neural structures was inductively coordinated by the dorsal mesoderm, to which they gave the term "the organizer" (see Kao & Elinson, 1988, and Stewart & Gerhart, 1990, for recent reviews). Based on Spemann's experiments, de Beer (1937) concluded that the development of the mesenchymal proto-neurocranium "...must be dependent on the organizer, or on the brain or on both" (p. 477). More recent genetic analysis has shown that early morphogenesis of the dorsal mesoderm (the so-called 'organizer') is regulated by a group of inducer bone morphogenetic proteins (BMPs). Suzuki *et al.* (1994) blocked the normal BMP signaling pathway in salamander embryos by mutating the active gene, and observed a disruption of axial/neurocranial development. It is clear from these experiments that morphogenesis of the neurocranium depends upon inductive interactions and therefore epigenetic rather than intrinsic cellular control.

In another series of elegant experiments, Nicholas (1930) introduced rapid-growing foreign tissue in the region of the embryological midbrain to expand the formation of the developing brain. In response, the surrounding mesodermal mesenchyme altered its normal development to keep pace with the internally growing tissue. This opens up the possibility that morphogenesis of the

Reproduced with permission of the copyright owner. Further reproduction prohibited without permission.

neurocranium may also be susceptible to environmental (i.e., mechanical) signals in addition to epigenetic ones. At this time, there is no evidence to support Murray's (1936) hypothesis that morphogenesis of the neurocranium is under strict intrinsic genetic cellular control.

Skeletogenesis

The process by which mesenchymal condensations develop into bone is called skeletogenesis. This can occur in one of two ways. Bone can either develop directly from mesenchyme (intramembranous ossification), or a mesenchymal condensation can first transform into a cartilaginous model that will subsequently ossify into bone (endochondral ossification). In either case, the onset of osteogenesis or chondrogenesis is characterized by differentiation of the mesenchyme cells into osteogenic or chondrogenic cells, that subsequently deposit collagenous fibers and extracellular matrix, and then by the envelopment of these elements in a skeletogenic membrane (periosteum or perichondrium). Recent studies have demonstrated that certain BMPs act to stimulate both osteogenic and chondrogenic activity (Reddi & Cunningham, 1993).

Unlike avascular cartilaginous tissue, which receives nutrients through diffusion, bone requires vascularization for nutrient support. Osteogenesis, either of mesenchyme directly or of a cartilaginous precursor, thus proceeds via the invasion and proliferation of blood vessels that induce differentiation of pre-osteonic cells into osteoblasts (bone-depositing cells) or osteoclasts (bone-absorbing cells). These osteogenic cells are embedded within membranes that cover both the outer surface of the bone (periosteum) and the inner surface of the bone cavity (endosteum). Bone

Reproduced with permission of the copyright owner. Further reproduction prohibited without permission.

formation hence proceeds by the differential rate of osteoblastic and osteoclastic activities. Various dynamic combinations of these resorptive and depository activities over the external and internal surfaces of a bone constitute the basis of bone remodeling (*cf.* Brullé & Hugueny, 1845; Enlow, 1975).

The source of control stimuli that directs bone remodeling during skeletogenesis and throughout the growth and life-time maintenance of the bone has been the topic of much debate. As noted, Murray (1936) hypothesized that vertebrate skull remodeling is primarily influenced by extrinsic stimuli, most notably by mechanical loads produced when muscles contract. The view that bone responds to mechanical forces by alterations to its form is one of the major tenets of theoretical morphology (e.g., Howship, 1815; Wolff, 1892; Thompson, 1917; van der Klaauw, 1948; Herring, 1993). Yet, others have proposed that cranial form derives from a process of strict genetic control (e.g., Baume, 1961).

Skeletogenesis of the Desmocranium

The pre-skeletal elements of the desmocranium do not attain their ultimate form by the end of the morphogenetic process. Extensive growth and remodeling take place once the mesenchymal members are replaced by bone, with its attendant surface-covering osteogenic membranes.

For several decades beginning in the 1930s a popular view of craniofacial osteogenesis was that "...bones such as the mandible or maxilla, and all of their morphologic features, were... largely self-generated products..." that were "...governed by intrinsic programming residing within that bone's own bone-producing cells" (*cf.* Enlow, 1990:233). For example, Washburn (1947) reasoned

Reproduced with permission of the copyright owner. Further reproduction prohibited without permission.

that since ossification of the coronoid process of the mandible occurs prenatally, presumably before normal functioning of the temporalis muscle, that its origin involved "intrinsic factors in the mandible" (p. 244). But Spyropoulos (1977) and Rieppel (1987) have subsequently shown, at least in humans and lizards, that prenatal formation and ossification of the coronoid process is initiated from within the developing mass of the temporalis muscle anlage, quite apart from the rest of the mandible. Moreover, Humphrey (1971) found evidence of oral and facial muscle activity in human fetuses that correspond to craniofacial growth events. These observations indicate that environmental stimuli, such as mechanical loading, cannot be ruled out as a determinant of desmocranial skeletogenesis.

Numerous other studies have unequivocally demonstrated the importance of environmental (non-genetic) stimuli in the growth and development of the ossified desmocranium. Enlow (1986), following van der Klauuw (1952), has identified two main sources of mechanical stimuli acting on the developing skull: (1) growth enlargement, and (2) functional actions. Pressure from the growth of soft tissues, such as the eyes and brain, and the mechanical force generated by muscle pull can dramatically alter bone size and shape during development of the desmocranium. A recent review of the evidence supporting this view has been provided by Herring (1993).

An excellent example of how *growth* of a soft tissue structure can modify the bony desmocranium is afforded by experiments in which surgical alteration of the eyes of amphibians, birds and mammals resulted in accommodative changes in the growth of the bony orbit. Steinitz (1906) removed the eyes from early larvae of *Rana fusca*; Stone (1930) grafted embryonic eyes from the large-eyed *Amblystoma*

Reproduced with permission of the copyright owner. Further reproduction prohibited without permission.

tigrinum to the small-eyed *A. punctatum;* Coulombre *et al.* (1962) "drained" the vitreous fluid from the eye of a chick, surgically preventing it from attaining normal size; Tonneyck-Müller (1976) enucleated the chick eye altogether; and Buchman *et al.* (1994) eviscerated the orbital contents of kittens. All of these studies revealed that growth and remodeling of the bony orbit was altered to accommodate the larger or smaller (or obliterated) size of the eye by producing a correspondingly larger or smaller orbital cavity.[6]

Likewise, the growing brain directly affects the growth and remodeling of the neurocranium. Garol *et al.* (1978) observed minimal development of the bones of the neurocranium in anencephalics; whereas in hydrocephalics an enlargement of the neurocranium accompanies the enlarged brain. Moss (1976) found results consistent with these in his review of the experimental literature.

Enlow (1990) proposed that the growing brain affects the form of neurocranial bones in two ways: (1) expansion of the brain causes sutural separation resulting in tension in the sutural membranes, which, "...respond immediately by depositing new bone on the sutural edges" (p. 99); and (2) membrane-mediated remodeling occurs in response to brain enlargement that results in altering the curvature of calvarial bones to accommodate changes in brain form.

Studies of the effects of muscle force on the skeletal development of the desmocranium are numerous. Most involve comparisons of bone morphology between control specimens and those subject to paralysis, extirpations, or, in a few cases, transpositions of one or more masticatory muscles. In one of the earliest

---

[6] Schultz's (1940) finding that there was no correlation between eye size and orbital size in a sample of adult primates can be explained by the different growth rates of the eyeball (and brain) and facial skeleton in early compared to later stages of development (see Chapter 11, Box 11.1).

Reproduced with permission of the copyright owner. Further reproduction prohibited without permission.

demonstrations of these techniques, Pratt (1943) unilaterally removed the masseter muscle from one-week old rats, and found that the face grew asymmetrically, with the mandible deviating toward the operated side. Washburn (1947), in a similar experiment, removed the temporalis muscle from one side of neonatal rats. The coronoid process, which had been well developed at birth, disappeared on the operated side subsequent to temporalis muscle extirpation. These and other similar studies (see Box 2.4) demonstrate unequivocally that growth enlargement of soft tissues in combination with muscle forces acting on dermal bones not only determine the form of the bones, but in many instances, are necessary for their continued existence.

Skeletogenesis of the Chondrocranium

In contrast to the desmocranium, the phylogenetically ancient chondrocranium has long been regarded as an intrinsically controlled "template" to which the growth of the desmocranium must conform (Scott, 1954; DuBrul & Laskin, 1961; Kean & Houghton, 1982; Enlow, 1990). Recall that experiments by Steinitz (1906), in which the eyes of larvae of *Rana fusca* were removed, resulted in malformation of the orbits and braincase, both formed by elements of the desmocranium. However, these same experiments showed that the optic foramen, a feature of the sphenoidal chondrocranium, developed in spite of the absence of the optic nerve. The hypothesis that the development of the chondrocranium is regulated by intrinsic genetic stimuli is further supported by experiments in which various cartilaginous tissues (e.g., sphenooccipital synchondrosis: Dorenbos, 1972; nasal septum: Copray, 1986; Meckel's cartilage: Richmond & Dewiert, 1988) are shown to develop

Reproduced with permission of the copyright owner. Further reproduction prohibited without permission.

normally subsequent to *in vivo* or *in vitro* transplantation. Huang *et al.* (1996) have recently demonstrated, however, that TGF-alpha proteins play a inhibitory role in the development of the chondrocranium, suggesting at least some form of epigenetic permissive regulation.

And yet, numerous studies have shown that the cartilaginous basicranium is affected by mechanical "unloading" associated with brain agenesis, such as anencephaly and microcephaly. These disorders are reportedly characterized by an abnormal increase in cranial base angulation (Fields *et al.*, 1978), a decrease of synchondrosis length (Moss, 1976), and changes in the timing of chondrocranial ossification (Melsen & Melsen, 1980).

There are several interpretations of these and similar findings. One is that mechanical stresses produced by the brain are responsible for chondrocranial development (Moss, 1976; Demes, 1985; Enlow, 1990). A second related idea is that "the [cranial] base is constrained from adjusting its own shape significantly by virtue of its intimate relationship with the brain and the emerging cranial nerves" (Kean & Houghton, 1982; also see Kjaer, 1998). And third, the genes responsible for congenital disorders of brain development may have a functionally independent pleiotropic effect on basicranial development (*cf.* Vogt, 1867). This latter interpretation, however, is not supported by cases in which experimental or clinical alterations to the size or shape of the brain are associated with developmental changes of the basicranium. In a review of the relevant literature, Moss (1976) found that experimentally induced reductions of brain size were associated with alterations in cranial base angle and length. Furthermore, experimentally produced

Reproduced with permission of the copyright owner. Further reproduction prohibited without permission.

postural changes have also been linked to changes in chondrocranial form (Moss, 1961; Fanghänel, 1972).

Unlike dermal bones, which appear to be dependent on extrinsic stimuli for their initial formation, the bones of the chondrocranium can develop to some extent even in the absence of extrinsic stimuli, such as those provided by the developing brain (*cf.* Bromage, 1980). Enlow (1990) has aptly summarized our current state of knowledge as follows:

> ...the shape, size, and characteristics of the cranial base have evolved in direct phylogenetic association with the brain it supports... but the cranial base itself has presumably developed a genetic capacity for its own growth that is at least partially separate and independent of the brain and that may function without it during ontogenetic growth [p. 104].

Reproduced with permission of the copyright owner. Further reproduction prohibited without permission.

Reproduced with permission of the copyright owner. Further reproduction prohibited without permission.

Box 2.4 Summary of studies showing effects of mechanical stimuli on the development of desmocranial bones (1940-1998).

Reference	Taxon	Alteration	Effects on viscerocranium	Effects on neurocranium
Pratt (1943)	rat	masseter removed	mandibular angle reduced or lost	
Washburn (1947)	rat	temporalis removed	coronoid process diminished	temporal ridges lost
Watt & Williams (1951)	rat	soft diet	angular process small; mandibular thickness decreased; maxillary breadth decreased	
Avis (1959)	cat	temporalis removed	coronoid process diminished	temporal ridges lost
Avis (1959)	cat	temporalis partially removed	coronoid grow in direction of remaining muscle pull	
Avis (1961)	rat	masseter & med. pterygoid removed	mandibular angle lost	
Coulombre *et al* (1962)	chick	eye size reduction	orbit reduced to fit eye	orbit reduced to fit eye
Moore (1965)	rat	soft diet	angular process small	
Pai (1965)	mouse	dysgenic	palate clefted	
Boyd *et al.* (1967)	guinea pig	temporalis removed	no effects	
Moore (1967)	rat	masseter & med. pterygoid removed	mandibular angle diminished or lost; condylar process reduced	
Murray & Drachman (1969)	chick (embryo)	paralysis (drug-induced)	mandible longer	
Moss & Meehan (1970)	rat	temporalis removed	coronoid process diminished;	temporal ridges lost
Moss & Meehan (1970)	rat	temporalis partially removed	coronoid grow in direction of remaining muscle pull	

Box 2.4 Summary of studies showing effects of mechanical stimuli on the development of desmocranial bones (1940-1998).

Reference	Taxon	Alteration	Effects on viscerocranium	Effects on neurocranium
Adams *et al.* (1972)	monkey (rhesus)	retractile force (appliance) on maxilla	zygomatico-frontal suture resorption (normally depository)	
Moore (1973)	rat	masseter & med. pterygoid removed	mandibular angle diminished or lost; condylar process reduced	
Tonneyck-Müller (1976)	chick	eye enucleation	orbit reduced	orbit reduced
Walker & Quarles (1976)	mouse	tongue removed	palate changed shape	
Hall (1978)	mouse	myogenic arrest of lat. pterygoid mm.	condylar process failed to form	
Hall (1978)	mouse	hypertrophy of lat. pterygoid mm.	condylar process increased size	
Schumacher et al (1979)	dog; sheep	temporalis removed	coronoid process diminished	temporal ridges lost
Schumacher et al (1979)	dog; sheep	masseter removed	mandibular angle reduced	
Bouvier & Hylander (1981)	monkey	soft food diet	mandibular thickness reduced	
Herring & Lakars (1981)	mouse	paralysis	abnormal curvature of mandible	
Müller & Punt-van Manen (1982)	human	myotonic muscular dystrophy	mandible/maxilla narrow; palate deep	
Bouvier & Hylander (1982)	macaques	soft food diet	mandibular cartilage alterations	
Hendricksen *et al.* (1982)	primates	muscle alteration	deflection of mandibular angle	

Reproduced with permission of the copyright owner. Further reproduction prohibited without permission.

Box 2.4 Summary of studies showing effects of mechanical stimuli on the development of desmocranial bones (1940-1998).				
Reference	Taxon	Alteration	Effects on viscerocranium	Effects on neurocranium
Corruccini & Beecher (1982)	monkey (*Saimiri sciureus*)	soft food diet	reduced maxillary arch length to C^1; reduced maxillary breadth at M^1 & P^3; reduced palate depth; reduced maxillary breadth/length ratio	
Beecher *et al* (1983)	monkey (*Saimiri sciureus*)	soft food diet	jaw length unchanged; maxillary breadth reduced; palate deep	
Hohl (1983)	monkey (*M. nemestrina*)	temporalis & masseter transpositioned	facial prognathism increased	
Vilmann et al (1985)	mouse	paralysis; dystropia	mandible longer; condylar process smaller; angular process smaller	
Kilaridis (1986)	rat	soft diet		
Bouvier & Zimny (1987)*	rats	soft diet	condylar surface small	
Ingervall & Bitsanis (1987)	human	hard chewing (pine resin)	facial growth altered direction	
Teixeira *et al.* (1990)	rabbits	transposition of masseter mm.	alveolar bone resorption	
Katsaros *et al.* (1994)	rats	hard diet vs. soft diet	greater sutural width and increased interdigitations in hard diet group	
Chuang (1995)	rabbits	soft food diet	greater anterior superior growth rotation of maxilla; reduction of angular process of mandible and thinner mandibular body	

Reproduced with permission of the copyright owner. Further reproduction prohibited without permission.

Box 2.4 Summary of studies showing effects of mechanical stimuli on the development of desmocranial bones (1940-1998).				
Reference	Taxon	Alteration	Effects on viscerocranium	Effects on neurocranium
Yamamoto (1996)	rats	soft food diet	reduced bone apposition on the occlusal surface of the palate between the first molars, but an increased in the region between the third molars, indicating "a more anteriorly directed growth rotation of the palate"; reduced ossification rate of the midpalatal synchondrosis; inhibited lateral growth of the maxilla (ie. narrow maxillary arch).	
Kiliaridis *et al.* (1996)	rats	soft food diet	reduced mandibular mass	

Reproduced with permission of the copyright owner. Further reproduction prohibited without permission.

Distal Causal Mechanisms of Morphological Diversity

Morphological Diversity and the Aristotelian Legacy

Scientific attempts to understand morphological diversity began, in earnest, around the fourth century BC in the writings of the Greek philosophers (Russell, 1916). Aristotle (384-322 BC), acclaimed by many to be the founder of comparative anatomy, was the first to recognize the three great patterns of morphological diversity among organisms. The first is that organisms belonging to the major groups are built upon a common organization ("Unity of Plan") (*Historia Animalium*, tr. Thompson, 1910). The second, phrased in modern terminology, is that the form and function of structures of organisms are adeptly suited to their biological roles (i.e. "adaptation") (*De Partibus Animalium*, tr. Peck, 1937). And third, that prior to specialization toward their individual (and divergent) adult structures the embryos of various types of organisms are similarly general in form (later known as "von Baer's law") (*De Generatione Animalium*, tr. Peck, 1943). These observations eluded scientific explanation for more than two thousand years, until Darwin proposed his revolutionary theories of evolution.

Darwinism and Neo-Darwinism (Selectional Adaptation[7])

Darwin's great achievement was the integrated explanation he provided for Aristotle's empirical generalizations—his theories of transmutation, common descent and natural and sexual selection. It is clear from Darwin's writings that, in addition to phylogeny, ontogeny played a crucial role in his evolutionary thinking.

---

[7] I do not adopt the terminology proposed by Gould and Vrba (1982) to distinguish those features or processes that enhances fitness—"aptation"—from only those aptations due to selection—"adaptation." Instead, I use "adaptation" for the general meaning and "selectional adaptation," or other prefix, for the specific.

Reproduced with permission of the copyright owner. Further reproduction prohibited without permission.

For example, he explained the Unity of Plan among organisms by maintaining that early embryonic stages (during which the basic morphological organization of the organism is established) are conserved throughout phylogeny. "Thus, community in embryonic structure [and concomitantly, basic body plan] reveals community of descent..." (Darwin, 1859; reprint 1958:417). Darwin also took recourse in ontogeny to explain adaptation and the resemblances of embryos (Darwin, 1844, 1859). He recognized that heritable modifications of developmental pathways in the descendents of an ancestral form provided the variation upon which selection acted to preserve favorable phenotypes. This led him to the conclusion that since selection for novel developmental modifications is strongest at a later period of life when the organism is devoid of the protective environment of the egg or uterus, these later periods of maturation will appear much more divergent among related forms compared to earlier stages.

> Variation not coming on at a very early age, and being inherited at not a very early corresponding period, explains, as it seems to me, the grandest of all facts in natural history,... the resemblance of embryos [Darwin, 1860, reprint 1887:131].

Several authors have dedicated their careers to examining the nature of Darwin's *heritable developmental modifications* and its relation to genetical models of evolution (e.g., Garstang, 1922, 1928; de Beer, 1930, 1940, 1948). In an article published in 1958 to commemorate the centenary of the first public announcement of Darwin's theories,[8] de Beer summarized the Neo-Darwinian theory of morphological evolution as follows:

---

[8] The occasion was the reading of a paper, written jointly by Darwin and Wallace, to the Linnean Society of London on July 1, 1858 (Darwin & Wallace, 1959).

Reproduced with permission of the copyright owner. Further reproduction prohibited without permission.

> It is now clear that evolution proceeds by the production of variation due to the mutation of genes, and the permutation and recombination of genes brought about by random fertilization of germ cells. The products of this variation are acted upon by selection which preserves those collections of genes, or gene-complexes, that control the development of characters which endow their possessors with advantages in the conditions of their various habitats [de Beer, 1958b:171].

This Neo-Darwinian view of life assumes that morphological variation is the product of differential selection for characters whose development is controlled by the genome. All of the necessary information for the complete development of an individual *within a specified environmental context* is presumed to be present in the zygote. Gould (1977) has unfortunately assigned the term 'neopreformationism' to this genome-centered view of development. A misnomer since there is no manifestation of later-occurring form in the zygote.

Acclimation (Physiological Adaptation)

An alternative approach (favored by nineteenth century American paleontologists and, more recently, by some developmental biologists), while acknowledging that genes play an essential role in the development of form, places greater emphasis on the contributions of physiological response to external stimuli in bringing about morphological variability (Russell, 1916; Herring, 1993). This approach, which as we have seen is firmly established on empirical grounds, contends that variation of skeletal form is largely the product of differential skeletogenic response to varying environmental stimuli. (*cf.* Cope, 1888; Wolff, 1892; Moore, 1965, 1967; Gray, 1992).

The physiological approach to the skeleton has become synonymous with the "Functional Matrix" hypothesis first outlined by van der Klaauw (1948) and later

Reproduced with permission of the copyright owner. Further reproduction prohibited without permission.

developed more extensively by Moss (1962, 1968). In this hypothesis, as originally conceived, "...it is denied that any of the morphological attributes of skeletal tissues beyond specific cytodifferentiation are produced directly by the operation of encoded genetic information within the nuclei of any one or any group of scleroblastic cells" (Moss, 1973:192). It is acknowledged, of course, that gene action is involved in the production of skeletal tissues, but these skeletogenic activities are viewed as simple mechanical responses to the development and activities of the non-skeletal tissues and capsular spaces—"functional matrices"—that surround the skeletal elements. The growth of the brain, eyes, muscles, glands, blood vessels, nerves, and nasal, oral and pharyngeal cavities is seen to regulate the development of skeletal form (van der Klaauw, 1948; Moss, 1968). What the proponents of the functional matrix approach failed to realize is that results obtained on the desmocranium, which appeared to support their view, were not necessarily applicable to the chondrocranium or to the early stages of cranial development involving mesenchymal morphogenesis.

In a series of four articles published in recent issues of *American Journal of Orthodontic and Dentofacial Orthopaedics*, Moss (1997a, b, c d) attempted to revise the functional matrix theory to include intrinsic genetic and epigenetic regulation of craniofacial growth and development.[9] The conclusion of his review and theoretical analysis is that "...both genomic and epigenetic factors are necessary causes, that neither alone is also a sufficient cause, and that only the two, interacting together, furnish both the necessary and sufficient cause(s) of ontogenesis" (Moss,

[9] Moss does not follow the embryologic/genetic definitions of the terms 'genetic' and 'epigenetic.' He combines both of these mechanisms into a single category, which he calls 'genomic,' and he equates 'epigenetic' with 'environment' control (as defined here).

Reproduced with permission of the copyright owner. Further reproduction prohibited without permission.

1997d:410). But as in his previous theoretical work, Moss (1997c, d) failed to consider fully the importance of chronological and region-specific variation in the control of skeletal ontogenesis. Moss's views are consistent with a broader school of thought called "developmental constructionism" (e.g., Oyama, 1985; Gottlieb, 1991; Gray, 1992; Griffiths & Gray, 1994), a form of neoepigeneticism in which "[i]t is emphasized that 'phenotypes' are not *transmitted* from one generation to the next, e.g., in coded form in the genetic material, but that they are *constructed* anew in each generation through organism-environment interactions during development" (Mahner & Bunge, 1997:299; original italics)

As Herring (1993) has pointed out, the dichotomy between the Neo-Darwinian and physiological approaches...

> parallels the problem with the word "adaptation," which can be construed either in an evolutionary context implying that an inherited trait has been selected in a species, or in a physiological context, implying that a trait (not necessarily inherited) has been elicited by external stimuli during the life of an individual [p. 154].

The latter meaning of adaptation is often referred to as *acclimation* by physiologists (e.g., Frisancho, 1981). Often overlooked is the fact that Darwin himself was fully aware that acclimation was a major contributor to organic diversity. Consider the following excerpts from *On the Origin of Species*:

> When a variation is of the slightest use to any being, we cannot tell how much to attribute to the accumulative action of natural selection, and how much to the definite action of the conditions of life. Thus, it is well known to furriers that animals of the same species have thicker and better fur the further north they live; but who can tell how much of this difference may be due to the warmest-clad individuals having been favoured and preserved during many generations, and how much to the action of the

Reproduced with permission of the copyright owner. Further reproduction prohibited without permission.

> severe climate? For it would appear that climate has some direct action on the hair of our domestic quadrupeds. [1859, reprint 1958:132]
>
> On the whole, we may conclude that habit, or use and disuse, have, in some cases, played a considerable part in the modification of the constitution and structure; but that the effects have often been largely combined with, and sometimes overmastered by, the natural selection of innate variations. [1859, reprint 1958:139]

Biological Constraints (Non-adaptational)

In contrast to selection and acclimation, which lead to organic adaptation, biological constraints are mechanisms that channel morphological variation into a restricted pattern, often away from optimal form.[10] Atchley and Hall (1991) define biological constraint as any "...process, structure or function which restricts or confines the possible states or actions of individuals or systems" (p. 146). Numerous types of constraints have been named, many of which are so vaguely defined, and so carelessly employed, that the concept is in danger of becoming a wastebasket category for any organic property or process for which no adaptational explanation is immediately apparent (Smith, 1993). However, the concept is too powerful to ignore, and even necessarily vague treatments are, for now, preferable to none at all.

Several types of constraints have received the most attention. *Developmental constraints* are defined by Maynard Smith *et al.* (1985) as the "...bias in production of variant phenotypes or limitations on phenotypic variability caused by the structure, character, composition or dynamics of the developmental system" (also

---

[10] In theory, constraints may act to channel phenotypic variation toward adaptive forms as well as non-adaptive ones. Traditionally, however, constraint mechanisms have been defined in terms of the manifestation of non-adaptive, cross-taxonomically stable phenotypes. Not all students of evolution agree on the importance of constraints. Some argue that directional selection is strong enough to overcome nearly all biological constraints (e.g., Lande, 1986).

Reproduced with permission of the copyright owner. Further reproduction prohibited without permission.

see Alberch, 1983: 906; and Scharloo, 1987). *Genetic constraints* arise from "...those genetic aspects that prevent or reduce the potential for selection to result in the most direct ascent of the mean phenotype to an optimum" (*cf.* Clark, 1987 cited in Atchley & Hall, 1991:146). *Phylogenetic constraints* are said to occur when phenotypic diversity is restricted in a given clade by the composition and character of its ancestral gene pool (*cf.* Mayr, 1983; Schaefer & Lauder, 1986; Janis, 1990). These categories of constraint are not mutually exclusive. On the contrary, they represent three related aspects of the same phenomenon. A given developmental constraint can arise from a genetic one and give rise to a phylogenetically constrained patterns of morphological diversity. Thus, any given biological constraint can involve any combination of developmental, genetic and phylogenetic elements (but see Mahner & Bunge, 1997:364-365).

In the context of the model of morphology outlined here, biological constraints are defined as *limitations to one or more sources of morphological variation that either prevent selection or acclimation from attaining optimal-adaptive form, or direct the development of form in the absence of adaptational forces*. Sources of morphological variation, as discussed in the previous sections, include intrinsic genetic, epigenetic and environmental cellular control signals, and their concomitant cellular response activities. Biological constraints can result from any combination of limiting processes involving these ontogenetic activities. Since these are precisely the (proximate) mechanisms that lead to morphological variation, it follows that "[d]ifferent characters may be constrained, or biased, or influenced in regards to change differently given their genetic, epigenetic..., or adaptive foundations..." (Szalay & Bock, 1991).

Reproduced with permission of the copyright owner. Further reproduction prohibited without permission.

Intrinsic genetic and epigenetic constraints contribute to patterns of phenotypic variation through processes that limit variation in a gene pool and through pleiotropic effects of genes that govern cellular control. Genetic limitations can come about in several ways. Allele fixation is the most obvious, resulting in a total absence of genetic variation in a given population (see Maynard Smith *et al.*, 1985:272, for examples in *Drosophila*). Or certain genes (or gene-complexes), acting either intrinsically or epigenetically, can be limited in the sense that any mutations (or combination of mutations) will produce only a limited set of canalized phenotypic modifications, or none at all (Riska, 1986). In a series of elegant experiments Oster *et al.* (1988) mimicked the effects of mutation by manipulating the properties of cellular condensations, and in so doing demonstrated that only a limited variety of limb morphologies can arise (also see Alberch, 1983). Alberch & Gale (1983, 1985) similarly observed that the evolutionary loss of digits in amniotes nearly always follows a predictable pattern.

Unlike allele fixation and canalization, pleiotropy can yield constrained phenotypes through a process that does not depend on genetic limitations. Consider a gene active in the cells of a given structure for which no severe limitations on genetic (or by extension, phenotypic) variation exist. A mutation of the gene produces an advantageous trait that is subsequently selected for in the population. The gene in question may have a pleiotropic effect on a second trait that may or may not be adaptive in nature. This can occur if the gene itself is active in the cells of the second structure, or if the gene in the cells of the first structure produce morphogens that stimulate cellular activity in the second structure (what Wagner, 1989, calls "epigenetic traps"; also see Lande, 1980; Cowley & Atchley, 1992).

Reproduced with permission of the copyright owner. Further reproduction prohibited without permission.

According to Mayr (1970), non-adaptive "...structural detail may be merely an incidental by-product of a gene maintained in the gene pool for other [i.e., adaptive] physiological properties" (p. 94).

Such pleiotropic effects, on the morphological level, are expressed as correlated phenotypes: "...selection operating on one part of a structure may impose a set of correlated and nonadaptive modifications on other parts" (Gould, 1981:44). This leads to the interesting conclusion that *lack* of interspecific diversity for a given trait is not a necessary consequence of biological constraint (i.e., constraints can be operating on a highly variable trait). A constraint acting in this fashion may only become apparent when the morphospace distribution of one trait is viewed in relation to the second.

Pleiotropic effects of this type represent one of a variety of mechanisms that can yield allometric relationships (or correlated size constraints) between two or more traits. A classic example involves canine size in primates, a trait characterized by near normally distributed variation. Box 2.5 (top graph) shows that the univariate distribution of the log cube root of estimated canine volumes for a sample of 300 anthropoid specimens approximates a normal distribution. Yet, when plotted against maxillary arch length the constraining effect of facial size on canine size becomes apparent (Box 2.5, bottom).

Reproduced with permission of the copyright owner. Further reproduction prohibited without permission.

Box 2.5. Canine size distribution (above) and plot with maxillary length (below)

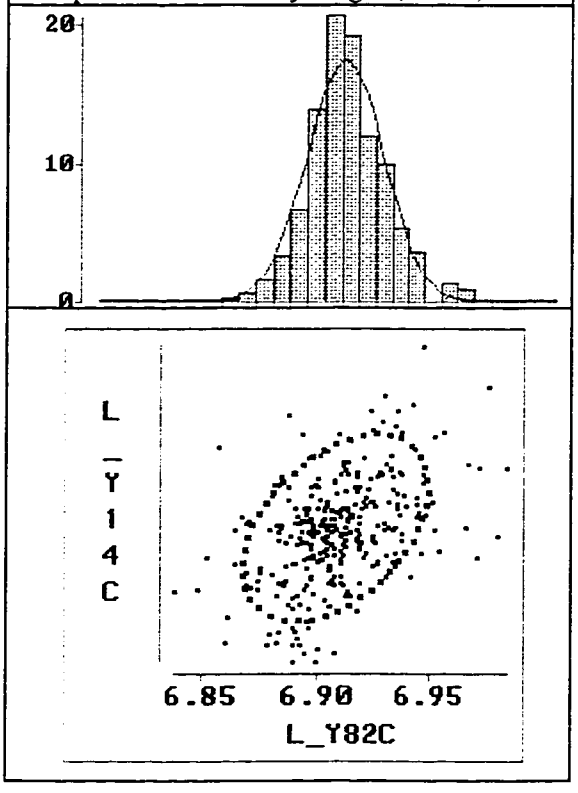

The concept of environmental constraint may seem counterintuitive at first. How can environmental control of cellular activity lead to non-adaptive phenotypes? The answer to this enigma lies in the understanding that there is a limited number of environmental signals that can stimulate a morphogenetic response.

Genetically mediated cellular response to the various types of control stimuli can also be a source of morphological variation, and therefore, of constraint. Regardless of the amount of genetic variation underlying cellular control stimuli, a lack of variation (or other limitation) in the genes that regulate cellular response activities can constrain subsequent phenotypic expression (*cf.* Wagner, 1989; Thomas & Reif, 1993). One such *response constraint* is the limited manner in which osteoblasts respond to mechanical forces (Bromage, 1986). Moskalewski *et al.*

Reproduced with permission of the copyright owner. Further reproduction prohibited without permission.

(1989) transplanted osteoblasts from various skeletal tissues and found that they all responded similarly to mechanical forces, although their respective response thresholds were somewhat different (also see Rubin & Lanyon, 1987; Frost, 1987).

Ontogeny, Phylogeny and Morphological Diversity

The trichotomy of morphological approaches outlined above (Neo-Darwinism, physiological acclimation, and constraint) emerged historically from a relative lack of knowledge concerning the inter-relationships of the various controls of morphogenic and skeletogenic activities. In effect, each of the three approaches makes different assumptions about two key issues pertaining to the cellular control of organic diversity: (1) the relative importance of each of the three types of control stimuli, and (2) the degree to which genetically coded *response* activities can and do vary.

The Neo-Darwinian (selectionist) view maintains that only those control stimuli and response activities that are heritable and thus subject to selection, play a significant role in ontogenetic regulation and the evolutionary production of morphological diversity. Hence, only intrinsic genetic and heritable epigenetic factors are seen as important in the evolution of skeletal diversity.

Since the Modern Synthesis no one has questioned that gene expression is involved in the development and growth of all connective tissues. Skeletogenesis proceeds by the production of enzymes and other proteins, adhesion molecules, and extracellular matrices through gene action (Atchely & Hall, 1991). Yet, proponents of the physiological approach reject the notion that skeletogenic cells are self-regulating. In the strictest form of this view intrinsic genetic control of skeletal

Reproduced with permission of the copyright owner. Further reproduction prohibited without permission.

development and growth is denied. The direction and magnitude of bone formation is thought to be regulated by signals external to skeletogenic cells, such as the mechanical forces imposed by muscles and growing organs. Thus, only environmental and, to a lesser extent, epigenetic factors are thought to play a primary role in the production of skeletal variation.

The constraint approach accepts the important roles played by selection and acclimation in the development and evolution of morphological diversity, but points to the many ways in which non-adaptive phenotypes can arise. Whether constraints are true "causes" of morphological variation or simply properties of systems that set conditions under which certain phenotypes are more or less likely to arise, is a matter of semantics.[11] Either way, constraints have the same *effect* as selection and acclimation—they channel phenotypic variation toward certain distributions and away from others, and are therefore classified together as distal causal mechanisms (see more Chapter 3).

It is of interest to note that Darwin himself, in *Origin of Species*, recognized all three of these causal mechanisms of morphological variation.

Conclusions

To understand the processes responsible for inter-individual and cross-taxonomic morphological variation, one first has to discern the processes responsible for the development of form in a single organism. Inter-individual variation arises from differences in the myriad developmental pathways that can vary during the ontogeny of an organism. At their core, these developmental processes involve the behavior

Reproduced with permission of the copyright owner. Further reproduction prohibited without permission.

of populations of cells that mitotically divide, migrate, alter structure, engage in cell-cell and cell-matrix communication, and produce extra-cellular products through gene action. The timing and character of these cellular behaviors are choreographed and guided by information emanating from within the cell (intrinsic signals), as well as from sources outside the cell (epigenetic and environmental signals). It is clear that the type of signals received by each cell population varies throughout ontogeny and by skeletal position.

Instrinsic and epigenetic sources of cellular information appear to be most important during the early stages of skull ontogeny (i.e., during morphogenesis), although this may be more so for the viscerocranium than for the neurocranium. When mesenchymal cells begin to differentiate into osteogenic and chondrogenic cells, with their attendant skeletogenic membranes, environmental signals (especially mechanically induced signals) begin to take over the further growth and remodeling of the skull. These mechanical signals are presumed to be mediated by genetically regulated response engines within the target cells. However, unlike the desmocranium, the chondrocranium appears to retain some aspects of intrinsic control during these later stages of skeletogenesis.

There are several reasons behind the emphasis in this review on the *source* of the control signals as opposed to their *content*. The processes of morphogenesis and skeletogenesis, and their respective roles in development, comprise an organismic level of organization that entail mechanisms of proximate causation of organic form and form variation. Higher-order mechanisms operating at organismic and

---

11 Although Mahner & Bunge (1997) concede that biological features can be explained in terms of biomechanical or developmental constraints (p. 166), they prefer to call such constraints 'determinants' rather than causal mechanisms.

Reproduced with permission of the copyright owner. Further reproduction prohibited without permission.

superorganismic levels of organization, which include selection, acclimation, and constraint, are classed as distal causes. Contingencies between proximate and distal causal mechanisms are determined by the sources of control stimuli. Selection can only effect change in a manner that influences the morphological variation of succeeding generations by acting on heritable sources of control, which include intrinsic and epigenetic stimuli, and genetically mediated cellular responses. Acclimation involves only non-heritable sources of control (environmental stimuli), but can evoke a heritable cellular response. Constraints can act via, or operate on, any type of control stimuli. Genetic drift, pleiotropy, canalization and polygenic effects all involve constraints imposed on heritable sources of cellular control. Polyphenism, allometric scaling and other biomechanical agents of constraint can act via non-heritable source stimuli.

Based on these relationships and knowledge of the chronological and regional patterns of morphogenetic and skeletogenetic control during development, I outline in the next chapter a research design aimed at elucidating the roles and relative contributions of the various higher-order causal agents and mechanisms in the production of anthropoid nasomaxillary diversity.

Reproduced with permission of the copyright owner. Further reproduction prohibited without permission.

PART II

Operational Framework

Reproduced with permission of the copyright owner. Further reproduction prohibited without permission.

Chapter 3. Research Design

The important question about methods is not 'how' but 'why.'

Tukey, 1954:36

Introduction

At the outset, I stated that the objective of the present investigation is to account for nasomaxillary morphological variation among extant anthropoid primates. I further qualified this statement with the remark that only distal nomological causal mechanisms will be examined. Historical causes of morphological diversity, and proximate mechanisms underlying nasomaxillary form are not included in the study. Therefore, only a proportion of the total variation can potentially be explained. A *comparative* research design was chosen for the current study because it is (1) in accord with the stated research objectives, and (2) well suited to explore distal nomological causal mechanisms.

As a prelude to a discussion on methodological issues I begin this chapter with a brief foray into the nature of explanation in evolutionary morphology. This includes a more in-depth discussion of nomological versus historical explanation, and comparison of proximate versus distal causation. I then describe the research design used in this study and take inventory of its strengths and weaknesses in relation to the theoretical and conceptual framework erected in Chapter 2. I show that the method is best suited to explore distal nomological causal mechanisms and agents.

Reproduced with permission of the copyright owner. Further reproduction prohibited without permission.

Explanation and Causality in Evolutionary Morphology

> *Before it is possible to test any idea or model in morphology, and indeed even before it is possible to formulate properly any hypothesis, it is necessary to understand the nature of explanation in biology.*
>
> Bock, 1988:205

There are many different perspectives on what constitutes a valid explanation in science in general, and in evolutionary biology in particular, and I make no attempt to review them all here (see Dullemeijer, 1974, and Bock, 1988, for more in-depth reviews). The purpose of this section is to define useful terms and to clarify my views on where current research stands with respect to epistemological issues in evolutionary morphology. For the most part I equate "explanation," or more properly "tentative explanation," with "hypothesis." As I see it, the key issues about what constitutes a valid scientific hypothesis are those of falsifiability, causality, and circularity.

Falsifiability

According to Popper (1957), any valid scientific hypothesis must be falsifiable. Popper initially regarded evolutionary biology, like geology and cosmology, as being outside the realm of science because he assumed that past events can never be falsified by current empirical observations (Popper, 1957, 1959; Lewontin, 1968). Several evolutionary biologists (e.g. Dullemeijer, 1972; Mayr, 1982; Bock, 1988; Szalay & Bock, 1991) have criticized Popper for failing to realize that phenomena (or patterns thereof) in the "historical sciences" are the result of

Reproduced with permission of the copyright owner. Further reproduction prohibited without permission.

processes operating at two levels: nomological and historical.[1] Nomological processes are governed by natural laws, that, given certain boundary conditions, will operate *predictably* throughout a defined realm of time and space—examples include valley formation through river erosion, the birth of neutron stars, and the processes of speciation, natural selection, and Mendelian inheritance. Hypotheses stated in terms of nomological processes are known as nomological-deductive explanations[2] (N-D Es) and are certainly falsifiable (*cf.* Bock & von Wahlert, 1963; Bock, 1973; Dullemeijer, 1985). In contrast, historical occurrences are based on unique events ensuing from random or semi-random contingencies, and while they may have a profound impact on the outcome of phenomena, they are generally not predictable (Mayr, 1982). Preadaptations and biogeographical distributions resulting from contingent geological events are examples of historical phenomena.[3] Hypotheses formulated to account for historical phenomena ("historical narrative explanations" or H-N Es) are considered to be operationally unfalsifiable. They are tested on the basis of a probabilistic model of corroborating empirical evidence (*cf.* Nagel, 1961; Sober, 1988; Szalay & Bock, 1991). Another important point emphasized by Bock (1988) and Szalay and Bock

---

[1] Various other terms have been proposed for these dual concepts (e.g. "functional" vs "evolutionary": Dullemeijer, 1980), and I view most of them as misleading, especially the use of the term "functional" in this context. I shall therefore use the terminology employed in Szalay & Bock (1991), which is the most conceptually, as well as semantically, accurate.

[2] As far as I can determine, this concept was first described by Hempel (1962) who contrasted deduction from nomological principles with induction from empirical relations.

[3] A useful way of distinguishing between the two types of processes is to conduct a mind experiment in which the history of life on Earth is "rerun" from the beginning. How different would a second run of life's history turn out to be? Certainly there would be many differences in the outcomes, and most of these would be due to differences in the historical contingencies between the two runs. But we would also expect to see many similarities, and most of these would be due to nomological processes operating over evolutionary time.

Reproduced with permission of the copyright owner. Further reproduction prohibited without permission.

(1991) is that any H-N E "...should be based on pertinent N-D Es, and these N-D Es, together with the pertinent empirical observations, form part of the chain of arguments used in testing the H-N E" (Szalay & Bock, 1991:7). In other words, a given H-N E can be falsified by falsification of a stipulated N-D E upon which the H-N E is based.

Popper (1957) was wrong about the alleged non-falsifiability of evolutionary biological phenomena because he failed to recognized that regular, predictable, nomological processes (both proximate and distal) are at the core of biological change and diversity. The following three quotations capture the role and importance of N-D Es in evolutionary morphology:

> Evolutionary explanations [H-N Es] in biology are absolutely dependent on prior functional explanations [N-D Es] in that no useful evolutionary explanation can be formulated in the absence of proper prior functional explanations—a point that is not realized by many evolutionary biologists, including most evolutionary morphologists [Bock, 1988:208].
>
> Functional explanations [N-D Es] in morphology are independent from evolutionary explanations [H-N Es], and are exceedingly useful in theoretical and practical morphological analysis [Bock, 1988:214].
>
> ...all conclusions about the relationships of organisms, about their phylogeny or classification... must be based on pertinent N-D Es. These should be, in our opinion, the detailed causal mechanisms of evolutionary change [Szalay & Bock, 1991:9].

In light of this epistemological background, it should be clear that the focus of the current research—the "causal mechanisms of evolutionary change"—require hypotheses framed in accordance with N-D Es.

Reproduced with permission of the copyright owner. Further reproduction prohibited without permission.

Causality

The role of causality in explanatory statements is even more contentious than that of falsifiability. Consider the following points of view: "The purpose of scientific theory is to understand causation" (Stolzenberg & Land, 1983:32). "The concept of cause is generally considered to be the most important one for the development of science" (Hutten, 1962:87). "The reason why physics has ceased to look for causes is that, in fact, there are no such things" (Russell, 1929:180). "It would be very healthy if more researchers abandon thinking of and using terms such as *cause* and *effect*" (Muthén, 1987:180). Despite this dichotomy of views regarding the validity and usefulness of causality, Nagel (1965) found in an analysis of explanatory research that even among investigators who reject the concept of causality, their work nonetheless implied causal thinking. This finding supports the view of Pedhazur (1997), with whom I agree, that "...the scientist's question of why a certain event has occurred carries with it an implication of causality" (p. 767). In short, causality is inherent in any statement of explanation (Heise, 1975).

To provide a nomological explanation of morphological diversity it has become common to distinguish between proximate and ultimate mechanisms of causation (Mayr, 1961; Hailman, 1982). Proximate causal mechanisms (PCMs), as described in Chapter 2, refer to the most immediate causes of skeletal form, the ontogenetic interactions between cellular control stimuli and cellular response that underlie the processes of morphogenesis and skeletogenesis in the production of morphological form. These are the causal processes acting within organisms that one can directly observe, and "...are often couched in the language of physiology and biochemistry" (Goldsmith, 1991:7). Ultimate causal mechanisms refer to

Reproduced with permission of the copyright owner. Further reproduction prohibited without permission.

those evolutionary processes that determine the historical origins and propagation of genotypes. Recently, Mahner and Bunge (1997) have rejected the concept of ultimate causation, based on the argument that...

> ...the history of [an individual's] genetic material are determinants of the developmental processes leading to its current morphology and behavior, but they do not cause it. What is true is that the history of a system provides some of the *conditions* or *circumstances* of the system's possible changes. Therefore, the expression 'ultimate cause' should be replaced by the expression *historical conditions*, or *distal cause* in the case of a genuine past cause [p. 40].

Selection, acclimation and constraint are *nomological causal mechanisms* in the sense that they are law-governed mechanisms that determine (and thus explain) morphological diversity. They are *distal* causal mechanisms (as distinct from proximal and ultimate causal mechanisms) in that they initiate, generate, trigger or channel chains of other causal events that lead to the effect of interest—i.e., they pertain to an understanding of *why* certain patterns arise rather than *how* a particular case of a general pattern is expressed (see Mahner & Bunge, 1997:107). Distal causal mechanisms (DCMs) are the forces that determine which proximate mechanisms are expressed and which are repressed. Adaptation by means of natural and sexual selection are obvious distal mechanisms. But if we broaden the meaning of adaptation beyond the realm of selection (see previous chapter), it is clear that acclimation is also a distal causal mechanism—it determines which proximate mechanisms are expressed and it invokes the concept of adaptation of organisms to their environment. I include also biological constraints under the rubric of distal causation because they act to express, repress proximate mechanisms, or to channel proximate mechanisms in a certain direction.

Reproduced with permission of the copyright owner. Further reproduction prohibited without permission.

I will have more to say about causation in the context of analytical techniques in Chapter 8.

Circularity

Circular causal explanations are of two types: (1) tautologous, and (2) circular, proper. Tautologous explanations are always true by virtue of their logical form (Copi, 1983); for example: "All carnivorous organisms eat at least one kind of meat". Circular explanations exhibit the property that the empirical observations employed as tests are completely dependent on the explanatory statement being tested (Szalay & Bock, 1991), such as testing a phylogenetic hypothesis using assumed homologous character states, where the assumption of homology is itself derived from the phylogenetic hypothesis.

A phenomenon in morphology often mistaken for a circular argument is the interdependence of form and function. In fact, this is a case in which the direction of causality is either uncertain (does form cause function or does function cause form?), or bi-directional (form effects function and function effects form). Here, it is the causal process itself that is potentially "circular," as in a positive or negative feedback loop, and not the explanation.

From the foregoing, it can be seen that explanations in biology formulated on the basis of nomological processes can indeed exhibit the properties of falsifiable, causality and non-circularity.

Explanation, Theory and Method

Despite disagreement by philosophers of science on what constitutes a valid explanation, there is wide agreement on the essential role of theory in both the

Reproduced with permission of the copyright owner. Further reproduction prohibited without permission.

formulation of hypotheses and the methods developed to test them. Hanson (1958) wrote: "The notions behind 'the cause x' and 'the effect y' are intelligible only against a pattern of theory, namely one which puts guarantees on inferences from x to y" (p. 64). Inferences from x to y are only possible when the causal processes involved in their relation are nomological in nature.

If explanation is beholden to established theory, method is subordinate to both. "All method...must fall out of well corroborated theory" (Szalay & Bock, 1991:1). "It is a model of causation among variables under study that determines, among other things the type of data to be collected and the method of analysis" (Pedhazur, 1997:768). Having devoted the previous chapter to nomological morphogenetic theory and having just discussed essential aspects of the nature of explanation in evolutionary morphology, I now turn to method.

Synchronic vs Diachronic Comparative Research

Synchronic comparative biology refers to a research design which employs "...the typical across taxa comparative analysis of contemporary species" (Pagel & Harvey, 1988:432). A diachronic comparative design, on the other hand, proceeds by the analysis of transformations accrued either by lineages over evolutionary time, or by individuals over their life cycles. Lewontin (1969), and later Lauder (1982) called these methods "equilibrium analysis" and "evolutionary analysis," respectively. The terms "horizontal" and "vertical" analysis have also been used to describe these methods.[4] In Chapter 6, I will develop the argument that a

[4]The terms "horizontal" and "vertical" are used to describe different methodological approaches and should not be confused with "horizontal and vertical evolution," which Mayr (1991) used to describe the duality of the evolutionary process.

Reproduced with permission of the copyright owner. Further reproduction prohibited without permission.

purely synchronic comparative approach is conceptually and analytically flawed, and its indiscriminate use can lead to inaccurate and potentially misleading inferences regarding nomological processes. In Chapter 7, I transform the data collected for this study so that it is compatible with a diachronic comparative approach.

Experimental vs Comparative Research

Comparative biology is often contrasted to its apparent antithesis, experimental biology, with the latter traditionally considered to be the more powerful approach. But statistical and technological advances over the past several decades have progressively broached the gap between the two research designs. All science is by its very nature comparative. Patterns are detected through systematic *comparison* of sets of observations; relationships are predicted against a backdrop of prevailing theory established by *comparative* means; and, hypotheses are tested by *comparing* expected with observed results. Experimental biology is as comparative as comparative biology.[5] At the heart of the difference between the two approaches is the issue of control. When, as is usually the case, there are multiple potential causes of a phenomenon the researcher must attempt to control the variance of the "confounding" or "nuisance" independent variables so that the variance of a "focal" independent variable can be isolated, and its effects on the dependent variable quantified. In an experimental design, the confounding independent variables are controlled by randomly assigning subjects to independent groups. When the groups are large, this usually ensures that the

[5] Recognition of this fact has prompted the use of the term "nonexperimental" in place of "comparative."

Reproduced with permission of the copyright owner. Further reproduction prohibited without permission.

within-groups variances of the confounding independent variables are equal across groups. The focal independent variable is then manipulated by the researcher so that it varies across groups. In this manner, any observed difference in the dependent variable between groups can be attributed to the focal independent variable. In a comparative design, subjects cannot be randomly assigned to groups—the groups are said to be intact or given—and the focal independent variable cannot be manipulated by the investigator. For this reason, comparative studies are said to lack the control and inferential power of experimental studies.

Two points are often overlooked when contrasting comparative and experimental designs. First, the portrayal of comparative methods as the less powerful second choice to experimental methods is misleading. This is cogently illustrated by Washburn and Detwiler (1943), who took the view that most problems in biological anthropology (and presumably other fields of biology) were "intractable" using comparative methods, and required the use of experimentation in order to be resolved. These authors noted two types of situations in particular "...in which comparative methods have proved inconclusive" (p. 172). One is a situation in which two hypotheses are mutually exclusive and diametrically opposed, and the other is "...when there are two or more equally reasonable theories which seem to explain the available facts" (p. 172). These authors appear to leave little left to investigate by comparative means! What they failed to recognize is that *the choice of method depends upon the character of the independent variables under investigation* (i.e., whether they are intrinsic or extrinsic). Intrinsic variables measure properties that cannot be separated from their subjects; examples include eye color, body size, and HIV serostatus.

Reproduced with permission of the copyright owner. Further reproduction prohibited without permission.

Extrinsic variables measure the familiar "treatment" dispensations or conditions that are externally applied to subjects; for example, exposure to radiation, ingestion of a given drug, or time spent on a tread-mill. Comparative methods are appropriate when the independent variables are either intrinsic or mixed intrinsic-extrinsic. Confounding independent variables cannot be randomized with respect to intrinsic variables and in such cases experimental methods fail to control for extraneous variance. For this reason, experimental methods are appropriate only when the focal independent variables are extrinsic.

The second, and related, point is that comparative designs are *not* devoid of control as often described, but rather, achieve control by different means. Whereas experimental designs control the variance of confounding variables by random assignment of subjects to treatment groups, comparative designs nullify confounding variables by means of *statistical control*. It is a well established, although little known, fact that statistical control of comparative data is heuristically and mathematically equivalent to experimental control. Sokal and Rohlf (1995) state the case as follows:

> *Statistical control* is an application... that is not widely known among biologists and represents a scientific philosophy that is not well established in biology outside agricultural circles. Biologists frequently categorize work as descriptive or experimental, implying that only the latter can be analytical. Statistical approaches applied to descriptive work can in some instances, however, take the place of experimental techniques quite adequately—occasionally they are even to be preferred [p. 489].

In evolutionary morphology, nature has already provided the comparative biologist with the longest running experiment in history—some 3.5 billion years—with

Reproduced with permission of the copyright owner. Further reproduction prohibited without permission.

ample variation to set up statistical control over practically any variable that can be operationalized. Since the vast majority of independent variables used in this study are of the intrinsic type, the appropriate research design is comparative. In those cases where extrinsic causal agents are examined (e.g., dietary preferences) results from comparative analyses will be compared to corresponding experimental results, with the expectation of concordant findings.

The limitations of the current study are not so much imposed by adopting a comparative research design, but rather, by the subject matter under investigation (i.e., osteological diversity of adult specimens). Therefore, the current research will permit very few, if any, tests of hypotheses pertaining to proximate causal agents. It is, however, well suited to fulfill the stated research objective, which is to explain anthropoid nasomaxillary variation in terms of a series of distal nomological causal agents.

K. K. Smith (1993:179) has expressed quite the opposite opinion, that while comparative synchronic morphology and related approaches "...allow quantitative assessment of hypotheses of morphological convergence or divergence, remove the effects of size, and allow study of a wide range of species..." such designs are not very adept at resolving the distal causes behind morphological patterns. She cites as an example, Radinsky (1981), who noted the relative constancy of the position of the carnassial tooth in utherian carnivorans, but was unable to resolve this phenomenon as due to adaptation or constraint. I obviously disagree with Smith in asserting that questions of distal causality in evolutionary morphology can be resolved, partly through the formulation, operationalization, and testing of specific causal hypotheses whose mode of

Reproduced with permission of the copyright owner. Further reproduction prohibited without permission.

causality can be deduced from established theoretical principles in evolutionary biology, and partly from analytical techniques involving multi-level structural modeling (see Chapter 8).

Conclusions

In contrast to Popper's (1957) early assertions regarding the shortcomings of the "historical" sciences, it is argued here that explanations regarding the causes of biological variation based on nomological processes do indeed satisfy the falsifiability criterion for valid scientific hypotheses.

It is further concluded that the concept of explanation in biology, like other branches of science, implies causality. That the concept of causality is a mental construct about the way in which the universe behaves, it is nonetheless essential for the development of models of asymmetrical and hierarchical relationships used to predict, control and understand phenomenological diversity and change.

The myth that comparative research is the less powerful, substandard alternative to experimental research is alive and well and living among us (see Mayr's excellent discussion on the subject, 1982, pp. 30-32). The choice of research designs is dictated, to a large degree, by the nature of the data being analyzed—some types of data are only compatible with a comparative design, whereas other types are amenable to experimental research.

In closing this chapter, I should like to emphasize that despite the focus on distal causal mechanisms in this study, knowledge of proximate mechanisms of morphological diversity is indispensable for several reasons: (1) distal and proximate causal mechanisms operate *together* in the production of variation via a

Reproduced with permission of the copyright owner. Further reproduction prohibited without permission.

complex and integrated relationship, (2) hypotheses concerning distal causes must conform to known proximate mechanisms, and (3) data regarding proximate mechanisms can be employed to formulate predictions pertaining to tests of distal causal hypotheses.

Reproduced with permission of the copyright owner. Further reproduction prohibited without permission.

Chapter 4. Sample

Introduction

Selecting the appropriate sample for comparative study is one of the most important, and often neglected, aspects of scientific research. There are many criteria that have to be considered in selecting an appropriate sample, many of them conflicting. For convenience, I discuss the selection of sample size and composition separately, although the two are clearly not independent from one another.

Sample Size

Determining the appropriate sample size (n) for a study is not a trivial matter. There are disadvantages in having a sample that is either too small or too large. "[B]y using few enough individuals you could never refute the null hypothesis" (Sokal & Rohlf, 1995:173). "[G]iven a sufficiently large sample, the likelihood of rejecting the null hypothesis is high" (Pedhazur, 1997:26). The optimal sample size, if such a thing exists, largely depends on the research design and analytical techniques employed in the study. Since several different analytical techniques are used in the present research the final sample size chosen will represent a compromise among the various techniques. I begin by reviewing several criteria that have been employed in determining appropriate sample sizes, followed by an examination of the formulae (based on these criteria) given for determining n associated with the analytical techniques used in this study (i.e., principal

Reproduced with permission of the copyright owner. Further reproduction prohibited without permission.

components analysis, analysis of variance and covariance, bivariate and partial regression, and covariance structural modeling).

Generally, the appropriate sample size for a given test is determined in one of two ways. The first is to reduce or optimize a given statistic by evaluating a formula containing both the statistic and sample size estimates (Approach 1). Dispersion statistics (e.g. variance, standard deviation, standard error, and confidence intervals) or derivatives of them (e.g. *F*-statistic) are often employed in this way. Since the formulae for calculating dispersion statistics differ with the statistic being estimated, different analytical techniques will call for different samples sizes (all else being equal) to maintain a given dispersion statistic. One statistic of particular importance in this regard is the standard error. Since:

$$s_{\bar{Y}} \propto 1/(n^{1/2}) \tag{4.1}$$

it is obvious that larger samples will reduce the standard error associated with a statistic (where $s_{\bar{Y}}$ is the standard error of a given statistic and s is the sample standard deviation). This is desirable because a smaller standard error is associated with an increased reliability that the sample statistic will be close to the population parameter. For descriptive statistics Marcus (1990:79) suggested that "...the required size of confidence intervals or standard errors should determine sample size."

$$n \propto (1/s_{\bar{Y}})^2 \tag{4.2}$$

For other types of analyses different dispersion statistics have been employed. For ANOVA, Sokal and Rohlf (1995) suggest an iterative approach, where *n* is the number of replicates needed for each of *a* groups to achieve a stipulated power and significance level when attempting to detect a given

Reproduced with permission of the copyright owner. Further reproduction prohibited without permission.

difference δ between group means:

$$n = 2\,(\sigma/\delta)^2\ \{t_{\alpha[v]} + t_{2(1\text{-}P)[v]}\}^2 \qquad (4.3)$$

where σ is the true standard deviation; and the t-values are taken from a two tailed t-table (see Sokal & Rohlf, 1995:263).

For correlation tests, Sokal and Rohlf (1995:578) give the formula for determining the appropriate sample size needed to detect a true difference between an observed and expected correlation as:

$$n = ((t_{\alpha[\infty]} + t_{2(1\text{-}P)[\infty]})/\zeta_1)^2 + 3 \qquad (4.4)$$

where ζ is the z-transformed expected value of the parametric correlation coefficient.

Rather than attempt to specify an expected coefficient, Milton (1986) recommended using the standard error of the t-statistic to determine the appropriate sample size for multiple regression. In her formula (equation 4.5 below), the anticipated overall R^2 of the model and the minimum *addition* to R^2 contributed by a variable entered last (Δr^2) must be specified:

$$n = ((t^2_{\alpha[\infty]}\ (1\text{-}R^2))/\Delta r^2) + k + 1 \qquad (4.5)$$

A second approach to determining appropriate sample size is to compare results of an analysis using the entire population (or at least a large sample) with results obtained using varying sizes of subsamples. The subsample size at which the results match those obtained with the larger sample is deemed appropriate (Approach 2). Analyses of this type pertaining to multiple regression have lent support to the often cited "rule of thumb" to use a minimum sample equal to 30

Reproduced with permission of the copyright owner. Further reproduction prohibited without permission.

times the number of independent variables that are entered into the regression equation (Pedhazur, 1997:26).

$$n = 30 \text{ x (\# of indep. vars in regression equation)} \quad (4.6)$$

In a re-sampling experiment using morphometric fowl data (n=276), Marcus (1990) showed that a sample of at least 8 to 10 times the number of variables was required to match the original interpretation of a principal components analysis using the full data set.

$$n = 10 \text{ x (\# of variables in PCA)} \quad (4.7)$$

The expressions of these formulae, using parameter estimates appropriate to this study, are presented in Box 4.1. An examination of the expression solutions reveal that (1) different analytical techniques may require different sample sizes (e.g., formulae 2 & 4 in Box 4.1), and (2) different *approaches* can lead to unique solutions regarding the appropriate sample size needed for the same analytical technique (e.g., formulae 4 & 5 for multiple regression). It is noteworthy that formulae 3 and 4 in Box 4.1 are quite similar in structure and lead to similar results (i.e. n=ca. 30 to 35) even though they were devised for different types of analyses: correlation and regression, respectively.

Both are based on properties of mathematical probability theory (Approach 1). In contrast, results based on Monte Carlo simulations using equivalency of interpretation as the main criteria (Approach 2) lead to higher sample size determinations.

Reproduced with permission of the copyright owner. Further reproduction prohibited without permission.

Box 4.1 Recommended sample sizes for various analytical techniques. Metric measures in mm.

(Formula) Source:	Rule or formula:	Study expression:	Recommended sample size
(1) Marcus, 1990	$n = (1 / s_{\bar{Y}})^2$	$n = (9.2/.5)^2$	$n = 339$
Descriptive statistics: s of 9.2 is average standard deviation of metric variables; $s_{\bar{Y}}$ is desired standard error based on .5 mm implied precision (see Chapter 5)			
(2) Sokal & Rohlf, 1995	$n = 2(\sigma/\delta)^2 \{t_{\alpha[v]} + t_{2(1-P)[v]}\}^2$	$n = 2(.28/.5)^2 (1.96+ 2.06)^2$	$n = 10$ (per group)
ANOVA: see test for details			
(3) Sokal & Rohlf, 1995	$n = (t_{\alpha[\infty]}+t_{2(1-P)[\infty]}/\zeta_1)^2 + 3$	$n = (1.96+2.58/.8)^2 + 3$	$n = 35$
Correlation coefficient: Study expression values based on those recommended by Sokal & Rohlf, 1995			
(4) Milton, 1986	$n=(t^2_{\alpha[\infty]} (1-R^2))/\Delta r^2)+k+1$	$n =$ ((3.84(.25))/.05)+10+1	$n = 30$
Multiple regression: Study expression values based on anticipated R^2 of .75, p = .01			
(5) Pedhazur, 1997	$n = 30$ x #vars	$n = 30$ x 10	$n = 300$
Multiple regression: The maximum number of ind. variables entered into a regression equation is 10			
(6) Marcus, 1990	$n = 10$ x #vars	$n = 10$ x 32	$n = 320$
Principal Components Analysis: The maximum # of variables entered into a given PCA is 35			

Presently there is no basis for favoring one or the other approach. Both have reciprocal advantages and disadvantages. The disadvantage of using Approach 1 is that *n* appears on both sides of the equation, and an iterative solution is therefore required. The disadvantage of Approach 2 is that interpretations using very large baseline samples may be biased towards committing Type I errors, and therefore assessment of interpretations obtained from subset samples on the basis of larger ones may be misleading.

The decision as to whether to use a sample size closer to 35 or one closer to 300 in multiple regression analysis and related techniques has important implications. In this study, the main analytical technique used to test nomological ultimate hypotheses is covariance structural modeling (CSM). A

Reproduced with permission of the copyright owner. Further reproduction prohibited without permission.

relatively large sample size is desirable for CSM analysis because it reduces the standard errors in connection with colinearity problems. But there is a potential down-side in using too large a sample that is unique to covariance structural modeling. An essential class of statistics used in CSM is the *fit measure*. Fit measures represent different scalar quantity statistics that summarize the differences between a given covariance structural model and the empirical data. Some fit measures, such as the Normed Fit Index (NFI) of Bentler and Bonett (1980), contain *n* in their formulae and are therefore affected by differences in sample size. Another popular fit measure is the adjusted goodness-of-fit index (AGFI), which was devised by Jöreskog and Sörbom to be "independent of sample size." However, Marsh, Balla and McDonald (1988) have demonstrated in Monte Carlo simulations that as *n* is increased the means obtained from the sampling distributions also increase. This implies that a high AGFI fit measure may be a consequence of a large sample rather than a true indicator of how well the model fits the data (*cf.* Bollen, 1990). In a recent review and evaluation of seven CSM incremental fit measures, Marsh, Balla and Hau (1996:351) recommended the Comparative Fix Index (CFI) formulated by Bentler (1990), partly because they found it to be "relatively unrelated to sample size." [1]

I argue in favor of a sample size that falls in the higher end of the acceptable range (*ca.* 300) for the following reasons. First, as I have already mentioned, a large sample size is desirable because it reduces standard errors associated with model colinearity (Schumacker & Lomax, 1996:26-27). Moreover, even if the CFI fit measure, or other indices, is somewhat affected by

[1] See Chapter 8 for a more detailed discussion of CSM fit statistics.

Reproduced with permission of the copyright owner. Further reproduction prohibited without permission.

sample size, a large sample will lead to an overestimation of the fit measure thereby increasing the likelihood of committing a Type I error. This is preferable to committing a Type II error due to underestimation of a fit statistic because the sample size is too small (see Chapter 8).

Second, simulation studies have shown that fit measures typically favor quantitative models with multiple complex parameters if the sample size is large, but favor simpler models if the sample size is small (Cudeck & Henly, 1991). This relationship between model complexity, sample size and goodness-of-fit is generally viewed as a weakness (e.g. Marsh, *et al.*, 1988). To address this problem, numerous fit measures have been devised (e.g., Bentler & Bonett, 1980; Mulaik *et al.*, 1989) that are down-weighted as a function of model complexity. A review of the literature on this topic, most of which emanates from the behavioral sciences, has convinced me that this way of thinking is wrong-headed. Simpler models generate better fit measures than more parameterized models when sample size is small because the reduced *df*-to-parameter ratio of the more complex models severely diminishes their power. On the other hand, more complex models generate higher fit measures than simpler ones when sample size is large because of the additive effects of the sums-of-squares (*SS*) each parameter contributes to the total explained *SS* of the model, thereby increasing the ratio of explained to unexplained model *SS*. This is obviously a problem if many parameters are included in the model without theoretical justification, just to beef-up the total explained variance. According to Cudeck and Henly (1991), this is precisely why using highly parameterized quantitative models with large samples is such a persistent problem in the behavioral sciences. They write:

Reproduced with permission of the copyright owner. Further reproduction prohibited without permission.

> It is not surprising that the choice of a model is not a particularly simple matter, especially because the underlying theory is often weak, measurements are of modest quality, distributions may be far from ideal, and subjects cannot be sampled in a completely random and representative way.

When structural models are soundly rooted in theory, that is, each included variable can be justified on theoretical grounds, and given sufficient power (i.e. large enough sample size) for the most complex model under evaluation, then simple and complex models alike are on an even playing field for goodness-of-fit tests. Since the present study will examine some fairly complex quantitative models (as required by underlying theory) a larger sample size (ca. 300) is appropriate. This sample size is in accord with most applications of covariance structural modeling in the research literature. Several recent surveys found that researchers applying CSM generally use a minimum sample of 150 and an average of between 250 to 500 (Boomsma, 1982; Ding *et al.*, 1995; Schumacker & Lomax, 1996).

The final reason for favoring a larger sample involves the issue of *units of analysis*. This issue revolves around the following question: are the measurements collected on individual specimens to be used as data points in the analysis or are species mean values to be used? For reasons I discuss in Chapter 8, I contend that both individual specimens and species (together) constitute the appropriate units of analysis. Since species (higher-level) are composed of individuals (lower-level), the number of individuals included in the sample should at least equal the larger recommended sample size (ca. 300), and we may apply the smaller recommended sample size (ca. 30 to 35) to species.

Reproduced with permission of the copyright owner. Further reproduction prohibited without permission.

The appropriate number of specimens per species that would allow reliable detection of between-groups mean differences was estimated using the formula given in Sokal and Rohlf (1981:263) (see this chapter, Box 4.1, formula 2). Using the mean coefficient of variation over all metric variables as an estimate of the true standard deviation, it was determined that a sample size of 10 will yield an 80% certainty of detecting non-random differences between two sample means at a significance level of 0.05. The small intraspecific variability relative to interspecific differences observed in the sample statistics indicate that this relatively small intraspecific sample size is justified (*cf.* Marcus, 1990).

Sample Composition

The study sample consists of 300 specimens of anthropoid primates, representing 37 species. Of these 37 species, 27 are represented by 10 specimens, while 10 species are represented by less than 10 specimens (see Box 4.2).[2] The complete list of specimens selected for study appears in Appendix F. All specimens included in the sample were wild-caught, adult, females. Only females were included in order to eliminate sex as a possible confounding variable. Males were excluded because they exhibit greater variation of canine size, an additional confounding influence on nasomaxillary form. All specimens were examined for signs of pathology or trauma that may have produced craniofacial deformation. Species were selected to meet four additional criteria or conditions: (1) that all living subfamilies of the suborder Anthropoidea be represented, (2) that species

[2] Species for which there were less than 10 adult females available, but which were considered important for the analysis were included. The analytical techniques detailed in Chapter 8 do not require a balanced design.

Reproduced with permission of the copyright owner. Further reproduction prohibited without permission.

diversity across subfamilies be adequately represented, (3) that comparative cases permitting contrasting combinations of variables be included, and (4) that appropriate specimens were available at the American Museum of Natural History (AMNH), or from the collections of the various campuses and institutions affiliated with the City University of New York (CUNY) and the New York Consortium of Evolutionary Primatology (NYCEP). Box 4.2 gives a classification, based on the phylogeny presented in Chapter 7, of the species selected for inclusion in this study.

Box 4.3 reports Chi-square results for sample proportionality at the infraorder, superfamily, and family levels. Results show that the proportion of platyrrhine and catarrhine species included in the sample does not significantly differ from their proportion in nature. At the family rank, cercopithecids are significantly under-represented, whereas hominidae are over-represented.

Reproduced with permission of the copyright owner. Further reproduction prohibited without permission.

Box 4.2. Classification of species included in the present study.

Order Primates
- Suborder Anthropoidea
  - Infraorder Platyrrhini
    - Superfamily Ateloidea
      - Family Atelidae
        - Subfamily Atelinae
          - Genus *Alouatta* (1/6)
            - A. palliata
          - Tribe Atelini
            - Genus *Ateles* (1/4)
              - A. geoffroyi
            - Genus *Lagothrix* (1/2)
              - L. lagothricha
            - Genus *Brachyteles* (1/1)
              - B. arachnoides*
        - Subfamily Pitheciinae
          - Genus *Callicebus* (1/3)
            - C. cupreus
          - Subtribe Pithecina
            - Genus *Pithecia* (2/5)
              - P. pithecia
              - P. monachus*
            - Genus *Chiropotes* (1/2)
              - C. satanas
            - Genus *Cacajao* (0/2)
      - Family Cebidae
        - Genus *Aotus* (1/1)
          - A. trivirgatus
        - Subfamily Cebinae
          - Genus *Cebus* (2/4)
            - C. apella
            - C. capucinus
          - Genus *Saimiri*
            - S. sciureus
        - Subfamily Callitrichinae
          - Genus *Saguinus* (1/10)
            - S. oedipus
          - Genus *Callithrix* (1/8)
            - C. pygmaea
          - Genus *Leontopithecus* (0/3)
          - Genus *Callimico* (1/1)
            - C. goeldii*
  - Infraorder Catarrhini
    - Superfamily Cercopithecoidea
      - Subfamily Cercopithecinae
        - Genus *Chlorocebus*
          - C. aethiops
        - Genus *Cercopithecus* (4/19)
          - C. mitis
          - C. ascanius
          - C. neglectus
        - Tribe Papionini
          - Genus *Miopithecus* (0/1)
          - Genus *Erythrocebus* (0/1)
          - Genus *Allenopithecus* (0/1)
        - Subtribe Papionina
          - Genus *Mandrillus* (0/2)
          - Genus *Theropithecus* (0/1)
          - Genus *Papio* (1/5)
            - P. hamadryas*
          - Genus *Lophocebus* (1/1)
            - L. albigena
          - Genus *Cercocebus* (0/4)
        - Subtribe Macacina
          - Genus *Macaca* (3/19)
            - M. nemestrina
            - M. fascicularis
            - M. mulatta
      - Subfamily Colobinae
        - Subtribe Colobina
          - Genus *Colobus* (1/4)
            - C. guereza
          - Genus *Procolobus* (1/2)
            - P. badius
        - Subtribe Presbytina
          - Genus *Pygathrix* (0/4)
          - Genus *Nasalis* (1/1)
            - N. larvatus*
          - Genus *Presbytis* (1/7)
            - P. melalophos
          - Genus *Semnopithecus* (2/9)
            - S. entellus*
            - S. cristata
    - Superfamily Hominoidea
      - Subfamily Hylobatinae
        - Genus *Hylobates* (2/9)
          - H. lar*
          - H. syndactylus
      - Subfamily Homininae
        - Genus *Pongo* (1/2)
          - P. pygmaeus*
        - Tribe Hominini
          - Genus *Gorilla* (1/1)
            - G. gorilla
          - Subtribe Hominina
            - Genus *Homo* (1/1)
              - H. sapiens
            - Genus *Pan* (2/2)
              - P. paniscus*
              - P. troglodytes

Underline=sampled; * <10 specimens

Reproduced with permission of the copyright owner. Further reproduction prohibited without permission.

Box 4.3. Chi-square goodness-of-fit test of sample proportions. Results in parenthesis were obtained when species represented by less than 10 specimens in the sample were excluded. ↑ significantly over represented; ↓ significantly under represented. *Tribe rank

Rank	Taxa	Observed Proportions	Exp. Prop.	G-Test	*df*	Prob.
Infraorder	Platyrrhini	39.0 (43.0)	36.0	.170	1	0.680
	Catarrhini	61.0 (57.0)	64.0	(.700)		(0.403)
Superfamily	Ateloidea	38.9 (42.9)	35.6	5.137	2	0.077
	Cercopithecoidae↓	41.7 (42.9)	55.0	(1.876)		(0.391)
	Hominoidea↑	19.4 (14.3)	09.4			
Family	Atelidae	19.4 (21.4)	16.8	12.982	4	0.011
	Cebidae	19.4 (21.4)	18.8	(5.892)		(0.207)
	Cercopithecidae↓	41.7 (42.9	55.0			
	Hylobatidae	5.6 (3.6)	06.0			
	Hominidae↑	13.9 (10.7)	03.4			
Subfamily	Atelinae	8.3 (10.7)	8.7	18.985	9	0.025
	Pitheciinae	11.1 (10.7)	8.1	(440.9)		(0.001)
	Cebinae↑	8.3 (10.7)	3.4			
	Callitrichinae↓	8.3 (7.1)	14.8			
	Aotinae	2.8 (3.6)	.7			
	Cercopithecinae↓	25.0 (28.5)	36.9			
	Colobinae	16.7 (14.3)	18.0			
	Hylobatinae	5.6 (3.6)	6.0			
	Ponginae*	2.8 (.0)	.7			
	Homininae*↑	11.1 (10.7)	2.7			

Among subfamilies, Cebinae is under-represented by about 5%, Callitrichinae is over-represented by 6.5%, Cercopithecinae is under-represented by about 12% and Homininae is over-represented by more than 8%. While these differences are statistically significant, I do not believe they are large enough to undermine the internal validity of the research results. Substantial care has been taken to analyze within-subfamily as well as between-subfamily data.

An additional concern related to sample composition was intraspecies variation. Although I attempted to select specimens from a single subspecies, this was not always possible. Of the 37 anthropoid species selected for analysis, 26 are represented by only one subspecies, while 11 are represented by more than one subspecies. To test whether the overall cranial morphology between the

Reproduced with permission of the copyright owner. Further reproduction prohibited without permission.

subspecies of a given species was significantly different I applied a technique from geometric morphometrics (*cf.* Bookstein, 1993). To illustrate this method I will use *Alouatta palliata* as an example. To secure 10 adult females that were in good condition I was compelled to select specimens from three different subspecies: *A. p. palliata*, *A. p. mexicana*, and *A. p. aequatorialis*. To test for inter-subspecies differences, I ran a series of Generalized Least-Squares (GLS) Procrustes superimpositions of 3D cranial landmark coordinates using *GRF-ND*, a morphometrics program written by Slice (1994; Rohlf & Slice, 1990). This procedure yields an optimum fit among a series of configurations and generates a consensus (or mean) configuration. For each GLS fit the program calculates the sum of the squared distances (Σd^2) between each landmark and the corresponding consensus landmark over all landmarks over all specimens. Since this is directly equivalent to a sum-of-squares in an analysis of variance, we can formulate an *F*-statistic by dividing the between-subspecies mean square ($\Sigma d^2/df$) by the pooled within-subspecies mean square, and test for significance in the normal way. Box 4.4 gives the results of this "Procrustes" ANOVA for each of the 11 species whose sample is composed of more than one subspecies. The results indicate no significant differences among subspecies within species in terms of overall cranial shape,[3] with the exception of *Ateles geoffroyi*. For comparison I ran the same test on a closely related pair of sister species: *Macaca fascicularis* and *Macaca mulatta*. I obtained an *F*-value of 3.11, which is significant at the $\alpha = 0.1$ level.

[3] Several other studies, using more conventional analysis, have similarly found very little inter-subspecific variation within species of macaques (e.g., Ikeda & Watanabe, 1966).

Reproduced with permission of the copyright owner. Further reproduction prohibited without permission.

More work is required before this morphogeometric technique can produce easily interpretable results.

Box 4.4. Tests of among-subspecies differences using analysis of variance of procrustes residuals

Subspecies group comparisons	**Mean Square, degrees of freedom =** (3p-7)/(3p-7)(2n-2)	**Morpho-geometric *F*-statistic and test of overall shape difference at p<.05**
Alouatta palliata palliata (n=3) *A. p. mexicana* (n=4) *A. p. aequatorialis* (n=3)	Betw. .00158 (320) Within .00292 (2240)	*F* = .52 (ns)
Ateles geoffroyi vellerosus (n=1) *A. g. ornatus* (n=1) *A. g. panamensis* (n=5) *A. g. geoffroyi* (n=3)	Betw. .00925 (320) Within .00432 (1920)	*F* = 2.14 (p<.01)
Cebus apella paraguayanus (n=6) *C. a. versutus* (n=4)	Betw. .00098 (320) Within .00348 (2560)	*F* = .28 (ns)
Cebus capucinus limitaneus (n=3) *C. c. imitator* (n=7)	Betw. .00093 (320) Within .00276 (2560)	*F* = .34 (ns)
Saimiri sciureus sciureus (n=7) *S. s. oerstedii* (n=3)	Betw. .00401 (320) Within .00445 (2560)	*F* = .90 (ns)
Aotus trivirgatus trivirgatus (n=5) *A. t. vociferus* (n=5)	Betw. .00055 (320) Within .00263 (2560)	*F*= .21 (ns)
Chlorocebus aethiops cynosuros (n=2) *C. a. johnstoni* (n=5) *C. a. centralis* (n=2) *C. a. hilgerti* (n=1)	Betw. .00224 (320) Within .00487 (1920)	*F* = .46 (ns)
Cercopithecus ascanius ascanius (n=5) *C. a. katangae* (n=5)	Betw. .00123 (320) Within .00436 (2560)	*F* = .28 (ns)
Macaca nemestrina nemestrina (n=6) *M. n. pagensis* (n=2)[4] *M. n. leonina* (n=2)	Betw. .00235 (320) Within .00366 (2240)	*F* = .64 (ns)
Papio hamadryas hamadryas (n=1) *P. h. ursinus* (n=1) *P. h. anubis* (n=5)	Betw. .00223 (320) Within .00528 (1280)	*F* = .42 (ns)
Semnopithecus cristata pyrrhus (n=4) *S. c. cristata* (n=4) *S. c. kohlbruggei* (n=2)	Betw. .00119 (320) Within .00315 (2240)	*F* = .38 (ns)

[4] Results of the morphogeometric analysis do not support the proposal that the Mentawa Island macaque (*M. n. pagensis*) is a separate species (Grove, 1993), although a larger sample size would be required for a more adequate test.

Reproduced with permission of the copyright owner. Further reproduction prohibited without permission.

I employed the method here simply to demonstrate that the variance of the among-subspecies shape residuals is no greater than the pooled within-subspecies variance, an indication of intraspecific homogeneity.[5] This ascertainment is of great importance because, as will be made clear, one of the theoretical assumptions of the multi-level analytical technique introduced in Chapter 8 is that of intraspecific homogeneity.

As theoretical and analytical modeling become more and more refined, sample size and composition will need to be tailored more precisely in accordance with model specifications. This will become exceedingly clear in Chapters 6-8 where I discuss the concepts of time-unstandardized phylogenetic effects and multi-level covariance structure modeling. In the next chapter, I describe the methods used to collect data from the sample specimens. Beginning on the following page I present photographs of 37 specimens, one per species, as a visual reference (Boxes 4.5-4.41, beginning on page 81). I encourage the reader to refer to these photographs often, as they are a rich visual supplement to the quantitative and qualitative descriptions and comparisons that follow.

Conclusions

The belief among applied researchers that 'the larger the sample size the better' is inaccurate for several reasons. Positive results obtained from excessively large samples can yield misleading conclusions (just as negative results due to samples that are too small can lead to incorrect inferences). The best examples are to be

[5] The only exception to this generalization is *Ateles geoffroyi*, whose among-subspecies variance was more than twice its pooled within-subspecies variance. This may suggest that one or more of the four subspecies sampled is nearing an incipient species level of divergence.

Reproduced with permission of the copyright owner. Further reproduction prohibited without permission.

found in clinical survey trials. Franceschi *et al.* (1998) administered a dietary questionnaire to 6,107 hospital patients, 1,953 of whom had cancer of the colon or rectum. One of the authors' conclusions was that individuals who consumed more cakes and desserts were 1.02 times more likely to have colorectal cancer. But with a sample size of over 6,000 even minute *and potentially biologically insignificant* differences in dessert consumption between cancer and noncancer patients is likely to have been statistically significant in the analysis.

While it is unlikely that investigators in the field of evolutionary morphology will be faced with the 'concern' of having a sample size of 6,000, the point is that decisions regarding the biological meaning of differences or associations revealed in a statistical analysis of data should be based on an understanding of the biology of the organisms involved, with a keen awareness of the effects of statistical power (and by implication, sample size) on the outcome of inferential tests. In fact, it has been argued that sample size and statistical power should be determined on the basis of an *a priori* assessment of the smallest biologically meaningful degree of difference between groups (e.g., Sokal and Rohlf, 1995), a topic I address in the next chapter. Moreover, the size of a sample must be tailored to the analytical techniques employed in a give research project.

Reproduced with permission of the copyright owner. Further reproduction prohibited without permission.

Box 4.5 *Alouatta palliata* [AMNH #18935]

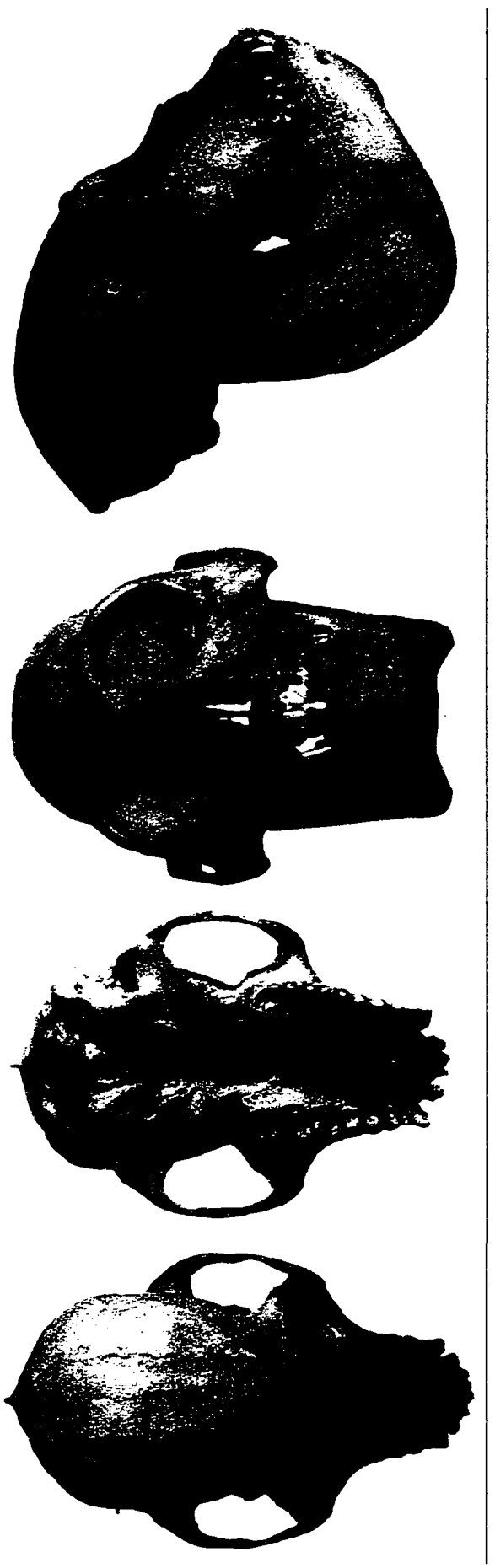

Box 4.6 *Ateles geoffroyi* [AMNH #177664]

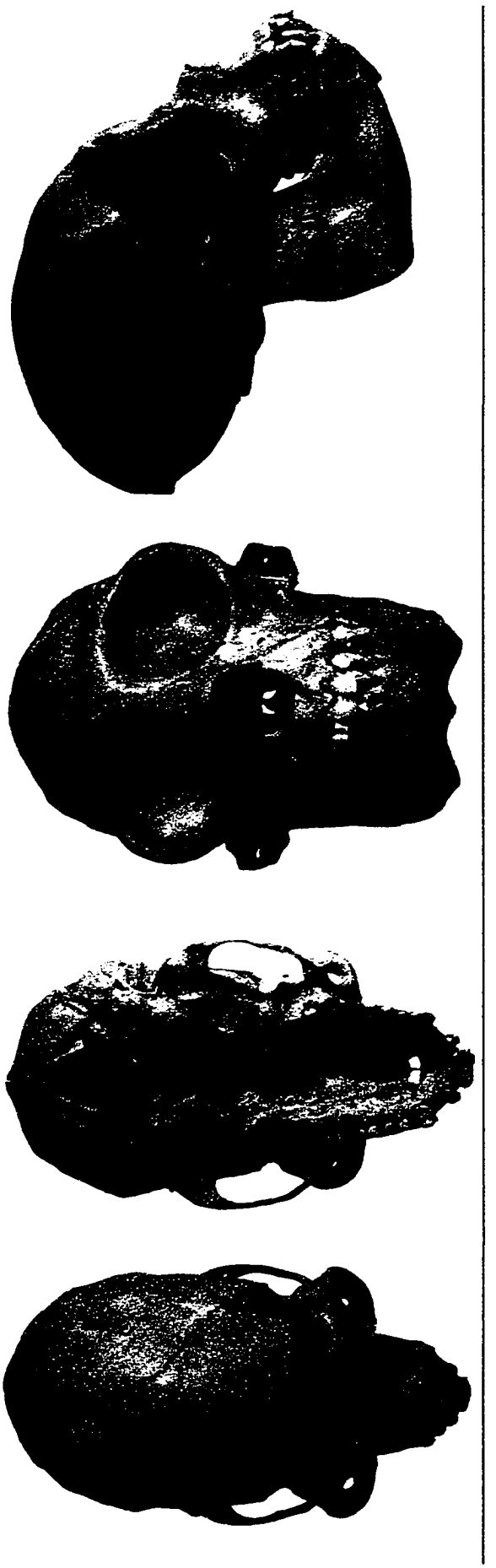

Reproduced with permission of the copyright owner. Further reproduction prohibited without permission.

Box 4.7 *Lagothrix lagothricha* [AMNH #73555]

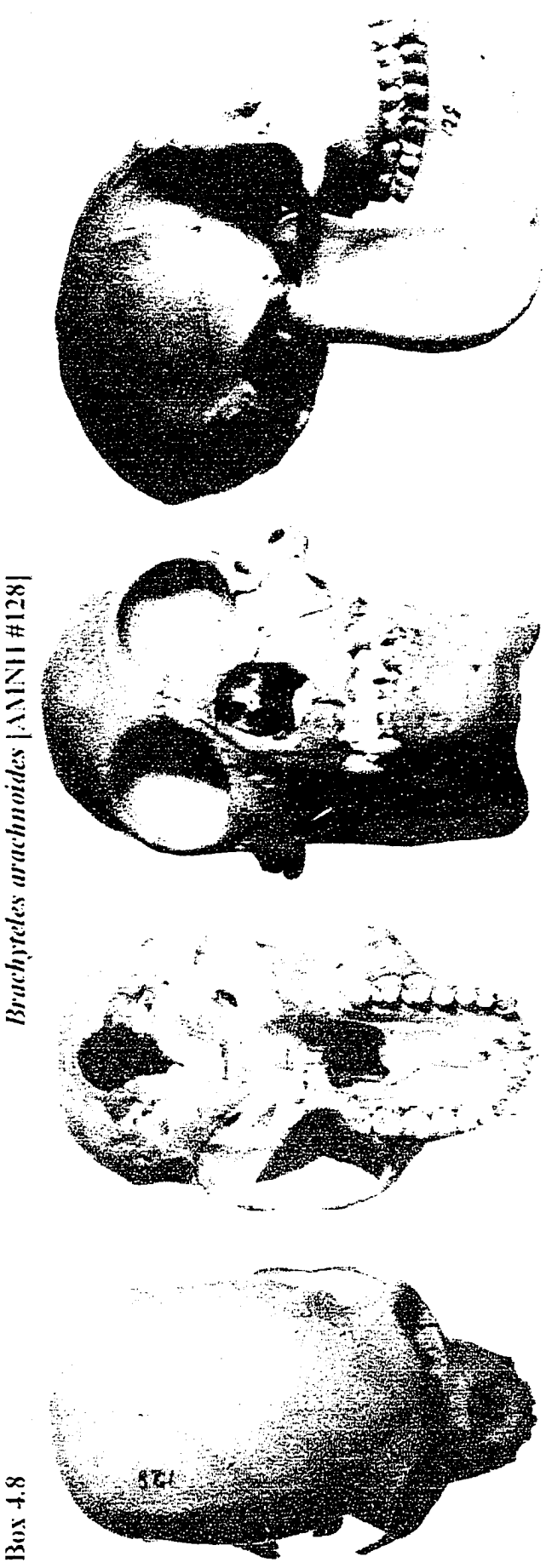

Box 4.8 *Brachyteles arachnoides* [AMNH #128]

Reproduced with permission of the copyright owner. Further reproduction prohibited without permission.

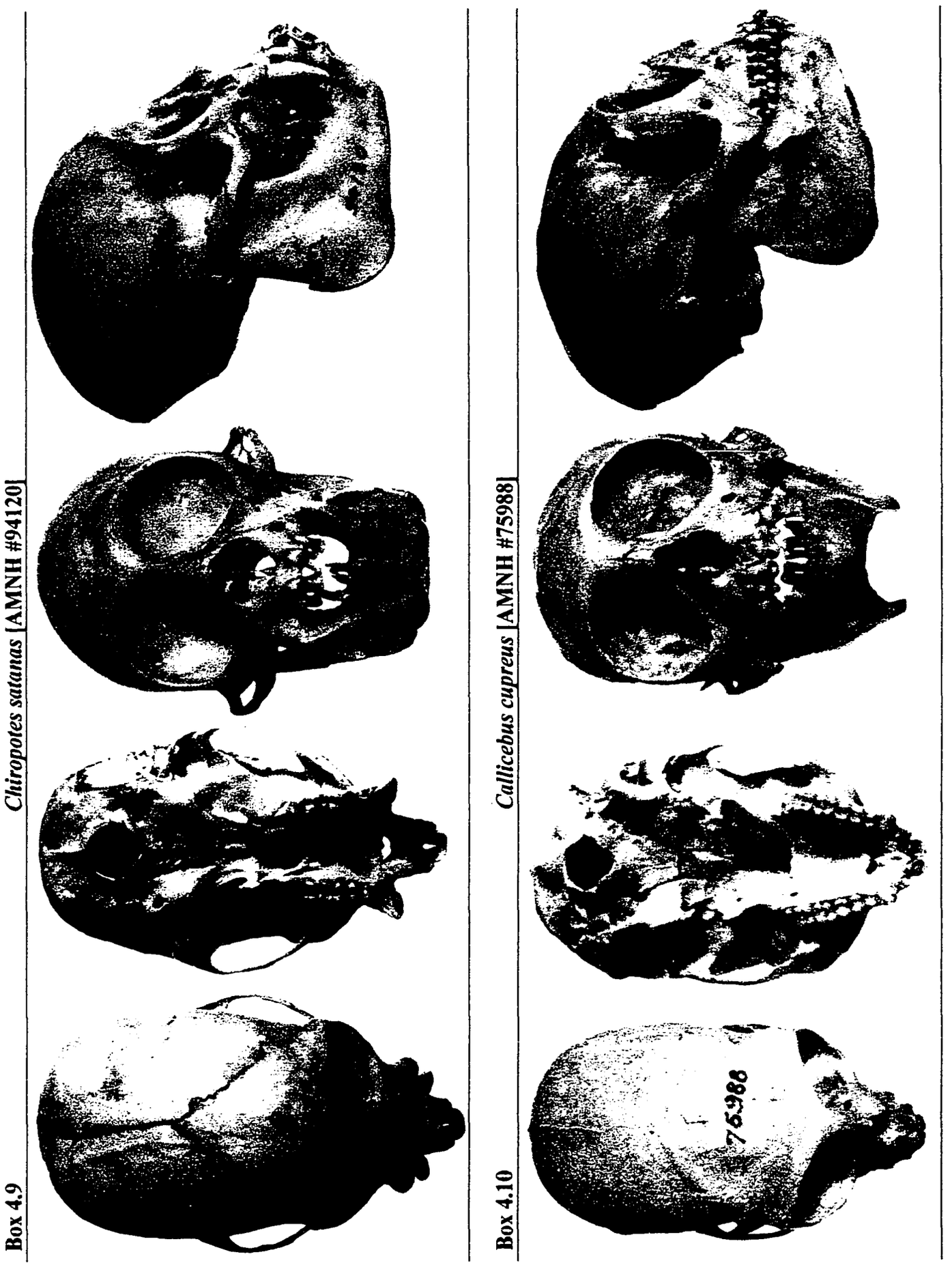

Reproduced with permission of the copyright owner. Further reproduction prohibited without permission.

Box 4.11 ***Pithecia pithecia***

Not available

Box 4.12 ***Pithecia monachus***

Not available

Reproduced with permission of the copyright owner. Further reproduction prohibited without permission.

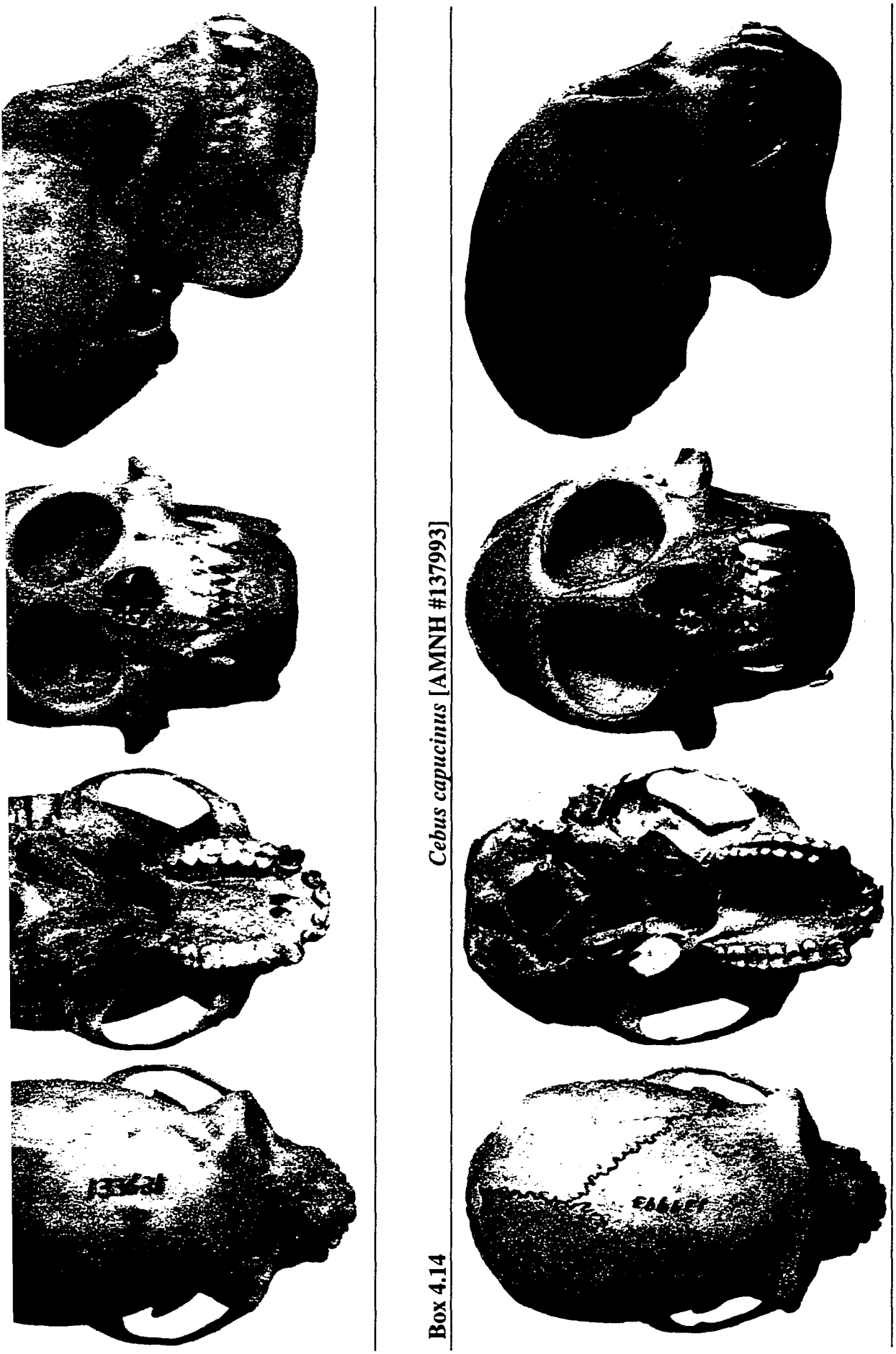

Box 4.14 *Cebus capucinus* [AMNH #137993]

Reproduced with permission of the copyright owner. Further reproduction prohibited without permission.

Box 4.20 *Saguinus oedipus* [AMNH #32702]

Reproduced with permission of the copyright owner. Further reproduction prohibited without permission.

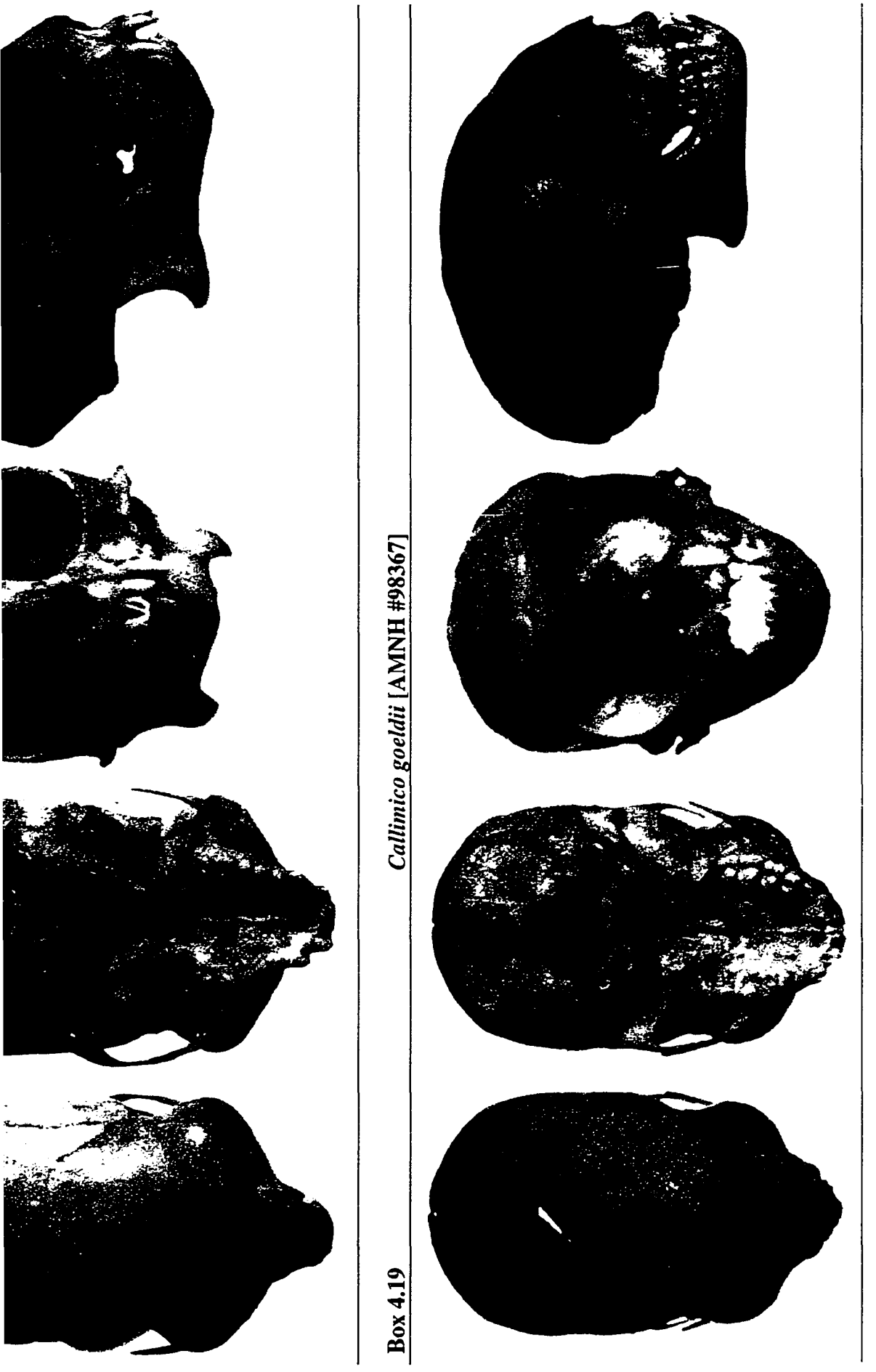

Box 4.19 *Callimico goeldii* [AMNH #98367]

Reproduced with permission of the copyright owner. Further reproduction prohibited without permission.

Box 4.20 *Chlorocebus aethiops* [AMNH #80789]

Box 4.21 *Cercopithecus neglectus* [AMNH #]

Not available

Reproduced with permission of the copyright owner. Further reproduction prohibited without permission.

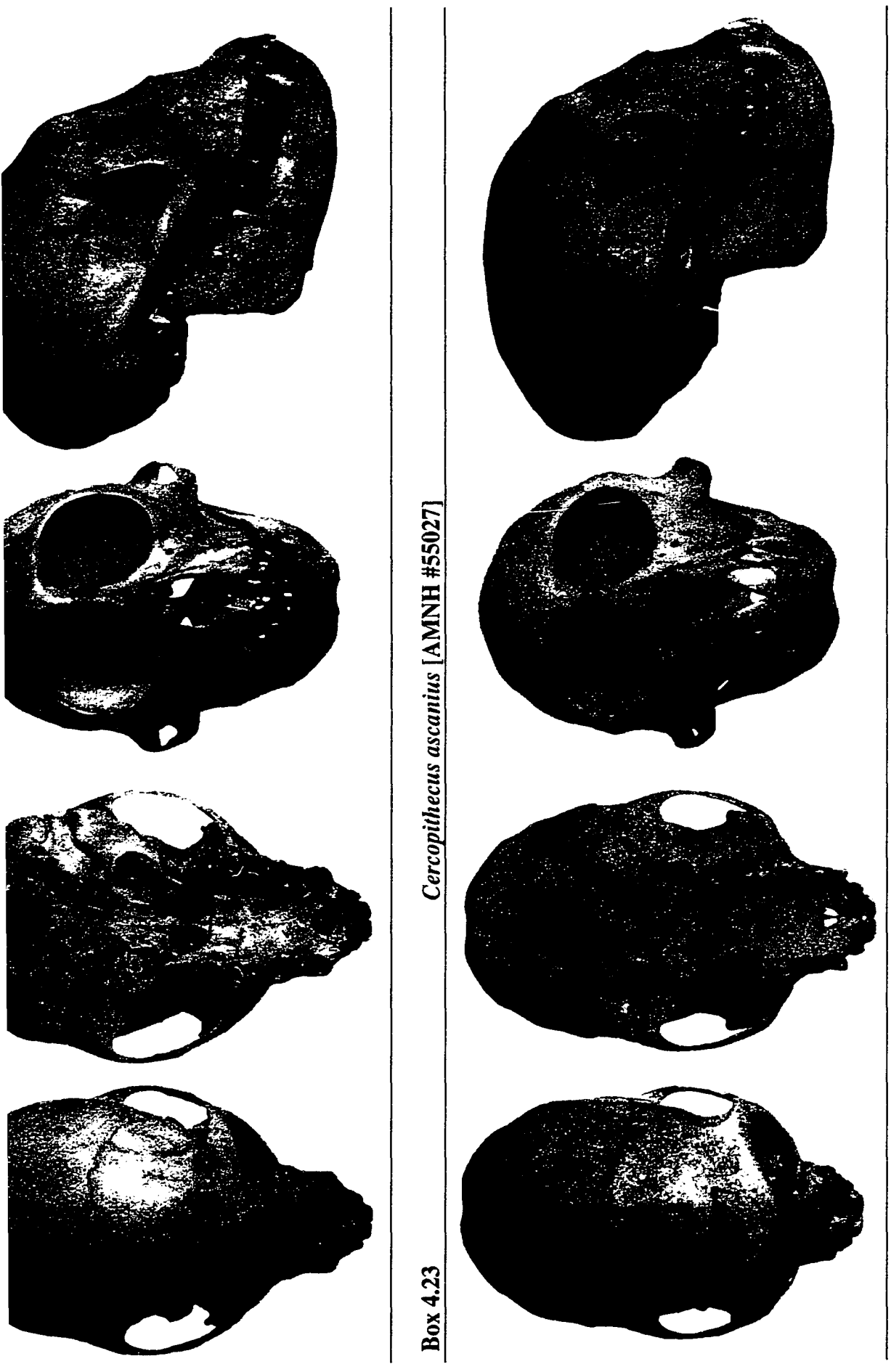

Box 4.23 *Cercopithecus ascanius* **[AMNH #55027]**

Reproduced with permission of the copyright owner. Further reproduction prohibited without permission.

Box 4.24 *Macaca nemestrina* [AMNH #57111]

Box 4.25 *Macaca fascicularis* [AMNH #102764]

Reproduced with permission of the copyright owner. Further reproduction prohibited without permission.

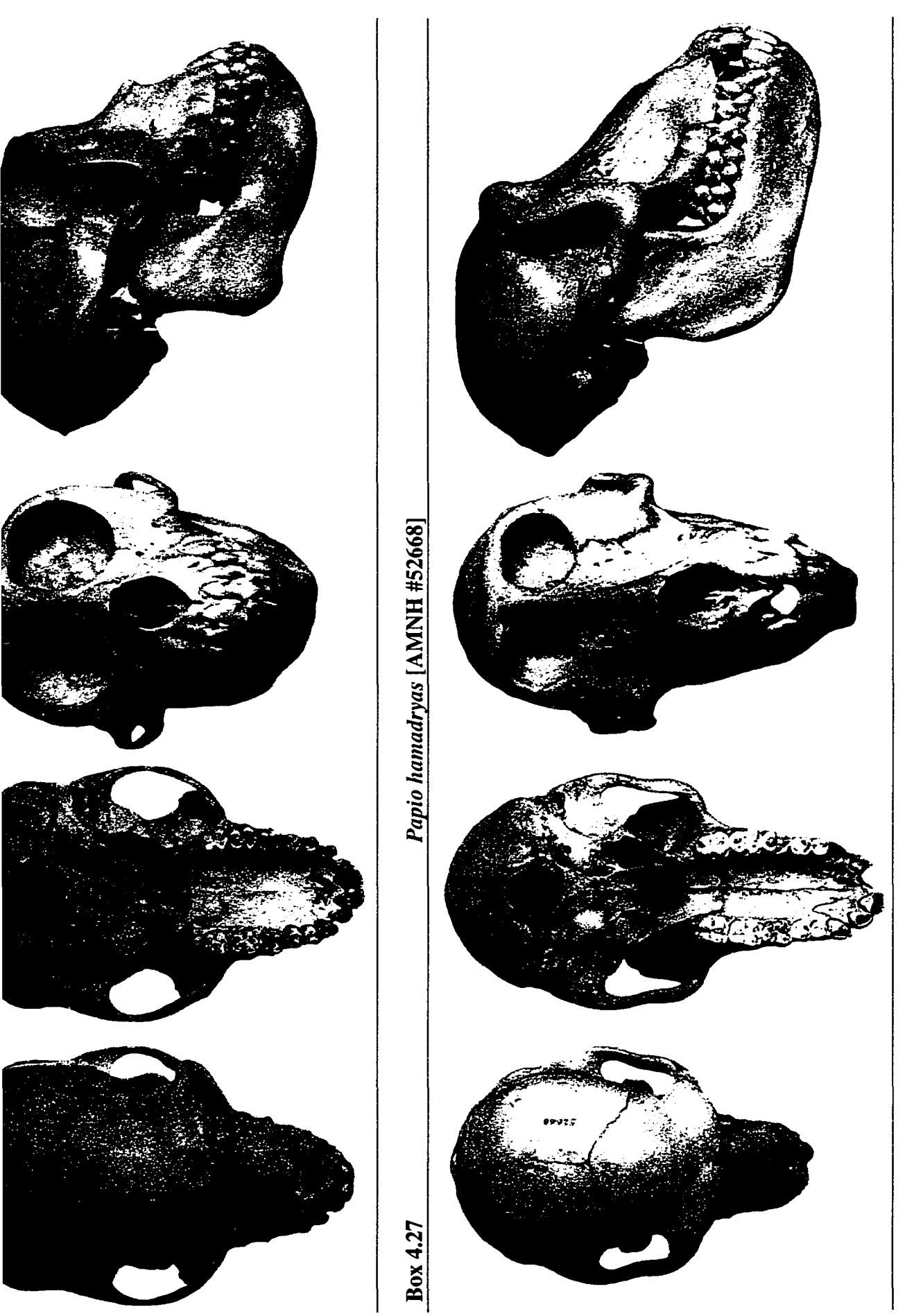

Box 4.27 *Papio hamadryas* [AMNH #52668]

Reproduced with permission of the copyright owner. Further reproduction prohibited without permission.

Box 4.28 *Lophocebus albigena* [AMNH #52613]

Box 4.29 *Procolobus guereza* [AMNH #52238]

Reproduced with permission of the copyright owner. Further reproduction prohibited without permission.

Box 4.30 *Procolobus badius* [AMNH #52267]

Box 4.31 *Nasalis larvatus* [AMNH #103465]

Reproduced with permission of the copyright owner. Further reproduction prohibited without permission.

Box 4.34 *Semnopithecus cristata* [AMNH #106588]

Box 4.35 *Pongo pygmaeus* [AMNH #200898]

Reproduced with permission of the copyright owner. Further reproduction prohibited without permission.

Box 4.36 *Hylobates lar* [AMNH #54659]

Box 4.37 *Hylobates syndactylus* [AMNH #102195]

Reproduced with permission of the copyright owner. Further reproduction prohibited without permission.

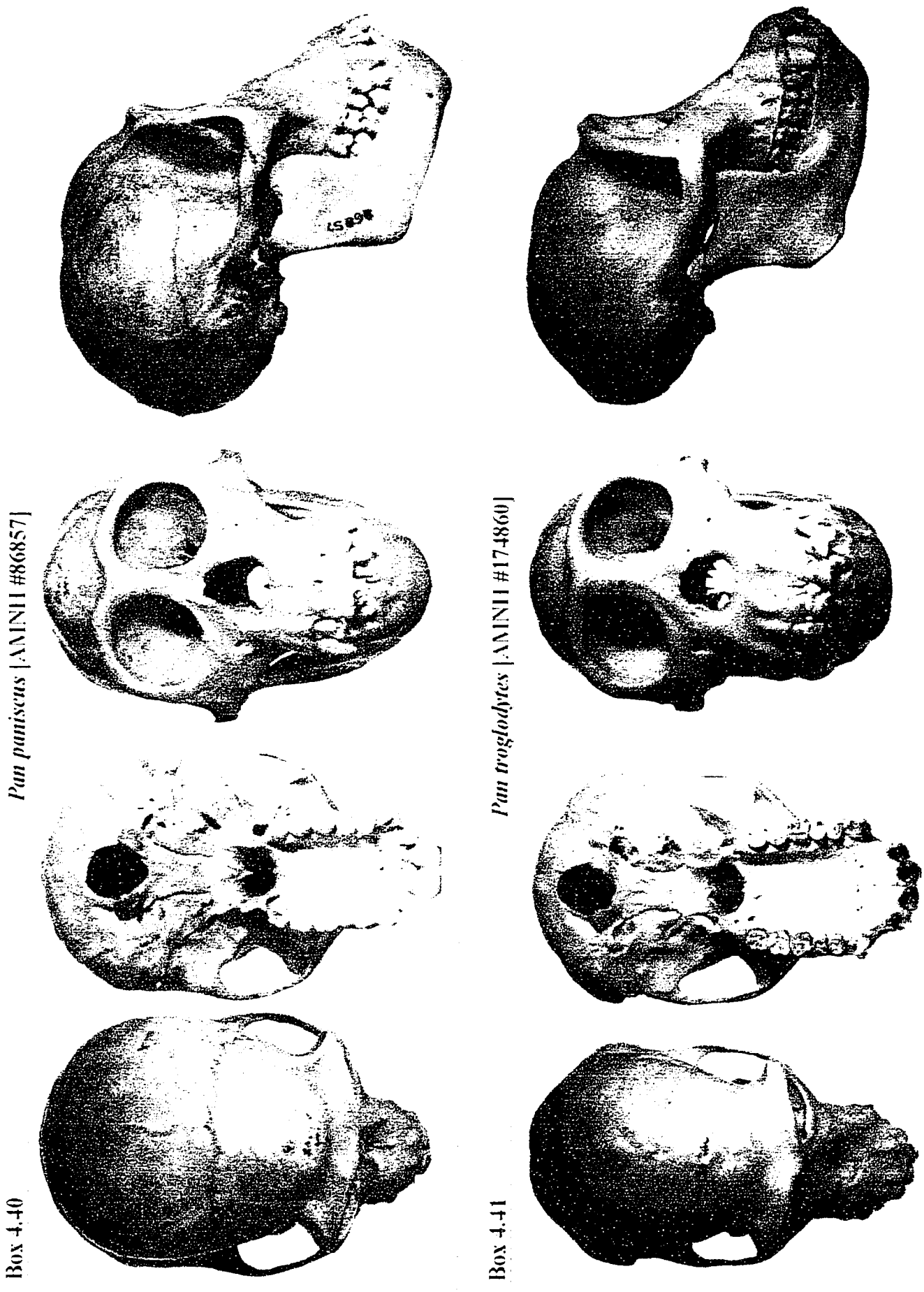

Reproduced with permission of the copyright owner. Further reproduction prohibited without permission.

Chapter 5. Data Collection Techniques

Introduction

The dependent and independent variables listed in Appendix B comprise the set of morphometric and ecological measurements that were employed to test the various nomological hypotheses examined in Chapters 9-15. Ecological and life history data (e.g., dietary preferences and life span) and some phenotypic data (e.g., olfactory bulb volumes and body size) were taken from the literature. All other data were collected directly from museum skulls. Measurements were calculated from 3D coordinate data digitized from the landmarks listed and described in Appendix A.

Three-dimensional coordinate data obtained using a Polhemus 3DRAW digitizer were combined with 2D coordinate data taken from lateral radiographs of each of the sample specimens. These two methods of procuring coordinate data are complimentary. The Polhemus 3DRAW was used to digitize *ectocranial* landmarks, whereas *endocranial* midline landmarks were digitized from the radiographs using a Summagraphics translucent digitizing tablet. Three ectocranial midline landmarks were also digitized from the radiographs and these were used to register and "snap" the two sets of coordinates in the same coordinate space. This was accomplished using *GRF-ND*, a scaling and superimpositioning software program developed by Slice (1994). This procedure resulted in a single *unified* configuration of 3D landmark coordinates for each specimen which combined both ectocranial and midline endocranial points. Each unified landmark configuration was then read into a program I wrote in SAS/IML (Interactive Matrix Language)

Reproduced with permission of the copyright owner. Further reproduction prohibited without permission.

that calculated the linear dimensions, ratios, angles, and estimated areas and volumes (i.e., morphometric variables) for each specimen (see Appendix D). The program also included a subroutine that applied analytic geometry and matrix algebra to the coordinate data configurations in order to model in three-dimensions the masticatory system of each specimen (see Chapter 14).

Protocol

The following data collection protocol was undertaken.

(1) ***Specimen procurement***. 290 nonhuman anthropoid skulls were procured from the osteological collections of the Mammalogy Department at the American Museum of Natural History (AMNH), and 10 human skulls were obtained from the von Luschan collection of the AMNH Anthropology Department. Specimens were signed-out in sets of 10, usually all members of a single species, and transported to the Department of Vertebrate Paleontology (DVP) for the first phase of data collection.

(2) ***3D landmark coordinate data collection***. A Polhemus 3DRAW 3D digitizer was used to collect ectocranial landmark data on the museum skulls. A list and description of the anatomical landmarks that were digitized directly from the skulls is given in Appendix A (landmarks 1-99). The coordinate data were read into a Lotus 1-2-3 spreadsheet using interface software written by Prof. Les Marcus. The data files were copied onto diskettes and transferred to a workstation computer for further handling.

(3) ***3D landmark coordinate data cleaning***. The 3D coordinate data were checked for errors visually by inspecting the superimposed configurations of

Reproduced with permission of the copyright owner. Further reproduction prohibited without permission.

conspecifics. When error-free these 3D images show tight clusters of points around each landmark. Digitization errors (e.g., digitizing landmarks out of sequence, or landmark misidentification) are clearly visible as points lying outside of their respective clusters. Specimens showing such anomalies were redigitized.

(4) ***Dry cranial weight and endocranial volume.*** After 3D digitization was complete, specimens were transported to the NYCEP[1] Quantification Laboratory (AMNH) where the remainder of the data collection was conducted. The cranium of each specimen was weighed to the nearest 0.1 grams using a Fisher Scientific digital analytical balance. Endocranial volume was quantified in ml using the method described by Montagu (1960; see Chapter 11, this study, for a detailed description of the method).

(5) ***Specimen radiography.*** To prepare each skull for radiography, plastilina clay was used to temporarily attach tiny metal fragments (gun shot) directly onto three landmarks: prosthion, bregma, and lambda. These landmarks were thus easily identifiable on subsequent radiographs as clear round dots. The mandible was also fitted to the cranium using plastilina. Specimens and radiographic film were held in proper orientation by a custom-made craniophor, designed and built by myself and Warren Pardi. Radiographs were taken using a Kramex DX-30N LBC portable x-ray unit onto Image Blue high resolution film. Two images were produced for each skull in *norma lateralis*. The first exposure was made of the specimen as described, and a second exposure was made after fine brass filings were poured into

[1] New York Consortium for Evolutionary Primatology.

Reproduced with permission of the copyright owner. Further reproduction prohibited without permission.

the endocranial cavity and shaken down to fill the olfactory recess.[2] This technique yielded radiographs in which the outlines of the olfactory recess and underlying cribriform plate were clearly visible (see Box 5.1). Particular care was taken to accurately label each film exposure with a unique specimen number that was cross-referenced with the museum number of that specimen. Exposure time and the distance between the cranial midline and the film surface were also recorded for each specimen.

Box 5.1. Positive contact lateral cephalograph of *Cebus capucinus* (AMNH 137993) showing anterior cranial fossa and olfactory recess filled with fine brass filings

(6) ***Radiographic processing***. The exposed radiographs were transferred from the film cassettes to a light-tight storage box and transported to Hunter

[2] Several earlier methods, including filling the anterior cranial fossa with a lead-based putty and spraying a radio-opaque liquid into the endocranial cavity, had failed to produce the desired results.

Reproduced with permission of the copyright owner. Further reproduction prohibited without permission.

College (CUNY), where the film was hand-processed in the Bioanthropology darkroom. The x-ray film (*Image Blue*) and processing chemicals (*Cine*) were obtained from the Ewen-Parker X-Ray Corporation, of Elmsford, NY. Once dry, each radiograph was carefully labeled with the species name, specimen number, exposure time and midline-to-film distance. Together with an earlier pilot study (McMahon, 1994), and preliminary test exposures, the total number of radiographic images taken and processed for this study was 853.

(7) ***2D cephalographic landmark coordinate data collection***. A translucent Summagraphics digitizing tablet was used to record the *xz* coordinate locations of a series of landmarks from each lateral cephalograph. Of the 14 landmarks recorded, 10 were endocranial midline landmarks, 3 were ectocranial midline landmarks which had been metalically labeled with gun shot (prosthion, bregma, and lambda), and the final landmark was porion (see Appendix A, landmarks 100-113). Each 2D specimen configuration was digitized three times, and the mean configuration for each specimen was saved to a separate file using an interface program written in *Basic* by Prof. Les Marcus.

(8) ***Transformation and unification of 3D and 2D landmark coordinates***. The next step was to "snap" together the 3D ectocranial configuration digitized using the Polhemus 3DRAW and the 2D endocranial-radiographic configuration taken from the same specimen with the Summagraphics. However, before this could be done several transformations and rigid rotations of the separate configurations were necessary. The first few transformations involved the 2D endocranial-radiographic coordinate configurations. Each configuration was first adjusted to correct for projection distortions inherent in the radiographs.

Reproduced with permission of the copyright owner. Further reproduction prohibited without permission.

Radiographic images are projections of an object, such as a skull, onto a flat film surface. Since the x-ray beam emanates from a single point, structures of the object lying away from the central x-ray beam will be projected as enlarged and distorted images, much the same way that shadow puppets can take on a size and shape disproportional to the hand that created them. Given knowledge of a few simple parameters (i.e., the midline-to-film distance, and the x-ray-source-to-midline distance), standard algorithms can be applied to the radiographic coordinates to correct for projection distortions (Wylie & Elsasser, 1948; Savara, 1965; see Appendix C). Each set of projection-corrected 2D coordinates was then converted to a 3D configuration by adding a vector of 0's for the *y* axis (the median axis). Each projection-corrected 3D endocranial-radiographic configuration was then rigidly superimposed (translated, rotated, and scaled) onto the 3D ectocranial configuration of the same specimen, using a least-squares criteria over the three common landmarks (prosthion, bregma, and lambda). Finally, the "unified" 3D landmark configurations (i.e., the combined ectocranial and midline endocranial coordinates) were translated and rotated (but not scaled) so that they were oriented in the proper Frankfort plane. Box 5.2 lists the various SAS programs and GRF-ND commands that were used. Appendix C presents an example of the foregoing transformations complete with SAS/IML program code, comments, and sample output.

(9) ***Calculation of research variates from unified landmark configurations.*** Once the unified landmark configurations were created, and checked for accuracy, they were read one-by-one into a SAS/IML program (see Appendix D) that calculated and wrote to an output file the values of variables 1 to 84 (in Appendix

Reproduced with permission of the copyright owner. Further reproduction prohibited without permission.

B), for a given specimen. Each generated variable thus recorded was appended to a master EXCEL spreadsheet for storage and later export to SAS for analysis. The full set of raw data is presented in Appendix E.

Box 5.2. Sheet used as guide for producing unified 3D morphometric landmark configurations.

STEPS FOR GENERATING MORPHOMETRIC DATA FROM RAW COORDINATES

* Make sure DD.OUT file in Excel is closed

** Make sure initial .WK1 file has 99 records

(1) Convert .WK1 file of 99 3D digitized landmark points to ASCII format file and copy it into appropriate directory,

e.g. C:\DISSDATA\CMITIS\CM52363**CM52363.PRN**

(2) Run the SAS program SNAP2.SAS to create a GRF-ND format file (e.g. **CM363.DTA**) that contains 2 configurations of 109x3 with appropriate missing (dummy) points (see Appendix C).

(3) Open GRF-ND and submit the following comands:

```
CD C:\DISSDATA\CMITIS\CM52363
D CM363.DTA
REF 1
STRICT ON
BACKSCALE
LS
SAVE RES CM363.RES
```

[NOTE: The above set of commands superimposes the cephalographic coordinate configuration onto the 3D ectocranial configuration. Since the two configurations share only 3 landmarks (prosthion, bregma, and lambda), these three landmarks are the basis of the superimposition. See Appendix C for a print-out of file CM363.RES.]

(4) Run the SAS/IML program SNAPCOMB.SAS to unify the ectocranial and cephalographic configurations into a single 109x3 configuration, and to create a GRF-ND formated file containing the unified configuration. e.g. **CM363G.DTA**

(5) Read the new unified configuration into GRF-ND and realign the points to anatomically correct position. Submit the following commands:

```
D CM363G.DTA
FR C:\DISSDATA\TRANS108.DIS
STRICT ON
LS
BACKSCALE
SAVE RES C:\DISSDATA\CMITIS\CM52363\CM52363C.RES
```

[NOTE: The above set of commands translates and rotates (but does not scale) the unified landmark configuration so that it is oriented in the Frankfort Horizontal. This is required because several measurements calculated from the coordinate configuration assume that it is oriented in this manner.]

(6) Run SAS/IML main variate calculation program DISS2.SAS on above .RES file

(7) Read resulting output file DD.OUT into EXCEL and and append to main data storage file DISSDATA.XLS.

Reproduced with permission of the copyright owner. Further reproduction prohibited without permission.

Diagrammatic Variable Depictions

Boxes 5.3A-5.3D present a series of cranial illustrations, photographs, and radiographic images that depict, anatomically, the morphometric variables used in this study (see Appendix A for a complete list and description of anatomical landmarks, and Appendix B for a list and description of morphometric variables). The key gives the variable (V) or landmark (L) number, label, name and dimensions of measurement [xyz].

Box 5.3A. Line drawings of *Pan paniscus* (AMNH 86857), frontal view, depicting several morphometric variables.

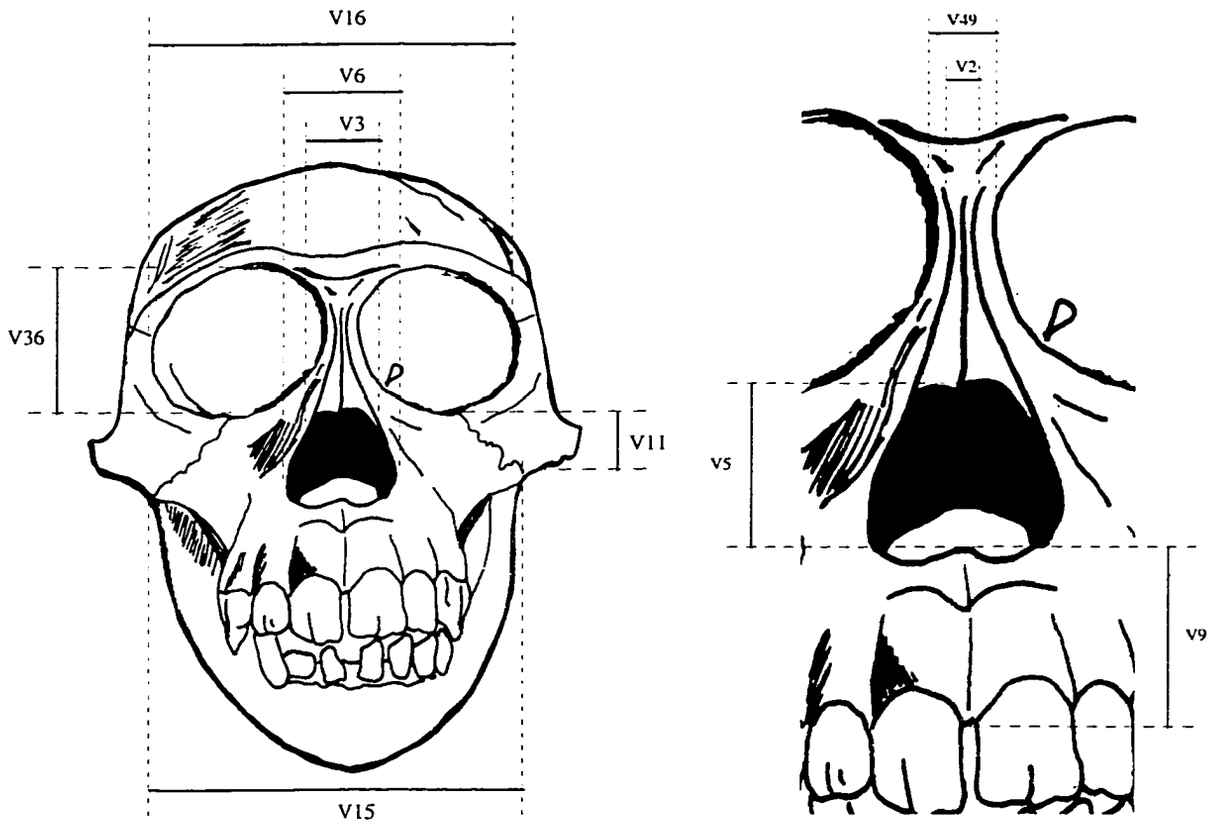

Key: **V2** (NASWDU) upper nasal bone width [y]; **V3** (NASWDL) lower nasal bone width [y]; **V5** (NSLAHT) anterior nasal aperture height [xyz]; **V6** (NSLAWD) anterior nasal aperture breadth [xyz]; **V9** (NLCLGT) nasoalveolar clivus length [xyz]; **V11** (ZYGOHT) zygomatic height [xy]; **V15** (BMAXWD) bimaxillary breadth [xyz]; **V16** (UMAXWD) upper facial breadth [xyz]; **V36** (ORBIHT) orbital height [xyz]; **V49** (IORBDS) interorbital distance [xyz]

Reproduced with permission of the copyright owner. Further reproduction prohibited without permission.

Box 5.3B. Line drawings and photo of *Pan paniscus* (AMNH 86857), basal and superior views, depicting several morphometric variables.

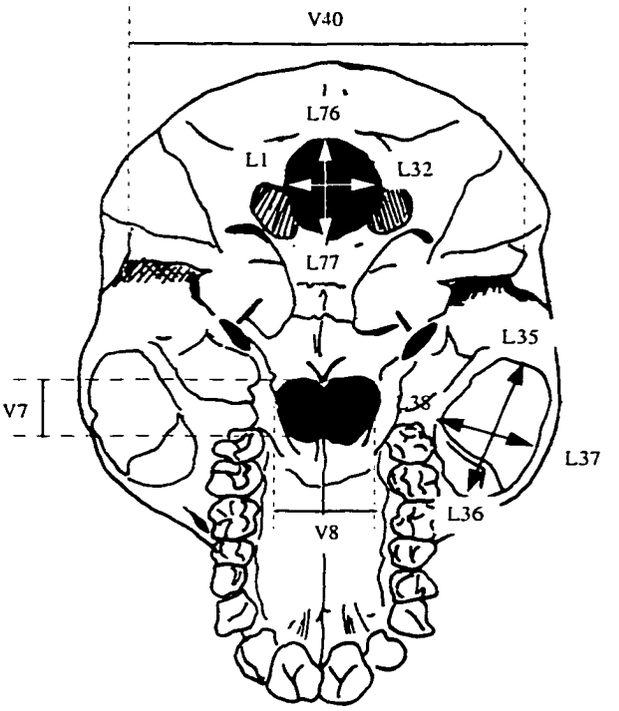

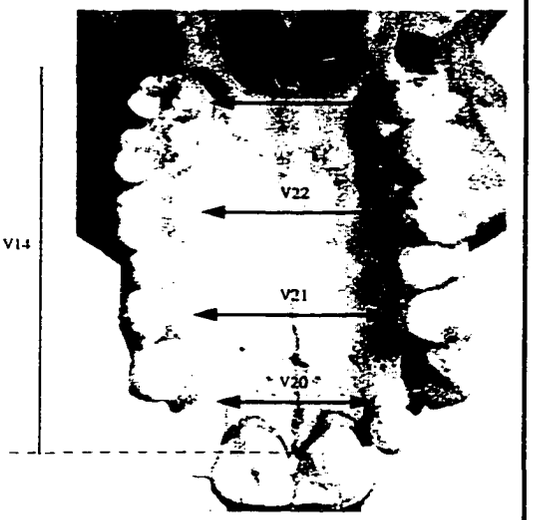

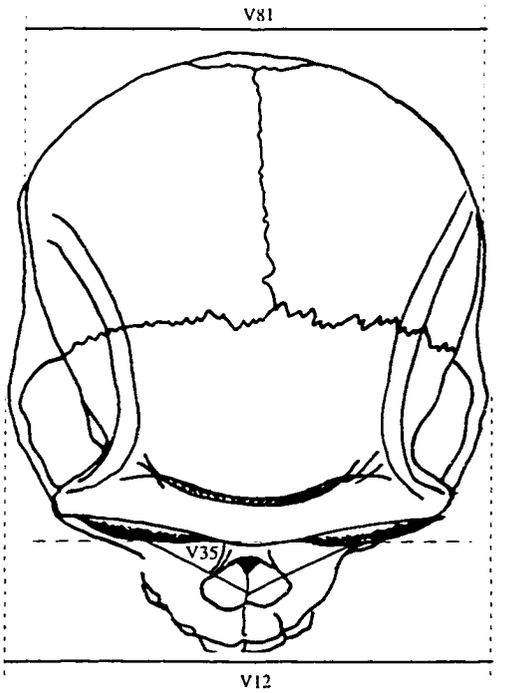

Key: **L1** (LLFORM) left, lateral-most foramen magnum margin; **L32** (RLFORM) right, lateral-most foramen magnum margin; **L35** (RPITFN) right, post.-most point of infratemporal foramen; **L36** (RAITFM) right, ant.-most point of infratemporal foramen; **L37** (RLITFN) right, lat.-most point of infratemporal foramen; **L38** (RMITFN) medial-most point of infratemporal foramen; **L76** (MOPIST) opisthion; **L77** (MBASIO) basion; **V7** (PNASHT) posterior nasal aperture height [xyz]; **V8** (PNASWD) posterior nasal aperture breadth [xyz]; **V12** (BZYGWD) bizygomatic breadth xyz]; **V14** (MXARCL) maxillary arch length [xz]; **V20** (I2PALW) inter-I2 palatal width [y]; **V21** (P3PALW) inter-P3 palatal width [y]; **V22** (M1PALW) inter-M1 palatal width [y]; **V23** (M3PALW) inter-M3 palatal width [y]; **V35** (PPNALO) paranasal plate orientation [xy]; **V40** (BIPORB) biporionic breadth [xyz]; **V81** (ENDOID) maximum neurocranial breadth dimension of endocranial index [xyz]

Reproduced with permission of the copyright owner. Further reproduction prohibited without permission.

Box 5.3C. Line drawing and radiographic image of *Pan paniscus* (AMNH 86857), lateral view, depicting morphometric landmarks, planes and variables.

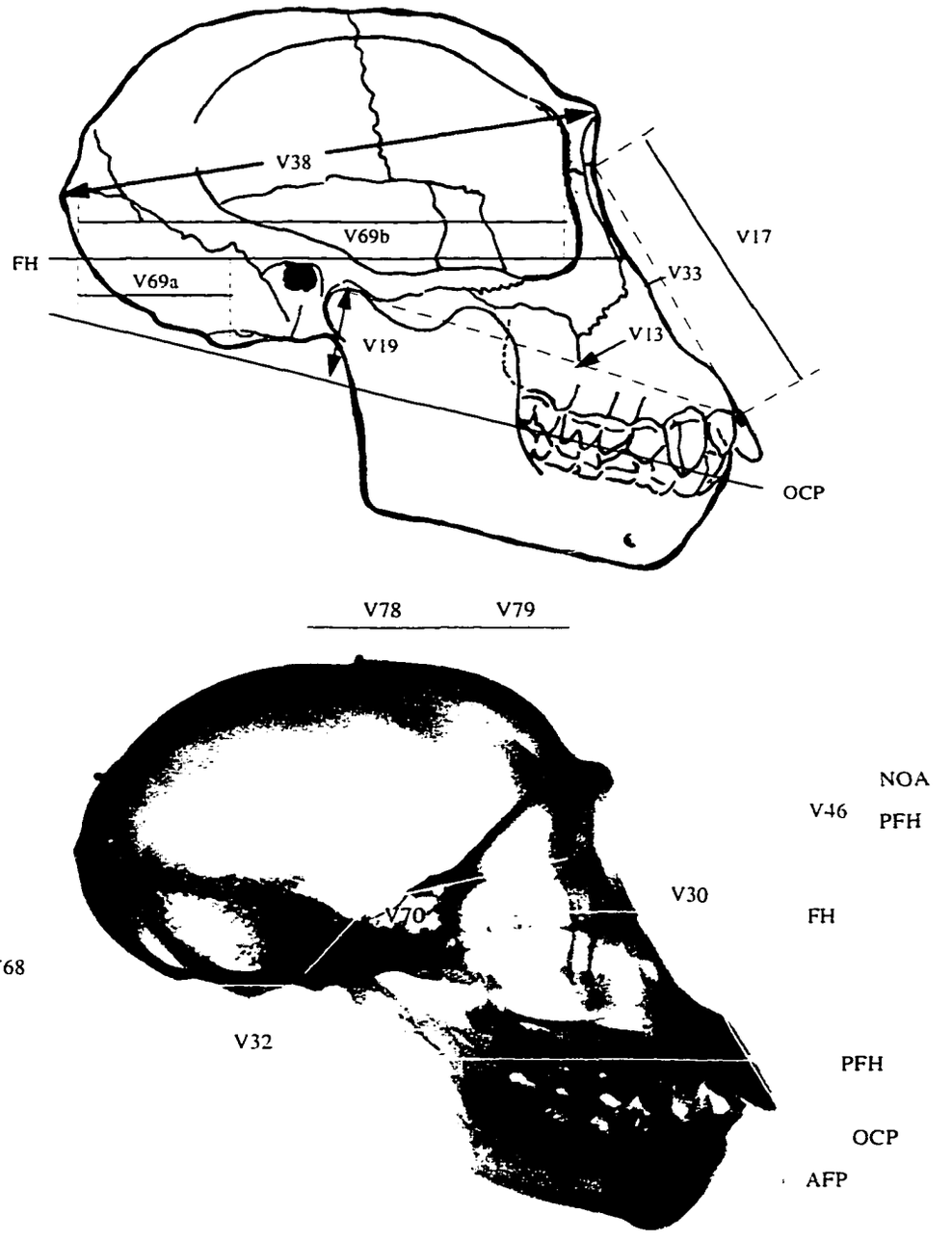

Key: **V13** (APZYGR) anteroposterior position of zygomatic root [xz]; **V17** (AFACHT) anterior facial length [xyz]; **V19** (RAMSHT) ramus height [xz]; **V30** (KROGAG) Krogman's angle of facial prognathism [xz]; **V32** (SLOPOC) occlusal slope relative to Frankfort plane [xz]; **V33** (FACCNV) facial convexity [xz]; **V38** (NCLGTH) neurocranial length [xyz]; **V46** (ORBTC1) orbital deflection [xz]; **V68** (SLOPFM) inclination of foramen magnum relative to Frankfort plane [xz]; **V69** (APOCND) anteroposterior position of occipital condyles V69a/V69b [xz]; **V70** (CBFLEX) cranial base flexion [xz]; **V78** (MCFLGT) middle cranial fossa length [xz]; **V79** (ACFLGT) anterior cranial fossa length [xz]; **AFP**, anterior facial plane; **FH**, Frankfort horizontal; **FMP**, foramen magnum plane; **NOA**, neutral orbital axis; **OCP**, occlusal plane; **PFH**, parallel Frankfort horizontal`

Reproduced with permission of the copyright owner. Further reproduction prohibited without permission.

Box 5.3D. Top: Lateral radiograph of *P. paniscus* indicating various landmarks (L), morphometric variables (V), and reference planes. Bottom. Lateral radiograph of *Procolobus badius* (AMNH #52267) showing olfactory recess and cribriform plane landmarks.

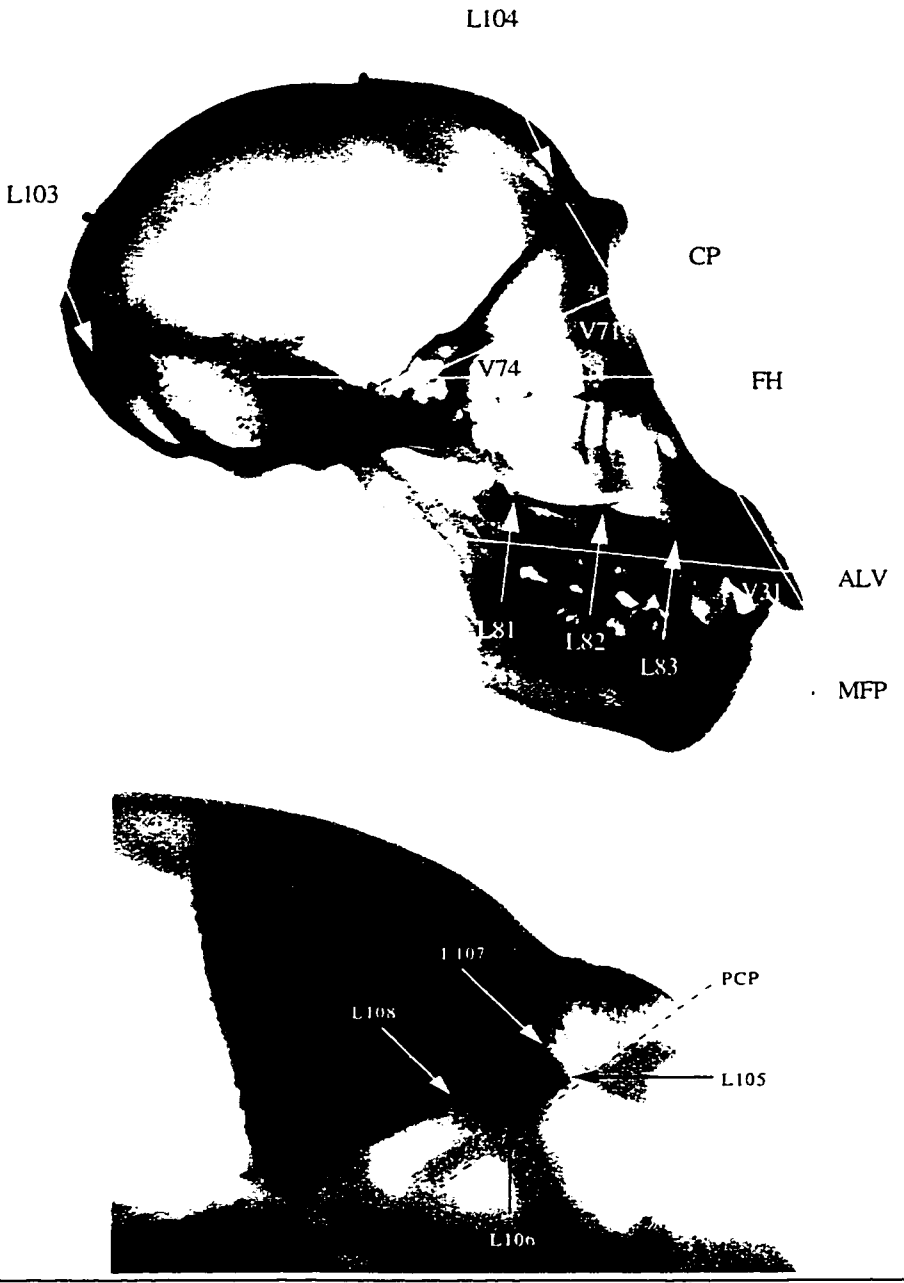

Key: **L81** (MPALM3) point on palatal midline between left and right M^3 ; **L82** (MPALM1) point on palatal midline between left and right M^1 ; **L83** (MPALP3) point on palatal midline between left and right P^3 ; **L103** (XPOSBR) posterior-most brain; **L104** (XANTBR) anterior-most brain; **L105** (XACRIB) anterior-most cribriform plate; **L106** (XPCRIB) posterior most cribriform plate; **L107** (XAOLFA) ant.-most point of olfactory fissure from anterior cranial fossa; **L108** (XPOLFA) post.-most point of olfactory fissure; **V31** (ENLOAG) Enlow's angle of facial prognathism; **V71** (ENLWCP) Enlow's cribriform plate-midfacial plane angle; **V74** (SLPCPF) inclination of cribriform plate relative to the Frankfurt Horizontal; **CP**, plane of cribriform plate; **FH**, Frankfurt Horizontal; **ALV**, dento-alveolar plane; **MFP**, midfacial plane; **PCP**, parallel cribriform plate plane

Reproduced with permission of the copyright owner. Further reproduction prohibited without permission.

The "Smallest Meaningful Measurement" and Measurement Error

Two important and related questions faced by researchers collecting biometric data are: (1) what is the correct scale of measurement? and, (2) how much measurement error is too much? These questions hinge on two operational concepts that are essential to comparative biological research—the *smallest meaningful measurement* and *measurement error.* I begin with a description of measurement error, since this concept leads logically to the other. There are two main *types* of measurement error—errors of accuracy and errors of precision. "Accuracy is *the closeness of a measured or computed value to its true value*; precision is *the closeness of repeated measurements of the same quantity* to each other" (Sokal & Rohlf, 1995:13). In addition, there are two main *sources* of measurement error: (1) measuring-instrument error, and (2) observer error.

Many investigators feel that it is essential to stipulate *a priori* the level of measurement error that will be deemed "acceptable" for a given study. Measurement error is undesirable, if unavoidable, as it can obstruct the investigator's ability to make substantive inferences about the traits of the subjects under study. It is one of the primary goals of the data collection technique to keep measurement error to a minimum. However, I view the tactic of setting an *a priori* "acceptable" level of measurement error as impractical in most instances. Not because reducing measurement error is unattainable, but because the criteria for setting such a limit is ambiguous.

The '*a priori*' approach maintains that some quantity exists that represents the *smallest biologically meaningful measurement* (SBMM) of a variable, and that

Reproduced with permission of the copyright owner. Further reproduction prohibited without permission.

measurement error above this quantity is unacceptable because it overlaps with and obscures small but substantive measurements. Although this statement is accurate, it is difficult to decide how such a quantity is to be assigned Is a difference of 0.01 mm in the nasal widths of two specimens of anthropoids biologically meaningful? What of a difference of 0.1 or 1 mm? Unless there is some good empirical or theoretical basis for setting a specific limit, any such designations are more or less arbitrary. Our only recourse is to take all available precautions to reduce measurement error and allow the empirically determined measurement error itself to dictate the *smallest statistically detectable measurement* (SSDM) in the data; or what Sokal and Rohlf (1995) refer to as "the smallest detectable difference." To reiterate, it is the degree of measurement error that determines the SSDM.

SBMM's and SSDM's are important concepts and deserve further consideration. Ideally we would like to keep the smallest detectable measurement at or below the quantity of the smallest biologically meaningful measurement. It is then up to the investigator to decide whether a true detected difference between groups or association between variables is great enough to be considered biologically meaningful. The frequently recited dogma that a given measurement or result may be statistically significant but not necessarily biologically meaningful has its foundations in such instances. This is of course preferable to the converse situation, in which the SSDM is *above* the level of the SBMM. In such cases, statistical tests will not be able to detect all of the biologically meaningful differences or associations in the data. Thus, *a priori* established measurement error levels, and consequently SSDMs, can only be set in relation to

Reproduced with permission of the copyright owner. Further reproduction prohibited without permission.

a known SBMM. Since SBMMs are for the most part unknown, there is no valid criteria for setting *a priori* measurement error levels. Despite the foregoing, conventional methods persist for establishing *a priori* measurement error levels based on some arbitrary criteria involving SSDMs.

Sokal and Rohlf (1981) phrase the SSDM question thus: "To how many significant figures should we record measurements?" They suggest the following method:

> If we array the sample by order of magnitude from the smallest individual to the largest one, an easy rule to remember is that *the number of unit steps from the smallest to the largest measurement in an array should usually be between 30 and 300* [Sokal & Rohlf, 1981:15].

These authors then suggest using the *implied limits principle*, which sets boundaries for acceptable measurement error as plus-or-minus one-half of the unit scale arrived at using the 30-to-300 rule. For example, if the 30-to-300 rule dictates that measurements be taken to the nearest 1 mm, then the acceptable measurement error is ± 0.5 mm; if measurements are to be taken to the nearest 0.1 mm, then the acceptable error is ± 0.05 mm, and so on.

I applied this method to the anthropoid data, but to offset the effects of including a few very large or a few very small specimens in the sample, I have opted to count the number of unit steps in two standard deviations of the data array, rather than taking the range difference. I found that for nearly every linear distance, square-root area, and cube-root volume, the appropriate scale is to the nearest millimeter. According to this method, then, the smallest statistically meaningful measurement is 1 mm. I then applied the principle of implied limits,

Reproduced with permission of the copyright owner. Further reproduction prohibited without permission.

as suggested by Sokal and Rohlf (1995:13), to arrive at an acceptable measurement error of less than 0.5 mm.

Although this approach is a frequently employed "rule-of-thumb," the dual approaches of the 30-to-300 rule and the implied limits principle do not gain much support on theoretical grounds. I have been unable to find a single study to support the notion that variate arrays covering less than 30 or more than 300 intervals yield biased or otherwise unreliable parameter estimates. From a practical standpoint, variables outside of the 30-to-300 interval range are quite frequently employed in data analyses, especially in the behavioral sciences and in clinical and biomedical research.[3] Moreover, it can be shown that the adoption of these methods can actually lead to measurements that are less accurate than if one were to use values consisting of several extra decimal places. Because of the base-10 scale of the metric system, implied precision limits are always constrained to plus-or-minus base-5 (0.5, 0.05, 0.005, etc..). If the actual precision is superior to base-5 (e.g., 0.2, 0.03, etc..) then measurements taken to more decimal places than indicated by the implied limits principle will yield more accurate quantities. For this reason, I report morphometric data to the nearest 0.1 mm (see Appendix F), and in so doing I do not imply a measurement error of 0.05 mm.

A more practical approach for determining the quantity of the smallest statistically detectable measurement, as I have already stated, is to calculate the measurement error and allow it to determine the appropriate SSDM. Once obtained, the SSDM is used to help determine the appropriate sample size for the study (for example, see Box 4.1, formula 2). Measurement error is clearly an

Reproduced with permission of the copyright owner. Further reproduction prohibited without permission.

important quantity in comparative research, and its quantification and assessment in relation to the present study is the subject of the next section.

Measurement Error Quantification

I earlier stated that there are two main *sources* of measurement error: measuring instrument error and observer error. In the present study, it is not possible to separate the effects of these two sources of error, since there was only one observer. But it was possible to quantify the separate error contributions of the various measurement instruments used to collect the data. I begin with an assessment of the accuracy of the various measurement devices, then proceed to an assessment of the precision of each.

Accuracy

The importance of taking accurate measurements is that such data are internally as well as externally valid. That is, not only can accurate measurements taken during the course of a research project be compared to each other, but they can also be combined with or compared to other accurate data from other research projects. One source of inaccuracy is a bias in the measuring instrument used. Instrument bias can affect the accuracy of the data in several different ways. A measuring device can yield consistently inaccurate readings over a series of scales, or it may yield scale-dependent inaccuracies. For example, a device may be shown to be accurate over a given scale (e.g., from 1 to 10 cm) but inaccurate over a different scale (e.g., 11 cm and over). Another potential source of bias unique to most

---

[3] Bentler & Chou (1987) have shown that variables with as low as four interval values give reasonably good results.

Reproduced with permission of the copyright owner. Further reproduction prohibited without permission.

digitizing devices derives from spatial inconsistencies within the measuring field. A digitizer may render accurate measurements in one part its field but inaccurate measurements in another. Each of these potential sources of instrument bias is examined in turn, for each of the devices employed.

The degree of inaccuracy attributable to instrument bias is difficult to quantify. For example, if the length of a structure is measured to be *precisely* 1.0 cm, how is one to be sure that the true length of the structure is not greater than or less than 1 cm. The standard method of testing the accuracy of a measuring device is to measure precisely a structure of known length, such as a calibration scale. If the device returns a measurement matching the known length of the scale then the device is assumed to be accurate (for the distance measured). Most devices can in fact be calibrated to such scales. However, when inconsistencies are observed one is never really sure whether they are due to instrument bias or to the inaccuracy of the scale. One way to address this problem is to measure a standard scale with several different instruments. If the instruments yield different results then at least one of them is biased, and the pattern of measurements observed may offer a clue as to which of the devices is giving inaccurate readings. If all of the devices return consistent (but unexpected) measurements there are two possible explanations: either they all happen to be biased in the same direction and to the same degree, or, more likely, the scale used as a standard is not accurate.

To assess the accuracy of the measuring devices employed in this study repeated decimeter measures were taken along a standard scale with three separate measuring devices: (1) the Polhemus 3DRAW digitizer, (2) the Summagraphics digitizing tablet, and (3) a set of Fowler digital calipers. A non-metallic calibration

Reproduced with permission of the copyright owner. Further reproduction prohibited without permission.

unit of known scale that is invariant under varying conditions of temperature, pressure and humidity was not available during the data collection phase of this study. In lieu of a true calibration scale, a Westcott Scientific acrylic millimeter-centimeter ruler was used as the standard scale. Results of the repeated measures are given in Box 5.4. It can be seen that the means of the different devices are not significantly different from each other (i.e., the 95% confidence intervals of the means overlap), but that all yield measurements that are significantly greater than 10 cm. The simplest explanation of these results is that the acrylic ruler used as the standard is inaccurate. If this presumption is true, then on average each 1 cm scale on the ruler is actually about 1.0017 cm in length. Further tests demonstrated that this magnitude of inaccuracy was consistent along the entire length of the 30 cm ruler.

Box 5.4. Descriptive statistics of repeated decimeter measurements.

	Mean (cm)	95% Confidence Intervals (CI)
Polhemus 3DRAW Digitizer	10.017 (n=200)	10.014, 10.020
Summagraphic Digitizer	10.016 (n=120)	10.0159,10.0161
Fowler Digital Calipers	10.015 (n=100)	10.012, 10.018

To assess the scale dependent accuracy of the 3DRAW digitizer, a series of 200 linear measurements were taken along the 30 cm acrylic ruler at 10, 20 and 30 cm intervals. The observed proportions of the means were then compared to the expected proportions. To quantify the effects of spatial inconsistencies, measurements were systematically taken in equal numbers in various regions of the digitizing field. Box 5.5 shows that the observed measurement proportions are not significantly different from expected. From these results I conclude that there is no significant scale dependent bias in the Polhemus digitizer. This procedure was

Reproduced with permission of the copyright owner. Further reproduction prohibited without permission.

repeated for the Summagraphics digitizing tablet, with similar results (see Box 5.6).

Box 5.5. Scale dependent inaccuracy assessment of the Polhemus 3DRAW digitizer			
	(A) 10 cm lengths	(B) 20 cm lengths	(C) 30 cm lengths
Mean	10.017	20.023	30.09
Standard Deviation	0.028	0.018	0.085
Expected proportion	C/A=3.0	B/A=2.0	C/B=1.5
Observed proportion	C/A=3.004 (ns)	B/A=1.999 (ns)	C/B=1.503 (ns)

Box 5.6. Scale dependent inaccuracy assessment of the Summagraphics digitizer			
	(A) 10 cm lengths	(B) 20 cm lengths	(C) 30 cm lengths
Mean	10.016	20.033	30.04
Standard Deviation	0.007	0.012	0.019
Expected proportion	C/A=3.0	B/A=2.0	C/B=1.5
Observed proportion	C/A=2.999 (ns)	B/A=2.000 (ns)	C/B=1.499 (ns)

There is yet another potential source of inaccuracy unique to digitizing devices that needs to be addressed. Because measurements are derived from information recorded in a *specific region* of the digitizing field the possibility exists that measurements of a given length taken in different regions of the field may yield inconsistent values. The Polhemus uses a magnetic field to "map out" a rectilinear coordinate system within which coordinates are recorded. Since this magnetic field can become distorted (by the introduction of a metal object, for example) it is possible that measurements may be accurately recorded in one area of the digitizing field but not in another. This potential source of error can be assessed by determining the extent to which the digitizer records a given (standard) quantity consistently throughout the coordinate field. In order to test for spatial inconsistency, the digitizing field of the Polhemus was divided into eighteen 10 cm^3 volumes (three across [x axis], two from top to bottom [y axis], and three high [z axis]). A series of linear decimeter distances (from 0 to 10 cm along the acrylic ruler) was then digitized in each of the eighteen volumes. Linear measures were

Reproduced with permission of the copyright owner. Further reproduction prohibited without permission.

recorded along the ruler in three orientations: along the *x*, *y*, and *z* axes. Ten repeated measures, each 10 cm in length, were recorded for each orientation in each volume—a total of 540 linear measurements. To reduce the effects of intraobserver error the means of repeated measures were calculated and used for assessing spatial inconsistency among the eighteen field volumes. It was therefore assumed (conservatively so) that each of the 54 mean values (18 regions x 3 orientations) represents an accurate measurement of the distance between the 0 and 10 cm hatch marks on the ruler. Any differences among mean values are thus interpreted as being caused by distortions in the magnetic field within the digitizing space. This was assessed by calculating the deviation of each of the 54 mean values from the grand mean. Box 5.7 shows the distribution of these deviations in the 18 cubic sectors of the digitizing field.

Box 5.7. Field distortions in 18 sectors of the Polhemus 3DRAW digitizer (in cm).

Upper field level		
x=-0.0022 y=-0.0073 **z=0.0438**	x=-0.0149 y=-0.0089 z=-0.0017	x=-0.0278 y=-0.0180 z=0.0074
x=-0.0099 y=-0.0276 z=0.0026	x=-0.0037 y=-0.0293 z=-0.0027	x=-0.0152 y=-0.0212 z=0.0268
Middle field level		
x=0.0290 y=-0.0098 z=-0.0225	x=0.0076 y= -0.0070 z=0.0176	x=-0.0287 y=0.0016 **z=0.0406**
x=-0.0080 y=-0.0178 z=0.0127	x=0.0142 y=-0.0102 z=0.0189	x=-0.0145 y=-0.0162 **z=0.0762**
Lower field level		
x=0.0266 y=0.0289 z=0.0001	x=0.0187 y=0.0173 z=0.0147	x=-0.0194 y=-0.0079 **z=0.0666**
x=0.0247 y=0.0048 z=0.0048	x=0.0163 y=-0.0114 z=0.0122	x=0.0048 y=-0.0102 **z=0.0958**

Reproduced with permission of the copyright owner. Further reproduction prohibited without permission.

It can be seen, with reference to Box 5.7, that there are no field distortions greater than 0.3 mm in the entire digitizing space in either the *x* or *y* axes. However, in the *z* (vertical) axis, the lower left corner and the middle and upper levels of the right side of the digitizing field exhibit distortions above 0.3 mm. Avoiding the right side and the lower left corner of the digitizing platform, there is still adequate space in that part of the field that is relatively "undistorted" to fit even the largest of the specimens used in this study (e.g., gorillas, chimps, humans and baboons).

The Summagraphics digitizer uses an electrical grid that covers the surface of the tablet to delineate the coordinate system of the digitizing field. Physical distortions or inconsistencies in the grid can lead to spatially dependent measurement bias. As with the Polhemus, this potential source of bias was evaluated by dividing the surface of the digitizing field into sectors, in this case six 10 cm^2 areas (three across [*x* axis], and two from top to bottom [*y* axis]). Once again, ten repeated measures, each a decimeter in length, were recorded for each orientation in each area—a total of 120 linear measurements. The deviations of each of the 12 mean values from the grand mean is reported in Box 5.8. It can be seen that there are no significant areas of field distortion among the six sectors—the largest distortion is 0.08 mm, with the mean around 0.03 mm.

Box 5.8. Field distortions in 6 sectors of the Summagraphics digitizer (in cm)

x=-0.0048 y=-0.0058	x=0.0083 y=0.0063	x=-0.0032 y=-0.0005
x=0.0027 y=-0.0053	x=0.0011 y=0.0005	x=-0.0011 y=-0.0025

Reproduced with permission of the copyright owner. Further reproduction prohibited without permission.

There is yet one further issue related to accuracy that must be addressed—the question of whether the anatomical structures recorded on lateral radiographs are an accurate representation of those of the actual specimen. Due to the effects of projection distortion the answer to this question must be no. However, you may recall that the landmark configurations used to calculate morphometric variables were corrected for projection distortions, and these corrected configurations are thus expected to accurately depict the locations of anatomical landmarks in relation to the actual specimens. To test this postulate, linear distances were calculated between three pairs of homologous landmarks (prosthion-prosthion, bregma-bregma, and lambda-lambda) after GLS superimposition of endocranial-radiographic landmarks onto ectocranial specimen landmarks (see Box 5.2, protocol step #7). Observed linear distances represent same-specimen intralandmark deviations due to radiographic inaccuracies. They are reported for each specimen in Appendix H. The average deviation over all 300 specimens was as follows: prosthion, 0.18 mm; bregma, 0.48 mm; lambda, 0.48 mm. The combined mean of 0.38 mm is taken to represent the measurement error associated with inaccuracies of the radiographic technique

Precision

Another term for precision is repeatability. It is a measure of the degree of similarity of repeated measurements of the same quantity, and is usually given as a standard deviation or variance estimate. Corner *et al.* (1992) tested the precision of the Polhemus and reported that the standard deviation of repeated measures was rarely over 0.3 mm. This level of precision is consistent with the value listed on

Reproduced with permission of the copyright owner. Further reproduction prohibited without permission.

the Polhemus specification sheet for the 3DRAW.

The precision of the Polhemus 3DRAW and the Summagraphics digitizers was quantified in two ways: (1) by repeated measures of a standard scale, and (2) by repeated measures of a sample specimen.

Standard scale repeated measures. A standard decimeter scale (from 0 to 10 cm on an acrylic ruler) was repeatedly digitized and the resulting coordinates were used to calculated linear distances and the standard deviation of the repeated measures. The results, which have already been reported in Box 5.4, give the standard deviation of repeated decimeter measures for the Polhemus 3DRAW as 0.28 mm, and for the Summagraphics as 0.07 mm.

The greater precision of the Summagraphics digitizer does not imply that measurements based on endocranial midline landmarks taken from lateral radiographs are more precise than measurements based on ectocranial landmarks taken directly from the specimens. The precision with which each morphometric measurement can be taken will vary depending upon the difficulty involved in locating the landmarks that describe the particular measurement. For example, it is reasonable to assume that a variable such as lower nasal bone width [Y3-NASWDL] can be measured with greater precision than a measurement such as middle cranial fossa length [Y78-MCFLGT], simply due to the more difficult task of locating and digitizing the landmarks defining the latter.

Specimen variables repeated measures. The second approach used to quantify measurement precision was the most crucial, since it involved actual research data. A single specimen (*Pongo pygmaeus*, AMNH #200898) was selected from among the study sample and subjected to the entire data collection protocol 30

Reproduced with permission of the copyright owner. Further reproduction prohibited without permission.

times, producing 30 repeated measures of each morphometric variable in the study. Selected statistics for each variable are given in Box 5.10. The average standard deviation over all variables was 0.32 mm. But this overall standard deviation obscures some interesting patterns. Box 5.9 gives a breakdown of standard deviations by measurement type (linear distance, area, volume, index, percentage, or angle) and landmark source (ectocranial or endocranial-radiographic). It can be seen that for linear distances, indices and percentages standard deviations are all under 0.3 (somewhat less for endocranial-radiographic variables, perhaps reflecting the superior precision of the Summagraphics digitizer). Cube root volumes performed the worst, with standard deviations around 1.5 mm. The other two types of data, square root areas and angles, exhibited standard deviations of 0.3 or lower when variables were derived exclusively from ectocranial landmarks, but had standard deviations over 0.6 when at least some endocranial-radiographic landmarks were employed. It would appear from Box 5.9 that variables calculated from endocranial-radiographic landmarks exhibit higher standard deviations for areas and angles than do variables constructed from ectocranial landmarks. However, closer examination of the results indicates that of the nine variables yielding high standard deviations (i.e., above 0.5), eight of them involved measurements of the olfactory apparatus. When measurements of the olfactory apparatus were excluded, variables that derived from endocranial-radiographic landmarks showed higher precision than variables calculated exclusively from ectocranial landmarks.

Reproduced with permission of the copyright owner. Further reproduction prohibited without permission.

Box 5.9. Summary of average standard deviations for various types of data (number of variables in parenthesis).

	Variables that employ ectocranial landmarks only	Variables that employ endocranial-radiographic landmarks
Linear Distances (mm)	0.20 (33)	0.13 (2)
Areas (square root mm)	0.16 (2)	0.62 (1)
Volumes (cube root mm)	1.55 (1)	1.43 (1)
Indices, Percentages	0.27 (13)	0.13 (3)
Angles (degrees)	0.30 (6)	0.75 (8)
Weighted Mean	0.25	0.58

The relatively high standard deviations of the angular measures of the olfactory apparatus (ca. 0.75) are mostly due to the short lengths of the cribriform plate and olfactory bulbs. The one of the two lines forming these angles is defined by the anterior-most and posterior-most points of the cribriform plate (or olfactory bulb recess). Since these points are so close together, very small deviations in locating and digitizing them can translate into quite large deviations in calculating the angles. In fact, it is quite remarkable that the standard deviations are as low as they appear.

These data can also help determine how many repeated measures of each specimen should be taken. If the mean and standard deviation over the 30 repeated measures are taken to represent the true "population"[4] mean (μ) and standard deviation (σ), then these parameters can be used to determine the confidence intervals for repeated measures different n size. For example, the mean and standard deviation for nasal bone length [Y1-NASLGT] were 35.18 mm and 0.23 mm, respectively (Box 5.10). If only one measurement is taken of this trait there is a

[4] In this case the population refers to a given collection of repeated measures of a single specimen under varying conditions of temperature, humidity, etc.

Reproduced with permission of the copyright owner. Further reproduction prohibited without permission.

95% chance that this value will fall between plus or minus 0.45 mm of the mean, 35.18 mm; since:

$$P\ \{Y - 1.96\sigma / n^{.5} \leq \mu \geq Y + 1.96\sigma / n^{.5}\ \} = 0.95 \qquad (5.1)$$

Likewise, there is a 95% chance that the mean of two repeated measures of nasal bone length will fall between plus or minus 0.32 of the true mean; and a similar change that the mean of three repeated measures of this trait will fall within 0.26 of the parametric mean. Therefore, the data in Boxes 5.9 and 5.10 indicate that all traits based on linear distances computed from both ectocranial and endocranial landmarks, as well as estimated areas computed from ectocranial landmarks require only a single measurement per specimen to fall within ca ± 0.50 mm of the true mean. However, volumetric measures require about 30 repeated measures per specimen to establish the same level of confidence. Angles calculated from endocranial landmarks require 3 repeated measures to attain 95% confidence intervals within 1 degree of the mean. Based on the foregoing, linear distances were calculated from a single digitization of each specimen in the sample, whereas measurements taken from endocranial-radiographic landmarks were calculated from the mean of 3 repeated digitizations per specimen. Volumetric measures were computed from the same coordinate configurations (i.e., 1 ectocranial and the mean of 3 endocranial).

Reproduced with permission of the copyright owner. Further reproduction prohibited without permission.

Box 5.10. Selected statistics for repeated measures (n=30) on single specimen (in mm)

Variable	SDev	Mean	SE30	Variable	SDev	Mean	SE30
NASLGT	0.23	35.18	0.04	ORBTCR	0.34	43.52	0.06
NASWDU	0.19	2.29	0.03	IORBDS	0.15	8.20	0.03
NASWDL	0.10	7.71	0.02	BFPUI1	0.18	30.53	0.03
NPMWDT	0.19	9.76	0.03	BFPUI2	0.20	31.14	0.04
NSLAHT	0.17	28.47	0.03	BFPUP3	0.22	37.77	0.04
NSLAWD	0.25	27.85	0.05	BFPUP4	0.33	41.43	0.06
PNASHT	0.17	30.25	0.03	BFPUM1	0.34	45.98	0.06
PNASWD	0.20	21.61	0.04	BFPUM2	0.36	53.61	0.07
NLCLGT	0.23	32.51	0.04	BFPUM3	0.35	64.26	0.06
ZYGOHT	0.12	25.99	0.02	ANTBFM	0.19	30.83	0.03
BZYGWD	0.18	122.38	0.03	PSTBFM	0.30	48.62	0.05
APZYGR	0.22	40.04	0.04	RELBFM	0.23	63.41	0.04
MXARCL	0.25	74.30	0.05	MAXBFM	0.26	43.54	0.05
BMAXWD	0.16	91.71	0.03	LEVADV	0.32	39.64	0.06
UMAXWD	0.30	73.04	0.05	TEMPMM	0.19	63.90	0.03
AFACHT	0.28	94.49	0.05	RMMEFF	0.25	96.59	0.05
PFACHT	0.21	51.00	0.04	APFMAG	0.22	21.03	0.04
RAMSHT	0.20	39.88	0.04	SLOPFM	0.38	28.21	0.07
I2PALW	0.21	23.04	0.04	APOCND	0.22	21.03	0.04
P3PALW	0.14	34.00	0.02	CBFLEX	0.50	173.51	0.09
M1PALW	0.14	32.46	0.03	ENLWCP	1.91	88.77	0.35
M3PALW	0.15	30.68	0.03	ENLWOB	1.36	85.02	0.25
I2PALD	0.21	1.13	0.04	SLPCPF	1.92	38.82	0.35
P3PALD	0.25	11.44	0.05	SLPCPO	1.82	46.74	0.33
M1PALD	0.19	12.95	0.03	SLPOBF	1.36	35.08	0.25
M3PALD	0.14	13.24	0.02	SLPOBO	1.38	43.00	0.25
PALLGT	0.30	76.69	0.05	MCFLGT	0.20	33.66	0.04
PALTHK	0.18	4.78	0.03	ACFLGT	0.11	20.94	0.02
KROGAG	0.25	129.11	0.05	FMAGSZ	0.12	26.14	0.02
ENLOAG	0.15	133.74	0.03	CEPHID	0.19	91.08	0.03
SLOPOC	0.19	7.92	0.03	CANINE	1.55	3.75	0.28
FACSIZ	0.39	249.10	0.07	OFBVOL	2.48	8.26	0.45
ORBIHT	0.18	37.38	0.03	OFBARE	1.07	5.83	0.20
CRLGTH	0.22	194.02	0.04	ORBSCR	0.37	13.26	0.07
NCLGTH	0.19	122.67	0.03				
BIPORB	0.25	104.45	0.05				
SKCNTR	0.32	634.62	0.06				
CRBTHK	0.14	2.40	0.03				

Reproduced with permission of the copyright owner. Further reproduction prohibited without permission.

Conclusions

The total measurement error for variables deriving from endocranial-radiographic landmarks can be calculated by taking the square root of the error variances contributed by radiographic inaccuracies (s=0.38 mm), measurement imprecision (s=0.13 mm), and measurement inaccuracies of the Summagraphics digitizer (s=0.03 mm). The total expected measurement error (for linear distances) for endocranial variables is thus: $(0.38^2 + 0.13^2 + 0.03^2)^{.5} = 0.40$ mm. For variables derived from ectocranially digitized landmarks, the total measurement error is the combined error due to potential inaccuracies (s=0.3 mm) and imprecision exhibited by the Polhemus 3DRAW digitizer (s=0.26 mm)—$(0.30^2 + 0.26^2)^{.5} =$ 0.40 mm. A reasonable estimate for the smallest statistically detectable measurement, overall, is therefore about 0.5 mm. In this particular case, the conventional rule-of-thumb method described by Sokal and Rohlf (1995) for determining the "smallest detectable difference" and the "acceptable" level of measurement error gave a similar solution to the more empirically-based method conducted here, although this need not have been the case. Repeated measures analysis of a single specimen yielded similar results, with the caveat that volumetric variables, angular variables calculated from endocranial-radiographic landmarks, and variables involving the olfactory apparatus may exhibit higher levels of measurement error.

Reproduced with permission of the copyright owner. Further reproduction prohibited without permission.

PART III

Analytical Framework

Reproduced with permission of the copyright owner. Further reproduction prohibited without permission.

Chapter 6. Phylogenetic Effects: Methods

> *We may falsely attribute to correlation of growth, structures which are common to whole groups of species, and which in truth are simply due to inheritance.*
>
> Darwin, 1859:141

Introduction

I cannot emphasize enough how pivotal the topic of phylogenetic effects is to the further integration of theory and method and to the substantive meaning of the research results that follow. I am about to transform the entire data set using methods that were unknown to comparative biologists only a few years ago. Many of the properties of these methods are still being described, developed, debated, or remain entirely unknown. In fact, several researchers have had the veracity to admit in print that they were not quite sure what the newly transformed data really mean (e.g., Martins & Garland, 1991). And yet, as I will demonstrate in the next section, not to apply any of these methods surely means that no further progress can be made using the synchronic comparative approach. We will have run into a brick wall. In order to elucidate the nomological processes responsible for nasomaxillary variation among extant anthropoids, the phylogeny of this group *must* be taken into account.

The obstacle I faced when I began investigating this issue was that none of the currently available methods were, in my opinion, adequately developed or tested to use "off the shelf," so to speak. Moreover, I found that much of the theoretical framework upon which these methods were built and almost the entire accompanying literature on "phylogenetic versus adaptive effects" was conceptually flawed. I therefore set out to examine these methods from both a conceptual and methodological perspective. I begin with a description of the problem that these

Reproduced with permission of the copyright owner. Further reproduction prohibited without permission.

methods address, then describe several of the more popular methods, and finally evaluate each based on their theoretical significance and practical value.

The Problem of Nonindependence in Comparative Analysis

Perhaps the best way to understand the nonindependence problem in comparative analysis is to compare it with experimental analysis. Experimentation is a powerful analytical technique capable of isolating the effects of at least *some* nomological processes on morphological variation. In Chapter 2, I summarized numerous experiments that demonstrated the effects of mastication, locomotion, ocular growth, and other nomological agents on craniofacial form (see Box 2.4). Under *optimum* circumstances experiments are designed so that each individual subject is identical to the others except with regard to the independent variable whose effect on the dependent variable is under study. In this way Bouvier and Zimny (1987) used genetically identical rats (a strain of clones) to isolate the effects of dietary variation on craniofacial form. In this design each subject in the experiment is regarded as an *independent* trial. Each dependent variate (e.g. craniofacial form of subject after being fed a given diet) represents an outcome dependent only on the independent variable, and *independent* of all other trials.

In a synchronic comparative design individuals (or other units of analysis such as species means) cannot be regarded as independent because of their shared common ancestry. Morphological variation will be clustered in accordance with a hierarchically structured phylogeny. Whereas in experimental designs similarities and differences of the dependent variable must be due to the effects of the independent variable, in a synchronic comparative design variation in the dependent

Reproduced with permission of the copyright owner. Further reproduction prohibited without permission.

variable may be due to common ancestry as well as the effects of the independent variable. This creates a serious analytical problem because statistical analyses estimating the association between traits assume that the data points are independent. Nonindependence of data points leads to an overestimation of the degrees of freedom in statistical tests, and, as a consequence, an increase in the Type I error rate (Ridley, 1983; Clutton-Brock & Harvey, 1984).

As Felsenstein (1985) has noted, a worst case scenario is when two or more traits appear to covary in a large number of species or individuals, when in fact this covariance can be traced back to only two ancestral lineages, each at the root of a monophyletic group. To illustrate this phenomenon, consider the continuous traits *maximum potential bite force at* M^1 [Y54-BFPUM1] and *slope of the olfactory bulbs relative to the occlusal plane* [Y77-SLPOBO] in catarrhines. When individual data points for these two traits are plotted, as shown in Box 6.1, a negative relationship can be detected (r=-0.29, p=.0001).

Box 6.1. Scatter plot of two traits in 177 catarrhines.

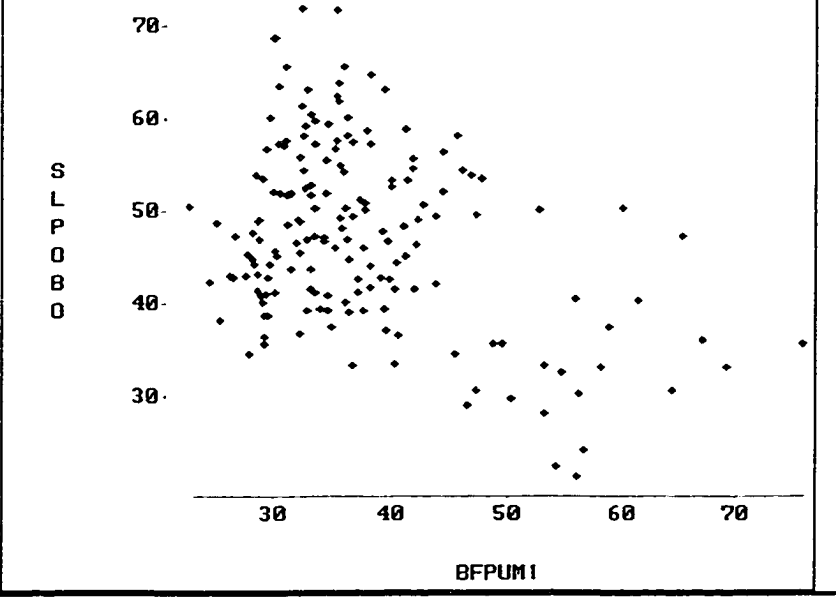

Reproduced with permission of the copyright owner. Further reproduction prohibited without permission.

If species means (n=24) are used as data points the correlation coefficient between BFPUM1 and SLPOBO is even greater (r=-0.55, p=.008). The same scatter plot is shown in Box 6.2, but this time with distinct markers identifying cercopithecoid (+) and hominoid (■) specimens. It can be seen that nearly all of the cercopithecoid specimens lie in the upper left sector of the plot whereas the hominoid specimens occupy the lower right sector. The significant correlation observed among individuals (or among species) with regard to the two traits is an artifact of the covariance between the traits at the superfamily level. There are neither 177 nor 24 independent data points represented on this scatter plot, but in fact two. Since n=2, the between-superfamily correlation cannot be tested for significance. Within each superfamily the correlation between the two traits is not significant (Cercopithecoidea: r=0.12, p=.16; Hominoidea: r=-0.009, p=.96).

Box 6.2. Same scatter plot as shown in Box 6.1, but with distinct markers for cercopithecoid and hominoid specimens.

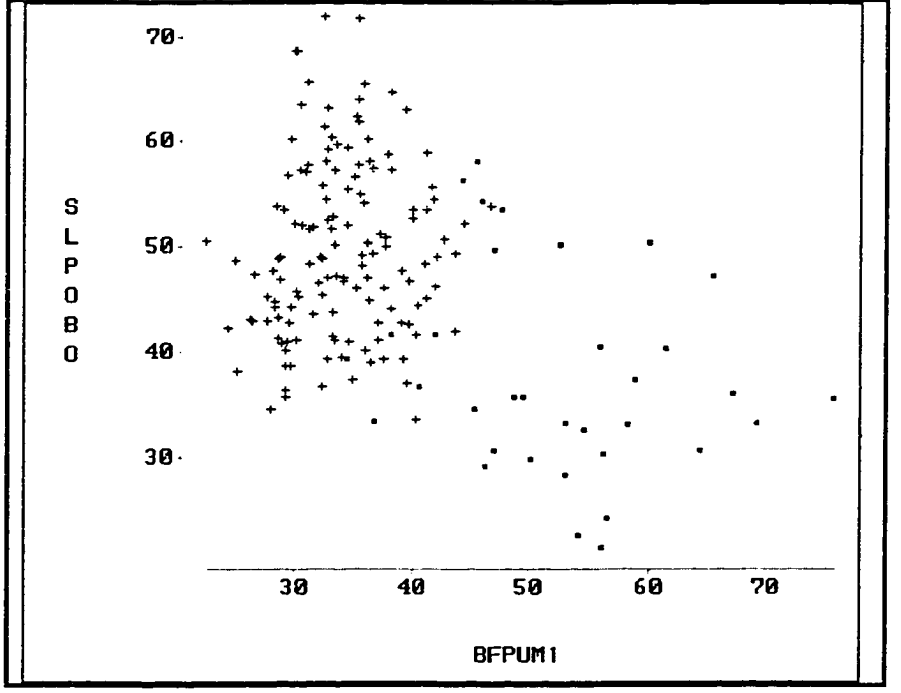

Reproduced with permission of the copyright owner. Further reproduction prohibited without permission.

In this example, an analysis using individuals or species means as data points led to a Type I error (rejection of the null hypothesis when it is true). While this case is an extreme example, it can be shown quantitatively that a shared phylogenetic topology among members of a taxon is sufficient to significantly increase the correlation among traits *even in the absence of any coadaptational effects*. To quantify this and other aspects of phylogenetic effects on the distribution and covariation of continuous traits I programmed a computer model to simulate the effects of phylogenetic topology, directional selection and random fluctuations on a set of hypothetical continuous traits.

Computer Simulated Phylogenies using *PHYLOMOD*

I wrote a customized phylogenetic simulation program (which I call *PHYLOMOD*) in SAS/IML (Interactive Matrix Language) because existing computer programs developed for this purpose were either unsuitable or unavailable.[1] Moreover, none of the previous simulation studies (e.g. Grafen, 1989; Rohlf *et al.*, 1990; Martins & Garland, 1991; Gittleman & Luh, 1992; Purvis *et al.*, 1994; Martins, 1996) that have examined the quantitative properties of phylogenetic effects on character distribution and covariation precisely conform to the theoretical and operational framework established in the previous chapters. A brief description of *PHYLOMOD* follows.

Each simulated phylogeny begins with a common ancestor, designated S_1 (Species 1), whose phenotypic trait value (Y) is 100 at T_0 (time zero). S_1 bifurcates into two new lineages, the vertical lengths of which are selected at

[1] The program is not included in an appendix because of its ungainly size (22,142 lines of code), but it can be furnished upon request.

Reproduced with permission of the copyright owner. Further reproduction prohibited without permission.

random from a range of between 3 to 6 time units. A uniform selective effect is assigned to each lineage equal to the length of the lineage multiplied by either -1 (negative directional selection), 0 (stabilizing selection), or +1 (positive directional selection). This uniform change per time unit value is also selected at random. In addition, a random fluctuation value is assigned (again, either -1, 0, or +1) for each time unit traversed by a lineage.[2] These three parameters—lineage length, uniform selectional change, and random fluctuation—combine to determine the value of Y for S_2 (the descendent of S_1). For example, if the length of a lineage derived from the common ancestor is randomly selected to be 5 time units, and the uniform value is +1, then the total *selective* change over the lineage will be equal to +5. If, over this same lineage, the random fluctuation values are +1, -1, 0, 0, -1, then the total change (selective and random) over the lineage will be +4 (5+1-1+0+0-1=4). Recall that the common ancestor began with a phenotypic trait value of 100. The descendent species S_2, located at the tip of the lineage just described, will exhibit a trait value of 104 (see S_1 and S_2 in Box 6.3). Each descendent species undergoes a similar bifurcation leading to the evolution of two more new lineages. The length and phenotypic change characterizing each lineage is determined following the same rules outlined above. Thus, ancestral lineages have no influence on the length or direction of descendent lineages. All lineages reach the present at T_{20}. The phenotypic values for trait Y exhibited by those species that reach T_{20} represent the measurements of trait Y taken from the extant members of the clade. Box 6.3 displays a simulated phylogeny generated in the

[2] In other phylogenetic simulations this type of random modification is referred to as a Brownian motion model of evolutionary change.

Reproduced with permission of the copyright owner. Further reproduction prohibited without permission.

manner described above.

To test the effects of a common tree topology (i.e., nonindependence) on trait covariance, the evolution of three traits (Y_1, Y_2, Y_3) was simulated for each phylogeny. *Each of the three traits follows an identical tree topology.*

Box 6.3. Multi-level Simulated Phylogeny. Trait Y_3. Tree Topology (Seed) 5. Selective Effect 5B. Random Effect 5C

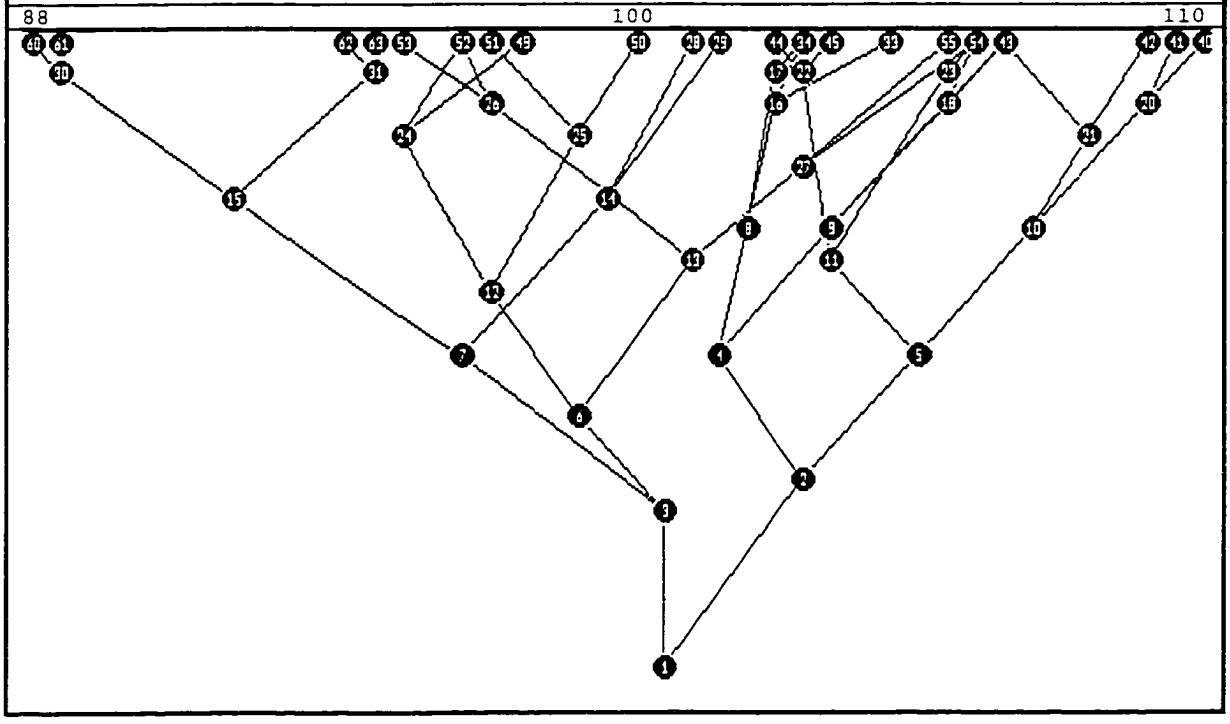

This is perhaps best visualized as the simultaneous evolution of the three traits over the course of a single "unfolding" phylogeny. The relational properties among traits Y_1, Y_2 and Y_3 with regard to tree topology and the two other model parameters are summarized in Box 6.4.

Box 6.4 Model parameters used for each trait in a given simulation

Model parameter/Trait	Trait Y_1	Trait Y_2	Trait Y_3
Tree Topology	A	A	A
Selective (Uniform) Effect	A	B	B
Random Effect	A	B	C

The pattern of selective change among the traits was established in order to

Reproduced with permission of the copyright owner. Further reproduction prohibited without permission.

compare coadaptational versus non-coadaptational relationships. For example, in each phylogenetic run, the uniform selective changes assigned to trait Y_1 were independent of those assigned to traits Y_2 and Y_3 (i.e., Y_1 has no coadaptational relationship with either Y_2 and Y_3). By contrast, traits Y_2 and Y_3 were assigned the same uniform selective changes along each of the lineages in the phylogeny (i.e., these traits exhibit a coadaptational relationship). Random fluctuations in all cases were assigned independently to each of the three traits. Without this random fluctuation, traits Y_2 and Y_3 would always be perfectly correlated (r=1.0) due to the identical selective effects operating on each.

For baseline comparison, I also ran single-level phylogenies for two continuous traits (K_1, K_2). In these simulations, the values of the two traits—K_1, K_2—were determined independently (i.e., they were assigned independent selective and random modification values). The subsequent (independent) relationship between K_1 and K_2 at T_{20} is analogous to the relationship between Y_1 and Y_2 or Y_1 and Y_3, with the exception that in the single-level phylogenies all of the species to reach T_{20} share a single most recent common ancestor (see Box 6.5).

Box 6.5: Single-level simulated phylogeny

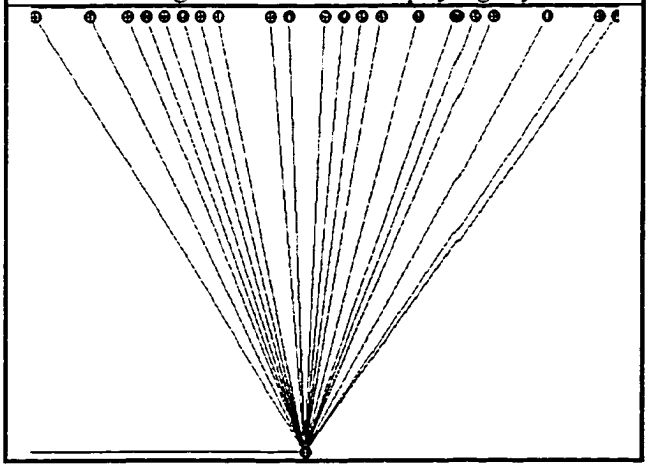

Reproduced with permission of the copyright owner. Further reproduction prohibited without permission.

The maximum attainable deviation from the ancestral morphotype of 100 in both the multi-level and single-level phylogenies is 40 (with a possible range of between 60 to 140). This maximum could only be reached if at each of the 20 time units the selective and random changes always went in one direction, negative or positive.

The 3 multi-level simulated trait vectors (Y_1 , Y_2 , and Y_3) and the 2 single-level simulated trait vectors (K_1 and K_2) that were produced each time the program was run were based on a series of random numbers generated using the SAS RANUNI random number generator function. This function requires a "seed" number that determines the sequence of random numbers subsequently applied to the simulation algorithms. The simulation program was run 400 times, beginning with seed number 1 and running sequentially to seed number 400. It was thus possible to "re-run" any given phylogeny by re-setting the appropriate seed value.

Properties of Computer Simulated Phylogenetic Effects

Let us now return to the nonindependence problem in comparative analysis. It should be clear that the single-level phylogeny, as illustrated in Box 6.5, is analogous to an experimental design. At the moment of multifurcation each new species (or individual) is (statistically) identical with regard to trait Y. We could, theoretically, separate these subjects into two or more groups and observe the effects of various assigned treatments, as in an experimental design. In the computer simulation each lineage is subjected to a unique selective and random "treatment" that determines its Y value at T_{20}. In this manner each variate of Y in a single-level phylogeny at T_{20} represents an independent data point. It should

Reproduced with permission of the copyright owner. Further reproduction prohibited without permission.

also be obvious that the variates of Y at T_{20} in the multi-level phylogenies (see Box 6.3) do not represent independent data points, due to the hierarchical structure of their ancestry.

To test whether a multi-level branching topology alone, for a pair of traits, can affect the strength of the covariance between them and lead to an increase in Type I error, I compared the correlation coefficients (and associated *p*-values) of trait vectors produced by a series of single-level phylogenies with those produced by multi-level phylogenies. It can be shown that the bivariate distribution of the trait vectors produced by both the multi-level phylogenies (Y_1, Y_2, Y_3) and the single-level phylogenies (K_1, K_2) is Gaussian, with a mean correlation coefficient of zero. Box 6.6 shows the univariate distribution of Y_1 over the 400 simulated phylogenies. Box 6.7 shows that the mean correlation coefficients for both the multi-level and the single-level phylogenies are covered by their respective 95% confidence intervals, as is the value of zero. In this regard the simulated data conform to theoretical expectations.

Box 6.6. Distribution of Y_1 over 400 simulated phylogenies

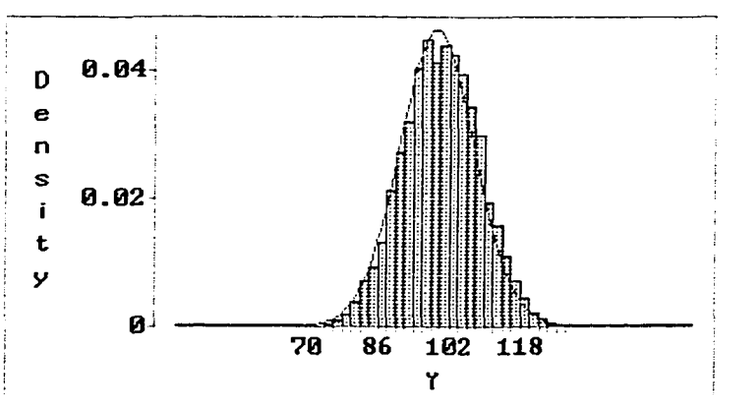

Reproduced with permission of the copyright owner. Further reproduction prohibited without permission.

The null hypothesis is that the Type I error rate (at α .05) for both the multi-level selectively independent trait pairs (Y_1 with Y_2, and Y_1 with Y_3) and the single-level selectively independent trait pairs (K_1 with K_2) will not be significantly different from .05. The simulation results confirm a significant increase in the Type I error rate—29.4%—in the multi-level phylogenies, which is greater than the error rate expected by chance alone (5%). Martins (1996) found a similar Type I error rate (31.4%) for simulated "raw species data" over a series of 15 and 42 species phylogenies. The Type I error rate for the trait vectors of the single-level phylogenies was 5.3%, not significantly different from that expected by chance.

Box 6.7: Parameter Estimations and Significance Test Predictions (Error Rate) Associated with Correlation Coefficients for Phylogenies with Independent and Nonindependent Data Points

Phylogeny Type/Parameter	Mean	Standard Error of Mean	95% Confidence Intervals for Mean	Type I Error Rate at 5% Significance Level
Single-level phylogenies (independent data points)	-0.0115	0.01	-0.032 to 0.008	5.3%
Multi-level phylogenies (nonindependent data points)	0.0114	0.016	-0.021 to 0.044	29.4%

The effect that multi-level topologies (and concomitantly, nonindependence of data points) have on the covariance between pairs of traits that are *selectively independent* can be seen by comparing the histograms displayed in Box 6.8. The left histogram plots the density of *p*-values for the correlation coefficients between traits Y_4 and Y_5 (single-level topology) and shows a nearly uniform distribution, as expected. The remaining histograms plot the density of *p*-values for traits Y_1 and Y_2 (middle) and Y_1 and Y_3 (right), and show a marked increase towards the lower values of *p* (reflecting an increase in the Type I error rate). All but 5 of the 400 correlations

Reproduced with permission of the copyright owner. Further reproduction prohibited without permission.

between Y_2 and Y_3 (the coadaptive traits) were significant at the 5% level.

Box 6.8: Histograms of the *p*-values of *r* for different phylogenies (see text for details)..

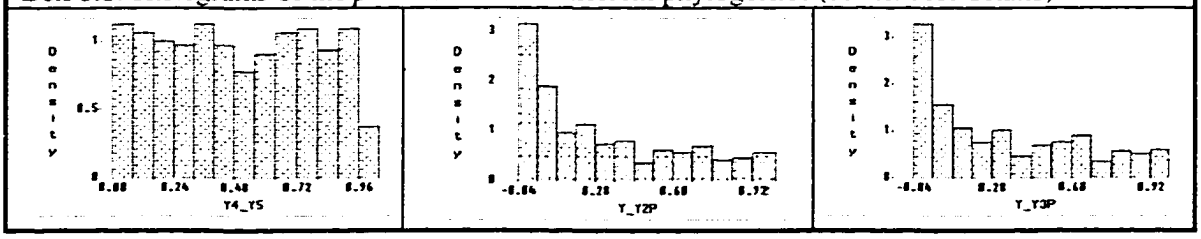

PHYLOMOD is an improvement over existing computer simulations in a number of respects. One major refinement is that the multi-level tree topology is free to vary for each simulated phylogeny. In previously published simulations the branching pattern of the phylogenies was set in advance, so only a few different topologies could be compared (e.g., Martins & Garland, 1991; Martins, 1996). As a consequence of the independently varying lengths of each of the node-to-node lineages in *PHYLOMOD* the number of lineages to reach the "present" (T_{20}) also varies from phylogeny to phylogeny. In a given phylogeny, some lineages may not reach T_{20} at all, while others may reach T_{20} before the 5th (and last) speciation event. These two model parameters simulate the evolutionary processes of extinction and asymmetrical speciation rates, respectively. Each phylogeny will thus produce a given "sample size" of between 0 to 32 species. However, since the probability of extinction is only 12%, most phylogenies will generate a sample size in the higher part of this range. The range of *n* for the 400 simulated phylogenies was between 17 and 32, with a median of 27.

As predicted by statistical theory, Type I error rates do not appear to be influenced by sample size. For example, no significant association was found between the *p*-values of the correlation coefficients for Y_1 and Y_2 and *n* over the

Reproduced with permission of the copyright owner. Further reproduction prohibited without permission.

400 simulated phylogenies; nor was there any pattern in Type I error rates among the *n*'s. This demonstrates that small sample sizes are no more or less likely to exhibit Type I error due to nonindependence of data points than are large sample sizes (at least within the range tested).

Methods Proposed to Solve the Nonindependence Problem

A variety of approaches have been advanced to solve the nonindependence problem in comparative biology—the so-called "nonindependence methods." These can be categorized into four main classes of methods: (1) higher taxonomic comparisons, (2) independent contrasts, (3) nested analysis of variance and covariance, and (4) autoregression. All possess limitations. The best one can do is to choose a method that is most compatible with the theoretical and operational framework of his or her research. Although I will focus mainly on the latter two of these classes, it will be instructive to give a brief account of the first two. For a more comprehensive review of these methods see Huey (1987), Pagel and Harvey (1988), Harvey and Pagel (1991), and Brooks and McLennan (1991).

Higher Taxonomic Comparisons

Clutton-Brock and Harvey (1977, 1984; Harvey & Clutton-Brock, 1985) were the first to propose the use of higher level taxonomic means as data points to avoid the problem of overestimation of the degrees of freedom in statistical tests. In an investigation of life-history variables among 135 species of primates, they used subfamily means as the units of analysis, remarking that "If analyses are performed at a lower level than the subfamily (the genus or the species), the sample size is increased but very little extra information in incorporated" (Harvey & Clutton-

Reproduced with permission of the copyright owner. Further reproduction prohibited without permission.

Brock, 1985:567). To identify the taxonomic level appropriate for analysis they employed a nested ANOVA and selected the level that contributed the greatest degree of variance to the dependent variable. One obvious difficulty with this method is that the greatest degree of variance may reside at different levels for different variables (Ridley, 1983). This is, in fact, a special case of a more general problem common to many nonindependence methods: the comparison among groups of different rank. I refer to this as the "cross-level comparison" problem.

Moreover, these authors and others who have followed their lead (e.g. Martin, 1979; Baker & Parker, 1979; Harvey & Mace, 1982; Ridley, 1983; Stearns, 1984; Dunham & Miles, 1985) appear to have been unaware of an entire body of statistical theory in the biomedical and behavioral sciences dealing with multi-level analysis (*cf.* Burstein, 1978; Roberts & Burstein, 1980; or for a recent review, Bryk & Raudenbush, 1992) and cross-level inference (Hannan & Burstein, 1974; Langbein & Lichtman, 1978; Kreft *et al.*, 1995). This work has shown that it is insufficient merely to isolate the group level at which most of the overall variance is accounted for. With hierarchically structured data, between-group analysis at one level is equivalent to the analysis of the pooled within-group data at a higher level. It has been shown that correlation and regression statistics using pooled within-group data is meaningful only when the separate regression slopes within each group do not significantly differ. Furthermore, it has been shown that using group means to make inferences about individual level properties renders misleading interpretations. Specifically, "[w]hen groups are formed on the basis of individuals' scores on the independent variable... using between-groups

Reproduced with permission of the copyright owner. Further reproduction prohibited without permission.

correlation to make inferences about individuals will be biased" (Pedhazur, 1997:685).

A variant of the higher-taxonomic comparisons method was devised by Ridley (1983) for discrete data. His method, referred to as the parsimony method, is based on the idea that the degrees of freedom in statistical tests should equal the number of independent origins of the character states of a given trait (Gittleman, 1981). Therefore, instead of using a nested ANOVA to identify the appropriate level for analysis, he applied cladistic methods to sort taxa into groups based on the shared derived condition of the dependent variable. Aside from the problems inherent in the principle of parsimony (*cf.* Camin & Sokal, 1965; Sober, 1988), Ridley's method embodies several critical flaws. First, clades whose members share a derived homology may be rooted at any level in the phylogeny, and we again run into the cross-level comparison problem. This renders the substantive interpretation of results difficult, at best. Second, the claim that "Ridley eliminates the effect of ancestry by his grouping procedure..." (Bell, 1989:554) is unwarranted. No account is taken of the potential influence of higher level ancestral effects. For example, consider the scenario in which the derived character states A, B and C arose as "independent" origins at the roots of clades 1, 2, and 3, respectively. If clades 1 and 2 share an immediate common ancestor not shared by clade 3, then character states A and B will have evolved from the same ancestral morphotype (under the same potential constraints) whereas character state C will have evolved from a different ancestral morphotype. Under such circumstances Ridley's data points are *not* independent. In all fairness, this problem is not unique to Ridley's method, but the parsimony approach accentuates

Reproduced with permission of the copyright owner. Further reproduction prohibited without permission.

the problem due to the extremes of rank designation permitted in the units of analysis.

It should be obvious from the foregoing discussion that higher taxonomic comparison methods are inadequate to deal with the problem of nonindependence in comparative biology. I now turn to a different approach that has received much attention in the recent literature.

The Method of Independent Contrasts

The conventional way of dealing with the problem of phylogenetic effects is to limit the comparison to pairs of sister taxa that are similar with respect to the variables the researcher wishes to control, but different in terms of the predictor variable whose effect is being studied (*cf.* Fleagle, 1977; Ward & Sussman, 1979). In an analysis of locomotor behavior and muscular anatomy in sister taxa of the genus *Presbytis*, Fleagle (1977) stated:

> Closely related animals with different behavior repertoires provide a natural experiment for the study of associations between behavior and morphology (e.g., Jolly and Gorton, '74: p. 814). Analysis of closely related, but behaviorally diverse species of a single genus gives a comparative perspective with the greatest possible control over phylogenetic heritage. [Fleagle, 1977:297]

Notice that this is actually a variant of Ridley's method applied at the alpha taxonomic level. Differences between sister taxa must represent instances of "independent" origins. But whereas the parsimony method compares groups of different rank, Fleagle's approach compares taxa at the same level. However, this method is weakened by the small number of species that share an immediate ancestor—usually two. The lack of statistical power inherent in this approach

Reproduced with permission of the copyright owner. Further reproduction prohibited without permission.

(n=2) is customarily compensated for by a more in-depth examination of the causal relations underlying the behavioral and morphological differences between species (e.g. Ward & Sussman, 1979). However, broad cross-taxonomic comparative analyses and narrower organism-centered analyses should not be thought of as competing approaches, but as complementary ones.

An extension of the conventional sister-taxon method was developed by Felsenstein (1985) to add statistical power to the approach while retaining its logical advantages. Felsenstein's method, known as the method of independent contrasts, uses the *difference* between trait values of sister taxa as data points in an analysis (also see Pagel, 1992). A major advantage of this method is that, unlike most other methods, no assumptions need to be made about the ancestral morphotypes below the species level (for example, using mean values of higher taxonomic groups). This effectively reduces one source of "measurement error" in the variables and should result in a decreased Type II error rate (i.e., increased statistical power). This prediction was confirmed in simulation studies conducted by Martin and Garland (1991), who found that the independent contrasts method had the lowest Type II error rates of any of the major nonindependence methods. Felsenstein's method has been acknowledged as one of the most statistically powerful and logically elegant methods to deal with the problem of nonindependence of data points (Harvey & Pagel, 1991). However, the method also suffers from some serious drawbacks. Because *differences* between species pairs are used as variates, the effective sample size (effective n) is one-half of that available with most other methods. To compensate for the small n, Felsenstein recommended enumerating contrasts between nodes at various levels of the

Reproduced with permission of the copyright owner. Further reproduction prohibited without permission.

phylogeny, not just among the branch tips. But in so doing, he unwittingly opened a Pandora's box of methodological problems. It not only required a complete knowledge of the ancestral morphotypes at each of the branch nodes (effectively eliminating one of the main advantages of the method) (Gittleman & Kot, 1990), but also fortuitously assumed a strictly symmetrical topology. When asymmetrical phylogenies are encountered "...comparisons are inevitably made between taxa of very different rank, with one datum representing a single species and another being the average of a whole family" (Bell, 1989:554). The cross-level comparison problem was thus let out of the box. Another major problem with Felsenstein's method is that the results, having been obtained from deviation variates, are difficult to interpret. One can say nothing about individuals, species, lineages or groups in comparison to others, since the variates have been displaced from the original units of analysis.

Nested Analysis of Variance and Covariance

Both the nested ANOVA method and the autoregression method (next section) are based on a common approach. Both methods attempt to partition the variance of a given trait Y into a "phylogenetic" component and a "nonphylogenetic" component. The effects of phylogeny can then be removed from the data, and analyses can proceed on the remaining "phylogenetic-free" component.

The nested ANOVA method takes advantage of the fact that the total variance of a given trait Y (s^2_{tY}) can be partitioned, at any level of the hierarchy, into the pooled within-group variance (s^2_{wY}) and the between-group variance (s^2_{bY}). Bell (1989), following methods established in quantitative genetics (*cf.* Lush, 1949; Roberts, 1967), proposed that the between-group variance at a given

Reproduced with permission of the copyright owner. Further reproduction prohibited without permission.

level is attributable to ancestry (=genetic component of quantitative genetics), whereas the pooled within-groups component is a measure of the variance due to function (=environmental component). The total phenotypic covariance between two traits, Y and X (s^2_{pYX}), can likewise be partitioned into genetic (s^2_{gYX}) and environmental (s^2_{eYX}) components. Once this is done it is a trivial matter to calculate the correlation or regression coefficient between the "environmental" components of traits Y and X:

$$r_{eYX} = s_{eYX} / (s^2_{eY} \; s^2_{eX})^{1/2} \quad (6.1)$$

$$b_{eYX} = s_{eYX} / s^2_{eX} \quad (6.2)$$

According to Bell, these coefficients measure the strength of association between traits Y and X due to "...the acquisition of adaptation through natural selection independent of ancestry" (Bell, 1989:562).

Phylogenetic Autoregression

A second approach to partitioning the total variance of a given trait Y into phylogenetic and nonphylogenetic components was advanced by Cheverud, Dow and Leutenegger (1985). Their method derives from a technique known as spatial autocorrelation, developed a decade earlier in the field of biogeography (*cf.* Cliff & Ord, 1973; Ord, 1975). Spatial autocorrelation attempts to measure effects that vary with distance. Cheverud, Dow and Leutenegger simply replaced spatial distance with genealogical distance among the species of a sample. Their method estimates the value of Y for species *j* as the weighted mean of all species (*j..n*) in the sample weighted by their genealogical distance to species *j*. The procedure thus requires the use of a weight matrix (W) stipulating the degree of relatedness among all pairs of

Reproduced with permission of the copyright owner. Further reproduction prohibited without permission.

species in the sample. The predicted Y produced by this formulation (Y'_j) represents the value of Y_j predicted from the phylogenetic structure underlying the sample. The procedure is repeated for all elements of vector $Y_{j..n}$. yielding $Y'_{j..n}$. This can be expressed in matrix notation as WY. According to Cheverud *et al.* (1985), the vector WY represents the phylogenetic value or component of $Y_{j..n}$, and the residuals (ϵ) of the regression of Y on WY represent the nonphylogenetic, or "specific," component. The complete regression equation is:

$$Y = \rho WY + \epsilon \qquad (6.3)$$

Since both Y and WY are on the same scale the intercept term is always zero. Y and WY are also standardized, which means that the square of the coefficient ρ is a measure of the proportion of the variance of Y accounted for by phylogeny (i.e., WY). This is true even though a maximum-likelihood (ML) procedure is used to estimate the regression slope because the dependent variable approximates a normal distribution (Sokal & Rohlf, 1995; this study, Chapter 8). The maximum-likelihood method is preferred because it yields asymptotically unbiased estimates (Eliason, 1993), and has been shown to be superior to other estimation methods when samples are small (Aneslin, 1982). According to Cheverud *et al.*(1985:1337), the specific component (ϵ_j) of Y_j represents "...the adaptation of a given species, independent of all other related species." Thus by removing WY from Y independence is restored to the data set in the form of the residual vector (ϵ). The residuals of any number of traits can be obtained using equation (6.3), and the covariance between residuals is said to measure the association between traits with the effects of phylogeny removed.

The W matrix in equation (6.3) can be constructed using any one of several

Reproduced with permission of the copyright owner. Further reproduction prohibited without permission.

different types of relatedness data. These can be grouped into two main categories: (1) taxonomic affinity data (or "rank-based" data), and (2) phylogenetic relatedness data (or "divergence-based" data). Taxonomic affinity data can be extracted from an inclusive hierarchical classification of the taxon under study. In their worked example, Cheverud *et al.* (1985) assigned the value 1 to congeneric species, and the values 0.5, 0.33, 0.25, 0.2, and 0.167 to pairs of species related at the family, superfamily, infraordinal, subordinal and ordinal levels, respectively. As these authors readily admitted, and others have reiterated, a "...classification system is not sufficiently detailed to show all of the structure in the phylogeny... The phylogenetic meaning of a given category varies from group to group: the insect genus *Drosophila* is thought to be as old as the mammalian order Primates" (Felsenstein, 1985:7). This is, in fact, another instance of the cross-level problem, although this time not involving comparisons but rather the unbalanced weightings of the W matrix. In other words, pairs of species that have different degrees of relatedness may be assigned equal weightings

Cross-level weightings are effectively eliminated with the use of phylogenetic relatedness data for the elements of the W matrix. Molecular genetic distances (e.g., sequence similarities, DNA hybridization) have been proposed as one source of phylogenetic relatedness (Cheverud *et al.*, 1985; Felsenstein, 1985: Gittleman & Kot, 1990), as have divergence distances (Lynch, 1991). However, these data are not always available for a given clade. Of all of the nonindependence methods described, the autoregression method has received the most attention in recent years.

Reproduced with permission of the copyright owner. Further reproduction prohibited without permission.

The Meaning of Phylogenetic and Nonphylogenetic Effects

At this point I think it imperative to step back and examine the *meaning* of what has been referred to as the "phylogenetic" and "nonphylogenetic" effects on the variance of a trait, or on the covariance between traits. The influence of the "phylogenetic" component has been described as, or described to include "...phylogenetic heritage" (Gittleman & Kot, 1990:227), "...phylogenetic inertia" (Felsenstein, 1985:6), "...phylogenetic burden" (Cheverud *et al.*, 1985:1341), "...phylogenetic constraint" (Cheverud *et al.*, 1985:1335), "...not evidence for phylogenetic constraint" (Bell, 1989:567), "...common inheritance" (Pagel & Harvey, 1988:415), "...common ancestry" (Pagel & Harvey, 1988:415), "...differences among ancestors" (Bell, 1989:570), "...microevolutionary" (Martins, 1996:1751), "...macroevolutionary" (Lynch, 1991:1065), and "..the influence of some hypothetical set of ancestral species" (Cheverud *et al.*, 1985:1337).

The so-called "nonphylogenetic" component has likewise been attributed to a hodgepodge of causes and consequences, including: "evolutionary change" (Pagel & Harvey, 1988), "evolutionary changes weighted... by the length of the branches" (Martins, 1996:1754), "evolutionary, ecological, or environmental... effects" (Gittleman & Kot, 1990:231), "natural selection in the current environment" (Felsenstein, 1985:6), "the acquisition of adaptation through natural selection independent of ancestry" (Bell, 1989:562), the "adaptive" component (Gittleman & Kot, 1990:238), "nonadaptive, evolutionary forces" (Cheverud *et al.*, 1985:1337), "functional effects" (Pagel & Harvey, 1988:430), "effects...attributable to function" (Bell, 1989:569), "habitus" (Cheverud *et al.*, 1985:1337), "genetic drift" (Cheverud *et al.*, 1985:1337), "random genetic drift of genes with pleiotropic effects" (Lynch,

Reproduced with permission of the copyright owner. Further reproduction prohibited without permission.

1991:1079), "passive changes in one variable owing to selection on another" (Pagel & Harvey, 1988:414), "variance component generated during the divergence of species within genera" (Bell, 1989:565), "specific effects" (Cheverud *et al.*, 1985:1338), "microevolutionary pattern" (Lynch, 1991:1065), "phenotypic, or homeostatic, responses to specific behavior patterns" (Ward & Sussman, 1979:576), and "the measurement error term" (Bell, 1989:565). Bell (1989) said it best when he described nonphylogenetic effects as due to "any...cause of modification" (p. 553).

The reader will perhaps tolerate the obvious displacement of the above quotes from their proper context when I reveal that my intent was not to deride, but to agree whole-heartedly with all of these statements. The so-called phylogenetic and nonphylogenetic components of phenotypic variance are all of these things, and more. *This is because the two components are not distinguishable on the basis of process, or the effects thereof, but rather, on the basis of chronology.* The phylogenetic component of the variance of a given trait represents all of the changes that have accrued in a clade, *through all known processes of modification*, up to a specified set of ancestors (I will later more formally introduce the term *Last Shared Ancestors*—LSA—for this set). The nonphylogenetic component represents all of the changes that have accrued, again, *through all known processes of modification*, from this set of ancestors to a specified set of descendents. In the next section, I enlarge this argument by introducing the concept of the *ancestrally centered phylogeny* (ACP). I will show that three of the four types of nonindependence methods discussed thus far—independent contrasts, nested ANOVA, and phylogenetic autoregression—can be viewed as special cases of the ACP.

Reproduced with permission of the copyright owner. Further reproduction prohibited without permission.

The Concept of the *Ancestrally Centered Phylogeny*

I have already demonstrated the effects that multi-level topologies have on the covariance between pairs of traits that are *selectively independent* (see Box 6.7). Yet, strictly speaking, it is not the topology alone that produces the problem of nonindependence of data points and elevated Type I error rates in comparative biology, but the *combined* effects of evolutionary change *within* a multi-level structured topology. A multi-level topology without change renders an absence of phenotypic variation. In such a case the structure of the phylogeny matters not at all. On the other hand, as we have seen, a single-level topology *with* evolutionary change yields data that are effectively independent. Viewed in this way, it becomes clear that *in order to restore independence to a set of cross-taxonomic trait values we need to remove from the data that component of the variance due to changes that have accrued within the multi-level structure of the phylogeny.*

To illustrate this, let us reconsider the single-level phylogeny (see Box 6.5). It has been shown (Felsenstein, 1985; this study) that the raw data points of such a phylogeny are independent. Thus, the raw data of a single-level phylogeny are exactly the type of data we are attempting to produce when we apply a nonindependence method to a set of cross-taxonomic data emanating from a multi-level phylogeny (i.e. the non-phylogenetic component). In fact, a good test of these methods is to apply them to data from a single-level phylogeny and see if the residuals they produce are equal to, or perfectly correlated with, the original data. In other words, since there is no phylogenetic effect in a single-level phylogeny these methods should remove nothing from the raw data. Box 6.9 gives results that show this to be true for the nested ANOVA and autoregression methods. Here,

Reproduced with permission of the copyright owner. Further reproduction prohibited without permission.

then, is a case in which we are certain that the residuals produced by the nested ANOVA and autoregression methods represent truly independent data points. Since these statistically independent residuals are equivalent to the raw data values of the single-level phylogeny, their properties should also be equivalent, and we can thus specify unequivocally the properties of the nonphylogenetic component. Another way of putting it, in less formalized logic, is that the single-level phylogeny provides an archetype after which to model the nonphylogenetic component of cross-taxonomic phenotypic variance.

Box 6.9. Application of Phylogenetic Autoregression method (top) and nested ANOVA (bottom) to data generated from a single-level phylogeny. Results show that the residuals are equivalent to (perfectly correlated with) the original data.

W	B	C	D	E	Y	WY	Model Equation	ϵ	r	p
B	1	1	1	1	1	7	$Y=1.0WY+\epsilon$	-6	1.0	.0001
C	1	1	1	1	5	7		-2		
D	1	1	1	1	9	7		2		
E	1	1	1	1	13	7		6		

	Y	T_1	Analysis of Variance						ϵ	r	p
B	1	1	Source	df	SS	MS	F	Prob>F	-6	1.0	.0001
C	5	1	Model	1	196	196	7.35	0.0731	-2		
D	9	1	Error	3	80	26.67			2		
E	13	1	Total	4	276				6		

This logic leads to the conclusion that the proper way to proceed to restore independence of data points to a multi-level phylogeny is to transform it into a single-level phylogeny. Any multi-level phylogeny can be collapsed into a single-level phylogeny in just three steps: (1) select a set of ancestral nodes whose ancestral morphotypes have been estimated (see the section on estimating ancestral morphotypes below); each selected ancestral node must be the direct ancestor to one extant species with no other intermediate ancestor of that species also selected (sister species may share an ancestral node), (2) if necessary, "prune" away all auxiliary branches leaving only those branches connecting the selected ancestral

Reproduced with permission of the copyright owner. Further reproduction prohibited without permission.

nodes with their extant descendent, (3a) "center" the selected ancestral nodes on a single vertical line while rigidly translating their attached lineages (time unstandardized centering); or, (3b) "center" the selected ancestral nodes on a single *point*, while rigidly translating their attached lineages, and scale each lineage to a common horizontal line (time standardized centering). A few examples will help clarify the procedure by which ancestrally centered phylogenies (ACPs) are constructed. Box 6.10 illustrates the construction of two ACPs from the same phylogeny from two different sets of ancestral nodes.

Box 6.10. Construction of *time-standardized* Ancetrally Centered Phylogenies (right) using two different sets of ancestral nodes (left).

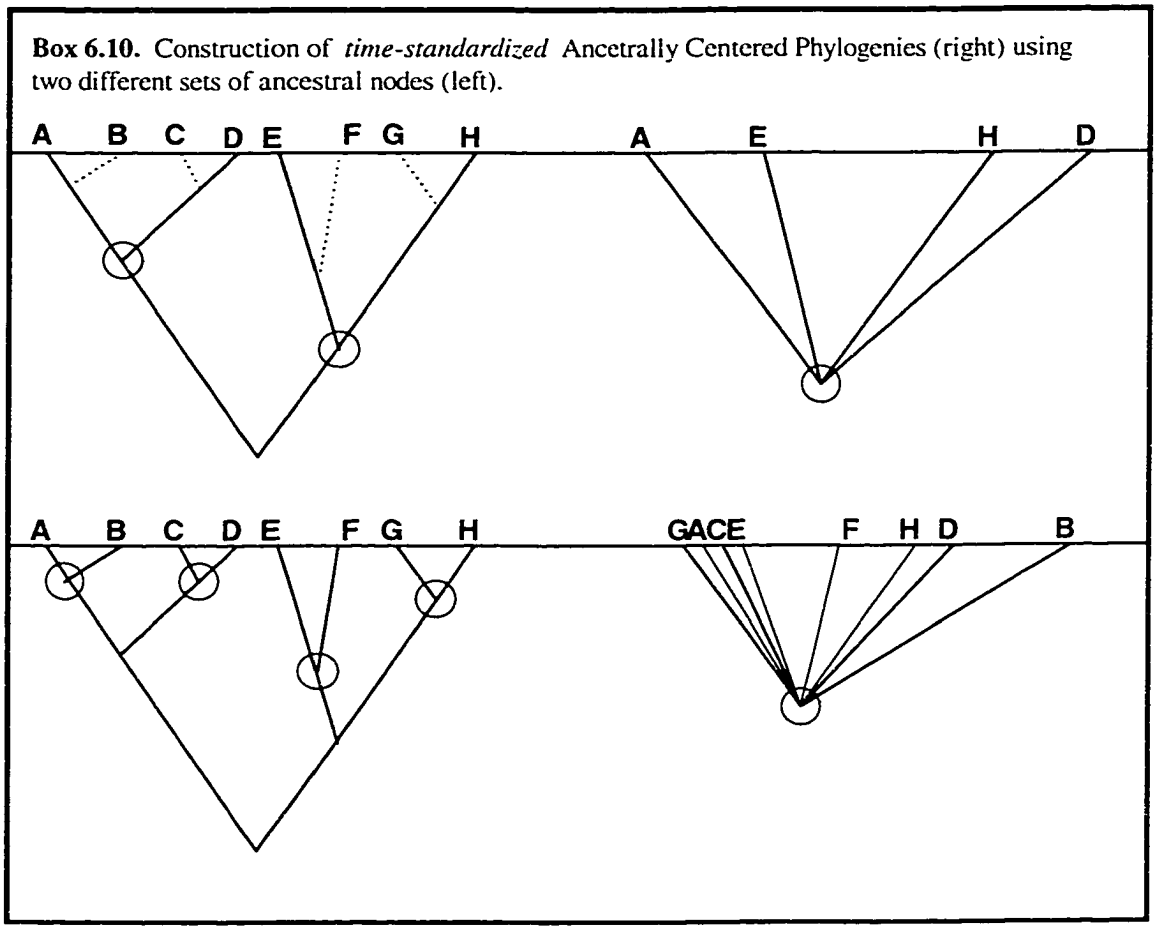

The upper left phylogeny in Box 6.10 shows two selected (circled) ancestral nodes, each giving rise to four extant species (A-D and E-H). Since each

Reproduced with permission of the copyright owner. Further reproduction prohibited without permission.

ancestral node gives rise to only two independent lineages, four lineages must be "pruned," one from each of the following pairs (A or B; C or D, E or F, G or H). In this example B, C, F and G have been pruned (dotted lines) leaving species A, D, E, and H, but any other appropriate combination could have been used. The two ancestral nodes are then centered (i.e., superimposed) and the attached lineages are rigidly translated and scaled to a horizontal line. When the ACP is scaled as described the vertical distance between the superimposed ancestral nodes and the horizontal line is unimportant because it does not affect the *relative* species values on the abscissa. The scaling procedure is equivalent to standardizing each Y value by lineage length. Moreover, if the central ancestral node is placed at coordinate 0 along the abscissa, then the Y values of the species along the horizontal line represent the amount of change in trait Y that has accrued along each lineage from the selected ancestor, standardized by lineage length (i.e., time).

I submit that this procedure is most effective when it is applied to the set of ancestral nodes representing the last common ancestors among extant sister taxa—I call this an *alpha* ACP (see Box 6.10, bottom). First, an alpha ACP requires no pruning because there are only two descendent lineages from each ancestral node, and both are independent. Second, since each species in the original phylogeny is represented in the alpha ACP there is no reduction of sample size. Finally, and most importantly, since the alpha ACP data represent, in this case, changes that have occurred only since the *most recent* ancestor, covariation estimates of this data with *current* ecological and behavioral data are more likely to be valid.

Reproduced with permission of the copyright owner. Further reproduction prohibited without permission.

The ACPs illustrated in Box 6.10 are standardized by lineage length, but this feature of the ACP is optional. Time-unstandardized ACPs corresponding to those in Box 6.10 are shown in Box 6.11. It can be seen that a time-unstandardized ACP is one in which the ancestral nodes have been vertically aligned or centered but not horizontally centered.

Box 6.11. Construction of *time-unstandardized* Ancestrally Centered Phylogenies (right) using two different sets of ancestral nodes (left). (Lower ACP is enlarged for ease of view)

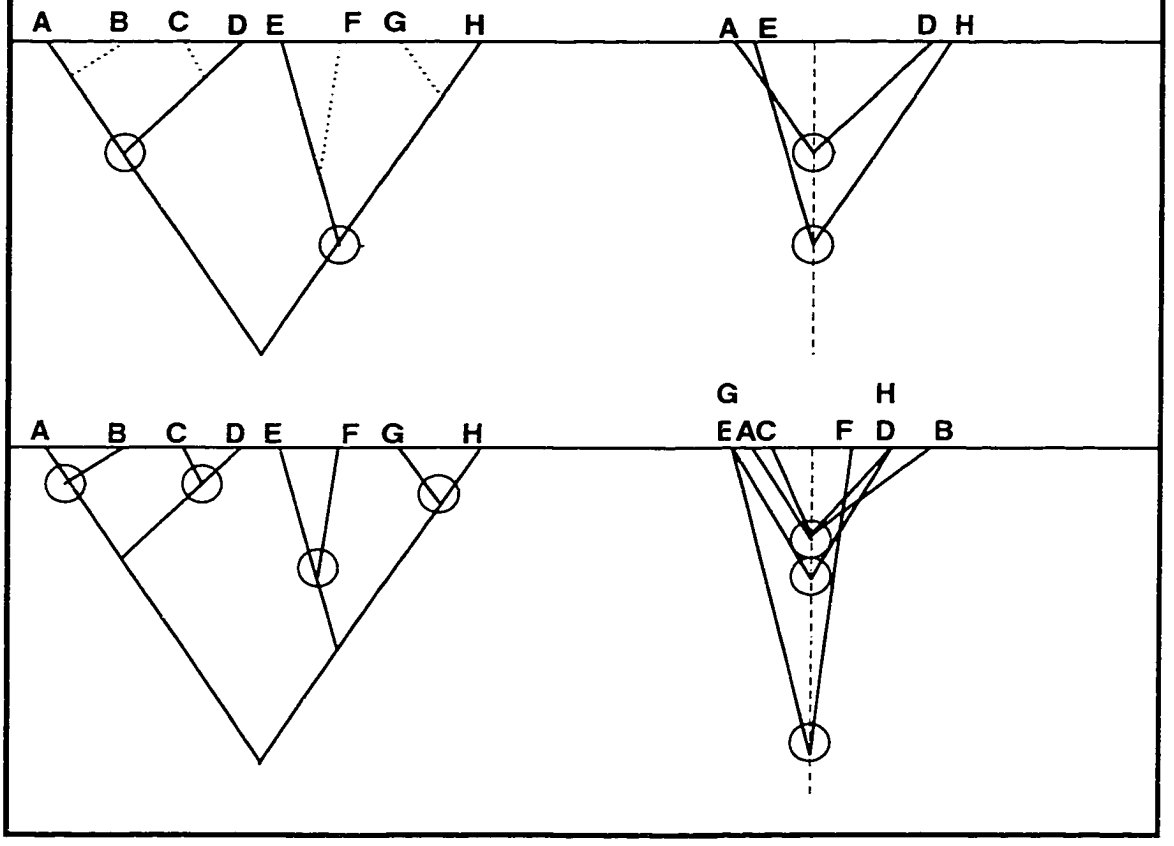

The Y vectors produced from time-standardized and time-unstandardized ACPs may differ because they measure different aspects of Y. A time-unstandardized Y value represents the *absolute* or *total* amount of change that has accrued over a linear (from ancestor to descendent), whereas a time-standardized Y

Reproduced with permission of the copyright owner. Further reproduction prohibited without permission.

value represents the *relative rate* of change accrued over a lineage. Time-standardized Y values are simply time-unstandardized values divided by lineage length. The distinction between time-standardized and time-unstandardized ACPs is important for two reasons. It will be shown that various nonindependence methods perform more efficiently either as time-standardized or time-unstandardized ACPs (I will return to this topic later). The distinction also has theoretical as well as practical significance. Time-unstandardized ACPs have several unfavorable properties. It turns out that time-unstandardized ACPs are more sensitive to sample composition than time-standardized ACPs. That is to say, if species are excluded from the original sample the time-unstandardized scores of those species remaining in the sample are more likely to change as a result. This effect is illustrated in Box 6.12, which shows two new ACPs (time-standardized, top right; time-unstandardized, bottom right) reconstructed with species D excluded from the original four species sample (Box 6.10 and 6.11, top). It can be seen that the Y values of species A, E, and H of the time-standardized ACPs are the same whether or not species D is included in the sample (compare Box 6.10 top right with Box 6.12 top right). In the time-unstandardized ACP, while species E and H are unaffected by the removal of species D, species A (the sister taxon to species D) has changed as a result. The Y value of species A has been shifted to the left (i.e., it has a greater negative value) after exclusion of species D from the sample (compare Box 6.10 top right with Box 6.12 bottom right). The reason for this is simple. Recall that the time-unstandardized ACP scores represent the total change accrued over a given lineage from ancestor to descendent. Descendent species with more distance ancestors are likely to have accumulated more change than species with more recent

Reproduced with permission of the copyright owner. Further reproduction prohibited without permission.

ancestors. In the current example, by removing species D from the sample the last common ancestor of species A was displaced to a more distant node, and this was reflected in the altered time-unstandardized ACP score for species A. In contrast, since the time-standardized ACP scores represent the *rate* of change over a given lineage, and the rate of change of species A was unaffected by the removal of species D.

Box 6.12. Comparison of *time-standardized* (top) and *time-ustandardized* (bottom) ACPs after exclusion of lineage D.

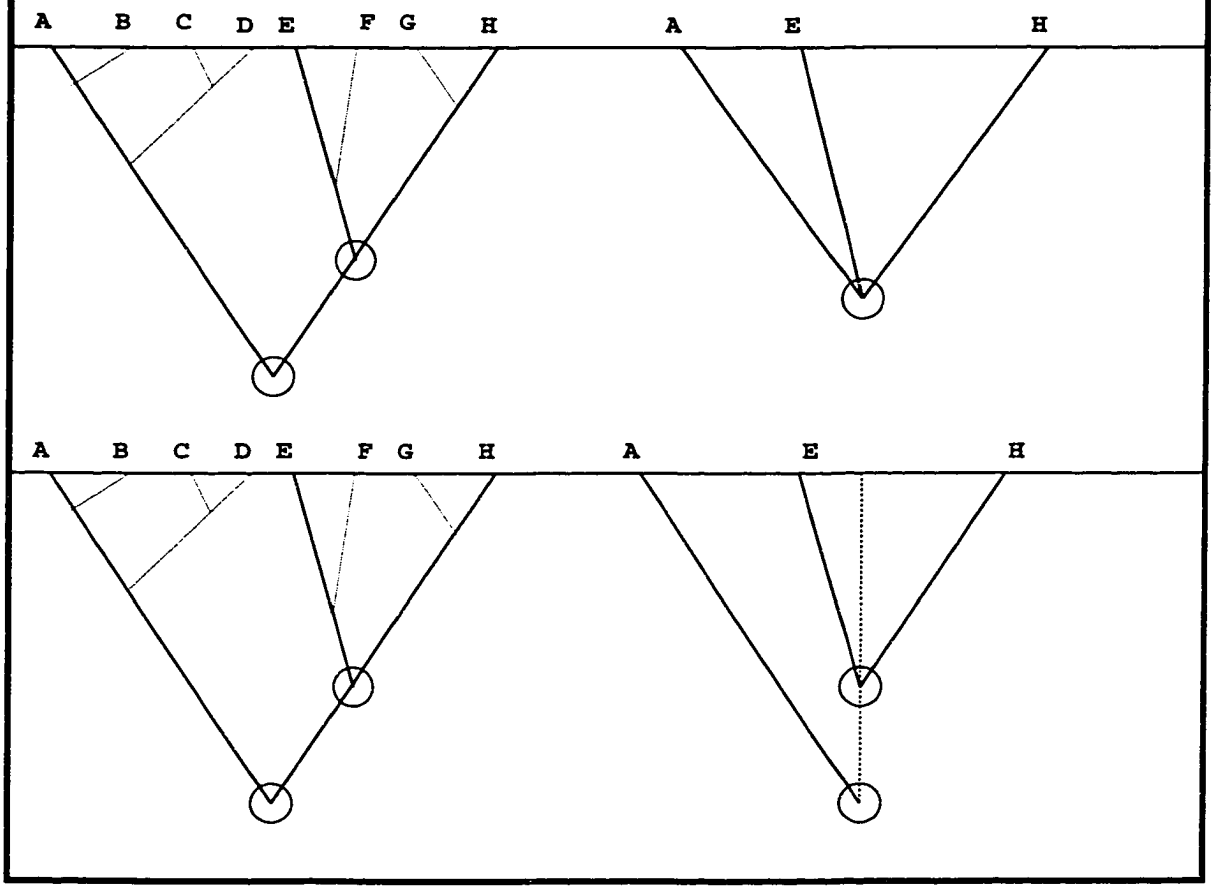

There are a number of interesting properties of ancestrally centered phylogenies, time-standardized or time-unstandardized, that should be noted. First, it is obvious that in constructing an ACP a multi-level phylogeny has been abridged

Reproduced with permission of the copyright owner. Further reproduction prohibited without permission.

to a single-level phylogeny whose data points are independent. And yet, in transforming the data to acquire independence the properties of the data have changed. In the original phylogeny, the Y values represent an inherent property of the species themselves. The data are entirely synchronic and, as we have seen, nonindependent. In the ancestrally centered phylogeny, the Y values represent *deviations of extant species from ancestral morphotypes* (real or estimated). The data have been transformed from a property inherent to species to a property involving change over a lineage (i.e., from ancestor to descendent). Hence, in order to restore independence to the data, it was necessary to introduce a diachronic element. This should be a vindication to those who have voiced concern over the efficacy of a strictly synchronic or "horizontal" analysis in comparative evolutionary biology (e.g., Szalay, personal communication). The foregoing discussion thus shows that even analytical techniques such as phylogenetic autoregression that on the surface appear to be strictly horizontal in character rely upon an implied knowledge or estimate of ancestral conditions.

The data generated from an ACP can be thought of either as a species-level property (i.e., the deviation of a given species from a given ancestor), or, just as aptly, a property of lineages (e.g., the rate of change of a trait unique to a given lineage). Therefore, it is equally justifiable to consider either the lineage or the species as the proper unit of analysis. Interestingly, Szalay and Bock (1991), two of the early architects of nomological thinking in evolutionary biology, arrived at essentially the same conclusion but from a completely independent set of logical premises. They do point out, however, that only species play a role in the evolutionary process, whereas phyletic lineages are simply the records of change

Reproduced with permission of the copyright owner. Further reproduction prohibited without permission.

in species taxa (ibid., p. 16). From a theoretical viewpoint it is thus most consistent to consider ACP data as species level data.

One of the most powerful features of the ancestrally centered phylogeny concept is that it can be used as a model to examine and assess properties of various nonindependence methods: *all valid nonindependence methods can be shown to be special cases of an ACP, whereas invalid methods do not conform to the ACP model.*

Higher taxonomic comparison methods, for example, do not conform to the concept of the ACP. They do not abridge multi-level phylogenies into single-level phylogenies. They do not introduce a diachronic element into the data. And they do not restore independence to the data points. On the other hand, data generated from an ACP, like the one shown in Box 6.10 (lower right), are equivalent to the pooled within-groups variance of a nested ANOVA, in which ancestral morphotypes are estimated as group means.

It can also be shown that the autoregression method is a variant of the ACP, in which each ancestral morphotype is estimated as a function of the weighted mean of all related species in the phylogeny. The residuals of an autoregression represent deviations of species' Y values from the estimated ancestral morphotypes. Recall that the W matrix used in an autoregression is a matrix of relatedness or affinity among pairs of species. The type of data used in a W matrix—taxonomic affinity data (rank-based W matrix) or phylogenetic relatedness data (divergence-based W matrix)—determines the criteria by which the ancestral morphotypes of the corresponding ACP are estimated. Thus, the nested ANOVA and autoregression methods are simply different approaches to

Reproduced with permission of the copyright owner. Further reproduction prohibited without permission.

estimating the ancestral morphotypes of an ACP. The independent contrasts method is also a special case of the ACP approach because the difference-values generated by the method simply represent the sum of sister-taxa absolute ACP scores.

The Problem of Estimating Ancestral Morphotypes

In light of the ACP concept it can be seen that the accuracy and power of the various nested ANOVA and autoregression methods depends upon the degree to which each can accurately estimate ancestral morphotypes. In general, these methods estimate ancestral morphotypes based on some form of averaging or weighted averaging over various sub-groups. As mentioned, the nested ANOVA uses the group mean, and as a consequence, the ancestral morphotypes of pairs of sister taxa will fall exactly in the middle of each pair. As a result, deviations from the ancestral morphotype will be equal in magnitude but opposite in sign for all pairs of sister taxa. In an alpha level analysis one species cannot have deviated any more or less from the ancestral morphotype than its sister. Autoregression is less restrictive, since *deviations* from the ancestral condition (=residuals of the autoregression) between sister taxa may be different in magnitude and may or may not be equal in sign. Therefore, autoregression methods are potentially better able to model certain features of the evolutionary process than analysis of variance methods—for example, differential rates of change in sister taxa and instances of parallelism.

Cheverud, Dow and Leutenegger (1985) apparently did not recognize this property of the autoregression method when they stated: "...if related species

Reproduced with permission of the copyright owner. Further reproduction prohibited without permission.

independently evolve similar trait values, our method assigns this independent adaptation to the phylogenetic value rather than the specific value" (p. 1340). This is not necessarily the case, however. Consider an instance in which sister taxa change in the same direction, but at different rates, away from a common ancestor (i.e. parallelism). If the method does a reasonable job at estimating the morphotype of this ancestor then the residuals of the autoregression will contain this parallel evolution (they will be of the same sign).

An analysis of parallelisms produced in the PHYLOMOD simulations showed that the autoregression method proposed by Cheverud *et al.* (1985) was in fact able to detect and assign parallelisms to the nonphylogenetic component of variance 63% of the time in comparison to 0% for the nested ANOVA method.

Convergence is a more serious problem. Convergence occurs when the same trait in two lineages evolves toward an intermediate form (for example, one small-bodied species and one large-bodied species both evolve toward medium size). Such a case is illustrated in Box 6.10. Species D and E in the upper left phylogeny have converged toward a similar form, perhaps due to some common evolutionary agent, such as diet. When this phylogeny is collapsed into an ACP (Box 6.10, top right) species D and E are assigned dissimilar trait values and opposite signs (E is negative, or to the left of the central ancestral point, and D is positive, or to the right of the central ancestral point). The ACP data would thus obscure any relationship between a causal agent (e.g., diet) and the trait under study.

The importance of parallelism and convergence in mammalian evolution is not completely known. Several workers have argued that parallelism involving

Reproduced with permission of the copyright owner. Further reproduction prohibited without permission.

craniofacial traits is not a common phenomenon among primates (Cheverud *et al.*, 1985) and other mammals (Wagner, 1989). In addition, Werdelin (1986) found no substantial convergences in a study comparing skull form among placental and marsupial carnivores: "In terms of the morphological composition of the functioning skull, convergence due to similar ecologies is of very minor significance." (p. 114).

Assessment of Nonindependence Methods by Phylogenetic Simulation

In order to measure the power and inferential reliability of several nested ANOVA and autoregression methods, I applied these methods to a series of phylogenetic simulations (see previous description). I evaluated the nested ANOVA method as described by Bell (1989) and three autoregression methods, each with a different type of W matrix.

In one autoregression equation I used the W matrix structure suggested by Cheverud *et al.* (1985). Recall that these authors assigned the value 1 to species that were congeneric, and the values 0.5, 0.33, 0.25, 0.2, and 0.167 to pairs of species related at the family, superfamily, infraordinal, subordinal and ordinal levels, respectively. This type of W matrix may be referred to as a *rank-based inclusive* W matrix. It is inclusive because all of the elements of the W matrix are non-zero (i.e., all of the species in the study contribute to the estimation of the ancestral morphotypes). The simulated phylogenies were designed to accommodate a maximum of five taxonomic levels and so the assigned values were truncated at the subordinal rank.

The second autoregression equation evaluated contained a W matrix structure proposed by Lynch (1991). Lynch suggested that each element in the W

Reproduced with permission of the copyright owner. Further reproduction prohibited without permission.

matrix be computed as the percentage of time that a given pair of species have shared a common ancestor going back to the beginning of the clade under study. As an example, he cites the relationship between *Homo* and *Pongo* within the order Primates. "[S]ince the root of the [primate] tree... is placed at 58 MYA and a split between *Homo* and *Pongo* is denoted at 13 MYA..." the element in the W matrix for this pair of species is (58-13)/58 = 0.78. In other words, *Homo* and *Pongo* shared a common primate ancestor for 78% of the time that primates have existed. Using this method, only the diagonal of the W matrix will contain 1s, and congenerics and more distantly related pairs of species will be assigned some fraction of 1 depending on how long they have shared a common ancestor. Thus, to express Lynch's W matrix a phylogeny with estimated divergence times is required. This, then, is an example of a *divergence-based inclusive* W matrix.

The third autoregression equation tested employed a W matrix structure that I developed based on the concept of the alpha ACP. Recall that the Y values produced by an alpha ACP represent a vector of the rates of change of trait Y over the lineages in the phylogeny connecting each extant species with its last immediate common ancestor. This last immediate ancestor may be the ancestor of only a pair of species, or it may be ancestral to a larger clade. In either case, only the member species of a given clade manifest Y values that are relevant to the estimation of the ancestral morphotype for the ancestor of that clade. The logic behind this is that only the trait values of the descendents of a given ancestor should be used to infer the ancestral condition. Strictly speaking, this is never the case when an autoregression method is used because the predicted values of Y (Y'=estimated ancestral values) are a function of the slope of the best fit line (ρ),

Reproduced with permission of the copyright owner. Further reproduction prohibited without permission.

and this slope is of course determined by the dispersion of Y and WY obtained from the entire phylogeny. However, since ρ is unity for the estimation of all Y' values the true equation Y'=ρWY is approximated by Y'=WY. The W matrix thus has a substantial influence on the estimation of the ancestral Y values in an alpha ACP model.

The residuals of an autoregression, as the differences between the observed trait values and the predicted trait values (Y-Y') represent the changes that have accrued over each of the lineages of the time-unstandardized alpha ACP. To convert these to time-standardized alpha ACP scores, each residual must be divided by the length of its respective lineage. Recall that WY is a vector with each element representing a linear combination of Y values weighted by the elements in the W matrix.

A W matrix most compatible with the alpha ACP concept will contain elements that assign a weight of 1 to all sister taxa of a given species, and a weight of 0 to all other species in the phylogeny. In this way, only the trait values of the descendents of a given ancestor are used to define WY, and, subsequently, Y'. For convenience, I refer to this type of W matrix as a *clade-based exclusive* W matrix. It is exclusive because only some of the elements of the W matrix are nonzero.

A numerical example will make the foregoing discussion more understandable. In Box 6.13, I specify the W matrices and the resulting WY, Y', ∈ and ∈/L vectors for each of the three types of autoregression models—rank-based inclusive, divergence-based inclusive and clade-based exclusive. A hypothetical phylogeny is given (Box 6.13, top left) consisting of extant species A - D and ancestral nodes 1-3. The raw Y values for the extant species of this phylogeny are

Reproduced with permission of the copyright owner. Further reproduction prohibited without permission.

given as A=1, B=5, C=9, and D=13; and the lineage lengths (L) are A=6, B=4, C=2, and D=2. The time-unstandardized ancestrally centered phylogeny is diagrammed directly below the hypothetical phylogeny. The Y values for the time-unstandardized ACP are A= -6, B= -4, C= -2, and D= 2. The Y values for the time-standardized ACP are A= -1, B= -1, C= -1, and D= 1.

Box 6.13. Comparison of the three types of W matrices in autoregression.

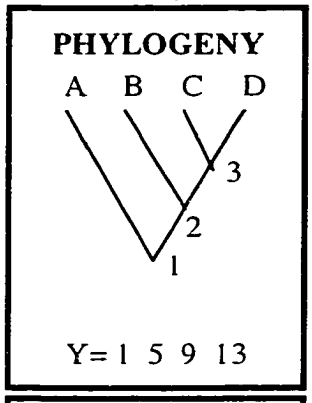

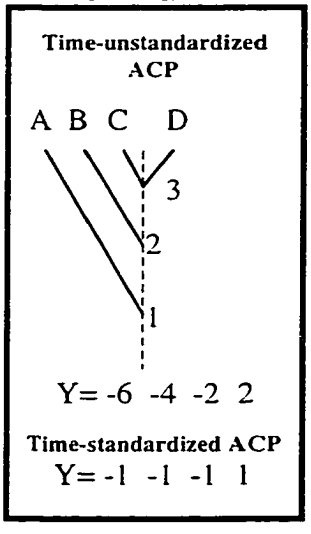

① Autoregression, Rank-based inclusive W matrix (row normalized) after Cheverud *et al.*, 1985

W	A	B	C	D	Wy	Y'	∈	∈/L
A	.49	.17	.17	.17	5.08	5.2	-4.2	-.7
B	.14	.44	.21	.21	6.96	7.1	-2.1	-.53
C	.12	.18	.35	.35	8.72	8.9	0.1	.05
D	.12	.18	.35	.35	8.72	8.9	4.1	2.1

② Autoregression, Divergence-based inclusive W matrix (row normalized) after Lynch, 1991.

W	A	B	C	D	Wy	Y'	∈	∈/L
A	.57	.14	.14	.14	4.43	4.5	-3.5	-.59
B	.11	.44	.22	.22	7.22	7.5	-2.5	-.61
C	.1	.2	.4	.3	8.6	8.9	.05	.02
D	.1	.2	.3	.4	9.0	9.4	3.6	1.8

③ Autoregression, Clade-based exclusive W matrix (row normalized) after present study.

W	A	B	C	D	Wy	Y'	∈	∈/L
A	.25	.25	.25	.25	7	5.5	-4.5	-.76
B	0	.33	.33	.33	9	7.1	-2.1	-.52
C	0	0	.5	.5	11	8.7	.3	.14
D	0	0	.5	.5	11	8.7	4.3	2.14

The elements of the first row of the W matrix represent the degree of relatedness between species A and all other species in the phylogeny. With regard to the rank-based W matrix the element AA is assigned a non-row-normalized

Reproduced with permission of the copyright owner. Further reproduction prohibited without permission.

value of 1, since species A is its own congeneric. The remaining elements of the first row are assigned the non-row-normalized value of 0.33 because species A is related to B, C and D at the superfamily level. Normalizing this first row of the rank-based W matrix yields the vector {0.49 0.17 0.17 0.17}. The elements of the second row of the W matrix represent the degree of relatedness between species B and all other species in the phylogeny. Element BA of the rank-based W matrix is assigned a non-row-normalized value of 0.33 since species B and A are related at the superfamily level. Element BB is assigned the non-row-normalized value of 1 since B is its own congeneric. Elements BC and BD are assigned the non-normalized value of 0.5 since species B is related to C and D at the family level. Normalizing the second row of the rank-based W matrix yields the vector {.14 .44 .21 .21}. The remaining row vectors, those for C and D, are calculated in a similar fashion.

With regard to the divergence-based W matrix, the element AA is assigned the non-normalized value 1 because it has shared a common ancestor with itself for 100% of the existence of the clade (in this example the clade length is given as 8). The remaining elements of the first row are assigned the non-row-normalized value of 0.25 because species A has shared a common ancestor with B, C and D for 25% of the existence of the clade. Normalizing this first row of the divergence-based W matrix yields the vector {.57 .14 .14 .14}. With reference to the second row, element BA is assigned a non-normalized value of .25 since species B and A have shared a common ancestor for 25% of the existence of the clade. Element BB is assigned the non-row-normalized value of 1 since B has shared an ancestor with itself for 100% of the existence of the clade. Elements BC

Reproduced with permission of the copyright owner. Further reproduction prohibited without permission.

and BD are assigned the non-row-normalized value of 0.5 since species B has shared a common ancestor with C and D for 50% of the existence of the clade. Normalizing the second row of the divergence-based W matrix yields the vector {.11 .44 .22 .22}. The remaining row vectors, those for C and D, are calculated in a similar fashion.

In the case of the clade-based W matrix, the elements of the first row of the W matrix do not represent the degree of relatedness between species A and all of the other species in the phylogeny. Recall that each row of the W matrix contains the weights applied to the calculation of the corresponding row elements of the WY vector, and the WY vector approximates the estimated ancestral morphotypes of species A - D, respectively. In other words, the first element of the WY vector represents the estimated Y value of the last immediate ancestor of species A (labeled node 1 in the ACP phylogram). Since node 1 is also the common ancestor of the entire clade, all of the member of the clade should be used to estimate the Y value of this ancestor. Thus, all of the elements of the first row of the clade-based W matrix are assigned a non-normalized value of 1. All of the species of the clade equally contribute to the estimate of the node 1 Y value. Normalizing this first row of the clade-based W matrix yields the vector {.25 .25 .25 .25}. The second row of the W matrix contains the weightings that contribute to the estimation of the Y value of the last immediate common ancestor of species B—node 2. Since only species B, C and D are descendent from ancestral node 2, then only these species should be involved in estimated the Y value of node 2. Hence, in the second row of the clade-based W matrix element BA is assigned 0 and elements BB, BC, and BD are assigned the non-normalized value 1. Normalizing the second

Reproduced with permission of the copyright owner. Further reproduction prohibited without permission.

row of the clade-based W matrix yields the vector {0 .33 .33 .33}. The remaining row vectors, those of C and D, are calculated in a similar fashion.

The vectors WY, Y', ϵ and ϵ/L were calculated using the autoregression method for each of the three types of W matrices (see Box 6.13). The vector of residuals ϵ corresponds to the time-unstandardized Y scores of the ACP (Y= -6 -4 -2 2). The residual scores from all three types of autoregressions correlated significantly with the time-unstandardized ACP scores (r >.99, p < .01). The vector of time-standardized residuals ϵ/L corresponds to the standardized Y scores of the ACP (Y= -1 -1 -1 1). The time-standardized residual scores from all three autoregressions likewise correlated significantly with the time-standardized ACP scores (r > .95, p < .05).

Although the three autoregression methods appear to correspond well to the ACP concept, the example was not given as a test of these methods, but merely to illustrate the differences among the three types of W matrices. To describe the properties and evaluate the effectiveness of the autoregression and nested ANOVA methods, and to confirm empirically the validity of the ACP approach, I applied each of these to a series of simulated phylogenies (with known properties) generated using PHYLOMOD.

Hypothesis Testing Effectiveness: Type I and Type II Error Rates

Recall that the multi-level simulated phylogenies described earlier produced phenotypic values for three traits (Y_1, Y_2, and Y_3), and that trait Y_1 was allowed to "evolve" independently of traits Y_2 and Y_3, but traits Y_2 and Y_3 shared a common directional "evolutionary" influence. A single-level phylogeny was also produced

Reproduced with permission of the copyright owner. Further reproduction prohibited without permission.

for each simulation run which yielded the independent phenotypes K_1 and K_2. From these initial parameters it can be seen that the null hypothesis (i.e., that no relationship exists) is the true hypothesis with regard to the covariance of Y_1 with Y_2, Y_1 with Y_3, and K_1 with K_2. A Type I error was counted as an instance in which the null hypothesis was rejected (as determined by a significant correlation) when in fact it was true, as in the case of the trait pairs just mentioned.

Type I error rates are reported for a variety of methods in Box 6.14. Results obtained by Martins (1996) and Gittleman and Luh (1992) are also given for comparison, although these represent the *average* Type I error rates over a series simulations using different parameters. The Type I error rate for the *raw* Y scores obtained in this study (0.294) is not substantially different from that obtained by Martins (1996) (0.318), even though her simulations were based on quite different parameters.

The Type I error rates obtained by Martins (1996) and Gittleman and Luh (1992) for the Independent Contrasts method of Felsenstein (1985) is also reported here, although this method was not tested using PHYLOMOD. When examining the results reported in Box 6.14, it should be kept in mind that truly independent data points are expected to yield a Type I error rate of 0.05, the rate expected due to chance alone. Thus, the Type I error rate of 0.294 obtained for the raw data correlations of Y_1 with Y_2 and Y_1 with Y_3 confirm that the raw data scores in a multi-level phylogeny are nonindependent.

Reproduced with permission of the copyright owner. Further reproduction prohibited without permission.

Box 6.14. Type I error rates for various nonindependence methods, for 800 simulation runs.

	Type I error at $\alpha = .05$			
	PHYLOMOD		Martins, 1996	Gittleman & Luh, 1992
Raw Data	.294		.318	------
	Time-standardized	Time-unstandardized		
Single-level phylogeny	.053 (ns)	------	------	------
ACP	.052 (ns)	.130	------	------
Independent Contrasts	------	------	.112	.09
Nested ANCOVA	------	.149	------	------
Rank-based autoregression	.239	.125 (.11-.14)	.177	.13
Divergence-based autoregression	.296	.115 (.10-.13)	------	.10
Clade-based autoregression	.126 (.11-.14)	.254	------	------

(ns)-not significantly different from .05. Confidence intervals are given in parenthesis.

The simulation results also confirm that the raw data points of a single-level phylogeny are indeed independent, as indicated by a Type I error rate (0.053) which is not significantly different from that expected by chance alone. All single-level phylogenies are, by their very nature, time-standardized phylogenies, and hence, no results are given under the "time-unstandardized" column for single-level phylogenies in Box 6.14.

Type I error rates are given for time-unstandardized as well as time-standardized ACPs. Recall that ACP scores represent the difference between trait values of an extant species and its last immediate common ancestor (from among those species included in the study). The calculation of ACP scores thus requires that ancestral morphotypes be known. It was possible to generate ACP scores from the phylogenetic simulations only because the Y values of all ancestral nodes were recorded for each simulation. I previously provided a logical argument leading to

Reproduced with permission of the copyright owner. Further reproduction prohibited without permission.

the conclusion that ACP scores are independent. However, the simulation test results show that only *time-standardized* ACP values resulted in a Type I error rate (0.052) that supports this argument. In contrast, the *time-unstandardized* ACP scores exhibited a Type I error rate (0.13) that is significantly greater than the expected 0.05 level. This is perhaps due to the fact that unstandardized ACPs are sensitive to relative node positions which are part of the phyletic topology (see earlier discussion).

Whereas the ancestral trait values must be known in the calculation of the ACP scores, the residuals generated by the nested ANOVA and autoregression techniques represent ACP scores whose values were calculated on the bases of *estimated* ancestral trait values. Each of these techniques is thus a special case of an ACP in which the role of the method is to estimate the ancestral trait values. This being the case, a straight-forward approach would be to analyze fossil specimens as a means of quantifying ancestral trait values. A alternative approach would be to include fossil specimens in the W matrix, following a structure that

Reproduced with permission of the copyright owner. Further reproduction prohibited without permission.

would allow for gaps in the paleontological record.[3]

The independent contrasts method of Felsenstein (1985), when restricted to extant species, is the only valid nonindependence method that does not require estimation of ancestral phenotypic conditions. Recall that the method may be thought of as a special case of the ACP, one in which the difference-values represent the sum of sister-taxa absolute ACP scores. Each sister-taxa pair contrast produces a truly independent value. Moreover, the method has the advantage that the independent values it generates are not based on potentially inaccurate ancestral morphotype estimates. Consistent with these auspicious theoretical properties, the independent contrasts method has yielded some of the lowest Type I error rates (0.112, 0.09) of any method tested by means of phylogenetic simulations (Gittleman & Luh, 1992; Martins, 1996). Perhaps time-standardized independent contrast scores would yield a Type I error rate not

---

[3] Consider a hypothetical example involving four living species (A-D) of a given clade related as follows: A(B(CD)). To improve ancestral morphotype estimates, two fossil species (E-F) are included in the analysis. Fossil species E is hypothesized to be close to the ancestral node of extant species C and D. Fossil species F is thought to be close to the ancestral node for the entire clade, and thus a good candidate for the last shared ancestor of species A. The fossil data can be incorporated into an *asymmetrical* W matrix (4x6, in this example) which contains extant species along the rows and both extant and fossil species along the columns (next page). Matrix multiplication of W and Y yields, in this example, a 4x1 array containing the estimated ancestral morphotype values for the extant species. Several different ways of utilizing the fossil data are possible: (1) a fossil trait value can be specified as the exclusive estimated ancestral morphotype, as in the case of fossil species E relative to extant species C and D; (2) a fossil trait can be included as one of several trait values that contribute to the estimation of an ancestral morphotype, as in the case of fossil species F relative to extant species A; or (3) fossil traits can be excluded from the estimation of an ancestral morphotype, as in the case of extant species B.

	A	B	C	D	E	F
A	1	.25	.25	.25	0	1
B	.25	1	.5	.5	0	0
C	0	0	0	0	1	0
D	0	0	0	0	1	0

Reproduced with permission of the copyright owner. Further reproduction prohibited without permission.

significantly different from 0.05. As noted previously, the main disadvantage of the alpha-level independent contrasts method, is that the degrees of freedom are virtually cut in half, making the method impractical for analysis of small samples.

Analysis of the PHYLOMOD simulations in Box 6.14 reveals that none of the nonindependence methods tested yielded Type I error rates of 0.05 or less. Therefore, the best that current methods can do is to reduce, not remove, the effects of phylogeny on cross-taxonomic phenotypic data. The nested ANCOVA method of Bell (1989) produced a Type I error rate of 0.149. About one-half of that observed for the raw data, but still about three times that expected by chance. Examination of the autoregression results shows an interesting, although not unexpected, pattern. The rank-based and divergence-based autoregression methods performed better with time-unstandardized residuals than with time-standardized residuals, whereas the clade-based autoregression method performed better with time-standardized residuals. Moreover, the best Type I error rates reported for each of the three autoregression methods (0.125, 0.115, 0.126) are not significantly different from one another.[4]

The Type I error rate for the time-unstandardized rank-based autoregression method reported by Gittleman and Luh (1992) is not significantly different from that reported here, although Martins (1996) found significantly higher rates in her simulation analyses. The Type I error rate reported in the present study for the time-unstandardized divergence-based autoregression method was also consistent with the

---

[4] This conclusion is based on the estimation that the confidence intervals for the Type I error rates of the three best methods overlap. Confidence intervals were calculated using Lilliefor's quantiles on the cumulative distribution function at the 5% level (*cf.* Sall & Lehman, 1996).

Reproduced with permission of the copyright owner. Further reproduction prohibited without permission.

corresponding rate published by Gittleman and Luh (1992).

The statistical power associated with a nonindependence method is important due to the serious consequences of committing a Type II error (β). Statistical power (1 - β) was calculated as the probability of rejecting the null hypothesis when it was false. The null hypothesis is known to be false in instances involving the correlation of Y_2 and Y_3, the two traits that were programmed to covary in the simulations. A simulated phylogeny in which the *p*-value of a correlation between Y_2 and Y_3 was greater than 0.05 was counted as a Type II error (β). Since a random element was introduced into the relationship between these two correlated traits, the strength of association varied from phylogeny to phylogeny. The average correlation and *p*-value between the time-standardized ACP scores of Y_2 and Y_3 (r=0.67; s =0.10; p=.00021) can be used as an indication of their true strength of association. The statistical power estimates of the various nonindependence methods (listed in Box 6.15) must be assessed relative to this level of covariance. Box 6.15 shows a number of interesting results. First, the power of the raw data values is quite high at .988, indicating that concerns about elevated Type II error rates due to phylogenetic effects are unwarranted (e.g., Gittleman & Kot, 1990). This makes intuitive sense when one understands that a common phylogenetic topology artificially enhances the covariance between two traits, thereby increasing the probability of rejecting a true null hypothesis (Type I error) but actually decreasing the probability of accepting a false null hypothesis (Type II error).

It is difficult to reconcile this result and interpretation with that of Martins (1996), however, who found from simulations involving 42 species that the statistical power of raw data correlations was much lower than the method-

Reproduced with permission of the copyright owner. Further reproduction prohibited without permission.

transformed data. She reports the power of two traits whose correlation was set at 0.75 to be around 0.50. Remarkably, Martins reports the power associated with the same two traits correlated at the same level (0.75) for simulations involving only 15 species to be around 0.65 (see Martins, 1996:1758). Clearly these findings violate statistical theory which stipulates that the power of a test will increase with the size of the sample (Sokal & Rohlf, 1995).

Box 6.15 Type II error rates for various nonindependence methods, for 400 simulation runs.

	Statistical Power (1 - β)	
Raw Data	.988	
	Time-unstandardized	Time-standardized
ACP	.993	.986
Nested ANCOVA	.975	------
Rank-based autoregression	.998	.923
Divergence-based autoregression	.980	.933
Clade-based autoregression	.988	.952

It is also of interest to note that the powers associated with tests involving the time-unstandardized residuals are greater than the powers associated with the time-standardized residuals, except in the case of the ACP scores for which there was no significant difference between the two.

I now turn to an assessment of the statistical estimates of the slope of the regression of Y on WY for each of the autoregression methods. Since the vectors Y and WY were standardized[5] prior to regression, the slope of the regression ρ is equivalent to the correlation coefficient *r*, and ρ-squared is equivalent to the coefficient

[5] The term "standardized" here is employed in the statistical sense, meaning a vector transformed to mean zero and unit variance, and it should not be confused with the concept of a "time-standardized" ACP.

Reproduced with permission of the copyright owner. Further reproduction prohibited without permission.

of determination R^2. This statistic can be interpreted as indicating the proportion of the variance of Y that can be accounted for by WY. Recall that WY represents the estimated morphotypes of the ancestors of a given set of descendents, or the so-called "phylogenetic component" of Cheverud *et al.* (1985). Box 6.16 gives the R^2 values for the three autoregression methods. The rank-based W matrix component accounted for about 77% of the variance of trait Y; the divergence-based W matrix method accounted for only about 65%; and the clade-based W matrix autoregression accounted for nearly 89% of the variance of Y. These statistics are comparable because each method was applied to precisely the same phylogenies.

Box 6.16. R^2 values for autoregression of Y on WY using the standardized regression coefficient, ρ. Standard errors are given in parenthesis. (n=2400)

Rank-based autoregression	0.772 (s_ρ=0.011)
Divergence-based autoregression	0.651 (s_ρ=0.014)
Clade-based autoregression	0.886 (s_ρ=0.010)
Actual ancestral scores	0.691 (s_ρ=0.009)

The benefit of simulation studies, of course, is that the parameters we are trying to estimate are known, and so our estimations can be evaluated. The parametric value ρ, and by extension R^2, can be determined by regression of Y on the *actual* ancestral values as determined by the simulations, which is precisely the vector quantity that the WY vectors are attempting to estimate. Calculated in this way, the parametric R^2 value indicates that the ancestral morphotypes of the last immediate ancestor of descendent species account for about 69% of the variance of extant species' Y values. The divergence-based autoregression method thus came closest to estimating the parametric R^2 value.

Reproduced with permission of the copyright owner. Further reproduction prohibited without permission.

Conclusions

The preceding analysis, together with similar findings of other recent studies, clearly demonstrate that the application of modern statistical techniques to cross-taxonomic data violates the assumption of observational independence, an occurrence that can lead to erroneous inferences regarding the hypothesized relationships among phenotypic traits. It was shown that several heretofore unrelated phylogenetic adjustment methods may in fact be regarded as belonging to one family. Specifically, all valid methods of restoring independence to the data—independent contrasts, nested ANOVA, and autoregression—are special cases of a general method (the ACP method), in which a multi-level phylogeny is collapsed into a single-level phylogeny. It was further shown, conceptually and analytically, that the nested ANOVA and autoregression methods can be viewed as (i.e. reduced to) techniques that estimate the ancestral morphotypes required of the ACP approach. The data produced by these methods represent an estimate of the degree of modification of a trait over a lineage from a specified ancestor to its extant descendent. Analyses employing the transformed data are thus inherently diachronic rather than synchronic in nature.

Consideration of the hypothesis testing reliability of the various nonindependence methods leads to the following assessments: (1) the nested ANCOVA method had a slightly higher Type I error rate and slightly lower statistical power compared to several forms of the autoregression method; (2) the rank-based and divergence-based inclusive autoregression methods with time-unstandardized residuals performed the best, having relatively low Type I error rates and relatively high statistical power. That the rank-based W matrix

Reproduced with permission of the copyright owner. Further reproduction prohibited without permission.

performed nearly as well as the divergence-based W matrix confirms earlier findings that the autoregression method is "...robust to inaccurate topological and branch length information" (Martins, 1996:1759; also see Gittleman & Kot, 1990; Gittleman & Luh, 1992, Purvis *et al.*, 1994). However, the divergence-based method was superior to the other autoregression methods in estimating the true parametric regression coefficient, or the proportion of variance of Y accounted for by the "phylogenetic component"; (3) the clade-based exclusive autoregression method using time-standardized residuals ranked among the best for Type I error, but it exhibited a slightly lower statistical power, and it overestimated the R^2 value of the phylogenetic effect.

When ancestral morphotypes are known the ACP method can restore independence to the data. This suggests that comparative analyses of cross-taxonomic data cannot proceed without reliable information about ancestral morphotypes, indicating that fossil specimens be included in nomological analyses. A method was outlined for the incorporation of fossil data into an ACP/autoregression approach.

The effectiveness of the time-unstandardized divergence-based autoregression method in both hypothesis testing and parametric estimation make it a clear choice for application in the current study. In the next chapter I apply this autoregression technique to the anthropoid data collected for this study.

Reproduced with permission of the copyright owner. Further reproduction prohibited without permission.

Chapter 7. Phylogenetic Effects: Application

Introduction

In the present chapter, I apply the divergence-based inclusive autoregression/ACP method (using time-unstandardized residuals) to the anthropoid data collected previously (see Chapter 5). The first step in this process was to establish a working phylogenetic hypothesis for the species included in the study sample. A W matrix was then constructed based on the phylogenetic hypothesis, and the raw data[1] were entered into the autoregression equation, as described in the previous chapter. Finally, some descriptive analyses were undertaken to compare the results obtained here with those of other similar studies, and to compare the raw data with the residuals obtained from the autoregression/ACP procedure.. The residuals, or "nonphylogenetic" component, from the autoregression/ACP procedure are analyzed in more detail in Chapter 8.

Anthropoid Phylogenetic Hypothesis

In order to account for the effects of ancestry on anthropoid craniofacial variation a working phylogenetic hypothesis must be specified. I shall not here review the extensive literature pertaining to anthropoid phylogeny, as this is beyond the scope of this investigation. However, to *justify* the phylogeny I adopted, a brief review of some of the major conclusions reached by others is given below.

The division of anthropoids into two major monophyletic clades—Platyrrhini (New World monkeys) and Catarrhini (Old World monkeys and apes)—is well

[1] The raw data were first "cleaned" by searching for and eliminating error outliers (see Chapter 8).

Reproduced with permission of the copyright owner. Further reproduction prohibited without permission.

established on genetic, phenotypic, paleontological and biogeographical evidence (see Szalay & Delson, 1979). The time of divergence of the common anthropoid ancestor into these two major clades has been estimated at about 40 MYA (Shoshani *et al.*, 1996). The origin of anthropoids is thought to have occurred at roughly 60 MYA.

Within Platyrrhini there is ample evidence to indicate that *Ateles*, *Brachyteles* and *Lagothrix* form a monophyletic group—Tribe Atelini, Gray, 1825 (Sarich & Cronin, 1976; Szalay & Delson, 1979; Rosenberger, 1984). Porter *et al.* (1995) have recently provided DNA sequence data that support earlier contentions (e.g. Szalay & Delson, 1979) of a sister-group relationship between *Brachyteles* and *Lagothirx* within Atelini. There is some dispute regarding the timing of the divergences involved. For example, Sarich and Cronin (1980) maintain that the lineages within Atelini began to diverge at about 5 MYA, whereas Rosenberger (1984) contends on paleontological grounds that the divergence was closer to 14 MYA. The genus *Alouatta* is the sister taxon to Atelini, and the four genera are together placed in the Subfamily Atelinae, Gray, 1825 (Szalay & Delson, 1979). The time of divergence of the lineage leading to *Alouatta* is also open to debate, with Sarich and Cronin (1980) placing the event at 10 MYA and Rosenberger (1984) double that at 20 MYA.

Several studies have demonstrated that *Pithecia*, *Chiropotes* and *Cacajao* also form a monophyletic group—Subtribe Pitheciina, Mivart 1865 (*cf.* Szalay & Delson, 1979)—with *Chiropotes* and *Cacajao* sharing a more recent common ancestor within Pitheciina (Sarich & Cronin, 1980; Rosenberger, 1984; Porter *et al.*, 1995). In this case, Sarich and Cronin (1980) and Rosenberger (1984) agree that the

Reproduced with permission of the copyright owner. Further reproduction prohibited without permission.

ancestor of *Pithecia* split from the *Chiropotes/Cacajoa* common ancestor at about 4-5 MYA. There is also wide agreement on the placement of *Callicebus* (Subtribe Callicebina, Pocock 1925) as a sister taxon to Pitheciina (Szalay & Delson, 1979; Rosenberger, 1981; Porter *et al.*, 1995; Shoshani *et al.*, 1996; Horovitz *et al.*, 1998; but for contra view see Ford, 1986). Callicebina and Pitheciina together form the Subfamily Pitheciinae, Mivart 1865 (Szalay & Delson, 1979; Shoshani *et al.*, 1996). Rosenberger (1984) argued that the ancestors of Callicebina and Pitheciina diverged about 25 MYA, and this view is supported by the reconstruction of relative branch lengths based on DNA sequence data (Porter *et al.*, 1995).

Evidence from a variety of sources, morphological and molecular, indicate that the two major Subfamilies Atelinae and Pitheciinae form a clade—classified under the Family Atelidae, Gray 1825 (Szalay & Delson, 1979; Rosenberger, 1981; Ford, 1986; Porter *et al.*, 1995; Shoshani *et al.*, 1996; Horovitz *et al.*, 1998). However, the time of divergence of the two Subfamilies has been under disputed. Once again, Rosenberger's estimate based on paleontological evidence (ca. 28 MYA) is nearly double that of Sarich and Cronin (ca. 17 MYA) whose estimate is based on molecular data.

A second major group of platyrrhines is classified under the Family Cebidae. Here again, there are some points of disagreement about the relationships among genera and at higher levels. Most agree that the genera *Callithrix* and *Cebuella* are sister taxa; indeed, Groves (1993) has argued that one species of *Cebuella* (*C. pygmaea*) should be subsumed under the genus *Callithrix*. *Callithrix* forms a clade with three other closely related neotropical primates—*Callimico*, *Leontopithecus* and *Saguinus*. Together these genera constitute the Subfamily Callitrichinae,

Reproduced with permission of the copyright owner. Further reproduction prohibited without permission.

Thomas 1903. Molecular evidence indicates that *Callithrix* is most closely related to *Callimico*, with *Leontopithecus* and *Saguinus* forming a sister clade (Sarich & Cronin, 1978, 1980; Porter *et al.*, 1995; Pastorini *et al.*, 1998); whereas morphological evidence suggests that *Callithrix* is closest to *Leontopithecus*, *Saguinus* and then *Callimico*, in that order (Rosenberger, 1981; Ford, 1986). Shoshani *et al.* (1996) were unable to resolve this dispute in a recent analysis. Here I use the topology given by Porter *et al.* (1995) and the estimated divergence times reported by Sarich and Cronin (1978).

The systematic placement of the platyrrhine genera *Aotus*, *Cebus* and *Saimiri* has been the subject of dispute. Rosenberger (1981) places *Aotus* within the Pitheciinae, and *Cebus* and *Saimiri* as a subfamily within Cebidae. Porter *et al.* (1995) position all three genera within Cebidae as equidistant sister-taxa to Callitrichinae. Ford (1986) established two new subfamily groups to accommodate these taxa which she views as separate from both the atelids and callitrichines. Several studies support the notion of a clade comprised of *Cebus* and *Saimiri* (Subfamily Cebinae, Bonaparte 1831) situated within Cebidae (Szalay & Delson, 1979; Baba *et al.*, 1980; Rosenberger, 1981; Harada *et al.*, 1995; Shoshani *et al.*, 1996; Horovitz *et al.*, 1998). The divergence of these two genera from a common ancestor is estimated by Sarich and Cronin (1978) to have occurred around 17 MYA, but estimated branch lengths based on nucleotide sequencing data (Porter *et al.*, 1995) support Rosenberger's (1981) interpretation of the paleontological evidence for an earlier divergence, ca. 25 MYA. There is also lack of agreement on the systematic placement of *Aotus* (*cf.* Hugot, 1998). Szalay and Delson (1979) and Rosenberger (1981) place *Aotus* in the subfamily Pitheciinae in the Family Atelidae,

Reproduced with permission of the copyright owner. Further reproduction prohibited without permission.

but Shoshani *et al.* (1996), who conducted a more comprehensive study, assign *Aotus* to the Family Cebidae. Porter *et al.* (1995) also place *Aotus* in the Family Cebidae, and, in addition, provide evidence to link this genus to the Cebinae. There is general agreement that the lineage leading to *Aotus* is about as old as those leading to *Cebus* and *Saimiri* (Sarich & Cronin, 1978; Rosenberger, 1984; Porter *et al.*, 1995).

The Catarrhini are divided into two major clades at the Superfamily level—Cercopithecoidea (Old World monkeys) and Hominoidea (apes). The cercopithecoids are further divided into two subfamilies—Colobinae (the leaf-eating monkeys) and Cercopithecinae (the cheek pouch monkeys).

In a recent review of the evolutionary history of Colobinae, Delson (1994) provided a tentative phylogeny for this group, which may be summarized as follows. Sometime during the middle Miocene (ca. 13 MYA) the common ancestor of colobines gave rise to two major subgroups, the African colobines (Subtribe Colobina, Blyth 1875) and the Eurasian colobines (Subtribe Presbytina, Gray 1825). African colobus monkeys are classified into two genera—*Colobus* and *Procolobus*—whose ancestors diverged from a common form during the late Pliocene (ca. 2-3 MYA). In Eurasia, colobus monkeys are divided into three main groups. One is composed of members of the genus *Pygathrix*, which includes the subgenera *Pygathrix* and *Rhinopithecus*. A second includes two species of the genus *Nasalis*. And a third is made up of three genera, *Presbytis*, *Semnopithecus*, and *Trachypithecus*, with the latter two forming a clade within this group. Divergence times are not well known, but Delson (1994) estimated that the three main groups of Eurasian colobus monkeys became distinct sometime during the mid-Pliocene.

Reproduced with permission of the copyright owner. Further reproduction prohibited without permission.

The other major group of Old World monkeys, the cercopithecinae, is a large one composed of many genera. Mitochondrial DNA analysis by Disotell *et al.* (1992) has confirmed earlier immunological work by Cronin and Sarich (1976) in placing *Papio* and *Theropithecus* together in a monophyletic clade (contra Strasser & Delson, 1987, but see Delson, 1992). The mangabeys, close relatives to the baboons, are probably not monophyletic as once assumed. Both morphological (Groves, 1978; Strasser & Delson, 1987) and molecular (Cronin & Sarich, 1976; Dutrillaux, 1979) data indicate that the mangabey genus *Lophocebus* is a sister group of the *Papio/Theropithecus* clade. The other mangabey genus, *Cercocebus*, has recently been aligned with the genus *Mandrillus*. These genera compose the Subtribe Papionina, Burnett 1828 (Szalay & Delson, 1979). The chronology of speciation events for the Papionina are sketchy at best, but can be outlined as follows: (1) *Theropithecus-Papio* divergence at ca. 4 MYA, (2) *Lophocebus* split from *Theropithecus-Papio* ancestor at ca. 5 MYA, (3) *Cercocebus-Mandrillus* ancestor diverged from *Theropithecus-Papio-Lophocebus* ancestor ca. 6 MYA (Cronin & Sarich, 1976; Delson, 1992).

The Subtribe Macacina, which contains all members of the genus *Macaca*, forms a sister group to the Papionina (Goodman & Moore, 1971; Szalay & Delson, 1979; Disotell *et al.*, 1992). The ancestors of these two clades diverged sometime between 8 to 6 MYA (Delson, 1980; 1992). The relationships among species of living macaques have not been clearly established, but several attempts have been made to understand the genealogy of this group. In one interpretation, macaques are divided into four main groups, one in northern Africa (the "sylvanus" group) and three in Asia (the "fascicularis," "silenus," and "sinica" groups) (Fooden, 1980;

Reproduced with permission of the copyright owner. Further reproduction prohibited without permission.

Delson, 1980). This interpretation has been largely supported, with a few alterations, in a recent study using high-resolution restriction site mapping of mitochondrial ribosomal genes (Morales & Melnick, 1998). Divergence of species within the Asian groups likely occurred during the early to middle Pleistocene, while the major groups themselves differentiated in the latter part of the Miocene (Nozawa *et al.*, 1977; Cronin *et al.*, 1980; Delson, 1980).

In addition to Papionina and Macacina, the cercopithecinae include a third subtribe, Cercopithecina, which includes the guenon monkeys, genus *Cercopithecus*, and several related forms, including *Allenopithecus*, *Miopithecus*, *Erythrocebus*, and *Chlorocebus* (Szalay & Delson, 1979; Delson, 1992). The guenons are a closely related group of African monkeys having evolved only in the last one or two million years (Kingdon, 1974). Their genealogy is not only disputed, it is unclear as to how many true species of the genus exist. For example, Struhsaker (1988) has reported observing hybridization between *Cercopithecus ascanius* and *C. mitis* in the Kabale Forest, Uganda. It is also unclear at this time how the other genera of cercopithecina are related to the guenons (Delson, 1992).

Compared to other anthropoid groups the phylogeny of the Superfamily Hominoidea is relatively well established. Hominoids last shared a common ancestor with cercopithecoids around 25 MYA (Gingerich, 1984). The ancestors of living *Hylobates* and *Pongo* were the first to branch off from the hominoid line at around 20 MYA and 15 MYA, respectively (Andrews & Martin, 1987). Evidence from a variety of sources over the last twenty years has demonstrated a close relationship among *Gorilla*, *Pan* and *Homo* (*cf.* Goodman *et al.*, 1982). The majority of the evidence at this time favors a sister-group relationship between

Reproduced with permission of the copyright owner. Further reproduction prohibited without permission.

chimps and humans, to the exclusion of the gorilla (Maeda, 1988; Koop *et al.*, 1989; Goodman *et al.*, 1990; 1994; Saitou, 1991; Shoshani *et al.*, 1996). The gorilla ancestor is estimated to have split from the chimp-human clade sometime around 9 MYA (Sibley, 1992), and the estimated divergence of the chimp and "human" lines is set around 5.5 MYA. Here I employ the classification proposed by Goodman *et al.* (1990), which names the *Gorilla-Pan-Homo* clade Tribe Hominini, and the *Pan-Homo* clade Subtribe Hominina.

From the foregoing, a working phylogenetic hypothesis was devised for the 37 anthropoid species included in this study (see Box 7.1). One of the advantages of the divergence-based inclusive autoregression method is that it is fairly robust to phylogenetic inaccuracies as long as the main branches of the phylogeny are well established (Martins, 1996). Since all of the species included in the sample contribute to some degree to the estimation of the ancestral morphotypes, errors due to misspecification of sister-taxa relations only bias a proportion of the estimate. Therefore, if several of the relationships and divergence times specified in the phylogeny adopted here should turn out to be inaccurate, this would not necessarily invalidate the analyses.

Application of the Autoregression Method to the Sample Data

With the specification of a working phylogeny, the next step was to construct a W matrix of interspecific relationships to be used in the autoregression equation, which you will recall is expressed as:

$$Y = \rho WY + \epsilon \qquad (7.1)$$

Based on the phylogenetic simulation results of the previous chapter, I

Reproduced with permission of the copyright owner. Further reproduction prohibited without permission.

choose to apply the divergence-based W matrix of Lynch (1991) in the autoregression equation. The non-row-normalized version of this W matrix is reproduced in Box 7.2, with species row and column labels added for reference. As per the simulation procedures, the W matrix was row-normalized prior to matrix multiplication with the Y variable vectors. The vector terms Y and WY were both standardized to zero mean and unit variance prior to running the autoregression. The residual variates represent the estimated accumulated change in a given trait (Y), expressed in variance units, for a given species from the origin of the ancestral lineage of that species (LSA) to the present, relative to the other ancestral lineages represented in the working phylogeny.[2]

[2] Henceforth I will use the following shorthand terms: *Last Shared Ancestor* (LSA) for the last common ancestor of a given extant species shared with one or more other species in the sample; *Extant lineage* or *Post-LSA*, for the lineage extending from a given extant species back to its LSA; *Ancestral lineage* or *Pre-LSA*, for the lineage extending from a given LSA to the last common ancestor of the entire sample group.

Reproduced with permission of the copyright owner. Further reproduction prohibited without permission.

Box 7.1. Working anthropoid phylogeny used to construct relationship (W) matrix for phylogenetic autoregression application.

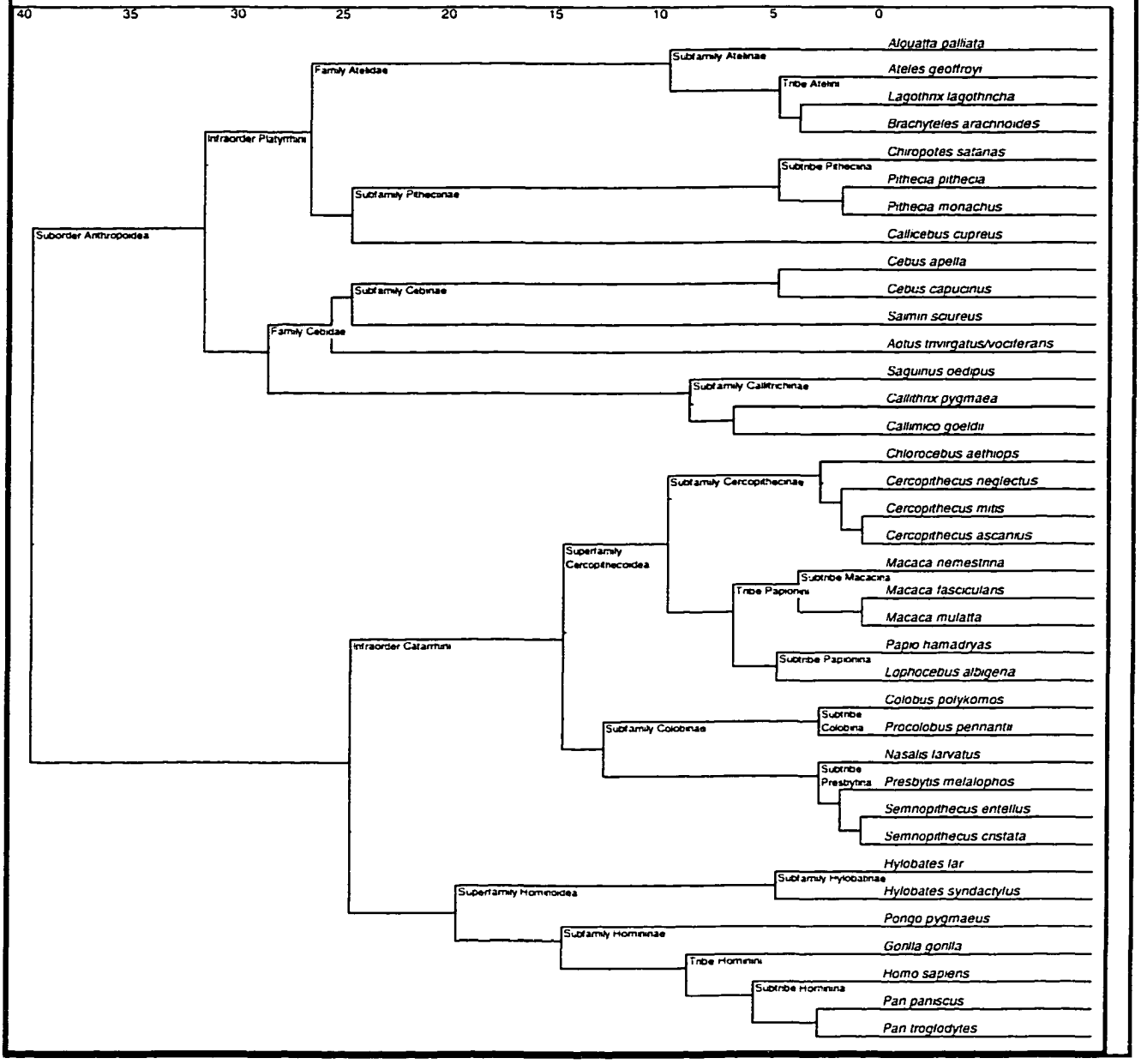

Reproduced with permission of the copyright owner. Further reproduction prohibited without permission.

Box 7.2. W matrix of interspecies relationships based on anthropoid working phylogeny (Box 7.1) after method proposed by Lynch (1991).

	Alouatta palliata	*Ateles geoffroyi*	*Lagothrix lagothricha*	*Brachyteles arachnoides*	*Chiropotes satanas*	*Pithecia pithecia*	*Pithecia monachus*	*Callicebus cupreus*	*Cebus apella*	*Cebus capucinus*	*Saimiri sciureus*	*Aotus trivirgatus/vociferans*	*Saguinus oedipus*	*Callithrix pygmaea*	*Callimico goeldii*	*Chlorocebus aethiops*	*Cercopithecus neglectus*	*Cercopithecus mitis*	*Cercopithecus ascanius*
Alouatta palliata	1.0	.83	.83	.83	.55	.55	.55	.55	.47	.47	.47	.47	.47	.47	.47	.17	.17	.17	.17
Ateles geoffroyi	.83	1.0	.92	.92	.55	.55	.55	.55	.47	.47	.47	.47	.47	.47	.47	.17	.17	.17	.17
Lagothrix lagothricha	.83	.92	1.0	.93	.55	.55	.55	.55	.47	.47	.47	.47	.47	.47	.47	.17	.17	.17	.17
Brachyteles arachnoides	.83	.92	.93	1.0	.55	.55	.55	.55	.47	.47	.47	.47	.47	.47	.47	.17	.17	.17	.17
Chiropotes satanas	.55	.55	.55	.55	1.0	.92	.92	.58	.47	.47	.47	.47	.47	.47	.47	.17	.17	.17	.17
Pithecia pithecia	.55	.55	.55	.55	.92	1.0	.97	.58	.47	.47	.47	.47	.47	.47	.47	.17	.17	.17	.17
Pithecia monachus	.55	.55	.55	.55	.92	.97	1.0	.42	.47	.47	.47	.47	.47	.47	.47	.17	.17	.17	.17
Callicebus cupreus	.55	.55	.55	.55	.58	.58	.42	1.0	.47	.47	.47	.47	.47	.47	.47	.17	.17	.17	.17
Cebus apella	.47	.47	.47	.47	.47	.47	.47	.47	1.0	.92	.58	.57	.52	.52	.52	.17	.17	.17	.17
Cebus capucinus	.47	.47	.47	.47	.47	.47	.47	.47	.92	1.0	.58	.57	.52	.52	.52	.17	.17	.17	.17
Saimiri sciureus	.47	.47	.47	.47	.47	.47	.47	.47	.58	.58	1.0	.57	.52	.52	.52	.17	.17	.17	.17
Aotus trivirgatus/vociferans	.47	.47	.47	.47	.47	.47	.47	.47	.57	.57	.57	1.0	.52	.52	.52	.17	.17	.17	.17
Saguinus oedipus	.47	.47	.47	.47	.47	.47	.47	.47	.52	.52	.52	.52	1.0	.85	.85	.17	.17	.17	.17
Callithrix pygmaea	.47	.47	.47	.47	.47	.47	.47	.47	.52	.52	.52	.52	.85	1.0	.88	.17	.17	.17	.17
Callimico goeldii	.47	.47	.47	.47	.47	.47	.47	.47	.52	.52	.52	.52	.85	.88	1.0	.17	.17	.17	.17
Chlorocebus aethiops	.17	.17	.17	.17	.17	.17	.17	.17	.17	.17	.17	.17	.17	.17	.17	1.0	.95	.95	.95
Cercopithecus neglectus	.17	.17	.17	.17	.17	.17	.17	.17	.17	.17	.17	.17	.17	.17	.17	.95	1.0	.97	.97
Cercopithecus mitis	.17	.17	.17	.17	.17	.17	.17	.17	.17	.17	.17	.17	.17	.17	.17	.95	.97	1.0	.98
Cercopithecus ascanius	.17	.17	.17	.17	.17	.17	.17	.17	.17	.17	.17	.17	.17	.17	.17	.95	.97	.98	1.0
Macaca nemestrina	.17	.17	.17	.17	.17	.17	.17	.17	.17	.17	.17	.17	.17	.17	.17	.83	.83	.83	.83
Macaca fascicularis	.17	.17	.17	.17	.17	.17	.17	.17	.17	.17	.17	.17	.17	.17	.17	.83	.83	.83	.83
Macaca mulatta	.17	.17	.17	.17	.17	.17	.17	.17	.17	.17	.17	.17	.17	.17	.17	.83	.83	.83	.83
Papio hamadryas	.17	.17	.17	.17	.17	.17	.17	.17	.17	.17	.17	.17	.17	.17	.17	.83	.83	.83	.83
Lophocebus albigena	.17	.17	.17	.17	.17	.17	.17	.17	.17	.17	.17	.17	.17	.17	.17	.83	.83	.83	.83
Colobus polykomos	.17	.17	.17	.17	.17	.17	.17	.17	.17	.17	.17	.17	.17	.17	.17	.75	.75	.75	.75
Procolobus pennantii	.17	.17	.17	.17	.17	.17	.17	.17	.17	.17	.17	.17	.17	.17	.17	.75	.75	.75	.75
Nasalis larvatus	.17	.17	.17	.17	.17	.17	.17	.17	.17	.17	.17	.17	.17	.17	.17	.75	.75	.75	.75
Presbytis melalophos	.17	.17	.17	.17	.17	.17	.17	.17	.17	.17	.17	.17	.17	.17	.17	.75	.75	.75	.75
Semnopithecus entellus	.17	.17	.17	.17	.17	.17	.17	.17	.17	.17	.17	.17	.17	.17	.17	.75	.75	.75	.75
Semnopithecus cristata	.17	.17	.17	.17	.17	.17	.17	.17	.17	.17	.17	.17	.17	.17	.17	.75	.75	.75	.75
Hylobates lar	.17	.17	.17	.17	.17	.17	.17	.17	.17	.17	.17	.17	.17	.17	.17	.58	.58	.58	.58
Hylobates syndactylus	.17	.17	.17	.17	.17	.17	.17	.17	.17	.17	.17	.17	.17	.17	.17	.58	.58	.58	.58
Pongo pygmaeus	.17	.17	.17	.17	.17	.17	.17	.17	.17	.17	.17	.17	.17	.17	.17	.58	.58	.58	.58
Gorilla gorilla	.17	.17	.17	.17	.17	.17	.17	.17	.17	.17	.17	.17	.17	.17	.17	.58	.58	.58	.58
Homo sapiens	.17	.17	.17	.17	.17	.17	.17	.17	.17	.17	.17	.17	.17	.17	.17	.58	.58	.58	.58
Pan paniscus	.17	.17	.17	.17	.17	.17	.17	.17	.17	.17	.17	.17	.17	.17	.17	.58	.58	.58	.58
Pan troglodytes	.17	.17	.17	.17	.17	.17	.17	.17	.17	.17	.17	.17	.17	.17	.17	.58	.58	.58	.58

Reproduced with permission of the copyright owner. Further reproduction prohibited without permission.

Box 7.2. Continued.

	Macaca nemestrina	*Macaca fascicularis*	*Macaca mulatta*	*Papio hamadryas*	*Lophocebus albigena*	*Colobus polykomos*	*Procolobus pennantii*	*Nasalis larvatus*	*Presbytis melalophos*	*Semnopithecus entellus*	*Semnopithecus cristata*	*Hylobates lar*	*Hylobates syndactylus*	*Pongo pygmaeus*	*Gorilla gorilla*	*Homo sapiens*	*Pan paniscus*	*Pan troglodytes*
Alouatta palliata	.17	.17	.17	.17	.17	.17	.17	.17	.17	.17	.17	.17	.17	.17	.17	.17	.17	.17
Ateles geoffroyi	.17	.17	.17	.17	.17	.17	.17	.17	.17	.17	.17	.17	.17	.17	.17	.17	.17	.17
Lagothrix lagothricha	.17	.17	.17	.17	.17	.17	.17	.17	.17	.17	.17	.17	.17	.17	.17	.17	.17	.17
Brachyteles arachnoides	.17	.17	.17	.17	.17	.17	.17	.17	.17	.17	.17	.17	.17	.17	.17	.17	.17	.17
Chiropotes satanas	.17	.17	.17	.17	.17	.17	.17	.17	.17	.17	.17	.17	.17	.17	.17	.17	.17	.17
Pithecia pithecia	.17	.17	.17	.17	.17	.17	.17	.17	.17	.17	.17	.17	.17	.17	.17	.17	.17	.17
Pithecia monachus	.17	.17	.17	.17	.17	.17	.17	.17	.17	.17	.17	.17	.17	.17	.17	.17	.17	.17
Callicebus cupreus	.17	.17	.17	.17	.17	.17	.17	.17	.17	.17	.17	.17	.17	.17	.17	.17	.17	.17
Cebus apella	.17	.17	.17	.17	.17	.17	.17	.17	.17	.17	.17	.17	.17	.17	.17	.17	.17	.17
Cebus capucinus	.17	.17	.17	.17	.17	.17	.17	.17	.17	.17	.17	.17	.17	.17	.17	.17	.17	.17
Saimiri sciureus	.17	.17	.17	.17	.17	.17	.17	.17	.17	.17	.17	.17	.17	.17	.17	.17	.17	.17
Aotus trivirgatus/vociferans	.17	.17	.17	.17	.17	.17	.17	.17	.17	.17	.17	.17	.17	.17	.17	.17	.17	.17
Saguinus oedipus	.17	.17	.17	.17	.17	.17	.17	.17	.17	.17	.17	.17	.17	.17	.17	.17	.17	.17
Callithrix pygmaea	.17	.17	.17	.17	.17	.17	.17	.17	.17	.17	.17	.17	.17	.17	.17	.17	.17	.17
Callimico goeldii	.17	.17	.17	.17	.17	.17	.17	.17	.17	.17	.17	.17	.17	.17	.17	.17	.17	.17
Chlorocebus aethiops	.83	.83	.83	.83	.83	.75	.75	.75	.75	.75	.75	.58	.58	.58	.58	.58	.58	.58
Cercopithecus neglectus	.83	.83	.83	.83	.83	.75	.75	.75	.75	.75	.75	.58	.58	.58	.58	.58	.58	.58
Cercopithecus mitis	.83	.83	.83	.83	.83	.75	.75	.75	.75	.75	.75	.58	.58	.58	.58	.58	.58	.58
Cercopithecus ascanius	.83	.83	.83	.83	.83	.75	.75	.75	.75	.75	.75	.58	.58	.58	.58	.58	.58	.58
Macaca nemestrina	1.0	.93	.93	.88	.88	.75	.75	.75	.75	.75	.75	.58	.58	.58	.58	.58	.58	.58
Macaca fascicularis	.93	1.0	.98	.88	.88	.75	.75	.75	.75	.75	.75	.58	.58	.58	.58	.58	.58	.58
Macaca mulatta	.93	.98	1.0	.88	.88	.75	.75	.75	.75	.75	.75	.58	.58	.58	.58	.58	.58	.58
Papio hamadryas	.88	.88	.88	1.0	.92	.75	.75	.75	.75	.75	.75	.58	.58	.58	.58	.58	.58	.58
Lophocebus albigena	.88	.88	.88	.92	1.0	.75	.75	.75	.75	.75	.75	.58	.58	.58	.58	.58	.58	.58
Colobus polykomos	.75	.75	.75	.75	.75	1.0	.95	.78	.78	.78	.78	.58	.58	.58	.58	.58	.58	.58
Procolobus pennantii	.75	.75	.75	.75	.75	.95	1.0	.78	.78	.78	.78	.58	.58	.58	.58	.58	.58	.58
Nasalis larvatus	.75	.75	.75	.75	.75	.78	.78	1.0	.95	.95	.95	.58	.58	.58	.58	.58	.58	.58
Presbytis melalophos	.75	.75	.75	.75	.75	.78	.78	.95	1.0	.97	.97	.58	.58	.58	.58	.58	.58	.58
Semnopithecus entellus	.75	.75	.75	.75	.75	.78	.78	.95	.97	1.0	.98	.58	.58	.58	.58	.58	.58	.58
Semnopithecus cristata	.75	.75	.75	.75	.75	.78	.78	.95	.97	.98	1.0	.58	.58	.58	.58	.58	.58	.58
Hylobates lar	.58	.58	.58	.58	.58	.58	.58	.58	.58	.58	.58	1.0	.92	.67	.67	.67	.67	.67
Hylobates syndactylus	.58	.58	.58	.58	.58	.58	.58	.58	.58	.58	.58	.92	1.0	.67	.67	.67	.67	.67
Pongo pygmaeus	.58	.58	.58	.58	.58	.58	.58	.58	.58	.58	.58	.67	.67	1.0	.75	.75	.75	.75
Gorilla gorilla	.58	.58	.58	.58	.58	.58	.58	.58	.58	.58	.58	.67	.67	.75	1.0	.85	.85	.85
Homo sapiens	.58	.58	.58	.58	.58	.58	.58	.58	.58	.58	.58	.67	.67	.75	.85	1.0	.90	.90
Pan paniscus	.58	.58	.58	.58	.58	.58	.58	.58	.58	.58	.58	.67	.67	.75	.85	.90	1.0	.95
Pan troglodytes	.58	.58	.58	.58	.58	.58	.58	.58	.58	.58	.58	.67	.67	.75	.85	.90	.95	1.0

Reproduced with permission of the copyright owner. Further reproduction prohibited without permission.

The average autoregression slope estimate over all variables was 0.67, and so the overall coefficient of determination (R^2), a measure of the proportion of the total variation that can be explained by ancestral effects, was 0.45. This value is very close to the values obtained by Cheverud *et al.* (1985) in their phylogenetic rank-based autoregression analysis of several phenotypic and ecological traits among primate families. These authors reported the following R^2 estimates: sexual dimorphism, 0.47; body size, 0.45; mating system, 0.38; habitat, 0.32. Cheverud *et al.*'s estimated R^2 for body size (0.45) is remarkably similar to the value obtained here for body weight (0.46), and both are consistent with the R^2 values reported for the phylogenetic effects on carnivoran body weight (Nowak & Paradiso, 1983: 0.46; Wayne *et al.*, 1989: 0.43). Even the body size of some species of birds appear to be affected by phylogeny to the same degree, as demonstrated by the phylogenetic R^2 reported for the Grey-crowned Babble *Pomatostomus* (Edwards & Kot, 1995: 0.46).

Of the 94 morphometric variables studied, only 7 yielded phylogenetic R^2 values under 0.25. These include: 'Enlow's angle of facial prognathism' [Y31-ENLOAG], 'olfactory bulb volume' [Y43-OFBVOL], 'inclination of the foramen magnum' [Y68-SLOPFM], 'Enlow's cribriform plate-midfacial plane angle' [Y71-ENLWCP], 'inclination of the cribriform plate relative to the Frankfurt Horizontal' [Y74-SLPCPF], 'inclination of the cribriform plate relative to the occlusal plane' [Y75-SLPCPO], and 'relative anterior cranial fossa length' [Y79-ACFLGT]. It is of interest to note that 5 of the 7 variables with R^2 values below 0.25 are related to the olfactory apparatus in some way.

To interpret these results we must answer the question: What is the meaning of R^2 in the context of phylogenetic autoregression? The answer depends on

Reproduced with permission of the copyright owner. Further reproduction prohibited without permission.

whether individual measurements are used as the basic unit of analysis or species (or higher-taxonomic level) means are used as the basic unit of analysis. You may recall that the *linear* regression R^2 is equivalent to the ratio of the among-groups variance to the total variance (Pedhazur, 1997), which in quantitative genetics is used as a measure of heritability. According to Cheverud *et al.* (1985:1347), "Values of R^2 ... represent the proportion of variance among primates that is due to phylogenetic relationships... and is thus the cross-species 'heritability.'" I contend that such an interpretation is only valid when the *groups* being analyzed are at the species or population level, and, consequently, the within-groups unit of analysis (i.e. the input data) is at the individual level. In comparative analysis, just as in experimental analysis, the only way to isolate environmental causes of phenotypic variation is to analyze the variance among individual organisms that are genetically homogeneous. Therefore, autoregression or ANOVA methods that use species (or higher taxonomic) means as input data do not produce R^2 values that isolate an "environmental" component of the overall variance. I will have more to say on this topic in the context of analytical techniques in Chapter 8.

Edwards and Kot (1995) interpreted Babbler songbird traits having low R^2 values (such as tarsus length) as being "more labile" (p. 1141) than traits exhibiting higher coefficients of determination (such as wing length). Although their interpretation is valid in an analysis involving among- and within-species or population variance, it is not valid when higher taxonomic means are used as the within-groups unit of analysis. When species mean values are used as the basic unit of analysis for isolating phylogenetic affects (as they are here and in most other autoregression studies), the following ratio applies:

Reproduced with permission of the copyright owner. Further reproduction prohibited without permission.

$$R^2 = (\sigma_{\text{pre-LSAM}}) / ((\sigma_{\text{pre-LSAM}}) + (\sigma_{\text{post-LSAM}})) \quad (7.2)$$

where $\sigma_{\text{pre-LSAM}}$ is the total variance accumulated from the origin of the study group to the last shared ancestral morphotypes (LSAMs), and $\sigma_{\text{post-LSAM}}$ is the total variance accumulated from the LSAMs to the extant species phenotype. Thus, traits with relatively low autoregression R^2 are those that exhibit a relatively high post-to-pre-LSAM ratio.

What processes produce such a high degree of variation in extant lineages compared to ancestral lineages? The answer, I propose, lies in the following paradox: most phylogenies exhibit the property that extant lineages are relatively short-lived compared to the long time-span traversed by ancestral lineages. For example, the average extant lineage length for the 37 species of anthropoids is only 6.5 million years, which is rather short compared to the average pre-LSA ancestral lineage length of 53.5 million years. It seems reasonable to assume that, given a stochastic model of genetic and phenotypic modification, more variation will accumulate over the ancestral lineages than will accumulate over the extant lineages, leading to high phylogenetic R^2 values. However, there is one type of trait that, paradoxically, could have the opposite effect under certain conditions. Traits that have a tendency to fluctuate randomly could appear to change little when measured over a long period, but could chance to modify significantly over the short run.

If the autoregression procedure was successful then the residuals will have the following properties: (1) they will represent independent data points, and (2) they will represent the total accumulated (genetic) change, in variance units, from the last shared ancestor to a given extant species (i.e., over each extant lineage). In Chapter 8, I show how the phylogenetic autoregression residuals can be used to

Reproduced with permission of the copyright owner. Further reproduction prohibited without permission.

create a multi-level data set whose structural relations provide the empirical evidence required to test nomological distal causal models.

An Illustrated Example of the Autoregression/ACP Technique

To better illustrate how the autoregression/ACP technique partitions ancestral effects from the data and concomitantly restores independence to the data points, I examine the covariance relationship between two traits before and after the procedure. The two traits that will serve as example are: (1) Enlow's olfactory bulb angle [Y72-ENLWOB], which is the angle of the olfactory apparatus relative to the mid-facial plane, and (2) palatal depth at P^3 [Y25-P3PALD]. I purposefully selected two traits that would not be expected to covary in any way. There is no *a priori* theoretical justification for predicting a relationship between these two traits. However, a glance at Box 7.3 shows the opposite. When ENLWOB is regressed against P3PALD using the log of the raw data, the regression coefficient (-0.73) is significant at the $p < .0001$ level. A closer examination of the scatter plot in Box 7.3 reveals that most of the data points occupying the upper left quadrant of the graph represent catarrhines (■), whereas most of the points in the lower right quadrant represent platyrrhines (+). The slope of the regression line is therefore an artifact of the differences between these two major groups, and it is not an indication of an association between the two traits among 37 independent data points. This is a classic example of phylogenetic effects causing a Type I error (a similar example was given in Chapter 6, Boxes 6.1 and 6.2).

Reproduced with permission of the copyright owner. Further reproduction prohibited without permission.

Box 7.4 shows the scatter plot of the same two traits, but this time using the log of the residuals from the divergence-based autoregression procedure. The regression coefficient (-0.22) has an associated *p*-value of 0.09, which is not significant at the 0.05 level. It can be seen that the data points for catarrhines and platyrrhines now more or less overlap. In this particular instance the divergence-based autoregression method successfully partitioned out the phylogenetic component from the data.

Box 7.3. Regression of two traits using log raw data.

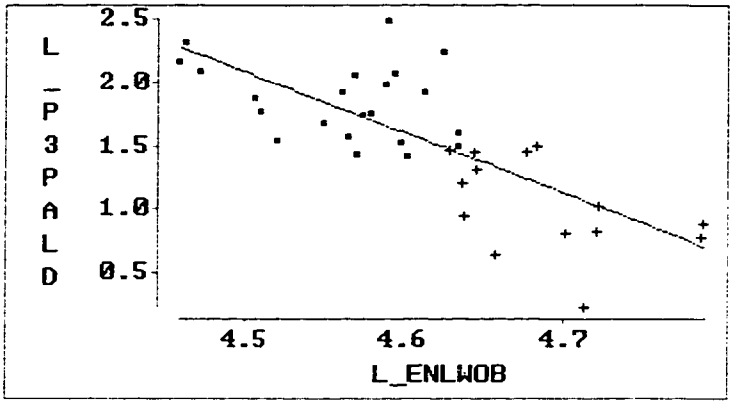

Box 7.4. Regression of two traits using log transformed phylogenetic autoregression residuals.

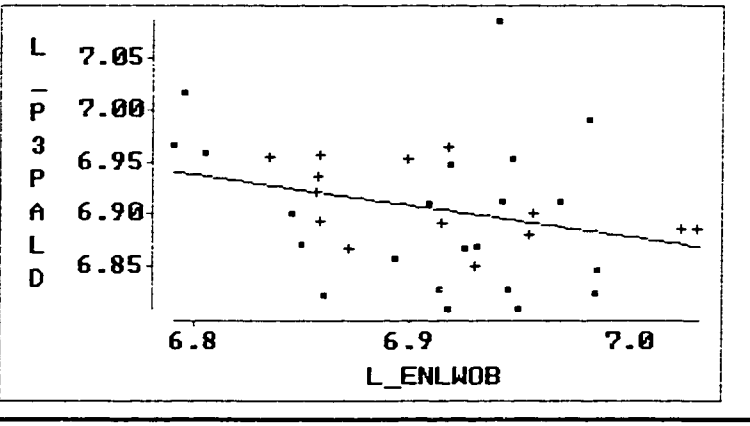

Reproduced with permission of the copyright owner. Further reproduction prohibited without permission.

Conclusions

In this chapter a working anthropoid phylogenetic hypothesis was presented (Box 7.1) and justified. The phylogeny was used to construct a W matrix essential for the application of the autoregression/ACP procedure described in Chapter 6. The results of this procedure were consistent with those of previous studies. It was found, for example, that the average regression slope was 0.67, and that the average proportion of variance accounted for by ancestry was 45%.

In the next Chapter, I demonstrate how the residuals obtained from an alpha-level phylogenetic autoregression procedure can be used in a multi-level covariance structural analysis to test hypotheses regarding the nomological causal mechanisms responsible for anthropoid nasomaxillary diversity.

Reproduced with permission of the copyright owner. Further reproduction prohibited without permission.

Chapter 8. Data Analysis Techniques and Assumptions

Introduction

Pierre Simon Laplace (1749-1827), a close colleague of George Cuvier, and one of France's most illustrious mathematicians and scientists at the turn of the nineteenth century, is well known for having solved one of the most vexing problems in the history of celestial mechanics. For over a century, attempts by astronomers to explain the observed fluctuations in the orbital motions of Saturn and Jupiter repeatedly met with failure. It was not until Laplace (1787) applied what was then a newly devised analytical technique—linear multivariate analysis—did a solution compatible with Newtonian gravitational theory reveal itself.[1] Stigler (1986:31-32) wrote of Laplace's discovery: "Laplace's success in this celebrated problem was in considerable part a statistical triumph, a model of the ways in which analyses of data suggested by theory may in turn suggest hypotheses requiring further theoretical development and then observational confirmation." There have been countless other instances in the history of science, some well known but many not, in which advancements were made only after the implementation of a novel analytical perspective or technique (e.g., Galton, 1886). Phenomenological patterns resulting from natural processes are often hidden deep within observational data, and reliance on mathematics to reveal these hidden patterns is part of modern science. Nevertheless, problems can arise because most modern analytical techniques are

[1] For a fascinating chronicle of Laplace's professional life revolving around the Paris Académie des Sciences see Hahn, 1971, and, for a detailed analysis of Laplace's mathematical contributions see Stigler, 1986.

Reproduced with permission of the copyright owner. Further reproduction prohibited without permission.

based on assumptions regarding the properties of the data; assumptions that are often not met. Interpretations of statistical results must be based on many considerations, foremost among them is their meaningfulness. The purpose of this chapter is to illustrate how the data employed in this study were prepared for analyses, and to describe the analytical approach (along with its attendant assumptions) used to test nomological distal hypotheses concerning anthropoid nasomaxillary diversity.

Data Preparation

Four phases of data preparation and transformation were undertaken in the present study. The first phase involved data cleaning, and identification of error outliers. The second phase involved transformation of the data to remove ancestral evolutionary effects using the phylogenetic autoregression/alpha ACP method. In the third phase the phylogenetically adjusted individual level data were partitioned into among-species (i.e., autoregression residuals) and within-species components in order to produce multi-level data sets. The multi-level data sets were used in the majority of subsequent multivariate analyses. Finally, phase four dealt with transformation of the data to better satisfy the assumptions of the analytical techniques used in this study. I list the four phases of data preparation at the outset so that the reader will have a clear understanding of the order in which they were performed. The remainder of this chapter is organized logically by concept rather than chronologically by task, and so the various data transformations appear out of their proper sequence.

I begin with a discussion on the construction and analysis of multi-level data

Reproduced with permission of the copyright owner. Further reproduction prohibited without permission.

sets, and the usefulness of this technique in comparative and evolutionary biology. I then show how multi-level analysis is compatible with the general linear model by integrating it with multiple regression analysis. Next, I reveal the asymmetrical relationship between statistical and theoretical inference, and show how a structured form of multi-level regression—multi-level covariance structure analysis—is compatible with this dynamic and permits the testing of nomological hypotheses involving multiple causal pathways operating at different levels.

Constructing Multi-Level Data Sets

In this section I illustrate graphically how the raw morphometric data were transformed into multiple data sets that were subsequently used in multivariate analyses and hypothesis testing. For simplicity, I show the transformation of only one variable—maxillary arch length [Y14-MXARCL]—but it should be kept in mind that each of the eighty-five morphometric variables listed in Appendix B underwent a similar transformation. MXARCL is measured as the linear distance (in the xz plane) between prosthion and alveolon (see Box 5.3B).

The first step in preparing the data was to calculate a vector of raw species means, which I shall denote as Y_m. A phylogenetic autoregression was then run using a row-normalized inclusive divergence-based W matrix (given in Box 7.2). The equation for the autoregression is:

$$Y_m = \rho W Y_m + \epsilon_m \qquad (8.1)$$

Recall that vectors Y_m and WY_m are standardized prior to autoregression.

Two important new vectors were produced from the autoregression procedure: (1) a vector of standardized predicted Y_m scores (Y'_m), and (2) a vector

Reproduced with permission of the copyright owner. Further reproduction prohibited without permission.

of standardized residuals (ϵ_m). The Y'_m scores represent the estimated last shared ancestral (LSA) values of Y ($Y'_m = Y_{LSA}$). The raw individual specimen values of maxillary arch length (Y_i), the raw species means (Y_m), and the estimated last shared ancestral morphotypes (Y_{LSA}) are depicted graphically in the phenogram in Box 8.1. The lineages connecting the ancestral nodes (bottom tips of lines) with extant species (top tips of lines along horizontal dotted line) have been drawn in proportion to their lengths, as estimated from the working hypothesis shown in Box 7.1. Other lineages could have been drawn; for example, the lineage connecting the *Pan* LSA and *Homo* LSA, but the purpose of the phenograms depicted in Boxes 8.1 and 8.2 is to demonstrate how the data were transformed, not to provide a comprehensive phylogeny.

In both phenograms (Boxes 8.1 and 8.2), the lower tips of the ancestral lineages correspond to the predicted Y values resulting from the phylogenetic autoregression procedure (denoted Y_{LSA}). Subtracting the predicted Y_{LSA} scores from the species means (Y_m) yields a vector of autoregression residuals (ϵ_m). These residuals correspond to a new set of species means ($Y_{m[ACP]} = Y_M$), which were adjusted according to the method of the ancestrally centered phylogeny (ACP). Since an ancestrally centered phylogeny is a special case of a single-level phylogeny, the new set of species means (Y_M) represent a set of independent data points. The individual level raw variates (Y_i) (distributed along the solid horizontal line in Box 8.1) are rigidly translated along with the species means during ACP modeling, thus forming a new set of individual level variates ($Y_{i[ACP]} = Y_V$), defined by the equation:

$$Y_V = Y_M + (Y_i - Y_m) \qquad (8.2)$$

Reproduced with permission of the copyright owner. Further reproduction prohibited without permission.

The component (Y_i - Y_m) represents the pooled within-species variates (Y_Q); and thus:

$$Y_V = Y_M + Y_Q \quad (8.3)$$

The new ACP-transformed individual level variates, Y_V, are not, strictly speaking, independent data points, since they result from a two-level topological hierarchy (ancestor-descendent lineages and deviation of individuals from species means).[2] However, the variance of Y_V can be partitioned in accordance with this topology into two components, the among-species variance (σY_M) and the pooled within-species variance (σY_Q). Each of the two components taken separately is composed of vectors of independent data points. It should also be clear that:

$$Y_V = Y_M + Y_Q = Y_b + Y_w \quad (8.4)$$

where *b* denotes the between-groups vector and *w* represents the pooled-within groups vector. [3]

---

[2] A generalized estimating equation (GEE) estimator could be used for analysis of the Y_V data, since parameter estimates generated using this method take group (e.g., species) affiliation into account. Currently, however, the GEE line fitting estimator is not available in SAS/CALIS, the covariance structural modeling module of SAS.

[3] The reader may find it useful to refer to the Reference Glossary and Special Symbols section at the front of the thesis, for a quick reference guide to the notation convention used throughout this and subsequent chapters.

Reproduced with permission of the copyright owner. Further reproduction prohibited without permission.

Reproduced with permission of the copyright owner. Further reproduction prohibited without permission.

Box 8.1. Phenogram showing the distribution of maxillary arch length (mm) for individual specimens (Y_i), species means (Y_m), and last shared ancestors estimated using phylogenetic autoregression (Y_{LSA}). Only 11 of the 37 anthropoid species are depicted for ease of view.

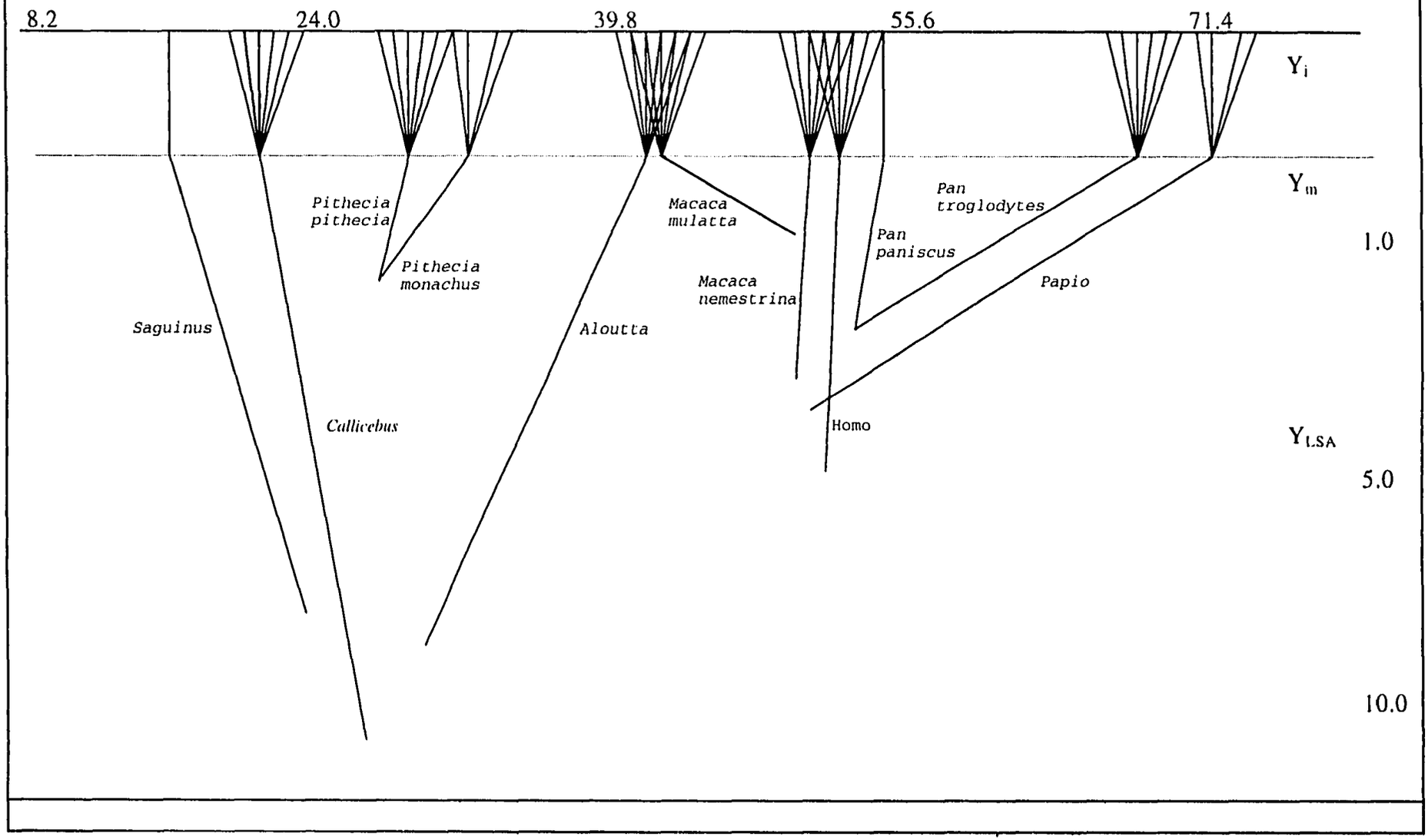

Reproduced with permission of the copyright owner. Further reproduction prohibited without permission.

Box 8.2. Ancestrally centered phylogeny (time unstandardized) of the phenogram shown in Box 8.1. The ancestral values (Y_{LSA}) have been horizontally centered (they are now a vector of 0's), and their attached lineages along with individual variates have been rigidly translated accordingly. The new Y_M variates are equivalent to the residuals of the phylogenetic autoregression, and the Y_V variates are a linear combination of the residual scores Y_M and the pooled within-species distributions Y_Q.

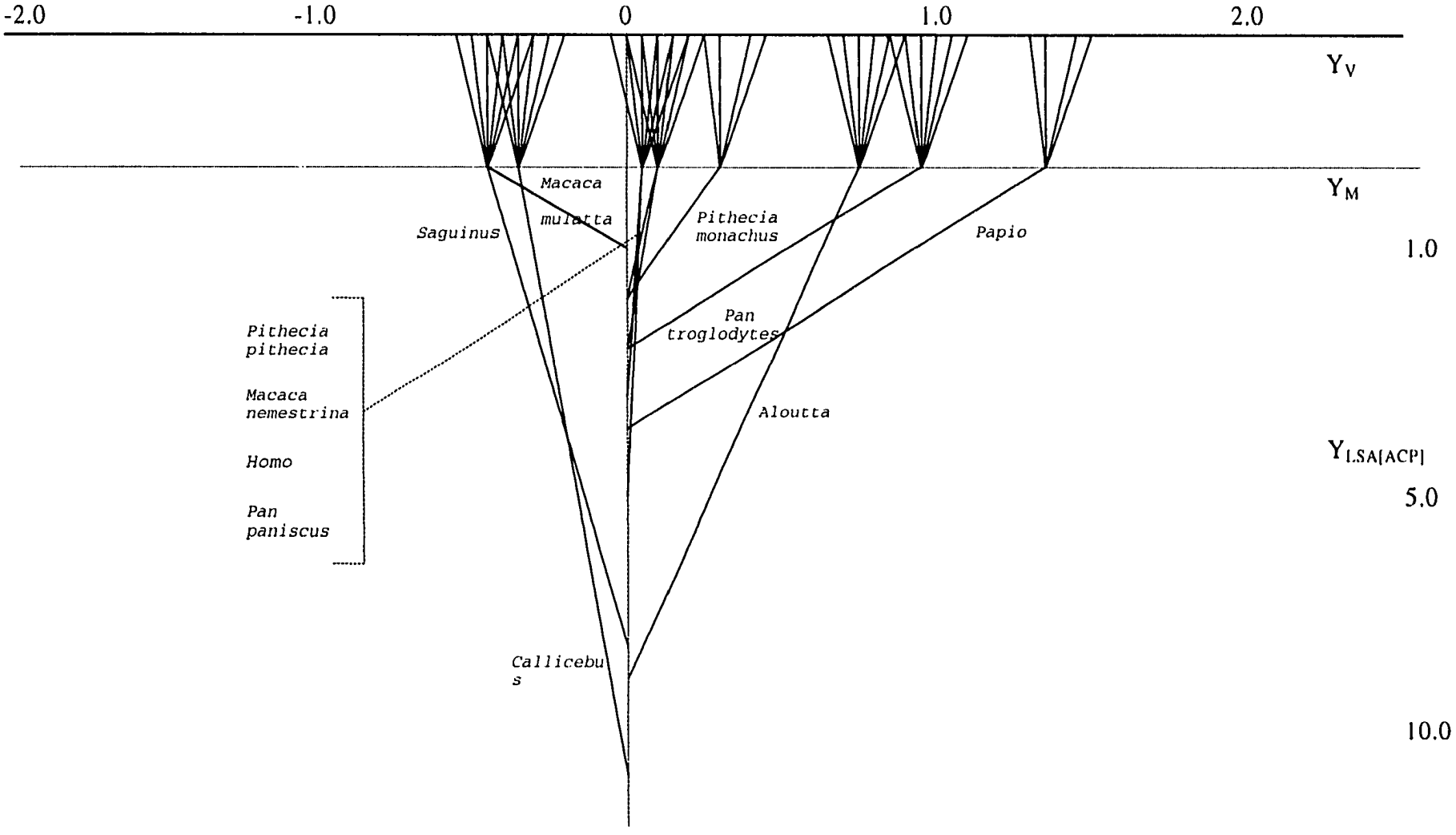

Multi-Level Analysis

Multi-level data analyses were devised over three decades ago (e.g., Hartley & Rao, 1967) as a means for dealing with the complex statistical problems associated with hierarchically nested data distributions. The last decade, in particular, has witnessed a surge in the development of multi-level approaches (e.g., Bock, 1989; Bryk & Raudenbush, 1993; Longford, 1993; McArdle & Hamagami, 1996). These methods grew out of a debate, mostly in the behavioral sciences, concerning the appropriate level or unit of analysis in cases involving multiple levels of aggregate data. Pedhazur (1997) recounts how a consensus was finally reached:

> Awareness that...[analyses at different levels]...may yield different results led to attempts to answer the question about the appropriate unit of analysis. However, it was soon realized that preoccupation with this question was imprudent, as the choice of one level to the exclusion of another may result in either masking certain effects or in showing effects when none existed. Accordingly, efforts were directed to the development of analytic approaches commensurate with the multilevel models called for in studies involving more than one level [p. 710].

A similar debate has not yet been waged in the biological sciences, and, with few exceptions, we have failed to take advantage of the lessons learned and subsequent advances made by our colleagues in other disciplines.[4] In most cross-taxonomic comparative studies, species mean values are the preferred unit of analysis (e.g., Ravosa, 1988). As I demonstrated in Chapter 6, tests of nomological hypotheses using raw species means can be biased if higher-level phylogenetic effects are ignored. Another common mistake is when inferences are made about

[4] One exception is in quantitative genetics where certain multi-level techniques have been adopted. I suspect that some of these techniques may have been introduced by the behavioral scientists who entered the field of behavioral genetics in the 1970s.

Reproduced with permission of the copyright owner. Further reproduction prohibited without permission.

individual-level properties based on analysis of higher taxonomic units, a type of cross-level inference termed the "ecological fallacy" by Robinson (1950). Moreover, ignoring within-species variance is to ignore a potentially critical source of biological information.

Justification for using species mean values as the sole units of analysis stems largely from misconceptions surrounding the observation that in most higher taxa there is much greater genetic and morphological variation among than within species (except when sexual dimorphism is extensive). This fact is explained by the homogeneous nature of the selective pressures that operate among individuals within a species—mutation, heterosis and other mechanisms of population variability aside. As a consequence, higher taxonomic diversity is often modeled analytically after a Model II ANOVA design in which differences among groups (i.e., species) are viewed as arising from different "treatments" (i.e., evolutionary forces), but variation within groups, that is, variation around the group mean, is largely seen as "random noise"—the so-called "error variance" in statistical parlance. From this perspective, *group means* take on central importance and thus many researchers feel justified in using species mean values as data points in comparative quantitative analysis.

There are two main traps that researchers fall into when adopting this strategy. The first is that they neglect to make a distinction between the *units of analysis* and the *units of comparison*. In an ANOVA, group means are the units of comparison (the aim is to compare differences among groups), but *individual* variates remain the units of analysis. Without individual measurements as the basic units of analysis there can be no statistical tests for among-group

Reproduced with permission of the copyright owner. Further reproduction prohibited without permission.

comparisons. Removing individual variates from data analysis and using only species means as data points obviates statistically meaningful among-group comparisons—there is no basis upon which to make meaningful interpretations of among-group differences. Moreover, the individual is also the *object of measurement*, and for this reason a loss of information and decreased analytical power accompanies the use of any supra-individual unit of analysis.

But an even greater misconception is the view that within-species variation is due to random (genetic) 'noise' around the species mean. As I discussed in Chapter 2 there are many non-random mechanisms of morphological change that operate at the level of the individual—epigenetic control of morphogenesis, acclimation, and some developmental constraints, for example. Moreover, the morphogenetic mechanisms that act to produce variation within a species (e.g., acclimation) are different from those that act to produce variation among species (e.g., selection).[5] Bell (1989) extended this argument to the covariance between traits:

> The covariance within species is in one sense fundamentally different from the taxonomic [i.e., among-taxa] components of covariance. It is only within a species that correlations between characters attributable to ancestry can be broken down by cross-fertilization and crossing-over [p. 565].

Morphological change on both levels—the individual and the species—must be included in an analysis of the nomological causal mechanisms of organic

[5] While debate continues over the proper unit of selection (e.g., Sober, 1984), it is clear that the proper unit of *change* effected by selection is the population or species.

Reproduced with permission of the copyright owner. Further reproduction prohibited without permission.

diversity.[6]

A similar logical and analytical approach is taken in quantitative genetics (*cf.* Plomin, *et al.*, 1980), in which the total variance of a phenotypic trait (P) is partitioned into genetic (G) and environmental (E) components:

$$\sigma_P = \sigma_G + \sigma_E + 2[cov(G)(E)] + (\sigma_{GxE}) \quad (8.5)$$

where σ_P is the total phenotypic variance, σ_G is the genetic variance component represented by the among-group variance, σ_E is the environmental variance component represented by the pooled within-groups variance, cov(G)(E) is the covariance term, and σ_{GxE} is an interaction term (which is not necessarily multiplicative). The genetic variance component represents that part of the total variance of a trait that is heritable, while the environmental component represents that part of the total variance that is nonheritable (Roberts, 1967). Therefore only nomological mechanisms that operate on populations or species (i.e., selection and some forms of specific constraints) will have an effect on the σ_G component, whereas only nomological mechanisms that operate on the organismic level (i.e., acclimation and some forms of developmental constraints) will have an effect on the σ_E component.

Equation 8.5 can be expressed in linear regression notation as follows:

$$Y = \alpha + \beta_G Y_G + \beta_E Y_E = \alpha + \beta_b Y_b + \beta_w Y_w \quad (8.6)$$

Here, a vector of morphological trait values Y is accounted for by the linear (additive) combination of an intercept term, α (which equals 0 when all scores are standardized), a regression coefficient function of a vector of group means, $\beta_b Y_b$,

[6] Higher taxonomic levels of morphological change could also have been included in the multi-level analysis, for example to test proposed macroevolutionary hypotheses.

Reproduced with permission of the copyright owner. Further reproduction prohibited without permission.

and a regression coefficient function of a vector of pooled within-groups values, $\beta_w Y_w$. It can be shown that both regression coefficients, β_b and β_w, in Equation 8.6 are equal to one, and so the equation can be simplified as $Y = Y_b + Y_w$, which is equivalent to Equation 8.4. The multi-level data sets produced by the autoregression/alpha ACP procedure are thus compatible with quantitative genetic modeling and interpretation.

This same basic model is used in multi-level analysis to account for the individual (total) variation of a dependent variable (Y) in terms of the separate among-groups and within-groups effects of one or more independent variables ($X_i...X_j$).

$$Y = \alpha + \beta_b X_b + \beta_w X_w + \epsilon \quad (8.7)$$

Notice that Equations 8.6 and 8.7 are identical except that a distinct independent variable X has replaced variable Y on the right side of Equation 8.7. A residual term has also been added to Equation 8.7 since it is not expected that all of the variation of Y will be accounted for by regression on the among-groups and within-groups values of X. Furthermore, the regression coefficients are not restricted to unity and thus cannot be dropped from the equation (see McArdle & Hamagami, 1996, and, Pedhazur, 1997, for a more detailed discussion on multi-level regression analysis).

Multiple Regression Approach

The multi-level technique described in the preceding section is a special case of a general linear model (GLM) method known as multiple regression analysis. The multiple regression approach is the most appropriate for pursuing the objectives of

Reproduced with permission of the copyright owner. Further reproduction prohibited without permission.

the present research—to explain morphological diversity in terms of multiple causal relationships.

Statistical techniques, no matter how well conceived and applied, do not in themselves yield research results. They are simply tools wielded by the investigator to reveal patterns in the data that substantiate, or not, well formulated theory. In the present case, the morphogenetic theory presented in Chapter 2 renders logical predictions about the conditional and causal relationships between nasomaxillary traits and distal causal agents (DCAs) acting by way of specific distal mechanisms of change (DCMs). Consistent with this approach, variables were differentiated into dependent and independent variables. Variation in a given dependent variable, Y, measuring some aspect of nasomaxillary form, is explained in terms of its covariance relations to a series of independent variables, X_1, X_2,...X_j, operationalized on the basis of one or more distal causal agents (DCAs). The multiple regression approach permitted tests of predicted relationships among dependent and independent variables, while controlling for the effects of other variables. Thus, although only a tool, it is an exceedingly powerful tool in aiding investigative research. But testing predicted outcomes statistically is not the same as testing scientific hypotheses substantively. Failure to recognize this fact has been the source of much confusion, and some points of clarification must be made before I can proceed.

Hypothesis Testing

Confusion about the roles of hypothesis formulation, prediction and interpretation of results in scientific research involving bivariate and multivariate data analysis

Reproduced with permission of the copyright owner. Further reproduction prohibited without permission.

(including multiple regression analysis) continues to persist in the literature. I have already discussed in some detail the properties of valid scientific hypotheses (see Chapter 3). Simply stated, hypotheses are tentative falsifiable explanations based on specified causal and conditional relations. These causal relations must conform to known empirical patterns, but are not themselves overt. One cannot observe or measure causation directly. Predictions, on the other hand, must be observable and measurable. Hypothesized relations are specified within a theoretical and conceptual framework in the language of causation, whereas predicted relations are specified within an operational and analytical framework in the language of association (e.g., correlation or covariance).

Confusion arises when hypothesized relations and predicted relations are placed on the same epistemological level, when in fact they should be separated. For example, conventional use of the term "null hypothesis" in statistics is a misnomer since it actually refers to a *prediction* regarding the *statistical association* (or lack thereof) between two or more operationalized variables. It does not involve explanation, causation, or other properties of a valid scientific hypothesis. Mistakenly imparting to operationalized predictions properties of valid scientific hypotheses (e.g., the "null hypothesis") leads to confusion regarding interpretations of test outcomes. Interpretations of tests of statistical predictions are not equivalent to interpretations of tests of scientific hypotheses.

We are often warned, and rightly so, that correlation does not signify causation; but an important aspect of the relationship between the two is often omitted, namely, that *lack of correlation does indicate a lack of causation.* In a

Reproduced with permission of the copyright owner. Further reproduction prohibited without permission.

discussion of the uses of regression analyses in biological research Sokal and Rohlf (1995:487) state:

> Although a significant regression of Y on X does not prove that changes in X are the cause of variations in Y, the converse statement is true. When we find no significant regression of Y on X, we may infer that the deviations of X do not affect Y.

This asymmetrical relationship between statistical association (whether correlation, regression or covariation) and causation precisely parallels Popper's (1959) falsification criterion as applied to tests of scientific hypotheses: hypotheses of cause-and-effect can never be proved (observed association ≠ causation) only disproved (lack of association = lack of causation).

Box 8.3. Relationship between test outcomes of scientific hypotheses and statistical predictions (simple case).

Scientific Hypothesis Statement	X causes Y	
Statistical Prediction	If X causes Y is true, then X will be statistically associated (i.e., correlate, regress, covary) with Y	
Statistical Prediction Test Outcome	Accept prediction that X is statistically associated with Y (in conventional terms: "accept the alternative hypothesis")	Reject the prediction that X is statistically associated with Y (in conventional terms: "accept the null hypothesis")
Scientific Hypothesis Test Outcome	Fail to refute scientific hypothesis	Refute scientific hypothesis

The relationship between association and causation is in fact a special case of the more general relationship between *scientific hypotheses* and *statistical prediction* (see Box 8.3). As discussed previously, a scientific hypothesis is a tentative explanation of a given phenomenon. In its simplest form it is posed as a cause-and-effect statement: factor or process X causes phenomenon Y (see Bock, 1988). If the scientific hypothesis that X causes Y is true, then the statistical

Reproduced with permission of the copyright owner. Further reproduction prohibited without permission.

prediction that X and Y are associated will also be true. Conventionally, there are only two outcomes to a statistical prediction test: (1) "variables X and Y are not significantly associated" (the null "hypothesis" [=prediction] is then accepted), or (2) "variables X and Y are significantly associated" (the alternative "hypothesis" [=prediction] is then accepted).[7] If X is found to be associated with Y we *accept* the statistical prediction, but we *fail to reject* the scientific hypothesis. In other words the test of the scientific hypothesis is *indecisive*, which simply implies that we cannot eliminate it from the pool of potentially viable scientific hypotheses purported to explain Y. If X is found not to be associated with Y we *reject* the statistical prediction (i.e., accept the null "hypothesis"), and we can in this case also *reject* the scientific hypothesis that X causes Y. The test of the scientific hypothesis in this instance is *decisive*, and we can eliminate it from the pool of potentially viable scientific hypotheses that may account for Y (given that all of the assumptions of the test are met and all of the specifications of the model satisfied).

Covariance Structure Analysis

In a more complex arrangement, depending on the theoretical framework, the relationship between a given DCA and nasomaxillary form can involve several "subrelationships" among causal and conditional factors. For example, mastication can theoretically affect nasomaxillary form via several pathways of interconnected

[7] If one rejects the null 'hypothesis' (=prediction) that X and Y are not significantly associated, by logical deduction one must *accept* the alternative 'hypothesis,' since the two 'hypotheses' are exhaustive *and* mutually exclusive. Therefore, the two possible outcomes of a test for significance are: (1) acceptance of the null 'hypothesis' that the variables are not associated *or* (2) acceptance of the alternative 'hypothesis' that the variables are associated.

Reproduced with permission of the copyright owner. Further reproduction prohibited without permission.

relationships involving the properties of the food items eaten, muscle recruitment and use, properties of the mechanical system, bite force magnitude and distribution, and induced craniofacial strain patterns (see Box 14.1). In a complex case such as this the statistical model of predicted relations developed for testing must reflect the complexity and content of the scientific hypothesis (i.e. the theoretical causal model).

A powerful multiple regression technique designed to test models involving complex relationships among several dependent and independent variables is structural equation modeling (SEM). A special case of SEM, and the technique most suitable for this study, is covariance structure modeling[8] (Wright, 1934; Tukey, 1954; Heise, 1975; Li, 1975; Hatcher, 1994). In covariance structural analysis the researcher formulates a set of equations that specify parameters to model the predicted associations among relevant operationalized variables in accordance with a causal scientific hypothesis. The causal hypothesis can be depicted as a path diagram, such as the one shown in Box 8.4. Once all the parameter estimates of the covariance structure model are identified they are combined to form a predicted (or "model-implied") variance-covariance matrix, denoted Σ. The model-implied predictions are tested by assessing how well the covariance structure model (summarized by Σ) fits the empirical data (represented by the sample covariance matrix, *S*).

Since both multi-level analysis and covariance structure modeling are subsumed under the general linear model (GLM), they can be combined into an integrated analysis (McArdle & Goldsmith, 1990; Muthén, 1994; McArdle &

[8] Covariance structure modeling is a refinement of a technique known as path analysis developed by Wright (1934). Some researchers regard path analysis as the first step in covariance structure modeling (e.g. SAS Inc., 1997), while others use the terms synonymously.

Reproduced with permission of the copyright owner. Further reproduction prohibited without permission.

Hamagami, 1996). Accordingly, the multi-level regression Equation 8.7, can be transformed into a covariance structure model, represented in Box 8.5 as a path diagram.

Box 8.4. Path diagram illustrating causal hypothesis relating population density and mortality rate to the size of a population of houseflies. (Adopted from Sokal & Rohlf .1995:647).

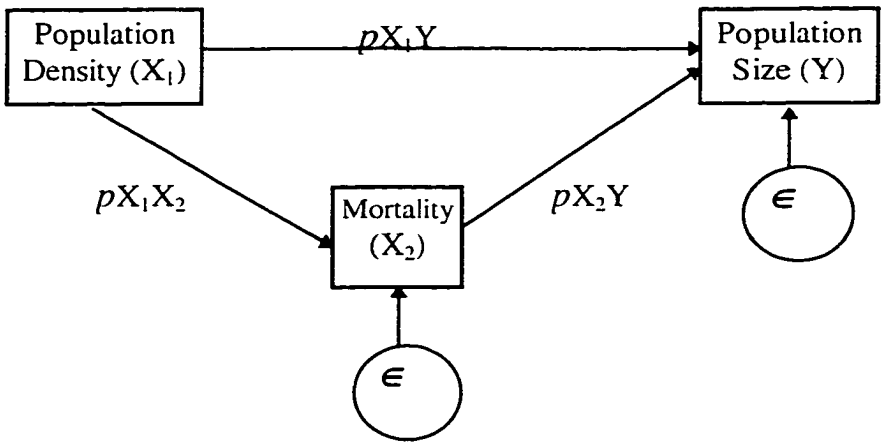

Theory-dependent causal hypotheses and corresponding covariance structure models were formulated for each of the five DCAs examined in this study, as well as for the structural growth relationships among the nasomaxillary variables (see Chapter 9). In accordance with the foregoing discussion of scientific hypotheses testing, if any of the predictions specified in a covariance structure model did not fit the data then they were subsequently rejected. In such cases, the corresponding DCA was either refuted as a potential cause of anthropoid nasomaxillary variation, or the hypothesis involving the DCA was modified such that its corresponding structure model conformed to the data. If, on the other hand, the predictions of a given model fit the empirical data they were subsequently accepted, and the DCA was not refuted as a potential causal agent.

Reproduced with permission of the copyright owner. Further reproduction prohibited without permission.

Box 8.5. Path diagram of multi-level analysis for one independent

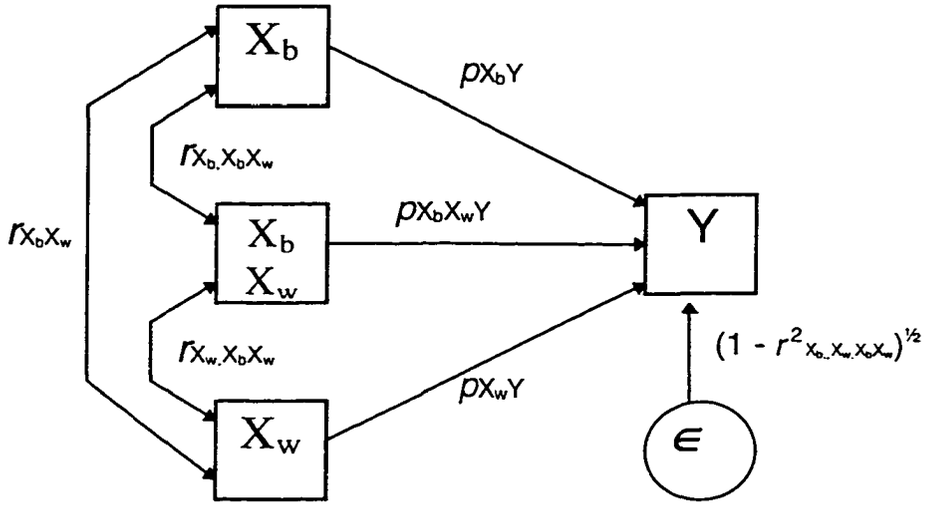

When the model tested is consistent with the true model, the one that generated the data, it is said to be properly specified. Misspecification occurs when the theoretical model (and subsequently, the structural model) is not correctly constructed; that is, when relevant variables are omitted from the structural equations or when irrelevant variables are included in the structural equations.

There are a number of methods available to reveal specification errors in covariance structure models. Parameter estimates that are not statistically different from zero may indicate that the independent variable associated with the estimate is irrelevant and should be dropped from the equation (i.e., the hypothesized causal pathway between the independent variable and the dependent variable should be reconsidered). Two recently developed procedures called the Wald test and the Lagrange multiplier test can quantify the significance of entire sets of parameters

Reproduced with permission of the copyright owner. Further reproduction prohibited without permission.

for a given model. The Wald test helps identify paths that should be deleted from the model, whereas the Lagrange multiplier test identifies paths that should possibly be added to the model (Hatcher, 1994).

Another approach is to examine the residual matrix obtained by taking the difference between the observed covariance matrix *S* and the model-implied covariance matrix Σ. Standardized residuals larger than 1.96 indicate that the observed covariance is not well explained by the model (Schumacker & Lomax, 1996).

Finally, there are numerous *fit statistics* that indicate the degree to which the model as a whole is consistent with the data (nonincremental fit indices), or whether one model provides a better fit compared to an alternative model (incremental fit indices). The most common model fit method is chi-square, but it has been shown to be sensitive to sample size. Schumacker and Lomax (1996) report that "...as sample size increases (generally above 200), the χ^2 test has a tendency to indicate a significant probability level" (p. 125), meaning that the test will find differences between the theoretically-based model and the data, even when the model fit the data reasonably well. Another popular nonincremental fit measure is the Goodness-of-Fit Index (GFI) (Jöreskog & Sörbom, 1989). The GFI measures the proportion of variance and covariance in the data covariance matrix, *S*, that is accounted for by the model-implied covariance matrix, Σ. An "adjusted" GFI (AGFI) was developed to take the model degrees of freedom into account (Jöreskog & Sörbom, 1993). Marsh, Balla and Hau (1996) have recently undertaken a thorough evaluation of the properties and effectiveness of various incremental fit indices in structural equation modeling. They concluded that two

Reproduced with permission of the copyright owner. Further reproduction prohibited without permission.

fit statistics in particular—the Comparative Fit Index of Bentler (1990) and the Normed Tucker Lewis Index (Marsh *et al.*, 1996)—exhibit several desirable properties. They are relatively unaffected by sample size, and their bias in relation to model complexity is known.

The problem with the current 'crop' of fit indices is that they fail to distinguish known spurious correlations from nonspurious correlations. Excluding known spurious relationships from the structural model (in accordance with theory) will result in a lower fit measure compared to models in which such relationships are included (contra theory) because the former will not account for as much of the observed covariance as the latter. I shall return to this point briefly in Chapter 15.

Once specification errors have been revealed, the model (i.e. operationalized causal hypothesis) can be respecified (i.e. modified) and retested against the data.

Assumptions of Multi-Level Covariance Structural Modeling

The analytical approach described in the previous sections assumes that the data exhibit certain properties. These assumptions include the following: (1) the model is free of specification errors, (2) the independent variables are free of collinearity, (3) the data points are independent, (4) the data are free of outliers and influential observations, (5) the data conform to a multivariate normal distribution, and (6) the relationships among variables are linear.

Reproduced with permission of the copyright owner. Further reproduction prohibited without permission.

(1) Absence of Specification Errors

Given the complexity involved in constructing covariance structural models with many parameters, it is common practice to build a complex model gradually, adding one set of parameters at a time (Schumacker & Lomax, 1996). I adopted this approach, systematically adding each of the five DCAs one at a time until arriving at a *general structural model* that includes all five causal agents (see Chapter 15).

The five DCAs examine—body size scaling, brain form, olfaction, locomotion and mastication—do not comprise an exhaustive list of potential causal agents. I have not, for example, examined the possible influence of gape, dental morphology, and thermoregulation, to name a few, on nasomaxillary diversity. In omitting these factors I have potentially committed specification errors (i.e. the omission of relevant independent variables from the covariance structure model). The effects that this type of misspecification have on tests of hypotheses depend upon whether or not the omitted variables are correlated with those already included in the covariance structure model. Substantial correlation among omitted and included independent variables can bias the regression coefficients of the latter.

The direction of the bias is important since the decisive outcome of the test is to refute the hypothesis. Thus, I would rather mistakenly fail to refute an incorrect hypothesis than to mistakenly refute a correct hypothesis, although neither error is desirable. In terms of the statistical prediction outcomes this translates into trying to avoid committing Type II errors (see Sokal & Rohlf, 1995:159). An overestimation bias of the regression coefficient due to omission

Reproduced with permission of the copyright owner. Further reproduction prohibited without permission.

specification errors is therefore more acceptable than an underestimation bias, since the latter is more likely to lead to a Type II error. Pedhazur (1997) has shown that the direction and magnitude of bias in such cases depends upon the signs and sizes (respectively) of the correlation coefficients between omitted and included independent variables.

If the omitted relevant variables are not correlated with those in the equation then there is no effect on the regression coefficients of the latter. However, omitting such variables from the structural equation model can still lead to an increase of the standard errors associated with the regression coefficients thereby reducing the sensitivity of their statistical tests of significance (Pedhazur, 1997). One way to offset increases in standard errors due to omission of non-correlated independent variables is to increase sample size (see Chapter 4), since:

$$s_{St} \propto 1 / n^{½} \tag{8.8}$$

where s_{St} is the standard error of a statistic, s is the standard deviation and n is the sample size. An advantage of using the multi-level approach is that sample sizes are much larger compared with analyses of group (e.g., species) means.

(2) Absence of Collinearity

Exact collinearity occurs when one independent variable is a linear combination of any set of other independent variables. Exact collinearity is rare, and usually only occurs when the same variable is mistakenly entered twice, perhaps in different units. Near collinearity, however, is common, and it can lead to serious problems in data analysis and interpretation. Strictly speaking, collinearity is not a violation of the assumptions of multiple regression and related techniques, but in the presence of collinearity variances

Reproduced with permission of the copyright owner. Further reproduction prohibited without permission.

for the parameter estimates may be inflated, and the parameters can be very sensitive to small changes in the data (i.e., the data are said to be unstable or ill-conditioned). High collinearity can thus render the parameter estimates (and hence one's results) meaningless.

Diagnosing collinearity is an essential, but often overlooked, part of data analysis. Unfortunately, many researchers mistakenly confuse collinearity with correlation, and finding little or no correlation among independent variables declare the data free of collinearity and proceed with the analysis. Yet it has been shown that high or even exact collinearity may exist among a set of variables in which no pair has a significantly high correlation (Stewart, 1987).

Belsley *et al.* (1980) developed a method for identifying collinearity based on the singular value decomposition (SVD) of the data matrix. In their method a "condition index" statistic identifies ill-conditioned components of the data, and variables that load highly on components associated with a high condition index (i.e. components with near-zero eigenvalues) are said to exhibit collinearity (Belsley, 1990).

There is little practical benefit to running a condition index collinearity diagnostic before the theoretical model and concomitant structural equations have been fully specified. This is because the results of an SVD collinearity test can change depending on which specific variables are included in the model. A series of condition index collinearity diagnostics were run in conjunction with model respecification in Chapter 15.

Reproduced with permission of the copyright owner. Further reproduction prohibited without permission.

(3) Independence of Data Points

The issue of independent data points has been addressed in detail in Chapters 6 and 7. It was shown that nonindependence can be substantially reduced in data derived from a cross-taxonomic sample using the autoregression/ACP procedure. Further, the multi-level data sets created by this procedure—the among-species and the pooled within-species data sets—are each a special case of a single-level phylogeny and thus characterized by independent data points. As I have previously noted, the individual-level data set (Y_V in Box 8.2) is, strictly speaking, composed of nonindependent data, since a hierarchical structure underlies its expression—it is the additive combination of the two single-level data sets. However, in the covariance structure models individual level variables $Y_{V\,i..j}$ are represented as dependent variables whose sums-of-squares are partitioned into components based on one or both of the two single-level data sets. Hence, nonindependent data points are always partitioned into variance components whose underlying data points are independent. Care will need to be taken when interpreting inferential results involving those few cases in which individual level data comprise exogenous variables (i.e., variables that are not dependent in the model).

(4) Absence of Outliers and Influential Data Points

A feature of non-normally distributed data is the potential for outliers and influential data points. The reliability of tests of theoretical models against empirical data in covariance structure modeling is especially adversely affected by outliers (Schumacker & Lomax, 1996). The occurrence of a single outlier can be

Reproduced with permission of the copyright owner. Further reproduction prohibited without permission.

sufficient in many cases to alter statistical test results (Wilcox, 1998).

Identification of outliers and influential data points, tests of assumptions concerning probability distribution normality, and data scale transformation go hand-in-hand. Outliers can affect the outcome of a test of normality, normality can be affected by the scale of the data (e.g., metric or log-scaled) and scale transformation can affect which variates are identified as outliers. To circumvent this catch-twenty-two a series of steps were followed in an attempt to generate data vectors that were normally distributed and free of outliers and influential data points. The first step in this process was identify and deal with outliers.

An outlier is an extreme variate whose value lies far from the sample mean. Sokal and Rohlf (1995:407) suggest applying the formula for calculating the standard deviate as a method of outlier identification.

$$\text{standard deviate} = (Y_i - \bar{Y})/(s) \qquad (8.9)$$

where Y_i is the ith variate of a vector, $\bar{Y}$ is the vector mean and s is the standard deviation. Critical values for standard deviate distributions have been published (Grubbs, 1969) so that any given ratio can be tested for significance. I propose a simpler form of this method using the formula:

$$d_i = (Y_i - \bar{Y})/(s \times 3) \qquad (8.10)$$

When individual variates (Y_i) are greater than 3 times the standard deviation (s) from the mean ($\bar{Y}$) the value of this expression is greater than unity. We would expect less than 1% (actually, 0.0023) of such deviates to fall within the normal probability distribution, and so values of d_i of 1 or greater can be said to be significant at the 0.003 level. This method assumes that the data are normally

Reproduced with permission of the copyright owner. Further reproduction prohibited without permission.

distributed, but even if the normality assumption is violated Equation 8.10 can be used as a heuristic tool to guide the investigator in identifying 'suspect' deviates.

Outliers may be due to measurement errors, or data entry or instrument errors ('error outliers'), or they may represent a truly deviate character variate ('true outliers'). It is important to make a distinction between these two types of outliers because each is handled differently. When searching a diverse cross-taxonomic sample for error outliers it is advisable to analyze the within-species data.[9] Error outliers can remain hidden within a large varied sample. For example, if I mistakenly record the endocranial volume of a specimen of *Callimico goeldii* as 100 ml instead of 10 ml, the error variate will likely fall within the normal distribution of the entire cross-taxonomic sample, but will be revealed as an outlier in an analysis of the within-species data. In such an analysis each variate is evaluated relative to the mean and standard deviation of its own species.

Several outliers were identified using the method denoted by Equation 8.9 and traced back to observer error. These errors were corrected by recollecting or re-entering the data. This step was undertaken prior to entry of the data into the phylogenetic autoregression analysis (see Chapter 7). Other outliers were detected that could not be traced to measurement error. A list of true univariate outliers for the raw and log transformed phylogenetically-adjusted data is given in Box 8.6. Multivariate influential outlier analysis was conducted in conjunction with covariance structural modeling, and is presented in Chapter 15.

---

[9] When the within-species samples are small (generally under 30), the pooled within-species data can be used instead.

Reproduced with permission of the copyright owner. Further reproduction prohibited without permission.

Box 8.6. True univariate outliers for raw and log transformed pooled within-species data, n=300 (in units of d_i , see Equation 21)

Var #	Raw data		Log transformed data		
	No. of outliers	Mean d_i	No. of outliers	Mean. d_i	Specimens exhibiting true outliers (d_i)
Y1	3	1.55	3	1.37	CA55030 (1.11), MN57111 (1.10), PT90293 (1.89)
Y2	2	1.21	2	1.20	LL75291 (1.19), PT90292 (1.20)
Y3	2	1.15	1	1.19	PT201469 (1.19)
Y5	2	1.38	2	1.27	GG1472 (1.31), PT89355 (1.23)
Y6	2	1.30	2	1.19	PP200898 (1.10), HSVL5281 (1.27)
Y7	1	1.51	2	1.18	CA52621 (1.09), GG167340 (1.28)
Y9	2	1.37	2	1.23	HSVL642 (1.41), PT174860 (1.06)
Y11	1	1.34	1	1.24	PT90191 (1.24)
Y12	2	1.29	2	1.15	GG214108 (1.20), PT89354 (1.09)
Y14	2	1.18	3	1.12	CA55030 (1.13), HSVL642 (1.14), PT174860 (1.10)
Y15	2	1.40	2	1.22	PP201811 (1.36), GG214108 (1.08)
Y16	1	1.79	1	1.52	GG214108 (1.52)
Y17	3	1.24	2	1.29	CA55030 (1.42), HSVL642 (1.16)
Y18	3	1.18	2	1.08	AG24172 (1.06), HSVL4927 (1.09)
Y19	1	1.27	1	1.07	MN106050 (1.07)
Y21	2	1.19	1	1.09	PP201811 (1.09)
Y23	2	1.30	1	1.35	PT201469 (1.35)
Y24	2	1.49	1	1.52	PA52674 (1.52)
Y25	5	1.30	3	1.29	PP201811 (1.11), GG81652 (1.55), HSVL2396 (1.22)
Y26	2	1.18	1	1.09	PP201811 (1.09)
Y27	2	1.28	1	1.12	GG214108 (1.12)
Y29	2	1.52	2	1.37	MF102764 (1.11), PT167345 (1.63)
Y30	2	1.08	2	1.07	CA55030 (1.05), HSVL2385
Y31	1	1.29	2	1.29	CA55030 (1.29), HSVL642 (1.30)
Y33	1	1.24	1	1.24	GG214108 (1.24)
Y34	2	1.18	1	1.17	PH52674 (1.17)
Y36	1	1.09	1	1.09	MN106050 (1.09)
Y37	3	1.12	1	1.06	GG214108 (1.06)
Y38	4	1.28	3	1.17	GG167340 (1.16), GG214108 (1.29), HSVL3449 (1.07)
Y40	3	1.34	2	1.29	GG214108 (1.41), HSVL5281 (1.17)
Y41	2	1.22	1	1.16	PH52668 (1.16)
Y42	3	1.81	2	1.96	CN189380 (2.35), PP200898 (1.58)
Y43	2	1.32	2	1.28	PP201811 (1.54), GG214108 (1.25)
Y44	4	1.40	4	1.30	PP201811 (1.54), GG167340 (1.43), GG214108 (1.09), HSVL2385 (1.14)
Y46			1	1.07	CP74369 (1.07)
Y49	1	1.87	1	1.66	GG214108 (1.66)
Y50	1	1.35	1	1.20	GG167340 (1.20)

Reproduced with permission of the copyright owner. Further reproduction prohibited without permission.

Box 8.6. True univariate outliers for raw and log transformed pooled within-species data, n=300 (in units of d_i , see Equation 21)

Var #	Raw data		Log transformed data		
	No. of outliers	Mean d_i	No. of outliers	Mean. d_i	Specimens exhibiting true outliers (d_i)
Y51	1	1.44	1	1.28	GG167340 (1.28)
Y52	1	1.33	1	1.18	GG167340 (1.18)
Y53	1	1.34	1	1.19	GG167340 (1.19)
Y54	2	1.19	2	1.12	MN106050 (1.09), GG167340 (1.15)
Y56	1	1.44	1	1.22	GG54356 (1.22)
Y57	1	1.40	1	1.24	GG167340 (1.24)
Y58	1	1.15			
Y60	1	1.22	1	1.07	GG167340 (1.07)
Y61	1	1.19	1	1.11	CP239606 (1.11)
Y63	1	1.34	1	1.25	MN106050 (1.25)
Y65	1	1.14			
Y68	1	1.16	1	1.14	CM98320 (1.14)
Y72	1	1.26	1	1.16	PP200900 (1.16)
Y76	1	1.42	1	1.23	PP200900 (1.23)
Y78	2	1.22	1	1.26	CN189380 (1.26)
Y79	1	1.10	1	1.10	HSVL2396 (1.10)
Y80	2	1.49	2	1.33	GG167340 (1.27), GG214108 (1.40)
Y82	1	1.09	1	1.06	CA161107 (1.06)
Y83	4	1.92	4	1.83	GG214108 (2.35), HS998452 (1.62), HSVL3449 (2.28), HSVL4927 (1.08)
Y84	2	1.54	2	1.33	PP201811 (1.25), HSVL4927 (1.42)
Sum/ mean	107	1.32	87	1.24	

Results of the outlier detection analysis can be summarized as follows: (1) of the 84 craniometric variables examined, 57 were shown to have at least one true outlier, (2) log transformation resulted in a 23% reduction in the number of outliers present in the data, from 107 to 87, (3) the total number of deviant outliers in the logged data [87] was only slightly higher than what is expected by chance alone [300*84*0.0027=68], (4) log transformation of the data reduced the mean d_i value of outliers only slightly (from 1.32 to 1.24), and (5) for many craniometric traits, the same few specimens, mostly large-bodied hominoids, contributed the

Reproduced with permission of the copyright owner. Further reproduction prohibited without permission.

outlying variates.

It has become increasingly clear that outliers pose a serious problem in data analysis, especially with regard to parametric estimations and their standard errors. Wilcox (1998) has cogently demonstrated that even a single outlier can render coefficients meaningless, even under fairly typical conditions. Outliers are also one of the major causes of collinearity, which can also render misleading estimates and both Type I and Type II errors. Outliers that have this sort of impact on data analysis are called "influential" outliers.

Influential data points are variates that have "...a demonstrably larger impact on the calculated values of various estimates (coefficients, standard errors, *t*-values, etc.) than is the case for most of the other observations" (Belsley, Kuh & Welsch, 1980:11). Several regression-based tests have been developed to aid in the identification of influential observations (e.g., *h* statistic, Cook's D, DFBETA). However, the only true test of an influential data point is to determine whether its presence or absence affects the outcome of a statistical test of significant, at a given alpha level. It is important to emphasize that influential data points are test specific. A given datum may be influential in one test setting but uninfluential vis-à-vis a different test.

Sokal and Rohlf (1995) recommend a three step procedure for detecting and testing influential observations based on the idea that influence is due to a combination of two properties: leverage and residuality. Leverage is a measure of the relative impact that a given variate exerts on the estimation of a coefficient, and residuality is a measure of the deviation of a variate from its predicted value. In the first step of the procedure, leverage coefficients (also called hat coefficients,

Reproduced with permission of the copyright owner. Further reproduction prohibited without permission.

denoted *h*) are computed for each variate of the independent variables in multidimensional space (*cf.* Hoaglin & Welsch, 1978; Hoaglin, 1992). In the second step, variables with high values of *h* are examined for residuality. Sokal and Rohlf (1995) suggest an inspection of the standardized residual, but studentized residuals may be more appropriate (SAS, 1990).[10] Finally, variates that exhibit both high leverage and residuality are evaluated by testing for a significant change to the value of the regression coefficient before and after removal of the suspect observation(s).

Opinions vary as to how to handle influential data points and other outliers in regression-based analyses (*cf.* Kruskal, 1988). There appears to be a growing consensus against removing them from the data, although such "trimming" strategies are still widely used (e.g., Judd & McClelland, 1989). An alternative to data "trimming" is a procedure called "winsorizing," in which outliers are replaced by their nearest less-deviant neighbor (Sokal & Rohlf, 1995). This approach has the advantage of retaining both the original sample size and the rank order of the data, while reducing the influence of extreme deviates on parameter estimates and test outcomes. The disadvantage is that estimates of the coefficient of multiple determination, R^2, will be artificially high. More recently, attempts have been made to develop regression estimation procedures that are resistant to the effects outliers (Wilcox, 1998). The benefits of using a resistant estimator are that the original data need not be tampered with at all (i.e., trimmed or winzorized), R^2

[10] The *h*-statistic is computed as $h = 1/n + (X_i - X)^2/\Sigma x^2$. Hoaglin and Welsch (1978) suggest that values of *h* above $4/n$ be considered excessive. The studentized residual approximates the ratio of the residual to its standard error. For the precise formula see SAS, 1990, p. 1418. Studentized residuals greater than 2 are considered high.

Reproduced with permission of the copyright owner. Further reproduction prohibited without permission.

estimates are unaffected, and the valuable information contained in outlying observations is not lost. Resistant (or robust) estimating procedures have not yet made there way into commercially available statistical software packages.

(5) Multivariate Distribution Normality

One of the necessary conditions for covariance structural modeling is that the data be normally distributed (Hatcher, 1994; Schumacker & Lomax, 1996). According to Hatcher (1994), "Although parameter estimates may be correct with non-normal data, the statistical tests... (such as the model chi-square test and significance tests for path coefficients) assume a multivariate normal distribution" (p. 148). Hence, in this section I examine and quantify some of the distribution properties of various forms of the anthropoid data.

One of the main normality issues with regard to regression-based approaches concerns the choice of a line fitting procedure. Covariance structural modeling is a form of Model II multiple regression, in which the use of ordinary least squares (OLS) can lead to biased parameter estimates (Sokal & Rohlf, 1995). An alternative estimation method, maximum-likelihood (ML), has been shown to produce more reliable parameter estimates (e.g., regression coefficients and error terms) even when the assumption of distribution normality is violated (Browne, 1982, 1984; Anderson & Gerbing, 1988; SAS Inc., 1997). However, use of the maximum-likelihood method with non-normally distributed data can lead to an over- or underestimation of standard errors (Boomsma, 1983, 1986; Bollen, 1989), and to inaccurate model fit statistics (SAS Inc., 1997). Boomsma (1983) demonstrated via simulation studies that standard errors of covariance structure

Reproduced with permission of the copyright owner. Further reproduction prohibited without permission.

parameter estimates were too small when the population distribution was skewed. Wilcox (1998) has recently shown that even slight deviations from normality can lead to underestimations of standard errors as low or lower than one-tenth their true value.

The Shapiro-Wilk statistic (W-statistic) was used to test for normality since it is appropriate for samples under 2000 (SAS Inc., 1993; Cody & Smith, 1997). Normality tests were performed on various forms of the data, including raw, autoregression/ACP adjusted, log transformed and size scaled. The results of these tests are presented in Box 8.8. Only the *p*-values of the W-statistic that were *not* significant at the 0.01 level are reported (i.e., those variables that were not significantly different from normal). *P*-values of less than 0.01, indicating variables that deviated significantly from normality, were left blank for ease of visualization. Tests of normality are presented according to data type (YV=individual level data, YM=species mean data, YQ=pooled within-species data) and scale (R=raw data, T=autoregression/ACP adjusted data, L=log transformed autoregression/ACP adjusted data). The W-statistic was not reported since its value holds little information, and can actually be misleading (*cf.* SAS Inc., 1992:627). A relatively low α level (0.01) was chosen because the Shapiro-Wilk test is rather conservative, and variables generating *p*-values greater than 0.01 appear to approximate normality quite well. Observe, for example, the histogram in Box 8.7, which shows that the frequency distribution for the variable 'anterior cranial fossa length' [ΔYV79-ACFLGT] closely approximates a normal distribution, even though it is associated with a relatively low Shapio-Wilk *p*-value (0.03).

Reproduced with permission of the copyright owner. Further reproduction prohibited without permission.

Box 8.7. Frequency distribution for ACFLGT (YV79).

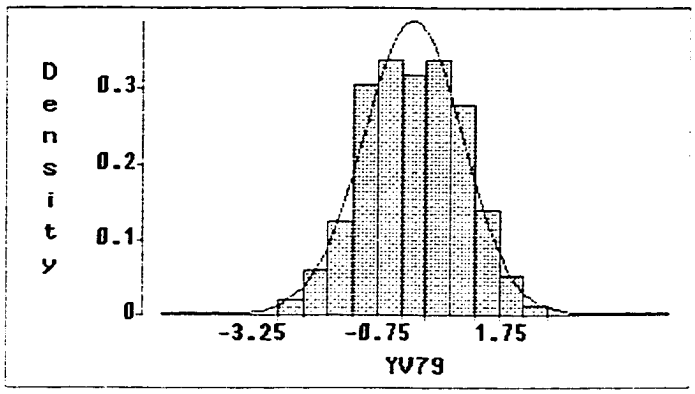

Several trends are apparent in the normality test results presented in Box 8.8. First, species mean data are, on average, more normally distributed than individual level data, while pooled within-species data approximate normality best. Second, autoregression/ACP adjustment, on average, significantly improved distribution normality over the raw data, for both the individual level and species mean vectors (recall that individual data points around the species mean were rigidly translated during the autoregression/ACP procedure, and thus the pooled-within species distribution was not affected by phylogenetic adjustment). Third, natural log transformation of the autoregression/ACP adjusted data, on average, did not significantly improve normality of the individual level variables, but did confer a slight increase of normality to the species means and pooled-within species data sets.

Reproduced with permission of the copyright owner. Further reproduction prohibited without permission.

Box 8.8. Results of Shapiro-Wilk tests of normality for morphometric variables. W-statistic *p*-values of 0.01 or greater are given. Shaded variables are those in which all three log transformed data sets are normally distributed. *#* indicates variables that are not linear distances.

		Individual-level			Among-species			Pooled within-species		
#	Variable:	RYV	TYV	LYV	RYM	TYM	LYM	RYQ	TYQ	LYQ
1	NASLGT									
2	NASWDU					0.381	0.47			
3	NSLWDL				0.223	0.054	0.069			0.029
4	NPMWDT			0.161	0.41	0.764	0.921	0.628	0.628	0.32
5	NSLAHT				0.649	0.059	0.143			
6	NSLAWD					0.072	0.155	0.024	0.024	0.383
7	PNASHT					0.072	0.21			0.102
8	PNASWD				0.016		0.02			
9	NLCLGT						0.013			
10	ZYGARE					0.015	0.054	0.342	0.342	0.19
11	ZYGOHT				0.018	0.177	0.39	0.055	0.055	0.257
12	BZYGWD		0.183		0.019	0.011	0.027			0.149
13	APZYGR			0.01		0.874	0.642	0.728	0.728	0.654
14	MXARCL				0.056	0.015	0.049			
15	BMAXWD						0.028	0.095	0.095	0.918
16	UMAXWD				0.016		0.018	0.034	0.034	0.217
17	AFACHT							0.094	0.094	0.672
18	PFACHT							0.017	0.017	0.208
19	RAMSHT							0.259	0.259	0.203
20	I2PALW						0.01	0.023	0.023	
21	P3PALW							0.067	0.067	0.588
22	M1PALW									0.018
23	M3PALW									
24	I2PALD				0.011	0.04	0.139			
25	P3PALD				0.121	0.103	0.279			
26	M1PALD						0.01			
27	M3PALD									
28	PALLGT					0.017	0.062			0.103
29	PALTHK			0.084	0.119	0.385	0.579			0.358
30	KROGAG				0.48			0.423	0.423	0.583
31	ENLOAG				0.066	0.02		0.916	0.916	0.182
32	SLOPOC			0.019	0.765	0.709	0.87	0.614	0.614	0.635
33	FACCNV		0.105	0.176	0.249	0.988	0.954	0.969	0.969	0.946
34	FACSIZ						0.016	0.17	0.17	0.361
35	PPNALO		0.098		0.08	0.998	0.988	0.23	0.23	0.181
36	ORBIHT						0.019	0.424	0.424	0.463
37	CRLGTH						0.015			
38	NCLGTH									0.385
39	BCLGTH				0.031		0.023	0.062	0.062	0.175
40	BIPORB						0.017			0.038
41	SKCNTR						0.014	0.052	0.052	0.235
42	CRBTHK					0.08	0.309			
43	OFBVOL						0.033			
44	OFBARE					0.047	0.104			
45	ORBSCR	0.191	0.035		0.209	0.367	0.203	0.484	0.484	0.4
46	ORBTC1	0.071			0.927	0.159	0.028	0.465	0.465	0.912

Reproduced with permission of the copyright owner. Further reproduction prohibited without permission.

Box 8.8. Results of Shapiro-Wilk tests of normality for morphometric variables. W-statistic *p*-values of 0.01 or greater are given. Shaded variables are those in which all three log transformed data sets are normally distributed. *#* indicates variables that are not linear distances.

		Individual-level			Among-species			Pooled within-species		
47	ORBTC2	0.421	0.731	0.597	0.674	0.799	0.797	0.772	0.772	0.272
48	ORBA12	0.328	0.085	0.042	0.145	0.484	0.244	0.036	0.036	0.296
49	IORBDS					0.057	0.127			0.595
50	BFPUI1				0.17	0.06	0.138	0.276	0.276	0.437
51	BFPUI2				0.181	0.073	0.17	0.551	0.551	0.713
52	BFPUP3				0.202	0.079	0.16	0.985	0.985	0.975
53	BFPUP4				0.164	0.055	0.117	0.975	0.975	0.981
54	BFPUM1				0.135	0.037	0.08	0.758	0.758	0.892
55	BFPUM2				0.332	0.104	0.254	0.081	0.081	0.348
56	BFPUM3				0.236	0.211	0.447	0.206	0.206	0.689
57	ANTBFM				0.177	0.065	0.152	0.424	0.424	0.593
58	PSTBFM				0.131	0.09	0.201	0.698	0.698	0.763
59	RELBFM		0.148	0.511	0.078	0.503	0.753	0.974	0.974	0.818
60	MAXBFM				0.148	0.103	0.224	0.636	0.636	0.756
61	APMASS	0.029	0.357	0.174	0.396	0.74	0.88	0.812	0.812	0.28
62	APTEMP	0.142	0.54	0.417	0.262	0.357	0.57	0.54	0.54	0.57
63	LEVADV		0.921	0.767	0.051	0.024	0.108	0.867	0.867	0.894
64	TEMPMM				0.124	0.251	0.416	0.864	0.864	0.972
65	CFORCE				0.165	0.038	0.1	0.598	0.598	0.727
66	RMMEFF	0.141	0.046		0.519	0.513	0.163	0.626	0.626	0.534
67	APFMAG					0.025	0.151	0.179	0.179	0.042
68	SLOPFM	0.268	0.215	0.537	0.135	0.231	0.338	0.959	0.959	0.943
69	APOCND				0.027	0.044	0.175	0.454	0.454	0.313
70	CBFLEX							0.015	0.015	
71	ENLWCP	0.019		0.637		0.03	0.192	0.871	0.871	0.206
72	ENLWOB	0.38	0.948	0.908	0.406	0.833	0.621	0.992	0.992	0.999
73	ENLOBO					0.58	0.442	0.427	0.427	
74	SLPCPF	0.728	0.523	0.05	0.929	0.136	0.03	0.155	0.155	
75	SLPCPO	0.197			0.695	0.064	0.013	0.768	0.768	0.376
76	SLPOBF		0.427	0.599	0.051	0.512	0.4	0.997	0.997	1
77	SLPOBO	0.926	0.834	0.693	0.81	0.74	0.55	0.974	0.974	0.972
78	MCFLGT		0.233	0.018	0.015	0.758	0.514	0.717	0.717	0.913
79	ACFLGT		0.03	0.016		0.23	0.264	0.686	0.686	0.26
80	FMAGSZ									
81	CEPHID	0.325	0.808	0.366	0.631	0.953	0.785	0.752	0.752	0.737
82	CANINE							0.258	0.258	0.374
83	DSKWGT									
84	BRNSIZ									0.011
85	OFBVLM									
86	STBRWT									
87	GESTAT									
88	BIRTHI				0.023	0.687	0.743			
89	LIFESP				0.055	0.152	0.095			
91	IMBIDX									
92	HDDIET				0.033					
94	BODYWT									
Means		.049	.087	.081	.137	.186	.21	.335	.335	.371

Reproduced with permission of the copyright owner. Further reproduction prohibited without permission.

More than a few variables did not follow these general patterns. About one-half of the variables were non-normally distributed in both raw and autoregression/ACP adjusted form, and in about 3% of cases raw data variables lost normality after phylogenetic adjustment. All other variables, however, either retained (43%) or gained (8%) normality subsequent to the phylogenetic adjustment (Box 8.9).

Box 8.9. Summary of effects of phylogenetic autoregression/ACP method on normality of multi-level data sets (260 variables).

Raw Data	Phylogenetically Adjusted Data	% of 260 variables
Non-normal	Non-normal	46%
Non-normal	Normal	8%
Normal	Non-normal	3%
Normal	Normal	43%

Of the 92 autoregression/ACP adjusted variables examined, only 18 were normally distributed at all three levels (individual, species means, and pooled within-species). The majority of the non-normally distributed variables, especially at the individual level, were highly skewed to the right.

Log transformation of the phylogenetically adjusted data yielded only nominal improvement. Log transformation often makes frequency distributions that are skewed to the right more symmetrical (Sokal & Rohlf, 1995). Yet, only 22 of the 92 log transformed variables exhibited a normal distribution at all three data levels (see shaded variables in Box 8.8). Box 8.10 summarizes the effects of log transformation of the autoregression/ACP adjusted data. For 85% of the multi-level variables, normality tests were unchanged after log transformation (38% remained non-normal and 47% remained normal). The distribution of 11% of the

Reproduced with permission of the copyright owner. Further reproduction prohibited without permission.

variables were changed from non-normal to normal, whereas 4% went from normal to non-normal subsequent to log transformation.

Box 8.10. Summary of effects of log transformation on normality of phylogenetically adjusted multi-level data sets.

Phylogenetically Adjusted Data	Log transformed	% of 92 variables
Non-normal	Non-normal	38%
Non-normal	Normal	11%
Normal	Non-normal	4%
Normal	Normal	47%

Box 8.11 presents box plots and frequency histograms for twelve selected variables. In addition to the raw data, autoregression/ACP adjusted data, and log transformed autoregression/ACP data, size standardized variables are also graphically displayed. Changes in the distribution properties of the selected variables can be compared by inspecting box plots and histograms along rows (across columns). The first two rows of plots depict distributions of the variable 'nasal process of maxilla width' [Y4-NPMWDT]. This variable is representative of raw measurements whose distribution is skewed to the right. In this instance, autoregression/ACP adjustment brings the distribution closer to normality, but the W-statistic p-value is still less than 0.01. Natural log transformation of the autoregressed residuals finally results in probability distribution normality. The variable 'bizygomatic breadth' [Y12-BZYGWD] is also highly skewed to the right in raw data form. Phylogenetic adjustment of the data transform it into a scale that is normally distributed (according to the Shapiro-Wilk test), but log transformation reverts the data back to non-normality! Two of the variables displayed in Box 8.11 [Y33-FACCNV, Y59-RELBFM] illustrate instances in which the raw data are non-

Reproduced with permission of the copyright owner. Further reproduction prohibited without permission.

normally distributed, autoregression/ACP adjustment renders the data normal, and log transformation further enhances the degree of normality. Many of the individual-level variables represented in Box 8.11, like bimaxillary breadth [Y15-BMAXWD], palatal width at M^1 [Y22-M1PALW], palatal depth at M^1 [Y26-M1PALD], maximum bite force potential at M^1 [Y54-BFPUM1], foramen magnum area [Y80-FMAGSZ], dry cranial weight [Y83-DSKWGT], and endocranial volume [Y84-BRNSIZ], remained skewed to the right despite phylogenetic and log transformation (although it is clear that a slight improvement has been rendered). Several non-linear raw measures, such as the angle of cranial base flexion [Y70-CBFLEX], are highly skewed to the *left*, and were not improved by phylogenetic adjustment or log transformation.

These results show that for this sample of anthropoid primates conventional craniometric measurements, especially individual level data, do not always conform to the assumption of distribution normality. The phylogenetic autoregression/ACP method and log transformation together conferred a slight improvement of distributional properties: about 16% of the variables were converted from non-normality to normality. Yet 37% of the multi-level variables remained non-normally distributed subsequent to the two transformations. However, geometric scaling (see Chapter 10) effectively rendered 62 of the 84 (74%) linear and nonlinear variables normally distributed at all levels.

Reproduced with permission of the copyright owner. Further reproduction prohibited without permission.

Reproduced with permission of the copyright owner. Further reproduction prohibited without permission.

Box 8.11. Box plots and frequency histograms of selected variables in various scales (individual level data, n=300).

Raw Data	Autoregression/ACP Adjusted	Log Transformed ACP Data	Geometric Size Adjusted
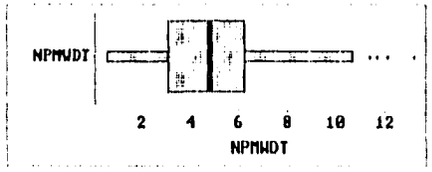	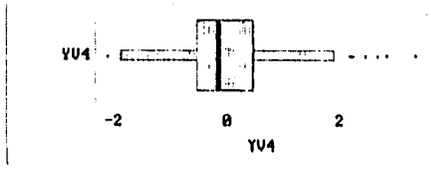	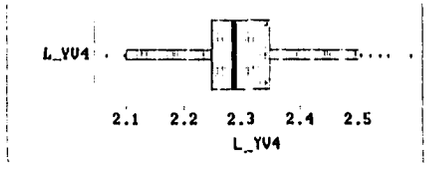	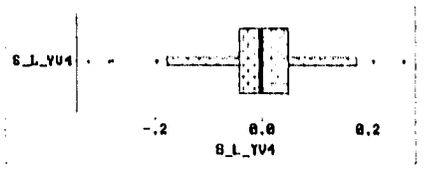
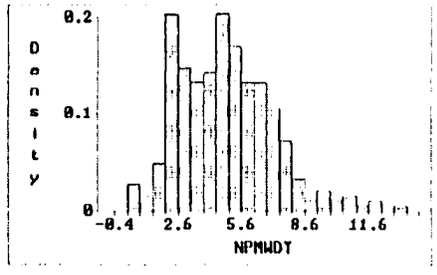	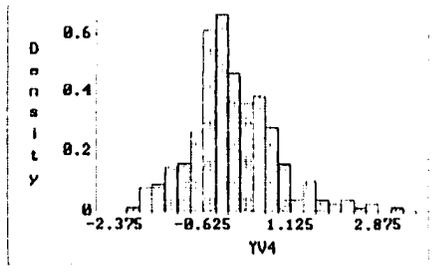	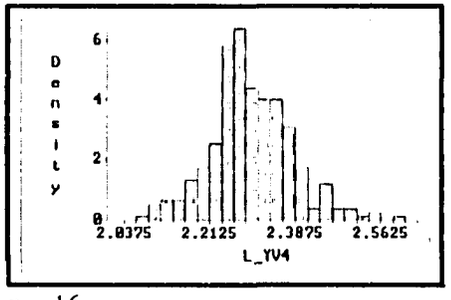	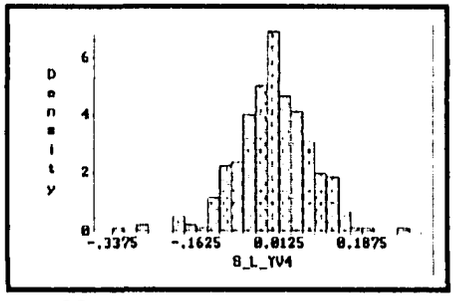
p <.01	p <.01	p =.16	p = .28
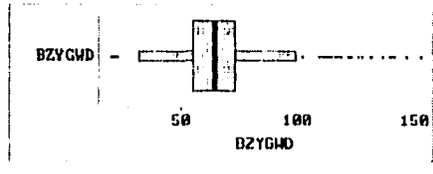	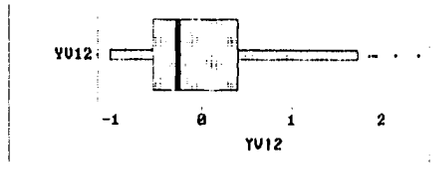	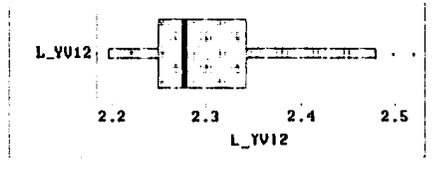	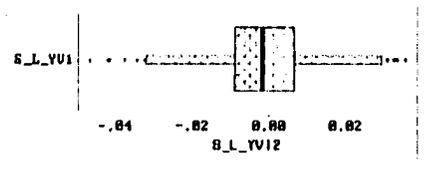
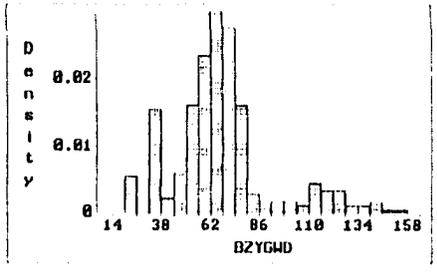	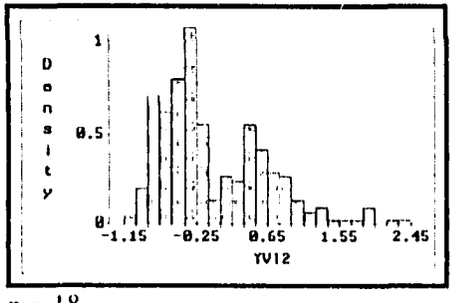	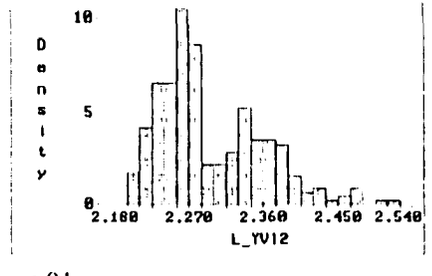	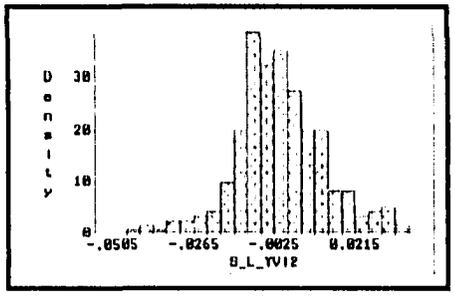
p <.01	p =.18	p <.01	p = .09

Box 8.11. Box plots and frequency histograms of selected variables in various scales (individual level data, n=300).

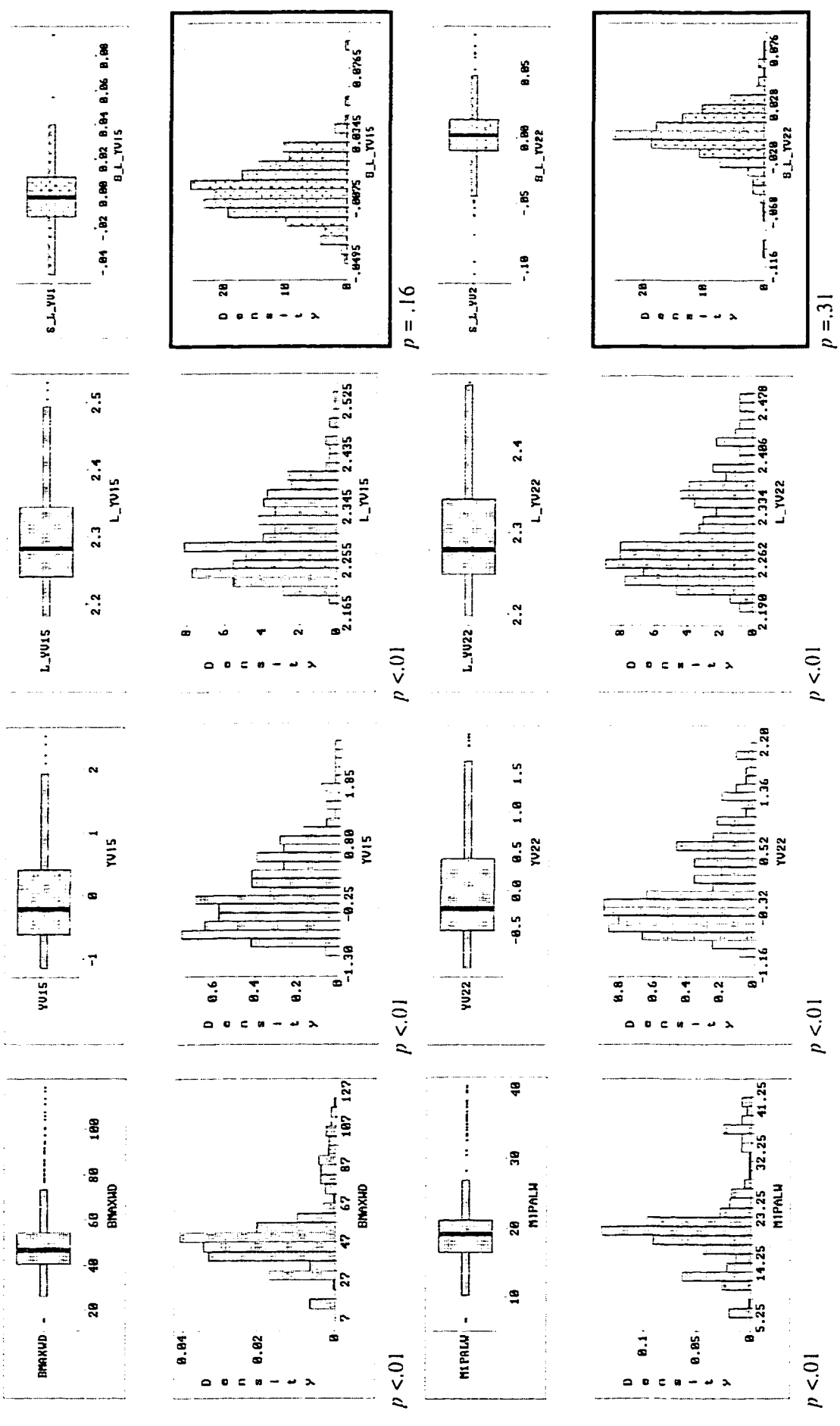

Reproduced with permission of the copyright owner. Further reproduction prohibited without permission.

Box 8.11. Box plots and frequency histograms of selected variables in various scales (individual level data, n=300).

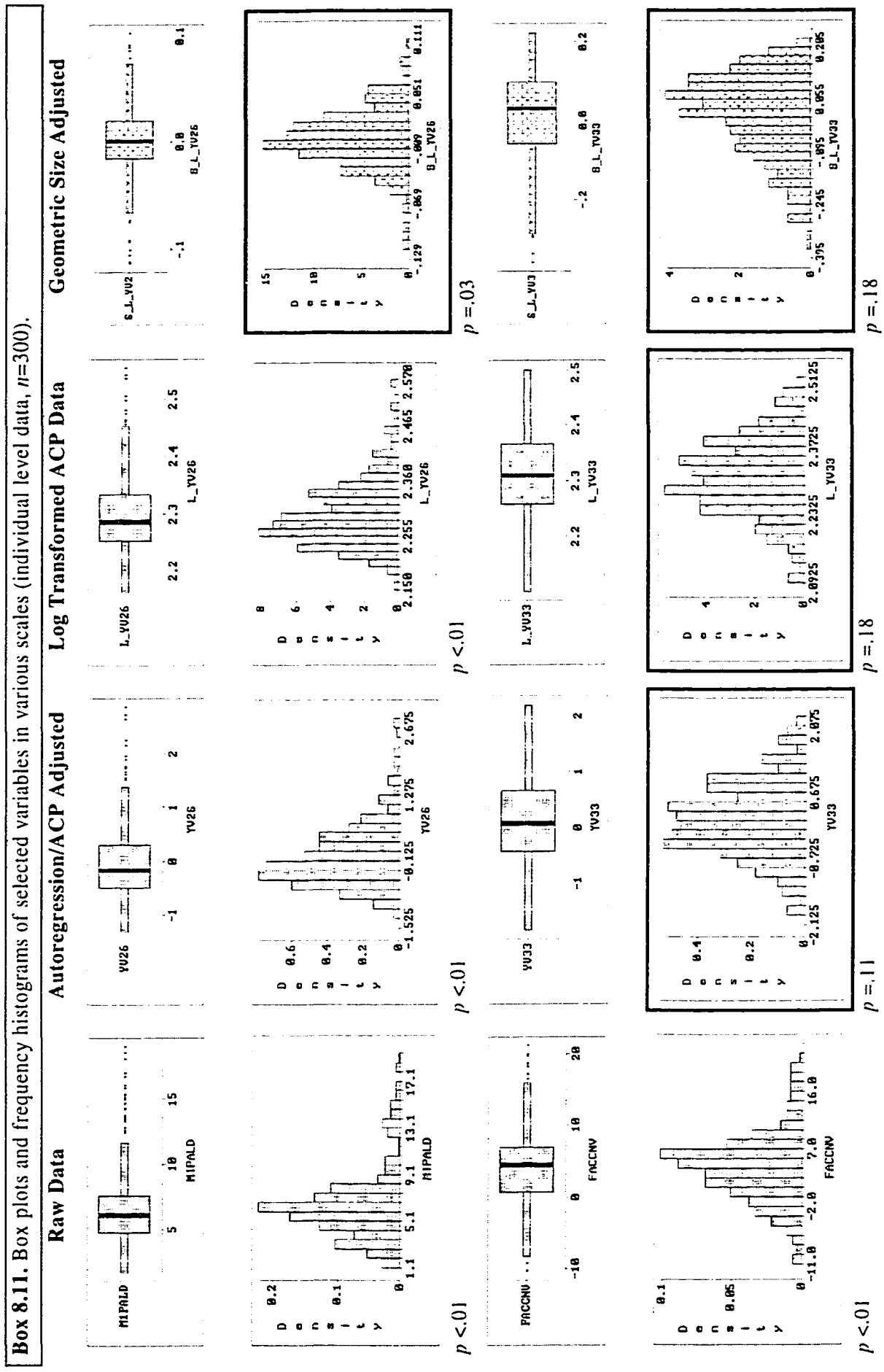

Reproduced with permission of the copyright owner. Further reproduction prohibited without permission.

Box 8.11. Box plots and frequency histograms of selected variables in various scales (individual level data, n=300).

Raw Data	Autoregression/ACP Adjusted	Log Transformed ACP Data	Geometric Size Adjusted	
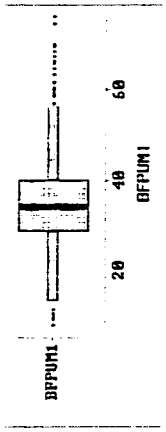	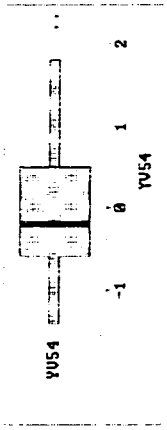	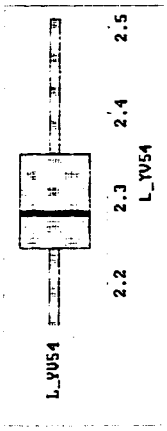	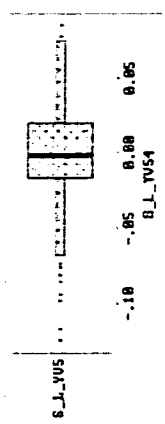	
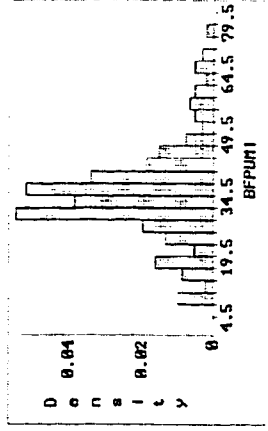	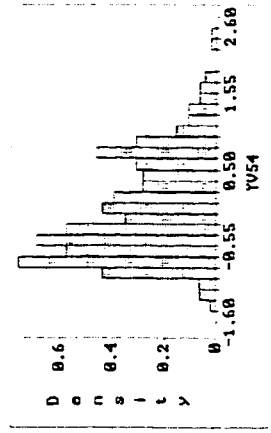	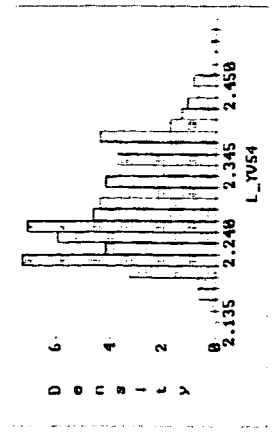	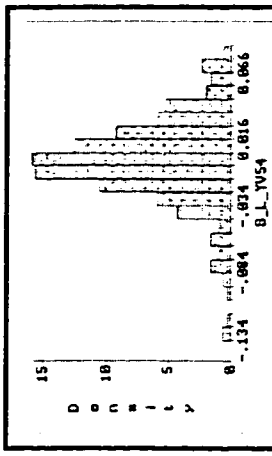	p <.01
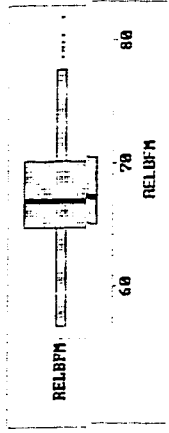	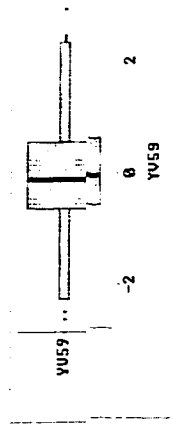	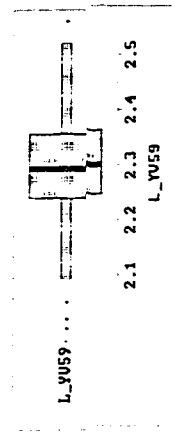	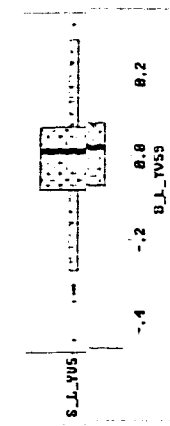	p <.01
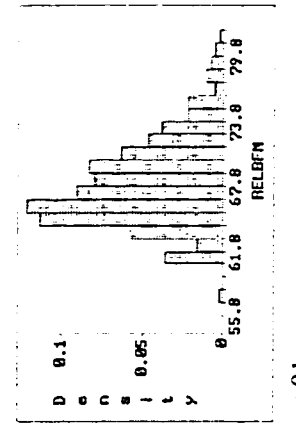	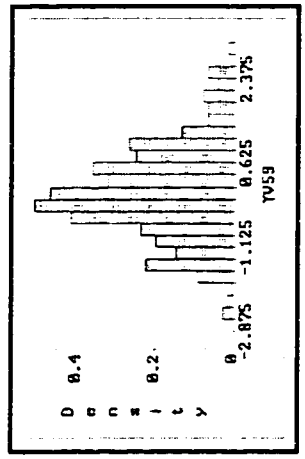	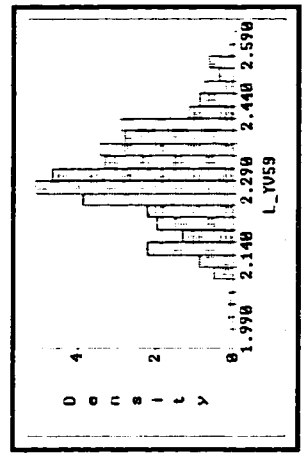	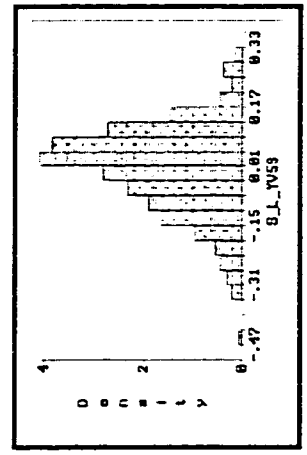	p =.51
				p =.51
				p =.15
				p <.01

Reproduced with permission of the copyright owner. Further reproduction prohibited without permission.

Box 8.11. Box plots and frequency histograms of selected variables in various scales (individual level data, n=300).

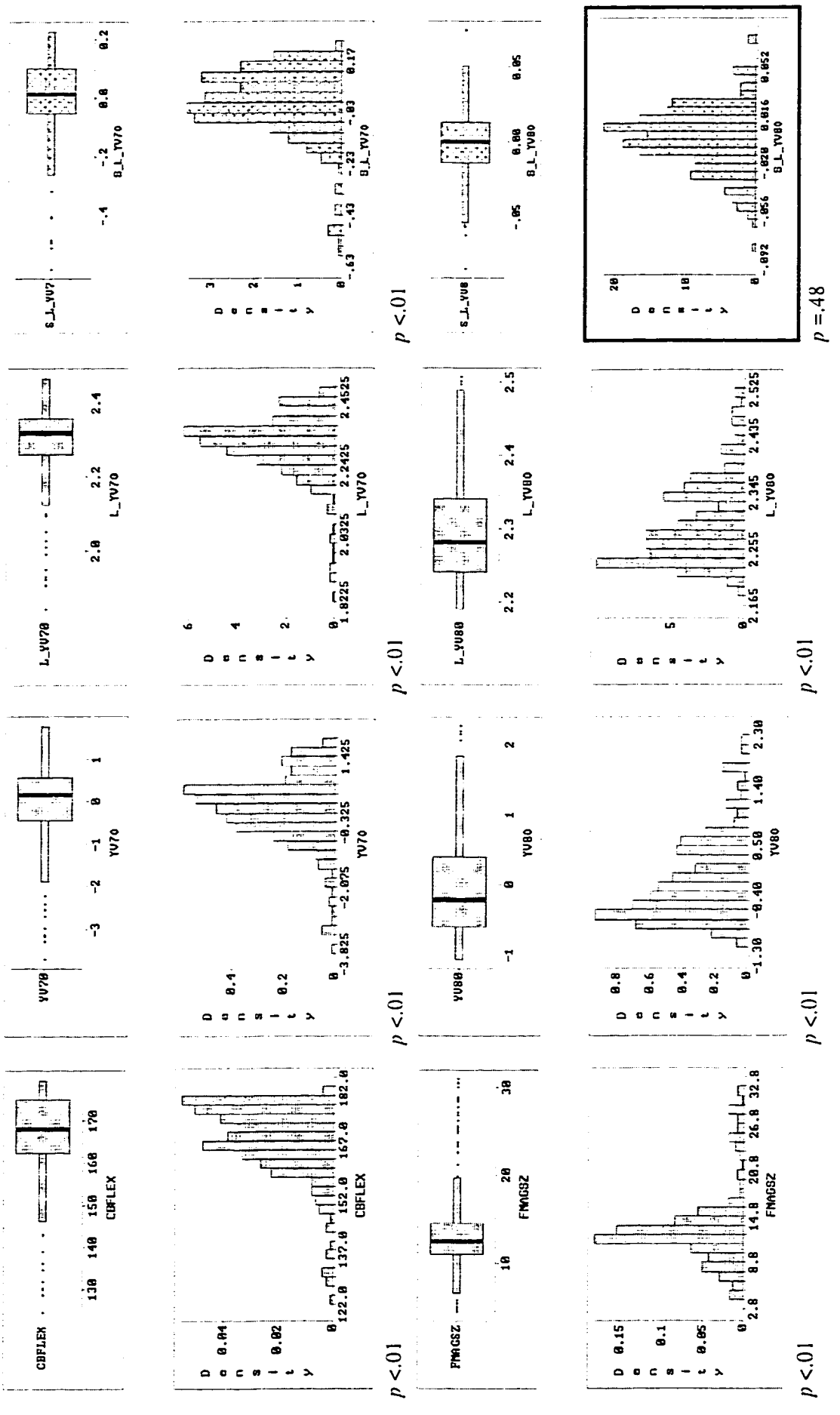

Reproduced with permission of the copyright owner. Further reproduction prohibited without permission.

Box 8.11. Box plots and frequency histograms of selected variables in various scales (individual level data, n=300).

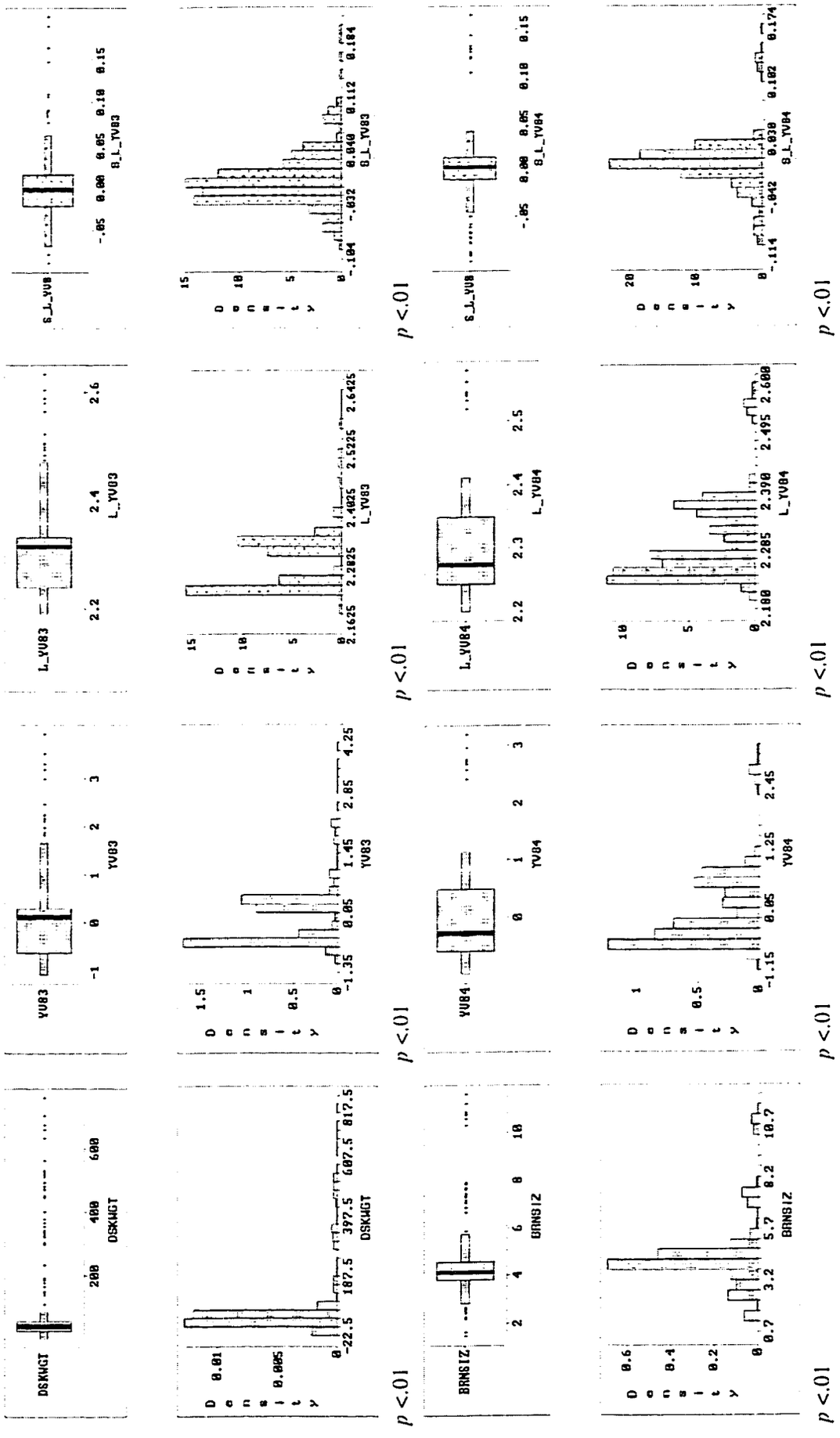

Reproduced with permission of the copyright owner. Further reproduction prohibited without permission.

There are several procedures available to deal with the problem of data non-normality. One is to use an asymptotically distribution-free (ADF) estimation method that does not depend upon the normality assumption, such as weighted least squares (WLS), rather than the maximum likelihood (ML) method (Raykov & Wildaman, 1995). Such a strategy could potentially solve the problem of unreliable standard errors and fit statistics associated with ML estimation under conditions of multivariate non-normality, but at a cost. ADF estimation methods typically require very large sample sizes (Schumacker & Lomax, 1996). Yet another solution is the use of a bootstraping method, which employs iterative resampling procedures to estimate test statistics and standard errors in combination with the ML line fitting estimation (Yung & Bentler, 1996). Boomsma (1986), Ichikawa and Konishi (1995), and Yung and Bentler (1996) established in simulation studies that the bootstrap provides less biased estimates of standard errors than conventional methods as long as sample sizes are close to or greater than $n = 300$. However, bootstrapping methods in structural equation modeling are currently not available on most statistical software programs.

(6) Test for Curvilinear Relationships

There are many possible forms of non-linear relationships, but by far the most common in biology is the curvilinear relationship. Curvilinear relationships can be described by a polynomial function, which in regression notation is expressed as:

$$Y' = a + b_1X + b_2X^2 + b_3X^3 + \ldots \quad (8.10)$$

Equation 8.10 uses increasing powers of X, each with a unique regression coefficient, in place of multiple independent variables. Addition of the power terms

Reproduced with permission of the copyright owner. Further reproduction prohibited without permission.

in the equation renders the best fit curved line to the data. A legitimate test of linearity is to determine whether the increment in the proportion of variance accounted for by inclusion of the quadratic term, b_2X^2, to the zero order equation is significant. In other words, does a curvilinear regression equation explain a significantly greater proportion of the variance of the dependent variable than a strictly linear equation? This can be tested using an *F* ratio for the quadratic term, defined as the sum-of-squares associated with the quadratic term divided by the mean square error (*cf.* Pedhazur, 1997).

The significant incrementation *F* ratio test for non-linearity was performed on all pairs of variables in the study for which a linear relationship was hypothesized. The results are presented in the context of covariance structural modeling and substantive hypothesis testing in Chapter 15.

Conclusions

In modern inferential analysis, hypotheses are evaluated by rendering predictions concerning the relationships among relevant operationalized variables, and testing these predictions against empirical observation. Therefore, all forms of inferential analyses (including regression, correlation, analysis of variance, analysis of frequencies and other general linear model methods) represent models, or sets of predictions, deduced from the hypotheses being tested. The structure of these mathematical models must conform to the structure of the causal relationships specified in the corresponding hypotheses. Thus, bivariate regression models, for example, imply a hypothesis in which a single causal factor or agent influences the phenotype under study. Likewise, conventional multiple regression analyses

Reproduced with permission of the copyright owner. Further reproduction prohibited without permission.

+model hypotheses in which multiple causal agents effect a given phenotype, and each agent is independent of the others. If the true relationships, or hypotheses, are not properly modeled then the model is misspecified (i.e., causal paths among relevant variables are omitted from the model or irrelevant paths are included in the model), a condition that can produce biased parameter estimates leading to incorrect inferences.

These considerations prompted Bookstein *et al.* (1985) to comment: "In our view, versions of Sewall Wright's general technique of path analysis are the only meaningful models available for the analysis of multivariate morphometric data" (p. 101). Path analysis, and its modern counterpart, covariance structure analysis, were developed to facilitate the modeling of complex causal relationships typical of morphological processes.

Multi-level analysis was developed to model hierarchical systems, and its use in morphology is well suited to model the various causal mechanisms discussed in Chapter 2. An analytical approach was developed here that integrates the phylogenetic autoregression/alpha ACP procedure outlined in Chapters 6 and 7 with covariance structure modeling and multi-level analysis. At the core of this approach is the bi-level partitioning of variance into within- and between-species components, whose underlying statistics and interpretation of parameters are consistent with those of quantitative genetics. The assumptions of this integrated approach were examined.

The foregoing does not imply that bivariate and other simple analyses have no place in comparative biological research. Such analyses are useful for exploratory analysis, revealing trends, and quantifying descriptive and

Reproduced with permission of the copyright owner. Further reproduction prohibited without permission.

distributional properties of the data. They may also be used to perform preliminary tests specific hypotheses, although test outcomes should be viewed as tentative. Simple bivariate, partial multivariate, and factor analytic techniques were employed in Chapters 9 through 14. In Chapter 15, an integrated structural model is presented based, in part, on previous preliminary analyses and, in part, on underlying morphogenetic theory.

Reproduced with permission of the copyright owner. Further reproduction prohibited without permission.

NOTE TO USERS

Page(s) missing in number only; text follows. Page(s) were microfilmed as received.

This reproduction is the best copy available

UMI

Reproduced with permission of the copyright owner. Further reproduction prohibited without permission.

PART IV

Nomological Hypothesis Testing (Constraints)

Reproduced with permission of the copyright owner. Further reproduction prohibited without permission.

Chapter 9:

Structural Growth Constraints on Nasomaxillary Form

If we regard the face and cranium as an entity—and, in the final analysis, we must—it follows that growth is inter-relational. Hence the growth in any given part will find a reflection in the part most intimately associated with it.

Krogman, 1931:357

Introduction

I have previously argued that there are three main nomological distal causal mechanisms (DCMs) in evolutionary morphology: selection, acclimation and constraint. In Chapter 2, I presented evidence in support of the assertion that DCMs effect nasomaxillary change by altering developmental choreographies (i.e., proximate causal mechanisms) or favoring certain variant choreographies over others. Mediating this change, to a large extent, is the prerequisite that organisms interact with their environment in a manner that ensures survival and reproduction. This imperative favors the development of nasomaxillary traits that can adequately perform (within the boundaries set by a particular niche) the primary biological roles of olfaction, locomotion and mastication. I also argued that changes in non-nasomaxillary structures or systems, especially those involving the brain and overall body size, can constrain nasomaxillary variation through pleiotropic, epigenetic or structural proximate mechanisms. It follows that changes in one *nasomaxillary* character, from whatever cause, may induce or constrain changes in a *second nasomaxillary* character. It is this structural and developmental integration of the nasomaxillary complex to which I now turn my attention.

At the heart of this issue is the question: Are nasomaxillary characters (such

Reproduced with permission of the copyright owner. Further reproduction prohibited without permission.

as palatal depth, facial prognathism, maxillary arch length and nasal aperture width) free to vary independently of each other, each affected separately by a unique combination of causal agents, or is it that changes in one nasomaxillary character impose constraints on how other nasomaxillary characters can vary? If the latter is correct, then it may not be necessary to postulate one or more DCAs operating directly on each and every nasomaxillary character. Or at the very least, some of the observed variation of the nasomaxillary complex may be explained in terms of intra-nasomaxillary growth processes and relationships.

It is therefore necessary, before considering the effects of exogenous agents on nasomaxillary form, to consider the integrated relationships among nasomaxillary characters. I have developed a four step procedure for modeling the effects of structural growth constraints on nasomaxillary form. The procedure begins with a principal components analysis of the log delta-transformed adult nasomaxillary variables [ΔL_YV1-ΔL_YV35]. The PCA revealed a distinct pattern of intercorrelations among specific variables. I next performed a series of ontogenetic shape analyses of selected nasomaxillary landmarks intended to reveal correlated growth changes among traits during craniofacial development. A review of the craniofacial growth literature was then conducted in order to (a) assess the reliability of the ontogenetic shape analysis, and (b) determine whether the observed correlated growth changes can be explained in terms of structural growth constraints. Finally, specific relationships between ontogenetic patterns of correlated nasomaxillary growth and nomological patterns of adult nasomaxillary variation and covariation were examined.

Implementation of these four steps helped determine the covariances that are

Reproduced with permission of the copyright owner. Further reproduction prohibited without permission.

best explained in terms of intra-nasomaxillary structural growth constraints. The hypothesized relationships were expressed in the form of a covariance structural model as described in Chapter 8. This constituted the "seed" model that was subsequently expanded, revised and tested in Chapters 10 through 15.

Principal Components Analysis of Nasomaxillary Variables

Principal components analysis (PCA) is an exploratory and data reduction procedure that permits the researcher to glimpse the underlying structure of the data. It is a factor analytic technique that summarizes the correlational relationships among a set of variables in terms of orthogonal factors or components. The technique was used here to identify those nasomaxillary characters that appear to covary independently of size, and to give clues to the possible structural interdependencies among these characters.

Box 9.1 reports the eigenvalues of the correlation matrix for the 35 nasomaxillary variables included in the PCA. The eigenvalues indicate the proportion of the total variance that is explained by each component. In the analysis, each variable is scaled to one unit of variance, and so the total variance among all variables is 35 units. The eigenvalue 21.03 for the 1st Principal Component, $PC_{(1)}$, indicates that this factor accounts for 60% of the total variance of the original variables. As shown in Box 9.1, $PC_{(2)}$ accounts for an additional 10% of the total variance, and $PC_{(3)}$ explains an additional 6%. Each successive principal component accounts for less of the total variance.

At some point the eigenvalues become so low as to be statistically nonsignificant. However, when factoring a correlation matrix conventional

Reproduced with permission of the copyright owner. Further reproduction prohibited without permission.

statistical test procedures are no longer valid (Dillon & Goldstein, 1984) and cannot be used to determine the number of significant principal components.

Box 9.1. Eigenvalues and accounted-for variance of log delta-transformed individual level (ΔL_YV) nasomaxillary variables (correlation matrix used in PCA; n=300).

PC	Eigen-value	Proportion of Total Variance Explained	Cumulative Proportion Explained	PC	Eigen-value	Proportion of Total Variance Explained	Cumulative Proportion Explained
1	21.03	.601	.60	19	.12	.003	.98
2	3.48	.099	.70	20	.12	.003	.99
3	1.96	.056	.76	21	.08	.002	.99
4	1.24	.035	.79	22	.08	.002	.99
5	1.03	.029	.82	23	.06	.001	.99
6	.89	.025	.85	24	.05	.001	.99
7	.72	.021	.87	25	.04	.001	.99
8	.67	.019	.89	26	.04	.001	1.00
9	.63	.017	.90	27	.03	.001	1.00
10	.53	.015	.92	28	.03	.001	1.00
11	.44	.013	.93	29	.03	.001	1.00
12	.31	.009	.94	30	.02	.001	1.00
13	.30	.009	.95	31	.01	.000	1.00
14	.25	.007	.96	32	.01	.000	1.00
15	.24	.007	.96	33	.01	.000	1.00
16	.21	.006	.97	34	.00	.000	1.00
17	.19	.005	.97	35	.00	.000	1.00
18	.13	.004	.98				

Horn (1965) proposed a method for determining the number of components to retain that involves comparing the curve of the ordered eigenvalues (called a 'scree plot') of the actual data with the corresponding curve (or line) for a set of randomly generated, independently distributed data. The random data are sampled from a population whose correlation structure is an identity matrix (i.e., one in which each variable has an *r*-value of 0 with every other variable). Due to sampling error, the ordered eigenvalues of the random data will range from greater than one to less than one, with the mid-point component having an eigenvalue equal to one. When the ordered eigenvalue curves for the actual data and the random data

Reproduced with permission of the copyright owner. Further reproduction prohibited without permission.

are superimposed, the point at which they cross separates the real data components whose eigenvalues are greater than that expected by chance alone from those that are likely due to sampling error. Box 9.2 shows Horn's superimposed scree plot method applied to the anthropoid nasomaxillary data.

Box 9.2. Horn's scree plot criterion for retaining principal components applied to nasomaxillary variables.

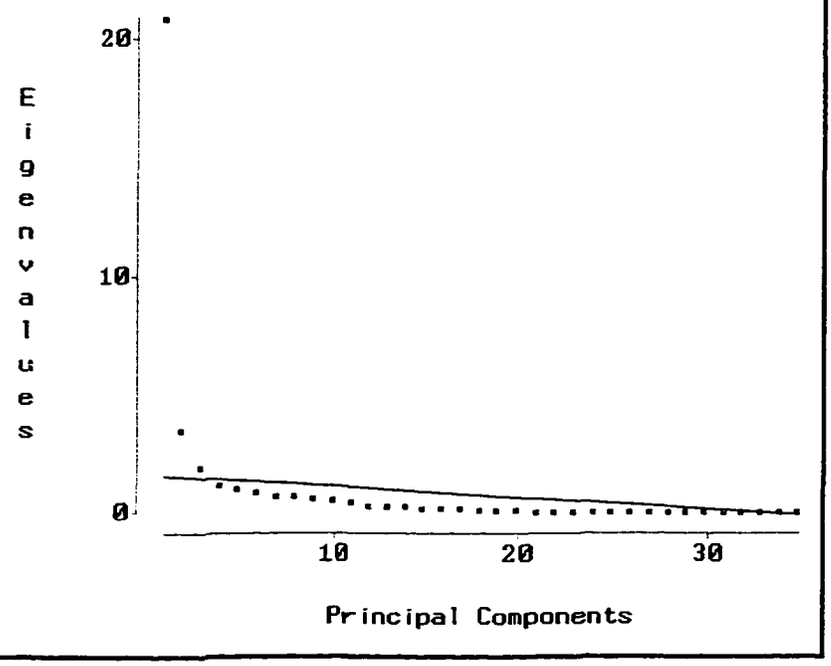

The dots in the scree plot in Box 9.2 represent eigenvalues for the 35 principal components of the actual data. The solid line connects the coordinates of eigenvalues and principal components for the random independent data. It can be seen that only the first three principal components of the nasomaxillary data are above the solid line. Thus, only $PC_{(1)}$-$PC_{(3)}$ have eigenvalues greater than that expected by chance.

In this and all subsequent PCAs, the component loadings were examined (*R*-type analysis) because the goal of the analyses was to summarize the correlation

Reproduced with permission of the copyright owner. Further reproduction prohibited without permission.

structure among the variables, and to describe the underlying dimensionality of the data, both as an aid to data reduction and as an exploratory tool. All component loadings derive from a varimax (orthogonal-simple structure) rotation of the initial principal components (see Cody & Smith, 1997:258). Correlation matrices were employed in all cases.

Box 9.3 lists the component loadings for the first three principal components of the anthropoid nasomaxillary data. Each vector of component loadings represents a new "factor" variable whose scale denotes the highest set of correlations (or maximum multidimensional variance) with the original variables. Since each eigenvector is determined on the basis of *orthogonal* principal axes of the 35-dimensional data plot, the principal components are uncorrelated. The component loadings of $PC_{(1)}$ thus represent standardized zero-order correlations of each of the original variables with the "new" first principal component variable; the component loadings of $PC_{(2)}$ represent the standardized partial correlations between each of the original variables and the "new" second principal component variable, with the variation from the first principal component removed; and the loadings of $PC_{(3)}$ represent the standardized partial correlations between the original variables and the "new" third principal component, with variation from the first two principal components removed (Marcus, 1990; Pedhazur, 1997; Cody & Smith, 1997).

The scatter plot of the first two principal component loadings is displayed in Box 9.4. It is clear from this graphic that the first principal component corresponds to a "size factor," a finding consistent with many other morphometric analyses (e.g., Jolicoeur, 1963; Blackith & Reyment, 1971; Shea, 1983; Marcus, 1990;

Reproduced with permission of the copyright owner. Further reproduction prohibited without permission.

Atchley, 1993).[1]

Box 9.3. Component loadings for the first three principal components of the nasomaxillary variables.

Variable	$PC_{(1)}$	$PC_{(2)}$	$PC_{(3)}$	Variable	$PC_{(1)}$	$PC_{(2)}$	$PC_{(3)}$
ΔL_YV1	0.750	0.474	0.239	ΔL_YV19	0.886	-0.075	-0.149
ΔL_YV2	0.145	-0.249	0.213	ΔL_YV20	0.907	0.127	-0.109
ΔL_YV3	0.789	-0.056	0.190	ΔL_YV21	0.93	-0.087	-0.169
ΔL_YV4	0.416	-0.462	-0.067	ΔL_YV22	0.927	-0.205	-0.055
ΔL_YV5	0.857	0.024	-0.132	ΔL_YV23	0.894	-0.258	0.046
ΔL_YV6	0.940	-0.072	0.031	ΔL_YV24	0.510	0.098	0.605
ΔL_YV7	0.876	0.055	0.131	ΔL_YV25	0.736	0.009	0.270
ΔL_YV8	0.860	-0.266	0.107	ΔL_YV26	0.902	-0.136	0.003
ΔL_YV9	0.843	-0.091	-0.113	ΔL_YV27	0.885	-0.107	-0.112
ΔL_YV10	0.964	0.011	-0.005	ΔL_YV28	0.927	0.227	-0.175
ΔL_YV11	0.856	0.206	0.143	ΔL_YV29	0.345	0.293	-0.058
ΔL_YV12	0.962	-0.144	-0.082	ΔL_YV30	0.122	0.640	-0.600
ΔL_YV13	-0.223	-0.685	0.070	ΔL_YV31	0.005	0.877	-0.222
ΔL_YV14	0.933	0.241	-0.142	ΔL_YV32	0.235	0.262	0.440
ΔL_YV15	0.95	-0.119	-0.03	ΔL_YV33	-0.300	0.183	0.630
ΔL_YV16	0.909	-0.298	-0.01	ΔL_YV34	0.990	0.034	-0.018
ΔL_YV17	0.94	0.233	0.040	ΔL_YV35	0.302	0.730	0.381
ΔL_YV18	0.950	-0.085	-0.071				

If the component loadings are taken to represent correlation coefficients (Marcus, 1990; Cody & Smith, 1997), then only loadings equal to or greater than 0.32 are significant (at $\alpha = .05$) for this data set. The dotted vertical line drawn through the bivariate plot in Box 9.4 separates the $PC_{(1)}$ loadings at this value. Notice that all of the variables measured as linear distances load significantly on $PC_{(1)}$ (they are to the right of the dotted vertical line), whereas all of the shape variables (i.e.,

[1] Shea (1983) has correctly pointed out that $PC_{(1)}$ is an "allometric" size factor (see Chapter 10).

Reproduced with permission of the copyright owner. Further reproduction prohibited without permission.

angles or ratios) do not load significantly on $PC_{(1)}$. The only exception to this rule is upper nasal bone width [Y2-NASWDU], which is linear yet has a $PC_{(1)}$ score of below 0.32.

Box 9.4. Plot of $PC_{(1)}$ and $PC_{(2)}$ component loadings of ΔL_YV data.

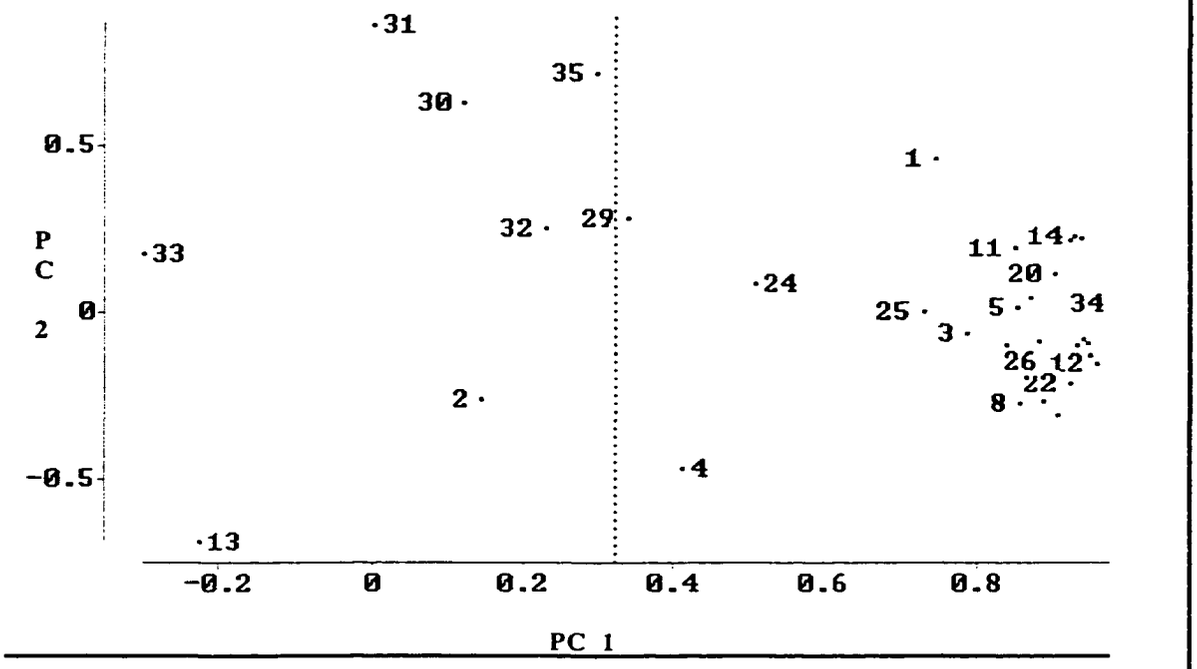

If the first principal component represents a size factor, then $PC_{(2)}$ and $PC_{(3)}$, which are orthogonal to $PC_{(1)}$, represent "size-independent" factors. An analysis of the second and third principal components, which together account for one-third of the remaining variance, may indicate substantive relationships among nasomaxillary characters after controlling for size. Marcus (1990) has cautioned that "...there is no special reason to search for biological sources of variation and covariation explained in the principal component analysis" (p. 89). Gibson *et al.* (1984), Marcus (1990), Atchley (1993), and Smith (1993) have found in separate principal components analyses of vertebrate morphometric data that there was no

Reproduced with permission of the copyright owner. Further reproduction prohibited without permission.

clear pattern of relations among variables beyond the first principal component. Marcus (per. comm.) has pointed out that these studies were based on relatively small sample sizes, and that other studies, such as Wright's (1968) path analysis of chicken bone metrics, have produced some meaningful results.

My view is that we should expect on first principles that "biological sources" are responsible for observed patterns of variation and covariation in the data. If biologically meaningful interpretations cannot be made of analytical results, then either the data or the analysis, or both, may be flawed. We have already encountered one potential source of error in the effects that multi-level phylogenies have on the correlational structure of a data matrix. Phylogenetic simulation studies (e.g., Martins, 1996; this study, Chapter 6) have shown that multi-level phylogenetic topologies result in a high degree—30% or more—of false significant correlations among the variables (i.e., an elevated Type I error rate). This amount of inaccuracy in a correlation or covariance matrix could be sufficient to obscure biologically meaningful patterns in principal components and other analyses that employ correlation or covariance matrices (e.g. structural equation modeling).

Analysis of the second and third principal components of the autoregressed/ACP-adjusted, log-transformed data reveal several patterns that are biologically interpretable. Box 9.5 presents the scatter plot of $PC_{(2)}$ against $PC_{(3)}$. As in Box 9.4, the dotted lines separate significant from nonsignificant areas of the bivariate plot. In this case the four corner areas indicate significance with both principal components, the center area indicates nonsignificance with both principal components and the four center perimeter areas represent significance on only one

Reproduced with permission of the copyright owner. Further reproduction prohibited without permission.

principal component. Box 9.6 lists the variables located in significant areas of the PCA plot.

Box 9.5. Plot of $PC_{(2)}$ and $PC_{(3)}$ component loadings of ΔL_YV data (size independent).

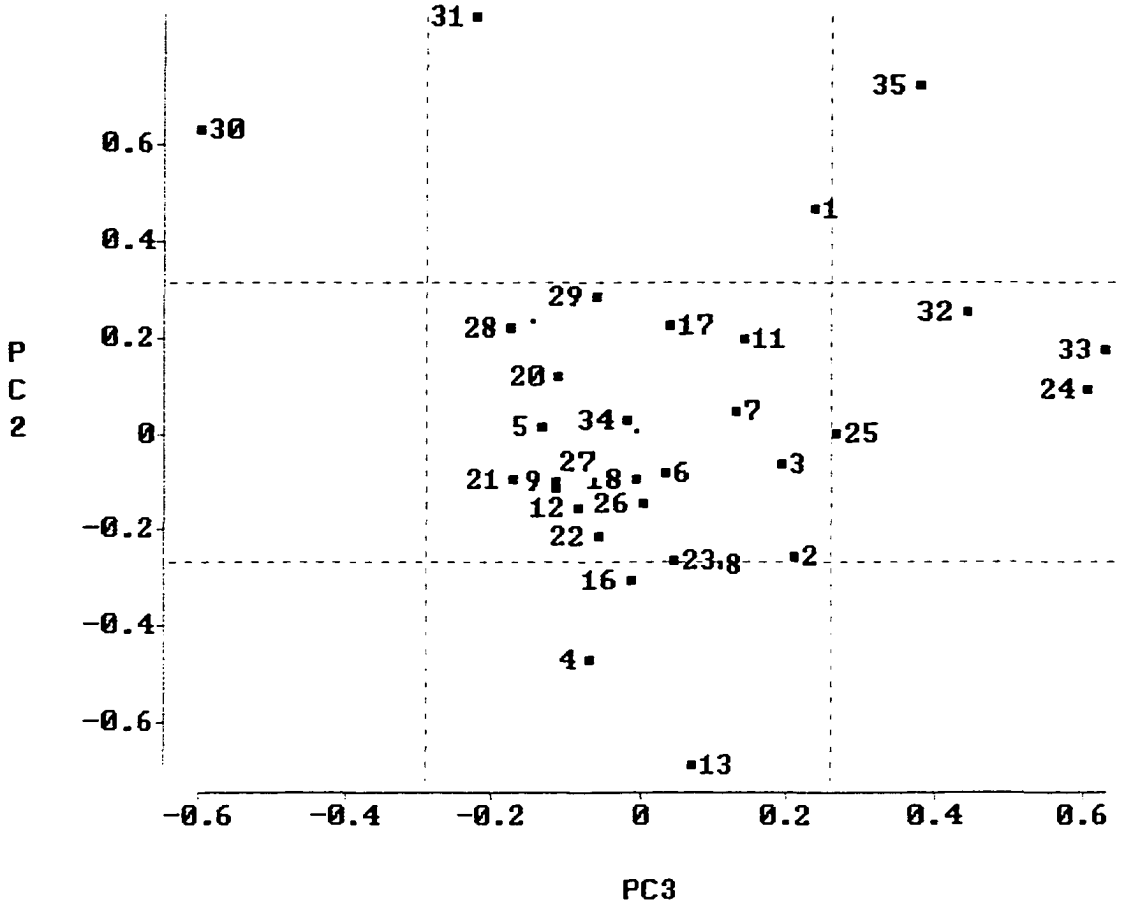

The results indicate that $PC_{(2)}$ contrasts facial prognathism, nasal bone length and paranasal plate orientation (all with high positive loadings) with superior and posterior facial breadth, and zygomatic root position (all with high negative loadings). In other words, anthropoids that have evolved or developed high facial prognathism, also tend to have relatively long nasal bones, sagittally oriented paranasal plates, narrow upper and posterior facial breadth, and a more posteriorly

Reproduced with permission of the copyright owner. Further reproduction prohibited without permission.

positioned zygomatic root. $PC_{(3)}$ in part contradicts $PC_{(2)}$ in that it associates at least one measure of facial prognathism with reduced paranasal plate orientation. $PC_{(3)}$ further associates facial prognathism with a shallow anterior palate, an occlusal surface oriented parallel to the Frankfort plane, and pronounced facial concavity.

Box 9.6. Summary of scatter plot of $PC_{(2)}$ and $PC_{(3)}$.

	PC3-High Neg	PC3-Low	PC3-High Pos
PC2-High Pos.	Krogman's Angle (Y30)	Enlow's Angle (Y31) Nasal Bone Length (Y1)	Paranasal Plate Orientation (Y35)
PC2-Low		All other nasomaxillary variables (Y3, Y5, Y6, Y7, Y9, Y10, Y11, Y14, Y15, Y17, Y18, Y19, Y20, Y21, Y27, Y28, Y29, Y34)	Palatal Depth I2 (Y24) Palatal Depth P3 (Y25) Occlusal Plane (Y32) Facial Convexity (Y33)
PC2-High Neg		Upper Nasal Bone Width (Y2); Nasal Process of Maxilla Width (Y4); Posterior Nasal Aperture Breadth (Y8); Bizygomatic Breadth (Y12); A-P Position of Zygomatic Root (Y13); Upper Facial Breadth (Y16); Palatal Width M1 (Y22); Palatal Width M3 (Y23)	

Data Reduction

The foregoing PCA revealed several "clusters" of highly intercorrelated variables. To the extent that the variables contained within each cluster measure the same basic attribute of the organism they are redundant and may be reduced in number for subsequent analyses. The following nasomaxillary variables were excluded from subsequent analyses for this reason. (1) *Upper nasal bone width* [Y2-NASWDU]: part of a cluster of facial breadth variables; redundant with interorbital distance. (2) *Lower nasal bone width* [Y3-NASWDL]: redundant with nasal aperture breadth. (3) *Zygomatic estimated area* [Y10-ZYGARE]: redundant with zygomatic

Reproduced with permission of the copyright owner. Further reproduction prohibited without permission.

height, which appears to be an adequate measure of zygomatic size. (4) *Bimaxillary breadth* [Y15-BZYGWD]: part of a cluster of collinear facial breadth variables. (5) *Inter-P^3 palatal width* [Y21-P3PALW]: redundant with inter-I^2 palatal width and inter-M^1 palatal width. (6) *Palatal length* [Y28-PALLGT]: redundant with maxillary arch length.[2] (7) *Palatal thickness at M^1* [Y29-PALTHK]: unreliable measurement (see Chapter 5). (8) *Facial size* [Y34-FACSIZ]: collinear with several other important variables including maxillary arch length and anterior facial length.

Examination of Size Independent Residual Correlation Matrix

The purpose of the principal components analysis of the preceding section was to reveal the underlying structure of the data and aid in data reduction. The analysis showed that three orthogonal components or factors account for 76% of the total variance in the data. It also revealed several collinear clusters of variables (e.g., a 'posterior facial breadth' cluster). Despite its obvious usefulness the results of a PCA can be deceptive.

In the preceding PCA the orthogonality constraint was imposed in order to extract size-independent second and third-order components from the data. In so doing, variables whose correlational properties fall between major orthogonal components (i.e., they are moderately correlated with both size and second or third component variables) may have been obscured in the analysis.[3] PCA is not very

---

[2] Oyen (1984) concluded with respect to *Papio* that the growth of palatal length relative to maxillary length remains constant (p. 348).

[3] It is for this reason that various authors (e.g., Hatcher, 1994; Cody & Smith, 1996) have noted that oblique rotation methods often yield more substantively meaningful factors.

Reproduced with permission of the copyright owner. Further reproduction prohibited without permission.

good at isolating the most meaningful character-by-character relationships in the data. If the number of variables is manageable, a thorough examination of the size-independent residual correlation matrix[4] may yield some important insights obscured by the PCA (see Box 9.7). In this manner, two key nasomaxillary variables were detected that were concealed by the PCA orthogonality constraint—maxillary arch length [Y14-MXARCL] and anterior facial length [Y17-AFACHT]. Even after accounting for cranial size (see Chapter 10), these two characters correlated significantly with over half of the nasomaxillary variables under study. Moreover, both features play prominent roles in current models of primate craniofacial growth (*cf.*, Krogman, 1974; Enlow, 1990). Maxillary arch length and anterior facial length were therefore added to the list of nasomaxillary characters already identified by the PCA for further ontogenetic shape analysis.

[4] In the present context the *size independent residual correlation matrix* refers to the correlation matrix of the residuals of each nasomaxillary character after regression on cranial centroid size. It will be shown in Chapter 10 that centroid size and the $PC_{(1)}$ size factor are nearly equivalent.

Reproduced with permission of the copyright owner. Further reproduction prohibited without permission.

Box 9.7. Scatter plot matrix of nasomaxillary residuals on cranial size. Species means raw data (n=37).

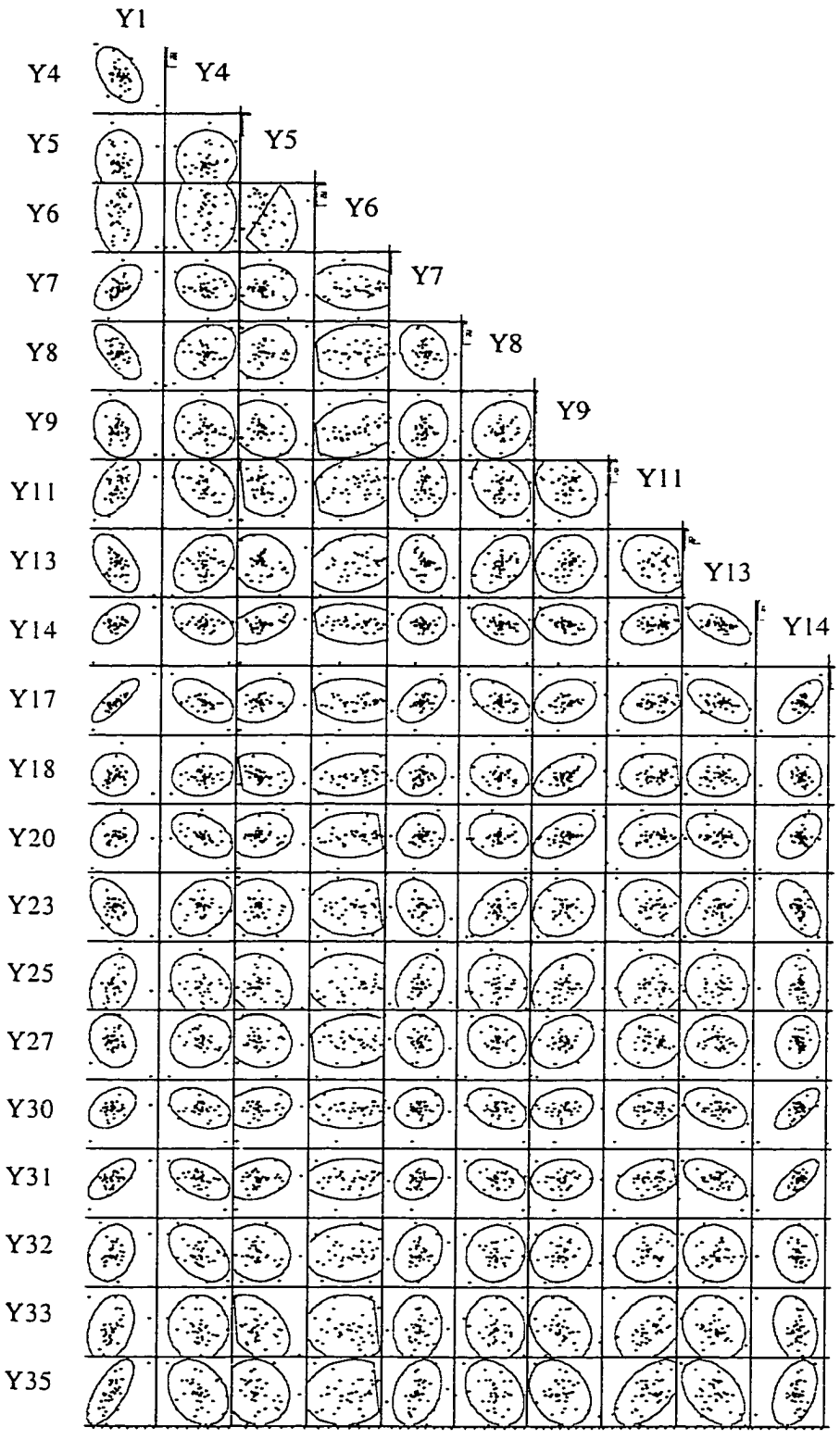

Reproduced with permission of the copyright owner. Further reproduction prohibited without permission.

Box 9.7. (continued from previous page)

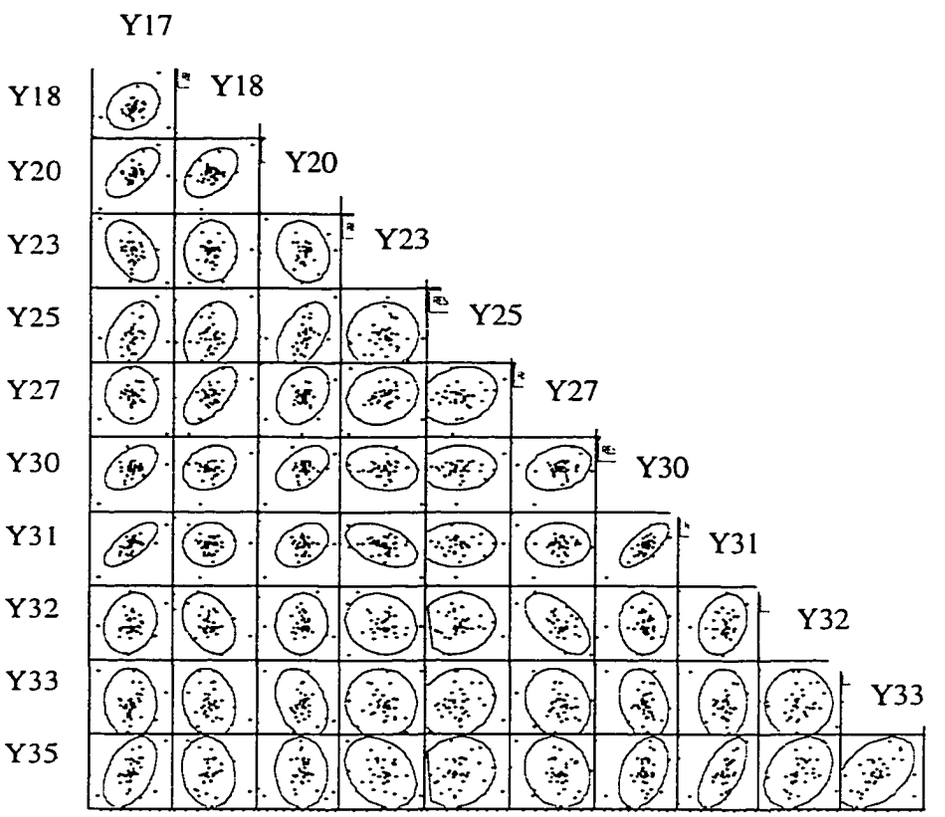

Ontogenetic Nasomaxillary Shape Analyses

The covariances among nasomaxillary traits revealed by the PCA and residual correlation matrix may have resulted from structural growth constraints. Ontogenetic growth relationships are often at the root of relationships observed among craniofacial traits in adults, both within and among taxa (Gould, 1966; Albrecht, *et al.*, 1979). Presley (1993) has cogently summarized the connection between ontogenetic and phylogenetic variation thus: "Our perception of phylogeny has always been of changing form. This change in form must reflect effects on developmental processes of which adult form is only the final manifestation" (p.

Reproduced with permission of the copyright owner. Further reproduction prohibited without permission.

372). To help quantify the ontogenetic patterns that might account for the observed interrelationships among nasomaxillary traits in adults, I conducted a series of ontogenetic shape analyses.

The ontogenetic shape analyses reported in this section were intended to reveal correlated growth changes among nasomaxillary variables, defined on the basis of adult traits. Analyses involved, but were not confined to, those traits that exhibited high loadings on size-independent components of the PCA (see Boxes 9.5 and 9.6), or significance in the residual correlation matrix.

Three separate ontogenetic shape analyses were undertaken. The first involved an examination of growth-related changes in the shape of the anthropoid lateral facial profile. This analysis was intended to shed light on the interrelations among facial prognathism, occlusal plane orientation and the lengths of the maxillary arch and the anterior and posterior facial planes. The second shape analysis focused specifically on developmental changes related to the shape of the maxillary arch. Ontogenetic patterns revealed in the analysis might help explain observed nomological relationships between facial breadth and numerous other characters. The third and final shape analysis was devoted to spatially correlated relationships among facial breadth, nasal bone length, and midfacial projection.

In order to quantify changes in craniofacial shape during ontogeny, a series of infant anthropoid crania were digitized for baseline comparison with adults. Known males were excluded from the sample. A list of the specimens used in the analyses is given in Box 9.8. All but 9 of the 27 genera represented in the adult sample were also represented in the infant sample.

Reproduced with permission of the copyright owner. Further reproduction prohibited without permission.

Box 9.8. List of infant anthropoid specimens used in ontogenetic shape analysis.

Species	AMNH #	Dental Developmental Stage
Alouatta palliata	128112	di1-2, dc, dm1-3 erupted; M1 in crypt
Ateles geoffroyi	17216	di1-2 erupted; dc, dc, dm1-3 in crypt
Lagothrix lagothrica	63934	di1-2, dc, dm1-2 erupted; dm3 in crypt
Chiropotes satanas	41948	di1-2, dc, dm1-3 erupted; M1 in crypt
Callicebus cupreus	63933	di1-2, dc, dm1-3 erupted; M1 in crypt
Cebus apella	369778	di1-2 erupted; dc, dc, dm1-3 in crypt
Cebus capucinus	177077	di1-2, dc, dm1 erupted; dm2-3, M1 in crypt
Chlorocebus aethiops	80788	di1-2 erupted; dc, dm1-2 in crypt
Cercopithecus neglectus	52427	di1-2, dc, dm1-2 erupted; M1 in crypt
Cercopithecus mitis	52366	di1-2, dc, dm1-2 in crypt
Cercopithecus ascanius	52534	di1-2, dc, dm1 erupted; dm2 in crypt
Macaca nemestrina	103727	di1-2, dc, dm1-2 erupted; M1 in crypt
Macaca fascicularis	100275	I1, dc, dm1-2, M1 erupted; I2, M2 in crypt
Macaca mulatta	60067	di1-2, dc, dm1-2 erupted; M1 in crypt
Papio hamadryus	80776	di1-2, dc, dm1 erupted; dm2, M1 in crypt
Lophocebus albigena	52610	di1-2, dc, dm1 erupted; dm2, M1 in crypt
Colobus guereza	52235	di1-2, dc, dm1-2 erupted; M1 in crypt
Procolobus badius	52274	di1-2, dc, dm1-2 in crypt
Presbytis melalophos	106607	di1-2, dc, dm1-2 erupted; M1 in crypt
Hylobates lar	148203	di1-2, dc, dm1-2 erupted; M1 in crypt
Pongo pygmaeus	200899	di1-2, dc, dm1-2 erupted; M1 in crypt
Gorilla gorilla	28273	di1-2, dc, dm1-2 erupted; M1 in crypt
Homo sapiens	84329	di1-2, dc, dm1-2 in crypt
Pan troglodytes	51385	di1-2, dc, dm1-2 in crypt

The cross-sectional ontogenetic analysis that follows should be viewed with caution. With a sample of only 24 infant specimens representing 6 anthropoid families, the power of the analysis is weak and the chance of error high. The accuracy and validity of the analysis rests on both empirical and logical grounds. Empirical in that the ratio of within-species to among-species variance is sufficiently low to permit generalizations on the basis of a few representative specimens; and logical in that information pertaining to form change can be deduced from a comparison of objects at chronological end points. Every attempt has been made to cross-validate the results uncovered here with those of previous studies.

And yet, it is the paucity of available information on anthropoid craniofacial growth that has necessitated an independent investigation in the first place. The

Reproduced with permission of the copyright owner. Further reproduction prohibited without permission.

statement by Hall and Hanken (1993) that "...for the vast majority of vertebrate species, few if any features of skull development have been formally documented..." is as true of anthropoids as any other vertebrate group . Most anthropoid craniofacial growth studies have been confined to a limited number of species, typically *Macaca*, *Papio*, the Great Apes and humans. Moore's (1981) comment that "With few exceptions, detailed information about postnatal growth in the remaining primate species is lacking" (p. 38) is as true today as is was two decades ago. Moreover, the studies that have been conducted typically focus on one or a few characters, such as palatal growth or basicranial growth. Nevertheless, there are enough pieces of the puzzle in place to begin to see at least the outline of a recognizable pattern, and the current analysis is a preliminary attempt to bridge some of the more isolated pieces.

Ontogenetic Shape Analysis I. Facial Profile.

As an aid to quantify and visualize the structural relationships among selected nasomaxillary traits, I employed Vogel's (1968) concept of the facial triangle, defined here in lateral view by the points nasion, prosthion and maxillary tuberosity. A line connecting prosthion to orbitale (Frankfort Horizontal) was also introduced to depict the position of the facial triangle relative to the postural orientation of the cranium (see Box 9.9). A least squares optimization fit of the infant facial triangle coordinates revealed much less variation of facial form at this early stage of ontogeny compared to adults, an observation well documented for many other biological traits (*cf.*, de Beer, 1937).

Least squares coordinate superimpositions were performed separately on infant

Reproduced with permission of the copyright owner. Further reproduction prohibited without permission.

and adult specimens using *GRF-ND* software (Slice, 1994). The infant facial triangles were then superimposed on adult profiles, using the mean configurations for fourteen anthropoid taxa. The superimposition of infant on adult profiles was not based on least squares or other minimization criteria, nor did it follow the conventional practice of registration on a single landmark (e.g., sella); it was undertaken simply to provide a visual aid in comparing differences in facial orientation and shape between infants and adults of the same taxa.[5] Quantification of shape change proceeded by comparison of the infant and adult landmark configurations, and was therefore independent of the method of superimposition. The superimposed facial profiles are shown in Box 9.9. The dotted lines represent infant facial profiles and the solid lines depict adult mean configurations for the specified taxa. The dots clustered around consensus landmarks represent individual specimen coordinate points.

Analysis of the shape differences between mean infant and adult facial forms indicates that nearly all of the variation in anthropoid facial profiles derives from two fundamental growth processes (in addition to overall growth enlargement). These processes include: (1) *facial displacement rotation*: an overall forward "translocational" rotation of the entire facial triangle, and (2) *differential facial growth*: the differential rate of bone remodeling and displacement at several key sites of craniofacial growth (i.e., nasomaxillary sutures, maxillary tuberosities, etc.) primarily affecting the anterior, posterior and alveolar facial planes (Enlow, 1975).

[5] This approach follows Enlow (1966), who developed a method of "visual" superimposition based on observed patterns of facial growth and remodeling.

Reproduced with permission of the copyright owner. Further reproduction prohibited without permission.

Ontogenetic shape changes resulting from these two growth processes were quantified from the coordinates and profiles displayed in Box 9.9, as follows. Facial rotation was measured as the angle between the posterior facial plane of the infant triangle and the corresponding plane of the adult triangle after alignment of each on the Frankfort horizontal. Relative rates of growth of the three facial planes making up the facial triangle (maxillary arch, and posterior and anterior facial planes) were determined trigonometrically. There is one optimal pattern of differential growth that can account for changes in facial shape from infant to adult in each taxon, and this pattern is given by the difference in corresponding angles opposite the three planes (Anton, 1984).

Results of the facial profile shape analysis are reported in Box 9.10 in the form of a line chart comparing patterns of facial rotation and relative facial growth among 13 anthropoid taxa. Facial rotation values range from 0° in *Hylobates* to 25° in Cercopithecinae. With respect to relative facial profile growth, three distinct patterns were discerned: (a) a pattern in which growth of the anterior facial plane is greater than that of the maxillary arch, and both are greater than that of the posterior facial plane (observed in Papionina, Cercopithecinae, Macacina, Colobina, *Pongo*, *Gorilla* and *Pan*); (b) a pattern in which the growth of the maxillary arch is greater than that of the anterior facial plane, and both are greater than that of the posterior facial plane (observed in Atelinae, Pithecinae, Presbytina, and Hylobatinae), and (c) a pattern in which growth of the posterior facial plane is greater than that of the maxillary arch, and both are greater than that of the anterior facial plane (observed exclusively in *Homo*). A factor analytic clustering procedure confirmed the distinctiveness of these three craniofacial growth patterns (see Box 9.11).

Reproduced with permission of the copyright owner. Further reproduction prohibited without permission.

Box 9.9. Superimpositions of infant (dotted line) and adult (solid line) facial profiles for various taxa.

Subfamily: Atelinae

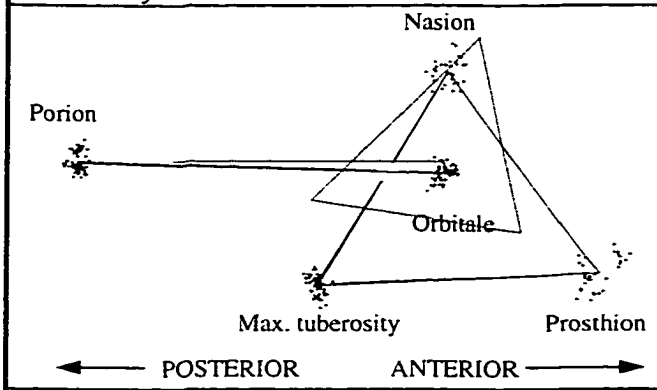

Subfamily: Pithecinae

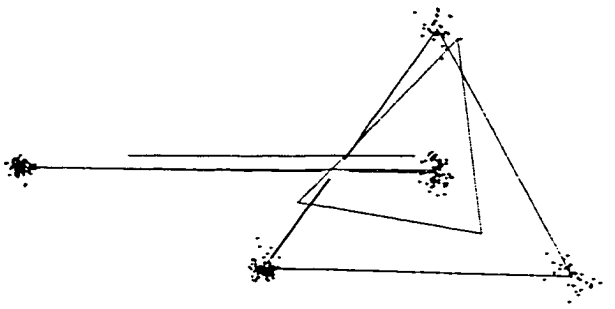

Subfamily: Cebinae

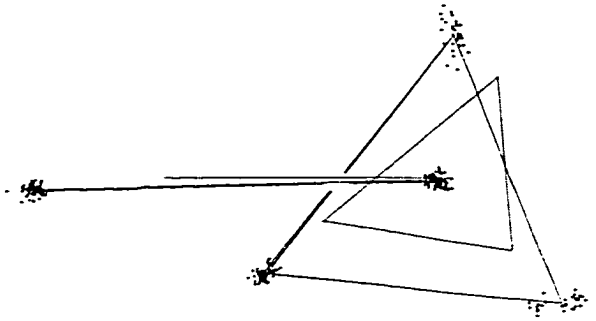

Subfamily: Callitrichinae

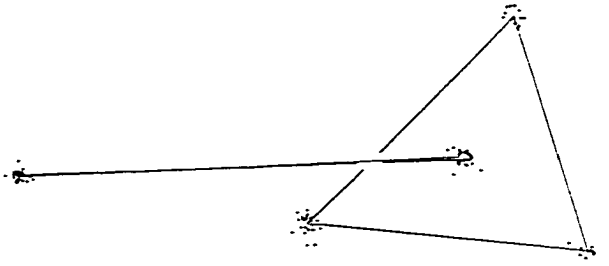

Tribe: Cercopithecini

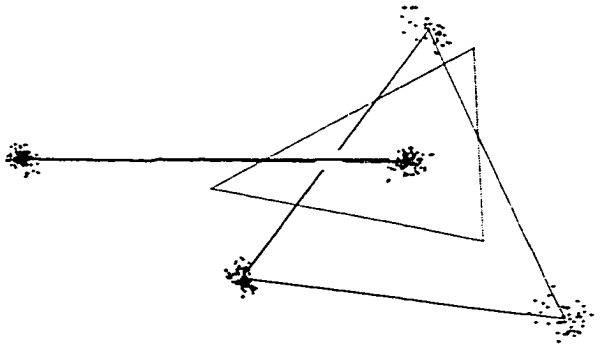

Subtribe: Macacina

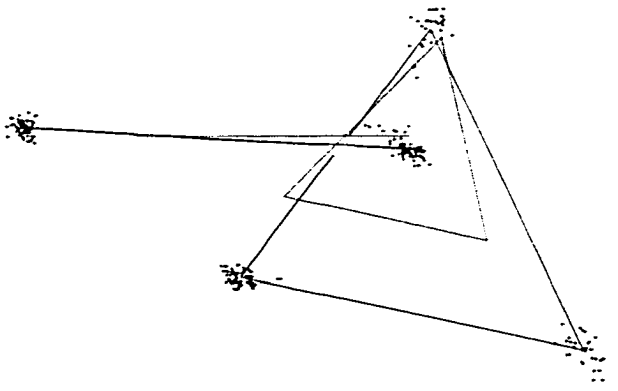

Reproduced with permission of the copyright owner. Further reproduction prohibited without permission.

Subtribe: Papionina	Subtribe: Colobina
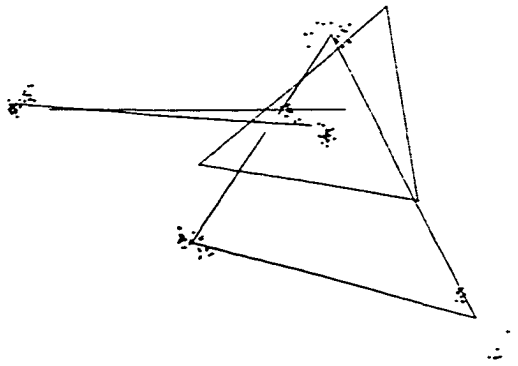	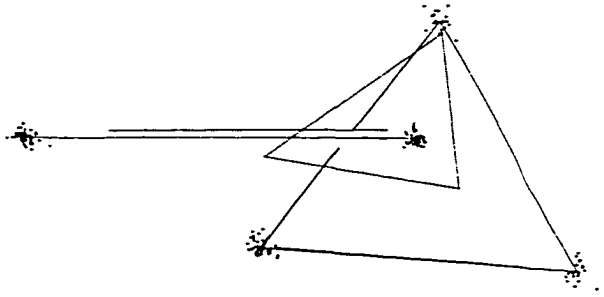
Subtribe: Presbytina	**Subfamily: Hylobatinae**
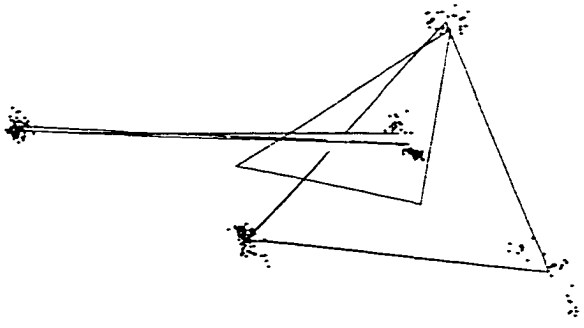	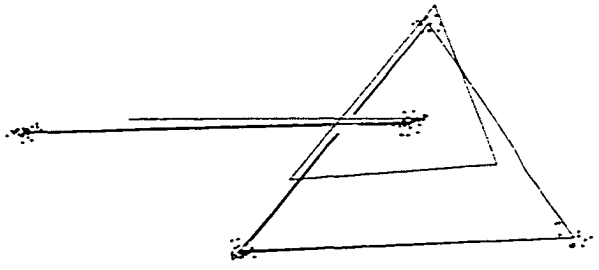
Genus: *Pongo*	**Genus: *Gorilla***
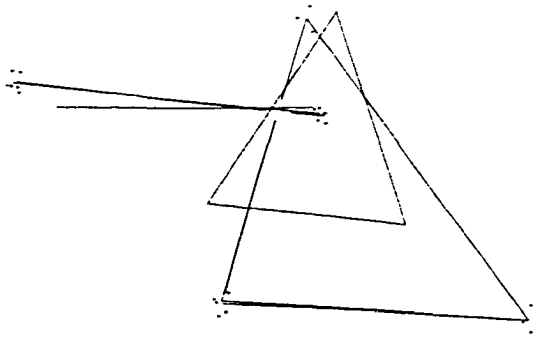	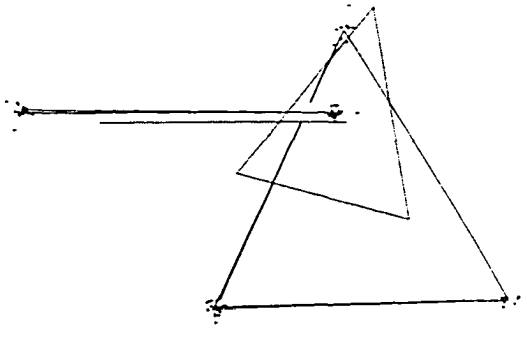
Genus: *Homo*	**Genus: *Pan***
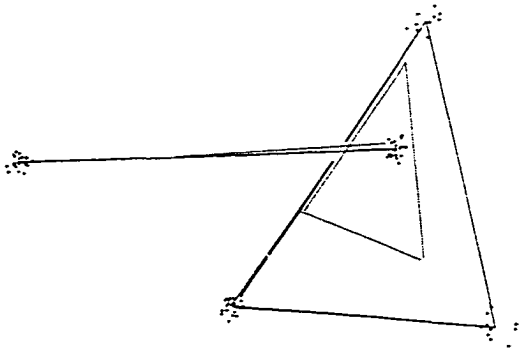	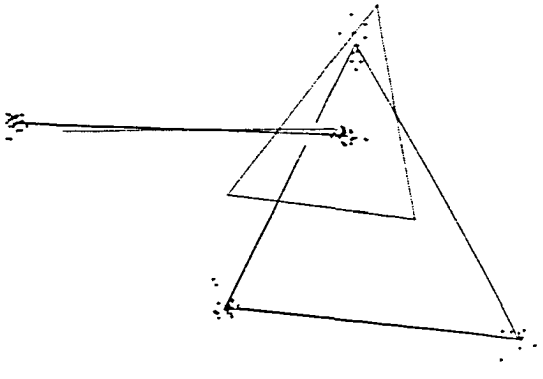

Reproduced with permission of the copyright owner. Further reproduction prohibited without permission.

Box 9.10. Line chart depicting results of ontogenetic shape analysis of anthropoid facial profiles. FR: facial rotation in degrees from infant to adult; PF: relative growth of posterior facial plane; PA: relative growth of palate; AF: relative growth of anterior facial plane.

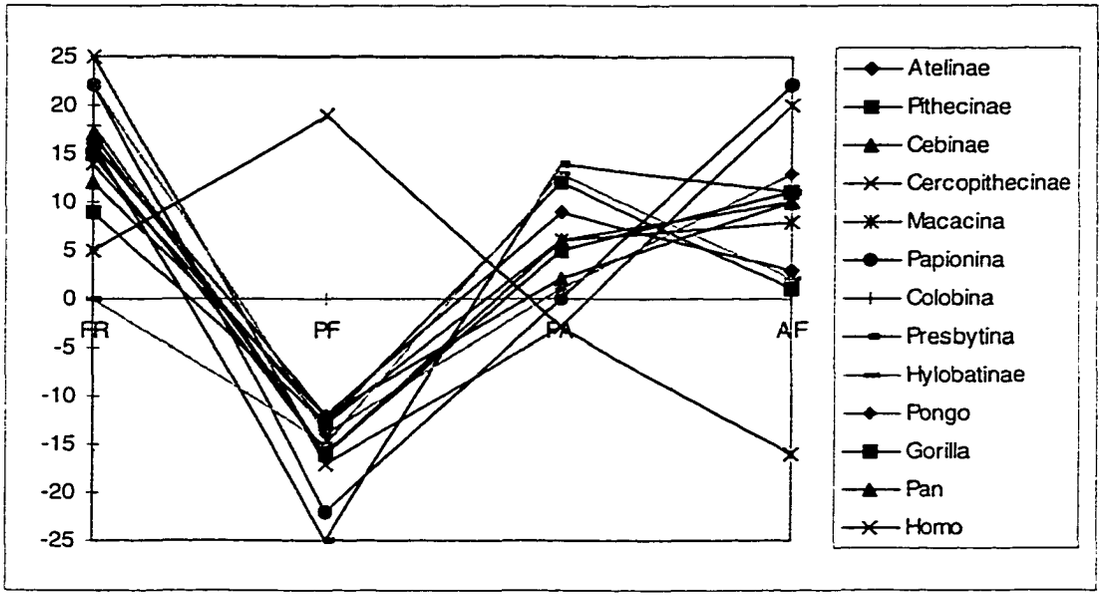

While informative, these results do not establish the existence of correlated growth changes. They do show that several distinct patterns of facial growth are expressed among different anthropoid groups. Each of these growth patterns may be associated with a correspondingly distinct set of structural growth constraints.

Reproduced with permission of the copyright owner. Further reproduction prohibited without permission.

Box 9.11. Plot of factor scores showing patterns of facial profile growth in anthropoids (n=24).

Initial Factor Method: Principal Factors

Plot of Factor Pattern for FACTOR1 and FACTOR2

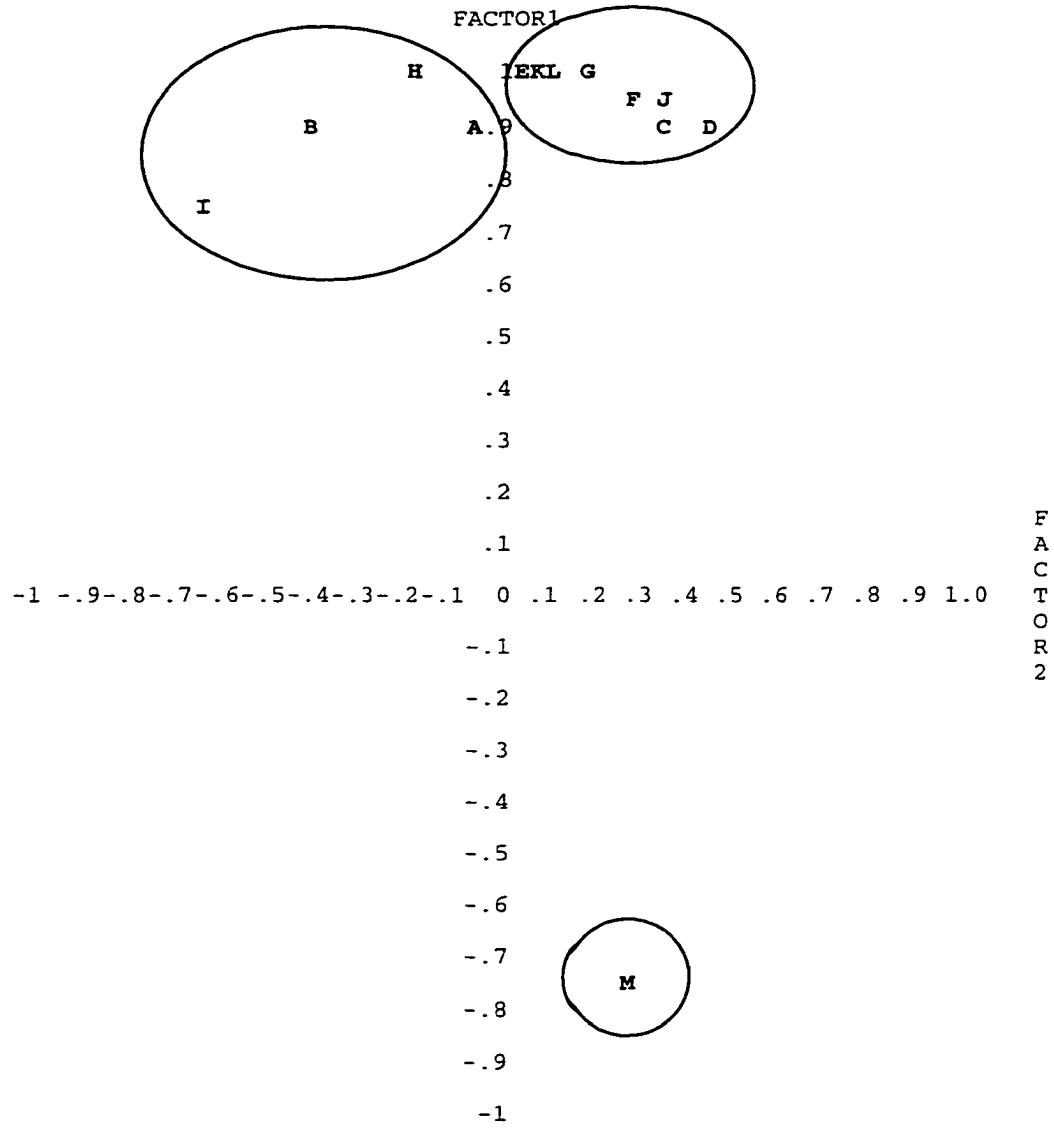

A=Atelinae; B=Pithecinae; C=Cebinae; D=Cercopithecinae; E=Macacina; F=Papionina
G=Colobina; H=Presbytina; I=Hylobatinae; J=*Pongo*; K=*Gorilla*; L=*Pan*; M=*Homo*

Reproduced with permission of the copyright owner. Further reproduction prohibited without permission.

Ontogenetic Shape Analysis II. Maxillary Arch.

A potential growth constraint is apparent in the relationship between maxillary arch length and breadth. To visualize how the shape of the maxillary arch changes from infant to adult, the length-to-breadth ratio is depicted as a triangle with prosthion, and left and right maxillary tuberosities at the vertices. Rather than use a least squares optimization fit as in the preceding analysis, the maxillary triangles of both the infant and adult specimens were scaled, translated and rotated to a common baseline—left to right maxillary tuberosities. Thus, only prosthion remained free to vary. Mean infant and adult maxillary shapes were then distinguished by drawing separate triangles for each. The results, shown in Box 9.12, indicate that in all 13 anthropoid taxa examined there is an increase in the length of the maxillary arch relative to breadth from infant to adult. Box 9.13 graphically depicts the vectors of relative maxillary growth (change in length-to-breadth ratio) for the 13 taxa.[6] Only 3 taxa are not covered by the 99% confidence interval around the overall anthropoid mean growth slope. Papionina and Pitheciinae exhibit a maxillary length-to-breadth growth vector significantly higher than the mean, whereas Atelinae displays a growth vector that is significantly lower than the overall mean. Although the growth vector in the modern human sample is not significantly different from the anthropoid mean, humans stand out in possessing a low absolute maxillary length-to-breadth ratio.

---

[6] The "growth slopes" depicted in Box 9.13 should be viewed with caution. The vectors were calculated on the basis of only a few (and in some cases only one) infant specimens per taxon.

Reproduced with permission of the copyright owner. Further reproduction prohibited without permission.

Box 9.12. Bimaxillary tuberosity baseline superimpositions of infant (dotted line) and adult (solid line) maxillary arch shapes for various anthropoid taxa.

Subfamily: Atelinae.

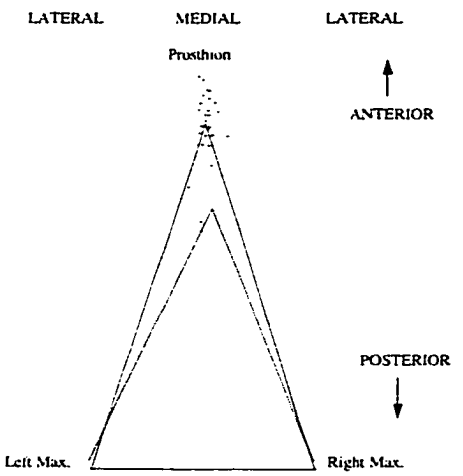

Subfamily: Pithecinae

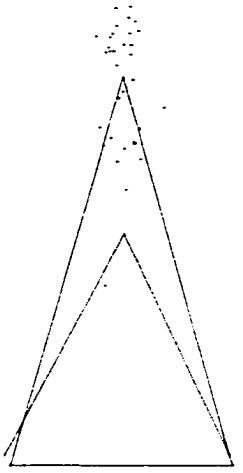

Subfamily: Cebinae

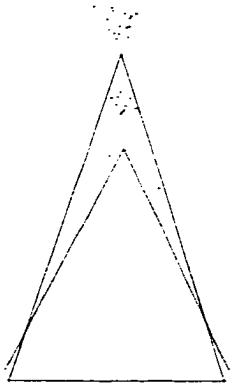

Subfamily: Callitrichinae

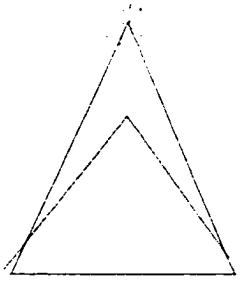

Tribe: Cercopithecini

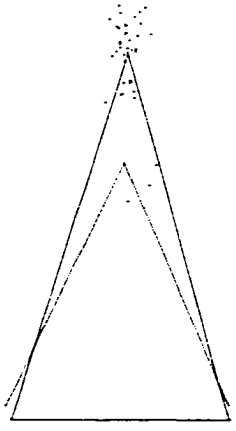

Subtribe: Macacina

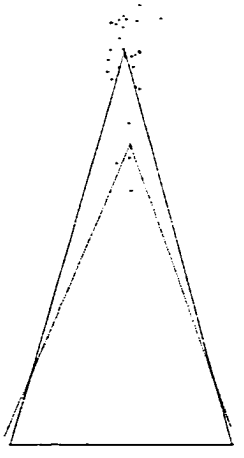

Reproduced with permission of the copyright owner. Further reproduction prohibited without permission.

Subtribe: Papionina	Subtribe: Colobina
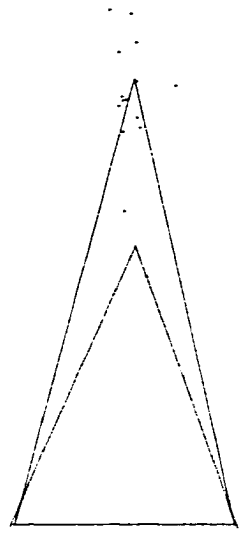	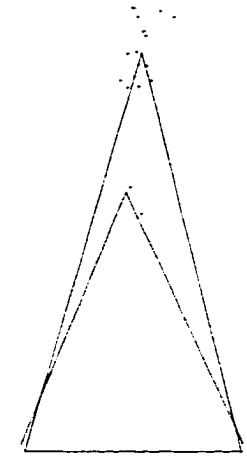
Subtribe: Presbytina	Subfamily: Hylobatinae
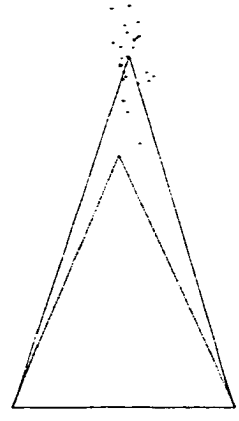	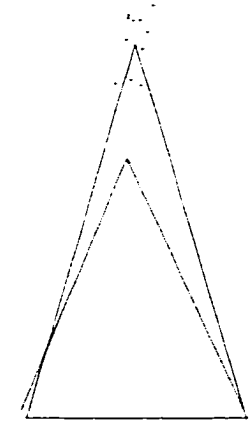
Genus: *Pongo*	Genus: *Gorilla*
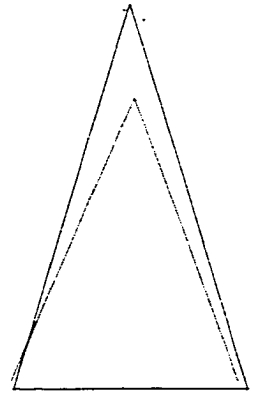	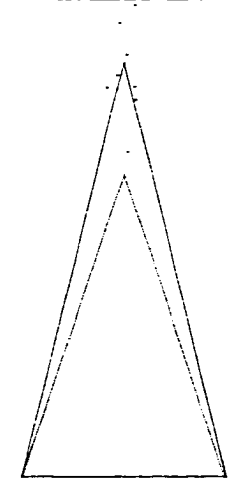

Reproduced with permission of the copyright owner. Further reproduction prohibited without permission.

Genus: *Homo*	Genus: *Pan*
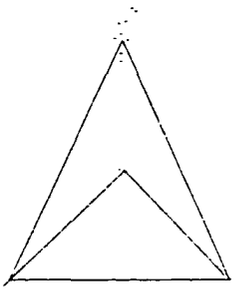	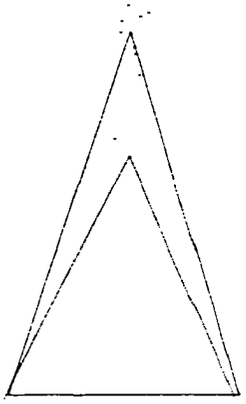

Box 9.13. Vectors of relative maxillary growth (change in length-to-breadth ratio) for the anthropoid 13 taxa (n=24)

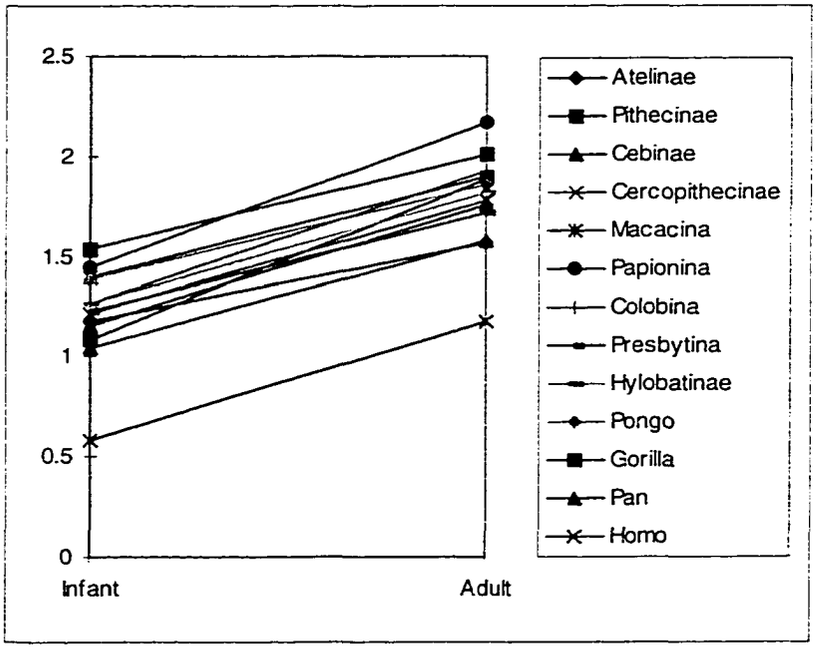

Reproduced with permission of the copyright owner. Further reproduction prohibited without permission.

Ontogenetic Shape Analysis III. Nasal/Mid-Facial Region

According to the results of the PCA there exist a number of size-independent associations involving nasomaxillary characters of the nasal/mid-facial region. To determine whether these inter-adult associations are also expressed as ontogenetic covariances, a shape analysis was carried out on two triangular elements of the midface. One triangle was defined by the landmarks nasion-rhinion-prosthion (the "midline anterior facial triangle"), and a second triangle was defined by left orbitale-rhinion-right orbitale (the "bilateral midfacial triangle"). Since the two triangles lie on perpendicular planes it is not possible to view them both in a single graphic. There is, however, a way around this limitation. By superimposing landmark configurations containing both triangles to a common baseline—left orbitale-right orbitale—then rotating them to align on the Frankfort horizontal, and viewing the resultant superimpositions in lateral view, it was possible to visualize shape variation in both triangular elements at once (see Box 9.14).

Outlines of the mean adult (solid lines) and infant (short-dotted lines) configurations are presented in Box 9.14 after superimposition in the manner described. The midline anterior facial triangles are easily observed and compared. But because the bilateral midfacial triangles are laid "flat" in lateral view we can see only their lateral edges which appear as straight lines from orbitale to rhinion. However, since all the landmark configurations are scaled to a common biorbitale length, the relative lengths of the orbitale-rhinion lines adequately represent shape variability of the midfacial triangles: the longer the length of the orbitale-rhinion line the greater the length-to-width ratio of the triangle. The Frankfort horizontal (long-dotted lines) is shown for reference.

Reproduced with permission of the copyright owner. Further reproduction prohibited without permission.

The anterior facial triangles depict the degree of facial convexity in lateral profile. It can be seen that adult Pitheciinae exhibits the greatest degree of facial convexity, whereas *Pongo* exhibits the greatest degree of facial concavity. Adults of Colobina, Presbytina, and Hylobatinae all display relatively flat anterior facial profiles (neither convex nor concave), while the remaining taxa show only slight facial convexity.

A downward rotation of the entire anterior facial triangle is apparent from infant to adult in the majority of taxa examined (the main exceptions are Pitheciinae and Cebinae). The analysis also confirms the forward translocational rotation of the anterior facial plane detected in the facial profile shape comparisons. There appears to be a substantial amount of variability in the shape of the bilateral midfacial triangle, which depicts the projection of the nasal bridge in relation to the lower orbital margins. The paranasal plates tend to project outward, thereby increasing in relative length in Pitheciinae, *Macaca*, Papionina, *Pongo* and *Gorilla*, while remaining constant or decreasing in the remaining taxa.

Reproduced with permission of the copyright owner. Further reproduction prohibited without permission.

Box 9.14. Biorbitale baseline superimpositions of infant (short-dotted line) and adult (solid line) nasal\mid-facial shapes for various anthropoid taxa (long-dotted line is Frankfort plane).

Subfamily: Atelinae.

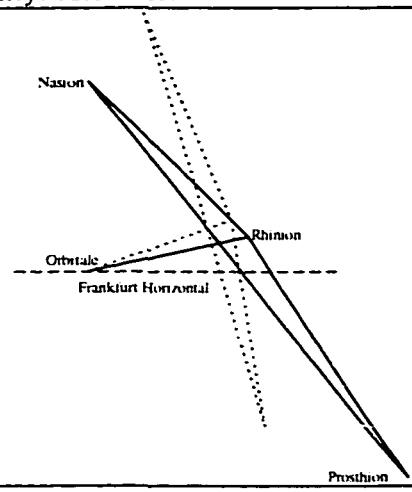

Subfamily: Pitheciinae

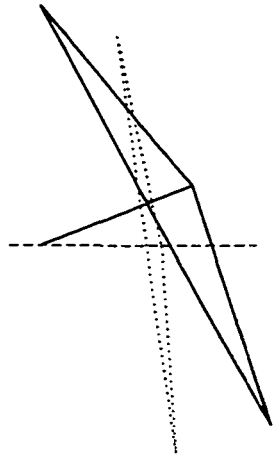

Subfamily: Cebinae

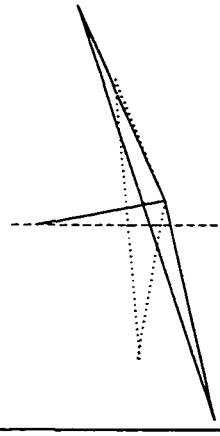

Subfamily: Callitrichinae

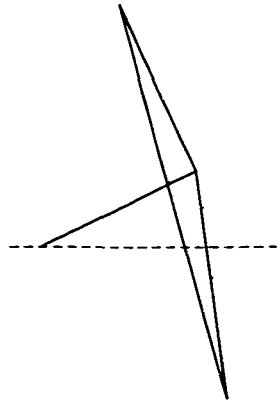

Tribe: Cercopithecini

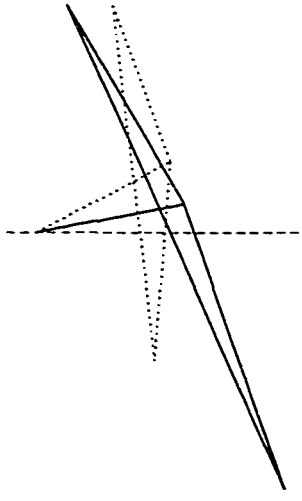

Subtribe: Macacina

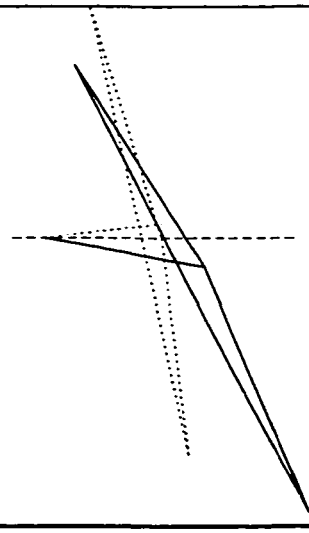

Reproduced with permission of the copyright owner. Further reproduction prohibited without permission.

Subtribe: Papionina	Subtribe: Colobina
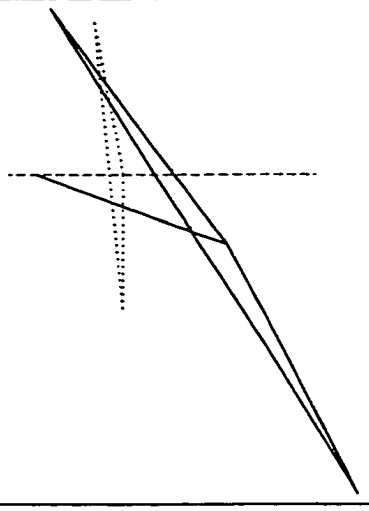	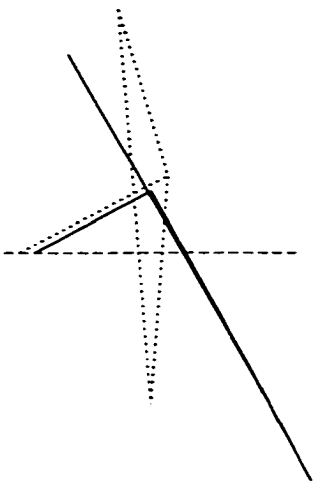
Subtribe: Presbytina	**Subfamily: Hylobatinae**
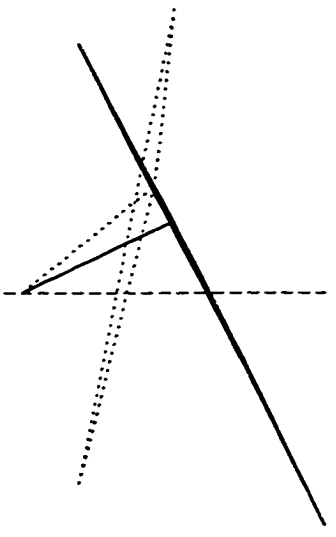	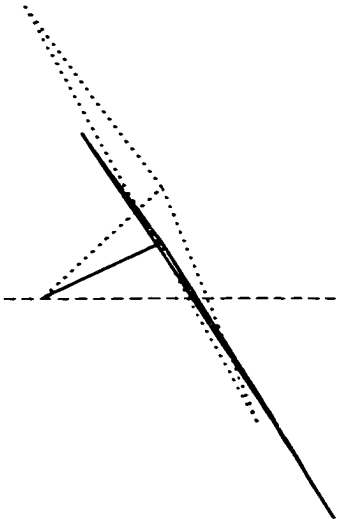
Genus: *Pongo*	**Genus: *Gorilla***
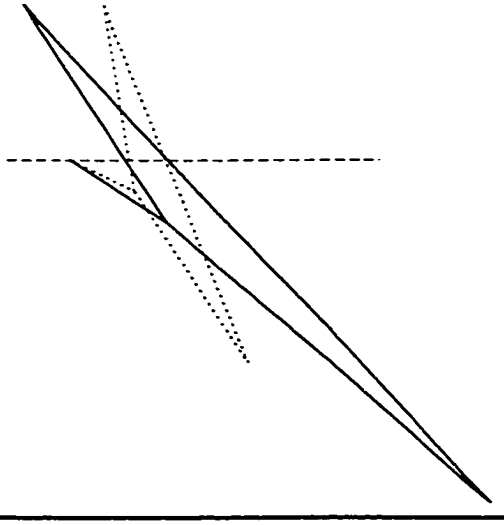	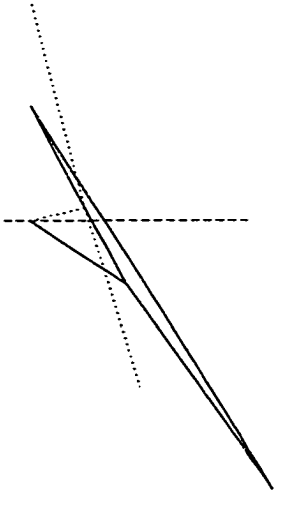

Reproduced with permission of the copyright owner. Further reproduction prohibited without permission.

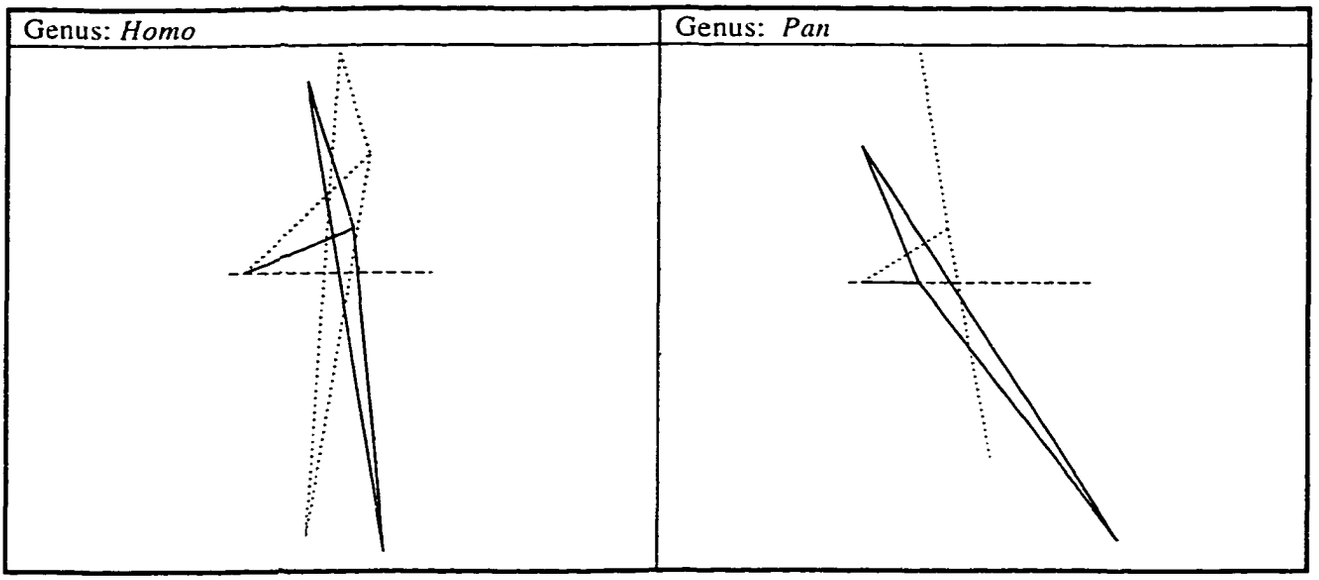

Summary of Anthropoid Nasomaxillary Growth Correlations

Associations among growth variables (i.e., correlated changes in the shape and relative size of traits from infant to adult) depicted in the shape diagrams in Boxes 9.10, 9.12 and 9.14 are summarized in the form of a correlation matrix and in a series of scatter plots presented in Boxes 9.15 and 9.16. Most of the correlated growth detected in the bi-sectional analysis involved changes related to facial length (maxillary arch and anterior facial elongation), facial prognathism, paranasal projection, and facial rotation. Conspicuously absent from the list of characters involved in correlated growth were those related to facial breadth, palatal depth and features typically associated with masticatory function (such as anteroposterior zygomatic root position and occlusal slope).

Reproduced with permission of the copyright owner. Further reproduction prohibited without permission.

Reproduced with permission of the copyright owner. Further reproduction prohibited without permission.

Box 9.15. Correlation matrix of size-independent nasomaxillary growth variables (Species mean raw data; n=24) (*p*-values in parenthesis).

Nasomaxillary variables	(1)	(2)	(3)	(4)	(5)	(6)	(7)	(8)	(9)	(10)	(11)	(12)	(13)
(1) Nasal bone length [Y1-NASLGT]	1.0												
(2) Maxillary arch length [Y14-MXARCL]	.65 (.001)	1.0											
(3) A-P zygomatic root [Y13-APZYGR]	-.32 (.12)	-.40 (.05)	1.0										
(4) Anterior facial length [Y17-AFACHT]	.82 (.001)	.86 (.001)	-.26 (.22)	1.0									
(5) Palatal width at M3 [Y23-M3PALW]	.21 (.33)	.48 .02)	-.18 (.40)	.33 (.12)	1.0								
(6) Palatal depth at P^3 [Y25-P3PALD]	.20 (.35)	.19 (.37)	.16 (.46)	.46 (.02)	.10 (.63)	1.0							
(7) Krogman's angle [Y30-KROGAG]	.06 (.77)	.37 (.07)	-.07 (.76)	.25 (.24)	.16 (.44)	.04 (.84)	1.0						
(8) Enlow's angle [Y31-ENLOAG]	.63 (.001)	.66 (.001)	-.16 (.45)	.65 (.001)	.29 (.16)	-.03 (.91)	.43 (.04)	1.0					
(9) Occlusal plane [Y32-SLOPOC]	.76 (.001)	.46 (.02)	-.19 (.37)	.62 (.001)	.24 (.26)	.07 (.75)	-.24 (.26)	.47 (.02)	1.0				
(10) Facial convexity [Y33-FACCNV]	.09 (.68)	-.30 (.16)	.21 (.32)	-.08 (.71)	-.45 (.03)	-.01 (.96)	-.44 (.03)	-.13 (.56)	.15 (.48)	1.0			
(11) Paranasal plate [Y35-PPNALO]	.70 (.001)	.59 (.003)	-.40 (.05)	.55 (.005)	.01 (.99)	.05 (.82)	-.16 (.47)	.23 (.28)	.54 (.007)	.29 (.17)	1.0		
(12) Facial rotation [Y95-FACROT, new variable]	.34 (.10)	.26 (.23)	.00 (.99)	.49 (.02)	.02 (.93)	.52 (.01)	.63 (.001)	.31 (.15)	.01 (.98)	-.29 (.17)	-.09 (.68)	1.0	
(13) Post. facial height [Y96-PASFHT, new variable]	-.02 (.92)	.16 (.46)	-.07 (.76)	.10 (.63)	.23 (.28)	.33 (.12)	.05 (.83)	.06 (.77)	-.23 (.29)	-.49 (.02)	-.12 (.58)	.24 (.26)	1.0

Box 9.16. Scatter plot matrix of nasomaxillary growth variables showing 95% density ellipses. See Box 9.15 for variables names corresponding to cell numbers. (Species mean raw data) Created with JMP Ver. 3.0 software.

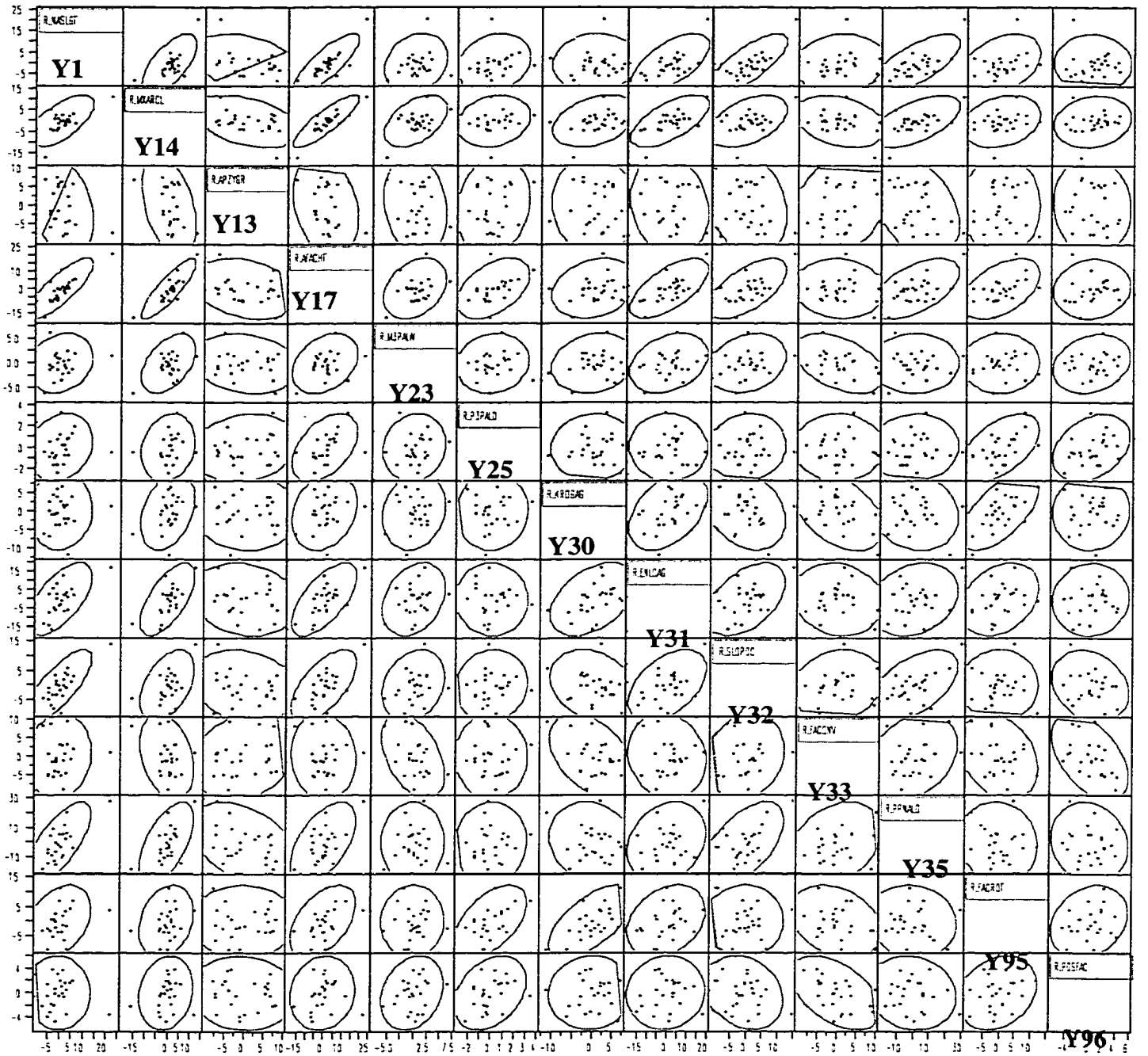

Reproduced with permission of the copyright owner. Further reproduction prohibited without permission.

Evidence for Structural Growth Constraints

As stated in the introduction, the objective of this chapter is to determine whether any of the observed correlations among nasomaxillary traits in the adult delta-transformed data defined in Chapter 8 can be explained, at least in part, in terms of structural growth constraints. The pattern of nomological correlations among adult anthropoid nasomaxillary traits was revealed using principal components analysis, which identified two size-independent factors relating a suite of characters (Box 9.5). Further information was gained from an examination of the size-independent residual correlation matrix (Box 9.8). A series of ontogenetic shape analyses further revealed that several of these inter-adult relationships are also expressed as growth correlations (Boxes 9.15 & 9.16). In the present section I assess whether any of these growth correlations can be explained in terms of structural constraints. What follows is a character-by-character analysis of the theoretical and empirical evidence bearing on the nature of the observed patterns of correlated growth. Such correlated growth patterns were further compared with the multivariate correlations of the logged delta-transformed adult data (see Boxes 9.5 and 9.7).

(1) ***Nasal bone length.*** In the principal components analysis of the adult data (Box 9.5), nasal bone length was positively associated with both Krogman's and Enlow's angle of facial prognathism, and paranasal plate orientation; and negatively associated with the anteroposterior position of the zygomatic root and posterior facial breadth. High positive correlations between nasal bone length and anterior facial length, and to a lesser extent maxillary arch length, were further revealed in the residual matrix (Box 9.7).

Reproduced with permission of the copyright owner. Further reproduction prohibited without permission.

The ontogenetic shape analysis indicated that some of these evolutionary associations are also expressed as correlated growth, while others are not (Box 9.15). Size-independent growth of nasal bone length was found *not* to be associated with Krogman's angle, zygomatic root position, or facial breadth. However, an increase in nasal bone length during ontogeny was shown to be associated with an increase in anterior facial length, maxillary arch length, Enlow's angle of facial prognathism and in the development of sagittally projecting paranasal plates. One additional growth correlation involving nasal bone length, which was not apparent in the adult data, included an association with occlusal plane orientation.

With the exception of paranasal plate orientation, it is difficult to conceive how changes in nasal bone length could impose or constrain changes in these other characters during craniofacial development. The literature on craniofacial growth lends no support to such a connection. More likely, the pattern of correlated growth related to nasal bone length is part of a more general trend involving growth of the entire anterior face (the nomological correlation between nasal bone length and anterior facial length is extremely high: $r = 0.84$, $p < .0001$).

The relationship between nasal bone length and paranasal projection is discussion in the section dealing with the paranasal plates.

(2) ***Anterior facial length***. Examination of the species means adult residual matrix (Box 9.7) indicates that anterior facial length (Y17) shows a high degree of nomological covariance with nasal bone length (Y1), maxillary arch length (Y14), Enlow's angle (Y31) (positive correlations), and posterior nasal aperture breadth (Y8) (negative correlation). Ontogenetically, it can be seen with reference to Box 9.15 that anterior facial growth is associated with essentially the same suite of

Reproduced with permission of the copyright owner. Further reproduction prohibited without permission.

nasomaxillary variables as nasal bone growth: it is positively correlated with maxillary arch length, Enlow's angle, paranasal plate orientation, and occlusal slope. In addition, anterior facial elongation covaries ontogenetically with degree of facial rotation and anterior palatal depth.

Several of these ontogenetic associations can be explained in terms of structural growth constraints. A disproportionately high rate of anterior facial growth (i.e., elongation between nasion and prosthion) relative to the maxillary arch (maxillary tuberosity to prosthion) and posterior face (nasion to maxillary tuberosity) produces several related structural effects, as depicted in Box 9.17. These include: (a) an increase in Enlow's angle of facial prognathism, (b) an increase in the slope of the occlusal plane, and (c) an increase in maxillary arch length. The model further predicts that anterior facial growth will *not* be correlated with Krogman's angle of facial prognathism, nor would it affect posterior facial height; and in fact no such growth correlations are observed in the ontogenetic data.

Recall that the first shape analysis revealed that this pattern of facial profile growth (i.e., a disproportionately high rate of anterior facial growth) is exhibited in Cebinae, Cercopithecinae, Colobina, *Pongo*, *Gorilla* and *Pan*. Unfortunately, there is very little evidence in the literature bearing on taxonomic differences in facial growth rates and patterns.

Reproduced with permission of the copyright owner. Further reproduction prohibited without permission.

Box 9.17. Diagrammatic model of anterior facial elongation.

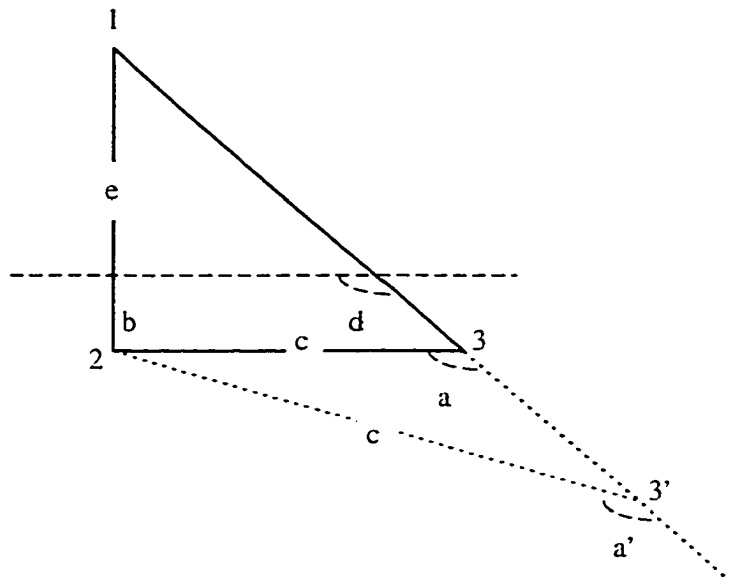

Key: 1, nasion; 2, maxillary tuberosity; 3, prosthion; 3', prosthion after facial growth; a, Enlow's angle of facial prognathism; a', Enlow's angle after facial growth; b, alveolar-posterior facial plane angle; c, maxillary arch length; c', maxillary arch after facial growth; d, Krogman's angle of facial prognathism; e, posterior facial length

In one notable exception, Krogman (1931) demonstrated that the anterior facial plane of *Pan troglodytes* grew some 46% in length from infancy to maturity, whereas maxillary length grew by only 26% during the same period. These values correspond well to the predicted values based on the model of facial growth shown in Box 9.17. A few simple calculations show that if the anterior facial length of the *Pan* infant facial profile (see Box 9.9) is extended by 46% (from point 3 to point 3' in Box 9.17), the maxillary arch would need to grow by 29% (c to c') to maintain its counterpart position, a value close to Krogman's observed value of 26%. On the other hand, Swindler, Sirianni and Tarrant (1973) found that the maxillary arch in *Macaca* and *Papio* grew 6% to 9% faster than the anterior face, but this finding is not strictly comparable to the results reported here because it derives from a shorter growth period—from age 3 months to 3 years. Nevertheless, it is clear that due to

Reproduced with permission of the copyright owner. Further reproduction prohibited without permission.

the structural integration of the anterior facial plane and the maxillary arch, changes in one will produce concurrent changes in the other.

The positive correlation between anterior facial growth and Enlow's angle is also predicted by the model portrayed in Box 9.18. As prosthion is progressively displaced from nasion during craniofacial growth (3 to 3') the lower obtuse angle formed by the anterior facial plane and the occlusal plane (which approximates Enlow's angle) also increases (from a to a').[7] Conversely, the internal acute angle nasion-prosthion-maxillary tuberosity decreases proportionately during anterior facial growth. This makes it difficult to interpret the observed positive growth correlation between anterior facial length and anterior palatal depth, since growth of the former should produce a physical constraint on the amount of space available for the development of the anterior palate (see Box 9.18).

Anterior facial growth also covaries with paranasal plate orientation and degree of facial rotation. With regard to the former, I will subsequently show that the correlation is spurious, due solely to the shared covariance of each with nasal bone length. If a structural growth constraint exists between anterior facial length and facial rotation it is likely due to the effects of the latter, and so I defer this topic for a later discussion.

(3) ***Maxillary arch/palate length***. Like anterior facial length, maxillary arch length appears to play an important role in the evolutionary integration and correlated growth of the nasomaxillary complex. Maxillary arch length covaries evolutionarily with anterior facial length, nasal bone length, facial prognathism (both measures),

---

[7] The adult manifestation of the relationship between anterior facial growth and Enlow's angle is particularily noticable in *Papio hamadryas*, *Macaca nemestrina*, and (at the other extreme) in *Homo* (see Boxes 4.5 & 9.10).

Reproduced with permission of the copyright owner. Further reproduction prohibited without permission.

anteroposterior position of the zygomatic root, and palatal breadth. All of these inter-adult correlations are also expressed as growth correlations. Two additional ontogenetic correlations concerning maxillary arch length, which were not apparent in the delta-transformed data, involve occlusal slope and paranasal plate orientation.

Comparative analysis of the ontogenetic sample indicates that a pattern of facial growth characterized by a disproportionately high rate of forward maxillary elongation is exhibited by Atelinae, Pithecinae, Presbytina, and Hylobatinae. Unfortunately, there is even less ontogenetic data pertaining to these taxa than for the cercopithecines and Great Apes. The structural consequences of disproportionate maxillary arch growth is shown in Box 9.18. The growth model predicts that an increase in the length of the maxillary arch (from point 3 to 3') will lead to an increase in Enlow's angle (a to a'), Krogman's angle (d to d'), and anterior facial length (compare 1 to 3 with 1 to 3'). The model further predicts that *no* ontogenetic association will be found between maxillary arch length (2 to 3, or 2 to 3') and occlusal slope (b) or posterior facial height (e).

Box 9.18. Diagrammatic model of maxillary arch elongation.

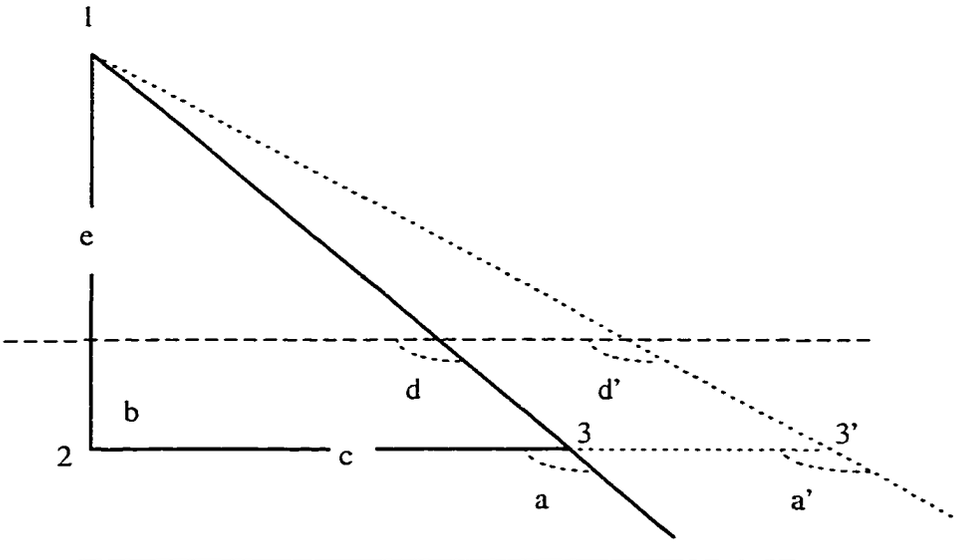

Reproduced with permission of the copyright owner. Further reproduction prohibited without permission.

Only one of the model predictions is inconsistent with the ontogenetic data. The observed association between forward maxillary arch growth and occlusal slope is not predicted by the model. It may be that the correlation is a spurious one, brought about by the relationship of both characters with anterior facial growth. When a partial correlation is carried out on two traits, with anterior facial length controlled for in the analysis, the association between maxillary arch length and occlusal slope disappears.

Three additional growth correlations involving maxillary arch length, not addressed in the model shown in Box 9.18, include positive relationships with both paranasal plate orientation and posterior facial breadth, and a negative relationship with anteroposterior position of the zygomatic root.

With regard to the latter correlation, if maxillary arch growth occurs primarily anterior to the zygomatic root, then the root will appear to be shifting in a progressively posterior direction, and the observed negative correlation can be explained in terms of a particular growth mechanism. However, primate craniofacial growth studies indicate the opposite, that the primary site of maxillary arch growth occurs posterior to the zygomatic root. Enlow (Enlow & Bang, 1965; Enlow 1990), in his investigation of facial growth mechanisms, determined that "...horizontal lengthening of the bony maxillary arch is produced by growth at the maxillary tuberosity" (1990:77). In support of this conclusion, histological studies have demonstrated that fine cancellous nonlamellar tissue is deposited at the maxillary tuberosities, a type of bone that facilitates rapid growth (Enlow, 1963). In a craniofacial growth study of olive baboons ranging in age from infants to adults, Oyen (1984), in agreement with Enlow, found that growth in the posterior portion of

Reproduced with permission of the copyright owner. Further reproduction prohibited without permission.

the maxilla "...along the transverse palatine suture and in the region of the maxillary tuberosities..." contributed more to the development of the palate than did growth at the anterior portion of the maxillary arch (p. 349). King and Schneiderman (1993) concluded that growth at the transverse palatine suture appeared to modulate overall palatal development in *Macaca mulatta*. But other studies have demonstrated that growth of the anterior and posterior portions of the palate occur independently, at least in cercopithecids (e.g., Moore, 1949; Swindler & Sirianni, 1973; Byrd & Swindler, 1980), indicating that differential growth rather than growth modulation may be the mechanism by which the posterior region of the palatal dominates overall palatal growth.

If this growth pattern holds for the majority of anthropoids then one would expect a positive rather than a negative correlation between maxillary arch elongation and zygomatic root position, since the zygoma would be displaced anteriorly by the deposition of newly formed bone at the maxillary tuberosities. Enlow (1990) noted that "...as the maxillary tuberosity grows and lengthens posteriorly, the whole maxilla is simultaneously carried anteriorly"(p. 62), presumably bringing the lower part of the zygoma along with it. That the zygoma does not migrate anteriorly with the displacement of the maxillary arch during development is due to the compensatory apposition of bone at the zygomaticomaxillary suture, or rather, to the differential rates of apposition at the zygomaticomaxillary and zygomaticotemporal sutures (Adams *et al*, 1972; Enlow, 1975).

A second growth mechanism mediating the posterior drift of the zygoma during ontogeny is a bone remodeling pattern characterized by resorption on the

Reproduced with permission of the copyright owner. Further reproduction prohibited without permission.

anterior surface of the zygoma and deposition on the posterior surface (Enlow, 1966). "As a result, the attachment of the arch to the facial skeleton is relocated backwards" (Moore, 1981:48). Given the complex choreography of growth and remodeling that underlies the negative evolutionary and ontogenetic association between maxillary arch elongation and zygomatic root position, it is unlikely that this relationship is produced by a simple structural constraint. The biological significance of the backwards drift of the zygomatic root that attends forward maxillary growth is a mystery yet to be solved, and we will have to look for adaptive rather than structural explanations.

A positive correlation between maxillary arch length and paranasal plate orientation is apparent in the ontogenetic data. However, a close examination of the bivariate scatter plot with regard to these two characters shows that the correlation may be due to the effects of two influential data points, representing *Homo* and *Papio*, located in the extreme corners of the plot (see Box 9.20). The relationship between maxillary arch length and width is discussed in the section dealing with posterior facial breadth.

(4) *Facial rotation*. Although the term "facial rotation" is typically used (e.g., Moss, 1958) there is no single point around which the downward and forward "translocation" of the nasomaxillary complex pivots. Enlow (1990) attributed much of the facial rotation he observed in primates to the relatively high degree of anteroinferior displacement of the posterior part of the face compared to the anterior portion—a process he called "displacement rotation of the maxilla" (p. 119). Experimental and comparative research, mainly by Moss (1958; Moss & Greenberg, 1955) and Enlow (Enlow & McNamara, 1973; Enlow, 1975), has established a clear

Reproduced with permission of the copyright owner. Further reproduction prohibited without permission.

link between displacement rotation of the nasomaxilla and the reorientation of the middle and anterior cranial fossae, especially the planum sphenoideum and the cribriform plate, a topic I revisit in Chapter 12.

Several expected structural growth correlates of facial rotation are depicted in Box 9.19. As the nasomaxillary complex rotates or translocates forward, as it does in all anthropoids with the possible exception of *Hylobates*, Krogman's angle of prognathism concomitantly increases as does the slope of the occlusal plane. Ontogenetic shape comparisons (Box 9.9) and growth correlations (Box 9.15) indicate that forward rotation of the nasomaxilla during development is indeed associated with an increase in Krogman's angle, but it does not appear to be associated with a change in the slope of the occlusal plane. The lack of correspondence between facial rotation and occlusal reorientation is perhaps explained in relation to anterior facial growth.

The growth correlation between facial rotation and anterior facial elongation suggests that anthropoids exhibiting extensive facial rotation compensate by increasing their rate of anterior facial growth, which serves to maintain the slope of the occlusal plane within certain limits; limits that are perhaps set by the biomechanical exigencies of mastication (see Chapter 14). This pattern of 'balanced' facial growth and rotation can be observed in every major anthropoid group. This "balancing mechanism" hypothesis was proposed independently for *Macaca mulatta* by Nielsen *et al.* (1989), who noted that "...differential vertical dentoalveolar development almost completely masked the rotation of the occlusal plane that results from the rotation of the jaws, which created the impression that the occlusal plane is stable during growth" (p. 405). Bravo *et al.* (1989) have also

Reproduced with permission of the copyright owner. Further reproduction prohibited without permission.

documented the relative invariance of the occlusal plane angle throughout ontogeny in the rhesus macaque.

Box 9.19. Diagrammatic model of facial rotation.

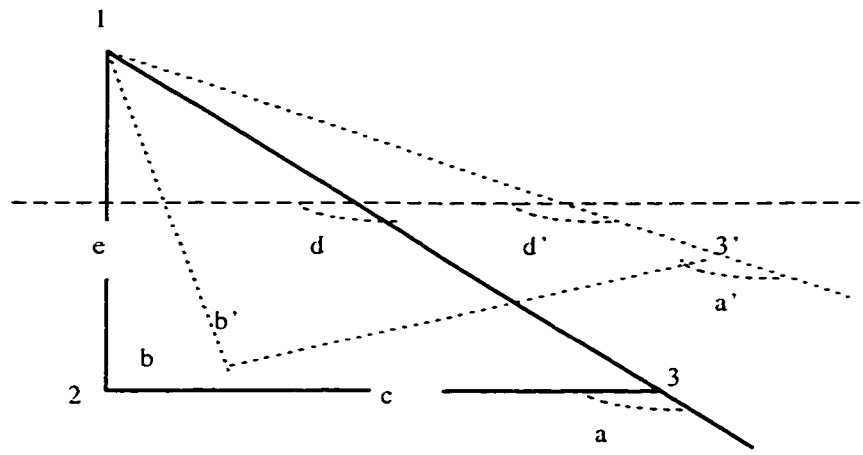

A predicted consequence of facial rotation and compensatory coordinated anterior facial elongation is that the acute angle formed by the anterior facial and alveolar planes will diminish, leaving less space for the development of the anterior palate. In fact, the opposite appears to be the case. A deep anterior palate is associated with both facial rotation and anterior facial growth, a relationship that cannot be explained in terms of a structural growth constraint.

(5) ***Anteroposterior position of the zygomatic root.*** I have already discussed the evidence bearing on the relationship between anteroposterior maxillary growth and zygomatic root position during development. The only other variable related to zygomatic root position is paranasal plate orientation. The observed negative correlation between these two traits (which is expressed both evolutionarily and ontogenetically) indicates that as the zygoma drifts to a relatively posterior position in prognathic anthropoids the paranasal plates project outward in sagittal

Reproduced with permission of the copyright owner. Further reproduction prohibited without permission.

orientation. It is likely that both growth correlations involving zygomatic root position—the one with maxillary length and the other with paranasal orientation—initiate from the same inter-regional growth and remodeling pattern: the forward and downward growth of the anterior maxillary/nasal region and the concomitant relative posterior drift of the zygoma/lower orbital region (refer to the ontogenetic shape outlines in Box 9.14).

(6) ***Paranasal plate orientation***. Analysis of the delta-transformed size-independent anthropoid data revealed that a sagittal projection of the paranasal plates is associated with Enlow's angle of facial prognathism, nasal bone length, anterior palatal depth, occlusal plane orientation and facial convexity; and negatively associated with posterior facial width and anteroposterior position of the zygomatic root. Of these nomological relationships several were also found to be expressed as growth correlations, while others were not. Ontogenetically, paranasal plate orientation was shown to be positively correlated with nasal bone length and occlusal plane orientation, and negatively correlated with the position of the zygomatic root. In addition, the angle of the paranasal plates covaried ontogenetically with maxillary arch length and anterior facial length.

One might also have expected the degree of facial rotation to influence paranasal plate orientation, but this does not appear to be the case. In most anthropoid taxa, the shifting axis of facial rotation during nasomaxillary growth, although dynamic, is confined to the midface, at or close to rhinion or nasomaxillare.[8] As a consequence, while the lower face becomes more protrusive

[8] The one exception to this generality is witnessed in Cebinae, whose axis of anterior facial rotation is more superiorly located,closer to nasion.

Reproduced with permission of the copyright owner. Further reproduction prohibited without permission.

with facial rotation the upper face (including the superior orbital margins) retracts. This process can, and often does, occur without significant change to the paranasal plates (for example in Atelinae, Cercopithecini, and Presbytina). But along with nasomaxillary rotation, the anterior facial plane translocates downward in many taxa, and it is this downward movement of the entire anterior face during ontogeny that corresponds to the sagittal projection of the paranasal plates. This covariance can easily be seen in several of the shape diagrams in Box 9.14. Notice that instances of increased paranasal projection during craniofacial growth (i.e., a long orbitale-nasomaxillare chord in adults compared to infants) occur almost exclusively in taxa which exhibit a downward movement of nasomaxillare from above to below the Frankfort horizontal (see especially Macacina, Papionina, and *Gorilla*).[9] The downward movement of the anterior face in relation to the neurocranial-orbital axis along with nasal bone elongation produces a displacement of the lower border of the nasals (rhionion and nasomaxillare) in relation to the lower orbital rim (orbitale), and it is this displacement that yields an increase in the sagittal projection of the paranasal plates. Nasal bone elongation can thus account for at least part of the variance observed in the orientation of the paranasal plates.[10]

The significant association between paranasal plate orientation and orientation of the occlusal plane is also apparent in both data sets. However, no mechanisms of craniofacial growth can be identified that would support the hypothesis of a structural growth constraint relating the two traits.

---

[9] The exception to this rule is Pitheciinae, a taxon whose adults show a substantial increase in paranasal plate projection but lack the usual accompanying downward remodeling of the anterior face.

Reproduced with permission of the copyright owner. Further reproduction prohibited without permission.

(7) ***Posterior facial breadth***.[11] In the analysis of adult traits, posterior facial breadth correlated positively with zygomatic root position, and negatively with nasal bone length, maxillary arch length, facial prognathism, and paranasal plate orientation. Similar associations have been described previously for a variety of taxa. Species with relatively wide faces are also typified by short, relatively orthognathic faces with zygomatic roots positioned anteriorly on the maxillary corpus (e.g., selected species of *Canis*: Weidenreich, 1941; *Paranthropus*: Robinson, 1954; *Cebus*: Kinzey, 1974; *Homo*, Scott, 1959; Enlow & Azuma, 1975). Conversely, species with narrow faces exhibit the opposite suite of traits (e.g., *Papio*: Swindler & Sirianni, 1973). There are too many exceptions, however, to explain this general tendency in terms of a few simple growth constraints.[12] In any event, few of these nomological correlations are manifest in terms of correlated growth. The only two characters to covary ontogenetically with posterior facial breadth are maxillary arch length (positive growth correlation) and degree of facial convexity (negative growth correlation) (see Boxes 9.12, 9.14 & 9.15).

Although the growth relationship between maxillary arch length and breadth has been studied extensively in primates, most of the research has focused on the

---

[10] The relationship between nasal bone length and paranasal plate orientation is a good example of a class of structural relationships known as 'topographical correlations' (Solow, 1966), which are due to the modification of a shared landmark (in this case the lower border of the nasals).

[11] Many of the nasomaxillary linear traits in the mediolateral dimension appear to measure some aspect of facial breadth (e.g., posterior nasal aperture breadth, bizygomatic breadth, upper facial breadth and palatal width at M^3). These traits all load highly on the second principal component of the PCA, indicating a high degree of collinearity. They are all measuring the same basic underlying characteristic—posterior facial breadth. To avoid the analytical problems associated with data collinearity and to simplify inferential interpretations, a single character, palatal width at M^3, was selected to represent posterior facial breadth in the current analysis.

[12] Exceptions include *Chiropotes santanas*, whose facial skeleton is both relatively narrow and orthognathic, and *Brachyteles arachnoides*, whose face is at once wide and prognathic.

Reproduced with permission of the copyright owner. Further reproduction prohibited without permission.

allometric relationship between the two traits. These studies have shown that maxillary length grows with positive allometry in relation to breadth, a finding that is confirmed in the present study (see Box 9.12). But an allometric growth relationship is not the same as a structural growth relationship. Allometric growth is a description of the relative exponential rates of growth of a pair of traits[13] as measured by the *slope of a regression line* relating the logged data. A structural growth relationship, on the other hand, is assessed more on the basis of the *strength of association* between two traits, such that their ratio of change covaries over a sample. A close examination of the bivariate plot of maxillary length to breadth growth, adjusted for cranial size, shows that the significant correlation between them is due to a pair of influential data points (*Homo* and *Papio*) located at the extreme opposite corners of the plot (Box 9.20, left). When either or both of these outliers is excluded from the analysis the relationship between maxillary length and breadth is no longer significant at the 0.05 level (Box 9.20, right). This signifies that variation in the growth of one facial dimension can not explain any of the growth variation in the other dimension.

[13] Allometry can involve the regression of two traits (*character allometry*), or, as conventionally defined, the regression of one trait on body size (*body size allometry*) (see Chapter 10).

Reproduced with permission of the copyright owner. Further reproduction prohibited without permission.

Box 9.20. Scatter plots and regression lines for maxillary length to breadth growth. Dotted lines depict by 95% confidence ellipses

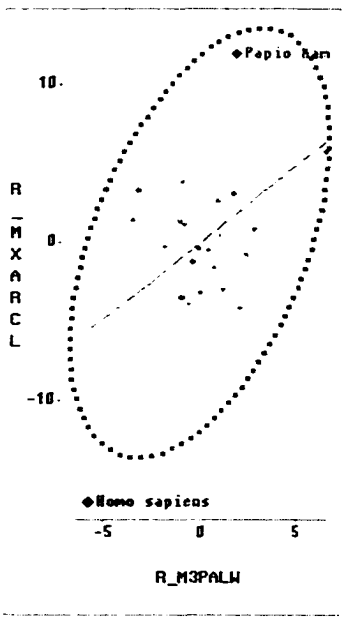

With *Homo* & *Papio*: r=0.48 (p=.02)

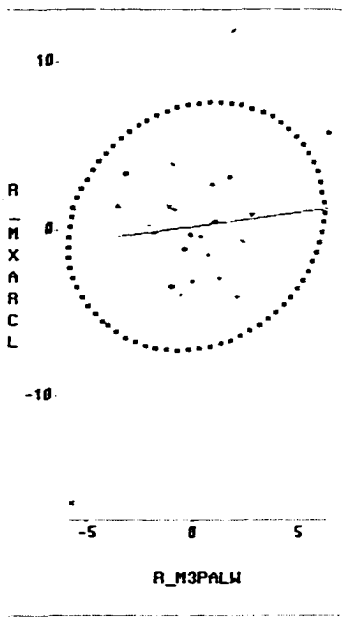

Excluding *Homo* & *Papio*: r=0.14 (p=.54)

Further dissociating facial length from breadth, Goss *et al.* (1983) found in both *Callithrix* and *Homo* that the onset and completion of growth is distinct for each dimension, with the growth of facial breadth completed much earlier than length. Oyen (1984) further showed that anteroposterior maxillary growth is episodic and related to dental emergence during development, whereas mediolateral maxillary growth follows a more gradual progression. The bulk of the current evidence thus favors the (null) hypothesis that no structural growth constraint exists between maxillary arch length and breadth.

The analysis shows that anthropoids who develop relatively wide faces also typically develop concave or dished anterior facial profiles (e.g., *Pan*, *Gorilla*), and conversely, those who exhibit relatively narrow faces develop convex or projecting facial profiles (e.g., *Macaca*, *Lophocebus*). But here again, the strength of

Reproduced with permission of the copyright owner. Further reproduction prohibited without permission.

association is rather weak, and there is no known structural growth mechanism that can account for this trend.

(8) ***Facial prognathism***. The notion that there is no single best measure of "facial prognathism," and that different definitions of this character might produce very different results, compelled me to examine two distinctly defined measures of this important variable. Both quantify the orientation of the face, but each to a different reference plane.[14] Krogman's angle (1931) measures the inclination of the anterior facial plane (nasion to prosthion) relative to the Frankfort horizontal, while Enlow's angle (1975) measures the orientation of the midfacial plane (anterior-most frontal lobe to prosthion) relative to the occlusal plane. [15]

The degree of correspondence between the two measures of facial prognathism is determined by (a) the confluence between the anterior-most brain and nasion, which is fairly tight in most anthropoids, although the separation of the two points may be substantial in some taxa, and (b) the degree of parallelism between the Frankfurt horizontal and the occlusal plane. As we have seen, the occlusal slope is maintained within a rather confined range of variance, both across

---

[14] Operationalizations of "facial prognathism" abound in the morphometric literature (e.g., Krogman, 1931; Smith, 1984; Bilsborough & Wood, 1998; Fleagle, 1988; Conroy, 1990; Poirier, Stini & Wrenden, 1994). The vast majority are shape variables (i.e., angles, ratios or indices) that attempt to quantify in some way the degree of "forward protrusion of the lower face and jaw" (Poirier *et al*, 1994). The main difference among the various definitions is in how the investigator defines "forward." In the pilot study for this project (McMahon, 1994), I examined four different measures of facial prognathism and found that each was characterized by a different correlational structure with other variables. Factor analysis showed that the different measures of prognathism could be separated on the basis of reference plane.

[15] Enlow himself never explicitly described this measure of facial prognathism—but it was defined on the basis of anatomical landmarks that he viewed as important for the growth and remodeling of the facial skeleton.

Reproduced with permission of the copyright owner. Further reproduction prohibited without permission.

taxa[16] and during ontogeny.[17] It is this constraint on occlusal orientation that is largely responsible for the observed topographical correlation between the two measures of facial prognathism.

Given that the two indicators of facial prognathism are measuring the same basic attribute, only from difference reference planes, is it remarkable to note that each is correlated with such different suites of characters. Ontogenetically, Enlow's angle covaries with maxillary arch length, anterior facial length, and occlusal slope, while Krogman's angle does not. Conversely, Krogman's angle covaries with facial convexity and facial rotation, while Enlow's angle does not (Box 9.15).

The negative correlation between Krogman's angle and facial convexity is persistent in the data. It occurs in both the adult and ontogenetic samples. Numerous examples of this association in anthropoids come immediately to mind; from modern humans with our orthognathic nasally convex faces, to *Alouatta* and *Pongo* with their hyperprognathic concave faces (see Boxes 4.5-4.41). In fact, it was Krogman (1931) himself who first described and attempted to explain the "dished" face of the orangutan: "In the Orang there is a relatively greater growth in the alveolar region than in the orbito-nasal and the alveolar region tilts forward and upward as though bridled by the lack of comparable growth in the orbito-nasal region" (p. 348). Enlow (1975) has suggested that a similar process of differential upper and lower facial growth and remodeling can account for much of the variation in facial prognathism observed among primates. The extent of this craniofacial

---

[16] The standard deviation of occlusal plane orientation (Y32-SLOPOC) across the entire anthropoid sample is less than 5 degrees. A test of angular invariance, which is formally introduced in Chapter 11, indicates that a constraint is operating on the slope of the occlusal plane.

Reproduced with permission of the copyright owner. Further reproduction prohibited without permission.

growth process may thus account for at least part of the covariance between prognathism and facial convexity.

(9) ***Palatal depth.*** Given the close structural integration of the naxomaxillary complex, the relative lack of covariance between palatal depth and other traits is quite remarkable, and the few associations that do exist are difficult to interpret. Ontogenetically, *anterior* palatal depth is significantly correlated with anterior facial length and facial rotation. I have noted previously that anterior facial elongation and facial rotation exhibit a correlated growth pattern that acts to maintain a relatively stable occlusal plane orientation during ontogeny. If increased anterior palatal depth is a secondary consequence of this mechanism it is difficult to reconcile with theory (see earlier discussion).

Anterior palatal depth (e.g., inter-P^3 depth) also shows a high positive correlation with nasoalveolar clivus length. The greatest inclination of the palate along the midline, in the majority of anthropoids, occurs from prosthion to a point between the third premolars (4 to 5 in Box 9.21); from this point back to staphylion the palate continues to ascend but at a much reduced incline (5 to 6, in Box 9.21). The juxtaposition of the oral and nasal cavities and the placement of the anterior nasal aperture must attain a balance in competing to fulfill their respective biological roles of mastication and respiration. The close correspondence between the depth of the anterior palate and nasoalveolar clivus length (3 to 4 in Box 9.21) may be a consequence of this biological imperative. The relationship is shown graphically in Box 9.21. The lines connect cranial landmarks (numbered) as seen in

---

[17] Among the twenty-four anthropoid species that comprise the ontogenetic sample, the maximum degree of occlusal plane rotation reached about 10° from infant to adult (with *Gorilla* exhibiting the greatest amount of anterosuperior rotation and *Papio* the greatest anteroinferior rotation).

Reproduced with permission of the copyright owner. Further reproduction prohibited without permission.

lateral view. The configuration of points depicts the mean anthropoid form. This diagram shows that the close correspondence between inter-P^3 palatal depth (shortest distance between dotted line and point 5) and nasoalveolar clivus length (3 to 4) is a consequence of the juxtaposition of the nasal and oral cavities.

Box 9.21. Mean anthropoid form in lateral view. Lines connect cranial landmarks (numbered). Dotted line represents the alveolar plane.

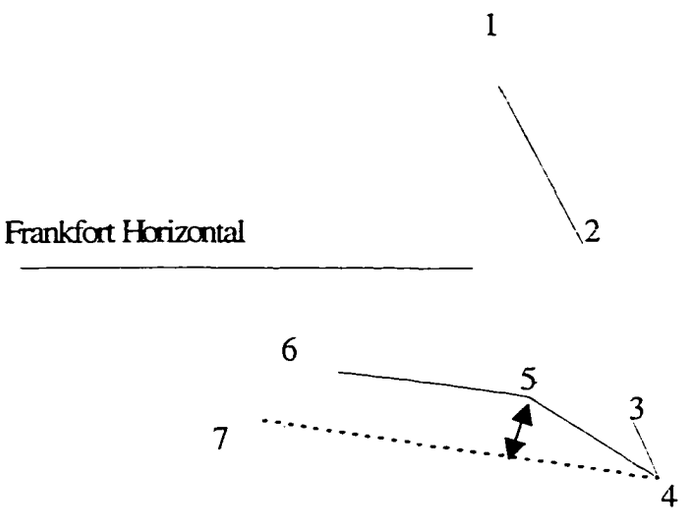

Key: 1, nasion; 2, rhinion; 3, subnasale; 4, prosthion; 5, inter P^3 midline point; 6, staphylion; 7, maxillary tuberosity.

Posterior palatal depth correlates quite highly with posterior facial height (r = 0.63, p<.0001). Since both characters occupy the same physical space at the back of the palate, it is easy to see how nomological modifications to one could effect structurally induced changes in the other.

(10) ***Slope of the occlusal plane***. I have already discussed several growth relationships involving this character. To recap, the angle of the occlusal plane relative to the Frankfort horizontal is ontogenetically correlated with nasal bone length, anterior facial length, maxillary arch length, Enlow's angle of facial prognathism, and paranasal plate orientation. The model of craniofacial growth

Reproduced with permission of the copyright owner. Further reproduction prohibited without permission.

shown in Box 9.17 illustrates how occlusal slope relates to anterior facial growth (and by extension, nasal bone growth), and Enlow's angle.[18] The correlation between occlusal slope and maxillary arch elongation disappears when controlling for anterior facial growth in a partial regression, indicating the association is a spurious one.

(11) ***Posterior facial height.*** Several correlated growth relationships involving posterior facial height have already been discussed (e.g., with posterior palatal depth). A related correlation, expressed in both the delta and ontogenetic data sets, occurs between posterior facial height and ramus height. Ramus height is defined after Lucas (1981) as the distance from condylion to the occlusal plane, perpendicular to the occlusal plane. Both dimensions—posterior facial height and ramus height—share the occlusal plane as their lowest point, and since their most superior points (superior-maxillary tuberosity[19] and condylion, respectively) usually lie roughly the same distance from the occlusal plane,[20] the two measures often correspond. In fact, the three variables ramus height, posterior facial height, and posterior palatal depth are nearly interchangeable.

---

[18] The counteracting effects of facial rotation are not shown in Box 19.17, but presumably they are not exact enough to completely nullify the effects of anterior facial growth on both Enlow's angle and occlusal orientation.

[19] The precise description of this landmark is the superior-most extent of the inferior orbital fissure (see Appendix A).

[20] The possible exception to this rule is the Papionini (*Macaca*, *Papio* and *Lophocebus*) whose occlusal planes are at an unusually high angle relative to the Frankfort horizontal, a configuration that produces lower metric values for ramus height compared to posterior facial height.

Reproduced with permission of the copyright owner. Further reproduction prohibited without permission.

Conclusions

The cross-sectional ontogenetic analysis of 24 anthropoid species conducted here confirmed several previously documented morphogenetic patterns of craniofacial growth, including the forward translocational rotation of the maxilla and the positive allometric growth of maxillary length relative to width. Several other features of anthropoid nasomaxillary development were also revealed. It was shown that facial profile shape change during growth follows one of three basic patterns: (1) anterior facial growth predominance, (2) maxillary arch growth predominance, or (3) posterior facial growth predominance. Moreover, the analysis indicated that the degree of facial rotation during growth might be related to mode of facial profile development. Species that exhibited predominant anterior facial growth also manifest greater facial forward rotation from infancy to maturity (12.5°) compared to species that exhibited predominant maxillary arch growth (8.5°). This finding, along with the observation that the degree of facial rotation is correlated with anterior facial growth but not with maxillary arch growth suggests that anterior facial elongation proceeds in conjunction with facial rotation in such a manner as to maintain a relatively stable orientation of the occlusal plane. In other words, species characterized by extensive facial rotation must also manifest a correspondingly high degree of anterior facial elongation to ensure that the slope of the occlusal plane remains in a functionally stable orientation.

In addition, the ontogenetic analysis revealed a number of potential structural growth constrains. These include the following: (1) disproportionately rapid growth of the anterior face (nasion to prosthion) leads to an increase in Enlow's angle of

Reproduced with permission of the copyright owner. Further reproduction prohibited without permission.

facial prognathism, an increase in the downward (from back to front) slope of the occlusal plane, and an increase in maxillary arch length (these constraits are especially apparent in Cebinae, Cercopithecinae, Colobina, *Pongo*, *Gorilla* and *Pan*), (2) disproportionately rapid growth of the maxillary arch (maxillary tuberosity to prosthion) leads to an increase in facial prognathism (both Enlow's and Krogman's angles) and anterior facial length (these constraits are especially apparent in Atelinae, Pithecinae, Presbytina, and Hylobatinae), (3) a forward and upward rotation of the face leads to an increase in Krogman's angle of facial prognathism, (4) the downward movement (due to remodeling) of the entire anterior face relative to the Frankfort plane, combined with anterior facial growth, especially that of the nasal bones, leads to an increase in the sagittal orientation of the paranasal plates (this constraint is especially apparent in Atelinae, Macacina, Papionina, *Pongo* and *Gorilla*), (5) anterior facial elongation combined with facial rotation centered around rhinion/nasomaxillaire produces a relative retraction of the naso-orbital region and a protraction of the anterior facial/alveolar region, which in turn, leads to anterior facial concavity (or reduction of convexity), (6) anterior palatal depth appears to constrain nasoalveolar clivus length, (7) posterior facial height appears to constraint posterior palatal depth and ramus height.

Reproduced with permission of the copyright owner. Further reproduction prohibited without permission.

Chapter 10. Body Size Scaling

Introduction

Immortalized for his contributions to physics, cosmology, mathematics and experimentation, Galileo is little known for his many contributions to comparative biology. In true Renaissance form, he applied his insights and innovations to the pursuit of knowledge in many fields, including the organic. In 1609 he not only trained his telescope on the moons of Jupiter, but began publishing observations of insects and other small animals and plants made with the aid of a compound microscope (McKenzie, 1967). It is not surprising, then, that Galileo should have applied his expertise in mechanics and motion to the study of organic form. This work is contained in his last major treatise—*Two New Sciences Pertaining to Mechanics and Local Motion*, which he published in 1638 at the age of seventy-four while still under house arrest in his villa in Arcetri near Florence.

Among the eclectic contributions included in the treatise, Galileo laid the foundation for what Thompson (1917) later called the "principle of similitude," the idea that organisms of different size require disproportionate structural dimensions in order to maintain mechanical and functional equivalence. He demonstrated, for example, not only that the short thick limb bones of large terrestrial animals were necessary to support their excessive weight, but that they were mechanically equivalent to the relatively long narrow limbs of smaller animals. Except for notable contributions by Herbert Spencer (1864), D'Arcy Thompson (1917), and Julian Huxley (1932), the importance of an organism's size in determining its form,

Reproduced with permission of the copyright owner. Further reproduction prohibited without permission.

physiology, and behavior has only recently begun to be understood. Hard and soft tissue structure, locomotor behavior, respiratory and thermoregulatory physiology, metabolism, fluid conservation, maturation rates, auditory communication, diet, and even life span are all in some way affected by body size (Thompson, 1917; Calder, 1984; Schmidt-Neilsen, 1984).

Despite its obvious importance, there have been surprisingly few studies on the effects of body size on primate craniofacial form (Cochard, 1985), and most of these have dealt with the scaling of dental dimensions to body size (e.g., Kay, 1976; Corruccini & Henderson, 1978; Gingerich *et al.*, 1982). The purpose of this chapter is to clarify and quantify the effects of body size (or, more accurately, cranial size) on nasomaxillary morphology among anthropoid primates, within the theoretical, operational and analytical framework established in the preceding chapters.

Before proceeding with an analysis of the anthropoid data and comparing the results with those of similar studies, I first critically review several important concepts related to body size scaling. From this analysis I conclude that the traditional concept of "body size" conflates several distinct aspects of size, each of which have a different effect on organic form. I further argue that the conventional model used to quantify the relationship between size and shape (i.e., Huxley's allometric equation) is inherently misspecified and as a consequence yields potentially inaccurate and misleading results. Finally, a general size factor is applied to the anthropoid metric data, in order to quantify the effects of scaling on craniofacial morphology and to generate a new set of size-independent variables for subsequent analyses.

Reproduced with permission of the copyright owner. Further reproduction prohibited without permission.

Isometry and Allometry

The next few sections were not intended as a simple review of conventional concepts concerning body size scaling (in that case I would simply have referred the reader to capable articles by Cock, 1966; Gould, 1971; Schmidt-Nielsen, 1984; Shea, 1985; and Jungers, 1985). Rather, I have attempted to clarify some misconceptions regarding the meaning, operationalization and relationships among the fundamental concepts of isometry, allometry, size, and shape.

The study of the effects of size on the morphology of organisms revolves around the twin concepts of isometry and allometry. Jungers, Falsetti and Wall (1995) define isometry as the preservation of shape among organisms of different sizes, or, "geometric similarity," as they call it (p. 139). Allometry, on the other hand, is defined as an instance in which shape changes as a function of size (Jungers, *et al.*, 1995), or, alternatively, as the study of the consequences of size with respect to shape (Gould, 1966). Isometry and allometry thus describe specific relationships between size and shape. These biological formulations have their origins in, and are consistent with, concepts first developed in geometry. Geometric treatments depict isometry as "...a transformation [such as a scale transformation] which preserves... the relative distances between all pairs of points" in a coordinate system (Graening & Nibbelink, 1975:503; also see Marcus *et al.*, 1996).

The relationship between body size and shape has been modeled after Huxley's (1932) allometric power equation:

$$Y = a + bX^k \qquad (10.1)$$

or its logarithmic equivalent (where a=0):

Reproduced with permission of the copyright owner. Further reproduction prohibited without permission.

$$(\log)Y = (\log)b + k\ (\log)X \qquad (10.2)$$

where Y is a character variable (e.g., chord), X is a variable representing body size, *a* is the intercept term, *b* is the value of Y when X =1, and k is the exponential relation of Y to X. Isometry is a special case of the allometric equation where *a* = 0 and k = 1:

[isometry in raw form:] $Y = 0 + bX^1$ (10.3)

[isometry in log form:] $(\log)Y = (\log)b + 1.0\ (\log)X$ (10.4)

The Coefficient and Power Terms. When raw data are used the coefficient *b* is arbitrary and depends only on the scales of X and Y (e.g., converting inches to centimeters in one of the variables will alter the slope). In the bivariate plots presented in Box 10.1, the variables X (body size) and Y (character dimension) have been set to a common scale and calibrated (e.g., when X is equal to 1, Y is also equal to 1), thus eliminating the need for the *b* coefficient. For uncalibrated data, the *b* coefficient effectively re-scales Y to be proportional with X. The power function k is the ratio Y/X re-scaled. The term k thus measures the relative increase of Y with respect to X. Proportional increases in Y relative to X are signified by k=1 (isometry), and when k is greater than or less than 1 linear increases in X are associated with exponential increases in Y (allometry). Isometry therefore occurs when Y increases only as a multiple of X (e.g., $Y = 1.0X^1$, $Y=2.0X^1$, $Y=0.5X^1$, and so on), and not to the power of X. Regardless of the proportionality of Y to X in the equation, allometry occurs when Y increases to the power of X (e.g., $Y=1.0X^2$, $Y=2.0X^2$, $Y=bX^{.75}$, and so on). Isometry can thus be recognized in a bivariate plot of the raw data as a linear fit, assuming the intercept *a* = 0 (Box 10.1, A), and allometry can be identified as a curvilinear fit of the raw

Reproduced with permission of the copyright owner. Further reproduction prohibited without permission.

data (Box 10.1, C, E). With respect to log-log data, the power term k of X in the raw data becomes the regression coefficient of logX. Hence, for log data isometry is indicated by a slope of 1.0 (Box 10.1, B), whereas allometry is indicated by a slope greater than or less than 1.0 (Box 10.1, D, F).

Box 10.1. Bivariate plots of pairs of size variables under conditions of isometry and allometry.

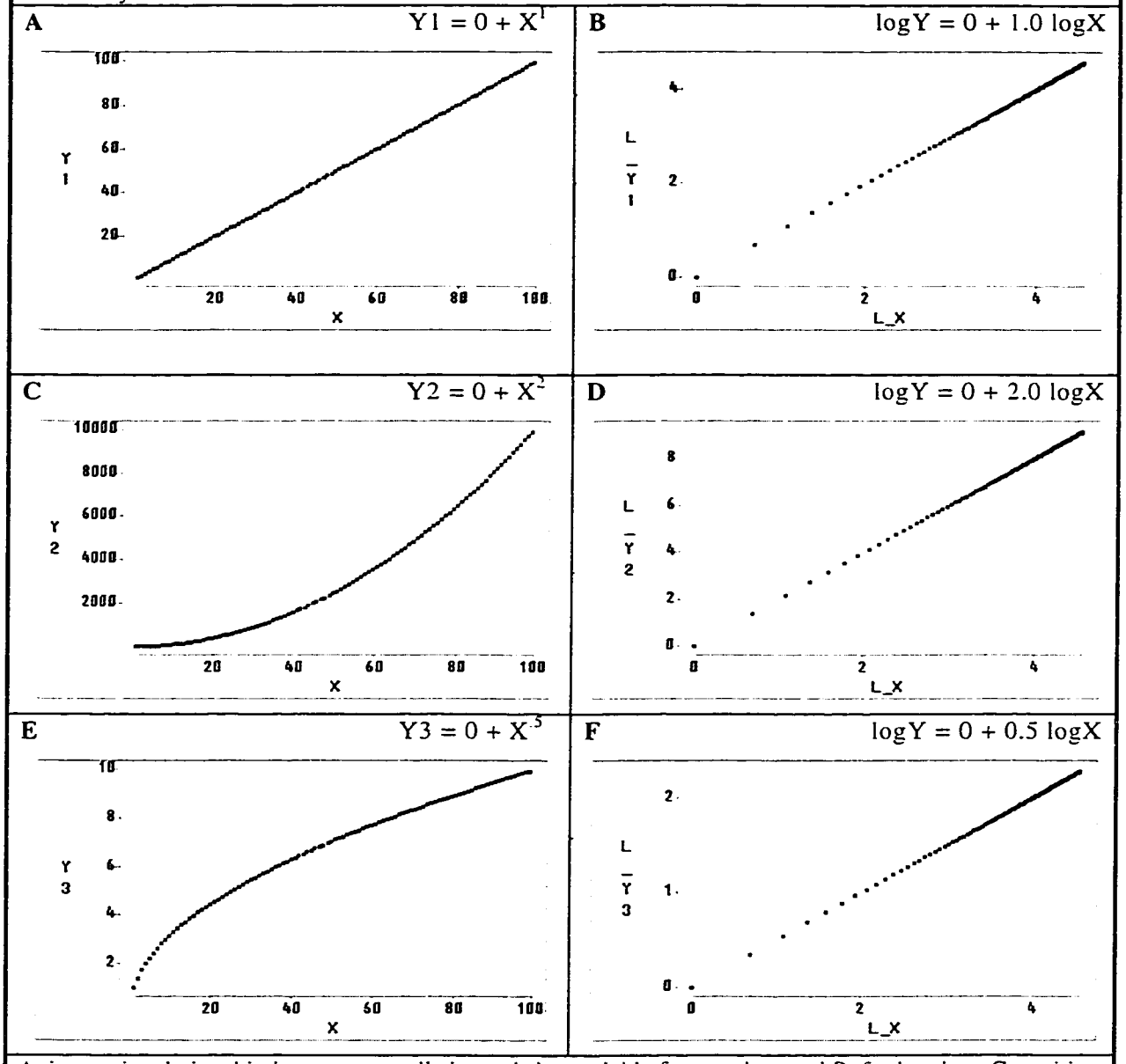

A, isometric relationship between overall size and size variable for raw data, and B, for log data; C, positive allometric relationship between overall size and size variable for raw data, and D, for log data; E, negative allometric relationship between overall size and size variable for raw data, and F, for log data.

Reproduced with permission of the copyright owner. Further reproduction prohibited without permission.

When the slope of the log-log regression coefficient is greater than 1 (i.e., $k > 1.0$) the allometric relationship between size and the character variable is said to be "positive" (Box 10.1, D), and when the slope is less than 1 (i.e., $k < 1.0$) the allometric relationship is said to be "negative" (Box 10.1, F).

The Intercept Term. A special case of allometry exists when an intercept term, *a*, is introduced into the allometric power equation. It can be seen with reference to the bivariate plot in Box 10.2, A, that when Y increases in proportion to X (that is, k=1) there exists a linear relationship between Y and X. But it is also true that in such cases, given a nonzero intercept, the relationship between Y and X, although linear, is not isometric: the regression coefficient of logX is not equal to 1.0 (see Box 10.2, B). Notice that when the intercept term is removed, as in the examples in Box 10.1, A and B, the isometric relationship between Y and X is restored. Another feature of this type of allometry—which I call *spurious allometry*[1] —is that the presence of an intercept term in the raw data equation yields a *curvilinear* relationship between logY and logX, whereas in the absence of an intercept term the log-log relationship is always linear.

[1] This type of allometric relationship has been called "linear allometry" by Jungers, *et al.* (1995), but the term "spurious allometry" is more consistent with my argument (presented in a later section) that in such cases the true *effect* of X on Y is isometric, and that the apparent allometry is spurious in the same way that a correlation between two variables can be spurious.

Reproduced with permission of the copyright owner. Further reproduction prohibited without permission.

10.2. Bivariate plots of size variables under conditions of isometry and allometry, when the intercept term in the allometric equation $Y=a+bX^k$ is not equal to 0 (e.g., $a=10$).

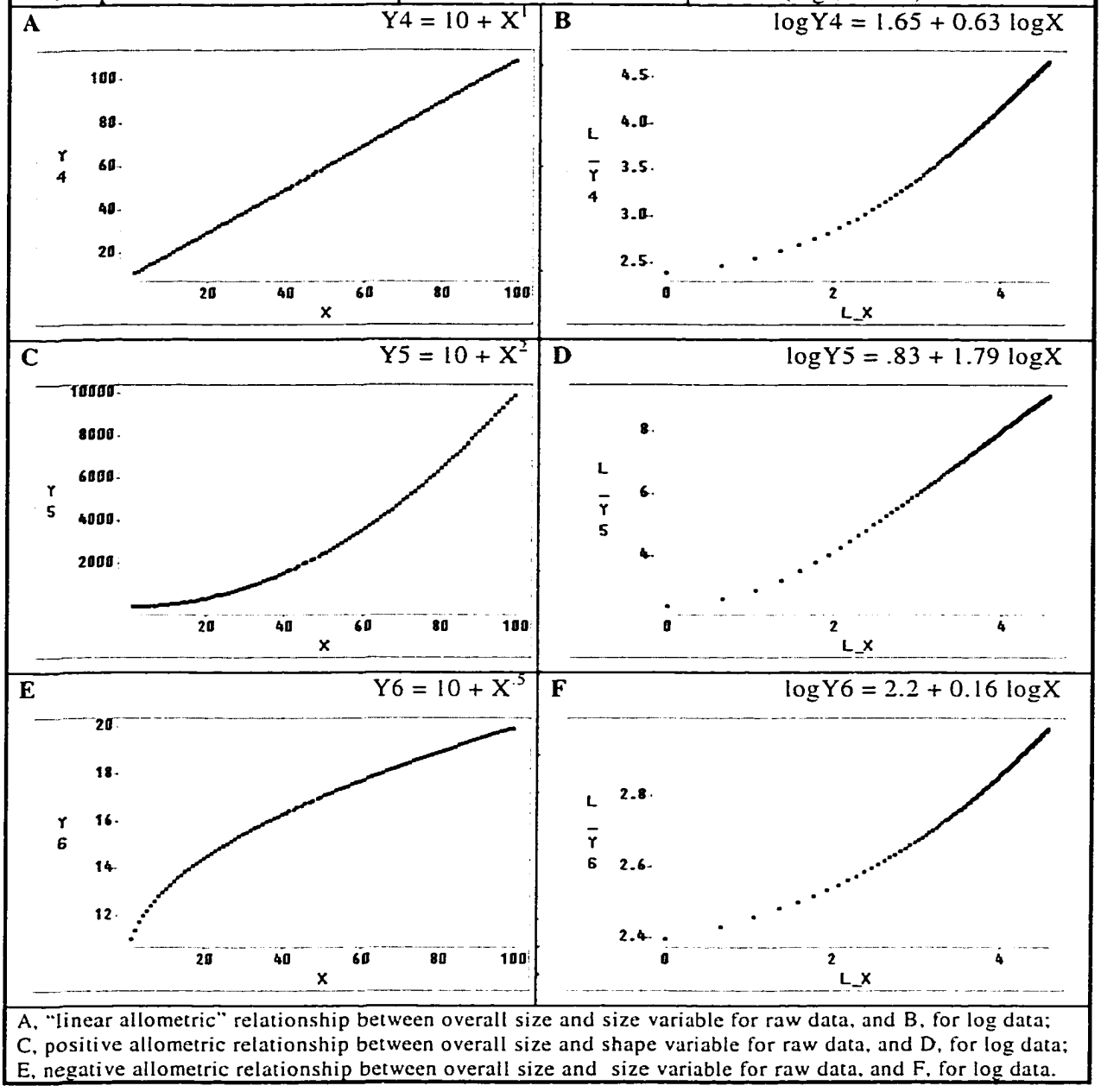

A, "linear allometric" relationship between overall size and size variable for raw data, and B, for log data; C, positive allometric relationship between overall size and shape variable for raw data, and D, for log data; E, negative allometric relationship between overall size and size variable for raw data, and F, for log data.

The effects of adding or subtracting a constant value to Y on the relationship between Y and X can easily be understood with reference to a simple trigonometric example. Consider the three triangles displayed in Box 10.3, A, B and C. The length of the base of each triangle is taken to represent X, and the height of each

Reproduced with permission of the copyright owner. Further reproduction prohibited without permission.

triangle is Y. The *increase* of Y to X among the three triangles is proportional, but in each case a constant value, 1, has been added to Y. The general allometric equation for this example is: $Y=1 + 1.0X^1$.

Box 10.3. Series of triangles showing how intercept term produces spurious allometry

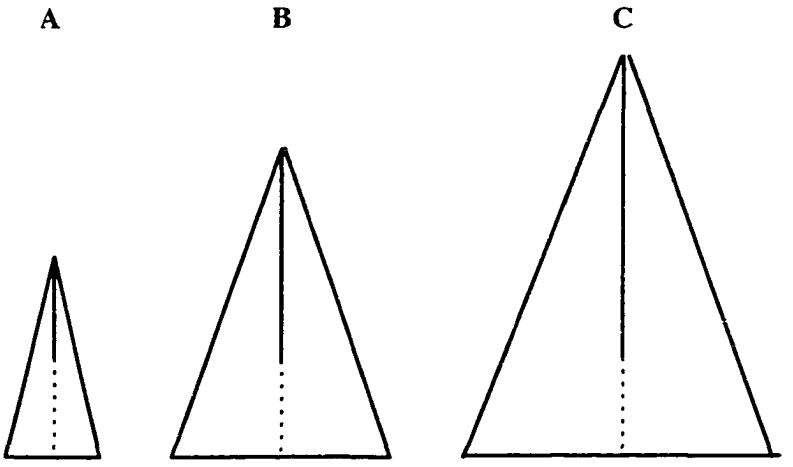

	$2=1+1^1$	$3=1+2^1$	$4=1+3^1$
Ratio *a*/Y	.50	.33	.25
Ratio Y/X	2.0	1.5	1.33

Notice that the proportion of the constant $a=1$ (dotted line) to Y (total vertical height, solid plus dotted line) gets progressively smaller as the triangles increase in size: from 50% to 33% to 25%. Because the added value is constant, it contributes progressively less to height (Y) as overall size (X) increases. The result is that the ratio Y/X, rather than remaining constant, gets progressively smaller with size, producing a negative allometric effect. In like manner, subtracting a constant from Y will produce a positive allometric effect. Numerical examples showing the effects of the sign of *a* on the relationship between X and Y are given in Box 10.4.

Reproduced with permission of the copyright owner. Further reproduction prohibited without permission.

Box 10.4. Numerical examples of how the properties of *a* (intercept) affect the relationship between X (body size) and Y (shape variable), when *a* is constant.

Properties of *a*	Numerical example: Y = *a* + X			Equation solution:	Relationship between X and Y
Property 1: *a* is constant and equal to 0	1	0	1	Y = 0 + X	Isometric
	2	0	2		
	3	0	3	logY=1.0 logX	
	4	0	4		
Property 2: *a* is constant and greater than 0	2	1	1	Y = 1 + X	Negative Allometric
	3	1	2		
	4	1	3	logY=.68+.66 logX	
	5	1	4		
Property 3: *a* is constant and less than 0	2	-1	1	Y = -1 + X	Positive Allometric
	3	-1	2		
	4	-1	3	logY= -1.1 +1.6 logX	
	5	-1	4		

Two further points can be made about Huxley's allometric equation: (1) it can be shown that adding *any* additional term to the standard allometric equation, be it a constant intercept term (*a*) or a variable term such as a second independent variable (X_2) will produce an allometric relationship between X and Y, and (2) the interpretation of this type of observed linear allometry (i.e., whether it is considered to be actual or spurious) depends upon one's research objective. I will return to these points presently.

Shape

In biology, shape refers to the geometric properties of an organism that are invariant to changes of orientation and scale (*cf.* Bookstein, 1978; Humphries *et al.*, 1981). It may not come as a surprise to learn that the vast majority of allometric studies do not, in fact, examine the relationship between body size and shape. For example, one of the most common applications of allometry in morphology is the quantification of the relative rates of growth of two different structures or organs of the same individual; or, alternatively, the relative dimensions of two structures

Reproduced with permission of the copyright owner. Further reproduction prohibited without permission.

across individuals of different size. These types of studies, which I call *character allometry*, do not measure body size, nor do they include a shape variable per se. Rather, body size (X) and shape (Y) are replaced by variables that measure the dimensions of two characters (e.g., maxillary length and bizygomatic breadth). Morphometric character variables measured as linear distances, areas or volumes are *not* shape variables,[2] and studies that quantify their covariance are not about the relationship between size and shape. This distinction is not simply semantic. I will show later in this chapter that treating character variables as if they were shape variables has led to serious misconceptions in applied morphology.

In "character allometry," shape is represented by the ratio Y/X and "size" is represented by the X character. Such an analysis reveals nothing about body size-related changes in the characters; it is purely a description of the change in the relative dimensions of the characters (Y/X) over increasing dimensions of one of them (X). *Body size allometry*, in which X is intended to be a measure of overall organic size, is formulated in much the same way. The Y variable is typically a character dimension rather than a shape variable, and shape is therefore represented as the ratio of the character dimension to body size. Although the use of this type of body size allometry is widespread in morphological studies, some workers have raised serious objections to its use. Cheverud *et al.* (1986), apparently not realizing they were referring to standard allometric practice, stated: "Previous suggestions that a ratio of some chosen character to overall size be used as a measure of shape

[2] A good definition of a "shape variable" is given by Slice *et al*, 1996: "Any measure of the geometry of a biological form, or the image of a form, that does not change under similarity transformations: translations, rotations, and changes of geometrical scale (enlargements or reductions). Useful shape variables include angles, ratios of distances, and any of the sets of shape coordinates that arise in geometric morphometrics" (p. 547).

Reproduced with permission of the copyright owner. Further reproduction prohibited without permission.

(Alberch *et al.*, 1979) are unsatisfactory, since they lead to a mathematical confounding of size and shape (Atchley *et al.*, 1976)."

The importance of the conceptual and analytical separation of size and shape becomes clear when we understand that the outcome obtained using a character dimension for the Y term in the allometric equation is different from the outcome obtained when a true shape variable is used for the Y term. Box 10.5 shows the results of a simulated allometric analysis under varying conditions of isometry versus allometry, raw versus log data, and size versus shape for the Y variable. The analysis was conducted on a simple geometric form—a right-angle triangle—but the principles apply equally well to more complex morphological forms. In each of the 8 bivariate plots presented in Box 10.5 (A-H) the X variable on the abscissa is the square root of the area of the triangle, a measure of the triangle's overall size. On the ordinate, the dependent variable is either the linear distance of one of the sides of the triangle (denoted Y) (see Box 10.5, A, B, E, F), or the ratio (denoted R) of Y to another side, Y' (see Box 10.5, C, D, G, H). Y is thus a character dimension whereas R is a shape variable. The smallest triangle had the measurements: Y=2, Y'=1, and X=1. This starting triangle was then scaled both isometrically (Y, R) and allometrically (Y2, R2), and the values of X, Y and R at various sizes of X were regressed and plotted.

Reproduced with permission of the copyright owner. Further reproduction prohibited without permission.

Box 10.5. Allometric equations and bivariate plots under varying conditions.

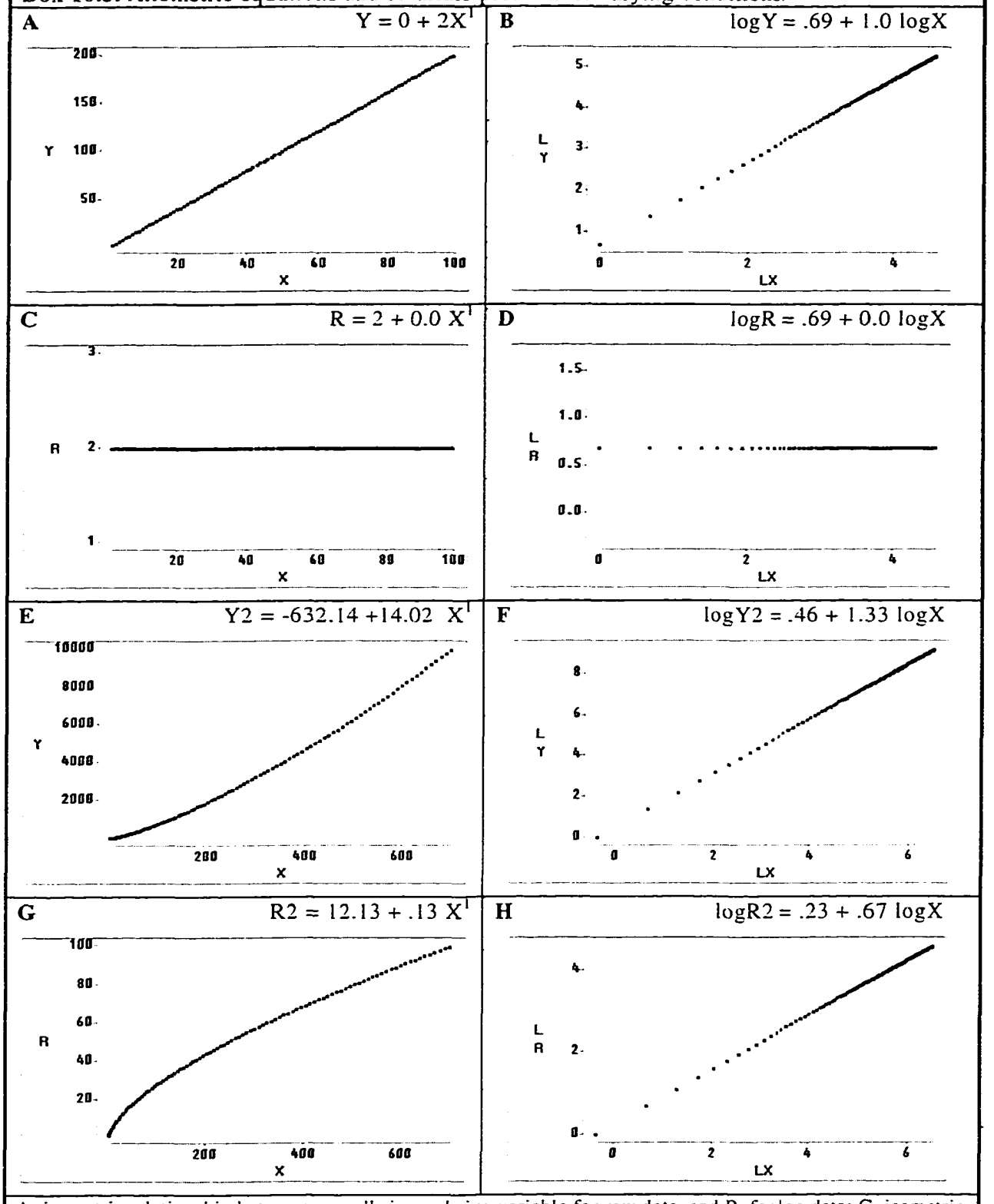

A, isometric relationship between overall size and size variable for raw data, and B, for log data; C, isometric relationship between overall size and shape variable for raw data, and D, for log data; E, allometric relationship between overall size and size variable for raw data, and F, for log data; G, allometric relationship between overall size and shape variable for raw data, and H, for log-log data.

Reproduced with permission of the copyright owner. Further reproduction prohibited without permission.

The bivariate plots in Box 10.5, A and B, which depict the isometric relationship between a character dimension (Y) and overall size (X), show the familiar signs of isometry: intercept =0 and power =1 in raw data form (plot A), and slope =1 for the log-log data (plot B). The results are much different when the character dimension (Y) is replaced by the shape variable (R), as shown in Box 10.5, C and D. In both raw and log data form, the regression of X on R yields a flat line (slope=0), indicating that R is invariant to changes in X (also see the discussion on angular invariance in Chapter 11).[3]

The distinct results associated with a character dimension compared to a shape variable are also apparent in the allometric case, in which the shape of the triangle changes with size. Bivariate plots E and F, in Box 10.5, illustrate the case of positive allometry between the character dimension (Y2) and overall size (X). But when the shape variable (R2) is substituted for the character dimension (Y) the relationship turns from positive allometry to negative allometry (Box 10.5, bivariate plots G & H).

The foregoing analysis shows that the results of an allometric study need to be interpreted differently depending on whether a character dimension or a shape variable is used in the study. Moreover, it demonstrates that character variables and shape variables must be treated differently with regard to their relationship with size.

---

[3] With naturally occurring data there will be some dispersion about the regression line. A zero-slope bivariate regression line, regardless of the dispersion, is conventionally interpreted to mean that no relationship exists between the two variables. However, it can be seen that in an allometric study in which a shape variable is regressed against a linear measure of body size a zero-slope regression line indicates isometry only when the data are homoscedastic and characterized by low variance (i.e., the dispersion is elliptical rather than circular).

Reproduced with permission of the copyright owner. Further reproduction prohibited without permission.

Size

The appropriate meaning and measure of size, or body size, is an issue in need of critical reexamination. In this section I demonstrate that the concept of "size," as conventionally conceived, confounds two distinct types of effects: (1) scale, geometric size, or simply "size" (*senso stricto*), and (2) size-related quantity, or just "quantity" for short. The former refers to the spatial dimensions of an organism, whereas the latter covers a multitude of properties associated with scale (weight and surface area-to-volume ratio are two examples). While highly correlated, the two classes of size—scale and quantity—influence the phenotypic properties of organisms via distinct causal pathways. Scale is mediated almost exclusively via intrinsic genetic and epigenetic mechanisms (such as paracrinal hormonal stimulation), while various size-related quantities operate predominantly via environmental mechanisms (see Chapter 2). Weight, for example, a size-related quantity, effects change in skeletal tissues through the action of applied strain, an extracellular proximate mechanism.

The distinctiveness of scale and quantity is best demonstrated in cases in which the effects of one or the other are absent. Skeletal elements of developing rats subjected to weightlessness during growth, for example, increase in scale but are lacking the normal skeletal properties associated with weight-bearing induced growth (Bromage *et al.*, 1997).

The properties of an appropriate measure of body size (i.e., scale) have already been alluded to in the context of geometric transformations. A measure of size that is consistent with the geometric formulations of isometry and allometry is one that corresponds to the concept of scale transformation. Scale transformations

Reproduced with permission of the copyright owner. Further reproduction prohibited without permission.

involve two components: (1) the center of the object (or configuration of points) undergoing the transformation—known as the *center of similitude* under conditions of isometry, and (2) a scale factor. The scale factor is a measure of the magnitude of the vectors connecting the center of an object with various points depicting the object's form. The scale factor is thus equivalent to the sum of the distances between the center and each of the points in the configuration of points depicting the object. An equivalent but more commonly used measure, known as *centroid size*, is taken as the square root of the sum of the squared distances between the center and each point of the configuration.[4] Doubling the centroid size of an object under isometry (i.e., increasing the magnitude while maintaining the relative directions of the point vectors) will produce a doubling of the point to point dimensions of that object. Centroid size is thus a proper measure of organic size in allometric studies.

It can further be shown that other proper measures of size are special cases of centroid size under varying conditions of point density and object dimensionality. At one extreme of point density is the special case in which just two points are used to represent an object. In this case centroid size is tantamount to the raw distance between the two points, which corresponds directly to the conventional practice of using a given linear distance, such as cranial length, as a proxy for size. However, it is obvious that this measure of size will be accurate only if the object it represents is perfectly symmetrical (a circle or a sphere), and even then only under certain conditions. At the other extreme of point density,

---

[4] An alternative, and equivalent, measure of centroid size is the sum of all the squared interpoint distances (Bookstein, 1992).

Reproduced with permission of the copyright owner. Further reproduction prohibited without permission.

consider the special case in which the object is virtually covered with points, and there is a seemingly infinite number of vectors connecting the center of similitude to these points. It can be shown that in such cases, centroid size will be proportional to the square root of the area of a 2-dimensional object, or the cube root of the volume of a 3-dimensional object (but see Bookstein, 1992, Sec. 5.5).

In applied allometry, the points to be included in the calculation of centroid size should be numerous and evenly distributed over the object under study—a condition that is not always possible to meet. The use of areas or volumes, when available, is ideal not only because all potential points are represented but because each measured point or subset of points contributes so little to the overall measure of size that any given character variable (e.g., point-to-point distance) can be regarded as independent with respect to centroid size. At the other extreme, using only a small subset of points in a morphometric analysis can yield severe collinearities between the character variables and centroid size.

Bookstein (e.g., Bookstein *et al.*, 1985, Bookstein, 1992) advocates a different measure of size in applied allometry. He suggests that a factor analytic model be employed to construct a latent variable, which he calls *general size*, the scores of which are "...constructed from the linear measures themselves, with no reference to any external standard of age, length, or mass" (Bookstein, 1992:97). This general size factor is computed so that it explains as much of the observed covariances among the manifest variables as possible (i.e., the principle factor). One could argue that this approach is flawed because it *a priori* assumes that all of the covariance explained by the first principal factor is due to a joint dependence on size alone, to the exclusion of other potential contributing factors. Bookstein

Reproduced with permission of the copyright owner. Further reproduction prohibited without permission.

justifies this assumption with the contention that other potential sources of covariance contribute very little to the major factor. "Only a small part of the covariance expresses functional regulation, morphological integration, shape differences between subgroups at constant size, or other specifically biological processes or constraints" (Bookstein, 1992:96).

Centroid size and general size are, in fact, variant methods of measuring the same overall scaling factor associated with a given set of landmarks configurations. Box 10.6 shows the close correspondence between centroid size and general size (R^2=.992) of the landmark coordinates and interlandmark distances for the 300 adult anthropoid specimens included in this study. Centroid size will be used in subsequent analyses as a measure of overall body size, or, more accurately, of overall skull size.

Box 10.6. Regression of log *centroid size* (ΔL_YV41) against *general size* factor scores of log interdistance measures (ΔFACTOR1) (n=300, R^2 = 0.9997).

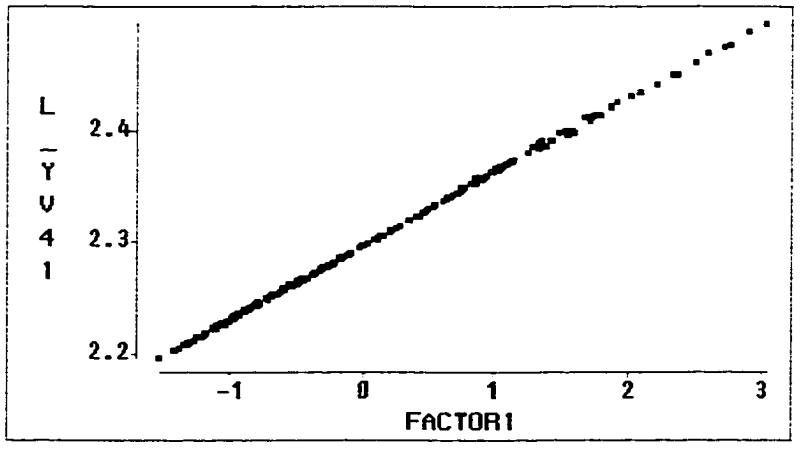

Most morphologists use body weight, or some estimator of body weight, as the preferred measure of size in allometric research. For these workers there is

Reproduced with permission of the copyright owner. Further reproduction prohibited without permission.

good news and there is bad news. The bad news is that body weight is not consistent with the geometric scale formulation of size. Weight is a size-associated quantity whose effects on the properties of bone parallel applied muscle force. Weight can approximate size only to the extent that it is correlated with volume (recall that cube root volume *is* an appropriate measure of size in three dimensions); and since the various tissues, fluids, and gasses that make up vertebrate organisms have different densities (e.g., bone, brain, blood, air), which occur in different proportions, one cannot assume that weight will be an equivalent measure of volume. A glance at Box 10.7, which contains the scatter plot of log skull centroid size [Y41-SKCNTR] against log dry cranial weight [Y83-DSKWGT], indicates that while dry bone weight is a reasonably good predictor of geometric size for most taxa it overestimates size for the genus *Homo*.

Box 10.7. Regression of log *centroid size* against log *dry cranial weight* (n=300, R^2 = .979).

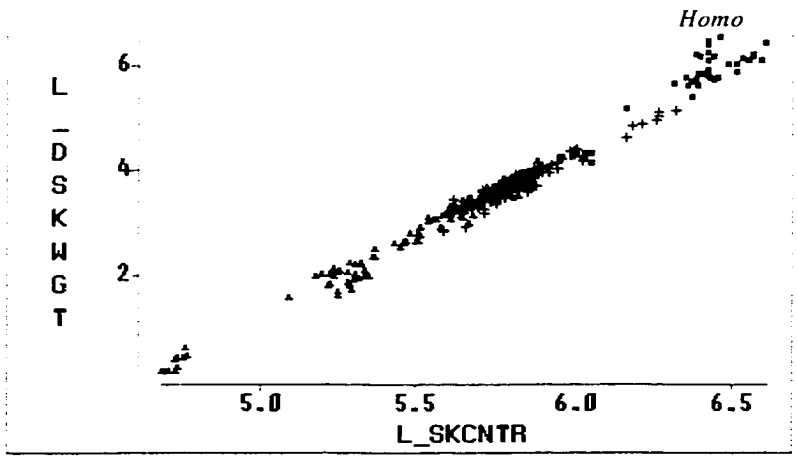

The good news is that body weight is usually unavailable, or difficult to obtain, anyway, whereas the best proxies for body size—centroid size and general size—are easily obtained from coordinate data and interlandmark distances,

Reproduced with permission of the copyright owner. Further reproduction prohibited without permission.

respectively. This "good" news is tempered somewhat by the fact that body weight, although not a proper measure of geometric size, is itself a potential factor influencing certain characters, especially those skeletal structures that respond to weight-induced strain. Fortunately for craniologists, few if any bones of the skull are true weight-bearing bones comparable to limb bones.

Evolutionary and Biological Significance of Isometry and Allometry

Allometric studies generally fall into three main categories: (a) growth allometry is the study of the effects of size on shape during ontogeny, (b) intraspecific allometry is the study of size-related differences among adults within a species, and (c) interspecific allometry is the study of size-related differences among adults across taxa. Intraspecific and interspecific allometric relationships obtain from alterations (i.e., changes in the timing or rate) of allometric growth patterns (McKinney, 1988), a process known as heterochrony (as defined by de Beer, 1930). Shea (1983), for example, found that certain interspecific allometric relationships among African apes could be explained by cessation or extension of growth along a single allometric slope. Leutenegger and Masterson (1989) likewise found that observed patterns of intraspecific allometry in *Pongo pygmaeus* were in large part due to heterochronic alterations of a common allometric growth trajectory.

Although proximate mechanisms are the immediate causes of allometric growth, causal agents operating via distal mechanisms determine which growth patterns become expressed. Variation in these expressed patterns produces the size-related differences among adults that are observed both within and between species. But the biological and evolutionary meaning of observed allometric

Reproduced with permission of the copyright owner. Further reproduction prohibited without permission.

relationships is often unclear. "Why, for example, should the well-known 0.66 slope for interspecific brain weight-body weight allometry indicate the requirement for functionally equivalent brain size? Functional equivalence could just as well be a slope of 0.60 (or any other value)" (Smith, 1984:R156). The eventual solution to this quandary begins with the understanding that overall size (i.e. geometric body size) is only one of several causal agents acting on a given character dimension. A given character (Y) is thus constrained by changes in overall body size (X) and at the same time modified by other causal agents ($Z_{i..j}$) associated with one or more biological roles (see Box 10.8).

Box 10.8 Effects of causal agents on size-related changes in shape.

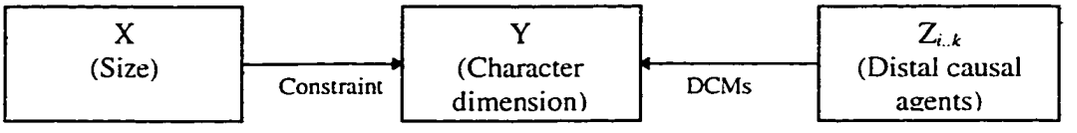

I contend that the true relationship between overall size and a given character dimension is always isometric, and that the apparent positive or negative allometry between size and the character is an artifact of model misspecification. In other words, in the absence of any additional causal agents ($Z_{i..j,}$) increases in body size will result in corresponding isometric increases in a given character dimension. But if one or more causal agents, in addition to body size, are acting to effect change in the character, then it will appear as though the relationship between the character and body size is that of allometry.

The dual influences of X and $Z_{i..j}$ on Y in Box 10.8 can be expressed in linear form as

Reproduced with permission of the copyright owner. Further reproduction prohibited without permission.

$$Y = a + bX + b_iZ_i + b_jZ_j + e \quad (10.5)$$

Recall that Huxley's allometric equation governing the relationship between X and Y for raw data is $Y = a + bX^k$. Assume that the true relationship between X and Y is isometric, in which case both the power function k and the intercept term a can be discarded, and we are left with

$$Y = bX, \quad (10.6)$$

or equivalently,

$$\log Y = a + 1.0 \log X. \quad (10.7)$$

But if X is not the sole cause of Y, then an error term must be added which contains residuals representing the effects of one or more relevant variables not included in the model (as well as random effects):

$$Y = bX + e \quad (10.8)$$

Alternatively, the relevant independent variables may be entered into the equation directly.

$$Y = bX + b_iZ_i + b_jZ_j + e' \quad (10.9)$$

In such a case, the zero-order model, the one which contains body size as the sole independent variable (formula 10.6), is misspecified, and the regression coefficient k of the log-log expression will be inaccurate.

Moreover, the nature of the relationship between the relevant missing independent variables $Z_{i..j}$ and X will determine the zero-order relationship between X and Y. Box 10.9 gives several examples. In each of the three cases the true model is $Y = 1.0X + .75Z$ (see Equations 1, 7, and 13). In the first example (Case 1) Y is a function of both X and Z, and Z is random with respect to X. The second example (Case 2) is the same as the first, except that Z is tightly correlated

Reproduced with permission of the copyright owner. Further reproduction prohibited without permission.

with X (r = .99). In Case 3, Z is perfectly correlated with X. According to the zero-order raw data and log-log equation solutions for Cases 1 and 2 the relationship between X and Y is allometric—the coefficients of logX are not equal to 1 (see Equations 2, 3, 8, and 9).

An important point to recognize in the preceding examples is that the inclusion of independent variable Z in the true model is equivalent (in terms of producing spurious allometry) to the inclusion of a non-zero intercept term in the allometric equation (see Box 10.2). In both models Y is linear with respect to X in raw data form, but the inclusion of the extra term (intercept a or independent variable Z) in the equation produces a log-log coefficient that is less than or greater than 1. Hence, the first two cases in Box 10.9 are examples of spurious allometry (see previous section).

The observed allometry between X and Y in Equations 2 and 8 of Box 10.9 is spurious in the same way that a spurious correlation can exist between two variables. "When two variables are correlated solely because they are both affected by... [a third variable], the correlation is said to be spurious. Once the effects of the... [third variable] are controlled, or removed from the two variables, the correlation between them vanishes" (Pedhazur, 1997:158). In a similar manner, when two variables are allometrically related solely because both are associated with a third variable (or a constant), the allometric relationship may be said to be spurious. The obvious question is: Just as a spurious correlation vanishes with control of the third relevant variable, does spurious allometry vanish once the effects of the other independent variables are controlled or removed? The answer depends on the method of control. If variable Z is controlled for using multiple

Reproduced with permission of the copyright owner. Further reproduction prohibited without permission.

regression, in which partial regression coefficients are produced, then the answer is no. This is because in multiple regression a "...coefficient such as b_{Yj} denotes the regression coefficient of Y on variable X_j that one would expect if all the other variables in the regression equation had been held constant experimentally" (Sokal & Rohlf, 1995:612). And we have already seen that a constant in the equation produces an allometric effect in the log-log data, even though the relationship between Y and X is linear in raw data form.

However, there is another method equivalent to multiple partial regression that obviates extraneous terms in the solution equation—incremental regression. Recall that the multiple regression of Y on X controlling for Z is equivalent to regression of the residuals of Y on X, where the residuals were obtained by regression of each with Z. Since only the residuals are involved in the regression equation, extraneous terms are excluded and the spurious allometry produced by them vanishes. Equations 6 and 12 in Box 10.9 show how the true isometric relationship between X and Y is revealed using the incremental regression approach.

Another important point, alluded to earlier, is that the concept of spurious allometry applies only to explanatory research. In studies in which the objective is purely descriptive or predictive (that is, the question being asked is simply: "Does Y covary with X isometrically or allometrically?"), it matters not whether the observed allometry is real or spurious. In such studies the zero-order model, the one containing only X, is entirely appropriate. However, *if the objective of the analysis is explanatory, (that is, the question being asked is: "What are the effects of X on Y?"), then the zero-order model is inappropriate and potentially*

Reproduced with permission of the copyright owner. Further reproduction prohibited without permission.

misleading. The problem is a serious one since most allometric research is explanatory in nature (recall Gould's definition of allometry as the "study of the consequences of size with respect to shape").

Reproduced with permission of the copyright owner. Further reproduction prohibited without permission.

Reproduced with permission of the copyright owner. Further reproduction prohibited without permission.

Box 10.9. Comparison of three different equation solutions for various known relationships between Y (character dimension, dep. var.), X (overall size, ind. var.) and Z (causal agent, ind. var.).

Properties of Z with respect to X	True model (Y is isometric with X):	Misspecified zero-order equation solution:	Fully specified first-order equation solution	Fully specified, incremental equation solution	Apparent relationship between X and Y based on zero-order solution
Case 1: Z is random with respect to X	**[1]** $Y = 1.0X + .75Z$	**[2]** $\log Y = 3.1 + .37 \log X + e$ ($R^2 = .48$; se $bX = .038$) **[3]** $Y = 36.18 + .96X + e$ ($R^2 = .66$; se $bX = .07$)	**[4]** $\log Y = 1.7 + .39 \log X + .34 \log Z + e$ ($R^2 = .84$; se $bX = .021$, $bZ = .023$) **[5]** $Y = 1.0X + .75Z$ ($R^2 = 1.0$; se $bX = 0$, $bZ = 0$)	**[6]** $\log Y = 1.0 \log X$ ($R^2 = 1.0$) $Y = 1.0X$	Allometric (spurious)
Case 2: Z is imperfectly correlated with X (in this example $r = .99$)	**[7]** $Y = 1.0X + .75Z$ (given: $Z = 1.5X$ + RAND)	**[8]** $\log Y = 1.14 + .91 \log X + e$ ($R^2 = .99$; se $bX = .008$) **[9]** $Y = 3.58 + 2.12X + e$ ($R^2 = .99$; se $bX = .007$)	**[10]** $\log Y = .47 + .37 \log X + .65 \log Z + e$ ($R^2 = 1.0$; se $bX = .005$; $bZ = .005$) **[11]** $Y = 1.0X + .75Z$ ($R^2 = 1.0$; se $bX = 0$, $bZ = 0$)	**[12]** $\log Y = 1.0 \log X$ ($R^2 = 1.0$) $Y = 1.0X$	Allometric (spurious)
Case 3: Z is perfectly correlated with X ($r = 1.0$)	**[13]** $Y = 1.0X + .75Z$ (given: $Z = 1.5X$)	**[14]** $\log Y = .75 + 1.0 \log X$ ($R^2 = 1.0$; se =0) **[15]** $Y = 2.125X$ ($R^2 = 1.0$; se =0)	**[16]** $\log Y = .75 + 1.0 \log X$ ($R^2 = 1.0$; se =0) **[17]** $Y = 2.125X$ ($R^2 = 1.0$; se =0)	Not applicable, since all residuals equal 0.	Isometric

In the context of explanatory morphometry, the only valid test of isometry is the demonstration of linearity between X and Y in raw data form, under conditions of full model specification (see Box 10.9, Equations 5 & 11), or incremental regression control of confounding variables in either raw or log data form (Equations 6 & 12).

The preceding discussion and analysis indicates that previous studies in which size is reported as having an "allometric" affect on various morphological characters, may be inaccurate due to the following pitfalls: (1) the confounding of size (i.e., scale) with size-related quantities, (2) the use of inherently misspecified zero-order allometric equations (i.e., omitting of other relevant independent variables from the equation), and (3) failure to make a distinction between descriptive and explanatory allometric research.

The above considerations clear the way for the proposition that changes in geometric size effect strictly isometric changes in character dimensions. The statement that organismic form will tend to develop and evolve isometrically in the absence non-scale nomological causal agents ($Z_{i..j}$) is not a metaphysical construct, it is an hypothesis that can in principle be tested. D'Arcy Thompson (1917) himself provided evidence bearing on this issue in his encyclopedic volume *On Growth and Form*. He elegantly summarized the *allometric effects of weight* on skeletal form, while providing a crucial observation on the separate *isometric effects of size*.

> ...if a matchstick be 2 in. long and a similar beam 6 ft. (or 36 times as long), the latter will sag under its own weight thirteen hundred times as much as the other. To counteract this tendency, as the size of an animal increases, the limbs tend to become thicker and shorter and the whole skeleton bulkier and heavier; bones make up some 8 per cent of the body of mouse or wren, 13 or 14 per cent of goose or dog, and 17 or 18 per cent of the body of man. Elephant and

Reproduced with permission of the copyright owner. Further reproduction prohibited without permission.

> hippopotamus have grown clumsy as well as big, and the elk is of necessity less graceful than the gazelle. It is of high interest, on the other hand, to observe how little the skeletal proportions differ in a little porpoise and a great whale, even in the limbs and limb-bones; for the whole influence of gravity has become negligible, or nearly so, in both of these [Thompson, 1917; reprint 1994, p. 20].

In this one passage Thompson has struck at the heart of the issue. It is weight, not size, that causes the disproportionate growth of limb bones in terrestrial animals of different scale. If weight is removed as a causal factor, as has occurred for the most part in the development and evolution of aquatic mammals, size by itself will effect only isometric changes in organic structure.

Further evidence comes from clinical cases or experiments in which organisms with excessive growth hormone levels increase in overall body size (gigantism) but maintain cranial proportionality (e.g., Savostin-Asling *et al.*, 1980; Pirinen *et al.*, 1994). In such cases, as the size of an animal increases (or if large animals are compared with smaller ones) cranial structures tend to increase isometrically. However, the same structure may be diverted from isometry (toward allometry) in order to maintain an adequate level of performance of one or more of its biological roles (Wolf *et al.*, 1991).

Modeling the Isometric Effects of Size

In a recent review article, Jungers *et al.* (1995) evaluated a dozen different methods of "size-adjustment" for continuous data in morphometric allometry. Although their objective was different from mine—theirs was to "correctly identify individuals of the same shape," whereas mine is to quantify the effects of size on a given character and control for size in order to isolate the effects of other causal agents—their analysis raises some interesting points. To summarize, these authors recommend

Reproduced with permission of the copyright owner. Further reproduction prohibited without permission.

against the use of residuals from an *empirically-based* regression on size as a means of size-adjustment or size-correction. According to their analysis, a family of methods based on Mosimann's (1970; 1975; Mosimann & James, 1979) shape ratios is best suited to handle a variety of allometry problems. In its most basic form, the Mosimann shape ratio is denoted as Y/X, where Y is a character dimension and X is an appropriate measure of size (e.g., centroid size, geometric mean). It can be shown that the log of this ratio, (log)Y/X, is equivalent to taking the residuals of (log)Y on (log)X with a regression slope set to 1.0:

$$(\log)Y = 1.0(\log)X + e \qquad (10.10)$$

or, alternatively, as the difference between the logged values,

$$e = (\log)Y - (\log)X. \qquad (10.11)$$

Yet another equivalent Mosimann-type size-adjustment can be obtained by altering Burnaby's (1966) method of removing size from a data matrix. Rather than projecting the logged data onto a plane orthogonal to the first principal component of a PCA (the "size" factor), as suggested by Burnaby, the data are projected orthogonal to an isometric plane (Rohlf & Bookstein, 1987; Jungers & Cole, 1992). What all of these methods have in common is that they partial out that part of the variance of a given character dimension, Y, that can be accounted for by *isometric* size variation.

As a size-independent measure, the Mosimann isometric log residual has several advantages, both theoretical and analytical. On the side of theory, it is consistent with the hypothesis advanced here that the effect of size on a character dimension is always isometric. One of the main criticisms of employing residuals from an unconstrained model, that is, one in which the slope is determined

Reproduced with permission of the copyright owner. Further reproduction prohibited without permission.

empirically, is that "...the potential for a functional or adaptive explanation of a point *on* a regression line is just as great as for a point *off* the line" (Smith, 1984:R157). To get around this problem, Smith advocated "...the use of a priori theoretical equations rather than empirical ones" (1984:R157). As an example, Smith referred to a study by McMahon (1975) who argued on theoretical grounds that the slope of long bone length to diameter in terrestrial mammals should be 0.67.

> Continuing with McMahon's demonstration of elastic similarity on long bones, he considers slopes such as 0.640 and 0.624 (overall forelimb and hindlimb slopes for Bovidae) to support the theoretically expected slope of 0.67. So why are the actual slopes different? Either because elastic similarity is modified by some other effect or because elastic similarity is the only factor and the 0.640 and 0.624 slopes represent sampling error. In either case, the relative size of individual specimens should be calculated from a slope of 0.67. If some other effect is involved, correction of relative size to a slope of 0.67 will allow study of the remaining factor, since the data will be known to be corrected purely for elastic similarity [Smith, 1984: R157].

The Mosimann method of obtaining isometric log residuals is the application of the same approach to the modeling of size on a given character variable.

Analytically, Mosimann's isometric log residuals have several advantages over other methods. Since the slope is theoretically prescribed rather than empirically computed, all of the problems attendant with line fitting procedures—assumptions of normality, effects of influential observations on slope estimation, coefficient standard errors, and the like—are at once eliminated. Another benefit is that the method can easily be incorporated into the multi-level design adopted in this study. I have already mentioned that the isometrically constrained regression of log X on log Y produces a residuals vector (e) that is equal to (log)Y - (log)X (see Equations 10.10 & 10.11). The isometric regression of centroid size [Y41-SKCNTR]

Reproduced with permission of the copyright owner. Further reproduction prohibited without permission.

on all three of the multi-level data sets (individual level, V; species means, M; and pooled-within species, Q) can therefore be performed without losing the structured linear relationship among the levels (i.e., V=M+Q). Hence,

$$(\log)YV = 1.0(\log)SKCNTR + e_V \quad (10.12a)$$

$$(\log)YM = 1.0(\log)SKCNTR + e_M \quad (10.12b)$$

$$(\log)YQ = 1.0(\log)SKCNTR + e_Q \quad (10.12c)$$

then,

$$e_V = e_M + e_Q \quad (10.12d)$$

and the multi-level analysis can proceed as outlined in Boxes 8.1 and 8.2.

In accordance with Mosimann's size modeling method, log skull centroid size was isometrically regressed on the logs of all linear character variables (i.e., linear distances, square root areas, and cube root volumes) used in the present study. The residuals from these regressions were then employed in subsequent covariance structure analyses. Shape variables were not regressed isometrically on size because they are expected to remain constant under conditions of isometric size variation. Shape variables, of course, may be influenced by size-related changes to one or more associated biological roles.

Reproduced with permission of the copyright owner. Further reproduction prohibited without permission.

Bivariate Scatter Plots

Box 10.10. Scatter plots of log skull centroid size against log nasomaxillary dependent variables.

Nasal bone length (ΔYV1-NASLGT)
Empirical slope 0.83

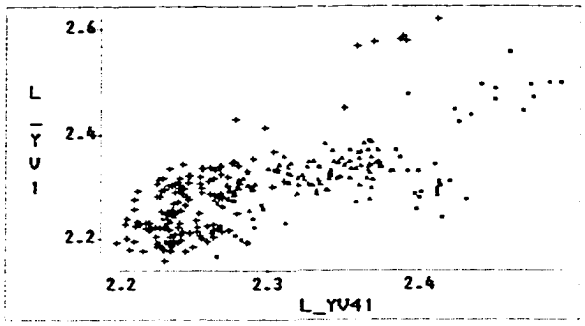

Upper nasal bone width (ΔYV2-NASWDU)
Empirical slope 0.20

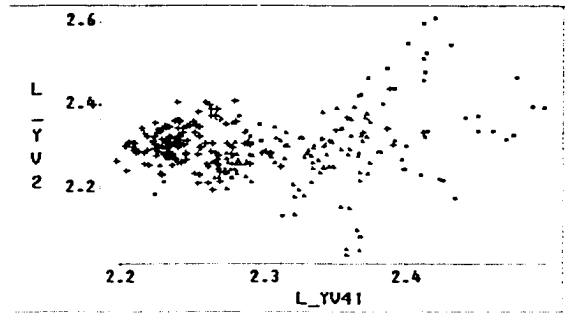

Lower nasal bone width (ΔYV3-NASWDL)
Empirical slope 0.84

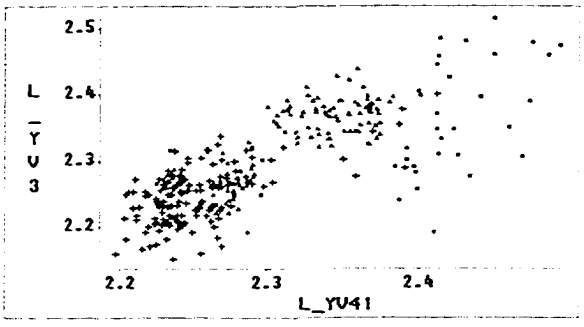

Nasal process of maxilla width (ΔYV4-NPMWDT)
Empirical slope 0.58

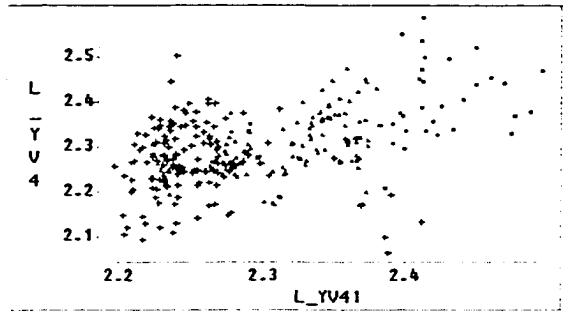

Nasal aperture height (ΔYV5-NSLAHT)
Empirical slope 0.76

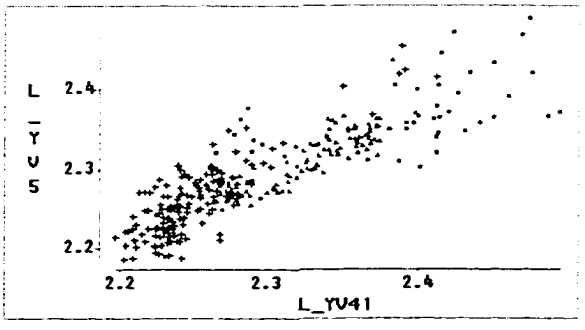

Nasal aperture breadth (ΔYV6-NSLAWD)
Empirical slope 1.02*

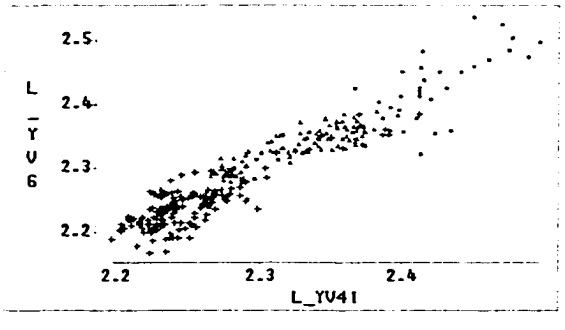

Reproduced with permission of the copyright owner. Further reproduction prohibited without permission.

Box 10.10. Scatter plots of log skull centroid size against log nasomaxillary dependent variables.

Posterior nasal aperture height (ΔYV7-PNASHT)
Empirical slope 0.98*

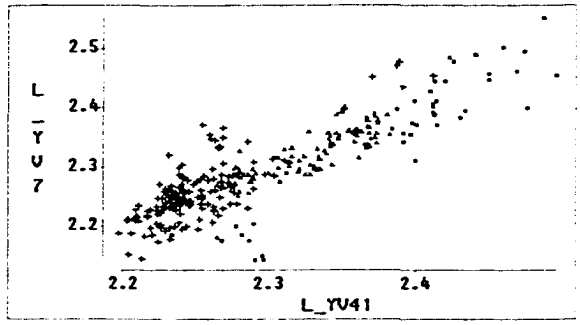

Posterior nasal aperture breadth (ΔYV8-PNASWD)
Empirical slope 0.93

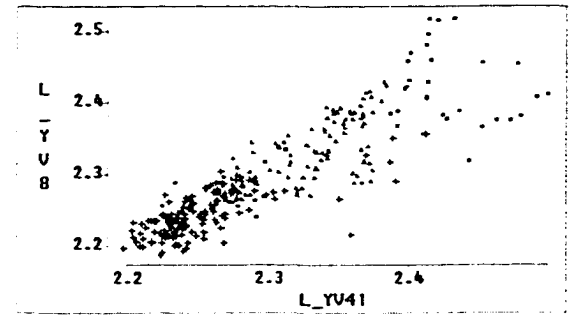

Nasoalveolar clivus length (ΔYV9-NLCLGT)
Empirical slope 0.88

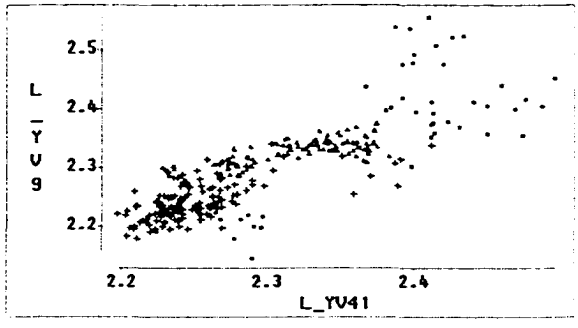

Zygomatic estimated area (ΔYV10-ZYGARE)
Empirical slope 1.03*

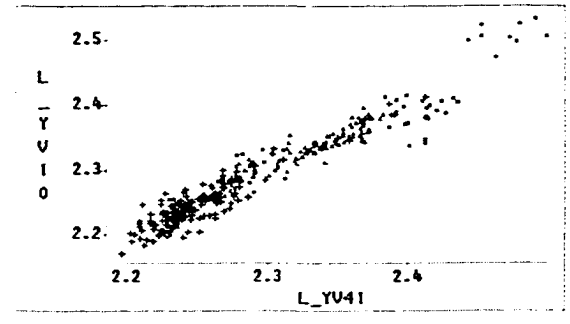

Zygomatic height (ΔYV11-ZYGOHT)
Empirical slope 0.99*

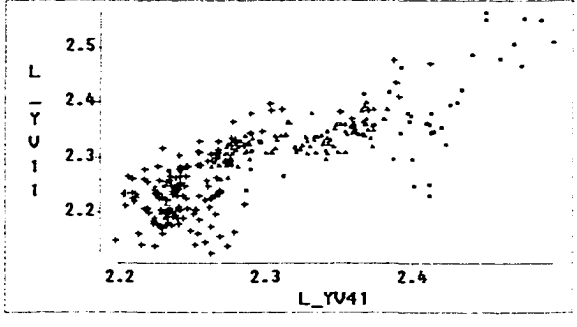

Bizygomatic breadth (ΔYV12-BZYGWD)
Empirical slope 0.95

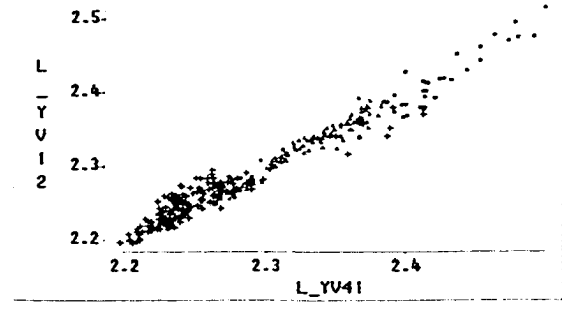

Maxillary arch length (ΔYV14-MXARCL)
Empirical slope 0.90

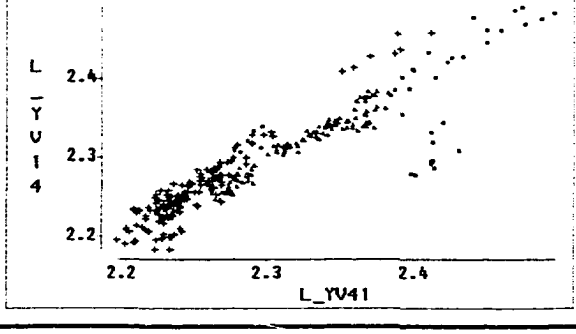

Bimaxillary breadth (ΔYV15-BMAXWD)
Empirical slope 0.99*

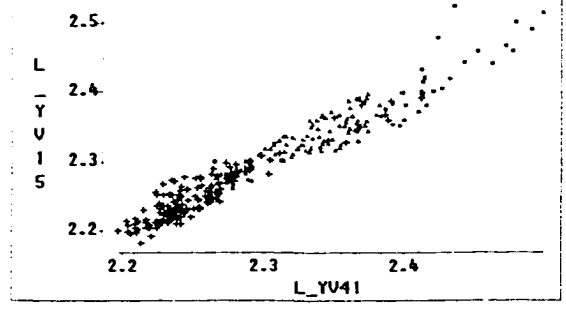

Reproduced with permission of the copyright owner. Further reproduction prohibited without permission.

Box 10.10. Scatter plots of log skull centroid size against log nasomaxillary dependent variables.

Upper facial breadth (ΔYV16-UMAXWD)
Empirical slope 0.95

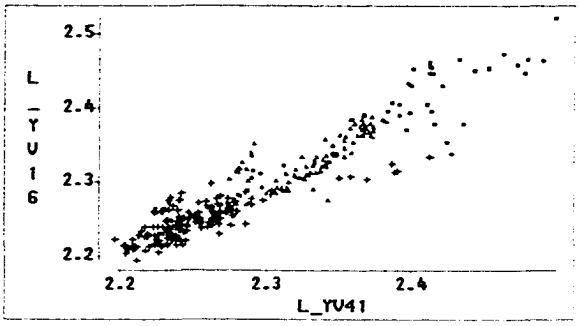

Anterior facial length (ΔYV17-AFACHT)
Empirical slope 0.92

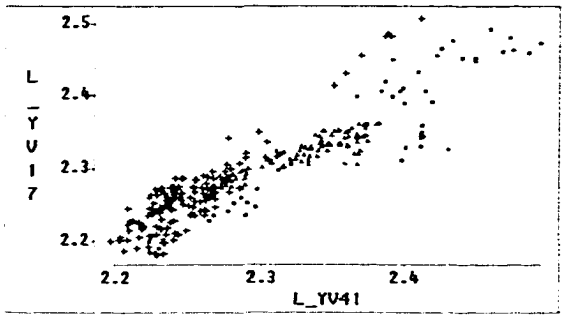

Posterior facial height (ΔYV18-PFACHT)
Empirical slope 0.96

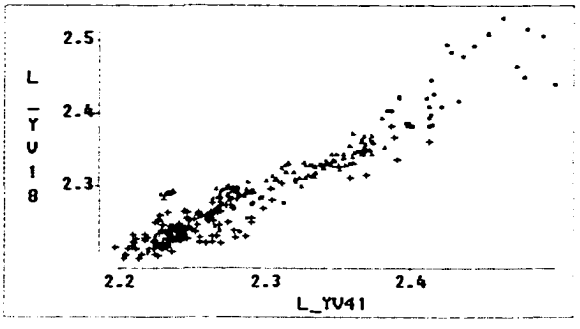

Ramus height (ΔYV19-=RAMSHT)
Empirical slope 0.96

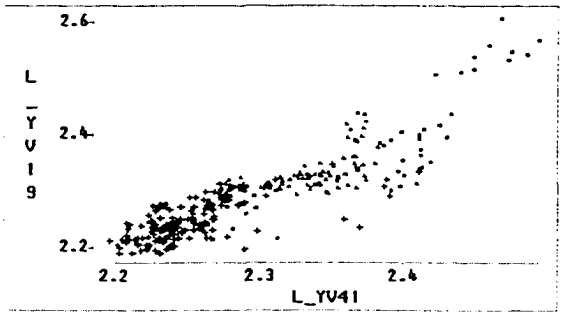

Inter-I^2 palatal width (ΔYV20-I2PALW)
Empirical slope 0.85

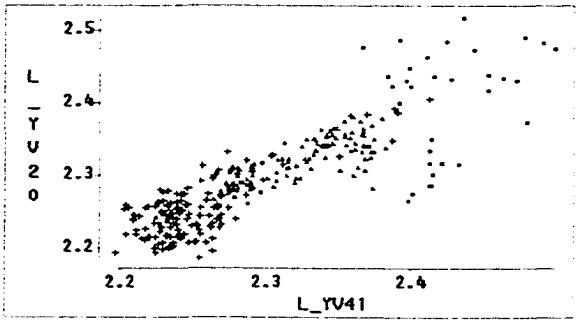

Inter-P^3 palatal width (ΔYV21-P3PALW)
Empirical slope 0.92

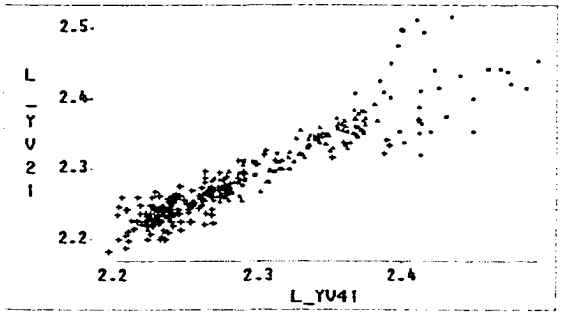

Inter-M^1 palatal width (ΔYV22-M1PALW)
Empirical slope 0.92

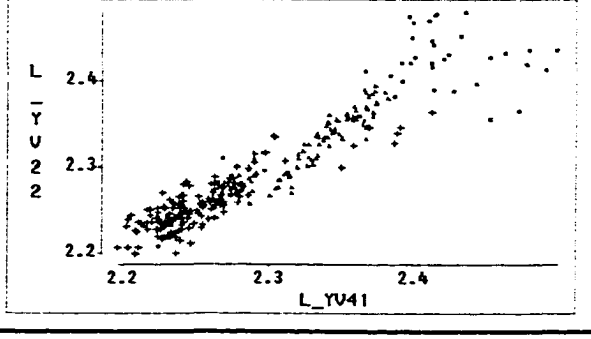

Inter-M^3 palatal width (ΔYV23-M3PALW)
Empirical slope 0.98*

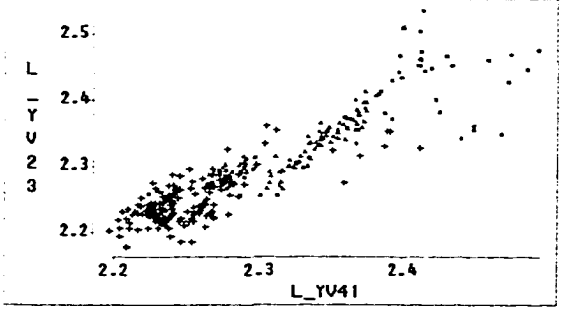

Reproduced with permission of the copyright owner. Further reproduction prohibited without permission.

Box 10.10. Scatter plots of log skull centroid size against log nasomaxillary dependent variables.

Palatal depth at I^2 (ΔYV24-I2PALD)
Empirical slope 0.62

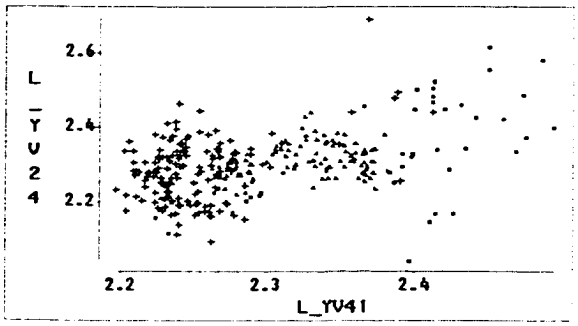

Palatal depth at P^3 (ΔYV25-P3PALD)
Empirical slope 0.69

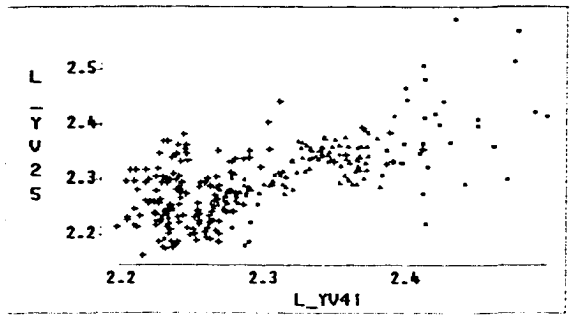

Palatal depth at M^1 (ΔYV26-M1PALD)
Empirical slope 0.88

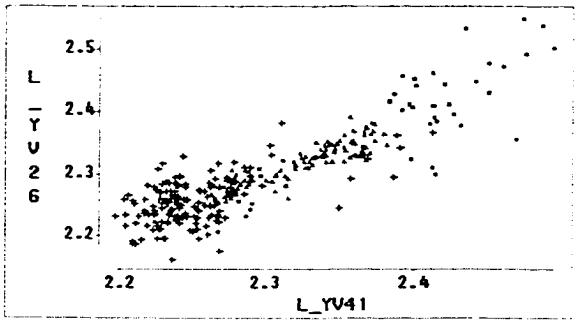

Palatal depth at M^3 (ΔYV27-M3PALD)
Empirical slope 0.94

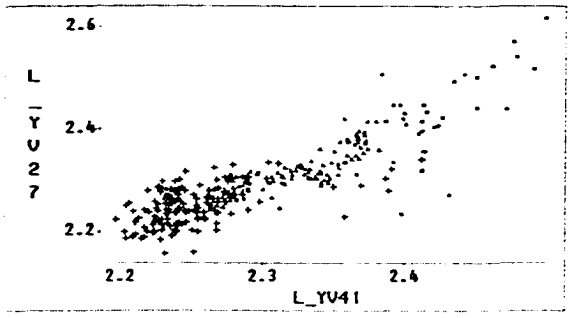

Reproduced with permission of the copyright owner. Further reproduction prohibited without permission.

Proportion of Variance Accounted for by Isometric Size Effect

The ground work has now been laid to quantify, as well as partition, the proportion of variance of the dependent nasomaxillary variables that can be accounted for by isometric size variation. Not unexpectedly, a glance at Box 10.11 clearly shows that isometric size variation explains a great deal of the variation of nasomaxillary morphology among anthropoid primates. In Box 10.11 dependent variables are listed in order of *R*-square. Aside from facial centroid size [Y34-FACSIZ], which by definition is nearly collinear with cranial centroid size, the order of the variables reveals a particular pattern.

If we read the *R*-squared values like a student grade sheet, the "A" variables, those with nearly all of their variance account for by size, measure mainly facial breadth, the "B" variables palatal length and width, and the "C" variables palatal height. The "failing" variables, those with less than 60% of their variance accounted for by size, consist largely of nasal and anterior palatal dimensions.

Reproduced with permission of the copyright owner. Further reproduction prohibited without permission.

Box 10.11. Error variance, total variance and *R*-square values for selected nasomaxillary dependent character variables isometrically regressed on skull centroid size, using ACP/Phylogenetically-adjusted log data. Variables are listed in ascending order of *R*-square. Shape variables are shaded.

Dep. Variable	Model Error Variance	Total Variance	R-squared
ΔL_YV34-FACSIZ	.000119	.004507	.97
ΔL_YV12-BZYGWD	.000180	.004568	.96
ΔL_YV15-BMAXWD	.000297	.004685	.94
ΔL_YV10-ZYGARE	.000387	.004774	.92
ΔL_YV16-UMAXWD	.000509	.004896	.90
ΔL_YV18-PFACHT	.000520	.004908	.89
ΔL_YV22-M1PALW	.000531	.004919	.89
ΔL_YV6-NASAWD	.000634	.005021	.87
ΔL_YV21-P3PALW	.000636	.005023	.87
ΔL_YV14-MXARCL	.000737	.005124	.86
ΔL_YV28-PALLGT	.000814	.005202	.85
ΔL_YV17-AFACHT	.000823	.005211	.84
ΔL_YV23-M2PALW	.000912	.005299	.83
ΔL_YV5-NSLAHT	.001090	.005478	.80
ΔL_YV26-M1PALD	.001091	.005479	.80
ΔL_YV8-PNASWD	.001158	.005545	.79
ΔL_YV20-I2PALW	.001169	.005557	.79
ΔL_YV19-RAMSHT	.001247	.005634	.78
ΔL_YV7-PNASHT	.001373	.005760	.76
ΔL_YV27-M3PALD	.001367	.005755	.76
ΔL_YV9-NLCLGT	.001726	.006114	.72
ΔL_YV3-NASWDL	.002135	.006522	.67
ΔL_YV11-ZYGOHT	.002164	.006552	.67
ΔL_YV25-P3PALD	.002861	.007249	.61
ΔL_YV1-NASLGT	.003368	.007756	.57
ΔL_YV4-NPMWDT	.006235	.010623	.41
ΔL_YV24-I2PALD	.006517	.10905	.40
ΔL_YV2-NASWDU	.008334	.012722	.35
ΔL_YV32-SLOPOC			.00
ΔL_YV30-KROGAG			.00
ΔL_YV35-PPNALO			.00
ΔL_YV13-APZYGR			.00
ΔL_YV33-FACCNV			.00
ΔL_YV31-ENLOAG			.00

Reproduced with permission of the copyright owner. Further reproduction prohibited without permission.

Conclusions

The most important thesis advanced in this chapter is the argument that when conducting explanatory research the allometric equation, as conventionally conceived and applied, will yield inaccurate results (i.e., incorrect allometric coefficient) concerning the effects of body size on organic form when other causal agents are operating on the character under investigation, especially when these other causal agents are correlated to some degree with overall size. In modern statistical terms this simply means that the traditional allometric equation contains specification errors, because it omits relevant independent variables from the model.

To adjust for the effects of scale differences among members of a sample, Mosimann log-log isometric residuals were calculated for each morphometric variable. Each residual vector represents the unexplained portion of the variance of a trait (Y) after all members of the sample have been scaled to unity.

Reproduced with permission of the copyright owner. Further reproduction prohibited without permission.

Chapter 11. Brain Form

Introduction

The squirrel monkey, genus *Saimiri*, holds a special fascination for craniofacial biologists due to its many parallel characteristics with humans. Members of this genus have flat orthognathic faces upon which their noses protrude from between close-set eyes. The vertebral column supports the head from well beneath the neurocranium. They have relatively weak masticatory musculature, small canines and simplified molars which process an eclectic but relatively soft food diet of fruits and animal prey. They are diurnal, extremely vocal and travel in large mixed groups. But their most striking resemblance to humans is in their brains. Next to people, squirrel monkeys have the largest brains relative to body size of any living primate. They have high, vertical foreheads, a manifestation of their large globular neocortex, and extensive flexion of the cranial base.

At the turn of the century it began to dawn on European morphologists that the striking resemblances between humans and squirrel monkeys were more than coincidental, that the suite of parallel characters may somehow be related through a common cause (e.g., Ameghino, 1909). In this chapter, I review the work of several researchers, mainly Weidenreich (1941) and Enlow (1975), who have shed light on this problem through their broader investigations of the effects of the brain on the growth and evolution of mammalian cranial form. Numerous hypotheses have appeared in the literature that purport to explain nasomaxillary variation in terms of differences in brain size, shape and allometry. Here I review several of the more germane hypotheses which are then operationalized and tested against the

Reproduced with permission of the copyright owner. Further reproduction prohibited without permission.

anthropoid data.

Literature Review

In Chapter 2, I presented evidence indicating that the growth and morphology of the brain has a tremendous influence on the morphology of both the neurocranium and the face. This was first systematically demonstrated by German morphologists at the turn of the 20th century. Studer (1901), for example, observed a relationship between body size, relative brain size and facial morphology in a sample of prehistoric dogs. The small "dwarf" dogs had relatively large globular brains and small, frail faces, whereas the larger dogs had relatively small brains and large, projecting snouts. Following Studer, other German comparative anatomists documented similar patterns in a variety of paleontological and modern mammalian samples (e.g., Lange, 1924; Hecker, 1926, 1927; Schultz, 1926; Møllison 1926; Wagner, 1929; Robb, 1935). But it was Weidenreich's treatise entitled "The Brain and Its Role in the Phylogenetic Transformation of the Human Skull," published in 1941, that put together under one cover all of the available evidence then known on the effects of brain growth and evolution on the morphology of the skull. Although his analyses were rather unsophisticated by modern standards of statistical inference, his method of comparing carefully selected pairs of specimens manifesting parallel character divergences conveyed a convincing argument for the primacy of the brain as a determinant of skull form.

Weidenreich (1941) observed that mammalian brain size is negatively allometrically related to body size: large mammals have relatively smaller brains

Reproduced with permission of the copyright owner. Further reproduction prohibited without permission.

compared to small mammals.[1] He further found that the relatively larger brains of smaller animals were associated with a suite of cranial characteristics that included: (1) an orthognathic face, (2) a foramen magnum that is wide and horizontally oriented, (3) a reduced or missing olfactory recess, (4) a short maxillary arch, (5) reduced maxillary height, (6) a high, globular forehead, (7) brachycrany, (8) an occlusal plane rotated up anteriorly in relation to the Frankfort horizontal, (9) teeth that are small and have "simplified" cusp morphology, (10) reduced or missing frontal sinuses, (11) reduced or missing supra-orbital tori, (12) reduced or missing cranial super-structures, (13) late closure of cranial sutures, (14) expanded anterior cranial fossae and anterior lobes of the brain, (15) a reduced masticatory apparatus, and (16) reduced post-orbital constriction. This list of features covers nearly every major morphological element of the skull. To Weidenreich, then, the relative size of the brain was the primary factor determining skull form—all other features, including tooth morphology, derive from relative brain size.

Weidenreich (1941) described this pattern in a wide range of mammalian taxa, including domesticated dogs and cats, wild carnivorans, horses, primates, and cetaceans. In every comparison between large and small forms (intraspecific or interspecific) he showed that increased relative brain size was associated with the aforementioned "gracile" suite of cranial characteristics. So ubiquitous was this association that he regarded it as the "...expression of a biological law of general validity" (*ibid.*, p. 378).

In the tradition of German morphology, the majority of Weidenreich's

[1] Weidenreich's analysis was descriptive rather than explanatory, and it was therefore appropriate for him to report on *allometric* relations to size (see relevant discussion in Chapter 10).

Reproduced with permission of the copyright owner. Further reproduction prohibited without permission.

work is descriptive, but hidden among the carefully dispensed observations, as though in a series of afterthoughts, are several ancillary attempts at explanation. One of the more perspicacious of these involved the neurological consequences of differences in body surface area-to-volume ratio; a second involved differences in the rate and timing of brain growth and the effects that these differences have on craniofacial variation; and a third was concerned with the relationship between brain size and shape in the development of craniofacial form.

Drawing from earlier work by Brandt (1898) and Anthony (1928), Weidenreich (1941) suggested that the amount of neuronal tissue in the brain corresponds, at least in part, to the number of nerve fibers required by the connective tissue, such as the dermal layer of the skin. He thus reasoned that "...since the body of small animals has a relatively larger surface than that of the large ones, the supply of nerve fibers must be more abundant" (Weidenreich, 1941:405).

Weidenreich also provided a mechanism by which smaller animals developed relatively larger brains. By the late 1930s developmental craniologists had unequivocally demonstrated that in the early ontogeny of mammals the brain grows at a much faster rate than the facial skeleton (positive allometry). In most mammals in general, and large ones in particular, at some stage of development there is a shift of growth patterns such that brain growth becomes diminished relative to facial growth (negative allometry).[2] Weidenreich proposed that in humans and "dwarf types" this relative growth shift is either slowed or absent

[2] This pattern of relative neurocranial and facial growth has subsequently been confirmed for various species of anthropoids (e.g., Krogman, 1931; Schultz, 1962; Enlow, 1966; Passingham, 1975; Sirianni & Newell-Morris, 1980; Nanda, *et al.*, 1987; Pucciarelli, *et al.*, 1990).

Reproduced with permission of the copyright owner. Further reproduction prohibited without permission.

altogether[3] (see Box 11.1). To account for the interdependent growth of the brain and face Weidenreich invoked a principle first enunciated by Goethe, the eighteenth century German transcendental morphologist, whose "law of compensation" stated that "...to no part can anything be added, without something being taken away from another part, and *vice versa*" (cited in Russell, 1916:49).[4] Applying Goethe's principle to the growth of the mammalian skull, Weidenreich (1941) argued that in smaller mammals "...the enlargement of the brain and the cranium...[occurs]...at the expense of the remaining skull" (p. 350). "The greater the space required by the brain, the more other parts of the skull must suffer and necessarily yield to that need" (p. 367).

Box 11.1. Weidenreich's (1941) conception of relative brain and facial growth in large and small mammals.

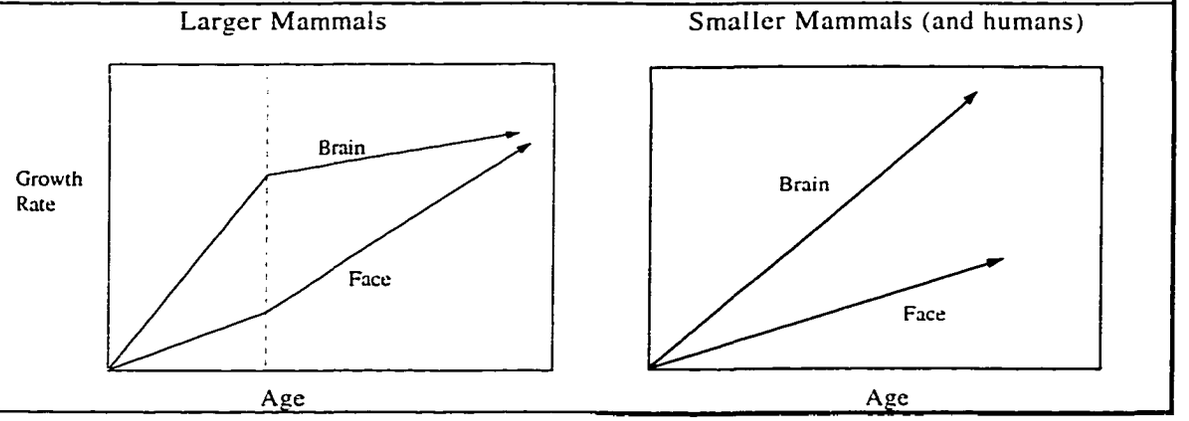

A more concise statement regarding anthropoid cranial development was provided by Weidenreich several chapters later, but nowhere in his treatise did he

---

[3] To explain why humans align with small mammals in this regard Weidenreich appealed to Bolk's (1926) *fetalisationstheorie*.

[4] Weidenreich did not cite Goethe or credit him for the idea, but it is difficult to conceive that he would not have been aware of Goethe's prior contribution.

Reproduced with permission of the copyright owner. Further reproduction prohibited without permission.

offer an explanation as to *why* larger animals needed relatively larger facial structures.[5] He stated,

> It is a well known fact that in ontogenetic development the nervous system is first to be differentiated and that its rate of growth exceeds that of all other organs. As long as this rate remains unchanged, the brain determines the proportions of the two main constituents of the skull, brain case and face, the former predominating, the latter restricted. Subsequently during development the moment will arrive when the growth of the central nervous system becomes diminished or ceases entirely. Then the hitherto restricted organs become "propulsive" and the proportions reverse. This is what occurs in great apes at a certain period of their postnatal life, approximately at the time when the deciduous dentition is fully erupted. In man, however, the growth rate [of the brain] which in general is already considerably higher than in anthropoids, remains unchanged, or its reduction covers a longer period and thereby exerts an arresting influence on the face as long as the growth is active [Weidenreich, 1941:412]

Weidenreich's second hypothesis focused on the relationship between the size and shape of the brain—larger brains relative to body size tend to be more globular and brachycephalic—and correlated characteristics of the face. But here as elsewhere in Weidenreich's work causal statements are vague and circuitous. The question of how brain shape might affect facial form would not receive formal treatment for several decades, with the publication of a seminal paper by Enlow and McNamara (1973). Weidenreich instead resorted to an analogy in which he compared the influence of the shape of the brain on craniofacial morphology to the growth of the liver, whose form is determined by a "...topographical relation to adjacent organs" (*ibid.*, p. 421).

---

[5] The Jarman-Bell principle, that large and small mammals have very different nutritional requirements was advanced more than two decades later (Bell, 1971; Jarman 1974), and so could not have been used by Weidenreich to explain his observation of the relationship between body size and masticatory size.

Reproduced with permission of the copyright owner. Further reproduction prohibited without permission.

The vagueness of Weidenreich's explanations is understandable and should not detract from the importance of his work, for although the edifice of the Modern Synthesis had by 1940 been erected, developmental biology, so crucial to an understanding of brain-skull interrelations, had been excluded from the amalgam. And yet, it is precisely the lack of a definitive causal treatment in Weidenreich's work that rendered it out of vogue with many of his contemporaries. It is a curious fact that, despite the strength of the evidence he presented and the elegance with which he painstakingly uncovered the numerous morphological patterns, Weidnedriech's work, which took a full year to complete, seems largely to have been ignored. Only two years after its publication, Washburn and Detwiler (1943) declared that the determinants of cranial form remained a complete mystery: "Is the shape of the cranium due to the brain, to the muscles of mastication, or to both of these and still other factors?" (p. 171). Weidenreich's analysis, while given its customary citation in most reviews of the subject through the 1940s and 50s, was never regarded as a major advance in our understanding of craniofacial diversity. By the 1960s, Weidenreich's work was routinely neglected. Little or no discussion of his findings on brain form and cranial morphology can be found in any of the leading anthropological or morphological texts through to the present day (e.g., von Koenigswald, 1966; Aiello & Dean, 1990; Hanken & Hall, 1993).

Perhaps this state of affairs is not surprising given the intellectual currents that were operating at the time of its publication. At that time two very different paradigms concerning cranial morphogenesis were competing for preeminence, and Weidenreich's results provided neither ammunition nor armor for either. Spemann's (1938) grafting experiments had demonstrated, just a few years earlier,

Reproduced with permission of the copyright owner. Further reproduction prohibited without permission.

that components of the embryonic viscerocranium were self-differentiating. By contrast, experiments by Pratt and others (e.g., Pratt, 1943; Washburn, 1947) were showing the plasticity of the craniofacial skeleton in relation to muscle force. Weidenreich's "biological law" did not fit neatly into either of these two general view of cranial morphogenesis.

Ironically, another body of work initiated in the mid-1940s that could have revived Weidenreich's ideas had the opposite effect. In a series of papers published between 1946 and 1952, van der Klaauw laid down a set of theoretical premises that bridged the gap between Weidenreich's observations and prevailing theory by incorporating both mechanical and non-mechanical influences on skull growth into a single morphogenetic model (e.g., van der Klaauw, 1948, 1952, *passim*). This work later inspired the development of the "functional matrix" theory of Moss (1962, 1968), as well as the work on skull growth, remodeling and architecture by Enlow. Van der Klaauw's ideas might have been adopted to show that brain growth and shape-change could influence skull form via both epigenetic and mechanical mechanisms, thereby providing the basis for integrating Weidenreich's work into the synthesis of modern morphogenetic theory. But van der Klaauw's (1946) insistence that the neurocranium and splanchnocranium were functionally independent systems effectively negated this possibility. Following van der Klaauw's lead, a series of influential articles appeared in the literature which endorsed the concept of functional independence of the brain and face (e.g., Kummer, 1952; Hofer, 1952; Starck, 1954; Biegert, 1957, 1963), further abrogating the influence of Weidenreich's study.

Not encumbered by the dominant German school of thought, Enlow shared

Reproduced with permission of the copyright owner. Further reproduction prohibited without permission.

Weidenreich's holistic view of the skull as an integrated unit. His work, with various colleagues, was published in a series of papers in the late 1960s and early 70s, culminating in a text in 1975. A trained bone histologist, Enlow was concerned with the underlying remodeling processes involved in skull growth and development. His work revealed for the first time the proximate mechanisms behind Cuvier's "principle of correlations." For every part there is one or more counterparts, whose growth, remodeling and form must coincide in order for the organism to maintain a viable, functioning system. Enlow was thus interested in the design of the mammalian skull in terms of the integrated remodeling patterns of bones, and the development of the soft tissues that enveloped them. He encountered, like Weidenreich before him, the numerous correspondences between the form of the brain and that of the facial skeleton.

> The ontogenetic and phylogenetic development of the cerebrum, importantly, involves a range of topographic variations which appear to be associated with corresponding, characteristic differences in facial structure and topography, both among mammals in general and among specific human ethnic groups [Enlow & McNamara, 1973:256].

Enlow not only confirmed many of Weidenreich's original observations, but went further by attempting to explain them in terms of growth processes and developmental constraints. He argued, for example, that the degree of horizontal and vertical rotation of the orbital axis in anthropoids was a morphologic response to differential rates of growth of the frontal and temporal lobes of the cerebrum.

> Among the anthropoids an obliquely upward but straight forward (medially rotated) placement of the eye sockets is associated with their smaller frontal and prefrontal lobes but sizable temporal lobes, respectively [Enlow & McNamara, 1973:258].

Reproduced with permission of the copyright owner. Further reproduction prohibited without permission.

Whereas van der Klaauw (1946) regarded the olfactory bulbs as belonging to the facial skeleton,[6] Enlow (Enlow & McNamara, 1973; Enlow, 1975) recognized that the olfactory apparatus, as a direct extension of the brain, had a intimate relationship with both the brain and the facial skeleton. The olfactory-ethmoid complex was regarded by Enlow as one of the key elements to an understanding of the correspondence between neurocranial and facial form. In a comparative sample of mammals, Enlow and McNamara (1973) observed that specimens with relatively large brains, particularly those with expanded frontal lobes, had a marked horizontal orientation of the olfactory bulbs and underlying cribriform plate, and a correspondingly vertical (or orthognathic) facial profile.

> A relationship exists between the size of the cerebrum, the alignment of the olfactory bulbs, and the corresponding over-all alignment of the facial plane. As a general rule, the facial profile is approximately perpendicular to the cribriform plates [Enlow & McNamara, 1973:260]

It is of interest to note that T. H. Huxley (1896), some seventy-seven years earlier, had observed much the same phenomenon in another series of mammalian skulls.

> ...if a series of sections of mammalian skulls, intermediate between a Rodent and a Man (Fig. 29), be examined, it will be found that... the "olfactory angle"... become[s] more obtuse [i.e., horizontal]; and that the "cranio-facial angle," becomes more acute [i.e., vertical] by the bending down, as it were, of the facial axis upon the cranial axis. At the same time, the roof of the cranium becomes more and more arched, to allow of the increasing height of the cerebral hemispheres... [T.H. Huxley, 1896:194] [7]

---

[6] van der Klaauw (1946) stated: "...the upper-jaw as well as the olfactory organ develop, in accordance with their function, in the rostral part of the skull, and thus go together" (p. 34).

[7] Bolk (1909) was also headed in this direction when he stated: "...the facial skull, first situated before the cerebral skull, is displaced underneath it, after which it is shortened" (p. 370).

Reproduced with permission of the copyright owner. Further reproduction prohibited without permission.

Huxley's reference to the arched, high cerebral hemispheres associated with facial orthognathism, is a clear harbinger of Weidenreich's later, more systematic, observations on brain size and shape.

Whereas Huxley's and Weidenreich's accounts were purely descriptive, Enlow proposed a causal mechanism to explain these morphological patterns. According to Enlow and McNamara (1973), as the frontal lobes expand, the cribriform plate is pushed into a more horizontal position. Because of the intimate connection between the olfactory apparatus, the cribriform plate, the ethmoid, and the entire nasomaxillary complex, the orientation of the olfactory bulbs establishes the growth trajectory of the face. The degree of facial prognathism, according to this hypothesis, is structurally determined by the relative expansion of the frontal lobes of the brain: "The downward rotation of the olfactory bulbs and the whole anterior cranial floor by the enlarged frontal lobes of the cerebrum has caused a corresponding downward rotation of the nasomaxillary complex" (Enlow, 1990:167).

Earlier experimental results obtained by Moss (1958) appear to contradict Enlow's hypothesis of the effects of olfactory bulb/cribriform plate rotation on craniofacial morphology. Moss performed a series of extirpation experiments on rats in which he removed the olfactory lobes at various stages of development, then compared craniofacial growth and morphology of the operated rats with controls. He concluded:

> The rotation of the cribriform does not depend functionally on the concurrent rotation of the olfactory lobes. Indeed, it would appear that the cribriform rotation is accelerated in the absence of these lobes. Accordingly, we may conclude that, in the rat, the rotation

Reproduced with permission of the copyright owner. Further reproduction prohibited without permission.

> of the cribriform plate is intrinsic. It is related to other processes of facial skeletal growth and functionally uncorrelated with the processes of neural growth. [Moss, 1958:82]

But consistent with Enlow's hypothesis, Moss has observed "...a close interrelation between the cribriform and palatal rotations", an observation anticipating Enlow's later reports of the correlated orientations of the cribriform plate and nasomaxillary complex. To Moss, there was no question that the cribriform plate, and the whole of the ethmoid bone, participated in the rotation of the lower face. In contrast to Enlow, however, he viewed this rotation as independent of the growth and configuration of the brain and olfactory apparatus. If anything, the olfactory lobes impeded facial rotation (Moss, 1958:84).

In a second structural relationship observed by Enlow (e.g., Enlow and Azuma, 1975), prosthion was found to lie invariably at the intersection of two planes: the midfacial plane, and another formed by a line passing through the most inferior point of the brain and maxillary tuberosity (IBMP, inferior brain-to-maxilla plane). Thus, the length and to some extent the projection of the face is constrained by the posteroinferior expansion of the cerebellum, since the inferior growth of the maxilla does not normally extend beyond (or stop short of) the level of the inferior-most extension of the brain. According to Enlow, then, the position of prosthion relative to the neurocranium can be predicted from neurocranial morphology alone.[8]

Enlow (1975, 1990) proposed that these relatively invariant geometrical relationships set minimum and maximum growth boundaries for various elements

---

[8] Among mammals, nonhuman anthropoids seem to be an exception to this rule: they are characterized by vertical hypoplasia of prosthion relative to IBMP (Enlow & Azuma, 1975). Bromage (1992) has demonstrated an increase in anterior maxillary hypoplasia (AMH) across dental age groups of *Pan troglodytes*, and has also reported sexual dimorphism for this trait.

Reproduced with permission of the copyright owner. Further reproduction prohibited without permission.

of the craniofacial skeleton, thereby greatly influencing overall skull form. In a recent morphometric study of cercopithecids, however, Ravosa and Shea (1994) contend that most of the brain-face relationships reported by Enlow (Enlow & McNamara, 1973; Enlow & Azuma, 1975) exhibit too much variation to be considered "constraints" on craniofacial growth.

Another proposed influence of the brain on craniofacial form is said to operate via the cranial base. That the growth and morphology of the facial skeleton is affected by changes in the cranial base is a long-standing and widely accepted tenet of craniofacial biology (DuBrul & Laskin, 1961; Enlow, 1975, Moore, 1981a; Herring, 1993). The relative growth of the anterior portion of the cranial base, for example, has been associated with degree of facial rotation and facial prognathism in several studies (e.g., Swindler *et al.*, 1973; Cheverud & Richtsmeier, 1986).

The related question of whether or not the brain can effect changes in the cranial base, for years a debated issue (*cf.*, Spatz, 1970), appears recently to have been resolved. In Chapter 2, in the section entitled "Skeletogenesis of the Chondrocranium," I summarized the current evidence on this issue, which supports the contention that basicranial morphology can be influenced by the growth of the brain (also see reviews by Moss, 1976; Herring, 1993; and this study, Chapter 13).

In conjunction with his hypotheses regarding the effects of brain growth on facial morphology via the frontal-olfactory-ethmoid complex, Enlow (e.g., Enlow & Hunter, 1968; Enlow & McNamara, 1973; Enlow, 1975) proposed a similar brain-face relationship operating via the cranial base. Enlow & McNamara (1973:257) suggested that "...cranial base flexure is a secondary skeletal adaptation to the

Reproduced with permission of the copyright owner. Further reproduction prohibited without permission.

shape of the brain..." caused by "...expansion of the anterior, middle, and posterior portions of the cerebrum around a much slower-growing hypothalamus, pons, and brain stem..."[9] The degree of cranial base flexion, in turn, establishes the basis for "...a chain of other factors that have characteristic topographic results in the configuration of the face" (*ibid.*, p. 267). A more detailed analysis of the role of the cranial base in the development and evolution of cranial form is presented in Chapter 13. The contributions of Weidenreich and Enlow form the basis for an integrated theory of the nomological effects of the brain on craniofacial form. This theory is summarized and dissected into its component parts in the next section

Hypotheses Formulation

The hypotheses discussed in the preceding section can be summarized as follows. Differences in body size relate to differences in brain size such that smaller mammals have relatively larger brains. The relatively larger brains of smaller mammals take on a more globular shape (1) in order to maximize the limited space to which they must conform, and (2) due to the differential growth of the midbrain and surrounding neocortex. Pressure from the expansion of the neocortex around the slower growing midbrain pushes the anterior and posterior portions of the cranial base together resulting in an increase in cranial base flexion and a more horizontally oriented anterior cranial floor. Expansion of the frontal lobes, in particular, produces a downward movement of the entire anterior cranial floor, and in particular a more horizontal orientation of the olfactory bulbs and underlying cribriform plates. Due to the intimate connection between the olfactory apparatus,

[9] Pucciarelli *et al.* (1990) cite evidence supporting the view that different parts of the brain grow at different rates.

Reproduced with permission of the copyright owner. Further reproduction prohibited without permission.

the ethmoid, and the nasomaxillary complex, the downward horizontal movement of the anterior cranial floor translates into a more vertically oriented (and thus short and orthognathic) facial skeleton.

The above narrative is actually composed of several distinct hypotheses, which can each be tested independently (see Box 11.2). These statements can be combined in various ways to formulate more comprehensive multi-premise compound nomological hypotheses. For example, Hypotheses C and D can be combined to form a more complete narrative.

Box 11.2. Hypothesis statements regarding the effects of brain growth and form on craniofacial variation.

Description of Hypothesis:	Source:
(A) As body size increases brain size becomes relatively smaller (negative allometry).	Weidenreich, 1941
(B) As relative brain size increases the shape of the brain becomes more brachycephalic.	Weidenreich, 1941
(C) As the frontal lobes expand with increasing relative brain size the olfactory bulbs (and cribriform plate) are pushed into a more horizontal position.	Enlow & McNamara, 1973
(D) The cribriform plate and midfacial plane maintain an invariant perpendicular angular relationship across taxa. Therefore, as the cribriform plate becomes more horizontal the facial plane translates into a more vertical (orthognathic) profile.	Enlow & McNamara, 1973
(E) As the frontal lobes of the brain expand the orbits are forced into a more horizontal orientation.	Cartmill, 1972; Enlow & McNamara, 1973
(F) As the temporal lobes expand anteriorly the orbits are forced medially, reducing interorbital (intranasal) distance.	Enlow, 1975
(G) As relative brain size increases a compressive force exerted on the cranial base leads to an increase in cranial base flexion.	Biegert, 1957

Reproduced with permission of the copyright owner. Further reproduction prohibited without permission.

Operationalization of Variables

In order to assess the hypotheses summarized in Box 11.2, it was necessary to deduce testable predictions regarding statistically significant covariances among sets of operationalized variables (see Chapter 8). In this section, relevant variables were defined and the predicted bivariate relationships specified (see Box 11.7).

Body size

In accordance with the concepts developed in Chapter 10, centroid size [Y41-SKCNTR] was used as the measure of overall body size in the current analysis.

Brain size and relative brain size

Endocranial volume [Y83-BRNSIZ] was used as a measure of absolute brain size. Volumetric measurements were obtained for each of the 300 specimens in the adult anthropoid sample using the method described by Montagu (1960:52). First, plastilina was applied to cover the basicranial foramina, and where needed, cotton was inserted into the nasal and orbital cavities. Mustard seed (measured in ml) was then poured into the endocranial cavity through the foramen magnum, which had been left uncovered. A test-tube vibrator was used to agitate the skull to ensure consistent settling of the seed. Once filled to the brim of the foramen magnum, the mustard seed was emptied into a graduated cylinder, agitated as before, and measured for volume in ml. This process was repeated for each specimen and the average of the two volumetric measurements was recorded.

The reliability of the endocranial volumetric data obtained in this manner was assessed by comparing the results with those of previous studies. Box 11.3

Reproduced with permission of the copyright owner. Further reproduction prohibited without permission.

lists the species mean endocranial volumes collected here with comparable data published by Stephan *et al.* (1981) and Rowe (1996). The scatter plot for the logged data is presented in Box 11.4. The species mean endocranial volumes obtained in this study are not statistically different from previously published measures of anthropoid brain size. This finding lends support to the view that individual endocranial volumetric measurements may represent a relatively accurate measure of brain size.

Relative brain size[10] was calculated in the manner described for other character dimensions, as the Mosimann log-log isometric residual, or in this case as the residual of the log cube root endocranial volume regressed isometrically against log centroid size (see Chapter 10).

[10] Unless otherwise stated, the term "relative" in the context of variable description refers to the measure of the variable standardized by centroid size as described in Chapter 10.

Reproduced with permission of the copyright owner. Further reproduction prohibited without permission.

Box 11.3. Data comparing endocranial volume measures from this study with previously published female adult brain weight data.

Anthropoid species:	Endocranial volume, this study (ml)	Previously published mean adult brain weight (g)	Anthropoid species:	Endocranial volume, this study (ml)	Previously published mean adult brain weight (g)
A. palliata	52	54	*M. nemestrina*	97	106
A. geoffroyi	100	110	*M. fascicularis*	60	69
L. lagothricha	94	99	*M. mulatta*	77	94
B. arachnoides	112	120	*P. hamadryas*	167	188
C. satanas	55	53	*L. albigena*	94	104
P. pithecia	32	32	*C. polykomos*	75	77
P. monachus	40	37	*P. pennantii*	75	78
C. cupreus	16	19	*N. larvatus*	87	96
C. apella	66	71	*P. melalophos*	75	80
C. capucinus	69	79	*S. entellus*	85	135
S. sciureus	26	24	*S. cristata*	63	64
A. trivirgatus	16	18	*H. lar*	110	105
S. oedipus	10	10	*H. syndactylus*	131	122
C. pygmaea	4	5	*P. pygmaeus*	383	413
C. goeldii	11	11	*G. gorilla*	422	503
C. aethiops	59	60	*H. sapiens*	1260	1290
C. neglectus	64	71	*P. paniscus*	291	307
C. mitis	65	75	*P. troglodytes*	379	408
C. ascanius	63	67			

Box 11.4. Log-log regression of anthropoid endocranial volume against published brain weight.

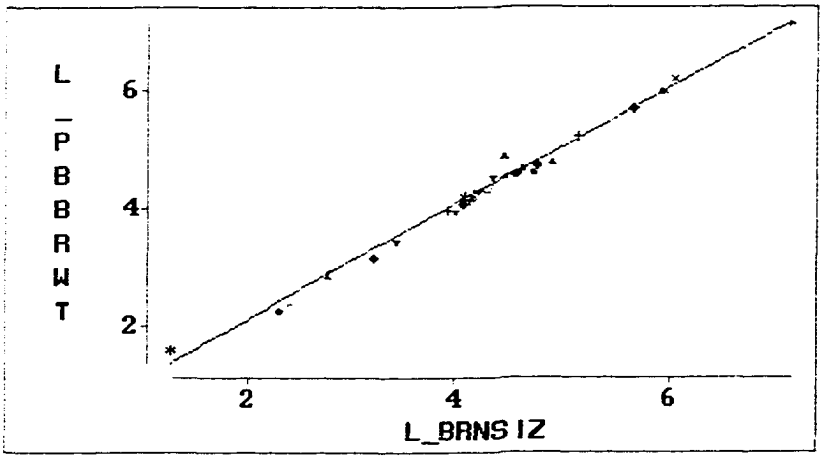

Log-log data regression: Slope=0.99; R^2=0.99. S.E. L_BRNSIZ=0.016.

Reproduced with permission of the copyright owner. Further reproduction prohibited without permission.

Relative frontal and temporal lobe sizes

For the craniologist interested in the evolution of the brain it is an unfortunate circumstance that "[i]nformation on changes in different parts of the brain can only be derived indirectly from comparisons of the brains of living species" (Passingham, 1975). Not even endocasts, when available, permit measurement of the various lobes of the neocortex. To make matters worse, good comparative samples of fresh (preserved) primate brains and skulls are difficult to obtain, and as a consequence the subdivisions of the neocortex in living anthropoids have not been adequately quantified. No reliable data exist that could be used to study the morphological consequences of differential neocortical growth and evolution. In attempting to operationalize "frontal lobe size" from dry skulls we are admittedly shooting in the dark. And yet, there are enough cues to make us hopeful that we are at least shooting in the right direction.

The closest osteological vestiges of the neocortical segments are the cranial fossae. According to Enlow and Azuma (1975) and Moore (1981a), the anterior, middle, and posterior cranial fossae provide a good measure of the anteroposterior dimension of the frontal, temporal and posterior lobes, respectively. Studies of brain malformations further indicate that size abnormalities of the various lobes of the brain are reflected in correspondingly malformed cranial fossae (Siebert *et al.*, 1987). Relative frontal lobe size was thus estimated as the ratio of the anteroposterior length of the anterior cranial fossae to total endocranial length [Y79-ACFLGT]; and relative temporal lobe size was defined as the ratio of the length of the middle cranial fossae to total endocranial length [Y78-MCFLGT] (see Box 5.3C).

Reproduced with permission of the copyright owner. Further reproduction prohibited without permission.

Cribriform plate and olfactory bulb orientation

In describing the orientation of the olfactory bulbs Enlow and McNamara (1973:262) drew a line through the "...anterior and posterior ends of the concave cribriform plates..." as a convenient way of establishing the tangent to the curvature of the bulbs. This operationalization presents a problem when applied to cephalographic analysis. Due to its light construction, the ends of the cribriform plates, and quite often the cribriform plates themselves, are obscured in lateral radiographs (see Box 11.5A). Enlow solved this problem by examining specimens whose calvaria were resected, exposing the anterior cranial floor. He then used metallic markers to label the anterior and posterior ends of the cribriform plate, which were then easily identifiable in lateral radiographs. Encountering the same problem, Cramer (1977) painted the cribriform plate with liquid barium, a radio-opaque substance, in order to make this thin structure visible on radiographs.

The problem of misidentification of the end-points of the cribriform plates in lateral radiographs is compounded in specimens in which the front and back edges of the plates are very close together (as they are in cercopithecids). In such cases even small errors in locating the plate ends can lead to large errors in describing the angular orientation of the plates. For this study, a novel method was devised to aid in the identification of the cribriform plates in lateral radiographs. Prior to radiography, a measured amount of fine brass filings was poured into the endocranial cavity through the foramen magnum and shaken down into the olfactory recess. Once the specimen had been radiographed the filings were removed from the endocranial cavity and a second radiograph was taken. By comparing the two radiographs the location of the olfactory recess and cribriform

Reproduced with permission of the copyright owner. Further reproduction prohibited without permission.

plates could be identified unambiguously (see Box 11.5B). The relevant olfactory landmarks were then digitized from the radiographs (see Box 5.3D) and the inclination of the cribriform plate relative to various planes (e.g., the Frankfort horizontal [Y74-SLPCPF] and the midfacial plane [Y71-ENLWCP])was calculated with relatively high precision (see Chapter 4). The advantage of this method is that it can be used with specimens whose calvaria are intact.

Radiographs produced in this manner also clearly reveal the olfactory recess in relation to the anterior cranial fossa, and by extension, the juxtaposition of the frontal and olfactory lobes. A line connecting the anterior-most and posterior-most junctions of the olfactory recess and anterior cranial fossae thus provides a second measure of olfactory bulb orientation [Y72-ENLWOB].

Box 11.5. Lateral radiographs of *Papio hamadryas* (AMNH #52668) without (A) and with (B) brass filings in the olfactory recess.

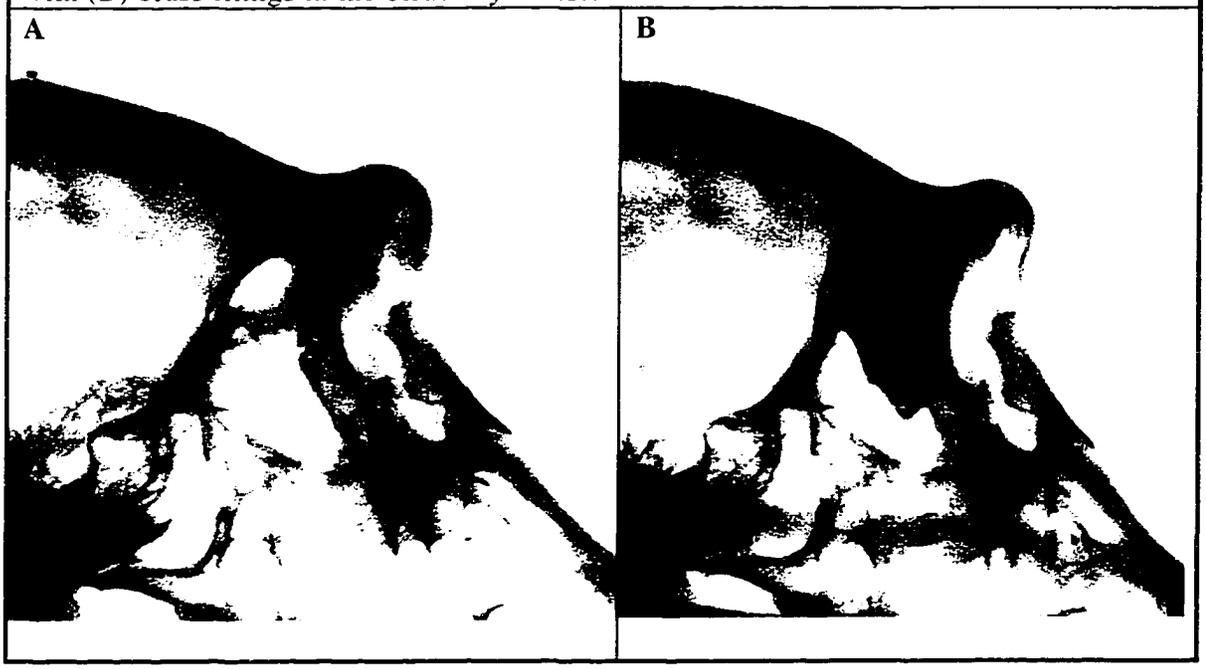

Reproduced with permission of the copyright owner. Further reproduction prohibited without permission.

Midfacial-cribriform angle

Enlow and McNamara (1973:261) defined the "midfacial plane" as a line "...drawn from the anterosuperiormost point on the endocranial surface of the frontal bone (or of the olfactory fossa in those species in which the olfactory bulbs protrude well beyond the cerebrum) down to the anteroinferiormost point of the premaxilla (superior prosthion)." The "anterosuperiormost point on the endocranial surface," which I refer to simply as *anterior-most brain*,[11] is operationally defined as the point of first contact between a line swung posteriorly from a pivot on prosthion and the endocranial cavity. The midfacial-cribriform angle [Y71-ENLWCP], as the name implies, is the angle formed by the midfacial plane and cribriform plates in lateral view (see Box 5.3D).

Horizontal and vertical orbital orientation, and interorbital distance

Attempts to estimate dimensional and positional properties of the eyes from the orbital morphology of dry skulls have met with limited success. As I have already mentioned in Chapter 2, Schultz (1940) demonstrated that orbital cavity size does not correspond to eyeball size in adult primates; and Cartmill (1972) argued that "...neither visual nor optic orientation can be directly inferred from the orientation of the orbits" (p. 109). Analysis and inferential results are therefore restricted to *orbital* variation and covariation with other variables.

Some confusion has arisen with respect to the terminology used to describe orbital morphology and orientation. DuBrul (1965) distinguished between the properties of *convergence* and *rotation* of the optic cavities. He argued that early in primate evolution the orbits converged (came closer together) and rotated medially

Reproduced with permission of the copyright owner. Further reproduction prohibited without permission.

to produce binocular vision. The independence of orbital convergence and rotation, according to DuBrul, is manifest in larger primates in which "...increase in size has apparently resulted in a secondary separation of the orbits while still maintaining the critical parallel relation between the visual axes..." (p. 273).

Cartmill (1972) defined three variables related to the position and orientation of the orbits of mammals. In his scheme, *convergence* is the degree to which the orbital planes are parallel, as measured by the "...dihedral angle between the mid-sagittal plane and the plane of the [mediolateral] orbital margin" (p. 109). *Interorbital breadth* is the distance between the orbits "as expressed in orbital diameters" (*ibid.*, p. 109). And *frontation* is a measure of the degree to which the orbits face forward rather than upward, as indicated by the "...angle between the nasion-inion line and the line along which orbital and mid-sagittal planes intersect" (*ibid.*, p. 109). Notice that Cartmill's use of the term convergence is equivalent to DuBrul's concept of rotation, whereas Dubrul's use of the term convergence is essentially what Cartmill meant by interorbital distance. To avoid (or perhaps contribute to the) confusion I have adopted a new set of terms—parallelism, intranasal breadth, and deflection—which are defined in Box 11.6.

---

[11] Bolk (1909:366) called this point "fronton," but I prefer the more descriptive term.

Reproduced with permission of the copyright owner. Further reproduction prohibited without permission.

Box 11.6. Definition of terms and variables used to measure orbital orientation.			
New terminology	Cartmill's (1972) terminology	DuBrul's (1965) terminology	Definition
Orbital parallelism (or sagittal-coronal orientation)	Convergence	Rotation (or frontation)	The degree to which the orbital axes are oriented parallel to each other. Angle between left and right orbital axes.
Intranasal breadth (or interorbital distance)	Interorbital distance	Convergence (or migration)	The distance between the orbits, measured as the inter-dacryon distance.
Orbital deflection (or transverse-coronal orientation)	Frontation		The degree to which the orbital axes are "deflected" from a horizontal orientation. Angle between orbital axes and Frankfort horizontal.

Cranial base flexion

Flexion, or bending, of the cranial base has long been of interest to craniofacial morphologists; a preoccupation likely due to its uniquely acute angle in humans as compared to other mammals. Cranial base flexion is typically defined as the angle formed by the clivus (which traverses the sphenooccipital synchondrosis) and the planum sphenoideum (which traverses the sphenoethmoidal synchondrosis) (e.g., Spatz, 1970; Duterloo & Enlow, 1970; Ravosa & Shea, 1994).[12] Numerous studies have demonstrated that growth-related alterations in cranial base angulation involve a complex choreography of differential growth at the sphenooccipital, sphenoethmoidal, and midsphenoidal synchondroses, as well as remodeling of the hypophyseal fossa and adjacent sphenoidal elements (Scott, 1958; Michejda, 1971; Sirianni & Van Ness, 1978; Moore, 1978; Dean & Wood, 1984; Enlow, 1990). For the present study, cranial base flexion [Y70-CBFLEX] was measured as the angle formed at sella by a line connecting basion with sella and a second line joining sella

Reproduced with permission of the copyright owner. Further reproduction prohibited without permission.

with the anterior-most point of the cribriform plate (see Box 5.3C). Keep in mind that as this angle—"cranial base angle"— becomes smaller, cranial base *flexion* increases.

Endocranial index

To quantify the shape of the brain, a width-by-length ratio was used which closely approximates the cranial index. Bass (1971:63) defined the cranial index as "...a numerical device for expressing the ratio of the breadth of the skull to the length (in percent)." Specifically, cranial index is the ratio of bi-euryon distance (maximum neurocranial breadth, see Box 5.3B) to the distance between glabella and opisthocranion (maximum neurocranial length, see Box 5.3C) expressed as a percent. However, because of the variable development of the frontal sinuses and supraorbital tori, anteriorly, and the nuchal ridges, posteriorly, glabella and opisthocranion can be situated either near to or some distance away from the endocranial cavity. The cranial index is not, and was never intended to be, a valid measure of brain shape. The *endocranial index* [Y81-ENDOID] replaces glabella and opisthocranion with corresponding endocranial landmarks—anterior-most brain and posterior-most brain, respectively (see Box 5.3D). Since parietal bone thickness is relatively invariant, bi-euryon length remains a reasonable proxy for maximum endocranial breadth.

---

[12] Several other definitions of cranial base flexion have appeared in the literature: Janis (1990) has proposed "the angle between the basioccipital bone and the palate," and Solow & Tallgren (1976) and Sirianni & Van Ness (1978) advocate the angle formed by basion-sella-nasion.

Reproduced with permission of the copyright owner. Further reproduction prohibited without permission.

Statistical Predictions

Predicted statistical associations between pairs of traits, deduced from previously formulated hypotheses are listed in Box 11.7.

Box 11.7. Predicted bivariate associations deduced from hypotheses statements.

Expected statistical associations and predictions.	Hypo-thesis
Endocranial volume [ΔL_Y81] ← Centroid size [ΔL_Y41] (Prediction: Larger anthropoids will have *relatively* smaller brains compared to smaller anthropoids)	(A)
Endocranial index [ΔL_Y81] ← Relative endocranial volume [ΔS_L_Y84] (Prediction: Anthropoids with *relatively* larger brains will have more globular brains)	(B)
Cribriform plate orientation [ΔL_Y74] ← Anterior cranial fossa length [ΔS_L_Y78] (Prediction: Anthropoids with relatively large frontal lobes will have more horizontally oriented cribriform plates)	(C)
Cribriform plate orientation [ΔL_Y74] ← Relative endocranial volume [ΔS_L_Y84] (Prediction: Anthropoids with relatively large brains will manifest horizontally oriented cribriform plates)	(C)
Cribriform plate ∠ Midfacial plane [Y71] (Prediction: Invariant 90° angle maintained between the two planes)	(D)
Prognathism [ΔL_Y30, ΔL_Y31] ← Cribriform plate orientation [ΔL_Y74] (Prediction: Anthropoids with horizontally oriented cribriform plate will exhibit relative orthognathism)	(D)
Orbital deflection [ΔL_Y46] ← Anterior cranial fossa length [ΔL_Y79] (Prediction: Anthropoids with relatively large frontal lobes will exhibit less orbital deflection, i.e. more horizontal orbital axes)	(E)
Intranasal breadth [ΔS_L_Y49] ← Middle cranial fossa length [ΔL_Y78] (Prediction: Anthropoids with relatively large temporal lobes will show a reduced interorbital distance)	(F)
Cranial base flexion [ΔL_Y70] ← Relative endocranial volume [ΔS_L_Y84] (Prediction: Anthropoids with relatively large brains will manifest a greater degree of cranial base flexion	(G)
Posterior facial orientation [ΔL_Y95] ← Anterior cranial fossa length [ΔL_Y79] (Prediction: Anthropoids with extended anterior cranial bases will exhibit greater facial rotation)	Ad hoc
Prognathism [ΔL_Y30, ΔL_Y31] ← Endocranial index [ΔL_Y81] (Prediction: Anthropoids with relatively globular brains will tend be more orthognathic)	Ad hoc

Reproduced with permission of the copyright owner. Further reproduction prohibited without permission.

Preliminary and Exploratory Analysis

Before attempting to integrate relevant endocranial variables into the covariance structural model (see Chapter 15), some exploratory analysis of the interrelations among nasomaxillary and endocranial variables is warranted. A principal components analysis and a series of bivariate regressions were performed on selected variables and the results are presented and discussed in the following sections.

Effects of Size-Related Quantity on Brain Size

Weidenreich's observation that larger mammals tend to have relatively smaller brains is confirmed for the anthropoid sample. As the scatter plots in Box 11.8 shows, the regression slope of log delta cube root endocranial volume against log delta centroid size is 0.92 indicating that increases in brain size do not keep pace with increases in body size. The cluster of points labeled "x" in the bivariate plot represent outlying specimens of *Homo*, which deviate substantially from the regression line in a manner that suggests a much larger brain than would be expected on the basis of body size. If *Homo* is removed from the analysis (see Box 11.9) the slope estimate becomes 0.78, a result more consistent with that of Martin (1982) who found a scaling coefficient of 0.75 for a diverse sample of mammals. However, an analysis of the error around the regression line (Box 11.9) indicates heteroscedasticity and non-normality of the residuals. In fact, there appears to be a bimodal distribution with *Alouatta*, *Ateles*, *Lagothrix*, *Chiropotes*, *Cebus* and *Pan* all contributing to a 'line' of residuals above the common regression line. When anthropoid infraorders are plotted separately, the slopes of the regression lines are

Reproduced with permission of the copyright owner. Further reproduction prohibited without permission.

quite different (catarrhines: *b*=0.66, R2=0.94; platyrrhines: *b*=0.93, R2=0.84). Within catarrhines the residuals appear to be normally distributed, but there is minimal overlap between Cercopithecoidea and Hominoidea. Within platyrrhines, *Alouatta* is an obvious outlier, with an endocranial volume much lower than expected on the basis of size.

The preceding analysis indicates that while brain size covaries with negative allometry in relation to body size, there are substantial differences in covariances among anthropoid taxa, both at the infraordinal and subinfraordinal levels. In accordance with the tenets set forth in Chapter 10, these allometric regression lines are interpreted as evidence for the operation of one or more distal causal agents (related to body size) affecting brain size in such a way that larger animals tend to have relatively smaller brains compared to smaller animals. Clearly much more work is needed to understand which size-related causal agents are involved and how the nomological processes determining brain size vary in different anthropoid taxa. However, since the primary objective of this chapter is to understand how brain size and form influence nasomaxillary morphology, a descriptive account of the relationship between brain size and body size will be sufficient.

Reproduced with permission of the copyright owner. Further reproduction prohibited without permission.

Box 11.8. Regression of log delta cube root endocranial volume against log delta centroid size. Slope = 0.92 (95% CI: 0.86, 0.97), R-square = .77. Residual-by-predicted plot, upper right; Residual density plot, lower right. (Entire anthropoid sample: n=300)

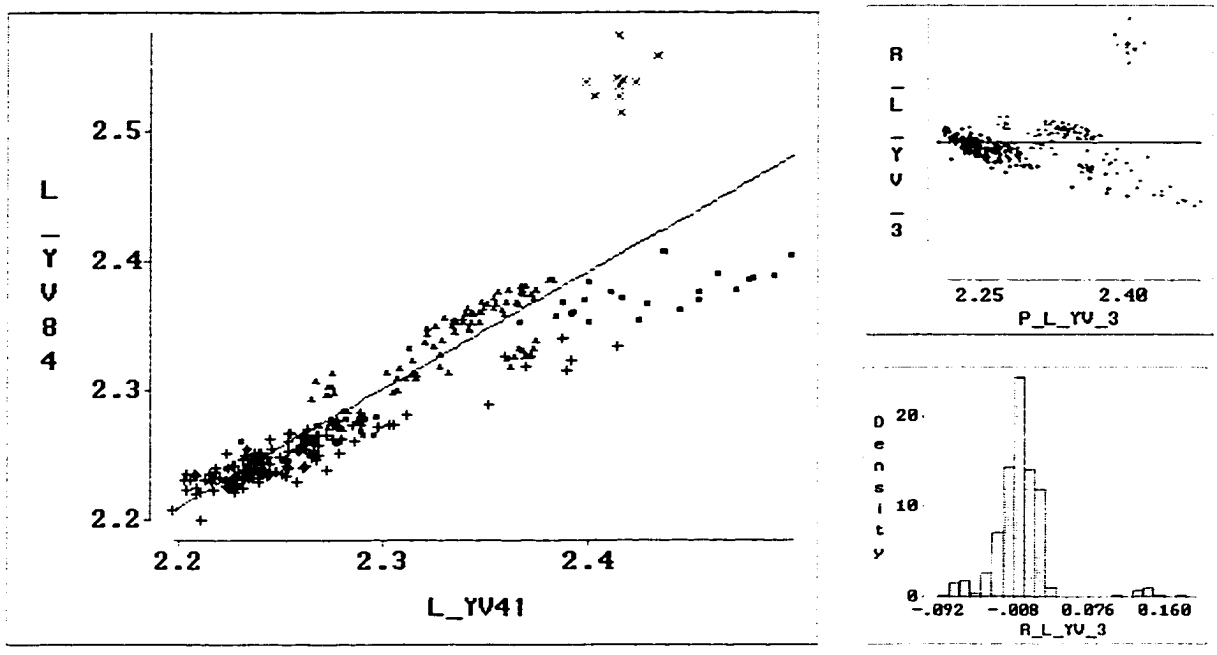

Box 11.9. Regression of log delta cube root endocranial volume against log delta centroid size. Slope = 0.78 (95% CI: 0.74, 0.81), R-square = 0.86. Residual-by-predicted plot, upper right; Residual density plot, lower right. (Entire anthropoid sample except *Homo*; n=290)

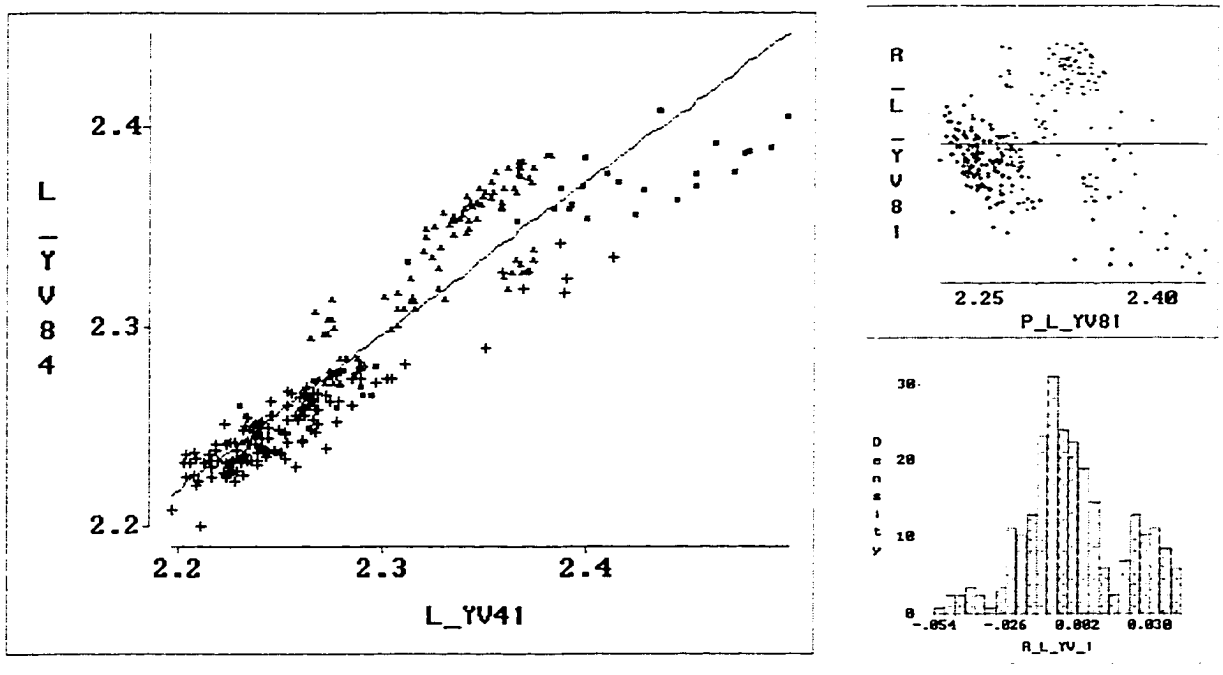

Reproduced with permission of the copyright owner. Further reproduction prohibited without permission.

Box 11.10. Regression of log delta cube root endocranial volume against log delta centroid size. Slope = 0.66 (95% CI: 0.63, 0.68), R-square = 0.94. Residual-by-predicted plot, upper right; Residual density plot, lower right. (Entire catarrhine sample except *Homo*; n=173)

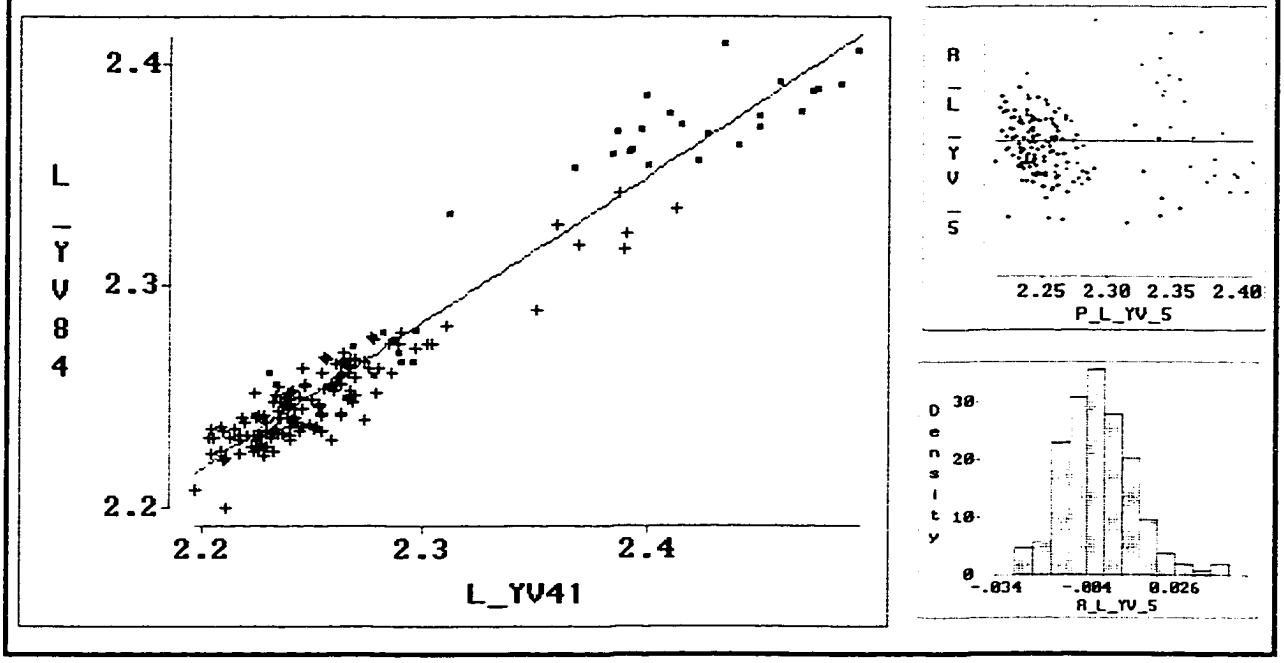

Box 11.11. Regression of log delta cube root endocranial volume against log delta centroid size. Slope = 0.93 (95% CI: 0.85, 1.00), R-square = 0.84. Residual-by-predicted plot, upper right; Residual density plot, lower right. (Platyrrhine sample; n=117)

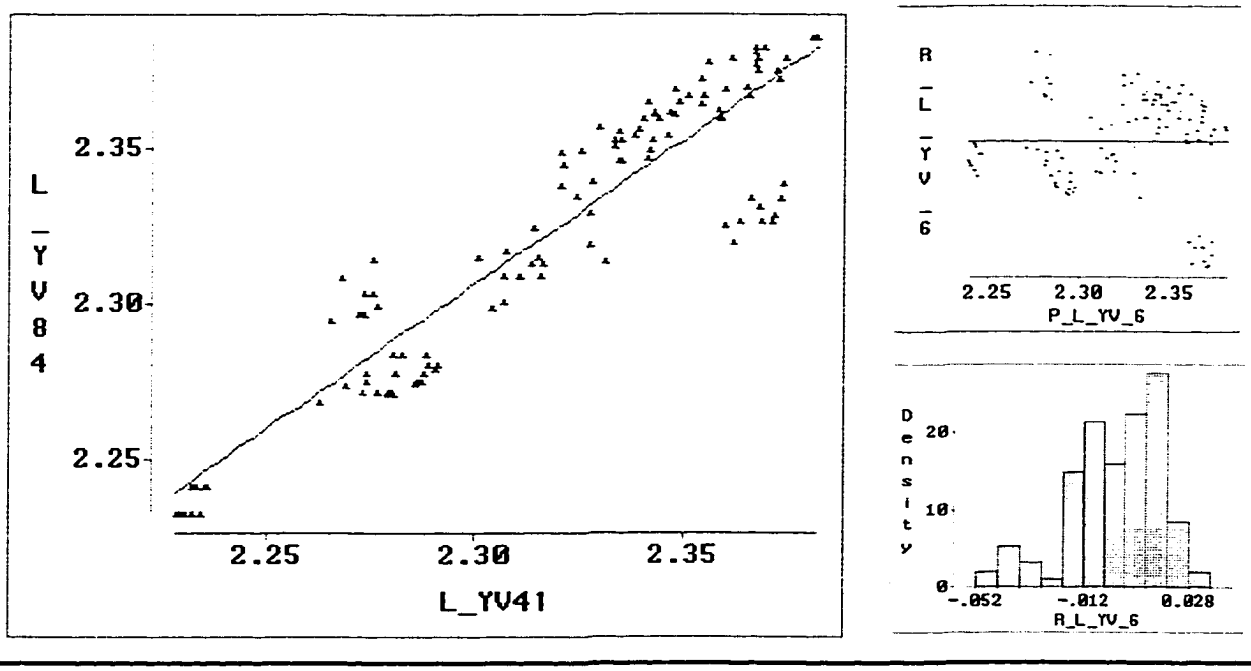

Reproduced with permission of the copyright owner. Further reproduction prohibited without permission.

Principal Components Analysis of Endocranial and Nasomaxillary Variables

Box 11.12 reports the eigenvalues for the 26 endocranial and nasomaxillary variables included in the PCA. The first two principal components were retained for examination. The eigenvalue for $PC_{(1)}$ indicates that this factor accounts for 62% of the total variance of the original variables, and $PC_{(2)}$ accounts for an additional 13%. In contrast to the PCA performed in Chapter 9, the first principal component of the current analysis does not represent a size factor, since all of the included variables are either shape variables or Mosimann isometric residuals.

Box 11.12. Eigenvalues and accounted-for variance of log delta endocranial and nasomaxillary variables (n=300; correlation matrix used in PCA).

PC	Eigenvalue	Proportion of Variance Explained	Cumulative Proportion Explained	PC	Eigenvalue	Proportion of Variance Explained	Cumulative Proportion Explained
1	16.07	.618	.62	14	0.03	.002	1.00
2	3.28	.126	.74	15	0.02	.001	1.00
3	2.24	.086	.83	16	0.02	.001	1.00
4	1.64	.063	.89	17	.00	.000	1.00
5	0.86	.033	.93	18	.00	.000	1.00
6	0.59	.023	.95	19	.00	.000	1.00
7	0.44	.017	.97	20	.00	.000	1.00
8	0.36	.014	.98	21	.00	.000	1.00
9	0.29	.011	.99	22	.00	.000	1.00
10	0.26	.010	1.00	23	.00	.000	1.00
11	0.21	.008	1.00	24	.00	.000	1.00
12	0.09	.004	1.00	25	.00	.000	1.00
13	0.07	.003	1.00	26	.00	.000	1.00

Box 11.13 lists the component loadings for the first two (orthogonally rotated) principal components; the corresponding scatter plot is displayed in Box 11.14. The dotted vertical and horizontal lines drawn through the bivariate plot in Box 11.14 separate significant from nonsignificant component loadings.

Reproduced with permission of the copyright owner. Further reproduction prohibited without permission.

Box 11.13. Component loadings for the first two principal components of the combined endocranial and nasomaxillary variables (varimax rotation).

Variable	$PC_{(1)}$	$PC_{(2)}$	Variable	$PC_{(1)}$	$PC_{(2)}$
ΔS_L_YV1	0.351	0.863	ΔL_YV30	0.846	-0.063
ΔS_L_YV5	0.265	0.020	ΔL_YV31	0.811	0.364
ΔS_L_YV6	0.001	0.059	ΔL_YV32	-0.167	0.378
ΔS_L_YV9	0.048	0.025	ΔL_YV33	-0.188	0.373
ΔS_L_YV11	0.206	0.485	ΔL_YV35	0.332	0.555
ΔL_YV13	-0.489	-0.370	ΔL_YV95	0.445	0.236
ΔS_L_YV14	0.796	0.308	ΔL_YV70	0.618	0.021
ΔS_L_YV15	0.066	-0.113	ΔL_YV74	0.676	-0.070
ΔS_L_YV17	0.463	0.790	ΔL_YV76	0.506	-0.061
ΔS_L_YV18	0.033	0.145	ΔL_YV78	0.577	0.019
ΔS_L_YV19	0.320	-0.174	ΔL_YV79	0.013	-0.524
ΔS_L_YV22	-0.213	-0.216	ΔL_YV81	-0.428	0.008
ΔS_L_YV26	0.035	0.006	ΔS_L_YV84	-0.859	-0.092

Box 11.14. Bivariate plot of first two principle components (PC1, PC2)

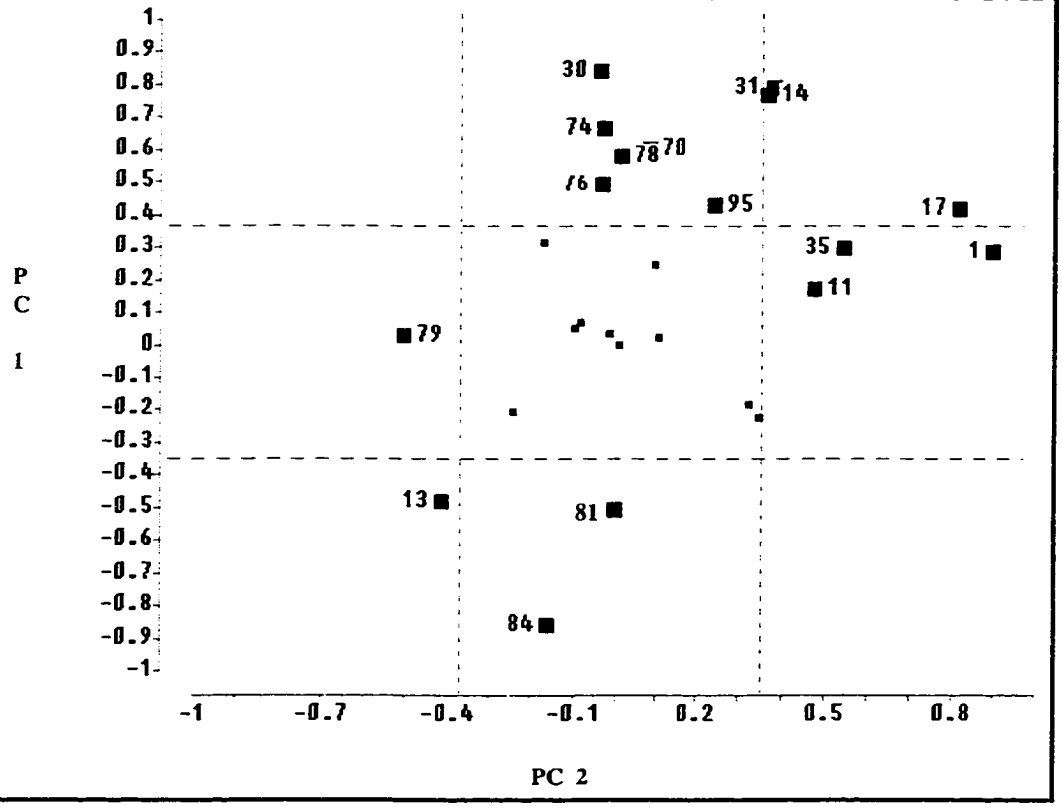

Variables that load highly (and positively) on $PC_{(1)}$ include maxillary arch length [ΔS_L_YV14], anterior facial length [ΔS_L_YV17], both Krogman's [ΔL_YV30]

Reproduced with permission of the copyright owner. Further reproduction prohibited without permission.

and Enlow's [ΔL_Y31] angles of facial prognathism, posterior facial angle [ΔL_YV95], cranial base flexion [ΔL_YV70], orientation of the cribriform plate [ΔL_YV74], orientation of the olfactory bulbs [ΔL_YV76], and middle cranial fossa length [ΔS_L_YV78]. All of these variables relate to the anteroposterior elongation of either the basicranial or facial elements. Contrasted to these variables are three characters that load highly (and negatively) on $PC_{(1)}$—relative endocranial volume [ΔS_L_YV84], endocranial index [ΔL_YV81], and anteroposterior position of the zygomatic root [ΔL_YV13],. Thus, $PC_{(1)}$ indicates that anthropoids with *relatively* large brains exhibit (1) zygomatic roots that are anteriorly located, (2) short orthognathic faces, (3) substantial cranial base flexion, (4) a horizontal orientation of the olfactory bulbs and cribriform plate, (5) shortened middle cranial fossae, and (6) brachyendocrany.

$PC_{(2)}$ contrasts nasal bone length [ΔS_L_YV1], zygoma height [ΔS_L_YV11], maxillary arch length [ΔS_L_YV14], anterior facial length [ΔS_L_YV17], Enlow's angle of facial prognathism [ΔL_YV31], and paranasal plate orientation [ΔL_YV35], all with high positive loadings, against anteroposterior position of zygomatic root [ΔL_YV13] and anterior cranial fossa length [ΔS_L_YV79], with high negative loadings. These findings suggest that anthropoids with relatively short anterior cranial fossae and posteriorly placed zygomatic roots also tend to exhibit long, prognathic faces, substantial zygomatic vertical height and sagittally oriented paranasal plates.

Bivariate and Multiple Regression Analysis

To further examine trait covariances and tentatively test predictions of trait relationships, bivariate regressions were conducted. The results are presented in

Reproduced with permission of the copyright owner. Further reproduction prohibited without permission.

Box 11.15. Two points must be made concerning the regression coefficients and significance tests in the following analysis. First, since the data are somewhat heterogeneous, with the residuals exhibiting various levels of heteroscedasticity and non-normality, the regression coefficients and associated *p*-values must be viewed with extreme caution. Accordingly, the *p*-values are perhaps best considered as 'heuristic guides' rather than conclusive tests (unless it can be shown in specific cases that the data conform to the assumptions required of inferential testing). To contend with this problem, bivariate analyses were repeated using various subgroups in order to determine whether the slope of a common regression line held for the lower-level taxa making up the larger group. Second, the morphogenetic theory of skull development and evolution indicates that the majority of nasomaxillary characters are influenced by several causal agents. Therefore, most bivariate models will likely be misspecified (i.e., omit relevant independent variables), and their regression coefficients may thus be inaccurate. Results of full model covariance structure analyses are presented in Chapter 15. Despite these problems, bivariate analyses are essential to an understanding of the structure of the relationships among dependent and independent variables and as an exploratory tool for asking more informed questions and refining nomological hypotheses.

Reproduced with permission of the copyright owner. Further reproduction prohibited without permission.

Reproduced with permission of the copyright owner. Further reproduction prohibited without permission.

Box 11.15. Endocranial volume [ΔL_YV84] ← Centroid size [ΔL_YV41]				
Taxon	Maximum likelihood regression coefficient (95% CI) and associated p-value	Shapiro-Wilk test for normality of residuals	Brown & Forsythe's test for residual homoscedasticity	Somers' D nonparametric measure and test of association
Anthropoids (n=300)	0.92 (0.86, 0.97) p<.0001	0.79 p< .0001	43.50 p< .0001	0.80 p < .05
Platyrrhini (n=117)	0.93 (0.85, 0.99) p<.0001	0.93 p< .0001	5.50 p=.001	0.72 p < .05
Atelidae (n=65)	0.90 (0.76, 1.04) p<.0001	0.91 p< .0002	2.68 p=.055	0.65 p < .05
Cebidae (n=52)	1.05 (0.97, 1.13) p<.0001	0.97 p< .44	2.51 p=.07	0.69 p< .05
Catarrhini (n=183)	0.89 (0.81, 0.97) p<.0001	0.71 p< .0001	22.35 p < .0001	0.74 p < .05
Cercopithecoidea (n=137)	0.56 (0.51, 0.59) p<.0001	0.97 p= .30	0.95 p = .42	0.65 p < .05
Cercopithecinae (n=87)	0.57 (0.53, 0.61) p<.0001	0.98 p= .56	0.95 p = .42	0.74 p < .05
Colobinae (n=50)	0.38 (0.22, 0.54) p<.0001	0.96 p= .18	0.98 p = .41	0.40 p < .05
Hominoidea (n=46)	0.86 (0.57, 1.14) p<.0001	0.79 p< .0001	1.91 p = .14	0.57 p < .05

Box 11.16. Endocranial index [ΔL_YV81] ← Relative endocranial volume [ΔS_L_YV84]				
Taxon	Maximum likelihood regression coefficient (95% CI) and associated p-value	Shapiro-Wilk test for normality of residuals	Brown & Forsythe's test for residual homoscedasticity	Somers' D nonparametric measure and test of association
Anthropoids (n=300)	1.01 (0.75, 1.27) p < .0001	0.98 p = .52	0.61 p = .61	0.22 p < .05
Platyrrhini (n=117)	0.36 (-0.50, 1.24) p = .40	0.97 p = .22	0.30 p = .82	0.11 ns
Atelidae (n=65)	-0.98 (-2.05, 0.10) p = .07	0.94 p = .01	1.80 p = .16	-0.12 ns
Cebidae (n=52)	3.23 (1.73, 4.74) p = .0001	0.98 p = .82	1.70 p = .18	0.34 p < .05
Catarrhini (n=183)	1.11 (0.85, 1.37) p = .0001	0.96 p = .01	1.59 p = .19	0.32 p < .05
Cercopithecoidea (n=137)	1.12 (0.52, 1.72) p = .0002	0.95 p = .0002	0.58 p = .63	0.21 p < .05
Cercopithecinae (n=87)	0.77 (0.10, 1.44) p = .02	0.91 p = .0001	0.18 p = .91	0.15 p < .05
Colobinae (n=50)	2.52 (1.24, 3.81) p = .0001	0.96 p = .25	0.31 p = .82	0.29 p < .05
Hominoidea (n=46)	1.12 (0.77, 1.45) p = .0001	0.94 p = .02	1.10 p = .36	0.46 p < .05

Reproduced with permission of the copyright owner. Further reproduction prohibited without permission.

Box 11.17. Cribriform plate orientation [ΔL_YV74] ← Anterior cranial fossa length [ΔL_YV79]

Taxon	Maximum likelihood regression coefficient (95% CI) and associated p-value	Shapiro-Wilk test for normality of residuals	Brown & Forsythe's test for residual homoscedasticity	Somers' D nonparametric measure and test of association
Anthropoids (n=300)	-0.04 (-0.16, 0.08) p = .49	0.98 p = .08	3.08 p = .03	-0.05 ns
Platyrrhini (n=117)	-0.36 (-0.68, -0.04) p = .03	0.97 p = .054	1.51 p = .21	-0.17 p < .05
Atelidae (n=65)	-0.39 (-0.83, 0.05) p = .08	0.95 p = .020	1.79 p = .16	-0.16 ns
Cebidae (n=52)	-0.32 (-0.80, 0.15) p = .17	0.97 p = .38	0.29 p = .83	-0.19 p < .05
Catarrhini (n=183)	0.07 (-0.05, 0.18) p = .24	0.96 p = .0005	1.10 p = .35	0.01 ns
Cercopithecoidea (n=137)	-0.04 (-0.15, 0.07) p = .45	0.98 p = .78	0.04 p = .99	-0.06 ns
Cercopithecinae (n=87)	-0.15 (-0.30, -0.01) p = .04	0.98 p = .62	0.19 p = .91	-0.16 p < .05
Colobinae (n=50)	0.07 (-0.17, 0.32) p = .54	0.97 p = .60	0.75 p = .53	-0.05 ns
Hominoidea (n=46)	0.35 (0.06, 0.63) p = .01	0.94 p = .03	3.78 p = .02	0.18 ns

Box 11.18. Cribriform plate orientation [ΔL_YV74] ← Relative endocranial volume [ΔS_L_YV84]

Taxon	Maximum likelihood regression coefficient (95% CI) and associated p-value	Shapiro-Wilk test for normality of residuals	Brown & Forsythe's test for residual homoscedasticity	Somers' D nonparametric measure and test of association
Anthropoids (n=300)	-1.87 (-2.16, -1.59) p = .0001	0.98 p = .31	2.10 p = .09	-0.46 p < .05
Platyrrhini (n=117)	-4.96 (-5.85, -4.07) p = .0001	0.98 p = .94	3.62 p = .02	-0.53 p < .05
Atelidae (n=65)	-5.34 (-6.34, -4.34) p = .0001	0.97 p = .36	0.87 p = .46	-0.60 p < .05
Cebidae (n=52)	-5.35 (-7.33, -3.37) p = .0001	0.95 p = .08	1.06 p = .37	-0.47 p < .05
Catarrhini (n=183)	-1.46 (-1.71, -1.23) p = .0001	0.98 p = .74	0.62 p = .60	-0.37 p < .05
Cercopithecoidea (n=137)	-1.09 (-1.72, -0.46) p = .0007	0.98 p = .72	1.21 p = .31	-0.26 p < .05
Cercopithecinae (n=87)	-0.65 (-1.35, 0.05) p = .07	0.98 p = .36	0.70 p = .55	-0.23 p < .05
Colobinae (n=50)	-2.86 (-4.22, -1.51) p = .0001	0.99 p = .89	0.09 p = .96	-0.36 p < .05
Hominoidea (n=46)	-1.54 (-1.76, -1.36) p = .0001	0.97 p = .42	0.39 p = .76	-0.54 p < .05

Reproduced with permission of the copyright owner. Further reproduction prohibited without permission.

Box 11.19. Cribriform plate orientation [ΔL_YV74] ← Endocranial index [ΔL_YV81]

Taxon	Maximum likelihood regression coefficient (95% CI) and associated p-value	Shapiro-Wilk test for normality of residuals	Brown & Forsythe's test for residual homoscedasticity	Somers' D nonparametric measure and test of association
Anthropoids (n=300)	-0.36 (-0.50, -0.23) p = .0001	0.98 p = .40	1.08 p = .35	-0.17 p < .05
Platyrrhini (n=117)	-0.26 (-0.52, 0.00) p = .05	0.97 p = .07	0.42 p = .73	-0.12 p = .05
Atelidae (n=65)	-0.05 (-0.43, 0.32) p = .77	0.95 p = .04	0.91 p = .44	-0.01 ns
Cebidae (n=52)	-0.51 (-0.88, -0.15) p = .005	0.99 p = .97	0.64 p = .59	-0.26 p < .05
Catarrhini (n=183)	-0.44 (-0.59, -0.31) p = .0001	0.98 p = .14	1.51 p = .21	-0.23 p < .05
Cercopithecoidea (n=137)	-0.25 (-0.42, -0.07) p = 005	0.98 p = .68	0.06 p = .98	-0.14 p < .05
Cercopithecinae (n=87)	-0.20 (-0.41, 0.02) p = .07	0.98 p = .58	0.15 p = .93	-0.10 ns
Colobinae (n=50)	-0.32 (-0.60, -0.03) p = .03	0.96 p = .15	0.19 p = .91	-0.22 p < .05
Hominoidea (n=46)	-0.65 (-0.90, -0.21) p = .0001	0.98 p = .73	4.26 p = .01	-0.34 p < .05

Box 11.20. Cribriform plate orientation [ΔL_YV74] ← Cranial base angle [ΔL_YV70]

Taxon	Maximum likelihood regression coefficient (95% CI) and associated p-value	Shapiro-Wilk test for normality of residuals	Brown & Forsythe's test for residual homoscedasticity	Somers' D nonparametric measure and test of association
Anthropoids (n=300)	0.45 (0.34, 0.56) p = .0001	0.97 p = .17	1.88 p = .13	0.26 p < .05
Platyrrhini (n=117)	0.27 (-0.09, 0.63) p = .14	0.96 p = .02	0.26 p = .85	0.15 p < .05
Atelidae (n=65)	0.59 (-0.04, 1.22) p = .07	0.96 p = .11	0.72 p = .72	0.12 ns
Cebidae (n=52)	0.00 (-0.46, 0.46) p = .99	0.96 p = .23	0.85 p = .48	0.10 ns
Catarrhini (n=183)	0.46 (0.37, 0.55) p = .0001	0.98 p = .39	0.61 p = .61	0.30 p < .05
Cercopithecoidea (n=137)	0.28 (0.13, 0.44) p = .0004	0.98 p = .48	0.82 p = .49	0.21 p < .05
Cercopithecinae (n=87)	0.12 (-0.08, 0.31) p. = .23	0.98 p = .59	0.34 p = .80	0.12 ns
Colobinae (n=50)	0.68 (0.43, 0.94) p = .0001	0.99 p = .99	0.25 p = .86	0.40 p < .05
Hominoidea (n=46)	0.57 (0.45, 0.68) p = .0001	0.95 p = .11	3.19 p = .03	0.40 p < .05

Reproduced with permission of the copyright owner. Further reproduction prohibited without permission.

Box 11.21. Cribriform plate orientation [ΔL_YV74] ← Middle cranial fossa length [ΔL_YV78]

Taxon	Maximum likelihood regression coefficient (95% CI) and associated p-value	Shapiro-Wilk test for normality of residuals	Brown & Forsythe's test for residual homoscedasticity	Somers' D nonparametric measure and test of association
Anthropoids (n=300)	0.40 (0.26, 0.45) p = .0001	0.97 p = .0004	2.64 p = .049	0.17 p < .05
Platyrrhini (n=117)	0.60 (0.32, 0.89) p = .0001	0.97 p = .04	0.84 p = .47	0.22 p < .05
Atelidae (n=65)	0.82 (0.35, 1.28) p = .0001	0.96 p = .07	0.85 p = .47	0.26 p < .05
Cebidae (n=52)	0.43 (0.07, 0.79) p = .02	0.96 p = .16	0.52 p = .67	0.16 ns
Catarrhini (n=183)	0.59 (0.43, 0.75) p = .0001	0.98 p = .50	2.94 p = .03	0.26 p < .05
Cercopithecoidea (n=137)	0.34 (0.16, 0.62) p = .0002	0.99 p = .97	1.01 p = .39	0.22 p < .05
Cercopithecinae (n=87)	0.19 (-0.04, 0.43) p = .10	0.98 p = .78	0.19 p = .91	0.11 ns
Colobinae (n=50)	0.56 (0.29, 0.83) p = .0001	0.97 p = .28	0.94 p = .43	0.40 p < .05
Hominoidea (n=46)	1.09 (0.80, 1.39) p = .0001	0.96 p = .29	2.82 p = .05	0.36 p < .05

Box 11.22. Facial prognathism (Krogman's angle) [ΔL_YV30] ← Cribriform plate orientation [ΔL_YV74]

Taxon	Maximum likelihood regression coefficient (95% CI) and associated p-value	Shapiro-Wilk test for normality of residuals	Brown & Forsythe's test for residual homoscedasticity	Somers' D nonparametric measure and test of association
Anthropoids (n=300)	0.40 (0.33, 0.47) p = .0001	0.96 p = .0001	6.54 p = .0003	0.32 p < .05
Platyrrhini (n=117)	0.31 (0.23, 0.39) p = .0001	0.96 p = .16	1.69 p = .17	0.37 p < .05
Atelidae (n=65)	0.42 (0.31, 0.52) p = .0001	0.97 p = .43	0.33 p = .80	0.46 p < .05
Cebidae (n=52)	0.14 (0.04, 0.24) p = .004	0.96 p = .18	1.58 p = .21	0.24 p < .05
Catarrhini (n=183)	0.63 (0.53, 0.73) p = .0001	0.99 p = .93	8.22 p = .0001	0.38 p < .05
Cercopithecoidea (n=137)	0.34 (0.22, 0.45) p = .0001	0.97 p = .11	4.44 p = .005	0.32 p < .05
Cercopithecinae (n=87)	0.28 (0.14, 0.43) p = .0001	0.97 p = .28	1.16 p = .33	0.27 p < .05
Colobinae (n=50)	0.42 (0.23, 0.61) p = .0001	0.96 p = .17	3.48 p = .02	0.40 p < .05
Hominoidea (n=46)	0.91 (0.76, 1.05) p = .0001	0.96 p = .21	1.48 p = .23	0.44 p < .05

Reproduced with permission of the copyright owner. Further reproduction prohibited without permission.

Box 11.23. Facial prognathism (Enlow's angle) [ΔL_YV31] ← Cribriform plate orientation [ΔL_YV74]				
Taxon	Maximum likelihood regression coefficient (95% CI) and associated p-value	Shapiro-Wilk test for normality of residuals	Brown & Forsythe's test for residual homoscedasticity	Somers' D nonparametric measure and test of association
Anthropoids (n=300)	0.53 (0.44, 0.63) p = .0001	0.94 p = .0001	6.70 p = .0002	0.36 p < .05
Platyrrhini (n=117)	0.43 (0.35, 0.51) p = .0001	0.98 p = .71	1.13 p = .34	0.52 p < .05
Atelidae (n=65)	0.48 (0.37, 0.59) p = .0001	0.99 p = .91	0.76 p = .52	0.51 p < .05
Cebidae (n=52)	0.36 (0.25, 0.47) p = .0001	0.98 p = .53	0.24 p = .87	0.53 p < .05
Catarrhini (n=183)	0.76 (0.61, 0.92) p = .0001	0.97 p = .02	14.54 p = .0001	0.27 p < .05
Cercopithecoidea (n=137)	0.38 (0.19, 0.57) p = .0001	0.96 p = .002	8.02 p = .0001	0.23 p < .05
Cercopithecinae (n=87)	0.37 (0.13, 0.60) p = .002	0.95 p = .004	2.83 p = .04	0.23 p < .05
Colobinae (n=50)	0.43 (0.13, 0.74) p = .005	0.94 p = .03	8.79 p = .0001	0.26 p < .05
Hominoidea (n=46)	1.11 (0.90, 1.32) p = .0001	0.93 p = .007	2.61 p = .06	0.41 p < .05

Box 11.24. Facial prognathism (Krogman's angle) [ΔL_YV30] ← Cranial base angle [ΔL_YV70]				
Taxon	Maximum likelihood regression coefficient (95% CI) and associated p-value	Shapiro-Wilk test for normality of residuals	Brown & Forsythe's test for residual homoscedasticity	Somers' D nonparametric measure and test of association
Anthropoids (n=300)	0.38 (0.30, 0.46) p = .0001	0.98 p = .33	8.11 p = .0001	0.14 p < .05
Platyrrhini (n=117)	0.22 (0.03, 0.41) p = .02	0.97 p = .18	0.35 p = .79	0.15 p < .05
Atelidae (n=65)	0.59 (0.22, 0.96) p = .001	0.92 p = .0004	0.15 p = .93	0.29 p < .05
Cebidae (n=52)	0.07 (-0.10, 0.25) p = .40	0.95 p = .04	1.23 p = .31	0.11 ns
Catarrhini (n=183)	0.44 (0.36, 0.52) p = .0001	0.99 p = .93	12.59 p = .0001	0.21 p < .05
Cercopithecoidea (n=137)	0.16 (0.04, 0.29) p = .009	0.97 p = .10	4.06 p = .009	0.16 p < .05
Cercopithecinae (n=87)	-0.03 (-0.17, 0.12) p = .70	0.98 p = .08	2.08 p = .11	-0.01 ns
Colobinae (n=50)	0.58 (0.38, 0.77) p = .0001	0.97 p = .47	5.12 p = .004	0.49 p < .05
Hominoidea (n=46)	0.58 (0.46, 0.71) p = .0001	0.95 p = .10	1.51 p = .21	0.32 p < .05

Reproduced with permission of the copyright owner. Further reproduction prohibited without permission.

Box 11.25. Facial prognathism (Krogman's angle) [ΔL_YV30] ← Relative endocranial volume [ΔS_L_YV84]

Taxon	Maximum likelihood regression coefficient (95% CI) and associated p-value	Shapiro-Wilk test for normality of residuals	Brown & Forsythe's test for residual homoscedasticity	Somers' D nonparametric measure and test of association
Anthropoids (n=300)	-1.59 (-1.78, -1.40) p = .0001	0.98 p = .05	6.85 p = .0002	-0.35 p < .05
Platyrrhini (n=117)	-2.46 (-1.95, -2.45) p = .0001	0.97 p = .27	0.29 p = .29	-0.34 p < .05
Atelidae (n=65)	-3.22 (-3.82, -2.61) p = .0001	0.98 p = .49	0.72 p = .54	-0.44 p < .05
Cebidae (n=52)	-1.88 (-2.67, -1.08) p = .0001	0.97 p = .42	0.48 p = .70	-0.35 p < .05
Catarrhini (n=183)	-1.57 (-1.76, -1.38) p = .0001	0.96 p = .0004	8.57 p = .0001	-0.48 p < .05
Cercopithecoidea (n=137)	-1.82 (-2.21, -1.41) p = .0001	0.96 p = .001	4.83 p = .003	-0.45 p < .05
Cercopithecinae (n=87)	-1.46 (-1.88, -1.02) p = .0001	0.96 p = .06	0.91 p = .43	-0.42 p < .05
Colobinae (n=50)	-3.28 (-4.13, -2.43) p = .0001	0.96 p = .22	1.36 p = .27	-0.50 p < .05
Hominoidea (n=46)	-1.51 (-1.78, -1.23) p = .0001	0.97 p = .34	1.57 p = .21	-0.43 p < .05

Box 11.26. Facial prognathism (Krogman's angle) [ΔL_YV30] ← Endocranial index [ΔL_YV81]

Taxon	Maximum likelihood regression coefficient (95% CI) and associated p-value	Shapiro-Wilk test for normality of residuals	Brown & Forsythe's test for residual homoscedasticity	Somers' D nonparametric measure and test of association
Anthropoids (n=300)	-0.30 (-0.40, -0.20) p = .0001	0.95 p = .0001	7.77 p = .0001	-0.16 p < .05
Platyrrhini (n=117)	-0.01 (-0.15, 0.13) p = .88	0.97 p = .07	1.78 p = .15	0.00 ns
Atelidae (n=65)	0.02 (-0.20, 0.25) p = .83	0.94 p = .006	2.12 p = .11	-0.03 ns
Cebidae (n=52)	-0.09 (-0.24, 0.06) p = .22	0.95 p = .07	0.32 p = .81	-0.07 ns
Catarrhini (n=183)	-0.46 (-0.58, -0.33) p = .0001	0.92 p = .0001	5.93 p = .0007	-0.23 p < .05
Cercopithecoidea (n=137)	-0.23 (-0.36, -0.10) p = .0001	0.96 p = .002	0.65 p = .58	-0.18 p < .05
Cercopithecinae (n=87)	-0.14 (-0.30, 0.02) p = .08	0.96 p = .06	1.38 p = .26	-0.13 ns
Colobinae (n=50)	-0.38 (-0.60, -0.16) p = .0005	0.96 p = .16	5.77 p = .002	-0.26 p < .05
Hominoidea (n=46)	-0.69 (-0.94, -0.44) p = .0001	0.95 p = .06	1.84 p = .15	-0.33 p < .05

Reproduced with permission of the copyright owner. Further reproduction prohibited without permission.

Box 11.27. Orbital deflection [ΔL_YV46] ← Anterior cranial fossa length [ΔL_YV79]

Taxon	Maximum likelihood regression coefficient (95% CI) and associated p-value	Shapiro-Wilk test for normality of residuals	Brown & Forsythe's test for residual homoscedasticity	Somers' D nonparametric measure and test of association
Anthropoids (n=300)	0.01 (-0.10, 0.12) p = .83	0.94 p = .0001	0.83 p = .47	-0.02 ns
Platyrrhini (n=117)	0.14 (-0.15, 0.43) p = .35	0.97 p = .17	1.09 p = .35	0.05 ns
Atelidae (n=65)	-0.25 (-0.58, 0.09) p = .15	0.96 p = .07	4.93 p = .004	-0.04 ns
Cebidae (n=52)	0.68 (0.22, 1.13) p = .002	0.96 p = .10	0.11 p = .95	0.24 p < .05
Catarrhini (n=183)	0.02 (-0.09, 0.14) p = .72	0.88 p = .0001	2.18 p = .09	-0.03 ns
Cercopithecoidea (n=137)	-0.06 (-0.15, 0.04) p = .22	0.97 p = .17	1.39 p = .25	-0.06 ns
Cercopithecinae (n=87)	0.00 (-0.14, 0.14) p = .97	0.97 p = .27	1.94 p = .13	0.00 ns
Colobinae (n=50)	-0.17 (-0.34, -0.01) p = .04	0.96 p = .16	1.16 p = .33	-0.17 p < .05
Hominoidea (n=46)	0.26 (-0.06, 0.59) p = .11	0.94 p = .02	2.31 p = .09	0.06 ns

Box 11.28. Orbital deflection [ΔL_YV46] ← Endocranial index [ΔL_YV81]

Taxon	Maximum likelihood regression coefficient (95% CI) and associated p-value	Shapiro-Wilk test for normality of residuals	Brown & Forsythe's test for residual homoscedasticity	Somers' D nonparametric measure and test of association
Anthropoids (n=300)	-0.33 (-0.46, -0.20) p = .0001	0.96 p = .0001	3.14 p = .03	-0.14 p < .05
Platyrrhini (n=117)	-0.20 (-0.43, 0.04) p = .09	0.99 p = .84	0.66 p = .58	-0.13 p < .05
Atelidae (n=65)	-0.30 (-0.57, -0.03) p = .03	0.96 p = .13	10.43 p = .0001	-0.07 ns
Cebidae (n=52)	0.09 (-0.31, 0.48) p = .67	0.95 p = .08	1.78 p = .16	0.06 ns
Catarrhini (n=183)	-0.42 (-0.56, -0.27) p = .0001	0.92 p = .0001	1.62 p = .18	-0.17 p < .05
Cercopithecoidea (n=137)	-0.09 (-0.24, 0.07) p = .26	0.98 p = .24	0.43 p = .73	-0.04 ns
Cercopithecinae (n=87)	-0.03 (-0.24, 0.17) p = .76	0.97 p = .24	1.01 p = .39	0.00 ns
Colobinae (n=50)	-0.18 (-0.39, 0.04) p = .10	0.97 p = .41	1.09 p = .36	-0.11 ns
Hominoidea (n=46)	-0.77 (-1.03, -0.51) p = .0001	0.95 p = .08	0.95 p = .42	-0.42 p < .05

Reproduced with permission of the copyright owner. Further reproduction prohibited without permission.

Box 11.29. Orbital deflection [ΔL_YV46] ← Cranial base angle [ΔL_YV70]

Taxon	Maximum likelihood regression coefficient (95% CI) and associated p-value	Shapiro-Wilk test for normality of residuals	Brown & Forsythe's test for residual homoscedasticity	Somers' D nonparametric measure and test of association
Anthropoids (n=300)	0.54 (0.45, 0.64) p = .0001	0.97 p = .01	2.63 p = .05	0.29 p < .05
Platyrrhini (n=117)	0.53 (022, 085) p = .0008	0.97 p = .11	1.23 p = .30	0.25 p < .05
Atelidae (n=65)	1.26 (0.87, 1.64) p = .0001	0.97 p = .32	4.31 p = .008	0.43 p < .05
Cebidae (n=52)	-0.14 (-0.61, 0.33) p = .55	0.96 p = .17	1.50 p = .23	-0.08 ns
Catarrhini (n=183)	0.53 (0.44, 0.62) p = .0001	0.98 p = .63	4.93 p = .002	0.27 p < .05
Cercopithecoidea (n=137)	0.36 (0.23, 0.49) p = .0001	0.98 p = .36	1.67 p = .18	0.28 p < .05
Cercopithecinae (n=87)	0.37 (0.21, 0.53) p = .0001	0.98 p = .44	2.11 p = .11	0.29 p < .05
Colobinae (n=50)	0.33 (0.12, 0.54) p = .002	0.98 p = .66	1.79 p = .16	0.29 p < .05
Hominoidea (n=46)	0.59 (0.44, 0.73) p = .0001	0.97 p = .55	1.00 p = .40	0.28 p < .05

Box 11.30. Intranasal distance [ΔS_L_YV49] ← Middle cranial fossa length [ΔL_YV78]

Taxon	Maximum likelihood regression coefficient (95% CI) and associated p-value	Shapiro-Wilk test for normality of residuals	Brown & Forsythe's test for residual homoscedasticity	Somers' D nonparametric measure and test of association
Anthropoids (n=300)	-0.08 (-0.16, -0.01) p = .02	0.95 p = .0001	1.86 p = .14	-0.06 ns
Platyrrhini (n=117)	-0.06 (-0.15, 0.03) p = .16	0.97 p = .13	4.53 p = .004	-0.08 ns
Atelidae (n=65)	-0.14 (-0.28, -0.01) p = .04	0.96 p = .14	0.58 p = .63	-0.10 ns
Cebidae (n=52)	0.01 (-0.11, 0.13) p = .89	0.93 p = .004	2.55 p = .07	-0.07 ns
Catarrhini (n=183)	-0.19 (-0.30, -0.08) p = .0006	0.96 p = .0002	3.34 p = .02	-0.13 p < .05
Cercopithecoidea (n=137)	-0.08 (-0.21, 0.04) p = .20	0.97 p = .03	15.93 p = .0001	-0.09 ns
Cercopithecinae (n=87)	-0.28 (-0.40, -0.15) p = .0001	0.93 p = .0003	4.19 p = .008	-0.36 p < .05
Colobinae (n=50)	0.21 (0.10, 0.33) p = .0002	0.96 p = .10	0.51 p = .68	0.35 p < .05
Hominoidea (n=46)	-0.34 (-0.58, -0.10) p = .004	0.86 p = .0001	2.04 p = .12	-0.28 p < .05

Box 11.31. Orbital parallelism [ΔL_YV45] ← Middle cranial fossa length [ΔL_YV78]				
Taxon	Maximum likelihood regression coefficient (95% CI) and associated p-value	Shapiro-Wilk test for normality of residuals	Brown & Forsythe's test for residual homoscedasticity	Somers' D nonparametric measure and test of association
Anthropoids (n=300)	-0.08 (-0.20, 0.04) p = .17	0.97 p = .01	0.48 p = .70	-0.04 ns
Platyrrhini (n=117)	0.15 (-0.07, 0.37) p = .18	0.97 p = .05	0.81 p = .49	0.07 ns
Atelidae (n=65)	0.19 (-0.08, 0.46) p = .16	0.98 p = .78	2.26 p = .09	0.10 ns
Cebidae (n=52)	0.16 (-0.20, 0.53) p = .38	0.93 p = .06	0.27 p = .84	0.06 ns
Catarrhini (n=183)	0.03 (-0.10, 0.16) p = .70	0.98 p = .31	1.85 p = .14	0.05 ns
Cercopithecoidea (n=137)	0.12 (-0.03, 0.27) p = .10	0.99 p = .85	0.75 p = .52	0.10 ns
Cercopithecinae (n=87)	0.06 (-0.14, 0.26) p = .57	0.99 p = .93	0.87 p = .46	0.04 ns
Colobinae (n=50)	0.23 (0.01, 0.44) p = .04	0.97 p = .36	0.45 p = .72	0.19 < .05
Hominoidea (n=46)	-0.25 (-0.51, 0.01) p = .06	0.98 p = .63	0.06 p = .98	-0.10 ns

Box 11.32. Cranial base angle [ΔL_YV70] ← Relative endocranial volume [ΔS_L_YV84]				
Taxon	Maximum likelihood regression coefficient (95% CI) and associated p-value	Shapiro-Wilk test for normality of residuals	Brown & Forsythe's test for residual homoscedasticity	Somers' D nonparametric measure and test of association
Anthropoids (n=300)	-1.63 (-1.90, -1.35) p = .0001	0.96 p = .0001	2.78 p = .04	-0.21 p < .05
Platyrrhini (n=117)	-0.84 (-1.46, -0.23) p = .006	0.92 p = .0001	1.76 p = .16	-0.14 p < .05
Atelidae (n=65)	-0.52 (-1.13, 0.09) p = .09	0.88 p = .0001	2.34 p = .08	-0.12 ns
Cebidae (n=52)	-0.57 (-2.04, 0.91) p = .44	0.92 p = .004	1.30 p = .28	-0.10 ns
Catarrhini (n=183)	-1.70 (-2.03, -1.37) p = .0001	0.95 p = .0001	6.30 p = .0004	-0.18 p < .05
Cercopithecoidea (n=137)	0.32 (-0.35, 0.99) p = .34	0.97 p = .04	3.08 p = .03	-0.03 ns
Cercopithecinae (n=87)	1.22 (0.48, 1.96) p = .001	0.95 p = .005	2.44 p = .07	0.12 ns
Colobinae (n=50)	-3.3 (-4.37, -2.28) p = .0001	0.98 p = .84	0.69 p = .57	-0.46 p < .05
Hominoidea (n=46)	-2.07 (-2.46, -1.67) p = .0001	0.96 p = .23	0.64 p = .59	-0.50 p < .05

Reproduced with permission of the copyright owner. Further reproduction prohibited without permission.

Box 11.33. Cranial base angle [ΔL_YV70] ← Endocranial index [ΔL_YV81]				
Taxon	Maximum likelihood regression coefficient (95% CI) and associated p-value	Shapiro-Wilk test for normality of residuals	Brown & Forsythe's test for residual homoscedasticity	Somers' D nonparametric measure and test of association
Anthropoids (n=300)	-0.31 (-0.43, -0.18) p = .0001	0.91 p = .0001	4.01 p = .008	-0.12 p < .05
Platyrrhini (n=117)	-0.18 (-0.31, -0.05) p = .006	0.93 p = .0001	1.19 p = .31	-0.16 p < .05
Atelidae (n=65)	-0.21 (-0.34, -0.08) p = .001	0.94 p = .008	5.71 p = .002	-0.21 p < .05
Cebidae (n=52)	-0.04 (-0.28, 0.19) p = .71	0.93 p = .01	0.39 p = .76	-0.01 ns
Catarrhini (n=183)	-0.40 (-0.58, -0.20) p = .0001	0.89 p = .0001	3.38 p = .02	-0.14 p < .05
Cercopithecoidea (n=137)	-0.08 (-0.26, 0.10) p = .38	0.96 p = .01	0.78 p = .51	-0.13 p < .05
Cercopithecinae (n=87)	0.16 (-0.07, 0.40) p = .17	0.94 p = .002	1.28 p = .29	-0.04 ns
Colobinae (n=50)	-0.48 (-0.71, -0.24) p = .0001	0.97 p = .40	0.20 p = .90	-0.36 p < .05
Hominoidea (n=46)	-0.73 (-1.13, -0.33) p = .0002	0.94 p = .04	2.22 p = .10	-0.23 p < .05

Box 11.34. Cranial base angle [ΔL_YV70] ← Middle cranial fossa length [ΔL_YV78]				
Taxon	Maximum likelihood regression coefficient (95% CI) and associated p-value	Shapiro-Wilk test for normality of residuals	Brown & Forsythe's test for residual homoscedasticity	Somers' D nonparametric measure and test of association
Anthropoids (n=300)	0.43 (0.30, 0.56) p = .0001	0.94 p = .0001	3.79 p = .01	0.14 p < .05
Platyrrhini (n=117)	0.15 (0.00, 0.31) p = .045	0.90 p = .0001	0.69 p = .57	0.15 p < .05
Atelidae (n=65)	0.35 (0.18, 0.52) p = .0001	0.92 p = .0001	2.73 p = .05	0.27 p < .05
Cebidae (n=52)	-0.04 (-0.27, 0.19) p = .72	0.94 p = .02	1.31 p = .28	0.03 ns
Catarrhini (n=183)	0.83 (0.64, 1.02) p = .0001	0.94 p = .0001	2.89 p = .04	0.26 p < .05
Cercopithecoidea (n=137)	0.32 (0.13, 0.50) p = .0007	0.97 p = .11	0.44 p = .72	0.20 p < .05
Cercopithecinae (n=87)	0.09 (-0.17, 0.35) p = .48	0.93 p = .0002	0.26 p = .85	0.06 ns
Colobinae (n=50)	0.64 (0.43, 0.85) p = .0001	0.98 p = .63	2.27 p = .09	0.50 p < .05
Hominoidea (n=46)	1.64 (1.25, 2.04) p = .0001	0.97 p = .34	0.40 p = .76	0.43 p < .05

Reproduced with permission of the copyright owner. Further reproduction prohibited without permission.

Reproduced with permission of the copyright owner. Further reproduction prohibited without permission.

Box 11.35. Maxillary arch length [ΔS_L_YV14] ← Relative endocranial volume[ΔS_L_YV84]

Taxon	Maximum likelihood regression coefficient (95% CI) and associated p-value	Shapiro-Wilk test for normality of residuals	Brown & Forsythe's test for residual homoscedasticity	Somers' D nonparametric measure and test of association
Anthropoids (n=300)	-0.57 (-0.63, -0.51) p = .0001	0.95 p = .0001	5.79 p = .0007	-0.34 p < .05
Platyrrhini (n=117)	-0.30 (-0.38, -0.21) p = .0001	0.96 p = .009	0.33 p = .80	-0.31 p < .05
Atelidae (n=65)	-0.33 (-0.45, -0.21) p = .0001	0.96 p = .14	3.66 p = .02	-0.35 p < .05
Cebidae (n=52)	-0.27 (-0.42, -0.12) p = .0003	0.97 p = .26	0.56 p = .64	-0.26 p < .05
Catarrhini (n=183)	-0.60 (-0.68, -0.51) p = .0001	0.92 p = .0001	9.54 p = .0001	-0.28 p < .05
Cercopithecoidea (n=137)	-0.61 (-0.75, -0.46) p = .0001	0.95 p = .0007	2.58 p = .06	-0.29 p < .05
Cercopithecinae (n=87)	-0.57 (-0.68, -0.45) p = .0001	0.98 p = .45	0.12 p = .94	-0.39 p < .05
Colobinae (n=50)	-0.79 (-1.13, -0.45) p = .0001	0.95 p = .07	0.65 p = .59	-0.37 p < .05
Hominoidea (n=46)	-0.58 (-0.70, -0.47) p = .0001	0.94 p = .02	1.07 p = .37	-0.24 p < .05

Box 11.36. Maxillary arch length [ΔS_L_YV14] ← Cranial base angle [ΔL_YV70]

Taxon	Maximum likelihood regression coefficient (95% CI) and associated p-value	Shapiro-Wilk test for normality of residuals	Brown & Forsythe's test for residual homoscedasticity	Somers' D nonparametric measure and test of association
Anthropoids (n=300)	0.17 (0.14, 0.19) p = .0001	0.96 p = .0001	15.36 p = .0001	0.28 p < .05
Platyrrhini (n=117)	0.04 (0.01, 0.07) p = .009	0.98 p = .32	1.71 p = .17	0.19 p < .05
Atelidae (n=65)	0.07 (0.02, 0.12) p = .01	0.93 p = .01	1.93 p = .13	0.23 p < .05
Cebidae (n=52)	0.02 (-0.01, 0.05) p = .31	0.96 p = .0001	1.55 p = .21	0.12 ns
Catarrhini (n=183)	0.19 (0.16, 0.22) p = .0001	0.98 p = .18	22.89 p = .0001	0.20 p < .05
Cercopithecoidea (n=137)	0.02 (-0.03, 0.06) p = .48	0.97 p = .04	9.03 p = .0001	0.05 ns
Cercopithecinae (n=87)	-0.06 (-0.10, -0.01) p = .01	0.98 p = .43	5.70 p = .001	-0.12 ns
Colobinae (n=50)	0.13 (0.06, 0.20) p = .0003	0.95 p = .06	0.67 p = .57	0.30 p < .05
Hominoidea (n=46)	0.25 (0.21, 0.29) p = .0001	0.98 p = .60	0.59 p = .62	0.52 p < .05

Reproduced with permission of the copyright owner. Further reproduction prohibited without permission.

Box 11.37. Maxillary arch length [ΔS_L_YV14] ← Cribriform plate orientation [ΔL_YV74]

Taxon	Maximum likelihood regression coefficient (95% CI) and associated p-value	Shapiro-Wilk test for normality of residuals	Brown & Forsythe's test for residual homoscedasticity	Somers' D nonparametric measure and test of association
Anthropoids (n=300)	0.12 (0.10, 0.15) p = .0001	0.90 p = .0001	4.87 p = .003	0.29 p < .05
Platyrrhini (n=117)	0.04 (0.03, 0.05) p = .0001	0.98 p = .53	1.98 p = .12	0.35 p < .05
Atelidae (n=65)	0.05 (0.03, 0.07) p = .0001	0.96 p = .06	2.75 p = .05	0.41 p < .05
Cebidae (n=52)	0.03 (0.01, 0.05) p = .0004	0.96 p = .09	3.33 p = .03	0.23 p < .05
Catarrhini (n=183)	0.21 (0.16, 0.25) p = .0001	0.96 p = .002	13.96 p = .0001	0.20 p < .05
Cercopithecoidea (n=137)	0.05 (0.01, 0.10) p = .02	0.97 p = .05	4.04 p = .009	0.14 p < .05
Cercopithecinae (n=87)	0.03 (-0.01, 0.08) p = .16	0.94 p = .0003	1.21 p = .31	0.12 ns
Colobinae (n=50)	0.09 (0.03, 0.16) p = .005	0.98 p = .63	5.00 p = .004	0.25 p < .05
Hominoidea (n=46)	0.34 (0.28, 0.41) p = .0001	0.96 p = .21	2.32 p = .09	0.37 p < .05

Box 11.38. Maxillary arch length [ΔS_L_YV14] ← Middle cranial fossa length [ΔL_YV78]

Taxon	Maximum likelihood regression coefficient (95% CI) and associated p-value	Shapiro-Wilk test for normality of residuals	Brown & Forsythe's test for residual homoscedasticity	Somers' D nonparametric measure and test of association
Anthropoids (n=300)	0.14 (0.11, 0.18) p = .0001	0.91 p = .0001	12.04 p = .0001	0.13 p < .05
Platyrrhini (n=117)	0.06 (0.03, 0.08) p = .0001	0.97 p = .10	0.78 p = .51	0.29 p < .05
Atelidae (n=65)	0.06 (0.02, 0.11) p = .002	0.94 p = .01	1.85 p = .15	0.29 p < .05
Cebidae (n=52)	0.05 (0.03, 0.07) p = .0001	0.98 p = .68	0.67 p = .57	0.29 p < .05
Catarrhini (n=183)	0.28 (0.22, 0.33) p = .0001	0.94 p = .0001	11.38 p = .0001	0.29 p < .05
Cercopithecoidea (n=137)	0.14 (0.09, 0.18) p = .0001	0.97 p = .36	2.09 p = .10	0.27 p < .05
Cercopithecinae (n=87)	0.08 (0.03, 0.13) p = .002	0.95 p = .008	1.04 p = .38	0.24 p < .05
Colobinae (n=50)	0.21 (0.15, 0.26) p = .0001	0.97 p = .48	0.67 p = .57	0.47 p < .05
Hominoidea (n=46)	0.46 (0.34, 0.58) p = .0001	0.95 p = .12	1.54 p = .22	0.30 p < .05

Reproduced with permission of the copyright owner. Further reproduction prohibited without permission.

Box 11.39. Partial regression of cribriform plate orientation [ΔL_YV74] on endocranial volume [ΔS_L_YV84] and endocranial index [ΔL_YV81

Taxon	ML partial regression coefficient (95% CI, and p-value) of cribriform plate orientation on relative endocranial volume controlling for endocranial index	ML partial regression coefficient (95% CI, and p-value) of cribriform plate orientation on endocranial index controlling for relative endocranial volume	Shapiro-Wilk test for normality of residuals	Brown & Forsythe's test for residual homoscedasticity
Anthropoids (n=300)	-1.80 (-2.11, -1.49) p = .0001	-0.07 (-0.20, 0.05) p = .24	0.98 p = .46	1.15 p = .33
Platyrrhini (n=117)	-4.89 (-5.77, -4.02) p = .0001	-0.18 (-0.36, 0.00) p = .053	0.99 p = .95	1.57 p = .20
Atelidae (n=65)	-5.67 (-6.62, -4.72) p = .0001	-0.33 (-0.55, -0.12) p = .002	0.98 p = .61	1.08 p = .36
Cebidae (n=52)	-5.01 (-7.31, -2.71) p = .0001	-0.11 (-0.47, 0.26) p = .56	0.95 p = .07	0.98 p = .42
Catarrhini (n=183)	-1.35 (-1.63, -1.06) p = .0001	-0.11 (-0.24, 0.03) p = .12	0.99 p = .79	0.18 p = .91
Cercopithecoidea (n=137)	-0.89 (-1.55, -0.24) p = .007	-0.17 (-0.35, 0.00) p = .052	0.98 p = .80	0.55 p = .65
Cercopithecinae (n=87)	-0.53 (-1.24, 0.19) p = .14	-0.16 (-0.38, 0.06) p = .15	0.98 p = .50	0.13 p = .94
Colobinae (n=50)	-2.70 (-4.25, -1.15) p = .0005	-0.06 (-0.36, 0.23) p = .66	0.98 p = .81	0.48 p = .69
Hominoidea (n=46)	-1.54 (-1.85, -1.23) p = .0001	0.00 (-0.19, 0.19) p = .96	0.97 p = .42	0.42 p = .74

Box 11.40. Partial regression of cribriform plate orientation [ΔL_YV74] on cranial base angle [ΔL_YV70] and endocranial volume [ΔS_L_YV84]

Taxon	ML partial regression coefficient (95% CI, and p-value) of cribriform plate orientation on cranial base angle controlling for relative endocranial volume	ML partial regression coefficient (95% CI, and p-value) of cribriform plate orientation on relative endocranial volume controlling for cranial base angle	Shapiro-Wilk test for normality of residuals	Brown & Forsythe's test for residual homoscedasticity
Anthropoids (n=300)	0.13 (0.01, 0.24) p = .03	-1.67 (-2.01, -1.33) p = .0001	0.98 p = .50	3.98 p = .008
Platyrrhini (n=117)	-0.09 (-0.35, 0.18) p = .52	-5.04 (-5.95, -4.12) p = .0001	0.99 p = .98	2.58 p = .06
Atelidae (n=65)	0.16 (-0.24, 0.56) p = .42	-5.26 (-6.27, -4.24) p = .0001	0.98 p = .45	0.91 p = .44
Cebidae (n=52)	-0.11 (-0.48, 0.27) p = .57	-5.41 (-7.40, -3.42) p = .0001	0.96 p = .10	1.05 p = .38
Catarrhini (n=183)	0.23 (0.13, 0.33) p = .0001	-1.07 (-1.37, -0.79) p = .0001	0.98 p = .69	0.00 p = .99
Cercopithecoidea (n=137)	0.31 (0.16, 0.46) p = .0001	-1.19 (-1.79, -0.59) p = .0001	0.99 p = .79	0.64 p = .59
Cercopithecinae (n=87)	0.20 (0.00, 0.40) p = .047	-0.89 (-1.62, -0.16) p = .02	0.98 p = .53	0.43 p = .73
Colobinae (n=50)	0.54 (0.21, 0.89) p = .001	-1.06 (-02.72, 0.60) p = .20	0.99 p = .94	0.36 p = .78
Hominoidea (n=46)	0.14 (-0.02, 0.31) p = .07	-1.23 (-1.63, -0.84) p = .0001	0.97 p = .36	0.51 p = .68

Box 11.41. Partial regression of facial prognathism [ΔL_YV30] on cranial base angle [ΔL_YV70] and cribriform plate orientation [ΔL_YV74]

Taxon	ML partial regression coefficient (95% CI, and p-value) of facial prognathism (Krogman's angle) on cranial base angle controlling for cribriform plate orientation	ML partial regression coefficient (95% CI, and p-value) of facial prognathism (Krogman's angle) on cribriform plate orientation controlling for cranial base angle	Shapiro-Wilk test for normality of residuals	Brown & Forsythe's test for residual homoscedasticity
Anthropoids (n=300)	0.24 (0.16, 0.32) p = .0001	0.31 (0.24, 0.38) p = .0001	0.98 p = .61	6.17 p = .0004
Platyrrhini (n=117)	0.14 (-0.02, 0.30) p = .08	0.30 (0.22, 0.38) p = .0001	0.97 p = .051	0.78 p = .51
Atelidae (n=65)	0.36 (0.08, 0.64) p = .01	0.39 (0.28, 0.49) p = .0001	0.97 p = .42	0.58 p = .68
Cebidae (n=52)	0.07 (-0.09, 0.24) p = .37	0.14 (0.04, 0.24) p = .004	0.97 p = .35	0.72 p = .55
Catarrhini (n=183)	0.23 (0.15, 0.32) p = .0001	0.45 (0.34, 0.57) p = .0001	0.99 p = .90	7.96 p = .0001
Cercopithecoidea (n=137)	0.07 (-0.04, 0.19) p = .22	0.32 (0.19, 0.44) p = .0001	0.98 p = .25	7.23 p = .0002
Cercopithecinae (n=87)	-0.06 (-0.20, 0.07) p = .36	0.29 (0.15, 0.44) p = .0001	0.97 p = .11	0.75 p = .53
Colobinae (n=50)	0.45 (0.21, 0.69) p = .0001	0.18 (-0.03, 0.39) p = .09	0.98 p = .58	2.53 p = .07
Hominoidea (n=46)	0.20 (0.04, 0.37) p = .01	0.67 (0.44, 0.91) p = .0001	0.97 p = .39	1.04 p = .38

Reproduced with permission of the copyright owner. Further reproduction prohibited without permission.

Bivariate Scatter Plots

Selected bivariate scatter plots are presented in Box 11.42. Refer to Boxes 11.15-11.32 for parameter estimates of the regression slopes.

Box 11.42 Scatter plots of delta log endocranial and nasomaxillary variables.

Endocranial index ← Rel. endocranial volume

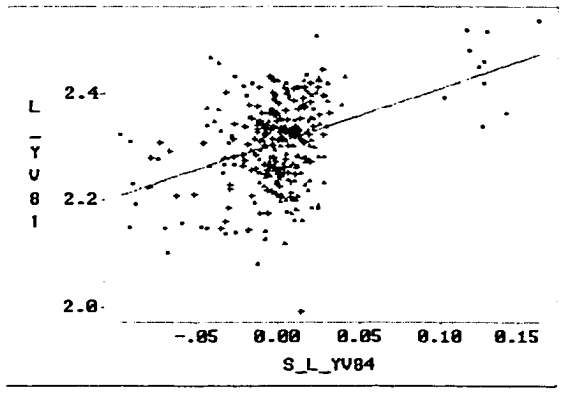

Cribriform orientation ← Rel. endocranial vol.

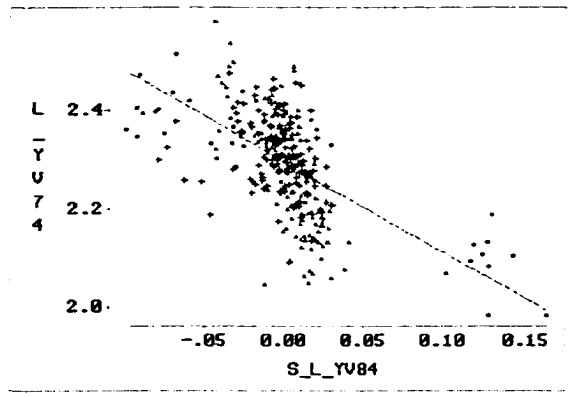

Cranial base flexion ← Rel. endocranial volume

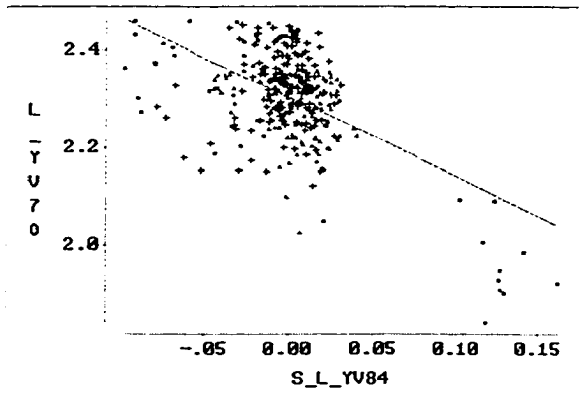

M. cranial fossa length ← Rel. endocranial vol.

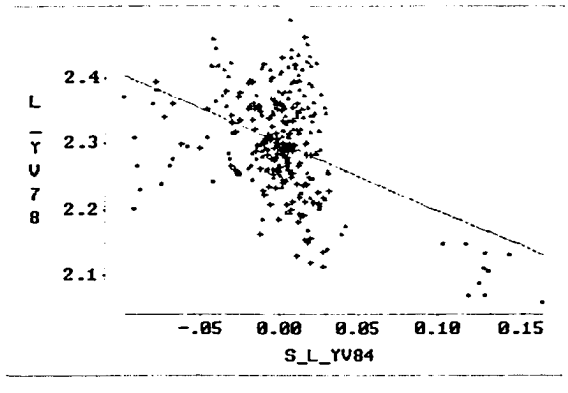

Endocranial index ← M. cranial fossa length

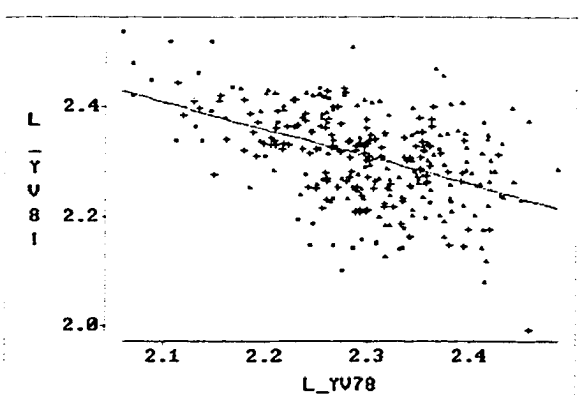

Ant. cranial fossa length ← Rel. endocranial vol.

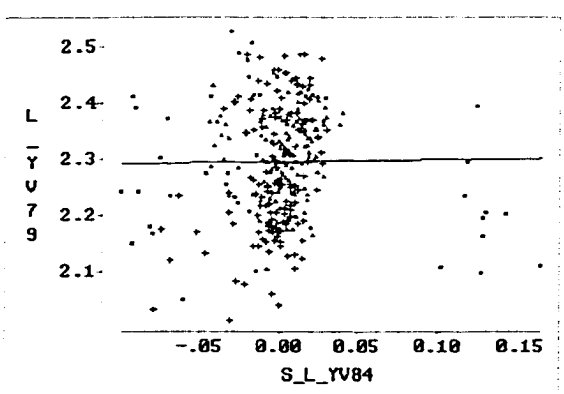

Reproduced with permission of the copyright owner. Further reproduction prohibited without permission.

Box 11.42 Scatter plots of delta log endocranial and nasomaxillary variables.

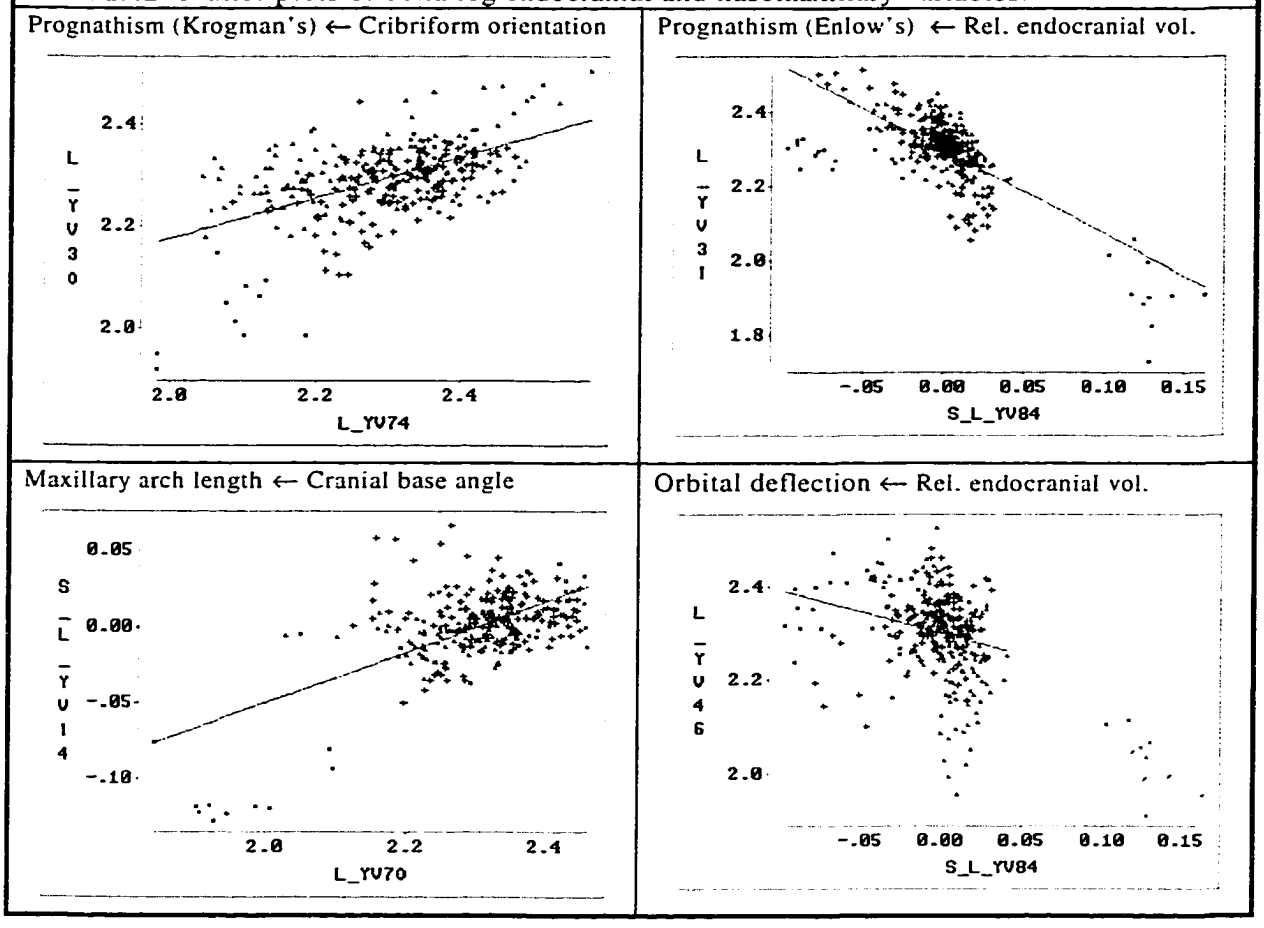

Midfacial-Cribriform Angle and the Concept of Angular Invariance

A key elements of Enlow's hypotheses on the effects of brain size and shape on craniofacial form is the relationship between the inclination of the olfactory bulbs (and underlying cribriform plates) and the nasomaxillary complex. Recall that Enlow and McNamara (1973) observed that "...more than thirty species representing different rodents, lagomorphs, marsupials, primates, carnivores, and artiodactyls... all show an approximately perpendicular relationship..." between the cribriform plane and midfacial plane. The maintenance of this relatively invariant 90° during craniofacial growth implies that any change in the orientation of the cribriform

Reproduced with permission of the copyright owner. Further reproduction prohibited without permission.

plates will have a corresponding rigid translational effect on the orientation of the midfacial plane.

Means and standard deviations of the midfacial-cribriform angle are reported for various taxa in Box 11.37. It can be seen that the mean for all anthropoids in the sample is not significantly different from 90°(at α=0.05), nor are the subgroup means for Platyrrhini and Hominoidea. Cercopithecoids, however, exhibit a midfacial-cribriform angle that is significantly lower than 90°, although only by a few degrees.

Box 11.43. Means and standard deviation (SD) for midfacial-cribriform angle for various anthropoid taxa.

Taxonomic group	Mean angle (95% CI)	SD (in degrees)
Anthropoidea (n=300)	89.3 (88.5, 90.0)	5.7
Platyrrhini (n=117)	90.8 (89.4, 92.3)	6.1
Catarrhini (n=183)	88.2 (87.1, 89.4)	5.5
Cercopithecoidea (n=137)	87.8 (86.9, 88.8)	5.7
Colobinae (n=50)	87.9 (86.3, 89.4)	5.4
Cercopithecinae (n=87)	87.8 (86.6, 89.1)	5.9
Hominoidea (n=46)	89.3 (87.9, 90.8)	4.8

The implication of Enlow's observations and hypothesis is that some biological constraint is acting on certain elements of the craniofacial skeleton to maintain an approximately perpendicular angle between the midfacial plane and cribriform plates. The relationships among biological constraints, angular invariance, isometry and inferential testing are complex, and a misunderstanding of these concepts has led to some confusion in the literature.

First, it should be made clear that geometric invariance (*senso stricto*) and isometry are equivalent descriptive concepts with respect to shape variables (see Box 10.5, C & D). In Chapter 10, I argued that isometry will result if (1) no causal

Reproduced with permission of the copyright owner. Further reproduction prohibited without permission.

agents are acting on the shape variable in question other than a scaling effect (the character is said to be "selectively neutral" in Neo-Darwinian terms), or (2) a biological constraint strong enough to predominate over other nomological agents is acting on the shape variable, or the competing and equally opposed causal agents are acting on a given shape variable (e.g., stabilizing selection). In practice it is difficult to determine which of these processes is responsible for a given incident of observed isometry. But regardless of which process is responsible for geometrical invariance (or isometry), some variation is inevitable, and the pattern of this variation may give us some clues as to which mechanism is involved. We might expect, for example, that in the case of scaling isometry, variance will be small and dispersion random. By contrast, in the case of geometrical invariance due to the operation of one of more biological constraints or competing forces, while variance may also be small dispersion may be nonrandom. This is because the strength and operation of such constraints can vary in the face of changing nomological forces. In other words, constraints are often conditional, varying in strength and regulatory properties with size, physiology, environmental conditions, or taxonomic affinity (genetic background). In analytical language this phenomenon is called an *interaction effect* (i.e., when the effect of a given independent variable on the dependent variable changes at each level of a third variable). For example, Cheng *et al.* (1997) have shown that the effects of mechanical loads on bone deposition and resorption vary depending on the levels of estrogen, testosterone, prostanoid and prostaglandin hormones in the body. This raises the possibility that biological constraints on bone growth and morphogenesis may differ between males and female, among age groups, or even among different taxa with varying physiological

Reproduced with permission of the copyright owner. Further reproduction prohibited without permission.

properties and requirements (see discussion on biological constraints in Chapter 2, p. 42).

Failure to recognize this property of the variation produced in association with morphogenetic constraints has led to some confusion and misapplications in evolutionary morphology. Since the pattern of variation generated by scale isometry is different from that produced by constraint invariance, it follows that standard tests for the former do not equally apply to the latter. Consequently, the question of how much variation is 'acceptable' in order to recognize the existence of a biological constraint has yet to be adequately addressed.

A recent examination of these issues is provided by Ravosa and Shea (1994), who devised four criteria for assessing angular invariance. These included: (1) no significant correlation between the proposed invariant angle and size, (2) no significant differences between the angular means of various subtaxa, (3) a low angular standard deviation compared to other angles, and (4) a low angular coefficient of variation (CV) compared to other angles. Three of the four criteria can be readily dismissed. The notion that character invariance resulting from a morphogenetic constraint on form should not be correlated with size holds no theoretical or analytical credibility. As I have already mentioned, such non-random variation is expected if interactive effects are in operation. Ravosa and Shea (1994) have conflated invariance with independence, and isometry due to scaling effects with geometric invariance due to constraint. By adhering to a strict criterion of invariance that is independent of covariate interaction effects (i.e., taxa or size, and one could also include sex, age, habitat, etc.), these authors provide an untenable model for the identification of biological constraints, a model that contains no

Reproduced with permission of the copyright owner. Further reproduction prohibited without permission.

provisions for examining how a given constraint behaves under varying genetic and environmental conditions.

Aside from these theoretical and substantive objections, there are, in addition, several analytical problems with their choice of analyses. Since the correlation coefficient is partly determined by the variance of the variables under study it cannot be used as an independent test of the degree of variability exhibited by a character. Likewise, ANOVA tests for mean differences among taxa are invalid tests of invariance because they are variance standardized. In an ANOVA the among-groups variance is assessed in relation to the total (pooled within-groups) variance, and therefore, variables with high total variance are no more or less likely to exhibit significant mean differences among taxa than variables with low total variance. More informative would have been Cochran's C or the Bartlett-Box test for homogeneity of variance. Use of the coefficient of variation (CV) with angular measures is an even more obvious transgression of morphological analysis. The CV was designed as a measure of variability that takes into account the size of the structures being measured (Pearson, 1956). It is valid only when applied to size-dependent variables such as linear distances; and it is invalid when applied to angles and other shape variables that are size-independent. Simpson *et al.* (1960) aptly expressed this principle as follows: "The valid use of *V* [coefficient of variation] depends on the assumption that variation as a biological function is relative to absolute size or, in terms of distributions, that absolute dispersion increases in direct proportion to the mean [size]" (p. 90). Since the variances of angular measures are not expected to covary with their means, "...use of the coefficient of variability in comparisons involving the variability of morphological relationships [such as

Reproduced with permission of the copyright owner. Further reproduction prohibited without permission.

'angular relationships'] can lead to completely erroneous conclusions" (Zingeser, 1973:248).

Measures of dispersion (such as the standard deviation) remain the only valid measures of variability for angular data. But how is one to determine the level of variability that is acceptably low enough to indicate the operation of a biological constraint? Ravosa and Shea (1994:808), who collected data on 15 angular variables, suggested that "...a SD that falls in the lowest one-third of... all 15 angular SDs..." may be taken to indicate angular invariance. But this seems rather arbitrary—why the lowest one-third as opposed to the lowest one-quarter or one-half? Enlow and McNamara (1973), and later Enlow and Azuma (1975), implied that relative invariance is exhibited by angular measures characterized by a standard deviation of 6° or less (which is actually quite similar to the mark of 6.3° eventually adopted by Ravosa and Shea), although these authors give no justification for this particular cut-off point. The standard deviation of 5.7° for the midfacial-cribriform angle of the *total* anthropoid sample fits either of these criteria for relative invariance.

Ravosa and Shea (1994) reported a mean of 90° and a standard deviation (SD) of 12.37° for the midfacial-cribriform angle in a sample of cercopithecid monkeys (n=79). These authors consider this magnitude of variance too great to

Reproduced with permission of the copyright owner. Further reproduction prohibited without permission.

be deemed "invariant," or act as a constraint on craniofacial growth.[13]

The mean midfacial-cribriform angle computed for all 300 anthropoid specimens in this study is 89.3°, which is not significantly different from the 90° degree angle reported by both Enlow and McNamara (1973) and Ravosa and Shea (1994). The standard deviation for the entire sample was found to be 5.7°, similar to the value of 6° reported for a smaller but more diverse sample of mammals by Enlow and McNamara (1973) but less than half the standard deviation reported by Ravosa and Shea (1994).

The discrepancy between studies may be due to dissimilar measurement techniques. In both the present investigation and that of Enlow and McNamara (1973) some form of labeling technique was used to aid in the identification of the cribriform plate (brass filings and lead markers, respectively). Ravosa and Shea (1994) used no such method, a shortcoming that may have introduced additional measurement error into the data. High measurement error, since it is random, will

---

[13] In fact, Ravosa and Shea (1994) used two distinct sets of landmarks to identify the cribriform plate, which they called (A) and (B). They define cribriform plate (A) as a "line connecting the anteriormost and posteriormost aspects of the cribriform plate at the ethmoid/nasal cavity junction," and (B) was taken as the "line connecting the anteriormost and posteriormost aspects of the cribriform plate at the anterior cranial base" (p. 819). For comparison, I used the data for their cribriform plate/midfacial angle (A), which appears to correspond closest to Enlow's original definition. They report a smaller standard deviation (9.84°) for their cribriform plate/midfacial plane (B) measurement. The authors justify the use of the two separate measures "...so as to represent variation adequately in this region... especially since Enlow did not specify to which portions of the cribriform plate a plane must be fit" (p. 819). Two points must be made. First, Enlow and McNamara (1973) specified precisely and in great detail how a plane should be fit to the cribriform plate. They provided photographs of midsagittally sectioned skulls, lateral radiographs, and headfilm tracings each with arrows or other markers indicating the precise locations of the landmarks used to define the cribriform plate (e.g., *ibid.*, Figs. 4, 5 & 6). Extensive word descriptions are also given in numerous publications (e.g. Enlow & McNamara, 1973, p.265; Enlow, 1975; Enlow & Azuma, 1975, p. 227). The second point is that there is no need to distinguish separate pairs of endpoints of the cribriform plate, one pair at the anterior cranial base and the other at the ethmoid/nasal cavity. The cribriform plate is a thin wafer of bone with distinct anterior and posterior ends. What Ravosa and Shea might have mistaken for as a second pair of plate ends is likely the anteriormost and posteriormost junctions of the olfactory recess with the anterior cranial floor, and not the cribriform plate itself.

Reproduced with permission of the copyright owner. Further reproduction prohibited without permission.

not affect the mean, but it will lead to overestimated measures of dispersion (such as standard deviation), a pattern consistent with Ravosa and Shea's reported results.

To test for geometrical invariance due to constraint, a more biologically and analytically valid approach is to ask the question: Is the degree of angular variability low enough to produce a coordinated effect between the two planes whose intersection forms the angle in question? A given angle is invariant, or more correctly 'constrained,' if each of the two arms forming the angle, measured against a common reference plane, yields a regression coefficient significantly different from zero (assuming that the two arm-to-reference plane angles exhibit sufficient variance). For example, a 'perfect' constraint will be manifest as a constant angle, and in such cases the slope of the regression between the two arms (each measured in degrees from a common baseline) will be equal to -1.0 because each increase of 1° in one arm will translate to a decrease of 1° in the other. This is shown diagrammatically in Box 11.44: if angle c to c' is constrained, then as the complex rotates (solid to dotted lines), for every 1° increase in angle b to b' there will be a corresponding 1° decrease in angle a to a'.

Box 11.44. If angle *c* to *c'* remains constant, an increase of 1° from angle *a* to *a'* will result in a decrease of 1° in angle *b* to *b'*.

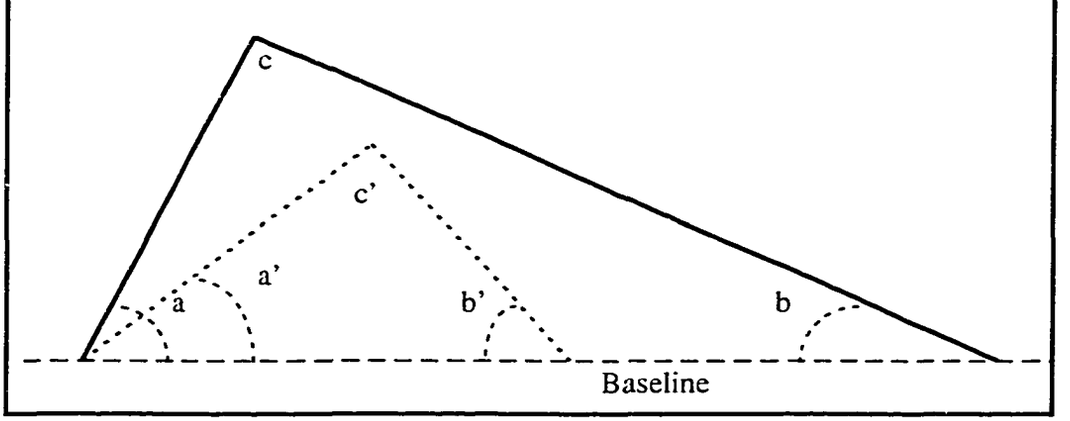

Reproduced with permission of the copyright owner. Further reproduction prohibited without permission.

Empirical regression slopes, measured in the manner described, that are not significantly different from -1.0 indicate a perfect constraint-mediated interdependence between the arms forming the angle in question, and this interdependence is manifested as angular invariance

This regression-based test of angular invariance was applied to eight of the angular variables included in the present investigation,[14] and the results are given in Box 11.45.

Box 11.45. Angular variables listed in order of increasing standard deviation (SD).

Angle	Mean	SD	Regression-based Test of Angular Invariance
(NA) Horizontal orbital orientation [Y45-ORBSCR]	21.0	3.10	NA (bilateral angle)
*Angle of orbital TC rotations [Y48-ORBA12]	82.4	4.65	-1.45 (-1.61, -1.30), R^2=0.53, $p < .01$
*Orbital deflection [Y46-ORBTC1]	19.6	4.90	-0.89 (-1.00, -0.78), R^2=0.46, $p < .01$
*Occlusal plane [Y32-SLOPOC]	9.2	4.95	-0.72 (-0.80, -0.63), R^2=0.49, $p < .01$
*Cribriform-midfacial angle [Y71-ENLWCP]	89.3	5.70	-0.87 (-0.93, -0.84), R^2=0.54, < = .01
Angle of facial prognathism [Y31-ENLOAG]	126.3	6.85	0.06 (-0.01, 0.13), R^2=0.01, ns
Inclination of foramen magnum [Y68-SLOPFM]	20.8	7.47	-0.05 (-0.27, 0.17), R^2=0.00, ns
Slope of cribriform plate to occlusal plane [Y75-SLOCPO]	39.7	8.70	-0.09 (-0.31, 0.13), R^2=0.02, ns
Cranial base flexion [Y70-CBFLEX]	167.2	10.12	0.05 (-0.02, 0.11), R^2=0.01, ns
(NA) Paranasal plate orientation [Y35-PPNALO]	40.1	10.92	NA (bilateral angle)

An obvious pattern emerges from the data presented in Box 11.45: angles whose SDs are greater than 6° fail the regression-based test of angular invariance, whereas angles with SD below this threshold yield positive results. Whether this

[14] It should be noted that the regression-based test of constraint-mediated invariance is also valid for bilateral angles but because the principle of bilateral symmetry is associated with different expected angular relationships the coefficient is expected to be *positive* and significantly different from zero.

Reproduced with permission of the copyright owner. Further reproduction prohibited without permission.

pattern is a consequence of some underlying trigonometric function, some general biological rule, or shear coincidence will require further investigation. The foregoing analysis supports Enlow's original hypothesis that the 90° angle maintained between the cribriform plate and the midfacial plane is due to the operation of a biological constraint.

Preliminary Tests of Hypotheses

Several of the hypotheses listed in Box 11.2 gain at least preliminary support from the PCA and bivariate regression results.

Hypothesis (A). The predicted negative association between endocranial volume and centroid size is confirmed for the anthropoid data (see Boxes 11.8 - 11.11, 11.15). Thus, Weidenreich's (1941) hypothesis that body size influences the size of the brain such that larger mammals tend to have relatively smaller brains cannot be rejected with respect to anthropoids. There are, however, certain exceptions: *Homo sapiens* exhibits a much larger brain size than would be expected on the basis of body size (or, more correctly, a much greater increase in brain size than would be expected on the basis of increased body size, from its last shared ancestor [LSA]). Moreover, the regression slope of log delta cube root endocranial volume on log delta centroid size is not homogeneous across anthropoid taxa. The nomological relationship tends to be nearly isometric in New World monkeys (Boxes 11.11, 11.15), especially Cebids; whereas among catarrhines the slope indicates a negative allometric relationship (Boxes 11.10, 11.15).

Hypothesis (B). Both the PCA results and the bivariate regression analysis confirms the prediction that endocranial index is positively correlated with relative

Reproduced with permission of the copyright owner. Further reproduction prohibited without permission.

endocranial volume. Weidenreich's (1941) hypothesis that the relative size of the brain affects its shape such that mammals with larger brains relative to body size exhibit brachycephaly cannot be rejected with respect to anthropoids. The one exception to this generalization appears to be Atelidae, for which no relationship between brain size and shape is apparent in the data (Box 11.16).

Hypothesis (C). The statistical prediction that cribriform plate orientation will covary with anterior cranial fossa length is tentatively rejected on the basis of the PCA and regression results (Box 11.17). The hypothesis of Enlow and McNamara (1973) that expansion of the frontal lobes of the brain forces the underlying cribriform plates into a more horizontal orientation is therefore refuted with respect to anthropoids.[15] [16] However, the related predictions that cribriform plate orientation will be negatively correlated with both relative endocranial volume and endocranial index can be accepted on the basis of the preceding analyses (Boxes 11.18 & 11.19). The atelids again appear to be an exception to the general anthropoid rule that as the brain becomes more globular (i.e. brachyendocephalic) the cribriform plate becomes more horizontally oriented. Thus, Enlow's (1975) hypotheses that relative brain size and brain shape affect the orientation of the cribriform plate, or more specifically, that large relative brain size and globular brains produce horizontally oriented cribriform plates, cannot be refuted with respect to the majority of anthropoid primates.

---

[15] The prediction appears to hold for cercopithecines, but even here the association is weak (see Box 11.17)

[16] This hypothesis test outcome assumes that relative anterior cranial fossa length is a valid measure of frontal lobe size.

Reproduced with permission of the copyright owner. Further reproduction prohibited without permission.

Hypothesis (D). The regression-based test for invariance confirmed the predictions that the cribriform-midfacial angle exhibits statistically significant angular invariance, and that the mean angle is not significantly different from 90°. Based on this evidence I conclude that Enlow and McNamara's (1973) hypothesis that the angle formed by the cribriform plates and the midfacial plane is constrained to approximate a 90° angle cannot be refuted with respect to anthropoids.

The second component of Hypothesis (D) predicts that cribriform plate orientation will be positively associated with both measures of facial prognathism (Boxes 11.22 & 11.23). This prediction can be confirmed on the basis of the PCA and bivariate regression results. In fact, the observed association between cribriform plate orientation and facial prognathism is quite consistent across anthropoid groups: there are no exceptions here. Hence, the hypothesis advanced by Enlow and McNamara (1973) that changes in the orientation of the cribriform plate, due to its invariant relationship with the midfacial plane, can effect changes in the degree of facial prognathism cannot be rejected for anthropoids.

Hypothesis (E). Hypothesis E predicts that orbital deflection will be negatively associated with relative anterior cranial fossae length. However, since no such association was found (with the possible exception of Cebidae, see Box 11.27), this prediction is rejected. Therefore, the hypothesis advance by Cartmill (1972), and later by Enlow and McNamara (1973), that expansion of the frontal lobes of the brain causes a reduction in the vertical deflection of the orbits can be refuted with respect to anthropoids. The related hypothesis that the shape of the brain has an effect on orbital deflection in anthropoids can also be refuted, since no significant association was found between orbital deflection and endocranial index (Box 11.28).

Reproduced with permission of the copyright owner. Further reproduction prohibited without permission.

The only craniometric variable found to be associated with orbital deflection was cranial base angle: the wider the angle the greater the upward deflection of the orbits (here again, cebids are the one exception; see Box 11.29).

Hypothesis (F). The statistical prediction, deduced from Hypothesis F, that intranasal breadth will be negatively associated with relative middle cranial fossae length is not supported for all anthropoid taxa. The data reveal no relationship within platyrrhines, and a conflicting pattern within catarrhines. The expected negative association is apparent within cercopithecines and hominoids, but colobine monkeys manifest the opposite trend (Box 11.30). As a consequence, Enlow's (1975) hypothesis that the relative expansion of the temporal lobes force the orbits closer together may be consistent with some, but not all, anthropoid groups. The related hypothesis that relative temporal lobe size has an effect on orbital parallelism was also tested and refuted (again, assuming that relative cranial fossa length is an accurate proxy for neocortical lobes size) (Box 11.31).

Hypothesis (G). Biegert's (1957) hypothesis that an increase in relative brain size produces an increase in cranial base flexion predicts that relative endocranial volume will be negatively correlated with cranial base angle. An examination of the results in Box 11.32 reveals a complex picture. While the slope of the regression line is significantly different from zero (and in a negative direction) for Anthropoidea (and the infraordinal subgroups Platyrrhini and Catarrhini), many of the taxonomic groups within these major taxa show no statistically significant relationship between relative brain size and cranial base flexion. For instance, the within-group analyses of Atelidae, Cebidae, and Cercopithecinae failed to reveal any significant relationships between these two characters. By contrast Colobinae and

Reproduced with permission of the copyright owner. Further reproduction prohibited without permission.

Hominoidea both manifest strong significant negative associations: the greater the relative brain size the smaller the cranial base angle (Box 11.32). Since the prediction cannot be confirmed for all anthropoid groups, Biegert's hypotheses can be refuted, at least in terms of a nomological agent that is ubiquitous for all Higher Primates. Nor can the case be made for an anthropoid-wide nomological effect of brain shape (as measured by endocranial index) on cranial base flexion: analyses reveal significant associations between brachyendocephaly and cranial base flexion in all anthropoid groups except Cebidae and Cercopithecinae (Box 11.33).

Conclusions

Exploratory and confirmatory analyses of the anthropoid data tentatively confirm (i.e., fail to refute) several proposed hypotheses relating to the effects of the brain on nasomaxillary form. Weidenreich's (1941) hypothesis that relative brain size is one of the key determinants of craniofacial morphology appears to hold for anthropoid primates. Further, the data are consistent with the hypothesis that the influence of relative brain size on nasomaxillary form is mediated through the chondrocranium, specifically the spheno-ethmoid complex. Enlow and McNamara's (1973) hypothesis that relative brain size effects a more horizontal orientation of the olfactory bulbs and underlying cribriform plates cannot be rejected. However, at this time it is not clear how relative brain size influences cribriform plate alignment. The hypothesis that expansion of the frontal lobes pushes the plates into a more horizontal orientation is not supported by the anthropoid data. However, due to the lack of confidence regarding the accuracy of the variable 'relative anterior fossa length' as a measure of relative frontal lobe size, I recommend that this hypothesis

Reproduced with permission of the copyright owner. Further reproduction prohibited without permission.

be given consideration in future research, with more refined operationalization of this character.

Nor does the degree of brachyendocrany (i.e., width-to-length ratio of the endocranial cavity) appear to have an effect on cribriform plate orientation, independently of relative brain size (Box 11.39). In other words, brachyendocephalic brains do not exhibit a more horizontal orientation of the cribriform plates than do dolichoendocephalic brains of the same size. On the other hand, relatively larger brains do exhibit more horizontal cribriform plates than relatively smaller brains, even when their shapes are the same. Apparently, some as yet unknown property of relative brain size may be responsible for cribriform plate orientation. Perhaps an analysis of the relative contributions of the M-level and Q-level components of the data will shed some light on the nomological mechanisms involved in this unresolved process (see Chapter 15).

The analyses failed to refute Enlow and McNamara's (1973) hypothesis that a biological constraint acts to maintain an invariant 90° angle between the cribriform plate and the midfacial plane, a constraint that underlies the covariance between these traits and helps explain much of the variation of facial prognathism observed in anthropoids.

The previous analyses are also consistent with the hypothesis, first introduced in the context of craniofacial growth in Chapter 9, that as facial prognathism increases, the anterior facial skeleton must also increase in order to maintain the slope of the occlusal plane within functionally acceptable limits (Boxes 11.29, 11.31). Furthermore, due to the part-counterpart relationship between the

Reproduced with permission of the copyright owner. Further reproduction prohibited without permission.

anterior face and the maxillary arch, increases in one must be matched by corresponding increases in the other.

Relative brain size and temporal lobe length do appear to have an effect on cranial base flexion in some, but not all, anthropoid taxa. Increased brain size and/or shortening of the temporal lobes is associated with cranial base flexion in Atelidae, Colobinae and Hominoidea.

It is of interest that, when the effects of relative brain size are taken into account, cranial base flexion has no effect on cribriform plate orientation (except perhaps in colobine monkeys) (see Box 11.40). This is surprising given the close connection between the sphenoid and ethmoid bones. Together these bones form the anterior segment of the chondrocranium. They articulate over a wide area of contact that appears as the spheno-ethmoidal synchondrosis on the endocranial surface of the planum sphenoideum. That the cranial base and cribriform plates do not covary independently of relative brain size indicates a degree of independent development of these two closely articulated skeletal elements.

Another interesting finding is that the degree of facial prognathism covaries with cribriform plate orientation regardless of the degree of cranial base flexion in all major anthropoid taxa except Colobinae (Box 11.41). Thus, the orientation of the cribriform plate (and presumably also the ethmoid) and cranial base flexion appear to affect facial prognathism somewhat independently.

The various hypotheses attributing the position and orientation of the orbits to relative brain size, brain shape or relative frontal lobe size were rejected with regard to anthropoid primates. No significant anthropoid-wide associations were found between orbital deflection, orbital parallelism or intranasal breadth on the one

Reproduced with permission of the copyright owner. Further reproduction prohibited without permission.

hand, and relative endocranial volume, endocranial index, anterior cranial fossa length or middle cranial fossa length on the other.

I must emphasize that the results of the preceding analyses and the conclusions based on these results are preliminary and tentative. The potential effects of other causal agents, such as olfaction, locomotion and mastication, have not been included in the various models examined in this chapter. Inclusion of these agents in subsequent models may change the results of tests of association between brain form and nasomaxillary morphology. In addition, no distinction was made in this chapter concerning the separate effects of M-level and Q-level causal mechanisms (see Chapter 8). These issues will be addressed more fully in Chapter 15.

Reproduced with permission of the copyright owner. Further reproduction prohibited without permission.

Reproduced with permission of the copyright owner. Further reproduction prohibited without permission.

NOMOLOGICAL MECHANISMS OF ANTHROPOID NASOMAXILLARY DIVERSITY

by

James M. McMahon

VOLUME II

A dissertation submitted to the Graduate Faculty in Anthropology in partial fulfillment of the requirement for the degree of Doctor of Philosophy, The City University of New York

1999

Reproduced with permission of the copyright owner. Further reproduction prohibited without permission.

PART V

Nomological Hypothesis Testing (Adaptations)

Reproduced with permission of the copyright owner. Further reproduction prohibited without permission.

Chapter 12. Olfaction

Introduction

The sense of smell has played a major role in the evolution of animal life on Earth. Phylogenetically, olfaction is found in insects and (independently) in all major vertebrate groups (Orton, 1878; Wallace, 1973). Olfactory mechanisms play a primary role in the survival and reproductive behavior of most fish and reptiles, but are poorly developed in birds (Romer & Parsons, 1985). In mammals, the importance of olfaction varies from virtually nonexistent in whales and some microchiropteran bats to predominant in moles, and in some carnivorous and herbivorous species (Barton *et al.*, 1995; Eisthen, 1997). Compared to other mammals, Higher Primates are not generally thought to possess a well developed sense of smell, but recent evidence suggests that the importance of olfaction in anthropoid lifeways may have been underestimated (Zeller, 1987).

The maxillary part of the olfactory organ is closely tied structurally to the nasal cavity and intranasal space. Typically, the upper one-third of the nasal cavity, which includes the superior nasal conchae and the nasal roof and superior lateral and medial walls, is lined with olfactory mucosa, a wet spongy tissue containing the olfactory receptors. Accordingly, the size of the nasal cavity may be due, at least in part, to the size of the olfactory apparatus (van der Klauuw, 1946). In this chapter I review several hypotheses relating to the effects of olfactory bulb size and olfactory acuity on the morphology of the nasomaxillary complex. These hypotheses are operationalized and tested against the anthropoid data.

Reproduced with permission of the copyright owner. Further reproduction prohibited without permission.

Literature Review

The degree to which an organism relies on its sense of smell (i.e. olfactory acuity) and the concomitant size of its olfactory apparatus has long been thought to determine particular features of nasomaxillary form. Best known of the evolutionary scenarios that purport to explain nasomaxillary diversity in terms of olfactory acuity and size is the "arboreal hypothesis" of Sir Grafton Elliot Smith (1912) and Frederick Wood Jones (1916).

Smith (1912) viewed the primitive mammalian cerebrum as having two distinct parts: the *archepallium*, the part of the brain devoted to the sense of smell[1] and the *neopallium*, the part devoted to all other (i.e., non-olfactory) senses. Smith postulated that the primitive vertebrate cerebrum was dominated by the archepallium. With the rise of mammals the neopallium increased in size, but still occupied only about one-half of the cerebral cortex—the sense of smell remained predominant. All this changed, according to Smith, with the evolution of arboreal mammals. "Once... a creature left the solid earth and took to an aquatic or an arboreal life... the guidance of the olfactory sense lost much of its usefulness" (Smith, cited in Jones, 1916:153-4). F. Wood Jones, who had studied under Smith, would later expand on this point:

> In the olfactory parts of the brain, and in the sensory olfactory apparatus itself, the atrophy in the arboreal stock is extremely well marked, and smell impressions play but little part in the more important roles in the lives of the Primates [Jones, 1916:154-5].

---

[1] Other paleoanatomists (e.g., Romer & Parsons, 1985) make a distinction between the *archipallium* and *paleopallium*, and consider the olfactory part of the brain contiguous with the latter. Perhaps to avoid confusion the term *rhinencephalon* has more recently been adopted to refer to the olfactory organ.

Reproduced with permission of the copyright owner. Further reproduction prohibited without permission.

The transition from a *two-dimensional* terrestrial substrate to a *three-dimensional* arboreal substrate seems to have been the key element leading to the purportedly reduced olfactory acuity of the primates. As William Howells (1959) later commented,

> The air that blankets the unbroken ground surface is a world of smell, but in the trees there is less for scent to cling to, and the paths of travel are narrow. Therefore the power of smell has hardly more than an aesthetic excuse for being [Howells, 1959:125].

To Smith and Jones, the adaptive advantage of the neopallium over the archepallium in an arboreal habitat was sufficient to initiate a series of evolutionary events that transformed the overall morphology of the primates. In early mammals, a projecting snout not only aided in the function of smell, but was also the main tactile apparatus.

> A primitive Mammal may be said to "nose" its way about the world, and it "noses" its path through life in more senses than one. Just as its nose leads the way, and gives the first impression of novel objects by permitting the animal to become acquainted with their scent, so it gives the second impression of them by importing to the animal a knowledge of their "feel." Such an animal is guided to an object by olfactory stimuli from the nose; afterwards, it tests the object with its snout [Jones, 1916:157].

According to this scenario, the recession of the snout that accompanied a reduction of the olfactory apparatus thus created a void of tactile sensation. But another morphological change associated with arboreality was evolving that would helped fill this void. Primate hands and feet were becoming more dexterous to allow for the grasping of branches required of an arboreal life. The primary tactile sense was relocated from the snout to the ever-more dexterous hands.

Reproduced with permission of the copyright owner. Further reproduction prohibited without permission.

> The greatest difference between the process of gathering tactile impressions by the snout region, and receiving them by the hand, is that in the latter case the examination of a novel object is carried out to a far greater extent under the observation of the eyes. It is true that when the snout region is the tactile organ, the object tested is brought into greater proximity with the eyes; but it is exposed to a far more limited and restricted view than when it is examined by the hand. Tactive impressions from the examining hand become correlated with visual impressions as simultaneous observations. Visual sensations will gain an added possibility as avenues of education, and their pallial representation will, in all probability, be augmented [Jones, 1916:166].

It was a fortunate state of affairs, the scenario continues, that one of the consequences of a receding snout was orbital convergence, which further enhanced "visual sensations" by facilitating stereoscopic vision.

The arboreal theory of primate evolution can be criticized on both logical and empirical grounds. In a classic paper published in 1972, Cartmill both critically examined the arboreal theory and proposed a new scenario to explain several features of the primate nasomaxillary skeleton. Cartmill first challenged the assumption that the sense of smell is of little use to arboreal mammals. Jones' (1916) contention that "...scent glands diminish steadily in those stocks which are truly arboreal," and that "no trail of scent is laid among the branches of a tree..." (p. 154) was no longer tenable in light of observations of arboreal primate scent marking behaviors, such as those exhibited by the brown lemur (*cf.*, Napier and Napier, 1967; Harrington, 1979). He further noted that "...strepsirhines have presumably had as much time to adapt to life in the trees as haplorhines have; but they have a much better-developed olfactory apparatus" (Cartmill, 1972:113).

Cartmill argued that orbital convergence and increased stereoscopic vision

Reproduced with permission of the copyright owner. Further reproduction prohibited without permission.

were not a consequence of a reduced olfactory apparatus and receding snout, but rather, the cause of it. According to his "visual predation" hypothesis, selection for enhanced visual acuity in the context of predatory behavior was the primary selective force underlying the evolution of primate nasomaxillary morphology. Reduction of the olfactory apparatus and a receding snout are seen as consequences of orbital convergence required for enhanced stereoscopic vision.

Hypotheses Formulation

While the arboreal and visual predation hypotheses were formulated to explain primate macroevolutionary trends and primate differentiation from other mammals, their main tenets can also be applied to account for diversity within primates, since both arboreality and visual predation vary within the Order. Both hypotheses are nomological in nature and therefore open to evaluation in the context of the current investigation. The two causal hypotheses are summarized graphically as a pair of path diagrams, which are presented in Box 12.1.

It is clear that not all of the causal pathways predicted by these alternative hypotheses can be tested here. I have no data relating to degree of arboreality, relative tactile and visual sensory perception, visual predation behavior, or, for that matter, extent of stereoscopic vision. What remains is the proposed effects of olfaction on the morphology of the nasomaxillary complex (common to both hypotheses), and the relationship of orbital convergence to both olfaction and nasomaxillary morphology (unique to each hypothesis). Additionally, the hypothesized relationship between the size of the neocortex and the olfactory apparatus can be tested.

Reproduced with permission of the copyright owner. Further reproduction prohibited without permission.

Of primary concern here are the essential roles of olfactory acuity and olfactory size in the evolution and development of nasomaxillary form. One would like to know whether reliance on the sense of smell effects fundamental changes in craniofacial morphology, and if so, what specific changes, and to what extent. Components of the arboreal and visual predation hypotheses that relate to the preceding questions are summarized in Box 12.2.

Box 12.1 Path diagrams comparing the "arboreal" and "visual predation" hypotheses.

Arboreal hypothesis of Smith (1912) and Jones (1916)

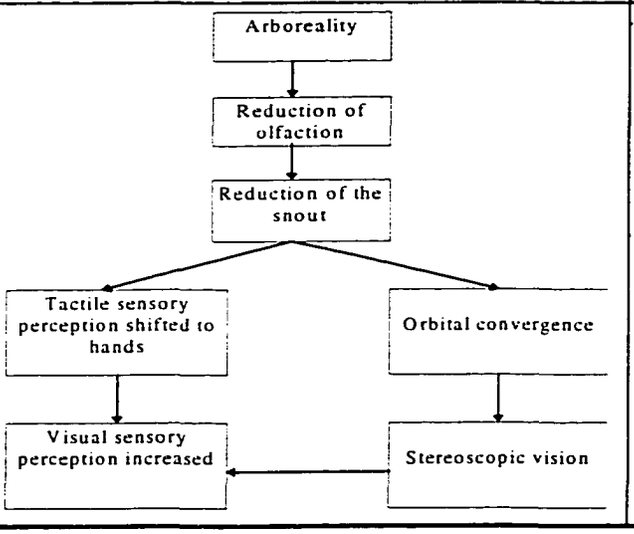

Visual predation hypothesis of Cartmill (1972)

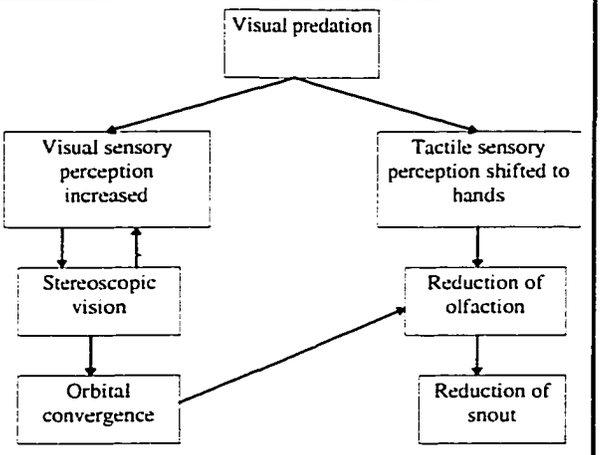

Reproduced with permission of the copyright owner. Further reproduction prohibited without permission.

Box 12.2. Hypotheses statements regarding the effects of olfactory size and acuity on craniofacial variation.	
Description of Hypothesis:	Source:
(A) As the olfactory apparatus diminished with continued disuse in an arboreal setting interorbital distance became smaller	Smith, 1912; Jones, 1916; Stadtmuller, 1936
(B) As the olfactory apparatus diminished with continued disuse in an arboreal setting the nasomaxillary complex reduced in size	Smith, 1912; Jones, 1916; Cartmill, 1972
(C) As the nasomaxillary complex reduced in size interorbital distance became smaller.	Smith, 1912; Jones, 1916
(D) As interorbital distance become smaller due to orbital convergence (i.e., parallelism) concomitant with stereoscopic vision the olfactory apparatus diminished	Cartmill, 1972
(E) As the neocortex increased in size the olfactory apparatus diminished	Smith, 1912; Jones, 1916; Cartmill, 1972

Operationalization of Variables

Variables that measure "reduction of the snout" or "nasomaxillary dimensions" have already been defined, and include the list of dependent nasomaxillary variables that are the primary focus of this study. The attribute "orbital convergence" in the context of Jones' (1916) writings meant both intranasal distance and orbital parallelism—no distinction was made between the two. For the characters describing orbital placement and orientation I have continued to use the terminology and operationalizations described in Chapter 11. Neocortical size was measured as endocranial volume minus olfactory recess volume. The properties referred to as "olfactory acuity" and "olfactory size," however, require detailed description and operationalization.

Olfactory bulb size and olfactory acuity

Radinsky (1975) has suggested that the "...size of the olfactory bulb (relative to body weight)... ...provides a rough indicator of the importance of the sense of smell in a given species" (p. 657). The olfactory bulbs constitute only one of a number of

Reproduced with permission of the copyright owner. Further reproduction prohibited without permission.

distinct components of the rhinencephalon, which together function in the sense of smell. The nasal cavity component of the olfactory apparatus is the *olfactory epithelia*, which contain specialized chemoreceptor neurons that line the roof and superior medial walls of the nasal cavity (Negus, 1958). The axons of these receptor neurons, collectively called the *olfactory nerves*, transmit through perforations in the cribriform plate to synapse with specialized nerve cells that compose the *olfactory bulbs*. The axons of olfactory bulb neurons form the *olfactory tract* which runs posteriorly before dividing into three *olfactory striae*, each of which lead to a different complex of the brain.

Obtaining separate measures for each of these olfactory apparatus components is not possible without detailed histological analysis. Epithelia dimensions, for example, are nearly impossible to measure accurately on dry skulls, at least without the aid of CAT scans. This is unfortunate, since the epithelial membrane is in immediate contact with the medial ethmoidal walls and might thus have a direct influence on nasal cavity size. It is reasonable to assume, however, that the volume of the olfactory bulbs will be proportional to the area of the olfactory epithelia, since there should exist a correspondence in the number of neurons in each of these components; although I am unaware of any empirical studies that have tested this assumption.

Despite these caveats it may still be possible to obtain fair estimates of olfactory bulb size from dry skulls. Two separate quantities were defined and collected from the anthropoids sample: (1) olfactory recess volume, and (2) cribriform plate area. In humans, the olfactory bulbs and tracts are pressed against the anterior cranial floor by the overlying frontal lobes of the brain. This is in

Reproduced with permission of the copyright owner. Further reproduction prohibited without permission.

contrast to most nonhuman primates, whose olfactory bulbs and tracts extend away from the anterior neocortex to form a distinct olfactory cavity, or recess. When filled with brass filings, a radioopaque material, the olfactory recess is clearly visible in radiographs and its volume can be estimated from the 3D coordinate configurations of combined ectocranial and endocranial landmarks (see Chapters 5 & 11, and Appendix B).

One potential problem with using olfactory recess volume as an estimate of olfactory bulb size is that the cavity contains the olfactory tracts as well as the bulbs. The size of the tracts may be independent of the size of the bulbs, since the *length* of the former reflect the distance between the olfactory bulbs and the point at which the olfactory striae enter the neocortex. Hence, it is possible to conceive of two organisms having equal olfactory epithelia areas and olfactory bulb volumes, but having different olfactory tract lengths. In such a case, the two organisms would differ with respect to olfactory recess volume despite having equally sized olfactory bulbs.

A better approach to estimating olfactory bulb size from dry skulls, and one that bypasses the problem of olfactory tract variability, is to measure the area of the cribriform plates. Ontogenetically, growth of the cribriform plates have been shown to keep pace with the growth of the olfactory bulbs in rats (Moss, 1958; but see Forster, 1927 for contrasting view). Moreover, the cribriform plates are perforated by foramina that transmit the olfactory nerves from the site of sensory reception to the olfactory bulbs, which are an extension of the brain. Thus, the role of the cribriform plate with respect to the olfactory bulbs is precisely parallel to that of the foramen magnum with respect to the brain. Just as the area of the

Reproduced with permission of the copyright owner. Further reproduction prohibited without permission.

foramen magnum can be used to predict or estimate brain size (see Box 12.3), so too can the area of the cribriform plates be employed to estimate the size of the olfactory bulbs.

Box 12.3. Scatter plot and regression line of log cube root endocranial volume (L_BRNSIZ) against log square root foramen magnum size (L_FMAGSZ) (log raw data; n=300). r = 0.964, p=.0001; prediction equation: L_BRNSIZ = -0.94 + 0.93 L_FMAGSZ

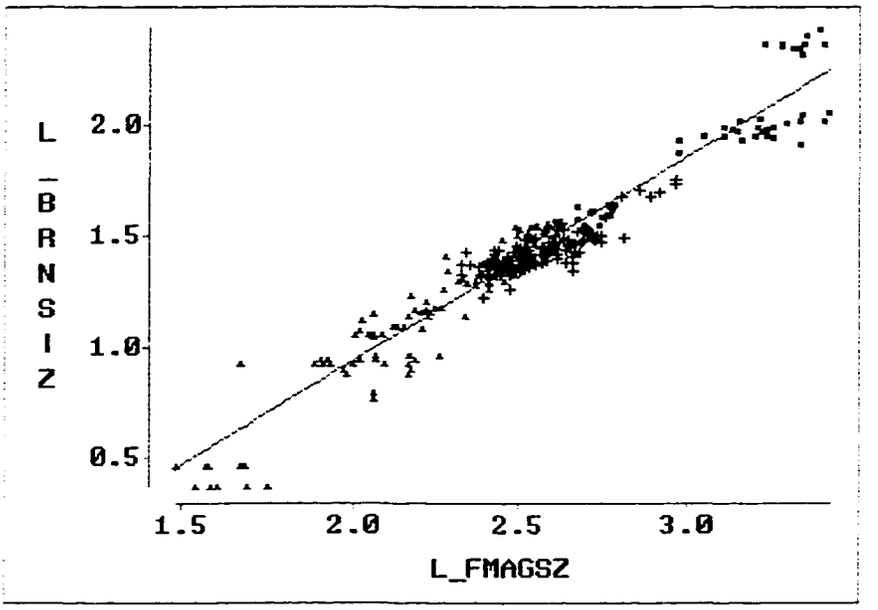

Fortunately, it was possible to assess the validity of the proposed estimates. Stephan, Frahm and Baron (1981) have quantified olfactory bulb volumes for 27 species of anthropoids from serial sections of whole brains. Twenty-one of the 27 species are included in the current anthropoid sample. It was therefore possible to regress histologically quantified olfactory volumes against the two craniometric olfactory variables described here, to see if either, both, or neither provide reliable estimates of olfactory bulb size. The results, reported in Boxes 12.4-12.6, show that olfactory cavity volume corresponds more closely to Stephan *et al.*'s (1981) measure of olfactory bulb volume. The *R*-squared values for olfactory cavity

Reproduced with permission of the copyright owner. Further reproduction prohibited without permission.

volume and cribriform plate area (this study) regressed against olfactory bulb volumes (Stephan *et al.*, 1981) are 0.67 and 0.46, respectively. Both are considerably lower than the *R*-squared obtained for foramen magnum area against endocranial volume (R^2=0.93). It is difficult to tell whether the lower predictive power of the former is due to the fact that the regressions were computed from the means of two different studies each using different samples, from measurement error, or from invalid operationalization. One would like to regress olfactory bulb volume against cribriform plate area measured from the same individuals, and it is not unreasonable to expect that such an analysis would yield a higher *R*-square, but this remains to be tested.

Box 12.4. Correlation coefficients and prediction equations for two measures of olfactory bulb size regressed on cube root olfactory bulb volumes for 21 species of anthropoids published by Stephan *et al.*, 1981.

Estimate of olfactory bulb size	Description:	*r*	*p*	Empirical prediction equation
Log cube root olfactory cavity estimated volume	length x height x width of olfactory recess	0.82	.0001	predicted=0.46+0.93
Log square root estimated cribriform plate area	length x width of cribriform plate	0.68	.0016	predicted=0.25+1.04

There is another caveat that has an even more important impact on the interpretation of the results. Stephan *et al.* (1981) never made explicit in their paper whether or not they separated the olfactory tracts from the olfactory bulbs when quantifying the "bulbous olfactorius volume." For good reason, I suspect they did not. Combining the olfactory bulbs and tracts into a single quantifiable component makes sense histologically, since the two components are contiguous and simply contain different parts of the same cells (Telford & Bridgman, 1989). From my own experience dissecting primate brains, I have observed that it is often

Reproduced with permission of the copyright owner. Further reproduction prohibited without permission.

difficult to tell precisely where the bulbs end and the tracts begin.

The results reported in Boxes 12.4-12.6 support this supposition, for the following two reasons. (1) As noted above, the olfactory bulb volumes published by Stephan *et al.* (1981) more closely correspond to measures of olfactory recess volume (this study), which include both bulbs and tracts, than to cribriform plate area, which should reflect olfactory bulb size alone. (2) The dispersion of the data around the regression line is consistent with the interpretation. For instance, in attempting to predict bulb size from a quantity that includes both bulbs and tracts, we would expect to see an overestimation of olfactory bulb size in species having longer than normal olfactory tracts and an underestimation of olfactory bulb size in species having shorter than normal olfactory tracts. In fact, this is precisely the pattern that appears when Stephan *et al*'s (1981) "olfactory bulb" volume is regressed on cribriform plate area. The three largest residual outliers from this regression— *Papio* (below the regression line) and, *Hylobates* and *Homo* (above the regression line)—follow the expected pattern (see Box 12.5). A careful examination of the radiographs indicate that *Papio* has one of the longest olfactory recesses (and presumably, correspondingly long olfactory tracts) of any anthropoid; whereas *Hylobates* and *Homo* exhibit relatively short olfactory recesses. It can be seen with reference to Box 12.5 that Stephan *et al.*'s data overestimate olfactory bulb size for *Papio*, while yielding underestimations for *Hylobates* and *Homo*. The other outliers also fit the pattern quite well.

Box 12.6 contains the regression plot of Stephan *et al.*'s "olfactory bulb" volume against olfactory cavity volume (this study). It can be seen that the 3 outliers identified in the earlier regression fall much close to the new regression

Reproduced with permission of the copyright owner. Further reproduction prohibited without permission.

line. If the foregoing analysis and interpretation is accurate, then cribriform plate area is a reasonable proxy for olfactory bulb size.

Box 12.5. Scatter plot and regression line of log square root cribriform plate area (L_CRIBAR) against log cube root bulbous olfactorius volume (L_OFBVLP) (log raw species mean data; n=21), from Stephan *et al.*, 1981.

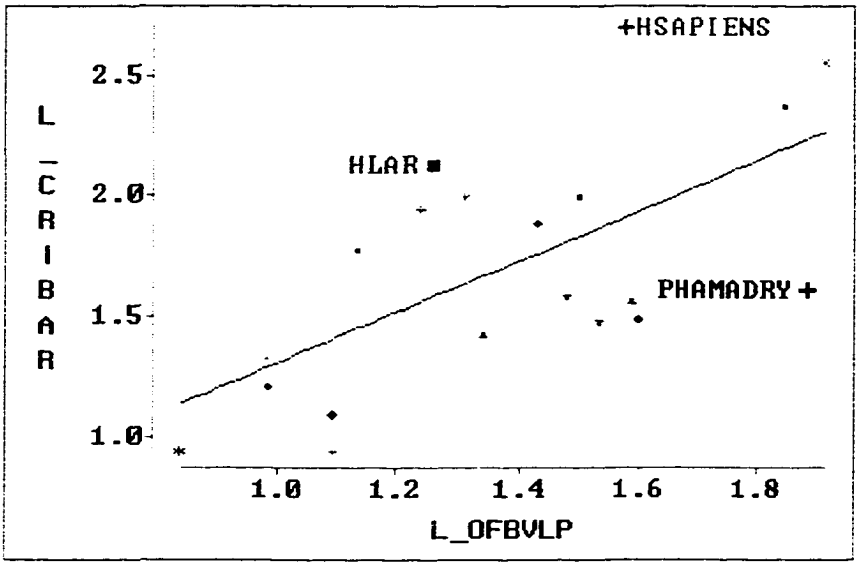

Box 12.6. Scatter plot and regression line of log cube root olfactory cavity volume (L_OLFBVL) against log cube root bulbous olfactorius volume (L_OFBVLP) (log raw species mean data; n=21).

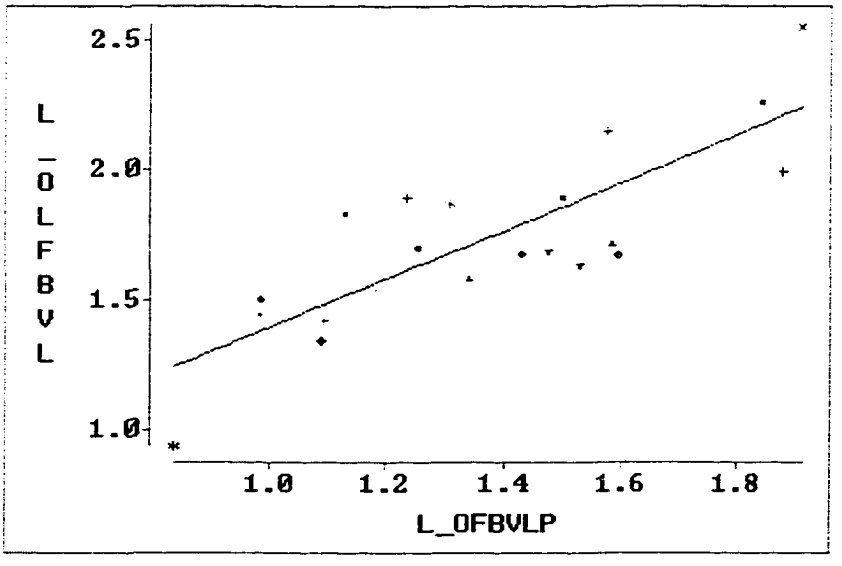

Reproduced with permission of the copyright owner. Further reproduction prohibited without permission.

In keeping with Radinsky's (1975) definition, olfactory acuity was measured as:

$$\text{(log) cribriform plate area}^{.5} - \text{(log) endocranial volume}^{.33} \qquad (12.1)$$

The reader may recall from Chapter 10 that this formulation produces a Mosimann isometric log residual, which is the log equivalent to standardization by size, in this case by endocranial size. Olfactory acuity is thus measured as olfactory bulb size after isometric standardization for brain size.

As a further check on the validity of the proposed operationalizations, a list of anthropoid species ordered by olfactory acuity was compared with known attributes of olfactory behavior and physiology. Box 12.7 ranks the 37 anthropoid species included in this study on the basis of olfactory acuity. The data reported by Stephan *et al.* (1981) was used to compute a comparable olfactory acuity score (olfactory bulb volume/brain volume),[2] and a rank index score was then assigned to each of the two sets of olfactory acuity scores for ease of comparison.

[2] To facilitate communication the olfactory acuity variable computed from cribriform plate areas (this study) is henceforth referred to as CRIBS, and the olfactory acuity scores computed from the published data on bulbus olfactorius volume by Stephan *et al.* (1981) is referred to as LOBES.

Reproduced with permission of the copyright owner. Further reproduction prohibited without permission.

Box 12.7. Ranking of sample species based on olfactory acuity (see text for details)

#	Species	Rank index CRIBILOBE		Comments
1	*C. pygmaea*	97	90	Frequent scent marking (Fleagle, 1988)
2	*S. oedipus*	94	81	Frequent scent and urine marking, especially by females (Hershkovitz, 1977). No sternal marking (Epple *et al*, 1993), but scent used for individual recognition (Epple *et al*, 1982).
3	*A. trivirgatus*	91	95	Well developed olfactory system. Urine and glandular secretions (Zeller, 1987), used mostly for intergroup communication (Wright, 1994). Urine washing (Jolly, 1972).
4	*A. palliata*	89	33	Well developed olfactory system. Odor producing scent glands (Crockett & Eisenberg, 1987). Urine washing (Neville *et al* 1988)
5	*C. cupreus*	86	52	Sternal scent marking (Mason, 1968), especially by males in association with territorial defense (Kinzey, 1981)
6	*P. badius*	83	23	No extensive olfactory behavior documented
7	*H. syndactylus*	81		No extensive olfactory behavior documented
8	*H. lar*	78	9	No extensive olfactory behavior documented
9	*C. polykomos*	75		No extensive olfactory behavior documented
10	*C. geoldii*	73	85	Frequently mark trails with urine and scent-mark with sternal secretions (Hershkovitz, 1977)
11	*S. entellus*	70		No extensive olfactory behavior documented
12	*A. geoffroyi*	67	38	Sternal marking of trees and individual recognition (Jolly, 1972)
13	*B. arachnoides*	64		Urine washing (Milton, 1984)
14	*L. lagotricha*	62	28	Sternal marking of trees and individual recognition (Jolly, 1972)
15	*P. monachus*	59	47	No extensive olfactory behavior documented
16	*P. pithecia*	56		No extensive olfactory behavior documented
17	*N. larvatus*	54	4	No extensive olfactory behavior documented
18	*G. gorilla*	51	14	No extensive olfactory behavior documented
19	*S. cristatus*	48		No extensive olfactory behavior documented
20	*P. melalopos*	45		No extensive olfactory behavior documented
21	*C. capucinus*	43		Use sternal scent glands to mark trees and use for individual recognition (Jolly, 1972). Well developed olfactory system in association with urine washing (Zeller, 1987)
22	*C. mitis*	40	76	No extensive olfactory behavior documented
23	*S. sciureus*	37	57	Well developed olfactory; urine washing (Zeller, 1987)
24	*C. apella*	35		Use sternal scent glands to mark trees and for individual recognition (Jolly, 1972). Urine marking (Freese & Oppenheimer, 1981)
25	*P. paniscus*	32		No extensive olfactory behavior documented
26	*C. neglectus*	29		Scent marking with sternal secretions, especially by males (Feistner, 1991; Loireau & Gautier-Hion, 1988)
27	*C. aethiops*	27		Territorial marking and recognition behavior (Gartlan & Brain, 1968)
28	*P. troglodytes*	24	19	No extensive olfactory behavior documented
29	*C. ascanius*	21	71	No extensive olfactory behavior documented
30	*M. mulatta*	18	42	No scent marking, but olfactory cues associated with sexual behavior (Michael & Keverne, 1968; Goldfoot, 1982)
31	*C. satanas*	16		No extensive olfactory behavior documented
32	*M. fascicularis*	13		No extensive olfactory behavior documented
33	*M. nemestrina*	10		No extensive olfactory behavior documented
34	*L. albigena*	8	61	No extensive olfactory behavior documented
35	*H. sapiens*	5	0	No extensive olfactory behavior documented
36	*P. hamadryus*	2	66	No extensive olfactory behavior documented
37	*P. pygmeaus*	0		No extensive olfactory behavior documented

Reproduced with permission of the copyright owner. Further reproduction prohibited without permission.

Callithix pygmaea, *Callimico goeldii*, *Saguinus oedipus* and *Aotus trivirgatus* are all known to have well developed olfactory systems and all three Neotropical primates rank high on both olfactory acuity scores. There is also abundant evidence that *Alouatta palliata* and *Callicebus cupreus* produce glandular secretions in association with olfactory behavior in a number of contexts. These species rank high on the cribriform olfactory acuity score (CRIBS), but mid to low on the Stephan olfactory acuity score (LOBES). Colobine monkeys (*P. badius*, *C. polykomos*, *S. entellus* and *N. larvatus*) and *Hylobates* (*H. lar* and *H. syndactylus*) rank relatively high on CRIBS, but I can find no reference in the literature to suggest that these species exhibit any special facility or need for advanced olfactory acuity. The LOBES index faired better, ranking *H. lar*, *P. badius* and *N. larvatus* relatively low. *Gorilla* was also ranked relatively higher on the CRIBS score (compared to the LOBES score). Both the CRIBS and LOBES scores appear to have under-ranked the Cebinae (*Cebus capucinus*, *C. apella* and *Saimiri sciureus*), which were assigned mid to low rankings despite evidence of fairly well developed olfactory systems and related behaviors in this group. On the plus side, the moderate to high CRIBS scores for the Atelini are in accord with olfactory behaviors reported for this groups (in contrast to the low LOBES scores). Scent marking with sternal secretion glands and urine washing are common to *Ateles geoffroyi*, *Lagothrix lagothricha* and *Brachyteles arachnoides*. The lower one-third of the CRIBS order (i.e., species with presumed low olfactory acuity) also appears to be consistent with published behavioral data.[3] However, *Cercopithecus*

[3] Although the low ranking *C. neglectus*, *C. aethiops* and *M. mulatta* have all been observed engaging in scent marking behavior, the extent of this behavior is either limited or unknown.

Reproduced with permission of the copyright owner. Further reproduction prohibited without permission.

ascanius, *Lophocebus albigena*, and *Papio hamadryus* (which all ranked in the bottom one-third of the CRIBS order) are ranked high by the LOBES index despite the lack of evidence to indicate a correspondingly high olfactory acuity.

Overall, the CRIBS rank index performed relatively better than the LOBES index when evaluated against the literature on olfactory-related behavior. The CRIBS index overrated 13% and underrated 8% of the sample species with regard to olfactory acuity, compared to 24% overrated and 14% underrates for the LOBES index.

While both the CRIBS and LOBES indices yield lower mean scores for catarrhines than for platyrrhines, the difference is significant (at alpha=.05) only for the CRIBS scores (see Box 12.8). Thus, the CRIBS index as a measure of olfactory acuity is more consistent with observed anthropoid behavior and ecology, which indicates that New World monkeys exhibit a much greater reliance on the sense of smell than do Old World monkeys and hominoids.

Box 12.8. Comparison of mean olfactory acuity scores for platyrhines and catarrhines.

Taxon	Mean CRIBS score (95% CL)	Mean LOBES score (95% CL)
Platyrrhini	37.9 (32.2, 43.8)	84.5 (53.7, 116.3)
Catarrhini	68.9 (46.6, 90.5)	158.7 (93.6, 223.8)

Reproduced with permission of the copyright owner. Further reproduction prohibited without permission.

Statistical Predictions

Predicted statistical associations between trait pairs deduced from the preceding hypotheses are listed in Box 12.9.

Box 12.9. Predicted bivariate associations deduced from hypotheses statements.	
Expected statistical associations and predictions.	Hypo-thesis
Intranasal breadth [ΔS_L_Y49] ← Cribriform plate area [ΔS_L_Y44] (Prediction: Anthropoids with large olfactory bulbs will exhibit greater intranasal distance compared to anthropoids with small olfactory bulbs)	(A)
Nasomaxillary dimensions [ΔS_L_Y1-ΔL_Y35] ← Cribriform plate area [ΔS_L_Y44] (Predictions: Anthropoids with larger olfactory bulbs will exhibit greater nasomaxillary linear dimensions and different shape characteristics compared to anthropoids with smaller olfactory bulbs)	(B)
Intranasal breadth [ΔS_L_Y49] ← Nasomaxillary dimensions [ΔS_L_Y1-ΔL_Y35] (Predictions: Anthropoids with larger snout dimensions will exhibit greater intranasal breadth compared to anthropoids with smaller snout dimensions)	(C)
Intranasal breadth [ΔS_L_Y49] ← Orbital parallelism [ΔL_Y45] (Prediction: Anthropoids with greater intranasal breadths will exhibit less orbital parallelism)	(D)
Cribriform plate area [ΔS_L_Y44] ← Intranasal breadth [ΔS_L_Y49] (Prediction: Anthropoids with greater intranasal breadths will exhibit larger olfactory bulbs compared to anthropoids with narrower intranasal breadths)	(D)
Cribriform plate area [ΔS_L_Y44] ← Rel. endocranial volume [ΔS_L_Y84] (Prediction: Anthropoids with larger relative brain size will exhibit smaller olfactory bulbs compared to anthropoids with smaller relative brain size)	(E)

Preliminary and Exploratory Analysis

In the previous section the objective was to assess the validity and accuracy of craniometric estimates of olfactory size and acuity among anthropoids. In accordance with this objective, raw data were used in the analysis. In this and subsequent sections, nomological comparative analyses are undertaken and use of the raw data is not appropriate (see Chapter 6). All subsequent analyses in the current chapter were conducted using the logged delta-transformed data.

Reproduced with permission of the copyright owner. Further reproduction prohibited without permission.

Preliminary analyses include (1) a description of the relationship between olfactory bulb size (log delta square root cribriform area) and brain size (log delta cube root endocranial volume), and (2) an examination of the bivariate scatter plots and correlational structure (i.e., PCA) between olfactory acuity and anthropoid nasomaxillary variables.

Body Size, Brain Size and Olfactory Bulb Size

The traditional view of the evolutionary relationship between the brain and the olfactory apparatus in primates maintains that a shift of sensory modalities, from olfactory to visual and tactile perception, ultimately led to an increase in the size of the neocortex and a corresponding decrease in the organs of smell. The negative allometric relationship between brain size and olfactory size implied by this view is elegantly illustrated by Radinsky (1975) in a comparison of the hedgehog (*Erinaceus*), the thick-tailed bush baby (*Otolemur*), and the squirrel monkey (*Saimiri*). Endocasts of these species (diagrammed in his Fig. 1, p. 657), arranged in order of size, show a graded series of increasing brain size and dwindling olfactory lobes (relative to brain size).[4]

It is presumed that the same relationship holds within Anthropoidea. It is known, for instance, that platyrrhines rely to a greater extent on the sense of smell than do catarrhines, and, given the emphasis on advanced neocortical functions by hominoids, it is not unreasonable to expect a further reduction in olfactory bulb size in apes and humans.

---

[4] It is of interest to note that body weight progresses in reverse order, with the hedgehog weighing the most and *Saimiri* weighing the least. Radinsky's (1975) classic comparison is therefore an unwitting example corroborating Weidenreich's (1941) hypothesis that smaller mammals tend to have relatively larger brains.

Reproduced with permission of the copyright owner. Further reproduction prohibited without permission.

The scatter plot and regression slope of endocranial volume against cribriform plate area confirms the predicted negative allometric association between the two characters (Box 12.10).[5] Thus, in general, anthropoids with absolutely larger brains tend to have proportionally smaller olfactory bulbs compared to anthropoids with absolutely smaller brains. But this is only part of the picture. Recall from Chapter 11 that larger anthropoids tend to have *absolutely* larger, but *relatively* smaller brains, compared to smaller anthropoids. Therefore, when scaled to the same overall (centroid) size smaller anthropoids tend to have relatively larger brains *and* larger olfactory bulbs compared to larger anthropoids (Boxes 12.11 & 12.12).

Box 12.10. Regression scatter plot of log delta cube root endocranial volume (L_YV84) against log delta square root cribriform plate area (L_YV44). (95% confidence limits around slope in parenthesis.) (n=300)

Slope 0.86 (0.79, 0.93), $R^2 = 0.64$

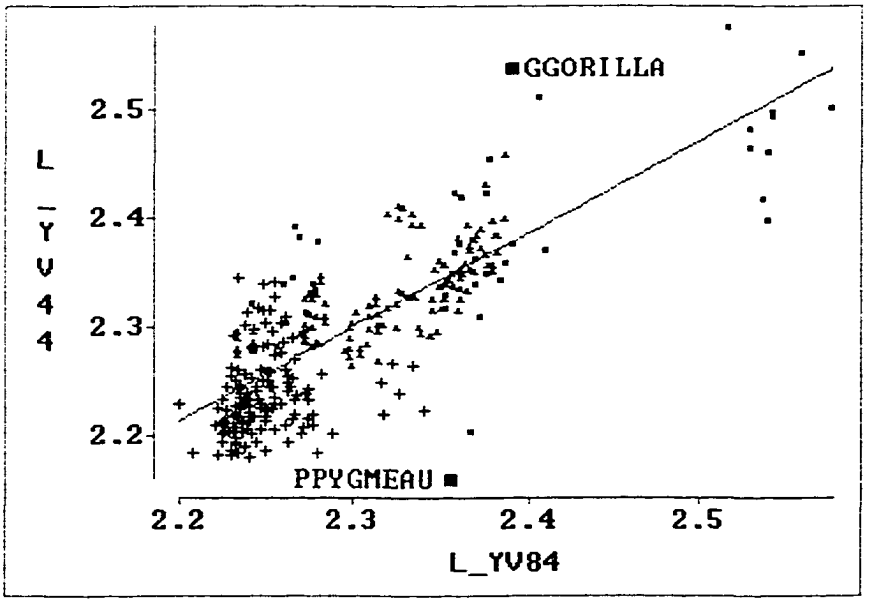

[5] The *raw data* log-log regression of brain size on olfactory bulb size yields a slope estimate that is not significantly different from 1.0, indicating an isometric relationship between these two variables in anthropoids. However, within superfamilies the slope varies from 0.47 in cercopithecoids to 0.85 in ceboids, suggesting that the isometric relationship is based on a line connecting only a few major groups.

Reproduced with permission of the copyright owner. Further reproduction prohibited without permission.

Box 12.11. Regression scatter plot of log delta centroid size (L_YV41) against log delta square root cribriform plate area (L_YV44). (95% confidence limits around slope in parenthesis.) (n=300)

Slope 0.85 (0.76, 0.93) p = .0001, R^2 = 0.56

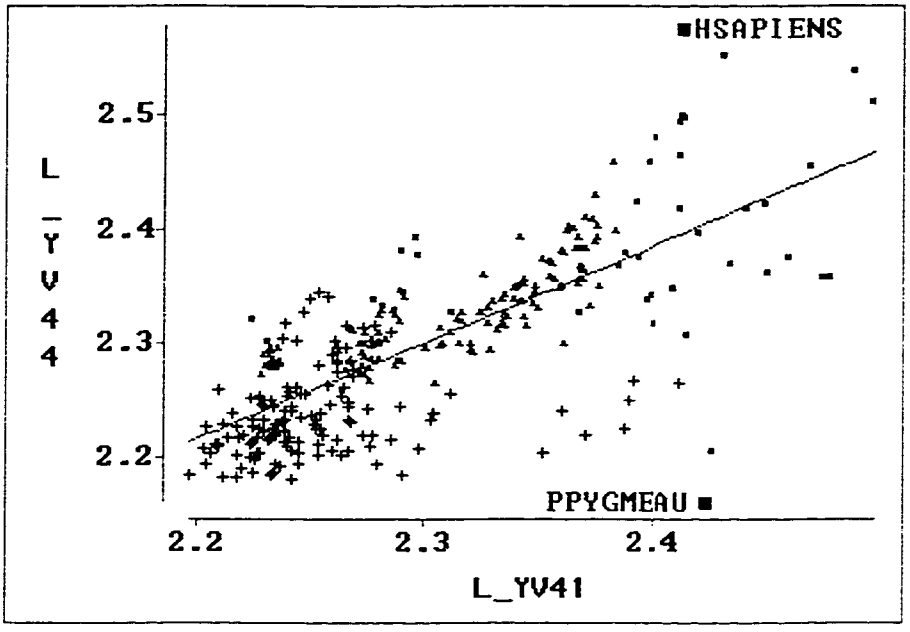

Box 12.12. Regression scatter plot of log delta cube root relative endocranial volume (ΔS_L_YM84) against log delta square root relative cribriform plate area (ΔS_L_YV44). (95% confidence limits around slope in parenthesis.) (n=300)

Slope 1.18 (1.00, 1.38), R^2 = 0.21

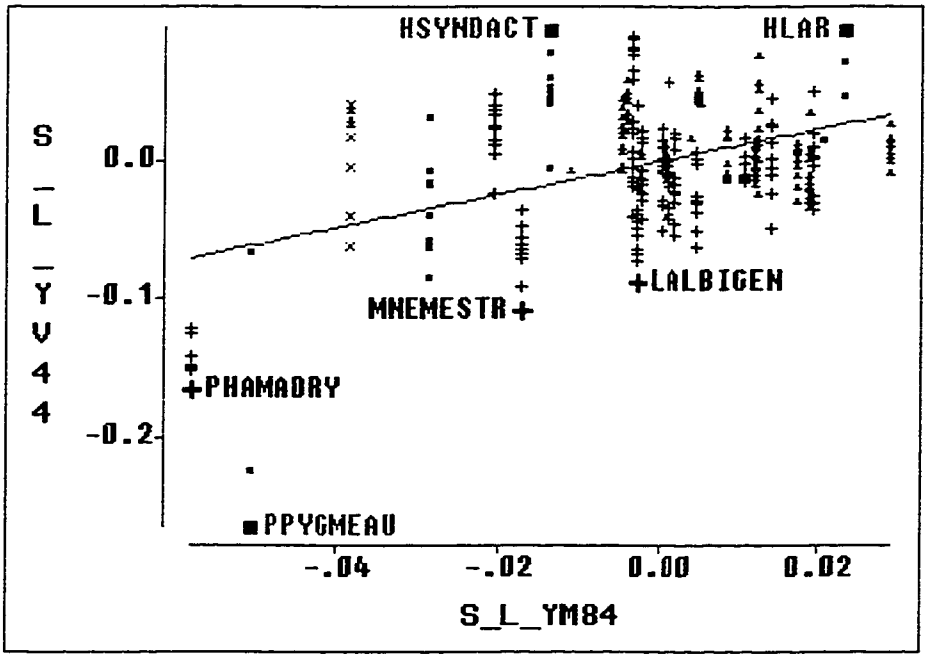

Reproduced with permission of the copyright owner. Further reproduction prohibited without permission.

Principal Components Analysis of Olfactory and Nasomaxillary Variables

Box 12.13 reports the eigenvalues for the 29 olfactory and nasomaxillary variables included in the PCA. Again, only the first two principal components were retained for examination. The first principal component accounted for 24% of the total variance of the variables, and the second principal component accounted for an additional 11%. All variables were log delta-transformed and either shape variables or Mosimann isometric residuals (recall that in the case of the latter the prefix 'S_' was added to the variable designation).

Box 12.13. Eigenvalues and accounted-for variance of log delta V-level olfactory and nasomaxillary variables (n=300; correlation matrix used in PCA).

PC	Eigenvalue	Proportion of Variance Explained	Cumulative Proportion Explained	PC	Eigenvalue	Proportion of Variance Explained	Cumulative Proportion Explained
1	6.92	.239	.24	16	0.44	.015	.92
2	3.10	.107	.35	17	0.40	.014	.93
3	2.50	.086	.43	18	.36	.012	.94
4	2.21	.076	.51	19	.31	.011	.95
5	2.15	.074	.58	20	.29	.010	.96
6	1.67	.058	.64	21	.24	.008	.97
7	1.35	.047	.69	22	.23	.008	.98
8	1.16	.040	.73	23	.16	.005	.99
9	1.08	.037	.76	24	.13	.004	.99
10	0.87	.030	.79	25	.11	.004	.99
11	0.81	.028	.82	26	.10	.004	.99
12	0.65	.022	.84	27	.04	.001	.99
13	0.61	.021	.86	28	.02	.001	.99
14	0.59	.020	.89	29	.01	.00	1.00
15	0.50	.017	.90				

Box 12.14 lists the component loadings for the first two principal components, and the corresponding scatter plot is displayed in Box 12.15.

Reproduced with permission of the copyright owner. Further reproduction prohibited without permission.

Box 12.14. Component loadings for the first two principal components of the combined olfactory and nasomaxillary variables (after varimax rotation).

Variable	$PC_{(1)}$	$PC_{(2)}$	Variable	$PC_{(1)}$	$PC_{(2)}$
ΔS_L_YV1	0.802	-0.145	ΔS_L_YV21	0.043	0.268
ΔS_L_YV4	-0.481	0.195	ΔS_L_YV23	-0.444	-0.048
ΔS_L_YV5	0.150	0.086	ΔS_L_YV25	0.187	-0.056
ΔS_L_YV6	0.044	0.278	ΔS_L_YV27	0.038	0.593
ΔS_L_YV7	0.335	-0.234	ΔL_YV30	0.616	0.461
ΔS_L_YV8	-0.469	-0.152	ΔL_YV31	0.785	0.246
ΔS_L_YV9	0.020	0.255	ΔL_YV32	0.177	-0.559
ΔS_L_YV11	0.528	0.030	ΔL_YV33	0.017	-0.126
ΔL_YV13	-0.654	-0.006	ΔL_YV35	0.667	-0.123
ΔS_L_YV14	0.769	0.241	ΔL_YV45	-0.128	0.268
ΔS_L_YV15	-0.028	0.158	ΔS_L_YV44	-0.685	0.394
ΔS_L_YV16	-0.717	0.303	ΔB_L_YV44	-0.233	0.719
ΔS_L_YV17	0.843	-0.065	ΔS_L_YV49	-0.702	0.441
ΔS_L_YV18	0.127	0.409	ΔL_YV95	0.571	0.109
ΔS_L_YV19	0.125	0.734			

Box 12.15 contains the scatter plot of the first two principal components. As before, the dotted lines separate "significant" from "nonsignificant" component loadings.

Box 12.15. Bivariate plot of first two principal components (PC1, PC2)

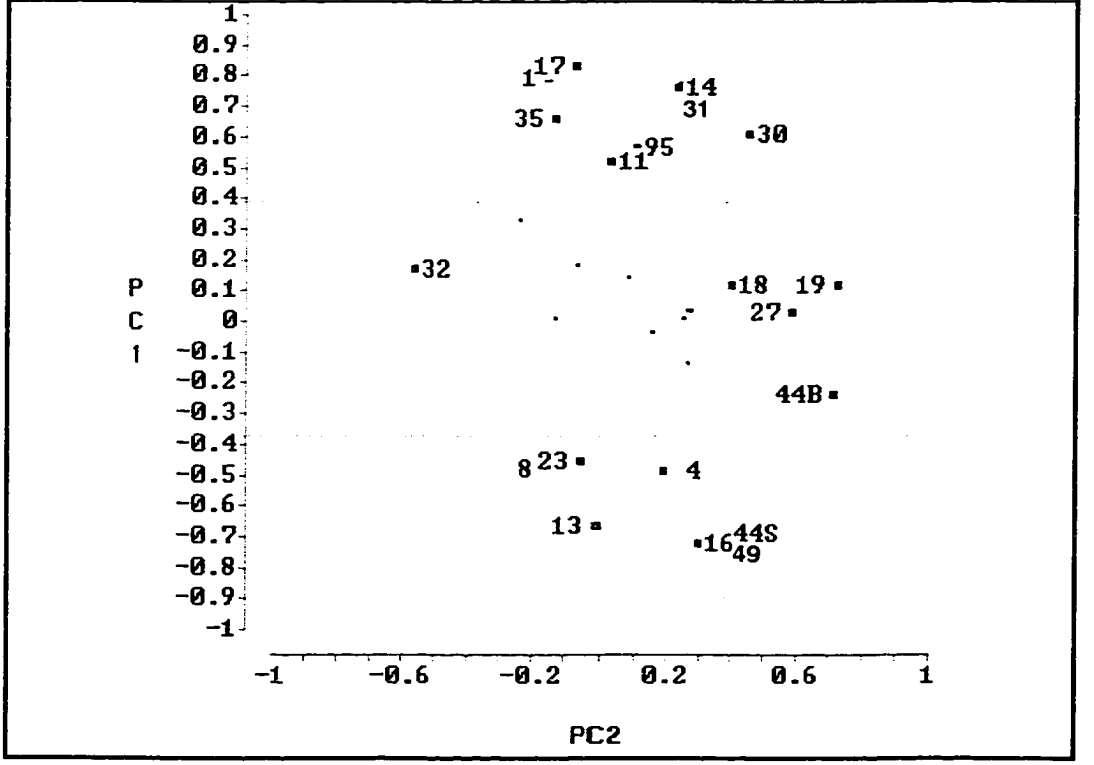

Reproduced with permission of the copyright owner. Further reproduction prohibited without permission.

The nasomaxillary variables that loaded highly (and positively) on $PC_{(1)}$ in the current analysis were generally the same as those that loaded highly on $PC_{(1)}$ in Chapter 11. They include nasal bone length [ΔS_LYV1], maxillary arch length [ΔS_LYV14], anterior facial length [ΔS_L_YV17], both Krogman's [ΔL_YV30] and Enlow's [ΔL_YV31] angle of facial prognathism, and posterior facial angle [ΔL_YV95]. Zygomatic height [ΔS_L_YV11] and paranasal plate orientation [ΔL_YV35] also contributed significantly to $PC_{(1)}$. Loading negatively on $PC_{(1)}$ were the nasomaxillary variables nasal process of maxilla width [ΔS_L_YV4], posterior nasal aperture breadth [ΔS_L_YV8], anteroposterior position of zygomatic root [ΔL_YV13], upper facial breadth [ΔS_L_YV16], inter-M^3 palatal width [ΔS_L_YV23], olfactory bulb size [ΔS_L_YV44], and intranasal distance [ΔS_L_YV49].

$PC_{(1)}$ thus contrasts facial prognathism and length against intranasal and choanal width and olfactory bulb size. Taken together with the results of previous chapters, it appears that an increase in body size is associated with a relatively small, dolichocephalic brain and even smaller olfactory bulbs which are vertically oriented, and a long, prognathic face. Smaller anthropoids in addition to having relatively larger olfactory bulbs tend to have relatively wide cranial bases, and wide maxillary arches and intranasal distances. This finding runs counter to the traditional view that large olfactory bulbs are associated with a longer more prognathic face. Empirical support for the traditional view is seen in the examples of horses and deer, which exhibit extreme nasomaxillary prognathism and are also known to have large olfactory systems (Orton, 1878). But cats also have extensively developed olfactory organs and yet are rather orthognathic compared to other mammals. At the moment, the scope of the present findings are limited to

Reproduced with permission of the copyright owner. Further reproduction prohibited without permission.

anthropoids.

It is also of interest to note which variables are not associated with olfactory bulb size. One might have expected anterior nasal breadth or height, or perhaps paranasal plate orientation to be positively correlated with olfactory bulb size, but no such association was revealed in either the PCA or subsequent regression analysis (see Box 12.32). [6]

$PC_{(2)}$ contrasts occlusal slope [ΔL_YV32] against ramus height [ΔS_L_YV18], palatal depth at M^3 [ΔS_L_YV27], facial prognathism (Enlow's angle) [ΔL_YV31], and olfactory acuity (olfactory bulb size relative to brain size) [ΔB_L_YV44].[7] Most of these variables have to do with the configuration and juxtaposition of the palate. $PC_{(2)}$ may thus delineate some type of craniometric-dietary factor.

Diet and Olfactory Acuity

To explore the hypothesis of a connection between diet and olfactory acuity, each of the 37 species in the anthropoid sample was assigned to one of ten dietary categories based on dietary information reported in Harding (1981) and Rowe (1996). These categories are described in more detail in Chapter 14. Mean olfactory acuity scores and 95% confidence intervals are reported for each dietary category in Box 12.16. Dietary regimes fall into two main non-overlapping groups, one with olfactory acuity scores above zero and the other with scores below zero. The group with high olfactory acuity scores includes the dietary categories of gumnivory, insectivory, folivory and frugivory. The group with low olfactory

---

[6] Although a negative association was found between paranasal plate orientation and olfactory bulb size in cercopithecines.

Reproduced with permission of the copyright owner. Further reproduction prohibited without permission.

scores includes omnivory, equal frugivory/insectivory, gramnivory and hard food specialists. Very little is known of the role of olfaction in locating and selecting food items among anthropoids. The results of the foregoing analysis make biological and ecological sense in that one would expect hard food items and seeds to be less odorous than fruits, gums, insects and leaves. However, it is not clear why anthropoids who supplement their mostly fruit-eating diets with insects (e.g., *Saimiri, Cebus*) should score low while both insectivory and frugivory are ranked high.

Box 12.16. Means and 95% confidence intervals for olfactory acuity scores by dietary category (n=300).

Dietary Category	Olfactory Acuity Mean & 95% CI	
Gumnivore	4.8	4.2, 5.5
Insectivore [8]	3.8	
Folivore w/ fruit	3.0	2.0, 4.1
Folivore	2.9	0.9, 5.0
Frugivore	1.8	0.8, 2.9
Frugivore/Omnivore	-1.2	-2.1, -0.4
Gramnivore	-1.3	-2.5, 0.1
Frugivore w/ insects	-2.5	-3.2, -1.8
Hard food specialist	-5.1	-6.8, -3.3
Omnivore	-5.6	-9.6, -1.5

Bivariate Regression Analysis

To further examine trait covariances and test predictions of trait relationships, bivariate regressions were conducted. The results are presented in Boxes 12.17 to 12.35 (see Chapter 11 for details of the analysis). Separate regressions were

[7] The variable code prefix "B_" indicates that the variable has been log isometrically standardized by brain size.

Reproduced with permission of the copyright owner. Further reproduction prohibited without permission.

conducted for anthropoid subtaxa, and for selected regressions the unique contributions of the M-level and Q-level components of the data are also given (see Chapter 8).

[8] The only true insectivore in the anthropoid sample is *S. oedipus*, which is represented by a single specimen.

Reproduced with permission of the copyright owner. Further reproduction prohibited without permission.

Box 12.17 Intranasal distance [ΔS_L_YV49] ← Cribriform plate area [ΔS_L_YV44]					
Taxon	Level of analysis	Maximum likelihood regression coefficient (95% CI) and associated p-value	Shapiro-Wilk test for normality of residuals	Brown & Forsythe's test for residual homoscedasticity	Somers' D nonparametric measure and test of association
Anthropoids (n=300)	V	0.85 (0.78, 0.91) p = .0001	0.98 p = .051	0.18 p = .91	0.58 p < .05
	M	0.98 (0.91, 1.05) p = .0001	0.97 p = .01	0.70 p = .55	0.57 p < .05
	Q	0.48 (0.37, 0.60) p = .0001			0.17 p < .05
Platyrrhini (n=117)	V	1.02 (0.84, 1.20) p = .0001	0.97 p = .06	1.65 p = .18	0.53 p < .05
	M	1.39 (1.15, 1.61) p = .0001	0.96 p = .004	1.28 p = .28	0.51 p < .05
	Q	0.65 (0.42, 0.88) p = .0001			0.20 p < .05
Atelidae (n=65)	V	0.86 (0.59, 1.13) p = .0001	0.92 p = .0005	1.91 p = .14	0.47 p < .05
	M	1.30 (0.78, 1.82) p = .0001	0.91 p = .0001	3.11 p = .03	0.42 p < .05
	Q	0.71 (0.40, 1.01) p = .0001			0.30 p < .05
Cebidae (n=52)	V	1.27 (1.05, 1.47) p = .0001	0.98 p = .65	1.83 p = .15	0.62 p < .05
	M	1.51 (1.32, 1.69) p = .0001	0.97 p = .49	1.11 p = .35	0.87 p < .05
Catarrhini (n=183)	V	0.84 (0.77, 0.91) p = .0001	0.98 p = .19	0.13 p = .94	0.62 p < .05
	M	0.97 (0.90, 1.05) p = .0001	0.96 p = .0005	0.47 p = .70	0.64 p < .05
	Q	0.44 (0.31, 0.57) p = .0001			0.17 p < .05
Cercopithecoidea (n=137)	V	0.93 (0.84, 1.02) p = .0001	0.97 p = .04	0.44 p = .72	0.62 p < .05
	M	1.06 (0.97, 1.16) p = .0001	0.95 p = .0002	1.15 p = .33	0.65 p < .05
	Q	0.45 (0.27, 0.62) p = .0001			0.15 p < .05
Cercopithecinae (n=87)	V	0.84 (0.75, 0.92) p = .0001	0.98 p = 53	0.38 p = .76	0.66 p < .05
	M	0.95 (0.87, 1.03) p = .0001	0.99 p = .99	0.74 p = .53	0.66 p < .05
	Q	0.45 (0.30, 0.61) p = .0001			0.19 p < .05
Colobinae (n=50)	V	0.58 (0.36, 0.79) p = .0001	0.96 p = .24	1.65 p = .19	0.41 p < .05
	M	0.70 (0.41, 0.99) p = .0001	0.98 p = .62	2.60 p = .06	0.37 p < .05
	Q	0.44 (0.13, 0.74) p = .005			0.25 p < .05
Hominoidea (n=46)	V	0.75 (0.61, 0.88) p = .0001	0.95 p = .09	0.96 p = .42	0.62 p < .05
	M	0.88 (0.73, 1.02) p = .0001	0.95 p = .10	0.54 p = .65	0.75 p < .05
	Q	0.44 (0.22, 0.67) p = .0001			0.17 ns

Reproduced with permission of the copyright owner. Further reproduction prohibited without permission.

Box 12.18. Nasal bone length [ΔS_L_YV1] ← Cribriform plate area [ΔS_L_YV44]					
Taxon	Level of analysis	Maximum likelihood regression coefficient (95% CI) and associated p-value	Shapiro-Wilk test for normality of residuals	Brown & Forsythe's test for residual homoscedasticity	Somers' D nonparametric measure and test
Anthropoids (n=300)	V	-0.57 (-0.68, -0.46) p = .0001	0.97 p = .07	8.83 p = .0001	-0.30 p < .05
	M	-0.79 (-0.92, -0.67) p = .0001	0.97 p = .0001	10.82 p = .0001	-0.42 p < .05
Platyrrhini (n=117)	V	0.15 (-0.06, 0.35) p = .14	0.95 p = .002	6.30 p = .0005	0.11 p < .05
	M	0.31 (0.03, 0.59) p = .03	0.96 p = .03	2.27 p = .08	0.10 ns
Atelidae (n=65)	V	-0.10 (-0.39, 0.20) p = .52	0.96 p = .08	1.86 p = .14	-0.03 ns
Cebidae (n=52)	V	0.33 (0.10, 0.56) p = .005	0.97 p = .35	3.44 p = .02	0.26 p < .05
	M	0.46 (0.21, 0.71) p = .0002	0.99 p = .89	3.64 p = .02	0.39 p < .05
Catarrhini (n=183)	V	-0.67 (-0.81, -0.62) p = .0001	0.97 p = .03	6.39 p = .0004	-0.41 p < .05
	M	-0.91 (-1.06, -0.77) p = .0001	0.95 p = .0001	5.06 p = .002	-0.54 p < .05
Cercopithecoidea (n=137)	V	-0.94 (-1.10, -0.79) p = .0001	0.95 p = .0007	0.38 p = .76	-0.44 p < .05
	M	-1.18 (-1.33, -1.03) p = .0001	0.96 p = .003	1.92 p = .13	-0.62 p < .05
Cercopithecinae (n=87)	V	-0.84 (-1.02, -0.67) p = .0001	0.97 p = .19	5.61 p = .002	-0.37 p < .05
	M	-1.04 (-1.22, -0.86) p = .0001	0.96 p = .04	4.43 p = .006	-0.54 p < .05
Colobinae (n=50)	V	-0.13 (-0.37, 0.12) p = .30	0.94 p = .03	0.52 p = .67	-0.09 ns
	M	-0.26 (-0.59, 0.07) p = .11	0.94 p = .04	3.37 p = .03	-0.21 p < .05
Hominoidea (n=46)	V	-0.30 (-0.50, -0.10) p = .002	0.99 p = .95	2.01 p = .13	-0.29 p < .05
	M	-0.49 (-0.71, -0.29) p = .0001	0.99 p = .98	6.27 p = .001	-0.57 p < 0.5

Reproduced with permission of the copyright owner. Further reproduction prohibited without permission.

Reproduced with permission of the copyright owner. Further reproduction prohibited without permission.

Box 12.19 Nasal process of maxilla width [ΔS_L_YV4] ← Cribriform plate area [ΔS_L_YV44]

Taxon	Level of analysis	Maximum likelihood regression coefficient (95% CI) and associated p-value	Shapiro-Wilk test for normality of residuals	Brown & Forsythe's test for residual homoscedasticity	Somers' D nonparametric measure and test
Anthropoids (n=300)	V	0.63 (0.47, 0.79) p = .0001	0.99 p = .88	2.03 p = .11	0.20 p < .05
	M	0.73 (0.54, 0.92) p = .0001	0.99 p = .89	3.43 p = .02	0.17 p < .05
	Q	0.36 (0.05, 0.67) p = .02			0.07 ns
Platyrrhini (n=117)	V	0.55 (0.15, 0.95) p = .006	0.98 p = .31	4.77 p = .004	0.16 p < .05
	M	0.52 (-0.04, 1.09) p = .06	0.98 p = .30	3.51 p = .02	0.14 p < .05
	Q	0.58 (0.01, 1.15) p = .04			0.09 ns
Atelidae (n=65)	V	0.82 (0.27, 1.37) p = .003	0.97 p = .35	2.20 p = .10	0.23 p < .05
	M	1.11 (0.02, 2.20) p = .04	0.97 p = .36	1.37 p = .26	0.20 ns
	Q	0.72 (0.09, 1.35) p = .02			0.15 ns
Cebidae (n=52)	V	-0.38 (-0.78, 0.03) p = .06	0.96 p = .19	1.53 p = .22	-0.20 ns
Catarrhini (n=183)	V	0.74 (0.56, 0.93) p = .0001	0.99 p = .79	1.36 p = .25	0.30 p < .05
	M	0.89 (0.68, 1.10) p = .0001	0.99 p = .91	0.38 p = .77	0.29 p < .05
Cercopithecoidea (n=137)	V	1.11 (0.84, 1.38) p = .0001	0.98 p = .47	0.69 p = .56	0.31 p < .05
	M	1.30 (1.00, 1.59) p = .0001	0.98 p = .70	0.36 p = .78	0.24 p < .05
Cercopithecinae (n=87)	V	1.18 (0.79, 1.58) p = .0001	0.97 p = .23	0.16 p = .92	0.24 p < .05
	M	1.43 (0.99, 1.86) p = .0001	0.98 p = .49	2.04 p = .11	0.17 ns
Colobinae (n=50)	V	0.55 (0.11, 0.98) p = .01	0.96 p = .16	0.13 p = .94	0.22 p < .05
Hominoidea (n=46)	V	0.49 (0.27, 0.71) p = .0001	0.99 p = .94	0.40 p = .76	0.41 p < .05
	M	0.60 (0.34, 0.85) p = .0001	0.98 p = .77	0.17 p = .91	0.48 p < .05

Box 12.20 Anterior nasal aperture height [ΔS_L_YV5] ← Cribriform plate area [ΔS_L_YV44]

Taxon	Level of analysis	Maximum likelihood regression coefficient (95% CI) and associated p-value	Shapiro-Wilk test for normality of residuals	Brown & Forsythe's test for residual homoscedasticity	Somers' D nonparametric measure and test of association
Anthropoids (n=300)	V	-0.02 (-0.09, 0.05) p = .59	0.98 p = .09	3.66 p = .01	0.03 ns
Platyrrhini (n=117)	V	0.11 (0.00, 0.23) p = .07	0.98 p = .69	0.45 p = .71	0.13 ns
Atelidae (n=65)	V	0.09 (-0.07, 0.26) p = .26	0.94 p = .006	2.08 p = .11	0.08 ns
Cebidae (n=52)	V	0.04 (-0.12, 0.20) p = .63	0.97 p = .43	0.80 p = .50	0.05 ns
Catarrhini (n=183)	V	0.01 (-0.09, 0.10) p = .85	0.96 p = .002	5.16 p = .002	0.13 p < .05
Cercopithecoidea (n=137)	V	0.13 (0.04, 0.23) p = .006	0.98 p = .50	0.22 p = .88	0.22 p < .05
Cercopithecinae (n=87)	V	0.04 (-0.08, 0.17) p = .47	0.98 p = .52	0.14 p = .94	0.14 ns
Colobinae (n=50)	V	0.41 (0.21, 0.61) p = .0001	0.97 p = .41	0.44 p = .72	0.35 p < .05
Hominoidea (n=46)	V	-0.04 (-0.22, 0.14) p = .66	0.97 p = .49	1.45 p = .24	-0.01 ns

Reproduced with permission of the copyright owner. Further reproduction prohibited without permission.

Box 12.21. Anterior nasal aperture breadth [ΔS_L_YV6] ← Cribriform plate area [ΔS_L_YV44]

Taxon	Level of analysis	Maximum likelihood regression coefficient (95% CI) and associated p-value	Shapiro-Wilk test for normality of residuals	Brown & Forsythe's test for residual homoscedasticity	Somers' D nonparametric measure and test of association
Anthropoids (n=300)	V	0.06 (0.01, 0.12) p = .03	0.99 p = .99	3.31 p = .02	0.07 ns
	M	0.08 (0.01, 0.14) p = .02	0.99 p = .99	4.29 p = .006	0.04 ns
Platyrrhini (n=117)	V	0.04 (-0.10, 0.17) p = .56	0.96 p = .03	2.26 p = .08	0.03 ns
Atelidae (n=65)	V	-0.23 (-0.41, -0.04) p = .01	0.97 p = .41	1.44 p = .0.24	-0.21 p < .05
	M	-0.89 (-1.20, -0.57) p = .0001	0.97 p = .28	0.89 p = .45	-0.40 p < .05
Cebidae (n=52)	V	0.24 (0.11, 0.37) p = .0004	0.99 p = .90	1.93 p = .14	0.31 p < .05
	M	0.30 (0.16, 0.45) p = .0001	0.99 p = .98	2.69 p = .06	0.53 p < .05
Catarrhini (n=183)	V	0.03 (-0.3, 0.09) p = .43	0.99 p = .81	2.74 p = .04	0.02 ns
Cercopithecoidea (n=137)	V	0.05 (-0.03, 0.13) p = .23	0.98 p = .40	1.14 p = .33	0.04 ns
Cercopithecinae (n=87)	V	0.15 (0.05, 0.24) p = .002	0.97 p = .37	1.51 p = .22	0.19 p < .05
	M	0.15 (0.04, 0.26) p = .006	0.97 p = .26	1.94 p = .13	0.14 ns
Colobinae (n=50)	V	0.23 (0.08, 0.38) p = .002	0.97 p =.29	0.97 p = .41	0.28 p < .05
	M	0.21 (0.00, 0.41) p = .045	0.96 p = .20	0.42 p = .74	0.33 p < .05
	Q	0.26 (0.04, 0.49) p = .02			0.21 p < .05
Hominoidea (n=46)	V	-0.01 (-0.13, 0.11) p = .81	0.97 p = .33	2.43 p = .08	-0.13 ns

Box 12.22 Posterior nasal aperture height [ΔS_L_YV7] ← Cribriform plate area [ΔS_L_YV44]

Taxon	Level of analysis	Maximum likelihood regression coefficient (95% CI) and associated p-value	Shapiro-Wilk test for normality of residuals	Brown & Forsythe's test for residual homoscedasticity	Somers' D nonparametric measure and test of association
Anthropoids (n=300)	V	-0.20 (-0.28, -0.12) p = .0001	0.96 p = .0001	3.69 p = .01	-0.12 p < .05
Platyrrhini (n=117)	V	0.11 (-0.3, 0.24) p = .11	0.97 p = .052	0.71 p = .54	0.13 ns
Atelidae (n=65)	V	0.00 (-0.19, 0.19) p = .99	0.97 p = .21	1.45 p = .24	-0.01 ns
Cebidae (n=52)	V	0.10 (-0.07, 0.27) p = .22	0.92 p = .002	0.92 p = .43	0.20 ns
Catarrhini (n=183)	V	-0.24 (-0.35, -0.14) p = .0001	0.97 p = .04	4.88 p = .003	-0.19 p < .05
Cercopithecoidea (n=137)	V	-0.18 (-0.31, -0.05) p = .005	0.96 p = .004	0.96 p = .41	-0.11 ns
Cercopithecinae (n=87)	V	-0.26 (-0.38, -0.14) p = .0001	0.98 p = .72	0.06 p = .98	-0.14 ns
Colobinae (n=50)	V	-0.02 (-0.41, 0.37) p = .93	0.91 p = .0006	0.42 p = .74	-0.00 ns
Hominoidea (n=46)	V	-0.24 (-0.41, -0.06) p = .006	0.96 p = .14	0.89 p = .45	-0.23 p < .05
	M	-0.32 (-0.52, -0.11) p = .002	0.96 p = .12	1.11 p = .36	-0.21 ns

Box 12.23. Posterior nasal aperture breadth [ΔS_L_YV8] ← Cribriform plate area [ΔS_L_YV44]

Taxon	Level of analysis	Maximum likelihood regression coefficient (95% CI) and associated p-value	Shapiro-Wilk test for normality of residuals	Brown & Forsythe's test for residual homoscedasticity	Somers' D nonparametric measure and test of association
Anthropoids (n=300)	V	0.22 (0.15, 0.29) p = .0001	0.97 p = .03	1.36 p = .25	0.13 p < .05
	M	0.33 (0.25, 0.41) p = .0001	0.98 p = .18	4.34 p = .005	0.19 P < .05
Platyrrhini (n=117)	V	0.05 (-0.16, 0.26) p = .67	0.95 p = .002	0.50 p = .68	0.00 ns
Atelidae (n=65)	V	0.15 (-0.20, 0.51) p = .39	0.92 p = .0003	2.17 p = .10	0.09 ns
	M	0.89 (0.21, 1.57) p = .009	0.92 p = .0003	6.72 p = .0005	0.31 p < .05
Cebidae (n=52)	V	-0.12 (-0.30, 0.05) p = .17	0.97 p = .27	2.71 p = .055	-0.06 ns
Catarrhini (n=183)	V	0.23 (0.14, 0.31) p = .0001	0.97 p = .09	1.50 p = .21	0.16 p < .05
	M	0.33 (0.24, 0.42) p = .0001	0.98 p = .47	6.12 p = .0006	0.21 p < .05
Cercopithecoidea (n=137)	V	0.21 (0.12, 0.29) p = .0001	0.96 p = .02	3.62 p = .01	0.11 ns
	M	0.26 (0.16, 0.36) p = .0001	0.98 p = .20	3.22 p = .02	0.07 ns
Cercopithecinae (n=87)	V	0.40 (0.29, 0.51) p = .0001	0.95 p = .01	2.00 p = .12	0.28 p < .05
	M	0.52 (0.40, 0.64) p = .0001	0.98 p = .54	3.23 p = .03	0.37 p < .05
Colobinae (n=50)	V	-0.05 (-0.20, 0.11) p = .57	0.97 p = .30	3.59 p = .02	-0.06 ns
Hominoidea (n=46)	V	0.25 (0.07, 0.42) p = .005	0.98 p = .72	2.17 p = .11	0.26 p < .05
	M	0.40 (0.20, 0.60) p = .0001	0.96 p = .14	0.53 p = .67	0.54 p < .05

Box 12.24 Maxillary arch length [ΔS_L_YV14] ← Cribriform plate area [ΔS_L_YV44]

Taxon	Level of analysis	Maximum likelihood regression coefficient (95% CI) and associated p-value	Shapiro-Wilk test for normality of residuals	Brown & Forsythe's test for residual homoscedasticity	Somers' D nonparametric measure and test
Anthropoids (n=300)	V	-0.21 (-0.27, -0.12) p = .0001	0.86 p = .0001	7.86 p = .0001	-0.20 p < .05
	M	-0.27 (-0.33, -0.20) p = .0001	0.86 p = .0001	13.79 p = .0001	-0.27 p < .05
Platyrrhini (n=117)	V	-0.06 (-0.12, 0.02) p = .15	0.97 p = .08	1.95 p = .13	-0.06 ns
Atelidae (n=65)	V	-0.10 (-0.21, 0.00) p = .05	0.97 p = .30	0.75 p = .53	-0.08 ns
	M	-0.27 (-0.48, -0.06) p = .01	0.97 p = .25	2.84 p = .05	-0.24 p < .05
Cebidae (n=52)	V	0.04 (-0.05, 012) p = .40	0.95 p = .03	2.23 p = .10	0.03 ns
Catarrhini (n=183)	V	-0.22 (-0.29 -0.14) p = .0001	0.85 p = .0001	7.51 p = .0001	-0.18 p < .05
	M	-0.27 (-0.40, -0.19) p = .0001	0.87 p = .0001	10.16 p = .0001	-0.26 p < .05
Cercopithecoidea (n=137)	V	-0.20 (-0.27, -0.14) p = .0001	0.96 p = .002	0.74 p = .53	-0.27 p < .05
	M	-0.24 (-0.18, -0.24) p = .0001	0.96 p = .002	5.89 p = .0008	-0.38 p < .05
Cercopithecinae (n=87)	V	-0.28 (-0.33, -0.22) p = .0001	0.98 p = .35	1.18 p = .32	-0.43 p < .05
	M	-0.34 (-0.40, -0.28) p = .0001	0.98 p = .68	1.05 p = .38	-0.57 p < .05
Colobinae (n=50)	V	0.21 (0.06, 0.36) p = .007	0.94 p = .03	1.37 p = .26	0.24 p < .05
	M	0.42 (0.23, 0.61) p = .0001	0.95 p = .04	2.68 p = .06	0.36 p < .05
Hominoidea (n=46)	V	-0.19 (-0.36, -0.02) p = .02	0.91 p = .0009	4.74 p = .006	-0.05 ns
	M	-0.25 (-0.45, -0.25) p = .01	0.92 p = .004	1.77 p = .32	-0.15 ns

Reproduced with permission of the copyright owner. Further reproduction prohibited without permission.

Box 12.25 Upper facial breadth [ΔS_L_YV16] ← Cribriform plate area [ΔS_L_YV44]					
Taxon	Level of analysis	Maximum likelihood regression coefficient (95% CI) and associated p-value	Shapiro-Wilk test for normality of residuals	Brown & Forsythe's test for residual homoscedasticity	Somers' D nonparametric measure and test
Anthropoids (n=300)	V	0.27 (0.23, 0.31) p = .0001	0.98 p = .10	0.75 p = .52	0.34 p < .05
	M	0.34 (0.29, 0.38) p = .0001	0.98 p = .03	3.71 p = .01	0.38 p < .05
	Q	0.08 (0.01, 0.16) p = .03			0.08 p < .05
Platyrrhini (n=117)	V	0.29 (0.17, 0.42) p = .0001	0.95 p = .0002	0.91 p = .44	0.30 p < .05
	M	0.56 (0.40, 072) p = .0001	0.96 p = .006	11.06 p = .0001	0.46 p < .05
Atelidae (n=65)	V	0.15 (0.02, 0.27) p = .02	0.97 p = .22	0.45 p = .72	0.22 p < .05
	M	0.43 (0.19, 0.66) p = .0004	0.95 p = .04	3.36 p = .02	0.27 p < .05
Cebidae (n=52)	V	0.52 (0.29, 0.76) p = .0001	0.94 p = .02	3.10 p = .04	0.39 p < .05
	M	0.70 (0.45, 0.93) p = .0001	0.97 p = .24	1.61 p = .20	0.59 p < .05
Catarrhini (n=183)	V	0.28 (0.23, 0.32) p = .0001	0.98 p = .17	1.45 p = .23	0.41 p < .05
	M	0.34 (0.29, 0.39) p = .0001	0.98 p = .34	2.50 p = .06	0.47 p < .05
	Q	0.10 (0.01, 0.18) p = .02			0.12 p < .05
Cercopithecoidea (n=137)	V	0.32 (0.26, 0.38) p = .0001	0.96 p = .01	0.03 p = .99	0.43 p < .05
	M	0.39 (0.33, 045) p = .0001	0.97 p = .04	5.97 p = .0008	0.52 p < .05
Cercopithecinae (n=87)	V	0.36 (0.30, 0.42) p = .0001	0.98 p = .10	0.75 p = .52	0.51 p < .05
	M	0.44 (0.38, 0.50) p = .0001	0.98 p = .41	1.04 p = .38	0.59 p < .05
Colobinae (n=50)	V	0.02 (-0.12, 0.16) p = .79	0.94 p = .03	1.21 p = .32	0.04 ns
Hominoidea (n=46)	V	0.24 (0.16, 031) p = .0001	0.95 p = .07	2.04 p = .12	0.39 p < .05
	M	0.29 (0.20, 038) p = .0001	0.96 p = .13	1.11 p = .36	0.53 p < .05

Reproduced with permission of the copyright owner. Further reproduction prohibited without permission.

Reproduced with permission of the copyright owner. Further reproduction prohibited without permission.

Box 12.26 Anterior facial length [ΔS_L_YV17] ← Cribriform plate area [ΔS_L_YV44]

Taxon	Level of analysis	Maximum likelihood regression coefficient (95% CI) and associated p-value	Shapiro-Wilk test for normality of residuals	Brown & Forsythe's test for residual homoscedasticity	Somers' D nonparametric measure and test of association
Anthropoids (n=300)	V	-0.32 (-0.37, -0.27) p = .0001	0.97 p = .007	1.75 p = .16	-0.30 p < .05
	M	-0.42 (-0.48 -0.37) p = .0001	0.97 p = .002	3.93 p = .009	-0.42 p < .05
Platyrrhini (n=117)	V	0.16 (0.05, 0.27) p = .004	0.92 p = .0001	3.74 p = .01	0.22 p < .05
	M	0.28 (0.13, 0.44) p = .0003	0.93 p = .0001	3.01 p = .03	0.21 p < .05
Atelidae (n=65)	V	0.02 (-0.15, 0.19) p = .81	0.95 p = .02	4.48 p = .0007	0.05 ns
Cebidae (n=52)	V	0.23 (0.11, 0.34) p = .0001	0.96 p = .12	4.22 p = .01	0.38 p < .05
	M	0.31 (0.19, 0.43) p = .0001	0.98 p = .84	3.07 p = .04	0.58 p < .05
Catarrhini (n=183)	V	-0.37 (-0.44, -0.31) p = .0001	0.97 p = .006	1.19 p = .31	-0.45 p < .05
	M	-0.49 (-0.55, -0.42) p = .0001	0.96 p = .001	0.18 p = .91	-0.57 p < .05
Cercopithecoidea (n=137)	V	-0.39 (-0.47, -0.31) p = .0001	0.97 p = .12	0.59 p = .62	-0.39 p < .05
	M	-0.49 (-0.57, -.041) p = .0001	0.96 p = .002	4.06 p = .009	-0.55 p < .05
Cercopithecinae (n=87)	V	-0.38 (-0.46, -0.30) p = .0001	0.98 p = .68	2.17 p = .10	-0.35 p < .05
	M	-0.46 (-0.55, -0.38) p = .0001	0.96 p = .047	0.94 p = .42	-0.48 p < .05
Colobinae (n=50)	V	0.12 (-0.01, 0.25) p = .07	0.98 p = .60	1.05 p = .38	0.13 ns
Hominoidea (n=46)	V	-0.32 (-0.41, -0.23) p = .0001	0.98 p = .66	1.11 p = .36	-0.58 p < .05
	M	-0.43 (-0.52, -0.34) p = .0001	0.99 p = .98	1.34 p = .27	-0.68 p < .05

Box 12.27 Posterior facial height [ΔS_L_YV18] ← Cribriform plate area [ΔS_L_YV44]

Taxon	Level of analysis	Maximum likelihood regression coefficient (95% CI) and associated p-value	Shapiro-Wilk test for normality of residuals	Brown & Forsythe's test for residual homoscedasticity	Somers' D nonparametric measure and test of association
Anthropoids (n=300)	V	0.01 (-0.4, 0.05) p = .79	0.95 p = .0001	5.44 p = .001	0.03 ns
Platyrrhini (n=117)	V	0.40 (0.25, 0.54) p = .0001	0.96 p = .02	8.96 p = .0001	0.24 p < .05
	M	0.77 (0.59, 0.95) p = .0001	0.95 p = .0001	6.07 p = .0007	0.27 p < .05
Atelidae (n=65)	V	0.02 (-0.14, 0.17) p = .83	0.93 p = .0007	0.98 p = .41	0.03 ns
Cebidae (n=52)	V	0.78 (0.59, 0.99) p = .0001	0.95 p = .07	1.29 p = .29	0.45 p < .05
	M	0.98 (0.78, 1.18) p = .0001	0.94 p = .02	2.57 p = .06	0.66 p < .05
Catarrhini (n=183)	V	-0.05 (-0.10, 0.00) p = .05	0.97 p = .01	4.77 p = .0003	-0.08 ns
Cercopithecoidea (n=137)	V	0.09 (0.03, 0.16) p = .003	0.97 p = .02	1.32 p = .27	0.05 ns
Cercopithecinae (n=87)	V	0.24 (0.17, 0.31) p = .0001	0.98 p = .45	1.33 p = .27	0.27 p < .05
	M	0.30 (0.22, 0.38) p = .0001	0.97 p = .14	3.69 p = .02	0.27 p < .05
Colobinae (n=50)	V	0.05 (-0.08, 0.18) p = .43	0.92 p = .003	0.47 p = .71	0.10 ns
Hominoidea (n=46)	V	-0.20 (-0.29, -0.12) p = .0001	0.98 p = .68	1.35 p = .27	-0.32 p < .05
	M	-0.28 (-0.38, -0.18) p = .0001	0.97 p = .31	3.58 p = .02	-0.41 p < .05

Reproduced with permission of the copyright owner. Further reproduction prohibited without permission.

Box 12.28 Inter M^1 palatal width [ΔS_L_YV22] ← Cribriform plate area [ΔS_L_YV44]					
Taxon	Level of analysis	Maximum likelihood regression coefficient (95% CI) and associated p-value	Shapiro-Wilk test for normality of residuals	Brown & Forsythe's test for residual homoscedasticity	Somers' D nonparametric measure and test of association
Anthropoids (n=300)	V	0.07 (0.02, 0.12) p = .01	0.97 p = .002	4.52 p = .004	0.03 ns
Platyrrhini (n=117)	V	0.07 (-0.02, 0.17) p = .14	0.98 p = .58	2.59 p = .06	0.06 ns
Atelidae (n=65)	V	0.14 (0.00, 0.28) p = .05	0.98 p = .49	1.02 p = .39	0.19 p < .05
	M	0.55 (0.29, 0.80) p = .0001	0.98 p = .59	0.64 p = .59	0.29 p < .05
Cebidae (n=52)	V	-0.13 (-0.23, -0.03) p = .01	0.97 p = .28	0.16 p = .93	-0.24 p < .05
	M	-0.18 (-0.29, -0.07) p = .001	0.98 p = .61	1.21 p = .32	-0.29 p < .05
Catarrhini (n=183)	V	0.09 (0.03, 0.15) p = .006	0.97 p = .02	6.38 p = .0004	0.08 ns
Cercopithecoidea (n=137)	V	0.14 (0.07, 0.21) p = .0001	0.98 p = .27	3.25 p = .02	0.12 ns
Cercopithecinae (n=87)	V	0.29 (0.20, 0.37) p = .0001	0.98 p = .57	1.53 p = .21	0.30 p < .05
	M	0.36 (0.27, 0.45) p = .0001	0.99 p = .88	1.30 p = .28	0.46 p < .05
Colobinae (n=50)	V	-0.05 (-0.18, 0.08) p = .46	0.98 p = .77	0.60 p = .61	-0.05 ns
Hominoidea (n=46)	V	0.05 (-0.09, 0.19) p = .49	0.97 p = .54	4.46 p = .008	0.05 ns

Box 12.29 Palatal depth at M^1 [ΔS_L_YV26] ← Cribriform plate area [ΔS_L_YV44]					
Taxon	Level of analysis	Maximum likelihood regression coefficient (95% CI) and associated p-value	Shapiro-Wilk test for normality of residuals.	Brown & Forsythe's test for residual homoscedasticity	Somers' D nonparametric measure and test of association
Anthropoids (n=300)	V	0.03 (-0.04, 0.11) p = .37	0.98 p = .05	1.49 p = .22	0.02 ns
Platyrrhini (n=117)	V	0.25 (0.13, 0.37) p = .0001	0.97 p = .20	0.72 p = .54	0.24 p < .05
	M	0.44 (0.27, 0.60) p = .0001	0.97 p = .14	1.42 p = .24	0.26 p < .05
Atelidae (n=65)	V	0.13 (-0.05, 0.31) p = .15	0.97 p = .33	1.28 p = .29	0.14 ns
Cebidae (n=52)	V	0.32 (0.18, 0.046) p = .0001	0.95 p = .06	0.12 p = .95	0.29 p < .05
	M	0.43 (0.29, 0.57) p = .0001	0.98 p = .59	0.48 p = .69	0.46 p < .05
Catarrhini (n=183)	V	0.03 (-0.07, 0.12) p = .60	0.98 p = .21	1.02 p = .39	0.01 ns
Cercopithecoidea (n=137)	V	0.21 (0.08, 0.34) p = .001	0.98 p = .64	0.78 p = .51	0.12 ns
	M	0.22 (0.08, 0.36) p = .002	0.98 p = .64	0.50 p = .68	0.10 ns
Cercopithecinae (n=87)	V	0.54 (0.39, 0.68) p = .0001	0.98 p = .74	0.10 p = .96	0.35 p < .05
	M	0.62 (0.45, 0.78) p = .0001	0.99 p = .97	0.09 p = .96	0.45 p < .05
Colobinae (n=50)	V	0.04 (-0.19, 0.27) p = .73	0.97 p = .42	0.03 p = .99	0.07 ns
Hominoidea (n=46)	V	-0.12 (-0.28, 0.03) p = .11	0.97 p = .32	0.69 p = .56	-0.20 p < .05

Reproduced with permission of the copyright owner. Further reproduction prohibited without permission.

Box 12.30 Facial prognathism (Krogman's angle) [ΔL_YV30] ← Cribriform plate area [ΔS_L_YV44]

Taxon	Level of analysis	Maximum likelihood regression coefficient (95% CI) and associated p-value	Shapiro-Wilk test for normality of residuals	Brown & Forsythe's test for residual homoscedasticity	Somers' D nonparametric measure and test of association
Anthropoids (n=300)	V	-0.40 (-0.57, -0.23) p = .0001	0.94 p = .0001	8.76 p = .0001	-0.06 ns
Platyrrhini (n=117)	V	0.02 (-0.22, 0.49) p = .92	0.97 p = .08	1.89 p = .13	0.07 ns
Atelidae (n=65)	V	-0.19 (-0.95, 0.057) p = .62	0.93 p = .0008	9.79 p = .0001	0.01 ns
Cebidae (n=52)	V	0.19 (-0.30, 0.69) p = .43	0.95 p = .05	0.11 p = .95	0.06 ns
Catarrhini (n=183)	V	-0.58 (-0.76, -0.39) p = .0001	0.90 p = .0001	6.91 p = .0002	-0.20 p < .05
	M	-0.75 (-0.95, -0.54) p = .0001	0.93 p = .0001	6.57 p = .0003	-0.29 p < .05
Cercopithecoidea (n=137)	V	-0.35 (-0.54, -0.16) p = .0004	0.96 p = .001	3.35 p = .02	-0.18 p < .05
	M	-0.41 (-0.62, -0.19) p = .0003	0.95 p = .0007	4.68 p = .003	-0.25 p < .05
Cercopithecinae (n=87)	V	-0.59 (-0.81, -0.37) p = .0001	0.97 p = .13	2.25 p = .09	-0.36 p < .05
	M	-0.72 (-0.96, -0.47) p = .0001	0.96 p = .05	4.49 p = .006	-0.46 p < .05
Colobinae (n=50)	V	0.11 (-0.40, 0.62) p = .66	0.92 p = .002	0.20 p = .89	0.01 ns
Hominoidea (n=46)	V	-0.76 (-1.15, -0.36) p = .0001	0.89 p = .0003	3.32 p = .03	-0.31 p < .05
	M	-1.05 (-1.50, -0.62) p = .0001	0.95 p = .09	4.31 p = .01	-0.45 p < .05

Box 12.31 Facial convexity [ΔL_YV33] ← Cribriform plate area [ΔS_L_YV44]

Taxon	Level of analysis	Maximum likelihood regression coefficient (95% CI) and associated p-value	Shapiro-Wilk test for normality of residuals	Brown & Forsythe's test for residual homoscedasticity	Somers' D nonparametric measure and test of association
Anthropoids (n=300)	V	0.17 (-0.01, 0.34) p = .06	0.97 p = .09	0.60 p = .61	0.01 ns
Platyrrhini (n=117)	V	0.31 (-0.28, 0.89) p = .29	0.96 p = .004	0.52 p = .67	0.07 ns
Atelidae (n=65)	V	-0.76 (-1.46, -0.07) p = .03	0.99 p = .89	1.00 p = .39	-0.15 ns
Cebidae (n=52)	V	1.73 (0.78, 2.66) p = .0003	0.95 p = .06	3.80 p = .02	0.29 p < .05
	M	2.41 (1.43, 3.86) p = .0001	0.96 p = .19	1.19 p = .32	0.46 p < .05
Catarrhini (n=183)	V	0.21 (0.03, 0.39) p = .02	0.98 p = .12	1.95 p = .12	0.01 ns
Cercopithecoidea (n=137)	V	-0.27 (-0.47, -0.06) p = .009	0.98 p = .33	0.22 p = .89	-0.21 p < .05
	M	-0.43 (-0.65, -0.21) p = .0002	0.98 p = .21	0.14 p = .94	-0.38 p < .05
Cercopithecinae (n=87)	V	0.18 (-0.04, 0.40) p = .10	0.99 p = .84	0.74 p = .53	0.04 ns
Colobinae (n=50)	V	0.14 (-0.19, 0.47) p = .40	0.99 p = .97	1.39 p = .26	0.01 ns
Hominoidea (n=46)	V	0.73 (0.47, 1.00) p = .0001	0.95 p = .09	0.59 p = .62	0.52 p < .05
	M	1.00 (0.71, 1.28) p .0001	0.97 p = .28	0.59 p = .63	0.61 p < .05

Reproduced with permission of the copyright owner. Further reproduction prohibited without permission.

Box 12.32 Paranasal plate orientation [ΔL_YV35] ← Cribriform plate area [ΔS_L_YV44]

Taxon	Level of analysis	Maximum likelihood regression coefficient (95% CI) and associated p-value	Shapiro-Wilk test for normality of residuals	Brown & Forsythe's test for residual homoscedasticity	Somers' D nonparametric measure and test of association
Anthropoids (n=300)	V	-0.53 (-0.73, -0.33) p = .0001	0.94 p = .0001	3.13 p = .03	-0.17 p < .05
	M	-0.67 (-0.90, -0.44) p = .0001	0.93 p = .0001	4.24 p = .0006	-0.22 p < .05
Platyrrhini (n=117)	V	-0.13 (-0.49, 0.24) p = .49	0.98 p = .43	4.29 p = .007	-0.04 ns
Atelidae (n=65)	V	0.03 (-0.52, 0.58) p = .91	0.97 p = .17	1.84 p = .15	0.03 ns
Cebidae (n=52)	V	-0.29 (-0.77, 0.19) p = .23	0.97 p = .26	1.66 p = .19	-0.06 ns
Catarrhini (n=183)	V	-0.75 (-0.98, -0.51) p = .0001	0.94 p = .0001	3.57 p = .02	-0.30 p < .05
	M	-0.96 (-.123, -0.69) p = .0001	0.93 p = .0001	5.10 p = .002	-0.41 p < .05
Cercopithecoidea (n=137)	V	-1.36 (-1.69, -1.03) p = .0001	0.93 p = .0001	0.89 p = .45	-0.36 p < .05
	M	-1.69 (-2.04, -1.33) p = .0001	0.92 p = .0001	2.44 p = .07	-0.55 p < .05
Cercopithecinae (n=87)	V	-1.22 (-1.52, -0.91) p = .0001	0.96 p = .03	0.16 p = .92	-0.36 p < .05
	M	-1.50 (-1.82, -1.17) p = .0001	0.95 p = .002	0.44 p = .73	-0.58 p < .05
Colobinae (n=50)	V	0.41 (-0.33, 1.15) p = .27	0.97 p = .43	1.43 p = .25	0.14 ns
Hominoidea (n=46)	V	-0.15 (-0.43, 0.12) p = .26	0.95 p = .08	4.20 p = .01	-0.04 ns

Box 12.33 Orbital parallelism [ΔL_YV45] ← Cribriform plate area [ΔS_L_YV44]

Taxon	Level of analysis	Maximum likelihood regression coefficient (95% CI) and associated p-value	Shapiro-Wilk test for normality of residuals	Brown & Forsythe's test for residual homoscedasticity	Somers' D nonparametric measure and test of association
Anthropoids (n=300)	V	0.31 (0.13, 0.48) p = .0007	0.97 p = .003	0.73 p = .53	0.12 p < .05
	M	0.27 (0.06, 0.48) p = .01	0.97 p = .005	0.93 p = .43	0.04 ns
	Q	0.41 (0.06, 0.76) p = .02			0.08 p < .05
Platyrrhini (n=117)	V	1.67 (1.11, 2.23) p = .0001	0.98 p = .25	0.26 p = .85	0.31 p < .05
	M	2.94 (2.23, 3.66) p = .0001	0.97 p = .08	2.40 p = .07	0.37 p < .05
Atelidae (n=65)	V	0.76 (0.11, 1.40) p = .02	0.97 p = .31	0.41 p = .74	0.18 p < .05
Cebidae (n=52)	V	2.95 (2.02, 3.87) p = .0001	0.98 p = .88	3.73 p = .02	0.44 p < .05
	M	3.95 (3.10, 4.80) p = .0001	0.97 p = .31	2.53 p = .07	0.49 p < .05
Catarrhini (n=183)	V	0.32 (0.16, 0.48) p = .0001	0.98 p = .66	1.12 p = .34	0.14 p < .05
	M	0.29 (0.11, 0.47) p = .002	0.98 p = .68	1.63 p = .19	0.07 ns
	Q	0.42 (0.11, 0.73) p = .008			0.10 p < .05
Cercopithecoidea (n=137)	V	0.26 (0.05, 0.47) p = .02	0.99 p = .90	0.21 p = .88	0.10 ns
Cercopithecinae (n=87)	V	0.00 (-0.29, 0.29) p = .99	0.99 p = .93	1.37 p = .26	-0.01 ns
Colobinae (n=50)	V	0.83 (0.43, 1.22) p = .0001	0.96 p = .16	1.76 p = .17	0.25 p < .05
	M	1.11 (0.58, 1.63) p = .0001	0.96 p = .14	0.77 p = .52	0.20 ns
Hominoidea (n=46)	V	0.43 (0.19, 0.67) p = .0004	0.99 p = .91	1.34 p = .27	0.42 p < .05
	M	0.42 (0.13, 0.71) p = .004	0.99 p = .90	0.46 p = .71	0.35 p < .05
	Q	0.45 (0.01, 0.90) p = .04			0.16 ns

Reproduced with permission of the copyright owner. Further reproduction prohibited without permission.

Box 12.34. Facial (centroid) size [ΔS_L_YV34] ← Intranasal distance [ΔS_L_YV49]

Taxon	Maximum likelihood regression coefficient (95% CI) and associated p-value	Shapiro-Wilk test for normality of residuals	Brown & Forsythe's test for residual homoscedasticity	Somers' D nonparametric measure and test of association
Anthropoids (n=300)	-0.10 (-0.12, -0.08) p = .0001	0.97 p = .002	6.89 p = .0002	-0.18 p < .05
Platyrrhini (n=117)	0.08 (0.05, 0.12) p = .0001	0.97 p = .09	4.02 p = .007	0.35 p < .05
Atelidae (n=65)	0.07 (0.03, 0.11) p = .0001	0.96 p = .05	1.14 p = .34	0.24 p < .05
Cebidae (n=52)	0.09 (0.04, 0.14) p = .0005	0.89 p = .0001	2.54 p = .07	0.36 p < .05
Catarrhini (n=183)	-0.14 (-0.16, -0.12) p = .0001	0.95 p = .0001	6.93 p = .0002	-0.43 p < .05
Cercopithecoidea (n=137)	-0.14 (-0.16, -0.12) p = .0001	0.98 p = .68	14.01 p = .0001	-0.44 p < .05
Cercopithecinae (n=87)	-0.16 (-0.19, -0.12) p = .0001	0.98 p = .53	19.83 p = .0001	-0.24 p < .05
Colobinae (n=50)	-0.00 (-0.04, 0.03) p = .81	0.97 p = .45	0.23 p = .87	0.02 ns
Hominoidea (n=46)	-0.13 (-0.19, 0.07) p = .0001	0.92 p = .006	0.95 p = .42	-0.40 p < .05

Box 12.35. Intranasal distance [ΔS_L_YV49] ← Orbital parallelism [ΔL_YV45]

Taxon	Maximum likelihood regression coefficient (95% CI) and associated p-value	Shapiro-Wilk test for normality of residuals	Brown & Forsythe's test for residual homoscedasticity	Somers' D nonparametric measure and test of association
Anthropoids (n=300)	0.17 (0.10, 0.24) p = .0001	0.94 p = .0001	0.98 p = .40	0.17 p < .05
Platyrrhini (n=117)	0.17 (0.10, 0.24) p = .0001	0.97 p = .07	3.18 p = .03	0.26 p < .05
Atelidae (n=65)	0.11 (-0.02, 0.23) p = .09	0.96 p = .14	1.20 p = .32	0.14 p < .05
Cebidae (n=52)	0.19 (0.12, 0.27) p = .0001	0.96 p = .12	3.27 p = .03	0.35 p < .05
Catarrhini (n=183)	0.31 (0.19, 0.43) p = .0001	0.96 p = .0002	1.66 p = .18	0.18 p < .05
Cercopithecoidea (n=137)	0.21 (0.07, 0.35) p = .003	0.95 p = .0005	0.87 p = .46	0.14 p < .05
Cercopithecinae (n=87)	0.05 (-0.09, 0.20) p = .45	0.90 p = .0001	0.71 p = .54	0.04 ns
Colobinae (n=50)	0.29 (0.14, 0.43) p = .0001	0.96 p = .11	1.59 p = .20	0.32 p < .05
Hominoidea (n=46)	0.54 (0.32, 0.77) p = .0001	0.92 p = .005	2.81 p = .0.051	0.36 p < .05

Box 12.36. Intranasal distance [ΔS_L_YV49] ← Anterior facial length [ΔS_L_YV17]

Taxon	Maximum likelihood regression coefficient (95% CI) and associated p-value	Shapiro-Wilk test for normality of residuals	Brown & Forsythe's test for residual homoscedasticity	Somers' D nonparametric measure and test of association
Anthropoids (n=300)	-0.96 (-1.14, -0.55) p = .0001	0.97 p = .0003	0.55 p = .65	-0.29 p < .05
Platyrrhini (n=117)	1.03 (0.68, 1.39) p = .0001	0.97 p = .10	2.24 p = .09	0.32 p < .05
Atelidae (n=65)	0.92 (0.46, 1.38) p = .0001	0.98 p = .79	5.11 p = .003	0.27 p < .05
Cebidae (n=52)	1.50 (0.74, 2.25) p = .0001	0.97 p = .27	0.45 p = .72	0.39 p < .05
Catarrhini (n=183)	-1.23 (-1.40, -1.05) p = .0001	0.96 p = .0002	3.44 p = .02	-0.50 p < .05
Cercopithecoidea (n=137)	-1.32 (-1.52, -1.12) p = .0001	0.97 p = .06	2.95 p = .04	-0.50 p < .05
Cercopithecinae (n=87)	-1.27 (-1.53, -1.02) p = .0001	0.96 p = .03	0.29 p = .83	-0.36 p < .05
Colobinae (n=50)	0.01 (-0.55, 0.56) p = .99	0.97 p = .49	3.09 p = .04	0.07 ns
Hominoidea (n=46)	-1.37 (-1.80, -0.94) p = .0001	0.95 p = .05	3.00 p = .04	-0.54 p < .05

Reproduced with permission of the copyright owner. Further reproduction prohibited without permission.

Box 12.37. Intranasal distance [ΔS_L_YV49] ← Facial prognathism (Krogman's angle) [ΔL_YV30]

Taxon	Maximum likelihood regression coefficient (95% CI) and associated p-value	Shapiro-Wilk test for normality of residuals	Brown & Forsythe's test for residual homoscedasticity	Somers' D nonparametric measure and test of association
Anthropoids (n=300)	-0.16 (-0.23, -0.09) p = .0001	0.96 p = .0001	3.54 p = .02	-0.06 ns
Platyrrhini (n=117)	0.00 (-0.10, 0.10) p = .99	0.97 p = .13	1.25 p = .30	0.04 ns
Atelidae (n=65)	0.00 (-0.11, 0.11) p = .94	0.96 p = .10	3.41 p = .02	0.03 ns
Cebidae (n=52)	-0.06 (-0.28, 0.17) p = .62	0.92 p = .003	0.05 p = .98	-0.05 ns
Catarrhini (n=183)	-0.28 (-0.37, -0.18) p = .0001	0.97 p = .03	7.61 p = .0001	-0.17 p < .05
Cercopithecoidea (n=137)	-0.19 (-0.33, -0.04) p = .01	0.96 p = .007	10.48 p = .0001	-0.14 p < .05
Cercopithecinae (n=87)	-0.39 (-0.53, -0.25) p = .0001	0.92 p = .0001	4.56 p = .005	-0.36 p < .05
Colobinae (n=50)	0.16 (0.02, 0.30) p = .03	0.97 p = .30	4.55 p = .007	0.17 p < .05
Hominoidea (n=46)	-0.31 (-0.45, -0.17) p = .0001	0.93 p = .01	1.41 p = .25	-0.37 p < .05

Box 12.38. Intranasal distance [ΔS_L_YV49] ← Paranasal plate orientation [ΔL_YV35]

Taxon	Maximum likelihood regression coefficient (95% CI) and associated p-value	Shapiro-Wilk test for normality of residuals	Brown & Forsythe's test for residual homoscedasticity	Somers' D nonparametric measure and test of association
Anthropoids (n=300)	-0.20 (-0.26, -0.14) p = .0001	0.95 p = .0001	0.87 p = .45	-0.25 p < .05
Platyrrhini (n=117)	0.12 (-0.01, 0.25) p = .07	0.97 p = .22	13.54 p = .0001	0.11 p < .05
Atelidae (n=65)	0.16 (0.01, 0.31) p = .04	0.98 p = .62	2.55 p = .06	0.15 p < .05
Cebidae (n=52)	0.06 (-0.18, 0.29) p = .63	0.93 p = .006	2.24 p = .10	0.02 ns
Catarrhini (n=183)	-0.30 (-0.37, -0.23) p = .0001	0.94 p = .0001	2.26 p = .08	-0.43 p < .05
Cercopithecoidea (n=137)	-0.31 (-0.37, -0.26) p = .0001	0.97 p = .011	2.14 p = .10	-0.51 p < .05
Cercopithecinae (n=87)	-0.32 (-0.40, -0.24) p = .0001	0.93 p = .0002	3.04 p = .03	-0.40 p < .05
Colobinae (n=50)	-0.06 (-0.16, 0.04) p = .24	0.97 p = .54	4.29 p = .009	0.01 ns
Hominoidea (n=46)	-0.20 (-0.47, 0.07) p = .14	0.88 p = .0001	0.02 p = .99	-0.13 ns

Box 12.39. Orbital parallelism [ΔL_YV45] ← Facial (centroid) size [ΔS_L_YV34]

Taxon	Maximum likelihood regression coefficient (95% CI) and associated p-value	Shapiro-Wilk test for normality of residuals	Brown & Forsythe's test for residual homoscedasticity	Somers' D nonparametric measure and test of association
Anthropoids (n=300)	0.66 (-0.18, 151) p = .12	0.97 p = .02	0.88 p = .45	0.14 p < .05
Platyrrhini (n=117)	5.02 (2.92, 7.11) p = .0001	0.98 p = .46	4.25 p = .007	0.24 p < .05
Atelidae (n=65)	0.42 (-2.34, 3.08) p = .75	0.98 p = .69	6.02 p = .002	0.03 ns
Cebidae (n=52)	9.41 (6.29, 12.52) p = .0001	0.98 p = .78	0.94 p = .42	0.47 p < .05
Catarrhini (n=183)	-0.47 (-1.23, 0.29) p = .22	0.98 p = .37	0.09 p = .97	-0.01 ns
Cercopithecoidea (n=137)	0.51 (-0.54, 1.56) p = .34	0.99 p = .84	0.79 p = .50	0.06 ns
Cercopithecinae (n=87)	1.58 (0.22, 2.94) p = .02	0.99 p = .98	0.07 p = .98	0.24 p < .05
Colobinae (n=50)	2.31 (-1.66, 6.29) p = .24	0.96 p = .24	6.24 p = .001	0.08 ns
Hominoidea (n=46)	-1.58 (-2.76, -0.39) p = .008	0.98 p = .69	0.22 p = .88	-0.18 ns

Bivariate Scatter Plots

Box 12.40. Scatter plots of delta log cribriform plate area against delta log nasomaxillary dependent variables. See Box 12.14 for fit estimates.

Nasal bone length

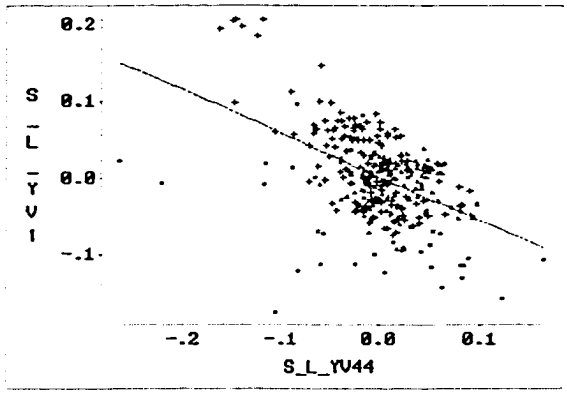

Anterior nasal aperture breadth

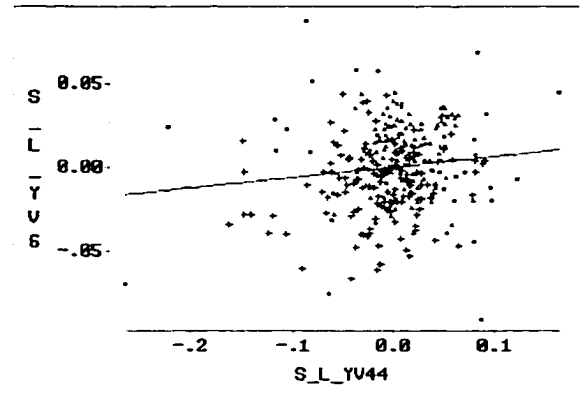

Maxillary arch length

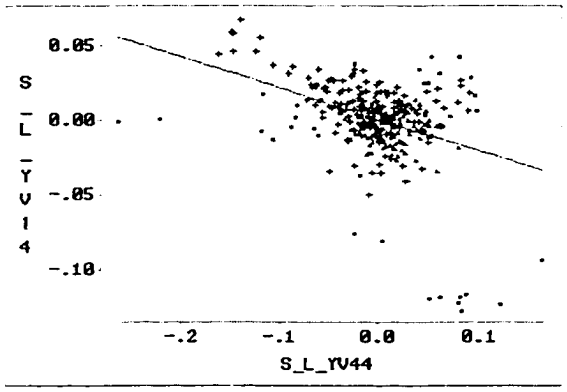

Upper facial breadth

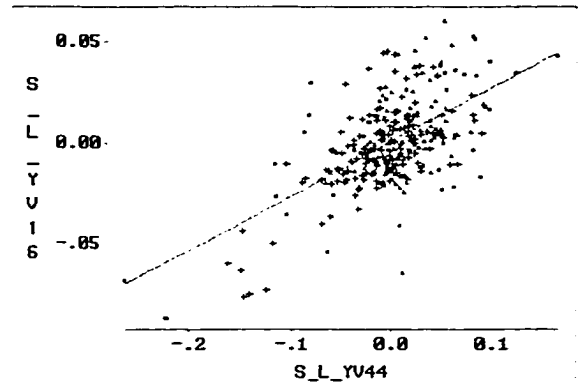

Anterior facial length

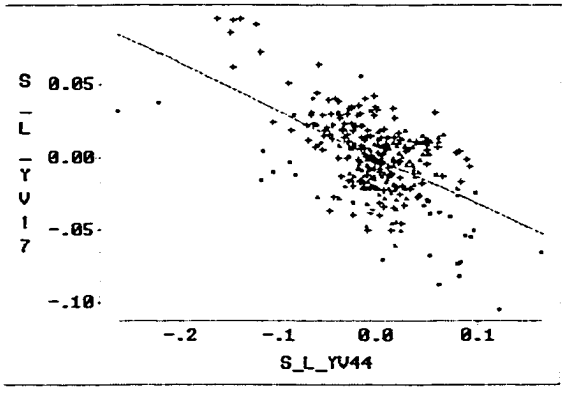

Facial prognathism (Krogman's angle)

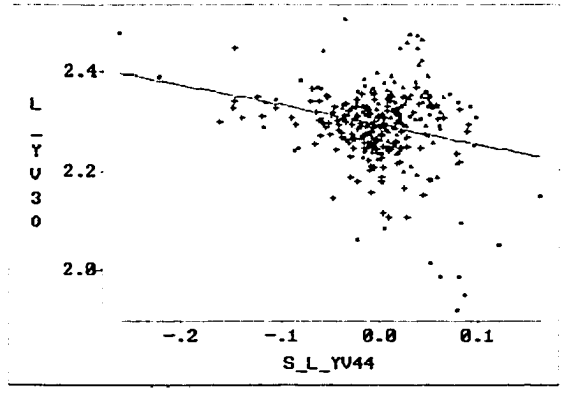

Reproduced with permission of the copyright owner. Further reproduction prohibited without permission.

Box 12.40. Scatter plots of delta log cribriform plate area against delta log nasomaxillary dependent variables. See Box 12.14 for fit estimates.

Paranasal plate orientation

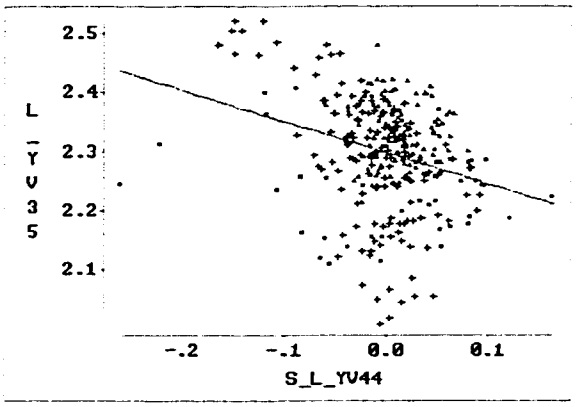

Intranasal distance

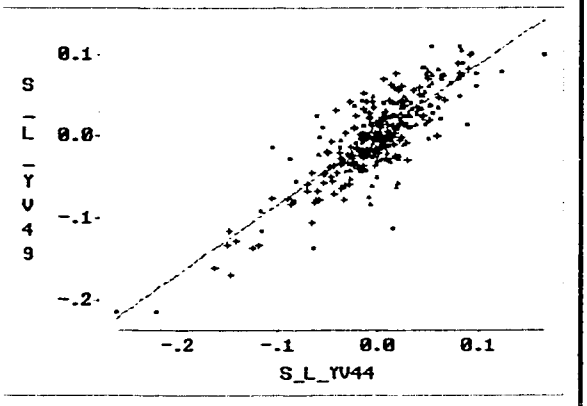

Box 12.41. Scatter plots of delta log intanasal breadth against delta log nasomaxillary dependent variables. See Box 12.14 for fit estimates

Orbital parallelism

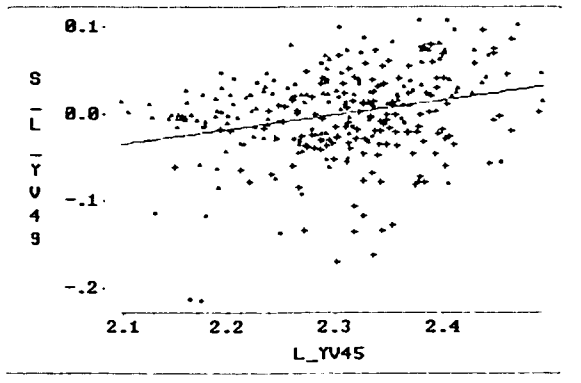

Maxillary arch length

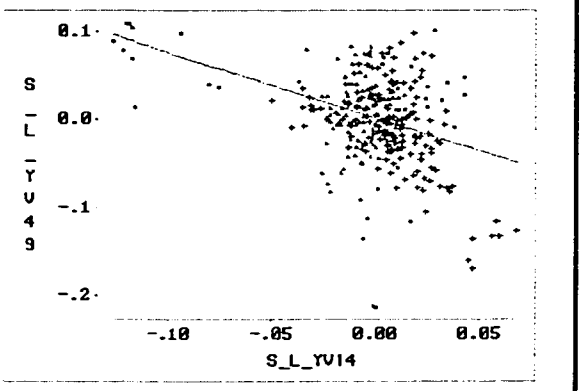

Anterior facial length

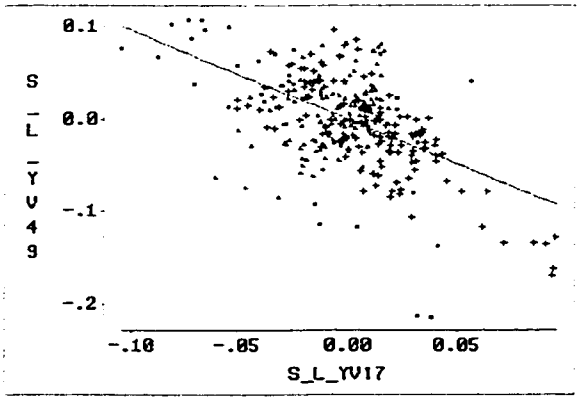

Krogman's angle of facial prognathism

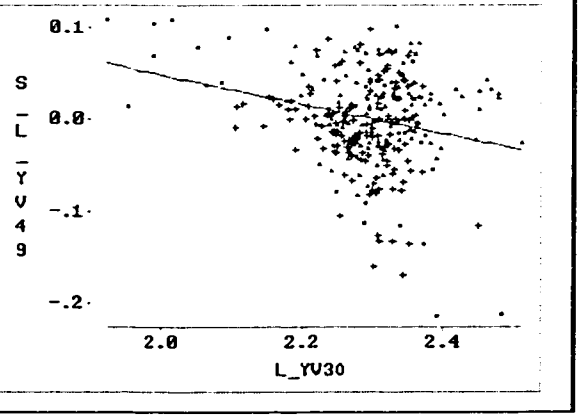

Reproduced with permission of the copyright owner. Further reproduction prohibited without permission.

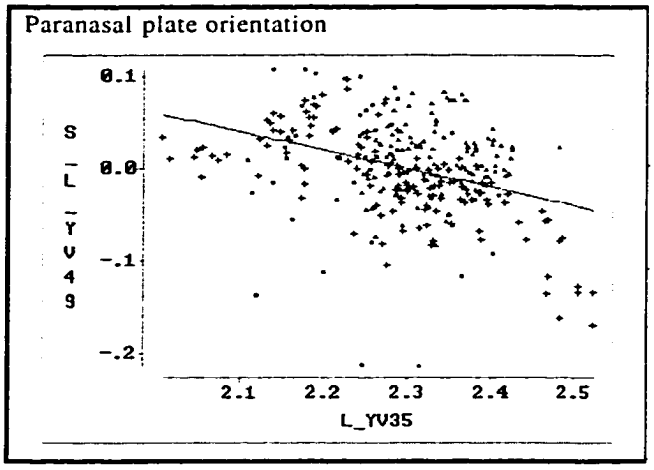

Preliminary Tests of Hypotheses

The preceding preliminary analyses may shed some light on the validity of the arboreal and visual predation hypotheses of primate evolution. With respect to olfactory and related nasomaxillary variables it appears that several of the predictions made by each hypotheses can be refuted, with others are not inconsistent with the anthropoid craniometric data.

Hypothesis (A). The predicted positive association between cribriform plate area and intranasal breadth is confirmed for the anthropoid data (see Box 17). In fact, intranasal breadth is the only nasomaxillary character that exhibits a consistent positive association with cribriform plate area in all anthropoid taxa examined. Thus, Smith's (1912) hypothesis that olfactory apparatus size has an effect on interorbital distance cannot be rejected with respect to anthropoids. However, the alternative hypothesis that decreasing intranasal breadth produces a corresponding decrease in olfactory bulb size can also not be rejected.

Hypothesis (B). Apart from intranasal breadth, the bivariate regression results reveal much heterogeneity, both anatomically and taxonomically, in the

Reproduced with permission of the copyright owner. Further reproduction prohibited without permission.

relationships between olfactory bulb size (i.e., cribriform plate area) and nasomaxillary characters. Of the 16 nasomaxillary characters examined (for association with cribriform plate area) atelids exhibited only 5 positive (mostly facial breadth measures) and 2 negative significant associations, while cebids displayed 9 positive and 1 negative association (see Boxes 12.17-12.33). Among catarrhines, the following patterns emerged: (1) most subgroups, especially cercopithecinae, displayed positive associations between cribriform plate area and facial width variables; (2) cercopithecines and hominoids generally displayed negative associations between cribriform plate area and facial length characters (e.g., nasal bone length, posterior nasal aperture height, anterior facial length, and facial prognathism); and, (3) colobines typically showed no association between cribriform plate area and facial length or depth measures.

Thus, the prediction that cribriform plate area is positively correlated with various dimensions of the nasomaxilla does not hold across major anthropoid taxa. One can only state that most anthropoids that evolve *relatively* large olfactory bulbs also tend to evolve relatively broad faces, especially upper facial breadth measures, such as nasal process of maxilla width [Y4-NPMWDT] and bi-zygofrontale breadth [Y16-UMAXWD]. Accordingly, the hypothesis advanced by Smith (1912), Jones (1916), and Cartmill (1972) that an increase or decrease in relative olfactory bulb size produces a corresponding increase or decrease in the relative anteroposterior dimensions of the snout can be rejected with respect to anthropoids.

Moreover, analysis of the separate M-level and Q-level effects of olfactory bulb size on nasomaxillary form indicate that, with few exceptions, the M-level component of the data is the sole significant contributor of the covariance. This

Reproduced with permission of the copyright owner. Further reproduction prohibited without permission.

suggests that the observed associations between relative olfactory bulb size and upper facial width in anthropoids is due to selectional, rather than acclimational, nomological mechanisms.

Hypothesis (C). Smith (1912) and Jones (1916) hypothesized that a decrease in interorbital distance produced a corresponding decrease in the size of the nasomaxillary complex in primates. This hypothesis predicts that intranasal breadth [S_L_YV49] will be positively associated with nasomaxillary size in anthropoids. A glance at Box 12.34 shows that the predicted association holds for platyrrhines but that the opposite trend (i.e., a negative association between intranasal distance and nasomaxillary size) is apparent for cercopithecines and hominoids, while colobines exhibit no significant association at all. It must also be noted that intranasal distance has very little explanatory power for both platyrrhines and catarrhines, accounting for less than 3 percent of the variation in facial size. These results suggest that intranasal distance has little effect on the dimensions of the nasomaxillary complex in anthropoids.

Hypothesis (D). Cartmill's (1972) hypothesis that greater orbital parallelism causes a corresponding decrease in interorbital distance, which in turn results in a reduction of olfactory apparatus size cannot be rejected with respect to anthropoid primates. The significant positive association between intranasal breadth and cribriform plate area has already been noted (see Box 12.17). The other prediction of Cartmill's hypothesis, that orbital parallelism and intranasal breadth are positively associated, is also here confirmed, for all anthropoid taxa, with the exception, once again, of the cercopithecines (see Box 12.35).

Reproduced with permission of the copyright owner. Further reproduction prohibited without permission.

Hypothesis (E). The relationships among body size, brain size and olfactory bulb size are rather complex. Anthropoids with absolutely larger brains tend to have proportionally smaller olfactory bulbs. Since large-bodied anthropoids tend to have absolutely larger, but relatively smaller, brains compared to small-bodied anthropoids, the latter not only have relatively larger brains but also relatively larger olfactory bulbs. For example, although gorillas have absolutely larger brains than do squirrel monkeys, they have smaller brains relative to body (centroid) size, and smaller olfactory bulbs in proportion to brain size. Therefore, the hypothesis that an increase in brain size *relative* to body size produces a *decrease* in *relative* olfactory bulb size can be rejected with respect to anthropoids (it is absolute brain size that is associated with proportionally smaller olfactory bulbs). However, the opposite hypothesis that increases in *relative* brain size are associated with proportionally larger olfactory bulbs cannot be rejected.

Conclusions

Both the "arboreal" and "visual predation" scenarios of primate craniofacial evolution rely on the presumed nomological relationships between olfactory apparatus size and nasomaxillary and orbital form. Each of these hypotheses is composed of two separate components, one unique and one common. The unique components relate the olfactory apparatus size and olfactory acuity to the placement and orientation of the orbits. The arboreal theory contends that selective forces acting to reduce olfactory apparatus size lead to corresponding reductions in interorbital distance and increased orbital parallelism. By contrast, the visual predation theory purports that selective forces acting to bring the visual axes into a

Reproduced with permission of the copyright owner. Further reproduction prohibited without permission.

parallel alignment lead to subsequent reductions of interorbital distance and olfactory apparatus size. Results of the current analysis cannot reject either of these two postulates (both are consistent with the craniometric nomological data), and the choice between them must rely on other sources of evidence (see Cartmill, 1972).

The common component of the two scenarios is that regardless of the causal agents responsible for effecting changes in interorbital distance and olfactory apparatus size, such changes lead to subsequent changes in nasomaxillary morphology. However, the analyses conducted here indicate that relative olfactory apparatus size has a positive effect only on upper nasomaxillary breadth in most, but not all, anthropoids. Few consistent (anthropoid-wide) patterns were found with regard to the relationships between most nasomaxillary characters, on the one hand, and olfactory apparatus size, intranasal breadth or orbital parallelism, on the other (see Boxes 12.18-12.39).

The traditional view that evolutionary increases in brain size are accompanied by decreases in the size of the olfactory apparatus is accurate only if one considers absolute increases in brain size (orangutans have absolutely larger brains than pygmy marmosets but possess smaller olfactory bulb/brain size ratios). However, when viewed in terms of *relative brain size*, the trend is reversed: anthropoids with larger brains relative to body size tend to have larger olfactory bulb/brain size ratios (thus, pygmy marmosets have both larger brains relative to body size and larger olfactory bulbs relative to brain size compared to orangutans).

Reproduced with permission of the copyright owner. Further reproduction prohibited without permission.

Chapter 13. Locomotion and Posture

Introduction

According to Schultz (1955), comparative study of the position of the foramen magnum in primates, and its functional significance, began with the work of Josephi in 1787. Observations in the nineteenth century relating locomotor behavior[1] to craniofacial morphology (e.g., Huxley, 1896) were soon followed by the realization that the former does not have a *direct* affect on the latter. Beginning with Bolk (1915) locomotion was hypothesized to have only an *indirect* effect on nasomaxillary form, particularly through the mediating influence of the cranial base. Opinions about the role of the cranial base in the development and evolution of skull form played a central role in the formulation of hypotheses regarding the effects of locomotor behavior on craniofacial morphology. The dominant, but by no means exclusive, view of the cranial base through most of the last two centuries has been one of an intrinsically programmed template upon which both the neurocranium and splanchnocranium develop. It is not surprising, then, that many investigators viewed locomotor style as having little or not affect on either the cranial base or the face (e.g., Biegert, 1957). Against this dogmatic tradition, proponents of a less stringent formulation of cranial development were generally unavailing. By the 1960s and 70s, however, experimental and comparative evidence had begun to accumulate indicating that extrinsic factors such as posture could indeed have an effect on the cranial base (e.g., Björk, 1972), and presumably

Reproduced with permission of the copyright owner. Further reproduction prohibited without permission.

other features of the skull. At about the same time investigators began to suspect that the growth of the brain might also have an effect on the development of the cranial base (e.g., Biegert, 1957).

Differences in research design and methodology have made it difficult to reconcile conflicting evidence regarding the role of locomotor behavior in the development and evolution of cranial form. Moreover, most of the studies that have examined this issue have been conducted on rats or other small nonprimate mammals, and the external validity of this research to anthropoids is unknown. In this chapter I evaluate several hypotheses relating locomotor behavior and cranio-cervical morphology (i.e., the relative position and inclination of the foramen magnum) to the ontogeny and evolution of the brain, cranial base and facial skeleton. Following a review of the relevant literature, hypotheses were formulated and operationalized, and statistical predictions deduced from these hypotheses were test against the anthropoid data.

Literature Review

Numerous studies have sought a correspondence between locomotor behavior and craniofacial morphology (e.g., Bolk, 1915; Weidenreich, 1924; DuBrul, 1950, 1962, 1964; DuBrul & Sicher, 1954;). In the majority of these studies, aspects of locomotor behavior were not observed directly, but inferred from cranio-cervical characteristics—most notably the anteroposterior position and inclination of the foramen magnum.

---

[1] Locomotor behavior is defined by the coordinated patterns of mechanical movement exhibited by an organism that enable it to travel in its environment. Postural behavior relates to the position of the limbs and the carriage of the body (including the head) both during movement as well as at rest.

Reproduced with permission of the copyright owner. Further reproduction prohibited without permission.

As early as 1862, the German anatomist Welcker observed a correspondence between the anteroposterior position of the foramen magnum and the degree of facial prognathism among a series of mammalian skulls: the more posterior the spinal opening the more prognathic the specimen. T. H. Huxley (1896) later reported a similar correlation between the *slope* of the foramen magnum and the degree of facial prognathism in a series of human and other mammalian skulls. It thus seemed reasonable to hypothesize that the observed relationship between the placement and orientation of the foramen magnum and facial prognathism was due to locomotor behavior . Schultz (1955) expressed the prevailing consensus of his time with reference to modern humans: "Today there exists wide-spread agreement ...that in adult recent man the atlanto-occipital joint lies farther forward and the face projects less far forward than in any other adult mammal and that these conditions are somehow connected with man's erect posture" (p. 99).

But if the postural and locomotor style of humans influenced the placement of the foramen magnum, should not the same be true of nonhuman primates? On this question agreement among investigators dissolved. In 1909, Bolk declared that "...there is no direct causal relation between the position of the foramen magnum and the development of the biped gait" in primates (p. 370). He cited as evidence the observation that the siamang (*Hylobates syndactylus*), which he considered to be "...more skilled in biped walking than any other [non-human] Primate" (p. 370), had one of the most occipitally placed spinal columns of all anthropoids. He later revised this view in a paper published in 1915, in which he introduced his "fetalisationstheorie," a forerunner of the modern concept of neoteny. Bolk (1915)

Reproduced with permission of the copyright owner. Further reproduction prohibited without permission.

proposed that upright posture prevented the backward migration of the foramen magnum during growth, a phenomenon observed in the apes and other primates. But he did not attempt to reconcile this hypothesis with his earlier observations on siamangs. Subsequent comparative analyses have provided some evidence supporting a causal relationship between the angle of head carriage or degree of pronograde posture and the disposition of the foramen magnum in primates and other mammals (e.g., Weidenreich, 1941; DuBrul, 1950; Scott, 1958; Michejda & Lamey, 1971; Adams & Moore, 1975). However, at least as many arguments and observations have been advanced that deny any relationship between locomotor behavior and cranio-cervical articulation (e.g., Biegert, 1957; Cartmill, 1972).

Three main hypotheses have been advanced to explain the role of locomotor style and cranio-cervical morphology in the development and evolution of craniofacial morphology. The first of these postulates that the relative proportions and juxtaposition of the face and neurocranium are optimally adapted to balance the head under varying locomotor and postural conditions (Jones, 1916; DuBrul, 1977, 1979). Schultz (1942) treated the mechanics of head support as a Class I lever, with the fulcrum at the occipital condyles. Using this model he was able to experimentally calculate the amount of nuchal muscle force required to balance the head in a variety of primates. To test Schultz's model, Adams and Moore (1975) estimated nuchal muscle force by measuring the muscle attachment area on dry skulls. Although these authors determined that modern humans possess considerably more nuchal musculature than is necessary to balance the head, their data generally supported Schultz's Class I lever model of head balance in primates. These studies have demonstrated, however, that neither head posture nor the

Reproduced with permission of the copyright owner. Further reproduction prohibited without permission.

placement of the occipital condyles impose constraints on craniofacial morphology—it appears that the nuchal musculature can easily balance even the most prognathic, occipitally supported heads. Adams and Moore (1975) further pointed out that while both modern humans and their hominine ancestors exhibit horizontally oriented and anteriorly placed occipital condyles, early hominines were rather prognathic whereas modern humans are extremely orthognathic (also see Dean & Wood, 1982). If locomotor behavior imposed constraints on craniofacial morphology, one would not expect to observe this amount of facial variation in two closely related posturally similar species. Moreover, the inferred relationship between posture and craniofacial form—posteriorly placed occipital condyles and facial prognathism—is the opposite of what one would expect for optimal head balance. Primates with posteriorly placed occipital condyles should exhibit facial orthognathism, not prognathism, so that the center of gravity is shifted back towards the atlanto-occipital joint, thus maintaining a more efficiently balanced head. In sum, there is little or no evidence in favor of the "head balance" hypothesis of craniofacial morphology and a multitude of evidence against it.

The second main hypothesis focuses on cranial base flexion as a link between locomotor behavior and craniofacial form (Huxley, 1867; Björk 1972; Fanghänel, 1972; Solow & Tallgren, 1976). During development most mammals undergo a posterior migration of the foramen magnum and a concomitant extension of the cranial base (Bolk, 1909, 1915; Schultz, 1942, 1955; Ashton & Zuckerman, 1952, 1956; Björk 1955; Moore *et al.*, 1973; Michejda, 1975, 1997; Bravo *et al.*, 1989; Masters, *et al.*, 1991). Michejda and Lamey (1971) suggested that variation in the timing of fusion of the midsphenoid synchondrosis is one mechanism by

Reproduced with permission of the copyright owner. Further reproduction prohibited without permission.

which cranial base flexion or extension is achieved during development. This synchondrosis fuses much earlier in humans (at or just prior to birth) compared to other primates, thus preventing extension of the cranial base during postnatal development (Ford, 1958; Scott, 1958). The opposite pattern is apparent in the spheno-ethmoidal synchondrosis which remains active in humans well into the juvenile stage, whereas in nonhuman primates it fuses at birth (Scott, 1958; Baume, 1968). Moore (1981) has pointed out that the pattern of growth of the spheno-ethmoidal synchondrosis parallels that of neural growth in primates: both cease at birth in most nonhuman primates but remain active until about age six in humans. By contrast, the sphenooccipital synchondrosis follows a somatic growth pattern, remaining osteogenically active in humans well into adolescence (Latham, 1966, 1972; but see Michejda, 1975 for contrasting evidence).

The sphenooccipital synchondrosis is thought to be one of the principal growth sites of the cranial base. In a revealing experiment, DuBrul and Laskin (1961) surgically removed the sphenooccipital synchondroses from a series of young rats thereby diminishing the degree of cranial base extension attained during growth. Compared to controls the operated rats exhibited cranial characteristics paralleling those of bipedal hominines (p. 122). These experimentally-induced cranial alterations included a shortening and downward rotation of the face, a more horizontal orientation of the cribriform plate, a more globular shape of the braincase, an inferior migration of the nuchal crest and nuchal plane, and a more

Reproduced with permission of the copyright owner. Further reproduction prohibited without permission.

anteriorly positioned, horizontally oriented foramen magnum.[2] These features, in fact, mirror the condition of fetal rats more than "bipedal hominids."

DuBrul and Laskin's (1961) experimental results indicate that growth of the cranial base during ontogeny influences the position of the foramen magnum and numerous other features of craniofacial and neurocranial morphology (also see Butow, 1990). These authors argued not only that variation in the rates of growth and timing of fusion of the chondrocranial synchondroses explained the observed patterns of overall mammalian skull form (an argument first proposed by Biegert, 1957), but that these patterns represent adaptations to specific shifts in locomotor behavior. The primary influence of the cranial base on the development of the foramen magnum also has gained some support from clinical research. For instance, Hecht *et al.* (1989) demonstrated that the abnormal development of the foramen magnum that characterizes achondroplasia is due to the "abnormal placement and premature fusion of the [endochondral] synchondroses" (p. 528).

In another informative experiment, Moss (1961) literally turned the work of DuBrul and Laskin on its head. Using a procedure first devised by Pratt (1943), Moss investigated the ontogenetic effects of locomotor behavior on cranial form in a series of experiments in which 3 day old rats were made "bipedal" by forelimb amputation. The experimental rats, as well as a group of controls, were killed at 90 days old and x-rayed, and the resulting cephalographs were compared. Moss (1961)

---

[2] It is equally instructive to note what DuBrul and Laskin (1961) observed *not* to differ between operated rats and controls. For instance, it is clear from their Fig. 10, p. 131 that the angle between the cribriform plate and "frontal bone" was approximately 90° in both groups, as predicted by Enlow's developmental constraint hypothesis (see Chapter 11). The slope of the occlusal plane also remained unchanged in the operated rats. This implies that in the normal rats the occlusal plane is adjusted to maintain an invariant orientation despite the forward rotation of the nasomaxillary complex. A similar adjustment mechanism for the occlusal plane was inferred for anthropoids in Chapter 9.

Reproduced with permission of the copyright owner. Further reproduction prohibited without permission.

found that the bipedal rats did *not* display a downward rotation of the face to compensate for an upwardly directed cranium, but just the opposite—cranial base extension and facial prognathism were increased in the experimental rats compared to controls. Moss (1961:305) noted that...

> "...in the rat there are definite alterations of cranial form with age. The neonatal rat facial skull is strongly flexed ventrally relative to the neural skull (i.e., is klinorhynchal). With age the entire facial skull rotates upwards until it comes to lie anterior to the neural skull and virtually in the same plane (Moss, '58a). Our present data make it appear that in rats with the forelimbs removed this process is accentuated...

The experimental results of DuBrul and Laskin (1961) and Moss (1961) present a consistent picture: if the cranial base is surgically prevented from undergoing extension, the foramen magnum will not undergo its normal posterior migration; and, if locomotor behavior is modified to an orthograde mode, extension of the cranial base is accelerated rather than constrained. It would thus appear that while intrinsically mediated properties of the cranial base can affect both craniofacial variation and the location at which the spinal cord enters the cranium, locomotor behavior can also influence the cranial base. Consistent with this view, Fanghänel (1972) reported observing cranial base modifications in rats that were experimentally induced to ambulate bipedally. And Björk (1972) reported cranial base extension in human subjects whose head posture had been clinically altered. The experimental and clinical evidence are thus inconsistent with regard to the relationship between posture and cranial base flexion.

The direction of causality, it seems, can also be reversed with regard to craniofacial morphology and the cranial base. Jackson *et al.* (1979) conducted an

Reproduced with permission of the copyright owner. Further reproduction prohibited without permission.

experiment in which an anteriorly directed external force was applied to the growing maxilla of *Macaca nemestrina*. The investigators found that changes in the cartilaginous synchondroses of the cranial base occurred in association with maxillary retrusion in response to the applied anterior force.

It is important to note that these experimental results apply to the question of whether or not the basicranium responds via acclimation to locomotor-related environmental stimuli. If the proximate mechanisms orchestrating the development of the cranial base are mediated by intrinsic genetic signals then one would not expect to see compensatory changes in the cranial base due to experimentally induced alterations of posture. On the other hand, if environmental signals (such as those derived from mechanical tension and compression) play a role in the growth and remodeling of the cranial base, then one *would* expect to see such compensatory changes. And yet, regardless of whether or not the cranial base is capable of acclimative change, a nomological relationship between head carriage and cranial base flexion may be established through adaptation.[3] It is still possible that cranial base flexion is an adaptation whose role is to adjust the position of the foramen magnum to ensure proper orientation of the face in response to shifting locomotor behavior. I believe this is what DuBrul and Laskin (1961) had in mind when they stated:

> Any mutations tending to shift growth patterns toward those we have produced experimentally (i.e. retardation of timing or rate of growth of spheno-occipital synchondrosis), will better balance a skull on a vertical column. Such mutations are certainly subject

[3] This is a good example of an instance in which experimental studies are useful for testing one hypothesis (acclimative change of the cranial base to locomotor behavior), but comparative research is required to test another (selectional adaptation of the cranial base to locomotor behavior).

Reproduced with permission of the copyright owner. Further reproduction prohibited without permission.

> to strong selection pressure in animals that are phylogenetically shifting their orientation in the gravitational field toward the vertical [DuBrul & Laskin, 1961:124]

A third hypothesis concerns the effects of relative brain size on the association between locomotion, cranial base morphology and craniofacial form. Dabelow (1929, 1931), a former student of Bolk, in attempting to explain the patterns reported by his mentor, pointed out that brain-to-body size ratio was correlated with cranial base shortening and flexion—all are substantial in fetal primates but weaken progressively into adulthood, whereas in humans these traits remain high throughout development (Bolk, 1915). Biegert (1957, 1963) was the first to advance the hypothesis that a relatively large brain actually induces cranial base flexion, and other subsequent alterations of cranial morphology (also see Moss, 1958; Cramer, 1977; Kean & Houghton, 1982). In Chapter 2, I briefly reviewed the comparative and experimental literature on the effects of the brain on chondrocranial development (see the section entitled "Skeletogenesis of the Chondrocranium"). I concluded that the bulk of the evidence favors the Dabelow-Biegert hypothesis that a reduction of relative brain size causes a corresponding decrease in cranial base flexion. The reader may recall from Chapter 11 that extension of the cranial base was found to be associated with diminished relative brain size among some, but not all, anthropoids. Thus, the comparative nomological evidence presented here is not entirely consistent with previous comparative, experimental and clinical findings.

The influence of the brain on the cranial base may be due to mechanical unloading of the chondrocranium, as Demes (1985) and others have suggested, or

Reproduced with permission of the copyright owner. Further reproduction prohibited without permission.

it may be brought about by constraints imposed by the emerging cranial nerves, as Kean and Houghton (1982) have asserted. Whatever the mechanism, relative brain size appears to be capable of inducing changes in cranial base morphology, and the chondrocranium itself appears to effect changes in other cranial characteristics. Disruption of the normal extension and elongation of the cranial base produced experimentally by DuBrul and Laskin (1961) caused the skull to retain many of its prenatal characteristics *despite changes in relative brain size.*

Cranial capacity may also play a role in determining the location and orientation of the foramen magnum (*cf.*, Bolk, 1909; 1910; Radinsky, 1967; Michejda 1971, 1975). Masters, Falk and Gage (1991) measured and compared 378 endocasts of rhesus monkeys and determined that "...percent increase in cranial capacity in *M. mulatta* appears comparable to percent change in position of foramen magnum" (p. 78). But DuBrul (1950) found that the associations among locomotor behavior, position of the foramen magnum and cranial base flexion observed in a series of lagomorph skulls were entirely independent of relative brain size. This conclusion is also supported by Weidenreich's (1934, 1941) observations of various other mammals: "The roominess of the brain case in dwarf dogs does not influence, for example, the position of the foramen magnum or the evenness of the base" (Weidenreich, 1941:419). These observations suggest that the observed influence of relative brain size on the disposition of the foramen magnum is mediated by the cranial base.

A related hypothesis is that the shape of the brain, not absolute or relative brain size, determines the anteroposterior location at which the spinal cord enters the cranium. Bolk (1909), however, found no correspondence between the position

Reproduced with permission of the copyright owner. Further reproduction prohibited without permission.

of the foramen magnum and the degree of brachycephalic or dolichocephalic skull properties in a sample of modern humans. He concluded: "[M]y results do not indicate that in man there exists a relation between the position of the foramen magnum and the shape of the skull..." (p. 371).

The foregoing hypotheses are summarized in the form of two alternative path diagrams, presented in Box 13.1 below. The main difference between the two models has to do with the relationship, or direction of causality, between cranial base flexion and foramen magnum disposition. The "cranial base" hypothesis maintains that one or more distal causal agent (brain shape, relative brain size and/or locomotor behavior) affects both foramen magnum disposition and nasomaxillary morphology via the mediating effects of the cranial base. The "cranio-cervical" hypothesis, on the other hand, holds that some combination of the same causal agents have a direct effect on the position of the foramen magnum, which, in turn, produces modifications in the cranial base and facial skeleton.

Reproduced with permission of the copyright owner. Further reproduction prohibited without permission.

Box 13.1. Path diagrams comparing alternative hypotheses.

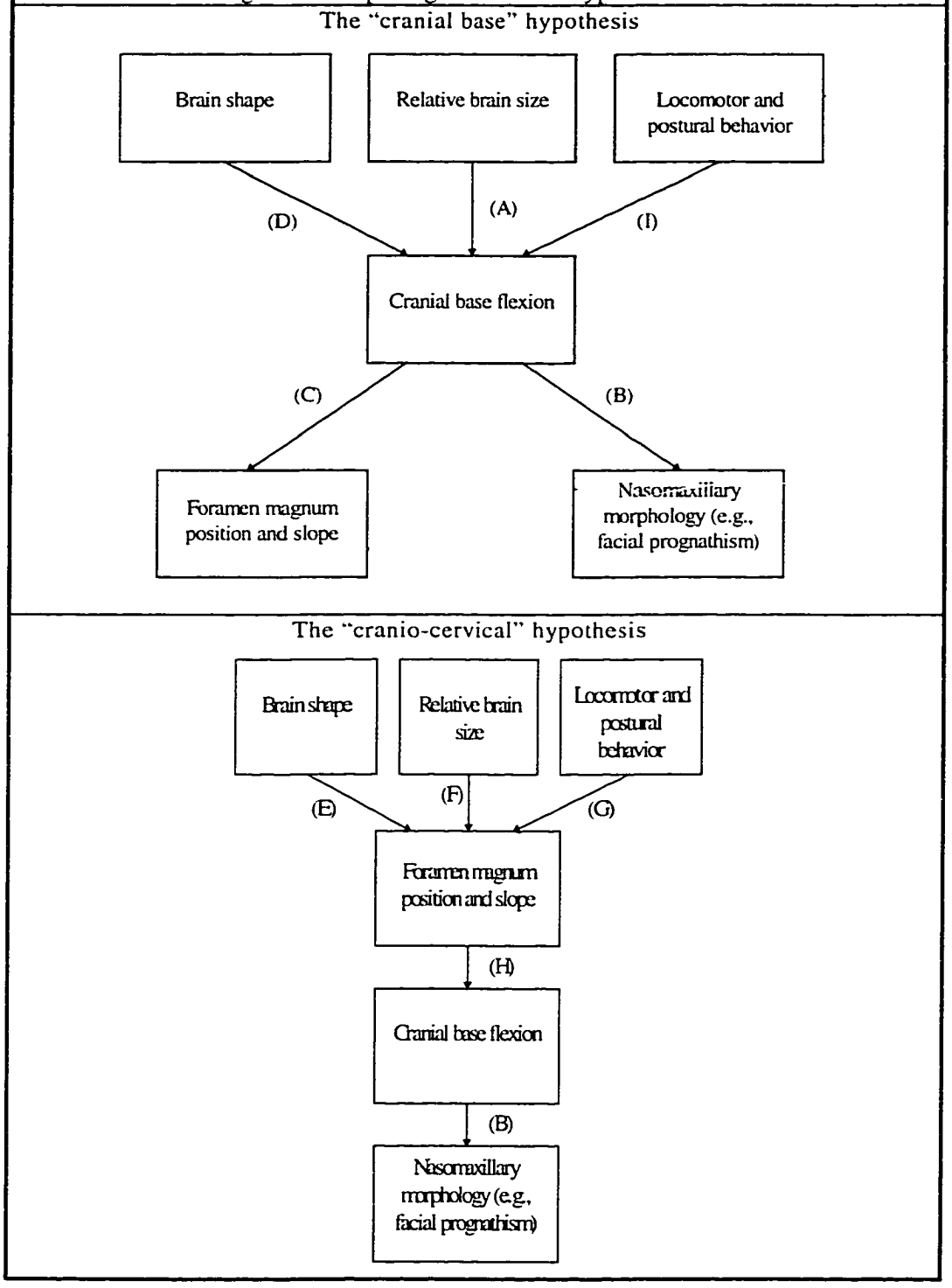

Reproduced with permission of the copyright owner. Further reproduction prohibited without permission.

Hypotheses Formulation

Hypotheses pertaining to the relationships among locomotion, cranio-cervical morphology, cranial base flexion, and relative brain size and shape in the development and evolution of cranial form are stated in Box 13.2. Each of the hypotheses statements correspond to one of the causal pathways (or its null alternative) contained in the models depicted in Box 13.1.

Box 13.2. Hypotheses statements regarding the effects of locomotor-related traits craniofacial variation.

Description of Hypothesis:	Source:
(A) Postural and locomotor behavior determines the location or angle at which the spinal cord enters the cranium. The more orthograde the posture, the more anterior the placement of the foramen magnum (see Box 13.1, Path G)	Bolk, 1915
(B) There exists no causal relationship between postural and locomotor behavior and the location or angle at which the spinal cord enters the cranium	Biegert, 1957
(C) Cranial base flexion is an adaptation to mode of locomotion. Selection for erect posture results in selection of increased cranial base flexion (Box 13.1, Path I)	DuBrul & Laskin, 1961
(D) Cranial base flexion is an acclimational response to changes in postural and locomotor behavior. Orthograde posture induces a greater degree of flexion of the cranial base (Box 13.1, path I)	Fanghanel, 1972; Björk, 1972
(E) Cranial base flexion is incapable of an acclimational response to changes in postural and locomotor behavior	DuBrul & Laskin, 1961; Moss, 1961
(F) No causal relationship exists, either selective or acclimative, between locomotion and cranial base flexion	Biegert, 1957
(G) The degree of cranial base flexion determines the location or angle at which the spinal cord enters the cranium. The more acute the flexion the more anterior the foramen magnum (Box 13.1, path C)	Huxley, 1867; DuBrul & Laskin, 1961
(H) The location or angle at which the spinal cord enters the cranium determines degree of cranial base flexion. The more anterior the relative position of the foramen magnum the more acute the angle of the cranial base (Box 13.1, path H)	
(I) A large brain relative to body size causes the foramen magnum to be anteriorly positioned (Box 13.1, path F)	Masters *et al.*, 1991
(J) There is no cause-and-effect relationship between relative brain size and the location at which the spinal cord enters the brain	DuBrul, 1950
(K) A large brain relative to body size induces flexion of the cranial base (Box 13.1, path A)	Dabelow, 1929; Biegert, 1957
(L) There is no cause-and-effect relationship between relative brain size and cranial base flexion	Weidenriech, 1941

Reproduced with permission of the copyright owner. Further reproduction prohibited without permission.

Box 13.2. Hypotheses statements regarding the effects of locomotor-related traits craniofacial variation.	
Description of Hypothesis:	Source:
(M) The shape of the brain determines the location and inclination at which the spinal cord enters the cranium. The more brachycephalic the shape of the brain the more anterior the position of the foramen magnum (Box 13.1, path E)	This study
(N) There is no cause-and-effect relationship between brain shape and the location and inclination at which the spinal cord enters the cranium	Bolk, 1909
(O) The degree of cranial base flexion determines various properties of nasomaxillary form (e.g., facial prognathism) (Box 13.1, path B)	Huxley, 1963; Weidenriech, 1947

Operationalization of Variables

Only variables related to cranio-cervical morphology are operationalized in this section. All other variables relevant to the preceding hypotheses have already been defined elsewhere.[4] Two variables intended to measure the location and inclination at which the spinal cord enters the cranium were defined as follows:

Anteroposterior position of the occipital condyles

This variable quantifies the location of the atlanto-occipital joint along the anteroposterior axis of the neurocranium. It was defined as the distance between the posterior-most point of the endocranium to the occipital condyles divided by endocranial length, expressed as a percent (see Box 5.3C). All distances were measured parallel to the Frankfurt horizontal. The more anterior the condyles in relation to the length of the brain the greater the value of the index. I refer to this measurement as the "condylar index."

Many variations of this index have appeared in the literature and no attempt is made here to review them all (good summaries can be found in Bolk, 1909; Schultz,

[4] Nasomaxillary variables: Chapters 5 & 9; cribriform plate orientation, cranial base flexion, brain shape (endocranial index), relative brain size (endocranial volume): Chapters 5 & 11.

Reproduced with permission of the copyright owner. Further reproduction prohibited without permission.

1955; and Luboga & Wood, 1990). I used the maxima of curvature of the occipital condyles to mark the vertebral position, rather than a landmark associated with the foramen magnum (e.g., basion), because of the importance of the atlanto-occipital joint in relation to head carriage and postural behavior (Senyurek, 1938; Schultz, 1942, 1955; Le Gros Clark, 1950). There is general agreement that the anteroposterior position of the condyles (or foramen magnum) should be measured in relation to the neurocranium, not total cranial length. This is especially important when the objective of the study is to examine possible relationships between postural behavior and craniofacial morphology—measurements of one should not include dimensions of the other.[5] Endocranial landmarks were used to represent neurocranial length due to the inherent residual variability associated with ectocranial landmarks (e.g., glabella and opisthocranion). Luboga and Wood (1991) examined the position of the foramen magnum relative to three different measures of cranial length and found that the index based on endocranial landmarks gave the most consistent results.

---

[5] An instructive example of how misleading results can obtain from ill defined craniometric variables is provided by Adams and Moore (1975). These authors examined the position of the occipital condyles in modern humans, African apes, and early hominids and concluded that *Australopithecus* fell closer to the ape range in having occipital condyles that were posteriorly positioned, while *Paranthropus* was more similar to modern humans in having anteriorly placed condyles. Since both early hominids are thought to have been bipedal, but only *Australopithecus* is characterized by marked facial prognathism, these results seemed to indicate that the anteroposterior position of the foramen magnum covaries with facial prognathism but not with locomotor behavior! However, it is clear that this conclusion derives from the method used by Adams and Moore to measure the relative position of the occipital condyles against *total cranial length* (which included facial length). This method will nearly always yield a correlation between foramen magnum position and facial prognathism because the same dimension—length of the face—contributes heavily to both measures. Almost by definition, more prognathic individuals will have more posteriorly placed occipital condyles relative to overall cranial length. Dean and Wood (1982) re-examined this issue using a measure of foramen magnum position that was independent of the facial skeleton. Their analysis revealed conclusively that both *Australopithecus* and *Paranthropus* were more similar to modern humans than to *Gorilla* with respect to the position of the foramen magnum.

Reproduced with permission of the copyright owner. Further reproduction prohibited without permission.

Slope of the foramen magnum

Typically the slope of the foramen magnum is measured as the angle between a line connecting basion and opisthion and a given baseline (*cf.* Bolk, 1910). Various baselines, some quite imaginative, have been used. Broca (1897) proposed the neutral orbital axis as a suitable baseline, whereas Bolk (1910) preferred a line connecting the anterior-most point of the cribriform plate ("fronton") to the posterior-most endocranium ("occipiton"). I have adopted the Frankfort horizontal as a reference plane for measuring the angle of the foramen magnum, following Huber (1902) and, more recently, Luboga and Wood (1990).

Locomotor behavior

In order to properly evaluate the hypothesis that locomotor and postural behaviors influence the position and inclination of the foramen magnum, an enormous amount of data on the temporal variation of the relative angulation of the skull, cervical column, and thoracic axis for a variety of activities in a diverse sample of primates would need to be collected and analyzed. The practical obstacles of such a study are prohibitive, although a good model is provided by Dunbar and Badam (1998).

Until a more refined analysis is forthcoming, the best we can do is to look for differences in cranio-cervical properties among locomotor categories. Based on a review of the behavioral literature, I scored each of the 37 species in the anthropoid sample on 8 locomotor activities including bipedality, quadrupedality, suspension, leaping, vertical clinging and leaping, climbing, branch walking, and knuckle-walking. For each activity a given species scored 1.0 if the activity was a major part of its locomotor repertoire and 0 if it was not. The scores are presented in Box 13.3.

Reproduced with permission of the copyright owner. Further reproduction prohibited without permission.

Box 13.3. Sample anthropoid species and a check-list of their main locomotor activities. B, bipedality; Q, quadrupedality; S, suspension; L, leaping; VCL, vertical clinging and leaping; C, climbing; W, branch walking; K, knuckle-walking.

Rank	Species	B	Q	S	L	VCL	C	W	K	
1.	*H. sapiens*	✔								
2.	*C. geoldii*		✔			✔				1
3.	*S. sciureus*		✔		✔			✔		2
4.	*M. nemestrina*		✔							3
5.	*M. fascicularis*		✔		✔					4
6.	*M. mulatta*		✔							4
7.	*P. paniscus*	✔	✔				✔		✔	5, 6
8.	*A. trivirgatus*		✔		✔		✔	✔		4
9.	*C. pygmaea*		✔			✔				7
10.	*C. capucinus*		✔		✔					8
11	*P. hamadryas*		✔							4
12.	*P. melalophos*		✔		✔		✔	✔		9
13.	*C. aethiops*		✔							4
14.	*L. albigena*		✔				✔	✔		4, 22
15.	*C. apella*		✔		✔					8
17.	*C. ascanius*		✔				✔			4, 22
16.	*S. oedipus*		✔			✔				7
18.	*C. neglectus*		✔					✔		4
19.	*C. mitis*		✔				✔			4, 22
20.	*C. cupreus*		✔		✔		✔	✔		4
22.	*P. badius*		✔		✔					10, 21, 22
21.	*P. pithecia*		✔		✔		✔	✔		11
23.	*N. larvatus*		✔		✔		✔			4, Pers. Ob
24.	*A. geoffroyi*		✔				✔	✔		12
26.	*P. troglodytes*		✔	✔	✔		✔		✔	
25.	*H. lar*			✔						13, Pers Ob
27.	*S. cristata*		✔		✔		✔			Pers. Obs.
28.	*S. entellus*		✔					✔		4
29.	*P. pygmeaus*		✔	✔			✔		✔	14
30.	*C. satanas*		✔		✔		✔	✔		15
31.	*G. gorilla*		✔				✔		✔	6
32.	*P. monachus*		✔				✔	✔		11
33.	*L. lagothrica*		✔	✔			✔			16
34.	*B. arachnoides*		✔	✔	✔			✔		17
35.	*H. syndactylus*			✔						18
36.	*A. palliata*		✔				✔	✔		19
37.	*C. guereza*		✔		✔		✔			20, 22

1, Pook & Pook, 1981; **2**, Baldwin & Baldwin, 1981; **3**, Caldecott, 1986; **4**, Rowe, 1996; **5**, Doran, 1993; **6**, Doran 1996; **7**, Hershkovitz, 1977; **8**, Freese & Oppenheimer, 1981; **9**, Fleagle, 1978; **10**, Struhsaker, 1975; **11**, Buchanan *et al.* 1981; **12**, van Roosmalen & Klein,1988; **13**, Roonwal & Mohnot, 1977; **14**, Nowak, 1991; **15**, Ford, 1994; **16**, Ramirez, 1988; **17**, Nishimura *et al.*, 1988; **18**, Curtin & Chivers, 1978; **19**, Neville *et al.*, 1988; **20**, Rose, 1978; **21**, McGraw, 1998; **22**, Gebo & Chapman, 1995.

Reproduced with permission of the copyright owner. Further reproduction prohibited without permission.

Statistical Predictions

The hypothesis statements listed in Box 13.2 render specific predictions regarding statistical associations among sets of operationalized variables. These statistical predictions are presented in Box 13.4 below.

Box 13.4. Predicted bivariate and multivariate associations deduced from hypotheses statements.

Expected associations:	Corresponding hypotheses
Disposition of foramen magnum [YM68-SLOPFM, YM69-APOCND] ← Locomotor categories [BIPED, QUAD, SUSP, LEAP, VCL, CLIMB, WALK, KNUC]	(A)
Cranial base flexion [YM70-CBFLEX] ← Locomotor categories [BIPED, QUAD, SUSP, LEAP, VCL, CLIMB, WALK, KNUC]	(C)
Disposition of foramen magnum [YV68-SLOPFM, YV69-APOCND] ← Cranial base flexion [YV70-CBFLEX]	(G)
Cranial base flexion [YV70-CBFLEX] ← Disposition of foramen magnum [YV68-SLOPFM, YV69-APOCND]	(H)
Disposition of foramen magnum [YV68-SLOPFM, YV69-APOCND] ← Relative endocranial volume [YV84-BRNSIZ]	(I)
Cranial base flexion [YV70-CBFLEX] ← Relative endocranial volume [YV84-BRNSIZ]	(K)
Disposition of foramen magnum [YV68-SLOPFM, YV69-APOCND] ← Endocranial index [YV81-ENDOID]	(M)
Nasomaxillary variables ← Cranial base flexion [YV70-CBFLEX]	(O)

Preliminary and Exploratory Analyses

The results of several preliminary analyses are presented and discussed in this section. Aside from the presentation of relevant species mean raw data (Box 13.6), analyses include (1) an examination of the correspondence between foramen magnum disposition and modes of locomotion, (2) an examination of the relationship between body size and features of the cranio-cervical joint, (3) a principal components analysis intended to clarify the underlying structure relating condylar index, foramen magnum slope and other relevant cranial and

Reproduced with permission of the copyright owner. Further reproduction prohibited without permission.

nasomaxillary variables, and (4) preliminary tests of statistical predictions using bivariate and partial multiple regression analysis. Before beginning the analyses, however, it will be informative to examine the relationship between the two variables used to quantify the disposition of the cranio-cervical joint—condylar index and inclination of the foramen magnum.

Correspondence Between Position and Slope of Foramen Magnum

Topinard (1891) first noted the high degree of correlation between the anteroposterior position and the slope of the foramen magnum. Bolk (1910:533) later commented that "..a shifting of the For. magn. and a change in the angle go hand in hand during the individual development. For in human beings as well as in Anthropoids the shifting backwards diminishes the angle of inclination." [6] Masters *et al.* (1991) found that in the rhesus monkey the rate and timing of change to both the position and angle of the foramen magnum were virtually simultaneous. From this evidence they concluded that the two features are likely "...linked to one process..." (p. 79). Regression of the delta log species means of the two variables in anthropoids confirms the close correspondence between the two traits (see Box 13.5). The regression line between foramen magnum inclination [ΔL_YM68] and condylar index [ΔL_YM69] is not significantly different from isometry, which indicates that the same set of causal agents may be operating on the two characters (see the relevant discussion in Chapter 10).

The two greatest outliers in the bivariate plot are *Pan paniscus*, whose FM inclination is more horizontal than would be expected for its anteroposterior

Reproduced with permission of the copyright owner. Further reproduction prohibited without permission.

location, and *Alouatta palliata*, whose FM slope is more vertical than predicted on the basis of its location.

Box 13.5. Regression plot of delta log condylar index (ΔL_YM69) against delta log foramen magnum slope (ΔL_YM68). Slope -0.93 (-1.19, -0.69), R^2 = 0.62

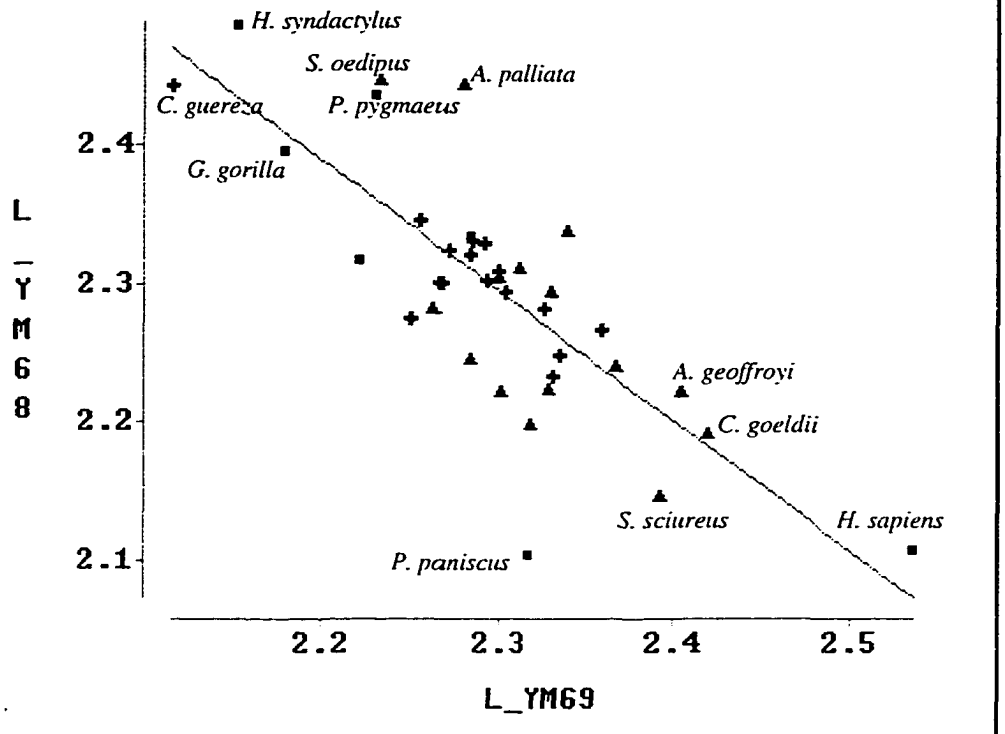

Comparison of Raw Data with Previously Published Results

Measurements of anthropoid foramen magnum position and inclination have been reported by Bolk (1909, 1910), Schultz (1942, 1955), Biegert (1957), Adams and Moore (1975), and Luboga and Wood (1990). I have not reprinted these authors' published data because the different measurement techniques and indices used preclude meaningful numerical comparison. A brief word comparison will have to

[6] Bolk (1910) measured the inclination of the foramen magnum in relation to a line drawn perpendicular to the long axis of the neurocranium. His reference to a "diminished angle of inclination" therefore refers to a foramum magnum that is becoming more vertical.

Reproduced with permission of the copyright owner. Further reproduction prohibited without permission.

suffice. The raw measurements for condylar index and foramen magnum slope are given in Box 13.6.

Consistent across studies is the finding that modern human crania exhibit the most anteriorly positioned occipital condyles and the most horizontally oriented foramen magnum (*H. sapiens* is in fact the only primate known to exhibit a forward facing foramen magnum). Schultz (1955) found that, next to modern humans, *Saimiri* had the most anteriorly place foramen magnum, but he did not include Goeldi's monkey (*Callimico goeldii*) in his sample. This Neotropical primate has a condylar index of 41, making it statistically indistinguishable from *Saimiri* with a condylar index of 38.

Surprisingly, the three macaque species included in the present sample ranked just below *Homo*, *Callimico* and *Saimiri* in terms of the anterior placement and horizontal inclination of the foramen magnum. All three exhibit statistically indistinguishable condylar indices and foramen slopes. What makes this observation all the more intriguing is that the locomotor behaviors of *M. nemestrina* and *M. fascicularis* are reportedly quite distinct despite their close phylogenetic relationship. Rodman (1979) described the locomotor specializations of the two congeneric species as follows:

> Sympatric *Macaca fascicularis* and *M. nemestrina* of Borneo coexist, in spite of similar frugivorous diets, by occupying habitats that differ in density of food sources. A primary specialization for foraging on widely dispersed food sources is terrestrial travel by *M. nemestrina*, in contrast to arboreal travel by *M. fascicularis* in the richer habitat [Rodman, 1979:51].

But Caldecott (1986) observed that another population of Pig-tailed macaques (*M. nemestrina*) spent less than 10% of the time on the ground, and even engaged in a

Reproduced with permission of the copyright owner. Further reproduction prohibited without permission.

considerable amount of suspensory behavior. This raises the concern that locomotor mode may be population-specific rather than species-specific.

Whereas Biegert (1957) reported that *Aotus*, *Cebus* and *Ateles* were similar to *Saimiri* in the anterior placement of the foramen magnum, the data presented here indicate that only *C. geoldii* displays a condylar index as high or higher than *Saimiri*. By comparison, while *Aotus* and *Cebus* ranked quite high on the condylar index, *Ateles* ranked rather low (24th of 37).

Two other congeneric pairs of species show divergent patterns of foramen magnum disposition, a finding reported in previous studies. Bolk (1910), Le Gros Clark (1950), Schultz (1955), Cramer (1977), and Luboga and Wood (1990) all detected a much more anteriorly placed and horizontally oriented foramen magnum in *Pan paniscus* compared to *P. troglodytes*.[7] Both Bolk (1909, 1910) and Schultz (1955) reported a parallel divergence in *Hylobates*, with *H. lar* displaying a more anterior and less vertical foramen magnum than was apparent for *H. syndactylus*. In fact, the siamang was found in this and previous studies to possess one of the most posteriorly placed and vertically oriented foramina of all anthropoids, second only to the howler monkey (*Alouatta*). The above observations are evident in the results presented in Box 13.6. *Colobus guereza* was also found to exhibit an extremely low condylar index, but comparable data have not been published for this species.

---

[7] Luboga & Wood (1990), in fact, reported finding no difference between the two species of *Pan* in terms of foramen magnum slope, but did report a difference in position.

Reproduced with permission of the copyright owner. Further reproduction prohibited without permission.

Box 13.6. Species mean raw condylar index and foramen magnum slope. Rank order and 95% confidence limits (parenthesis) are also given.

Species	Rank	Mean Condylar Index	Rank	Mean FM Slope
H. sapiens	1.	48.4 (45.9, 50.9)	1.	-6.5 (-9.2, -3.8)
C. geoldii	2.	41.3	9.	17.2
S. sciureus	3.	37.9 (36.0, 39.7)	3.	12.9 (9.6, 16.1)
M. nemestrina	4.	33.2 (30.8, 35.4)	6.	16.2 (12.5, 19.9)
M. fascicularis	5.	31.4 (30.0, 32.8)	5.	15.0 (11.6, 18.4)
M. mulatta	6.	31.2 (29.3, 33.0)	4.	14.1 (10.9, 17.2)
P. paniscus	7.	30.9	2.	6.1
A. trivirgatus	8.	30.3 (28.2, 32.4)	7.	16.4 (12.1, 20.6)
C. pygmaea	9.	29.5 (27.4, 31.6)	27.	23.4 (19.9, 27.7)
C. capucinus	10.	28.9 (27.4, 30.5)	11.	17.7 (15.3, 20.1)
P. hamadryas	11	28.8 (26.6, 31.0)	12.	18.1 (15.5, 20.7)
P. melalophos	12.	28.2 (26.8, 29.7)	10.	17.5 (15.0, 20.1)
C. aethiops	13.	28.0 (26.1, 30.0)	16.	19.3 (16.3, 22.3)
L. albigena	14.	27.9 (26.7, 29.1)	21.	20.6 (18.0, 23.1)
C. apella	15.	27.7 (25.8, 29.6)	14.	19.1 (18.2, 20.0)
C. ascanius	17.	27.0 (25.4, 28.5)	22.	20.8 (17.7, 23.8)
S. oedipus	16.	27.0	36.	35.5
C. neglectus	18.	26.1 (24.3, 27.9)	20.	20.4 (16.4, 24.4)
C. mitis	19.	25.8 (24.2, 27.5)	13.	18.7 (15.9, 21.5)
C. cupreus	20.	25.7 (23.8, 27.7)	17.	19.3 (13.3, 25.2)
P. badius	22.	25.5 (22.8, 28.3)	15.	19.2 (17.2, 21.2)
P. pithecia	21.	25.5 (24.3, 26.6)	23.	20.8 (16.4, 25.2)
N. larvatus	23.	25.4 (23.9, 26,9)	19.	20.2 (18.4, 22.1)
A. geoffroyi	24.	24.9 (23.3, 26.5)	24.	20.9 (19.3, 22.5)
P. troglodytes	26.	24.7 (21.4, 28.0)	18.	19.6 (16.3, 23.0)
H. lar	25.	24.7 (21.9, 27.5)	26.	22.3 (12.3, 32.3)
S. cristata	27.	23.6 (22.1, 25.1)	25.	22.1 (18.6, 25.5)
S. entellus	28.	23.2	8.	17.1
P. pygmeaus	29.	23.2 (12.5, 34.0)	33.	29.3 (23.0, 35.6)
C. satanas	30.	22.9 (21.7, 24.1)	28.	24.2 (21.9, 26.4)
G. gorilla	31.	21.1 (19.0, 23.1)	30.	25.7 (22.4, 28.9)
P. monachus	32.	20.7 (17.5, 23.9)	29.	25.2 (15.4, 34.9)
L. lagothrica	33.	20.0 (18.4, 21.5)	32.	28.7 (26.8, 30.6)
B. arachnoides	34.	17.8	31.	26.9
H. syndactylus	35.	16.3 (15.0, 17.6)	35.	34.1 (31.3, 36.9)
A. palliata	36.	16.0 (13.3, 18.7)	37.	36.9 (32.9, 40.8)
C. guereza	37.	14.4 (12.2, 16.7)	34.	29.7 (25.9, 33.5)

Reproduced with permission of the copyright owner. Further reproduction prohibited without permission.

Several findings reported here differ from those found previously. Schultz (1955), for example, ranked both *Papio hamadryas* and *Lophocebus albigena* low on his "condylion index," signifying that these species have relatively posterior occipital condyles, whereas the results obtained here place these species in the top half of the order (11th and 14th of 37, respectively) with relatively anterior condyles.

Among the Great Apes, several investigators have found no significant difference between *Gorilla* and *Pan troglodytes* in the disposition of the foramen magnum (e.g., Adams & Moore, 1975). In the present study, *Pan* ranked higher than *Gorilla* on both the mean raw condylar index and foramen magnum slope, but their respective means were not significantly different. Nor were any significant differences detected between *Pongo* and either *Gorilla* or *Pan troglodytes* in either condylar index or foramen magnum slope.

The Effects of Locomotion on the Disposition of the Foramen Magnum

It has often been assumed that the relative location and inclination at which the spinal cord enters the cranium is associated with postural and locomotor behavior, but no such association has ever been unequivocally demonstrated. Indeed, several investigators have adamantly denied that such an association exists. Beigert (1957), for instance, asserted that the forward position of the foramen magnum in humans is not related to bipedality, but is rather a consequence of the flexion of the cranial base in association with a relatively large brain. Cartmill (1972) also found no evidence linking posture with features of the cranial base: "The placement of the

Reproduced with permission of the copyright owner. Further reproduction prohibited without permission.

foramen magnum shows no correlation with posture, as Biegert (1957) and others have repeatedly shown" (p. 118).

The near-universal observation that the foramen magnum and occipital condyles migrate posteriorly with age in primates and other mammals has been used by both sides of the argument to support their respective positions. Ashton and Zuckerman (1952, 1956) investigated the age-related changes that occur in the position of the occipital condyles in *Gorilla* and *Pan*. They observed that the condyles became more posteriorly located with age but were unable to observe any obvious differences in posture or head carriage between younger and older apes. Adams and Moore (1975) challenged this claim contending that "In the apes, the young tend to move by brachiation and thus have habitual posture of the spine closer to the vertical than in the 'knuckle walking' adults" (p. 582). Michejda and Lamey (1971) have reported observing an age-related transition of locomotor behavior in *Macaca mulatta*, from predominantly erect posture and bipedal locomotion in infants to exclusive quadrupedalism in juveniles and adults. Doran (1997) has documented a more complex ontogenetic transition in locomotor behavior in mountain gorillas and common chimpanzees. Johnson and Shapiro (1998) recently examined the relationship between locomotor mode and vertebral anatomy in several neotropical monkeys and hylobatids. Their data show no obvious correspondence between vertebral morphology and cranio-cervical disposition. To further muddy the waters, results from experiments intended to shed light on the relationship between locomotion and cranial morphology have either been inconclusive or contradictory (e.g., Moss, 1961; Fanghänel, 1972).

Reproduced with permission of the copyright owner. Further reproduction prohibited without permission.

A list of species and their locomotor activities has already been presented in Box 13.3. This data was examined using multiple regression analysis in which each of the 8 locomotor categories served as a dummy-coded independent variable. The results are given in Boxes 13.7 and 13.8. Since I was attempting to *explain* variation in the position of the occipital condyles and inclination of the foramen magnum in terms of locomotor activity, the delta-transformed data were used in the analysis.

Box 13.7. SAS output of multiple regression of delta log condylar index on delta log locomotor activities for 37 species of anthropoids.

Model: MODEL1
Dependent Variable: L_YM69

Analysis of Variance

Source	DF	Sum of Squares	Mean Square	F Value	Prob>F
Model	8	0.09384	0.01173	3.013	0.0143
Error	28	0.10902	0.00389		
C Total	36	0.20286			

Root MSE	0.06240	R-square	0.4626
Dep Mean	2.29924	Adj R-sq	0.3090
C.V.	2.71389		

Parameter Estimates

Variable	DF	Parameter Estimate	Standard Error	T for H0: Parameter=0	Prob > |T|
INTERCEP	1	2.123026	1.28520962	1.652	0.1097
L_BIPED	1	0.540179	0.17646801	3.061	0.0048
L_QUAD	1	0.058630	0.16616850	0.353	0.7269
L_SUSP	1	0.001007	0.20215474	0.005	0.9961
L_LEAP	1	-0.044561	0.13722513	-0.325	0.7478
L_VCL	1	-0.147397	0.17841086	-0.826	0.4157
L_CLIMB	1	-0.181539	0.15721016	-1.155	0.2580
L_WALK	1	0.035018	0.14687625	0.238	0.8133
L_KNUC	1	-0.184575	0.18059827	-1.022	0.3155

Evolutionary regression of condylar index (Box 13.7) and foramen magnum slope (Box 13.8) on locomotor variables indicate that only bipedality is a significant explanatory variable among anthropoids. One could thus predict bipedality from either the location of the occipital condyles or the inclination of

Reproduced with permission of the copyright owner. Further reproduction prohibited without permission.

the foramen magnum. None of the other locomotor activities significantly accounted for cranio-cervical location or inclination. Once the effects of phylogeny are removed from the data, there remains a substantial amount of variation in foramen magnum disposition across the various locomotor repertoires.

Box 13.8. SAS output of multiple regression of delta log foramen magnum slope on delta log locomotor activities for 37 species of anthropoids

Model: MODEL2
Dependent Variable: L_YM68

Analysis of Variance

Source	DF	Sum of Squares	Mean Square	F Value	Prob>F
Model	8	0.14483	0.01810	3.501	0.0064
Error	28	0.14478	0.00517		
C Total	36	0.28961			

Root MSE	0.07191	R-square	0.5001
Dep Mean	2.29727	Adj R-sq	0.3572
C.V.	3.13017		

Parameter Estimates

Variable	DF	Parameter Estimate	Standard Error	T for H0: Parameter=0	Prob > |T|
INTERCEP	1	4.204534	1.48107048	2.839	0.0083
L_BIPED	1	-0.794034	0.20336104	-3.905	0.0005
L_QUAD	1	-0.241734	0.19149192	-1.262	0.2172
L_SUSP	1	0.010178	0.23296232	0.044	0.9655
L_LEAP	1	-0.166464	0.15813769	-1.053	0.3015
L_VCL	1	0.142720	0.20559997	0.694	0.4933
L_CLIMB	1	0.182892	0.18116837	1.010	0.3214
L_WALK	1	-0.046818	0.16925961	-0.277	0.7841
L_KNUC	1	0.083616	0.20812073	0.402	0.6909

Reproduced with permission of the copyright owner. Further reproduction prohibited without permission.

The Effects of Locomotion on Cranial Base Angle

Box 13.9 shows that bipedality is also the only locomotor category able to account for a significant proportion of the variance of cranial base angle.

Box 13.9. SAS output of multiple regression of delta log cranial base angle on delta log locomotor activities for 37 species of anthropoids

Model: MODEL3
Dependent Variable: L_YM7O

Analysis of Variance

Source	DF	Sum of Squares	Mean Square	F Value	Prob>F
Model	8	0.19662	0.02458	7.754	0.0001
Error	28	0.08874	0.00317		
C Total	36	0.28536			

Root MSE	0.05630	R-square	0.6890
Dep Mean	2.29780	Adj R-sq	0.6002
C.V.	2.45008		

Parameter Estimates

Variable	DF	Parameter Estimate	Standard Error	T for HO: Parameter=0	Prob > |T|
INTERCEP	1	4.380786	1.15954520	3.778	0.0008
L_BIPED	1	-0.829579	0.15921344	-5.210	0.0001
L_QUAD	1	0.033002	0.14992098	0.220	0.8274
L_SUSP	1	0.214826	0.18238858	1.178	0.2488
L_LEAP	1	-0.155483	0.12380761	-1.256	0.2196
L_VCL	1	-0.280358	0.16096632	-1.742	0.0925
L_CLIMB	1	0.114162	0.14183857	0.805	0.4277
L_WALK	1	0.059536	0.13251507	0.449	0.6567
L_KNUC	1	-0.062008	0.16293985	-0.381	0.7064

The Effects of Body Size on the Disposition of the Foramen Magnum

According to the theoretical tenets developed in Chapter 10, isometry between overall size (e.g., centroid size) and a shape variable (e.g., angle, ratio, etc.) is characterized by a zero slope log-log regression line with homoscedastic dispersion and low variance. In other words, under conditions of isometry the mean value of the shape variable will not change with changes in body size.

Reproduced with permission of the copyright owner. Further reproduction prohibited without permission.

Moreover, isometry indicates either that no size-related causal agents have acted on the shape variable under investigation, or that the shape variable has attained an equilibrium with respect to two or more agents (see Chapter 10, Box 10.8). Alternatively, a significant non-zero log-log regression slope signifies that one or more size-related causal agents have had an effect on the shape variable.

The log-log regression of the cranio-cervical shape variables on centroid size yielded a coefficient of zero, but exhibited considerable heteroscedacticity and high variance (Boxes 13.10 & 13.11). Therefore, it can be concluded that both condylar index and foramen magnum slope have no relationship with size. However, if specimens of *Homo sapiens* are excluded from the analysis (*H. sapiens* are outliers in having large bodies and anteriorly placed FM), the regression slope is significant (b = 0.19, 95% CI: 0.02, 0.37), but the R-square remains low (R^2= 0.02).

Box 13.10 Regression plot of log delta centroid size (ΔL_YV41) against delta log foramen magnum slope (ΔL_YV68). Slope: 0.00 (-0.17, 0.17), R^2 = 0.00, heteroscedastic. (n=300)

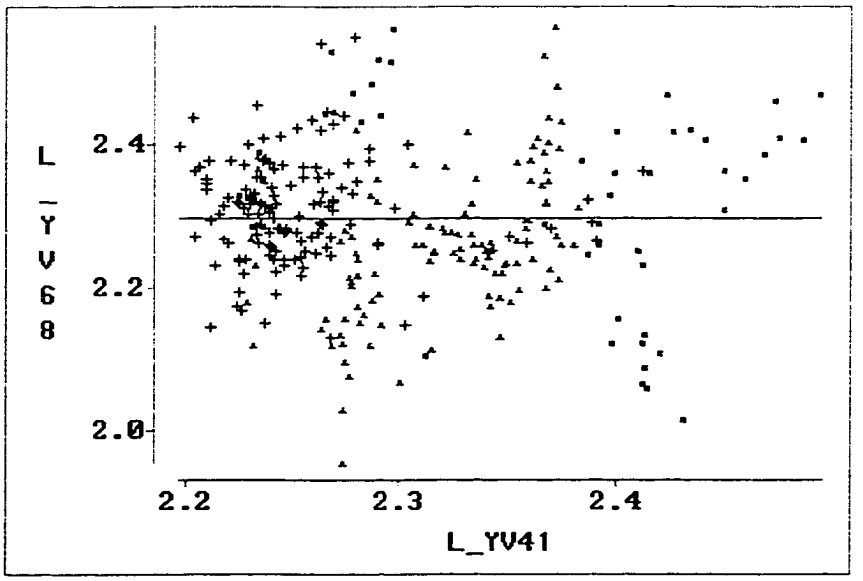

Reproduced with permission of the copyright owner. Further reproduction prohibited without permission.

Box 13.11 Regression plot of log delta centroid size (ΔL_YV41) against delta log condylar index (ΔL_YV69). Slope: 0.13 (-0.01, 0.28), R^2 = 0.01, heteroscedastic. (n=300)

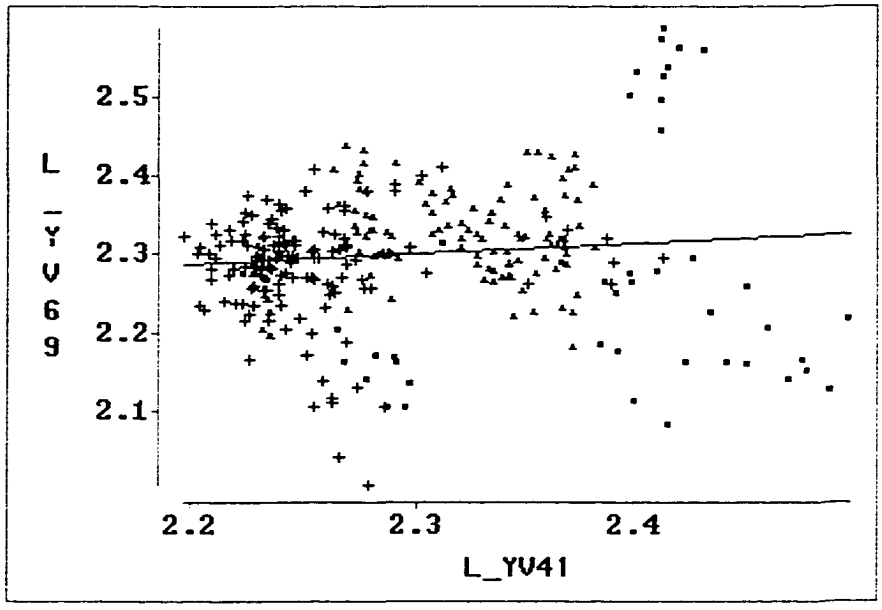

Previous allometric analysis involving these variables have yielded inconsistent results. Luboga and Wood (1991), in a craniometric study of *Pan* and *Homo*, found that cranial size (i.e., the geometric mean of 41 linear measurements) regressed isometrically with foramen magnum inclination, but allometrically with foramen magnum position: larger crania tended to have more posteriorly situated foramina (p. 75).

When these authors examined within-species variation they found that both the position and slope of the foramen magnum were significantly greater than isometry. "The implication is that within modern human crania there is an allometric trend such that larger crania have a relatively more posteriorly located foramen magnum..." (p. 73). Interestingly, they observed the same allometric pattern in *Pan paniscus*, but not in *P. troglodytes*, which exhibited isometric relationships with respect to the same

Reproduced with permission of the copyright owner. Further reproduction prohibited without permission.

variables. Based on this report I examined the allometric properties of the pooled within-species anthropoid data. I found no significant relationship between skull size and either condylar index (slope= -0.33, 95% CI: -0.77, 0.11, R^2=.01) or foramen magnum inclination (b= 0.47, 95% CI: -0.23, 1.17, R^2=0)

Principal Components Analysis of Cranio-cervical and Craniofacial Variables

Thirty-six craniometric variables were selected for principal components analysis, including the two cranio-cervical variables—condylar index and foramen magnum slope—and 34 relevant endocranial and nasomaxillary variables. The aim of the analysis was to examine correlational patterns of foramen magnum disposition to other relevant characteristics of the cranium. The eigenvalues for the 36 variables are given in Box 13.12. Only the first two principal components were retained for examination. The first principal component accounted for 23% of the total variance of the variables, and the second principal component accounted for an additional 13%.

Box 13.12. Eigenvalues and accounted-for variance of log delta V-level cranio-cervical and craniofacial variables (n=300; correlation matrix used in PCA).

PC	Eigen-value	Proportion of Variance Explained	Cumulative Proportion Explained	PC	Eigenvalue	Proportion of Variance Explained	Cumulative Proportion Explained
1	8.42	0.234	0.234	19	0.45	0.012	0.910
2	4.63	0.128	0.363	20	0.40	0.011	0.921
3	2.85	0.079	0.442	21	0.36	0.010	0.931
4	2.31	0.064	0.506	22	0.34	0.009	0.941
5	2.12	0.059	0.565	23	0.29	0.008	0.949
6	1.59	0.044	0.608	24	0.25	0.007	0.955
7	1.40	0.039	0.647	25	0.23	0.007	0.962
8	1.31	0.036	0.684	26	0.23	0.006	0.969
9	1.77	0.032	0.716	27	0.21	0.006	0.975
10	1.10	0.030	0.747	28	0.19	0.005	0.980
11	0.92	0.025	0.772	29	0.17	0.005	0.985
12	0.84	0.023	0.796	30	0.14	0.004	0.989
13	0.73	0.020	0.816	31	0.12	0.003	0.992
14	0.70	0.019	0.836	32	0.11	0.003	0.995
15	0.62	0.017	0.853	33	0.08	0.002	0.997
16	0.54	0.015	0.868	34	0.04	0.001	0.999
17	0.53	0.015	0.883	35	0.03	0.001	0.999
18	0.50	0.014	0.897	36	0.01	0.000	1.000

Reproduced with permission of the copyright owner. Further reproduction prohibited without permission.

As in previous PCAs, all variables were log delta-transformed and either shape variables or Mosimann isometric residuals. Box 13.13 lists the component loadings for the first two principal components of the PCA.

Box 13.13. Component loadings for the first two principal components of the combined cranio-cervical, endocranial and craniofacial variables (after varimax rotation)

Variable	$PC_{(1)}$	$PC_{(2)}$	Variable	$PC_{(1)}$	$PC_{(2)}$
ΔS_L_YV1	0.148	0.830	ΔS_L_YV27	0.356	-0.201
ΔS_L_YV4	-0.137	-0.474	ΔL_YV30	0.738	0.293
ΔS_L_YV5	0.345	-0.022	ΔL_YV31	0.577	0.608
ΔS_L_YV6	-0.084	0.069	ΔL_YV32	-0.417	0.471
ΔS_L_YV7	-0.207	0.493	ΔL_YV33	-0.307	0.212
ΔS_L_YV8	-0.454	-0.269	ΔL_YV35	0.030	0.780
ΔS_L_YV9	-0.037	-0.011	ΔL_YV45	0.091	-0.177
ΔS_L_YV11	0.053	0.555	ΔL_YV46	0.644	0.093
ΔL_YV13	-0.370	-0.540	ΔS_L_YV49	-0.143	-0.686
ΔS_L_YV14	0.723	0.479	ΔL_YV68	0.722	-0.177
ΔS_L_YV15	0.132	-0.133	ΔL_YV69	-0.852	0.155
ΔS_L_YV16	-0.201	-0.703	ΔL_YV70	0.736	0.077
ΔS_L_YV17	0.268	0.793	ΔL_YV74	0.689	0.059
ΔS_L_YV18	0.001	0.079	ΔL_YV78	0.485	0.301
ΔS_L_YV19	0.409	-0.138	ΔL_YV79	0.216	-0.592
ΔS_L_YV21	0.293	-0.162	ΔL_YV81	-0.435	-0.140
ΔS_L_YV23	-0.365	-0.329	ΔS_L_YV84	-0.822	-0.365
ΔS_L_YV25	-0.082	0.210	ΔL_YV95	0.268	0.500

Box 13.14 displays the scatter plot of the first two principal components. Once again, the dotted lines separate 'significant' from 'nonsignificant' component loadings. It is informative to compare the PCA results from Chapters 11 and 12 with the PCA results of the current analysis. The variables that contribute significantly to $PC_{(1)}$ in the current PCA are, for the most part, the same that loaded highly on $PC_{(1)}$ in Chapter 11 (Box 11.11). This component contrasts relative brain size [YV84] and brain shape [YV81] against characteristics of the chondrocranium (i.e., cranial base flexion [YV70], cribriform plate orientation [YV74], middle cranial fossa length [YV78]) and nasomaxillary complex (i.e., facial prognathism

Reproduced with permission of the copyright owner. Further reproduction prohibited without permission.

[YV30, YV31] and maxillary length [YV14]). It can be seen with reference to the PCA plot in Box 13.14 that both condylar index [YV69] and foramen magnum slope [YV68] strongly align with this component. A second component that has remained relatively stable across analyses was first revealed as $PC_{(2)}$ in Chapter 11 (Box 11.11), then resurfaced as $PC_{(1)}$ in Chapter 12 (Box 12.13), and has now reappeared as $PC_{(2)}$ (Box 13.14). This component contrasts facial length (i.e., nasal bone length [YV1], anterior facial length [YV17], and zygomatic height [YV11]), posterior facial angle [YV95], and paranasal plate orientation [YV35] with naso-orbital breadth (i.e., nasal process of maxilla width [YV4], upper facial breadth [YV16], and intranasal breadth [YV49]), zygomatic root position[YV13], and anterior cranial fossa length [YV79]). This components appears to be orthogonal to the component defined by relative brain size and shape.

Box 13.14. Bivariate plot of first two principal components (PC 1, PC 2)

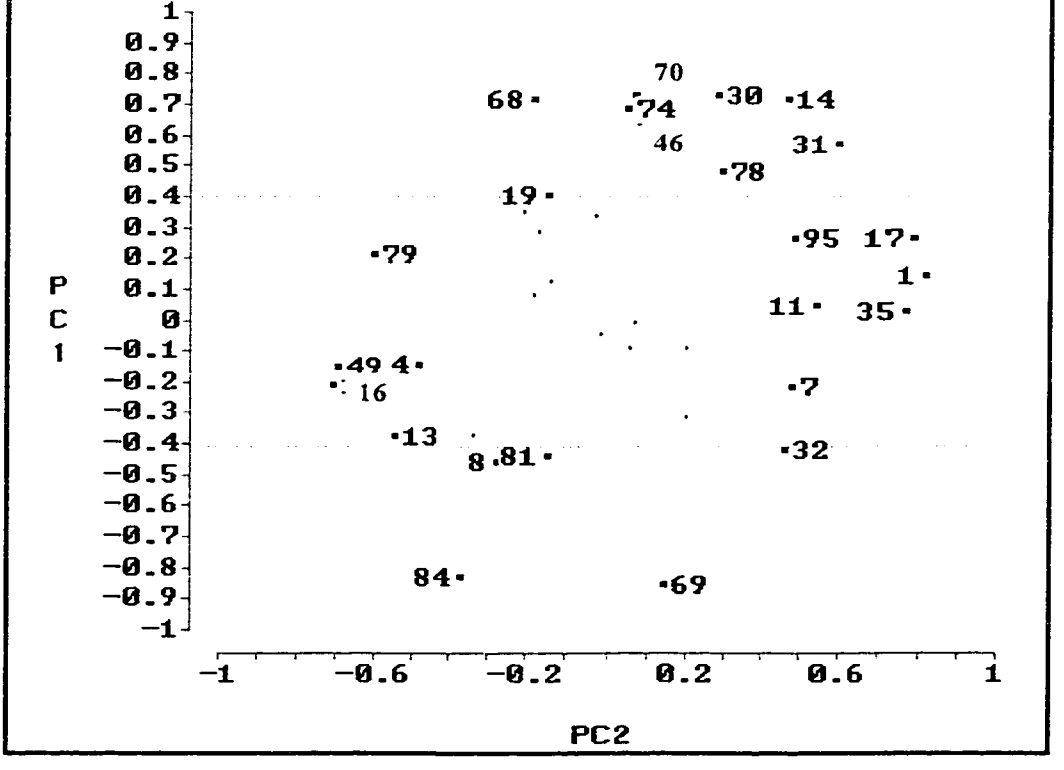

Reproduced with permission of the copyright owner. Further reproduction prohibited without permission.

It is noteworthy that foramen magnum position and slope should be correlated with characteristics of the brain, chondrocranium, and facial protrusion, since these are precisely the variables that have been hypothesized to be causally related in some fashion. In the next section, I examine specific bivariate and multivariate relationships in the context of evaluating particular hypotheses.

Bivariate and Multiple Regression Analysis

To further examine trait covariances and to test statistical predictions (see Box 13.4), bivariate and multiple regressions were conducted. The results are given in Boxes 13.15-13.24, and selected scatter plots are displayed in Boxes 13.25 and 13.26.

Reproduced with permission of the copyright owner. Further reproduction prohibited without permission.

Box 13.15 Predicted bivariate statistical associations and properties deduced from hypotheses statements. (n=300)

Predicted bivariate associations (dependent variable in bold)	Regression slope (95% CL) and test of significant association, R^2 (p-value)
Cranial base flexion [ΔL_YV70] ←	
*Slope of foramen magnum [ΔL_YV68]	0.48 (0.38, 0.57) R^2 = 0.24 (p < .01)
*A-P position of occipital condyles [ΔL_YV69]	-0.68 (-0.79, -0.57) R^2 = 0.34 (p < .01)
Endocephalic index [ΔL_YV81]	-0.31 (-0.43, -0.18) R^2 = 0.07 (ns)
*Relative endocranial volume [ΔS_L_YV84]	-1.60 (-1.90, -1.35) R^2 = 0.31 (p < .01)
Slope of foramen magnum [L_YV68] ←	
*Cranial base flexion [ΔL_YV70]	0.50 (0.40, 0.61) R^2 = 0.24 (p < .01)
Endocephalic index [ΔL_YV81]	-0.26 (-0.39, -0.13) R^2 = 0.05 (ns)
*Relative endocranial volume [ΔS_L_YV84]	-1.54 (-1.83, -1.25) R^2 = 0.26 (p < .01)
A-P position of occipital condyles [ΔL_YV69] ←	
*Cranial base flexion [ΔL_YV70]	-0.51 (-0.58, -0.43) R^2 = 0.34 (p < .01)
*Endocephalic index [ΔL_YV81]	0.39 (0.28, 0.49) R^2 = 0.15 (p < .05)
*Relative endocranial volume [ΔS_L_YV84]	1.61 (1.39, 1.83) R^2 = 0.41 (p < .01)
Nasomaxillary dimensions ← A-P position of occipital condyles [ΔL_YV69]	
Nasal bone length [ΔS_L_YV1] ←	0.00 (-0.08, 0.08) R^2 = 0.00 (ns)
Anterior nasal aperture breadth [ΔS_L_YV6] ←	0.03 (0.01, 0.06) R^2 = 0.01 (ns)
Posterior nasal aperture breadth [ΔS_L_YV8] ←	0.11 (0.07, 0.16) R^2 = 0.08 (ns)
***Maxillary length [ΔS_L_YV14] ←**	-0.17 (-0.20, -0.14) R^2 = 0.29 (p < .01)
Upper facial breadth [ΔS_L_YV16] ←	0.03 (0.00, 0.06) R^2 = 0.02 (ns)
Anterior facial length [ΔS_L_YV17] ←	-0.05 (-0.08, 0.01) R^2 = 0.02 (ns)
***Facial prognathism [ΔL_Y30] ←**	-0.45 (-0.54, -0.36) R^2 = 0.24 (p < .01)
***Occlusal slope [ΔL_YV32] ←**	0.40 (0.30, 0.51) R^2 = 0.16 (p < .05)
Paranasal plate orientation [ΔL_YV35] ←	0.12 (0.00, 0.24) R^2 = 0.01 (ns)
***Orbital declination [ΔL_YV46] ←**	-0.49 (-0.61, -0.37) R^2 = 0.17 (p < .05)
Nasomaxillary dimensions ← Cranial base flexion [ΔL_YV70]	
Nasal bone length [ΔS_L_YV1] ←	0.17 (0.11, 0.23) R^2 = 0.08 (p < .05)
Anterior nasal aperture breadth [ΔS_L_YV6] ←	-0.01 (-0.04, 0.02) R^2 = 0.00 (ns)
Posterior nasal aperture breadth [ΔS_L_YV8] ←	-0.09 (-0.13, -0.05) R^2 = 0.07 (p < .05)
***Maxillary length [ΔS_L_YV14] ←**	0.17 (0.14, 0.19) R^2 = 0.37 (p < .01)
Upper facial breadth [ΔS_L_YV16] ←	-0.05 (-0.07, -0.02) R^2 = 0.04 (p < .05)
Anterior facial length [ΔS_L_YV17] ←	0.09 (0.06, 0.12) R^2 = 0.10 (p < .05)
***Facial prognathism [ΔL_Y30] ←**	0.38 (0.30, 0.46) R^2 = 0.22 (p < .01)
Occlusal slope [ΔL_YV32] ←	-0.27 (-0.36, -0.17) R^2 = 0.09 (p < .05)
Paranasal plate orientation [ΔL_YV35] ←	0.05 (-0.06, 0.16) R^2 = 0.00 (ns)
***Orbital deflection [ΔL_YV46] ←**	0.55 (0.45, 0.64) R^2 = 0.28 (p < .01)

Reproduced with permission of the copyright owner. Further reproduction prohibited without permission.

Box 13.16. Predicted bivariate statistical associations and properties deduced from hypotheses statements.

Predicted multivariate associations (dependent variable in bold)	Regression slope, t-statistic and test of significance (df = 35)
Facial prognathism-Krogman [ΔL_YV30] ← model *R*-square = 0.50	
A-P position of occipital condyles [ΔL_YV69]	0.00 t = 0.01 ns
Cranial base flexion [ΔL_YV70]	0.09 t = 2.00 ns
Cribriform plate orientation [ΔL_YV74]	0.14 t = 3.56 ($p < .01$)
Endocranial index [ΔL_YV81]	-0.03 t = -0.77 ns
Relative endocranial volume [ΔS_L_YV84]	-1.15 t = -7.96 ($p < .01$)
Maxillary arch length [ΔS_L_YV14] ← model *R*-square = 0.58	
A-P position of occipital condyles [ΔL_YV69]	-0.01 t = -0.43 ns
Cranial base flexion [ΔL_YV70]	0.08 t = 6.03 ($p < .01$)
Cribriform plate orientation [ΔL_YV74]	0.01 t = 0.75 ns
Endocranial index [ΔL_YV81]	0.02 t = 1.39 ns
Relative endocranial volume [ΔS_L_YV84]	-0.43 t = -9.39 ($p < .01$)
Posterior Nasal Aperture Breadth [ΔS_L_YV8] ← model *R*-square = 0.34	
A-P position of occipital condyles [ΔL_YV69]	-0.02 t = -0.79 ns
Cranial base flexion [ΔL_YV70]	0.00 t = 0.35 ns
Cribriform plate orientation [ΔL_YV74]	0.03 t = 1.67 ns
Endocranial index [ΔL_YV81]	-0.06 t = -2.89 ($p < .01$)
Relative endocranial volume [ΔS_L_YV84]	0.72 t = 10.08 ($p < .01$)
Cranial base flexion [ΔL_YV70] ← model *R*-square = 0.40	
A-P position of occipital condyles [ΔL_YV69]	-0.44 t = -6.25 ($p < .01$)
Cribriform plate orientation [ΔL_YV74]	0.05 t = 0.98 ns
Endocranial index [ΔL_YV81]	0.02 t = 0.33 ns
Relative endocranial volume [ΔS_L_YV84]	-0.85 t = -4.44 ($p < .01$)
Slope of foramen magnum [ΔL_YV68] ← model *R*-square = 0.32	
Cranial base flexion [ΔL_YV70]	0.30 t = 5.14 ($p < .01$)
Relative endocranial volume [ΔS_L_YV84]	-1.04 t = -6.04 ($p < .01$)
A-P position of occipital condyles [ΔL_YV69] ← model R-square = 0.49	
Cranial base flexion [ΔL_YV70]	-0.29 t = -6.63 ($p < .01$)
Relative endocranial volume [ΔS_L_YV84]	1.14 t = 9.01 ($p < .01$)

Reproduced with permission of the copyright owner. Further reproduction prohibited without permission.

Box 13.17. Maxillary arch length [ΔS_L_YV14] ← Cranial base angle [ΔL_YV70]					
Taxon	Level of analysis	Maximum likelihood regression coefficient (95% CI) and associated p-value	Shapiro-Wilk test for normality of residuals	Brown & Forsythe's test for residual homoscedasticity	Somers' D nonparametric measure and test of association
Anthropoids (n=300)	V	0.17 (0.14, 0.19) p = .0001	0.96 p = .0001	15.36 p = .0001	0.28 p < .05
	M	0.23 (0.20, 0.25) p = .0001	0.94 p = .0001	10.77 p = .0001	0.34 p < .05
Platyrrhini (n=117)	V	0.04 (0.01, 0.07) p = .009	0.98 p = .32	1.71 p = .17	0.19 p < .05
	M	0.13 (0.08, 0.18) p = .0001	0.96 p = .008	10.43 p = .0001	0.34 p < .05
Atelidae (n=65)	V	0.07 (0.02, 0.12) p = .01	0.93 p = .01	1.93 p = .13	0.23 p < .05
	M	0.15 (0.08, 0.22) p = .0001	0.97 p = .19	2.05 p = .12	0.29 p < .05
Cebidae (n=52)	V	0.02 (-0.01, 0.05) p = .31	0.96 p = .0001	1.55 p = .21	0.12 ns
	M	0.71 (0.56, 0.86) p = .0001	0.96 p = .11	0.52 p = .67	0.45 p < .05
Catarrhini (n=183)	V	0.19 (0.16, 0.22) p = .0001	0.98 p = .18	22.89 p = .0001	0.20 p < .05
	M	0.23 (0.20, 0.27) p = .0001	0.95 p = .0001	41.03 p = .0001	0.20 p < .05
Cercopithecoidea (n=137)	V	0.02 (-0.03, 0.06) p = .48	0.97 p = .04	9.03 p = .0001	0.05 ns
Cercopithecinae (n=87)	V	-0.06 (-0.10, -0.01) p = .01	0.98 p = .43	5.70 p = .001	-0.12 ns
Colobinae (n=50)	V	0.13 (0.06, 0.20) p = .0003	0.95 p = .06	0.67 p = .57	0.30 p < .05
	M	0.18 (0.10, 0.26) p = .0001	0.95 p = .09	0.49 p = .69	0.36 p < .05
Hominoidea (n=46)	V	0.25 (0.21, 0.29) p = .0001	0.98 p = .60	0.59 p = .62	0.52 p < .05
	M	0.28 (0.24, 0.31) p = .0001	0.93 p = .007	0.83 p = .48	0.57 p < .05

Reproduced with permission of the copyright owner. Further reproduction prohibited without permission.

Box 13.18. Facial prognathism (Krogman's angle) [ΔL_YV30] ← Cranial base angle [ΔL_YV70]					
Taxon	Level of analysis	Maximum likelihood regression coefficient (95% CI) and associated p-value	Shapiro-Wilk test for normality of residuals	Brown & Forsythe's test for residual homoscedasticity	Somers' D nonparametric measure and test of association
Anthropoids (n=300)	V	0.38 (0.30, 0.46) p = .0001	0.98 p = .33	8.11 p = .0001	0.14 p < .05
	M	0.51 (0.41, 0.60) p = .0001	0.99 p = .64	6.37 p = .0003	0.14 p < .05
Platyrrhini (n=117)	V	0.22 (0.03, 0.41) p = .02	0.97 p = .18	0.35 p = .79	0.15 p < .05
	M	0.82 (0.49, 1.15) p = .0001	0.98 p = .31	5.23 p = .002	0.21 p < .05
Atelidae (n=65)	V	0.59 (0.22, 0.96) p = .001	0.92 p = .0004	0.15 p = .93	0.29 p < .05
	M	1.38 (0.94, 1.82) p = .0001	0.95 p = .02	4.52 p = .006	0.40 p < .05
Cebidae (n=52)	V	0.07 (-0.10, 0.25) p = .40	0.95 p = .04	1.23 p = .31	0.11 ns
	M	2.75 (1.56, 3.94) p = .0001	0.97 p = .37	0.57 p = .64	0.28 p < .05
Catarrhini (n=183)	V	0.44 (0.36, 0.52) p = .0001	0.99 p = .93	12.59 p = .0001	0.21 p < .05
	M	0.53 (0.44, 0.62) p = .0001	0.99 p = .97	8.26 p = .0001	0.21 p < .05
Cercopithecoidea (n=137)	V	0.16 (0.04, 0.29) p = .009	0.97 p = .10	4.06 p = .009	0.16 p < .05
	M	0.20 (0.3, 0.37) p = .02	0.97 p = .14	6.22 p = .0005	0.13 p < .05
Cercopithecinae (n=87)	V	-0.03 (-0.17, 0.12) p = .70	0.98 p = .08	2.08 p = .11	-0.01 ns
Colobinae (n=50)	V	0.58 (0.38, 0.77) p = .0001	0.97 p = .47	5.12 p = .004	0.49 p < .05
	M	0.72 (0.52, 1.00) p = .0001	0.98 p = .86	1.90 p = .14	0.58 p < .05
Hominoidea (n=46)	V	0.58 (0.46, 0.71) p = .0001	0.95 p = .10	1.51 p = .21	0.32 p < .05
	M	0.64 (0.52, 0.76) p = .0001	0.98 p = .73	2.09 p = .12	0.33 p < .05

Reproduced with permission of the copyright owner. Further reproduction prohibited without permission.

Box 13.19. Occlusal slope [ΔL_YV32] ← Cranial base angle [ΔL_YV70]

Taxon	Level of analysis	Maximum likelihood regression coefficient (95% CI) and associated p-value	Shapiro-Wilk test for normality of residuals	Brown & Forsythe's test for residual homoscedasticity	Somers' D nonparametric measure and test of association
Anthropoids (n=300)	V	-0.27 (-0.36, -0.17) p = .0001	0.98 p = .60	1.91 p = .13	-0.32 p < .05
	M	-0.36 (-0.47, -0.25) p = .0001	0.98 p = .53	1.24 p = .29	-0.30 p < .05
Platyrrhini (n=117)	V	-0.18 (-0.38, 0.02) p = .07	0.98 p = .58	0.62 p = .60	-0.12 p < .05
	M	-0.53 (-0.89, -0.17) p = .004	0.98 p = .73	0.91 p = .44	-0.15 p < .05
Atelidae (n=65)	V	-0.54 (-0.88, -0.20) p = .002	0.97 p = .80	0.76 p = .52	-0.25 p < .05
	M	-1.06 (-1.51, -0.60) p = .001	0.97 p = .25	3.76 p = .02	-0.24 p < .05
Cebidae (n=52)	V	-0.07 (-0.31, 0.16) p = .53	0.98 p = .68	1.23 p = .31	-0.07 ns
	M	-2.44 (-4.02, -0.68) p = .006	0.97 p = .52	0.27 p = .85	-0.24 p < .05
Catarrhini (n=183)	V	-0.24 (-0.35, -0.14) p = .0001	0.97 p = .07	2.55 p = .06	-0.18 p < .05
	M	-0.30 (-0.42, -0.19) p = .0001	0.98 p = .25	5.41 p = .001	-0.22 p < .05
Cercopithecoidea (n=137)	V	-0.31 (-0.50, -0.11) p = .002	0.97 p = .06	1.15 p = .32	-0.23 p < .05
	M	-0.59 (-0.85, -0.34) p = .0001	0.98 p = .22	4.01 p = .009	-0.20 p < .05
Cercopithecinae (n=87)	V	-0.27 (-0.50, -0.05) p = .02	0.97 p = .15	1.72 p = .17	-0.22 p < .05
	M	-0.76 (-1.09, -0.43) p = .0001	0.97 p = .11	2.28 p = .09	-0.18 p < .05
Colobinae (n=50)	V	-0.50 (-0.84, -0.16) p = .003	0.98 p = .55	1.05 p = .38	-0.37 p < .05
	M	-0.56 (-0.95, -0.18) p = .003	0.98 p = .56	1.02 p = .39	-0.23 p < .05
Hominoidea (n=46)	V	-0.24 (-0.36, -0.11) p = .0001	0.98 p = .68	1.63 p = .19	-0.17 ns
	M	-0.26 (-0.38, -0.13) p = .0001	0.97 p = .30	2.63 p = .06	-0.20 p < .05

Reproduced with permission of the copyright owner. Further reproduction prohibited without permission.

Box 13.20. Orbital deflection [ΔL_YV46] ← Cranial base angle [ΔL_YV70]					
Taxon	Level of analysis	Maximum likelihood regression coefficient (95% CI) and associated p-value	Shapiro-Wilk test for normality of residuals	Brown & Forsythe's test for residual homoscedasticity	Somers' D nonparametric measure and test of association
Anthropoids (n=300)	V	0.55 (0.45, 0.64) p = .0001	0.97 p = .01	2.63 p = .05	0.29 p < .05
	M	0.72 (0.61, 0.83) p = .0001	0.98 p = .28	7.19 p = .0001	0.37 p < .05
Platyrrhini (n=117)	V	0.53 (022, 085) p = .0008	0.97 p = .11	1.23 p = .30	0.25 p < .05
	M	2.03 (1.54, 2.51) p = .0001	0.97 p = .17	10.41 p = .0001	0.46 p < .05
Atelidae (n=65)	V	1.26 (0.87, 1.64) p = .0001	0.97 p = .32	4.31 p = .008	0.43 p < .05
	M	2.34 (1.94, 2.73) p = .0001	0.96 p = .10	2.75 p = .05	0.54 p < .05
Cebidae (n=52)	V	-0.14 (-0.61, 0.33) p = .55	0.96 p = .17	1.50 p = .23	-0.08 ns
Catarrhini (n=183)	V	0.53 (0.44, 0.62) p = .0001	0.98 p = .63	4.93 p = .002	0.27 p < .05
	M	0.62 (0.53, 0.72) p = .0001	0.99 p = .95	4.93 p = .002	0.26 p < .05
Cercopithecoidea (n=137)	V	0.36 (0.23, 0.49) p = .0001	0.98 p = .36	1.67 p = .18	0.28 p < .05
	M	0.52 (0.35, 0.69) p = .0001	0.98 p = .46	2.72 p = .047	0.29 p < .05
Cercopithecinae (n=87)	V	0.37 (0.21, 0.53) p = .0001	0.98 p = .44	2.11 p = .11	0.29 p < .05
	M	0.65 (0.41, 0.89) p = .0001	0.98 p = .53	2.73 p = .049	0.32 p < .05
Colobinae (n=50)	V	0.33 (0.12, 0.54) p = .002	0.98 p = .66	1.79 p = .16	0.29 p < .05
	M	0.36 (0.12, 0.60) p = .003	0.98 p = .70	1.66 p = .19	0.33 p < .05
Hominoidea (n=46)	V	0.59 (0.44, 0.73) p = .0001	0.97 p = .55	1.00 p = .40	0.28 p < .05
	M	0.63 (0.48, 0.78) p = .0001	0.99 p = .93	0.56 p = .65	0.23 p < .05

Reproduced with permission of the copyright owner. Further reproduction prohibited without permission.

Box 13.21. Condylar index [ΔL_YV69] ← Cranial base angle [ΔL_YV70]					
Taxon	Level of analysis	Maximum likelihood regression coefficient (95% CI) and associated p-value	Shapiro-Wilk test for normality of residuals	Brown & Forsythe's test for residual homoscedasticity	Somers' D nonparametric measure and test of association
Anthropoids (n=300)	V	-0.51 (-0.59, -0.43) p = .0001	0.95 p = .0001	7.10 p = .0001	-0.31 p < .05
	M	-0.71 (-0.79, -0.62) p = .0001	0.97 p = .0001	5.42 p = .001	-0.37 p < .05
Platyrrhini (n=117)	V	-0.12 (-0.28, 0.05) p = .16	0.98 p = .30	3.79 p = .01	-0.13 p < .05
	M	-0.47 (-0.77, -0.17) p = .002	0.96 p = .02	1.11 p = .35	-0.14 p < .05
Atelidae (n=65)	V	-0.55 (-0.77, -0.34) p = .0001	0.98 p = .53	1.28 p = .29	-0.33 p < .05
	M	-1.02 (-1.28, -0.76) p = .0001	0.97 p = .33	1.79 p = .16	-0.45 p < .05
Cebidae (n=52)	V	0.01 (-0.23, 0.25) p = .93	0.96 p = .19	1.37 p = .26	-0.05 ns
	M	-3.46 (-5.16, -1.76) p = .0001	0.98 p = .56	0.58 p = .63	-0.17 ns
Catarrhini (n=183)	V	-0.55 (-0.64, -0.46) p = .0001	0.96 p = .003	2.25 p = .08	-0.34 p < .05
	M	-0.70 (-0.79, -0.61) p = .0001	0.97 p = .02	2.19 p = .09	-0.42 p < .05
Cercopithecoidea (n=137)	V	-0.31 (-0.45, -0.17) p = .0001	0.93 p = .0001	1.52 p = .0.21	-0.21 p < .05
	M	-0.62 (-0.79, -0.44) p = .0001	0.97 p = .03	4.17 p = .007	-0.29 p < .05
Cercopithecinae (n=87)	V	-0.11 (-0.23, 0.01) p = 0.08	0.98 p = .46	1.57 p = .20	-0.17 p < .05
	M	-0.35 (-0.52, -0.17) p = .0001	0.98 p = .54	1.11 p = .35	-0.26 p < .05
Colobinae (n=50)	V	-0.89 (-1.12, -0.65) p = .0001	0.97 p = .36	1.89 p = .15	-0.48 p < .05
	M	-1.15 (-1.37, -0.92) p = .0001	0.99 p = .99	1.24 p = .31	-0.55 p < .05
Hominoidea (n=46)	V	-0.74 (-0.85, -0.63) p = .0001	0.95 p = .07	0.79 p = .50	-0.57 p < .05
	M	-0.80 (-0.90, -0.70) p = .0001	0.94 p = .03	0.61 p = .62	-0.56 p < .05

Reproduced with permission of the copyright owner. Further reproduction prohibited without permission.

Reproduced with permission of the copyright owner. Further reproduction prohibited without permission.

Box 13.22. Cranial base angle [ΔL_YV70] ← Relative endocranial volume [ΔL_YV69]

Taxon	Level of analysis	Maximum likelihood regression coefficient (95% CI) and associated p-value	Shapiro-Wilk test for normality of residuals	Brown & Forsythe's test for residual homoscedasticity	Somers' D nonparametric measure and test of association
Anthropoids (n=300)	V	-1.63 (-1.90, -1.36) p = .0001	0.96 p = .0001	2.87 p = 04	-0.21 p < .05
	M	-1.74 (-1.99, -1.43) p = .0001	0.96 p = .0001	4.24 p = .006	-0.21 p < .05
Platyrrhini (n=117)	V	-0.85 (-1.46, -0.23) p = .006	0.92 p = .0001	1.76 p = .16	-0.14 p < .05
	M	-0.95 (-1.60, -0.30) p = .0001	0.92 p = .0001	4.05 p = .009	-0.17 p < .05
Atelidae (n=65)	V	-0.52 (-1.13, 0.09) p = .09	0.88 p = .0001	2.34 p = .08	-0.12 ns
	M	-0.69 (-1.31, -0.03) p = .04	0.90 p = .0001	1.67 p = .19	-0.16 p < .05
Cebidae (n=52)	V	-0.57 (-2.04, 0.91) p = .44	0.93 p = .004	1.30 p = .28	-0.10 ns
	M	-0.39 (-1.99, 1.20) p = .62	0.93 p = .005	0.99 p = .40	-0.08 ns
Catarrhini (n=183)	V	-1.70 (-2.03, -1.37) p = .0001	0.95 p = .0001	6.29 p = .0001	-0.18 p < .05
	M	-1.78 (-2.11, -1.44) p = .0001	0.95 p = .0001	4.77 p = .003	-0.16 p < .05
Cercopithecoidea (n=137)	V	0.32 (-0.35, 0.99) p = .34	0.97 p = .04	3.09 p = .03	-0.03 ns
	M	0.51 (-0.24, 1.26) p = .18	0.97 p = .02	1.11 p = .34	0.02 ns
Cercopithecinae (n=87)	V	1.22 (0.48, 1.46) p = .001	0.95 p = .005	2.44 p = .07	0.12 ns
	M	1.52 (0.72, 2.32) p = .0002	0.93 p = .0001	0.53 p = .66	0.10 ns
Colobinae (n=50)	V	-3.32 (-4.36, -2.28) p = .0001	0.98 p = .84	0.68 p = .56	-0.46 p < .05
	M	-4.72 (-5.83, -3.59) p = .0001	0.96 p = .15	1.34 p = .27	-0.34 p < .05
Hominoidea (n=46)	V	-2.06 (-2.45, -1.67) p = .0001	0.96 p = .23	0.64 p = .59	-0.40 p < .05
	M	-2.01 (-2.49, -1.70) p = .0001	0.94 p = .04	0.24 p = .86	-0.37 p < .05

Box 13.23. Partial regression of condylar index [ΔL_YV69] on cranial base angle [ΔL_YV70] and relative endocranial volume [ΔS_L_YV84]

Taxon	ML partial regression coefficient (95% CI, and p-value) of condylar index on cranial base angle controlling for relative endocranial volume	ML partial regression coefficient (95% CI, and p-value) of condylar index on relative endocranial volume controlling for cranial base angle	Shapiro-Wilk test for normality of residuals.	Brown & Forsythe's test for residual homoscedasticity
Anthropoids (n=300)	-0.28 (-0.37, -0.20) p = .0001*	1.13 (0.89, 1.39) p = .0001*	0.96 p = .0001	5.81 p = .0007
Platyrrhini (n=117)	-0.04 (-0.20, 0.12) p = .63	1.13 (0.57, 1.69) p = .0001*	0.98 p = .42	1.77 p = .16
Atelidae (n=65)	-0.45 (-0.63, -0.27) p = .0001*	1.27 (1.72, 1.27) p = .0001*	0.99 p = .85	1.13 p = .34
Cebidae (n=52)	0.05 (-0.19, 0.27) p = .67	1.88 (0.67, 3.08) p = .002	0.98 p = .85	0.47 p = .71
Catarrhini (n=183)	-0.33 (-0.43, -0.23) p = .0001*	1.05 (0.77, 1.33) p = .0001*	0.97 p = .006	6.07 p = .0006
Cercopithecoidea (n=137)	-0.32 (-0.46, -0.18) p = .0001*	0.74 (0.19, 1.29) p = .008	0.94 p = .0001	4.31 p = .006
Cercopithecinae (n=87)	-0.09 (-0.22, 0.03) p = .15*	-0.16 (-0.62, 0.31) p = .51	0.98 p = .54	1.05 p = .37
Colobinae (n=50)	-0.58 (-0.87, -0.29) p = .0001*	2.27 (0.85, 3.70) p = .001*	0.99 p = .90	1.78 p = .16
Hominoidea (n=46)	-0.41 (-0.58, -0.24) p = .0001*	0.96 (0.55, 1.37) p = .0001*	0.95 p = .06	1.06 p = .38

Box 13.24. Multiple regression of cranial base angle [ΔL_YV70] on condylar index [ΔL_YV69], endocranial index [ΔL_YV81], and relative endocranial volume [ΔS_L_YV84]

Taxon	ML partial regression coefficient (95% CI, and p-value)			Shapiro-Wilk test for normality of residuals	Brown & Forsythe's test for residual homoscedasticity
	Cranial base angle on condylar index controlling for endocranial index and relative endocranial volume	Cranial base angle on endocranial index controlling for condylar index and relative endocranial volume	Cranial base angle on relative endocranial volume controlling for condylar index andendocranial index		
Anthropoids (n=300)	-0.45 (p = .0001)*	0.02 (p = .76)*	-0.92 (p = .0001)*	0.96 p = .21	0.19 p = .90
Platyrrhini (n=117)	0.03 (p = .75)*	-0.17 (p = .009)*	-0.82 (p = .01)*	0.93 p = .0001	1.10 p = .39
Atelidae (n=65)	-0.46 (p = .0005)*	-0.14 (p = .04)*	0.04 (p = .90)	0.96 p = .16	4.21 p = .009
Cebidae (n=52)	0.08 (p = .65)	-0.02 (p = .89)	-0.65 (p = .47)	0.93 p = .01	1.24 p = .30
Catarrhini (n=183)	-0.61 (p = .0001)*	0.14 (p = .09)*	-0.88 (p = .0001)*	0.97 p = .09	1.78 p = .15
Cercopithecoidea (n=137)	-0.42 (p = .0001)*	0.01 (p = .91)*	0.07 (p = .08)	0.98 p = .24	1.13 p = .34
Cercopithecinae (n=87)	-0.30 (p = .09)*	0.13 (p = .27)	-1.04 (p = .007)*	0.95 p = .005	0.21 p = .89
Colobinae (n=50)	-0.39 (p = .0003)*	-0.11 (p = .27)*	-1.40 (p = .03)*	0.99 p = .96	1.09 p = .36
Hominoidea (n=46)	-0.80 (p = .0001)*	0.21 (p = .12)*	-0.85 (p = .03)*	0.98 p = .79	0.27 p = .84

Reproduced with permission of the copyright owner. Further reproduction prohibited without permission.

Bivariate Scatter Plots

Selected bivariate scatter plots are presented in Box 13.25, below.

Box 13.25 Scatter plots of delta log condylar index against various delta log craniofacial variables. See Box 13.14 for fit estimates. (n=300)

Condylar index against cranial base flexion

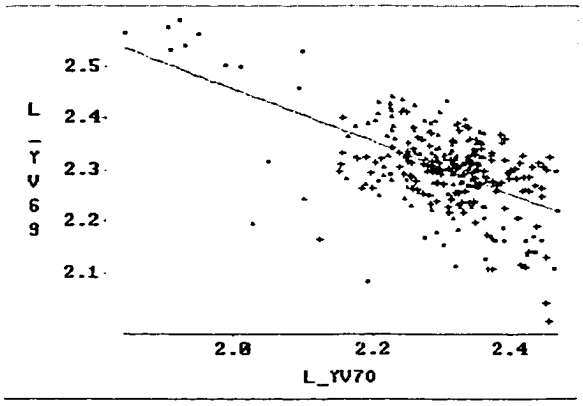

Condylar index against endocranial volume

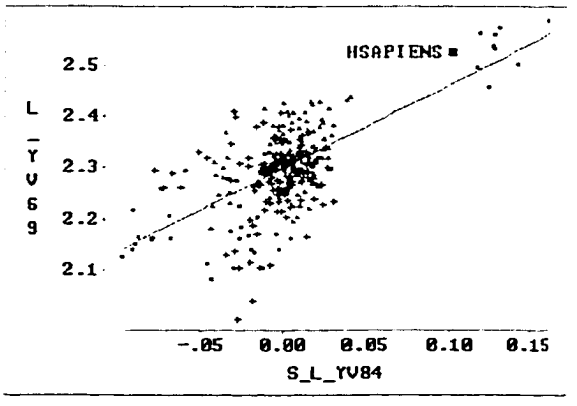

Condylar index against endocephalic index

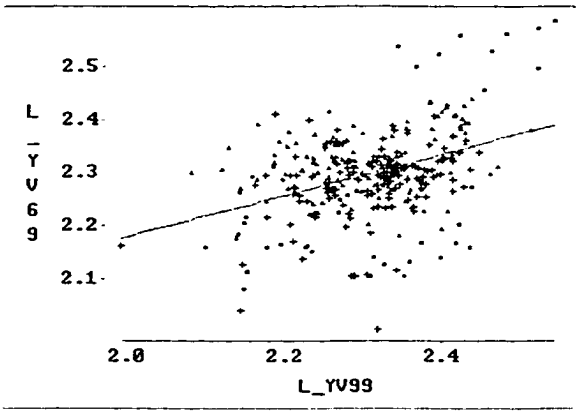

Condylar index against maxillary arch length

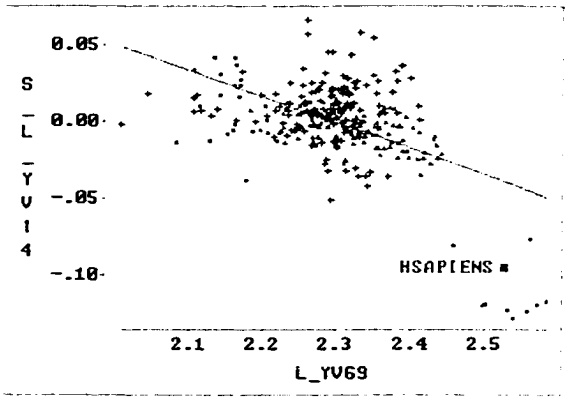

Condylar index against anterior facial length

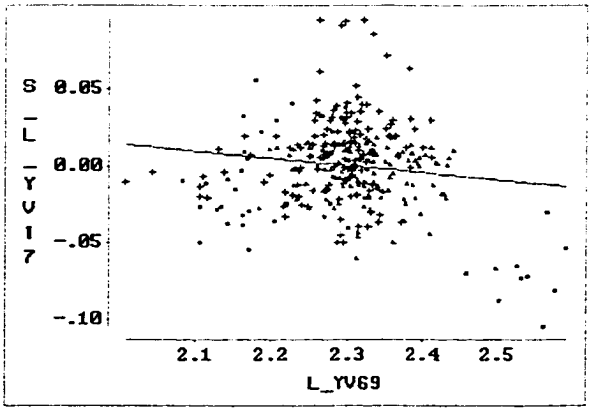

Condylar index against facial prognathism (Krogman's angle)

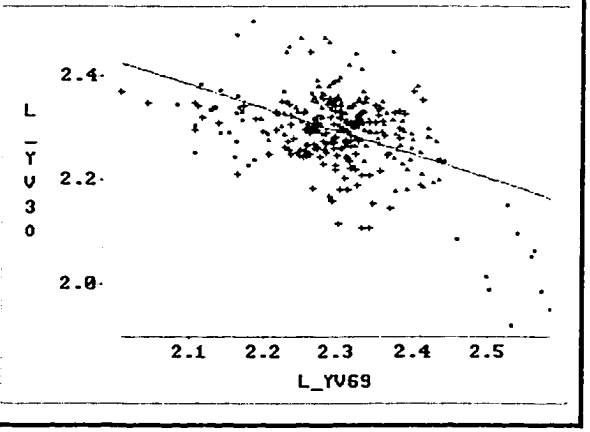

Reproduced with permission of the copyright owner. Further reproduction prohibited without permission.

Box 13.25 Scatter plots of delta log condylar index against various delta log craniofacial variables. See Box 13.14 for fit estimates. (n=300)

Condylar index against occlusal slope

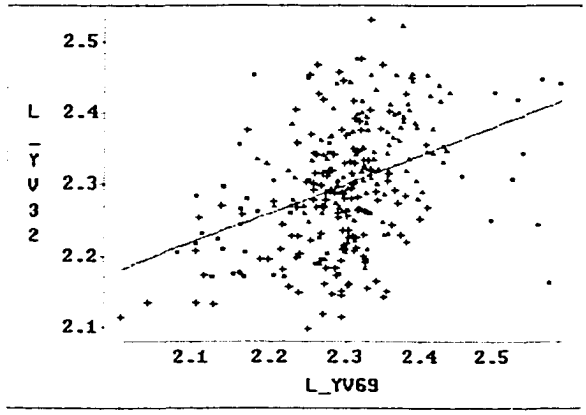

Condylar index against orbital deflection

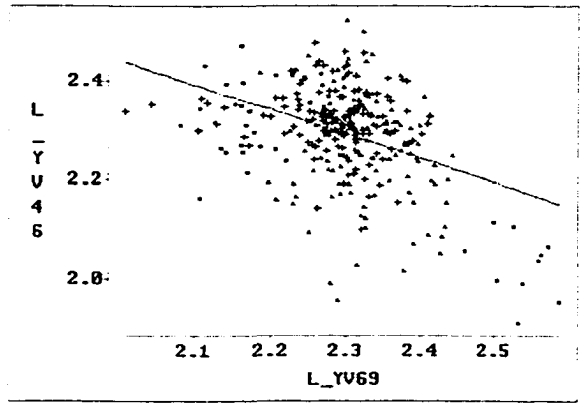

Box 13.26 Scatter plots of delta log cranial base flexion against various delta log craniofacial variables. See Box 13.14 for fit estimates. (n=300)

Cranial base flexion against endocranial volume

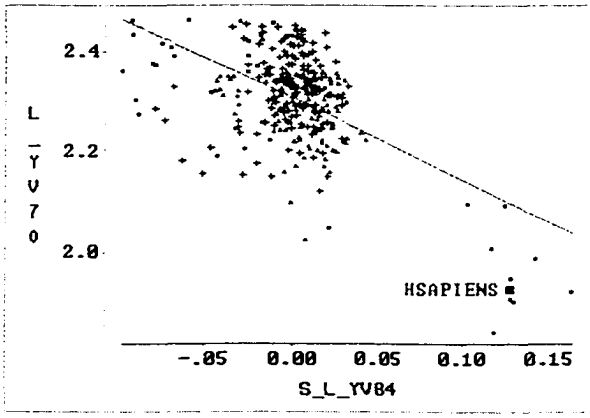

Cranial base flexion against endocranial index

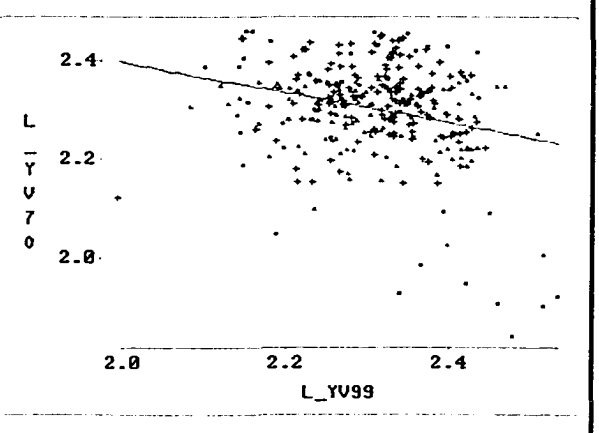

Cranial base flexion against maxillary arch length

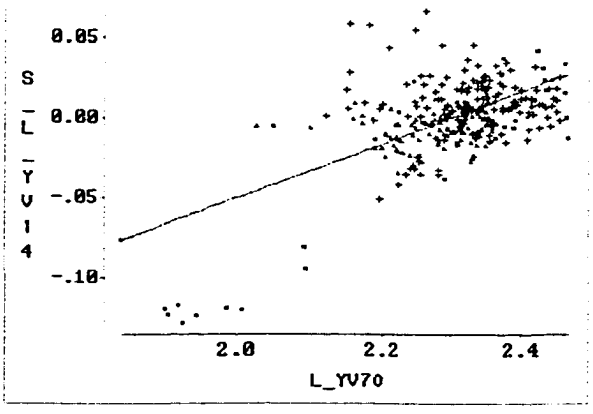

Cranial base flexion against anterior facial length

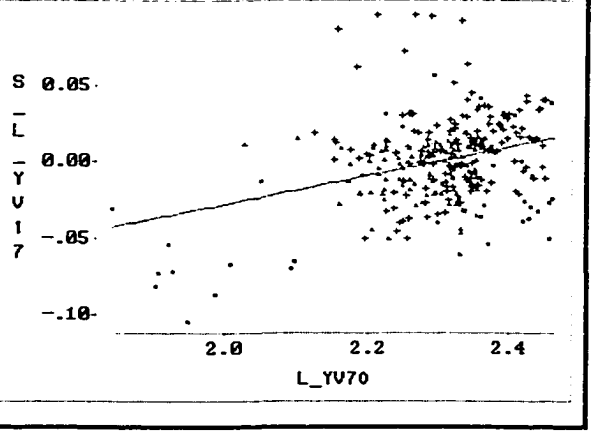

Reproduced with permission of the copyright owner. Further reproduction prohibited without permission.

Box 13.26 Scatter plots of delta log cranial base flexion against various delta log craniofacial variables. See Box 13.14 for fit estimates. (n=300)

Cranial base flexion against facial prognathism (Enlow's angle

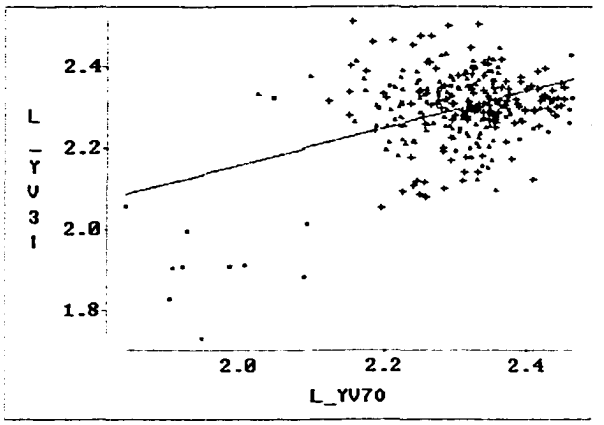

Cranial base flexion against occlusal slope

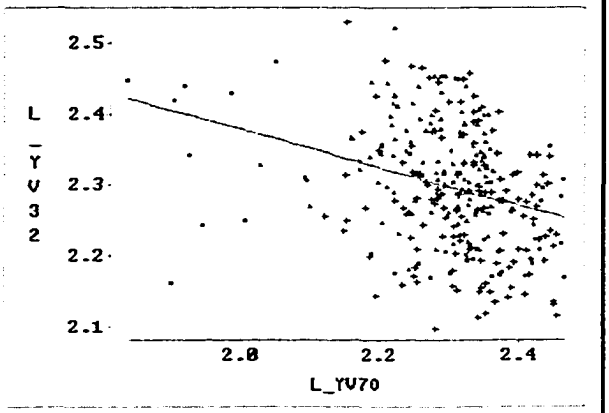

Cranial base flexion against orbital deflection

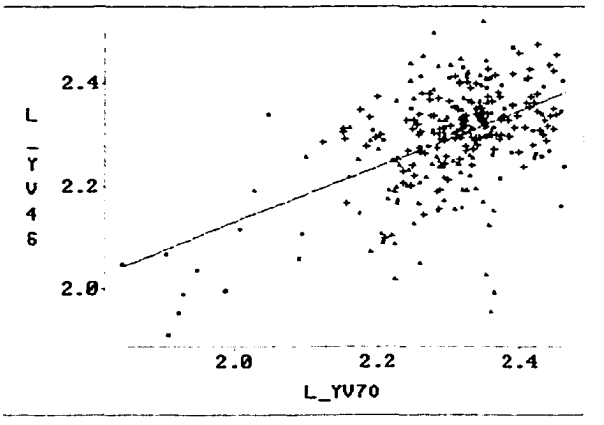

Cranial base flexion against facial rotation

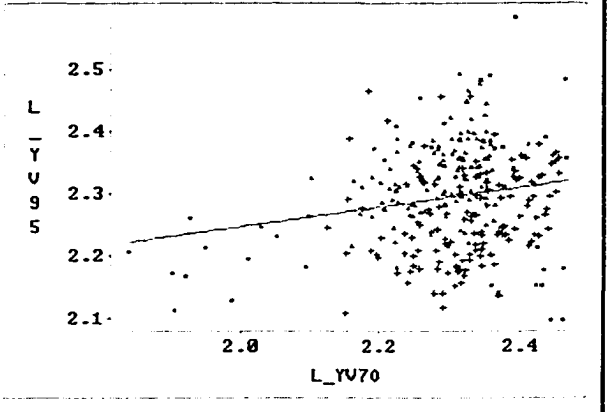

Preliminary Tests of Hypotheses

For convenience, Hypotheses A through O, in Box 13.2, were be divided into 3 groups: (1) hypotheses regarding the causal agents influencing foramen magnum position and slope; (2) hypotheses regarding the causal agents influencing cranial base flexion; and (3) hypotheses regarding the effects of cranial base flexion on nasomaxillary form.

Group 1 Hypotheses: Influences on Foramen Magnum Disposition.

(Hypotheses A, B, G, I, J & M, Box 13.2). The 'cranio-cervical' hypothesis of

Reproduced with permission of the copyright owner. Further reproduction prohibited without permission.

nasomaxillary form postulates that changes in relative brain size and/or brain shape, and locomotor behavior produce corresponding changes in the disposition of the foramen magnum. An alternative explanation, according to the 'cranial base' hypothesis, is that the position and slope of the foramen magnum are determined by cranial base anatomy—primarily by the degree of cranial base flexion.

With regard to locomotor behavior, I have already presented evidence that only bipedality has a direct effect on the position and inclination of the foramen magnum in anthropoids (see Boxes 13.7 & 13.8). The bivariate and multiple regression results reported here show that changes in relative endocranial volume effect changes in condylar index, independent of degree of cranial base flexion (in all anthropoid groups save cercopithecinae) (Box 13.23). Thus, anthropoids that exhibit relatively large brains also tend to exhibit more anteriorly located occipital condyles, independent of the degree of cranial base flexion. Likewise, anthropoids (with the possible exception of cebids and cercopithecines) that display extensive flexion of the cranial base also tend to manifest more anteriorly located occipital condyles, regardless of the relative size of the brain (Box 13.23). Relative brain size and cranial base flexion thus appear to effect the disposition of the foramen magnum independently. This finding is inconsistent with the 'cranial base' postulate that relative brain size has only an indirect effect on the foramen magnum (i.e., an effect that is strictly mediated by the cranial base).

Group 2 Hypotheses. Influences on Cranial Base Angle. *(Hypotheses C, D, E, F, H, K, & L, Box 13.2).* Biegert (1957) and DuBrul (1950) disagreed on the cause of cranial base flexion. Biegert postulated that relative brain size was the determining factor responsible for cranial base angulation (Box 13.1, path A),

Reproduced with permission of the copyright owner. Further reproduction prohibited without permission.

whereas neither Weidenreich (1941) nor DuBrul (1950) viewed relative brain size as the determining factor in the development and evolution of the cranial base or of the position of the foramen magnum, preferring instead to regard the chondrocranium as intrinsically regulated. Bolk (1915) and Björk (1972) argued that an anteriorly located and horizontally oriented spinal cord (and thus, foramen magnum) produces cranial base flexion (Box 13.1, path H), not the other way around, as asserted by Biegert (1957), DuBrul and Laskin (1961).

The crucial distinction between the 'cranial base' and 'cranio-cervical' hypotheses of nasomaxillary form is in the causal agent or agents that (purportedly) effect change in the cranial base. According to the 'cranial base' hypothesis, changes in brain size/shape and locomotor behavior effect changes to the angulation of the cranial base. Proponents of the 'cranio-cervical' hypothesis, on the other hand, view these agents as acting only indirectly on the cranial base through the mediating effects of the position and orientation of the spinal cord and vertebral column.

The results of the present analysis show little evidence to suggest that, apart from bipedality, locomotor behavior has any effect (direct, indirect or otherwise) on the angulation of the cranial base (Box 13.9). Results of the multiple regression analysis indicate that at least relative brain size has a direct effect on the cranial base, independent of the position of the foramen magnum (Box 13.24). Therefore, the 'cranio-cervical' postulate that relative brain size effects cranial base angulation only indirectly through the disposition of the spinal cord/vertebral column can be rejected. Moreover, analysis of the multi-level data further indicate that the

Reproduced with permission of the copyright owner. Further reproduction prohibited without permission.

influence of the brain on the cranial base operates via selectional rather than acclimational mechanisms.

The auxiliary hypothesis that brain shape determines cranial base angulation is not supported by the data: endocranial index is not significantly correlated with cranial base flexion. Perhaps some aspect of brain shape other than width-to-length ratio affects the cranial base.

Group 3 Hypotheses: Effects of cranial base angulation on nasomaxillary form. *(Hypothesis O, Box 13.2).* DuBrul and Laskin (1961), in agreement with Biegert (1957), hypothesized that variation in the angulation of the cranial base was responsible for numerous characteristics of the facial skeleton (Box 13.1, paths B and C). Thus, both the 'cranial base' and 'cranio-cervical' hypotheses of nasomaxillary form predict significant correlations between the degree of cranial base flexion and such characters as facial prognathism, maxillary length, and orbital deflection

Regression of nasomaxillary characters on cranial base angle showed that degree of cranial base flexion accounted for a significant proportion of the variance of nasal bone length, anterior facial length, maxillary length, facial prognathism, posterior nasal aperture breadth, upper facial breadth, occlusal slope, and orbital deflection (Box 13.15). It must be noted, however, that certain subtaxa did not always conform to the general anthropoid tendency. Cercopithecinae, for instance, did not manifest the general anthropoid tendency, exhibited in all other major groups, of a positive association between cranial base angle and both maxillary arch length and facial prognathism, (Box 13.17 & 13.18). Likewise, members of cebidae displayed no significant association between cranial base angle and orbital

Reproduced with permission of the copyright owner. Further reproduction prohibited without permission.

deflection, whereas all other major anthropoid taxa exhibited a significant positive association between these two characters (Box 13.20).

The relationship between nasomaxillary characters and properties of the cranial base has focused primarily on the degree cranial base flexion. However, the potential effects of other properties of the cranial base on nasomaxillary form should not be excluded. Three nasomaxillary variables that loaded significantly on the first two principal components of the PCA were selected as the dependent variables in a series of multiple regression models. The nasomaxillary variables were Krogman's angle of facial prognathism, maxillary arch length, and posterior nasal aperture width. In each model, condylar index, cranial base flexion, cribriform plate orientation, and relative brain size and brain shape were entered as the independent variables. In each of the three regressions relative brain size retained its significance with the dependent variable, indicating that relative brain size may be the initiating causal agent affecting craniofacial form.

When the set of independent variables were regressed on facial prognathism only relative brain size and cribriform plate orientation were significant; with maxillary arch length as the dependent variable only relative brain size and cranial base flexion retained significance; and with posterior nasal aperture breadth as the dependent variable only relative brain size and brain shape were significant. In all three models the relative position of the occipital condyles was not significant at the 0.05 level.

From these preliminary analyses it appears that relative brain size affects specific properties of nasomaxillary morphology though different cranial modalities.

Reproduced with permission of the copyright owner. Further reproduction prohibited without permission.

We shall see if this tentative hypothesis, depicted as a path diagram in Box 13.27, holds up to covariance structure analysis in Chapter 15.

Box 13.27 Heuristic path diagram of showing hypothesized relationships between selected neural, basicranial and facial properties.

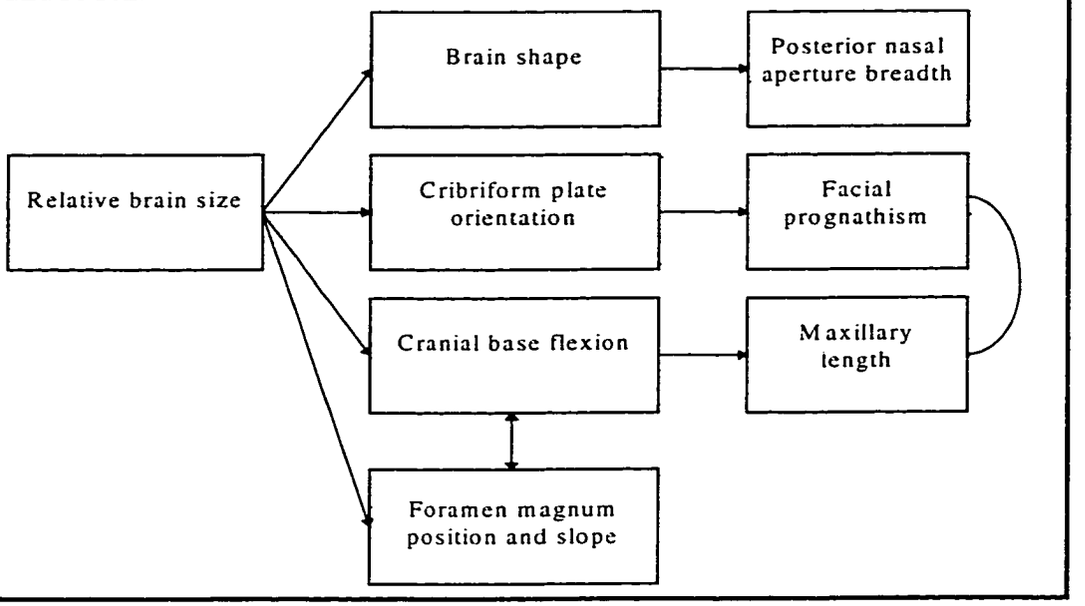

Conclusions

The main questions surrounding the debate on the effects of locomotion on craniofacial morphology in anthropoids are: whether or not locomotor or postural behavior in fact produce any effects at all on cranial morphology; and if so, what are their nature, and how are they mediated (e.g., through changes in the position and inclination of the foramen magnum, or changes in the cranial base). Few experiments have been conducted that have attempted to isolate the effects of locomotion on craniofacial morphology in mammals, but those that have been undertaken have shown that changes to locomotor and postural behavior do appear to have an effect, albeit slight, on craniofacial form (e.g., Moss, 1961; Fanghänel, 1972). Due to the problem of operationalizing and measuring locomotor and

Reproduced with permission of the copyright owner. Further reproduction prohibited without permission.

postural behavior in primates, few cross-taxonomic studies have been conducted that investigate the association between aspects of locomotion and nasomaxillary morphology. In the present investigation, no association was found between the position of the occipital condyles or the slope of the foramen magnum and any of seven locomotor variables, including quadrupedality, suspensory behavior, leaping, vertical clinging and leaping, climbing, walking, and knuckle-walking. Bipedality alone was significantly associated with an anteriorly located and horizontally oriented foramen magnum.

The disposition of the foramen magnum was further found to be associated with a suite of cranial characteristics that tend to be expressed collectively. Thus, for example, anthropoids with relatively large brains tend also to possess broad, short faces, flexed cranial bases, horizontally oriented olfactory bulbs, and anteriorly positioned occipital condyles. By contrast, anthropoids with relatively small brains tend to have narrow, long faces, extended cranial bases, vertically oriented olfactory bulbs, and posteriorly placed occipital condyles (see Box 13.14).

Results obtained in the current analysis are most consistent with the 'cranial base' hypothesis (Box 13.1), in which the development of the chondrocranium, perhaps in association with the growth of the brain, effects changes in both nasomaxillary morphology and the disposition of the foramen magnum.

Reproduced with permission of the copyright owner. Further reproduction prohibited without permission.

Chapter 14. Diet and Mastication

Introduction

In this chapter I depart from the established format of first presenting a literature review, then formulating a series of hypothesis statements which are subsequently evaluated through analyses of the empirical data. Rather, I begin by presenting an *a priori* model of dietary and masticatory effects on craniofacial form, then review some of the key studies that have contributed conceptually and empirically towards its formulation. Finally, I evaluate specific hypotheses within the context of the model against the anthropoid data through the standard process of operationalization, prediction and statistical analyses. The reasons for this departure are twofold: (1) the process by which diet and mastication affect craniofacial form is rather complex and clarification of the main features of this process early on facilitate a better understanding of the significance of the research literature, and (2) the multitude of applied methodologies and research designs in the field of craniofacial biomechanics make it difficult to follow a strictly inductive, heuristic presentation style.

The preliminary results from this chapter, which is directed toward uncovering the dietary and masticatory factors responsible for nasomaxillary variation among anthropoids, are incorporated into the covariance structural model developed and evaluated in Chapter 15.

Reproduced with permission of the copyright owner. Further reproduction prohibited without permission.

Model of Dietary and Masticatory Effects on Nasomaxillary Form

The properties of food items consumed by anthropoids and other mammals impose specific requirements on the biomechanics of the masticatory apparatus (Ahlgren 1966; Hiiemae and Crompton 1971; Luschei and Goodwin 1974; Herring, 1976; Bouvier & Hylander, 1981; Iwasaki, 1989). Biomechanical explanations of nasomaxillary form assume that skeletal morphology (as the hard tissue component of the musculoskeletal masticatory apparatus) will reflect acclimations and adaptations that establish maximum mechanical efficiency to cope with these requirements (Hylander *et al.*, 1997). It is argued here that two properties of masticatory function, in particular, play a critical role in establishing mechanical efficiency: (1) the magnitude and distribution of bite forces, and (2) tooth morphology. While the latter was not specifically incorporated into the present analysis it has been considered in the interpretation of results.

Biomechanical properties of the masticatory system can affect craniofacial form directly through the generation of external loads (bite forces) and bone deformations (strains) that stimulate osteogenic activity (acclimation via environmental stimulus; e.g., Rubin & Lanyon, 1987; Zahrowski & Turley, 1992; Lanyon, 1996), or through selection of growth processes that lead to mechanically advantageous forms (adaptation via intrinsic genetic and epigenetic stimuli; e.g., Cole, 1992). Finally, bone growth and remodeling[1] patterns can result from paracrinal signals, from muscle or endocrine cells, for example, that are affected

[1] Remodeling refers to the dynamic resorptive and depository activities of osteogenic cells over the external, internal and intracortical surfaces of a bone which operate to produce various bone properties (e.g., Haversian density) and act to shape skeletal elements (*cf.* Brullé & Hugueny, 1845; Enlow, 1975).

Reproduced with permission of the copyright owner. Further reproduction prohibited without permission.

by diet (e.g., Riesenfeld, 1975; Miller *et al.*, 1988; Heinrichs *et al.*, 1997).

Acclimation. Organisms can adapt[2] to environmental forces through acclimation (distal causal mechanism involving phenotypic adaptation through the interaction of biological role, environmental stimuli, and various proximate mechanisms; see Chapter 2). In the context of diet and mastication, osteogenic bone remodeling occurs in response to strain patterns (Box 14.1, A, path C) that result from the magnitude and distribution[3] of bite forces (path B) transmitted during mastication (Iwasaki, 1989; Daegling & Hylander, 1997). Existing bone morphology itself affects strain patterns to a large degree (path D). Changes in nasomaxillary morphology produced by the remodeling process can also influence properties of the mechanical system (path E), for example, the load-to-lever arm ratio or the orientation of the occlusal plane. In this way a positive feedback system is initiated in which changes in the mechanical system lead to changes in bite force patterns (path F), which, as previously described, lead to modifications in the pattern of craniofacial strain (path B) and further bone remodeling (path C). Alterations of masticatory muscle recruitment and use can also affect myological properties of the mechanical system directly (path I). It is important to recognize that all of these changes are initiated by a dietary shift which requires modification to existing masticatory behavior and mechanical properties to cope with the new dietary regime.

---

[2] The term 'adapt' is used here in the broader sense, introduced in Chapter 2, meaning any phenotypic modification initiated through operation of environmental forces and which enhances an organism's survival or reproduction.

[3] This includes both temporal and spatial distribution.

Reproduced with permission of the copyright owner. Further reproduction prohibited without permission.

Adaptation. Nasomaxillary morphology can also change (adapt) through selection of individuals with craniofacial growth patterns that yield mechanically advantageous properties in the context of shifting dietary regimes. Selection will primarily act on two properties: the magnitude and distribution of applied bite force (Box 14.1, B, path 1) and dental morphology (path 2). These two properties work in conjunction to ensure efficient procurement and processing of food items. Any phenotypes that contribute to these primary ones will be concurrently selected. These include: the soft tissue properties of the masticatory apparatus that affect bite force and distribution (such as masticatory muscle mass and attachment sites) (path 3) and properties of the nasomaxillary skeleton that affect mechanical properties (such the load-to-lever arm ratio or the orientation of the occlusal plane) (path 4).

Reproduced with permission of the copyright owner. Further reproduction prohibited without permission.

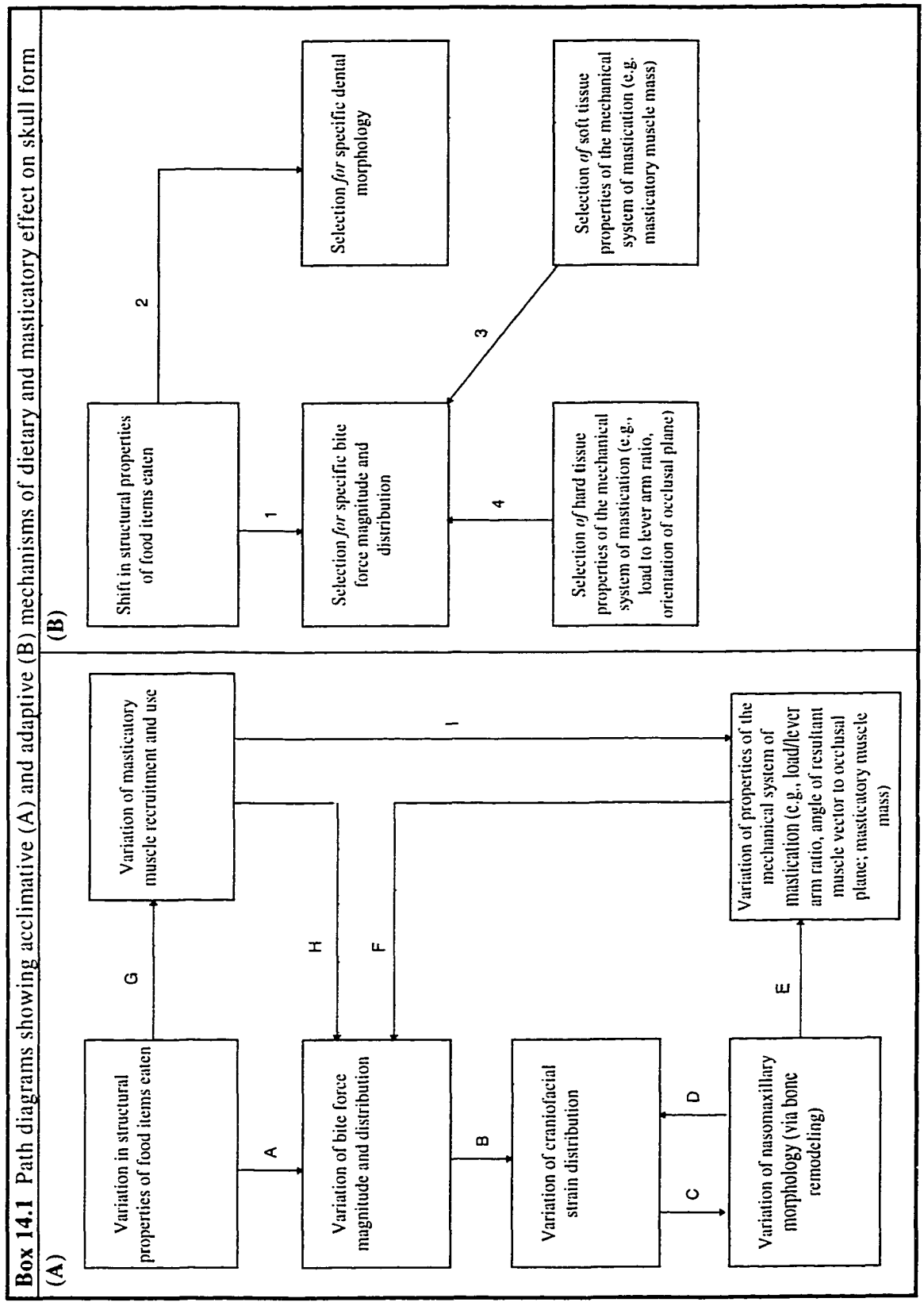

Reproduced with permission of the copyright owner. Further reproduction prohibited without permission.

Literature Review

A considerable literature has accumulated on the ecological and biological roles of diet and mastication in the production of nasomaxillary variation. Given the complexity of the problem, investigators have had to be remarkably versatile in probing for answers, often using a variety of techniques and approaches. To facilitate the review of this literature I have developed a classification of standard research methods designed to correspond to the functional models depicted in Box 14.1. The classification, which is presented in Box 14.2, is constructed around two research modes (A, nonexperimental; and, B, experimental) and four main approaches (I, analysis of dietary effects; II, analysis of occlusal forces; III, analysis of strain patterns; and, IV, analysis of mechanical properties). Each approach focuses on a different node, or series of nodes, in the networks of causal pathways depicted in the masticatory models (Box 14.1).

Reproduced with permission of the copyright owner. Further reproduction prohibited without permission.

Box 14.2. Classification of standard research methods in craniofacial masticatory mechanics and ecomorphology. Modes: A, nonexperimental; B, experimental.

Method	Description	Examples
IA	Examination of observed covariance between diet and craniofacial morphology	Jolly, 1970; Kinzey, 1974; DuBrul, 1977; Roberts & Tattersall, 1977; Shea, 1983; Sakka, 1984
IB	Examination of covariance between experimentally controlled diet and craniofacial morphology.	Watt & Williams, 1951; Moore, 1965; Bouvier & Hylander, 1981; Beecher & Corruccini, 1981; Corruccini & Beecher, 1982; Beecher *et al*, 1983; Kiliaridis, 1986; Bouvier & Zimny, 1987; Ingervall & Bitsanis, 1987; Iwasaki, 1989; Katsaros *et al*., 1994; Chuang, 1995; Yamamoto, 1996; Kiliaridis *et al*., 1996
IIA	Examination of observed covariance between patterns of occlusal force and facial morphology	Preushoft et al, 1986; Demes, 1987; Demes & Creel, 1988; Kiliaridis *et al*., 1993; Ciochon *et al*., 1997
IIB	Examination of covariance between experimentally controlled patterns of occlusal force and facial morphology	Adams *et al*, 1972; Jackson *et al*., 1979; Saijo & Sugimura, 1993
IIIA	Examination of covariance between masticatory strain patterns inferred from engineering principles and craniofacial morphology.	Gorke, 1904; Barth, 1919; Richter, 1920; Bluntschli, 1926; Sicher & Tandler, 1928; Couly, 1976; Roberts & Tattersall, 1974; Sicher & DuBrul, 1975; Thomason & Russell, 1986; Vinyard & Ravosa, 1998
IIIB	Examination of covariance between experimentally controlled masticatory strain patterns and craniofacial morphology	Endo, 1965, 1966, 1973; Hylander, 1979; Buckland-Wright 1978; Kakudo & Amano 1968; Iwasaki, 1989; Oyen & Tsay, 1991; Herring & Mucci, 1991
IVA	Examination of covariance between observed properties of the mechanical system of mastication and craniofacial morphology	Demes & Creel, 1988; van Spronsen *et al*., 1991; Ruf *et al*., 1994; Raadsheer *et al*., 1996
IVB	Examination of covariance between experimentally altered properties of the mechanical system of mastication and craniofacial morphology	Pratt, 1943; Washburn, 1947; Avis, 1959, 1961; Boyd *et al*, 1967; Moss & Meehan, 1970; Moore, 1973; Madeira *et al*., 1976; Hall, 1978; Schumacher *et al*, 1979; Muller & Punt-van Manen, 1982; Hohl, 1983; Carlson & Schneiderman, 1983Vilmann *et al*, 1985; Teixeira *et al*., 1990

Reproduced with permission of the copyright owner. Further reproduction prohibited without permission.

Methods IA and IB. Studies using Method IA attempt to find a correspondence between interspecific dietary variation and variation of craniofacial form. Typically, these studies make no distinction between acclimational and adaptational processes, and assume that both are in operation. This approach focuses on the presumed causal relationship between the properties of food items consumed and craniofacial morphology, bypassing all intermediate steps (see Box 14.1). Such analyses may be likened to studies that search for a correlation between the incidence of smoking and the rate of lung cancer. In both cases a *possible* causal relationship can be established, but in neither case is any light shed on the fundamental mechanisms underlying the relationship.

The first systematic Method IA studies on primates compared tough or hard object food eaters with other less specialized dietary preferences. Investigators found that a diet of hard object foods was associated with relative orthognathy, pronounced facial height and bizygomatic breadth, and reduced anterior dentition (e.g. Jolly, 1970; Kinzey, 1974; DuBrul, 1977; Roberts & Tattersall, 1977; Sakka, 1984). But a number of subsequent Method IA studies have found no correspondence between dietary diversity and craniofacial form (e.g., Smith & Redford, 1990; Janis, 1990). Shea (1983), for instance, compared African ape craniofacial forms and found no correspondence between nasomaxillary features (such as palate length, facial height, and bimaxillary breadth) and dietary specializations for frugivory (*Pan troglodytes*) or folivory (*Gorilla gorilla*). Shea attributes these apparent contradictory findings in the research literature to the different effects produced by the various properties of food items. For example, the properties of food items eaten by gorillas and chimpanzees may differ in ways that

Reproduced with permission of the copyright owner. Further reproduction prohibited without permission.

require different tooth morphologies in the two genera, but not necessarily a reorganization of the masticatory-craniofacial complex. Reorganization of this type may be associated with dietary changes involving the consistency or hardness of the food items consumed (Shea, 1983).

Studies utilizing Method IB seek to find a correspondence between experimentally varied diet and variation in craniofacial form. Typically, two or more groups of the same homogeneous species are fed different diets during part of their growth period and their resulting morphologies are compared. This technique differs from the first in that any observed differences in craniofacial form among groups are attributed solely to acclimational processes.

In all of the Method IB studies reviewed here animals fed a "soft diet" exhibited a reduction of maxillary breadth and a high arched palate compared to controls or animals fed a "hard diet" (e.g., Watt & Williams, 1951; Beecher & Corruccini, 1981; Yamamoto, 1996: rats; Beecher *et al.*, 1983: squirrel monkeys). In a review article summarizing this evidence, Herring (1993) stated that "...reduction in muscle forces, whether due to defects in the muscles or to reduced use, has a consistent effect on skull morphology. The bones are little reduced in length, but they are slender and the viscerocranium as a whole is narrower than normal" (p. 184). While her assessment is accurate with regard to bone thickness and facial breadth, the effects of diet on facial length cannot be so easily dismissed. Kiliaridis (1986) reported that rats fed a soft diet exhibited a more "orthocranial" facial morphology, and Corruccini and Beecher (1982) observed that squirrel monkeys fed a soft diet exhibited a reduced maxillary length compared to a hard diet control group. But Chuang (1995), in a similar experiment with lagomorphs,

Reproduced with permission of the copyright owner. Further reproduction prohibited without permission.

found that "...a more anterior superior growth rotation of the upper jaw occurred in the rabbits fed with soft diet" (p. 458). Chuang's results are more consistent with that of Katsaros *et al.* (1994), who found histological evidence of increased apposition in the anterior facial sutures of rats fed a soft dietary regime.[4] And in a recent study of Yucatan minipigs, Ciochon *et al.* (1997) reported that animals fed a soft diet exhibit increased facial prognathism as well as maxillary arch narrowing, compared to controls.

Methods IIA and IIB. Studies characterized by Method II attempt to find a correspondence between bite force patterns and craniofacial form. This method concentrates on the presumed causal relationship between bite force magnitude and distribution on the one hand and craniofacial variation on the other (see Box 14.1, A, B).

The crucial role of bite force patterns in eliciting a remodeling response in the facial skeleton has been well documented empirically (see Ringqvist, 1973). The observed functional connection between bite force and skeletogenesis has lead most workers to the conclusion that "...there exists a direct relationship between the structure of the oro-facial skeleton and the... resultant (bite) forces produced at the teeth during mastication" (Roberts and Tattersall, 1974:2).

Demes and Creel (1988) observed that most interspecific variation in bite force results primarily from differences in masticatory muscle mass, with only a small portion of the variation due to differences in the mechanical efficiency of the

---

[4] While "wide facial sutures" and sutural apposition was found to occur by Droschl (1975) during *backwards* rotation of the nasomaxilla with artificially applied retrusive force, this growth condition does not occur during normal growth. Sutural apposition during normal facial growth coincides with displacement of the conjoining bones due to remodeling patterns during growth (Enlow, 1990). Therefore, maxillary sutural apposition is consistent with a model of facial growth elongation.

Reproduced with permission of the copyright owner. Further reproduction prohibited without permission.

masticatory apparatus.[5] High masseter lever efficiency, however, has been associated with increased facial height, and a more anterior position of both the masseter origin and zygomatic root (Rak 1983; Smith 1986). Demes and Creel also demonstrated that facial orthognathism is associated with a bite force distribution in which "...incisor bite force relative to molar bite force is high" (p. 667). This finding is consistent with the results of Kiliaridis *et al.* (1993), who documented a correspondence between a high incisal bite force and a relatively short anterior face in a group of human subjects.

Preushoft *et al.* (1986) tested the hypothesis that the coronal cross-sectional area of the maxillary bone will increase posteriorly, following the same curve as the maximal bite forces along the tooth row. In each of several primate species, these authors found "...a fair coincidence between the pattern of shearing forces and the arrangement of bone material, or shape-dictated strength properties of the upper jaw" (p. 259).

van der Klaauw (1946:18) suggested that facial prognathism in mammals is associated with "...strong development of the jaws," presumably due to high masticatory forces. In support of this view, Dechow and Carlson (1990) found that in macaques "facial length" increased isometrically with bite force. They argued that as adult male faces become more prognathic, muscle attachments migrate anteriorly maintaining a relatively constant lever arm ratio; and further, that "...masticatory muscle growth occurs in such a way as to maintain maximal bite forces that are proportional to a given facial size" (Dechow & Carlson, 1990:230).

---

[5] A similar conclusion was reached by Sasaki *et al.* (1989) in a study of the relationships between properties of the masticatory system and bite force in a group of human subjects.

Reproduced with permission of the copyright owner. Further reproduction prohibited without permission.

Methods IIIA and IIIB. Studies using Method III attempt to find a correspondence between patterns of bone strain and craniofacial form (Weijs, 1980). This type of analysis focuses on the presumed causal relationship between bone strain, osteogenic activity and craniofacial morphology (Box 14.1, A, path C). Typically, Method IIIA analyses employ engineering principles to work backwards, inferring strain patterns and bite forces from observed skeletal morphology. Craniofacial form is then explained in terms of a structural solution (i.e., adaptation) to a given strain pattern.

The German morphologists Görke (1904) and Richter (1920) were among the first to propose that the craniofacial skeleton served as a structural framework to absorb masticatory forces. These and subsequent authors (e.g., Roberts & Tattersall, 1974) have advanced various models of facial biomechanics with proposed medial and bilateral paths of stress dissipation leading from the maxillary occlusal surface towards the calvaria. A more modern example is provided by Demes (1987). Using the concept known as St. Venant's principle, which states that bending strains become small when the length of a beam is small in comparison to its depth, she surmised that a convex facial profile (e.g., Neanderthals) is an adaptation to resist high bending strains caused by great anterior bite forces (see her diagram, p.301).

Endo (1965, 1966) concluded that "theoretical deductions" of this type were of little use, and decided that an experimental analysis of strain (Method IIIB) would yield more reliable results. He attached electric strain gauges to dry gorilla and human skulls and measured the direction and magnitude of deformation of the facial skeleton during simulated biting. Endo (1966, 1973) found a more complex

Reproduced with permission of the copyright owner. Further reproduction prohibited without permission.

pattern of stress dissipation in the splanchnocranium than had been predicted by the engineering models. First, the *magnitude* of strain changed dramatically in relation to the placement of the bite point along the tooth row. Higher overall magnitudes of strain were recorded for anterior compared with posterior tooth biting. The *patterns* of strain also changed with bite point location. During anterior biting the highest magnitudes of strain were located directly under the bite point, along the lateral nasal margins, below the infraorbital margins and across the inferior aspect of the zygomatics. When the bite point was shifted to the first molar, the greatest magnitudes of strain occurred on the alveolar process above the bite point, and along the inferior margin of the zygomatic root on the ipsilateral side.

Extreme caution must be taken when interpreting patterns of strain in relation to masticatory function. Bone strain is proportional to transmitted bite force (Box 14.1, A, path B) and inversely proportional to bone volume or thickness (path D). Bone strain thus derives as the ratio of transmitted force over bone thickness.

$$\text{bone stain} = \text{applied force}/\text{bone thickness} \qquad (14.1)$$

While this formulation is an oversimplification, it nonetheless underscores the role of strain in the development of skeletal form. As a structural material, bone fails when strain becomes excessive. Strain must therefore be kept under a critical maximum for the organism to function (physiologically) and survive. It can be seen with reference to Equation 14.1 that if a change in diet leads to an increase in bite force, strain will increase proportionally. Increased bone strain induces osteogenic activity leading to greater bone thickness, which in turn brings the strain back to its previously safe levels (acclimation). Or, those individuals with variant growth

Reproduced with permission of the copyright owner. Further reproduction prohibited without permission.

patterns that yield thicker bones will be at a selective advantage and propagate that trait (adaptation). This process of maintaining an equilibrium of strain magnitudes in bone is referred to as the "functional equivalence" hypothesis of bone morphology (Rubin & Lanyon, 1985; Biewener *et al.*, 1986).[6] The hypothesis states that "[m]echanically adaptive bone modeling and remodeling can be regarded as a homeostatic mechanism regulating functional bone strains at each location throughout the skeleton" (Lanyon, 1996:37S). With respect to mastication, "...this hypothesis predicts that during chewing and biting there should be relatively high and near uniform amounts of strain throughout the facial skeleton" (Hylander & Johnson, 1997:203), a prediction confirmed in several experimental studies (e.g., Saijo & Sugimura, 1993).

How, then, are we to interpret the heterogeneous strain patterns observed in the facial skeleton by Endo and others (e.g., Bouvier & Hylander, 1981, 1996; Hylander *et al.*, 1991; Rubin & Lanyon, 1985, 1987)? Hylander and Johnson (1997) argue that facial morphology represents a compromise solution to several competing biological requirements and thus "...it is unlikely that all facial bones are especially designed so as to minimize bone tissue and maximize strength for countering masticatory loads" (p. 203). Another possibility is that ultrastructural properties of bone (e.g., collagen fiber orientation) work together with macrostructural properties (e.g., gross morphology) in localized areas to optimally dissipate patterns of induced strain (*cf.* Bromage, 1992; Rubin *et al.*, 1994; McMahon *et al.*, 1995)

---

[6] For a good example of functional equivalence with regard to the morphology of the mandibular symphysis see Vinyard & Ravosa, 1998.

Reproduced with permission of the copyright owner. Further reproduction prohibited without permission.

It follows that variation of strain patterns alone tells us little about the relationship between nasomaxillary form and dietary or masticatory differences among individuals or among species. Interindividual differences in bone deformation might be due to different bite force patterns applied to similar morphologies, or alternatively, to different morphologies subjected to similar bite force patterns. Even with a constant bite force, individuals with seemingly very different facial forms can display quite similar patterns of strain, as found by Endo (1966, 1973) for humans and gorillas. In this case, the orthognathic but slightly built human face appears to be mechanically equivalent to the more prognathic but robustly built gorilla face in coping with experimentally induced occlusal forces. This outcome is in fact predicted by the functional equivalence hypothesis in conjunction with the positive feedback mechanism depicted in Box 14.1, A, paths C & D, in which strain is maintained below a critical level. Nor is the absence or diminished magnitude of bone strain an indication of weak masticatory stress. A strongly build skeletal element may be dissipating a great deal of masticatory induced stress, but because of its robust construction may not exhibit a correspondingly high level of strain (as an example, see the discussion of circumorbital morphology, stress and strain patterns in Picq & Hylander, 1989).

Methods IVA and IVB. Studies employing Method IV seek to correlate properties of the mechanical system with properties of craniofacial morphology (Weijs, 1980). This method attends to the presumed causal relationship between properties of the mechanical system of mastication and craniofacial morphology (Box 14.1, A, paths F, B & C; B, paths 3 & 4).

Reproduced with permission of the copyright owner. Further reproduction prohibited without permission.

Three of the most important biomechanical properties of the masticatory system include: (1) the magnitude and direction of forces exerted by the muscles of mastication (primarily the temporalis and masseter/lateral pterygoid mm.), (2) the angle between the resultant muscle vector and the occlusal plane, and (3) the load-to-lever arm ratio, or mechanical efficiency of the resultant muscle vector.

Comparative studies (Method IVA), which have focused mainly on modern humans, typically explore how differences in craniofacial morphology affect the mechanical efficiency of the masticatory apparatus, or how differences in some properties of the mechanical system (e.g., muscle mass) correspond to differences in facial morphology. For example, van Spronsen *et al.* (1991) analyzed serial MRI scans of 21 human skulls and found a positive correlation between masticatory muscle mass and facial breadth, but no association between muscle mass and either anterior facial length or posterior facial height. Raadsheer *et al.* (1996), however, examined various cephalometric and masticatory properties of 329 modern human subjects and found that masseter muscle mass was negatively correlated with anterior facial length and maxillary arch length. While these findings lead to the conclusion that masticatory function plays a role in the development of craniofacial form, one must also entertain the possibility that the correlations are spurious due to the association of both masticatory muscle mass and cranial morphology with overall body size (Cachel, 1984; this study, Chapter 10).

In an inter-deme study, Hylander (1977) found that Eskimos, who have anteriorly positioned temporalis and masseter muscles, are relatively orthognathic, and consequently "...compared to other human populations, the Eskimo masticatory apparatus is mechanically more efficient in generating vertical occlusal forces" (p.

Reproduced with permission of the copyright owner. Further reproduction prohibited without permission.

149). Hylander argued that this craniofacial form was an "...adaptation to reduce the bending moments acting on the facial skeleton in order to more effectively dissipate excessively large biting forces in the anterior region of the skull" (p. 147). But an alternative explanation is that facial orthognathy in Eskimos is an adaptation to increase the load-to-lever arm ratio thus *allowing* a greater bite force required of their diet (Waugh, 1937; Collins, 1951; Shea, 1983).

Most experimental Method IV studies involve analyses of the morphological consequences induced by altering the muscles of mastication. For example, complete removal of the masseter muscles in rats (Pratt, 1943; Avis 1961; Moore, 1967, 1973), dogs, and sheep (Schumacher *et al.*, 1979) result in a reduction of bone at the mandibular angle and the condylar processes, but had little effect on nasomaxillary morphology. Removal or transection of the temporalis mm. in the rat (Washburn, 1947; Moss & Meehan, 1970), cat (Avis, 1959), dog, and sheep (Schumacher *et al.*, 1979) caused a reduction of the coronoid process and loss of the temporal ridges, but again, appeared to have had little or no effect on nasomaxillary form (*cf.* Boyd *et al*, 1967). Perhaps, as Guelinckx *et al.* (1986) have suggested, when one muscle group is inoperative the others compensate, thus maintaining overall strain patterns. Carlson and Schneiderman (1983), however, found that detachment of the masseter muscles in a young adult rhesus monkey produced significantly less anterior displacement of the maxilla compared to controls. These results are not necessarily contradictory. Because the masseter muscle attachments are located further forward on the cranium compared to the temporalis muscle attachments, removal of the latter would not be expected to affect the anterior limit of the maximum resultant vector (MRV). By contrast,

Reproduced with permission of the copyright owner. Further reproduction prohibited without permission.

removal of the masseter muscles would shift the MRV backward forcing a "less anterior displacement of the maxilla" in order to maintain the various relationships of the mechanical system (see Greaves, 1978; this Chapter).

In cases in which both major muscle groups are affects, such as in humans with myotonic muscular dystrophy (Müller & Punt-van Manen, 1982) and dystrophic mice (Vilmann et al., 1985), a narrower-than-normal maxilla and deep arched palate has been observed. Hohl (1983) transposed both the temporalis and masseter muscles in *Macaca nemestrina* to a more anterior location and observed a redirected cranial growth pattern that reoriented the face upward and outward relative to the braincase. This observation is also consistent with Greaves' triangle of support model, which will be introduced in a subsequent section.

Summary. Since an organism must be able to process preferred or available food items to survive, its dental morphology, mechanical properties of mastication and bite force patterns are dictated by the structural properties of its food. During mastication bone strain must be kept below a certain level to avoid critical bone failure. Facial skeletal morphology will thus reflect a compromise between these two, sometimes competing, requirements. In the face of a shifting diet it is predicted that nasomaxillary morphology will change in order to (1) alter the properties of the mechanical system thereby producing optimal bite force magnitudes and patterns appropriate to the new diet, and (2) modify the morphology of the facial skeleton to maintain bone strain magnitudes under the critical maximum.

Reproduced with permission of the copyright owner. Further reproduction prohibited without permission.

Hypotheses Formulation

Hypotheses regarding the role of diet and mastication in the development and evolution of craniofacial form are summarized in Box 14.3. While all of the hypotheses listed are consistent with the general model of masticatory effects depicted in Box 14.1, the specific relationships hypothesized are in some cases contradictory.

Box 14.3. Hypotheses statements regarding the effects of mastication properties on craniofacial variation.

Description of Hypothesis:	Source:
(A) Diet of hard food items requires large bite force magnitudes (and concomitantly large masticatory muscles) for food tritiation.	Kinzey, 1974
(B) Pronounced bizygomatic breadth due to large temporalis muscles associated with high bite force magnitudes.	Jolly, 1970
(C) Reduction of masticatory muscle mass and a soft food diet result in a reduction of maxillary breadth	Watt & Williams, 1951; van Spronsen *et al.*, 1991; Muller & Punt-van Manen, 1982; Vilmann *et al.*, 1985
(D) Facial orthognathism and reduced facial length is an adaptation to increase bite force magnitudes, especially at the anterior dentition.	Jolly, 1970; Hylander, 1977
(E) Facial orthognathism and reduced facial length is associated with decreased masticatory muscle mass.	Carlson & Schneiderman, 1983; Raadsheer *et al.*, 1996
(F) Facial orthognathism and reduced facial length is an adaptation to a hard food diet	Chuang, 1995; Ciochon *et al.*, 1997
(G) Facial morphology is not affected by changes to masticatory muscle mass	Washburn, 1947; van Spronsen *et al.*, 1991;
(H) Pronounced facial height is an adaptation to increase the mechanical efficiency of the masticatory lever system.	Rak, 1983
(I) No difference in masticatory properties between frugivores and folivores	Shea, 1983
(J) Anteriorly placed zygomatic root position caused by the anterior placement of the masseter mm resulting in increased mechanical efficiency	Smith, 1986
(K) Anteriorly placed temporalis and masseter muscle attachments an adaptation to produce large anterior bite force magnitudes	Hylander, 1977
(L) Anterior migration of masticatory muscle attachments result in increased facial prognathism and length	Hohl, 1983
(M) Palatal depth increases in response to a soft food diet	Watt & Williams, 1951

Reproduced with permission of the copyright owner. Further reproduction prohibited without permission.

Box 14.3. Hypotheses statements regarding the effects of mastication properties on craniofacial variation.	
Description of Hypothesis:	Source:
(N) Pronounces facial height is an adaptation to increase the mechanical efficiency of the masticatory lever system	Rak, 1983
(O) Facial convexity is an adaptation to dissipate high anterior bite force magnitudes.	Deme, 1987
(P) Palatal depth increases in response to reduced masticatory muscle force	Muller & Punt-van Manen, 1982; Vilmann *et al.*, 1985
(Q) Bite force magnitudes are isometric with facial size. This condition is brought about by an isometric relationship between masticatory muscle mass and facial size, and an anterior migration of the muscle attachment sites with increased facial length.	Dechow & Carlson, 1990

Consider, for example, the following hypotheses from Box 14.3. Hypothesis F: facial orthognathism is an adaptation to a hard food diet; Hypothesis A: a hard food diet requires a large masticatory muscle mass; Hypothesis E: an increase in masticatory muscle mass results in facial *prognathism*.

Operationalization of Variables

Many of the variables relevant to the hypotheses listed in Box 14.3 have been defined in previous chapters. The path models contained in Box 14.1 provide a good overview of the masticatory variables that require operationalization, within their theoretical context. Several of the variables contained in these models cannot be included in the present investigation due to limitations of cost, time, or to the research design itself. For example, measurement of bone strain has not been undertaken, nor has quantification of masticatory muscle recruitment during chewing in living animals. Likewise, variation in the properties of food items eaten can only be inferred from information on the behavioral ecology of anthropoid species, with all the attendant problems of meta-analysis. What remains are the properties of the mechanical system, inferred bite force patterns, and nasomaxillary

Reproduced with permission of the copyright owner. Further reproduction prohibited without permission.

morphology. While the present analysis therefore falls short of being comprehensive, it nonetheless encompasses Methods IA, IIA and IVA, and is thus broader in scope than most previous nonexperimental studies.

Properties of food items eaten

Ten variables were operationalized to measure dietary differences among anthropoid species. These variables fall into three categories. (1) Each species in the sample was assigned a "hardness index" value based on the estimated average hardness of the food items consumed in its diet [YM92-HDDIET]. (2) Each species was assigned to one of nine dietary categories based on the percentages of major food types consumed [YM93-CTDIET]. (3) The estimated percentages of 8 major food types consumed by each species were obtained from the literature and recorded [DVERT, DINSEC, DFRUIT, DSEED, DBUD, DLEAF, DROOT, DGUM].

Dietary Categories. Kay (1984) cautioned that dietary categories are rather arbitrary constructs with no consensus among either behavioralists or anatomists, and further advised that each study should tailor its dietary categories to suite its own research goals (also see Rosenberger, 1992). Taking heed of this advice, nine dietary categories were defined as follows: (1) Hard food specialist (HF): species whose diet is derive from mostly hard food items such as seeds, nuts, and roots. (2) Leaf eater with fruit supplement (LF): species whose diet consists of at least 60% leaf products and at least 10% fruit. (3) Folivore (FV): diet consisting of at least 60% leaf products and less than 10% of any other category. (4) Frugivore (FR): species whose diet consists of at least 60% fruit and less than 15% of any other category. (5) Fruit omnivore (FO): species that consume mostly fruit, but also consumes food items from at least 4 other categories. (6) Fruit eater with insect

Reproduced with permission of the copyright owner. Further reproduction prohibited without permission.

supplement (FB): species whose diet consists of at least 60% fruit and at least 25% insects. (7) Omnivore (O): species that consume food items from at least 6 of the 8 categories with no one category providing more than 40% of the diet. (8) Insectivore (IN): species whose diet consists of at least 50% insects. (9) Gumnivore (GM): species whose diet consists of at least 50% gums. The dietary percentage data and dietary category assignments are given in Box 14.4.

Percentages of food types eaten. The proportion of 8 classes of food items in the diet of each of the 37 anthropoid species was estimated from data reported in the primate behavior ecology literature (see references in Box 14.4). The 8 food classes included: (A) vertebrate animals [DVERT], (B) invertebrate animals [DINSEC], (C) fruit [DFRUIT], (D) seeds and nuts [DSEED], (E) buds, flowers and young leaves [DBUD], (F) mature leaves [DLEAF], (G) roots and tubers [DROOT], and (H) gums [DGUM] (see Box 14.4).

Hardness index. To assess the impact of the structural properties of food items on masticatory and morphological attributes a dietary hardness variable was constructed. Each of the food classes was assigned a hardness value based on a 5 scale ordinal classification as follows: (1) soft: fruits, buds, flowers and young leaves; (2) medium soft: invertebrates; (3) medium: gums; (4) medium hard: vertebrates and mature leaves, (5) hard: roots, tubers, seeds and nuts. A dietary hardness value was computed for each species by taking the sum of the hardness values of the food items consumed weighted by the percentages of each food class in the diet. The results are given in Box 14.4.

Reproduced with permission of the copyright owner. Further reproduction prohibited without permission.

Box 14.4. Dietary properties for anthropoid sample. (A) vertebrate animals, (B) invertebrate animals, (C) fruit, (D) seeds and nuts, (E) buds, flowers and young leaves, (F) mature leaves, (G) roots and tubers, and (H) gums. Cat, dietary categories; HI, Hardness index

Species	(A)	(B)	(C)	(D)	(E)	(F)	(G)	(H)	Cat	HI	References:
A. palliata	.00	.00	.12	.00	.64	.19	.00	.05	LF	153	1, 2, 3, 4
A. geoffroyi	.02	.00	.71	.10	.15	.02	.00	.00	FR	205	4, 5
L. lagothrica	.00	.00	.68	.07	.03	.15	.00	.06	FR	222	1, 6
B. arachnoides	.00	.00	.32	.08	.09	.51	.00	.00	LF	228	1, 4, 7
C. satanas	.00	.00	.20	.75	.03	.00	.00	.01	HF	309	8, 9
P. pithecia	.02	.00	.59	.33	.06	.00	.00	.00	FO	247	10, 11
P. monachus	.00	.00	.55	.38	.03	.04	.00	.00	FO	256	1
C. cupreus	.00	.00	.20	.00	.40	.40	.00	.00	LF	180	12
C. apella	.07	.05	.50	.30	.05	.05	.00	.00	FO	260	13
C. capucinus	.04	.20	.65	.03	.02	.05	.00	.01	FB	214	1, 14
S. sciureus	.00	.31	.65	.03	.00	.04	.00	.00	FB	212	15
A. trivirgatus	.00	.10	.60	.00	.15	.15	.00	.00	FR	192	1
S. oedipus	.10	.50	.27	.02	.00	.00	.00	.10	IN	236	16
C. pygmaea	.00	.17	.16	.01	.00	.00	.00	.67	GM	304	17, 18
C. geoldii	.34	.00	.33	.00	.00	.00	.00	.33	--	317	19
C. aethiops	.04	.02	.32	.32	.15	.15	.00	.00	O	248	1, 20
C. neglectus	.00	.10	.41	.37	.03	.09	.00	.00	FO	257	21
C. mitis	.03	.14	.55	.07	.00	.19	.00	.02	FO	229	22, 23
C. ascanius	.10	.18	.62	.00	.00	.07	.00	.03	FB	228	1, 21
M. nemestrina	.12	.00	.48	.30	.04	.06	.00	.03	FO	278	1, 24
M. fascicularis	.09	.00	.64	.09	.09	.09	.00	.00	FR	227	1
M. mulatta	.00	.05	.60	.03	.25	.03	.00	.04	FO	187	1, 25
P. hamadryas	.05	.00	.25	.25	.05	.05	.35	.00	HF	350	1, 20,
L. albigena	.11	.15	.66	.00	.03	.05	.00	.00	FB	221	1, 26
C. guereza	.00	.00	.25	.00	.25	.50	.00	.00	LF	200	27, 28
P. badius	.00	.00	.00	.00	.33	.67	.00	.00	FV	200	28
N. larvatus	.02	.00	.30	.20	.03	.46	.00	.00	LF	256	1, 29
P. melalophos	.00	.00	.25	.17	.50	.08	.00	.00	LF	179	30
S. entellus	.03	.00	.24	.00	.25	.38	.00	.10	LF	215	31
S. cristata	.00	.00	.10	.00	.10	.80	.00	.10	FV	265	1
H. lar	.00	.13	.50	.00	.18	.19	.00	.00	FO	191	1, 32
H. syndactylus	.03	.00	.31	.00	.30	.36	.00	.00	LF	194	33
P. pygmeaus	.15	.00	.60	.00	.25	.25	.00	.00	FO	267	1
G. gorilla	.03	.00	.57	.00	.10	.10	.17	.03	FO	256	1, 34
H. sapiens	.40	.00	.15	.25	.20	.00	.00	.00	O	297	35
P. paniscus	.05	.00	.80	.00	.05	.05	.05	.00	FR	222	1
P. troglodytes	.03	.03	.58	.05	.08	.23	.00	.00	FO	217	34, 36

1, Rowe, 1996; **2**, Estrada, 1984; **3**, Neville *et al.*, 1988; **4**, Strier, 1992; **5**, Chapman, 1987; **6**, Peres, 1994; **7**, Nishimura; **8**, Kinzey, 1992; **9**, van Roosmalen *et al.*, 1981; **10**, Buchanan *et al.*, 1981; **11**, Kinzey & Norconk, 1993; **12**, Robinson et al., 1987; **13**, Eisenberg, 1989; **14**, Freese *et al.*, 1981; **15**, Baldwin & Baldwin, 1981; **16**, Hershkovitz, 1977; **17**, Soini, 1993; **18**, Harrison & Tardif, 1988; **19**, Pook & Pook, 1981; **20**, Happel, 1988; **21**, Gautier-Hion, 1988; **22**, Cords, 1987; **23**, Lawes *et al.*, 1990; **24**, Caldecott, 1986; **25**, Richard, 1989; **26**, Butynski, 1990; **27**, Struhsaker & Oates, 1975; **28**, Clutton-Brock, 1975; **29**, Yeager, 1989; **30**, Davies *et al.*, 1988; **31**, Bennett & Davies, 1994; **32**, Raemaekers, 1979; **33**, Curtin & Chivers, 1978; **34**, Tutin *et al.*, 1991; **35**, Southgate, 1991; **36**, Goodall, 1996

Reproduced with permission of the copyright owner. Further reproduction prohibited without permission.

Bite force magnitude and distribution: Greaves' triangle of support model

According to Demes and Creel (1988:657), "Bite force is one of the most important variables governing the efficiency of the masticatory apparatus." Since the mechanical properties of the masticatory system determine the bite force patterns produced during mastication, knowledge of the mechanical properties of mastication allows one to estimate the maximum bite forces (MBF) generated along the tooth row. Maximum bite forces were calculated for each tooth along the upper right quadrant of the dental arch for each of the 300 specimens in the anthropoid sample using Greaves' (1978) three-dimensional "triangle of support" model of masticatory function. Greaves modeled the working mandible as a plate having three points of contact with the cranium—the left and right temporomandibular joints (TMJs) and the unilateral bite point. He depicted the mandible as a Class III lever with one or both of the TMJs as the fulcrum and the bite point as the load. The force acting on the lever system is determined by the combined forces of the muscles of mastication which can be resolved into a single resultant vector. Greaves (1973) argued that for the system to remain stable the resultant force must stay within the triangle of support. "If it does not, one of the three contact points will tend to be separated as the system rotates around the other two points" (p. 273). The resultant force magnitude and location can be altered by varying the combination of masticatory muscles that contract at any given moment. Greaves explained:

> Muscle forces of 10 units on the working side and from zero to 10 units on the balancing side are assumed below for simplicity. Because of these simplifying restrictions, the muscle resultant has a minimum value of 10 units situated directly over the chewing

Reproduced with permission of the copyright owner. Further reproduction prohibited without permission.

> side when the balancing side muscles are inactive. As the balancing side muscle force increases, the muscle resultant increases and moves medially, reaching its maximum value of 20 units in the midline when the balancing side is fully active" [*ibid.*, p. 273]. [7]

The triangle of support model accounts for several otherwise anomalous properties of masticatory function that have been observed in experimental and clinical studies. The first of these is the observation that the balancing (or contralateral) side TMJ, rather than the working side TMJ, manifests the highest reaction forces during normal mastication (Hylander, 1979; Weijs, 1980; Iwasaki, 1989; Throckmorton & Dechow, 1994; Marks *et al.*, 1997),[8] which indicates, under the assumptions of the lever model, that this side acts as the fulcrum. While Greaves' model permits any point between the left and right TMJs to act as the effective fulcrum, maximum bite forces are attained only when the contralateral side TMJ

---

[7] Greaves' model, as originally proposed, assumes that both the ipsilateral and contralateral side chewing muscles will reach peak magnitude simultaneously during centric occlusion when the masticatory muscle resultant resides at the midline. Electromyographic studies have shown, however, that peak masseter and temporalis muscle forces do not coincide during maximum intercuspation (Hiiemae, 1978; Hylander *et al.*, 1992). The pattern of muscle recruitement and activty responsible for jaw excursion during mastication is complex. The key to Greaves' model is not so much that all elevator muscles reach *peak* magnitude during the power stroke, but that the muscles coordinate to attain *maximum* possible force given the constraint that these same muscles are operating to move and position the jaw during the closing phase of the cycle. Even with this qualifier the basic principles of the model remain sound.

[8] Only two studies that I know of report higher reaction forces at the ipsilateral TMJ. Ferrario and Sforza (1994) contend that "reaction forces... do not always load the balancing-side joint more than the working-side joint", but this conclusion was based on their own theoretical model, not empirical data. Boyd *et al.* (1990) measured TMJ reaction forces with implanted remote signaling piezoelectric foil transducers in two unconstrained stump-tailed monkeys (*Macaca arctoides*) over an 8 day period. They found that "[f]orces were greater on the working (food) side than on the nonworking (balancing) side ..." However, in one of the animals they reported an oral dysfunction that interfered with mastication.

Reproduced with permission of the copyright owner. Further reproduction prohibited without permission.

acts as the fulcrum.[9] A series of simplified diagrams may help clarify several properties of Greaves' model (Box 14.5).

In the diagrams in Box 14.5 the skull is depicted in basal view with the balancing side TMJ represented by a black circle and the working side TMJ by a white circle. The dotted vertical line depicts the midline and the square boxes represent occlusal tooth surfaces on the right side of the skull (the solid square is the bite point tooth). Dotted lines connect the left and right TMJ and the ipsilateral TMJ with the bite point. The solid line linking the effective fulcrum with the bite point represents the mechanical lever arm. The masticatory muscle resultant must pass through this line in order to constitute a Class III lever system. The numerical values in the diagrams represent estimated bite force magnitudes at the bite point for various positions of the resultant muscle vector.

Box 14.5, A, gives three bite force magnitudes (13.4, 12.3 and 10.0) when the bite point is located at the middle tooth (solid square). Using Greaves' value of 10.0 units for unilateral muscle force, each of the three bite force magnitudes shown in Box 14.5, A, represents the bite force at the bite point predicted by the model when the resultant muscle vector is located at the corresponding number along the lever arm. For instance, when the resultant is situated at the point where the midline crosses the lever arm (i.e., the decimal point of the numerical value 13.4) the predicted maximum bite force at the bite point is 13.4 (solid square). When the resultant is shifted along the lever arm towards the bite point such that it is located at the decimal point of the numerical value 12.3, then the predicted bite

[9] Hylander (1975) came to the same conclusion on both mechanical and empirical grounds, and predicted that reaction forces should be greater on the balancing side than on the working side.

Reproduced with permission of the copyright owner. Further reproduction prohibited without permission.

force at the bite point is 12.3. Likewise, when the resultant passes directly through the bite point (i.e., the decimal point in the solid box) the maximum bite force is 10.0.

The maximum potential bite force is greatest at the midline because both left and right side masticatory muscles contribute equally to the generation of forces at the occlusal surface. When the resultant is directly over the bite point the lever system reaches maximum lever efficiency but the force exerted by the balancing-side muscles will have been decreased to allow for the lateral movement of the resultant vector. Maximum bite force (MBF) at a given tooth is thus calculated as the product of total masticatory muscle force and mechanical efficiency. The model does not always predict that MBF magnitudes will be greatest when the resultant muscle vector is located at the midline. In mammals that possess relatively long maxillary arches, mechanical efficiency is reduced too much by having the resultant vector located along the midline, and the MBF actually increases as the resultant is relocated towards the bite point (thereby increasing mechanical efficiency).

The diagram in Box 14.5, B, illustrates how MBF magnitudes change as the resultant muscle vector migrates from medial to lateral. Located at the midline the resultant vector produces a bite force of 13.4 units at the bite point (20 units muscle force x 0.662 mechanical efficiency). When the resultant is shifted laterally, the effective fulcrum also changes from the balancing-side TMJ to a point mid-way between the two TMJs (E). This produces a slight increase of mechanical efficiency, but reduces the total applied muscle force to 14 units. The MBF in this case is 9.3 (14 units muscle force x 0.668 mechanical efficiency). Finally, if the

Reproduced with permission of the copyright owner. Further reproduction prohibited without permission.

resultant muscle vector is moved to a position directly behind the bite point, thus shifting the effective fulcrum further toward the ipsilateral TMJ (E*), the load-to-lever arm ratio is again slightly increased, but not enough to compensate for the decrease in total muscle force. The bite force in this case falls to just 6.8 units (10 units working-side muscle force x 0.680 mechanical efficiency).

Greaves (1978) further argued that there are anterior and posterior limits to the movement of the resultant muscle vector, which are defined by muscle attachments and oral function. He argued on mechanical grounds that the posterior limit of the resultant should coincide with the distal end of the tooth row. The resultant is thus physically constrained to move within a small area of the triangle of support. The position of this area in relation to the bite tooth, and the left and right TMJs determine the optimal location of the resultant vector for producing the maximum bite force at a given tooth. That the masticatory muscle resultant vector changes with bite point, and throughout the chewing cycle, in association with alterations of muscle recruitment and activity patterns has been demonstrated electromyographically in several mammalian species (Hylander *et al.*, 1987, 1992; Dessem, 1989; Throckmorton *et al*, 1990; Erhardson *et al.*, 1993; Spencer, 1998).

The figure in Box 14.5, C, illustrates that MBF is attained at the posterior molars when the resultant muscle vector is directly over the bite point. Recall that the greatest total muscle force is attained when the resultant passes through the midline. However, the resultant vector cannot move medial to the bite point without exiting the triangle of support (point X along the arrow) thereby causing a dislocation at the working side TMJ. Theoretically, a resultant muscle vector located at the intersection of the midline and the balancing TMJ/bite point lever

Reproduced with permission of the copyright owner. Further reproduction prohibited without permission.

arm (X*) will produce the greatest bite point magnitude, but for posteriorly positioned teeth this point may be beyond the physical posterior limit of the resultant. In such a case, the only mechanically advantageous location for the resultant vector is directly over the bite point, which, as we have seen, yields a bite force magnitude of 10.0 units.

The situation is reversed when the bite point is located at the anterior dentition (Box 14.5, D). In this case the masticatory muscle resultant may encounter an anterior physical limit prior to reaching either the midline/lever arm intersect (X) or the bite point (B). The most advantageous location of the resultant, according to the model, will be along the midline at the anterior limit of the resultant vector (11.8).[10] This results in an effective fulcrum that lies between the TMJs (E), and yields a maximum bite force magnitude of 11.8.

The triangle of support model predicts that the greatest magnitude of bite force will occur not at the most posterior bite point, as conventional lever models predict, but at a tooth anterior to this point, from which bite force magnitudes will decrease in either direction along the tooth row. This prediction has been confirmed in experimental studies in which the maximum bite force has been shown to reside at M^1-M^2 (Mansour & Reynik, 1975; Prium *et al.*, 1980; Erhardson *et al.*, 1993).

Several authors have suggested modifications to Greaves' model (e.g., Smith *et al.*, 1986; Spencer, 1998), and I propose several here. In the model, as the

---

[10] The idea that the posterior portion of the temporalis muscle is dominant during incisal biting (as predicted by Gingerich's, 1979, link theory) is not consistent with results obtained from EMG investigations. For example, Latif (1957) and Weolfel *et al.* (1960) found that while both the anterior and posterior portions of the temporalis mm. were active during incisal biting, it was usually the anterior portion that was most active (*cf.* Hylander, 1975).

Reproduced with permission of the copyright owner. Further reproduction prohibited without permission.

resultant is shifted laterally towards the ipsilateral side it decreases in magnitude due to the diminishing contribution of the contralateral muscles. But Greaves made no adjustment for magnitude as the resultant vector migrates anteroposteriorly along the midline. Maximum masticatory muscle contraction will resolve into a single resultant vector passing through a point along the midline (the "maximum resultant vector" or MRV). Any deviation of the resultant from the MRV, either mediolaterally or anteroposteriorly, can only be achieved by a reduction in muscle force. Adding this new variable to the model has the following consequence: in the majority of cases, in order to produce the maximum bite force at any given tooth the masticatory muscle resultant will not deviate in the anteroposterior direction from the MRV location. However, as the bite point moves further back along the tooth row at some point the resultant muscle vector must begin to migrate laterally to stay within the triangle of support, until it finally passes through the bite point, usually at the posterior-most tooth.

This configuration is depicted in Box 14.5, E, which shows that the lever arms of the four most anterior teeth pass through MRV, but that the lever arm for the posterior-most tooth does not. The masticatory muscle resultant is thus obligated to move laterally (see arrow) until it resides within the triangle of support, which in this case is directly over the tooth. This model-implied transition of the resultant vector is consistent with the pattern of ipsilateral TMJ reaction forces observed by Hylander (1979): "During biting along the premolars or first two molars a compressive reaction force acts about the ipsilateral TMJ; however, when the bite point is positioned along the M3, the ipsilateral TMJ has either very little compressive stress, no stress, or it is loaded in tension" (p. 433). Since the

Reproduced with permission of the copyright owner. Further reproduction prohibited without permission.

muscle resultant is directly over the bite point at the last molar, the lever mechanics are momentarily suspended and there is either no fulcrum point, or the f ulcrum point is positioned exclusively at the contralateral TMJ.

In contrast to the previous diagrams, the numbers in the solid boxes in diagram 14.5, E, represent the bite force magnitudes at each tooth when the resultant is located at MRV, with the exception of the posterior tooth at which the resultant is located directly on the tooth. The muscle force applied to the first four teeth is 20 units, since in each case the applied resultant is located at MRV. The increase in bite force moving distally along the tooth row (8.0, 8.6, 10.1, 12.4 units) is due to an increase in mechanical efficiency (i.e., an increase in the load-to-lever arm ratio)—from only 40% at the anterior-most tooth to 62% at the penultimate tooth. The decrease in bite force at the distal-most tooth (10.9 units) is due to the lateral migration of the muscle resultant as discussed above.

The triangle of support model explains another feature of anthropoid dental morphology that was not mentioned by Greaves (1978), who applied his model to selenodont artiodactyls, or by subsequent authors—namely, the shape of the dental arcade. The typical (but not the only) shape of the anthropoid dental arcade is a para-ellipse (i.e., an ellipse cut-off to one side of center). In many species, the molars thus curve inward (medially) in as one proceeds toward the distal end of the tooth row. The medial convergence of the posterior-most molars can be viewed as an adaptation to maximize the bite force by increasing the contribution of the contralateral side masticatory muscles. Recall that, according to Greaves' model, a medial shift in the resultant vector is achieved by an increase in the magnitude of the contralateral side jaw adductor muscles, which results in an overall increase of

Reproduced with permission of the copyright owner. Further reproduction prohibited without permission.

the resultant force. Shifting the posterior molars medially increases the maximum bite force by placing the tooth in a location at which the balancing-side masticatory muscles can contribute to the overall bite force.

Box 14.5, F, gives the maximum bite force magnitudes for a matrix of potential tooth positions in the upper right quadrant. The tooth location exhibiting the greatest bite force in each row has been shaded. Several patterns emerge from this diagram. First, it can be seen that there is very little mediolateral variation in bite force magnitude at the anterior teeth (incisors). Second, the location of the greatest bite forces for the next three rows (canine, premolars and anterior molars) is not along the medial-most column, but lateral to it, in this example about half-way between the midline and right TMJ. Third, the greatest bite force magnitudes for the posterior-most rows (i.e., molars) occurs medial to that of the premolars and anterior molars. Finally, the diagram shows that there is little benefit to having the tooth row extend posterior to the MRV. In each column of the matrix in diagram 14.5, F, the MBF decreases in the posterior-most row. That the pattern of shaded boxes does not correspond precisely to the actual mean anthropoid dental arcade shape indicates that maxillary arch form is a compromise solution involving other causal agents. For example, there is presumably a constraint on how far medially the distal molars can be located before they begin to interfere with respiration, vocalization and swallowing. Nonetheless, the model helps explain the para-elliptical shape of the dental arcade of most anthropoids.

Reproduced with permission of the copyright owner. Further reproduction prohibited without permission.

Box 14.5. Diagrams showing properties of Greaves' "triangle of support" model of masticatory function.

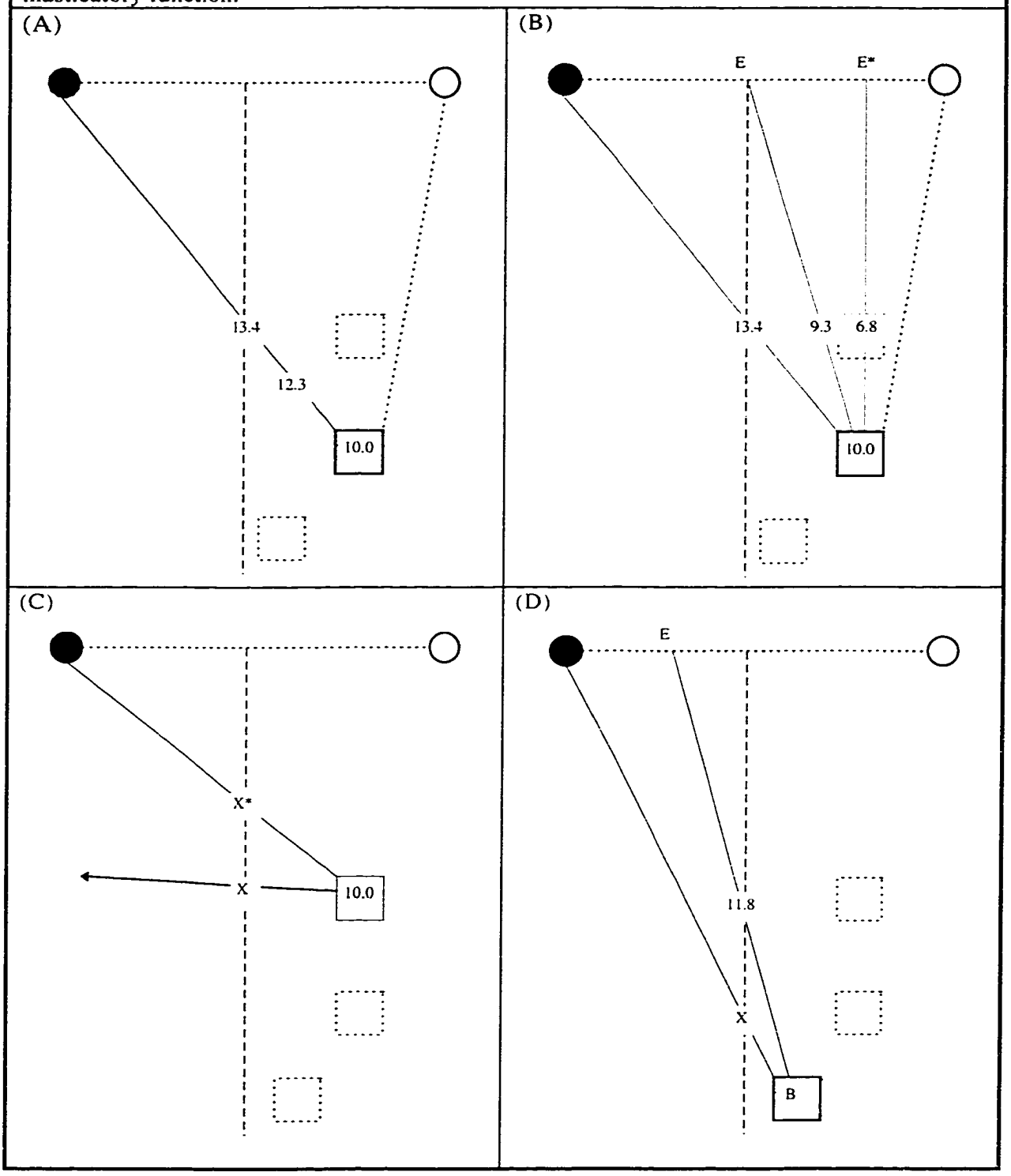

Reproduced with permission of the copyright owner. Further reproduction prohibited without permission.

Box 14.5. Diagrams showing properties of Greaves' "triangle of support" model of masticatory function.

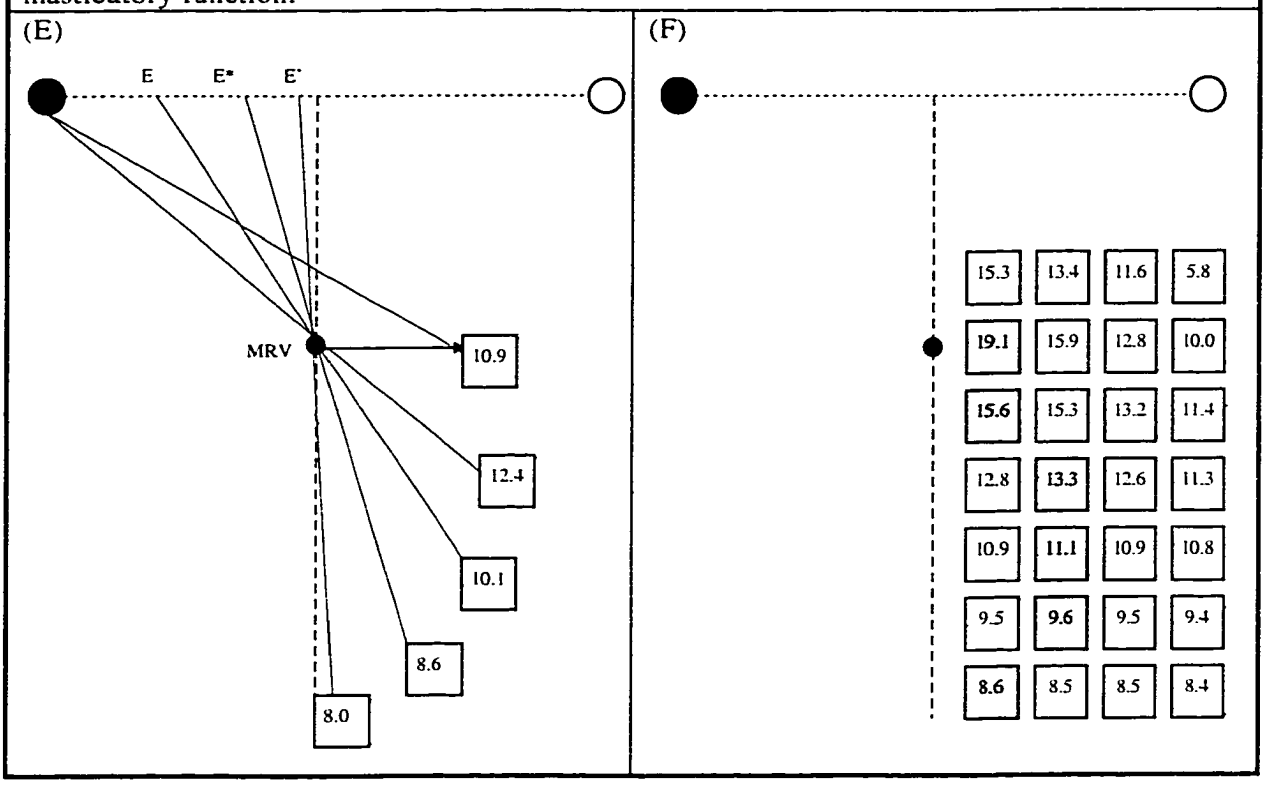

Applying three-dimensional analytic geometry to the 3D landmark coordinate data, I wrote a computer program in SAS Interactive Matrix Language (IML), based on Greaves' model, that calculated the maximum bite force at each tooth in the upper right quadrant for each of the 300 anthropoid specimens in the study sample.[11] The species mean data are presented in Box 14.6.

Surprisingly, there have been very few studies that have experimentally quantified maximum bite force magnitudes for various bite points along the tooth row, even in humans. It is therefore not possible at this time to adequately test the estimated MBFs derived from Greaves' model against experimentally observed MBFs of the same species. Of the studies that have published *in vivo* bite force data (e.g., Mansour & Reynik, 1976; Hylander, 1986; Oyen & Tsay, 1991;

Reproduced with permission of the copyright owner. Further reproduction prohibited without permission.

Erhardson *et al.*, 1993) few were conducted under conditions of normal masticatory function. For instance, Dechow and Carlson (1990) reported bite force magnitudes measured with a transducer at three different tooth locations in 132 rhesus macaques, but the animals were anesthetized and bite force was measured during unilateral muscle stimulation. In a study of occlusal forces generate by human subjects, Mansour and Reynick (1976) reported that "...the force at the second molar was approximately 10% greater than that at the first molar" (p. 114), which is not significantly different from the 9.2% mean increase in MBF (at M^2 compared with M^1) estimated for the 10 human crania examined here.

Once maximum bite force estimates had been calculated, it was a trivial matter to compute several other relevant variables. These included: anterior bite force magnitude [Y57-ANTBFM]: the average MBF of the upper right maxillary incisors; posterior bite force magnitude [Y58-PSTBFM]: the average MBF of upper right P^3 through M^3; relative anterior-to-posterior bite force [Y59-RELBFM]: index ANTBFM/PSTBFM x 100; maxillary bite force magnitude [Y60-MAXBFM]: average maximum bite force over all bite points (I^1-M^3). The species mean raw MBF data are presented in Box 14.6, below.

---

[11] The program is reproduced in full in Appendix D, under the variable names BFPUI1 to BFPUM3.

Reproduced with permission of the copyright owner. Further reproduction prohibited without permission.

Box 14.6. Species mean maximum bite force magnitudes for I^1 through M^3 of the right upper dental quadrant.

Anthropoid species:	BFPUI1	BFPUI2	BFPUP3	BFPUP4	BFPUM1	BFPUM2	BFPUM3
A. palliata	26.5	27.3	35.3	38.6	43.5	41.2	36.6
A. geoffroyi	24.2	25.3	32.6	35.0	36.0	32.7	30.5
L. lagothricha	25.4	26.3	33.8	36.5	38.5	35.2	32.5
B. arachnoides	25.5	26.1	32.7	36.0	40.5	38.5	35.4
C. satanas	17.6	18.5	26.3	28.9	30.6	28.4	25.7
P. pithecia	15.5	16.4	22.1	23.8	25.9	24.6	22.2
P. monachus	17.1	18.2	24.6	26.7	28.8	26.3	23.9
C. cupreus	13.6	14.4	17.9	19.4	20.9	19.2	17.7
C. apella	19.5	20.3	27.8	30.5	33.6	30.5	27.6
C. capucinus	19.1	20.0	27.1	29.7	33.2	32.0	28.6
S. sciureus	11.4	12.0	15.9	17.4	17.5	15.7	14.5
A. trivirgatus	10.1	10.8	13.8	15.0	16.5	15.6	14.3
S. oedipus	12.9	13.9	19.1	18.2	16.2	15.1	12.1
C. pygmaea	6.8	7.1	8.8	9.5	9.7	8.5	7.7
C. goeldii	10.4	10.9	14.1	15.6	16.6	14.7	13.4
C. aethiops	16.4	17.3	22.3	24.2	27.2	29.3	25.7
C. neglectus	19.5	20.6	26.2	28.6	32.1	34.4	30.0
C. mitis	19.5	20.7	26.4	28.6	32.2	33.3	29.6
C. ascanius	17.9	18.9	23.7	25.9	29.3	31.7	27.6
M. nemestrina	24.0	25.0	31.2	33.7	37.9	41.1	36.7
M. fascicularis	17.9	18.9	23.5	25.6	28.9	32.7	28.9
M. mulatta	20.3	21.2	25.5	27.9	31.5	37.3	33.8
P. hamadryas	26.8	28.0	34.5	37.5	42.1	50.0	43.3
L. albigena	21.8	23.5	30.4	33.1	37.0	42.2	36.4
C. guereza	23.6	24.6	30.7	33.6	37.6	42.7	37.6
P. badius	22.6	23.8	29.7	32.4	36.6	43.6	38.8
N. larvatus	22.5	23.4	28.0	30.7	34.7	40.5	35.5
P. melalophos	25.9	27.1	32.7	35.6	40.2	44.1	37.2
S. entellus	24.1	25.0	30.4	33.2	37.3	44.2	40.8
S. cristata	21.8	22.7	27.5	30.0	33.5	38.7	35.7
H. lar	23.5	24.4	31.5	34.1	37.4	35.8	32.6
H. syndactylus	28.6	29.4	37.5	41.1	46.0	49.6	44.3
P. pygmaeus	44.3	46.0	57.0	62.3	69.3	70.7	62.6
G. gorilla	38.5	39.6	49.8	55.4	63.5	76.2	68.5
H. sapiens	35.1	36.4	42.2	46.1	51.8	55.1	48.8
P. paniscus	27.7	29.4	38.2	42.1	47.9	49.2	43.5
P. troglodytes	38.5	39.9	51.2	55.8	61.4	61.0	55.7

Reproduced with permission of the copyright owner. Further reproduction prohibited without permission.

Mechanical properties of the masticatory system. A number of mechanical properties of the masticatory apparatus, as defined by Greaves' model, were also computed. Resolution of the masticatory muscle resultant required estimates of the vectors of the left and right masseter and temporalis muscles.[12] These vectors were based on, but slightly modified from, the craniometric system of muscle attachment points developed by Dechow and Carlson (1990: see p. 223, Fig. 2). The anteroposterior position of the masseter muscle vector [Y61-APMASS] and the temporalis muscle vector [Y62-APTEMP] were each calculated independently as the load-to-lever arm ratio (expressed as a percent) with the bite point at I^1. The load-to-lever arm ratio was also calculated for the combined masseter and temporalis muscle resultant, as previously described [Y63-LEVADV]. Temporalis muscle mass [Y64-TEMPMM] was estimated as the average elliptical area of the left and right infratemporal foramina (*cf.* Horowitz & Shapiro, 1955; Weijs, 1980; Deme & Creel, 1988; Cole, 1992). The "occlusal efficiency" of the resultant masticatory muscle force [Y66-RMMEFF] was based on the angle between the resultant vector and the occlusal plane. A perpendicular angle was assumed to transfer all of the resultant muscle force to the bite force, and deviations from 90° were assumed to diminish

[12] Muscle recruitement and activity during mastication is not limited to the temporalis and masseter muscles. The medial pterygoid is another major muscle of mastication. Since its line of action runs parallel to that of the masseter no additional vector calculations were included in the model for this muscle. It was possible, however, to include the muscle force contribution of the medial pterygoid to the resultant vector because it has been shown that the cross-sectional area of this muscle is highly correlated with the cross-sectional area of the masseter (Sasaki *et al.*, 1989). The lateral pterygoid muscles have been shown to be important for refining and restricting the movements of the mandibular condyles during chewing (Hylander *et al*, 1987). More complex modeling of the masticatory muscles is certainly possible (consider, for example Osborn's, 1995, 16 muscle model), but since, according to some estimates, the temporalis and masseter/med. pterygoid muscles contribute about 94% of the total masticatory muscle force (Dechow & Carlson, 1990), little is gained by the added complexity in the context of an *in vitro* craniometric study.

Reproduced with permission of the copyright owner. Further reproduction prohibited without permission.

muscle-to-bite force efficiency (Turnbull, 1970; Kay & Hiiemae, 1974). Dean (1986) defined the occlusal plane in terms of the planes of the dental wear facets and found a correspondence between the orientation of a given facet and the superficial masseter muscles. However, it must be kept in mind that primates engage in both downward (Phase I) and upward (Phase II) tritiational contact during the power stroke of mastication, and the planes of the wear facets involved in the two phases are at very different angles. Current evidence does not support the contention that the masticatory muscle resultant maintains a 90° angle to the wear facets during both phases of the power stroke (*cf.* Koolstra *et al.*, 1988; van Eijden, 1991).

Statistical Predictions

The hypotheses listed in Box 14.3 each render one or more predictions regarding the statistical associations among relevant operationalized variables. These statistical predictions are presented in the table in Box 14.7.

Reproduced with permission of the copyright owner. Further reproduction prohibited without permission.

Reproduced with permission of the copyright owner. Further reproduction prohibited without permission.

Box 14.7. Table of predicted statistical associations between masticatory and nasomaxillary variables. [Ref. #] source (study type).

Dependent Nasomaxillary Variable	Pred Corr	Reference and Research Design: Properties of the Masticatory System					
		Anterior bite force magnitude [Y57]	Posterior bite force magnitude [Y58]	Relative ant.-to-post. bite force magnitude [Y59]	A-P position of masseter/ temporalis [Y61/Y62]	Mechanical lever efficiency [Y63]	Temporalis muscle mass [Y64]
Facial prognathism	pos	**[1]** 3 (IB), 13 (IVB)	**[2]** 3 (IB), 13 (IVB)		**[3]** 15 (IVB)		
	neg	[4] 4 (IB), 1 (IA)	[5] 4 (IB), 1 (IA)	[6] 6 (IIA)	[7] 16 (IVA)		[8] 11 (IVA)
	null	[9] 2 (IB), 12 (IVB)	[10] 2 (IB), 12 (IVB)				[11] 10 (IVA)
Anterior facial length	pos	**[12]** 3 (IB), 13 (IVB)	**[13]** 3 (IB), 13 (IVB)		**[14]** 15 (IVB)		
	neg	[15] 4 (IB), 1 (IA)	[16] 4 (IB), 1 (IA)	[17] 6 (IIA)	[18] 16 (IVA)		[19] 11 (IVA)
	null	[20] 2 (IB), 12 (IVB)	[21] 2 (IB), 12 (IVB)				[22] 10 (IVA)
Maxillary arch length	pos	**[23]** 3 (IB), 13 (IVB)	**[24]** 3 (IB), 13 (IVB)		**[25]** 15 (IVB)		
	neg	[26] 4 (IB), 1 (IA)	[27] 4 (IB), 1 (IA)	[28] 6 (IIA)	[29] 16 (IVA)		[30] 11 (IVA)
	null	[31] 2 (IB), 12 (IVB)	[32] 2 (IB), 12 (IVB)				[33] 10 (IVA)
Facial vertical height	pos	**[34]** 1 (IA)	**[35]** 1 (IA)			**[36]** 5 (IIA) 6 (IIA)	
Bizygomatic breadth	pos	**[37]** 1 (IA), 2 (IB), 14 (IVB)	**[38]** 1 (IA), 2 (IB), 14 (IVB)				**[39]** 10 (IVA)
Maxillary arch breadth	pos	**[40]** 1 (IA), 2 (IB), 14 (IVB), 18 (IIIA)	**[41]** 1 (IA), 2 (IB), 14 (IVB), 18 (IIIA)				**[42]** 10 (IVA)
Bimaxillary breadth	pos	**[43]** 1 (IA), 2 (IB), 14 (IVB)	**[44]** 1 (IA), 2 (IB), 14 (IVB)				**[45]** 10 (IVA)
Palatal depth at P^3	neg	[46] 2 (IB)	[47] 2 (IB)				
Palatal depth at M^1	neg	[48] 2 (IB)	[49] 2 (IB)				
Palatal depth at M^3	neg	[50] 2 (IB)	[51] 2 (IB)				
Facial convexity	pos	**[52]** 9 (IIIA)		**[53]** 9 (IIIA)			
Zygomatic height	pos						**[54]** 8 (IIA)
Zygomatic root position	pos					**[55]** 5 (IIA)	
Ant nasal aperture brdth.	pos.		**[56]** 9 (IIIA)				
	neg.	[57] 16 (IVA); 17 (IIIA)					
Nasal pros. maxilla wdth	pos	**[58]** 17 (IIIA)		**[59]** 17 (IIIB)			
Paranasal plate angle	pos	**[60]** 9 (IIIA)					

1, Jolly, 1970; Kinzey, 1974 (IA); 2, Beecher et al., 1983 (IB); 3, Kiliaridis, 1986 (IB); 4, Chuang, 1995 (IB); 5, Rak, 1983 (IIA); 6, Demes & Creel, 1988; 7, Preushoft et al., 1986; 8, ? (IIA); 9, Deme, 1987 (IIIA); 10, van Spronsen et al., 1991 (IVA); 11, Raadsheer et al., 1996; 12, Pratt, 1943 (IVB); 13, Carlson & Schneiderman, 1983 (IVB); 14, Muller & Punt-van Manen, 1982 (IVB); 15, Hohl, 1983 (IVB); 16, Hylander, 1977 (IVA); 17, Endo, 1970 (IIIA); 18, Thomason & Russell, 1986 (IIIA) [A=non-experimentsl; B=experimental]

Preliminary and Exploratory Data Analysis

The results of a preliminary analyses of the anthropoid dietary and craniometric data are presented and discussed in this section. Analyses include (1) an examination of the effects of body size on dietary preferences, masticatory mechanics, and maximum bite force patterns, (2) quantification of the relationship between properties of the masticatory apparatus and maximum bite force magnitude and distribution, (3) an examination of the association between masticatory mechanics and bite force, (4) an examination of the relationship between maximum bite force and nasomaxillary morphology, and (5) a principal components analysis aimed at elucidating the relationships among masticatory variables and other relevant craniofacial variables.

Effects of Body Size on Dietary Preferences

The relationship between body size and diet has been well documented in primates as well as in other mammals (Kurland & Pearson, 1986). Smaller mammals have relatively higher basal metabolic rates and therefore require more energy-rich sources of food compared to larger mammals, although smaller mammals do not require the abundance of food that larger mammals require. Food items like insects are an ideal source of energy for small primates, but do not occur in the abundance needed to sustain large primates. On the other hand, foods such as foliage and roots are found in abundance and are therefore ideal for large primates, but are too energy-poor to sustain small primates. A good summary of this principle, known as the Jarman-Bell principle, is provided by Richard (1985, p. 184).

A multiple regression analysis of the *raw* log craniometric and behavioral

Reproduced with permission of the copyright owner. Further reproduction prohibited without permission.

data was conducted to see if the dietary preferences of anthropoids predict body size. The results (Box 14.8) indicate that percent consumption of insects and exudates predicts small body size, whereas percent consumption of vertebrate fauna and underground plant parts such as roots, tubers, and corms, predicts large body size. The dietary consumption of fruits, seeds, leaves, buds and flowers were not significant predictors of body size.

An analysis of the raw categorical data led to much the same conclusion. The mean raw centroid size for frugivorous anthropoids (299.7) is not significantly different from that of folivorous anthropoids (327.9). These findings contradict those of Clutton-Brock and Harvey (1977a) who concluded that frugivores tend to be smaller than folivores. The categorical data presented here signify only that gumnivores and insectivores tend to be significantly smaller than other dietary groups, and that omnivores tend to be significantly larger. The mean centroid sizes (and their 95% confidence limits and samples sizes) for the nine dietary groups are given in Box 14.9.

Reproduced with permission of the copyright owner. Further reproduction prohibited without permission.

Box 14.8. SAS output of multiple regression of raw log dietary variables on raw log skull centroid size for 37 species of anthropoids

Model: MODEL1
Dependent Variable: L_SKCNTR log(SKCNTR)

Analysis of Variance

Source	DF	Sum of Squares	Mean Square	F Value	Prob>F
Model	8	3.33508	0.41689	6.309	0.0001
Error	28	1.85029	0.06608		
C Total	36	5.18538			

Root MSE	0.25706	R-square	0.6432
Dep Mean	5.77128	Adj R-sq	0.5412
C.V.	4.45419		

Parameter Estimates

Variable	DF	Parameter Estimate	Standard Error	T for H0: Parameter=0	Prob > |T|
INTERCEP	1	5.564485	0.29687784	18.743	0.0001
L_ VERT	1	1.648538	0.65656488	2.511	0.0181
L_INSECT	1	-1.628130	0.58888453	-2.765	0.0100
L_FRUIT	1	0.532402	0.43695383	1.218	0.2332
L_SEED	1	-0.279058	0.49143679	-0.568	0.5747
L_BUD	1	0.027375	0.07768234	0.352	0.7272
L_LEAF	1	0.499940	0.51574879	0.969	0.3407
L_ROOT	1	2.365174	0.88520998	2.672	0.0124
L_GUM	1	-1.541177	0.59059858	-2.610	0.0144

Box 14.9. Means and 95% confidence intervals for raw skull centroid size by dietary category.

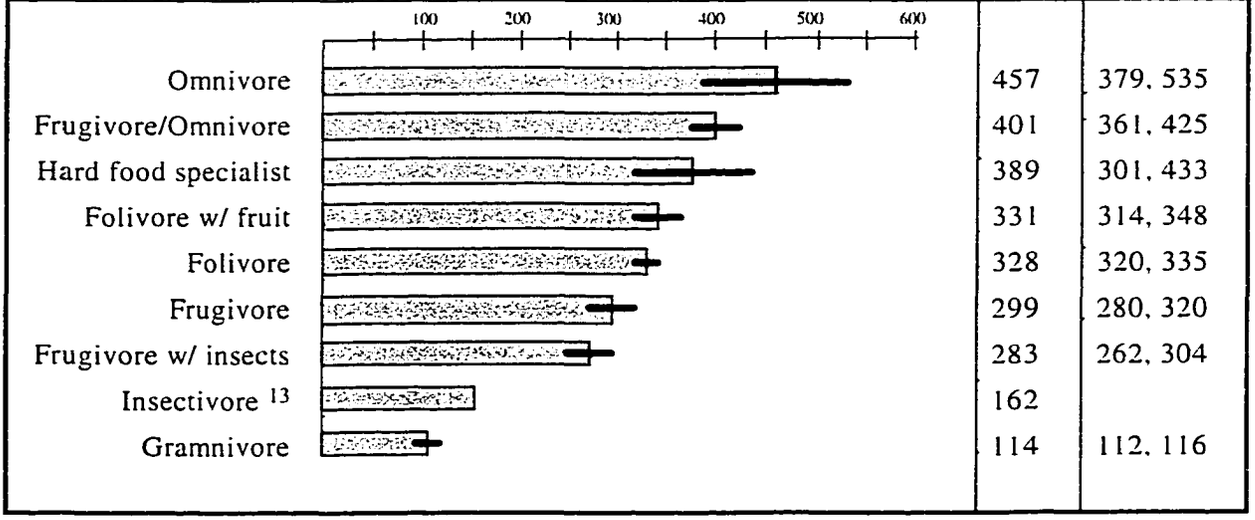

[13] The only true insectivore in the anthropoid sample is *S. oedipus*, which is represented by a single specimen.

Reproduced with permission of the copyright owner. Further reproduction prohibited without permission.

Effects of Body Size on Masticatory Mechanics and Maximum Bite Force

In addition to describing the relationship between body size and features of masticatory morphology and behavior, another topic that must be addressed is the role of size in mediating the relationship between masticatory features and craniofacial morphology. In previous chapters, linear variables were scaled to a common centroid size by transforming them into Mosimann isometric log residuals. But it is not clear that the same approach should be taken with respect to linear masticatory variables.[14] There are good arguments for the use of both absolute and relative masticatory force measures in nomological analysis. For example, in order to masticate palm nuts, a relatively hard food item favored by mangabeys like *Lophocebus albigena*, a primate must be capable of generating high *absolute* bite forces. The pygmy marmoset may generate a higher bite force *relative to body size* than a mangabey, but that's not going to help it crack open a palm nut. On the other hand, the principle of functional equivalence dictates that *relative* bite forces are what is essential for inducing strain-related osteogenic bone response: small absolute bite forces dissipated by a small facial skeleton can lead to the same morphogenetic response as large absolute bite forces dissipated by a comparatively larger facial skeleton (*cf.* Biewener, 1989). This interpretation mandates that *absolute* MBF values be used when examining relationships between the properties of anthropoid diets and attributes of the masticatory system, but that *relative* measures be used in the analysis of the effects of masticatory forces and strain patterns on nasomaxillary form.

---

[14] The "linear" masticatory variables include all those variables that are measured in units of absolute force, and which are not expressed as a ratio.

Reproduced with permission of the copyright owner. Further reproduction prohibited without permission.

Another problem is the potential occurrence of spurious associations between dietary variables and masticatory attributes. The bivariate regression plots in Box 14.10 show the close association between MBF variables and body size (i.e., centroid size). It is also well established that body size greatly affects primate diets (Kurland & Pearson, 1986). Any covariance between diet and masticatory features observed in anthropoids may be due to the common influence of body size.

The regression plots presented in Box 14.11 yield several important results. One is that maximum bite fore magnitudes scale isometrically with size for the incisors and premolars (i.e., the 95% confidence interval covers the 1.0 regression coefficient), although the molars fall just short of isometry. This is somewhat unexpected since it has been demonstrated in previous chapters that small-bodied anthropoids tent to have relatively wide, orthognathic faces, and we would therefore expect size-related differences in MBF patterns. For example, facial orthognathy should produce a greater anterior-to-posterior bite force ratio due to the reduced load-to-lever arm ratio in short-faced forms. However, this does not appear to be the case. Analysis of the anthropoid craniometric data revealed no significant correlation between degree of facial prognathism and either mechanical lever advantage or anterior-to-posterior bite force ratio. This indicates that the resultant masticatory muscle vector is located in the same relative position between the temporomandibular joints and the anterior dentition regardless of the length or projection of the snout.

Recall that Greaves (1978) argued on biomechanical grounds that the resultant vector will reside at or close to the distal-most end of the tooth row (along the anteroposterior axis). In a slight modification of Greaves' model I propose that

Reproduced with permission of the copyright owner. Further reproduction prohibited without permission.

resultant vector should pass through a line connecting the points of centric occlusion of the last molars. Resultant vectors were estimated empirically for each of the 300 specimens in the anthropoid sample on the basis of craniometrically determined muscle attachment points. A 3D analysis of these vectors showed that the average anteroposterior location of the resultants was between the second and third upper molars. It can be seen with reference to the skull photographs in Box 14.9 that this point is almost always mid-way between the TMJ and prosthion, regardless of the size of the skull.

Box 14.9. Skull photographs in basal view showing line connecting TMJ with prosthion (thick bold line), the midway point on this line (dotted vertical line), lever arm from largest molar to TMJ, and MRV. **A**, *C. mitis*; **B**, *S. sciureus*; **C**, *M. nemestrina*; **D**, *P. melalophos*

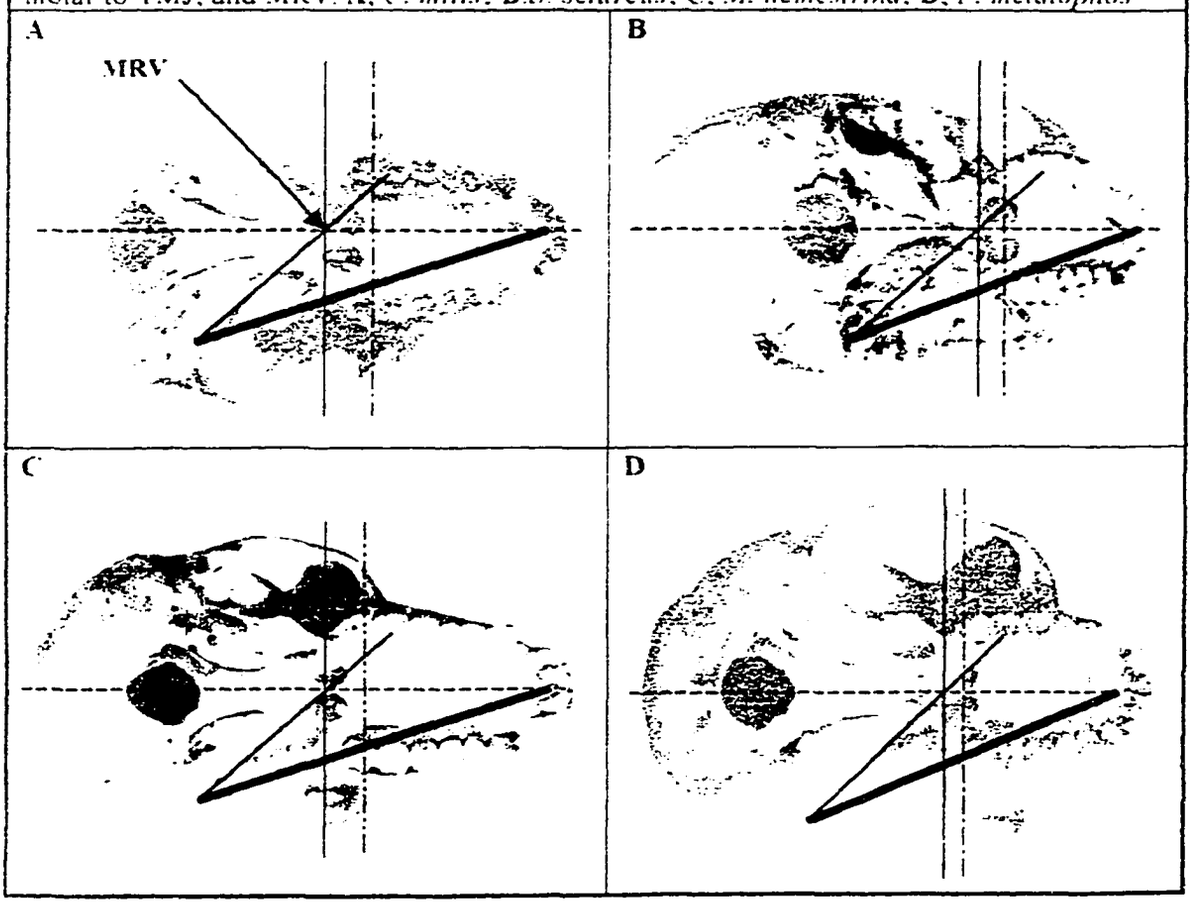

Reproduced with permission of the copyright owner. Further reproduction prohibited without permission.

This interpretation is consistent with the bivariate analysis of masticatory efficiency and body size. In order to maintain a mechanically efficiency isometry, relative increases in maxillary length and facial prognathism must be accompanied by an expansion of the cranial base and pharyngeal space. The principal components analysis conducted in Chapter 13 confirms this postulate, showing that relative maxillary arch length and facial prognathism covary with relative middle cranial fossa length and cranial base extension (see Box 13.16). It is of interest to note in this context that the anteroposterior position of the zygomatic root, long considered to be a indicator of the anterior extent of masticatory muscle action, does not participate in the isometric relationship between maxillary length, middle cranial fossa length and muscle resultant position. It has already been shown (see Chapter 9) that as the maxillary arch increases in length (both evolutionarily and ontogenetically) the relative position of the zygomatic root becomes more posteriorly displaced. Therefore, zygomatic root position is not a reliable indicator of the anterior extent of masticatory muscle action—there is only a very weak association between A-P zygomatic root position and masticatory muscle lever advantage (b=0.09, $R^2 < 0.02$, $p = .02$).

The foregoing analysis suggests that even though facial anteroposterior dimensions scale allometrically with body size, essential masticatory properties scale isometrically with size.

Reproduced with permission of the copyright owner. Further reproduction prohibited without permission.

Box 14.11. Scatter plots of delta log skull centroid size against delta log masticatory attributes. .

MBF at I^1: Slope = 0.95 (0.89, 1.01), R^2 = 0.78

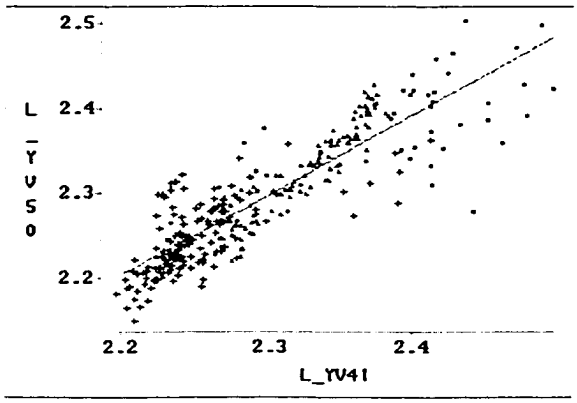

MBF at I^2: Slope = 0.94 (0.89, 1.01), R^2 = 0.78

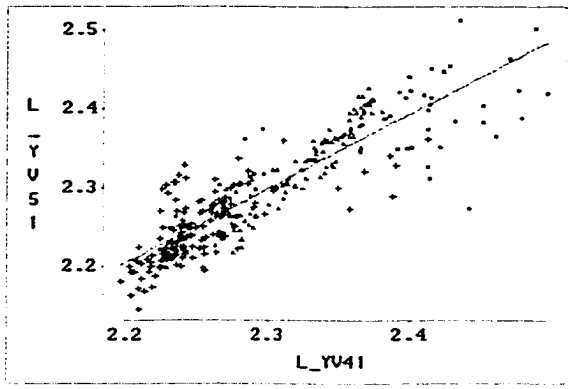

MBF at P^3: Slope = 0.95 (0.89, 1.02), R^2 = 0.75

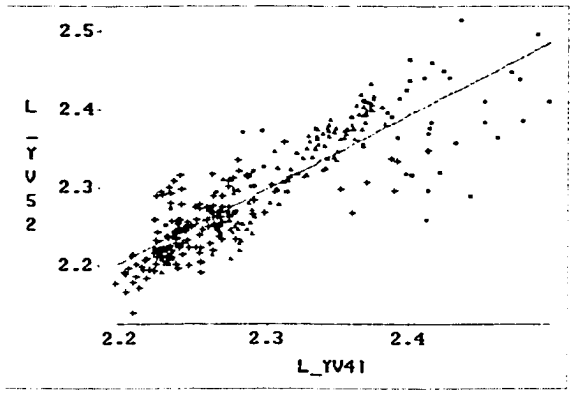

MBF at P^4: Slope = 0.95 (0.89, 1.01), R^2 = 0.76

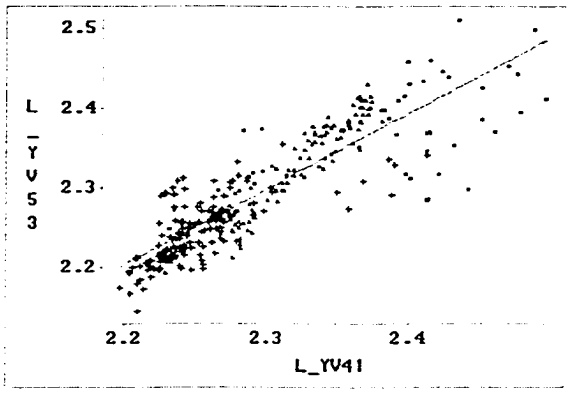

MBF at M^1: Slope = 0.93 (0.87, 0.99), R^2 = 0.78

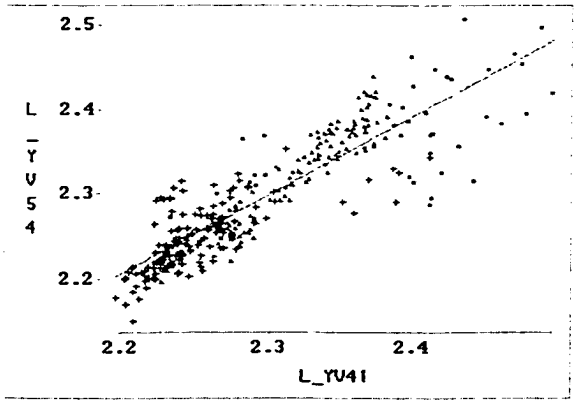

MBF at M^2: Slope = 0.88 (0.83, 0.93), R^2 = 0.80

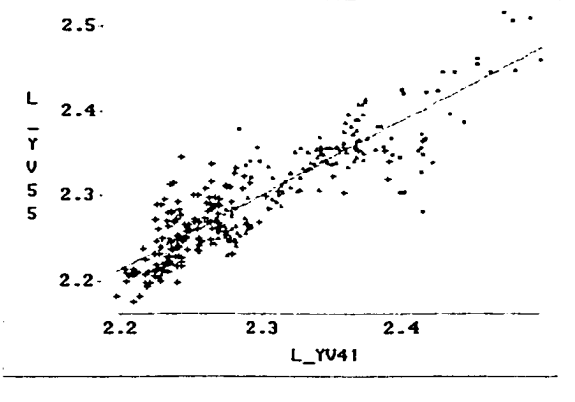

Reproduced with permission of the copyright owner. Further reproduction prohibited without permission.

Box 14.11. Scatter plots of delta log skull centroid size against delta log masticatory attributes. .

MBF at M^3: Slope = 0.92 (0.86, 0.97), R^2 = 0.78

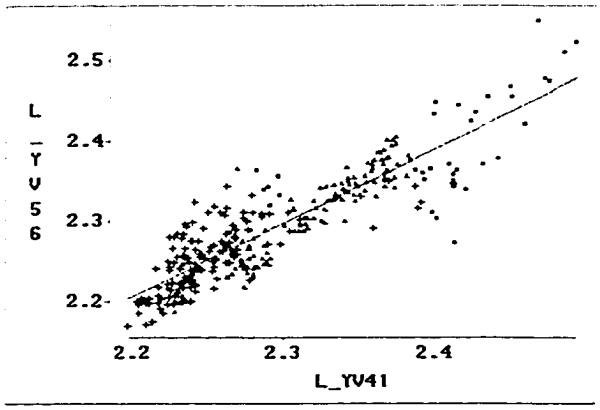

Anterior MBF: Slope = 0.95 (0.89, 1.01), R^2 = 0.78

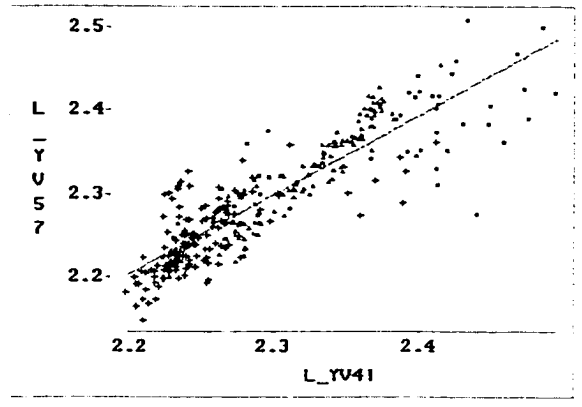

Posterior MBF: Slope = 0.94 (0.89, 0.99), R^2 = 0.80

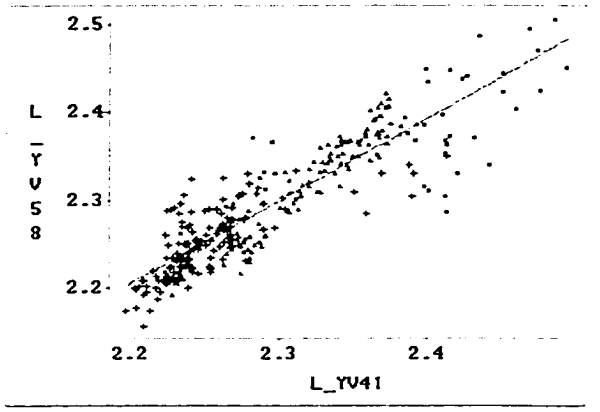

A/P MBF: Slope = -0.16 (-0.32, 0.01), R^2 = 0.01

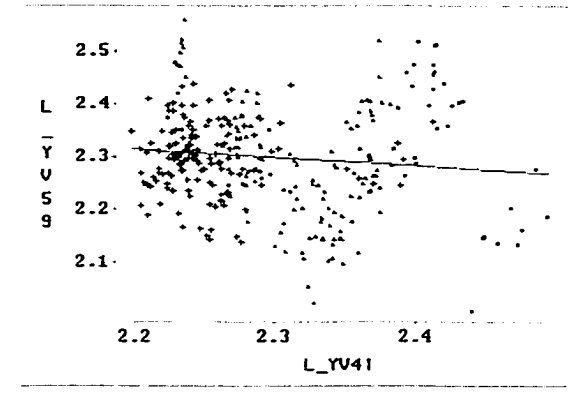

Total MBF: Slope = 0.94 (0.89, 1.00), R^2 = 0.80

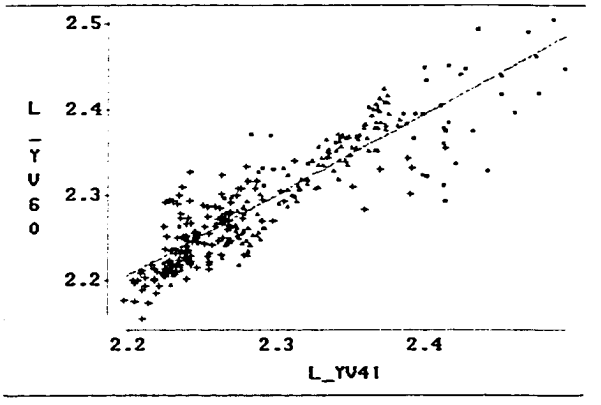

Masseter position: -0.04 (-0.32, 0.01), R^2 = 0.00

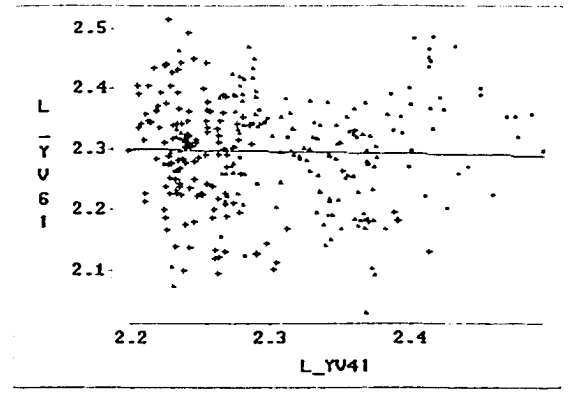

Reproduced with permission of the copyright owner. Further reproduction prohibited without permission.

Box 14.11. Scatter plots of delta log skull centroid size against delta log masticatory attributes. .

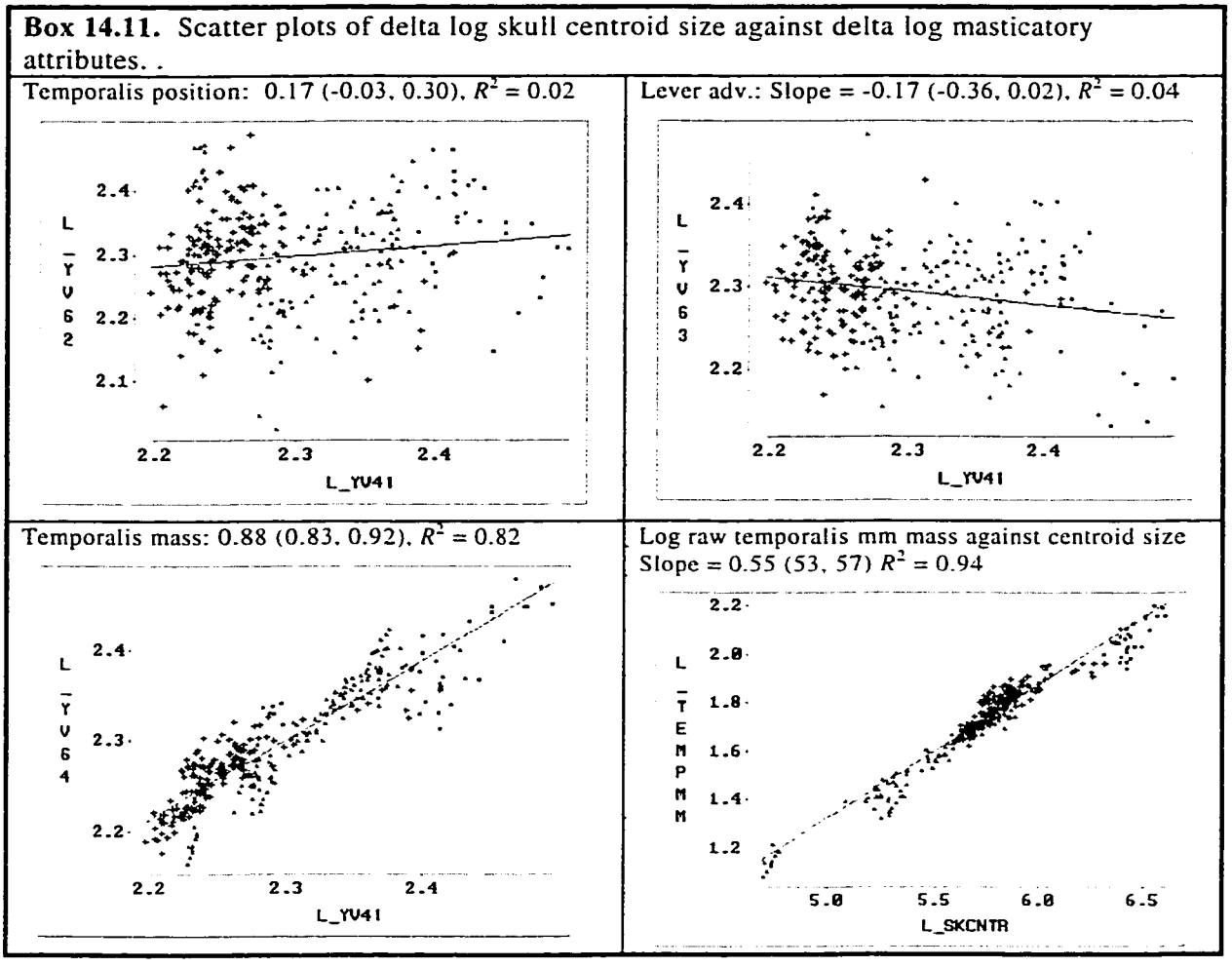

Effects of Diet on Masticatory Mechanics and Maximum Bite Force

The models presented in Box 14.1 include a causal pathway between the properties of food items consumed by anthropoids and properties of the mechanical system of mastication (paths A.G and A.I). The structure and consistency of food items can also influence the magnitude and distribution of maximum bite forces at different bite points along the tooth row (paths A.A and B.1). In this section, I examine the relationship between dietary preference and masticatory function in anthropoids. Three types of dietary information were analyzed: (1) hardness of food items consumed, (2) percent of food types consumed, and (3) dietary categories.

Reproduced with permission of the copyright owner. Further reproduction prohibited without permission.

Hardness of Food Items Consumed

The analyses in this section (see results Box 14.12) were intended to examine the predicted relationships between properties of food items consumed and properties of the masticatory apparatus (paths A & GI, Box 14.1; Hypothesis A & C, Box 14.3). Regression of various bite force and masticatory properties on dietary hardness {L_YM92} revealed no significant associations among the variables (see Box 14.12). How are we to reconcile this finding with the principle that the masticatory and food procurement behaviors of certain anthropoids demand specific mechanical attributes of the masticatory system? There are two plausible solutions: (1) the analysis and conclusions are accurate and therefore the hypothesis is incorrect, or (2) the analysis is flawed and the hypothesis remains untested. In fact, in this instance, the latter may be the case.

Although the accuracy of the craniometric data has been thoroughly examined (see Chapter 5), the accuracy of the "hardness index" variable is perhaps low enough to obscure any meaningful results. One example will suffice to make this point clear. Fruit consumption contributed very little to the hardness index because it was designated a "soft" food type. But it is well known that anthropoids consume fruit from a wide variety of plant species, under varying climatic conditions and seasons. Some of these fruits are indeed soft having thin membranous outer skins and soft fleshy pulp inside; whereas other fruits have tough protective coverings and dense or fibrous pulp (Richard, 1985; Dumont, 1997). Variation in the consistency of the fruit eaten by anthropoids make a generalization regarding the "hardness of fruit" quite meaningless—one need only consider the

Reproduced with permission of the copyright owner. Further reproduction prohibited without permission.

consistency of an apple and a pealed banana. More refined analyses are required to adequately quantify the variation in the physical properties of fruit and other food types in anthropoid diets (*cf.*, Bouvier & Hylander, 1982; Beecher, Corruccini & Freeman, 1983; Kinzey & Norconk, 1993). Nothing tried, nothing gained.

Given the problems associated with the operationalization of food item consistency, Kinzey's (1974) hypothesis that large bite force magnitudes are an adaptation to a diet of hard food items cannot be rejected.

Box 14.12. Predicted bivariate statistical associations and properties deduced from hypotheses statements.

Predicted bivariate associations (dependent variable in bold)	Regression slope (95% CL) and test of significant association, R^2 (p-value)
Maximum bite force magnitudes ← Dietary hardness index [L_YM92]	
Anterior bite force [L_YV57]	0.22 (0.11, 0.33) R^2 = 0.05 (ns)
Posterior bite force [L_YV58]	0.19 (0.08, 0.31) R^2 = 0.04 (ns)
Relative A-P bite force [L_YV59]	0.12 (-0.03, 0.28) R^2 = 0.01 (ns)
Maxillary bite force [L_YV60]	0.20 (0.09, 0.31) R^2 = 0.04 (ns)
A-P position of masseter muscle [L_YV61]	-0.12 (-0.27, 0.03) R^2 = 0.01 (ns)
A-P position of temporalis muscle [L_YV62]	0.24 (0.11, 0.37) R^2 = 0.04 (ns)
Lever efficiency [L_YV63]	0.02 (-0.11, 0.07) R^2 = 0.00 (ns)
Temporalis muscle mass [L_YV64]	0.22 (0.11, 0.38) R^2 = 0.06 (ns)
Resultant vector efficiency [L_YV66]	0.34 (0.20, 0.47) R^2 = 0.08 (ns)

Percent of Food Types Consumed

Analyses of the relationship between dietary composition and properties of the masticatory apparatus (see results Box 14.13) test the same set of hypotheses as the previous section, but make no assumptions regarding the consistency of the various food types. Multiple regression of percent food types eaten against masticatory properties indicate only a few associations, all involving gumnivory or insectivory. Percent of exudates in the diet was found to be significantly associated with

Reproduced with permission of the copyright owner. Further reproduction prohibited without permission.

increased anterior-to-posterior bite force ratio and reduced temporalis muscle mass. This latter association is likely due to the effects of body size: in accordance with the Jarman-Bell principle, gumnivores tend to be small-bodied and therefore have smaller absolute masticatory muscle mass. That percent consumption of exudates is significantly associated with high anterior-to-posterior bite force magnitudes is consistent with gumnivore feeding behavior. Marmosets, for example, often gouge holes in the bark and phloem of trees to induce exudate flow, a task that presumably requires strong relative anterior bite forces. In a recent ecomorphological study, Dumont (1997) concluded: "Exudate feeder skulls and dentaries exhibit a combination of features that reflect the high stresses encountered by the anterior dentition through bark gouging behavior" (p. 187).

Percent consumption of insects in the diet was found to be associated with increased load-to-lever arm ratio, or mechanical efficiency. This finding does not appear to coincide with any proposed hypothesis of trophic function. Maynard Smith and Savage (1959) explained several of the observed differences in the masticatory apparatus of carnivores and herbivores as adaptations to their respective diets. Carnivores tend to develop large, anteriorly placed temporalis muscles and inferiorly placed mandibular condyles (relative to the occlusal plane), features which produce fast-closing jaws able to resist anteriorly directed forces from struggling prey. The data presented in Box 14.13 do not support the Maynard Smith and Savage hypothesis when applied to anthropoids. Neither temporalis muscle mass nor ramus height show a significant association with percent of insects or vertebrate fauna in the diet.

Reproduced with permission of the copyright owner. Further reproduction prohibited without permission.

Box 14.13. SAS output of multiple regression of delta log masticatory and dietary variables

Dep. Var.: Ant. bite force, L_YM57

Analysis of Variance

Source	DF	Sum of Squares	Mean Square	F Value	Prob>F
Model	8	0.04426	0.00553	1.273	0.2967
Error	28	0.12170	0.00435		
C Total	36	0.16596			

Root MSE	0.06593	R-square	0.2667
Dep Mean	2.30001	Adj R-sq	0.0572
C.V.	2.86636		

Parameter Estimates

Variable	DF	Parameter Estimate	Standard Error	T for H0: Parameter=0	Prob > |T|
INTERCEP	1	4.636212	3.27314621	1.416	0.1677
L_DVERT	1	0.010943	0.20127443	0.054	0.9570
L_DINSEC	1	-0.221763	0.19417018	-1.142	0.2631
L_DFRUIT	1	-0.244825	0.30173561	-0.811	0.4240
L_DSEED	1	-0.171189	0.25372731	-0.675	0.5054
L_DBUD	1	-0.076291	0.24873525	-0.307	0.7614
L_DLEAF	1	-0.128755	0.26286201	-0.490	0.6281
L_DROOT	1	0.095156	0.18301522	0.520	0.6072
L_DGUM	1	-0.279179	0.16766410	-1.665	0.1070

Dep. Var.: Post. bite force, L_YM58

Analysis of Variance

Source	DF	Sum of Squares	Mean Square	F Value	Prob>F
Model	8	0.04404	0.00551	1.303	0.2822
Error	28	0.11829	0.00422		
C Total	36	0.16233			

Root MSE	0.06500	R-square	0.2713
Dep Mean	2.30015	Adj R-sq	0.0631
C.V.	2.82582		

Parameter Estimates

Variable	DF	Parameter Estimate	Standard Error	T for H0: Parameter=0	Prob > |T|
INTERCEP	1	4.897832	3.22704163	1.518	0.1403
L_DVERT	1	-0.056570	0.19843933	-0.285	0.7777
L_DINSEC	1	-0.234678	0.19143515	-1.226	0.2305
L_DFRUIT	1	-0.242227	0.29748545	-0.814	0.4224
L_DSEED	1	-0.180486	0.25015338	-0.722	0.4766
L_DBUD	1	-0.102973	0.24523164	-0.420	0.6778
L_DLEAF	1	-0.139024	0.25915941	-0.536	0.5959
L_DROOT	1	0.125525	0.18043732	0.696	0.4924
L_DGUM	1	-0.299172	0.16530243	-1.810	0.0811

Dep. Var.: Rel A-P bite force, L_YM59

Analysis of Variance

Source	DF	Sum of Squares	Mean Square	F Value	Prob>F
Model	8	0.07035	0.00879	1.494	0.2042
Error	28	0.16487	0.00589		
C Total	36	0.23522			

Root MSE	0.07673	R-square	0.2991
Dep Mean	2.29840	Adj R-sq	0.0988
C.V.	3.33856		

Parameter Estimates

Variable	DF	Parameter Estimate	Standard Error	T for H0: Parameter=0	Prob > |T|
INTERCEP	1	-0.934969	3.80969265	-0.245	0.8079
L_DVERT	1	0.272534	0.23426809	1.163	0.2545
L_DINSEC	1	0.118192	0.22599928	0.523	0.6051
L_DFRUIT	1	0.123882	0.35119724	0.353	0.7269
L_DSEED	1	0.093554	0.29531925	0.317	0.7538
L_DBUD	1	0.210603	0.28950887	0.727	0.4730
L_DLEAF	1	0.106065	0.30595133	0.347	0.7314
L_DROOT	1	-0.103375	0.21301576	-0.485	0.6312
L_DGUM	1	0.584598	0.19514823	2.996	0.0057

Dep. Var.: A-P position of masseter, L_YM61

Analysis of Variance

Source	DF	Sum of Squares	Mean Square	F Value	Prob>F
Model	8	0.01917	0.00240	0.473	0.8645
Error	28	0.14180	0.00506		
C Total	36	0.16098			

Root MSE	0.07116	R-square	0.1191
Dep Mean	2.29908	Adj R-sq	-0.1326
C.V.	3.09536		

Parameter Estimates

Variable	DF	Parameter Estimate	Standard Error	T for H0: Parameter=0	Prob > |T|
INTERCEP	1	3.749819	3.53320033	1.061	0.2976
L_DVERT	1	0.092714	0.21726584	0.427	0.6728
L_DINSEC	1	-0.041790	0.20959716	-0.199	0.8434
L_DFRUIT	1	-0.190742	0.32570875	-0.586	0.5628
L_DSEED	1	-0.237455	0.27388615	-0.867	0.3933
L_DBUD	1	-0.173242	0.26849747	-0.645	0.5240
L_DLEAF	1	0.007167	0.28374660	0.025	0.9800
L_DROOT	1	-0.162237	0.19755592	-0.821	0.4185
L_DGUM	1	0.074676	0.18098515	0.413	0.6830

Dep. Var.: A-P position of temporalis, L_YM62

Analysis of Variance

Source	DF	Sum of Squares	Mean Square	F Value	Prob>F
Model	8	0.06823	0.00853	2.518	0.0335
Error	28	0.09483	0.00339		
C Total	36	0.16307			

Root MSE	0.05820	R-square	0.4184
Dep Mean	2.29899	Adj R-sq	0.2523
C.V.	2.53140		

Parameter Estimates

Variable	DF	Parameter Estimate	Standard Error	T for H0: Parameter=0	Prob > |T|
INTERCEP	1	4.872399	2.88936957	1.686	0.1028
L_DVERT	1	0.093844	0.17767498	0.528	0.6015
L_DINSEC	1	-0.336279	0.17140371	-1.962	0.0598
L_DFRUIT	1	-0.356612	0.26635709	-1.339	0.1914
L_DSEED	1	-0.108907	0.22397776	-0.486	0.6306
L_DBUD	1	-0.329054	0.21957103	-1.499	0.1452
L_DLEAF	1	-0.069024	0.23204142	-0.297	0.7683
L_DROOT	1	-0.277394	0.16155667	-1.717	0.0970
L_DGUM	1	0.264207	0.14800547	1.785	0.0851

Dep. Var.: Lever efficiency, L_YM63

Analysis of Variance

Source	DF	Sum of Squares	Mean Square	F Value	Prob>F
Model	8	0.04597	0.00575	2.662	0.0261
Error	28	0.06045	0.00216		
C Total	36	0.10641			

Root MSE	0.04646	R-square	0.4320
Dep Mean	2.30064	Adj R-sq	0.2697
C.V.	2.01955		

Parameter Estimates

Variable	DF	Parameter Estimate	Standard Error	T for H0: Parameter=0	Prob > |T|
INTERCEP	1	-0.690387	2.30678204	-0.299	0.7669
L_DVERT	1	0.165728	0.14185013	1.168	0.2525
L_DINSEC	1	0.436306	0.13684335	3.188	0.0035
L_DFRUIT	1	0.211436	0.21265114	0.994	0.3286
L_DSEED	1	0.239374	0.17881682	1.339	0.1915
L_DBUD	1	0.170693	0.17529862	0.974	0.3385
L_DLEAF	1	0.064533	0.18525459	0.348	0.7302
L_DROOT	1	-0.046306	0.12898178	-0.359	0.7223
L_DGUM	1	0.058944	0.11816292	0.499	0.6218

Reproduced with permission of the copyright owner. Further reproduction prohibited without permission.

Box 14.13. SAS output of multiple regression of delta log masticatory and dietary variables

Dep. Var.: Temporalis muscle mass, L_YM64

Analysis of Variance

Source	DF	Sum of Squares	Mean Square	F Value	Prob>F
Model	8	0.04720	0.00590	1.729	0.1354
Error	28	0.09557	0.00341		
C Total	36	0.14277			

Root MSE	0.05842	R-square	0.3306
Dep Mean	2.30053	Adj R-sq	0.1394
C.V.	2.53955		

Parameter Estimates

Variable	DF	Parameter Estimate	Standard Error	T for H0: Parameter=0	Prob > |T|
INTERCEP	1	5.024991	2.90060819	1.732	0.0942
L_DVERT	1	-0.059374	0.17836608	-0.333	0.7417
L_DINSEC	1	-0.276998	0.17207041	-1.610	0.1187
L_DFRUIT	1	-0.239290	0.26739312	-0.895	0.3785
L_DSEED	1	-0.155603	0.22484896	-0.692	0.4946
L_DBUD	1	-0.165422	0.22042508	-0.750	0.4592
L_DLEAF	1	-0.116958	0.23294397	-0.502	0.6195
L_DROOT	1	0.133918	0.16218507	0.826	0.4159
L_DGUM	1	-0.305012	0.14858116	-2.053	0.0495

Dep. Var.: Resultant efficiency, L_YM66

Analysis of Variance

Source	DF	Sum of Squares	Mean Square	F Value	Prob>F
Model	8	0.05542	0.00693	1.166	0.3533
Error	28	0.16633	0.00594		
C Total	36	0.22175			

Root MSE	0.07707	R-square	0.2499
Dep Mean	2.29852	Adj R-sq	0.0356
C.V.	3.35321		

Parameter Estimates

Variable	DF	Parameter Estimate	Standard Error	T for H0: Parameter=0	Prob > |T|
INTERCEP	1	2.222445	3.82660333	0.581	0.5660
L_DVERT	1	0.038416	0.23530797	0.163	0.8715
L_DINSEC	1	-0.423165	0.22700246	-1.864	0.0728
L_DFRUIT	1	0.179984	0.35275616	0.510	0.6139
L_DSEED	1	0.178897	0.29663013	0.603	0.5513
L_DBUD	1	-0.095252	0.29079396	-0.328	0.7457
L_DLEAF	1	0.086104	0.30730941	0.280	0.7814
L_DROOT	1	0.161331	0.21396131	0.754	0.4571
L_DGUM	1	-0.093210	0.19601446	-0.476	0.6381

All data are delt log transformed. L_DVERT, vertebrate fauna; L_DINSEC, invertebrate fauna; L_DFRUIT, fruit; L_DSEED, seeds and nuts; L_DBUD, buds, stems, flowers and young leaves; L_DLEAF, mature leafs; L_ROOT, underground plants; L_DGUM, exudates.

The prediction that fruit and gum eaters require greater anterior bite force and that leaf and insect eaters require greater posterior bite force (e.g., Richard, 1985) is not consistent with the evidence presented here. While a shift towards gumnivory is associated with a high anterior bite force *relative to posterior bite force*, absolute anterior MBF is quite low. The results of the present analysis signify that masticatory mechanics do not necessarily become specialized to conform to an increase or decrease of a given food type. Most anthropoids appear to be generalists when it comes to masticatory mechanics. Specialization is more likely to occur in the dental morphology of specific anthropoids (Kay, 1976, 1977; Richard, 1985:190-194). Consistent with this view, Smith (1993) has argued that variation of dental morphology together with stability of masticatory mechanics marks the evolution of the mammalian trophic apparatus.

Reproduced with permission of the copyright owner. Further reproduction prohibited without permission.

Dietary Categories

Tukey's multiple comparison ANOVA, modified by Kramer (1956) to handle unequal group sizes, was applied to the masticatory data to test for significant differences among dietary groups (see Dunnett, 1980; SAS Inc., 1990:944-948). The results are presented in Box 14.14, and can be summarized as follows. (1) Maximum anterior and posterior bite force magnitudes (examined separately) were found to be significantly greater in hard object feeders, fruit/omnivores, leaf with fruit eaters, and frugivores compared to gumnivores. (2) The anterior-to-posterior bite force index was greatest in gumnivores, second greatest, although significantly less, in omnivores, and least in hard object feeders. (3) The anterior placement of masseter muscle attachment was found to be greatest in omnivores and least in hard object feeders and insectivores, whereas the anterior attachment of the temporalis muscle was greatest in gumnivores (significantly greater than all other dietary groups save omnivores) and least in fruit with insect eaters and insectivores. (4) Insectivores are distinct from all other dietary types (with the possible exception of gumnivores) in having the greatest lever efficiency. (5) With respect to temporalis muscle mass, hard food eaters exhibit significantly greater cross sectional area than gumnivores (a pattern no doubt related to body size) (6) Finally, due to the fact that insectivores are represented by a single specimen, nonsignificance of mean differences between this dietary category and others should not be taken to imply equality of group means. The results also support the conclusion of Shea (1983) who found no significant differences in masticatory morphology between frugivorous chimpanzees and folivorous gorillas (Hypothesis I, Box 14.1).

Reproduced with permission of the copyright owner. Further reproduction prohibited without permission.

Reproduced with permission of the copyright owner. Further reproduction prohibited without permission.

Box 14.14. SAS output of Tukey's studentized range test for differences among multiple means (V-level anthropoid data).

Dep. Var.: Ant. bite force, L_YV57

Tukey's Studentized Range (HSD) Test for variable: L_YV57

NOTE: This test controls the type I experimentwise error rate.

Alpha= 0.05 Confidence= 0.95 df= 290 MSE= 0.004661
Critical Value of Studentized Range= 4.420

Comparisons significant at the 0.05 level are indicated by '***'.

CTDIET Comparison	Simultaneous Lower Confidence Limit	Difference Between Means	Simultaneous Upper Confidence Limit	
FO - FV	0.00023	0.05303	0.10583	***
FO - GM	0.01879	0.08996	0.16112	***
LF - GM	0.01347	0.08627	0.15906	***
FR - GM	0.01054	0.08579	0.16105	***
HF - GM	0.01984	0.10488	0.18991	***

Means with the same letter are not significantly different.

Tukey Grouping			Mean	N	CTDIET
	A		2.32514	17	HF
	A	C	2.31022	89	FO
	A	C	2.30653	61	LF
	A	C	2.30606	41	FR
B	A	C	2.29931	1	IN
B	A	C	2.27893	20	O
B	A	C	2.27041	40	FB
B		C	2.25719	20	FV
B			2.22027	10	GM

Dep. Var: Post. bite force, L_YV58

Tukey's Studentized Range (HSD) Test for variable: L_YV58

NOTE: This test controls the type I experimentwise error rate.

Alpha= 0.05 Confidence= 0.95 df= 290 MSE= 0.004342
Critical Value of Studentized Range= 4.420

Comparisons significant at the 0.05 level are indicated by '***'.

CTDIET Comparison	Simultaneous Lower Confidence Limit	Difference Between Means	Simultaneous Upper Confidence Limit	
HF - FV	0.001765	0.069699	0.137632	***
HF - GM	0.042378	0.124448	0.206517	***
FO - GM	0.035572	0.104255	0.172938	***
LF - GM	0.025547	0.095804	0.166061	***
FR - GM	0.017452	0.090083	0.162713	***

Means with the same letter are not significantly different.

Tukey Grouping			Mean	N	CTDIET
	A		2.33370	17	HF
	A	C	2.31351	89	FO
	A	C	2.30506	61	LF
	A	C	2.29934	41	FR
B	A	C	2.29842	1	IN
B	A	C	2.27534	40	FB
B	A	C	2.26673	20	O
B		C	2.26401	20	FV
B			2.20926	10	GM

Reproduced with permission of the copyright owner. Further reproduction prohibited without permission.

Box 14.14. SAS output of Tukey's studentized range test for differences among multiple means (V-level anthropoid data).

Dep. Var.: Rel A-P bite force, L_YV59

Tukey's Studentized Range (HSD) Test for variable: L_YV59

NOTE: This test controls the type I experimentwise error ra

Alpha= 0.05 Confidence= 0.95 df= 290 MSE= 0.00682
Critical Value of Studentized Range= 4.420

Comparisons significant at the 0.05 level are indicated by '**

CTDIET Comparison		Simultaneous Lower Confidence Limit	Difference Between Means	Simultaneous Upper Confidence Limit	
GM	- O	0.02653	0.12649	0.22646	***
GM	- FR	0.08379	0.17482	0.26585	***
GM	- LF	0.09318	0.18124	0.26930	***
GM	- FO	0.13207	0.21815	0.30423	***
GM	- FV	0.12070	0.22066	0.32063	***
GM	- FB	0.15368	0.24494	0.33619	***
GM	- HF	0.19580	0.29866	0.40152	***
O	- FO	0.02779	0.09166	0.15553	***
O	- FV	0.01255	0.09417	0.17579	***
O	- FB	0.04776	0.11844	0.18913	***
O	- HF	0.08702	0.17217	0.25731	***
FR	- FB	0.01275	0.07012	0.12748	***
FR	- HF	0.04938	0.12384	0.19829	***
LF	- FB	0.01118	0.06370	0.11621	***
LF	- HF	0.04663	0.11742	0.18820	***
FO	- HF	0.01219	0.08051	0.14882	***

Means with the same letter are not significantly different.

Tukey Grouping	Mean	N	CTDIET
A	2.49937	10	GM
B	2.37287	20	O
B C	2.32454	41	FR
B C	2.31813	61	LF
C D	2.28121	89	FO
C D E	2.27870	20	FV
D E	2.25443	40	FB
A B C D E	2.22903	1	IN
E	2.20071	17	HF

Dep. Var.: A-P position of masseters, L_YV61

Tukey's Studentized Range (HSD) Test for variable: L_YV61

NOTE: This test controls the type I experimentwise error rate.

Alpha= 0.05 Confidence= 0.95 df= 290 MSE= 0.006926
Critical Value of Studentized Range= 4.420

Comparisons significant at the 0.05 level are indicated by '***'.

CTDIET Comparison		Simultaneous Lower Confidence Limit	Difference Between Means	Simultaneous Upper Confidence Limit	
O	- LF	0.03323	0.10025	0.16727	***
O	- GM	0.01498	0.11572	0.21645	***
O	- FR	0.05181	0.12275	0.19369	***
O	- FO	0.05995	0.12432	0.18868	***
O	- HF	0.04523	0.13104	0.21684	***
FV	- FR	0.00026	0.07120	0.14214	***
FV	- FO	0.00841	0.07277	0.13714	***
FB	- FO	0.00697	0.05648	0.10599	***

Means with the same letter are not significantly different.

Tukey Grouping	Mean	N	CTDIET
A	2.39623	20	O
A B	2.34468	20	FV
A B C	2.32839	40	FB
B C D	2.29597	61	LF
B C D	2.28051	10	GM
C D	2.27348	41	FR
D E	2.27191	89	FO
B C E	2.26519	17	HF
A B C E	2.22730	1	IN

Reproduced with permission of the copyright owner. Further reproduction prohibited without permission.

Box 14.14. SAS output of Tukey's studentized range test for differences among multiple means (V-level anthropoid data).

Dep. Var.: A-P position of temporalis, L_YV62

Tukey's Studentized Range (HSD) Test for variable: L_YV62

NOTE: This test controls the type I experimentwise error rate.

Alpha= 0.05 Confidence= 0.95 df= 290 MSE= 0.005735
Critical Value of Studentized Range= 4.420

Comparisons significant at the 0.05 level are indicated by '***'.

CTDIET Comparison	Simultaneous Lower Confidence Limit	Difference Between Means	Simultaneous Upper Confidence Limit	
GM - FV	0.00662	0.09829	0.18996	***
GM - FO	0.04956	0.12850	0.20744	***
GM - LF	0.05324	0.13399	0.21474	***
GM - FR	0.05853	0.14201	0.22549	***
GM - HF	0.05514	0.14947	0.24380	***
GM - FB	0.06965	0.15333	0.23702	***
GM - IN	0.00817	0.25641	0.50466	***
O - FB	0.00662	0.07144	0.13626	***

Means with the same letter are not significantly different.

Tukey Grouping	Mean	N	CTDIET
A	2.42516	10	GM
A B	2.34327	20	O
B C	2.32687	20	FV
B C	2.29666	89	FO
B C	2.29117	61	LF
B C	2.28315	41	FR
B C	2.27569	17	HF
C	2.27183	40	FB
B C	2.16875	1	IN

Dep. Var.: Lever efficiency, L_YV63

Tukey's Studentized Range (HSD) Test for variable: L_YV63

NOTE: This test controls the type I experimentwise error rate.

Alpha= 0.05 Confidence= 0.95 df= 290 MSE= 0.002729
Critical Value of Studentized Range= 4.420

Comparisons significant at the 0.05 level are indicated by '***'.

CTDIET Comparison	Simultaneous Lower Confidence Limit	Difference Between Means	Simultaneous Upper Confidence Limit	
IN - FB	0.017485	0.182791	0.348097	***
IN - O	0.016281	0.183590	0.350900	***
IN - FO	0.024389	0.188581	0.352773	***
IN - HF	0.023257	0.191269	0.359280	***
IN - FR	0.040616	0.205873	0.371129	***
IN - LF	0.042100	0.206710	0.371321	***
IN - FV	0.051373	0.218683	0.385993	***
GM - FV	0.000925	0.064162	0.127399	***

Means with the same letter are not significantly different.

Tukey Grouping	Mean	N	CTDIET
A	2.48919	1	IN
A B	2.33467	10	GM
B C	2.30640	40	FB
B C	2.30560	20	O
B C	2.30061	89	FO
B C	2.29792	17	HF
B C	2.28332	41	FR
B C	2.28248	61	LF
C	2.27051	20	FV

Reproduced with permission of the copyright owner. Further reproduction prohibited without permission.

Box 14.14. SAS output of Tukey's studentized range test for differences among multiple means (V-level anthropoid data).

Dep. Var.: Temporalis muscle mass, L_YV64

Tukey's Studentized Range (HSD) Test for variable: L_YV64

NOTE: This test controls the type I experimentwise error rate.

Alpha= 0.05 Confidence= 0.95 df= 290 MSE= 0.003518
Critical Value of Studentized Range= 4.420

Comparisons significant at the 0.05 level are indicated by '***'.

CTDIET Comparison	Simultaneous Lower Confidence Limit	Difference Between Means	Simultaneous Upper Confidence Limit	
HF - FB	0.001198	0.054866	0.108535	***
HF - GM	0.074561	0.148435	0.222310	***
FO - GM	0.066300	0.128125	0.189949	***
LF - GM	0.057271	0.120513	0.183754	***
FR - GM	0.046837	0.112215	0.177592	***
O - GM	0.023211	0.095004	0.166797	***
FB - GM	0.028031	0.093569	0.159107	***
FV - GM	0.020578	0.092371	0.164164	***

Means with the same letter are not significantly different.

Tukey Grouping	Mean	N	CTDIET
A	2.33421	17	HF
A B	2.31390	89	FO
A B	2.30629	61	LF
A B	2.29799	41	FR
A B	2.28078	20	O
B	2.27935	40	FB
A B	2.27815	20	FV
A B C	2.26291	1	IN
C	2.18578	10	GM

Dep. Var.: Rel. temporalis muscle mass, S_L_YV64

Tukey's Studentized Range (HSD) Test for variable: S_L_YV64
NOTE: This test controls the type I experimentwise error rate.

Alpha= 0.05 Confidence= 0.95 df= 290 MSE= 0.000425
Critical Value of Studentized Range= 4.420

Comparisons significant at the 0.05 level are indicated by '***'.

CTDIET Comparison	Simultaneous Lower Confidence Limit	Difference Between Means	Simultaneous Upper Confidence Limit	
FV - FB	0.015258	0.032899	0.050539	***
FV - FO	0.020880	0.036820	0.052760	***
FV - FR	0.029421	0.046990	0.064558	***
FV - HF	0.029449	0.050698	0.071947	***
FV - O	0.050476	0.070846	0.091215	***
FV - GM	0.057131	0.082078	0.107026	***
LF - FB	0.006339	0.019444	0.032550	***
LF - FO	0.012659	0.023366	0.034073	***
LF - FR	0.020527	0.033535	0.046544	***
LF - HF	0.019577	0.037243	0.054909	***
LF - O	0.040794	0.057391	0.073989	***
LF - GM	0.046648	0.068624	0.090600	***
FB - O	0.020306	0.037947	0.055587	***
FB - GM	0.026406	0.049180	0.071953	***
FO - LF	-0.034073	-0.023366	-0.012659	***
FO - O	0.018086	0.034026	0.049965	***
FO - GM	0.023775	0.045258	0.066742	***
FR - O	0.006287	0.023856	0.041424	***
FR - GM	0.012371	0.035089	0.057807	***
HF - GM	0.005710	0.031381	0.057051	***

Means with the same letter are not significantly different.

Tukey Grouping	Mean	N	CTDIET
A	0.03581	20	FV
A	0.02236	61	LF
B	0.00292	40	FB
B	-0.00101	89	FO
A B C	-0.00609	1	IN
B	-0.01118	41	FR
B D	-0.01488	17	HF
C D	-0.03503	20	O
C	-0.04626	10	GM

Effects of Masticatory Mechanics on Maximum Bite Force

The analyses in this section were intended to examine the predicted relationships between properties of the masticatory apparatus and bite force magnitude and distribution (paths F & 3, Box 14.1). A series of analyses in which MBF magnitudes (adjusted for size) were regressed on properties of the masticatory system yielded the following results: (1) about 63% of the variation observed in anterior bite force was accounted for by the combination of lever efficiency and temporalis muscle mass, (2) approximately 72% of the variation in posterior bite force was accounted for by temporalis muscle mass alone, and (3) about 23% of the variation in anterior-to-posterior bite force ratio was accounted for by lever efficiency alone (see Box 14.15). Multiple regression analysis gave the same results.

Box 14.15. Predicted bivariate statistical associations and properties deduced from hypotheses statements.

Predicted bivariate associations (dependent variable in bold)	Regression slope (95% CL) and test of significant association, R^2 (p-value)
Anterior bite force [ΔS_L_YV57] ←	
A-P position of masseter muscle [ΔL_YV61]	-0.02 (-0.06, 0.02) R^2 = 0.00 (ns)
A-P position of temporalis muscle [ΔL_YV62]	0.00 (-0.04, 0.05) R^2 = 0.00 (ns)
Lever efficiency [ΔL_YV63]	0.23 (0.16, 0.30) R^2 = 0.14 (p < .05)
Temporalis muscle mass [ΔS_L_YV64]	0.84 (0.74, 0.94) R^2 = 0.49 (p < .01)
Resultant vector efficiency [ΔL_YV66]	-0.03 (-0.07, -0.02) R^2 = 0.00 (ns)
Posterior bite force [ΔS_L_YV58] ←	
A-P position of masseter muscle [ΔL_YV61]	-0.04 (-0.08, 0.00) R^2 = 0.01 (ns)
A-P position of temporalis muscle [ΔL_YV62]	-0.04 (-0.08, 0.00) R^2 = 0.01 (ns)
Lever efficiency [ΔL_YV63]	0.10 (0.04, 0.17) R^2 = 0.03 (ns)
Temporalis muscle mass [ΔS_L_YV64]	0.94 (0.88, 1.01) R^2 = 0.72 (p < .01)
Resultant vector efficiency [ΔL_YV66]	-0.04 (-0.08, -0.00) R^2 = 0.01 (ns)
Relative A-P bite force [ΔL_YV59] ←	
A-P position of masseter muscle [ΔL_YV61]	0.17 (0.05, 0.30) R^2 = 0.03 (ns)
A-P position of temporalis muscle [ΔL_YV62]	0.31 (0.18, 0.44) R^2 = 0.07 (ns)
Lever efficiency [ΔL_YV63]	0.86 (0.68, 1.04) R^2 = 0.23 (p < .01)
Temporalis muscle mass [ΔS_L_YV64]	-0.87 (-1.24, -0.48) R^2 = 0.06 (ns)
Resultant vector efficiency [ΔL_YV66]	-0.03 (-0.16, 0.10) R^2 = 0.00 (ns)

Reproduced with permission of the copyright owner. Further reproduction prohibited without permission.

Effects of Maximum Bite Force and Nasomaxillary Morphology

Predicted relationships between maximum bite force magnitudes and distribution and nasomaxillary features (path BC, Box 14.1) were examined using bivariate regression analysis. The results are given in Box 14.16, and can be summarized as follows:

(1) Anterior MBF does not explain a significant proportion of the variation of maxillary nasal process width among anthropoids. Thus, Endo's (1970) hypothesis (see Box 14.7, Predictions 58 & 59) that the enlargement of these processes represents an adaptation to dissipate large compressive forces produced during anterior biting is inconsistent with the anthropoid data.

(2) The hypothesis advanced by Demes (1987), that a rounded anterior nasal aperture is a structural adaptation to resist torsional rotation caused by heavy unilateral biting, is inconsistent with the results of the present analysis. While both anterior and posterior bite force magnitudes explain a small proportion of the variation in anterior piriform breadth, the M-level covariance is in the opposite direction from that predicted by Demes (Box 14.7, Prediction 56). Increased anterior bite force magnitude was found to be (significantly) negatively associated with anterior nasal aperture breadth in New World monkeys and apes (but not in Old World monkeys).

Consistent with this finding, Hylander (1977) hypothesized that high anterior bite forces are dissipated around either side of nasal aperture between the orbits to glabella. As a consequence, some anthropoid species (e.g., *Alouatta*)exhibit wide internasal distances and narrow anterior nasal apertures. In yet another example, Hylander (1977) observed that North American Eskimos

Reproduced with permission of the copyright owner. Further reproduction prohibited without permission.

possess both high anterior bite force and relatively narrow anterior nasal apertures, although he speculated that the cold climate could also have contributed to this attribute.

(3) It is not surprising that both anterior and posterior MBF magnitudes account for a significant proportion of the variance (22% and 39%, respectively) of relative bizygomatic breadth. This character is highly correlated with temporalis muscle mass ($r = 0.64$, $p < 0.0001$), which directly contributes to MBF. That both the Q-level and M-level portions of the data are significant is consistent with the observation that muscle mass and the bone with which it comes into contact are susceptible to both acclimational and selectional mechanisms of change. The positive association between maximum bite force and bizygomatic breadth is consistent across all major anthropoid taxa. Numerous experimental and nonexperimental studies have reported a positive relationship between MBF and bizygomatic breadth (see Box 14.3, Hypothesis B, and Box 14.6, Predictions 37-39).

(4) Anterior MBF accounted for a significant proportion of the variance (18%) of anteroposterior position of the zygomatic root. Recall from Chapter 9 that as the maxillary arch is displaced forward during growth the zygomatic root is not carried along with it. Rather, due to a combination of sutural apposition and bone remodeling the zygoma drifts posteriorly in relation to the maxillary arch. That both the M-level and, at least in some taxa, Q-level portions of the variance of anterior and posterior bite force were significant indicates that zygomatic root position is affected by both acclimational and selectional nomological mechanisms. Indeed, Hylander and Johnson (1997) found that the magnitude of strain along the

Reproduced with permission of the copyright owner. Further reproduction prohibited without permission.

zygomatic arch was highest near the root, and suggested that this was due to masseter muscle pull which is concentrated at the anterior end of the arch. Thus, the posteroinferior pull of the masseter could be at least partially responsible for the observed backwards migration (or lack of forward migration) of the zygoma during development. Anterior bite forces, in particular, will tend to augment this process because it has been shown that incisal biting causes tensile strain along the lateral aspect of the maxilla (Endo, 1973; Demes, 1987; Demes & Creel, 1988) and up along the frontal process of the zygoma (Endo, 1973; Oyen *et al.*, 1996), resulting in separation at the zygomaticomaxillary sutures. By contrast, molar biting results in either much lower tensile strain or compressive strain in these regions (e.g., Endo, 1973; Alexandridis *et al.*, 1985). The combined action of nasomaxillary bending and masseter muscle pull during incisal biting could partially account for the observed posterior drift of the zygoma during growth. However, the significant positive association between zygomatic root position and anterior MBF magnitudes indicates that as the zygoma drifts posteriorly MBF magnitudes at the anterior teeth diminish, establishing a negative feedback mechanism.

(5) The significant degree of correspondence between maxillary arch length and anterior-to-posterior bite force ratio (r = -0.49) can be explained topographically—that is, due to the nature of the mechanical system. A short maxillary arch will always produce a high anterior-to-posterior bite force ratio. Therefore, maxillary arch length is not necessarily an acclimational or selectional response to high relative anterior MBF. On the other hand, if a high anterior-to-posterior bite force ratio is required for a given dietary regime then one way to achieve it would be to shorten maxillary arch length.

Reproduced with permission of the copyright owner. Further reproduction prohibited without permission.

(6) Anterior MBF can explain a significant proportion of the variance (12-16%) of anterior facial length (including nasal bone length). There is a significant negative association between anterior bite force and anterior facial length for all of the anthropoid taxa examined, except hominoids. This finding confirms the prediction that anthropoids with relatively high anterior bite forces tend to have relatively short anterior faces and short nasal bones (Box 14.7, Prediction 15). However, only the M-level data are significant suggesting that the relationship is due to selectional nomological mechanisms. Therefore, hypotheses postulating either a positive (Kiliaridis, 1986) or negative (Chuang, 1995) *acclimational* effect of bite force on facial length do not gain support from this analysis. However, the hypothesis that reduced anterior facial length is an *adaptation* (albeit weak) to reduce bending strains on the anterior part of the facial skeleton (e.g., Jolly, 1970, Kinzey, 19) cannot be refuted at present.

(7) There are three main hypotheses regarding the relationship between posterior facial height (or "vertical" facial height) and masticatory mechanics. The first proposes that increased posterior facial height produces greater MBF magnitudes by altering the mechanical system (*cf.* Rak, 1983). For example, Demes and Creel (1988) have asserted that increased vertical facial height produces a high masseter lever arm ratio and thus higher MBFs (Box 14.7, Prediction 36). However, this postulate is not borne out by the anthropoid data—the correlation between posterior facial height and masticatory lever arm ratio is not statistically significant ($r = 0.08$, $p > 0.05$), nor is the correlation between ramus height and lever arm ratio or MBF. This finding is consistent with Greaves' triangle of support model, which predicts that no increase in mechanical advantage will be

Reproduced with permission of the copyright owner. Further reproduction prohibited without permission.

gained by an increase in vertical facial height. Similarily, Southard *et al.* (1990) in an analysis of masticatory factors influencing anterior bite force concluded that "the perpendicular distance from the top of the mandibular condyle to the occlusal plane" had no direct effect on the anterior component of occlusal force.

The second hypothesis is that greater posterior facial height is better suited to resist high strain magnitudes, due either to nasomaxillary bending caused by high anterior bite forces (Hylander, 1977; Rak, 1983; Demes & Creel, 1988), or to high posterior bite forces (Rak, 1983). Several studies have shown a correspondence between vertical facial height and masticatory function. Subsequent to the unilateral removal of the mandibular condyles of young rhesus and *Saimiri* monkeys, Sarnat (1973) found a reduction of vertical facial height and alveolar bone on the operated side compared to the unoperated side. However, these results do not provide support for the second hypothesis. Post-operative animals would have been forced to bite on the *operated side* (because the contralateral TMJ acts as the effective fulcrum during unilateral biting). Thus, the observation that only the operated side exhibited a reduction of posterior facial height is opposite of that predicted by the hypothesis. The results of the present analysis also contradict the hypothesis that posterior facial height helps resist high bite force magnitudes . A negative association between maximum bite force magnitudes and posterior facial height was found to exit in anthropoids (Box 14.16).

Rak (1983, p. 117) further proposed that the sheer size of the temporalis muscles necessitates increased vertical facial height. In fact, the anthropoid data show the opposite trend: temporalis muscle mass (as measured by the area of the infratemporal foramen) is negatively correlated with posterior facial height (r = -

Reproduced with permission of the copyright owner. Further reproduction prohibited without permission.

0.37, $p = 0.02$; $df = 36$). *Homo*, *Callithrix*, *Aotus* and *Saimiri*, for example, all have small temporalis muscles but high vertical faces relative to body size, whereas *Colobus*, *Hylobates* and *Brachyteles* all exhibit the opposite trend. Perhaps increased posterior facial height reflects an increase in the length of the masticatory musculature in compensation for reduced cross-sectional area.

(8) The evidence indicates a weak, but consistent, degree of covariance between palatal width and MBF magnitudes: specifically, anterior and posterior bite force accounts for roughly 10% of the variance of palatal width at P^3, and anterior-to-posterior bite force ratio explains 23% of the variance of inter-M^3 palatal width. Multi-level analysis shows that both the M-level and Q-level components of maximum bite force magnitude are significantly (positively) associated with maxillary width (e.g., Box 14.24). Thus, the anthropoid data support the hypothesis advanced by Thomason and Russell (1986) that the palate acts to resist torsional and bending forces generated during mastication. Moreover, the association between anterior-to-posterior bite force ratio and posterior palatal width may help explain an observation reported in Chapter 9—that relatively long maxillary arches also tend to be narrow, whereas short maxillary arches tend to be wide. The greater maximum anterior-to-posterior bite forces generated by specimens with short maxillary arches may be resisted by an increase in maxillary width.

I have already argued that the observed correlation between anterior-to-posterior MBF ratio and maxillary arch length is due to a topographical relationship. It follows that the correlation between anterior-to-posterior MBF ratio and maxillary arch width may be spurious, due to the common influence of

Reproduced with permission of the copyright owner. Further reproduction prohibited without permission.

maxillary arch length (assuming that maxillary length constrains width in some fashion). This interpretation may explain why Janis (1990), in a comparative study of ungulates, found no correspondence between palatal width and diet. However, consistent with the mechanical/functional interpretation, when anterior-to-posterior MBF ratio is regressed against maxillary width with the effects of maxillary length controlled for in the analysis, the two variables remain significantly correlated at $\alpha = 0.05$. Thus, the alternative hypothesis that increased maxillary breadth is an adaptation to resist the high anterior masticatory forces generated in anthropoids with relatively short faces cannot be rejected.

(9) Analysis of the anthropoid data indicate that only *anterior* palatal depth covaries significantly with MBF magnitudes (in all taxa but cercopithecoids). More specifically, MBF at I^2 was shown to be negatively correlated with palatal depth at I^2 ($r = -0.46$, $p < 0.01$, $df = 36$), and, MBF at P^3 was negatively correlated with palatal depth at P^3 ($r = -0.39$, $p < 0.05$, $df = 36$). These findings are consistent with the experimental results of Beecher *et al.* (1983) who reported that squirrel monkeys fed a soft food diet developed deep, arched maxillary palates compared to monkeys fed a diet of "naturally tough" food items. However, a multi-level analysis of the effects of I^2 MBF on anterior palatal depth yielded significant negative slopes only for the M-level component of the data, indicating that the association is maintain through selectional rather than acclimational nomological mechanisms, as predicted by Beecher *et al.*'s experiments. Nonetheless, anterior MBF appears to have a nomological effect (whether acclimational or selectional) on anterior palatal depth, such that high bite force magnitudes evoke shallow anterior palates.

Reproduced with permission of the copyright owner. Further reproduction prohibited without permission.

(10) Facial prognathism (both measures) covaried with MBF in the same way that maxillary arch length covaried with MBF: anterior-to-posterior MBF magnitude was found to be negatively correlated with facial prognathism. This finding is consistent with the predictions of Demes and Creel (1988; Box 14.7, Predictions 6 & 28). In addition, posterior MBF was found to be positively associated to Krogman's angle of facial prognathism, with the former accounting for about 10% of the variance in the latter. The positive relationship between posterior MBF and facial prognathism is consistent with previous observations by Carlson and Schneiderman (1983) and Kiliaridis (1986) (Box 14.7, Predictions 2 & 24). A multi-level analysis showed that only the M-level component of the data was significant, in all major anthropoid taxa except cercopithecines, for which no significant association was detected.

(11) M-level anterior and posterior maximum bite force magnitudes were found to be negatively associated with facial convexity (Boxes 14.27 & 14.28). Thus, there appears to be an evolutionary correspondence (driven by selectional mechanisms) between high relative MBF and concave facial profiles among anthropoids (with the exception of cercopithecines). This correspondence is most clearly manifest in *Pongo*, *Pan*, *Gorilla*, and *Allouatta*, which all exhibit high relative anterior bite force magnitudes and concave facial profiles (see Boxes 4..5, 4.35, 4.38, 4.41); and in the low relative bite force magnitudes and convex facial profiles of *Homo*, *Aotus*, *Saimiri*, *Callithrix* and *Callimico* (see Boxes 4.15, 4.16, 4.18, 4.19, 4.39) Interestingly, cercopithecines exhibit the exact opposite correspondence—there is a positive association between MBF and facial convexity. For example, *Papio hamadryas* exhibits relatively low delta posterior MBF

Reproduced with permission of the copyright owner. Further reproduction prohibited without permission.

magnitude and low facial convexity, whereas *Macaca nemestrina* exhibits both high MBF and facial convexity. Thus, only cercopithecines conform to the relationship proposed by Demes (1987) who predicted on the basis of engineering principles that high bite force magnitudes would best be resisted by a convex facial profile (Box 14.6, Predictions 52 & 53).

(12) A taxonomic distinction was also found regarding the relationship between anterior MBF magnitudes and paranasal plate orientation. All major catarrhine taxa exhibited a significant negative association between these two characters (M-level only), whereas cebids manifest a significant positive (M-level) association, and atelids no significant association. Thus, in catarrhines, coronal orientation of the paranasal plates appear to proffer a selective advantage with respect to the generation of high bite force magnitudes, especially anterior bite force magnitudes; while in cebids, sagittal orientation of the paranasal plates appear to have a similar effect. The positive association observed among cebids is consistent with that predicted by Demes (1987) (Box 14.7, Prediction 60), who argued that great anterior bite force magnitudes should be associated with sagittally oriented paranasal plates, as she had observed in Neanderthals. At the present, these taxon-specific differences in the nomological effects of mastication on nasomaxillary form remain unexplained.

Reproduced with permission of the copyright owner. Further reproduction prohibited without permission.

Box 14.16. Multi-level bivariate regressions of nasomaxillary characters on MBF properties.

Predicted bivariate associations (dependent variable in bold)	Regression slope (95% CL) and test of significant association, F-stat (p-value), and Model R^2
Nasal bone length [ΔS_L_YV1] ←	
Q-Level anterior bite force [ΔS_L_YQ57]	-0.24 (-0.53, 0.05) $F = 2.68$ (ns)
M-Level anterior bite force [ΔS_L_YM57]	-0.85 (-1.07, -0.62) $F = 53.49$ ($p < .01$)
	Model $R^2 = 0.16$
Q-Level posterior bite force [ΔS_L_YQ58]	-0.32 (-0.69, 0.04) $F = 2.94$ (ns)
M-Level posterior bite force [ΔS_L_YM58]	-0.57 (-0.81, -0.33) $F = 20.97$ ($p < .01$)
	Model $R^2 = 0.07$
Q-Level A-P bite force ratio [ΔL_YQ59]	-0.04 (-0.17, 0.09) $F = 0.30$ (ns)
M-Level A-P bite force ratio [ΔL_YM59]	-0.14 (-0.22, -0.06) $F = 12.83$ ($p < .01$)
	Model $R^2 = 0.04$
Nasal process of maxilla width [ΔS_L_YV4] ←	
Q-Level anterior bite force [ΔS_L_YQ57]	0.15 (-0.27, 0.58) $F = 0.51$ (ns)
M-Level anterior bite force [ΔS_L_YM57]	0.41 (0.08, 0.75) $F = 5.91$ ($p < .05$)
	Model $R^2 = 0.02$
Q-Level posterior bite force [ΔS_L_YQ58]	0.18 (-0.34, 0.69) $F = 0.44$ (ns)
M-Level posterior bite force [ΔS_L_YM58]	0.32 (-0.02, 0.66) $F = 3.31$ (ns)
	Model $R^2 = 0.01$
Q-Level A-P bite force ratio [ΔL_YQ59]	0.04 (-0.14, 0.22) $F = 0.21$ (ns)
M-Level A-P bite force ratio [ΔL_YM59]	0.11 (0.00, 0.21) $F = 3.84$ (ns)
	Model $R^2 = 0.01$
Anterior nasal aperture height [ΔS_L_YV5] ←	
Q-Level anterior bite force [ΔS_L_YQ57]	0.02 (-0.16, 0.20) $F = 0.04$ (ns)
M-Level anterior bite force [ΔS_L_YM57]	0.09 (-0.05, 0.23) $F = 1.68$ (ns)
	Model $R^2 = 0.01$
Q-Level posterior bite force [ΔS_L_YQ58]	0.06 (-0.15, 0.28) $F = 0.33$ (ns)
M-Level posterior bite force [ΔS_L_YM58]	0.19 (0.05, 0.33) $F = 6.84$ ($p < .01$)
	Model $R^2 = 0.02$
Q-Level A-P bite force ratio [ΔL_YQ59]	-0.00 (-0.08, 0.08) $F = 0.01$ (ns)
M-Level A-P bite force ratio [ΔL_YM59]	-0.02 (-0.06, 0.02) $F = 0.77$ (ns)
	Model $R^2 = 0.00$
Anterior nasal aperture breadth [ΔS_L_YV6] ←	
Q-Level anterior bite force [ΔS_L_YQ57]	0.11 (-0.02, 0.24) $F = 2.64$ (ns)
M-Level anterior bite force [ΔS_L_YM57]	-0.22 (-0.32, -0.12) $F = 17.56$ ($p < .01$)
	Model $R^2 = 0.06$
Q-Level posterior bite force [ΔS_L_YQ58]	0.22 (0.06, 0.38) $F = 7.21$ ($p < .01$)
M-Level posterior bite force [ΔS_L_YM58]	-0.20 (-0.31, -0.10) $F = 14.34$ ($p < .01$)
	Model $R^2 = 0.07$
Q-Level A-P bite force ratio [ΔL_YQ59]	-0.03 (-0.09, 0.02) $F = 1.34$ (ns)
M-Level A-P bite force ratio [ΔL_YM59]	-0.02 (-0.06, 0.01) $F = 1.94$ (ns)
	Model $R^2 = 0.01$

Reproduced with permission of the copyright owner. Further reproduction prohibited without permission.

Box 14.16. Multi-level bivariate regressions of nasomaxillary characters on MBF properties.	
Posterior nasal aperture height [ΔS_L_YV7] ←	
Q-Level anterior bite force [ΔS_L_YQ57]	-0.08 (-0.27, 0.12) $F = 0.64$ (ns)
M-Level anterior bite force [ΔS_L_YM57]	-0.32 (-0.47, -0.16) $F = 16.26$ ($p < .01$)
	Model $R^2 = 0.05$
Q-Level posterior bite force [ΔS_L_YQ58]	-0.09 (-0.33, 0.15) $F = 0.53$ (ns)
M-Level posterior bite force [ΔS_L_YM58]	-0.35 (-0.51, -0.20) $F = 19.76$ ($p < .01$)
	Model $R^2 = 0.06$
Q-Level A-P bite force ratio [ΔL_YQ59]	-0.02 (-0.11, 0.06) $F = 0.25$ (ns)
M-Level A-P bite force ratio [ΔL_YM59]	0.03 (-0.02, 0.08) $F = 1.31$ (ns)
	Model $R^2 = 0.01$
Posterior nasal aperture breadth [ΔS_L_YV8] ←	
Q-Level anterior bite force [ΔS_L_YQ57]	0.05 (-0.13, 0.24) $F = 0.30$ (ns)
M-Level anterior bite force [ΔS_L_YM57]	0.05 (-0.10, 0.19) $F = 0.40$ (ns)
	Model $R^2 = 0.00$
Q-Level posterior bite force [ΔS_L_YQ58]	0.11 (-0.12, 0.33) $F = 0.86$ (ns)
M-Level posterior bite force [ΔS_L_YM58]	-0.21 (-0.35, -0.06) $F = 7.58$ ($p < .01$)
	Model $R^2 = 0.03$
Q-Level A-P bite force ratio [ΔL_YQ59]	-0.02 (-0.09, 0.06) $F = 0.19$ (ns)
M-Level A-P bite force ratio [ΔL_YM59]	0.12 (0.08, 0.17) $F = 30.02$ ($p < .01$)
	Model $R^2 = 0.09$
Nasoalveolar clivus length [ΔS_L_YV9] ←	
Q-Level anterior bite force [ΔS_L_YQ57]	-0.07 (-0.29, 0.16) $F = 0.33$ (ns)
M-Level anterior bite force [ΔS_L_YM57]	0.14 (-0.04, 0.32) $F = 2.41$ (ns)
	Model $R^2 = 0.01$
Q-Level posterior bite force [ΔS_L_YQ58]	-0.10 (-0.38, 0.17) $F = 0.55$ (ns)
M-Level posterior bite force [ΔS_L_YM58]	-0.02 (-0.20, 0.16) $F = 0.07$ (ns)
	Model $R^2 = 0.00$
Q-Level A-P bite force ratio [ΔL_YQ59]	-0.00 (-0.10, 0.09) $F = 0.00$ (ns)
M-Level A-P bite force ratio [ΔL_YM59]	0.11 (0.05, 0.16) $F = 14.09$ ($p < .01$)
	Model $R^2 = 0.05$
Zygomatic height [ΔS_L_YV11] ←	
Q-Level anterior bite force [ΔS_L_YQ57]	-0.09 (-0.33, 0.15) $F = 0.51$ (ns)
M-Level anterior bite force [ΔS_L_YM57]	-0.46 (-0.65, -0.27) $F = 21.95$ ($p < .01$)
	Model $R^2 = 0.07$
Q-Level posterior bite force [ΔS_L_YQ58]	-0.09 (-0.39, 0.22) $F = 0.30$ (ns)
M-Level posterior bite force [ΔS_L_YM58]	-0.27 (-0.47, -0.08) $F = 7.24$ ($p < .01$)
	Model $R^2 = 0.02$
Q-Level A-P bite force ratio [ΔL_YQ59]	-0.03 (-0.14, 0.08) $F = 0.31$ (ns)
M-Level A-P bite force ratio [ΔL_YM59]	-0.12 (-0.18, -0.06) $F = 13.92$ ($p < .01$)
	Model $R^2 = 0.05$

Reproduced with permission of the copyright owner. Further reproduction prohibited without permission.

Box 14.16. Multi-level bivariate regressions of nasomaxillary characters on MBF properties.

Bizygomatic breadth [ΔS_L_YV12] ←	
Q-Level anterior bite force [ΔS_L_YQ57]	0.11 (0.05, 0.17) $F = 11.21$ ($p < .01$)
M-Level anterior bite force [ΔS_L_YM57]	0.22 (0.17, 0.27) $F = 72.21$ ($p < .01$)
	Model $R^2 = 0.22$
Q-Level posterior bite force [ΔS_L_YQ58]	0.15 (0.09, 0.22) $F = 18.87$ ($p < .01$)
M-Level posterior bite force [ΔS_L_YM58]	0.30 (0.26, 0.35) $F = 168.25$ ($p < .01$)
	Model $R^2 = 0.39$
Q-Level A-P bite force ratio [ΔL_YQ59]	0.01 (-0.02, 0.04) $F = 0.21$ (ns)
M-Level A-P bite force ratio [ΔL_YM59]	-0.04 (-0.06, -0.03) $F = 29.05$ ($p < .01$)
	Model $R^2 = 0.09$
Anteroposterior position of zygomatic root [ΔS_L_YV13] ←	
Q-Level anterior bite force [ΔS_L_YQ57]	0.56 (0.16, 0.96) $F = 7.39$ ($p < .01$)
M-Level anterior bite force [ΔS_L_YM57]	1.26 (0.94, 1.58) $F = 60.35$ ($p < .01$)
	Model $R^2 = 0.18$
Q-Level posterior bite force [ΔS_L_YQ58]	0.49 (-0.03, 1.02) $F = 3.39$ (ns)
M-Level posterior bite force [ΔS_L_YM58]	0.82 (0.47, 1.16) $F = 21.40$ ($p < .01$)
	Model $R^2 = 0.08$
Q-Level A-P bite force ratio [ΔL_YQ59]	0.26 (0.08, 0.45) $F = 7.50$ ($p < .01$)
M-Level A-P bite force ratio [ΔL_YM59]	0.17 (0.06, 0.27) $F = 8.88$ ($p < .01$)
	Model $R^2 = 0.05$
Maxillary arch length [ΔS_L_YV14] ←	
Q-Level anterior bite force [ΔS_L_YQ57]	-0.15 (-0.30, -0.01) $F = 4.29$ ($p < .05$)
M-Level anterior bite force [ΔS_L_YM57]	-0.03 (-0.14, 0.09) $F = 0.21$ (ns)
	Model $R^2 = 0.02$
Q-Level posterior bite force [ΔS_L_YQ58]	-0.07 (-0.24, 0.11) $F = 0.54$ ($p < .01$)
M-Level posterior bite force [ΔS_L_YM58]	0.26 (0.14, 0.37) $F = 19.27$ ($p < .01$)
	Model $R^2 = 0.06$
Q-Level A-P bite force ratio [ΔL_YQ59]	-0.11 (-0.16, -0.05) $F = 14.77$ ($p < .01$)
M-Level A-P bite force ratio [ΔL_YM59]	-0.14 (-0.18, -0.11) $F = 78.15$ ($p < .01$)
	Model $R^2 = 0.24$
Anterior facial length [ΔS_L_YV17] ←	
Q-Level anterior bite force [ΔS_L_YQ57]	-0.10 (-0.24, 0.05) $F = 1.80$ (ns)
M-Level anterior bite force [ΔS_L_YM57]	-0.38 (-0.49, -0.26) $F = 42.14$ ($p < .01$)
	Model $R^2 = 0.12$
Q-Level posterior bite force [ΔS_L_YQ58]	-0.14 (-0.32, 0.05) $F = 2.09$ (ns)
M-Level posterior bite force [ΔS_L_YM58]	-0.25 (-0.37, -0.13) $F = 16.95$ ($p < .01$)
	Model $R^2 = 0.06$
Q-Level A-P bite force ratio [ΔL_YQ59]	-0.01 (-0.08, 0.06) $F = 0.07$ (ns)
M-Level A-P bite force ratio [ΔL_YM59]	-0.05 (-0.08, -0.01) $F = 5.24$ ($p < .05$)
	Model $R^2 = 0.02$

Reproduced with permission of the copyright owner. Further reproduction prohibited without permission.

Box 14.16. Multi-level bivariate regressions of nasomaxillary characters on MBF properties.	
Posterior facial height [ΔS_L_YV18] ←	
Q-Level anterior bite force [ΔS_L_YQ57]	-0.06 (-0.18, 0.06) $F = 0.93$ (ns)
M-Level anterior bite force [ΔS_L_YM57]	-0.12 (-0.21, -0.02) $F = 5.62$ ($p < .05$)
	Model $R^2 = 0.02$
Q-Level posterior bite force [ΔS_L_YQ58]	-0.10 (-0.25, 0.05) $F = 1.75$ (ns)
M-Level posterior bite force [ΔS_L_YM58]	-0.13 (-0.23, -0.04) $F = 7.29$ ($p < .01$)
	Model $R^2 = 0.03$
Q-Level A-P bite force ratio [ΔL_YQ59]	0.01 (-0.04, 0.06) $F = 0.12$ (ns)
M-Level A-P bite force ratio [ΔL_YM59]	0.06 (0.03, 0.09) $F = 15.36$ ($p < .01$)
	Model $R^2 = 0.05$
Ramus height [ΔS_L_YV19] ←	
Q-Level anterior bite force [ΔS_L_YQ57]	0.11 (-0.08, 0.30) $F = 1.29$ (ns)
M-Level anterior bite force [ΔS_L_YM57]	-0.04 (-0.19, 0.11) $F = 0.24$ (ns)
	Model $R^2 = 0.01$
Q-Level posterior bite force [ΔS_L_YQ58]	0.16 (-0.07, 0.39) $F = 1.90$ (ns)
M-Level posterior bite force [ΔS_L_YM58]	0.12 (-0.03, 0.27) $F = 2.46$ (ns)
	Model $R^2 = 0.01$
Q-Level A-P bite force ratio [ΔL_YQ59]	0.02 (-0.06, 0.10) $F = 0.17$ (ns)
M-Level A-P bite force ratio [ΔL_YM59]	-0.04 (-0.10, 0.00) $F = 3.33$ (ns)
	Model $R^2 = 0.01$
Inter-I^2 palatal width [ΔS_L_YV20] ←	
Q-Level anterior bite force [ΔS_L_YQ57]	-0.15 (-0.34, 0.03) $F = 2.67$ (ns)
M-Level anterior bite force [ΔS_L_YM57]	0.01 (-0.13, 0.16) $F = 0.03$ (ns)
	Model $R^2 = 0.01$
Q-Level posterior bite force [ΔS_L_YQ58]	-0.11 (-0.33, 0.11) $F = 0.93$ (ns)
M-Level posterior bite force [ΔS_L_YM58]	0.15 (0.00, 0.29) $F = 3.77$ (ns)
	Model $R^2 = 0.02$
Q-Level A-P bite force ratio [ΔL_YQ59]	-0.08 (-0.16, 0.00) $F = 4.03$ ($p < .05$)
M-Level A-P bite force ratio [ΔL_YM59]	0.06 (-0.11, -0.02) $F = 6.74$ ($p < .01$)
	Model $R^2 = 0.03$
Q-Level I^2 maximum bite force [ΔS_L_YQ51]	-0.12 (-0.27, 0.02) $F = 2.84$ (ns)
M-Level I^2 maximum bite force [ΔS_L_YM51]	-0.14 (-0.20, -0.08) $F = 23.93$ ($p < .01$)
	Model $R^2 = 0.08$
Inter-P^3 palatal width [ΔS_L_YV21] ←	
Q-Level anterior bite force [ΔS_L_YQ57]	-0.05 (-0.18, 0.08) $F = 0.56$ (ns)
M-Level anterior bite force [ΔS_L_YM57]	0.32 (0.22, 0.42) $F = 37.66$ ($p < .01$)
	Model $R^2 = 0.11$
Q-Level posterior bite force [ΔS_L_YQ58]	-0.03 (-0.18, 0.13) $F = 0.11$ (ns)
M-Level posterior bite force [ΔS_L_YM58]	0.31 (0.21, 0.42) $F = 34.73$ ($p < .01$)
	Model $R^2 = 0.10$
Q-Level A-P bite force ratio [ΔL_YQ59]	-0.03 (-0.09, 0.03) $F = 0.85$ (ns)
M-Level A-P bite force ratio [ΔL_YM59]	0.01 (-0.03, 0.04) $F = 0.08$ (ns)
	Model $R^2 = 0.00$
Q-Level P^3 maximum bite force [ΔS_L_YQ52]	0.00 (-0.11, 0.11) $F = 0.00$ (ns)
M-Level P^3 maximum bite force [ΔS_L_YM52]	-0.01 (-0.05, 0.03) $F = 0.22$ (ns) $R^2 = 0.00$

Reproduced with permission of the copyright owner. Further reproduction prohibited without permission.

Box 14.16. Multi-level bivariate regressions of nasomaxillary characters on MBF properties.	
Inter-M^1 palatal width [ΔS_L_YV22] ←	
Q-Level anterior bite force [ΔS_L_YQ57]	-0.03 (-0.15, 0.09) $F = 0.30$ (ns)
M-Level anterior bite force [ΔS_L_YM57]	0.23 (0.14, 0.32) $F = 23.69$ ($p < .01$)
	Model $R^2 = 0.08$
Q-Level posterior bite force [ΔS_L_YQ58]	-0.04 (-0.19, 0.11) $F = 0.31$ (ns)
M-Level posterior bite force [ΔS_L_YM58]	0.10 (0.01, 0.20) $F = 4.18$ ($p < .05$)
	Model $R^2 = 0.02$
Q-Level A-P bite force ratio [ΔL_YQ59]	-0.01 (-0.06, 0.05) $F = 0.04$ (ns)
M-Level A-P bite force ratio [ΔL_YM59]	0.07 (0.04, 0.10) $F = 23.29$ ($p < .01$)
	Model $R^2 = 0.07$
Q-Level M^1 maximum bite force [ΔS_L_YQ54]	-0.02 (-0.13, 0.09) $F = 0.12$ (ns)
M-Level M^1 maximum bite force [ΔS_L_YM54]	-0.05 (-0.09, -0.02) $F = 7.43$ ($p < .01$)
	Model $R^2 = 0.02$
Inter-M^3 palatal width [ΔS_L_YV23] ←	
Q-Level anterior bite force [ΔS_L_YQ57]	0.12 (-0.04, 0.28) $F = 2.00$ (ns)
M-Level anterior bite force [ΔS_L_YM57]	0.11 (-0.01, 0.24) $F = 2.99$ (ns)
	Model $R^2 = 0.02$
Q-Level posterior bite force [ΔS_L_YQ58]	0.03 (-0.17, 0.22) $F = 0.06$ (ns)
M-Level posterior bite force [ΔS_L_YM58]	-0.16 (-0.29, -0.03) $F = 6.12$ ($p < .05$)
	Model $R^2 = 0.02$
Q-Level A-P bite force ratio [ΔL_YQ59]	0.10 (0.04, 0.16) $F = 9.40$ ($p < .01$)
M-Level A-P bite force ratio [ΔL_YM59]	0.15 (0.12, 0.19) $F = 67.30$ ($p < .01$)
	Model $R^2 = 0.21$
Q-Level M^3 bite force [ΔS_L_YQ56]	0.03 (-0.12, 0.19) $F = 0.19$ (ns)
M-Level M^3 bite force [ΔS_L_YM56]	-0.08 (-0.13, -0.03) $F = 9.33$ ($p < .01$)
	Model $R^2 = 0.03$
Palatal depth at I^2 [S_L_YV24] ←	
Q-Level anterior bite force [ΔS_L_YQ57]	-0.21 (-0.62, 0.19) $F = 1.06$ (ns)
M-Level anterior bite force [ΔS_L_YM57]	-1.12 (-1.44, -0.80) $F = 47.33$ ($p < .01$)
	Model $R^2 = 0.14$
Q-Level posterior bite force [ΔS_L_YQ58]	-0.04 (-0.54, 0.46) $F = 0.03$ (ns)
M-Level posterior bite force [ΔS_L_YM58]	-1.09 (-1.41, -0.76) $F = 41.83$ ($p < .01$)
	Model $R^2 = 0.12$
Q-Level A-P bite force ratio [ΔL_YQ59]	-0.13 (-0.31, 0.06) $F = 1.72$ (ns)
M-Level A-P bite force ratio [ΔL_YM59]	-0.01 (-0.12, 0.10) $F = 0.04$ (ns)
	Model $R^2 = 0.01$
Q-Level I^2 maximum bite force [ΔS_L_YQ51]	-0.24 (-0.55, 0.08) $F = 2.16$ (ns)
M-Level I^2 maximum bite force [ΔS_L_YM51]	-0.55 (-0.67, -0.43) $F = 75.54$ ($p < .01$)
	Model $R^2 = 0.21$

Reproduced with permission of the copyright owner. Further reproduction prohibited without permission.

Box 14.16. Multi-level bivariate regressions of nasomaxillary characters on MBF properties.

Palatal depth at P^3 [ΔS_L_YV25] ←	
Q-Level anterior bite force [ΔS_L_YQ57]	-0.03 (-0.32, 0.26) $F = 0.05$ (ns)
M-Level anterior bite force [ΔS_L_YM57]	-0.13 (-0.36, 0.10) $F = 1.23$ (ns)
	Model $R^2 = 0.00$
Q-Level posterior bite force [ΔS_L_YQ58]	-0.02 (-0.37, 0.33) $F = 0.01$ (ns)
M-Level posterior bite force [ΔS_L_YM58]	-0.17 (-0.40, 0.06) $F = 2.08$ (ns)
	Model $R^2 = 0.01$
Q-Level A-P bite force ratio [ΔL_YQ59]	0.01 (-0.11, 0.14) $F = 0.40$ (ns)
M-Level A-P bite force ratio [ΔL_YM59]	0.03 (-0.04, 0.10) $F = 0.60$ (ns)
	Model $R^2 = 0.00$
Q-Level P^3 maximum bite force [ΔS_L_YQ52]	0.06 (-0.15, 0.28) $F = 0.35$ (ns)
M-Level P^3 maximum bite force [ΔS_L_YM52]	-0.30 (-0.38, -0.22) $F = 52.23$ ($p < .01$)
	Model $R^2 = 0.15$
Palatal depth at M^1 [S_L_YV26] ←	
Q-Level anterior bite force [ΔS_L_YQ57]	-0.02 (-0.20, 0.16) $F = 0.06$ (ns)
M-Level anterior bite force [ΔS_L_YM57]	0.06 (-0.08, 0.20) $F = 0.59$ (ns)
	Model $R^2 = 0.00$
Q-Level posterior bite force [ΔS_L_YQ58]	0.06 (-0.27, 0.16) $F = 0.26$ (ns)
M-Level posterior bite force [ΔS_L_YM58]	0.06 (-0.08, 0.21) $F = 0.82$ (ns)
	Model $R^2 = 0.00$
Q-Level A-P bite force ratio [ΔL_YQ59]	0.03 (-0.05, 0.10) $F = 0.46$ (ns)
M-Level A-P bite force ratio [ΔL_YM59]	0.04 (-0.01, 0.08) $F = 2.58$ (ns)
	Model $R^2 = 0.01$
Q-Level M^1 maximum bite force [ΔS_L_YQ54]	0.04 (-0.13, 0.20) $F = 0.18$ (ns)
M-Level M^1 maximum bite force [ΔS_L_YM54]	-0.11 (-0.16, -0.05) $F = 14.04$ ($p < .01$)
	Model $R^2 = 0.05$
Palatal depth at M^3 [S_L_YV27] ←	
Q-Level anterior bite force [ΔS_L_YQ57]	0.08 (-0.12, 0.28) $F = 0.65$ (ns)
M-Level anterior bite force [ΔS_L_YM57]	0.10 (-0.06, 0.25) $F = 1.47$ (ns)
	Model $R^2 = 0.01$
Q-Level posterior bite force [ΔS_L_YQ58]	0.03 (-0.22, 0.27) $F = 0.04$ (ns)
M-Level posterior bite force [ΔS_L_YM58]	0.17 (0.02, 0.33) $F = 4.55$ ($p < .05$)
	Model $R^2 = 0.02$
Q-Level A-P bite force ratio [ΔL_YQ59]	0.08 (0.00, 0.17) $F = 03.59$ (ns)
M-Level A-P bite force ratio [ΔL_YM59]	0.03 (-0.02, 0.08) $F = 1.06$ (ns)
	Model $R^2 = 0.02$
Q-Level M^3 maximum bite force [ΔS_L_YQ56]	0.08 (-0.12, 0.27) $F = 0.59$ (ns)
M-Level M^3 maximum bite force [ΔS_L_YM56]	-0.04 (-0.11, 0.02) $F = 1.65$ (ns)
	Model $R^2 = 0.01$

Reproduced with permission of the copyright owner. Further reproduction prohibited without permission.

Box 14.16. Multi-level bivariate regressions of nasomaxillary characters on MBF properties.	
Krogman's angle of facial prognathism [ΔL_YV30] ←	
Q-Level anterior bite force [ΔS_L_YQ57]	0.27 (-0.16, 0.69) $F = 1.51$ (ns)
M-Level anterior bite force [ΔS_L_YM57]	0.39 (0.05, 0.72) $F = 5.10$ ($p < .05$)
	Model $R^2 = 0.02$
Q-Level posterior bite force [ΔS_L_YQ58]	0.40 (-0.10, 0.89) $F = 2.43$ (ns)
M-Level posterior bite force [ΔS_L_YM58]	0.93 (0.61, 1.26) $F = 31.17$ ($p < .01$)
	Model $R^2 = 0.10$
Q-Level A-P bite force ratio [ΔL_YQ59]	-0.01 (-0.17, 0.16) $F = 0.00$ (ns)
M-Level A-P bite force ratio [ΔL_YM59]	-0.38 (-0.48, -0.28) $F = 57.07$ ($p < .01$)
	Model $R^2 = 0.16$
Enlow's angle of facial prognathism [L_YV31] ←	
Q-Level anterior bite force [ΔS_L_YQ57]	0.17 (-0.40, 0.55) $F = 0.34$ (ns)
M-Level anterior bite force [ΔS_L_YM57]	-0.36 (-0.81, 0.09) $F = 2.45$ (ns)
	Model $R^2 = 0.01$
Q-Level posterior bite force [ΔS_L_YQ58]	0.12 (-0.58, 0.82) $F = 0.11$ (ns)
M-Level posterior bite force [ΔS_L_YM58]	0.31 (-0.16, 0.77) $F = 1.67$ (ns)
	Model $R^2 = 0.01$
Q-Level A-P bite force ratio [ΔL_YQ59]	0.07 (-0.17, 0.30) $F = 0.30$ (ns)
M-Level A-P bite force ratio [ΔL_YM59]	-0.36 (-0.49, -0.22) $F = 25.27$ ($p < .01$)
	Model $R^2 = 0.08$
Occlusal slope [L_YV32] ←	
Q-Level anterior bite force [ΔS_L_YQ57]	-0.65 (-1.12, -0.18) $F = 7.38$ ($p < .01$)
M-Level anterior bite force [ΔS_L_YM57]	-0.13 (-0.50, 0.24) $F = 0.48$ (ns)
	Model $R^2 = 0.03$
Q-Level posterior bite force [ΔS_L_YQ58]	-0.87 (-1.43, -0.31) $F = 9.14$ ($p < .01$)
M-Level posterior bite force [ΔS_L_YM58]	-0.49 (-0.86, -0.13) $F = 6.85$ ($p < .01$)
	Model $R^2 = 0.05$
Q-Level A-P bite force ratio [ΔL_YQ59]	-0.10 (-0.31, 0.10) $F = 0.99$ (ns)
M-Level A-P bite force ratio [ΔL_YM59]	0.04 (-0.07, 0.16) $F = 0.51$ (ns)
	Model $R^2 = 0.01$
Facial convexity [ΔL_YV33] ←	
Q-Level anterior bite force [ΔS_L_YQ57]	0.10 (-0.29, 0.49) $F = 0.26$ (ns)
M-Level anterior bite force [ΔS_L_YM57]	-0.16 (-1.46, -0.85) $F = 54.21$ ($p < .01$)
	Model $R^2 = 0.15$
Q-Level posterior bite force [ΔS_L_YQ58]	0.02 (-0.44, 0.48) $F = 0.01$ (ns)
M-Level posterior bite force [ΔS_L_YM58]	-1.35 (-1.65, -1.04) $F = 74.91$ ($p < .01$)
	Model $R^2 = 0.20$
Q-Level A-P bite force ratio [ΔL_YQ59]	0.07 (-0.11, 0.25) $F = 0.54$ (ns)
M-Level A-P bite force ratio [ΔL_YM59]	0.12 (0.01, 0.22) $F = 4.77$ ($p < .05$)
	Model $R^2 = 0.02$
Paranasal plate orientation [ΔL_YV35] ←	

Reproduced with permission of the copyright owner. Further reproduction prohibited without permission.

Box 14.16. Multi-level bivariate regressions of nasomaxillary characters on MBF properties.	
Q-Level anterior bite force [ΔS_L_YQ57]	0.01 (-0.45, 0.47) $F = 0.00$ (ns)
M-Level anterior bite force [ΔS_L_YM57]	-1.46 (-1.83, -1.10) $F = 62.55$ ($p < .01$)
	Model $R^2 = 0.17$
Q-Level posterior bite force [ΔS_L_YQ58]	-0.09 (-0.67, 0.50) $F = 0.08$ (ns)
M-Level posterior bite force [ΔS_L_YM58]	-1.20 (-1.58, -0.81) $F = 37.29$ ($p < .01$)
	Model $R^2 = 0.11$
Q-Level A-P bite force ratio [ΔL_YQ59]	0.06 (-0.15, 0.27) $F = 0.30$ (ns)
M-Level A-P bite force ratio [ΔL_YM59]	-0.28 (-0.40, -0.15) $F = 19.30$ ($p < .01$)
	Model $R^2 = 0.06$

Reproduced with permission of the copyright owner. Further reproduction prohibited without permission.

Reproduced with permission of the copyright owner. Further reproduction prohibited without permission.

Box 14.17 Nasal process of maxilla width [ΔS_L_YV4] ← Anterior bite force magnitude [ΔS_L_YV57]

Taxon	Level of analysis	Maximum likelihood regression coefficient (95% CI) and associated p-value	Shapiro-Wilk test for normality of residuals	Brown & Forsythe's test for residual homoscedasticity	Somers' D nonparametric measure and test of association
Anthropoids (n=300)	V	0.31 (0.05, 0.58) p = .02	0.98 p = .50	0.34 p = .79	0.04 ns
	M	0.41 (0.08, 0.75) p = .01	0.98 p = .60	1.67 p = .17	0.04 ns
Platyrrhini (n=117)	V	-0.57 (-0.99, -0.14) p = .009	0.97 p = .07	1.54 p = .21	-0.15 p < .05
	M	-0.93 (-1.45, -0.42) p = .0004	0.97 p = .21	5.29 p = .0002	-0.14 p < .05
Atelidae (n=65)	V	-0.41 (-1.07, 0.24) p = .21	0.97 p = .41	0.92 p = .44	-0.09 ns
Cebidae (n=52)	V	0.30 (-0.18, 0.77) p = .20	0.95 p = .06	0.72 p = .55	0.15 ns
Catarrhini (n=183)	V	0.58 (0.26, 0.90) p = .0004	0.98 p = .54	1.28 p = .28	0.14 p < .05
	M	0.85 (0.44, 1.26) p = .0001	0.99 p = .89	1.74 p = .16	0.14 p < .05
Cercopithecoidea (n=137)	V	1.09 (0.66, 1.50) p = .0001	0.99 p = .76	1.63 p = .18	0.23 p < .05
	M	1.49 (0.97, 2.00) p = .0001	0.99 p = .93	1.64 p = .18	0.23 p < .05
Cercopithecinae (n=87)	V	1.32 (0.51, 2.21) p = .001	0.99 p = .94	3.05 p = .03	0.09 ns
	M	2.47 (1.28, 3.64) p = .0001	0.98 p = .69	1.26 p = .29	-0.03 ns
Colobinae (n=50)	V	0.34 (-0.12, 0.79) p = .14	0.94 p = .03	0.87 p = .46	0.11 ns
	M	0.41 (-0.18, 1.01) p = .16	0.95 p = 0.3	0.91 p = .43	0.25 p < .05
Hominoidea (n=46)	V	-0.12 (-0.57, 0.32) p = .58	0.98 p = .84	1.64 p = .20	-0.08 ns

Box 14.18 Anterior nasal apertue breadth [ΔS_L_YV6] ← Anterior bite force magnitude [ΔS_L_YV57]

Taxon	Level of analysis	Maximum likelihood regression coefficient (95% CI) and associated p-value	Shapiro-Wilk test for normality of residuals	Brown & Forsythe's test for residual homoscedasticity	Somers' D nonparametric measure and test of association
Anthropoids (n=300)	V	-0.10 (-0.17, -0.01) p = .02	0.99 p = .95	0.23 p = .87	-0.13 p < .05
	M	-0.22 (-0.33, -0.12) p = .0001	0.99 p = 85	0.29 p = .83	-0.22 p < .05
Platyrrhini (n=117)	V	-0.40 (-0.53, -0.28) p = .0001	0.98 p = .39	0.55 p = .65	-0.34 p < .05
	M	-0.62 (-0.76, -0.48) p = .0001	0.98 p = .47	1.08 p = .36	-0.51 p < .05
Atelidae (n=65)	V	-0.44 (-0.63, -0.25) p = .0001	0.98 p = .80	0.35 p = .79	-0.34 p < .05
	M	-0.83 (-1.07, -0.59) p = .0001	0.98 p = .47	0.65 p = .58	-0.51 p < .05
Cebidae (n=52)	V	-0.17 (-0.34, -0.01) p = .03	0.95 p = .05	0.40 p = .75	-0.15 ns
	M	-0.29 (-0.48, -0.10) p = .002	0.97 p = .24	1.67 p = .19	-0.33 p < .05
Catarrhini (n=183)	V	-0.05 (-0.15, 0.05) p = .29	0.98 p = .68	0.47 p = .70	-0.09 ns
	M	-0.18 (-0.30, -0.5) p = .005	0.99 p = .95	1.73 p = .16	-0.20 p < .05
Cercopithecoidea (n=137)	V	-0.05 (-0.06, 0.06) p = .40	0.98 p = .29	1.35 p = .26	-0.09 ns
Cercopithecinae (n=87)	V	0.08 (-0.10, 0.26) p = .40	0.98 p = .66	0.85 p = .47	0.00 ns
Colobinae (n=50)	V	0.12 (-0.04, 0.29) p = .13	0.99 p = .89	2.22 p = .10	0.16 ns
Hominoidea (n=46)	V	-0.03 (-0.23, 0.17) p = .75	0.97 p = .49	0.20 p = .89	-0.06 ns
	M	-0.26 (-0.52, -0.01) p = .04	0.98 p = .67	0.46 p = .71	-0.22 p < .05

Box 14.19 Bizygomatic breadth [ΔS_L_YV12] ← Anterior bite force magnitude [ΔS_L_YV57]

Taxon	Level of analysis	Maximum likelihood regression coefficient (95% CI) and associated p-value	Shapiro-Wilk test for normality of residuals	Brown & Forsythe's test for residual homoscedasticity	Somers' D nonparametric measure and test of association
Anthropoids (n=300)	V	0.18 (0.14, 0.22) p = .0001	0.98 p = .30	2.09 p = .10	0.27 p < .05
	M	0.22 (0.17, 0.27) p = .0001	0.98 p = .17	4.69 p = .003	0.23 p < .05
	Q	0.11 (0.05, 0.14) p = .0008			0.11 p < .05
Platyrrhini (n=117)	V	0.15 (0.09, 0.21) p = .0001	0.98 p = .72	2.62 p = .054	0.30 p < .05
	M	0.19 (0.11, 0.26) p = .0001	0.98 p = .56	4.17 p = .008	0.29 p < .05
Atelidae (n=65)	V	0.14 (0.03, 0.25) p = .009	0.99 p = .90	0.37 p = .77	0.21 p < .05
	M	0.17 (0.01, 0.32) p = .03	0.99 p = .91	0.10 p = .95	0.14 ns
Cebidae (n=52)	V	0.20 (0.15, 0.26) p = .0001	0.98 p = .78	1.62 p = .20	0.49 p < .05
	M	0.29 (0.24, 0.35) p = .0001	0.97 p = .32	0.86 p = .47	0.58 p < .05
Catarrhini (n=183)	V	0.19 (0.14, 0.24) p = .0001	0.98 p = .61	1.53 p = .21	0.29 p < .05
	M	0.24 (0.18, 0.31) p = .0001	0.98 p = .36	2.68 p = .048	0.22 p < .05
	Q	0.12 (0.03, 0.20) p = .005			0.11 p < .05
Cercopithecoidea (n=137)	V	0.27 (0.21, 0.33) p = .0001	0.97 p = .047	0.44 p = .72	0.40 p < .05
	M	0.38 (0.32, 0.45) p = .0001	0.99 p = .74	0.99 p = .40	0.36 p < .05
Cercopithecinae (n=87)	V	0.20 (0.11, 0.30) p = .0001	0.96 p = .02	1.27 p = .28	0.20 p < .05
	M	0.39 (0.26, 0.52) p = .0001	0.95 p = .02	0.59 p = .62	0.00 ns
Colobinae (n=50)	V	0.19 (0.10, 0.28) p = .0001	0.98 p = .68	0.17 p = .91	0.33 p < .05
	M	0.28 (0.17, 0.40) p = .0001	0.97 p = .36	3.86 p = .01	0.46 p < .05
Hominoidea (n=46)	V	0.07 (-0.02, 0.16) p = .10	0.94 p = .04	4.66 p = .007	0.19 ns
	Q	0.17 (0.04, 0.29) p = .007	0.96 p = .24	0.81 p = .49	0.02 p < .05

Reproduced with permission of the copyright owner. Further reproduction prohibited without permission.

Box 14.20 Bizygomatic breadth [ΔS_L_YV12] ← Posterior bite force magnitude [ΔS_L_YV58]

Taxon	Level of analysis	Maximum likelihood regression coefficient (95% CI) and associated p-value	Shapiro-Wilk test for normality of residuals	Brown & Forsythe's test for residual homoscedasticity	Somers' D nonparametric measure and test of association
Anthropoids (n=300)	V	0.26 (0.22, 0.30) p = .0001	0.98 p = .17	2.12 p = .10	0.38 p < .05
	M	0.30 (0.26, 0.35) p = .0001	0.98 p = .04	3.68 p = .01	0.37 p < .05
	Q	0.15 (0.08, 0.22) p = .0001			0.12 p < .05
Platyrrhini (n=117)	V	0.24 (0.19, 0.29) p = .0001	0.96 p = .02	2.61 p = .054	0.48 p < .05
	M	0.28 (0.22, 0.34) p = .0001	0.96 p = .03	2.57 p = .058	0.46 p < .05
	Q	0.11 (0.01, 0.21) p = .03			0.12 ns
Atelidae (n=65)	V	0.33 (0.23, 0.42) p = .0001	0.98 p = .067	0.24 p = .86	0.48 p < .05
	M	0.45 (0.33, 0.57) p = .0001	0.98 p = .54	0.06 p = .98	0.41 p < .05
	Q	0.15 (0.01, 0.29) p = .03			0.16 p < .05
Cebidae (n=52)	V	0.21 (0.16, 0.25) p = .0001	0.98 p = .55	1.17 p = .33	0.56 p < .05
	M	0.24 (0.20, 0.28) p = .0001	0.98 p = .73	0.50 p = .68	0.58 p < .05
Catarrhini (n=183)	V	0.27 (0.22, 0.33) p = .0001	0.98 p = .35	2.14 p = .09	0.37 p < .05
	M	0.31 (0.25, 0.37) p = .0001	0.97 p = .03	3.00 p = .03	0.32 p < .05
	Q	0.16 (0.07, 0.25) p = .0003			0.12 p < .05
Cercopithecoidea (n=137)	V	0.36 (0.30, 0.42) p = .0001	0.98 p = .23	0.67 p = .57	0.46 p < .05
	M	0.47 (0.40, 0.53) p = .0001	0.97 p = .13	0.47 p = .70	0.48 p < .05
	Q	0.10 (0.00, 0.19) p = .056			0.05 ns
Cercopithecinae (n=87)	V	0.28 (0.18, 0.38) p = .0001	0.97 p = .16	0.87 p = .46	0.23 p < .05
	M	0.45 (0.32, 0.57) p = .0001	0.96 p = .02	0.71 p = .54	0.20 p < .05
Colobinae (n=50)	V	0.30 (0.19, 0.40) p = .0001	0.97 p = .34	1.00 p = .40	0.46 p < .05
	M	0.43 (0.31, 0.54) p = .0001	0.98 p = .086	2.22 p = .09	0.61 p < .05
Hominoidea (n=46)	V	0.14 (0.06, 0.28) p = .0005	0.94 p = .02	0.13 p = .94	0.26 p < .05
	M	0.10 (0.00, 0.20) p = .047	0.93 p = .01	1.09 p = .36	0.07 ns
	Q	0.23 (0.09, 0.37) p = .001			0.29 p < .05

Reproduced with permission of the copyright owner. Further reproduction prohibited without permission.

Box 14.21 Anterior facial length [ΔS_L_YV17] ← Anterior bite force magnitude [ΔS_L_YV57]

Taxon	Level of analysis	Maximum likelihood regression coefficient (95% CI) and associated p-value	Shapiro-Wilk test for normality of residuals	Brown & Forsythe's test for residual homoscedasticity	Somers' D nonparametric measure and test of association
Anthropoids (n=300)	V	-0.27 (-0.36, -0.18) p = .0001	0.95 p = .0001	5.84 p = .0007	-0.26 p < .05
	M	-0.38 (-0.49, -0.26) p = .0001	0.93 p = .0001	16.62 p = .0001	-0.36 p < .05
Platyrrhini (n=117)	V	-0.38 (-0.49, -0.28) p = .0001	0.97 p = .18	6.21 p = .0006	-0.37 p < .05
	M	-0.56 (-0.67, -0.44) p = .0001	0.96 p = .01	1.40 p = .24	-0.54 p < .05
Atelidae (n=65)	V	-0.42 (-0.58, -0.26) p = .0001	0.98 p = .51	2.81 p = .045	-0.36 p < .05
	M	-0.75 (-0.95, -0.56) p = .0001	0.97 p = .38	2.66 p = .055	-0.51 p < .05
Cebidae (n=52)	V	-0.19 (-0.33, -0.05) p = .008	0.95 p = .09	1.19 p = .33	-0.19 p < .05
	M	-0.28 (-0.45, -0.12) p = .0007	0.95 p = .047	4.39 p = .008	-0.33 p < .05
Catarrhini (n=183)	V	-0.23 (-0.36, -0.11) p = .0002	0.97 p = .008	7.18 p = .0001	-0.20 p < .05
	M	-0.32 (-0.47, -0.16) p = .0001	0.95 p = .0001	16.93 p = .0001	-0.26 p < .05
Cercopithecoidea (n=137)	V	-0.57 (-0.68, -0.46) p = .0001	0.98 p = .48	5.14 p = .002	-0.38 p < .05
	M	-0.84 (-0.94, -0.72) p = .0001	0.98 p = .31	2.15 p = .09	-0.47 p < .05
Cercopithecinae (n=87)	V	-0.46 (-0.63, -0.28) p = .0001	0.97 p = .29	8.09 p = .0001	-0.15 p < .05
	M	-0.87 (-1.12, -0.62) p = .0001	0.96 p = .06	11.13 p = .0001	-0.05 ns
Colobinae (n=50)	V	-0.30 (-0.41, -0.19) p = .0001	0.97 p = .36	0.65 p = .58	-0.38 p < .05
	M	-0.49 (-0.61, -0.38) p = .0001	0.98 p = .71	0.06 p = .98	-0.56 p < .05
Hominoidea (n=46)	V	0.12 (-0.10, 0.33) p = .28	0.97 p = .31	0.11 p = .95	0.13 ns
	M	0.31 (0.03, 0.59) p = .03	0.94 p = .05	0.09 p = .96	0.05 ns

Reproduced with permission of the copyright owner. Further reproduction prohibited without permission.

Box 14.22 Anteroposterior position of zygomatic root [ΔL_YV13] ← Anterior bite force magnitude [ΔS_L_YV57]

Taxon	Level of analysis	Maximum likelihood regression coefficient (95% CI) and associated p-value	Shapiro-Wilk test for normality of residuals	Brown & Forsythe's test for residual homoscedasticity	Somers' D nonparametric measure and test of association
Anthropoids (n=300)	V	1.00 (0.74, 1.25) p = .0001	0.98 p = .054	4.97 p = .002	0.21 p < .05
	M	1.26 (0.94, 1.57) p = .0001	0.97 p = .007	7.91 p = .0001	0.17 p < .05
	Q	0.56 (0.16, 0.97) p = .006			0.09 p < .05
Platyrrhini (n=117)	V	0.39 (0.08, 0.69) p = .01	0.97 p = .13	2.57 p = .057	0.11 ns
	M	0.13 (-0.23, 0.50) p = .47	0.98 p = .43	1.59 p = .20	0.02 ns
	Q	0.84 (0.35, 1.34) p = .0008			0.19 p < .05
Atelidae (n=65)	V	0.01 (-0.43, 0.46) p = .95	0.97 p = .29	0.95 p = .42	-0.03 ns
	M	-0.70 (-0.29, -0.12) p = .02	0.97 p = .21	1.54 p = .21	-0.14 ns
	Q	0.72 (0.14, 1.30) p = .01			0.15 ns
Cebidae (n=52)	V	0.74 (0.26, 1.22) p = .002	0.98 p = .64	0.47 p = .69	0.18 ns
	M	0.57 (0.00, 1.15) p = .048	0.97 p = .28	0.05 p = .99	0.10 ns
	Q	1.09 (0.27, 1.93) p = .008			0.27 p < .05
Catarrhini (n=183)	V	1.06 (0.74, 1.38) p = .0001	0.98 p = .20	3.44 p = .02	0.24 p < .05
	M	1.42 (1.01, 1.83) p = .0001	0.97 p = .01	5.32 p = .002	0.16 p < .05
	Q	0.50 (0.00, 1.00) p = .05			0.07 ns
Cercopithecoidea (n=137)	V	1.97 (1.62, 2.31) p = .0001	0.98 p = .34	1.21 p = .31	0.42 p < .05
	M	2.78 (2.42, 3.15) p = .0001	0.97 p = .48	1.18 p = .31	0.38 p < .05
	Q	0.48 (0.00, 0.97) p = .05			0.09 ns
Cercopithecinae (n=87)	V	1.86 (1.26, 2.45) p = .0001	0.97 p = .11	2.44 p = .07	0.35 p < .05
	M	3.39 (2.59, 4.18) p = .0001	0.96 p = .03	0.89 p = .44	0.19 p < .05
	Q	0.69 (0.00, 1.38) p = .048			0.13 ns
Colobinae (n=50)	V	1.88 (1.31, 2.44) p = .0001	0.97 p = .47	0.28 p = .83	0.45 p < .05
	M	3.05 (2.53, 3.58) p = .0001	0.94 p = .02	0.35 p = .78	0.73 p < .05
Hominoidea (n=46)	V	-0.13 (-0.68, 0.41) p = .63	0.94 p = .02	4.21 p = .01	-0.5 ns

Reproduced with permission of the copyright owner. Further reproduction prohibited without permission.

Box 14.23 Maxillary arch length [ΔS_L_YV14] ← Anterior-to-posterior bite force ratio [ΔS_L_YV59]

Taxon	Level of analysis	Maximum likelihood regression coefficient (95% CI) and associated p-value	Shapiro-Wilk test for normality of residuals	Brown & Forsythe's test for residual homoscedasticity	Somers' D nonparametric measure and test of association
Anthropoids (n=300)	V	-0.14 (-0.16, -0.11) p = .0001	0.89 p = .0001	12.39 p = .0001	-0.34 p < .05
	M	-0.14 (-0.18, -0.11) p = .0001	0.90 p = .0001	11.48 p = .0001	-0.27 p < .05
	Q	-0.11 (-0.16, -0.05) p = .0001			-0.18 p < .05
Platyrrhini (n=117)	V	-0.04 (-0.-6, -0.03) p = .0001	0.97 p = .13	6.23 p = .0006	-0.38 p < .05
	M	-0.04 (-0.06, -0.03) p = .0001	0.97 p = .06	4.69 p = .004	-0.26 p < .05
	Q	-0.06 (-0.09, -0.03) p = .0005			-0.17 p < .05
Atelidae (n=65)	V	-0.07 (-0.09, -0.05) p = .0001	0.97 p = .35	2.14 p = .10	-0.47 p < .05
	M	-0.07 (-0.10, -0.05) p = .0001	0.97 p = .33	2.37 p = .08	-0.30 p < .05
	Q	-0.07 (-0.11, -0.02) p = .002			-0.17 p < .05
Cebidae (n=52)	V	-0.02 (-0.04, -0.01) p = .006	0.91 p = .0004	0.52 p = .66	-0.35 p < .05
	M	-0.02 (-0.03, -0.01) p = .03	0.88 p = .0001	0.81 p = .49	-0.30 p < .05
	Q	-0.05 (-0.09, 0.00) p = .048			-0.23 p < .05
Catarrhini (n=183)	V	-0.26 (-0.31, -0.22) p = .0001	0.92 p = .0001	13.27 p = .0001	-0.46 p < .05
	M	-0.33 (-0.38, -0.28) p = .0001	0.92 p = .0001	8.36 p = .0001	-0.38 p < .05
	Q	-0.14 (-0.21, -0.07) p = .0001			-0.23 p < .05
Cercopithecoidea (n=137)	V	-0.18 (-0.22, -0.14) p = .0001	0.94 p = .0001	2.18 p = .09	-0.46 p < .05
	M	-0.25 (-0.31, -0.19) p = .0001	0.92 p = .0001	3.66 p = .01	-0.34 p < .05
	Q	-0.13 (-0.18, -0.07) p = .0001			-0.26 p < .05
Cercopithecinae (n=87)	V	-0.11 (-0.16, -0.05) p = .0001	0.92 p = .0001	0.11 p = .95	-0.33 p < .05
	M	-0.10 (-0.17, 0.02) p = .10	0.92 p = .0001	0.03 p = .99	-0.18 p < .05
	Q	-0.13 (-0.019, -0.06) p = .0002			-0.28 p < .05
Colobinae (n=50)	V	-0.23 (-0.27, -0.19) p = .0001	0.96 p = .21	2.86 p = .046	-0.69 p < .05
	M	-0.33 (-0.37, -0.28) p = .0001	0.98 p = .62	0.40 p = .75	-0.58 p < .05
	Q	-0.13 (-0.18, -0.09) p = .0001			-0.27 p < .05
Hominoidea (n=46)	V	-0.31 (-0.40, -0.21) p = .0001	0.92 p = .003	0.55 p = 65	-0.50 p < .05
	M	-0.34 (-0.44, -0.23) p = .0001	0.87 p = .0001	2.09 p = .12	-0.45 p < .05
	Q	-0.16 (-0.37, 0.06) p = .14			-0.22 p < .05

Reproduced with permission of the copyright owner. Further reproduction prohibited without permission.

Box 14.24 Inter-M^3 palatal width [ΔS_L_YV23] ← Anterior-to-posterior bite force ratio [ΔL_YV59]

Taxon	Level of analysis	Maximum likelihood regression coefficient (95% CI) and associated p-value	Shapiro-Wilk test for normality of residuals	Brown & Forsythe's test for residual homoscedasticity	Somers' D nonparametric measure and test of association
Anthropoids (n=300)	V	0.14 (0.11, 0.17) p = .0001	0.98 p = .08	1.53 p = .20	0.30 p < .05
	M	0.15 (0.12, 0.19) p = .0001	0.98 p = .08	0.93 p = .43	0.26 p < .05
	Q	0.10 (0.04, 0.16) p = .002			0.10 p < .05
Platyrrhini (n=117)	V	0.05 (0.03, 0.08) p = .0001	0.99 p = .83	1.23 p = .30	0.23 p < .05
	M	0.06 (0.03, 0.08) p = .0001	0.99 p = .82	1.53 p = .21	0.23 p < .05
Atelidae (n=65)	V	0.11 (0.07, 0.15) p = .0001	0.98 p = .82	2.23 p = .09	0.43 p < .05
	M	0.13 (0.08, 0.17) p = . 0001	0.98 p = .78	2.54 p = .06	0.46 p < .05
	Q	0.07 (0.00, 0.15) p = .05			0.09 ns
Cebidae (n=52)	V	0.00 (-0.02, 0.03) p = .77	0.96 p = .14	0.12 p = .94	0.08 ns
Catarrhini (n=183)	V	0.25 (0.19, 0.30) p = .0001	0.99 p = .85	2.28 p = .08	0.36 p < .05
	M	0.32 (0.25, 0.38) p= .0001	0.99 P = .81	0.38 P = .76	0.34 P < .05
	Q	0.13 (0.04, 0.21) p = .003			0.11 P < .05
Cercopithecoidea (n=137)	V	0.13 (0.07, 0.20) p = .0001	0.97 p = .16	1.15 p = .33	0.24 p < .05
	M	0.17 (0.06, 0.27) p = .0001	0.97 P = .10	1.01 P = .40	0.20 P < .05
	Q	0.11 (0.02, 0.20) p = .01			0.14 P < .05
Cercopithecinae (n=87)	V	0.16 (0.07, 0.26) p = .0005	0.94 p = .0005	0.12 p = .94	0.31 p < .05
	M	0.22 (0.07, 0.38) p = .004	0.93 p = .0001	0.45 p = .71	0.29 p < .05
	Q	0.13 (0.01, 0.24) p = .03			0.19 p < .05
Colobinae (n=50)	V	0.14 (0.06, 0.23) p = .0004	0.98 p = .56	1.03 p = .39	0.29 p < .05
	M	0.20 (0.09, 0.32) p = .0004	0.98 p = .60	2.32 p = .09	0.24 p < .05
Hominoidea (n=46)	V	0.34 (0.26, 0.43) p = .0001	0.97 p = .42	0.73 p = .54	0.60 p < .05
	M	0.38 (0.29, 0.47) p = .0001	0.98 p = .83	0.63 p = .59	0.54 p < .05

Reproduced with permission of the copyright owner. Further reproduction prohibited without permission.

Reproduced with permission of the copyright owner. Further reproduction prohibited without permission.

Box 14.25 Palatal depth at I^2 [ΔS_L_YV24] ← I^2 maximum bite force [ΔS_L_YV51]

Taxon	Level of analysis	Maximum likelihood regression coefficient (95% CI) and associated p-value	Shapiro-Wilk test for normality of residuals	Brown & Forsythe's test for residual homoscedasticity	Somers' D nonparametric measure and test of association
Anthropoids (n=300)	V	-0.75 (-1.01, -0.50) p = .0001	0.99 p = .73	2.53 p = .056	-0.25 p < .05
	M	-1.10 (-1.41, -0.78) p = .0001	0.98 p = .056	3.09 p = .027	-0.35 p < .05
Platyrrhini (n=117)	V	-0.91 (-1.23, -0.58) p = .0001	0.98 p = .64	3.61 p = .02	-0.28 p < .05
	M	-1.25 (-1.64, -0.87) p = .0001	0.98 p = .82	1.62 p = .19	-0.33 p < .05
Atelidae (n=65)	V	-1.50 (-2.00, -1.00) p = .0001	0.97 p = .40	1.50 p = .22	-0.40 p < .05
	M	-2.90 (-3.45, -2.35) p = .0001	0.99 p = .96	2.04 p = .12	-0.52 p < .05
Cebidae (n=52)	V	-0.50 (-0.93, -0.06) p = .0001	0.96 p = .15	1.53 p = .21	-0.15 ns
	M	-0.56 (-1.08, -0.03) p = .03	0.96 p = .13	0.93 p = .42	-0.12 ns
Catarrhini (n=183)	V	-0.69 (-1.02, -0.34) p = .0001	0.98 p = .32	3.01 p = .03	-0.22 p < .05
	M	-1.01 (-1.43, -0.57) p = .0001	0.97 p = .052	2.97 p = .03	-0.33 p < .05
Cercopithecoidea (n=137)	V	-0.79 (-1.17, -0.41) p = .0001	0.99 p = .95	0.41 p = .74	-0.21 p < .05
	M	-1.09 (-1.57, -0.63) p = .0001	0.99 p =. 96	0.51 p = .67	-0.35 p < .05
Cercopithecinae (n=87)	V	-0.06 (-0.63, 0.51) p = .83	0.98 p = .42	1.06 p = .37	0.02 ns
Colobinae (n=50)	V	-0.27 (-0.84, 0.30) p = .34	0.97 p = .32	0.69 p = .56	-0.06 ns
Hominoidea (n=46)	V	-0.79 (-1.36, -0.20) p = .0007	0.97 p = .44	1.83 p = .16	-0.28 p < .05
	M	-1.31 (-2.05, -0.57) p = .0004	0.94 p = .02	1.46 p = .24	-0.28 p < .05

Box 14.26 Krogman's angle of facial prognathism [ΔL_YV30] ← Anterior-to-posterior bite force ratio [ΔL_YV59]

Taxon	Level of analysis	Maximum likelihood regression coefficient (95% CI) and associated p-value	Shapiro-Wilk test for normality of residuals	Brown & Forsythe's test for residual homoscedasticity	Somers' D nonparametric measure and test of association
Anthropoids (n=300)	V	-0.29 (-0.37, -0.20) p = .0001	0.95 p = .0001	6.86 p = .0002	-0.19 p < .05
	M	-0.38 (-0.48, -0.28) p = .0001	0.97 p = .0002	19.68 p = .0001	-0.24 p < .05
Platyrrhini (n=117)	V	-0.16 (-0.26, -0.06) p = .002	0.97 p = .08	2.88 p = .039	-0.20 p < .05
	M	-0.18 (-0.29, -0.08) p = .0008	0.96 p = .03	7.24 p = .0002	-0.20 p < .05
Atelidae (n=65)	V	-0.19 (-0.37, -0.01) p = .04	0.94 p = .003	2.92 p= .04	-0.17 p < .05
	M	-0.27 (-0.47, -0.06) p = .009	0.92 p = .0005	4.44 p = .007	-0.20 p < .05
Cebidae (n=52)	V	-0.14 (-0.22, -0.05) p = .002	0.96 p = .15	1.66 p = .19	-0.29 p < .05
	M	-0.13 (-0.22, -0.04) p = .004	0.96 p = .15	1.37 p = .26	-0.26 p < 05
Catarrhini (n=183)	V	-0.41 (-0.54, -0.27) p = .0001	0.96 p = .0005	17.82 p = .0001	-0.14 p < .05
	M	-0.63 (-0.79, -0.48) p = .0001	0.98 p = .52	20.14 p = .0001	-0.15 p < .05
Cercopithecoidea (n=137)	V	-0.18 (-0.32, -0.03) p = .01	0.97 p = .11	2.71 p = .05	-0.10 ns
	M	-0.46 (-0.67, -0.25) p = .0001	0.98 p = .67	2.28 p = .08	-0.15 p < .05
Cercopithecinae (n=87)	V	-0.02 (-0.21, 0.17) p = .82	0.97 p = .14	1.21 p = .31	-0.02 ns
Colobinae (n=50)	V	-0.34 (-0.56, -0.12) p = .002	0.96 p = .18	1.76 p = .17	-0.25 p < .05
	M	-0.72 (-0.99, -0.46) p = .0001	0.95 p = .07	1.07 p = .37	-0.38 p < .05
Hominoidea (n=46)	V	-0.60 (-0.88, -0.32) p = .0001	0.97 p = .56	3.02 p = .04	-0.21 p < .05
	M	-0.71 (-1.01, -0.41) p = .0001	0.99 p = .93	1.92 p = .14	-0.18 ns

Box 14.27 Facial convexity [ΔL_YV33] ← Posterior bite force magnitude [ΔS_L_YV58]

Taxon	Level of analysis	Maximum likelihood regression coefficient (95% CI) and associated p-value	Shapiro-Wilk test for normality of residuals	Brown & Forsythe's test for residual homoscedasticity	Somers' D nonparametric measure and test of association
Anthropoids (n=300)	V	-0.93 (-1.19, -0.67) p = .0001	0.99 p = .67	1.05 p = .36	-0.27 p < .05
	M	-1.35 (-1.65, -1.04) p = .0001	0.98 p = .20	3.65 p = .01	-0.31 p < .05
Platyrrhini (n=117)	V	-1.71 (-2.17, -1.15) p = .0001	0.99 p = .86	2.09 p = .11	-0.31 p < .05
	M	-2.31 (-2.92, -1.71) p = .0001	0.99 p = .76	2.02 p = .11	-0.36 p < .05
Atelidae (n=65)	V	-0.08 (-1.69, 0.06) p = .065	0.99 p = .97	1.59 p = .20	-0.18 p < .05
	M	-1.62 (-2.72, -0.52) p = .003	0.99 p = .96	0.93 p = .43	-0.21 p < .05
Cebidae (n=52)	V	-2.86 (-3.58, -2.14) p = .0001	0.98 p = .61	0.57 p = .63	-0.57 p < .05
	M	-3.36 (-4.07, -2.64) p = .0001	0.96 p = .13	0.06 p = .98	-0.60 p < .05
Catarrhini (n=183)	V	-0.71 (-0.99, -0.41) p = .0001	0.97 p = .02	0.19 p = .90	-0.24 p < .05
	M	-1.03 (-1.37, -0.69) p = .0001	0.96 p = .002	1.96 p = .12	-0.30 p < .05
Cercopithecoidea (n=137)	V	-0.70 (-1.01, -0.38) p = .0001	0.99 p = .91	0.38 p = .77	-0.23 p < .05
	M	-1.07 (-1.44, -0.71) p = .0001	0.98 p = .51	1.29 p = .28	-0.34 p < .05
Cercopithecinae (n=87)	V	0.55 (0.11, 0.98) p = .01	0.98 p = .76	0.48 p = .69	0.13 ns
	M	0.80 (0.20, 1.40) p = .008	0.98 p = .70	0.56 p = .63	0.08 ns
Colobinae (n=50)	V	-0.51 (-0.90, -0.12) p = .009	0.98 p = .67	0.87 p = .46	-0.27 p < .05
	M	-0.84 (-1.32, -0.37) p = .0004	0.98 p = .56	0.58 p = .63	-0.28 p < .05
Hominoidea (n=46)	V	-0.92 (-1.47, -0.37) p = .0007	0.96 p = .12	0.10 p = .96	-0.20 ns
	M	-1.32 (-1.97, -0.68) p = .0001	0.96 p = .27	0.30 p = .82	-0.18 ns

Reproduced with permission of the copyright owner. Further reproduction prohibited without permission.

Box 14.28 Facial convexity [ΔL_YV33] ← Anterior bite force magnitude [ΔS_L_YV57]

Taxon	Level of analysis	Maximum likelihood regression coefficient (95% CI) and associated p-value	Shapiro-Wilk test for normality of residuals	Brown & Forsythe's test for residual homoscedasticity	Somers' D nonparametric measure and test of association
Anthropoids (n=300)	V	-0.68 (-0.93, -0.43) p = .0001	0.99 p = .84	5.18 p = .002	-0.24 p < .05
	M	-1.16 (-1.46, -0.84) p = .0001	0.98 p = .13	3.98 p = .008	-0.34 p < .05
Platyrrhini (n=117)	V	-1.51 (-2.08, -0.94) p = .0001	0.98 p = .73	3.93 p = .01	-0.24 p < .05
	M	-2.47 (-3.11, -1.83) p = .0001	0.98 p = .36	1.83 p = .15	-0.38 p < .05
Atelidae (n=65)	V	-0.71 (-1.51, 0.10) p = .08	0.99 p = .99	3.76 p = .02	-0.13 ns
	M	-1.91 (-2.97, -0.85) p = .0003	0.98 p = .77	0.63 p = .60	-0.36 p < .05
Cebidae (n=52)	V	-3.11 (-3.95, -2.27) p = .0001	0.99 p = .91	0.76 p = .51	-0.50 p < .05
	M	-4.49 (-5.27, -3.71) p = .0001	0.98 p = .76	0.60 p = .62	-0.60 p < .05
Catarrhini (n=183)	V	-0.44 (-0.72, -0.17) p = .001	0.97 p = .12	2.01 p = .11	-0.19 p < .05
	M	-0.78 (-1.12, -0.44) p = .0001	0.97 p = .005	3.29 p = .02	-0.28 p < .05
Cercopithecoidea (n=137)	V	-0.57 (-0.85, -0.29) p = .0001	0.99 p = .93	0.05 p = .98	-0.19 p < .05
	M	-0.97 (-1.30, -0.64) p = .0001	0.98 p = .59	1.47 p = .23	-0.31 p , .05
Cercopithecinae (n=87)	V	0.56 (0.17, 0.94) p = .004	0.99 p = .83	0.45 p = .71	0.15 p < 05
	M	0.91 (0.33, 1.49) p = .002	0.98 p = .57	0.13 p = .94	0.91 p < .05
Colobinae (n=50)	V	-0.42 (-0.73, -0.10) p = .0001	0.98 p = .56	3.52 p = .02	-0.23 p < .05
	M	-0.71 (-1.10, -0.32) p = .003	0.99 p = .91	0.51 p = .67	-0.32 p < .05
Hominoidea (n=46)	V	-0.43 (-0.99, 0.14) p = .12	0.97 p = .31	1.25 p = .30	-0.17 ns
	M	-0.77 (-1.51, -0.02) p = .04	0.97 p = .32	0.74 p = .53	-0.08 ns

Reproduced with permission of the copyright owner. Further reproduction prohibited without permission.

Reproduced with permission of the copyright owner. Further reproduction prohibited without permission.

Box 14.29 Paranasal plate orientation [ΔL_YV35] ← Anterior bite force magnitude [ΔS_L_YV57]

Taxon	Level of analysis	Maximum likelihood regression coefficient (95% CI) and associated p-value	Shapiro-Wilk test for normality of residuals	Brown & Forsythe's test for residual homoscedasticity	Somers' D nonparametric measure and test of association
Anthropoids (n=300)	V	-0.90 (-1.20, -0.61) p = .0001	0.97 p = .01	4.04 p = .008	-0.12 p < .05
	M	-1.46 (-1.83, -1.10) p = .0001	0.97 p = .006	8.32 p = .0001	-0.20 p < .05
Platyrrhini (n=117)	V	0.44 (0.05, 0.82) p = .02	0.98 p = .51	0.58 p = .62	0.15 p < .05
	M	0.68 (0.21, 1.14) p = .004	0.98 p = .74	2.90 p = .04	0.12 p < .05
Atelidae (n=65)	V	0.40 (-0.22, 1.03) p = .20	0.97 p = .20	1.30 p = .29	0.13 ns
	M	0.68 (-0.20, 1.56) p = .13	0.97 p = .22	1.73 p = .17	0.04 ns
Cebidae (n=52)	V	0.52 (0.00, 1.05) p = .05	0.95 p = .07	3.13 p = .03	0.22 p < .05
	M	0.92 (0.29, 1.54) p = .003	0.97 p = .36	2.40 p = .08	0.20 p < .05
Catarrhini (n=183)	V	-1.32 (-1.70, -0.99) p = .0001	0.97 p = .03	0.94 p = .42	-0.28 p < .05
	M	-2.22 (-2.62, -1.81) p = .0001	0.98 p = .55	5.76 p = .0009	-0.39 p < .05
Cercopithecoidea (n=137)	V	-2.01 (-2.47, -1.55) p = .0001	0.98 p = .61	0.16 p = .92	-0.30 p < .05
	M	-3.21 (-3.67, -2.75) p = .0001	0.98 p = .31	1.36 p = .26	-0.44 p < .05
Cercopithecinae (n=87)	V	-0.79 (-1.50, -0.09) p = .03	0.97 p = .28	2.42 p = .07	-0.04 ns
	M	-1.95 (-2.97, -0.94) p = .0001	0.98 p = .52	3.76 p = .01	-0.05 ns
Colobinae (n=50)	V	-1.57 (-2.19, -0.96) p = .0001	0.97 p = .28	1.25 p = .30	-0.38 p < .05
	M	-2.89 (-3.45, -2.34) p = .0001	0.97 p = .53	1.18 p = .33	-0.61 p < .05
Hominoidea (n=46)	V	-0.63 (-1.06, -0.19) p = .004	0.95 p = .05	0.56 p = .64	-0.22 p < .05
	M	-1.01 (-1.57, -0.45) p = .0003	0.94 p = .02	0.46 p = .71	-0.20 p < .05

Box 12.30. Facial (centroid) size [ΔS_L_YV34] ← Intranasal distance [ΔS_L_YV49]

Taxon	Maximum likelihood regression coefficient (95% CI) and associated p-value	Shapiro-Wilk test for normality of residuals.	Brown & Forsythe's test for residual homoscedasticity.	Somers' D nonparametric measure and test of association
Anthropoids (n=300)	-0.10 (-0.12, -0.08) p = .0001	0.97 p = .002	6.89 p = .0002	-0.18 p < .05
Platyrrhini (n=117)	0.08 (0.05, 0.12) p = .0001	0.97 p = .09	4.02 p = .007	0.35 p < .05
Atelidae (n=65)	0.07 (0.03, 0.11) p = .0001	0.96 p = .05	1.14 p = .34	0.24 p < .05
Cebidae (n=52)	0.09 (0.04, 0.14) p = .0005	0.89 p = .0001	2.54 p = .07	0.36 p < .05
Catarrhini (n=183)	-0.14 (-0.16, -0.12) p = .0001	0.95 p = .0001	6.93 p = .0002	-0.43 p < .05
Cercopithecoidea (n=137)	-0.14 (-0.16, -0.12) p = .0001	0.98 p = .68	14.01 p = .0001	-0.44 p < .05
Cercopithecinae (n=87)	-0.16 (-0.19, -0.12) p = .0001	0.98 p = .53	19.83 p = .0001	-0.24 p < .05
Colobinae (n=50)	-0.00 (-0.04, 0.03) p = .81	0.97 p = .45	0.23 p = .87	0.02 ns
Hominoidea (n=46)	-0.13 (-0.19, 0.07) p = .0001	0.92 p = .006	0.95 p = .42	-0.40 p < .05

Principal Components Analysis of Masticatory and Nasomaxillary Variables

To see how the masticatory variables relate to nasomaxillary variables, a principal components analysis was conducted. Box 14.31 reports the eigenvalues for the 38 variables examined. The first two principal components together account for only 34% of the total variance, and this should be kept in mind when assessing inter-variable relationships. Box 14.32 lists the component loadings for the first two principal components, and the corresponding scatter plot is displayed in Box 14.33.

Box 14.31. Eigenvalues and accounted-for variance of log delta masticatory and nasomaxillary variables (correlation matrix used in PCA) (n=300)

PC	Eigen-value	Proportion of Variance Explained	Cumulative Proportion Explained	PC	Eigen-value	Proportion of Variance Explained	Cumulative Proportion Explained
1	7.01	.184	.184	20	0.39	.010	.922
2	5.86	.154	.339	21	0.37	.010	.932
3	3.04	.080	.419	22	0.36	.009	.941
4	2.81	.074	.493	23	0.31	.008	.949
5	2.22	.059	.551	24	0.29	.008	.957
6	1.86	.049	.600	25	0.28	.007	.964
7	1.61	.042	.643	26	0.24	.006	.977
8	1.53	.040	.683	27	0.23	.006	.977
9	1.24	.033	.716	28	0.19	.005	.981
10	1.19	.031	.747	29	0.16	.004	.985
11	1.00	.026	.773	30	0.14	.004	.989
12	0.91	.024	.797	31	0.11	.003	.992
13	0.84	.022	.819	32	0.09	.002	.994
14	0.74	.019	.839	33	0.08	.002	.996
15	0.68	.018	.857	34	0.06	.002	.998
16	0.60	.016	.873	35	0.05	.001	.999
17	0.56	.015	.888	36	0.02	.001	.999
18	0.48	.013	.900	37	0.01	.000	1.000
19	0.42	.011	.911	38	0.00	.000	1.000

Reproduced with permission of the copyright owner. Further reproduction prohibited without permission.

Box 14.32. Component loadings for the first two principal components of masticatory and nasomaxillary variables.

Variable	$PC_{(1)}$	$PC_{(2)}$	Variable	$PC_{(1)}$	$PC_{(2)}$
ΔS_L_YV1	0.788	-0.285	ΔL_YV45	-0.089	-0.063
ΔS_L_YV4	-0.438	0.147	ΔL_YV46	0.404	0.395
ΔS_L_YV5	0.207	0.236	ΔS_L_YV49	-0.669	0.067
ΔS_L_YV6	-0.017	-0.156	ΔL_YV30	0.603	0.425
ΔS_L_YV7	0.310	-0.340	ΔL_YV31	0.793	0.124
ΔS_L_YV8	-0.488	-0.215	ΔL_YV32	0.235	-0.349
ΔS_L_YV9	-0.078	-0.108	ΔL_YV33	0.040	-0.432
ΔS_L_YV11	0.494	-0.171	ΔL_YV35	0.671	-0.336
ΔL_YV13	-0.676	0.179	ΔS_L_YV52	-0.110	0.817
ΔS_L_YV14	0.827	0.320	ΔS_L_YV56	0.018	0.910
ΔS_L_YV15	-0.048	0.321	ΔL_YV59	-0.440	-0.274
ΔS_L_YV16	-0.699	0.047	ΔS_L_YV60	-0.104	0.912
ΔS_L_YV17	0.800	-0.248	ΔL_YV61	-0.525	-0.097
ΔS_L_YV18	-0.007	-0.243	ΔL_YV62	-0.162	-0.144
ΔS_L_YV19	0.018	0.188	ΔL_YV63	-0.244	0.008
ΔS_L_YV21	0.008	0.289	ΔS_L_YV64	0.043	0.886
ΔS_L_YV23	-0.513	-0.184	ΔS_L_YV65	-0.012	0.949
ΔS_L_YV25	0.145	-0.159	ΔL_YV66	0.409	-0.164
ΔS_L_YV27	-0.057	0.115	ΔL_YM92	0.260	-0.148

Box 14.33. Bivariate plot of first two principal components (PC 1, PC 2)

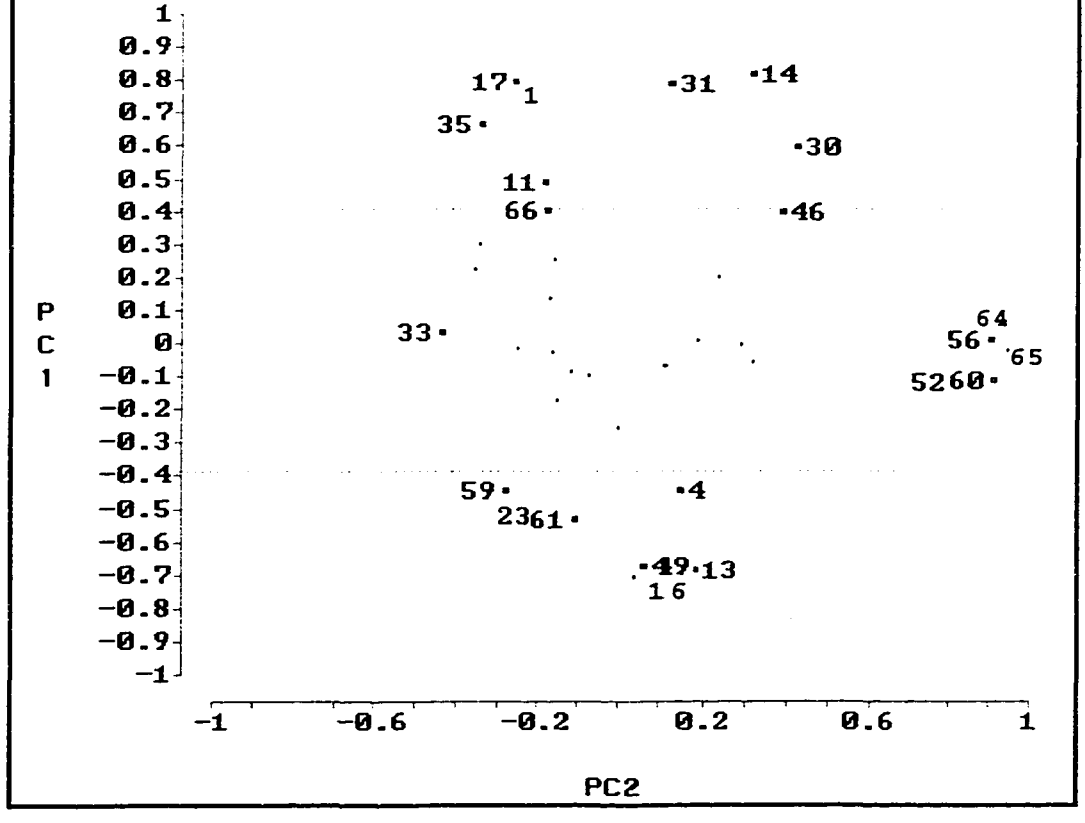

Reproduced with permission of the copyright owner. Further reproduction prohibited without permission.

Variables that load highly (and positively) on $PC_{(1)}$ include maxillary arch length [ΔS_L_Y14], anterior facial length [ΔS_L_Y17], both Krogman's [ΔL_Y30] and Enlow's [ΔL_Y31] angle of facial prognathism, zygoma height [ΔS_L_Y11], and (marginally) orbital deflection [ΔL_Y46] and resultant-occlusal efficiency [ΔL_Y66]. Most of these variables relate to the anteroposterior elongation of facial skeleton. Variables that load highly (and negatively) on $PC_{(1)}$ include (by order of loading importance) upper facial breadth [ΔS_L_16], anteroposterior position of the zygomatic root [ΔL_13], intranasal distance [ΔS_L_49], anteroposterior position of the masseter muscles [ΔL_61], inter-M^3 palatal width [ΔS_L_23], nasal process of maxilla width [ΔS_L_4], and relative anterior-to-posterior bite force magnitude. Thus, $PC_{(1)}$ indicates that anthropoids with forward projecting snouts have narrower faces, more posteriorly located zygomatic roots and masseter muscles relative to cranial size.

$PC_{(2)}$ contrasts facial convexity [ΔL_Y33] against maximum bite force magnitude [ΔS_L_Y52, ΔS_L_Y56, ΔS_L_Y60], and masticatory muscle mass [ΔS_L_Y64, ΔS_L_Y65]. This suggests that anthropoids generating greater bite force magnitudes relative to body size tend to exhibit more concave facial profiles.

Reproduced with permission of the copyright owner. Further reproduction prohibited without permission.

PART VI

Synthesis and Conclusions

Reproduced with permission of the copyright owner. Further reproduction prohibited without permission.

Chapter 15.
Nomological Models of Anthropoid Nasomaxillary Diversity

Introduction

One of the themes running through this thesis is that statistical tests of causal hypotheses take the form of mathematical models of the systems, conditions and phenomenological relationships being tested. In experimental designs, the investigator attempts to isolate one-to-one cause-and-effect relationships by manually controlling other confounding factors (either through block randomization or standardization of these factors). In such cases a simple bivariate association (e.g., significant correlation) is sufficient to render an inference regarding the relationship between the phenomena examined. However, in nonexperimental designs, simple bivariate statistical tests will not necessarily rending accurate inferences because of the possible influence of other relevant variables that have not been controlled for in the analysis (such models are said to be misspecified). The investigator must therefore attempt to control for covariates statistically by including them in the mathematical model of the causal hypothesis. Complex systems require complex models in order to render accurate inferences regarding predicted relationships.

In this chapter, I formulate and evaluate a series of integrated models, using manifest variables, which are based on both theoretical considerations and analytical results (presented in the previous chapters). First, a fully specified integrated model (i.e., one composed of all relevant nasomaxillary and explanatory variables)—Model I—was evaluated against the anthropoid data. Based on this evaluation, Model I was

Reproduced with permission of the copyright owner. Further reproduction prohibited without permission.

modified (i.e., respecified) producing a second, revised model—Model II—which was again tested against the empirical data. For heuristic proposes this final model was depicted in two parts, or submodels, each composed of selected causal pathways and depicted as a path diagram (see Boxes 15.13 & 15.14). The substantive meaning of these models was examined.

Model I (Initial Model): Estimation

The nomological hypotheses pertaining to nasomaxillary development and evolution formulated in Chapters 9 through 14 were integrated into a single structural model (Model I, Box 15.1).[1] As described in Chapter 8, structural models represent a series of specific predictions regarding the covariance relationships (hierarchically specified) of the system. In covariance structural modeling, the model-implied covariance matrix is compared with the empirical covariance matrix to assess the extent to which the theoretical model 'fits' the data. On the basis of this assessment the initial model usually requires respecification (and the theoretical model is consequently modified) to improve the model fit. Modification indices (i.e., the Lagrange multiplier index and the Wald index) generated in the analysis indicate which specific paths of the model to add or remove to improve model fit (Sörbom, 1989; Schumacker & Lomax, 1996). Respecification of the structural model is undertaken with reference to the modification indices, but all decisions as to whether a given causal path is added or removed from the model is guided by theory. The occurrence of influential observations and tests for curvilinearity are presented for the respecified model (Model II) only. Box 15.1 presents the SAS output listing

[1] Due to the great number of parameters (i.e., paths) estimated in Model I it was not practical to depict the model in terms of a path diagram.

Reproduced with permission of the copyright owner. Further reproduction prohibited without permission.

the parameter coefficients, standard errors and *t*-statistics for Model I covariance structural equations. *T*-values of 2.0 or greater indicate significant associations in the model.

Box 15.1. SAS/CALIS output. Model I. Covariance structure analysis, maximum likelihood estimation, manifest variable equations. Unstandardized path coefficients. (multi-level, log delta data; n=300)

```
S_L_YV1 =     1.7520*S_L_YV17 +  1.0000 E1
Std Err       0.0420 PV1V17
t Value      41.7002

S_L_YV4 =     0.7069*S_L_YM44 +  0.3558*S_L_YQ44 +  0.2063*S_L_YM57 +  0.1381*S_L_YQ57  +   1.0000 E4
Std Err       0.0952 PV4M44      0.1585 PV4Q44      0.1546 PV4M57      0.1977 PV4Q57
t Value       7.4248             2.2441             1.3340             0.6986

S_L_YV6 =     0.1125*S_L_YM44 +  0.0409*S_L_YQ44 -  0.3495*S_L_YM57 -  0.3514*S_L_YQ57 +
Std Err       0.0314 PV6M44      0.0522 PV6Q44      0.0517 PV6M57      0.0760 PV6Q57
t Value       3.5887             0.7833            -6.7601            -4.6233

          0.1065*S_L_YM58  +  0.6134*S_L_YQ58 +  1.0000 E6
Std Err   0.0128 PV6M58      0.0927 PV6Q58
t Value   8.2922             6.6208

S_L_YV8 =     0.3270*S_L_YM44 -  0.0785*S_L_YQ44 +  1.0000 E8
Std Err       0.0411 PV8M44      0.0684 PV8Q44
t Value       7.9551            -1.1480

S_L_YV9 =     0.2265*S_L_YV25 +  0.1689*S_L_YM7 +  1.0000 E9
Std Err       0.0413 PV9V25      0.0864 PV7M57
t Value       5.4872             1.9558

S_L_YV11=  -  0.4576*S_L_YM57 +  1.0000 E11
Std Err       0.0971 PV11M57
t Value      -4.7102

S_L_YV12=     0.3124*S_L_YM64 +  1.0000 E12
Std Err       0.0245 PV12M64
t Value      12.7789

L_YV13  =     1.9848*S_L_YM57 +  0.2915*S_L_YQ57 -  1.0329*S_L_YM64 +  0.7231*S_L_YQ64  +  1.0000 E13
Std Err       0.2290 PV13M57     0.2722 PV13Q57     0.2396 PV13M64     0.4926 PV13Q64
t Value       8.6681             1.0707            -4.3105             1.4679

S_L_YV14=  -  0.6787*S_L_YM57 -  0.6370*S_L_YQ57 +  0.5838*S_L_YM58 +  0.6423*S_L_YQ58 +
Std Err       0.0373 PV14M57     0.0548 PV14Q57     0.0093 PV14M58     0.0668 PV14Q58
t Value     -18.2046           -11.6258           63.0445             9.6145

              0.1881*L_YM70  +   0.0116*L_YQ70   +  1.0000 E14
Std Err       0.0117 PV14M70     0.0187 PV14Q70
t Value      16.0786             0.6207

S_L_YV17=     0.5490*S_L_YV14 -  0.0418*L_YV30  -   0.2729*S_L_YM44 +  0.0001*S_L_YQ44 -
Std Err       0.0408 PV17V14     0.0158 PV17V30     0.0236 PV17M44     0.0380 PV17Q44
t Value      13.4592            -2.6403           -11.5761            0.0030

          0.2675*S_L_YM57  -  0.0036*S_L_YQ57  +  1.0000 E17
Std Err   0.0382 PV17M57      0.0481 PV17Q57
t Value  -7.0089            -0.0738

S_L_YV19=  -  0.1837*L_YV32   +  0.7586*S_L_YV18 +  1.0000 E19
Std Err       0.0170 PV19V32     0.0635 PV19V18
t Value     -10.8172           11.9415

S_L_YV21=     0.2207*S_L_YM57 +  0.1086*S_L_YM58 +  1.0000 E21
Std Err       0.0521 PV21M57     0.0129 PV21M58
t Value       4.2340             8.3909
```

Reproduced with permission of the copyright owner. Further reproduction prohibited without permission.

Box 15.1. SAS/CALIS output. Model I. Covariance structure analysis, maximum likelihood estimation, manifest variable equations. Unstandardized path coefficients. (multi-level, log delta data; n=300)

```
S_L_YV22=     0.7778*S_L_YM57 -  0.6128*S_L_YM58 +  1.0000 E22
Std Err       0.0464 PV22M57     0.0115 PV22M58
t Value      16.7791           -53.2548

S_L_YV23=     0.1525*L_YM59   +  0.0982*L_YQ59   +  1.0000 E23
Std Err       0.0187 PV23M59     0.0319 PV23Q59
t Value       8.1331             3.0758

S_L_YV24=   - 1.1212*S_L_YM57 -  0.2133*S_L_YQ57 +  1.0000 E24
Std Err       0.1620 PV24M57     0.2070 PV24Q57
t Value      -6.9215            -1.0301

S_L_YV25=     0.6250*S_L_YV17 -  0.0117*S_L_YM58 +  0.0667*S_L_YQ58 +  1.0000 E25
Std Err       0.0960 PV25V17     0.0356 PV25M57     0.1702 PV25Q58
t Value       6.5083            -0.3275             0.3923

L_YV30  =     1.6163*S_L_YV14 +  0.4023*S_L_YM44 +  0.0118*S_L_YQ44 -  0.0377*S_L_YM57
Std Err       0.1075 PV30V14     0.0565 PV30M44     0.0870 PV30Q44     0.1132 PV30M57
t Value      15.0363             7.1231             0.1351            -0.3333

            - 0.1024*S_L_YQ57   +  0.4935*S_L_YM58 +  0.4350*S_L_YQ58 +  0.1174*L_YM74   +
Std Err       0.1440 PV30Q57     0.0665 PV30M58     0.1691 PV30Q58     0.0292 PV30M74
t Value      -2.5720             4.0230             1.8627            18.9894

            0.0761*L_YQ74   +  0.5261*L_YV95       +  1.0000 E30
Std Err     0.0408 PV30Q74     0.0277 PV30V95
t Value     0.7108             7.4213

L_YV31  =     1.9684*S_L_YV14 +  1.5133*S_L_YV17 +  0.5121*L_YV30   +  0.4005*S_L_YM44
Std Err       0.2020 PV31V14     0.1633 PV31V17     0.0467 PV31V30     0.0835 PV31M44
t Value       9.7463             9.2665            10.9773             4.7945

           - 0.0516*S_L_YQ44 +  0.9170*S_L_YM57 +  1.8458*S_L_YQ57 -  1.0070*S_L_YM58
Std Err       0.1073 PV31Q44     0.1604 PV31M57     0.1883 PV31Q57     0.1024 PV31M58
t Value      -0.4812             5.7160             9.8011            -9.8326

          - 1.7912*S_L_YQ58 -  0.1070*L_YM70  - 0.1192*L_YQ70     +  1.0000 E31
Std Err     0.2189 PV31Q58     0.0477 PV31M70   0.0537 PV31Q70
t Value    -8.1811            -2.2454          -2.2198

L_YV32  =     0.5908*S_L_YV17 -  0.1598*L_YV30   +  0.1043*L_YV95   -  0.2472*L_YM68
Std Err       0.1747 PV32V17     0.0412 PV32V30     0.0609 PV32V95     0.0588 PV32M68
t Value        3.3820            -3.8765             1.7108            -4.2040

           -  0.0421*L_YQ68      +  1.0000 E32
Std Err       0.0809 PV32Q68
t Value      -0.5197

L_YV33  =   - 0.0597*L_YV30   +  0.2345*S_L_YM44 +  0.0468*S_L_YQ44 -  0.1995*S_L_YM57 +
Std Err       0.0532 PV33V30     0.0919 PV33M44     0.1530 PV33Q44     0.1637 PV33M57
t Value      -1.1220             2.5510             0.3058            -1.2192

            0.4718*S_L_YQ57   -  1.1304*S_L_YM58 -  0.4775*S_L_YQ58 +  1.0000 E33
Std Err     0.2304 PV33Q57     0.0858 PV33M58     0.2829 PV33Q58
t Value     2.0484           -13.1679            -1.6878

L_YV35  =     0.8968*S_L_YV1  +  0.1102*S_L_YM44 -  0.1894*S_L_YQ44 -  0.6443*S_L_YM57 +
Std Err       0.0909 PV35V1      0.1108 PV35M44     0.1600 PV35Q44     0.1848 PV35M57
t Value       9.8630             0.9950            -1.1842            -3.4866

            0.5089*S_L_YQ57   -  0.1054*S_L_YM58 -  0.3704*S_L_YQ58 +  1.0000 E35
Std Err     0.2380 PV35Q57     0.0574 PV35M58     0.2877 PV35Q58
t Value     2.1379            -1.8363            -1.2873

S_L_YM44=     0.7036*S_L_YM84 +  1.0000 EM44
Std Err       0.0645 PM44M84
t Value      10.9062

S_L_YQ44=     0.4321*S_L_YQ84 +  1.0000 EQ44
Std Err       0.1777 PQ44Q84
t Value       2.4320
```

Reproduced with permission of the copyright owner. Further reproduction prohibited without permission.

Box 15.1. SAS/CALIS output. Model I. Covariance structure analysis, maximum likelihood estimation, manifest variable equations. Unstandardized path coefficients. (multi-level, log delta data; n=300)

```
L_YV45  =  -  0.5866*S_L_YV8   -  0.1768*S_L_YM44 +  0.2015*S_L_YQ44 +  0.0226*L_YM78   +
Std Err       0.1324 PV45V8       0.1079 PV45M44      0.1570 PV45Q44      0.0623 PV45M78
t Value      -4.4316             -1.6380             1.2834              0.3623

              0.0961*L_YQ78  +   1.9240*S_L_YV16 +  1.0000 E45
Std Err       0.0999 PV45Q78      0.1868 PV45V16
t Value       0.9626             10.3016

L_YV46  =     0.5128*L_YM70   +  0.0912*L_YQ70   +  0.2356*L_YM74   +  0.1402*L_YQ74
Std Err       0.0749 PV46M70      0.0863 PV46Q70      0.0709 PV46M74      0.0836 PV46Q74
t Value       6.8445              1.0557             3.3250              1.6766

            -  0.2350*S_L_YM84   -  0.1411*S_L_YQ84 +  1.0000 E46
Std Err       0.2120 PV46M84      0.5597 PV46Q84
t Value      -1.1082             -0.2520

S_L_YV49=     0.9625*S_L_YM44 +  0.4513*S_L_YQ44 +  0.0745*L_YV45   -  0.0044*L_YM78   +
Std Err       0.0353 PV49M44      0.0565 PV49Q44      0.0174 PV49V45      0.0222 PV49M78
t Value      27.2934              7.9915             4.2706             -0.1963

           0.0114*L_YQ78 +  1.0000 E49
Std Err    0.0359 PV49Q78
t Value    0.3174

S_L_YM57=     0.2055*L_YM63   +  0.7695*S_L_YM64 +  1.0000 EM57
Std Err       0.0220 PM57M63      0.0363 PM57M64
t Value       9.3501             21.2112

S_L_YQ57=     0.2581*L_YQ63   +  1.1851*S_L_YQ64 +  1.0000 EQ57
Std Err       0.0212 PM57Q63      0.0628 PM57Q64
t Value      12.1978             18.8844

S_L_YM58=     1.2929*S_L_YM64 +  1.0000 L_DGUM   +  1.0000 EM58
Std Err       0.1695 PM58M64
t Value       7.6294

S_L_YQ58=     1.1267*S_L_YQ64 +  1.0000 EQ58
Std Err       0.0559 PM58Q64
t Value      20.1667

L_YM59  =     0.6562*L_YM63   +  0.4642*L_DGUM   +  1.0000 EM59
Std Err       0.0952 PM59M63      0.0538 PV59GUM
t Value       6.8936              8.6215

L_YQ59  =     0.9631*L_YQ63   +  1.0000 EQ59
Std Err       0.0605 PQ59Q63
t Value      15.9157

L_YM62  =     0.3392*L_DGUM   -  0.2616*L_DINSEC -  0.1815*L_DROOT  +  1.0000 EM62
Std Err       0.0389 PV62GUM      0.0457 PV62INS      0.0372 PV62ROO
t Value       8.7269             -5.7280            -4.8852

L_YM63  =     0.2624*L_DINSEC +  1.0000 EM63
Std Err       0.0345 PM63INS
t Value       7.6053

S_L_YM64=  -  0.0455*L_DGUM   +  1.0000 EM64
Std Err       0.0196 PM64GUM
t Value      -2.3178

L_YV69  =  -  0.5010*L_YM70   +  0.0165*L_YQ70   +  0.7831*S_L_YM84 +  1.1043*S_L_YQ84 + 1.0000 E69
Std Err       0.0538 PV69M70      0.0638 PV69Q70      0.1371 PV69M84      0.3978 PV69Q84
t Value      -9.3180              0.2596             5.7126              2.7757

L_YM70  =     0.1784*L_YM78   -  0.0201*L_YM81   -  1.5078*S_L_YM84 +  1.0000 EM70
Std Err       0.0645 PM70M78      0.0784 PM70M81      0.1362 PM70M84
t Value       2.7651             -0.2560            -11.0674
```

Reproduced with permission of the copyright owner. Further reproduction prohibited without permission.

Box 15.1. SAS/CALIS output. Model I. Covariance structure analysis, maximum likelihood estimation, manifest variable equations. Unstandardized path coefficients.
(multi-level, log delta data; n=300)

```
L_YQ70  =     0.1040*L_YQ78   +  0.0262*L_YQ81   -  0.2715*S_L_YQ84 +  1.0000 EQ70
Std Err       0.0804 PQ70Q78     0.0534 PQ70Q81     0.3678 PQ70Q84
t Value       1.2937             0.4907            -0.7382

L_YM74  =     0.2435*L_YM70   -  0.1457*L_YM81   -  1.3116*S_L_YM84 +  1.0000 EM74
Std Err       0.0592 PM74M70     0.0750 PM74M81     0.1663 PM74M84
t Value       4.1132            -1.9426            -7.8855

L_YQ74  =  -  0.0448*L_YQ70   -  0.0024*L_YQ81   -  1.8331*S_L_YQ84 +  1.0000 EQ74
Std Err       0.0597 PQ74Q70     0.0519 PQ74Q81     0.3726 PQ74Q84
t Value      -0.7516            -0.0453            -4.9199

L_YM78  =  -  1.0436*S_L_YM84 +  1.0000 EM78
Std Err       0.1047 PM78M84
t Value      -9.9709

L_YQ78  =  -  1.0328*S_L_YQ84 +  1.0000 EQ78
Std Err       0.2751 PQ78Q84
t Value      -3.7546

L_YM81  =  -  0.3231*L_YM78   +  0.7215*S_L_YM84 +  1.0000 EM81
Std Err       0.0437 PM81M78     0.0914 PM81M84
t Value      -7.3873            7.8954

L_YQ81  =  -  0.5172*L_YQ78   -  0.2407*S_L_YQ84 +  1.0000 EQ81
Std Err       0.0817 PQ81Q78     0.3979 PQ81Q84
t Value      -6.3276           -0.6050

L_YV95  =     0.0090*L_YM70   +  0.2538*L_YQ70   +  0.1785*L_YM74   +  0.2072*L_YQ74 +  1.0000 E95
Std Err       0.0689 PV95M70     0.0890 PV95Q70     0.0641 PV95M74     0.0831 PV95Q74
t Value       0.1305             2.8512             2.7874             2.4933
```

Model I (Initial Model): Model Fit

In covariance structure analysis a causal model is formulated from underlying theory. To assess the efficacy of the theoretical model we want to determine how well the empirical data, that is, the sample covariance matrix (S) corresponds to the model-implied (or predicted) variance-covariance matrix (Σ). The criteria for assessment of model fit were discussed in detail in Chapter 8. Box 15.2 presents several fit indices for Model I (see Chapter 8 for a brief description of these indices; or refer to Marsh, Balla & Hau, 1996, for a more detailed discussion and analysis).

Reproduced with permission of the copyright owner. Further reproduction prohibited without permission.

Box 15.2. Various fit indices for Model I.	
Fit Index:	Estimate:
Chi-square (df=1340)	12690.37 (p=.0001)
Goodness of Fit Index (GFI)	0.480
Adjusted Goodness of Fit Index (AGFI)	0.381
Bentler's Comparative Fit Index (CFI)	0.339
Normed Tucker Lewis Index (NTLI)	0.322
Root Mean Square Residual (RMR)	0.0017

Chi-square is the only fit index associated with a statistical test of significance. The Model I chi-square p-value of 0.0001 indicates that the predicted variance-covariance matrix is significantly different (at the 0.05 level) from the empirical sample variance-covariance matrix: the causal model does not fit the empirical data well. However, in structural equation modeling the chi-square test is not very informative since it is highly sensitive to sample size. It has been shown that with sample sizes greater than about 200, the predicted and empirical variance-covariance matrices need to be nearly identical before the test yields nonsignificant results.

The next four indices—GFI, AGFI, CFI and NTLI—are more robust with respect to sample size, but provide no inference statistics. They all measure, to some extent, the amount of variance in the empirical data accounted for by the theoretical model. Values around 0.90 for these fit indices indicate a good model fit (Hatcher, 1994). The mean score over all four indices for Model I is 0.38. This fit value, while low, is not unfavorable at this stage considering that no attempt at model respecification has yet been made.

Model I (Initial Model): Modification Diagnostics

Model respecification is required when one or more of the components of the

Reproduced with permission of the copyright owner. Further reproduction prohibited without permission.

theoretical model, and corresponding structural equations, do not conform to the empirical relationships observed in the data. The theoretical model is then modified (and the corresponding structural model respecified) to be more consistent with the data. The modified model is then subjected to a second round of assessments to see whether respecification has improved the model fit (*cf.* single sample cross validation, Schumacher & Lomax, 1996, p. 109). This process is continued until a 'best fit' model is attained, which is consistent with underlying theory.

Four statistics in particular were used to guide model respecification in the present instance: (1) the *t*-values for the path coefficients in the model, (2) the condition index collinearity diagnostic, (3) the Lagrange multiplier test statistic, and (4) the Wald test statistic. Standard errors and *t*-statistics are given for each of the non-standardized path coefficients of the initial structural model presented in Box 15.1. The remaining three statistics are discussed below.

Model I (Initial Model): Collinearity Diagnostics

The condition index for the 39 independent endogenous modeled variables is presented in Box 15.3 (see Chapter 8). It can be seen that several variables load substantially (i.e., above 0.40) on each of the ill-conditioned components (25-40) of the index. As one might expect, the two measures of facial prognathism exhibit a perceptible (but low) level of near collinearity—the condition index values for Krogman's angle [ΔL_YV30] and Enlow's angle [ΔL_YV31] on component 38 are 0.38 and 0.40, respectively. The three Q-level maximum bite force variables, anterior MBF [ΔS_L_YQ57], posterior MBF [ΔS_L_YQ58] and anterior-to-posterior MBF ratio [ΔL_YQ59], all show relatively higher near collinearity; each with index values over

Reproduced with permission of the copyright owner. Further reproduction prohibited without permission.

0.80 on component 25. Finally, a low degree of near collinearity was observed between M-level cranial base angle [ΔL_YM70] (0.38), and relative middle cranial fossa length [ΔL_YM78] (0.41), on component 36. The observed near collinearities between these sets of variables makes sense both biologically and morphometrically.

Box 15.3. SAS output condition index collinearity diagnostics. Model I.

Number	Eigenvalue	Condition Index	Var Prop INTERCEP	Var Prop S_L_YV1	Var Prop S_L_YV8	Var Prop S_L_YV14	Var Prop S_L_YV16	Var Prop S_L_YV17
1	15.99832	1.00000	0.0000	0.0000	0.0000	0.0000	0.0000	0.0000
2	4.26159	1.93754	0.0000	0.0040	0.0065	0.0015	0.0060	0.0015
3	3.33596	2.18991	0.0000	0.0001	0.0002	0.0000	0.0007	0.0001
4	3.05680	2.28772	0.0000	0.0003	0.0044	0.0009	0.0001	0.0001
5	1.62745	3.13533	0.0000	0.0000	0.0001	0.0002	0.0000	0.0000
6	1.34030	3.45491	0.0000	0.0000	0.0080	0.0006	0.0001	0.0000
7	1.25489	3.57054	0.0000	0.0012	0.0046	0.0000	0.0027	0.0002
8	1.23710	3.59613	0.0000	0.0005	0.0561	0.0000	0.0034	0.0007
9	1.07493	3.85787	0.0000	0.0009	0.0025	0.0000	0.0002	0.0001
10	1.01848	3.96333	0.0000	0.0002	0.0034	0.0001	0.0124	0.0001
11	0.91954	4.17111	0.0000	0.0000	0.0091	0.0000	0.0063	0.0000
12	0.80742	4.45129	0.0000	0.0000	0.0059	0.0002	0.0000	0.0000
13	0.65390	4.94631	0.0000	0.0048	0.0180	0.0155	0.0771	0.0010
14	0.61129	5.11580	0.0000	0.0008	0.0197	0.0002	0.0002	0.0004
15	0.59240	5.19673	0.0000	0.0000	0.2773	0.0022	0.0598	0.0009
16	0.53855	5.45034	0.0000	0.0001	0.0395	0.0002	0.0004	0.0005
17	0.37077	6.56878	0.0000	0.0796	0.0224	0.0051	0.0056	0.0055
18	0.35815	6.68349	0.0000	0.0015	0.1450	0.0073	0.1852	0.0022
19	0.31637	7.11114	0.0000	0.0209	0.0107	0.0010	0.0048	0.0010
20	0.24386	8.09965	0.0000	0.0081	0.0009	0.0010	0.0064	0.0000
21	0.15727	10.08582	0.0000	0.0021	0.0546	0.0001	0.0191	0.0204
22	0.11198	11.95259	0.0000	0.2777	0.0605	0.0482	0.0845	0.0754
23	0.07334	14.76919	0.0000	0.0804	0.0080	0.2109	0.0269	0.1321
24	0.02597	24.81878	0.0000	0.0002	0.0069	0.0033	0.0056	0.0132
25	0.00683	48.40188	0.0000	0.0025	0.0001	0.0036	0.0000	0.0010
26	0.00175	95.68807	0.0000	0.0736	0.0089	0.0014	0.0819	0.0003
27	0.00120	115.47231	0.0000	0.0031	0.0055	0.0056	0.0000	0.0002
28	0.0008040	141.06176	0.0003	0.0055	0.0178	0.0009	0.0212	0.0041
29	0.0005467	171.06735	0.0000	0.0139	0.0438	0.0043	0.1886	0.0002
30	0.0004852	181.58915	0.0000	0.0022	0.0168	0.0144	0.0060	0.0066
31	0.0003980	200.48709	0.0003	0.0488	0.0300	0.0000	0.0001	0.0137
32	0.0003317	219.60738	0.0000	0.1880	0.0897	0.0221	0.0087	0.0710
33	0.0002865	236.31357	0.0003	0.0001	0.0021	0.0298	0.1108	0.0089
34	0.0002412	257.56586	0.0004	0.0026	0.0019	0.0839	0.0045	0.0011
35	0.0001275	354.26153	0.0015	0.0008	0.0012	0.0483	0.0332	0.0191
36	0.0001075	385.83559	0.0019	0.0031	0.0010	0.0146	0.0000	0.0000
37	0.0000999	400.20047	0.0001	0.0455	0.0006	0.0611	0.0060	0.0086
38	0.0000606	513.62592	0.0001	0.0455	0.0135	0.1746	0.0020	0.2609
39	0.0000537	546.03476	0.0028	0.0534	0.0008	0.2119	0.0006	0.3209
40	0.0000133	1096	0.9922	0.0280	0.0019	0.0251	0.0291	0.0277

Reproduced with permission of the copyright owner. Further reproduction prohibited without permission.

Box 15.3. SAS output condition index collinearity diagnostics. Model I.

Number	Var Prop S_L_YV18	Var Prop S_L_YV25	Var Prop L_YV30	Var Prop L_YV31	Var Prop L_YV32	Var Prop L_YV35	Var Prop S_L_YM44	Var Prop S_L_YQ44
24	0.0481	0.0162	0.0000	0.0000	0.0000	0.0000	0.0003	0.0000
25	0.0012	0.0090	0.0000	0.0000	0.0000	0.0000	0.0016	0.0221
26	0.0503	0.0292	0.0010	0.0042	0.0407	0.0238	0.0049	0.0004
27	0.0013	0.0010	0.0154	0.0005	0.1287	0.0010	0.0016	0.0011
28	0.0067	0.0055	0.0025	0.0012	0.0026	0.0068	0.0113	0.0046
29	0.0134	0.0077	0.0010	0.0002	0.1092	0.0025	0.0502	0.0002
30	0.0007	0.0050	0.0041	0.0551	0.0544	0.0661	0.0331	0.0016
31	0.0524	0.0002	0.0007	0.0194	0.0803	0.0620	0.0038	0.0030
32	0.0145	0.0723	0.0589	0.0015	0.0992	0.4312	0.0182	0.0070
33	0.0311	0.0068	0.0020	0.0255	0.0187	0.0784	0.0004	0.0053
34	0.0001	0.0017	0.0369	0.0527	0.0398	0.0317	0.0390	0.0001
35	0.0072	0.0062	0.0058	0.3152	0.2980	0.0051	0.0152	0.0031
36	0.1115	0.0108	0.0118	0.0502	0.0133	0.0938	0.0302	0.0000
37	0.0383	0.0256	0.0652	0.0213	0.0039	0.1455	0.0624	0.0005
38	0.0046	0.0021	0.4099	0.0145	0.0019	0.0404	0.0014	0.0062
39	0.1207	0.0267	0.3807	0.3982	0.0010	0.0100	0.0365	0.0026
40	0.0069	0.0223	0.0041	0.0402	0.1082	0.0017	0.0979	0.0075

Number	Var Prop L_YV45	Var Prop S_L_YM57	Var Prop S_L_YQ57	Var Prop S_L_YM58	Var Prop S_L_YQ58	Var Prop L_YM59	Var Prop L_YQ59	Var Prop L_YM62
24	0.0000	0.0767	0.0003	0.1705	0.0002	0.0000	0.0005	0.0000
25	0.0000	0.0003	0.8757	0.0007	0.8703	0.0000	0.8051	0.0000
26	0.0202	0.0008	0.0016	0.0073	0.0008	0.0040	0.0015	0.0001
27	0.0000	0.0075	0.0000	0.0136	0.0003	0.0029	0.0004	0.0012
28	0.2287	0.0012	0.0008	0.0106	0.0009	0.0001	0.0028	0.0213
29	0.1613	0.0065	0.0053	0.0235	0.0086	0.0005	0.0051	0.0093
30	0.0163	0.0023	0.0100	0.0020	0.0097	0.0006	0.0037	0.0714
31	0.1362	0.0088	0.0005	0.0077	0.0003	0.0179	0.0001	0.0503
32	0.0163	0.0000	0.0032	0.0058	0.0043	0.0010	0.0002	0.0859
33	0.3050	0.0159	0.0069	0.0273	0.0056	0.0071	0.0014	0.1144
34	0.0001	0.0134	0.0129	0.0095	0.0092	0.0222	0.0107	0.0051
35	0.0223	0.0279	0.0116	0.0073	0.0135	0.0885	0.0054	0.1016
36	0.0187	0.0096	0.0128	0.0610	0.0130	0.0048	0.0129	0.2210
37	0.0412	0.0085	0.0247	0.0251	0.0263	0.0353	0.0137	0.0121
38	0.0124	0.1920	0.0127	0.2588	0.0128	0.2408	0.0039	0.1724
39	0.0091	0.2378	0.0050	0.2035	0.0023	0.2563	0.0020	0.0412
40	0.0122	0.3666	0.0069	0.1641	0.0056	0.3179	0.0000	0.0927

Number	Var Prop L_YM63	Var Prop L_YQ63	Var Prop S_L_YM64	Var Prop S_L_YQ64	Var Prop L_YM68	Var Prop L_YQ68	Var Prop L_YV69	Var Prop L_YM70
24	0.0000	0.0001	0.2158	0.0002	0.0000	0.0007	0.0000	0.0000
25	0.0000	0.0145	0.0000	0.0410	0.0000	0.0054	0.0000	0.0000
26	0.0020	0.0000	0.0566	0.0002	0.0141	0.0054	0.0113	0.0063
27	0.0022	0.0001	0.0119	0.0002	0.0000	0.0001	0.0051	0.0017
28	0.0047	0.0011	0.0194	0.0000	0.0012	0.0012	0.0019	0.0318
29	0.0003	0.0003	0.0207	0.0066	0.0355	0.0079	0.1001	0.0229
30	0.0007	0.0001	0.0003	0.0000	0.0016	0.0002	0.0005	0.0064
31	0.0055	0.0023	0.0026	0.0017	0.0300	0.0007	0.0988	0.0048
32	0.0000	0.0003	0.0070	0.0019	0.0000	0.0001	0.0122	0.0209
33	0.0011	0.0006	0.0043	0.0038	0.0026	0.0017	0.0055	0.1730
34	0.0261	0.0039	0.0080	0.0009	0.0727	0.0265	0.2731	0.0178

Reproduced with permission of the copyright owner. Further reproduction prohibited without permission.

Box 15.3. SAS output condition index collinearity diagnostics. Model I.

35	0.0145	0.0022	0.0583	0.0135	0.2385	0.0003	0.0183	0.0145
36	0.1071	0.0080	0.1257	0.0021	0.1255	0.0120	0.0560	0.3840
37	0.2857	0.0016	0.1041	0.0000	0.0678	0.0054	0.0077	0.0131
38	0.3275	0.0000	0.0197	0.0009	0.3394	0.0215	0.1567	0.0491
39	0.0134	0.0152	0.0087	0.0104	0.0649	0.0043	0.1214	0.1674
40	0.2092	0.0013	0.0894	0.0016	0.0064	0.0195	0.1314	0.0862

Number	Var Prop L_YQ70	Var Prop L_YM74	Var Prop L_YQ74	Var Prop L_YM78	Var Prop L_YQ78	Var Prop L_YM81	Var Prop L_YQ81	Var Prop S_L_YM84
24	0.0084	0.0000	0.0000	0.0000	0.0008	0.0000	0.0001	0.0398
25	0.0010	0.0000	0.0051	0.0000	0.0076	0.0000	0.0016	0.0001
26	0.0030	0.0100	0.0002	0.0030	0.0063	0.0007	0.0017	0.0059
27	0.0074	0.0119	0.0198	0.0074	0.0012	0.0110	0.0009	0.0464
28	0.0086	0.0213	0.0000	0.0082	0.0015	0.0231	0.0001	0.0023
29	0.0007	0.0016	0.0231	0.0248	0.0008	0.0343	0.0032	0.0612
30	0.0024	0.2195	0.0041	0.0083	0.0035	0.0014	0.0000	0.0562
31	0.0006	0.0012	0.0011	0.0091	0.0045	0.0583	0.0097	0.0028
32	0.0029	0.0431	0.0014	0.0004	0.0003	0.0001	0.0002	0.0170
33	0.0253	0.1246	0.0001	0.0259	0.0001	0.0153	0.0007	0.0047
34	0.0098	0.0791	0.0005	0.0167	0.0113	0.0430	0.0110	0.0014
35	0.0009	0.0914	0.0009	0.0007	0.0010	0.1371	0.0032	0.0019
36	0.0003	0.0015	0.0007	0.4132	0.0008	0.0005	0.0007	0.0696
37	0.0009	0.0388	0.0033	0.2781	0.0005	0.4085	0.0000	0.0020
38	0.0032	0.1802	0.0044	0.0045	0.0293	0.0489	0.0002	0.0372
39	0.0061	0.1749	0.0025	0.0453	0.0064	0.1673	0.0048	0.4010
40	0.0005	0.0010	0.0047	0.1544	0.0305	0.0504	0.0047	0.0498

Number	Var Prop S_L_YQ84	Var Prop L_YV95
24	0.0002	0.0000
25	0.0038	0.0000
26	0.0095	0.0033
27	0.0070	0.0191
28	0.0001	0.0129
29	0.0003	0.0050
30	0.0001	0.0036
31	0.0113	0.0187
32	0.0002	0.0221
33	0.0037	0.0056
34	0.0160	0.0362
35	0.0032	0.0337
36	0.0352	0.0000
37	0.0125	0.0071
38	0.0000	0.1413
39	0.1206	0.6208
40	0.0068	0.0705

Reproduced with permission of the copyright owner. Further reproduction prohibited without permission.

Model I (Initial Model): Modification Indices (Lagrange Multiplier & Wald Tests)

As discussed in Chapter 8, two statistics are particularly useful in aiding the respecification process: the Lagrange multiplier, which indicates the bivariate relationships to add to the causal model in order to improve model fit, and the Wald statistic, which indicates which paths should be removed from the model to improve model fit. Box 15.4 lists the top Lagrange multipliers and Wald estimates associated with Model I.

Box 15.4. Lagrange multiplier and Wald statistics for respecification of Model I

Top Lagrange multipliers (Best causal pathways to add)	Top Wald estimates (Best causal pathways to remove)
(1) ΔS_L_YM64 ← ΔS_L_YM58	(1) CM68Q68 (cov)
(2) ΔS_L_YM58 ← ΔS_L_YV14	(2) CINSQ68 (cov)
(3) ΔS_L_YM58 ← ΔS_L_YV22	(3) CGUMQ63 (cov)
(4) ΔS_L_YQ58 ← ΔS_L_YQ57	(4) CROOQ68 (cov)
(5) ΔS_L_YM58 ← ΔL_YV33	(5) CROOQ63 (cov)
(6) ΔS_L_YM57 ← ΔS_L_YQ58	(6) CM68Q63 (cov)
(7) ΔS_L_YM58 ← ΔL_YV30	(7) CGUMQ68 (cov)
(8) ΔS_L_YM58 ← ΔL_YV31	(8) CINSQ63 (cov)
(9) ΔS_L_YM58 ← ΔS_L_YV17	(9) PV17Q44
(10) ΔS_L_YV21 ← ΔS_L_YV22	(10) PQ74Q81
(11) ΔS_L_YM64 ← ΔL_YM68	(11) CM84Q63 (cov)
(12) ΔS_L_YM44 ← ΔS_L_YV16	
(13) ΔL_YM70 ← ΔL_DROOT	
(14) ΔL_YV13 ← ΔS_L_YM84	
(15) ΔL_YM70 ← ΔL_YM68	
(16) ΔS_L_YM57 ← ΔL_DINSEC	
(17) ΔS_L_YM44 ← ΔS_L_YV16	
(18) ΔL_YV95 ← ΔS_L_YM84	
(19) ΔS_L_YV8 ← ΔS_L_YM84	
(20) ΔL_YV95 ← ΔL_DROOT	

Reproduced with permission of the copyright owner. Further reproduction prohibited without permission.

Model II (Respecified Model): Specification and Estimation

Of the 45 endogenous variables included in Model I, 34 were respecified based on the preceding path coefficient *t*-test results (Box 15.1), collinearity diagnostics (Box 15.3), and modification indices (Box 15.4). Box 15.5 provides a brief summary and justifications for model respecification.

Box 15.5. Model I to Model II respecification details.

Path	Respecification	Justification
ΔS_L_YV4 ← ΔS_L_YM57	Path removed	Nonsignificant path coefficient
ΔS_L_YV4 ← ΔS_L_YQ57	Path removed	Nonsignificant path coefficient
ΔS_L_YV6 ← ΔS_L_YQ44	Path removed	Nonsignificant path coefficient
ΔS_L_YV6 ← ΔS_L_YM57	Path removed	Nonsignificant path coefficient
ΔS_L_YV6 ← ΔS_L_YM58	Path removed	Nonsignificant path coefficient
ΔS_L_YV8 ← ΔS_L_YQ44	Path removed	Nonsignificant path coefficient
ΔS_L_YV8 ← ΔS_L_YM84	Path added	Lagrange multiplier test
ΔS_L_YV11 ← ΔS_L_YM57	Path removed	Simplify model
ΔS_L_YV12 ← ΔS_L_YQ64	Path added	Lagrange multiplier test
ΔL_YV13 ← ΔS_L_YQ57	Path removed	Nonsignificant path coefficient
ΔL_YV13 ← ΔS_L_YM64	Path removed	Non significant path coefficient
ΔL_YV13 ← ΔS_L_YV14	Path added	Topographic relationship
ΔS_L_YV14 ← ΔS_L_YM70	Path removed	Nonsignificant path coefficient
ΔS_L_YV14 ← ΔS_L_YQ70	Path removed	Nonsignificant path coefficient
ΔS_L_YV14 ← ΔS_L_YV17	Path added	Lagrange; structural constraint
ΔS_L_YV14 ← ΔL_YV30	Path added	Lagrange multiplier test
ΔS_L_YV16 ← ΔS_L_YM44	Path added	Lagrange multiplier test
ΔS_L_YV16 ← ΔS_L_YQ44	Path added	Lagrange multiplier test
ΔS_L_YV16 ← ΔS_L_YQ57	Path added	Lagrange multiplier test
ΔS_L_YV16 ← ΔS_L_YQ58	Path added	Lagrange multiplier test
ΔS_L_YV17 ← ΔS_L_YQ57	Path removed	Nonsignificant path coefficient
ΔS_L_YV17 ← ΔS_L_YQ44	Path removed	Nonsignificant coefficient, Wald
ΔS_L_YV17 ← ΔS_L_YV14	Path removed	Change causal model
ΔS_L_YV17 ← ΔS_L_YV18	Path added	Lagrange multiplier test
ΔS_L_YV17 ← ΔS_L_YQ58	Path added	Lagrange multiplier test
ΔS_L_YV21 ← ΔS_L_YM58	Path removed	Nonsignificant path coefficient
ΔS_L_YV22 ← ΔS_L_YM57	Path removed	Simplify model
ΔS_L_YV22 ← ΔS_L_YM58	Path removed	Simplify model
ΔS_L_YV23 ← ΔS_L_YM59	Path removed	Replace w/ M57 due to collinearity
ΔS_L_YV23 ← ΔS_L_YQ59	Path removed	Replace w/ Q57 due to collinearity
ΔS_L_YV23 ← ΔS_L_YM57	Path added	In place of M59
ΔS_L_YV23 ← ΔS_L_YQ57	Path added	In place of Q59
ΔS_L_YV23 ← ΔS_L_YM58	Path added	Lagrange multiplier test
ΔS_L_YV23 ← ΔS_L_YQ58	Path added	Lagrange multiplier test
ΔS_L_YV24 ← ΔS_L_YQ57	Path removed	Nonsignificant path coefficient
ΔS_L_YV25 ← ΔS_L_YQ58	Path removed	Nonsignificant path coefficient
ΔS_L_YV25 ← ΔS_L_YM57	Path added	Lagrange multiplier test
ΔS_L_YV27 ← ΔS_L_V18	Path added	Lagrange multiplier test

Reproduced with permission of the copyright owner. Further reproduction prohibited without permission.

Box 15.5. Model I to Model II respecification details.		
Path	Respecification	Justification
ΔL_YV30 ← ΔS_L_YV14	Path removed	Change causal model
ΔL_YV30 ← ΔS_L_YQ44	Path removed	Nonsignificant path coefficient
ΔL_YV30 ← ΔS_L_YM57	Path removed	Nonsignificant path coefficient
ΔL_YV30 ← ΔS_L_YQ57	Path removed	Nonsignificant path coefficient
ΔL_YV30 ← ΔL_YM70	Path added	Lagrange multiplier test
ΔL_YV31 ← all	Paths removed	Due to collinearity with V30
ΔL_YV32 ← ΔL_YV95	Path removed	Nonsignificant path coefficient
ΔL_YV32 ← ΔL_YM68	Path removed	Nonsignificant path coefficient
ΔL_YV32 ← ΔL_YQ68	Path removed	Nonsignificant path coefficient
ΔL_YV33 ← ΔS_L_YQ44	Path removed	Nonsignificant path coefficient
ΔL_YV33 ← ΔS_L_YM57	Path removed	Nonsignificant path coefficient
ΔL_YV33 ← ΔS_L_YM58	Path removed	Change causal model
ΔL_YV33 ← ΔS_L_YV35	Path added	Change causal model
ΔL_YV35 ← ΔS_L_YM44	Path removed	Nonsignificant path coefficient
ΔL_YV35 ← ΔS_L_YQ44	Path removed	Nonsignificant path coefficient
ΔL_YV35 ← ΔS_L_YM57	Path removed	Change causal model
ΔL_YV35 ← ΔS_L_YQ57	Path removed	Nonsignificant path coefficient
ΔL_YV35 ← ΔS_L_YQ58	Path removed	Nonsignificant path coefficient
ΔL_YV35 ← ΔL_YV30	Path added	Lagrange multiplier test
ΔL_YV45 ← ΔS_L_YM44	Path removed	Nonsignificant path coefficient
ΔL_YV45 ← ΔS_L_YQ44	Path removed	Nonsignificant path coefficient
ΔL_YV45 ← ΔS_L_YM78	Path removed	Nonsignificant path coefficient
ΔL_YV45 ← ΔS_L_YQ78	Path removed	Nonsignificant path coefficient
ΔL_YV46 ← ΔS_L_YQ70	Path removed	Nonsignificant path coefficient
ΔL_YV46 ← ΔS_L_YQ74	Path removed	Nonsignificant path coefficient
ΔL_YV46 ← ΔS_L_YM84	Path removed	Nonsignificant path coefficient
ΔL_YV46 ← ΔS_L_YQ84	Path removed	Nonsignificant path coefficient
ΔS_L_YV49 ← ΔS_L_YM78	Path removed	Nonsignificant path coefficient
ΔS_L_YV49 ← ΔS_L_YQ78	Path removed	Nonsignificant path coefficient
ΔS_L_YM58 ← ΔS_L_DGUM	Path removed	Nonsignificant coefficient; Wald
ΔL_YM59 ← all	Paths removed	Due to collinearity with M57
ΔL_YQ59 ← all	Paths removed	Due to collinearity with Q57
ΔL_YM62 ← all	Paths removed	Simplify model
ΔL_YM63 ← all	Paths removed	Simplify model
ΔS_L_YM64 ← all	Paths removed	Simplify model
ΔL_YV69 ← ΔL_YQ70	Paths removed	Nonsignificant path coefficient
ΔL_YM70 ← ΔL_YM81	Path removed	Nonsignificant path coeeficient
ΔL_YQ70 ← all	Paths removed	Nonsignificant path coefficients
ΔL_YM74 ← ΔL_YM81	Path removed	Nonsignificant path coefficient
ΔL_YQ74 ← ΔL_YQ70	Path removed	Nonsignificant path coefficient
ΔL_YQ74 ← ΔL_YQ81	Path removed	Nonsignificant path coefficient
ΔL_YM78 ← all	Path removed	Simplify model
ΔL_YQ78 ← all	Path removed	Simplify model
ΔL_YM81 ← ΔL_YM78	Path removed	Nonsignificant path coefficient
ΔL_YQ81 ← ΔL_YQ78	Path removed	Nonsignificant path coefficient
ΔL_YQ81 ← ΔS_L_YQ84	Path removed	Nonsignificant path coefficient
ΔL_YV95 ← all	Paths removed	Nonsignificant path coefficient; Simplify model

Reproduced with permission of the copyright owner. Further reproduction prohibited without permission.

Model II (Respecified Model): Estimation

Box 15.6 presents the parameter coefficients, standard errors and *t*-statistics for Model II covariance structural equations.

Box 15.6. SAS/CALIS output. Model II. Covariance structure analysis, maximum likelihood estimation, manifest variable equations. Unstandardized path coefficients. (multi-level, log delta data; n=300).

```
S_L_YV1 =     1.7541*S_L_YV17 +  1.0000 E1
Std Err       0.0590 PV1V17
t Value      29.7301

S_L_YV4 =     0.6856*S_L_YM44 +  0.3459*S_L_YQ44 +  1.0000 E4
Std Err       0.0956 PV4M44      0.1592 PV4Q44
t Value       7.1751             2.1735

S_L_YV6 =     0.0780*S_L_YM44 -  0.3232*S_L_YQ57 +  0.5778*S_L_YQ58 +  1.0000 E6
Std Err       0.0326 PV6M44      0.0792 PV6Q57      0.0963 PV6Q58
t Value       2.3917            -4.0810             6.0003

S_L_YV8 =     0.1235*S_L_YM44 +  0.5023*S_L_YM84 +  1.0000 E8
Std Err       0.0435 PV8M44      0.0574 PV8M84
t Value       2.8385             8.7501

S_L_YV9 =     0.2131*S_L_YV25 +  0.1544*S_L_YM57 +  1.0000 E9
Std Err       0.0418 PV9V25      0.0860 PV9M57
t Value       5.0944             1.7954

S_L_YV12=     0.3124*S_L_YM64 +  0.2651*S_L_YQ64 +  1.0000 E12
Std Err       0.0234 PV12M64     0.0518 PV12Q64
t Value      13.3332             5.1207

L_YV13  =  -  1.8553*S_L_YV14 +  1.2111*S_L_YM57 +  1.0656*S_L_YQ64 +  1.0000 E13
Std Err       0.0956 PV13V14     0.1207 PV13M57     0.2739 PV13Q64
t Value     -19.4112            10.0338             3.8901

S_L_YV14=     0.4543*S_L_YV17 +  0.1083*L_YV30   -  0.7603*S_L_YM57 -  0.6366*S_L_YQ57
Std Err       0.0286 PV14V17     0.0101 PV14V30     0.0357 PV14M57     0.0395 PV14Q57
t Value      15.8812            10.7485           -21.2670           -16.1371

           +  0.9725*S_L_YM58 +  0.6668*S_L_YQ58 +  1.0000 E14
 Std Err       0.0361 PV14M58     0.0484 PV14Q58
 t Value      26.9524            13.7769

S_L_YV16=     0.3363*S_L_YM44 +  0.0944*S_L_YQ44 -  0.2253*S_L_YQ57 +  0.2499*S_L_YQ58    +  1.0000 E16
Std Err       0.0226 PV16M44     0.0376 PV16Q44     0.0548 PV16Q57     0.0666 PV16Q58
t Value      14.8976             2.5092            -4.1089             3.7495

S_L_YV17=   0.0709*L_YV30   -  0.3631*S_L_YM44-  0.2712*S_L_YM57 - 0.1446*S_L_YQ58  +  0.2137*S_L_YV18 +  1.0000 E17
Std Err     0.0154 PV17V30    0.0282 PV17M44    0.0432 PV17M57    0.0655 PV17Q58      0.0503 PV17V18
t Value     4.6079          -12.8895          -6.2747           -2.2084               4.2464

S_L_YV19=  -  0.1837*L_YV32   +  0.7607*S_L_YV18 +  1.0000 E19
Std Err       0.0167 PV19V32     0.0636 PV19V18
t Value     -10.9950            11.9520

S_L_YV21=     0.3141*S_L_YM57 +  1.0000 E21
Std Err       0.0515 PV21M57
t Value       6.0972

S_L_YV23=     1.3966*S_L_YM57 +  0.3593*S_L_YQ57 -  1.4463*S_L_YM58 -  0.3448*S_L_YQ58    +  1.0000 E23
Std Err       0.0704 PV23M57     0.0802 PV23Q57     0.0719 PV23M58     0.0974 PV23Q58
t Value      19.8279             4.4830           -20.1248           -3.5389

S_L_YV24=  -  1.1286*S_L_YM57 +  1.0000 E24
Std Err       0.1627 PV24M57
t Value      -6.9378
```

Reproduced with permission of the copyright owner. Further reproduction prohibited without permission.

Box 15.6. SAS/CALIS output. Model II. Covariance structure analysis, maximum likelihood estimation, manifest variable equations. Unstandardized path coefficients. (multi-level, log delta data; n=300).

```
S_L_YV25=     0.7199*S_L_YV17 +  0.7123*S_L_YM57 -  0.6306*S_L_YM58 +  1.0000 E25
Std Err       0.1048 PV25V17     0.1456 PV25M57     0.1448 PV25M58
t Value       6.8698             4.8926            -4.3551

S_L_YV27=     0.5287*S_L_YV18 +  1.0000 E27
Std Err       0.0888 PV27V18
t Value       5.9562

L_YV30  =  -  0.3297*S_L_YM44 +  0.3143*S_L_YM58 +  0.3766*S_L_YQ58 +  0.2129*L_YM70
Std Err       0.0871 PV30M44     0.1345 PV30M58     0.2013 PV30Q58     0.0521 PV30M70
t Value      -3.7850             2.3364             1.8712             4.0854

           +  0.3234*L_YM74   +  0.1845*L_YQ74   +  1.0000 E30
Std Err       0.0485 PV30M74     0.0615 PV30Q74
t Value       6.6701             2.9990

L_YV32  =     0.8077*S_L_YV17 -  0.2280*L_YV30   +  1.0000 E32
Std Err       0.1848 PV32V17     0.0655 PV32V30
t Value       4.3718            -3.4782

L_YV33  =  -  0.1920*L_YV30   +  0.2713*L_YV35   +  0.3188*S_L_YM44 -  0.8757*S_L_YM58   +  1.0000 E33
Std Err       0.0586 PV33V30     0.0515 PV33V35     0.0990 PV33M44     0.1677 PV33M58
t Value      -3.2743             5.2709             3.2202            -5.2232

L_YV35  =     0.6910*S_L_YV1  +  0.3981*L_YV30   -  1.1744*S_L_YM58 +  1.0000 E35
Std Err       0.0722 PV35V1      0.0531 PV35V30     0.1540 PV35M58
t Value       9.5664             7.5006            -7.6248

S_L_YM44=     0.7042*S_L_YM84 +  1.0000 EM44
Std Err       0.0645 PM44M84
t Value      10.9163

S_L_YQ44=     0.4221*S_L_YQ84 +  1.0000 EQ44
Std Err       0.1777 PQ44Q84
t Value       2.3758

L_YV45  =  -  0.6403*S_L_YV8  +  1.7123*S_L_YV16 +  1.0000 E45
Std Err       0.1253 PV45V8      0.1860 PV45V16
t Value      -5.1089             9.2040

L_YV46  =     0.5735*L_YM70   +  0.2612*L_YM74   +  1.0000 E46
Std Err       0.0673 PV46M70     0.0626 PV46M74
t Value       8.5160             4.1729

S_L_YV49=     0.9631*S_L_YM44 +  0.4487*S_L_YQ44 +  0.0753*L_YV45   +  1.0000 E49
Std Err       0.0345 PV49M44     0.0564 PV49Q44     0.0184 PV49V45
t Value      27.9343             7.9557             4.0888

S_L_YM57=     0.2056*L_YM63   +  0.7699*S_L_YM64 +  1.0000 EM57
Std Err       0.0220 PM57M63     0.0363 PM57M64
t Value       9.3534            21.2197

S_L_YQ57=     0.2583*L_YQ63   +  1.1803*S_L_YQ64 +  1.0000 EQ57
Std Err       0.0212 PQ57Q63     0.0627 PQ57Q64
t Value      12.2076            18.8108

S_L_YM58=     0.9053*S_L_YM64 +  1.0000 EM58
Std Err       0.0276 PM58M64
t Value      32.8339

S_L_YQ58=     1.1292*S_L_YQ64 +  1.0000 EQ58
Std Err       0.0559 PQ58Q64
t Value      20.2141

L_YV69  =  -  0.5003*L_YM70   +  0.7833*S_L_YM84 +  1.4472*S_L_YQ84 +  1.0000 E69
Std Err       0.0538 PM69M70     0.1371 PM69M84     0.3977 PQ69Q84
t Value      -9.2999             5.7122             3.6389
```

Reproduced with permission of the copyright owner. Further reproduction prohibited without permission.

Box 15.6. SAS/CALIS output. Model II. Covariance structure analysis, maximum likelihood estimation, manifest variable equations. Unstandardized path coefficients. (multi-level, log delta data; n=300).

```
L_YM70  =     0.1897*L_YM78   -  1.5144*S_L_YM84 +  1.0000 EM70
Std Err       0.0593 PM70M78     0.1239 PM70M84
t Value       3.1972          -12.2185

L_YM74  =     0.2540*L_YM70   -  1.4467*S_L_YM84 +  1.0000 EM74
Std Err       0.0593 PM74M70     0.1512 PM74M84
t Value       4.2818           -9.5685

L_YQ74  =  -  1.8174*S_L_YQ84 +  1.0000 EQ74
Std Err       0.3720 PQ74Q84
t Value      -4.8859

L_YM81  =     1.0517*S_L_YM84 +  1.0000 EM81
Std Err       0.0861 PM81M84
t Value      12.2171
```

In the next few sections, I report the results of several diagnostic assessments of the respecified model (Model II). In keeping with the procedures outlined in Chapter 8, Model II relationships were examined for collinearity, curvilinearity, and influential observations.

Model II (Respecified Model): Diagnostics: Collinearity

The condition index for the 34 endogenous variables of Model II is presented in Box 15.7. The diagnostics revealed no near collinearity in the data.

Box 15.7. SAS output condition index collinearity diagnostics. Model II.

Collinearity Diagnostics

Number	Eigenvalue	Condition Index	Var Prop INTERCEP	Var Prop S_L_YV1	Var Prop S_L_YV4	Var Prop S_L_YV6	Var Prop S_L_YV8	Var Prop S_L_YV9
22	0.06856	13.23893	0.0000	0.0070	0.0026	0.0077	0.0281	0.0010
23	0.04221	16.87362	0.0000	0.5524	0.0113	0.0087	0.0092	0.3034
24	0.02216	23.28559	0.0000	0.0020	0.0002	0.0311	0.0008	0.0089
25	0.00128	97.06937	0.0000	0.0626	0.0014	0.0636	0.0006	0.0058
26	0.0008132	121.55895	0.0002	0.0011	0.0332	0.0160	0.0193	0.0001
27	0.0007711	124.83532	0.0000	0.0199	0.0119	0.0144	0.0157	0.0644
28	0.0005733	144.77336	0.0009	0.0323	0.0067	0.0051	0.0002	0.0016
29	0.0004572	162.11940	0.0000	0.0377	0.0002	0.0209	0.0996	0.0004
30	0.0004145	170.27359	0.0001	0.0236	0.0216	0.0276	0.0250	0.0272
31	0.0003375	188.69138	0.0010	0.0018	0.0001	0.0013	0.0016	0.0001
32	0.0003272	191.64000	0.0004	0.0002	0.0099	0.0089	0.0000	0.0775
33	0.0002344	226.40824	0.0008	0.0032	0.0083	0.0009	0.0257	0.0373
34	0.0001667	268.50842	0.0003	0.0169	0.0026	0.0083	0.0046	0.0245
35	0.0000255	686.23818	0.9962	0.1434	0.0096	0.0000	0.0010	0.0074

Reproduced with permission of the copyright owner. Further reproduction prohibited without permission.

Box 15.7. SAS output condition index collinearity diagnostics. Model II.

Number	Var Prop S_L_YV12	Var Prop L_YV13	Var Prop S_L_YV14	Var Prop S_L_YV16	Var Prop S_L_YV17	Var Prop S_L_YV19	Var Prop S_L_YV21	Var Prop S_L_YV23
24	0.2621	0.0000	0.1885	0.0063	0.0368	0.0038	0.0003	0.0540
25	0.0035	0.0001	0.0630	0.1158	0.0351	0.1798	0.0098	0.0009
26	0.0001	0.0689	0.1170	0.0168	0.0012	0.0004	0.0102	0.0035
27	0.0232	0.0000	0.0002	0.0623	0.0216	0.0010	0.0008	0.0001
28	0.0194	0.0840	0.0188	0.0165	0.0259	0.0204	0.0317	0.0159
29	0.0366	0.0165	0.0000	0.0799	0.0200	0.0047	0.0245	0.0447
30	0.0005	0.0962	0.0050	0.0253	0.0592	0.0736	0.0055	0.0011
31	0.0134	0.1459	0.0418	0.0148	0.0053	0.0410	0.0001	0.0455
32	0.0194	0.0402	0.0617	0.0077	0.0000	0.0017	0.0059	0.0176
33	0.0109	0.1664	0.0208	0.0039	0.0112	0.0041	0.0085	0.0006
34	0.0085	0.2720	0.1041	0.0184	0.0012	0.0027	0.0098	0.0007
35	0.0115	0.1097	0.1409	0.0159	0.0820	0.1237	0.0303	0.0528

Number	Var Prop S_L_YV24	Var Prop S_L_YV25	Var Prop S_L_YV27	Var Prop L_YV30	Var Prop L_YV32	Var Prop L_YV33	Var Prop L_YV35	Var Prop S_L_YM44
24	0.0001	0.0044	0.0037	0.0000	0.0000	0.0000	0.0000	0.0067
25	0.0006	0.0011	0.0007	0.0008	0.0830	0.0074	0.0156	0.0291
26	0.0219	0.0129	0.0105	0.0231	0.0401	0.0307	0.1182	0.0057
27	0.0001	0.0084	0.0011	0.0058	0.0733	0.0076	0.0114	0.0143
28	0.0016	0.0073	0.0005	0.0159	0.0207	0.3311	0.0310	0.0064
29	0.0402	0.0559	0.0276	0.0090	0.0076	0.3122	0.0062	0.0011
30	0.0134	0.0008	0.0011	0.0889	0.4262	0.0036	0.1337	0.0004
31	0.0015	0.0085	0.0005	0.0885	0.1590	0.0195	0.0157	0.0007
32	0.0000	0.0002	0.0092	0.0173	0.0204	0.0544	0.0954	0.0223
33	0.0063	0.0007	0.0971	0.2531	0.0653	0.0968	0.1173	0.0151
34	0.0261	0.0007	0.0008	0.3216	0.0942	0.1345	0.4163	0.0099
35	0.0041	0.0198	0.0023	0.1761	0.0103	0.0023	0.0390	0.0131

Number	Var Prop S_L_YQ44	Var Prop L_YV45	Var Prop L_YV46	Var Prop S_L_YV49	Var Prop S_L_YM57	Var Prop S_L_YQ57	Var Prop S_L_YM58	Var Prop S_L_YQ58
24	0.0032	0.0000	0.0000	0.0005	0.7497	0.2250	0.7225	0.2750
25	0.0014	0.0014	0.1843	0.0030	0.0258	0.0247	0.0210	0.0129
26	0.0006	0.0160	0.0051	0.0083	0.0047	0.0042	0.0150	0.0050
27	0.0090	0.3449	0.2291	0.0884	0.0140	0.0008	0.0307	0.0002
28	0.0082	0.0067	0.0530	0.0326	0.0412	0.0055	0.1338	0.0099
29	0.0242	0.3116	0.2694	0.0542	0.0015	0.0099	0.0025	0.0045
30	0.0001	0.0087	0.0644	0.0118	0.0009	0.0130	0.0015	0.0023
31	0.0003	0.2370	0.0046	0.0005	0.0000	0.0014	0.0002	0.0042
32	0.0026	0.0069	0.0010	0.0113	0.0181	0.0078	0.0072	0.0011
33	0.0001	0.0037	0.0019	0.0005	0.0244	0.0000	0.0183	0.0029
34	0.0099	0.0275	0.1819	0.0003	0.0001	0.0002	0.0006	0.0005
35	0.0001	0.0358	0.0053	0.0051	0.0155	0.0356	0.0011	0.0197

Continued on next page...

Reproduced with permission of the copyright owner. Further reproduction prohibited without permission.

Box 15.7. SAS output condition index collinearity diagnostics. Model II.

Number	Var Prop L_YV69	Var Prop L_YM70	Var Prop L_YM74	Var Prop L_YQ74	Var Prop L_YM81
24	0.0000	0.0000	0.0000	0.0102	0.0000
25	0.0399	0.0048	0.0447	0.0012	0.0137
26	0.0305	0.0105	0.0766	0.0000	0.0281
27	0.0028	0.0009	0.0416	0.0001	0.0089
28	0.0702	0.0483	0.0204	0.0024	0.0019
29	0.0438	0.0080	0.1347	0.0506	0.0054
30	0.0487	0.0001	0.0327	0.0154	0.0633
31	0.0391	0.0090	0.1161	0.0066	0.2251
32	0.3762	0.0488	0.3430	0.0017	0.0984
33	0.1246	0.3211	0.0189	0.0015	0.0053
34	0.0841	0.1531	0.0751	0.0018	0.1922
35	0.1402	0.3954	0.0960	0.0006	0.3577

Model II (Respecified Model): Diagnostics: Curvilinearity

Of the 80 bivariate relationships included in Model II, 7 show a significant increase in *R*-square when fit to a quadratic curvilinear model in comparison to a linear model. These were: (1) nasoalveolar clivus length regressed on M-level anterior MBF [R^2 increase of 15%], (2) maxillary arch length regressed on facial prognathism [R^2 increase 15%], (3) maxillary arch length regressed on M-level posterior MBF [R^2 increase 31%], (4) facial prognathism regressed on M-level posterior MBF [R^2 increase 15%], (5) paranasal plate orientation regressed on M-level posterior MBF [R^2 increase 12%], (6) M-level cranial base angle regressed on M-level middle cranial fossa length [R^2 increase of 37%], and (7) M-level cranial base angle regressed on M-level endocranial volume [R^2 increase16%]. Notice that 3 through 5 above all involve the relationship between posterior bite force and facial protrusion, and that 6 and 7 both concern the effects of brain size and form on cranial base flexion. Box 15.8 reports the linear model coefficient of determination for each of the bivariate components of Model II, and the incremental increase for

Reproduced with permission of the copyright owner. Further reproduction prohibited without permission.

the quadratic curvilinear fit.

Box 15.8. Model II R-square for linear fit of bivariate regressions, and increase of R-square due to quadratic curvilinear model.

Bivariate components of Model II	R^2 y=x	R^2 Δ y=x^2	Bivariate components of Model II	R^2 y=x	R^2 Δ y=x^2
ΔS_L_YV1 = ΔS_L_YV17	0.750	0.013	ΔS_L_YV25 = ΔS_L_YM58	0.007	0.060
ΔS_L_YV4 = ΔS_L_YM44	0.162	0.010	ΔS_L_YV27 = ΔS_L_YV18	0.104	0.006
ΔS_L_YV4 = ΔS_L_YQ44	0.010	0.010	ΔL_YV30 = ΔS_L_YM44	0.082	0.004
ΔS_L_YV6 = ΔS_L_YM44	0.021	0.020	**ΔL_YV30 = ΔS_L_YM58**	**0.094**	**0.150**
ΔS_L_YV6 = ΔS_L_YQ57	0.012	0.000	ΔL_YV30 = ΔS_L_YQ58	0.010	0.000
ΔS_L_YV6 = ΔS_L_YQ58	0.023	0.000	ΔL_YV30 = ΔL_YM70	0.285	0.100
ΔS_L_YV8 = ΔS_L_YM44	0.174	0.003	ΔL_YV30 = ΔL_YM74	0.307	0.000
ΔS_L_YV9 = ΔS_L_YV25	0.081	0.024	ΔL_YV30 = ΔL_YQ74	0.017	0.007
ΔS_L_YV9 = ΔS_L_YM57	**0.012**	**0.143**	ΔL_YV32 = ΔS_L_YV30	0.017	0.029
ΔS_L_YV8 = ΔS_L_YM84	0.323	0.040	ΔL_YV33 = ΔL_YV30	0.050	0.000
ΔS_L_YV12 = ΔS_L_YM64	0.353	0.026	ΔL_YV33 = ΔL_YV35	0.090	0.008
ΔS_L_YV12 = ΔS_L_YQ64	0.053	0.013	ΔL_YV33 = ΔS_L_YM44	0.013	0.000
ΔS_L_YV13 = ΔS_L_YV14	0.387	0.100	ΔL_YV33 = ΔS_L_YM57	0.154	0.020
ΔS_L_YV13 = ΔS_L_YM57	0.166	0.000	ΔL_YV35 = ΔS_L_YV1	0.351	0.010
ΔS_L_YV13 = ΔS_L_YQ64	0.023	0.032	ΔL_YV35 = ΔL_YV30	0.121	0.000
ΔS_L_YV14 = ΔS_L_YV17	0.393	0.055	**ΔL_YV35 = ΔS_L_YM58**	**0.112**	**0.123**
ΔS_L_YV14 = ΔL_YV30	**0.434**	**0.152**	ΔS_L_YM44 = ΔS_L_YM84	0.285	0.017
ΔS_L_YV14 = ΔS_L_YM57	0.000	0.036	ΔS_L_YQ44 = ΔS_L_YQ84	0.019	0.020
ΔS_L_YV14 = ΔS_L_YQ57	0.014	0.015	ΔL_YV45 = ΔS_L_YV8	0.022	0.000
ΔS_L_YV14 = ΔS_L_YM58	**0.061**	**0.307**	ΔL_YV45 = ΔS_L_YV16	0.164	0.015
ΔS_L_YV14 = ΔS_L_YQ58	0.000	0.002	ΔL_YV46 = ΔL_YM70	0.359	0.004
ΔS_L_YV16 = ΔS_L_YM44	0.419	0.012	ΔL_YV46 = ΔL_YM74	0.262	0.018
ΔS_L_YV16 = ΔS_L_YQ44	0.009	0.007	ΔS_L_YV49 = ΔS_L_YM44	0.685	0.000
ΔS_L_YV16 = ΔS_L_YQ57	0.000	0.000	ΔS_L_YV49 = ΔS_L_YQ44	0.059	0.020
ΔS_L_YV16 = ΔS_L_YQ58	0.000	0.000	ΔS_L_YV49 = ΔL_YV45	0.071	0.008
ΔS_L_YV17 = ΔS_L_YV18	0.040	0.020	ΔS_L_YM57 = ΔL_YM63	0.095	0.001
ΔS_L_YV17 = ΔL_YV30	0.456	0.002	ΔS_L_YM57 = ΔS_L_YM64	0.533	0.013
ΔS_L_YV17 = ΔS_L_YM44	0.420	0.000	ΔS_L_YQ57 = ΔL_YQ63	0.214	0.001
ΔS_L_YV17 = ΔS_L_YM57	0.120	0.026	ΔS_L_YQ57 = ΔS_L_YQ64	0.464	0.013
ΔS_L_YV17 = ΔS_L_YQ58	0.010	0.000	ΔS_L_YM58 = ΔS_L_YM64	0.783	0.000
ΔS_L_YV19 = ΔS_L_YV18	0.293	0.001	ΔS_L_YQ58 = ΔS_L_YQ64	0.576	0.005
ΔS_L_YV19 = ΔL_YV32	0.260	0.016	ΔL_YV69 = ΔL_YM70	0.482	0.006
ΔS_L_YV21 = ΔS_L_YM57	0.112	0.111*	ΔL_YV69 = ΔS_L_YM84	0.399	0.014
ΔS_L_YV23 = ΔS_L_YM57	0.011	0.040	ΔL_YV69 = ΔS_L_YQ84	0.012	0.004
ΔS_L_YV23 = ΔS_L_YQ57	0.007	0.041	**ΔL_YM70 = ΔL_YM78**	**0.202**	**0.371**
ΔS_L_YV23 = ΔS_L_YM58	0.000	0.021	**ΔL_YM70 = ΔS_L_YM84**	**0.452**	**0.158**
ΔS_L_YV23 = ΔS_L_YQ58	0.020	0.018	ΔL_YM74 = ΔL_YM70	0.349	0.000
ΔS_L_YV24 = ΔS_L_YM57	0.000	0.020	ΔL_YM74 = ΔS_L_YM84	0.470	0.002
ΔS_L_YV25 = ΔS_L_YV17	0.112	0.025	ΔL_YQ74 = ΔS_L_YQ84	0.074	0.003
ΔS_L_YV25 = ΔS_L_YM57	0.004	0.043	ΔL_YM81 = ΔL_YM84	0.336	0.002

Reproduced with permission of the copyright owner. Further reproduction prohibited without permission.

Model II (Respecified Model): Diagnostics: Influential Observations

In accordance with the three-step procedure for detecting and testing influential data points outlined in Chapter 8, observations exhibiting both high *h*-values and studentized residuals were selected for closer examination. Model II was then evaluated with and without the selected observations to see if their removal significantly changed the path coefficients. Typically, several potential influential observations were detected for each dependent variable in the diagnostic stage of the analysis, and in such cases it proved to be most efficient to compare test results before and after the entire set of suspected influential observations was removed from the data. If the path coefficients after removal of potentially influential observations were more than 2 standard errors away from the initial full sample coefficient, then the observations were deemed truly influential (I call this the "meta-test"). Box 15.9 reports the results of the three-stage diagnostic test for each of the submodels of Model II. The analysis revealed only one set of influential observations whose removal from Model II resulted in a change to a test of significance. When specimens of *Papio hamadryas* (#89361, 169141), *Hylobates syndactylus* (#102186), and *Gorilla gorilla* (#1472) were removed from Model II analysis the path coefficient leading from M-level relative anterior MBF [ΔS_L_YM57] to nasoalveolar clivus length [ΔS_L_YV9] was no longer significant (at α 0.05) (see Box 15.9).

Reproduced with permission of the copyright owner. Further reproduction prohibited without permission.

Box 15.9. Diagnostic and test for presence of influential observations with respect to coefficients of regression on each endogenous variable in Model II.

Endogenous Model II variables	Diagnostic: Specimen # with $h > 0.013$ and Rstudent > 2	Meta-test outcome
ΔS_L_YV1	*P. hamadryus* (89361)	negative
ΔS_L_YV4	*A. palliata* (66707); *P. hamadryus* (52668, 216520, 169141)	negative
ΔS_L_YV6	*G. gorilla* (54327); *H. sapiens* (4927)	negative
ΔS_L_YV8	*A. palliata* (176641); *P. hamadryus* (89361); *G. gorilla* (167337, 81652); *H. sapiens* (2385, 3445, 642)	negative
ΔS_L_YV9	*P. hamadryus* (89361, 169141); *H. syndactylus* (102186); *G. gorilla* (1472)	positive; ΔS_L_YM5 7 ns
ΔS_L_YV12	*H. sapiens* (3281)	negative
ΔL_YV13	*H. sapiens* (3281)	negative
ΔS_L_YV14	*P. hamadryas* (161115); *P. melalophos* (102744, 102890); *H. lar* (54659); *H. syndactylus* (102186, 102195, 102196, 102463, 106583); *G. gorilla* (54327); *H. sapiens* (3281, 4927, 5281); *P. troglodytes* (90293)	negative
ΔS_L_YV17	*C. neglectus* (86854); *P. hamadryus* (52668, 216250, 82097); *P. pygmaeus* (201811, 200898)	negative
ΔS_L_YV19	*A. palliata* (141852); *G. gorilla* (1472, 214108); *P. troglodytes* (90239)	negative
ΔS_L_YV21	*P. melalophos* (102886); *G. gorilla* (167340, 54327)	negative
ΔS_L_YV25	*P. hamadryus* (82097, 216250); *Homo sapiens* (2396, 4927, 5281)	negative
ΔS_L_YV27	*P. hamadryus* (89361); *C. guereza* (52226); *G. gorilla* (214108)	negative
ΔL_YV30	*A. palliata* (128109, 141852, 17231, 17250, 66707); *P. pygmaeus* (200900); *H. sapiens* (2793)	negative
ΔL_YV32	*A. palliata* (128109, 141852); *P. hamadryus* (52674)	negative
ΔL_YV33	none	negative
ΔL_YV35	none	negative
ΔS_L_YM44	none	negative
ΔL_YV45	*P. hamadryus* (169141); *G. gorilla* (167330)	negative
ΔL_YV46	*P. paniscus* (86857)	negative
ΔS_L_YV49	*G. gorilla* (214108); *H. sapiens* (4927); *P. troglodytes* (89355)	negative
ΔS_L_YM57	none	negative
ΔS_L_YQ57	*P. hamadryus* (52688); *H. syndactylus* (102721); *G. gorilla* (167339, 167340, 54327)	negative
ΔS_L_YM58	none	negative
ΔS_L_YQ58	*H. syndactylus* (102721, 102727); *G. gorilla* (167330)	negative
ΔL_YV69	*M. nemestrina* (106050); *C. guereza* (52245); *P. paniscus* (86857); *P. troglodytes* (201469, 89355)	negative
ΔL_YM70	*P. hamadryus* (52688; 89361, 216250, 82097, 161115, 52674, 169141)	negative
ΔL_YM74	none	negative
ΔL_YQ74	*C. badius* (52301)	negative
ΔL_YM78	none	negative
ΔL_YM81	*B. arachnoides* (80405); *P. pygmaeus* (200900, 201811, 200898)	negative

Reproduced with permission of the copyright owner. Further reproduction prohibited without permission.

Model II (Respecified Model): Model Fit: Model Fit Indices

To allow comparison between Model I and Model II goodness-of-fit, model fit indices are presented side-by-side for both models in Box 15.10. It can be seen that only moderate improvement in model fit has been achieved with respecification. The mean score over all four indices for Model II is 0.48 compared to 0.38 for Model I. This is still far short of the 0.90 fit index criterion recommended by Hatcher (1996) for a "good" model fit. However, fit indices must be interpreted with degree of parameterization in mind. It will be shown in subsequent sections that smaller less parameterized *submodels* of Model II score close to or over the 0.90 fit index threshold, despite the fact that the primary path relations being evaluated are the same.

Box 15.10. Various fit indices for Model II.

Fit Index:	Model I	Model II
Chi-square	12690.37 (p=.0001; df=1340)	7307 (p=.0001; df=820)
Goodness of Fit Index (GFI)	0.480	0.516
Adjusted Goodness of Fit Index (AGFI)	0.381	0.416
Bentler's Comparative Fit Index (CFI)	0.339	0.507
Normed Tucker Lewis Index (NTLI)	0.322	0.482
Root Mean Square Residual (RMR)	0.0017	0.0004
Mean fit index	0.38	0.480

Model II (Respecified Model): Model Fit: Model *R*-squared

Another method of assessing model fit, which is not adversely affected by model parameterization, is to examine the *R*-squared values associated with each endogenous variable in the model. Box 15.11 reports the proportion of variance accounted for, for each nasomaxillary dependent variable in Model II. The *R*-squared associated with isometric size effect is given separately from the *R*-squared

Reproduced with permission of the copyright owner. Further reproduction prohibited without permission.

associated with all other nomological agents, reflecting the hierarchical nature of the analysis. Total Model II R^2 is also reported in Box 15.11.

Box 15.11. Proportion of variance accounted for by isometric scale variation, structural growth constraints, and other nomological agents. Residual *R*-square given in parenthesis

Dep. Variable	Isometric Size *R*-square	Other nomological agents R^2	Total Model II *R*-square
Y1-NASLGT	0.57	0.74 (0.32)	0.89
Y2-NASWDU	0.35		0.35
Y3-NASWDL	0.67		0.67
Y4-NPMWDT	0.41	0.17 (0.10)	0.51
Y5-NSLAHT	0.80		0.80
Y6-NASAWD	0.87	0.13 (0.02)	0.89
Y7-PNASHT	0.76		0.76
Y8-PNASWD	0.79	0.34 (0.07)	0.86
Y9-NLCLGT	0.72	0.10 (0.03)	0.75
Y10-ZYGARE	0.92		0.92
Y11-ZYGOHT	0.67		0.67
Y12-BZYGWD	0.96	0.41 (0.02)	0.98
Y13-APZYGR	0.00	0.66 (0.66)	0.66
Y14-MXARCL	0.86	0.87 (0.12)	0.98
Y15-BMAXWD	0.94		0.94
Y16-UMAXWD	0.90	0.45 (0.05)	0.95
Y17-AFACHT	0.84	0.54 (0.09)	0.93
Y18-PFACHT	0.89		0.89
Y19-RAMSHT	0.78	0.45 (0.10)	0.88
Y20-I2PALW	0.79		0.79
Y21-P3PALW	0.87	0.11 (0.01)	0.88
Y22-M1PALW	0.89		0.89
Y23-M2PALW	0.83	0.65 (0.11)	0.83
Y24-I2PALD	0.40	0.14 (0.08)	0.48
Y25-P3PALD	0.61	0.16 (0.06)	0.67
Y26-M1PALD	0.80		0.80
Y27-M3PALD	0.76	0.11 (0.03)	0.79
Y30-KROGAG	0.00	0.45 (0.45)	0.45
Y32-SLOPOC	0.00	0.07 (0.07)	0.07
Y33-FACCNV	0.00	0.29 (0.29)	0.29
Y35-PPNALO	0.00	0.49 (0.49)	0.49

It can be seen that for some nasomaxillary characters a high proportion of their size-adjusted variance can be explained in terms of the nomological causal agents included in the model. For instance, 87% of the size-adjusted variation in delta

Reproduced with permission of the copyright owner. Further reproduction prohibited without permission.

relative maxillary arch length can be explained in terms of structural growth constraints involving anterior facial elongation and facial prognathism and the effects of selectional and acclimative nomological mechanisms acting on anterior and posterior bite force. However, a substantial proportion of the size-adjusted variation of other nasomaxillary characters remains unexplained. For example, only 10% of the size-adjusted variance of delta relative nasoalveolar clivus length can be explained by a spatial constraint involving palatal depth at P^3 and selection for increased anterior MBF.

Model II (Respecified Model): Analysis of Structured Covariance (ANSCOVA)

When data sampled across groups are fit to a linear model the common parameter estimates can be misleading if the within-group estimates are heterogeneous. For example, if the regression coefficient, *b*, of Y on X for the males of a given sample is *positive* significant, and the corresponding *b* for the females is *negative* significant, the common regression slope (male and females pooled) may well be zero and nonsignificant. The common regression line is meaningful, both in terms of inference and statistical control, only if the separate group coefficients are relatively homogeneous (Cochran, 1957; Huitema, 1980). It was therefore necessary to conduct an analysis of structured covariance (ANSCOVA) to assess the homogeneity of model parameters across anthropoid groups. Numerous authors have found that *standardized* path coefficients are taxon-specific and thus should not be used for comparisons across groups (e.g., Tukey, 1954; Turner & Stevens, 1959; Wright, 1960; Duncan, 1975; Pedhazur, 1997). I therefore report *unstandardized* coefficients in the ANSCOVA table.

Reproduced with permission of the copyright owner. Further reproduction prohibited without permission.

Two distinct group affiliations, one taxonomic the other developmental, were examined for heterogeneity of path coefficients.[2] Developmental Modes 1 and 2 were described in Chapter 9. Taxonomic subgroups included New World monkeys, Old World monkeys, and hominoids. While it is clear that substantial heterogeneity may exist within these major anthropoid subtaxa (as evidenced in the bivariate regression results), any further division into lower-level taxonomic groups would have severely limited the power of the analysis due to insufficient sample sizes. This is already evident in the ANSCOVA results for hominoids, with a sample size of only 46. Regard, for example, that the hominoid path coefficient for the effect of inter-P^3 palatal depth [ΔS_L_YV25] on nasoalveolar clivus length [ΔS_L_YV9] is 0.21, which matches the common anthropoid coefficient precisely, but because of the limited power associated with such a small sample (n=46), the coefficient is not significantly different from zero. The analysis of structured covariance results should therefore be considered tentative; that is, forming the basis of hypotheses to be tested more fully in lower level taxa.

Box 15.12 displays the ANSCOVA results as the common and within-group unstandardized path coefficients for the bivariate components of Model II. It can be seen that various within-group coefficients deviate significantly from the common estimate in terms of sign and significance. In Box 15.12, the shaded cells indicate path coefficients whose values are not significantly different from zero, and the asterisks indicate coefficients whose values are significantly different from the common coefficient. For example, the common and group path coefficients for the effects of M-level anterior MBF [ΔS_L_YM57] on anterior facial length [ΔS_L_YV17]

---

[2] Although the morphometric data was "adjusted" to remove phylogenetic effects (see Chapters 6 and7), taxonomic affinities can remain in the data due to macroevolutionary processes discussed in Chapter 9. I discuss this issue further in Chapter 16.

Reproduced with permission of the copyright owner. Further reproduction prohibited without permission.

reveal that the path coefficient of -0.61 for Old World monkeys is significantly different from the common coefficient of -0.27 (asterisk), and that the path coefficient of -0.03 for hominoids is both significantly different from the common coefficient (asterisk) and not significantly different from zero (shaded). Specific group heterogeneities will be discussed in the context of selected nasomaxillary characters in the following section.

Box 15.12. ANSCOVA table comparing *unstandardized* path regression coefficients for various groups. NWM=New World monkeys, OW= Old World monkeys.

Bivariate paths	Taxonomic and developmental subsamples					
	Complete Sample (n=300)	NWM (*n*=117)	OWM (n=137)	Hominoid (n=46)	Dev Mode_1 (n=170)	Dev Mode_2 (n=130)
ΔS_L_YV1 = ρΔS_L_YV17	1.75	1.48	2.00	1.15	2.07	1.58
ΔS_L_YV4 = ρΔS_L_YM44	0.69	0.52	1.29	0.59	0.97	0.52
ΔS_L_YV4 = ρΔS_L_YQ44	0.35	0.58	0.42	0.23	0.12	0.73
ΔS_L_YV6 = ρΔS_L_YM44	0.08	0.09	0.01	0.01*	0.11	0.11
ΔS_L_YV6 = ρΔS_L_YQ57	-0.32	-0.23	-0.09	-0.67	-0.52	-0.04
ΔS_L_YV6 = ρΔS_L_YQ58	0.58	0.29	0.16*	1.19	0.71	0.41
ΔS_L_YV8 = ρΔS_L_YM44	0.12	0.33	0.10	0.08	0.08*	0.18
ΔS_L_YV8 = ρΔS_L_YM84	0.50	0.66	0.65	0.51	0.67	0.40
ΔS_L_YV9 = ρΔS_L_YV25	0.21	0.38	0.23	0.21	0.03*	0.53
ΔS_L_YV9 = ρΔS_L_YM57	0.15	-0.76*	0.29	0.49	0.94*	-0.37*
ΔS_L_YV12 = ρΔS_L_YM64	0.31	0.22	0.61*	0.09	0.37	0.28
ΔS_L_YV12 = ρΔS_L_YQ64	0.27	0.19	0.26	0.34	0.23	0.31
ΔS_L_YV13 = ρΔS_L_YV14	-1.86	-1.55	-2.16	-1.49	-2.21	-1.68
ΔS_L_YV13 = ρΔS_L_YM57	1.21	0.18*	1.59	0.48	0.98	1.15
ΔS_L_YV13 = ρΔS_L_YQ64	1.07	1.35	0.84	1.13	1.24	0.73
ΔS_L_YV14 = ρΔS_L_YV17	0.45	0.19*	0.29	0.11	0.45	0.36
ΔS_L_YV14 = ρΔL_YV30	0.11	0.08	0.12	0.09	0.08	0.12
ΔS_L_YV14 = ρΔS_L_YM57	-0.76	-0.32*	-0.75	-0.94	-0.58	-1.00
ΔS_L_YV14 = ρΔS_L_YQ57	-0.64	-0.44*	-0.72	-0.60	-0.67	-0.57
ΔS_L_YV14 = ρΔS_L_YM58	0.97	0.42*	0.62*	1.85	0.62	1.24
ΔS_L_YV14 = ρΔS_L_YQ58	0.67	0.46	0.70	0.63	0.73	0.55
ΔS_L_YV16 = ρΔS_L_YM44	0.33	0.56	0.39	0.29	0.36	0.23
ΔS_L_YV16 = ρΔS_L_YQ44	0.09	0.03	0.08	0.12	0.11	0.08
ΔS_L_YV16 = ρΔS_L_YQ57	-0.23	-0.21	-0.24	-0.21	-0.34	-0.06
ΔS_L_YV16 = ρΔS_L_YQ58	0.25	0.21	0.23	0.28	0.30	0.19
ΔS_L_YV17 = ρΔS_L_YV18	0.21	0.37	0.00*	0.14	-0.11*	0.57
ΔS_L_YV17 = ρΔL_YV30	0.17	0.06	0.13	0.17	0.17	0.15
ΔS_L_YV17 = ρΔS_L_YM44	-0.36	-0.14*	-0.28	-0.30	-0.34	-0.39
ΔS_L_YV17 = ρΔS_L_YM57	-0.27	-0.38	-0.61*	-0.03*	-0.12	-0.18
ΔS_L_YV17 = ρΔS_L_YQ58	-0.14	-0.03	-0.12	-0.17	-0.17	-0.04
ΔS_L_YV19 = ρΔS_L_YV18	0.76	0.71	0.62	0.65	0.70	0.79

Reproduced with permission of the copyright owner. Further reproduction prohibited without permission.

ΔS_L_YV19 = ρΔL_YV32	-0.18	-0.13	-0.23	-0.41	-0.25	-0.12
ΔS_L_YV21 = ρΔS_L_YM57	0.31	-0.05*	0.13	0.87	0.66	0.30
ΔS_L_YV23 = ρΔS_L_YM57	1.40	0.86*	1.12	1.70	1.75	1.33
ΔS_L_YV23 = ρΔS_L_YQ57	0.36	0.41	0.61	0.62	0.47	0.73
ΔS_L_YV23 = ρΔS_L_YM58	-1.45	-0.79*	-1.14	-1.78	-1.59	-1.45
ΔS_L_YV23 = ρΔS_L_YQ58	-0.34	-0.48	-0.68	-0.62	-0.43	-0.87
ΔS_L_YV24 = ρΔS_L_YM57	-1.13	-1.29	-1.08	-1.31	-1.41	-0.91
ΔS_L_YV25 = ρΔS_L_YV17	0.72	0.57	0.29	0.44	0.09	0.74
ΔS_L_YV25 = ρΔS_L_YM57	0.71	-0.55*	2.71*	0.90	1.91*	1.26
ΔS_L_YV25 = ρΔS_L_YM58	-0.63	0.32*	-3.10*	-0.93	-1.89	-1.13*
ΔS_L_YV27 = ρΔS_L_YV18	0.53	0.54	0.58	0.62	0.47	0.59
ΔL_YV30 = ρΔS_L_YM44	-0.33	-0.31	-0.25	-0.35	-0.28	-0.71
ΔL_YV30 = ρΔS_L_YM58	0.31	0.99	-0.65*	1.28*	0.49	-0.57*
ΔL_YV30 = ρΔS_L_YQ58	0.38	0.73	0.24	0.44	0.21	0.65
ΔL_YV30 = ρΔL_YM70	0.21	0.06	-0.08	-0.32*	-0.31	0.54
ΔL_YV30 = ρΔL_YM74	0.32	0.36	0.70	0.67	0.27	0.42
ΔL_YV30 = ρΔL_YQ74	0.18	0.18	0.15	0.24	0.15	0.23
ΔL_YV32 = ρΔS_L_YV17	0.81	-0.41*	2.12*	0.74	1.44	1.33
ΔL_YV32 = ρΔS_L_YV30	-0.23	-0.28	-0.57	-0.44	-0.24	-0.24
ΔL_YV33 = ρΔL_YV30	-0.19	0.24*	-0.25	-0.34	-0.20	-0.24
ΔL_YV33 = ρΔL_YV35	0.27	0.54	0.40	0.37	0.33	0.25
ΔL_YV33 = ρΔS_L_YM44	0.32	-1.10*	0.15	0.65	0.61	0.12
ΔL_YV33 = ρΔS_L_YM58	-0.88	-3.56*	-0.03*	-0.85	-1.41	-0.57
ΔL_YV35 = ρΔS_L_YV1	0.69	0.69	0.99	0.24	0.88	0.80
ΔL_YV35 = ρΔL_YV30	0.40	0.10	0.39	0.27	0.33	0.54
ΔL_YV35 = ρΔS_L_YM58	-1.17	1.12*	-1.47	0.05*	-0.51	-1.74
ΔS_L_YM44 = ρΔS_L_YM84	0.70	-0.22*	1.44*	0.65	0.96	0.35
ΔS_L_YQ44 = ρΔS_L_YQ84	0.42	0.10	0.58	0.43	0.75	-0.08*
ΔL_YV45 = ρΔS_L_YV8	-0.64	-1.11	-0.30	-0.15	-0.78	-0.48
ΔL_YV45 = ρΔS_L_YV16	1.71	2.85*	0.68*	1.87	1.82	2.06
ΔL_YV46 = ρΔL_YM70	0.57	1.86*	0.48	-0.38*	0.17*	0.69
ΔL_YV46 = ρΔL_YM74	0.26	0.13	0.06	1.60*	0.48	0.14
ΔS_L_YV49 = ρΔS_L_YM44	0.96	1.44*	1.05	0.88	0.95	0.80
ΔS_L_YV49 = ρΔS_L_YQ44	0.45	0.66	0.42	0.44	0.47	0.42
ΔS_L_YV49 = ρΔL_YV45	0.08	0.02	0.08	0.22	0.06	0.13
ΔS_L_YM57 = ρΔL_YM63	0.21	0.11*	0.26	0.38	0.22	0.20
ΔS_L_YM57 = ρΔS_L_YM64	0.77	0.77	1.03	0.75	0.65	0.80
ΔS_L_YQ57 = ρΔL_YQ63	0.26	0.13*	0.32	0.40	0.29	0.22
ΔS_L_YQ57 = ρΔS_L_YQ64	1.18	0.98	1.3	1.59	1.13	1.23
ΔS_L_YM58 = ρΔS_L_YM64	0.91	0.84	1.17*	1.11	0.82	0.94
ΔS_L_YQ58 = ρΔS_L_YQ64	1.13	0.95	0.95	1.53	1.09	1.16
ΔL_YV69 = ρΔL_YM70	-0.50	-0.27	-0.68	-0.57	-0.52	-0.68
ΔL_YV69 = ρΔS_L_YM84	0.78	0.81	1.05	0.60	1.03	0.14
ΔL_YV69 = ρΔS_L_YQ84	1.45	1.89	0.39*	1.75	2.17	0.87*
ΔL_YM70 = ρΔL_YM78	0.19	0.18	0.96*	0.73	0.01*	0.02
ΔL_YM70 = ρΔS_L_YM84	-1.51	-0.72*	2.47*	-1.38	-0.56*	-2.44*
ΔL_YM74 = ρΔL_YM70	0.25	-0.14*	0.54	0.26	0.56	-0.26
ΔL_YM74 = ρΔS_L_YM84	-1.45	-5.51*	-1.06	-1.53	-1.41	-2.71*
ΔL_YQ74 = ρΔS_L_YQ84	-1.82	-1.57	-2.11	-1.34	-1.86	-1.88
ΔL_YM81 = ρΔL_YM84	1.05	0.50	1.22	1.14	1.30	0.86

Reproduced with permission of the copyright owner. Further reproduction prohibited without permission.

Model II (Respecified Model): Submodel Path Diagrams

Boxes 15.13 and 15.16 contain path diagrams showing selected causal pathways (arrows) relating relevant endogenous and exogenous variables in the model. Standardized path coefficients are given for each causal pathway. These path coefficients represent standard partial regression coefficients that estimate the strength of the cause and effect relationship between specific dependent and independent variables in the model (Sokal & Rohlf, 1995, p. 636). Although the path coefficients in the diagrams were calculated on the basis of the full model (i.e., Model II as shown in Box 15.6), in order to render the diagrams more comprehensible only selected causal pathways are shown. Covariances between exogenous variables are also not shown in the diagrams, although they were factored into the model. Residual coefficients (labeled with an "e" prefix) for each endogenous variable are given in the rounded boxes. Solid arrows represent causal pathways that are relatively robust and homogeneous across major anthropoid taxa. Dotted arrows, by contrast, depict causal pathways that are less stable and more heterogeneous across groups. The model fit indices reported for the two path diagrams give the values for each of the *submodels* depicted, not for the full model.

Model II Submodel A: Path Diagram and Character Synopses

Submodel A of Model II shows the main causal pathways relevant to the effects of (and relationship among) (1) relative brain form and cranial base morphology, (2) olfactory acuity, and (3) maximum bite force on anteroposterior dimensions of nasomaxillary skeleton (see Box 15.13).

Reproduced with permission of the copyright owner. Further reproduction prohibited without permission.

Box 15.13. Model II Submodel A. .

Model Fit Statistics: (for submodel components only)

Chi-square	311 (p=0.0001)
Goodness of Fit Index (GFI)	0.82
Adj. Goodness of Fit Index (AGFI)	0.61
Comparative Fit Index (CFI)	0.82
Normed Tucker Lewis Index (NTLI)	0.81

Full Model II Estimation.(all path coefficients are significant at $\alpha = 0.05$)

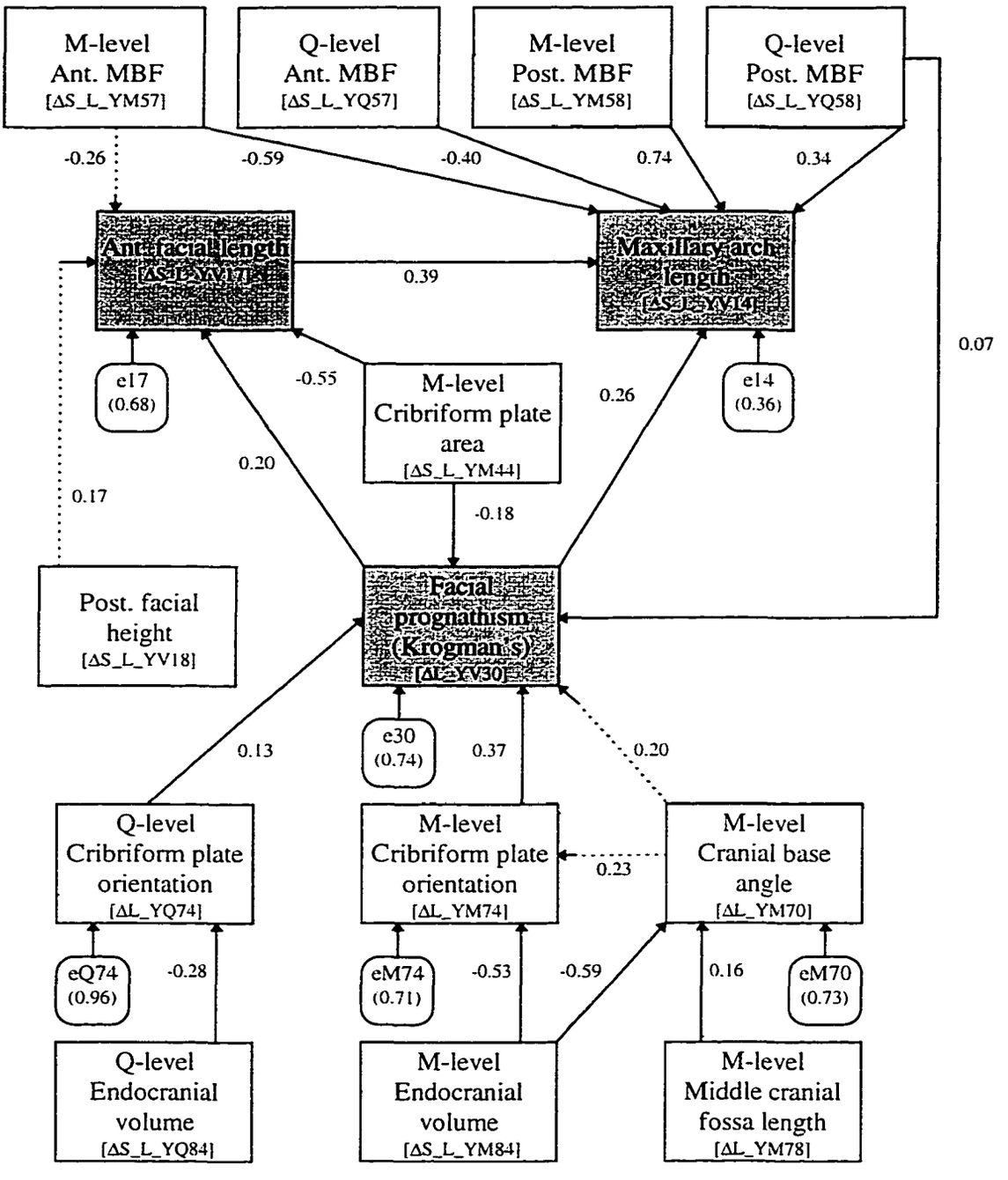

Reproduced with permission of the copyright owner. Further reproduction prohibited without permission.

Nasal bone length [Y1-NASLGT]

It must be noted that none of the three levels of the delta transformed data (V-level, Q-level and M-level) for nasal bone length conformed to a normal distribution. Nomological modeling of the anthropoid morphometric data indicate that 74% of the size-adjusted variance in delta nasal bone length can be accounted for in terms of a topographical growth constraint involving anterior facial elongation. The relationship between nasal bone length and anterior facial elongation is stable across anthropoid superfamilies and facial profile developmental modalities.

The ontogenetic shape analyses revealed growth correlations between nasal bone elongation, adjusted for cranial size, and maxillary arch length, facial prognathism, slope of the occlusal plane, and paranasal plate orientation. However, all of these growth correlations, with the possible exception of paranasal plate orientation, are part of a more general suite of growth correlations between these characters and anterior facial elongation.

Anterior nasal aperture height [Y5-NSLAHT]

The univariate distribution of this trait among anthropoids was not significantly different from normal for the V-level data, but was significantly different from normal for the Q- and M-level data. Modeled changes in piriform aperture height were not found to be affected by any structural growth constraints involving the characters examined. Body size scaling accounted for 80% of the total variation in anterior nasal aperture height among anthropoids, leaving 20% of the variance unexplained. After adjusting for size, evolutionary and developmental changes in anterior nasal aperture height were found not to be associated with any component

Reproduced with permission of the copyright owner. Further reproduction prohibited without permission.

of nasomaxillary or cranial variation (see PCA results, Boxes 11.11, 12.13, 13.13, 14.18). One might have expected that the same growth process that accounted for a significant proportion of the variation of nasal bone length (i.e. anterior facial elongation) could also explain anterior nasal aperture height. While the zero-order regression of anterior nasal aperture height on anterior facial elongation (delta V-level data) was significant at the 0.05 level, the R^2 was only 0.06. And when included in the full model, anterior facial elongation did not account for a significant proportion of the variation in anterior nasal aperture height.

Nasoalveolar clivus length **[Y9-NLCLGT]**

As with anterior nasal aperture height, nasoalveolar clivus length was univariate normal for the V-level data, but deviated significantly from normality for the Q- and M-level data. Two explanatory variables were retained in the final structural model to account for changes in size-adjusted nasoalveolar clivus length in anthropoids. It was shown in Chapter 9 that changes in inter-P^3 palatal depth are associated with changes in nasoalveolar clivus length, presumably through a spatial constraint involving the juxtaposition of the oral and nasal cavities in connection with their respective biological roles of mastication and respiration (see Box 9.21). It was found that changes in inter-P^3 palatal depth accounted for about 8% of the size-adjusted delta nasoalveolar clivus length. The main outliers in a regression of these two characters are contributed by *Pan troglodytes*, a species that exhibits much greater nasoalveolar clivus length than expected on the basis of inter-P^3 palatal depth. If specimens of *P. troglodytes* are excluded from the Model II CSM, the R-square increases to 15%.

Reproduced with permission of the copyright owner. Further reproduction prohibited without permission.

Initial structural modeling also indicated that delta nasoalveolar clivus length was associated with selectional (M-level) changes to anterior bite force magnitudes. However, this interpretation is highly suspect for the following reasons: in addition to the finding that the zero-order regression between the two characters was not significant ($\alpha = 0.05$) (see Box 14.16), in the multi-level structural model the proportion of variance accounted for was only 1% and the regression of nasoalveolar clivus length on anterior MBF conformed to a curvilinear rather than linear fit (see Box 15.9). Moreover, the significant association between the characters disappeared with the removal of 4 outlier specimens (see Box 15.10). Finally, the ANSCOVA results revealed that the unstandardized path coefficients between the two characters in Model II CSM were highly unstable, with positive values in some subgroups and negative valued in others.

Anterior facial length **[Y17-AFACHT]**

Although anterior facial length failed the Shapiro-Wilk test of normality for all three data levels, it can be seen with reference to the frequency distributions in Box 15.13 that this character approximates normality quite well, at least visually.

Box 15.14. Univariate frequency distributions of V-level, Q-level, and M-level anterior facial length anthropoid data.

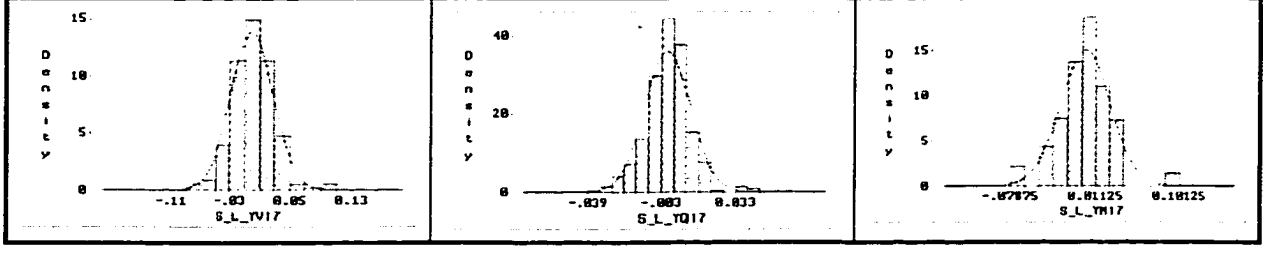

Correlated growth changes were found to occur between anterior facial length and maxillary arch length, palatal depth at P^3, facial prognathism, slope of the

Reproduced with permission of the copyright owner. Further reproduction prohibited without permission.

occlusal plane, paranasal plate orientation and facial rotation. A model of structural growth was developed in Chapter 9 in which an elongation of the anterior face imposes constraints on occlusal plane orientation and maxillary arch length (Box 9.17). In terms of specific growth constraints acting on anterior facial length, there appears to be a functional relationship between facial rotation, occlusal plane orientation and anterior facial growth. It was shown in Chapter 11 (Box 11.15) that the slope of the occlusal plane relative to the Frankfort horizontal exhibits angular invariance consistent with the hypothesis that the occlusal plane is constrained to be at a 10° angle to the FH (SD = 5°). Because nasomaxillary forward rotation during ontogeny tends to substantially decrease the occlusal angle thereby disrupting the constraint, anterior facial elongation can be viewed as a mechanism that compensates for the effects of facial rotation on occlusal reorientation. The effects of increased facial prognathism (a consequence of facial rotation—see Box 9.12) on anterior facial elongation are homogeneous across major anthropoid taxa (see Box 15.12), indicating that this mechanism may be wide-spread among anthropoids.

Another nomological agent found to have a consistent, but in this case negative, effect on anterior facial elongation across anthropoid groups is relative olfactory bulb size (i.e., relative cribriform plate area) (see Boxes 15.12 & 15.15). This finding runs counter to the postulate that a reduction of olfactory acuity initiated an evolutionary reduction of the nasomaxillary complex, a postulate elemental to both the 'arboreal' and 'visual predation' hypotheses of primate evolution. The preceding analyses indicate the opposite: that lineages marked by a reduction of olfactory bulbs size (relative to cranial centroid size) also exhibit an increase in relative anterior facial length (as well as an increase in facial

Reproduced with permission of the copyright owner. Further reproduction prohibited without permission.

prognathism). Obviously this runs counter to the hypotheses that an increase in the size of the olfactory apparatus requires a corresponding increase in the anterior dimension of the nasomaxillary complex in order to accommodate an enlargement of the nasal olfactory epithelia.

But why do evolutionary increases in olfactory bulb size produce decreases in anterior facial length? The answer may lie in the causal relationships between the brain, the olfactory apparatus, the cribriform plate and the rotation of the nasomaxillary complex. Recall from Chapters 11 and 12 that changes in relative olfactory bulb size and cribriform plate orientation are both dependent upon changes in brain size. It was further substantiated that changes in the orientation of the cribriform plate directly effect changes in facial prognathism and anterior facial length (through the mediating effects of facial rotation and constraints on the angular invariance of the cribriform plate and anterior facial plane). Therefore, the negative effects of olfactory bulb size on facial prognathism and anterior facial elongation can be viewed as an extension of the relationship between brain size and nasomaxillary morphology.

The covariance structural model indicates that two other properties are related to anterior facial length, although their effects are neither as strong nor as consistent as those already mentioned. First, the relationship between anterior bite force magnitude and anterior facial length. Mechanically, mammals with short anterior faces will be able to exert greater bite forces at the anterior dentition than comparably sized longer-faced mammals due to the increased lever efficiency in the former. Results of the analysis given in Chapter 14 (Box 14.15) indicate that only the M-level component of anterior bite force accounts for a significant proportion of

Reproduced with permission of the copyright owner. Further reproduction prohibited without permission.

the variance of anterior facial length—selection *for* increased anterior MBF results in selection *of* decreased anterior facial length (except in hominoids, for which no association was apparent). This suggests that while masticatory requirements for increased anterior bite force can operate via selection to reduce anterior facial length, the nasomaxilla does not respond to the same requirements through acclimative mechanisms. This interpretation conflicts with the results obtained in experimental studies that have demonstrated that dietary consistency has an effect on anterior facial growth in a variety of mammals (e.g., Chuang, 1995; Ciochon *et al.*, 1997). The significant association between M-level anterior bite force magnitudes and anterior facial length is consistent with previous observations regarding the correspondence between dietary specializations for hard food items and reduced anterior facial length (e.g., Kinzey, 1974).

Second, increases in posterior facial height are associated with corresponding increases in anterior facial length (except in catarrhines) (see Box 15.12). The relationship between anterior and posterior facial length in some, but not all, anthropoids can be understood in terms of the functional constraint operating to maintain the slope of the occlusal plane within functionally acceptable boundaries. Modifications in one plane of the face without compensatory modifications of the other will result in an aberrant slope of the occlusal plane. However, in terms of a craniofacial growth mechanism this is only true if the shape of the facial profile remains relatively uniform from infant to adult—as it is platyrrhines and, to a lesser extent, hominoids. In most cercopithecoids, however, this is not the case. The shape of the facial profile is much different in infants compared to that of adults, requiring a much different facial growth pattern. Several of the facial profile

Reproduced with permission of the copyright owner. Further reproduction prohibited without permission.

diagrams originally presented in Box 9.9 are reproduced in Box 15.15 for reference. It can be seen in both atelines and *Pan* that the transition from infant to adult form is characterized by a downward and forward translational rotation of the nasomaxillary complex and relatively uniform growth of the anterior and posterior facial planes and maxillary arch. By contrast, the cercopithecini and papionina facial profiles depicted in Box 15.15 suggest a different pattern of facial growth and remodeling. In addition to forward rotation of the nasomaxillary complex, these taxa are characterized by extensive elongation of the anterior face and maxillary arch but relatively little change in posterior facial height.

Box 15.15. Superimpositions of infant (dotted line) and adult (solid line) facial profiles for selected anthropoid taxa.

Subfamily: Atelinae

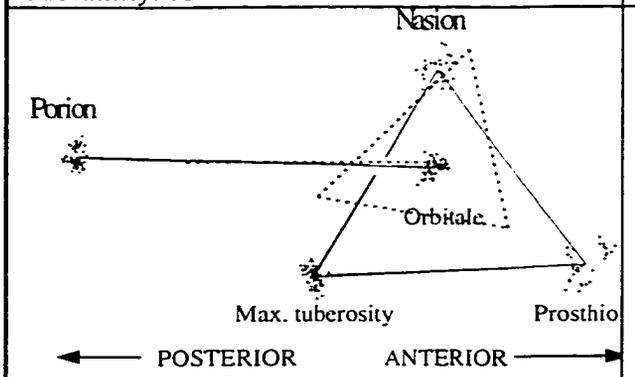

Tribe: Cercopithecini

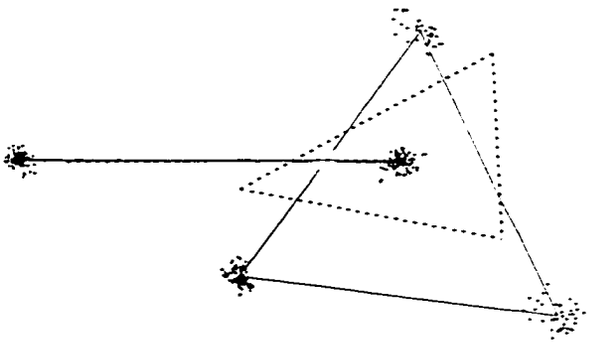

Subtribe: Papionina

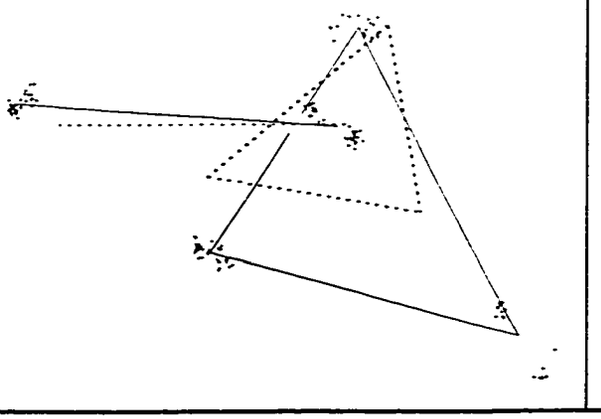

Genus: *Pan*

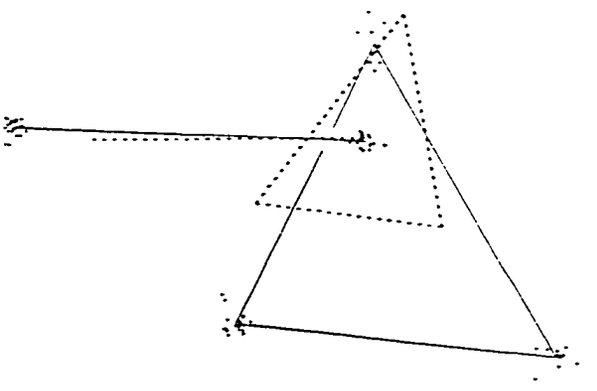

Reproduced with permission of the copyright owner. Further reproduction prohibited without permission.

In *Homo* little or no facial rotation is manifest and posterior facial elongation appears to be the primary mechanism by which the slope of the occlusal plane is maintained.

The foregoing analysis suggests that the key to understanding variation of size-adjusted anterior facial length in anthropoids is to understand (1) the causal agents that determine nasomaxillary rotation, (2) the mechanical requirements that impose constraints on the slope of the occlusal plane, and (3) the selectional pressures acting on maximum anterior bite force magnitudes. Together, these factors account for roughly two-thirds of the size-adjusted variance in anterior facial length in anthropoids (platyrrhines, 65%; catarrhines, 68%; hominoids, 62%).

Maxillary arch length **[Y14-MXARCL]**

Due to the counterpart relationship between anterior facial length and maxillary arch length, these two traits covary to a great extent. The question is whether the development and evolution of the anterior face imposes constraints on maxillary arch length or the direction of causality is reversed.

We have already seen that elongation of the anterior face may operate to counteract the effects of facial rotation on the slope of the occlusal plane, in which case maxillary arch elongation can be viewed as a counterpart response to the growth of the anterior face. However, if maxillary arch length is an adaptation in conjunction with maximum bite force requirements, or to accommodate a particularly large (or small) set of dentition (Oyen, 1984), then it is anterior facial growth and remodeling (and to some extent facial rotation itself) that is the

Reproduced with permission of the copyright owner. Further reproduction prohibited without permission.

counterpart response to maxillary arch elongation (cf. Krogman, 1931) (compare the facial profile diagrams in Boxes 9.17 & 9.18).

In contrast to Krogman (1931), who viewed facial rotation as stemming from posterior maxillary arch growth, Enlow (1966:298) contended that the "...forward translocation of the face during development is primarily a result of new bone growth at the sutures separating facial bones from the various other cranial bones lying behind them." In this latter formulation facial rotation produces tension on these sutures, including the pterygomaxillary fissure, thereby initiating growth through *primary displacement* (see Enlow, 1990, p. 51).

There may well be a bidirectional influence between the two counterpart elements (*cf.* Nanda *et al.*, 1987): the forward displacement of the nasomaxillary complex combined with anterior facial elongation may determine the anterior extent of the maxillary arch, but the extent of posterior maxillary growth through deposition at the maxillary tuberosities may be determined by the degree of cranial base extension and dentary and masticatory factors. For example, it has already been shown (Box 14.9) that the placement of the last molar is functionally/mechanically constrained to a point midway between the ipsilateral TMJ and prosthion. Maximum bite force magnitudes were also shown to be associated with maxillary arch length in the analyses presented in Chapter 14 (Box 14.15).

Consistent with this theoretical model, CSA Model II (Box 15.15) shows that both anterior and posterior maximum bite force magnitudes (M-level and Q-level), anterior facial elongation, and facial prognathism all have a significant effect on

Reproduced with permission of the copyright owner. Further reproduction prohibited without permission.

maxillary arch length.[3] Moreover, these effects are consistent across major taxa. Together, these causal agents account for 77% of the size-adjusted variance in maxillary arch length in New World monkeys, 94% in Old World monkeys, and 86% in hominoids.

Facial prognathism (Krogman's angle): **[Y30-KROGAG]**

Vogel (1968) listed facial prognathism as one of the four most important cranial characters for understanding the systematics and evolution of the primates (the others were: placement of the foramen magnum, position of the zygomatic arch in relation to the orbits, and properties of mandibular shape and construction). The main reason for this, I think, is that facial prognathism is the best static adult indicator of facial rotation. Of all the characters examined in the ontogenetic analysis (Chapter 9), facial prognathism had the highest correlation with facial rotation (Box 9.15). Another reason is that this character is highly variable in anthropoids, and this variability has yet to be adequately explained. I have already discussed the important effects of facial rotation, and by implication facial prognathism, on anterior facial elongation, occlusal orientation and maxillary arch length. But what causal agents conspire to determine facial prognathism?

Camper (1782) was the first to define and measure this character in primates, but his analysis was largely descriptive. Numerous researchers have subsequently shown, in a wide variety of mammalian taxa, that *cranial base extension* covarys with facial rotation and, concomitantly, with facial prognathism (e.g., Huxley, 1896; Weidenriech, 1947; DuBrul & Laskin, 1961; DuBrul, 1965; Vogel, 1968; Enlow &

[3] It is important to note, however, that both delta facial prognathism and M-level delta posterior MBF exhibit a curvilinear relationship with delta maxillary arch length (see Box 15.9).

Reproduced with permission of the copyright owner. Further reproduction prohibited without permission.

McNamara, 1973; Swindler, *et al.*, 1973; Solow & Tallgren, 1976; Moore, 1981). Others have pointed to the association between *dietary behavior or masticatory properties* and facial prognathism. CSA Model II confirms the importance of these two sets of causal agents on facial prognathism. The only masticatory variable to exhibit a consistent effect on facial prognathism was posterior MBF (particularly the Q-level data). This finding is consistent with the experimental results of Carlson and Schneiderman (1983) and Kiliaridis (1986), but runs counter to the results reported by Chuang (1995) and Ciochon *et al.* (1997) (see Chapter 14). It implies that great posterior bite force magnitudes generated during ontogeny have the capacity to induce an acclimational response characterized by increased facial prognathism. It should be noted, however, that the strength of this association is rather weak. The regression model containing both M- and Q-level posterior MBF accounts for just 10% of the variance of facial prognathism (see Box 14.16), and the standardized path coefficient connecting the two traits in the covariance structural model is only 0.07 (see Box 15.15).

By contrast, the effects of chondrocranial development and evolution on facial prognathism appear to be much stronger. Surprisingly, however, the CSA model indicates that *cranial base flexion* has no consistent direct effect on facial prognathism across anthropoid taxa or developmental modalities (see Box 15.12). On the other hand, *cribriform plate orientation* invokes a relatively strong influence on facial prognathism that is consistent across major anthropoid groups, for both the M-level and Q-level data. This finding indicates that it is not cranial base extension, per se, that initiates facial rotation and facial prognathism among anthropoids, as many have contended. Rather, as first suggested by Enlow and McNamara (1973), it

Reproduced with permission of the copyright owner. Further reproduction prohibited without permission.

is the vertical reorientation of the cribriform plate-ethmoid complex during ontogeny that is primarily responsible for nasomaxillary rotation and facial prognathism. The positive association between cranial base angle and facial prognathism revealed in Chapter 13 (see Box 13.18), does not retain its significance when the effects of cribriform plate orientation are controlled for in the covariance structural model.

These results would seem to contradict those obtained in experiments conducted by DuBrul and Laskin (1961), which clearly established a link between normal cranial base development and facial rotation/prognathism. Recall that these researchers surgically removed the sphenooccipital synchondroses from young rats and observed that the normal progression of cranial base extension and forward rotation of the nasomaxillary complex had been disrupted. However, it is also clear from the detailed diagrams provided by these authors that the orientation of the cribriform plates remained in a relatively horizontal orientation and that the 90° angle between the cribriform plate and mid-facial plane was preserved in the experimental rats (see Chapter 11). This suggests that while it is the orientation of the cribriform plate that determines the degree of facial rotation/prognathism, the development of the cranial base acts to facilitate cribriform plate movement, a hypothesis consistent with the CSA model (Box 15.13).

A third causal agent that has a direct effect on facial prognathism is relative olfactory bulb size. The covariance structural model (Model II) indicates that evolutionary increases in relative olfactory bulb size are associated with decreases in facial prognathism. As with the relationship between relative olfactory bulb size and anterior facial length, the negative relationship between relative olfactory bulb

Reproduced with permission of the copyright owner. Further reproduction prohibited without permission.

size and facial prognathism is best understood in terms of the association between the brain and the nasomaxillary complex. I shall return to this point presently.

Occlusal slope: **[Y32-SLOPOC]**

Although not shown in Submodel A, changes in occlusal slope during ontogeny are intimately related to facial rotation and anterior facial elongation. Using the regression-based test for angular invariance developed in Chapter 11, it was shown (Box 11.45) that the slope of the occlusal plane is constrained to maintain an angle of approximately 10° to the Frankfort horizontal. What little variation exists (SD 5°) across anthropoids is thus likely to be due to slight variations in the mechanism that maintains the angular invariance. Accordingly, variation of facial prognathism and anterior facial length account for a significant, but small (7%), proportion of the variance of occlusal orientation. I have already described in some detail the hypothesis that anterior facial elongation acts to counter the effects of facial rotation on occlusal slope, thereby maintaining the relative angular invariance of the latter (both ontogenetically and phylogenetically). The question remains: why should the occlusal plane be constrained to maintain its observed invariant orientation? It is not unreasonable to assume that the inclination of the occlusal plane may be regulated by requirements imposed by the masticatory system. Recall that Hohl (1983) surgically repositioned the attachment sites of the masseter and temporalis muscles in *Macaca nemestrina* and observed a readjustment in the orientation of the occlusal plane subsequent to postsurgical masticatory function.

The occlusal surface must be at a 90° angle to resultant muscle vector in order to fully translate muscle force into occlusal force. Since the resultant

Reproduced with permission of the copyright owner. Further reproduction prohibited without permission.

masticatory muscle vector is mostly determined by the masseter and temporalis adductor muscles, constraints on the physical attachments of these muscles may translate into constraints on occlusal plane orientation. Based on the three-dimensional model of masticatory function developed in Chapter 14 (*cf.* Greaves, 1978; Demes & Creel, 1988) the estimated resultant muscle vector roughly corresponds to a plane following the path of maximum postorbital constriction (MPC plane). It can be seen with reference to the skull photographs in Chapter 4 that the MPC plane approximates a 90° angle to the occlusal plane. The MPC further coincides with (1) maximum infratemporal foramen width, (2) the main bulk of the retro-orbital temporal fibers (McDevitt, 1989, p. 53), and (3) the anterior masseteric tubercle. The MPC plane is also situated just posterior to maxillary tuberosity, precisely at a point where the maximum resultant vector (MRV) is predicted to occur by Greaves' triangle of support model. Thus, the MPC (maximum postorbital constriction) plane appears to closely correspond to the MRV (maximum resultant vector) (see Chapter 14). Structural restrictions on the anatomical placement of the MPC, in conjunction with the need to maintain a 90° angle between the MPC/MRV plane and occlusal plane, impose constraints on the orientation of the latter.

The hypothesis of occlusal plane orientation outlined above differs markedly from the structural hypothesis advanced by Zingerser (1972), who argued that "the combined size and form of the upper face capsules determine the *basic* orientation of the maxillary tooth-bearing region" (p. 254).

Reproduced with permission of the copyright owner. Further reproduction prohibited without permission.

Model II, Submodel A Synopsis.

It can be seen with reference to the path diagram in Box 15.13, that the significant negative relationship between brain size and facial prognathism is mediated by changes in the chondrocranium, more specifically through changes in the orientation of the cribriform plate/ethmoid complex, with perhaps a moderating role of the basisphenoidal component of the chondrocranium. Facial rotation and facial prognathism, in turn, effect changes to anterior facial length and maxillary arch length.

This model of brain-chondrocranium-splanchnocranium interaction is supported by recent studies focusing on normal embryonic and fetal brain-face interrelations, and on the correlated effects of congenital cranial disorders, although most of these studies have been confined to human subjects. Investigation of normal human cranial ontogeny indicate a close interconnection between the development of the craniofacial skeleton and that of the brain (see Kjaer, 1995, for a recent review). Diewert and colleages (e.g., Diewert, Wang & Tait, 1993; Diewert, Lozanoff & Choy, 1993) have pieced together the major changes that occur in the spatial relations between the neural and facial components in the developing fetus. Consistent with the hypothesis of Enlow and McNamara (1973), these authors report that the most fundamental correlated growth changes occur between the ventral contour of the frontal aspect of the brain and the frontonasal prominences of the primate face.

Studies of craniofacial disorders have also been instrumental in elucidating the relationship between the brain and the face. As originally reported by Weidenreich (1941), and confirmed in more recent studies, microcephalic individuals typically

Reproduced with permission of the copyright owner. Further reproduction prohibited without permission.

exhibit many of the characteristics associated with the relatively smaller brains of larger mammals, including flattened calvaria and pronounced facial features. The correlated changes observed to occur between the size and shape of the brain and craniofacial characteristics associated with neurocranial disorders may result from pleiotropic gene anomolies (see Chapter 2), but in some specific disorders (e.g., atelencephaly) brain-face interrelations appear to be "...deformations rather then malformations" (Siebert *et al.*, 1987).

The intimate connections between the forebrain and the nasoethmoidal component of the face are also manifest in human cranial disorders. The vast majority of such disorders involve "...malformation of the forebrain..." and "...the basicranial skeleton anterior to the spheno-occipital junction..." (Kjaer *et al.*, 1991:846). Thus, both recent clinical data and the results of the current study support the hypotheses of Weidenriech (1941), Biegert (1957), and, particularly, Enlow and McNamara (1973), that interrelated changes in the size and shape of the brain and the orientation of the spheno-ethmoid complex play a central role in effecting changes to the morphology of the face.[4] According the Siebert *et al.* (1981), "...the spatial relationships of the bony and soft tissue components of the median face are guided and maintained by the ethmoid complex during morphogenesis" (p. 305)

Recent experiments by Haung, Solursh and Sandra (1996) help shed some light on the observed relationship between the development and evolution of the brain, the cranial base and the facial skeleton in mammals. These authors traced the expression of transforming growth factor alpha (TGF-alpha) in embryonic rats and found that these

Reproduced with permission of the copyright owner. Further reproduction prohibited without permission.

regulatory molecules first appeared in the neural fold then in the "...mesenchyme surrounding the olfactory bulb, within the olfactory bulb, the nasal capsule, vomeronasal organ, and vibrissal folicle" (Haung, *et al.*, 1996, p. 73). They further confirmed that TGF-alpha has an inhibitory effect on chondrogenesis. These findings suggest a further proximate mechanism by which increases in relative brain size and olfactory bulb size inhibit cranial base extension, thereby limiting vertical cribriform plate/ethmoidal reorientation and, concomitantly, facial prognathism.

Model II Submodel B: Path Diagram and Character Synopses

Submodel B of Model II shows the main causal pathways important for an understanding of anthropoid diversity in terms of selected facial breadth and depth measurements, and upper orbito-nasal morphology (see Box 15.16).

[4] For a review of recent studies focusing on the relationship between nerve tissue and craniofacial development see Kjaer, 1998.

Reproduced with permission of the copyright owner. Further reproduction prohibited without permission.

Box 15.16. Model II Submodel B.

Model Fit Statistics: (for submodel components only)

Chi-square	427 (p=0.0001)
Goodness of Fit Index (GFI)	0.87
Adj. Goodness of Fit Index (AGFI)	0.66
Comparative Fit Index (CFI)	0.88
Normed Tucker Lewis Index (*NTLI*)	0.85

Full Model II Estimation (all path coefficients are significant at $\alpha = 0.05$):

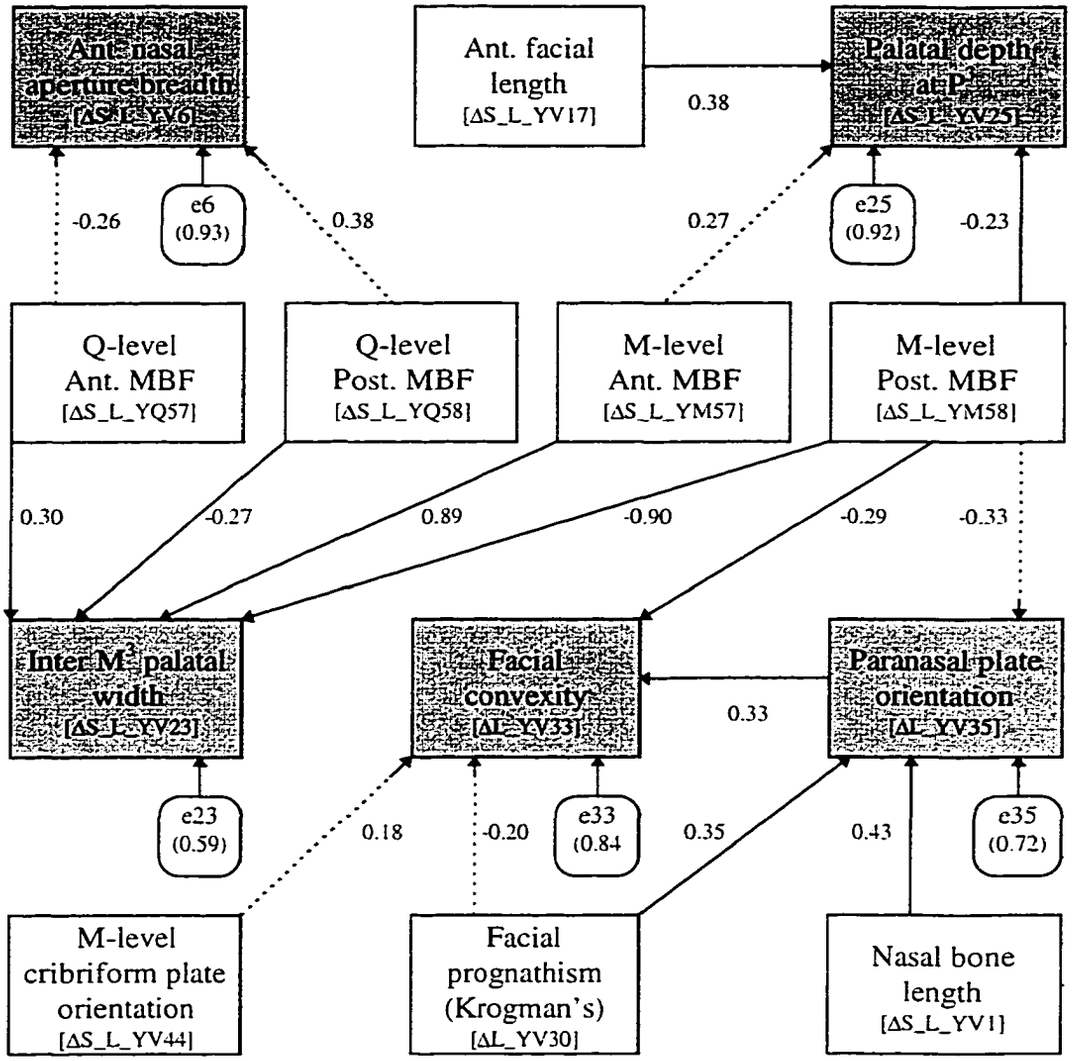

Reproduced with permission of the copyright owner. Further reproduction prohibited without permission.

Anterior nasal aperture breadth: **[Y6-NSLANWD]**

Various hypotheses have been proposed to explain primate and anthropoid variation in the shape of the anterior nasal aperture. Climatic-thermoregulator causal agents have also been proposed to account for piriform aperture breadth (e.g., Thomson & Buxton, 1923; Davies, 1932).

According to Covariance Structural Model II, two masticatory factors—Q-level anterior MBF and Q-level posterior MBF—can account for a significant proportion of the variation of anthropoid anterior nasal aperture breadth. In contrast to the bivariate results presented in Chapter 14, the best fit covariance structural model supports *both* the hypothesis of Demes (1987) and that of Hylander (1977), at least as far as the nomological mechanism of acclimation is concerned. Demes' (1987) hypothesis that a broad, rounded nasal aperture is a response to torsional masticatory forces caused by unilateral biting is consistent with the observed positive association between increased posterior MBF magnitude and increased anterior nasal aperture breadth (see Box 15.12). Hylander's (1977) hypothesis that a narrow anterior nasal aperture is best suited to dissipate extensive anterior bite force magnitudes is consistent with the observed negative association between increased anterior MBF magnitude and decreased anterior nasal aperture breadth (see Box 15.12). Therefore, relative anterior nasal aperture breadth represents a compromise "solution" to the engendered opposing forces of posterior unilateral bite force and anterior bite force.

However, these masticatory forces account for less than 15% of the size-adjusted variance of anterior nasal aperture breadth, indicating that other causal

Reproduced with permission of the copyright owner. Further reproduction prohibited without permission.

agents not included in the current model play an even more important role in the production of variation of this character. Although olfactory bulb size was found to be positively related to piriform aperture breadth among anthropoids, the ANSCOVA results indicate no significant relationship between these traits within major anthropoid taxa (see Box 15.12).

Inter-M^3 palatal width: **[Y23-M3PALW]**

All three levels of the delta log size-adjusted data for inter-M^3 palatal width deviate significantly from distribution normality, but there are no outliers for this character with regard to the independent variables included in the structural model. It was demonstrated in Chapter 9 that delta relative maxillary width is highly (negatively) correlated with delta maxillary length for all three data levels (V-level: r = -0.48, p = .001, n=300; M-level: r =-0.51, p = .001, n=37; Q-level: r = -0.28, p = .001; n=300). However, no biological growth constraint was discovered that could account for the observed covariance between maxillary length and breadth. Enlow (1965, p. 449) suggested that the specific orientation of the maxillary tuberosity during ontogeny could explain the negative allometric growth relationship between maxillary length and width. Because the maxillary tuberosities are oriented more posteriorly than laterally, accumulative bone deposition at these important growth sites will yield greater anteroposterior growth than lateral growth.

In Chapter 14 I presented evidence from experimental studies in which animals fed a "soft diet" exhibited a reduction of maxillary breadth compared to controls or animals fed a "hard diet" (e.g., Watt & Williams, 1951; Beecher & Corruccini, 1981; Yamamoto, 1996: rats; Beecher et al., 1983: squirrel monkeys).

Reproduced with permission of the copyright owner. Further reproduction prohibited without permission.

These results are consistent with the hypothesis that relatively wide maxillary arches are acclimations to high bite force magnitudes. This hypothesis gains support from the current structural covariance analysis, only if it is assumed that animals in the experiments just cited engaged primarily in incisal biting (and very little in molar or premolar mastication), a tenuous assumption, at best. The structural submodel represented diagrammatically in Box 15.16 indicates that selective and acclimational nomological mechanisms both operate to increase maxillary width in response to increased anterior bite force magnitude; but act to decrease maxillary width in response to increased posterior bite force magnitude. These results are consistent with Greaves' (1978) model of mammalian masticatory function. Recall that bite points located closer to the midline are capable of greater bite force magnitudes than bite points located further away from the midline, but that this condition only holds for the posterior dentition. There is no similar effect operating on the anterior dentition: changes in mediolateral position of the anterior teeth have little effect on maximum bite force magnitude (see Box 14.5, F).

The changes effected by Q-level and M-level anterior and posterior MBF magnitudes on inter-M^3 maxillary width are significant and consistent across the major anthropoid taxa. These masticatory causal agents account for 65% of the size-adjusted variance in maxillary width among anthropoids.

Reproduced with permission of the copyright owner. Further reproduction prohibited without permission.

Chapter 16. Conclusions and Applications

This concluding chapter is divided into three sections. The first contains a review of the major findings of the study, with an eye towards integration of the conclusions reached in each of the preceding chapters. The second provides a summary of the potential applications of the research findings, with a few brief examples. Finally, a few concluding remarks are given.

A. Major Research Findings

This study described and tested hypotheses relating to the effects of body size, brain form, olfaction, locomotion and mastication on the morphology of the nasomaxillary skeleton among extant Higher Primates.[1] A set of integrated operational and analytical procedures, consistent with current morphogenetic theory, was developed and applied in an attempt to delineate the nomological mechanisms (i.e., selection, acclimation, and constraints) responsible for anthropoid craniofacial diversity. The major findings of this study are summarized below:

Morphogenetic Theory

Cranial variation derives from differences in the patterns of growth and remodeling during ontogeny (Davidson, 1976; van Limborgh, 1982; Atchley & Hall, 1991). A review of the research literature (Chapter 2) revealed that during morphogenesis branchial arch mesenchyme (primordial viscerocranium) comes under increasing intrinsic and homeotic control, whereas permissive epigenetic and environmental

[1] Although this study was conducted exclusively on female specimens, it is argued that the external validity of the results extends to include males as well.

Reproduced with permission of the copyright owner. Further reproduction prohibited without permission.

signals regulate the morphogenesis of the dermal mesoderm (primordial neurocranium). Anatomically, intrinsic signals appear to play a greater role in the skeletogenesis of the chondrocranium, whereas development of the desmocranium is regulated largely by environmental signals originating from growing soft tissue and muscle contraction (Moss, 1976; Enlow, 1990; Herring, 1993).

I further argued in Chapters 2 and 3 that organic diversity derives from causal mechanisms operating on two levels—proximate and distal. Proximate causal mechanisms (PCM) include processes that characterize morphogenesis and skeletogenesis of the developing organism. Distal causal mechanisms (DCM) establish the distribution of traits in a population by determining which heritable proximate mechanisms become propagated or expressed through selection, acclimative response, or biological constraint. Different distal causal mechanisms determine nasomaxillary diversity via different proximate control mechanisms. Selection determines which intrinsically and epigenetically regulated proximate programs will be propagated and expressed. Acclimation operates via environmental control signals, although the response mechanism may have a genetic basis. Biological constraints can involve all three types of regulatory control.

Operational Framework

In 1943, Washburn and Detwiler published an influential paper in which they argued against the use of comparative research in biological anthropology, and presumably other fields of biology. They argued that tests of competing hypotheses could only be resolved using experimental designs. However, these and subsequent authors (e.g., K. Smith, 1993) have failed to realize that the choice of experimental vs.

Reproduced with permission of the copyright owner. Further reproduction prohibited without permission.

nonexperimental design is predicated on the nature of the research question, and on the causal mechanisms being studied. In Chapter 3, I argued that experimental designs in morphology are best suited to resolve questions regarding acclimative causal mechanisms, or, in some cases, the role of specific genes or cellular components in normal development and function (i.e., proximate causal mechanisms). Experimental designs, however, are poorly suited to address questions regarding selective nomological and historical causal mechanisms, for which comparative designs are well suited. For example, the question "How can we explain the observed diversity of canine size among primates?" cannot be resolved experimentally, because selective nomological and historical causal mechanisms likely played a much larger role in the evolution of canine morphology than did acclimative mechanisms.

In Chapter 4, I addressed the issue of sample size and composition in comparative morphology. Several methods for determining the appropriate size of a study sample were assessed in relation to specific analytical techniques. Based on this review, and on parameter estimates obtained from an initial pilot study (McMahon, 1994), I made the general recommendation that samples of at least 300 specimens be used for multiple regression, principal components analysis, and covariance structural modeling of craniometric data. The reader is referred to the formulae in Box 4.1, or to the tables provided by Cohen (1988), for more detailed recommendations based on specific test conditions.

I further suggested that studies employing cross-taxonomic data should attempt to sample proportionately from the major subtaxa constituting the clade. A chi-square test was introduced to assess goodness-of-fit of sample proportions (Box

Reproduced with permission of the copyright owner. Further reproduction prohibited without permission.

4.3). In multi-level analyses that include both among-species and within-species components, an attempt should also be made to ensure species homogeneity. The first option in this regard is to select specimens of the same subspecies from within each species. However, this is not always possible (as in the present study), and a geomorphometric analysis of variance test was introduced to assess the degree of overall cranial homogeneity within each polytypic species. The test results indicated that, with the exception of *Ateles*, including specimens from two or more subspecies did not substantially inflate the within-species cranial heterogeneity (see Box 4.4).

The importance of collecting precise, accurate data for analysis cannot be overstated. In Chapter 5, a novel method was presented for accurately combining ectocranial landmarks with endocranial radiographic landmarks to form a single coordinate configuration for each skull that contains both internal and external points in three-dimensions. Thus, this study contributes a large body of raw empirical data on anthropoid craniofacial morphology (see Appendix E). In all, the locations of 109 landmarks (including both ectocranial and endocranial coordinates) were recorded on 324 anthropoid crania (a total of 35,316 digitized points). From these coordinates, any number of constructed points, linear distances, angles, indices, and estimated areas and volumes can be calculated for future analysis.

Analytical Framework

A major problem faced by researchers conducting comparative analyses on samples drawn from multiple populations or species is that the data points are not statistically independent. This is because species are differentially related in

Reproduced with permission of the copyright owner. Further reproduction prohibited without permission.

accordance with the nested hierarchical topology of the underlying phylogeny. In Chapter 6, I demonstrated that in order to restore independence to the data a multi-level phylogeny must be collapsed into a single-level phylogeny. A technique called the ACP (ancestrally centered phylogeny) was introduced to achieve this goal. It was further shown using computer simulations that the ACP method fully restored independence to the data if, and only if, the ancestral morphotypes of the last shared ancestors (LSAs) of the extant species are known. Since ancestral morphotypes can never be known with certainty (except in simulations) they must be estimated. It was shown that current phylogenetic adjustment methods (e.g., nested ANOVA, phylogenetic autoregression, independent contrasts) are simply procedures by which LSA morphotypes are estimated from a sample dataset and a working phylogenetic hypothesis.

Once this is understood, the meaning of the phylogenetically adjusted data becomes clear: each transformed variate represents the amount of change that has accrued over a given lineage from the LSA to its extant descendent. Simple stated, a phylogenetically transformed datum measures the difference in trait values between an extant species and the estimated morphotype of its last shared ancestor. This metric corresponds precisely to Eldredge's (1989) concept of an *evolutionary trend*—"directional accumulations of (presumably) adaptive change" (p. 134).

Several important corollaries emerge from this insight. First, the crucial information in the procedure is the estimate of the ancestral morphotype—all other required information comes from direct observation and calculation. Recall that in the phylogenetic simulations, when the ancestral morphotypes are known, the ACP procedure completely restored independence to the virtual data. It follows that the

Reproduced with permission of the copyright owner. Further reproduction prohibited without permission.

method used to derive LSA morphotype estimates is critical. All current phylogenetic adjustment procedures (e.g., phylogenetic autoregression) estimate ancestral morphotypes solely from data obtained on extant forms. While these methods produced reasonable results in simulations (i.e., they reduced the Type I error rate from 0.30 to about 0.10), estimates of ancestral morphotypes will be greatly improved by incorporating fossil data into the analysis. For example, the autoregression procedure gave an estimate of 743 ml for the endocranial volume of the last shared ancestor of *Pan* and *Homo*. However, fossil evidence indicates that the last shared ancestor of *Pan* and *Homo* likely had an endocranial volume more similar to *Australopithecus*, around 400 ml. A method for incorporating both fossil and extant morphometric data into the analysis of phylogenetic effects using the ACP/autoregression approach with a rectangular W matrix was presented (although not applied in the current research).

Second, given that the use of raw data will increase the probability of committing a Type I error (i.e., finding significance when none exists), and correcting this problem by adjusting for phylogenetic effects transforms the data into *units of change*, it follows that all valid (i.e., phylogenetically adjusted) cross-taxonomic comparative research is inherently diachronic. Therefore, the distinction made between "vertical" and "horizontal" analyses in morphology is metaphysically ill-formed (e.g., Lewontin, 1969)

There is another element to this issue that has not been previously addressed, here or in the theoretical literature. Despite the success of the autoregression/ACP approach in simulation studies to partially restore independence to *virtual* data, analysis of *actual* anthropoid craniometric data reveal clear taxonomic clustering of

Reproduced with permission of the copyright owner. Further reproduction prohibited without permission.

the data points even after phylogenetic adjustment and correction for size. The reason for this occurrence is that there are two basic types of phylogenetic effects, and all current methods of phylogenetic adjustment, including the ACP method, remove only one type. The type of phylogenetic effect removed by the ACP and subordinate procedures, as discussed in Chapter 6, derives from the hierarchical branching pattern underlying multi-level phylogenies and may be referred to as a *topology* effect. The second type of phylogenetic effect, which is not removed by the ACP method, is what Mahner and Bunge (1997) refer to as *causal propensity*—"the propensity to acquire certain manifest properties under certain circumstances" (p. 9). Thus, while the autoregression/ACP procedure can partition and remove that part of the variance of a given trait due to inheritance from a common ancestor, it cannot remove an inherited *propensity* of a species or lineage to change in a certain direction, or to respond to selective pressures in a particular way. This concept corresponds to one particular definition of phylogenetic constraint (e.g., Mayr, 1983). According to K. Smith (1993), "Phylogenetic constraints arise because evolutionary change in a particular lineage is possible only within the functional and genetic context of the ancestors of the lineage" (p. 151). For instance, inheritance of extensive orbital deflection from a common ancestor can be removed from a pair of related species (if the ancestral condition is known), but it is not possible to remove an inherited "propensity" for both species to evolve increased orbital deflection in association with taxon-specific constraints involving cranial base mediation (as appears to have been the case with platyrrhines).

The notion that nomological mechanisms operate differently in different taxa is consistent with the morphogenetic framework established in Chapter 2, and

Reproduced with permission of the copyright owner. Further reproduction prohibited without permission.

with the biophilosophical foundations developed by Szalay and Bock (1991) and Mahner and Bunge (1997). Selection, acclimation and constraints operate within character-specific and taxon-specific boundary conditions defined by particular genetic and ecological landscapes.

On first principles we may assume that propensity effects will lead to inflated Type I error rates. One possible solution is to statistically control for taxon-specific proclivity effects by including dummy-coded taxon membership variables into a multiple regression or covariance structural model (in addition to delta transformation of the data!). However, a more informative approach, and the one adopted here, is to test nomological hypotheses within taxa across several levels. The advantages of this approach are numerous. It permits taxon-specific and level-specific phylogenetic constraints and boundary conditions to be identified and quantified. By tailoring models to specific taxa, more of the total variance can be accounted for and predicted values are more accurate. Further, taxon-specific propensity effects, once identified, can be interpreted in light of historical processes. The main disadvantage of the approach is that potentially large samples are required in order to ensure adequate power in analyses involving taxa of low rank.

In addition to quantifying taxon-specific nomological effects on nasomaxillary morphology, one of the objective of this research was to distinguish the effects of particular nomological mechanisms on nasomaxillary form. A multi-level analytic approach was developed in Chapter 8 that attempted to partition the effects of selection and acclimation on anthropoid craniofacial variation. This multi-level model was borrowed from quantitative genetics in which the total variance of a phenotypic trait is partitioned into "genetic" and "environmental" components.

Reproduced with permission of the copyright owner. Further reproduction prohibited without permission.

A review of proximate and distal nomological mechanisms responsible for craniofacial diversity (Chapter 2) revealed that only heritable (intrinsic genetic and epigenetic) morphogenetic control signals are associated with selectional change, whereas nonheritable (environmental) control signals are associated with acclimational change. Since only cytogenetic processes operating within species (i.e., recombination and crossing-over) are capable of disrupting correlations between characters attributable to selection, it follows that nomological mechanisms operating within species are qualitatively different from those operating between species (Bell, 1989). A multi-level model was thus developed, consistent with quantitative genetic analysis and interpretation, in which the total variation of a given trait (V-level) was partitioned into separate among-species (M-level) and pooled-within species (Q-level) components, in an attempt to distinguish selectional from acclimative effects on anthropoid nasomaxillary form.

To my knowledge, this particular approach has not been adopted in any previous craniometric analysis. Its efficacy is therefore unknown, and interpretation of the multi-level results with respect to nomological mechanisms should be viewed with caution. An integrated analytical approach was further developed (Chapter 8) that combines autoregression/ACP phylogenetic adjustment, taxon-specific multi-level nomological analysis, and covariance structural modeling.

Structural Growth Constraints

Nomological modeling of anthropoid nasomaxillary diversity began with an examination of structural growth constraints which are manifested as trait covariances among the delta-transformed variables. Growth data were calculated for

Reproduced with permission of the copyright owner. Further reproduction prohibited without permission.

selected characters by taking the difference between conspecific infant and adult (mean) measurements. Shape analyses of the ontogenetic data revealed several size-independent correlated growth processes or constraints (Box 9.15). They include: (1) changes in nasal bone length are structurally constrained by the degree of anterior facial elongation during growth; (2) changes in anterior facial length are associated with changes in facial rotation, such that these two growth events attain a compensatory equilibrium that maintains the orientation of the occlusal plane within functionally suitable limits; (3) changes in anterior facial length are associated with corresponding counterpart changes in maxillary arch length; (4) facial prognathism (Krogman's angle) is a structural manifestation of degree of facial rotation during growth; (5) the downward migration of the anterior face in relation to the Frankfort horizontal, in combination with facial rotation and nasal bone elongation, produces a displacement of the lower border of the nasals in relation to the lower orbital rim, thus determining the degree sagittal projection of the paranasal plates; (6) a pattern of craniofacial development characterized by differential upper and lower facial growth and remodeling structurally constrains both the degree of facial prognathism and facial convexity; (7) nasoalveolar clivus length is, in part, constrained by anterior palatal depth; (8) changes in posterior palatal depth are structurally constrained by growth-related changes in posterior facial height; (9) the slope of the occlusal plane is structurally and mechanically constrained to maintain an orientation at or close to 10° to the Frankfort horizontal; and, (10) the slope of the midfacial plane is constrained to maintain an angle of 90° to the plane of the

Reproduced with permission of the copyright owner. Further reproduction prohibited without permission.

cribriform plates. [2]

In addition to the preceding structural growth constraints, other well established patterns of facial growth were confirmed in the analysis, including the forward translocational rotation of the maxilla and the positive allometric growth of maxillary length to maxillary width.

Craniofacial Allometry

A somewhat unconventional approach to craniofacial allometry was advanced in Chapter 10. The conventional approach is to regress a linear character dimension (e.g., nasal bone length) on some cranial variable representing "size" (e.g., basicranial length). The slope of the regression line of the logged data is then taken to indicate whether "size" has an isometric or allometric effect on the character. Moreover, the regression R^2 is used to indicate the proportion of variance of the character that can be accounted for by "size," and the residuals are said to be "size-independent." In this approach, character values whose points fall on the regression line are considered to be fully explained by size. But as RJ Smith (1984) has pointed out, this does not constitute a valid explanation—why should "size," per se, affect craniofacial form in accordance with an allometric power function?

In Chapter 10, I advanced the argument that the solution lies in the realization that the concept of "size" embodies two distinct types: (1) $size_1$ (*stricto senso*) as a *measure of scale quantity* (e.g., volume, centroid size, geometric mean, general size), and (2) $size_2$ as a *scale-related quantity* (e.g., weight, surface area-to-volume ratio, basal metabolic rate). It was further argued that the effect of $size_1$

[2] The reader is also referred to Enlow (1990, Chapter 3), who has provided a comprehensive review of the correlated growth processes between the maxilla, mandible and cranial fossae.

Reproduced with permission of the copyright owner. Further reproduction prohibited without permission.

(e.g. centroid size) on a linear or shape variable will be such that isometry will be maintained, and that only scale-related quantities ($size_2$) will have an allometric effect on a morphometric character. I showed that empirically-derived allometric relationships between character variables and $size_1$ (in conventional analysis) are due to model misspecification: the omission of one or more relevant scale-related explanatory variables in the model. Moreover, it was shown that even a properly specified model (i.e., one that includes all relevant scale-related explanatory variables) will yield an allometric relationship between a character variable and $size_1$. This is because entering any additional terms to the standard allometric equation, whether a constant or one or more covariates, will transform a linear proportional relationship between a character variable and $size_1$ into an allometric relationship (see Boxes 10.2, 10.3 & 10.4). Such apparent allometric relationships are said to be *spurious*, in the same way that apparent correlations between variables can be spurious.

It is hypothesized that in a fully specified model the true relationship between a given character variable and $size_1$ will be that of isometry. For example, the observed allometric relationship between $size_1$ and cross-sectional long bone area will revert to isometry when the effects of weight ($size_2$) are incrementally removed from the data. Thus, it is not $size_1$ that has an allometric effect on cross-sectional long bone area, but weight ($size_2$). Likewise, observed allometric relationships between $size_1$ and craniofacial characters will revert to isometry when the effects of, say, endocranial volume ($size_2$) are removed from the data (i.e., when misspecification of the conventional allometric equation is corrected by

Reproduced with permission of the copyright owner. Further reproduction prohibited without permission.

incrementally removing the effects of relevant scale-related independent variables from the data).

Consistent with this approach is the Mosimann family of size-adjustment techniques, which removes that part of the variation of a trait due to isometric scaling (*cf.* Jungers et al., 1995). Moreover, the Mosimann log-log isometric regression technique was shown to be analytically consistent with the multi-level approach outlined in Chapter 8. Applied to the anthropoid craniometric data, the Mosimann procedure revealed that centroid size, as expected, accounted for a substantial proportion of the variance of most nasomaxillary traits (see Box 10.11). That portion of the variance which is unexplained by $size_1$, was examined in subsequent chapters to see if other causal agents, including scale-related quantities (i.e., $size_2$), could account for any of the remaining variance.

Brain Form and Nasomaxillary Morphology

Two scale-related quantities that can potentially affect nasomaxillary morphology are the shape and relative size of the brain.[3] Weidenreich's (1941) observation that larger mammals tend to have relatively smaller brains was confirmed for anthropoid primates. It was further shown that this negative allometric relationship between brain size and body size is much stronger in catarrhines than in platyrrhines. Weidenreich's (1941) hypothesis that relative brain size is the primary factor

---

[3] Brandt (1898), Anthony (1928), and Weidenreich (1941) provided a neurological explanation for the observed relationship between body size and brain size (see Chapter 11, p. 333). And, DuBrul and Laskin (1961) have argued that the relationship between body size and the shape of the brain is due to constraints imposed by parturition. The head of most fetal mammals is rounded because there is a need to fit "...the largest mass—the brain—into the smallest space—a sphere—within the restricting confines of the uterus" (DuBrul & Laskin, 1961:122). Once the head is clear of the birth canal the brain and the entire skull is free to elongate into its adult rectangular form.

Reproduced with permission of the copyright owner. Further reproduction prohibited without permission.

influencing craniofacial morphology in mammals cannot be rejected with respect to anthropoids. Specifically, it was shown that changes in relative brain size have a significant negative effect on changes to various nasomaxillary characters, including posterior facial angle (Box 11.14), facial prognathism (Box 11.25), maxillary arch length (Box 11.35), and posterior nasal aperture breadth (Box 15.6).

However, consistent with the hypotheses of Dabelow (1929), Biegert (1957), Huxley (1963), Weidenreich (1947), Enlow and McNamara (1973) and Enlow (1975), the current study confirmed that the effects of relative brain size on nasomaxillary morphology are mediated indirectly through changes to the chondrocranium. The best fit covariance structural model (Model II, Chapter 15) confirmed the hypothesis of Enlow and McNamara (1973) that cribriform plate orientation is the primary mediator between the development and evolution of the brain and nasomaxillary morphology. Multi-level analysis further indicated that changes in relative brain size and concomitant changes in cribriform plate orientation effect changes to nasomaxillary form through both acclimative and selective nomological processes. These results are consistent with current morphogenetic theory, which indicates that all three types of cellular control stimuli (intrinsic genetic, epigenetic and environmental) act to regulate morphogenesis of the viscerocranium and skeletogenesis of the chondrocranium (see Chapter 2).

The proposed invariant 90° angle between the cribriform plate and midfacial plane (see Enlow & McNamara, 1973), which translates changes in brain form to changes in facial growth vectors, was also confirmed for anthropoids. That this angle is biologically constrained was demonstrated using a regression-based test for angular invariance (Box 11.45). It was shown that although changes in cranial base

Reproduced with permission of the copyright owner. Further reproduction prohibited without permission.

angle can affect the orientation of the cribriform plate (especially in catarrhines), the latter has a strong and independent influence on nasomaxillary morphology. Covariance structural analysis indicated that cribriform plate orientation mainly effects changes in the nasomaxillary skeleton by influencing the degree of facial rotation during development (Box 15.13).

In Chapter 15, I reviewed some of the more recent clinical evidence indicating a close spatial, histological, and biochemical association between the anterior portion of the brain and the spheno-ethmoidal complex.

Olfaction and Nasomaxillary Morphology

Both the 'arboreal' (Smith, 1912; Jones, 1916) and the 'visual predation' (Cartmill, 1972) hypotheses of primate evolution maintain that a reduction of olfactory acuity resulted in a diminished size of the nasomaxillary complex. However, *if cribriform plate area is an accurate proxy for olfactory bulb size*, then this postulate can be rejected—*increased* olfactory acuity was found to be associated with a *reduction* of nasomaxillary size. On the other hand, relative olfactory bulb size appears to have a significant positive effect on various measures of craniofacial breadth, including nasal process of maxilla width, posterior nasal aperture breadth, upper facial breadth, and especially, interorbital breadth.

It was subsequently revealed that olfactory bulb size does not scale isometrically with brain size (Box 12.10). Anthropoids with larger brains tend to have relatively smaller olfactory bulbs; which means that small-bodied anthropoids tend to have both relatively larger brains and relatively larger olfactory bulbs compared to large-bodied anthropoids (Boxes 12.11 & 12.12). The observed

Reproduced with permission of the copyright owner. Further reproduction prohibited without permission.

negative relationship between body size and olfactory acuity may result from a common relationship with diet (*cf.* Barton, *et al.*, 1995). Gumnivores and insectivores exhibit a high degree of olfactory acuity and tend to be small-bodied, whereas gramnivores, hard food specialists and omnivores all exhibit a low degree of olfactory acuity and tend to be large-bodied (Box 12.16).

Locomotion and Nasomaxillary Morphology

Despite some early comparative work suggesting a causal link between the position of the foramen magnum and craniofacial morphology (e.g., Huxely, 1896), and experimental results indicating that changes in locomotor behavior can affect cranial form (e.g., Moss, 1961), I found no evidence to suggest that mode of locomotion has an effect on craniofacial morphology among anthropoid primates. In fact, the analysis showed no clear correspondence between locomotor behavior and foramen magnum position or slope, with the exception that bipedality was associated with a more anteriorly placed, horizontally oriented, foramen magnum (Boxes 13.7 & 13.8). But caution must be exercised even here. Several species, such as *Saimiri sciureus* (see Box 4.15) and *Callimico goeldii* (see Box 4.19), display anteriorly placed foramina approaching the human condition (see Box 13.6), yet exhibit no bipedal behavior.

Both of these species, however, exhibit large brains relative to body size and extensive cranial base flexion, properties shown to have an independent effect on the disposition of the foramen magnum (see Boxes 13.23 & 15.12). Anthropoids with relatively large brains and flexed cranial bases tend to have a foramen magnum that is anteriorly placed. The analysis further indicated that increased relative brain size

Reproduced with permission of the copyright owner. Further reproduction prohibited without permission.

affects foramen magnum disposition through both selectional and acclimational mechanisms (see Box 15.6).

The observed association between the disposition of the foramen magnum and various features of the face, first reported by Huxley (1896) and Bolk (1915) and confirmed here for anthropoids (see Box 13.14), is shown to be due to the common influence of the cranial base.

Diet, Mastication and Nasomaxillary Morphology

A model of the effects of diet and mastication on nasomaxillary form was presented in Chapter 14 (Box 14.1). In accordance with the morphogenetic theory outlined in Chapter 2, this model distinguished acclimational from selectional nomological mechanisms, and incorporated intrinsic, epigenetic and environmental sources of cellular control. A classification of research methods pertaining to mastication-related morphology was developed to facilitate a review of the relevant literature. Eight types of research methods were identified—four research approaches, each with a nonexperimental (A) and experimental (B) design mode (Box 14.2). The four research approaches included: (I) analysis of dietary effects on craniofacial form, (II) study of the effects due to occlusal forces, (III) analysis of craniofacial strain patterns, and (IV) analysis of mechanical properties. Types IA, IIA, and IVA were employed in the present research. The analysis required the estimation of maximum bite force (MBF) magnitudes along the tooth row. A modified version of Greaves' (1978) three-dimensional 'triangle of support' model of mastication was applied to the anthropoid craniometric data in order to calculate MBF.

Reproduced with permission of the copyright owner. Further reproduction prohibited without permission.

Several variables related to anthropoid diets were constructed from data obtained from the behavioral ecology literature. These included: hardness of food items consumed, percent food types consumed, and dietary categories. Morphogenetic theory predicts that anthropoid nasomaxillary morphology will change (via both acclimation and selection) in response to changes in the "hardness" of food items consumed. That no such correspondence was found may be due to the low accuracy of the "hardness" variable, rather than an absence of such an effect. M-level multiple regression of percent food types eaten against masticatory properties indicated that (1) percent exudates in the diet is significantly associated with increased anterior-to-posterior bite force ratio, and (2) percent consumption of insects is associated with increased load-to-lever arm ratio.

Several differences in the properties of the masticatory apparatus were found among anthropoids with different diets. Absolute maximum bite force was found to be greatest in hard object feeders, and species that consume considerable fruit. Anterior bite force to posterior bite force ratio was greatest in gumnivores and omnivores, as was the anterior attachment of the masticatory adductor muscles. Insectivores showed the greatest mechanical lever efficiency of the masticatory apparatus. Finally, hard object feeders had significantly greater masticatory muscle mass compared to gumnivores, but this difference is likely due to the smaller absolute body size of the latter.

Covariance structure analysis Model II (Chapter 15) revealed several significant associations between maximum bite force magnitude and nasomaxillary form among anthropoids. Several path relationships were found to be consistent across major anthropoid groups. These include: (1) an increase in anterior

Reproduced with permission of the copyright owner. Further reproduction prohibited without permission.

maximum bite force (MBF) is associated with an acclimational decrease in anterior nasal aperture breadth, whereas an increase in posterior MBF is associated with an acclimational increase in anterior nasal aperture breadth, (2) selection for increased anterior MBF is associated with more anteriorly placed zygomatic roots, (3) selection for, and acclimation to, increased anterior MBF is associated with decreased maxillary arch length; whereas, selection for, and acclimation to, increased posterior MBF is associated with increased maxillary arch length, (4) an increase in anterior MBF is associated with an acclimational decrease in upper facial breadth, whereas an increase in posterior MBF is associated with an acclimational increase in upper facial breadth, (5) selection for, and acclimation to, increased anterior MBF is associated with increased inter-M^3 palatal width; whereas, selection for, and acclimation to, increased posterior MBF is associated with decreased inter-M^3 palatal width, (6) selection for increased anterior MBF is associated with decreased palatal depth at I^2, (7) increased posterior MBF is associated with an acclimational increase in facial prognathism (Krogman's angle), and (8) temporalis muscle mass accounts for nearly half of the size-adjusted variance in bizygomatic breadth among anthropoids.

Selection for increased anterior bite force and acclimational response to masticatory muscle pull help explain the anterior migration of the zygomatic root in some anthropoids (e.g. *P. melalophos*). Selection for, and acclimation to, particular bite force patterns also account for a significant proportion of the size-adjusted variance of maxillary arch length and width (see Box 15.6). In general, an increase in anterior bite force magnitude is associated with a shorter, wider palate and

Reproduced with permission of the copyright owner. Further reproduction prohibited without permission.

orthognathic face; whereas an increase in posterior bite force is associated with a longer, narrower palate, and prognathic face.

Several of the findings above contradict those of earlier studies. For example, in previous experiments animals fed a soft food diet showed a reduction of maxillary breadth compared to controls. This finding appears to conflict with the results of the current analysis of the Q-level data which indicates that decreased maximum bite force *at the posterior dentition* is associated with a widening of the maxillary arch. However, decreased maximum bite force *at the anterior dentition* is associated with a narrowing of the maxillary arch. Perhaps the animals on which these experiments were conducted experienced a greater reduction of bite force on the anterior teeth with the introduction of a soft food diet, thus leading to a narrowing of the palate.

It was further shown that maximum bite force magnitudes scaled isometrically with centroid size for the incisors and premolars, but increased with negative allometry for the molars. In fact, this is another example of spurious allometry—increased body size is not *causing* exponentially smaller molar bite force magnitudes. Rather, the allometric relationship is due to the effects of a scale-related quantity—masticatory muscle mass. Increases in masticatory muscle mass do not quite keep pace with increases in body size, but are proportional to increases in molar MBF magnitudes (see Box 14.11).

Several hypotheses were advanced to explain characteristics of the dental arcade and dentition of anthropoids. For instance, the para-elliptical shape of the dental arcade in many anthropoid species (see Boxes 4.5-4.41) can be explained as an adaptation to increase maximum bite force at each tooth along the tooth row (see

Reproduced with permission of the copyright owner. Further reproduction prohibited without permission.

Box 14.5, F). Likewise, the relative sizes of the molar teeth along the tooth row roughly coincide with MBF magnitudes, as estimated by the 'triangle of support' model of mastication (see Box 14.9).

B. Applications

The primary applications of the research findings obtained in this study will be in the fields of anthropoid craniofacial biology, primate systematics, and paleobiology. A few brief examples are discussed below.

Anthropoid Craniofacial Biology: Why Do Baboons Have Such Long Snouts?

The extreme projection of the muzzle in baboons has been a persistent enigma in primate craniofacial morphology. There is little evidence that the extreme length of the snout is a mechanical adaptation related to mastication. Oyen, Walker and Rice (1979) have shown that in the olive baboon mechanical efficiency decreases dramatically during growth as the palate increases in length. Nor does an elongated muzzle appear to play much of a role in food procurement and preparation. Moreover, the olfactory acuity of *P. hamadryas* ranks low compared to other anthropoids, and I have found no reference in the literature to suggest any special olfactory behavior in this species.

Swindler, Sirianni and Tarrant (1973) found that *P. hamadryas cynocephalus* and *Macaca nemestrina* follow a similar growth trajectory, suggesting that the facial profile of the former is simply an allometrically scaled version of the latter. However, as I have argued in Chapter 10, the mere description of size allometry does not in itself constitute an explanation of form. In accordance with the concepts outlined in this study, it is hypothesized that relative brain size (a scale-related

Reproduced with permission of the copyright owner. Further reproduction prohibited without permission.

quantity) is responsible for the observed allometric relationship between body size and maxillary arch length among anthropoids. It can be seen with reference to the scatter plots in Boxes 16.1 and 16.2 that while the regression line of maxillary arch length on centroid size passes through the middle of the cluster of *P. hamadryas* points (Box 16.1), the same is true for relative brain size (Box 16.2).

An examination of the residuals (unexplained variance) from the covariance structural analysis in Chapter 15 shows that Model II also explains maxillary arch length in *P. hamadryas* quite well. Box 16.3 contains the residual-by-predicted plot for the full model (Model II). To isolate the effects of the non-masticatory variables, a residual-by-predicted plot produced using the same model but with maximum bite force variables removed is presented in Box 16.4. In both of these residual plots the prediction line passes close to the mean maxillary arch length for *P. hamadryas* (although in the full model, Box 16.3, the residual scores have a reduced variance).

The foregoing analysis demonstrates that the length of the palate in *Papio hamadryas* is close to what would be expected for a cercopithecoid primate of similar relative brain size and masticatory function.

Reproduced with permission of the copyright owner. Further reproduction prohibited without permission.

Box 16.1. Scatter plot and regression lines of log delta maxillary arch length [ΔL_YV14] against log delta centroid size [ΔL_YV41 (V-level data, n=300) Solid regression line=cercopithecoids; dotted regression line=platyrrhines

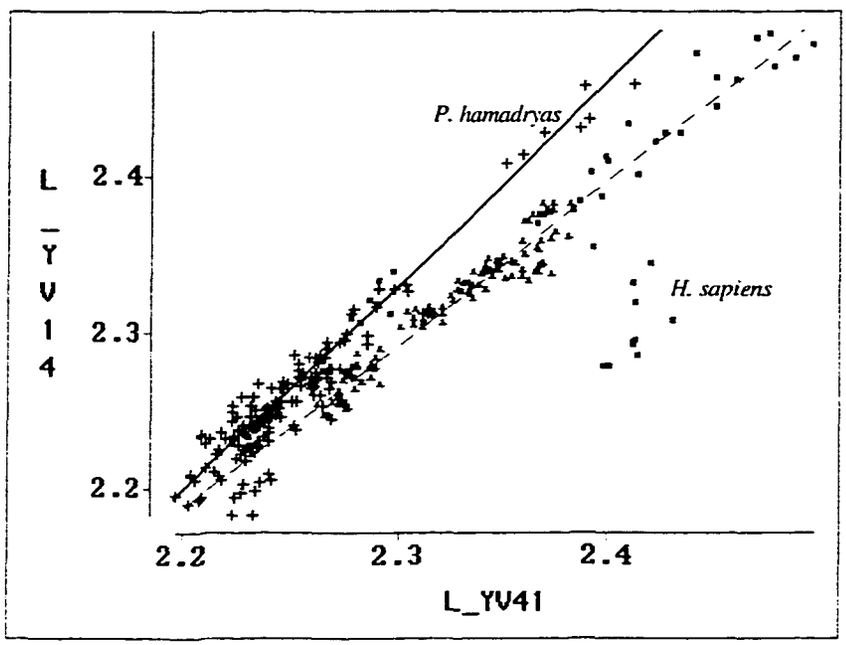

Box 16.2. Scatter plot and regression line of log delta relative maxillary arch length [ΔS_L_YV14] against log delta relative endocranial volume [ΔS_L_YV84] (V-level data; cercopithecoids only; n=137)

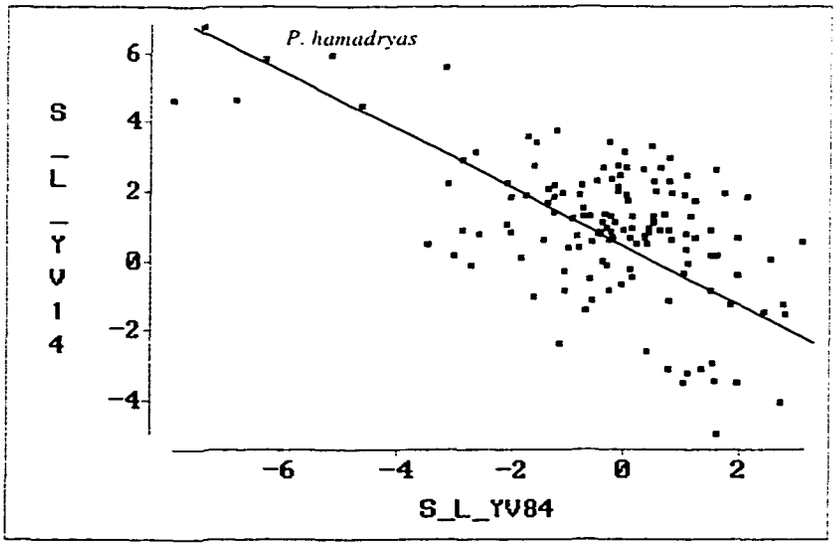

Reproduced with permission of the copyright owner. Further reproduction prohibited without permission.

Box 16.3. Residual-by-predicted plot for log delta relative maxillary arch length [ΔS_L_YV14] based on CSA full Model II (V-level data; cercopithecoids only; n=137)

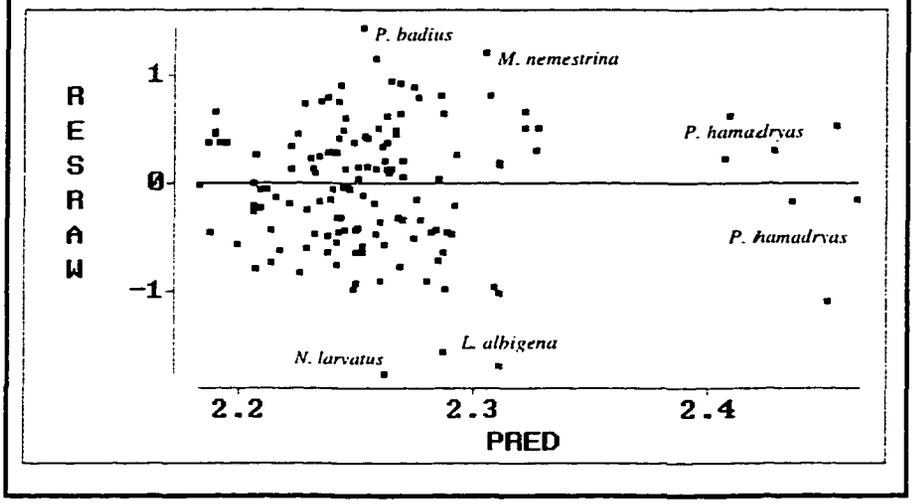

Box 16.4. Residual-by-predicted plot for log delta relative maxillary arch length [ΔS_L_YV14] based on CSA Model II with masticatory explanatory variables removed from the model (V-level data; cercopithecoids only; n=137)

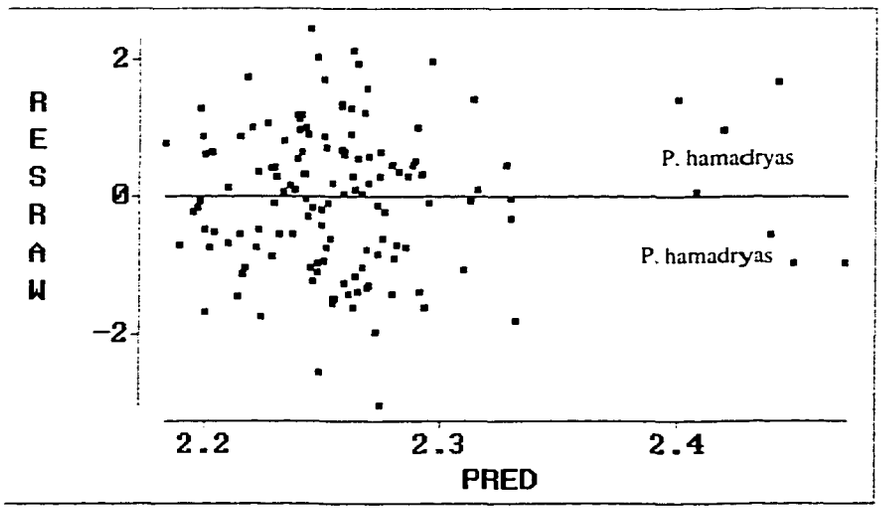

Reproduced with permission of the copyright owner. Further reproduction prohibited without permission.

Anthropoid Systematics

By quantifying the 'non-phylogenetic' or 'non-topological' nomological determinants of craniofacial form, this study contributes important information to the field of primate systematics. Phylogenetic hypotheses are based on assumptions of character homology (features that are similar due to inheritance from a common ancestor). In practice, tests of specific homology hypotheses are based on the comparison of numerous processes operating at different levels (e.g., histological, functional, historical). One important consideration is the likelihood that a feature is shared, not because of inheritance from a common ancestor, but because of the occurrence of similar adaptive responses to, or convergence involving, one or more biological roles (i.e., the shared feature is a homoplasy). As Szalay and Delson (1979) have noted: "Unique and special similarities which are judged unlikely to be convergent are hypothesized to be homologues of each other" (p. 561). Therefore, by providing evidence that specific character similarities across species are due to nomological processes, alternative explanations to homology are given for consideration.

Strasser and Delson (1987) provide a good example. In their cladistic analysis of cercopithecid relationships, these authors list 8 shared derived character states that describe the cercopithecine clade. The 8 traits are assumed to be independent in their analysis. The present study has shown, however, that 4 of the 8 traits—long nasal bone length, narrow interorbital distance, low cranial vault height, and long facial length—form part of an interrelated complex of characters that relate to body size and relative brain size. At the very least, these characters should be

Reproduced with permission of the copyright owner. Further reproduction prohibited without permission.

combined into a single 'feature' in the analysis (see Andrews & Martin, 1987). Shoshani *et al.* (1996), in a cladistic analysis of primates, recognized the interrelated nature of these characters by including facial length, nasal bone length, and interorbital distance into a single feature called "facial elongation" (p. 130). But these authors did not recognize that "muzzle length," and "braincase size" are also part of the same complex (also see Fleagle & Rosenberger, 1983, p. 145).

Similarities in these characters are more likely the result of nomological mechanisms involving relative brain size, than the *independent* historical inheritance of each character trait from a common ancestor. In fact, Strasser and Delson (1987) acknowledged that the character "facial length" is "probably of low phyletic value" (p. 94). But if this is true of facial length, then it is also true of the other related characters in the complex.

Anthropoid Paleobiology

Interpretation of the functional significance and associated biological roles of particular features of the skull of extinct anthropoids is drawn by analogy with living forms. Understanding the nomological agents and mechanisms responsible for craniofacial variation in extant species is thus essential to the paleobiological study of fossil specimens. No attempt will be made here to critically review earlier paleobiological interpretations in light of the present research findings (the size of the current study has already exceeded Mitchnerian proportions). Suffice it to say that the majority of paleobiological interpretations of extinct anthropoid nasomaxillary forms are explained in terms of a particular model of masticatory function (e.g., Miocene hominoids: Andrews & Martin, 1991, Schwartz & Conroy,

Reproduced with permission of the copyright owner. Further reproduction prohibited without permission.

1996; classic Neanderthals: Rak, 1986, Demes, 1987, Trinkaus, 1987, Spencer & Demes, 1993; early hominids: DuBrul, 1977, Ward & Molnar, 1980, Rak, 1983, Osborn, 1987) (also see Dumont, 1997).

While it is clear that trophic nomological agents play an important role in the development and evolution of specific craniofacial features, it is equally apparent from the results of this study that other nomological agents, such as craniofacial growth constraints, relative brain size and shape, and basicranial morphology, have an impact on all aspects of nasomaxillary form among the Higher Primates.

C. Final Remarks

It has always surprised me that the comparative method, which was originally developed for use in astronomy and celestial dynamics, and later adopted for use in behavioral and clinical research (to show, for example, that smoking causes cancer), has not gained wider acceptance in biology.[4] Clearly, there are obstacles unique to comparative analysis that must be addressed when sampling across taxa. While some of these obstacles are indeed formidable (for instance, the problem of data nonindependence and the confounding nature of size) they are not insurmountable. While comparative research is the most suitable design for testing hypotheses regarding evolutionary nomological agents and mechanisms, an alliance of experimental and nonexperimental research provides the most powerful and comprehensive approach to the study of biological diversity.

I have attempted to show that by adopting an integrated comparative approach to the study of morphological diversity, meaningful results can be attained.

Reproduced with permission of the copyright owner. Further reproduction prohibited without permission.

Obviously, there is much room for improvement. Future work will benefit greatly by incorporating fossil specimens into the M-level component of the data, and ontogenetic samples into the Q-level component. More detailed quantitative modeling of morphological features (especially those related to the shape of the brain and the morphology of the chondrocranium) is needed. This may be realized sooner rather than later, given recent advances and availability of medical imaging and image analysis technology. Combined with new ways to quantify organic form and form-change (i.e., geometric morphometrics) such developments will permit the various hypotheses examined here to be further refined and tested.

This study underscores the complexity of the nomological agents and mechanisms involved in the production of nasomaxillary diversity among vertebrates, in general, and anthropoid, in particular. Unifactorial explanations of anthropoid craniofacial morphology should be viewed with skepticism. The current research indicates that multiple nomological causal agents (primarily those related to structural growth constraints, body size, brain form, chondrocranial development, and mastication) interact, integrate, and operate via distal causal mechanisms to influence nasomaxillary form. These processes and the effects they produce are constrained by boundary conditions set by taxon-specific genetic, epigenetic and environmental landscapes, and the interaction among them.

---

[4] An anonymous reviewer of a grant proposal seeking support for this work wrote something to this effect: "So you collect a bunch of data on a bunch of skulls and find a bunch of correlations. So what?"

Reproduced with permission of the copyright owner. Further reproduction prohibited without permission.

PART VII

Appendices and Bibliography

Reproduced with permission of the copyright owner. Further reproduction prohibited without permission.

APPENDIX A: Anatomical Landmarks

No	Label	Landmark name and description
1	LLFORM	lat.-most foramen magnum margin
2	LPORIO	**porion, left**: outer upper margin of the external auditory canal
3	LSGLEN	**condylion, left**: estimated as the sup.-most point of the glenoid fossa
4	LPITFN	post.-most point of infratemporal foramen
5	LAITFN	ant.-most point of infratemporal foramen
6	LLITFN	**endozygion, left**: lat.-most point of infratemporal foramen
7	LMITFN	med.-most point of infratemporal foramen
8	LZYGMX	**zygomaxillare, left**: inf.-most point of zygomaxillary suture
9	LIZYGT	**zygotemporale, left**: inf.-most zygomatico-temporal suture
10	LLBRAC	**euryon, left**: lat.-most point on brain case
11	LZYGOR	**zygoorbitale, left**: zygomaxillary suture at inf. orbital margin
12	LATEMP	**frontotemporale, left**: ant.-most temporal line
13	LZYGMF	**zygofrontale, left**: zygomaticofrontal suture at orbital margin
14	LSORBM	**supraorbitale, left**: sup.-most point along superior orbital margin
15	LDACRY	**dacryon, left**: point of junction of the frontal, lacrimal and maxillary bones
16	LORBIT	**orbitale, left**: inf.-most point on orbital margin
17	LACONE	**orbital cone, left**: apex of cone-shaped orbit (post.-most point of superior orbital fissure)
18	LSORBF	sup.-most extent of the inferior orbital fissure (*superior* maxillary tuberosity)
19	LNMSNA	**nasomaxillare, left**: nasomaxillary suture at nasal aperture margin
20	LLALAR	**alare, left**: lat.-most point of nasal aperture
21	LFMNRE	**maxillofrontale, left**: sutural junction of the maxilla, frontal, and nasal bones
22	LZROOT	**zygomatic root, left**: inferior base of the attachment of the zygomatic process to the maxilla
23	LP3OCC	**P^3 mid-occlusal surface, left**:
24	LM3OCC	**M^3 mid-occlusal surface, left**: sup.-most point of the trigon basin
25	LMI2AJ	**I^2 endomolare, left**: med.-most I^2 alveolar junction
26	LMP3AJ	**P^3 endomolare, left**: med.-most P^3 alveolar junction
27	LMM1AJ	**M^1 endomolare, left**: med.-most M^1 alveolar junction
28	LMM3AJ	**M^3 endomolare, left**: med.-most M^3 alveolar junction
29	LMAXTB	**maxillary tuberosity, left**: post.-most point along alveolar surface behind distal molar
30	LLMPTP	lat.-most point on medial pterygoid plate
31	MNASLF	**nasal floor**: point on nasal floor just left of nasal septum between left and right M1s
32	RLFORM	lat.-most foramen magnum margin,
33	RPORIO	**porion, right**
34	RSGLEN	**condylion, right**
35	RPITFN	post.-most point of infratemporal foramen
36	RAITFN	ant.-most point of infratemporal foramen
37	RLITFN	**endozygion, right**
38	RMITFN	med.-most point of infratemporal foramen
39	RZYGMX	**zygo-maxillare, right**
40	RIZYGT	**zygo-temporale, right**
41	RLBRAC	**euryon, right**
42	RZYGOR	**zygo-orbitale, right**
43	RATEMP	**fronto-temporale, right**

Reproduced with permission of the copyright owner. Further reproduction prohibited without permission.

No	Label	Landmark name and description
44	RZYGMF	**zygo-frontale, right**
45	RSORBM	**supraorbitale, right**
46	RDACRY	**dacryon, right**
47	RORBIT	**orbitale, right**
48	RACONE	**orbital cone, right**
49	RSORBF	sup.-most extent of the superior orbital fissure
50	RNMSNA	**nasomaxillare, right**
51	RLALAR	**alare, right**
52	RFMNRE	**maxillofrontale, right**
53	RZROOT	**zygomatic root, left**
54	RP3OCC	**P^3 mid-occlusal surface, right**
55	RM3OCC	**M^3 mid-occlusal surface, right**
56	RMI2AJ	**I^2 endomolare, right**: med.-most I^2 alveolar junction
57	RMP3AJ	**P^3 endomolare, right**: med.-most P^3 alveolar junction
58	RMM1AJ	**M^1 endomolare, right**: med.-most M^1 alveolar junction
59	RMM3AJ	**M^3 endomolare, right**: med.-most M^3 alveolar junction
60	RMAXTB	***maxillary tuberosity, right***
61	RLMPTP	lat.-most point on medial pterygoid plate
62	RI1OCC	**I^1 occlusal surface, right**: mid-point of the wear facet
63	RI2OCC	**I2 occlusal surface, right**: mid-point of the wear facel
64	RP4OCC	**P4 occlusal surface, right**:
65	RM1OCC	**M1 occlusal surface, right**: sup.-most point of the trigon basin
66	RM2OCC	**M2 occlusal surface, right**: sup.-most point of the trigon basin
67	MPROST	**prosthion**: tip of the alveolar portion of the (pre)maxilla between the upper central incisors
68	MSBNAS	**nasospinale**: inf.-most point of nasal aperture at midline
69	MRHINI	**rhinion**: anteroinferior-most extent of the internasal suture
70	MNASIO	**nasion**: intersection of the frontal and internasal sutures
71	MGLABE	**glabella**: most prominent point along the midline between superior orbital margins
72	MBREGM	**bregma**: intersection of the coronal and sagittal sutures
73	MLAMBD	**lambda**: intersection of the sagittal and lambdoidal sutures
74	MOPISC	**opisthocranion**: post.-most point of cranium along midline in Frankfort horizontal
75	MINION	**inion**: center point of the external occipital protuberance
76	MOPIST	**opisthion**: post.-most point on the internal margin of the foramen magnum at midline
77	MBASIO	**endobasion**: ant.-most point on the internal margin of the foramen magnum at midline
78	MSPHBA	**sphenobasion**: spheno-occipital synchondrosis at midline
79	MHORMI	**hormion**: point on sphenoid bone at midline where left and right alae of vomer converge
80	MSTAPH	**staphylion**: intersection of line connecting ant.-most incurves of palatine bones and midline
81	MPALM3	point on palate midline between left and right M^3
82	MPALM1	point on palate midline between left and right M^1
83	MPALP3	point on palate midline between left and right P^3
84	MPALI2	point on palate midline between left and right I^2
85	LIOCCD	inf.-most point on occipital condyle, left
86	RIOCCD	inf.-most point on occipital condyle, right
87	LSZYGT	sup.-most zygomatico-temporal suture, left

Reproduced with permission of the copyright owner. Further reproduction prohibited without permission.

No	Label	Landmark name and description
88	RSZYGT	sup.-most zygomatico-temporal suture, right
89	RMASTO	center of origin of masseter along zygomatic arch, right
90	CRTIP	tip of right canine
91	CRMESO	mesial-most extent of right canine at alveolar border
92	CRDIST	distal-most extent of right canine at alveolar border
93	CRBUCO	buccal-most extent of right canine at alveolar border
94	CRLING	lingual-most extent of right canine at alveolar border
95	JLCORO	**coronoidale, left**: sup.-most point of the coronoid process
96	JLGONI	**gonion, left**: point of maximum curvature of the mandibular angle
97	JRCORO	**coronoidale, right**
98	JRGONI	**gonion, right**
99	LMASTO	center of origin of masseter along zygomatic arch
100	XENLBR	Enlow's "anterior-most brain"
101	XSELLA	**sella**: center of hypophyseal fossa as seen in lateral cephalogram
102	XANTMP	anterior-most temporal lobe
103	XPOSBR	posterior-most brain
104	XANTBR	anterior-most brain in Frankfort horizontal
105	XACRIB	ant.-most cribriform plate
106	XPCRIB	post.-most cribriform plate
107	XAOLFA	ant.-most point of olfactory fissure from anterior cranial fossa
108	XPOLFA	post.-most point of olfactory fissure from anterior cranial fossa
109	XENDBR	endobregma
110	XBREGM	bregma
111	XPROST	prosthion
112	XLAMBD	lambda
113	XPORIO	porion

Reproduced with permission of the copyright owner. Further reproduction prohibited without permission.

Reproduced with permission of the copyright owner. Further reproduction prohibited without permission.

APPENDIX B: Variable list and description

	Individual Landmark-based Y Variables	Dimensions	Quant	Description
1	Nasal bone length (NASLGT)	xyz	mm	Nasion [70] to rhinion [69]
2	Upper nasal bone width (NASWDU)	y	mm	Left frontomaxillonasal junction [21] to right frontomaxillonasal junction [52]
3	Lower nasal bone width (NASWDL)	y	mm	Left nasomaxillare [19] to right nasomaxillare [50]
4	Nasal process of maxilla width (NPMWDT)	xyz	mm	Avg. two distances: left dacryon [15] to left frontomaxillonasal junction [21]; and right dacryon [46] to right frontomaxillonasal junction [52]
5	Nasal aperture height (NSLAHT)	xyz	mm	Rhinion [69] to subnasale [68]
6	Nasal aperture breadth (NSLAWD)	xyz	mm	Left alare [20] to right alare [51]
7	Posterior nasal aperture height (PNASHT)	xyz	mm	Staphylion [80] to hormion [79]
8	Posterior nasal aperture breadth (PNASWD)	xyz	mm	Lat.-most pterygoid plate left [30] to lat.-most pterygoid plate right [61]
9	Nasoalveolar clivus length (NLCLGT)	xyz	mm	Subnasale [68] to prosthion [67]
10	Zygomatic estimated area (ZYGARE)	xyz	mm^2	Avg. of left and right zygomatic bone estimated surface area: if zygomatic is modeled as a rhomboid the area equals: .5 x (zygo-orbitale [11, 42] to inf.-most zygomatico-temporal suture [9, 40] x zygomaticofrontal suture at orbital margin [13, 44]) to zygomaxillare [8, 39])
11	Zygoma height (ZYGOHT)	xz	mm	Avg. of two distances: left zygo-orbitale [11] to left zygomaxillare [8]; and, right zygo-orbitale [42] to right zygomaxillare [39]
12	Bizygomatic breadth (BZYGWD)	xyz	mm	Left inf.-most zygomatico-temporal suture [9] to right inf.-most zygomatico-temporal suture [40]
13	Anteroposterior position of zygomatic root (APZYGR)	xz	percent	Average of two percentages: (a) (left zygomatic root [22] to left condylion [3]) / (left condylion [4] to prosthion [67]); and, (b) (right zygomatic root [53] to right condylion [34]) / (right condylion [34] to prosthion [67]) (Mastication)
14	Maxillary arch length (MXARCL)	xz	mm	Prosthion [67] to alveolon [constructed]
15	Bimaxillary breadth (BMAXWD)	xyz	mm	Left zygomaxillare [8] to right zygomaxillare [39]

Reproduced with permission of the copyright owner. Further reproduction prohibited without permission.

	Individual Landmark-based Y Variables	Dimensions	Quant	Description
16	Upper facial breadth (UMAXWD)	xyz	mm	Left zygomaticofrontal suture at orbital margin [13] to right zygomaticofrontal suture at orbital margin [44]
17	Anterior facial length (AFACHT)	xyz	mm	Nasion [70] to prosthion [67]
18	Posterior facial height (PFACHT)	xyz	mm	Avg. of two distances: Left maxillary tuberosity [29] to sup.-most extent of the inferior orbital fissure [18]; and, right maxillary tuberosity [60] to right sup.-most extent of the inferior orbital fissure [49]
19	Ramus height (RAMSHT)	xz	mm	Avg. of two distances: Left condylion [3] to occlusal plane (perp. to occlusal plane) [constructed]; and, right condylion [34] to occlusal plane (perp. to occlusal plane) [constructed]
20	Inter-I2 palatal width (I2PALW)	y	mm	Left med.-most point on I2 alveolar junction [25] to right med.-most point on I2 alveolar junction [56]
21	Inter-P3 palatal width (P3PALW)	y	mm	Left med.-most point on P3 alveolar junction [26] to right med.-most point on P3 alveolar junction [57]
22	Inter M1 palatal width (M1PALW)	y	mm	Left med.-most point on M1 alveolar junction [27] to right med.-most point on M1 alveolar junction [58]
23	Inter M3 palatal width M3PALW)	y	mm	Left med.-most point on M3 alveolar junction [28] to right med.-most point on M3 alveolar junction [59]
24	Palatal depth at I2 (I2PALD)	xz	mm	Palate midline at I2 [84] to midline intersection of I2-I2 alveolar junction [constructed]
25	Palatal depth at P3 (P3PALD)	xz	mm	Palate midline at P3 [83] to midline intersection of P3-P3 alveolar junction [constructed]
26	Palatal depth at M1 (M1PALD)	xz	mm	Palate midline at M1 [82] to midline intersection of M1-M1 alveolar junction [constructed]
27	Palatal depth at M3 (M3PALD)	xz	mm	Palate midline at M3 [81] to midline intersection of M3-M3 alveolar junction [constructed]
28	Palate length (PALLGT)	xz	mm	Prosthion [67] to staphylion [80]
29	Palatal thickness at M1 (PALTHK)	xz	mm	Line perpendicular to M3 palatal midline [81] and M1 palatal midline [82] to nasal floor [31]

	Individual Landmark-based Y Variables	Dimensions	Quant	Description
30	Krogman's angle of facial prognathism (KROGAG)	xz	degrees (angle)	Angle of two lines: (a) nasion [70] to prosthion [67], and (b) porion [2, 33] to orbitale [16, 47]
31	Enlow's angle of facial prognathism (ENLOAG)	xz	degrees (angle)	Angle of two lines: (a) ant. brain [100] to prosthion [67], and (b) maxillary tuberosity [29, 60] to prosthion [67]
32	Occlusal plane (SLOPOC)	xz	degrees (angle)	Angle of two lines: (a) occlusal surface of P3 [23, 54] to occlusal surface of M3 [24,55], and (b) porion [2, 33] to orbitale [16, 47]
33	Facial convexity (FACCNV)	xz	index	Ratio of (a) line perpendicular to nasion-prosthion through rhionion and, (b) nasion-prosthion (expressed as a percent); positive values indicate a convex facial shape, whereas negative values indicate a concave facial shape
34	Facial size (FACSIZ)	xyz	mm	Centroid size of facial landmarks 8, 11, 13, 14, 15, 17, 19, 20, 22, 25, 26, 27, 28, 29, 39, 42, 44, 45, 46, 48, 50, 51, 53, 56, 57, 58, 59, 60, 67, 68, 69, 70, and 80
35	Paranasal plate orientation (PPNALO)	xy	degrees (angle)	Average of left and right angles: angle of bizygo-orbitale line [11, 42] and left zygo-orbitale [11] to naso(pre)maxillary suture at nasal aperture margin [19]

Reproduced with permission of the copyright owner. Further reproduction prohibited without permission.

Reproduced with permission of the copyright owner. Further reproduction prohibited without permission.

	Individual Landmark-based X Variables	Dimensions	Quant	Description (Hypothesis)
36	Orbital height (ORBIHT)	xyz	mm	Avg. of two distances: left orbitale [16] to left sup.-most point along superior orbital margin [14]; and, right orbitale [47] to left sup.-most point along superior orbital margin [45] (Body Size)
37	Cranial length (CRLGTH)	xyz	mm	Prosthion [67] to opisthicranion [74] (Body Size)
38	Neurocranial length (NCLGTH)	xyz	mm	Glabella [71] to opisthicranion [74] (Body Size)
39	Basicranial length (BCLGTH)	xyz	mm	Nasion [70] to basion [77] (Body Size)
40	Biporionic breadth (BIPORB)	xyz	mm	Left porion [2] to right porion [33] (Body Size)
41	Skull centroid size (SKCNTR)	xyz	mm	Mean distance from each landmark to skull centroid [constructed] (Body Size)
42	Cranial bone thickness (CRBTHK)	xz	mm	Bregma [72] to endobregma [109] (Body Size)
43	Olfactory bulb (recess) volume (OFBVOL)	xyz	mm^3	((Length of perpendicular to ant. and post.-most points of olfactory junction [107, 108] x (length from ant.-most point of cribriform plate [105] to post.-most point of cribriform plate [106] + ant.-most point of olfactory junction [107] to post.-most point of olfactory junction [108]))/2) x (left dacryon [15] to right dacryon [46]) (Olfaction)
44	Olfactory bulb area (OFBARE)	xyz	mm^2	(((Ant.-most point of cribriform plate [105] to post.-most point of cribriform plate [106])+(ant.-most point of olfactory junction [107] to post.-most point of olfactory junction [108]))/2) x (left dacryon [15] to right dacryon [46]) (Olfaction)
45	Orbital sagittal-coronal rotation (orbital parallelism) (ORBSCR)	xy	degrees (angle)	Angle between two lines: (a) left orbital margin midpoint [constructed] to left orbital cone vertex [17]; (b) right orbital margin midpoint [constructed] to right orbital cone vertex [48] (Olfaction)
46	Orbital transverse-coronal rotation I (orbital deflection) (ORBTC1)	xz	degrees (angle)	Angle between two lines: (a) avg. left and right orbital margin midpoint [constructed] to avg. left and right orbital cone vertex [17, 48] (b) porion [2, 33] to orbitale [16, 47] (Olfaction)
47	Orbital transverse-coronal rotation II (ORBTC2)	xz	degrees (angle)	Angle between two lines: (a) orbitale [16, 47] to sup.-most point on orbital margin [14, 45] (b) porion [2, 33] to orbitale [16, 47] (Olfaction)

Reproduced with permission of the copyright owner. Further reproduction prohibited without permission.

	Individual Landmark-based X Variables	Dimensions	Quant	Description (Hypothesis)
48	Angle of orbital TC rotations (ORBA12)	xz	degrees (angle)	Angle between two lines: (a) orbitale [16, 47] to sup.-most point on orbital margin [14, 45] (b) orbital margin midpoint [constructed] to orbital cone vertex [17, 48]
49	Interorbital distance (IORBDS)	xyz	mm	Left dacryon [15] to right dacryon [46] (Olfaction)
50	Bite force potential at I1 (BFPUI1)	xyz	----	Maximum potential mechanical muscle force at I1 (Mastication)
51	Bite force potential at I2 (BFPUI2)	xyz	----	Maximum potential mechanical muscle force at I2 (Mastication)
52	Bite force potential at P3 (BFPUP3)	xyz	----	Maximum potential mechanical muscle force at P3 (Mastication)
53	Bite force potential at P4 (BFPUP4)	xyz	----	Maximum potential mechanical muscle force at P4 (Mastication)
54	Bite force potential at M1 (BFPUM1)	xyz	----	Maximum potential mechanical muscle force at M1 (Mastication)
55	Bite force potential at M2 (BFPUM2)	xyz	----	Maximum potential mechanical muscle force at M2 (Mastication)
56	Bite force potential at M3 (BFPUM3)	xyz	----	Maximum potential mechanical muscle force at M3 (Mastication)
57	Anterior bite force magnitude (ANTBFM)	xyz	----	Average maximum potential bite force of maxillary I1 and I2 (Mastication)
58	Posterior bite force magnitude (PSTBFM)	xyz	----	Average maximum potential bite force of maxillary P3, P4, M1, M2 and M3 (Mastication)
59	Relative anterior to posterior bite force (RELBFM)	xyz	ratio	Ratio: ANTBFM/PSTBFM x 100 (Mastication)
60	Maxillary bite force magnitude (MAXBFM)	xyz	----	Average maximum potential bite force of maxillary I1, I2, P3, P4, M1, M2 and M3 (Mastication)
61	Anteroposterior position of masseter muscles (APMASS)	xz	percent	(Mastication)
62	Anteroposterior position of temporalis muscles (APTEMP)	xz	percent	(Mastication)
63	Mechanical lever efficiency (LEVADV)	xyz	percent	Load arm/lever arm ratio at M1(Mastication)
64	Temporalis muscle mass (TEMPMM)	xyz	mm^2	Average of two areas (a) (π (left post. to ant. -infra-temporal foramen [4,5]/2) (left med. to lat.-infra-temporal foramen [6, 7]/2))^{½}; and, (b) (π (right post. to ant. -infra-temporal foramen [35, 36]/2) (right med. to lat.-infra-temporal foramen [37, 38]/2))^{½} (Mastication)

Reproduced with permission of the copyright owner. Further reproduction prohibited without permission.

	Individual Landmark-based X Variables	Dimensions	Quant	Description (Hypothesis)
65	Total resultant force of temporalis and masseter muscles (CFORCE)	xyz	---	Magnitude of resultant vector of temparalis and masseter muscles (Mastication)
66	Resultant masticatory muscle efficiency (RMMEFF)	xz	degrees (angle)	Angle of two lines: (a) resultant masticatory muscle vector [constructed], and (b) occlusal surface of P3, left-right [23, 54] to occlusal surface of M3, left-right [24, 55] (Mastication)
67	Anteroposterior position of foramen magnum (APFMAG)	xz	percent	Percent: post.-most brain [103] to lat.-most foramen magnum, left-right avg. [1, 32] / post.-most brain [103] to ant.-most brain [104] (Locomotion)
68	Inclination of foramen magnum (SLOPFM)	xz	degrees (angle)	Angle of two lines: (a) opisthion [76] to basion [77] and, (b) porion, left-right [2, 33] to orbitale, left-right [16, 47] (Locomotion)
69	Anteroposterior position of occipital condyles (APOCND)	xz	percent	Percent: post.-most brain [103] to inf.-most occipital condyle, left-right [85, 86] / post.-most brain [103] to ant.-most brain [104] (Locomotion)
70	Cranial base flexion (CBFLEX)	xz	degrees (angle)	Angle of two lines: (a) nasion [70] to sella [101], and (b) sella [101] to basion [77] (Locomotion)
71	Enlow's cribriform plate angle (ENLWCP)	xz	degrees (angle)	Angle of two lines (a) ant.-most cribriform plate [105] plate to post.-most cribriform plate [106] , and (b) ant.-most brain [100] to prosthion [67] (Encephalization)
72	Enlow's olfactory bulb angle (ENLWOB)	xz	degrees (angle)	Angle of two lines: (a) ant.-most junction of olfactory bulbs [107] to post.-most junction of olfactory bulbs [108], and (b) ant.-most brain [100] to prosthion [67] (Encephalization)
73	Enlow's olfactory bulb orientation (ENLOBO)	xz	degrees (angle)	Angle of two lines
74	Inclination of cribriform plate relative to Frankfort Horizontal (SLPCPF)	xz	degrees (angle)	Angle of two lines: (a) ant.-most cribriform plate [105] to post.-most cribriform plate [106], and (b) porion, left-right [2, 33] to orbitale [16, 47] (Encephalization)
75	Inclination of cribriform plate relative to occlusal plane (SLPCPO)	xz	degrees (angle)	Angle of two lines: (a) ant.-most cribriform plate [105] to post.-most cribriform plate [106], and(b) occlusal surface of P3, left-right [23, 54] to occlusal surface of M3, left-right [24, 55] (Encephalization)
76	Inclination of olfactory bulbs relative to Frankfort Horizontal (SLPOBF)	xz	degrees (angle)	Angle of two lines: (a) ant.-most junction of olfactory bulbs [107] to post.-most junction of olfactory bulbs [108], and (b) porion, left-right [2, 33] to orbitale [16, 47] (Encephalization)

	Individual Landmark-based X Variables	Dimensions	Quant	Description (Hypothesis)
77	Inclination of olfactory bulbs relative to occlusal plane (SLPOBO)	xz	degrees (angle)	Angle of two lines: (a) ant.-most junction of olfactory bulbs [107] to post.-most junction of olfactory bulbs [108], and (b) occlusal surface of P3, left-right [23, 54] to occlusal surface of M3, left-right [24, 55] (Encephalization)
78	Middle cranial fossa length (MCFLGT)	xz	percent	Percentage: porion, left-right [2, 33] to ant.-most middle cranial fossa [102] / post.-most brain [103] to ant.-most brain [104] (Encephalization)
79	Anterior cranial fossa length (ACFLGT)	xz	percent	Percentage: ant.-most middle cranial fossa [102] to ant.-most brain [104] / post.-most brain [103] to ant.-most brain [104] (Encephalization)
80	Foramen magnum size (FMAGSZ)	xyz	mm^2	[π (opisthion [76] to basion [77]/2) (left, lat.-most foramen magnum [1] to right, lat.-most foramen magnum [32]/2]$^{1/2}$ (Encephalization)
81	Brachyendocephalic index (ENDOID)	xyz	percent	Percentage: left lat.-most brain case [10] to right lat.-most brain case [41] / nasion [70] to opisthicranion [74] (Encephalization]
82	Canine size (CANINE]	xyz	mm^3	Canine base area [91, 92, 93, 94] x canine height: centroid of base points [constructed] to canine tip [90]

	Individual Non-Landmark X Variables	Factor		Description
83	Dry skull weight (DSKWGT)	---	grams	Weight of dry cranium
84	Brain size (BRNSIZ)		mm^3	Endocranial volume

Reproduced with permission of the copyright owner. Further reproduction prohibited without permission.

	Species Mean X Variables	Factor	Quant	Description and source
85	Olfactory bulb volume (OFBVLP)		mm^3	Actual measured olfactory bulb volumes; Stephan et al., 1981
86	Brain weight, in Rowe, 1996; Stephan et al. 1981 (STBRWT)		g	Brain weight published in Stephan et al. 1981
87	Gestation period (GESTAT)		days	Compiled by Rowe, 1996
88	Interbirth interval (BIRTHI)		months	Complied by Rowe, 1996
89	Life span (LIFESP)		years	Compiled by Rowe, 1996
90	Locomotor category (LOCCAT)		cat	Compiled by Rowe, 1996
91	Intermembral index (IMBIDX)		index	Compiled by Rowe, 1996
92	Hardness of food item in diet (HDDIET)		index	Rating of dietary hardness on scale between 1 (soft) and 3 (hard)
93	Dietary category (CTDIET)		cat	Ten dietary categories (see Chapter 7); Harding, 1981.
94	Body weight (BODYWT)		kg	Actual body weights: Compiled by Rowe, 1996
	New Variables	**Factor**	**Quant**	**Description and source**
95	Posterior facial angle (PFACAN)		degrees	angle between posterior facial plane and Frankfort horizontal

Reproduced with permission of the copyright owner. Further reproduction prohibited without permission.

APPENDIX C SAS/IML programs for constructing unified configurations

SNAP2.SAS: SAS/IML program to correct radiographic landmarks for projection distortions, and to prepare 3D and 2D landmarks for unification

```
FILENAME CURRENT
'C:\DISSDATA\CMITIS\CM52363';
DATA MKEEP;
 INFILE CURRENT(CM52363.PRN); /*File
containing 3D landmarks in ASCII format */
 INPUT  X Y Z;
DATA PROJC;
 INFILE CURRENT(XCM52363L.TXT); /* File
containing 2D landmarks in ASCII format */
 INPUT X Z;
PROC IML;
 USE PROJC;
 READ ALL INTO F;

 SF=62; /*Distance in mm between cranial
midline and film surface */

 /* Next series of lines translate 2D xray
configuration so that porion is at origin
*/

 DX=0-F[14,1];
 DZ=0-F[14,2];

 P1X=F[1,1]+DX;
 P1Z=F[1,2]+DZ;
 P2X=F[2,1]+DX;
 P2Z=F[2,2]+DZ;
 P3X=F[3,1]+DX;
 P3Z=F[3,2]+DZ;
 P4X=F[4,1]+DX;
 P4Z=F[4,2]+DZ;
 P5X=F[5,1]+DX;
 P5Z=F[5,2]+DZ;
 P6X=F[6,1]+DX;
 P6Z=F[6,2]+DZ;
 P7X=F[7,1]+DX;
 P7Z=F[7,2]+DZ;
 P8X=F[8,1]+DX;
 P8Z=F[8,2]+DZ;
 P9X=F[9,1]+DX;
 P9Z=F[9,2]+DZ;
 P10X=F[10,1]+DX;
 P10Z=F[10,2]+DZ;
 P11X=F[11,1]+DX;
 P11Z=F[11,2]+DZ;
 P12X=F[12,1]+DX;
 P12Z=F[12,2]+DZ;
 P13X=F[13,1]+DX;
 P13Z=F[13,2]+DZ;
 P14X=F[14,1]+DX;
 P14Z=F[14,2]+DZ;


 P1=P1X||0||P1Z;
 P2=P2X||0||P2Z;
 P3=P3X||0||P3Z;
 P4=P4X||0||P4Z;
 P5=P5X||0||P5Z;
 P6=P6X||0||P6Z;
 P7=P7X||0||P7Z;
 P8=P8X||0||P8Z;
 P9=P9X||0||P9Z;
 P10=P10X||0||P10Z;
 P11=P11X||0||P11Z;
 P12=P12X||0||P12Z;
 P13=P13X||0||P13Z;
 P14=P14X||0||P14Z;

B=P1//P2//P3//P4//P5//P6//P7//P8//P9//P10/
/P11//P12//P13//P14;
 /* B matrix contains landmark coordinates
centered at porion */

  O=1390-SF; /* 1390 is constant distance
in mm from x-ray source to midline plane
of specimen */
  M=1390;
  N=1390;

  /* Next series of lines adjust
coordinates to remove x-ray distortions
due to projection effects */

  E=O/(M*N-B[1,1]* B[1,2]);
  X=E * (N-B[1,2])*B[1,1];
  Z=E * (N-B[1,2])*B[1,3];
  C1=X||Z;

  E=O/(M*N-B[2,1]* B[2,2]);
  X=E * (N-B[2,2])*B[2,1];
  Z=E * (N-B[2,2])*B[2,3];
  C2=X||Z;

  E=O/(M*N-B[3,1]* B[3,2]);
  X=E * (N-B[3,2])*B[3,1];
  Z=E * (N-B[3,2])*B[3,3];
  C3=X||Z;

  E=O/(M*N-B[4,1]* B[4,2]);
  X=E * (N-B[4,2])*B[4,1];
  Z=E * (N-B[4,2])*B[4,3];
  C4=X||Z;
```

Reproduced with permission of the copyright owner. Further reproduction prohibited without permission.

```
E=O/(M*N-B[5,1]* B[5,2]);
 X=E * (N-B[5,2])*B[5,1];
 Z=E * (N-B[5,2])*B[5,3];
 C5=X||Z;

E=O/(M*N-B[6,1]* B[6,2]);
 X=E * (N-B[6,2])*B[6,1];
 Z=E * (N-B[6,2])*B[6,3];
 C6=X||Z;

E=O/(M*N-B[7,1]* B[7,2]);
 X=E * (N-B[7,2])*B[7,1];
 Z=E * (N-B[7,2])*B[7,3];
 C7=X||Z;

E=O/(M*N-B[8,1]* B[8,2]);
 X=E * (N-B[8,2])*B[8,1];
 Z=E * (N-B[8,2])*B[8,3];
 C8=X||Z;

E=O/(M*N-B[9,1]* B[9,2]);
 X=E * (N-B[9,2])*B[9,1];
 Z=E * (N-B[9,2])*B[9,3];
 C9=X||Z;

E=O/(M*N-B[10,1]* B[10,2]);
 X=E * (N-B[10,2])*B[10,1];
 Z=E * (N-B[10,2])*B[10,3];
 C10=X||Z;

E=O/(M*N-B[11,1]* B[11,2]);
 X=E * (N-B[11,2])*B[11,1];
 Z=E * (N-B[11,2])*B[11,3];
 C11=X||Z;

E=O/(M*N-B[12,1]* B[12,2]);
 X=E * (N-B[12,2])*B[12,1];
 Z=E * (N-B[12,2])*B[12,3];
 C12=X||Z;

E=O/(M*N-B[13,1]* B[13,2]);
 X=E * (N-B[13,2])*B[13,1];
 Z=E * (N-B[13,2])*B[13,3];
 C13=X||Z;

E=O/(M*N-B[14,1]* B[14,2]);
 X=E * (N-B[14,2])*B[14,1];
 Z=E * (N-B[14,2])*B[14,3];
 C14=X||Z;

 /*XADJ is new data matrix containing x-
ray projection corrected points. Notice
that C14, PORTION, has been dropped. Its
only purpose was to facilitate the
correction adjustment */

XADJ=C1//C2//C3//C4//C5//C6//C7//C8//C9//C
10//C11//C12//C13;


  /* Next series of lines saves new XADJ
matrix to a file */
   FILENAME OUT 'C:\DISSDATA\CM363XC.TXT';
   FILE OUT;

    do i=1 to nrow(XADJ);
     do j=1 to ncol(XADJ);
       put (XADJ[i,j]) 7.2 +3 @;
     end;
      put;
    end;
   CLOSEFILE OUT;

DATA MSNAP;
  INFILE 'C:\DISSDATA\CM363XC.TXT';
  INPUT X2 Z2;
  RUN;

 PROC IML;
  USE MSNAP;
  READ ALL INTO Q; /*Q matrix contains
projection corrected x-ray coordinates */

  USE MKEEP;
  READ ALL INTO P; /* P matrix contains
raw 3D landmark configuration */

  /* Next series of lines produces 2
configurations both 109 landmarks in
length. The first contains the P matrix
with 10 missing values attached to the
bottom. The second configuration contains
the Q matrix with prostion, bregma and
lambda in their proper locations and the
10 endocranial cephalographic landmarks at
the end, with missing values elsewhere */

   L=shape({-999 -999 -999},10,3);

   M=P//L;

   B=Q[1:13,1];
   C=Q[1:13,2];
   D=shape({0},13,1);
   E=B||D||C;

   A1=shape({-999 -999 -999},66,3);
   A2=E[12,]; /* Matching point for
prosthion, #67 */
   A3=shape({-999 -999 -999},4,3);
   A4=E[11,]; /* Matching point for
bregma, #72 */
```

Reproduced with permission of the copyright owner. Further reproduction prohibited without permission.

```
   *A5=shape({-999 -999 -999},3,3);
   A6=E[13,]; /* Matching point for
lambda, #73 */
   A7=shape({-999 -999 -999},26,3);
   A8=E[1:10,];
   A9=A1//A2//A3//A4//A6//A7//A8;

   ALL=M//A9;

   /* Next series of lines produces a GFR-
ND format file containing the two 109
landmark configurations */

    GRF1="'Snap file containing two 109 3D
digitized points";
    GRF2="1 2L 327 1 -999 DIM=3";
    GRF3="CM52363.PRN";
    GRF4="CM363XC.TXT";

   FILENAME OUT 'C:\DISSDATA\CM363.DTA';
   FILE OUT;
    PUT GRF1//GRF2//GRF3//GRF4//;
    do i=1 to nrow(all);
     do j=1 to ncol(all);
       put (all[i,j]) 7.2 +3 @;
     end;
     put;
    end;
   CLOSEFILE OUT;
```

Example file CM363.DTA: GRF-ND format file resulting from SNAP2.SAS program. The file contains two configurations of 109 landmark configurations each. The first configuration contains the raw coordinates of 3D ectocranial landmarks. The second configuration contains the coordinates taken from lateral radiographs. These cephalographic coordinates have been corrected for radiographic projection effects, and have been converted into 3D (from 2D) by adding a vector of 0's for the Y axis. The Y axis is the median plane. The file below was further used to unify the two configuration sets.

```
'Snap file containing two 109 3D digitized
points

1 2L 327 1 -999 DIM=3

CM52363.PRN
CM363XC.TXT

  -3.56      0.77      17.69
  -4.33      2.79      17.15
  -4.90      2.62      17.87
  -5.38      3.14      18.28
  -7.34      2.20      19.64
  -6.57      3.21      18.99
  -6.03      2.17      18.46
  -7.42      2.38      19.88
  -6.05      3.41      18.73
  -4.58      2.94      16.48
  -8.80      1.40      19.18
  -8.47      1.50      16.30
  -8.36      2.48      17.99
  -9.04      1.43      17.00
  -9.23      0.32      18.02
  -8.76      1.53      19.16
  -6.36      0.50      18.00
  -6.70      1.08      18.84
  -9.71      0.47      19.60
  -9.62      0.74      20.48
  -9.63      0.17      18.32
  -7.44      2.16      20.11
  -8.31      1.46      21.39
  -6.62      1.58      20.47
  -9.39      0.83      21.60
  -8.47      1.12      21.11
  -7.71      1.23      20.77
  -6.79      1.19      20.20
  -6.37      1.39      19.98
  -6.17      0.75      19.06
  -8.73      0.51      20.43
  -3.38     -0.57      17.75
  -4.28     -2.48      17.54
  -4.80     -2.33      18.11
  -5.26     -2.79      18.57
  -7.26     -1.69      19.95
  -6.63     -2.79      19.44
  -5.95     -1.96      18.62
  -7.38     -2.07      20.08
  -5.97     -3.04      19.02
  -4.92     -2.83      16.61
  -8.78     -1.20      19.32
  -8.43     -1.48      16.44
  -8.34     -2.32      18.24
  -9.01     -1.30      17.14
  -9.12     -0.22      18.06
  -8.81     -1.32      19.37
  -6.23     -0.33      18.10
  -6.67     -0.65      18.90
  -9.74     -0.19      19.62
  -9.62     -0.25      20.60
  -9.57     -0.07      18.11
  -7.35     -1.67      20.24
  -8.27     -0.82      21.53
  -6.62     -1.07      20.61
  -9.36     -0.19      21.66
  -8.43     -0.59      21.20
  -7.65     -0.69      20.84
  -6.76     -0.69      20.27
  -6.30     -0.83      20.02
```

Reproduced with permission of the copyright owner. Further reproduction prohibited without permission.

-6.19	-0.45	19.16	-999.00	-999.00	-999.00
-9.67	0.13	22.24	-999.00	-999.00	-999.00
-9.41	-0.22	22.11	-999.00	-999.00	-999.00
-7.95	-0.82	21.43	-999.00	-999.00	-999.00
-7.52	-0.94	21.18	-999.00	-999.00	-999.00
-7.01	-1.04	20.87	-999.00	-999.00	-999.00
-9.78	0.30	21.84	-999.00	-999.00	-999.00
-9.77	0.26	21.24	-999.00	-999.00	-999.00
-9.79	0.12	19.58	-999.00	-999.00	-999.00
-9.61	0.07	18.19	-999.00	-999.00	-999.00
-9.63	-0.02	17.34	-999.00	-999.00	-999.00
-6.74	-0.43	14.35	-999.00	-999.00	-999.00
-3.35	-0.06	14.42	-999.00	-999.00	-999.00
-2.63	-0.08	15.10	-999.00	-999.00	-999.00
-2.61	-0.08	15.15	-999.00	-999.00	-999.00
-2.74	0.12	17.12	-999.00	-999.00	-999.00
-3.96	0.14	18.06	-999.00	-999.00	-999.00
-4.94	0.09	18.42	-999.00	-999.00	-999.00
-5.99	0.10	18.60	-999.00	-999.00	-999.00
-7.11	0.18	19.58	-999.00	-999.00	-999.00
-7.13	0.18	19.58	-999.00	-999.00	-999.00
-8.03	0.20	20.16	-999.00	-999.00	-999.00
-8.72	0.19	20.58	-999.00	-999.00	-999.00
-9.48	0.25	21.47	-999.00	-999.00	-999.00
-3.34	0.75	18.05	-999.00	-999.00	-999.00
-3.26	-0.52	18.09	-999.00	-999.00	-999.00
-6.91	3.20	18.97	-999.00	-999.00	-999.00
-6.86	-2.89	19.30	-999.00	-999.00	-999.00
-6.55	-2.72	19.68	-999.00	-999.00	-999.00
-8.42	-0.84	22.42	-999.00	-999.00	-999.00
-9.12	-0.76	21.68	-999.00	-999.00	-999.00
-8.59	-0.77	21.39	-999.00	-999.00	-999.00
-8.94	-0.96	21.57	-999.00	-999.00	-999.00
-8.81	-0.52	21.50	-999.00	-999.00	-999.00
-6.41	2.68	18.50	-999.00	-999.00	-999.00
-4.19	2.38	20.32	-999.00	-999.00	-999.00
-6.23	-2.40	18.85	-999.00	-999.00	-999.00
-3.90	-1.37	20.64	-999.00	-999.00	-999.00
-6.69	3.16	19.43	-999.00	-999.00	-999.00
-999.00	-999.00	-999.00	-999.00	-999.00	-999.00
-999.00	-999.00	-999.00	-999.00	-999.00	-999.00
-999.00	-999.00	-999.00	-999.00	-999.00	-999.00
-999.00	-999.00	-999.00	-999.00	-999.00	-999.00
-999.00	-999.00	-999.00	-999.00	-999.00	-999.00
-999.00	-999.00	-999.00	-999.00	-999.00	-999.00
-999.00	-999.00	-999.00	-999.00	-999.00	-999.00
-999.00	-999.00	-999.00	-999.00	-999.00	-999.00
-999.00	-999.00	-999.00	-999.00	-999.00	-999.00
-999.00	-999.00	-999.00	-999.00	-999.00	-999.00
			-999.00	-999.00	-999.00
-999.00	-999.00	-999.00	-999.00	-999.00	-999.00
-999.00	-999.00	-999.00	-999.00	-999.00	-999.00
-999.00	-999.00	-999.00	-999.00	-999.00	-999.00
-999.00	-999.00	-999.00	-999.00	-999.00	-999.00
-999.00	-999.00	-999.00	-999.00	-999.00	-999.00
-999.00	-999.00	-999.00	-999.00	-999.00	-999.00
-999.00	-999.00	-999.00	-999.00	-999.00	-999.00

Reproduced with permission of the copyright owner. Further reproduction prohibited without permission.

```
-999.00   -999.00   -999.00
-999.00   -999.00   -999.00
  66.42      0.00    -18.41
-999.00   -999.00   -999.00
-999.00   -999.00   -999.00
-999.00   -999.00   -999.00
-999.00   -999.00   -999.00
  13.40      0.00     41.18
 -19.16      0.00     29.13
-999.00   -999.00   -999.00
-999.00   -999.00   -999.00
-999.00   -999.00   -999.00
-999.00   -999.00   -999.00
```

```
-6.170000   0.750000  19.060000
-8.730000   0.510000  20.430000
-3.380000  -0.570000  17.750000
-4.280000  -2.480000  17.540000
-4.800000  -2.330000  18.110000
-5.260000  -2.790000  18.570000
-7.260000  -1.690000  19.950000
-6.630000  -2.790000  19.440000
-5.950000  -1.960000  18.620000
-7.380000  -2.070000  20.080000
-5.970000  -3.040000  19.020000
-4.920000  -2.830000  16.610000
-8.780000  -1.200000  19.320000
-8.430000  -1.480000  16.440000
-8.340000  -2.320000  18.240000
-9.010000  -1.300000  17.140000
-9.120000  -0.220000  18.060000
-8.810000  -1.320000  19.370000
-6.230000  -0.330000  18.100000
-6.670000  -0.650000  18.900000
-9.740000  -0.190000  19.620000
-9.620000  -0.250000  20.600000
-9.570000  -0.070000  18.110000
-7.350000  -1.670000  20.240000
-8.270000  -0.820000  21.530000
-6.620000  -1.070000  20.610000
-9.360000  -0.190000  21.660000
-8.430000  -0.590000  21.200000
-7.650000  -0.690000  20.840000
-6.760000  -0.690000  20.270000
-6.300000  -0.830000  20.020000
-6.190000  -0.450000  19.160000
-9.670000   0.130000  22.240000
-9.410000  -0.220000  22.110000
-7.950000  -0.820000  21.430000
-7.520000  -0.940000  21.180000
-7.010000  -1.040000  20.870000
-9.780000   0.300000  21.840000 (PROSTHION)
-9.770000   0.260000  21.240000
-9.790000   0.120000  19.580000
-9.610000   0.070000  18.190000
-9.630000  -0.020000  17.340000
-6.740000  -0.430000  14.350000 (BREGMA)
-3.350000  -0.060000  14.420000 (LAMBDA)
-2.630000  -0.080000  15.100000
-2.610000  -0.080000  15.150000
-2.740000   0.120000  17.120000
-3.960000   0.140000  18.060000
-4.940000   0.090000  18.420000
-5.990000   0.100000  18.600000
-7.110000   0.180000  19.580000
-7.130000   0.180000  19.580000
-8.030000   0.200000  20.160000
-8.720000   0.190000  20.580000
-9.480000   0.250000  21.470000
-3.340000   0.750000  18.050000
-3.260000  -0.520000  18.090000
-6.910000   3.200000  18.970000
-6.860000  -2.890000  19.300000
-6.550000  -2.720000  19.680000
-8.420000  -0.840000  22.420000
-9.120000  -0.760000  21.680000
-8.590000  -0.770000  21.390000
-8.940000  -0.960000  21.570000
-8.810000  -0.520000  21.500000
-6.410000   2.680000  18.500000
-4.190000   2.380000  20.320000
-6.230000  -2.400000  18.850000
-3.900000  -1.370000  20.640000
-6.690000   3.160000  19.430000
-999.000000 -999.000000 -999.000000
-999.000000 -999.000000 -999.000000
-999.000000 -999.000000 -999.000
```

```
    -999.000000 -999.000000 -999.000000
    -999.000000 -999.000000 -999.000000
    -999.000000 -999.000000 -999.000000
```

```
   O=G[72,];
   P=G[181,];
   R=O-P;
   S=R[,1]+R[,2]+R[,3];
   W=SQRT(S**2);

   O=G[73,];
   P=G[182,];
   R=O-P;
   S=R[,1]+R[,2]+R[,3];
   Y=SQRT(S**2);

   ADD=T+W+Y;

   /* Next series of lines creates a
single configuration from the two separate
ectocranial and cephalographic
configurations by combining the first 99
coordinates from the former and the bottom
10 coordinates from the latter*/

   A=G[1:99,];
   B=G[209:218,];
   C=A//B;

   /* Next series of lines creates a file
containing the unified configuration */

   FILENAME OUT 'C:\DISSDATA\CM363G.DTA';
   FILE OUT;
    PUT GRF1;
    PUT QUOTE T W Y;
    PUT//GRF2//GRF3;
     do i=1 to nrow(C);
     do j=1 to ncol(C);
       put (C[i,j]) 7.2 +3 @;
     end;
     put;
    end;
   CLOSEFILE OUT;

   PRINT GRF3 T W Y ADD;
```

Example file CM363G.DTA: GRF-ND formate file that contains the unified configuration of the raw coordinates of both ectocranial and endocranial landmarks. Notice that the 3D linear distances between pairs of homologous landmarks are all under .03 cm-a very close fit.

```
'File with combined 3D digitized
ectocranial points and 2D xray points'
'Prosthion Bregma     Lambda
 0.029925  0.010856  0.019069
 1 1L 327 1 -999 DIM=3

CM363G.DTA
  -3.56      0.77     17.69
  -4.33      2.79     17.15
  -4.90      2.62     17.87
  -5.38      3.14     18.28
  -7.34      2.20     19.64
  -6.57      3.21     18.99
  -6.03      2.17     18.46
  -7.42      2.38     19.88
  -6.05      3.41     18.73
  -4.58      2.94     16.48
  -8.80      1.40     19.18
  -8.47      1.50     16.30
  -8.36      2.48     17.99
  -9.04      1.43     17.00
  -9.23      0.32     18.02
  -8.76      1.53     19.16
  -6.36      0.50     18.00
  -6.70      1.08     18.84
  -9.71      0.47     19.60
  -9.62      0.74     20.48
  -9.63      0.17     18.32
  -7.44      2.16     20.11
  -8.31      1.46     21.39
  -6.62      1.58     20.47
  -9.39      0.83     21.60
  -8.47      1.12     21.11
  -7.71      1.23     20.77
  -6.79      1.19     20.20
  -6.37      1.39     19.98
  -6.17      0.75     19.06
  -8.73      0.51     20.43
  -3.38     -0.57     17.75
  -4.28     -2.48     17.54
  -4.80     -2.33     18.11
  -5.26     -2.79     18.57
  -7.26     -1.69     19.95
  -6.63     -2.79     19.44
  -5.95     -1.96     18.62
  -7.38     -2.07     20.08
  -5.97     -3.04     19.02
  -4.92     -2.83     16.61
  -8.78     -1.20     19.32
  -8.43     -1.48     16.44
  -8.34     -2.32     18.24
  -9.01     -1.30     17.14
  -9.12     -0.22     18.06
  -8.81     -1.32     19.37
  -6.23     -0.33     18.10
  -6.67     -0.65     18.90
  -9.74     -0.19     19.62
  -9.62     -0.25     20.60
  -9.57     -0.07     18.11
  -7.35     -1.67     20.24
  -8.27     -0.82     21.53
```

Reproduced with permission of the copyright owner. Further reproduction prohibited without permission.

```
-6.62    -1.07    20.61
-9.36    -0.19    21.66
-8.43    -0.59    21.20
-7.65    -0.69    20.84
-6.76    -0.69    20.27
-6.30    -0.83    20.02
-6.19    -0.45    19.16
-9.67     0.13    22.24
-9.41    -0.22    22.11
-7.95    -0.82    21.43
-7.52    -0.94    21.18
-7.01    -1.04    20.87
-9.78     0.30    21.84
-9.77     0.26    21.24
-9.79     0.12    19.58
-9.61     0.07    18.19
-9.63    -0.02    17.34
-6.74    -0.43    14.35
-3.35    -0.06    14.42
-2.63    -0.08    15.10
-2.61    -0.08    15.15
-2.74     0.12    17.12
-3.96     0.14    18.06
-4.94     0.09    18.42
-5.99     0.10    18.60
-7.11     0.18    19.58
-7.13     0.18    19.58
-8.03     0.20    20.16
-8.72     0.19    20.58
-9.48     0.25    21.47
-3.34     0.75    18.05
-3.26    -0.52    18.09
-6.91     3.20    18.97
-6.86    -2.89    19.30
-6.55    -2.72    19.68
-8.42    -0.84    22.42
-9.12    -0.76    21.68
-8.59    -0.77    21.39
-8.94    -0.96    21.57
-8.81    -0.52    21.50
-6.41     2.68    18.50
-4.19     2.38    20.32
-6.23    -2.40    18.85
-3.90    -1.37    20.64
-6.69     3.16    19.43
-8.85    -0.33    16.66
-5.43     0.21    17.88
-6.72     0.14    18.41
-2.55     0.14    15.22
-8.79    -0.26    17.15
-8.72    -0.13    17.97
-8.32    -0.08    18.01
-8.68    -0.21    17.35
-8.23    -0.13    17.59
-6.75    -0.41    14.49
```

Example file CM52363C.DTA: GRF-ND result output file that contains the unified configuration of raw coordinates aligned to the Frankfort horizontal.

```
'File with combined 3D digitized
ectocranial points and 2D xray points'

** GRF_ND (c) 1992-94 dslice (revision 11-
01-94 +)
** FILE: CM363G.DTA   DATE: 4/21/97
TIME: 22:30:36
** Initial/Reference configuration 1
loaded from TRANS109.DIS
** LEAST-SQUARES FITTING: STRICT     TIME:
22:30:46
**     N  :          7
**     ād :    20.8029
**     ādý:    63.4581
** RESULTS

1 1L 327 1 -999.000000 DIM=3
CM363G.DTA

     -2.253733   0.645634  -1.001934
     -1.730821   2.709406  -0.344433
     -0.926544   2.499082  -0.769994
     -0.317600   2.996958  -0.994064
      2.006216   1.995756  -1.409118
      1.056236   3.036156  -1.184164
      0.338354   2.026890  -0.837571
      2.176174   2.160057  -1.610413
      0.478575   3.245597  -1.163133
     -1.761402   2.908817   0.357849
      3.158779   1.251507  -0.359884
      1.728087   1.543890   2.146295
      2.301715   2.403811   0.484944
      2.525821   1.434692   1.732174
      3.085902   0.260326   0.947460
      3.115826   1.381950  -0.366185
      0.440116   0.397608  -0.170873
      1.089517   0.923696  -0.848449
      4.148473   0.308822  -0.324503
      4.413957   0.516393  -1.185800
      3.569487   0.096192   0.839268
      2.281843   1.925121  -1.798400
      3.574666   1.152239  -2.583616
      1.661029   1.309379  -2.409834
      4.642352   0.525809  -2.309698
      3.607757   0.834729  -2.240553
      2.776798   0.956233  -2.233918
      1.706591   0.941459  -2.068574
      1.236598   1.149675  -2.045069
      0.683870   0.571354  -1.235108
      3.572631   0.276859  -1.472668
     -2.413144  -0.697907  -1.034908
     -1.692159  -2.575084  -0.357717
```

Reproduced with permission of the copyright owner. Further reproduction prohibited without permission.

-0.988513	-2.456665	-0.687351
-0.391050	-2.940100	-0.897419
2.003780	-1.907113	-1.456104
1.210162	-2.978972	-1.158970
0.274043	-2.105092	-0.730351
2.160196	-2.293270	-1.502114
0.435200	-3.209567	-1.014890
-1.472291	-2.850661	0.770430
3.161613	-1.351974	-0.316524
1.707608	-1.438955	2.208076
2.319200	-2.401776	0.579386
2.517775	-1.298620	1.780599
2.993396	-0.282756	0.904982
3.207251	-1.474652	-0.342355
0.348969	-0.439179	-0.256198
1.063057	-0.806598	-0.795718
4.175374	-0.350461	-0.285499
4.448172	-0.479393	-1.227496
3.428907	-0.129715	1.025019
2.200458	-1.905696	-1.688301
3.563238	-1.132338	-2.570200
1.681615	-1.343674	-2.355185
4.625073	-0.496241	-2.306024
3.584110	-0.877826	-2.220646
2.724200	-0.964734	-2.188986
1.682109	-0.939151	-2.014654
1.159167	-1.068643	-1.955802
0.725933	-0.632236	-1.236110
5.141644	-0.212123	-2.738840
4.846995	-0.556289	-2.697233
3.229672	-1.130341	-2.603803
2.734587	-1.239427	-2.534582
2.142656	-1.325660	-2.443031
5.088316	-0.013419	-2.340503
4.843516	-0.012296	-1.791165
4.209708	-0.037723	-0.250632
3.498860	0.005057	0.957616
3.183061	-0.026083	1.751531
-0.652415	-0.273821	3.391059
-3.738860	0.038907	1.973327
-4.135060	-0.038660	1.068779
-4.133869	-0.042396	1.015070
-3.239832	0.023889	-0.755270
-1.748929	-0.002117	-1.141185
-0.706967	-0.061796	-1.084136
0.329642	-0.048206	-0.838665
1.744998	-0.018627	-1.304597
1.763397	-0.018323	-1.296763
2.818865	-0.024490	-1.477735
3.618064	-0.052796	-1.592098
4.666714	-0.042466	-2.115096
-2.315332	0.597631	-1.417026
-2.389679	-0.673189	-1.397315
1.361056	3.032724	-1.031938
1.365607	-3.065619	-0.933516
1.231504	-2.926833	-1.415340
4.049680	-1.211086	-3.326622
4.404749	-1.069854	-2.379004
3.803419	-1.067987	-2.319856
4.193472	-1.264547	-2.334772
4.052140	-0.822809	-2.351873
0.710205	2.538662	-0.760653
-0.622894	2.080740	-3.279374
0.616057	-2.555530	-0.801289
-0.812793	-1.686355	-3.427469
1.338378	2.957908	-1.537396
2.195058	-0.300511	2.091296
-0.466211	0.102418	-0.405041
0.927285	0.015836	-0.381148
-4.158795	0.171344	0.912142
2.332750	-0.265224	1.613388
2.591314	-0.192885	0.824648
2.239650	-0.151837	0.627804
2.310562	-0.230746	1.383347
1.991649	-0.174258	0.981347
-0.588105	-0.263326	3.265146

Reproduced with permission of the copyright owner. Further reproduction prohibited without permission.

APPENDIX D: SAS/IML programs to calculate variables from configurations

DISS2.SAS: SAS/IML program using analytic geometry and matrix algebra to calculate morphometric variates from unified coordinate configuration. The program also contains a 3D model of mastication.

```
DATA DISS2;

  INFILE 'C:\DISSDATA\GGORILLA\GG1472\GG1472C.RES' FIRSTOBS=16;

  INPUT X Y Z;

 RUN;

  PROC IML;

    USE DISS2;
    READ ALL INTO B;

  /* Next 2 lines convert cm into mm */
  L=shape({10},1,1);
  K=B@L;


 /* ------------------------------------------------------------------ */
 /*Constructed xyz coordinates for use in subsequent programs*/
 /*-------------------------------------------------------------------*/
 /*1:MSY: Midsagittal Y-axis coordinate, should approximate zero */
   MSY=(K[67,2]+K[71,2]+K[76,2]+K[80,2])/4;

 /*2:MAXTMP: Alveolon: Maxillary tuberosity midpoint */
   XMAX=(K[29,1]+K[60,1])/2;
   ZMAX=(K[29,3]+K[60,3])/2;
   MAXTMP=XMAX||MSY||ZMAX;

 /*3:CONDMP: Condylion midpoint */
   XCON=(K[3,1]+K[34,1])/2;
   ZCON=(K[3,3]+K[34,3])/2;
   CONDMP=XCON||MSY||ZCON;

 /*4:ZYROMP: Zygomatic root midpoint */
   XZYR=(K[22,1]+K[53,1])/2;
   ZZYR=(K[22,3]+K[53,3])/2;
   ZYROMP=XZYR||MSY||ZZYR;

 /*5:BIPOR: Biporionic midpoint */
   XBIP=(K[2,1]+K[33,1])/2;
   ZBIP=(K[2,3]+K[33,3])/2;
   BIPOR=XBIP||MSY||ZBIP;

 /*6:BIORB: Biorbitale midpoint*/
   XORB=(K[16,1]+K[47,1])/2;
   ZORB=(K[16,3]+K[47,3])/2;
   BIORB=XORB||MSY||ZORB;

 /*7:ORBML: Orbital midpoint left*/
   XOML=(K[13,1]+K[14,1]+K[15,1]+K[16,1])/4;
   YOML=(K[13,2]+K[14,2]+K[15,2]+K[16,2])/4;
   ZOML=(K[13,3]+K[14,3]+K[15,3]+K[16,3])/4;
   ORBML=XOML||YOML||ZOML;
```

Reproduced with permission of the copyright owner. Further reproduction prohibited without permission.

```
 /*8:ORBMR: Orbital midpoint right*/
   XOMR=(K[44,1]+K[45,1]+K[46,1]+K[47,1])/4;
   YOMR=(K[44,2]+K[45,2]+K[46,2]+K[47,2])/4;
   ZOMR=(K[44,3]+K[45,3]+K[46,3]+K[47,3])/4;
   ORBMR=XOMR||YOMR||ZOMR;

 /*9:BIP3: Upper P3 occlusal surface midpoint*/
   XP3=(K[23,1]+K[54,1])/2;
   ZP3=(K[23,3]+K[54,3])/2;
   BIP3=XP3||MSY||ZP3;

 /*10:BIM3: Upper M3 occlusal surface midpoint*/
   XM3=(K[24,1]+K[55,1])/2;
   ZM3=(K[24,3]+K[55,3])/2;
   BIM3=XM3||MSY||ZM3;

 /*-------------------------------------------------------------------*/
 /*NASLGT: Nasal length: Linear distance: nasion - rhinion: TYPE 1 */
   NASLGT=SQRT((((K[70,1])-(K[69,1]))**2)+(((K[70,2])-(K[69,2]))**2)+(((K[70,3])-
(K[69,3]))**2));

 /*-------------------------------------------------------------------*/
 /*NASWDU: Upper nasal bone width: Left frontomaxillonasal junction to right
   frontomaxillonasal junction: TYPE 1 */
   NASWDU=SQRT(((K[21,2])-(K[52,2]))**2);

 /*-------------------------------------------------------------------*/
 /*NASWDL: Lower nasal bone width: Left nasomaxillare to right nasomaxillare:
   TYPE 1 */
   NASWDL=SQRT(((K[19,2])-(K[50,2]))**2);

 /*-------------------------------------------------------------------*/
 /*NPMWDT: Nasal process of maxilla width: Average Linear distance: left
   left dacryon to left frontomaxillonasal junction, and right dacryon to
   right frontomaxillonasal junction: TYPE 1 */
   LNPMWDT=SQRT((((K[15,1])-(K[21,1]))**2)+(((K[15,2])-(K[21,2]))**2)+(((K[15,3])-
(K[21,3]))**2));
   RNPMWDT=SQRT((((K[46,1])-(K[52,1]))**2)+(((K[46,2])-(K[52,2]))**2)+(((K[46,3])-
(K[52,3]))**2));
   NPMWDT=(LNPMWDT+RNPMWDT)/2;

 /*-------------------------------------------------------------------*/
 /*NSLAHT: Nasal aperture height: Linear distance: rhinion - subnasale:
   TYPE 1*/
   NSLAHT=SQRT((((K[68,1])-(K[69,1]))**2)+(((K[68,2])-(K[69,2]))**2)+(((K[68,3])-
(K[69,3]))**2));

 /*-------------------------------------------------------------------*/
 /*NSLAWD: Nasal aperture width: max. transverse breadth of nasal aperture
   (using alare): TYPE 1 */
   NSLAWD=SQRT(((K[20,2])-(K[51,2]))**2);

 /*-------------------------------------------------------------------*/
 /*PNASHT: Posterior nasal aperture length: Linear distance: staphylion -
   hormion (along midline): TYPE 1 */
   PNASHT=SQRT((((K[79,1])-(K[80,1]))**2)+(((K[79,2])-(K[80,2]))**2)+(((K[79,3])-
(K[80,3]))**2));

 /*-------------------------------------------------------------------*/
 /*PNASWD: Posterior nasal aperture breadth: max. distance between
   medial pterygoid plates: TYPE 1 */
   PNASWD=SQRT(((K[30,2])-(K[61,2]))**2);
```

Reproduced with permission of the copyright owner. Further reproduction prohibited without permission.

```
/*-----------------------------------------------------------------*/
/*NLCLGT: Nasoalveolar clivus length: Calculates linear distance between
  subnasale - prosthion: TYPE 1 */
  NLCLGT=SQRT((((K[67,1])-(K[68,1]))**2)+(((K[67,2])-(K[68,2]))**2)+(((K[67,3])-
(K[68,3]))**2));

/*-----------------------------------------------------------------*/
/*ZYGARE: Area within 4 point polygon outlining zygomatic bone: TYPE 2 */
/* If polygon is modeled as a rhombus, then the area is one half the
   product of the diagonals*/
  LEN1=SQRT((((K[11,1])-(K[9,1]))**2)+(((K[11,2])-(K[9,2]))**2)+(((K[11,3])-
(K[9,3]))**2));
  LEN2=SQRT((((K[13,1])-(K[8,1]))**2)+(((K[13,2])-(K[8,2]))**2)+(((K[13,3])-
(K[8,3]))**2));
  LZYGARE=.5*(LEN1*LEN2);

  LEN3=SQRT((((K[42,1])-(K[40,1]))**2)+(((K[42,2])-(K[40,2]))**2)+(((K[42,3])-
(K[40,3]))**2));
  LEN4=SQRT((((K[44,1])-(K[39,1]))**2)+(((K[44,2])-(K[39,2]))**2)+(((K[44,3])-
(K[39,3]))**2));
  RZYGARE=.5*(LEN3*LEN4);

  ZYGARE=(LZYGARE+RZYGARE)/2;

/*-----------------------------------------------------------------*/
/*ZYGOHT: Zygoma height: avg. left and right: zygo-orbitale to zygomaxillare
  in xz dimensions: TYPE 3 */
  ZYGOHL=SQRT((((K[8,1])-(K[11,1]))**2)+(((K[8,3])-(K[11,3]))**2));
  ZYGOHR=SQRT((((K[39,1])-(K[42,1]))**2)+(((K[39,3])-(K[42,3]))**2));
  /*Take average of linear distance of left and right measurments*/
  ZYGOHT=(ZYGOHL+ZYGOHR)/2;

/*-----------------------------------------------------------------*/
/*BZYGWD: Bizygomatic breadth: Linear distance:
  inf.-most zygomatico-temporal suture -
  inf.-most zygomatico-temporal suture: TYPE 1 */
  BZYGWD=SQRT(((K[9,2])-(K[40,2]))**2);

/*-----------------------------------------------------------------*/
/*APZYGR: Anteroposterior position of zygomatic root: Avg. of two percentages:
  left and right: condylion to zygomatic root divided by condylion to prosthion:
  TYPE 4 */

  /* N.B. The method below was used because you can't just take the linear
          distances on the x axis since the orientation of the skull is
          has the x axis parallel with the Frankfort horizontal; the program
          below calculates distances on prosthion to alveolor plane */

 /*The next 16 lines of code calculates the xz coordinates of the
   intersection point of two lines: (a) a line defined by OC, and
   (b) a line perpendicular to OC passing through point L */

 OC=MAXTMP//K[67,];
 L=CONDMP;

 SOC=(OC[1,3]-OC[2,3])/(OC[1,1]-OC[2,1]);
 SL=-(1/SOC);

 LX=5;  /* Assign arbitrary value */

 LZ=SL*(LX-L[,1])+L[,3];

     F=OC[1,1]-OC[2,1];
```

Reproduced with permission of the copyright owner. Further reproduction prohibited without permission.

```
      G=LX-L[,1];
      b1=(OC[1,3]-OC[2,3])/F;
      b2=(LZ-L[,3])/G;
        H=b2-b1;
      a1=OC[2,3]-b1*OC[2,1];
      a2=L[,3]-b2*L[,1];
        if H=0 then H=.000-1;
      LZN=(a1*b2-a2*b1)/H;
      LXN=(LZN-a1)/b1;

  CONDP=SQRT((((K[67,1])-(LXN))**2)+(((K[67,3])-(LZN))**2));

  OC=MAXTMP//K[67,];
  L=ZYROMP;

  SOC=(OC[1,3]-OC[2,3])/(OC[1,1]-OC[2,1]);
  SL=-(1/SOC);

  LX=5;  /* Assign arbitrary value */

  LZ=SL*(LX-L[,1])+L[,3];

      F=OC[1,1]-OC[2,1];
      G=LX-L[,1];
      b1=(OC[1,3]-OC[2,3])/F;
      b2=(LZ-L[,3])/G;
        H=b2-b1;
      a1=OC[2,3]-b1*OC[2,1];
      a2=L[,3]-b2*L[,1];
        if H=0 then H=.000-1;
      ZZN=(a1*b2-a2*b1)/H;
      ZXN=(ZZN-a1)/b1;

  CONDZ=SQRT((((LXN)-(ZXN))**2)+(((LZN)-(ZZN))**2));

  APZYGR=(CONDZ/CONDP)*100;

 /*-----------------------------------------------------------------*/
 /*MXARCL: Maxillary arch length: Linear distance: prosthion to alveolon:
   TYPE 3 */
   MXARCL=SQRT((((K[67,1])-(XMAX))**2)+(((K[67,3])-(ZMAX))**2));

 /*-----------------------------------------------------------------*/
 /*BMAXWD: Bimaxillary breadth: Linear distance: left zygomaxillare to right
   zygomaxillare: TYPE 1 */
   BMAXWD=SQRT(((K[8,2])-(K[39,2]))**2);

 /*-----------------------------------------------------------------*/
 /*UMAXWD: Upper facial breadth: Linear distance: left zygomaticofrontal to right
   zygomaticofrontal: TYPE 1 */
   UMAXWD=SQRT(((K[13,2])-(K[44,2]))**2);

 /*-----------------------------------------------------------------*/
 /*AFACHT: Anterior facial height: Linear distance: nasion to prosthion: TYPE 1 */
   AFACHT=SQRT((((K[67,1])-(K[70,1]))**2)+(((K[67,2])-(K[70,2]))**2)+(((K[67,3])-
(K[70,3]))**2));

 /*-----------------------------------------------------------------*/
 /*PFACHT: Posterior facial height: avg. left and right: maxillary tuberosity
   to sup.-most extent of inf orbital fissure in xyz dimensions:*/
   PFACHTL=SQRT((((K[18,1])-(K[29,1]))**2)+(((K[18,2])-(K[29,2]))**2)+(((K[18,3])-
(K[29,3]))**2));
```

Reproduced with permission of the copyright owner. Further reproduction prohibited without permission.

```
   PFACHTR=SQRT((((K[49,1])-(K[60,1]))**2)+(((K[49,2])-(K[60,2]))**2)+(((K[49,3])-
(K[60,3]))**2));
   PFACHT=(PFACHTL+PFACHTR)/2;

 /*-----------------------------------------------------------------*/
 /*RAMSHT: Ramus height: Avg. linear distance, condylion to occlusal
   plane (perp. to occlusal plane): avg. left and right: TYPE 2 */

 OCINDL={23 24};
 OC=K[OCINDL,];
 L=K[3,];

 SOC=(OC[1,3]-OC[2,3])/(OC[1,1]-OC[2,1]);
 SL=-(1/SOC);

 LX=5;  /* Assign arbitrary value */

 LZ=SL*(LX-L[,1])+L[,3];

     F=OC[1,1]-OC[2,1];
     G=LX-L[,1];
     b1=(OC[1,3]-OC[2,3])/F;
     b2=(LZ-L[,3])/G;
       H=b2-b1;
     a1=OC[2,3]-b1*OC[2,1];
     a2=L[,3]-b2*L[,1];
       if H=0 then H=.000-1;
     LZN=(a1*b2-a2*b1)/H;
     LXN=(LZN-a1)/b1;

 RAMSHTL=SQRT((((L[,1])-(LXN))**2)+(((L[,3])-(LZN))**2));

 OCINDL={54 55};
 OC=K[OCINDL,];
 L=K[34,];

 SOC=(OC[1,3]-OC[2,3])/(OC[1,1]-OC[2,1]);
 SL=-(1/SOC);

 LX=5;  /* Assign arbitrary value */

 LZ=SL*(LX-L[,1])+L[,3];

     F=OC[1,1]-OC[2,1];
     G=LX-L[,1];
     b1=(OC[1,3]-OC[2,3])/F;
     b2=(LZ-L[,3])/G;
       H=b2-b1;
     a1=OC[2,3]-b1*OC[2,1];
     a2=L[,3]-b2*L[,1];
       if H=0 then H=.000-1;
     LZN=(a1*b2-a2*b1)/H;
     LXN=(LZN-a1)/b1;

  RAMSHTR=SQRT((((L[,1])-(LXN))**2)+(((L[,3])-(LZN))**2));

  RAMSHT=(RAMSHTL+RAMSHTR)/2;

/*-----------------------------------------------------------------*/
/*I2PALW: Inter-I2 palatal width: min. distance between I2 alveolar
  junctions: TYPE 1 */
 I2PALW=SQRT(((K[25,2])-(K[56,2]))**2);
```

Reproduced with permission of the copyright owner. Further reproduction prohibited without permission.

```
/*-----------------------------------------------------------------*/
/*P3PALW: Inter-P3 palatal width: min. distance between P3 alveolar
  junctions: TYPE 1 */
 P3PALW=SQRT(((K[26,2])-(K[57,2]))**2);

/*-----------------------------------------------------------------*/
/*M1PALW: Inter-M1 palatal width: min. distance between M1 alveolar
  junctions: TYPE 1 */
 M1PALW=SQRT(((K[27,2])-(K[58,2]))**2);

/*-----------------------------------------------------------------*/
/*M3PALW: Inter-M3 palatal width: min. distance between M3 alveolar
  junctions: TYPE 1 */
 M3PALW=SQRT(((K[28,2])-(K[59,2]))**2);

/*-----------------------------------------------------------------*/
/*I2PALD: Palatal depth at I2: Distance between I2PAW line and palate
  along midline (perpendicular to occlusal plane): TYPE 5 */
/*XI2 is x-coord of midline-occlusal line point (I2), taken as avg.
  x-coord of LMI2AJ and RMI2AJ*/
XI2=((K[25,1])+(K[56,1]))/2;
/*ZI2 is z-coord of point I2, taken as avg. z-coord of LMI2AJ and
  RMI2AJ*/
ZI2=((K[25,3])+(K[56,3]))/2;
I2PALD=SQRT((((K[84,1])-(XI2))**2)+(((K[84,3])-(ZI2))**2));

/*-----------------------------------------------------------------*/
/*P3PALD: Palatal depth at P3: Distance between P3PAW line and palate
  along midline (perpendicular to occlusal plane): TYPE 5 */
/*XP3 is x-coord of midline-occlusal line point (P3), taken as avg.
  x-coord of LMP3AJ and RMP3AJ*/
XP3=((K[26,1])+(K[57,1]))/2;
/*ZP3 is z-coord of point P3, taken as avg. z-coord of LMP3AJ and
  RMP3AJ*/
ZP3=((K[26,3])+(K[57,3]))/2;
P3PALD=SQRT((((K[83,1])-(XP3))**2)+(((K[83,3])-(ZP3))**2));

/*-----------------------------------------------------------------*/
/*M1PALD: Palatal depth at M1: Distance between M1PAW line and palate
  along midline (perpendicular to occlusal plane): TYPE 5 */
/*XM1 is x-coord of midline-occlusal line point (M1), taken as avg.
  x-coord of LMM1AJ and RMM1AJ*/
XM1=((K[27,1])+(K[58,1]))/2;
/*ZM1 is z-coord of point M1, taken as avg. z-coord of LMM1AJ and
  RMM1AJ*/
ZM1=((K[27,3])+(K[58,3]))/2;
M1PALD=SQRT((((K[82,1])-(XM1))**2)+(((K[82,3])-(ZM1))**2));

/*-----------------------------------------------------------------*/
/*M3PALD: Palatal depth at M3: Distance between M3PAW line and palate
  along midline (perpendicular to occlusal plane): TYPE 5 */
/*XM3 is x-coord of midline-occlusal line point (M3), taken as avg.
  x-coord of LMM3AJ and RMM3AJ*/
XM3=((K[28,1])+(K[59,1]))/2;
/*ZM3 is z-coord of point M3, taken as avg. z-coord of LMM3AJ and
  RMM3AJ*/
ZM3=((K[28,3])+(K[59,3]))/2;
/*Just make the y-coord of point M3 equal to y-coord of MPALM3 which
  should be close to 0, or leave y-coord out of equation altogether,
  then calculate linear distance*/
M3PALD=SQRT((((K[81,1])-(XM3))**2)+(((K[81,3])-(ZM3))**2));

/*-----------------------------------------------------------------*/
```

Reproduced with permission of the copyright owner. Further reproduction prohibited without permission.

```
/*PALLGT: Palate length: linear distance: prosthion - staphylion:
  TYPE 1 */
  PALLGT=SQRT((((K[67,1])-(K[80,1]))**2)+(((K[67,3])-(K[80,3]))**2));

/*-------------------------------------------------------------------*/
/*PALTHK: Palatal thickness at M1: Linear distance, nasal floor to palatal
  floor (perp. to palatal floor)*/

 OCINDL={81 82};
 OC=K[OCINDL,];
 L=K[31,];

 SOC=(OC[1,3]-OC[2,3])/(OC[1,1]-OC[2,1]);
 SL=-(1/SOC);

 LX=5;  /* Assign arbitrary value */

 LZ=SL*(LX-L[,1])+L[,3];

     F=OC[1,1]-OC[2,1];
     G=LX-L[,1];
     b1=(OC[1,3]-OC[2,3])/F;
     b2=(LZ-L[,3])/G;
       H=b2-b1;
     a1=OC[2,3]-b1*OC[2,1];
     a2=L[,3]-b2*L[,1];
       if H=0 then H=.000-1;
     LZN=(a1*b2-a2*b1)/H;
     LXN=(LZN-a1)/b1;

  PALTHK=SQRT((((L[,1])-(LXN))**2)+(((L[,3])-(LZN))**2));


/*-------------------------------------------------------------------*/
/*KROGAG: Krogman's angle of facial prognathism: nasion - prosthion:
  Frankfort horizontal*/
/*The following equation has been tested for accuracy*/
 L1=XORB-XBIP;
 N1=ZORB-ZBIP;
 L2=K[67,1]-K[70,1];
 N2=K[67,3]-K[70,3];
 cosKROGA=((L1*L2)+(N1*N2))/((SQRT((L1**2)+(N1**2)))*
        (SQRT((L2**2)+(N2**2))));
 KROGAG=180-(arcos(cosKROGA)*180/3.14159265); /*This converts a cosine into
 degrees */



/*-------------------------------------------------------------------*/
/*ENLOAG: Enlow's angle of facial prognathism: ant. brain (Enlow) -
  prosthion - maxillary tuberosity: TYPE 9 */
/*The following equation has been tested for accuracy*/
 L1=K[67,1]-K[100,1];
 N1=K[67,3]-K[100,3];
 L2=K[67,1]-XMAX;
 N2=K[67,3]-ZMAX;
 cosENLOA=((L1*L2)+(N1*N2))/((SQRT((L1**2)+(N1**2)))*
        (SQRT((L2**2)+(N2**2))));
 ENLOAG=180-(arcos(cosENLOA)*180/3.14159265); /*This converts a cosine into
 degrees */


/*-------------------------------------------------------------------*/
```

Reproduced with permission of the copyright owner. Further reproduction prohibited without permission.

```
/*SLOPOC: Angle between Frankfort Horizontal and occlusal plane */
/*The following equation has been tested for accuracy*/
 L1=XBIP-XORB;
 N1=ZBIP-ZORB;
 L2=K[23,1]-K[24,1];
 N2=K[23,3]-K[24,3];
 cosSLOPO=((L1*L2)+(N1*N2))/((SQRT((L1**2)+(N1**2)))*
        (SQRT((L2**2)+(N2**2))));
 SLOPOCL=180-(arcos(cosSLOPO)*180/3.14159265); /*This converts a cosine into
 degrees */

 L1=XBIP-XORB;
 N1=ZBIP-ZORB;
 L2=K[54,1]-K[55,1];
 N2=K[54,3]-K[55,3];
 cosSLOPR=((L1*L2)+(N1*N2))/((SQRT((L1**2)+(N1**2)))*
        (SQRT((L2**2)+(N2**2))));
 SLOPOCR=180-(arcos(cosSLOPR)*180/3.14159265); /*This converts a cosine into
 degrees */

 SLOPOC=(SLOPOCL+SLOPOCR)/2;

/*-----------------------------------------------------------------*/
/* FACCNV: Facial convexity: Ratio: Dist1=line perpendicular to prosthion-nasion,
   through rhinion / Dist2=prosthion-nasion */

 OCINDL={67 70};
 OC=K[OCINDL,];
 L=K[69,];

 SOC=(OC[1,3]-OC[2,3])/(OC[1,1]-OC[2,1]);
 SL=-(1/SOC);

 LX=5;  /* Assign arbitrary value */

 LZ=SL*(LX-L[,1])+L[,3];

     F=OC[1,1]-OC[2,1];
     G=LX-L[,1];
     b1=(OC[1,3]-OC[2,3])/F;
     b2=(LZ-L[,3])/G;
       H=b2-b1;
     a1=OC[2,3]-b1*OC[2,1];
     a2=L[,3]-b2*L[,1];
       if H=0 then H=.000-1;
     LZN=(a1*b2-a2*b1)/H;
     LXN=(LZN-a1)/b1;

 FACPERP=SQRT((((L[,1])-(LXN))**2)+(((L[,3])-(LZN))**2));
 IF L[,1] < LXN THEN FACPERP = FACPERP*(-1);
 FACCNV=(FACPERP/AFACHT)*100;

/*-----------------------------------------------------------------*/
/*FACSIZ: Centroid size for selected facial points */

 INDS={8 11 13 14 15 17 19 20 22 25 26 27 28 29
      39 42 44 45 46 48 50 51 53 56 57 58 59 60
      67 68 69 70 80};
 FACK=K[INDS,];
 p=NROW(FACK);
 MX=(SUM(FACK[,1]))/p;
 MY=(SUM(FACK[,2]))/p;
 MZ=(SUM(FACK[,3]))/p;
```

Reproduced with permission of the copyright owner. Further reproduction prohibited without permission.

```
 M=MX||MY||MZ;
 R=REPEAT(M,p,1);
 Y=FACK-R;
 SS=Y`*Y;
 CS=trace(SS);
 FACSIZ=SQRT(CS);

/*-----------------------------------------------------------------*/
/*PPNALO:Average of left and right angles: angle of bizygo-orbitale
  line [11, 42] and left zygo-orbitale [11] to naso(pre)maxillary suture
  at nasal aperture margin [19] */
/*The following equation has been tested for accuracy*/

 L1=K[11,1]-K[42,1];
 N1=K[11,2]-K[42,2];
 L2=K[11,1]-K[19,1];
 N2=K[11,2]-K[19,2];
 cosPPNL=((L1*L2)+(N1*N2))/((SQRT((L1**2)+(N1**2)))*
        (SQRT((L2**2)+(N2**2))));
 PPNL=arcos(cosPPNL)*180/3.14159265; /*This converts a cosine into
 degrees */


 L1=K[42,1]-K[11,1];
 N1=K[42,2]-K[11,2];
 L2=K[42,1]-K[50,1];
 N2=K[42,2]-K[50,2];
 cosPPNR=((L1*L2)+(N1*N2))/((SQRT((L1**2)+(N1**2)))*
        (SQRT((L2**2)+(N2**2))));
 PPNR=arcos(cosPPNR)*180/3.14159265; /*This converts a cosine into
 degrees */

 PPNALO=(PPNL+PPNR)/2;

/*-----------------------------------------------------------------*/
/* ORBIHT: Orbital height: orbitale - sup.-most point along
   superior orbital margin, in z and x dimensions only (no mediolateral
   component, ie. along parasagittal plane): averaged over left and
   right points: TYPE 3 */
   ORBIL=SQRT((((K[14,1])-(K[16,1]))**2)+(((K[14,3])-(K[16,3]))**2));
   ORBIR=SQRT((((K[45,1])-(K[47,1]))**2)+(((K[45,3])-(K[47,3]))**2));
   ORBIHT=(ORBIL+ORBIR)/2;

/*-----------------------------------------------------------------*/
/*CRLGTH: Cranial length: Linear distance: prosthion - opisthocranion */
  CRLGTH=SQRT((((K[67,1])-(K[74,1]))**2)+(((K[67,2])-(K[74,2]))**2)+(((K[67,3])-
(K[74,3]))**2));

/*-----------------------------------------------------------------*/
/*NCLGTH: Neurocranial length: Linear distance: glabella - opisthocranion */
  NCLGTH=SQRT((((K[71,1])-(K[74,1]))**2)+(((K[71,2])-(K[74,2]))**2)+(((K[71,3])-
(K[74,3]))**2));

/*-----------------------------------------------------------------*/
/*BCLGTH: Basicranial length: Linear distance: nasion - basion */
  BCLGTH=SQRT((((K[70,1])-(K[77,1]))**2)+(((K[70,2])-(K[77,2]))**2)+(((K[70,3])-
(K[77,3]))**2));

/*-----------------------------------------------------------------*/
/*BIPORB: Biporionic breadth: Linear distance: left to right porion */
  BIPORB=SQRT(((K[2,2])-(K[33,2]))**2);

/*-----------------------------------------------------------------*/
```

Reproduced with permission of the copyright owner. Further reproduction prohibited without permission.

```
/* SKCNTR: Skull Centroid size: square root of the sum of squared distances of
   the total set of landmarks from their centroid: TYPE 6 */

 /*p=NROW(K); */
 K0=K[1:109,];
 MX=(SUM(K[1:109,1]))/109;
 MY=(SUM(K[1:109,2]))/109;
 MZ=(SUM(K[1:109,3]))/109;
 M=MX||MY||MZ;
 R=REPEAT(M,109,1);
 Y=K0-R;
 SS=Y`*Y;
 CS=trace(SS);
 SKCNTR=SQRT(CS);

/*-----------------------------------------------------------------*/
/*CRBTHK: Cranial bone thickness at bregma: linear distance between bregma
  and endobregma in xz plane */
  CRBTHK=SQRT((((K[72,1])-(K[109,1]))**2)+(((K[72,3])-(K[109,3]))**2));

/*-----------------------------------------------------------------*/
/*OFBVOL: Olfactory bulb volume: Area within 4 points x dacryon-dacryon */

 OCINDL={108 107};
 OC=K[OCINDL,];
 L=K[105,];

 SOC=(OC[1,3]-OC[2,3])/(OC[1,1]-OC[2,1]);
 SL=-(1/SOC);

 LX=5;  /* Assign arbitrary value */

 LZ=SL*(LX-L[,1])+L[,3];

     F=OC[1,1]-OC[2,1];
     G=LX-L[,1];
     b1=(OC[1,3]-OC[2,3])/F;
     b2=(LZ-L[,3])/G;
       H=b2-b1;
     a1=OC[2,3]-b1*OC[2,1];
     a2=L[,3]-b2*L[,1];
       if H=0 then H=.000-1;
     LZN=(a1*b2-a2*b1)/H;
     LXN=(LZN-a1)/b1;

  /*Olfactory recess area */
  HEIGHT=SQRT((((L[,1])-(LXN))**2)+(((L[,3])-(LZN))**2));
  DIST1=SQRT((((K[108,1])-(K[107,1]))**2)+(((K[108,3])-(K[107,3]))**2));
  DIST2=SQRT((((K[106,1])-(K[105,1]))**2)+(((K[106,3])-(K[105,3]))**2));
  OLFRA=.5*(HEIGHT*(DIST1+DIST2)); /*Equation for area of trapezoid */

  /*Olfactory recess volume */
  IORBDS=SQRT((((K[15,1])-(K[46,1]))**2)+(((K[15,2])-(K[46,2]))**2)+(((K[15,3])-
(K[46,3]))**2));
  OFBVOL=OLFRA*IORBDS;

/*-----------------------------------------------------------------*/
/*OFBARE: Olfactory bulb area: length of cribriform plate x dacryon-dacryon */
  CRIBLG=SQRT((((K[105,1])-(K[106,1]))**2)+(((K[105,2])-
(K[106,2]))**2)+(((K[105,3])-(K[106,3]))**2));
  OFBARE=CRIBLG*IORBDS;

/*-----------------------------------------------------------------*/
```

Reproduced with permission of the copyright owner. Further reproduction prohibited without permission.

```
 /*ORBSCR: Orbital sagittal-coronal rotation: Angle between orbital
   axis and mid-sagittal plane*/

 /*ORBSCRL: left ORBSCR angle */
 L1=XOML-K[17,1];
 N1=YOML-K[17,2];
 L2=K[67,1]-K[76,1];
 N2=K[67,2]-K[76,2];
 cosOSCRL=((L1*L2)+(N1*N2))/((SQRT((L1**2)+(N1**2)))*
        (SQRT((L2**2)+(N2**2))));
 ORBSCRL=arcos(cosOSCRL)*180/3.14159265; /*This converts a cosine into
 degrees */

/*ORBSCRR: right ORBSCR angle */
 L1=XOMR-K[48,1];
 N1=YOMR-K[48,2];
 L2=K[67,1]-K[76,1];
 N2=K[67,2]-K[76,2];
 cosOSCRR=((L1*L2)+(N1*N2))/((SQRT((L1**2)+(N1**2)))*
        (SQRT((L2**2)+(N2**2))));
 ORBSCRR=arcos(cosOSCRR)*180/3.14159265; /*This converts a cosine into
 degrees */

 ORBSCR=(ORBSCRL+ORBSCRR)/2;

/*-------------------------------------------------------------------*/
 /*ORBTC1: Orbital transverse-coronal rotation: Angle between orbital
   axis and Frankfort horiztonal*/

 /*ORBTCRL: left ORBTCR angle */
 L1=K[17,1]-XOML;
 N1=K[17,3]-ZOML;
 L2=XBIP-XORB;
 N2=ZBIP-ZORB;
 cosOTCRL=((L1*L2)+(N1*N2))/((SQRT((L1**2)+(N1**2)))*
        (SQRT((L2**2)+(N2**2))));
 ORBTCRL=arcos(cosOTCRL)*180/3.14159265; /*This converts a cosine into
 degrees */

/*ORBTCRR: right ORBTCR angle */
 L1=K[48,1]-XOMR;
 N1=K[48,3]-ZOMR;
 L2=XBIP-XORB;
 N2=ZBIP-ZORB;
 cosOTCRR=((L1*L2)+(N1*N2))/((SQRT((L1**2)+(N1**2)))*
        (SQRT((L2**2)+(N2**2))));
 ORBTCRR=arcos(cosOTCRR)*180/3.14159265; /*This converts a cosine into
 degrees */

 ORBTC1=(ORBTCRL+ORBTCRR)/2;

/*-------------------------------------------------------------------*/
 /*ORBTC2: Orbital transverse-coronal rotation: Angle between orbital
   axis and Frankfort horiztonal*/

 /*ORBTCRL: left ORBTCR angle */
 L1=K[16,1]-K[14,1];
 N1=K[16,3]-K[14,3];
 L2=XORB-XBIP;
 N2=ZORB-ZBIP;
 cosOTCL2=((L1*L2)+(N1*N2))/((SQRT((L1**2)+(N1**2)))*
        (SQRT((L2**2)+(N2**2))));
 ORBTCRL2=arcos(cosOTCL2)*180/3.14159265; /*This converts a cosine into
```

Reproduced with permission of the copyright owner. Further reproduction prohibited without permission.

```
 degrees */

/*ORBTCRR: right ORBTCR angle */
 L1=K[47,1]-K[45,1];
 N1=K[47,3]-K[45,3];
 L2=XORB-XBIP;
 N2=ZORB-ZBIP;
 cosOTCR2=((L1*L2)+(N1*N2))/((SQRT((L1**2)+(N1**2)))*
        (SQRT((L2**2)+(N2**2))));
 ORBTCRR2=arcos(cosOTCR2)*180/3.14159265; /*This converts a cosine into
 degrees */

 ORBTC2=(ORBTCRL2+ORBTCRR2)/2;

/*-------------------------------------------------------------------*/
 /*ORBA12: Angle between two lines of orbital transverse-coronal rotation:
   predicted to be a constant 90 degrees*/

 /*ORBA12L: left ORBA12 angle */
 L1=K[16,1]-K[14,1];
 N1=K[16,3]-K[14,3];
 L2=K[17,1]-XOML;
 N2=K[17,3]-ZOML;
 cosOTCAL=((L1*L2)+(N1*N2))/((SQRT((L1**2)+(N1**2)))*
        (SQRT((L2**2)+(N2**2))));
 ORBA12L=arcos(cosOTCAL)*180/3.14159265; /*This converts a cosine into
 degrees */

/*ORBA12R: right ORBA12 angle */
 L1=K[47,1]-K[45,1];
 N1=K[47,3]-K[45,3];
 L2=K[48,1]-XOMR;
 N2=K[48,3]-ZOMR;
 cosOTCAR=((L1*L2)+(N1*N2))/((SQRT((L1**2)+(N1**2)))*
        (SQRT((L2**2)+(N2**2))));
 ORBA12R=arcos(cosOTCAR)*180/3.14159265; /*This converts a cosine into
 degrees */

 ORBA12=(ORBA12L+ORBA12R)/2;



/*-------------------------------------------------------------------*/
/*IORBDS: Dacryon-dacryon: already defined */


/*-------------------------------------------------------------------*/
/*Universal estimates used for all teeth */
/*-------------------------------------------------------------------*/

/*1:TFORCE: Maximum muscle force of temporalis mm. */
/* Infratemporal foramen modeled as ellipse with muscle force = to area */

   TMLW=SQRT((((K[7,1])-(K[6,1]))**2)+(((K[7,2])-(K[6,2]))**2)+(((K[7,3])-
(K[6,3]))**2));
   TMLL=SQRT((((K[5,1])-(K[4,1]))**2)+(((K[5,2])-(K[4,2]))**2)+(((K[5,3])-
(K[4,3]))**2));
   TMFL=SQRT(3.14159265*(TMLW/2)*(TMLL/2));

   TMRW=SQRT((((K[37,1])-(K[38,1]))**2)+(((K[37,2])-(K[38,2]))**2)+(((K[37,3])-
(K[38,3]))**2));
   TMRL=SQRT((((K[35,1])-(K[36,1]))**2)+(((K[35,2])-(K[36,2]))**2)+(((K[35,3])-
(K[36,3]))**2));
```

Reproduced with permission of the copyright owner. Further reproduction prohibited without permission.

```
  TMFR=SQRT(3.14159265*(TMRW/2)*(TMRL/2));

  TFORCE=(TMFL+TMFR);


/*2: MFORCE: Maximum muscle force of masseter and med. pterygoid mm. */
  MFORCE=.94*TFORCE;

/*3: Calculated coordinates of temporal mm. attachments */
   TEMLX=(K[2,1]+K[12,1])/2;
   TEMLY=(K[2,2]+K[12,2])/2;
   TEMLZ=(K[2,3]+K[12,3])/2;

   TEMRX=((K[33,1])+(K[43,1]))/2;
   TEMRY=((K[33,2])+(K[43,2]))/2;
   TEMRZ=((K[33,3])+(K[43,3]))/2;

/*4:TMANGL: Below equation calculates angle in degrees between temporalis
      and masseter on left side: needed to calculate FORCE  */
     LL1=K[95,1]-TEMLX;
     NL1=K[95,3]-TEMLZ;
     LL2=K[96,1]-K[99,1];
     NL2=K[96,3]-K[99,3];
     cosTMANL=((LL1*LL2)+(NL1*NL2))/((SQRT((LL1**2)+(NL1**2)))*
        (SQRT((LL2**2)+(NL2**2))));    /* Degrees cosine of TMANG */
     TMANGL=arcos(cosTMANL)*180/3.14159265;
      /*The arcos function above gives result in radians, must multiply
        by 180/pie to convert to degrees */

/*5: TMANGR: Below equation calculates angle in degrees between temporalis
      and masseter on right side: needed to calculate FORCE */
     LR1=K[97,1]-TEMRX;
     NR1=K[97,3]-TEMRZ;
     LR2=K[98,1]-K[89,1];
     NR2=K[98,3]-K[89,3];
     cosTMANR=((LR1*LR2)+(NR1*NR2))/((SQRT((LR1**2)+(NR1**2)))*
        (SQRT((LR2**2)+(NR2**2))));    /* Degrees cosine of TMANG */
     TMANGR=arcos(cosTMANR)*180/3.14159265;
      /*The arcos function above gives result in radians, must multiply
        by 180/pie to convert to degrees */

    cosTMANG=(cosTMANL+cosTMANR)/2;

/*6: TMANG */
     TMANG=(TMANGL+TMANGR)/2;

/*7: FORCE: Total resultant force for masticatory muscles */
     FORCE=SQRT((TFORCE**2)+(MFORCE**2)+((2*TFORCE*MFORCE)*cosTMANG));
    /*Above equation for FORCE  on p. 16 of Harwood */

/*8: FANG = angle between resultant force vector and occlusal plane
         = REMASANG + MASOANG
     where:
           REMASANG = angle between resultant vector and masseter mm. vector
                 sin REMASANG = (TF / F) sin TMANG
           MASOANG = angle between masseter mm. vector and occlusal plane
              = midpoint of masseter origin to midpoint of masseter insertion by
                 P3 mid-occlusal surface - M3 mid-occlusal surface  */
       /*In the equations below:
       REMSANG= angle between left restultant vector and masseter vec.
       MASOANG= angle between left masseter vec. and occlusal plane
       FANG = angle between left resultant and occlusal plane */
```

Reproduced with permission of the copyright owner. Further reproduction prohibited without permission.

```
    /*REMSANG=angle between resultant vector and masseter mm. vector
                  sin REMSANG=(TFORCE/FORCE)sinTMANG */
     TMANGR=TMANG*.017453293;      /* Converts TMANG in degrees to radians*/
     SINREMS=(TFORCE/FORCE)*sin(TMANGR); /* Because SAS sin function is on radians
*/
                                        /*sin(TMANGRL)=sin(TMANGL) */

     REMSANG=arsin(SINREMS)*180/3.14159265;


     /*MASOANGL= angle between masseter mm. vector and occlusal plane
              = midpoint of masseter origin to midpoint of masseter insertion by
                  P3 mid-occlusal surface - M3 mid-occlusal surface */
      LL1=K[96,1]-K[99,1];
      NL1=K[96,3]-K[99,3];
      LL2=K[24,1]-K[23,1];
      NL2=K[24,3]-K[23,3];
      cosCMASL=((LL1*LL2)+(NL1*NL2))/((SQRT((LL1**2)+(NL1**2)))*
         (SQRT((LL2**2)+(NL2**2))));
      MASOANGL=arcos(cosCMASL)*180/3.14159265;

     /*MASOANGR= angle between masseter mm. vector and occlusal plane
              = midpoint of masseter origin to midpoint of masseter insertion by
                  P3 mid-occlusal surface - M3 mid-occlusal surface */
      LR1=K[98,1]-K[89,1];
      NR1=K[98,3]-K[89,3];
      LR2=K[55,1]-K[54,1];
      NR2=K[55,3]-K[54,3];
      cosCMASR=((LR1*LR2)+(NR1*NR2))/((SQRT((LR1**2)+(NR1**2)))*
         (SQRT((LR2**2)+(NR2**2))));
      MASOANGR=arcos(cosCMASR)*180/3.14159265;

      MASOANG=(MASOANGL+MASOANGR)/2;

      FANG=REMSANG+MASOANG;

      FANGLE=FANG;

 /*9: Origin coordinates of resultant vector RXi, RYi, RZi */

   p=2;  /*p=.5 1/3 distance between points */
          /*p=1 1/2 distance between points */
          /*p=2 2/3 distance between points */
          /*p=3 3/4 distance between points */
          /*p=4 4/5 distance between points */

    GONLX=(K[95,1]+(p*K[96,1]))/(1+p);
    GONLY=(K[95,2]+(p*K[96,2]))/(1+p);
    GONLZ=(K[95,3]+(p*K[96,3]))/(1+p);

    GONRX=(K[97,1]+(p*K[98,1]))/(1+p);
    GONRY=(K[97,2]+(p*K[98,2]))/(1+p);
    GONRZ=(K[97,3]+(p*K[98,3]))/(1+p);
    /*Above equations have been tested: source: Ilyan & Poznyak, p.22 */


  RXi=(K[95,1]+GONLX+K[97,1]+GONRX)/4;
  RYi=(K[95,2]+GONLY+K[97,2]+GONRY)/4;
  RZi=(K[95,3]+GONLZ+K[97,3]+GONRZ)/4;

  /* Ri=RXi||RYi||RZi; */
  /*Optionally, have resltant vector originate at ALVEOLON, see below */
```

Reproduced with permission of the copyright owner. Further reproduction prohibited without permission.

```
/*10: Occlusal end point coordinates of resultant vector RX, RY,RZ */

/* OC=BIP3//BIM3;
 L=Ri;

 SOC=(OC[1,3]-OC[2,3])/(OC[1,1]-OC[2,1]);
 SL=-(1/SOC); */

 LX=5;  /* Assign arbitrary value */

/* LZ=SL*(LX-L[,1})+L[,3];

     F=OC[1,1]-OC[2,1];
     G=LX-L[,1];
     b1=(OC[1,3]-OC[2,3])/F;
     b2=(LZ-L[,3])/G;
       H=b2-b1;
     a1=OC[2,3]-b1*OC[2,1];
     a2=L[,3]-b2*L[,1];
       if H=0 then H=.000-1;
     RZ=(a1*b2-a2*b1)/H;
     RX=(RZ-a1)/b1;
     RY=0; */

  /*Ro=RX||RY||RZ; */

 /*IN PLACE OF #10 and 11: ALTERNATIVE Ri and Ro, CALCULATED USING GREAVES'
   METHOD OF TAKING AS THE RESULTANT MUSCLE VECTOR A LINE PERPENDICULAR TO
   THE OCCLUSAL PLANE THROUGH ALVEOLON */

 OCINDL={54 55};
 OC=K[OCINDL,];
 L=MAXTMP;

 SOC=(OC[1,3]-OC[2,3])/(OC[1,1]-OC[2,1]);
 SL=-(1/SOC);

 LX=5;  /* Assign arbitrary value */

 LZ=SL*(LX-L[,1])+L[,3];

     F=OC[1,1]-OC[2,1];
     G=LX-L[,1];
     b1=(OC[1,3]-OC[2,3])/F;
     b2=(LZ-L[,3])/G;
       H=b2-b1;
     a1=OC[2,3]-b1*OC[2,1];
     a2=L[,3]-b2*L[,1];
       if H=0 then H=.000-1;
     LZN=(a1*b2-a2*b1)/H;
     LXN=(LZN-a1)/b1;

   Ri=LXN||MSY||LZN;
   Ro=MAXTMP;

 /*--------------------------*/
 /*Angle check, angle between Ri-Ro line and occlusal plane should be
   90 degrees */

  L1=K[54,1]-K[55,1];
  N1=K[54,3]-K[55,3];
  L2=LXN-MAXTMP[,1];
  N2=LZN-MAXTMP[,3];
```

Reproduced with permission of the copyright owner. Further reproduction prohibited without permission.

```
 cosANGCH=((L1*L2)+(N1*N2))/((SQRT((L1**2)+(N1**2)))*
       (SQRT((L2**2)+(N2**2))));
 ANGCH=arcos(cosANGCH)*180/3.14159265; /*This converts a cosine into
 degrees */



/*-------------------------------------------------------------------*/
/*Maximum potential mechanical bite force*/
/*= (FORCE cos FANG) x E
       -------------
            O

 E = load arm
    = distance B to C
 O = lever arm
    = distance A to C

 where:
   A = bite point
   B = point at which resultant vector crosses plane defined by left and
          right TMJ and bite point
   C = point at which extension of line A-B crosses TMJ-TMJ line */


/*B above requires 5 points, 2 to define the resultant vector and 3 to
  define plane (left and right TMJ and bite point)
  Let's call the XYZ coords of the vector points
  RXi,RYi, RZi and RX, RY, RZ */



  /*---------------------------------------- */
  /*FIND MAXIMUM BITE POINT FORCE FOR I1 = BFPUI1 */
  /*---------------------------------------- */

  BP=K[62,];
  BPX=BP[1,1];
  BPY=BP[1,2];
  BPZ=BP[1,3];

 /* Find B=xyz point at which resultant vector crosses plane defined by
  left and right TMJ and bite point */

  TMJL=K[3,];
  TMJR=K[34,];
  plane=TMJL//TMJR//BP;
  line=Ri//Ro;
  R1=j(3,1)||plane[,1:2];
  L1=plane[,3];
  s1=inv(R1)*L1; /* z intercept and x and y slope for given plane */
  newpt=j(1,3,0); /* saves place for random new point */
  pln2=line//uniform(newpt); /* plane made up of line and new random pt */
  R2=j(3,1)||pln2[,1:2];
  L2=pln2[,3];
  s2=inv(R2)*L2; /* z intercept and x and y for dummy plane 2 */
  pln3=line//uniform(newpt); /* dummy plane using another random third point */
  R3=j(3,1)||pln3[,1:2];
  L3=pln3[,3];
  s3=inv(R3)*L3;  /*third solution for plane 3 */
  S=(s1||s2||s3)`; /*  coefficient array putting solutions together */
  R4=S[,2:3]||j(3,1,-1);
  L4=-S[,1];
```

Reproduced with permission of the copyright owner. Further reproduction prohibited without permission.

```
    xyz=inv(R4)*L4;  /*final solution of x, y, z points in common */
    LEVX=xyz[1,1];
    LEVY=xyz[2,1];
    LEVZ=xyz[3,1];

    LEV=LEVX||LEVY||LEVZ;


    /* Find C, point at which extension of line A-B crosses TMJ-TMJ */
      F=BPX-LEV[,1];
      G=K[34,1]-K[3,1];
       if F=0 then F=.00001;
       if G=0 then G=.00001;
      b1=(BPZ-LEV[,3])/F;              /* b1 = slope of top line */
      b2=(K[34,3]-K[3,3])/G;             /* b2 = slope of bottom line */
        if b1=0 then b1=.00001;
        if b2=0 then b2=.00001;
        H=b2-b1;
      a1=LEV[,3]-b1*LEV[,1];              /* a1 = intercept of top line */
      a2=K[3,3]-b2*K[3,1];              /* a2 = intercept of bottom line */
        if H=0 then H=.000-1;
      TMJ2Z=(a1*b2-a2*b1)/H;               /* Zi = Z axis intercept of top and
bottom lines */
      TMJ2X=(TMJ2Z-a1)/b1;                 /* Xi = X axis intercept of top and
botom lines */

      F=BPX-LEV[,1];
      G=K[34,1]-K[3,1];
       if F=0 then F=.00001;
       if G=0 then G=.00001;
      b1=(BPY-LEV[,2])/F;              /* b1 = slope of top line */
      b2=(K[34,2]-K[3,3])/G;             /* b2 = slope of bottom line */
        if b1=0 then b1=.00001;
        if b2=0 then b2=.00001;
        H=b2-b1;
      a1=LEV[,2]-b1*LEV[,1];              /* a1 = intercept of top line */
      a2=K[3,2]-b2*K[3,1];              /* a2 = intercept of bottom line */
        if H=0 then H=.000-1;
      TMJ2Y=(a1*b2-a2*b1)/H;               /* Zi = Z axis intercept of top and
bottom lines */

      TMJ2=TMJ2X||TMJ2Y||TMJ2Z;

    /* Next lines of code finds xy coord for intersection of inter-
       maxillary tuberosity line and perpendicular through right
       masticatory mm. origin */


    RVEC=BP;

    OCINDL={29 60};
    OC=K[OCINDL,];
    L=RVEC;

    SOC=(OC[1,2]-OC[2,2])/(OC[1,1]-OC[2,1]);
    SL=-(1/SOC);

    LX=5;  /* Assign arbitrary value */

    LY=SL*(LX-L[,1])+L[,2];

     F=OC[1,1]-OC[2,1];
     G=LX-L[,1];
```

Reproduced with permission of the copyright owner. Further reproduction prohibited without permission.

```
      b1=(OC[1,2]-OC[2,2])/F;
      b2=(LY-L[,2])/G;
        H=b2-b1;
      a1=OC[2,2]-b1*OC[2,1];
      a2=L[,2]-b2*L[,1];
        if H=0 then H=.000-1;
      LYN=(a1*b2-a2*b1)/H;
      LXN=(LYN-a1)/b1;



    /* Find new xyz point at which "shifted" resultant vector crosses
       triangle of support */

    Mo=K[3,];

    MTL=K[29,];
    MTR=K[60,];
    plane=MTL//MTR//LEV;
    line=BP//Mo;
    R1=j(3,1)||plane[,1:2];
    L1=plane[,3];
    s1=inv(R1)*L1; /* z intercept and x and y slope for given plane */
    newpt=j(1,3,0); /* saves place for random new point */
    pln2=line//uniform(newpt); /* plane made up of line and new random pt */
    R2=j(3,1)||pln2[,1:2];
    L2=pln2[,3];
    s2=inv(R2)*L2; /* z intercept and x and y for dummy plane 2 */
    pln3=line//uniform(newpt); /* dummy plane using another random third point */
    R3=j(3,1)||pln3[,1:2];
    L3=pln3[,3];
    s3=inv(R3)*L3;  /*third solution for plane 3 */
    S=(s1||s2||s3)`; /*  coefficient array putting solutions together */
    R4=S[,2:3]||j(3,1,-1);
    L4=-S[,1];
    xyz=inv(R4)*L4;  /*final solution of x, y, z points in common */
    MLEVX=xyz[1,1];  /* MLEV for modified LEV */
    MLEVY=xyz[2,1];
    MLEVZ=xyz[3,1];

    MLEV=MLEVX||MLEVY||MLEVZ;



     LEVER=SQRT(((BPX)-TMJ2X)**2)+(((BPY)-TMJ2Y)**2)+(((BPZ)-TMJ2Z)**2));
     LOAD=SQRT(((LEV[,1])-TMJ2X)**2)+((LEV[,2])-TMJ2Y)**2)+((LEV[,3])-
TMJ2Z)**2));
     LEVER2=SQRT(((BPX)-K[3,1])**2)+(((BPY)-K[3,2])**2)+(((BPZ)-K[3,3])**2));
     LOAD2=SQRT(((K[3,1]-MLEV[,1])**2)+((K[3,2]-MLEV[,2])**2)+((K[3,3]-
MLEV[,3])**2));;

     LATRB=SQRT(((LEVX-LXN)**2)+((LEVY-LYN)**2));
     GRBR=SQRT(((MLEVX-LXN)**2)+((MLEVY-LYN)**2));
     FP=GRBR/LATRB*100;
     FPERC=(.90476+(.31286*FP)+(.00677*(FP**2)))/100; /* Quadratic equation
                                                         calculated from Greaves
1978 */
     FORCEH=FORCE/2;


    /*FANGRAD=FANG*.017453293; NOT USED: ASSUMING FANG TO BE 90 DEGREES */
```

Reproduced with permission of the copyright owner. Further reproduction prohibited without permission.

```
IF TMJ2Y>K[3,2] THEN BFPUI1=((((FORCEH*FPERC)+FORCEH))*LOAD2)/LEVER2;
ELSE BFPUI1=((FORCE)*LOAD)/LEVER;


 /*--------------------------------------- */
 /*FIND MAXIMUM BITE POINT FORCE FOR I2 = BFPUI2 */
 /*--------------------------------------- */

 BP=K[63,];
 BPX=BP[1,1];
 BPY=BP[1,2];
 BPZ=BP[1,3];

/* Find B=xyz point at which resultant vector crosses plane defined by
 left and right TMJ and bite point */

 TMJL=K[3,];
 TMJR=K[34,];
 plane=TMJL//TMJR//BP;
 line=Ri//Ro;
 R1=j(3,1)||plane[,1:2];
 L1=plane[,3];
 s1=inv(R1)*L1; /* z intercept and x and y slope for given plane */
 newpt=j(1,3,0); /* saves place for random new point */
 pln2=line//uniform(newpt); /* plane made up of line and new random pt */
 R2=j(3,1)||pln2[,1:2];
 L2=pln2[,3];
 s2=inv(R2)*L2; /* z intercept and x and y for dummy plane 2 */
 pln3=line//uniform(newpt); /* dummy plane using another random third point */
 R3=j(3,1)||pln3[,1:2];
 L3=pln3[,3];
 s3=inv(R3)*L3;  /*third solution for plane 3 */
 S=(s1||s2||s3)`; /*  coefficient array putting solutions together */
 R4=S[,2:3]||j(3,1,-1);
 L4=-S[,1];
 xyz=inv(R4)*L4;  /*final solution of x, y, z points in common */
 LEVX=xyz[1,1];
 LEVY=xyz[2,1];
 LEVZ=xyz[3,1];

 LEV=LEVX||LEVY||LEVZ;


 /* Find C, point at which extension of line A-B crosses TMJ-TMJ */
   F=BPX-LEV[,1];
   G=K[34,1]-K[3,1];
    if F=0 then F=.00001;
    if G=0 then G=.00001;
   b1=(BPZ-LEV[,3])/F;              /* b1 = slope of top line */
   b2=(K[34,3]-K[3,3])/G;             /* b2 = slope of bottom line */
     if b1=0 then b1=.00001;
     if b2=0 then b2=.00001;
     H=b2-b1;
   a1=LEV[,3]-b1*LEV[,1];              /* a1 = intercept of top line */
   a2=K[3,3]-b2*K[3,1];              /* a2 = intercept of bottom line */
     if H=0 then H=.000-1;
   TMJ2Z=(a1*b2-a2*b1)/H;               /* Zi = Z axis intercept of top and
bottom lines */
   TMJ2X=(TMJ2Z-a1)/b1;                 /* Xi = X axis intercept of top and
botom lines */

   F=BPX-LEV[,1];
   G=K[34,1]-K[3,1];
```

Reproduced with permission of the copyright owner. Further reproduction prohibited without permission.

```
        if F=0 then F=.00001;
        if G=0 then G=.00001;
       b1=(BPY-LEV[,2])/F;                /* b1 = slope of top line */
       b2=(K[34,2]-K[3,3])/G;               /* b2 = slope of bottom line */
         if b1=0 then b1=.00001;
         if b2=0 then b2=.00001;
         H=b2-b1;
       a1=LEV[,2]-b1*LEV[,1];                /* a1 = intercept of top line */
       a2=K[3,2]-b2*K[3,1];                /* a2 = intercept of bottom line */
         if H=0 then H=.000-1;
       TMJ2Y=(a1*b2-a2*b1)/H;                /* Zi = Z axis intercept of top and
bottom lines */

       TMJ2=TMJ2X||TMJ2Y||TMJ2Z;

      /* Next lines of code finds xy coord for intersection of inter-
         maxillary tuberosity line and perpendicular through right
         masticatory mm. origin */


      RVEC=BP;

      OCINDL={29 60};
      OC=K[OCINDL,];
      L=RVEC;

      SOC=(OC[1,2]-OC[2,2])/(OC[1,1]-OC[2,1]);
      SL=-(1/SOC);

      LX=5;  /* Assign arbitrary value */

      LY=SL*(LX-L[,1])+L[,2];

       F=OC[1,1]-OC[2,1];
       G=LX-L[,1];
       b1=(OC[1,2]-OC[2,2])/F;
       b2=(LY-L[,2])/G;
         H=b2-b1;
       a1=OC[2,2]-b1*OC[2,1];
       a2=L[,2]-b2*L[,1];
         if H=0 then H=.000-1;
       LYN=(a1*b2-a2*b1)/H;
       LXN=(LYN-a1)/b1;



     /* Find new xyz point at which "shifted" resultant vector crosses
        triangle of support */

     Mo=K[3,];

     MTL=K[29,];
     MTR=K[60,];
     plane=MTL//MTR//LEV;
     line=BP//Mo;
     R1=j(3,1)||plane[,1:2];
     L1=plane[,3];
     s1=inv(R1)*L1; /* z intercept and x and y slope for given plane */
     newpt=j(1,3,0); /* saves place for random new point */
     pln2=line//uniform(newpt); /* plane made up of line and new random pt */
     R2=j(3,1)||pln2[,1:2];
     L2=pln2[,3];
     s2=inv(R2)*L2; /* z intercept and x and y for dummy plane 2 */
```

Reproduced with permission of the copyright owner. Further reproduction prohibited without permission.

```
     pln3=line//uniform(newpt); /* dummy plane using another random third point */
     R3=j(3,1)||pln3[,1:2];
     L3=pln3[,3];
     s3=inv(R3)*L3;  /*third solution for plane 3 */
     S=(s1||s2||s3)`; /*  coefficient array putting solutions together */
     R4=S[,2:3]||j(3,1,-1);
     L4=-S[,1];
     xyz=inv(R4)*L4;  /*final solution of x, y, z points in common */
     MLEVX=xyz[1,1];  /* MLEV for modified LEV */
     MLEVY=xyz[2,1];
     MLEVZ=xyz[3,1];

     MLEV=MLEVX||MLEVY||MLEVZ;



      LEVER=SQRT((((BPX)-TMJ2X)**2)+(((BPY)-TMJ2Y)**2)+(((BPZ)-TMJ2Z)**2));
      LOAD=SQRT((((LEV[,1])-TMJ2X)**2)+(((LEV[,2])-TMJ2Y)**2)+(((LEV[,3])-
TMJ2Z)**2));
      LEVER2=SQRT((((BPX)-K[3,1])**2)+(((BPY)-K[3,2])**2)+(((BPZ)-K[3,3])**2));
      LOAD2=SQRT(((K[3,1]-MLEV[,1])**2)+((K[3,2]-MLEV[,2])**2)+((K[3,3]-
MLEV[,3])**2));;

      LATRB=SQRT(((LEVX-LXN)**2)+((LEVY-LYN)**2));
      GRBR=SQRT(((MLEVX-LXN)**2)+((MLEVY-LYN)**2));
      FP=GRBR/LATRB*100;
      FPERC=(.90476+(.31286*FP)+(.00677*(FP**2)))/100;

      FORCEH=FORCE/2;


     /*FANGRAD=FANG*.017453293; NOT USED: ASSUMING FANG TO BE 90 DEGREES */


    IF TMJ2Y>K[3,2] THEN BFPUI2=((((FORCEH*FPERC)+FORCEH))*LOAD2)/LEVER2;
    ELSE BFPUI2=((FORCE)*LOAD)/LEVER;



     /*-------------------------------------- */
     /*FIND MAXIMUM BITE POINT FORCE FOR P3 = BFPUP3 */
     /*-------------------------------------- */

     BP=K[54,];
     BPX=BP[1,1];
     BPY=BP[1,2];
     BPZ=BP[1,3];

    /* Find B=xyz point at which resultant vector crosses plane defined by
     left and right TMJ and bite point */

     TMJL=K[3,];
     TMJR=K[34,];
     plane=TMJL//TMJR//BP;
     line=Ri//Ro;
     R1=j(3,1)||plane[,1:2];
     L1=plane[,3];
     s1=inv(R1)*L1; /* z intercept and x and y slope for given plane */
     newpt=j(1,3,0); /* saves place for random new point */
     pln2=line//uniform(newpt); /* plane made up of line and new random pt */
     R2=j(3,1)||pln2[,1:2];
     L2=pln2[,3];
     s2=inv(R2)*L2; /* z intercept and x and y for dummy plane 2 */
```

Reproduced with permission of the copyright owner. Further reproduction prohibited without permission.

```
     pln3=line//uniform(newpt); /* dummy plane using another random third point */
     R3=j(3,1)||pln3[,1:2];
     L3=pln3[,3];
     s3=inv(R3)*L3;  /*third solution for plane 3 */
     S=(s1||s2||s3)`; /*  coefficient array putting solutions together */
     R4=S[,2:3]||j(3,1,-1);
     L4=-S[,1];
     xyz=inv(R4)*L4;  /*final solution of x, y, z points in common */
     LEVX=xyz[1,1];
     LEVY=xyz[2,1];
     LEVZ=xyz[3,1];

     LEV=LEVX||LEVY||LEVZ;


     /* Find C, point at which extension of line A-B crosses TMJ-TMJ */
       F=BPX-LEV[,1];
       G=K[34,1]-K[3,1];
        if F=0 then F=.00001;
        if G=0 then G=.00001;
       b1=(BPZ-LEV[,3])/F;              /* b1 = slope of top line */
       b2=(K[34,3]-K[3,3])/G;              /* b2 = slope of bottom line */
         if b1=0 then b1=.00001;
         if b2=0 then b2=.00001;
         H=b2-b1;
       a1=LEV[,3]-b1*LEV[,1];               /* a1 = intercept of top line */
       a2=K[3,3]-b2*K[3,1];               /* a2 = intercept of bottom line */
         if H=0 then H=.000-1;
       TMJ2Z=(a1*b2-a2*b1)/H;                /* Zi = Z axis intercept of top and
bottom lines */
       TMJ2X=(TMJ2Z-a1)/b1;                /* Xi = X axis intercept of top and
botom lines */

       F=BPX-LEV[,1];
       G=K[34,1]-K[3,1];
        if F=0 then F=.00001;
        if G=0 then G=.00001;
       b1=(BPY-LEV[,2])/F;              /* b1 = slope of top line */
       b2=(K[34,2]-K[3,3])/G;              /* b2 = slope of bottom line */
         if b1=0 then b1=.00001;
         if b2=0 then b2=.00001;
         H=b2-b1;
       a1=LEV[,2]-b1*LEV[,1];               /* a1 = intercept of top line */
       a2=K[3,2]-b2*K[3,1];               /* a2 = intercept of bottom line */
         if H=0 then H=.000-1;
       TMJ2Y=(a1*b2-a2*b1)/H;                /* Zi = Z axis intercept of top and
bottom lines */

       TMJ2=TMJ2X||TMJ2Y||TMJ2Z;

     /* Next lines of code finds xy coord for intersection of inter-
        maxillary tuberosity line and perpendicular through right
        masticatory mm. origin */


     RVEC=BP;

     OCINDL={29 60};
     OC=K[OCINDL,];
     L=RVEC;

     SOC=(OC[1,2]-OC[2,2])/(OC[1,1]-OC[2,1]);
     SL=-(1/SOC);
```

Reproduced with permission of the copyright owner. Further reproduction prohibited without permission.

```
LX=5;  /* Assign arbitrary value */

LY=SL*(LX-L[,1])+L[,2];

 F=OC[1,1]-OC[2,1];
 G=LX-L[,1];
 b1=(OC[1,2]-OC[2,2])/F;
 b2=(LY-L[,2])/G;
   H=b2-b1;
 a1=OC[2,2]-b1*OC[2,1];
 a2=L[,2]-b2*L[,1];
   if H=0 then H=.000-1;
 LYN=(a1*b2-a2*b1)/H;
 LXN=(LYN-a1)/b1;



/* Find new xyz point at which "shifted" resultant vector crosses
   triangle of support */

Mo=K[3,];

MTL=K[29,];
MTR=K[60,];
plane=MTL//MTR//LEV;
line=BP//Mo;
R1=j(3,1)||plane[,1:2];
L1=plane[,3];
s1=inv(R1)*L1; /* z intercept and x and y slope for given plane */
newpt=j(1,3,0); /* saves place for random new point */
pln2=line//uniform(newpt); /* plane made up of line and new random pt */
R2=j(3,1)||pln2[,1:2];
L2=pln2[,3];
s2=inv(R2)*L2; /* z intercept and x and y for dummy plane 2 */
pln3=line//uniform(newpt); /* dummy plane using another random third point */
R3=j(3,1)||pln3[,1:2];
L3=pln3[,3];
s3=inv(R3)*L3;  /*third solution for plane 3 */
S=(s1||s2||s3)`; /*  coefficient array putting solutions together */
R4=S[,2:3]||j(3,1,-1);
L4=-S[,1];
xyz=inv(R4)*L4;  /*final solution of x, y, z points in common */
MLEVX=xyz[1,1];  /* MLEV for modified LEV */
MLEVY=xyz[2,1];
MLEVZ=xyz[3,1];

MLEV=MLEVX||MLEVY||MLEVZ;



 LEVER=SQRT((((BPX)-TMJ2X)**2)+(((BPY)-TMJ2Y)**2)+(((BPZ)-TMJ2Z)**2));
 LOAD=SQRT((((LEV[,1])-TMJ2X)**2)+(((LEV[,2])-TMJ2Y)**2)+(((LEV[,3])-
TMJ2Z)**2));
 LEVER2=SQRT((((BPX)-K[3,1])**2)+(((BPY)-K[3,2])**2)+(((BPZ)-K[3,3])**2));
 LOAD2=SQRT(((K[3,1]-MLEV[,1])**2)+((K[3,2]-MLEV[,2])**2)+((K[3,3]-
MLEV[,3])**2));;

 LATRB=SQRT(((LEVX-LXN)**2)+((LEVY-LYN)**2));
 GRBR=SQRT(((MLEVX-LXN)**2)+((MLEVY-LYN)**2));
 FP=GRBR/LATRB*100;
 FPERC=(.90476+(.31286*FP)+(.00677*(FP**2)))/100;
 FORCEH=FORCE/2;
```

Reproduced with permission of the copyright owner. Further reproduction prohibited without permission.

```
/*FANGRAD=FANG*.017453293; NOT USED: ASSUMING FANG TO BE 90 DEGREES */


IF TMJ2Y>K[3,2] THEN BFPUP3=((((FORCEH*FPERC)+FORCEH))*LOAD2)/LEVER2;
ELSE BFPUP3=((FORCE)*LOAD)/LEVER;


/*---------------------------------------- */
/*FIND MAXIMUM BITE POINT FORCE FOR P4 = BFPUP4 */
/*---------------------------------------- */

BP=K[64,];
BPX=BP[1,1];
BPY=BP[1,2];
BPZ=BP[1,3];

/* Find B=xyz point at which resultant vector crosses plane defined by
 left and right TMJ and bite point */

TMJL=K[3,];
TMJR=K[34,];
plane=TMJL//TMJR//BP;
line=Ri//Ro;
R1=j(3,1)||plane[,1:2];
L1=plane[,3];
s1=inv(R1)*L1; /* z intercept and x and y slope for given plane */
newpt=j(1,3,0); /* saves place for random new point */
pln2=line//uniform(newpt); /* plane made up of line and new random pt */
R2=j(3,1)||pln2[,1:2];
L2=pln2[,3];
s2=inv(R2)*L2; /* z intercept and x and y for dummy plane 2 */
pln3=line//uniform(newpt); /* dummy plane using another random third point */
R3=j(3,1)||pln3[,1:2];
L3=pln3[,3];
s3=inv(R3)*L3;  /*third solution for plane 3 */
S=(s1||s2||s3)`; /*  coefficient array putting solutions together */
R4=S[,2:3]||j(3,1,-1);
L4=-S[,1];
xyz=inv(R4)*L4;  /*final solution of x, y, z points in common */
LEVX=xyz[1,1];
LEVY=xyz[2,1];
LEVZ=xyz[3,1];

LEV=LEVX||LEVY||LEVZ;


/* Find C, point at which extension of line A-B crosses TMJ-TMJ */
  F=BPX-LEV[,1];
  G=K[34,1]-K[3,1];
   if F=0 then F=.00001;
   if G=0 then G=.00001;
  b1=(BPZ-LEV[,3])/F;              /* b1 = slope of top line */
  b2=(K[34,3]-K[3,3])/G;             /* b2 = slope of bottom line */
    if b1=0 then b1=.00001;
    if b2=0 then b2=.00001;
    H=b2-b1;
  a1=LEV[,3]-b1*LEV[,1];              /* a1 = intercept of top line */
  a2=K[3,3]-b2*K[3,1];              /* a2 = intercept of bottom line */
    if H=0 then H=.000-1;
  TMJ2Z=(a1*b2-a2*b1)/H;               /* Zi = Z axis intercept of top and
bottom lines */
```

Reproduced with permission of the copyright owner. Further reproduction prohibited without permission.

```
      TMJ2X=(TMJ2Z-a1)/b1;                    /* Xi = X axis intercept of top and
botom lines */

      F=BPX-LEV[,1];
      G=K[34,1]-K[3,1];
       if F=0 then F=.00001;
       if G=0 then G=.00001;
      b1=(BPY-LEV[,2])/F;                  /* b1 = slope of top line */
      b2=(K[34,2]-K[3,3])/G;                  /* b2 = slope of bottom line */
        if b1=0 then b1=.00001;
        if b2=0 then b2=.00001;
        H=b2-b1;
      a1=LEV[,2]-b1*LEV[,1];                  /* a1 = intercept of top line */
      a2=K[3,2]-b2*K[3,1];                 /* a2 = intercept of bottom line */
        if H=0 then H=.000-1;
      TMJ2Y=(a1*b2-a2*b1)/H;                  /* Zi = Z axis intercept of top and
bottom lines */

      TMJ2=TMJ2X||TMJ2Y||TMJ2Z;

     /* Next lines of code finds xy coord for intersection of inter-
        maxillary tuberosity line and perpendicular through right
        masticatory mm. origin */


     RVEC=BP;

     OCINDL={29 60};
     OC=K[OCINDL,];
     L=RVEC;

     SOC=(OC[1,2]-OC[2,2])/(OC[1,1]-OC[2,1]);
     SL=-(1/SOC);

     LX=5;  /* Assign arbitrary value */

     LY=SL*(LX-L[,1])+L[,2];

      F=OC[1,1]-OC[2,1];
      G=LX-L[,1];
      b1=(OC[1,2]-OC[2,2])/F;
      b2=(LY-L[,2])/G;
        H=b2-b1;
      a1=OC[2,2]-b1*OC[2,1];
      a2=L[,2]-b2*L[,1];
        if H=0 then H=.000-1;
      LYN=(a1*b2-a2*b1)/H;
      LXN=(LYN-a1)/b1;



    /* Find new xyz point at which "shifted" resultant vector crosses
       triangle of support */

    Mo=K[3,];

    MTL=K[29,];
    MTR=K[60,];
    plane=MTL//MTR//LEV;
    line=BP//Mo;
    R1=j(3,1)||plane[,1:2];
    L1=plane[,3];
    s1=inv(R1)*L1; /* z intercept and x and y slope for given plane */
```

Reproduced with permission of the copyright owner. Further reproduction prohibited without permission.

```
     newpt=j(1,3,0); /* saves place for random new point */
     pln2=line//uniform(newpt); /* plane made up of line and new random pt */
     R2=j(3,1)||pln2[,1:2];
     L2=pln2[,3];
     s2=inv(R2)*L2; /* z intercept and x and y for dummy plane 2 */
     pln3=line//uniform(newpt); /* dummy plane using another random third point */
     R3=j(3,1)||pln3[,1:2];
     L3=pln3[,3];
     s3=inv(R3)*L3;  /*third solution for plane 3 */
     S=(s1||s2||s3)`; /*  coefficient array putting solutions together */
     R4=S[,2:3]||j(3,1,-1);
     L4=-S[,1];
     xyz=inv(R4)*L4;  /*final solution of x, y, z points in common */
     MLEVX=xyz[1,1];  /* MLEV for modified LEV */
     MLEVY=xyz[2,1];
     MLEVZ=xyz[3,1];

     MLEV=MLEVX||MLEVY||MLEVZ;



      LEVER=SQRT((((BPX)-TMJ2X)**2)+(((BPY)-TMJ2Y)**2)+(((BPZ)-TMJ2Z)**2));
      LOAD=SQRT((((LEV[,1])-TMJ2X)**2)+(((LEV[,2])-TMJ2Y)**2)+(((LEV[,3])-
TMJ2Z)**2));
      LEVER2=SQRT((((BPX)-K[3,1])**2)+(((BPY)-K[3,2])**2)+(((BPZ)-K[3,3])**2));
      LOAD2=SQRT(((K[3,1]-MLEV[,1])**2)+((K[3,2]-MLEV[,2])**2)+((K[3,3]-
MLEV[,3])**2));;

      LATRB=SQRT(((LEVX-LXN)**2)+((LEVY-LYN)**2));
      GRBR=SQRT(((MLEVX-LXN)**2)+((MLEVY-LYN)**2));
      FP=GRBR/LATRB*100;
      FPERC=(.90476+(.31286*FP)+(.00677*(FP**2)))/100;
      FORCEH=FORCE/2;


     /*FANGRAD=FANG*.017453293; NOT USED: ASSUMING FANG TO BE 90 DEGREES */


    IF TMJ2Y>K[3,2] THEN BFPUP4=((((FORCEH*FPERC)+FORCEH))*LOAD2)/LEVER2;
    ELSE BFPUP4=((FORCE)*LOAD)/LEVER;



     /*--------------------------------------- */
     /*FIND MAXIMUM BITE POINT FORCE FOR M1 = BFPUM1 */
     /*--------------------------------------- */

     BP=K[65,];
     BPX=BP[1,1];
     BPY=BP[1,2];
     BPZ=BP[1,3];

    /* Find B=xyz point at which resultant vector crosses plane defined by
     left and right TMJ and bite point */

     TMJL=K[3,];
     TMJR=K[34,];
     plane=TMJL//TMJR//BP;
     line=Ri//Ro;
     R1=j(3,1)||plane[,1:2];
     L1=plane[,3];
     s1=inv(R1)*L1; /* z intercept and x and y slope for given plane */
     newpt=j(1,3,0); /* saves place for random new point */
```

Reproduced with permission of the copyright owner. Further reproduction prohibited without permission.

```
pln2=line//uniform(newpt); /* plane made up of line and new random pt */
R2=j(3,1)||pln2[,1:2];
L2=pln2[,3];
s2=inv(R2)*L2; /* z intercept and x and y for dummy plane 2 */
pln3=line//uniform(newpt); /* dummy plane using another random third point */
R3=j(3,1)||pln3[,1:2];
L3=pln3[,3];
s3=inv(R3)*L3;  /*third solution for plane 3 */
S=(s1||s2||s3)`; /*  coefficient array putting solutions together */
R4=S[,2:3]||j(3,1,-1);
L4=-S[,1];
xyz=inv(R4)*L4;  /*final solution of x, y, z points in common */
LEVX=xyz[1,1];
LEVY=xyz[2,1];
LEVZ=xyz[3,1];

LEV=LEVX||LEVY||LEVZ;


/* Find C, point at which extension of line A-B crosses TMJ-TMJ */
  F=BPX-LEV[,1];
  G=K[34,1]-K[3,1];
   if F=0 then F=.00001;
   if G=0 then G=.00001;
  b1=(BPZ-LEV[,3])/F;              /* b1 = slope of top line */
  b2=(K[34,3]-K[3,3])/G;             /* b2 = slope of bottom line */
    if b1=0 then b1=.00001;
    if b2=0 then b2=.00001;
    H=b2-b1;
  a1=LEV[,3]-b1*LEV[,1];              /* a1 = intercept of top line */
  a2=K[3,3]-b2*K[3,1];              /* a2 = intercept of bottom line */
    if H=0 then H=.000-1;
  TMJ2Z=(a1*b2-a2*b1)/H;                /* Zi = Z axis intercept of top and
bottom lines */
  TMJ2X=(TMJ2Z-a1)/b1;                  /* Xi = X axis intercept of top and
botom lines */

  F=BPX-LEV[,1];
  G=K[34,1]-K[3,1];
   if F=0 then F=.00001;
   if G=0 then G=.00001;
  b1=(BPY-LEV[,2])/F;              /* b1 = slope of top line */
  b2=(K[34,2]-K[3,3])/G;             /* b2 = slope of bottom line */
    if b1=0 then b1=.00001;
    if b2=0 then b2=.00001;
    H=b2-b1;
  a1=LEV[,2]-b1*LEV[,1];              /* a1 = intercept of top line */
  a2=K[3,2]-b2*K[3,1];              /* a2 = intercept of bottom line */
    if H=0 then H=.000-1;
  TMJ2Y=(a1*b2-a2*b1)/H;                /* Zi = Z axis intercept of top and
bottom lines */

  TMJ2=TMJ2X||TMJ2Y||TMJ2Z;

/* Next lines of code finds xy coord for intersection of inter-
   maxillary tuberosity line and perpendicular through right
   masticatory mm. origin */


RVEC=BP;

OCINDL={29 60};
```

Reproduced with permission of the copyright owner. Further reproduction prohibited without permission.

```
OC=K[OCINDL,];
L=RVEC;

SOC=(OC[1,2]-OC[2,2])/(OC[1,1]-OC[2,1]);
SL=-(1/SOC);

LX=5;  /* Assign arbitrary value */

LY=SL*(LX-L[,1])+L[,2];

 F=OC[1,1]-OC[2,1];
 G=LX-L[,1];
 b1=(OC[1,2]-OC[2,2])/F;
 b2=(LY-L[,2])/G;
   H=b2-b1;
 a1=OC[2,2]-b1*OC[2,1];
 a2=L[,2]-b2*L[,1];
   if H=0 then H=.000-1;
 LYN=(a1*b2-a2*b1)/H;
 LXN=(LYN-a1)/b1;



/* Find new xyz point at which "shifted" resultant vector crosses
   triangle of support */

Mo=K[3,];

MTL=K[29,];
MTR=K[60,];
plane=MTL//MTR//LEV;
line=BP//Mo;
R1=j(3,1)||plane[,1:2];
L1=plane[,3];
s1=inv(R1)*L1; /* z intercept and x and y slope for given plane */
newpt=j(1,3,0); /* saves place for random new point */
pln2=line//uniform(newpt); /* plane made up of line and new random pt */
R2=j(3,1)||pln2[,1:2];
L2=pln2[,3];
s2=inv(R2)*L2; /* z intercept and x and y for dummy plane 2 */
pln3=line//uniform(newpt); /* dummy plane using another random third point */
R3=j(3,1)||pln3[,1:2];
L3=pln3[,3];
s3=inv(R3)*L3;  /*third solution for plane 3 */
S=(s1||s2||s3)`; /*  coefficient array putting solutions together */
R4=S[,2:3]||j(3,1,-1);
L4=-S[,1];
xyz=inv(R4)*L4;  /*final solution of x, y, z points in common */
MLEVX=xyz[1,1];  /* MLEV for modified LEV */
MLEVY=xyz[2,1];
MLEVZ=xyz[3,1];

MLEV=MLEVX||MLEVY||MLEVZ;



 LEVER=SQRT((((BPX)-TMJ2X)**2)+(((BPY)-TMJ2Y)**2)+(((BPZ)-TMJ2Z)**2));
 LOAD=SQRT((((LEV[,1])-TMJ2X)**2)+(((LEV[,2])-TMJ2Y)**2)+(((LEV[,3])-
TMJ2Z)**2));
 LEVER2=SQRT((((BPX)-K[3,1])**2)+(((BPY)-K[3,2])**2)+(((BPZ)-K[3,3])**2));
 LOAD2=SQRT(((K[3,1]-MLEV[,1])**2)+((K[3,2]-MLEV[,2])**2)+((K[3,3]-
MLEV[,3])**2));;
```

Reproduced with permission of the copyright owner. Further reproduction prohibited without permission.

```
  LATRB=SQRT(((LEVX-LXN)**2)+((LEVY-LYN)**2));
  GRBR=SQRT(((MLEVX-LXN)**2)+((MLEVY-LYN)**2));
  FP=GRBR/LATRB*100;
  FPERC=(.90476+(.31286*FP)+(.00677*(FP**2)))/100;
  FORCEH=FORCE/2;

  M1FP=FPERC;

 /*FANGRAD=FANG*.017453293; NOT USED: ASSUMING FANG TO BE 90 DEGREES */


IF TMJ2Y>K[3,2] THEN BFPUM1=((((FORCEH*FPERC)+FORCEH))*LOAD2)/LEVER2;
ELSE BFPUM1=((FORCE)*LOAD)/LEVER;

IF TMJ2Y>K[3,2] THEN LEVADV=LOAD2/LEVER2*100;
ELSE LEVADV=LOAD/LEVER*100;


 /*---------------------------------------- */
 /*FIND MAXIMUM BITE POINT FORCE FOR M2 = BFPUM2 */
 /*---------------------------------------- */

 BP=K[66,];
 BPX=BP[1,1];
 BPY=BP[1,2];
 BPZ=BP[1,3];

/* Find B=xyz point at which resultant vector crosses plane defined by
 left and right TMJ and bite point */

 TMJL=K[3,];
 TMJR=K[34,];
 plane=TMJL//TMJR//BP;
 line=Ri//Ro;
 R1=j(3,1)||plane[,1:2];
 L1=plane[,3];
 s1=inv(R1)*L1; /* z intercept and x and y slope for given plane */
 newpt=j(1,3,0); /* saves place for random new point */
 pln2=line//uniform(newpt); /* plane made up of line and new random pt */
 R2=j(3,1)||pln2[,1:2];
 L2=pln2[,3];
 s2=inv(R2)*L2; /* z intercept and x and y for dummy plane 2 */
 pln3=line//uniform(newpt); /* dummy plane using another random third point */
 R3=j(3,1)||pln3[,1:2];
 L3=pln3[,3];
 s3=inv(R3)*L3;  /*third solution for plane 3 */
 S=(s1||s2||s3)`; /*  coefficient array putting solutions together */
 R4=S[,2:3]||j(3,1,-1);
 L4=-S[,1];
 xyz=inv(R4)*L4;  /*final solution of x, y, z points in common */
 LEVX=xyz[1,1];
 LEVY=xyz[2,1];
 LEVZ=xyz[3,1];

 LEV=LEVX||LEVY||LEVZ;


 /* Find C, point at which extension of line A-B crosses TMJ-TMJ */
   F=BPX-LEV[,1];
   G=K[34,1]-K[3,1];
    if F=0 then F=.00001;
    if G=0 then G=.00001;
   b1=(BPZ-LEV[,3])/F;              /* b1 = slope of top line */
```

Reproduced with permission of the copyright owner. Further reproduction prohibited without permission.

```
      b2=(K[34,3]-K[3,3])/G;                /* b2 = slope of bottom line */
        if b1=0 then b1=.00001;
        if b2=0 then b2=.00001;
        H=b2-b1;
      a1=LEV[,3]-b1*LEV[,1];                /* a1 = intercept of top line */
      a2=K[3,3]-b2*K[3,1];                 /* a2 = intercept of bottom line */
        if H=0 then H=.000-1;
      TMJ2Z=(a1*b2-a2*b1)/H;                 /* Zi = Z axis intercept of top and
bottom lines */
      TMJ2X=(TMJ2Z-a1)/b1;                   /* Xi = X axis intercept of top and
botom lines */

      F=BPX-LEV[,1];
      G=K[34,1]-K[3,1];
       if F=0 then F=.00001;
       if G=0 then G=.00001;
      b1=(BPY-LEV[,2])/F;                 /* b1 = slope of top line */
      b2=(K[34,2]-K[3,3])/G;                 /* b2 = slope of bottom line */
        if b1=0 then b1=.00001;
        if b2=0 then b2=.00001;
        H=b2-b1;
      a1=LEV[,2]-b1*LEV[,1];                /* a1 = intercept of top line */
      a2=K[3,2]-b2*K[3,1];                 /* a2 = intercept of bottom line */
        if H=0 then H=.000-1;
      TMJ2Y=(a1*b2-a2*b1)/H;                 /* Zi = Z axis intercept of top and
bottom lines */

      TMJ2=TMJ2X||TMJ2Y||TMJ2Z;

     /* Next lines of code finds xy coord for intersection of inter-
        maxillary tuberosity line and perpendicular through right
        masticatory mm. origin */


     RVEC=BP;

     OCINDL={29 60};
     OC=K[OCINDL,];
     L=RVEC;

     SOC=(OC[1,2]-OC[2,2])/(OC[1,1]-OC[2,1]);
     SL=-(1/SOC);

     LX=5;  /* Assign arbitrary value */

     LY=SL*(LX-L[,1])+L[,2];

      F=OC[1,1]-OC[2,1];
      G=LX-L[,1];
      b1=(OC[1,2]-OC[2,2])/F;
      b2=(LY-L[,2])/G;
        H=b2-b1;
      a1=OC[2,2]-b1*OC[2,1];
      a2=L[,2]-b2*L[,1];
        if H=0 then H=.000-1;
      LYN=(a1*b2-a2*b1)/H;
      LXN=(LYN-a1)/b1;



    /* Find new xyz point at which "shifted" resultant vector crosses
       triangle of support */
```

Reproduced with permission of the copyright owner. Further reproduction prohibited without permission.

```
     Mo=K[3,];

     MTL=K[29,];
     MTR=K[60,];
     plane=MTL//MTR//LEV;
     line=BP//Mo;
     R1=j(3,1)||plane[,1:2];
     L1=plane[,3];
     s1=inv(R1)*L1; /* z intercept and x and y slope for given plane */
     newpt=j(1,3,0); /* saves place for random new point */
     pln2=line//uniform(newpt); /* plane made up of line and new random pt */
     R2=j(3,1)||pln2[,1:2];
     L2=pln2[,3];
     s2=inv(R2)*L2; /* z intercept and x and y for dummy plane 2 */
     pln3=line//uniform(newpt); /* dummy plane using another random third point */
     R3=j(3,1)||pln3[,1:2];
     L3=pln3[,3];
     s3=inv(R3)*L3;  /*third solution for plane 3 */
     S=(s1||s2||s3)`; /*  coefficient array putting solutions together */
     R4=S[,2:3]||j(3,1,-1);
     L4=-S[,1];
     xyz=inv(R4)*L4;  /*final solution of x, y, z points in common */
     MLEVX=xyz[1,1];  /* MLEV for modified LEV */
     MLEVY=xyz[2,1];
     MLEVZ=xyz[3,1];

     MLEV=MLEVX||MLEVY||MLEVZ;



      LEVER=SQRT((((BPX)-TMJ2X)**2)+(((BPY)-TMJ2Y)**2)+(((BPZ)-TMJ2Z)**2));
      LOAD=SQRT((((LEV[,1])-TMJ2X)**2)+(((LEV[,2])-TMJ2Y)**2)+(((LEV[,3])-
TMJ2Z)**2));
      LEVER2=SQRT((((BPX)-K[3,1])**2)+(((BPY)-K[3,2])**2)+(((BPZ)-K[3,3])**2));
      LOAD2=SQRT(((K[3,1]-MLEV[,1])**2)+((K[3,2]-MLEV[,2])**2)+((K[3,3]-
MLEV[,3])**2));;

      LATRB=SQRT(((LEVX-LXN)**2)+((LEVY-LYN)**2));
      GRBR=SQRT(((MLEVX-LXN)**2)+((MLEVY-LYN)**2));
      FP=GRBR/LATRB*100;
      FPERC=(.90476+(.31286*FP)+(.00677*(FP**2)))/100;
      FORCEH=FORCE/2;

      M2FP=FPERC;

     /*FANGRAD=FANG*.017453293; NOT USED: ASSUMING FANG TO BE 90 DEGREES */


    IF TMJ2Y>K[3,2] THEN BFPUM2=((((FORCEH*FPERC)+FORCEH))*LOAD2)/LEVER2;
    ELSE BFPUM2=((FORCE)*LOAD)/LEVER;


     /*-------------------------------------- */
     /*FIND MAXIMUM BITE POINT FORCE FOR M3 = BFPUM3 */
     /*-------------------------------------- */

     BP=K[55,];
     BPX=BP[1,1];
     BPY=BP[1,2];
     BPZ=BP[1,3];

    /* Find B=xyz point at which resultant vector crosses plane defined by
     left and right TMJ and bite point */
```

Reproduced with permission of the copyright owner. Further reproduction prohibited without permission.

```
TMJL=K[3,];
TMJR=K[34,];
plane=TMJL//TMJR//BP;
line=Ri//Ro;
R1=j(3,1)||plane[,1:2];
L1=plane[,3];
s1=inv(R1)*L1; /* z intercept and x and y slope for given plane */
newpt=j(1,3,0); /* saves place for random new point */
pln2=line//uniform(newpt); /* plane made up of line and new random pt */
R2=j(3,1)||pln2[,1:2];
L2=pln2[,3];
s2=inv(R2)*L2; /* z intercept and x and y for dummy plane 2 */
pln3=line//uniform(newpt); /* dummy plane using another random third point */
R3=j(3,1)||pln3[,1:2];
L3=pln3[,3];
s3=inv(R3)*L3;  /*third solution for plane 3 */
S=(s1||s2||s3)`; /*  coefficient array putting solutions together */
R4=S[,2:3]||j(3,1,-1);
L4=-S[,1];
xyz=inv(R4)*L4;  /*final solution of x, y, z points in common */
LEVX=xyz[1,1];
LEVY=xyz[2,1];
LEVZ=xyz[3,1];

LEV=LEVX||LEVY||LEVZ;


/* Find C, point at which extension of line A-B crosses TMJ-TMJ */
  F=BPX-LEV[,1];
  G=K[34,1]-K[3,1];
   if F=0 then F=.00001;
   if G=0 then G=.00001;
  b1=(BPZ-LEV[,3])/F;              /* b1 = slope of top line */
  b2=(K[34,3]-K[3,3])/G;              /* b2 = slope of bottom line */
    if b1=0 then b1=.00001;
    if b2=0 then b2=.00001;
    H=b2-b1;
  a1=LEV[,3]-b1*LEV[,1];               /* a1 = intercept of top line */
  a2=K[3,3]-b2*K[3,1];               /* a2 = intercept of bottom line */
    if H=0 then H=.000-1;
  TMJ2Z=(a1*b2-a2*b1)/H;                /* Zi = Z axis intercept of top and
bottom lines */
  TMJ2X=(TMJ2Z-a1)/b1;                /* Xi = X axis intercept of top and
botom lines */

  F=BPX-LEV[,1];
  G=K[34,1]-K[3,1];
   if F=0 then F=.00001;
   if G=0 then G=.00001;
  b1=(BPY-LEV[,2])/F;              /* b1 = slope of top line */
  b2=(K[34,2]-K[3,3])/G;              /* b2 = slope of bottom line */
    if b1=0 then b1=.00001;
    if b2=0 then b2=.00001;
    H=b2-b1;
  a1=LEV[,2]-b1*LEV[,1];               /* a1 = intercept of top line */
  a2=K[3,2]-b2*K[3,1];               /* a2 = intercept of bottom line */
    if H=0 then H=.000-1;
  TMJ2Y=(a1*b2-a2*b1)/H;                /* Zi = Z axis intercept of top and
bottom lines */

  TMJ2=TMJ2X||TMJ2Y||TMJ2Z;
```

Reproduced with permission of the copyright owner. Further reproduction prohibited without permission.

```
/* Next lines of code finds xy coord for intersection of inter-
   maxillary tuberosity line and perpendicular through right
   masticatory mm. origin */

RVEC=BP;

OCINDL={29 60};
OC=K[OCINDL,];
L=RVEC;

SOC=(OC[1,2]-OC[2,2])/(OC[1,1]-OC[2,1]);
SL=-(1/SOC);

LX=5;  /* Assign arbitrary value */

LY=SL*(LX-L[,1])+L[,2];

 F=OC[1,1]-OC[2,1];
 G=LX-L[,1];
 b1=(OC[1,2]-OC[2,2])/F;
 b2=(LY-L[,2])/G;
   H=b2-b1;
 a1=OC[2,2]-b1*OC[2,1];
 a2=L[,2]-b2*L[,1];
   if H=0 then H=.000-1;
 LYN=(a1*b2-a2*b1)/H;
 LXN=(LYN-a1)/b1;



/* Find new xyz point at which "shifted" resultant vector crosses
   triangle of support */

Mo=K[3,];

MTL=K[29,];
MTR=K[60,];
plane=MTL//MTR//LEV;
line=BP//Mo;
R1=j(3,1)||plane[,1:2];
L1=plane[,3];
s1=inv(R1)*L1; /* z intercept and x and y slope for given plane */
newpt=j(1,3,0); /* saves place for random new point */
pln2=line//uniform(newpt); /* plane made up of line and new random pt */
R2=j(3,1)||pln2[,1:2];
L2=pln2[,3];
s2=inv(R2)*L2; /* z intercept and x and y for dummy plane 2 */
pln3=line//uniform(newpt); /* dummy plane using another random third point */
R3=j(3,1)||pln3[,1:2];
L3=pln3[,3];
s3=inv(R3)*L3;  /*third solution for plane 3 */
S=(s1||s2||s3)`; /*  coefficient array putting solutions together */
R4=S[,2:3]||j(3,1,-1);
L4=-S[,1];
xyz=inv(R4)*L4;  /*final solution of x, y, z points in common */
MLEVX=xyz[1,1];  /* MLEV for modified LEV */
MLEVY=xyz[2,1];
MLEVZ=xyz[3,1];

MLEV=MLEVX||MLEVY||MLEVZ;


 LEVER=SQRT(((BPX)-TMJ2X)**2)+(((BPY)-TMJ2Y)**2)+(((BPZ)-TMJ2Z)**2));
```

Reproduced with permission of the copyright owner. Further reproduction prohibited without permission.

```
     LOAD=SQRT(((LEV[,1])-TMJ2X)**2)+(((LEV[,2])-TMJ2Y)**2)+(((LEV[,3])-
TMJ2Z)**2));
     LEVER2=SQRT(((BPX)-K[3,1])**2)+(((BPY)-K[3,2])**2)+(((BPZ)-K[3,3])**2));
     LOAD2=SQRT(((K[3,1]-MLEV[,1])**2)+((K[3,2]-MLEV[,2])**2)+((K[3,3]-
MLEV[,3])**2));;

     LATRB=SQRT(((LEVX-LXN)**2)+((LEVY-LYN)**2));
     GRBR=SQRT(((MLEVX-LXN)**2)+((MLEVY-LYN)**2));
     FP=GRBR/LATRB*100;
     FPERC=(.90476+(.31286*FP)+(.00677*(FP**2)))/100;
     FORCEH=FORCE/2;

     M3FP=FPERC;

    /*FANGRAD=FANG*.017453293; NOT USED: ASSUMING FANG TO BE 90 DEGREES */


   IF TMJ2Y>K[3,2] THEN BFPUM3=((((FORCEH*FPERC)+FORCEH))*LOAD2)/LEVER2;
   ELSE BFPUM3=((FORCE)*LOAD)/LEVER;

 /*-----------------------------------------------------------------*/
 /*ANTBFM: Average anterior bite force magnitude */
   ANTBFM=(BFPUI1+BFPUI2)/2;

 /*-----------------------------------------------------------------*/
 /*PSTBFM: Average posterior bite force magnitude */
   PSTBFM=(BFPUP3+BFPUP4+BFPUM1+BFPUM2+BFPUM3)/5;

 /*-----------------------------------------------------------------*/
 /*RELBFM: Relative posterior bite force magnitude */
   RELBFM=(ANTBFM/PSTBFM)*100;

 /*-----------------------------------------------------------------*/
 /*MAXBFM: Average bite force magnitude */
   MAXBFM=(BFPUI1+BFPUI2+BFPUP3+BFPUP4+BFPUM1+BFPUM2+BFPUM3)/7;

 /*-----------------------------------------------------------------*/
 /*APMASS: Expressed as a percent (ratio): First find xz coordinate (APM)
   intersection of two lines: TMJ to I1 and masseter insertion to origin:
   then take ratio of TMJ to APM over TMJ to I1 expressed as a percent */

      /* Find APM, xz point at which TJM TO I1 crosses masseter insertion
         to origin */
      F=K[89,1]-K[98,1];
      G=K[34,1]-K[62,1];
       if F=0 then F=.00001;
       if G=0 then G=.00001;
      b1=(K[89,3]-K[98,3])/F;              /* b1 = slope of top line */
      b2=(K[34,3]-K[62,3])/G;              /* b2 = slope of bottom line */
        if b1=0 then b1=.00001;
        if b2=0 then b2=.00001;
        H=b2-b1;
      a1=K[98,3]-b1*K[98,1];               /* a1 = intercept of top line */
      a2=K[62,3]-b2*K[62,1];               /* a2 = intercept of bottom line */
        if H=0 then H=.000-1;
      APMZ=(a1*b2-a2*b1)/H;                /* Zi = Z axis intercept of top and
bottom lines */
      APMX=(APMZ-a1)/b1;                  /* Xi = X axis intercept of top and botom
lines */

      TMJAPM=SQRT((((K[34,1])-(APMX))**2)+(((K[34,3])-(APMZ))**2));
      TMJI1=SQRT((((K[34,1])-(K[62,1]))**2)+(((K[34,3])-(K[62,3]))**2));
```

Reproduced with permission of the copyright owner. Further reproduction prohibited without permission.

```
      APMASS=(TMJAPM/TMJI1)*100;

 /*-----------------------------------------------------------------*/
 /*APTEMP: Expressed as a percent (ratio): First find xz coordinate (TPM)
   intersection of two lines: TMJ to I1 and temporalis insertion to origin:
   then take ratio of TMJ to TPM over TMJ to I1 expressed as a percent */

      /* Find TPM, xz point at which TJM TO I1 crosses masseter insertion
         to origin */
      F=TEMRX-K[97,1];
      G=K[34,1]-K[62,1];
       if F=0 then F=.00001;
       if G=0 then G=.00001;
      b1=(TEMRZ-K[97,3])/F;              /* b1 = slope of top line */
      b2=(K[34,3]-K[62,3])/G;             /* b2 = slope of bottom line */
        if b1=0 then b1=.00001;
        if b2=0 then b2=.00001;
        H=b2-b1;
      a1=K[97,3]-b1*K[97,1];              /* a1 = intercept of top line */
      a2=K[62,3]-b2*K[62,1];              /* a2 = intercept of bottom line */
        if H=0 then H=.000-1;
      TPMZ=(a1*b2-a2*b1)/H;               /* Zi = Z axis intercept of top and
bottom lines */
      TPMX=(TPMZ-a1)/b1;                 /* Xi = X axis intercept of top and botom
lines */

      TMJTPM=SQRT((((K[34,1])-(TPMX))**2)+(((K[34,3])-(TPMZ))**2));
      TMJI1=SQRT((((K[34,1])-(K[62,1]))**2)+(((K[34,3])-(K[62,3]))**2));

      APTEMP=(TMJTPM/TMJI1)*100;

 /*-----------------------------------------------------------------*/
 /*LEVADV: load arm/lever arm at M1 */
 /*Previously defined */

 /*-----------------------------------------------------------------*/
   TEMPMM=TFORCE;

 /*-----------------------------------------------------------------*/
 /*CFORCE: Magnitude of resultant vector of temporalis and masseter muscles*/
   CFORCE=FORCE;

 /*-----------------------------------------------------------------*/
 /*RMMEFF: Resultant mastictory muscle efficiency: angle between resultant
   mastictory muscle vector and occlusal plane: should be close to 90 degrees */
   RMMEFF=FANG;

 /*-----------------------------------------------------------------*/
 /*APFMAG: Anteroposterior position of foramen magnum */
   MIDFM=(K[1,1]+K[32,1])/2;
   POSTFM=SQRT((K[103,1]-MIDFM)**2);
   POSTANT=SQRT((K[103,1]-K[104,1])**2);
   APFMAG=POSTFM/POSTANT*100;

 /*-----------------------------------------------------------------*/
 /*SLOPFM: Slope of foramen magnum relative to Frankfort horizontal */

  L1=XORB-XBIP;
  N1=ZORB-ZBIP;
  L2=K[76,1]-K[77,1];
  N2=K[76,3]-K[77,3];
  cosSLPFM=((L1*L2)+(N1*N2))/((SQRT((L1**2)+(N1**2)))*
         (SQRT((L2**2)+(N2**2))));
```

Reproduced with permission of the copyright owner. Further reproduction prohibited without permission.

```
 SLOPFM=180-(arcos(cosSLPFM)*180/3.14159265); /*This converts a cosine into
 degrees */


/*-------------------------------------------------------------------*/
/*APOCND: Anteroposterior position of occipital condyles */
  MIDOC=(K[85,1]+K[86,1])/2;
  POSTFM=SQRT((K[103,1]-MIDOC)**2);
  POSTANT=SQRT((K[103,1]-K[104,1])**2);
  APOCND=POSTFM/POSTANT*100;

/*-------------------------------------------------------------------*/
/*CBFLEX: Cranial base flexion */

 L1=K[70,1]-K[101,1];
 N1=K[70,3]-K[101,3];
 L2=K[101,1]-K[77,1];
 N2=K[101,3]-K[77,3];
 cosCBF=((L1*L2)+(N1*N2))/((SQRT((L1**2)+(N1**2)))*
        (SQRT((L2**2)+(N2**2))));
 CBFLEX=180-(arcos(cosCBF)*180/3.14159265); /*This converts a cosine into
 degrees */

/*-------------------------------------------------------------------*/
/*ENLWCP: Enlowian cribriform plate angle */

 L1=K[105,1]-K[106,1];
 N1=K[105,3]-K[106,3];
 L2=K[100,1]-K[67,1];
 N2=K[100,3]-K[67,3];
 cosENCP=((L1*L2)+(N1*N2))/((SQRT((L1**2)+(N1**2)))*
        (SQRT((L2**2)+(N2**2))));
 ENLWCP=180-(arcos(cosENCP)*180/3.14159265); /*This converts a cosine into
 degrees */

/*-------------------------------------------------------------------*/
/*ENLWOB: Enlowian olfactory bulb angle */

 L1=K[107,1]-K[108,1];
 N1=K[107,3]-K[108,3];
 L2=K[100,1]-K[67,1];
 N2=K[100,3]-K[67,3];
 cosENCP=((L1*L2)+(N1*N2))/((SQRT((L1**2)+(N1**2)))*
        (SQRT((L2**2)+(N2**2))));
 ENLWOB=180-(arcos(cosENCP)*180/3.14159265); /*This converts a cosine into
 degrees */

/*-------------------------------------------------------------------*/
/*ENLOBO: Enlowian olfactory bulb orientation: angle between perpendicular
  of midpoint line through 4 olfactory bulb points, and midfacial plane */

 OLFX=(K[107,1]+K[108,1])/2;
 OLFZ=(K[107,3]+K[108,3])/2;
 CBPX=(K[105,1]+K[106,1])/2;
 CBPZ=(K[105,3]+K[106,3])/2;

 L1=OLFX-CBPX;
 N1=OLFZ-CBPZ;
 L2=K[100,1]-K[67,1];
 N2=K[100,3]-K[67,3];
 cosENCP=((L1*L2)+(N1*N2))/((SQRT((L1**2)+(N1**2)))*
        (SQRT((L2**2)+(N2**2))));
 ENLOBOA=(arcos(cosENCP)*180/3.14159265); /*This converts a cosine into
```

Reproduced with permission of the copyright owner. Further reproduction prohibited without permission.

```
 degrees */

 ENLOBO=180-ENLOBOA-90;

/*-----------------------------------------------------------------*/
/*SLPCPF: Slope of cribriform plate relative to Frankfort horizontal */

 L1=XORB-XBIP;
 N1=ZORB-ZBIP;
 L2=K[106,1]-K[105,1];
 N2=K[106,3]-K[105,3];
 cosSLPCP=((L1*L2)+(N1*N2))/((SQRT((L1**2)+(N1**2)))*
        (SQRT((L2**2)+(N2**2))));
 SLPCPF=180-(arcos(cosSLPCP)*180/3.14159265); /*This converts a cosine into
 degrees */

/*-----------------------------------------------------------------*/
/*SLPCPO: Slope of cribriform plate relative to occlusal plane */

 L1=BIP3[,1]-BIM3[,1];
 N1=BIP3[,3]-BIM3[,3];
 L2=K[106,1]-K[105,1];
 N2=K[106,3]-K[105,3];
 cosSLCPO=((L1*L2)+(N1*N2))/((SQRT((L1**2)+(N1**2)))*
        (SQRT((L2**2)+(N2**2))));
 SLPCPO=180-(arcos(cosSLCPO)*180/3.14159265); /*This converts a cosine into
 degrees */

/*-----------------------------------------------------------------*/
/*SLPOBF: Slope of olfactory bulbs relative to Frankfort horizontal */

 L1=XORB-XBIP;
 N1=ZORB-ZBIP;
 L2=K[108,1]-K[107,1];
 N2=K[108,3]-K[107,3];
 cosSLPOB=((L1*L2)+(N1*N2))/((SQRT((L1**2)+(N1**2)))*
        (SQRT((L2**2)+(N2**2))));
 SLPOBF=180-(arcos(cosSLPOB)*180/3.14159265); /*This converts a cosine into
 degrees */

/*-----------------------------------------------------------------*/
/*SLPOBO: Slope of olfactory bulbs relative to occlusal plane */

 L1=BIP3[,1]-BIM3[,1];
 N1=BIP3[,3]-BIM3[,3];
 L2=K[108,1]-K[107,1];
 N2=K[108,3]-K[107,3];
 cosSLOBO=((L1*L2)+(N1*N2))/((SQRT((L1**2)+(N1**2)))*
        (SQRT((L2**2)+(N2**2))));
 SLPOBO=180-(arcos(cosSLOBO)*180/3.14159265); /*This converts a cosine into
 degrees */

/*-----------------------------------------------------------------*/
/*MCFLGT: Middle cranial fossa length */
  MCFL=SQRT((BIPOR[,1]-K[102,1])**2);
  NCLG=SQRT((K[103,1]-K[104,1])**2);
  MCFLGT=MCFL/NCLG*100;

/*-----------------------------------------------------------------*/
/*ACFLGT: Anterior cranial fossa length */
  ACFL=SQRT((K[102,1]-K[104,1])**2);
  NCLG=SQRT((K[103,1]-K[104,1])**2);
  ACFLGT=ACFL/NCLG*100;
```

Reproduced with permission of the copyright owner. Further reproduction prohibited without permission.

```
 /*-------------------------------------------------------------------*/
 /*FMAGSZ: Foramen magnum size (area) */
   FMAGSZ=(3.14159265*((SQRT((((K[76,1])-(K[77,1]))**2)+(((K[76,2])-(K[77,2]))**2)+
        (((K[76,3])-(K[77,3]))**2)))/2)*((SQRT((((K[1,1])-(K[32,1]))**2)+
        (((K[1,2])-(K[32,2]))**2)+(((K[1,3])-(K[32,3]))**2)))/2));

 /*-------------------------------------------------------------------*/
 /*CEPHID: Cephalic index */
   LATBC=SQRT((((K[10,1])-(K[41,1]))**2)+(((K[10,2])-(K[41,2]))**2)+(((K[10,3])-
(K[41,3]))**2));
   NCLG=SQRT((((K[103,1])-(K[104,1]))**2)+(((K[103,2])-(K[104,2]))**2)+(((K[103,3])-
(K[104,3]))**2));
   CEPHID=LATBC/NCLG*100;

 /*-------------------------------------------------------------------*/
 /*CANINE: Estimated canine volume with canine modeled as a cone */
   BASW=(SQRT((((K[91,1])-(K[92,1]))**2)+(((K[91,2])-(K[92,2]))**2)+(((K[91,3])-
(K[92,3]))**2)))/2;
   BASL=(SQRT((((K[93,1])-(K[94,1]))**2)+(((K[93,2])-(K[94,2]))**2)+(((K[93,3])-
(K[94,3]))**2)))/2;
   RSQR=BASW*BASL;
   BASEMX=(K[91,1]+K[92,1]+K[93,1]+K[94,1])/4;
   BASEMY=(K[91,2]+K[92,2]+K[93,2]+K[94,2])/4;
   BASEMZ=(K[91,3]+K[92,3]+K[93,3]+K[94,3])/4;
   BASEM=BASEMX||BASEMY||BASEMZ;
   HEIGHT=SQRT((((BASEM[,1])-(K[90,1]))**2)+(((BASEM[,2])-
(K[90,2]))**2)+(((BASEM[,3])-(K[90,3]))**2));
   CANINE=(3.14159265*RSQR*HEIGHT)/3;

  /*-------------------------------------------------------------------*/

/*-------------------------------------------------------------------*/

   FILENAME DISSNI 'C:\DISSDATA\AA.OUT';
   FILE DISSNI LRECL=1000;
   PUT NASLGT 8.2 NASWDU 8.2 NASWDL 8.2 NPMWDT 8.2 NSLAHT 8.2 NSLAWD 8.2
       PNASHT 8.2 PNASWD 8.2 NLCLGT 8.2 ZYGARE 8.2 ZYGOHT 8.2 BZYGWD 8.2
       APZYGR 8.2 MXARCL 8.2 BMAXWD 8.2 UMAXWD 8.2 AFACHT 8.2 PFACHT 8.2
       RAMSHT 8.2 I2PALW 8.2 P3PALW 8.2 M1PALW 8.2 M3PALW 8.2 I2PALD 8.2
       P3PALD 8.2 M1PALD 8.2 M3PALD 8.2 PALLGT 8.2 PALTHK 8.2 KROGAG 8.2
       ENLOAG 8.2 SLOPOC 8.2 FACCNV 8.2 FACSIZ 8.2 PPNALO 8.2 ORBIHT 8.2
       CRLGTH 8.2 NCLGTH 8.2 BCLGTH 8.2 BIPORB 8.2 SKCNTR 8.2 CRBTHK 8.2
       OFBVOL 8.2 OFBARE 8.2 ORBSCR 8.2 ORBTC1 8.2 ORBTC2 8.2 ORBA12 8.2
       IORBDS 8.2 BFPUI1 8.2 BFPUI2 8.2
       BFPUP3 8.2 BFPUP4 8.2 BFPUM1 8.2 BFPUM2 8.2 BFPUM3 8.2 ANTBFM 8.2
       PSTBFM 8.2 RELBFM 8.2 MAXBFM 8.2 APMASS 8.2 APTEMP 8.2 LEVADV 8.2
       TEMPMM 8.2 CFORCE 8.2 RMMEFF 8.2 APFMAG 8.2 SLOPFM 8.2 APOCND 8.2
       CBFLEX 8.2
       ENLWCP 8.2 ENLWOB 8.2 ENLOBO 8.2 SLPCPF 8.2 SLPCPO 8.2 SLPOBF 8.2
       SLPOBO 8.2
       MCFLGT 8.2 ACFLGT 8.2 FMAGSZ 8.2 CEPHID 8.2 CANINE 8.2
       ;
    CLOSEFILE DISSNI;

/*
 PRINT NASLGT [format=5.1] NASWDU [format=5.1] NASWDL [format=5.1];
 PRINT NASWDT [format=5.1] NSLAHT [format=5.1] NSLAWD [format=5.1];
 PRINT PNASHT [format=5.1] PNASWD [format=5.1] NLCLGT [format=5.1];
 PRINT                     ZYGOHT [format=5.1] BZYGWD [format=5.1];
 PRINT APZYGR [format=5.1] APZYGR [format=5.1] MXARCL [format=5.1];
 PRINT BMAXWD [format=5.1] UMAXWD [format=5.1] AFACHT [format=5.1];
 PRINT PFACHT [format=5.1] RAMSHT [foramt=5.1] I2PALW [format=5.1];
```

Reproduced with permission of the copyright owner. Further reproduction prohibited without permission.

```
 PRINT P3PALW [format=5.1] M1PALW [format=5.1] M3PALW [format=5.1];
 PRINT 12PALD [format=5.1] P3PALD [format=5.1] M1PALD [format=5.1];
 PRINT M3PALD [format=5.1] PALLGT [format=5.1] PALTHK [format=5.2];
   BFPUI1 BFPUI2 BFPUP3 BFPUP4;
    BFPUM1 BFPUM2 BFPUM3;
*/


 /* EXAMPLE CODE FOR CALCULATING 3D ANGLE

   L1=K[11,1]-K[42,1];
  N1=K[11,2]-K[42,2];
  M1=K[11,3]-K[42,3];
  L2=K[11,1]-K[19,1];
  N2=K[11,2]-K[19,2];
  M2=K[11,3]-K[19,3];
  cosPPNY=((L1*L2)+(N1*N2)+(M1*M2))/((SQRT((L1**2)+(N1**2)+(M1**2)))*
         (SQRT((L2**2)+(N2**2)+(M2**2))));
  PPNY=180-(arcos(cosPPNY)*180/3.14159265);
  */
```

Reproduced with permission of the copyright owner. Further reproduction prohibited without permission.

Reproduced with permission of the copyright owner. Further reproduction prohibited without permission.

Appendix E. Specimen raw morphometric data.

	Genus	Species	Subspecies	CabDra	AMNH#	1 NASL GT	2 NAS WDU	3 NAS WDL	4 NPM WDT	5 NSLA HT	6 NSLA WD	7 PNAS HT	8 PNAS WD	9 NLCL GT	10 ZYGA RE	11 ZYG OHT	12 BZYG WD	13 APZY GR	14 MXA RCL	15 BMA XWD
1	*Alouatta*	*palliata*	*palliata*	46/3	128109	17.5	6.3	10.2	4.6	12.8	11.8	12.5	10.7	5.9	543.7	19.1	68.6	51.7	40.9	56.1
2	*Alouatta*	*palliata*	*palliata*	46/3	141852	16.5	10.2	10.7	1.2	11.9	12.3	10.9	9.2	7.9	491.8	16.1	70.3	52.5	41.4	56.7
3	*Alouatta*	*palliata*	*mexicana*	45/3	17230	20.5	8.9	10.4	0.6	13.8	10.9	10.4	10.6	5.6	468.2	16.6	70.3	52.3	42.1	56.4
4	*Alouatta*	*palliata*	*mexicana*	45/3	17231	20.2	8.1	11.4	2.6	12.7	10.9	12.1	9.6	6.0	470.0	15.5	64.8	51.6	41.0	51.3
5	*Alouatta*	*palliata*	*mexicana*	45/4	17236	18.5	7.3	9.9	3.5	13.4	11.2	9.3	9.1	5.8	414.6	16.1	67.6	52.4	40.2	53.8
6	*Alouatta*	*palliata*	*mexicana*	45/5	17250	18.6	7.7	10.1	4.7	14.2	11.3	11.4	10.4	6.5	437.0	14.3	70.4	52.3	41.3	55.6
7	*Alouatta*	*palliata*	*palliata*	46/4	176641	17.1	5.5	8.9	3.4	12.0	10.0	12.4	9.8	5.0	494.5	16.6	66.0	51.7	40.3	55.7
8	*Alouatta*	*palliata*	*aequatorialis*	44/3	18935	15.8	7.2	9.3	3.3	13.0	10.2	13.0	10.0	6.0	494.4	16.7	72.4	52.4	42.1	57.9
9	*Alouatta*	*palliata*	*aequatorialis*	43/2	62828	18.7	8.9	10.9	3.5	12.3	13.1	10.3	11.5	5.7	406.5	15.6	73.6	51.8	40.9	56.7
10	*Alouatta*	*palliata*	*aequatorialis*	43/3	66707	16.3	7.5	9.2	0.6	13.2	12.4	14.2	11.6	6.5	424.4	15.1	69.1	53.0	41.4	54.8
11	*Ateles*	*geoffroyi*	*vellerosus*	87/8	123280	16.1	6.3	8.6	6.6	15.2	10.6	14.0	16.4	8.1	513.4	16.7	64.6	54.8	34.4	47.7
12	*Ateles*	*geoffroyi*	*ornatus*	87/3	139829	15.5	6.3	9.4	5.4	13.5	11.9	12.2	14.8	6.6	400.9	16.0	62.0	57.1	33.8	46.8
13	*Ateles*	*geoffroyi*	*panamensis*	87/3	141980	13.1	6.0	10.5	3.5	13.0	12.3	11.5	16.2	5.7	381.8	16.1	66.1	55.4	35.5	47.6
14	*Ateles*	*geoffroyi*	*panamensis*	87/3	141981	15.2	6.8	9.0	2.4	13.4	10.4	12.3	14.2	5.3	378.4	15.7	58.3	55.0	35.6	42.3
15	*Ateles*	*geoffroyi*	*geoffroyi*	87/1	176644	15.3	4.1	10.0	6.5	14.5	11.8	12.0	15.9	8.8	430.8	18.4	62.6	52.4	38.1	48.8
16	*Ateles*	*geoffroyi*	*geoffroyi*	87/1	176646	14.0	7.9	8.7	4.4	15.1	10.3	12.1	15.1	6.4	295.1	14.0	56.0	50.3	32.9	40.5
17	*Ateles*	*geoffroyi*	*geoffroyi*	87/1	176647	15.8	8.1	9.0	4.7	15.3	10.0	15.1	15.1	6.5	366.2	16.8	55.5	52.0	33.9	40.6
18	*Ateles*	*geoffroyi*	*panamensis*	87/6	24172	14.5	5.4	10.6	6.1	14.3	12.0	14.1	15.6	10.5	491.6	17.3	66.8	51.6	38.2	50.8
19	*Ateles*	*geoffroyi*	*panamensis*	87/6	24173	15.5	4.7	8.9	3.4	15.2	11.7	13.6	14.7	8.9	492.9	16.7	67.3	52.3	38.8	46.1
20	*Ateles*	*geoffroyi*	*panamensis*	87/6	24176	15.7	3.7	9.5	5.9	13.7	10.8	12.8	14.6	5.9	387.0	15.5	59.4	52.8	36.9	43.4
21	*Lagothrix*	*lagothrica*	*poeppigii*	96/1	67697	9.6	0.6	10.5	3.7	14.6	10.8	10.5	14.4	4.2	406.5	17.1	64.7	52.5	34.7	47.1
22	*Lagothrix*	*lagothrica*	*poeppigii*	96/5	71768	11.5	1.3	10.1	2.7	14.3	12.8	12.0	13.8	5.2	455.3	17.3	64.0	57.8	35.3	47.7
23	*Lagothrix*	*lagothrica*	*poeppigii*	96/7	71776	14.3	1.3	10.1	2.7	13.6	11.2	10.7	13.6	6.3	476.8	18.8	66.3	56.1	35.3	49.5
24	*Lagothrix*	*lagothrica*	*poeppigii*	96/7	71779	13.2	1.6	10.3	3.7	13.7	11.8	10.7	15.3	4.4	495.7	18.3	65.7	55.4	34.7	46.6
25	*Lagothrix*	*lagothrica*	*poeppigii*	96/2	73555	14.9	0.4	10.6	4.3	14.3	12.8	12.1	14.8	6.5	404.5	16.6	64.3	54.6	34.8	48.9
26	*Lagothrix*	*lagothrica*	*poeppigii*	96/3	73556	8.9	0.7	9.0	5.0	14.5	11.1	11.0	14.7	5.5	398.6	16.5	64.0	55.4	34.2	48.0
27	*Lagothrix*	*lagothrica*	*poeppigii*	98/1	75291	14.7	5.6	10.8	2.8	13.6	12.2	13.8	14.2	7.4	445.5	17.1	65.2	55.9	37.1	48.6
28	*Lagothrix*	*lagothrica*	*poeppigii*	98/1	76393	13.3	2.8	10.0	2.5	14.0	12.4	12.2	13.8	6.6	413.0	16.0	59.8	53.9	34.3	41.7
29	*Lagothrix*	*lagothrica*	*poeppigii*	98/2	76395	15.7	4.6	8.3	2.2	13.4	10.6	13.5	15.8	7.1	422.3	16.8	65.6	53.9	37.9	47.3
30	*Lagothrix*	*lagothrica*	*poeppigii*	98/2	76396	11.9	2.7	10.5	3.5	13.1	12.3	11.6	14.2	8.5	450.0	17.0	61.9	55.4	36.4	45.9
31	*Brachyteles*	*arachnoides*	.	91/5	80405	14.5	5.4	11.0	4.2	20.9	13.8	11.9	17.2	4.7	515.8	18.4	70.6	56.4	42.2	54.2
32	*Chiropotes*	*satanas*	*chiropotes*	33/2	94118	12.1	4.0	8.9	3.1	10.2	12.0	6.4	9.1	5.2	296.9	12.8	55.5	56.9	30.7	39.3
33	*Chiropotes*	*satanas*	*chiropotes*	33/2	94120	15.2	3.6	10.5	3.4	9.9	11.0	8.0	8.9	6.2	288.6	12.9	55.4	56.2	30.2	38.6
34	*Chiropotes*	*satanas*	*chiropotes*	33/2	94122	11.9	4.2	8.4	2.1	11.5	9.1	6.9	7.0	6.2	300.9	13.5	54.5	57.1	30.5	37.6
35	*Chiropotes*	*satanas*	*chiropotes*	33/3	94125	12.9	5.1	9.7	2.5	10.9	9.2	6.4	8.3	5.7	274.3	13.6	51.3	55.7	29.5	38.5
36	*Chiropotes*	*satanas*	*chiropotes*	33/4	94129	12.2	4.5	7.9	4.1	11.5	11.0	6.9	8.8	7.9	324.9	14.5	55.9	54.9	32.4	41.2
37	*Chiropotes*	*satanas*	*chiropotes*	33/4	94130	10.3	2.5	9.7	3.6	11.5	10.5	6.7	8.3	6.9	315.2	14.4	54.9	57.7	30.4	37.2

						1	2	3	4	5	6	7	8	9	10	11	12	13	14	15
	Genus	Species	Subspecies	CabDra	AMNH#	NASL GT	NAS WDU	NAS WDL	NPM WDT	NSLA HT	NSLA WD	PNAS HT	PNAS WD	NLCL GT	ZYGA RE	ZYG OHT	BZYG WD	APZY GR	MXA RCL	BMA XWD
38	*Chiropotes*	*satanas*	*satanas*	33/5	95867	10.5	2.4	8.7	3.1	11.4	8.9	6.7	7.5	6.6	262.7	13.5	53.4	54.9	28.9	35.9
39	*Chiropotes*	*satanas*	*satanas*	33/6	96339	11.9	1.7	8.4	2.5	8.9	8.7	7.8	7.2	6.1	252.8	12.9	52.0	53.4	28.3	41.1
40	*Chiropotes*	*satanas*	*satanas*	33/6	96340	13.1	0.8	8.1	3.2	9.8	8.1	7.0	7.0	4.7	271.5	13.2	51.1	56.7	27.3	36.6
41	*Chiropotes*	*satanas*	*satanas*	33/6	96344	13.6	2.1	9.5	4.3	9.4	9.2	8.3	7.5	5.8	293.7	13.1	54.4	55.1	29.9	38.1
42	*Pithecia*	*pithecia*	*pithecia*	31/6	36321	16.1	4.4	10.2	2.0	8.8	10.8	8.3	9.4	6.1	287.4	16.1	48.8	56.2	28.1	41.5
43	*Pithecia*	*pithecia*	*pithecia*	31/6	36322	14.4	4.4	9.9	2.3	9.0	10.7	7.7	11.4	7.1	303.1	14.9	49.2	55.3	28.1	41.5
44	*Pithecia*	*pithecia*	*pithecia*	31/7	42417	15.9	4.9	9.1	0.6	7.4	10.1	5.7	10.4	5.1	258.1	14.3	46.7	51.5	28.6	36.6
45	*Pithecia*	*pithecia*	*pithecia*	31/8	42743	15.0	3.5	9.2	2.1	8.2	9.1	7.1	10.6	5.0	235.5	13.3	47.9	56.3	27.0	39.1
46	*Pithecia*	*pithecia*	*pithecia*	31/9	48123	14.7	3.8	9.3	1.9	7.8	9.9	8.1	10.8	6.4	226.9	12.8	47.0	54.7	28.2	38.1
47	*Pithecia*	*pithecia*	*pithecia*	32/1	48400	15.1	4.2	10.1	0.7	7.5	9.0	6.5	8.8	4.5	212.1	12.9	44.0	54.3	26.7	38.1
48	*Pithecia*	*pithecia*	*pithecia*	31/4	79383	12.5	5.3	10.0	1.9	8.4	9.4	7.7	9.3	6.2	329.1	16.0	46.8	53.5	27.9	37.1
49	*Pithecia*	*pithecia*	*pithecia*	31/4	79384	14.0	4.5	9.8	2.0	7.6	9.3	9.3	10.0	5.7	359.3	16.0	49.0	54.1	28.2	39.3
50	*Pithecia*	*pithecia*	*pithecia*	32/3	94132	17.4	4.8	9.9	0.9	7.5	10.6	9.1	10.8	6.3	297.5	14.7	46.4	54.5	26.6	40.5
51	*Pithecia*	*pithecia*	*pithecia*	32/3	94133	14.6	5.6	9.6	0.6	7.7	9.1	8.1	8.7	6.3	244.1	14.7	44.9	55.4	27.6	40.1
52	*Pithecia*	*monachus*	*monachus*	31/2	230798	16.4	1.8	10.9	5.3	9.6	11.1	7.5	10.8	6.3	291.5	14.1	50.5	54.2	31.0	41.0
53	*Pithecia*	*monachus*	*monachus*	31/2	239854	16.4	4.4	10.6	2.3	9.5	10.5	7.4	12.0	6.8	311.1	17.1	51.2	54.8	31.6	42.5
54	*Pithecia*	*monachus*	*monachus*	30/6	77822	15.4	5.1	11.4	2.4	10.1	10.0	11.1	10.7	5.9	312.3	14.6	52.9	52.1	31.9	39.7
55	*Pithecia*	*monachus*	*monachus*	31/1	98399	15.5	3.9	10.7	3.9	10.2	10.7	7.4	8.4	5.4	229.4	14.8	47.6	53.4	29.3	35.3
56	*Callicebus*	*cupreus*	.	24/5	174286	7.2	3.6	6.9	3.0	8.8	7.9	5.7	11.1	4.8	253.3	13.1	38.3	59.4	21.6	32.5
57	*Callicebus*	*cupreus*	.	24/7	72141	8.9	3.5	4.4	2.6	9.1	6.6	5.4	9.3	5.9	244.7	13.3	37.2	57.0	22.1	30.8
58	*Callicebus*	*cupreus*	.	24/6	75994	10.2	3.9	4.7	2.2	7.6	6.5	6.4	8.8	5.7	205.6	11.7	35.1	56.9	21.8	30.0
59	*Callicebus*	*cupreus*	.	24/5	76419	11.4	2.7	4.9	3.1	8.0	6.2	4.5	8.5	4.9	272.4	14.6	37.1	57.2	22.7	34.6
60	*Callicebus*	*cupreus*	.	24/5	76422	11.2	4.9	4.8	2.0	7.7	6.3	5.7	10.3	6.2	259.9	13.9	39.0	58.5	22.4	29.8
61	*Callicebus*	*cupreus*	.	24/5	98320	11.5	3.1	5.0	2.3	7.4	5.9	4.3	7.5	4.0	258.3	14.0	36.5	60.5	20.5	31.5
62	*Callicebus*	*cupreus*	.	24/5	98370	10.5	2.1	4.4	2.5	7.3	5.3	5.6	8.5	3.7	204.5	13.4	35.9	55.4	20.4	30.7
63	*Callicebus*	*cupreus*	.	24/6	98381	9.0	3.5	4.2	2.3	7.1	5.1	4.8	7.5	3.9	167.5	11.4	32.0	57.7	19.1	27.8
64	*Callicebus*	*cupreus*	.	24/5	98385	10.8	3.0	3.9	3.4	7.4	6.1	4.8	10.0	4.5	187.7	12.7	34.2	53.2	22.2	30.4
65	*Callicebus*	*cupreus*	.	24/4	98389	11.2	4.0	4.8	2.3	7.0	6.7	4.7	8.0	3.8	213.4	13.1	37.3	57.8	21.5	32.5
66	*Cebus*	*apella*	*paraguayanus*	75/1	133593	18.2	3.7	6.6	4.7	11.0	9.1	7.8	10.2	6.7	361.8	13.1	56.6	57.0	32.6	41.1
67	*Cebus*	*apella*	*paraguayanus*	75/3	133626	15.0	3.6	7.1	4.9	10.9	9.2	8.5	10.2	5.7	328.2	13.8	55.5	58.5	29.6	45.7
68	*Cebus*	*apella*	*paraguayanus*	75/4	133631	13.5	3.6	8.4	3.9	11.3	10.1	9.8	10.1	6.7	329.9	13.7	57.8	58.6	32.4	48.8
69	*Cebus*	*apella*	*paraguayanus*	75/4	133635	19.7	2.8	8.6	3.2	9.5	9.7	9.4	9.7	5.8	307.6	14.1	55.6	56.8	30.9	47.1
70	*Cebus*	*apella*	*versutus*	75/8	133736	11.0	2.1	8.3	3.0	11.3	9.7	9.1	10.1	6.7	303.9	13.0	55.0	59.3	32.2	44.7
71	*Cebus*	*apella*	*paraguayanus*	75/5	133864	10.8	3.0	8.5	4.3	9.8	9.1	9.4	10.2	6.5	330.7	13.5	55.0	56.7	31.2	47.0
72	*Cebus*	*apella*	*versutus*	75/9	136375	16.2	3.1	8.5	3.2	13.8	10.5	10.0	11.3	5.6	355.4	13.6	59.0	58.7	31.9	48.0
73	*Cebus*	*apella*	*versutus*	75/9	136383	14.2	2.3	6.9	4.8	13.1	10.4	10.1	9.8	5.6	331.9	14.5	57.2	56.8	32.3	48.4
74	*Cebus*	*apella*	*versutus*	75/1	136384	12.7	2.3	7.4	4.6	10.0	8.9	8.8	9.0	6.4	295.6	13.9	54.2	57.8	31.1	44.9

Reproduced with permission of the copyright owner. Further reproduction prohibited without permission.

	Genus	Species	Subspecies	CnhDra	AMNH#	1 NASL GT	2 NAS WDU	3 NAS WDL	4 NPM WDT	5 NSLA HT	6 NSLA WD	7 PNAS HT	8 PNAS WD	9 NLCL GT	10 ZYG ARE	11 ZYG OHT	12 BZYG WD	13 APZY GR	14 MXA RCL	15 BMA XWD
75	*Cebus*	*apella*	*paraguayanus*	75/1	136386	13.3	3.8	8.9	4.8	11.0	10.2	10.9	11.0	7.9	336.4	15.2	59.8	57.1	33.2	49.6
76	*Cebus*	*capucinus*	*limitaneus*	78/5	128119	16.8	2.3	9.0	6.7	11.5	11.5	13.7	13.2	7.5	323.2	12.3	58.3	55.9	34.2	41.4
77	*Cebus*	*capucinus*	*limitaneus*	78/5	128120	14.6	2.3	8.1	6.1	12.2	10.9	11.1	12.8	6.8	310.9	12.1	56.6	54.4	33.8	40.1
78	*Cebus*	*capucinus*	*limitaneus*	78/6	128145	13.0	3.8	8.1	5.3	13.7	12.1	13.4	13.5	6.1	312.3	12.7	56.4	55.3	33.7	41.1
79	*Cebus*	*capucinus*	*imitator*	77/3	137993	18.3	3.4	8.2	4.8	10.7	11.2	11.7	12.1	8.1	391.5	15.2	59.3	56.9	33.3	48.3
80	*Cebus*	*capucinus*	*imitator*	77/6	176630	13.2	2.4	10.4	4.7	12.0	12.2	11.3	13.1	5.7	315.4	12.9	55.9	55.8	33.0	40.0
81	*Cebus*	*capucinus*	*imitator*	77/1	19220	16.2	4.6	10.2	5.7	13.2	11.9	11.5	11.7	6.7	369.0	12.3	60.2	59.6	33.7	45.4
82	*Cebus*	*capucinus*	*imitator*	77/2	24429	17.9	3.0	10.8	7.4	11.6	12.6	11.6	13.1	6.5	408.2	14.3	60.5	57.4	35.8	47.0
83	*Cebus*	*capucinus*	*imitator*	77/5	28493	16.0	3.9	7.9	5.3	11.3	10.7	10.7	12.5	5.7	363.4	14.8	56.9	55.6	32.7	43.6
84	*Cebus*	*capucinus*	*imitator*	78/3	29610	11.1	3.9	8.2	4.9	12.6	10.7	11.4	11.9	7.0	325.4	13.4	54.1	54.7	32.7	42.1
85	*Cebus*	*capucinus*	*imitator*	78/3	29620	12.9	4.0	7.2	5.0	12.5	10.2	10.7	11.7	7.4	322.8	11.5	55.7	54.1	33.2	39.2
86	*Saimiri*	*sciureus*	*oerstedii*	103/7	26992	8.4	2.2	3.9	2.5	7.7	6.5	6.8	6.2	4.6	160.8	10.8	34.7	53.2	17.8	27.6
87	*Saimiri*	*sciureus*	*oerstedii*	103/7	26997	8.7	3.1	4.9	2.4	7.3	7.2	5.1	6.1	4.3	152.6	10.8	34.0	53.6	17.6	27.6
88	*Saimiri*	*sciureus*	*oerstedii*	103/8	27002	9.1	2.8	4.4	3.1	7.1	6.9	6.1	6.1	4.0	154.1	11.1	34.0	54.6	17.6	27.4
89	*Saimiri*	*sciureus*	*sciureus*	104/2	37468	8.0	1.7	2.4	2.6	6.9	6.2	5.1	6.8	3.7	146.8	11.1	32.3	57.9	16.6	28.5
90	*Saimiri*	*sciureus*	*sciureus*	104/6	64096	9.8	1.7	3.8	2.7	7.4	6.4	5.1	6.2	2.7	157.8	10.9	33.1	55.2	16.5	29.1
91	*Saimiri*	*sciureus*	*sciureus*	104/7	76871	10.4	1.8	3.1	5.0	7.4	6.8	5.4	6.4	3.9	198.5	11.4	34.6	57.9	17.5	26.1
92	*Saimiri*	*sciureus*	*sciureus*	104/5	80442	9.6	1.7	3.9	3.8	7.6	6.1	4.8	7.0	3.8	179.8	13.1	34.8	56.5	17.3	29.3
93	*Saimiri*	*sciureus*	*sciureus*	104/5	80443	11.2	1.9	4.3	2.6	6.8	7.9	5.5	6.8	4.4	182.0	11.5	34.8	55.5	18.2	28.9
94	*Saimiri*	*sciureus*	*sciureus*	104/3	94205	10.3	2.6	3.9	2.3	8.0	6.7	5.2	6.7	3.8	190.6	13.1	34.1	56.3	18.2	29.8
95	*Saim*	*sciureus*	*sciureus*	104/4	94210	11.6	2.2	2.9	2.0	7.6	6.7	5.1	6.2	3.3	176.0	12.1	34.2	56.6	17.7	29.8
96	*Aotus*	*trivirgatus*	*trivirgatus*	23/5	187963	11.1	3.8	5.6	3.4	6.6	8.1	6.1	7.7	3.3	194.7	13.1	37.8	53.3	22.6	32.2
97	*Aotus*	*trivirgatus*	*trivirgatus*	23/5	76915	12.0	2.8	3.8	2.8	9.0	7.9	6.0	7.5	2.5	186.1	10.8	35.7	49.5	23.1	29.6
98	*Aotus*	*trivirgatus*	*trivirgatus*	23/5	76919	11.2	2.1	2.4	3.0	8.4	6.2	5.4	7.4	2.4	146.8	9.6	34.6	53.0	20.4	28.5
99	*Aotus*	*trivirgatus*	*trivirgatus*	23/4	78587	11.9	3.1	4.4	3.2	9.7	8.5	6.6	7.4	3.9	230.5	13.7	37.2	56.2	23.5	32.4
100	*Aotus*	*trivirgatus*	*trivirgatus*	23/3	93078	12.6	2.6	3.7	2.5	7.4	6.1	6.3	6.7	2.7	214.0	13.4	36.6	57.2	20.2	31.1
101	*Aotus*	*trivirgatus*	*vociferus*	23/7	67692	11.0	2.1	4.1	2.0	7.3	6.7	6.8	6.4	2.4	181.0	13.4	35.8	51.9	21.9	29.7
102	*Aotus*	*trivirgatus*	*vociferus*	23/8	72058	10.9	3.2	4.6	3.0	8.5	7.1	7.0	7.7	3.5	195.7	11.6	38.6	57.7	21.7	31.8
103	*Aotus*	*trivirgatus*	*vociferus*	23/8	72061	13.9	2.6	3.8	2.7	8.4	6.5	6.3	8.4	3.0	228.7	12.3	38.2	55.9	21.5	31.8
104	*Aotus*	*trivirgatus*	*vociferus*	23/8	72063	12.3	4.0	4.2	2.6	8.0	6.6	6.2	6.9	3.3	191.8	13.6	36.1	54.7	21.9	29.8
105	*Aotus*	*trivirgatus*	*vociferus*	23/6	73417	12.6	2.6	2.6	3.6	7.6	6.1	8.9	7.8	2.2	185.9	13.2	35.2	54.1	21.7	30.2
106	*Saguinus*	*oedipus*	*oedipus*	3/14	32702	6.5	5.2	4.6	2.8	5.1	5.3	4.0	5.4	3.6	109.1	8.3	33.1	54.5	15.5	27.0
107	*Callithrix*	*pygmaea*	.	106/2	239606	4.8	2.9	3.0	1.8	3.7	3.5	2.7	3.8	1.8	51.5	4.6	21.4	58.8	10.2	15.5
108	*Callithrix*	*pygmaea*	.	106/2	44365	3.8	3.0	2.3	1.6	4.5	3.5	3.1	3.6	1.9	50.3	4.7	20.7	57.4	10.7	15.9
109	*Callithrix*	*pygmaea*	.	106/3	72036	4.2	2.6	2.6	2.5	3.5	3.5	2.2	4.0	2.6	45.0	4.9	20.3	55.2	10.5	15.4
110	*Callithrix*	*pygmaea*	.	106/3	72037	5.0	3.5	3.3	1.9	3.4	3.8	2.6	3.7	2.1	53.3	5.7	21.1	56.3	11.1	15.4

Reproduced with permission of the copyright owner. Further reproduction prohibited without permission.

	Genus	Species	Subspecies	CabDra	AMNH#	1 NASL GT	2 NAS WDU	3 NAS WDL	4 NPM WDT	5 NSLA HT	6 NSLA WD	7 PNAS HT	8 PNAS WD	9 NLCL GT	10 ZYGA RE	11 ZYG OHT	12 BZYG WD	13 APZY GR	14 MXA RCL	15 BMA XWD
111	*Callithrix*	*pygmaea*	.	106/2	73751	5.0	3.2	3.1	2.1	2.9	3.2	2.2	4.2	2.5	45.1	4.9	21.2	54.9	10.7	16.2
112	*Callithrix*	*pygmaea*	.	106/2	74056	4.6	2.9	3.6	2.0	3.3	3.3	2.7	4.4	2.9	58.9	5.2	21.6	55.2	11.3	16.1
113	*Callithrix*	*pygmaea*	.	106/2	74362	4.3	3.1	2.7	2.3	3.5	3.1	3.1	3.3	2.3	43.9	4.4	20.0	55.5	10.8	16.1
114	*Callithrix*	*pygmaea*	.	106/2	74365	5.5	3.2	3.0	1.8	3.4	3.4	2.5	3.4	2.4	48.4	4.5	20.2	54.8	11.0	14.9
115	*Callithrix*	*pygmaea*	.	106/2	74369	4.9	4.0	3.2	2.1	3.7	3.3	2.7	3.6	2.8	58.3	5.1	21.6	57.0	11.1	16.1
116	*Callithrix*	*pygmaea*	.	106/3	76328	5.0	3.8	3.3	1.0	3.3	3.5	3.2	3.7	2.5	53.3	5.0	22.7	55.6	11.7	15.7
117	*Callimico*	*geoldii*	.	106/1	183290	9.6	1.7	3.9	3.8	7.6	6.1	4.8	7.0	3.8	179.8	13.1	34.8	56.5	17.3	29.3
118	*Chlorocebus*	*aethiops*	*cynosuros*	26/7	116268	13.7	1.2	5.8	5.8	17.8	8.6	10.2	10.1	4.7	319.9	12.8	59.1	51.4	36.3	40.0
119	*Chlorocebus*	*aethiops*	*johnstoni*	26/13	161104	14.3	1.9	7.0	6.5	17.8	9.1	5.7	10.9	4.8	249.0	10.5	57.7	48.9	37.3	36.2
120	*Chlorocebus*	*aethiops*	*johnstoni*	26/13	161107	14.0	2.5	6.1	4.3	18.3	8.9	9.0	10.6	5.6	278.6	11.6	58.2	49.1	39.7	41.6
121	*Chlorocebus*	*aethiops*	*johnstoni*	26/11	27706	14.8	1.8	6.5	6.0	15.3	8.8	9.2	10.3	6.6	295.2	13.8	54.8	52.2	36.8	42.0
122	*Chlorocebus*	*aethiops*	*johnstoni*	26/10	34716	13.5	1.1	5.2	5.1	17.8	7.9	7.9	11.4	3.7	313.4	12.5	58.9	53.9	37.3	38.1
123	*Chlorocebus*	*aethiops*	*centralis*	26/3	52475	13.3	1.7	6.2	4.2	17.4	9.1	8.5	11.5	6.2	339.3	12.3	63.0	51.8	38.5	43.9
124	*Chlorocebus*	*aethiops*	*centralis*	26/3	52479	16.4	1.5	6.3	5.0	16.8	10.1	9.1	11.3	6.5	353.5	14.8	61.6	51.4	39.0	41.1
125	*Chlorocebus*	*aethiops*	*johnstoni*	26/11	54231	11.4	1.4	4.8	4.9	14.4	7.2	7.9	9.6	5.6	221.9	9.8	54.0	54.9	32.0	39.3
126	*Chlorocebus*	*aethiops*	*cynosuros*	26/5	80789	13.5	2.8	6.0	6.4	16.4	9.2	8.6	10.7	4.5	262.0	12.9	58.0	51.7	37.9	41.0
127	*Chlorocebus*	*aethiops*	*hilgerti*	26/8	83924	12.0	0.8	5.5	4.5	14.8	8.0	9.4	10.3	5.9	258.4	13.0	54.7	51.7	34.2	39.0
128	*Cercopithecus*	*neglectus*	.	32/6	52414	22.3	1.6	7.1	6.8	15.0	7.8	13.0	11.9	7.1	330.9	14.1	58.6	53.2	37.6	41.7
129	*Cercopithecus*	*neglectus*	.	32/6	52416	18.0	2.1	7.9	5.8	14.9	7.2	12.1	11.6	9.8	331.0	14.9	59.1	50.6	42.5	42.7
130	*Cercopithecus*	*neglectus*	.	32/8	52424	22.5	2.6	7.2	3.2	16.3	9.1	11.2	12.4	6.9	342.3	14.0	60.7	55.2	39.5	42.6
131	*Cercopithecus*	*neglectus*	.	32/8	52425	20.0	1.6	9.8	7.2	15.1	9.7	12.2	12.0	6.3	358.1	14.1	62.5	56.0	38.5	44.7
132	*Cercopithecus*	*neglectus*	.	32/12	52428	23.2	1.6	7.8	5.7	16.2	8.7	12.4	13.1	8.8	382.3	13.8	64.6	55.1	40.9	44.8
133	*Cercopithecus*	*neglectus*	.	33/1	52441	21.3	2.4	8.7	6.4	16.5	9.4	12.5	10.5	7.4	346.1	13.6	61.2	53.9	39.5	44.8
134	*Cercopithecus*	*neglectus*	.	32/11	55008	19.4	2.2	7.2	4.8	14.2	8.1	13.4	12.9	9.2	367.2	14.9	64.1	53.9	40.2	44.0
135	*Cercopithecus*	*neglectus*	.	32/10	86854	22.5	3.1	6.7	3.2	16.4	8.3	12.3	11.7	6.6	345.5	12.7	60.0	56.7	36.0	42.0
136	*Cercopithecus*	*neglectus*	.	32/6	200761	17.9	3.0	8.4	4.7	19.3	11.5	11.1	12.3	9.2	403.3	14.0	66.6	55.0	40.8	44.6
137	*Cercopithecus*	*neglectus*	.	32/9	189380	13.9	3.0	8.3	6.0	18.8	8.0	10.2	13.2	7.8	363.6	16.9	63.4	54.0	36.7	46.5
138	*Cercopithecus*	*mitis*	*stuhlmanni*	30/4	52350	16.9	2.1	6.1	5.6	19.7	10.4	14.0	11.6	7.1	385.6	16.6	62.6	53.7	39.5	44.6
139	*Cercopithecus*	*mitis*	*stuhlmanni*	30/5	52356	20.6	2.5	7.2	4.4	17.6	8.5	12.6	11.2	6.0	314.9	13.8	61.6	51.7	38.6	42.3
140	*Cercopithecus*	*mitis*	*stuhlmanni*	30/5	52357	18.7	1.7	9.3	4.8	17.6	13.0	11.4	12.5	7.8	332.1	16.8	61.8	53.1	42.1	45.1
141	*Cercopithecus*	*mitis*	*stuhlmanni*	30/5	52358	20.8	2.7	7.7	3.6	19.1	8.7	12.3	11.1	5.3	385.9	15.9	62.7	54.3	39.5	42.9
142	*Cercopithecus*	*mitis*	*stuhlmanni*	30/6	52363	14.0	2.3	6.6	5.0	16.7	10.0	14.9	12.0	6.0	357.8	15.7	64.6	53.1	39.1	44.5
143	*Cercopithecus*	*mitis*	*stuhlmanni*	30/7	52366	20.2	3.2	8.5	2.5	18.2	10.9	15.2	12.7	7.3	347.6	14.6	62.6	55.1	38.3	45.5
144	*Cercopithecus*	*mitis*	*stuhlmanni*	30/8	52372	16.7	2.2	7.8	5.3	16.9	9.2	11.6	11.6	5.4	288.0	13.6	64.3	52.4	38.1	45.2
145	*Cercopithecus*	*mitis*	*stuhlmanni*	30/9	52377	18.3	1.4	8.0	5.3	17.3	12.5	14.0	10.5	6.2	358.4	14.4	65.1	55.3	37.5	43.3
146	*Cercopithecus*	*mitis*	*stuhlmanni*	30/10	52382	16.9	2.1	7.0	4.1	16.7	8.6	11.7	11.7	7.5	374.5	16.0	61.7	52.2	40.0	42.5

Reproduced with permission of the copyright owner. Further reproduction prohibited without permission.

	Genus	Species	Subspecies	CabDra	AMNH#	1 NASL GT	2 NAS WDU	3 NAS WDL	4 NPM WDT	5 NSLA HT	6 NSLA WD	7 PNAS HT	8 PNAS WD	9 NLCL GT	10 ZYGA RE	11 ZYG OHT	12 BZYG WD	13 APZY GR	14 MXA RCL	15 BMA XWD
147	*Cercopithecus*	*mitis*	*stuhlmanni*	30/13	52406	19.8	2.4	8.8	4.2	17.8	10.3	13.8	13.0	5.7	369.7	15.2	66.7	51.8	39.3	41.1
148	*Cercopithecus*	*ascanius*	*ascanius*	28/6	51020	10.4	2.4	7.7	2.5	14.6	8.2	8.0	10.0	4.2	281.3	15.9	54.0	52.6	33.3	38.6
149	*Cercopithecus*	*ascanius*	*ascanius*	28/3	52531	13.8	1.7	7.7	2.1	13.9	8.8	9.7	10.0	4.7	327.7	16.6	57.5	53.6	35.7	42.3
150	*Cercopithecus*	*ascanius*	*ascanius*	28/5	52551	14.6	1.9	7.5	2.7	14.8	8.2	10.3	11.4	5.5	300.5	15.3	60.3	54.2	33.3	40.3
151	*Cercopithecus*	*ascanius*	*ascanius*	28/7	52557	15.2	2.1	7.5	2.3	13.6	8.6	6.1	11.3	3.3	261.2	14.2	54.8	55.4	33.8	40.7
152	*Cercopithecus*	*ascanius*	*ascanius*	28/8	52566	11.6	2.3	7.7	4.1	15.8	9.1	10.4	10.6	4.1	326.1	14.3	57.3	56.3	31.5	41.0
153	*Cercopithecus*	*ascanius*	*katangae*	28/11	55021	14.1	2.3	8.3	4.2	14.0	9.0	9.6	11.2	6.3	266.7	13.4	56.5	57.1	31.7	38.9
154	*Cercopithecus*	*ascanius*	*katangae*	28/12	55027	14.3	2.1	6.4	3.1	12.5	8.1	9.3	10.8	5.5	285.1	14.0	56.5	60.3	31.2	41.7
155	*Cercopithecus*	*ascanius*	*katangae*	28/13	55030	21.6	3.6	7.0	2.3	13.9	7.8	12.7	11.1	9.6	405.2	12.5	64.7	54.9	39.8	42.7
156	*Cercopithecus*	*ascanius*	*katangae*	28/13	55033	14.5	2.9	7.5	3.0	16.3	8.7	9.8	11.4	5.0	351.6	15.6	60.6	54.1	33.6	41.4
157	*Cercopithecus*	*ascanius*	*katangae*	28/12	55068	13.9	2.1	8.0	2.5	15.3	9.6	10.7	12.7	5.7	358.5	18.7	61.9	51.8	35.0	43.8
158	*Macaca*	*nemestrina*	*nemestrina*	10/12	102202	27.0	1.3	9.6	5.5	20.3	12.7	12.9	13.6	9.2	563.1	22.8	72.5	49.0	51.3	58.9
159	*Macaca*	*nemestrina*	*pagensis*	10/14	103398	25.5	1.1	7.0	7.1	16.4	10.6	12.6	12.2	8.9	438.5	17.8	68.1	51.5	43.4	49.7
160	*Macaca*	*nemestrina*	*pagensis*	10/14	103399	20.5	1.0	8.6	4.1	18.7	13.6	13.6	10.1	8.7	487.0	18.5	66.2	50.7	45.3	50.5
161	*Macaca*	*nemestrina*	*nemestrina*	10/7	103728	27.0	2.4	8.3	5.5	18.8	11.0	15.8	14.3	9.8	598.3	20.7	75.6	50.6	52.9	56.7
162	*Macaca*	*nemestrina*	*nemestrina*	10/9	106050	22.9	1.1	10.1	7.8	22.0	15.4	15.9	13.6	12.4	618.4	23.3	82.7	47.7	50.6	61.2
163	*Macaca*	*nemestrina*	*nemestrina*	10/10	106559	28.2	1.9	8.3	4.5	21.5	13.1	14.2	13.0	10.9	683.9	23.2	80.5	47.8	52.8	59.4
164	*Macaca*	*nemestrina*	*nemestrina*	10/10	106562	21.9	1.8	9.5	6.1	20.1	13.9	16.0	13.5	13.8	650.6	24.0	79.3	47.2	53.6	55.5
165	*Macaca*	*nemestrina*	*leonina*	10/5	11091	32.9	2.0	8.1	5.1	20.4	10.2	14.3	13.4	9.1	517.3	20.9	75.3	47.0	53.1	60.5
166	*Macaca*	*nemestrina*	*nemestrina*	10/3	57111	34.5	2.2	9.4	2.9	17.1	13.5	15.2	13.6	9.2	556.4	21.9	71.6	47.7	50.5	54.6
167	*Macaca*	*nemestrina*	*leonina*	10/4	83434	24.2	1.2	7.0	5.7	14.7	11.6	14.4	13.2	11.7	561.4	19.7	72.1	51.6	47.8	53.1
168	*Macaca*	*fascicularis*	*fascicularis*	5/18	102764	25.8	2.4	8.3	4.2	12.7	10.3	11.6	11.2	10.2	464.8	17.2	64.9	52.0	42.7	49.0
169	*Macaca*	*fascicularis*	*fascicularis*	5/10	103652	22.1	2.3	7.5	4.5	14.3	11.7	10.2	10.5	7.2	405.4	14.9	61.9	50.5	40.9	40.9
170	*Macaca*	*fascicularis*	*fascicularis*	5/11	103654	20.9	2.1	7.2	4.0	14.3	11.5	10.9	10.4	6.8	447.7	15.8	63.0	51.4	41.7	44.7
171	*Macaca*	*fascicularis*	*fascicularis*	5/11	103655	21.0	1.9	6.5	5.3	13.5	8.7	11.1	9.8	3.3	405.1	14.4	59.8	54.5	35.3	40.4
172	*Macaca*	*fascicularis*	*fascicularis*	5/11	103657	19.4	2.0	7.1	5.3	12.7	9.1	9.5	9.8	4.5	320.9	16.0	59.1	49.8	38.3	43.3
173	*Macaca*	*fascicularis*	*fascicularis*	5/12	103660	20.0	2.0	7.3	4.1	13.6	10.1	11.6	10.0	7.1	421.4	14.6	63.4	52.4	39.5	42.4
174	*Macaca*	*fascicularis*	*fascicularis*	5/12	103663	17.8	2.1	7.0	4.4	14.9	9.6	9.8	9.7	8.2	331.5	14.1	55.4	50.1	38.1	40.9
175	*Macaca*	*fascicularis*	*fascicularis*	5/7	107094	24.8	2.5	7.1	5.6	13.8	11.2	10.7	10.4	7.7	396.4	15.7	60.0	48.9	41.9	42.2
176	*Macaca*	*fascicularis*	*fascicularis*	5/7	107095	21.3	1.3	6.2	5.1	15.2	10.1	12.3	10.0	9.4	440.2	16.9	64.7	50.5	40.9	46.7
177	*Macaca*	*fascicularis*	*fascicularis*	5/8	107096	20.0	1.9	7.1	3.6	13.0	10.2	9.0	10.5	6.6	369.2	14.5	61.3	50.6	39.9	41.4
178	*Macaca*	*mulatta*	*mulatta*	8/9	112732	25.4	1.7	10.6	5.9	14.2	11.3	12.9	14.0	9.6	534.4	19.0	74.4	53.1	44.2	53.1
179	*Macaca*	*mulatta*	*mulatta*	9/1	112740	23.4	1.8	7.1	6.2	18.0	11.6	11.2	11.6	5.3	493.3	18.8	68.5	49.0	44.4	48.3
180	*Macaca*	*mulatta*	*mulatta*	9/3	112971	25.0	2.2	9.5	5.1	18.9	13.5	12.0	12.0	5.8	443.0	19.9	68.5	54.4	42.9	54.4
181	*Macaca*	*mulatta*	*mulatta*	8/9	112972	22.3	1.4	9.3	7.5	16.7	11.3	11.1	10.8	4.3	416.2	16.2	66.9	55.4	40.2	51.1
182	*Macaca*	*mulatta*	*mulatta*	8/8	163612	21.9	2.8	8.7	5.1	16.6	11.7	10.9	10.5	6.6	404.3	15.8	65.2	54.7	39.6	46.1

Reproduced with permission of the copyright owner. Further reproduction prohibited without permission.

	Genus	Species	Subspecies	CahDra	AMNH#	1 NASL GT	2 NAS WDU	3 NAS WDL	4 NPM WDT	5 NSLA HT	6 NSLA WD	7 PNAS HT	8 PNAS WD	9 NLCL GT	10 ZYGA RE	11 ZYG OHT	12 BZY GWD	13 APZY GR	14 MXA RCL	15 BMA XWD
183	*Macaca*	*mulatta*	*mulatta*	9/7	27573	21.3	2.8	8.6	10.7	16.8	9.8	13.2	11.5	7.4	454.7	18.3	68.2	54.6	38.6	48.8
184	*Macaca*	*mulatta*	*mulatta*	9/7	27574	21.5	2.4	8.3	7.7	17.5	11.6	11.0	9.5	4.5	391.9	15.4	68.5	52.2	40.9	48.3
185	*Macaca*	*mulatta*	*mulatta*	9/12	54679	22.2	1.1	8.0	9.1	16.7	10.5	11.2	11.4	5.3	410.7	14.7	67.0	55.2	39.8	47.9
186	*Macaca*	*mulatta*	*mulatta*	9/9	59987	23.8	3.5	8.2	6.8	17.0	10.5	11.5	12.7	8.7	417.9	17.2	66.1	54.4	42.8	48.2
187	*Macaca*	*mulatta*	*mulatta*	9/8	60038	22.2	0.1	8.2	6.7	18.0	11.3	12.6	10.3	7.0	440.3	17.3	68.4	50.0	41.6	46.0
188	*Papio*	*hamadryus*	*hamadryus*	20/5	52668	58.2	3.0	13.0	2.7	28.5	19.4	26.2	17.8	13.8	1044.2	28.8	99.4	47.5	76.7	78.5
189	*Papio*	*hamadryus*	*anubis*	EDU2/4	89361	51.7	4.0	8.7	6.5	22.8	15.9	19.2	10.8	8.3	742.0	22.2	85.4	47.2	68.9	65.6
190	*Papio*	*hamadryus*	*anubis*	EDU2/7	216250	53.4	3.3	11.3	2.1	28.7	17.4	27.5	15.8	11.7	997.1	29.2	91.5	44.2	71.8	73.5
191	*Papio*	*hamadryus*	*anubis*	EDU2/7	82097	52.9	2.2	9.1	3.9	29.0	17.3	24.9	14.4	12.2	917.4	24.7	102.0	44.6	72.8	77.7
192	*Papio*	*hamadryus*	*anubis*	EDU2/4	161115	38.2	3.2	9.5	5.5	27.6	17.0	22.2	13.2	12.6	757.2	23.1	91.5	44.3	67.8	73.0
193	*Papio*	*hamadryus*	*anubis*	EDU2/4	52674	52.7	3.0	11.0	3.4	25.1	19.5	26.0	16.3	10.3	887.2	23.2	96.1	44.7	71.3	76.7
194	*Papio*	*hamadryus*	*ursinus*	EDU2/7	169141	54.1	5.9	12.2	1.5	31.3	17.9	28.0	17.5	9.2	915.8	26.4	94.3	43.2	76.4	72.0
195	*Lophocebus*	*albigena*	*johnstoni*	15/11	52581	26.2	2.2	7.2	2.9	17.9	11.1	14.3	13.8	7.3	441.8	18.0	75.7	57.4	48.0	57.9
196	*Lophocebus*	*albigena*	*johnstoni*	16/3	52589	25.6	3.8	8.5	5.1	18.7	12.1	14.5	14.7	8.1	482.9	19.9	76.1	52.1	51.0	58.3
197	*Lophocebus*	*albigena*	*johnstoni*	15/5	52600	25.1	2.1	7.4	4.4	15.6	8.7	14.3	13.9	8.5	420.6	17.3	71.0	53.6	44.7	53.0
198	*Lophocebus*	*albigena*	*johnstoni*	15/5	52606	24.8	2.4	8.2	5.0	17.7	12.0	12.8	13.1	7.2	412.7	17.8	74.4	55.0	46.5	57.2
199	*Lophocebus*	*albigena*	*johnstoni*	15/5	52607	25.4	4.6	8.1	3.4	18.9	11.3	12.0	14.2	7.4	417.7	18.1	70.9	54.5	47.0	55.4
200	*Lophocebus*	*albigena*	*johnstoni*	15/7	52613	21.7	2.8	7.3	2.8	17.5	11.6	12.0	13.9	6.6	444.6	18.7	72.2	54.3	45.6	54.9
201	*Lophocebus*	*albigena*	*johnstoni*	15/10	52620	26.5	1.7	7.9	4.8	19.3	11.0	12.6	14.5	7.9	451.1	20.2	74.5	53.3	48.7	56.4
202	*Lophocebus*	*albigena*	*johnstoni*	15/11	52621	24.7	3.0	8.6	5.3	20.6	12.2	17.8	12.4	8.5	441.6	19.4	74.4	55.3	48.5	56.7
203	*Lophocebus*	*albigena*	*johnstoni*	16/4	52624	23.5	3.6	8.6	4.6	17.7	12.0	14.2	13.5	8.8	390.7	17.6	74.9	54.6	47.7	58.8
204	*Lophocebus*	*albigena*	*johnstoni*	16/4	52625	23.5	4.1	8.1	3.3	16.7	11.4	11.1	14.3	7.9	420.9	18.5	74.1	55.1	44.3	56.0
205	*Colobus*	*polykomos*	*wellensis*	51/5	52221	10.9	3.1	10.0	6.7	18.7	10.3	11.0	14.1	12.3	357.1	9.5	75.2	56.2	43.1	51.1
206	*Colobus*	*polykomos*	*wellensis*	51/6	52225	12.9	4.8	10.3	7.0	20.0	13.8	10.0	11.2	10.7	436.0	11.9	74.4	55.9	45.7	50.8
207	*Colobus*	*polykomos*	*wellensis*	51/7	52226	15.5	5.8	8.9	5.0	21.5	11.6	11.1	12.2	7.3	416.9	10.3	72.9	56.7	44.6	53.6
208	*Colobus*	*polykomos*	*wellensis*	51/7	52228	11.6	2.6	9.2	6.3	19.7	11.1	10.4	13.1	8.0	348.9	8.4	73.4	56.1	43.6	52.8
209	*Colobus*	*polykomos*	*wellensis*	51/10	52241	12.9	3.1	8.2	7.4	23.3	11.4	11.1	13.8	11.6	404.8	9.1	76.7	55.7	44.7	54.0
210	*Colobus*	*polykomos*	*wellensis*	51/11	52245	12.8	5.3	8.1	4.2	22.1	10.7	10.6	13.6	7.2	364.9	10.9	70.6	55.6	45.2	50.9
211	*Colobus*	*polykomos*	*wellensis*	51/12	52249	11.5	4.1	8.0	4.1	18.0	9.9	10.6	12.3	9.3	359.4	11.5	69.6	55.4	43.6	46.7
212	*Colobus*	*polykomos*	*wellensis*	51/4	52213	13.3	1.3	7.9	4.7	18.8	9.0	11.8	12.0	11.1	301.2	9.2	67.7	53.2	45.8	49.7
213	*Colobus*	*polykomos*	*wellensis*	51/6	52223	12.5	4.5	9.5	5.5	19.8	11.6	10.6	13.5	10.2	373.9	9.9	74.4	56.2	43.4	51.4
214	*Colobus*	*polykomos*	*wellensis*	51/9	52238	10.8	3.1	10.0	7.7	23.6	11.5	10.7	14.6	11.4	430.2	12.9	78.3	56.5	47.0	56.3
215	*Procolobus*	*pennantii*	*powelli*	46/2	52263	10.8	4.4	6.0	7.0	20.2	7.7	11.9	10.8	5.3	403.6	11.9	70.2	57.0	39.8	46.8
216	*Procolobus*	*pennantii*	*powelli*	46/3	52267	14.5	4.3	7.0	5.9	18.9	11.1	13.5	11.9	7.0	425.1	12.0	76.3	59.2	41.4	46.2
217	*Procolobus*	*pennantii*	*powelli*	46/4	52273	13.9	5.5	6.4	6.2	20.3	9.4	10.2	11.2	5.5	344.4	11.5	74.3	58.0	40.6	47.4
218	*Procolobus*	*pennantii*	*powelli*	46/5	52275	13.8	4.0	5.6	4.9	18.7	10.2	16.3	12.1	6.2	394.3	12.1	70.4	55.6	40.9	44.9

Reproduced with permission of the copyright owner. Further reproduction prohibited without permission.

	Genus	Species	Subspecies	CabDra	AMNH#	1 NASL GT	2 NAS WDU	3 NAS WDL	4 NPM WDT	5 NSLA IIT	6 NSLA WD	7 PNAS IIT	8 PNAS WD	9 NLCL GT	10 ZYGA RE	11 ZYG OHT	12 BZYG WD	13 APZY GR	14 MXA RCL	15 BMA XWD
219	*Procolobus*	*pennantii*	*powelli*	46/6	52280	12.4	3.1	8.2	7.6	19.4	11.0	11.1	12.3	9.0	358.5	12.5	73.4	59.9	43.3	48.4
220	*Procolobus*	*pennantii*	*powelli*	46/7	52283	13.5	5.6	6.7	6.0	19.6	11.3	13.6	12.8	6.0	430.9	13.3	76.7	56.3	45.7	49.6
221	*Procolobus*	*pennantii*	*powelli*	46/10	52301	11.9	5.0	7.1	7.6	18.5	11.5	13.8	10.9	9.8	419.5	10.2	76.6	58.5	43.7	48.8
222	*Procolobus*	*pennantii*	*powelli*	46/11	52305	10.0	4.0	5.9	8.1	17.9	8.5	13.1	10.7	6.5	380.6	10.4	71.7	58.8	43.0	44.1
223	*Procolobus*	*pennantii*	*powelli*	46/12	52310	12.4	5.4	7.1	8.1	20.3	10.8	14.9	11.7	6.8	438.9	12.6	77.8	58.9	45.5	49.6
224	*Procolobus*	*pennantii*	*powelli*	45/12	52257	13.6	5.1	7.1	6.4	20.1	9.7	13.8	11.5	8.9	446.2	13.4	76.7	55.0	44.2	48.1
225	*Nasalis*	*larvatus*	*larvatus*	45/4	103460	18.3	2.2	6.2	8.3	18.9	10.6	17.3	11.9	7.6	507.9	15.3	72.2	57.2	43.3	48.6
226	*Nasalis*	*larvatus*	*larvatus*	45/5	103464	18.2	0.9	7.8	5.2	19.1	11.2	15.5	13.2	6.4	485.7	14.0	73.2	55.3	42.2	48.0
227	*Nasalis*	*larvatus*	*larvatus*	45/5	103465	21.3	2.0	9.6	4.8	17.0	10.2	18.6	12.4	6.6	477.2	15.0	72.5	55.3	43.2	47.8
228	*Nasalis*	*larvatus*	*larvatus*	45/5	103466	18.8	0.5	5.8	6.1	18.8	10.1	18.0	13.7	6.6	430.8	13.4	70.7	55.4	41.6	48.9
229	*Nasalis*	*larvatus*	*larvatus*	45/6	103467	18.9	0.9	8.1	4.9	18.2	11.1	18.1	13.5	6.4	467.5	14.4	68.4	56.7	42.4	47.5
230	*Nasalis*	*larvatus*	*larvatus*	EDU	103668	19.3	1.3	4.6	4.9	16.6	9.2	19.7	12.2	5.1	434.2	13.5	66.6	56.8	43.2	46.5
231	*Nasalis*	*larvatus*	*larvatus*	EDU1/5	103669	18.4	1.5	5.0	4.8	18.8	9.9	19.4	12.0	7.3	469.7	13.9	71.8	54.0	44.1	50.3
232	*Nasalis*	*larvatus*	*larvatus*	EDU1/5	106033	16.8	1.5	6.8	6.0	18.7	11.4	18.2	11.8	4.3	468.6	13.8	71.9	59.2	39.2	51.1
233	*Nasalis*	*larvatus*	*larvatus*	EDU1/5	106034	18.6	2.6	5.4	4.9	18.0	10.7	17.2	15.0	6.3	443.7	13.5	69.7	57.6	40.5	50.6
234	*Presbytis*	*melalophos*	*sumatranus*	40/3	102744	11.8	2.3	6.2	6.8	14.3	10.0	10.4	9.8	7.7	348.5	11.5	70.2	68.3	32.7	53.4
235	*Presbytis*	*melalophos*	*sumatranus*	40/3	102746	12.1	4.3	6.3	4.7	14.4	10.6	12.4	9.7	6.1	346.3	12.1	70.5	66.3	33.1	52.2
236	*Presbytis*	*melalophos*	*sumatranus*	40/4	102751	10.9	1.8	7.5	5.0	13.9	10.5	11.2	11.1	6.3	370.0	12.4	73.5	66.4	33.5	50.8
237	*Presbytis*	*melalophos*	*sumatranus*	40/5	102752	9.9	4.0	7.3	5.3	13.9	9.6	10.6	10.0	6.4	325.7	12.3	69.0	67.2	32.0	53.9
238	*Presbytis*	*melalophos*	*sumatranus*	40/6	102760	9.1	2.5	5.9	6.3	12.8	8.5	12.8	9.9	5.5	367.1	11.0	71.3	69.2	29.8	49.9
239	*Presbytis*	*melalophos*	*sumatranus*	40/6	102762	7.4	3.9	6.8	7.1	14.7	9.1	11.2	10.5	4.8	334.8	10.5	67.0	66.7	32.6	49.8
240	*Presbytis*	*melalophos*	*sumatranus*	40/7	102882	9.7	3.4	6.0	5.5	13.1	8.5	10.2	9.5	5.0	297.8	11.3	66.2	67.0	31.5	49.7
241	*Presbytis*	*melalophos*	*sumatranus*	40/7	102884	9.4	1.2	5.9	7.0	13.5	8.3	10.7	10.6	4.4	317.4	10.6	70.4	66.3	31.7	52.8
242	*Presbytis*	*melalophos*	*sumatranus*	40/8	102886	11.2	3.0	6.3	4.2	14.5	8.9	11.2	10.8	4.0	345.8	11.8	69.3	65.5	32.0	50.4
243	*Presbytis*	*melalophos*	*sumatranus*	40/9	102890	11.2	3.2	6.2	7.5	13.6	8.6	10.8	9.2	4.0	286.1	10.9	68.4	68.1	29.8	50.5
244	*Semnopithecus*	*entellus*	*entellus*	38/9	163082	12.0	5.0	6.0	8.2	19.9	8.8	9.1	12.6	5.4	419.3	12.3	79.2	58.6	41.3	51.7
245	*Semnopithecus*	*cristata*	*pyrrhus*	37/7	102730	10.2	4.2	5.0	5.6	15.0	6.0	7.2	11.9	6.9	298.7	8.9	64.5	64.2	37.1	47.0
246	*Semnopithecus*	*cristata*	*pyrrhus*	37/7	102733	9.0	3.8	6.0	7.0	15.8	7.3	8.6	12.5	7.5	293.4	11.4	70.4	61.3	39.2	54.5
247	*Semnopithecus*	*cristata*	*pyrrhus*	37/8	102736	10.7	3.2	4.3	6.9	15.5	6.1	8.6	11.0	5.9	339.4	10.7	67.9	64.3	36.2	49.8
248	*Semnopithecus*	*cristata*	*pyrrhus*	37/9	102743	11.7	4.3	5.9	5.6	15.7	7.3	8.3	12.0	8.7	273.3	10.8	68.8	63.7	36.9	49.9
249	*Semnopithecus*	*cristata*	*cristata*	36/9	106042	9.1	3.8	4.8	5.8	14.6	6.6	7.7	11.5	5.2	264.7	9.0	62.8	64.9	34.0	45.8
250	*Semnopithecus*	*cristata*	*cristata*	36/10	106587	10.2	3.9	7.4	6.1	15.7	8.4	7.5	10.4	7.6	305.4	10.7	65.4	62.9	38.0	46.8
251	*Semnopithecus*	*cristata*	*cristata*	36/10	106588	9.8	3.7	5.6	6.2	16.1	7.1	8.5	10.9	5.8	299.7	10.8	63.2	64.9	35.2	45.3
252	*Semnopithecus*	*cristata*	*cristata*	37/1	106674	9.3	1.0	6.1	7.3	15.8	8.0	8.2	11.5	7.6	277.7	10.0	66.6	63.1	37.7	46.8
253	*Semnopithecus*	*cristata*	*kohlbruggei*	37/5	107570	15.2	3.9	6.7	4.8	16.3	8.5	9.4	11.4	5.9	390.5	12.1	72.9	63.0	38.0	51.7
254	*Semnopithecus*	*cristata*	*kohlbruggei*	37/5	107571	12.1	3.5	6.3	7.3	18.6	7.3	8.3	12.0	6.3	339.7	12.2	71.7	63.5	38.3	54.0

Reproduced with permission of the copyright owner. Further reproduction prohibited without permission.

	Genus	Species	Subspecies	CabDrn	AMNH#	1 NASL GT	2 NAS WDU	3 NAS WDL	4 NPM WDT	5 NSLA IIT	6 NSLA WD	7 PNAS IIT	8 PNAS WD	9 NLCL GT	10 ZYGA RE	11 ZYG OHT	12 BZY GWD	13 APZY GR	14 MXA RCL	15 BMA XWD
255	*Hylobates*	*lar*	*entelloides*	56/10	208985	11.0	5.3	12.1	4.5	15.0	12.7	8.7	16.1	8.1	506.7	18.4	66.8	53.4	40.5	48.7
256	*Hylobates*	*lar*	*entelloides*	57/3	31593	10.8	2.7	10.5	6.2	16.7	10.9	10.8	14.5	6.3	438.5	16.7	65.0	53.2	39.5	47.1
257	*Hylobates*	*lar*	*entelloides*	56/11	54659	11.1	3.4	10.5	5.7	13.5	12.2	12.8	13.5	7.3	506.1	16.8	63.9	55.1	40.0	47.6
258	*Hylobates*	*syndactylus*	*syndactylus*	59/10	102186	15.0	5.7	12.2	6.8	22.2	17.8	9.7	14.8	3.5	544.9	18.5	80.9	56.5	53.5	64.4
259	*Hylobates*	*syndactylus*	*syndactylus*	59/8	102188	11.1	6.1	8.1	5.8	26.0	15.1	8.1	15.2	8.0	591.5	16.3	79.5	57.4	54.0	60.7
260	*Hylobates*	*syndactylus*	*syndactylus*	59/9	102190	16.5	5.5	11.6	5.6	22.8	17.3	6.2	17.5	7.9	700.6	21.2	79.2	53.2	56.9	66.0
261	*Hylobates*	*syndactylus*	*syndactylus*	59/11	102195	12.2	6.6	9.8	6.8	23.6	14.0	9.4	14.5	5.6	744.1	20.0	74.5	56.8	52.1	57.8
262	*Hylobates*	*syndactylus*	*syndactylus*	59/12	102196	13.6	5.4	10.7	7.2	23.2	13.6	6.2	13.7	6.8	642.9	20.3	78.9	51.8	55.9	58.9
263	*Hylobates*	*syndactylus*	*syndactylus*	59/13	102463	12.2	6.6	9.8	6.8	23.6	14.0	9.4	14.5	5.6	744.1	20.0	74.5	56.8	52.1	57.8
264	*Hylobates*	*syndactylus*	*syndactylus*	59/4	102721	11.4	7.0	11.0	4.6	24.9	16.5	8.6	15.8	7.5	750.3	20.7	80.7	56.3	51.8	61.6
265	*Hylobates*	*syndactylus*	*syndactylus*	59/6	102727	13.6	4.0	10.5	5.5	19.5	14.4	8.1	16.4	7.5	612.2	19.9	74.1	55.2	49.5	60.5
266	*Hylobates*	*syndactylus*	*syndactylus*	59/2	106582	8.9	4.2	9.4	5.3	22.2	12.9	8.3	16.1	8.3	595.9	20.0	72.7	56.7	47.0	64.0
267	*Hylobates*	*syndactylus*	*syndactylus*	59/3	106583	17.3	6.5	9.9	5.5	18.5	15.5	6.6	15.1	6.7	771.5	21.3	86.6	55.2	52.6	65.6
268	*Pongo*	*pygmaeus*	*pygmaeus*	62/9	200900	37.7	3.9	13.8	6.6	34.2	21.1	30.5	22.0	21.9	1190.1	21.7	122.3	57.0	73.7	107.5
269	*Pongo*	*pygmaeus*	*pygmaeus*	62/1	201811	36.5	2.9	11.4	6.9	30.3	21.4	23.9	22.3	33.0	1180.5	27.9	131.9	54.8	74.8	118.4
270	*Pongo*	*pygmaeus*	*pygmaeus*	62/9	200898	34.9	3.8	12.4	8.1	28.3	27.7	30.0	21.7	32.9	1095.4	26.0	122.4	59.6	74.6	91.6
271	*Gorilla*	*gorilla*	*gorilla*	72/4	1472	43.3	6.9	16.0	6.6	35.6	31.0	31.7	26.5	20.2	1824.3	31.2	146.6	56.1	87.6	104.2
272	*Gorilla*	*gorilla*	*gorilla*	71/5	167330	42.6	8.1	18.8	11.3	26.3	29.3	28.0	21.5	24.0	1884.5	37.2	131.0	57.2	82.2	104.2
273	*Gorilla*	*gorilla*	*gorilla*	71/9	167337	50.7	7.2	14.6	9.5	28.2	29.9	32.1	22.1	26.7	1663.2	32.1	141.3	53.9	82.0	100.2
274	*Gorilla*	*gorilla*	*gorilla*	71/11	167339	43.3	8.0	16.3	8.4	25.8	28.6	31.2	19.1	24.5	1835.9	32.6	127.6	50.2	85.2	100.5
275	*Gorilla*	*gorilla*	*gorilla*	71/12	167340	43.7	8.8	18.8	7.7	26.4	30.2	36.2	23.9	24.0	2108.2	37.1	140.9	56.5	84.7	111.3
276	*Gorilla*	*gorilla*	*gorilla*	73/1	214108	43.5	8.6	19.3	10.0	26.8	32.0	28.6	24.1	27.5	1888.8	34.1	152.9	55.1	86.1	116.9
277	*Gorilla*	*gorilla*	*gorilla*	70/6	54327	40.1	7.2	21.0	9.2	31.3	35.0	28.7	26.7	20.5	2011.4	38.1	136.4	56.6	79.1	104.3
278	*Gorilla*	*gorilla*	*gorilla*	71/3	54356	37.7	6.7	13.0	9.3	33.9	34.1	29.1	22.1	23.5	1873.3	34.0	139.4	59.8	86.8	105.7
279	*Gorilla*	*gorilla*	*gorilla*	72/10	81652	40.6	10.7	19.5	7.4	30.4	32.5	24.6	22.4	24.8	2041.1	37.3	140.5	54.6	83.4	113.8
280	*Homo*	*sapiens*	*sapiens*	VL4/B3	998452	20.6	14.6	14.6	7.8	24.4	26.3	24.6	28.5	21.8	912.7	17.0	111.9	66.6	51.9	89.3
281	*Homo*	*sapiens*	*sapiens*	VL4/A1	2385	22.8	6.6	18.7	13.2	24.7	29.0	27.7	29.4	23.2	1106.8	23.5	116.5	61.6	55.9	93.6
282	*Homo*	*sapiens*	*sapiens*	VL5/A4	2396	21.3	11.9	18.2	9.9	27.1	25.9	24.9	24.2	20.2	942.5	18.1	118.8	64.8	57.9	90.7
283	*Homo*	*sapiens*	*sapiens*	VL4/B8	2462	18.2	4.6	12.3	12.1	26.4	24.5	22.6	25.0	16.8	1051.1	24.7	109.3	67.1	49.7	90.1
284	*Homo*	*sapiens*	*sapiens*	VL4/C9	2793	21.0	13.0	16.4	6.6	21.9	22.2	22.5	27.8	23.3	898.2	18.0	109.4	67.9	49.7	86.4
285	*Homo*	*sapiens*	*sapiens*	VL4/A2	3281	21.9	10.3	15.5	11.7	23.2	26.7	24.0	24.0	24.6	1096.7	24.4	122.1	69.2	51.7	97.5
286	*Homo*	*sapiens*	*sapiens*	VL5/A8	3449	19.9	12.9	19.6	10.6	24.9	26.7	23.3	30.7	21.3	1256.4	26.9	122.8	65.1	54.2	94.3
287	*Homo*	*sapiens*	*sapiens*	VL4/D8	4927	23.1	10.9	13.3	9.2	28.9	20.0	23.6	25.4	22.0	1177.1	25.7	112.8	62.9	52.3	89.7
288	*Homo*	*sapiens*	*sapiens*	VL4/A2	5281	22.3	12.3	19.8	10.6	26.1	30.9	25.1	30.8	20.8	1090.5	23.7	118.7	66.0	50.8	94.8
289	*Homo*	*sapiens*	*sapiens*	VL4/4-5	642	23.1	15.0	17.4	7.1	26.5	25.6	27.6	30.6	29.5	1157.0	24.1	116.3	60.6	59.9	90.7
290	*Pan*	*paniscus*	.	.	86857	15.6	3.2	14.4	4.1	22.7	19.4	16.8	20.0	19.9	687.0	19.1	96.7	57.2	54.2	69.4

Reproduced with permission of the copyright owner. Further reproduction prohibited without permission.

	Genus	Species	Subspecies	CnhDra	AMNH#	1 NASL GT	2 NAS WDU	3 NAS WDL	4 NPM WDT	5 NSLA HT	6 NSLA WD	7 PNAS HT	8 PNAS WD	9 NLCL GT	10 ZYGA RE	11 ZYG OHT	12 BZY GWD	13 APZY GR	14 MXA RCL	15 BMA XWD
291	*Pan*	*troglodytes*	*verus*	66/5	167343	21.2	5.6	12.6	7.9	25.6	23.9	21.2	24.8	35.1	1194.0	25.6	113.6	57.6	68.0	79.8
292	*Pan*	*troglodytes*	*verus*	66/7	167345	31.0	6.1	13.7	5.5	22.6	26.8	23.0	17.7	27.1	1082.4	27.9	102.0	57.6	65.3	78.6
293	*Pan*	*troglodytes*	*verus*	66/13	174860	26.4	4.8	9.4	9.8	26.0	23.6	26.3	21.2	36.7	1231.3	24.6	112.6	54.5	76.0	83.9
294	*Pan*	*troglodytes*	*verus*	66/10	201469	20.5	6.5	16.6	6.0	26.4	28.6	18.4	25.4	31.4	1057.8	20.6	113.7	53.8	71.9	81.6
295	*Pan*	*troglodytes*	*verus*	67/3	89351	29.1	9.1	12.6	7.2	29.1	25.3	21.8	25.0	24.4	1271.3	28.0	114.6	56.2	66.5	82.6
296	*Pan*	*troglodytes*	*verus*	67/4	89354	25.1	5.1	11.4	7.7	28.6	25.9	25.1	27.0	30.3	1280.7	25.2	125.7	56.0	72.4	89.6
297	*Pan*	*troglodytes*	*verus*	67/5	89355	16.9	7.4	14.1	6.9	32.0	27.6	22.3	27.1	32.6	1204.8	23.6	121.8	57.7	70.5	86.1
298	*Pan*	*troglodytes*	*verus*	66/2	90191	25.1	6.8	12.9	7.3	25.7	24.8	21.3	21.8	30.2	1249.8	31.1	111.1	56.8	70.6	80.5
299	*Pan*	*troglodytes*	*verus*	66/11	90292	27.8	11.6	11.0	4.2	22.5	23.6	24.2	22.8	35.2	1034.1	20.7	114.6	56.7	67.6	84.8
300	*Pan*	*troglodytes*	*verus*	66/12	90293	40.4	10.2	13.5	6.3	25.3	22.4	20.4	23.0	25.7	1144.0	23.5	117.1	57.8	62.7	86.5

Reproduced with permission of the copyright owner. Further reproduction prohibited without permission.

	16	17	18	19	20	21	22	23	24	25	26	27	28	29	30	31	32	33	34	35	36	37	38
	UMA XWD	AFA CHT	PFA CHT	RAM SHT	I2PA LW	P3PA LW	M1P ALW	M3P ALW	I2PA LD	P3PA LD	M1P ALD	M3P ALD	PAL LGT	PAL THK	KRO GAG	ENL OAG	SLO POC	FAC CNV	FAC SIZ	PPN ALO	ORBI HT	CRL GTH	NCL GTH
1	51.6	35.6	14.4	26.1	7.3	17.5	19.5	21.1	1.0	4.1	6.5	7.4	37.8	4.4	140.2	127.1	11.8	7.2	133.0	44.8	23.2	103.1	71.0
2	49.1	36.0	14.5	25.8	6.2	18.2	21.0	21.5	1.2	3.4	6.3	6.6	38.0	4.2	141.2	126.6	12.4	-0.5	132.3	43.1	23.1	103.7	71.9
3	50.2	39.0	12.6	19.7	8.1	16.5	19.4	20.6	1.4	3.4	5.4	6.8	38.3	4.3	134.1	129.3	2.6	5.2	131.2	46.1	22.2	104.1	73.1
4	49.6	38.0	11.9	22.3	7.5	15.9	18.8	20.2	0.8	2.7	4.9	5.5	38.0	3.4	141.2	131.9	10.0	4.3	127.2	45.5	21.9	104.4	72.4
5	52.9	37.2	9.9	20.3	8.8	15.3	18.5	19.0	1.4	3.8	5.6	6.7	38.0	3.9	136.4	131.7	6.5	5.1	127.1	47.0	22.6	102.5	72.5
6	52.5	38.7	12.0	22.6	8.5	17.3	19.1	19.9	1.2	3.7	6.2	7.2	38.5	3.5	138.7	130.7	8.8	6.5	132.0	45.8	22.8	106.3	74.7
7	47.8	33.3	15.0	23.6	7.0	15.6	19.3	20.3	1.2	2.9	5.8	6.8	35.0	1.7	138.3	127.6	9.6	9.9	127.4	43.2	21.6	101.3	71.0
8	50.5	34.4	13.4	24.2	8.6	17.8	19.9	22.1	0.6	4.1	6.7	8.1	36.9	0.8	138.7	127.2	7.5	5.7	133.2	48.2	22.3	106.7	74.9
9	51.0	35.7	13.5	19.9	8.6	19.4	21.1	22.4	1.4	2.8	5.3	7.2	36.7	2.7	139.6	126.9	4.8	1.4	128.3	45.6	21.6	102.9	71.7
10	50.1	35.4	11.9	20.7	9.0	19.3	20.7	19.3	0.8	3.0	5.1	5.9	38.0	1.8	144.4	130.0	6.1	2.5	129.4	41.8	21.9	106.0	72.0
11	50.0	39.0	13.7	14.2	8.3	17.0	18.9	22.1	1.5	5.4	6.8	7.3	30.6	1.3	116.1	123.8	10.4	6.6	125.9	41.0	22.8	112.4	86.4
12	52.6	35.4	11.4	9.8	9.2	17.1	18.7	20.4	1.6	3.7	5.0	6.7	30.0	2.1	116.7	120.3	11.2	3.5	119.2	31.6	22.0	105.1	82.2
13	51.6	31.6	13.0	13.3	9.0	19.1	20.6	20.7	1.0	4.6	6.5	6.2	30.1	1.3	120.9	117.5	6.1	4.2	121.5	34.9	19.2	108.8	86.0
14	49.4	33.7	9.4	11.4	9.1	18.0	18.7	19.8	1.4	3.6	5.2	6.7	28.7	1.5	119.8	120.2	6.5	5.8	116.1	35.9	21.0	105.2	83.4
15	54.7	37.8	11.4	11.7	10.5	19.3	21.5	23.5	0.9	4.6	6.3	6.7	35.0	3.5	122.6	128.4	9.9	9.8	129.1	37.4	23.4	111.9	86.3
16	48.6	35.5	9.6	10.1	8.3	16.3	17.0	18.8	1.3	4.4	5.6	6.2	25.9	1.6	115.8	121.5	12.0	1.5	112.3	32.1	21.6	97.5	74.5
17	49.7	37.0	8.8	13.7	7.5	15.6	16.9	18.3	1.2	4.9	5.8	6.0	26.5	1.7	117.0	121.3	5.3	7.5	117.5	33.5	23.0	102.6	79.4
18	53.9	38.9	17.6	14.3	11.0	20.1	20.9	23.0	1.9	5.0	6.2	8.1	33.6	1.8	118.4	120.1	11.5	-0.6	132.9	34.0	21.9	114.8	88.7
19	51.8	39.2	13.2	11.1	9.6	18.7	20.0	21.2	1.5	5.3	5.8	6.2	34.1	1.5	123.9	125.1	10.8	5.4	127.4	33.0	23.0	113.3	81.8
20	49.7	35.2	12.0	9.2	10.1	18.6	17.8	19.0	1.5	3.9	5.1	7.1	30.1	2.2	115.5	121.5	16.1	2.1	120.5	43.0	22.1	108.5	84.2
21	53.0	27.8	11.2	15.9	10.4	17.8	19.6	19.6	0.7	3.6	6.2	6.9	29.0	2.1	126.1	112.2	1.6	7.3	122.0	33.2	25.0	103.8	79.4
22	55.0	30.7	11.6	13.0	9.2	16.8	17.9	19.1	0.9	4.0	4.7	5.5	30.5	2.4	124.3	118.4	4.2	5.4	122.3	29.8	23.6	104.9	80.1
23	52.7	33.5	11.7	15.9	9.2	18.4	20.9	21.5	0.9	3.5	6.1	7.1	30.6	1.3	123.1	119.0	3.1	6.3	124.0	37.5	23.9	106.9	81.7
24	52.0	30.7	11.7	15.9	10.9	17.0	18.1	20.1	1.1	3.3	5.0	6.4	30.6	2.1	125.5	117.1	0.2	8.2	121.0	38.2	22.2	101.9	76.2
25	54.0	34.8	12.6	15.6	8.8	17.3	18.8	20.5	1.4	5.0	7.1	8.2	29.6	1.5	123.3	120.3	3.3	8.9	121.7	39.8	23.3	101.5	74.0
26	51.5	28.1	9.5	15.7	9.7	17.9	18.4	19.7	1.2	3.1	4.9	5.3	29.6	2.1	129.1	117.5	0.7	5.6	118.3	28.7	23.9	99.7	74.1
27	54.0	35.4	11.2	14.4	10.0	18.5	18.4	19.0	0.9	3.9	5.5	5.8	31.6	2.0	123.1	119.9	4.8	4.5	123.1	36.6	22.8	103.8	78.3
28	48.4	32.8	11.1	11.4	9.8	18.6	19.0	18.8	1.1	2.8	4.7	4.5	31.1	1.4	120.3	121.8	8.1	8.7	117.9	38.9	22.5	101.1	76.6
29	55.2	35.8	11.5	13.7	9.9	16.9	16.8	19.8	1.2	4.0	5.1	6.7	30.9	2.4	119.1	119.3	6.5	6.4	123.8	39.3	22.1	104.5	81.6
30	53.9	32.7	10.8	12.2	11.2	17.8	18.7	19.2	1.3	4.5	6.3	5.7	32.0	1.7	125.6	120.9	7.9	7.8	120.4	34.9	21.8	102.8	77.1
31	53.6	39.8	12.5	18.2	9.0	18.3	20.4	23.1	1.0	2.6	5.6	6.1	38.1	1.8	127.3	125.6	4.6	-2.5	134.3	35.5	22.5	110.5	80.0
32	37.9	26.4	5.5	9.9	9.1	16.1	14.9	14.2	1.9	4.0	3.9	4.4	27.3	0.9	119.1	116.0	7.7	2.2	99.5	30.6	19.2	80.4	63.9
33	39.8	29.8	5.8	8.6	8.3	14.5	14.0	13.9	2.1	4.4	4.5	4.2	25.9	1.7	120.6	119.3	12.1	6.8	101.2	35.3	20.0	86.0	65.8
34	36.1	28.3	6.1	8.7	7.7	13.6	13.6	13.0	1.3	3.4	4.0	3.9	26.9	2.4	116.4	117.3	9.2	5.9	96.6	34.3	18.8	83.5	64.8
35	40.4	28.5	4.2	5.3	8.6	15.3	14.9	13.5	2.2	4.8	4.5	4.4	25.8	2.9	118.4	115.6	14.1	5.8	97.9	31.9	20.4	82.2	64.8
36	40.3	30.2	6.6	9.4	8.3	15.5	14.9	13.9	1.9	4.3	5.3	4.8	28.7	1.5	119.5	120.7	10.4	3.6	103.4	32.3	19.3	84.8	63.5
37	38.4	27.0	5.8	9.5	8.0	14.4	13.7	13.2	1.3	3.5	4.5	4.1	27.2	1.7	117.5	119.0	9.3	4.7	97.6	30.0	18.9	86.0	66.3

Reproduced with permission of the copyright owner. Further reproduction prohibited without permission.

	16	17	18	19	20	21	22	23	24	25	26	27	28	29	30	31	32	33	34	35	36	37	38
	UMA XWD	AFA CHT	PFA CHT	RAM SHT	I2PA LW	P3PA LW	M1P ALW	M3P ALW	I2PA LD	P3PA LD	M1P ALD	M3P ALD	PAL LGT	PAL THK	KRO GAG	ENL OAG	SLO POC	FAC CNV	FAC SIZ	PPN ALO	ORBI HT	CRL GTH	NCL GTH
38	36.0	27.2	6.6	7.0	6.2	13.2	13.0	13.2	1.1	3.9	4.2	4.2	26.6	1.0	115.3	118.5	12.0	7.1	93.8	32.6	19.1	80.5	61.1
39	37.3	25.7	5.5	8.4	6.4	13.9	14.0	13.8	1.5	3.8	3.9	3.9	25.4	2.6	119.3	114.4	8.3	5.5	93.6	26.9	19.0	80.6	63.1
40	35.7	26.6	5.0	8.5	7.3	12.3	13.7	13.2	1.2	2.5	4.1	3.6	25.0	0.7	115.2	111.2	8.5	7.6	92.1	31.3	18.5	79.1	61.8
41	35.4	27.3	5.6	9.3	6.4	12.8	14.3	13.0	1.7	3.3	4.7	4.2	25.6	3.8	117.7	117.5	9.4	7.8	96.0	31.5	21.3	80.7	62.2
42	33.9	29.2	8.0	7.4	7.1	12.9	11.3	12.6	1.8	3.1	2.4	3.2	26.5	3.2	117.5	130.6	13.5	14.0	96.3	43.4	18.2	77.8	58.9
43	32.1	28.6	7.8	6.6	6.5	12.8	12.1	12.5	1.4	2.8	2.9	3.4	26.9	3.0	114.2	128.4	16.3	11.0	95.4	43.7	18.1	75.9	58.2
44	32.7	26.6	5.5	7.3	7.5	11.9	11.8	12.2	1.7	3.1	3.5	3.5	26.4	1.3	114.7	129.3	12.6	17.2	93.2	46.6	16.0	74.5	56.7
45	31.4	26.1	5.4	7.7	6.2	10.7	11.2	12.5	1.6	2.9	3.5	3.7	24.5	1.8	115.6	126.8	10.3	19.6	90.3	44.4	16.9	74.5	56.1
46	31.9	27.0	5.8	7.5	5.9	10.7	11.1	10.8	1.5	2.7	3.2	3.4	25.7	2.1	120.3	131.7	11.4	14.5	90.1	44.5	16.9	74.0	55.4
47	31.3	24.9	5.2	6.6	6.4	9.8	10.6	10.1	1.3	2.8	3.3	3.0	23.4	1.3	113.4	126.1	12.6	17.0	87.5	43.3	15.6	70.9	56.0
48	32.8	24.9	6.7	9.0	7.5	12.1	12.2	11.5	1.1	2.3	2.9	3.7	24.9	2.4	119.1	128.1	9.8	14.6	92.0	44.7	15.8	77.9	60.9
49	32.2	25.3	8.2	8.0	7.6	12.0	10.8	10.9	1.6	2.7	3.3	4.3	25.3	2.2	117.1	126.3	12.9	13.0	94.0	43.7	16.5	78.2	61.1
50	32.3	29.3	7.2	6.1	7.7	11.7	12.4	14.1	1.6	3.3	3.8	3.9	22.9	2.6	113.1	129.5	16.3	16.4	93.8	45.7	15.9	74.3	56.8
51	34.4	26.7	5.2	6.7	6.8	11.8	11.8	11.4	1.5	2.8	2.7	2.4	25.3	1.8	122.4	128.9	12.9	13.5	91.6	43.6	16.7	72.6	52.8
52	36.2	31.0	8.0	9.6	7.6	13.8	13.9	14.3	1.9	4.8	4.6	4.5	28.9	2.3	124.9	127.9	7.9	11.9	101.4	50.0	19.2	83.7	60.1
53	36.8	30.7	8.1	11.5	7.1	13.4	13.3	14.7	2.5	4.7	4.3	4.3	30.0	3.6	119.8	131.0	7.2	16.4	105.3	49.0	19.2	84.6	61.2
54	35.2	30.1	8.4	9.0	7.8	13.7	13.2	13.7	2.4	4.5	4.3	4.6	28.6	2.6	123.4	128.2	8.6	13.7	101.7	57.3	18.1	83.4	60.7
55	36.6	29.3	6.9	6.5	7.1	12.3	12.6	11.3	1.7	3.4	3.5	3.9	26.7	1.2	122.5	127.8	11.0	15.6	94.2	47.9	18.0	79.1	58.8
56	35.4	19.8	5.3	9.6	6.0	10.8	12.3	13.3	1.4	2.3	3.1	3.5	21.7	0.7	112.5	129.4	1.4	5.6	81.8	30.5	18.1	64.2	51.6
57	30.9	23.1	3.8	5.3	5.7	10.2	11.2	12.5	1.5	2.4	3.4	2.7	19.7	0.8	116.3	134.5	7.9	9.9	77.4	33.2	16.3	60.9	47.0
58	30.6	22.5	4.3	8.2	5.6	9.5	11.2	13.5	1.3	3.0	3.9	4.0	20.2	0.3	118.4	129.7	1.9	8.3	75.9	37.9	15.4	62.8	49.1
59	29.8	24.1	4.1	7.9	6.0	11.0	13.3	14.0	1.3	2.6	4.0	3.3	22.9	1.8	125.2	129.9	1.0	4.2	81.8	29.0	18.0	66.7	49.9
60	30.2	24.3	3.5	7.4	5.7	9.2	11.5	13.4	1.0	2.4	3.9	3.8	21.0	1.4	115.0	126.2	3.5	9.3	79.8	36.0	16.8	65.7	51.9
61	29.9	22.4	4.2	9.1	5.6	9.2	10.7	11.8	1.5	2.4	3.6	3.6	19.3	1.2	115.2	130.7	0.3	8.6	75.3	35.2	14.8	60.8	48.5
62	30.3	21.2	4.5	7.2	5.4	9.0	11.1	11.9	1.0	1.5	2.4	2.4	19.6	2.3	116.9	126.7	3.4	6.2	74.2	29.0	15.3	60.2	48.0
63	27.8	19.9	2.5	3.1	5.1	9.2	10.2	11.8	1.1	1.9	2.7	1.8	17.0	2.4	108.9	128.2	13.5	6.8	69.8	31.9	15.5	58.2	48.7
64	29.9	22.3	4.7	7.1	5.5	9.7	11.3	12.1	1.2	2.4	2.9	2.8	21.4	1.9	118.6	131.9	5.0	5.3	76.4	34.4	15.7	61.7	49.3
65	32.1	21.3	4.4	7.8	5.8	10.0	11.5	12.4	1.2	2.2	3.7	3.0	19.8	0.6	114.9	129.7	2.7	10.1	78.4	36.7	15.4	61.7	49.8
66	30.2	35.6	8.5	8.4	9.2	15.9	16.8	16.9	0.9	5.1	5.6	4.3	31.3	0.1	112.5	124.6	11.5	4.3	106.8	36.6	20.2	89.7	72.0
67	36.6	31.2	7.8	5.8	9.3	15.0	16.1	16.2	1.5	4.1	4.7	3.5	29.3	0.3	109.8	121.0	18.3	2.9	101.8	33.1	20.0	85.0	67.3
68	37.9	31.3	8.7	8.8	9.1	15.9	15.4	15.9	1.0	4.2	4.4	3.0	31.4	0.7	115.0	122.8	12.4	0.4	105.7	32.6	19.8	87.0	69.3
69	37.1	34.5	8.4	6.5	10.4	16.0	15.8	15.4	1.2	4.2	5.1	3.6	28.9	0.6	109.7	120.9	15.9	1.8	104.4	36.9	20.8	88.5	71.6
70	38.0	28.6	8.0	8.8	9.2	15.7	16.1	16.2	0.8	4.1	4.8	3.5	29.5	0.8	116.1	123.4	12.8	6.4	102.5	37.2	18.1	86.5	68.6
71	32.6	26.2	8.0	6.6	9.7	14.6	16.2	16.8	0.7	4.1	4.2	3.5	29.8	1.1	113.6	120.7	14.2	1.2	102.0	37.2	18.7	85.1	69.9
72	39.6	35.3	8.2	9.3	10.3	16.2	16.5	16.6	1.1	5.1	5.3	3.4	30.4	0.0	108.8	119.9	11.6	5.7	108.6	39.3	20.6	84.4	69.0
73	39.0	32.8	8.6	11.2	9.8	16.7	18.0	18.3	1.1	4.6	5.1	3.8	28.8	1.3	115.6	121.4	9.1	2.9	107.1	35.3	20.0	87.6	70.5
74	39.2	28.7	6.6	8.3	9.6	15.5	16.4	16.0	1.2	4.6	4.7	3.5	29.2	0.3	112.6	122.2	13.8	4.5	102.6	33.9	18.8	84.8	68.2

Reproduced with permission of the copyright owner. Further reproduction prohibited without permission.

	16	17	18	19	20	21	22	23	24	25	26	27	28	29	30	31	32	33	34	35	36	37	38
	UMA XWD	AFA CHT	PFA CHT	RAM SHT	I2PA LW	P3PA LW	M1P ALW	M3P. ALW	I2PA LD	P3PA LD	M1P ALD	M3P ALD	PAL LGT	PAL THK	KRO GAG	ENL OAG	SLO POC	FAC CNV	FAC SIZ	PPN ALO	ORBI HT	CRL GTH	NCL GTH
75	40.7	31.6	8.7	9.2	9.7	15.9	17.5	17.8	0.8	4.1	5.1	3.5	31.5	0.4	111.3	123.7	12.3	6.5	109.5	35.1	19.3	89.0	72.2
76	41.3	34.6	10.0	8.5	10.4	14.5	16.4	16.3	1.9	4.7	5.4	4.5	30.6	0.5	110.2	125.9	11.9	8.1	107.5	47.3	20.2	90.7	73.0
77	41.0	31.9	8.5	6.7	10.0	15.3	17.3	16.5	1.7	4.3	4.8	3.2	31.2	1.4	113.1	126.5	10.6	7.0	105.0	47.9	20.1	88.5	71.2
78	41.7	31.8	10.0	7.7	9.3	15.1	16.6	16.9	1.6	4.3	4.4	3.7	30.8	0.2	110.3	125.1	10.2	7.2	107.6	44.4	20.4	89.7	73.6
79	40.7	35.9	9.3	7.3	10.9	17.0	18.2	17.6	1.9	4.8	5.9	4.4	32.5	1.7	111.6	120.2	10.2	5.2	110.7	43.2	21.1	94.1	73.8
80	43.3	30.3	8.0	5.1	10.0	15.9	16.9	17.4	1.7	3.9	5.3	3.8	31.8	1.1	109.2	123.0	15.2	4.1	105.4	48.3	17.8	89.7	75.9
81	42.6	35.6	9.5	5.9	10.1	16.7	17.7	16.6	1.6	4.3	5.1	4.2	32.5	0.0	107.4	123.2	15.1	2.6	110.8	41.0	21.8	91.6	74.9
82	41.8	35.3	8.3	8.7	10.2	17.5	18.9	16.4	1.2	4.1	5.5	4.5	33.8	0.8	112.9	125.6	10.2	1.3	114.1	42.7	22.8	95.8	78.1
83	41.2	32.1	9.1	4.8	10.5	16.1	17.7	17.5	1.6	4.4	4.9	3.2	31.2	0.8	108.3	122.1	16.8	5.1	107.4	45.7	20.5	89.6	75.8
84	39.8	30.4	7.7	6.6	9.2	15.6	17.1	16.0	1.9	4.5	4.8	3.8	30.4	0.6	113.1	121.9	13.1	-0.9	103.5	40.3	19.1	88.2	73.0
85	38.5	32.3	7.7	6.6	9.3	16.1	17.4	17.5	1.6	4.6	5.0	4.0	29.6	0.3	112.5	126.2	14.2	4.7	104.2	40.8	19.3	88.0	71.2
86	27.2	19.3	3.1	4.6	6.1	9.9	11.6	13.6	1.2	2.4	3.3	2.6	17.7	0.0	105.7	120.1	11.5	10.1	69.6	37.0	14.7	63.9	52.7
87	28.0	18.7	3.5	4.9	5.7	10.8	12.0	13.0	0.9	2.2	3.4	2.5	15.6	0.1	106.1	116.4	9.5	9.0	68.9	36.4	14.4	60.7	51.4
88	27.8	19.6	2.7	3.7	6.0	9.4	11.4	12.7	1.1	2.1	3.3	2.7	15.7	1.2	104.0	120.0	13.4	8.0	68.6	35.9	14.9	60.8	51.9
89	24.5	18.4	3.6	3.5	6.8	10.1	11.6	12.6	0.9	1.6	2.3	2.0	15.1	0.7	103.1	115.6	14.4	3.0	65.4	27.5	13.2	56.8	48.6
90	27.0	19.5	2.8	2.7	5.6	9.0	11.0	11.8	1.1	1.8	2.2	1.7	15.0	0.2	102.1	117.9	16.0	7.7	66.8	31.0	14.8	58.6	51.6
91	27.1	20.9	3.5	4.9	6.0	9.7	11.1	12.4	1.0	1.4	2.4	2.1	15.6	0.5	104.5	119.3	10.2	5.7	67.3	31.2	14.6	61.7	52.3
92	27.4	20.1	2.0	4.2	6.0	10.2	11.6	12.5	1.1	2.3	3.2	2.3	15.0	0.4	102.3	117.7	11.7	8.7	68.9	30.2	14.0	60.8	54.4
93	27.2	21.9	3.8	5.0	6.2	10.2	11.7	12.6	0.9	1.9	2.4	1.7	16.4	0.5	104.3	118.9	10.2	5.1	69.9	32.9	14.4	57.3	48.9
94	26.7	21.3	2.4	3.1	6.9	10.1	12.4	13.3	1.1	1.8	2.5	1.9	16.1	0.3	101.7	120.4	15.1	7.9	69.3	34.1	12.6	60.9	51.7
95	26.4	22.0	3.5	4.1	6.0	9.7	12.1	13.0	0.6	1.6	2.9	2.2	15.9	0.5	106.5	121.1	12.1	7.1	70.6	30.2	14.3	59.2	48.6
96	41.2	19.5	3.1	6.7	6.3	12.5	14.4	14.5	1.0	2.5	3.1	3.3	19.0	2.1	112.6	129.8	4.9	18.5	86.2	33.4	18.8	61.9	51.4
97	38.3	22.5	2.5	6.5	7.1	10.0	11.9	12.8	0.9	2.2	2.9	3.6	18.4	1.2	117.8	129.9	2.5	14.8	83.3	31.1	20.6	61.3	46.5
98	35.5	20.5	1.6	4.3	5.9	10.0	11.5	12.0	1.2	1.9	2.8	2.2	16.0	1.5	116.8	126.6	6.4	19.6	77.4	33.5	18.8	59.5	49.4
99	43.9	24.1	3.1	6.5	7.5	11.6	12.7	12.8	0.9	2.5	3.3	3.9	19.9	0.6	114.4	132.8	5.0	15.9	88.1	31.1	21.7	63.4	49.6
100	39.6	21.3	2.3	6.4	6.2	10.7	11.7	11.7	0.9	2.4	3.1	3.0	16.8	0.9	110.4	124.6	2.6	18.6	82.1	29.5	20.4	58.6	50.6
101	37.1	19.3	2.9	6.3	7.1	10.7	11.9	11.9	1.3	2.3	2.7	2.7	17.5	1.3	114.0	124.9	4.9	18.6	79.9	34.6	18.5	61.9	49.1
102	41.9	21.4	2.8	7.1	6.0	10.4	12.5	13.2	1.2	2.6	3.3	3.5	17.4	1.5	114.7	127.6	1.3	18.2	83.8	32.2	20.8	62.0	51.7
103	37.9	23.3	3.1	5.9	6.4	11.6	12.3	12.9	0.5	3.0	3.3	2.7	18.8	0.2	114.9	126.7	4.8	21.1	84.6	32.4	20.6	60.5	50.4
104	37.5	22.0	3.0	5.8	6.6	11.8	12.5	12.4	1.1	3.2	3.2	2.9	18.1	1.4	112.7	133.0	7.2	19.6	81.7	36.3	18.4	59.1	49.2
105	37.8	20.8	2.2	4.6	6.6	10.4	11.8	12.3	0.5	2.0	2.6	2.3	17.9	0.2	116.0	131.9	7.6	19.8	80.5	30.6	19.7	60.8	47.5
106	25.9	14.9	2.1	4.0	4.7	10.1	10.9	12.0	0.8	2.2	2.6	2.5	15.6	2.9	107.3	124.9	6.6	4.4	60.1	37.2	10.6	49.6	42.5
107	20.9	10.1	1.3	1.1	3.6	5.7	6.6	7.8	0.6	1.1	1.7	1.9	10.7	0.2	99.2	122.4	5.3	6.9	41.8	37.9	9.2	34.1	30.7
108	19.7	10.1	1.9	1.3	2.8	5.8	6.7	7.6	1.1	1.4	1.9	2.4	11.2	1.3	100.7	123.0	6.3	6.2	42.1	38.3	8.5	34.8	31.1
109	18.9	9.8	1.5	0.8	3.4	6.0	6.5	7.8	0.4	1.6	2.0	2.4	10.7	1.2	107.6	126.4	8.8	9.4	39.8	32.9	8.0	33.9	29.1
110	19.6	10.3	1.7	1.1	2.9	6.3	6.6	7.2	0.4	1.2	1.9	2.1	11.2	0.7	100.3	129.9	8.0	8.4	41.1	37.5	7.5	34.6	30.5

Reproduced with permission of the copyright owner. Further reproduction prohibited without permission.

	16	17	18	19	20	21	22	23	24	25	26	27	28	29	30	31	32	33	34	35	36	37	38
	UMA XWD	AFA CHT	PFA CHT	RAM SHT	I2PA LW	P3PA LW	M1P ALW	M3P ALW	I2PA LD	P3PA LD	M1P ALD	M3P ALD	PAL LGT	PAL THK	KRO GAG	ENL OAG	SLO POC	FAC CNV	FAC SIZ	PPN ALO	ORBI HT	CRL GTH	NCL GTH
111	18.8	9.8	0.7	0.5	3.2	6.1	6.6	7.7	0.4	1.2	1.8	2.5	10.6	0.3	101.5	129.4	11.1	12.8	40.6	35.5	7.6	34.2	30.4
112	20.1	10.5	2.2	0.6	3.2	6.3	6.7	8.0	0.7	1.3	2.1	2.5	12.8	0.8	104.0	125.1	9.2	4.9	42.7	40.2	8.6	36.3	31.5
113	19.4	9.9	1.3	0.3	3.3	5.9	6.5	7.4	0.7	1.1	2.0	1.9	10.8	0.6	105.8	126.4	12.9	6.4	40.6	35.5	8.5	34.5	30.2
114	19.5	10.8	1.7	0.6	3.0	6.0	6.4	7.4	0.4	1.1	1.8	2.0	11.3	0.9	106.7	127.7	9.0	11.6	41.4	39.9	9.0	35.4	31.1
115	20.4	11.0	1.7	1.2	3.3	5.9	6.5	7.3	0.4	1.2	1.9	2.2	11.7	1.0	105.8	128.5	6.3	11.5	42.9	36.1	9.1	35.9	31.4
116	20.6	10.5	1.8	1.5	3.0	6.4	6.8	7.9	0.3	1.4	1.9	2.4	12.4	0.9	105.0	124.0	6.3	10.1	43.9	38.6	8.4	36.4	31.8
117	27.4	20.1	2.0	4.2	6.0	10.2	11.6	12.5	1.1	2.3	3.2	2.3	15.0	0.4	102.3	117.7	11.7	8.7	68.9	30.2	14.0	60.8	54.4
118	45.8	36.0	10.4	7.2	9.9	16.7	18.3	15.7	1.8	5.9	6.2	4.1	32.8	0.3	114.2	127.2	11.2	4.1	113.7	43.9	19.1	91.1	70.4
119	45.9	36.5	7.3	5.6	10.7	16.8	18.7	17.1	2.1	5.2	6.1	5.2	34.6	0.8	118.2	130.4	9.3	5.8	110.6	45.3	20.5	92.6	70.5
120	47.9	37.8	9.9	6.2	10.2	17.4	19.2	17.5	2.1	5.8	5.4	4.8	37.4	2.8	119.4	129.9	9.3	3.5	117.9	46.4	19.5	96.7	69.1
121	43.5	36.1	8.8	8.1	9.5	15.8	18.8	15.8	1.5	6.4	5.7	5.0	33.5	1.5	114.4	131.9	9.7	6.9	113.2	41.8	19.6	89.9	66.5
122	43.4	34.9	8.8	8.4	9.4	16.4	18.8	17.1	2.1	5.9	6.1	5.5	35.2	1.8	118.0	127.1	5.8	4.1	112.1	41.7	19.3	93.5	70.3
123	45.3	36.6	9.4	5.4	12.3	19.2	20.6	18.2	2.2	6.8	7.3	5.5	35.7	1.3	114.2	128.7	14.3	2.7	118.4	46.5	19.5	96.6	75.6
124	43.8	39.6	11.8	8.7	12.1	18.6	20.8	19.1	3.4	8.0	8.1	6.9	36.2	1.1	113.3	126.5	12.4	3.1	121.9	45.7	20.8	99.6	77.4
125	45.1	31.2	9.1	7.8	8.5	13.9	16.8	15.5	1.7	4.8	6.1	5.1	29.7	0.8	113.4	125.4	8.0	3.1	103.9	33.8	19.6	82.9	65.7
126	45.6	34.2	8.5	6.1	11.3	17.4	19.4	18.0	2.0	5.8	5.6	4.5	34.5	2.0	118.1	128.6	11.1	3.5	113.7	40.2	18.9	93.1	70.7
127	42.1	32.4	8.1	5.6	9.5	15.1	16.8	15.1	1.2	5.0	6.2	6.0	30.3	1.8	110.1	127.8	13.5	5.4	106.8	40.0	18.0	88.3	69.0
128	45.0	43.7	9.7	7.0	11.5	17.3	19.0	16.9	2.0	7.4	7.4	5.8	33.0	1.0	115.0	131.1	14.8	6.2	117.7	47.5	23.2	95.4	70.9
129	45.0	42.4	11.8	8.3	10.9	18.2	19.1	16.4	1.9	7.9	7.4	4.7	38.7	2.1	116.6	130.1	12.0	3.4	122.2	45.1	21.5	100.3	73.3
130	45.5	45.3	11.8	7.0	11.3	18.4	20.1	18.0	2.5	8.5	7.7	5.5	36.8	1.0	116.6	129.1	14.7	6.1	123.7	45.1	22.0	101.4	75.1
131	45.9	41.2	10.1	8.3	10.3	17.8	19.1	18.7	3.0	7.1	6.5	6.4	33.8	1.0	114.0	128.3	13.6	5.6	121.8	49.8	21.8	97.4	74.1
132	47.0	47.8	13.8	12.0	12.5	19.1	21.7	20.9	2.9	8.1	7.7	6.8	36.1	1.1	116.0	129.3	8.6	4.5	129.2	48.6	24.3	103.3	78.4
133	43.9	44.6	9.4	8.3	11.4	16.7	19.4	16.5	3.3	8.8	7.9	6.1	34.3	0.4	121.9	132.4	12.1	7.0	121.0	53.4	23.3	96.9	68.7
134	44.8	42.7	11.7	8.2	11.4	17.9	19.2	18.7	2.5	8.3	7.0	6.1	36.2	2.2	114.2	128.3	13.4	1.5	122.7	48.8	20.9	103.7	77.0
135	43.4	45.0	11.7	10.1	11.0	18.2	20.0	18.1	1.9	6.7	7.3	6.8	33.1	0.6	114.6	130.7	12.6	7.1	119.6	53.9	22.6	94.5	68.3
136	46.5	45.7	14.7	11.0	12.2	19.3	19.7	19.5	2.6	9.1	9.2	7.1	37.3	0.1	120.0	132.2	11.6	8.6	127.8	47.4	23.1	101.6	71.8
137	45.8	40.2	13.5	10.4	10.3	17.5	18.8	17.6	1.2	8.1	8.5	7.1	35.5	0.6	110.6	130.2	10.5	2.4	118.7	39.9	20.8	95.5	71.3
138	48.3	43.5	12.6	12.3	11.1	17.7	19.4	18.8	2.4	7.0	6.6	6.9	36.6	2.0	119.1	129.7	7.3	2.4	123.8	44.7	20.1	100.2	74.1
139	47.9	43.4	9.0	6.1	11.7	17.9	18.8	17.6	2.9	7.0	7.7	5.1	32.8	0.5	117.2	135.6	14.9	9.0	120.9	48.3	22.2	96.4	67.8
140	47.7	43.9	10.4	12.0	11.5	20.1	19.5	19.6	2.4	8.5	7.5	8.1	38.2	1.5	115.4	133.6	11.0	4.1	128.0	53.3	20.3	102.9	75.4
141	44.9	44.9	11.3	9.1	12.2	19.1	21.9	19.1	2.2	6.4	8.1	6.9	34.5	1.9	113.0	130.2	13.2	5.6	125.8	56.3	21.6	100.5	75.2
142	48.1	36.6	12.1	13.8	10.2	17.1	19.2	18.8	2.0	6.4	7.4	7.5	35.0	1.3	115.8	128.1	5.8	3.2	122.1	45.9	22.1	98.3	73.5
143	47.2	45.5	12.7	10.2	11.0	18.6	19.1	21.1	0.8	6.3	7.6	6.4	33.8	1.5	113.1	127.8	14.2	1.7	126.5	52.4	23.0	97.0	72.8
144	44.8	38.9	11.2	11.5	12.5	19.0	21.2	20.3	2.4	6.0	6.9	7.1	33.9	1.5	121.5	129.1	6.1	1.7	117.4	51.4	18.6	96.4	69.3
145	46.1	41.6	11.9	10.5	11.7	18.9	20.3	19.9	3.1	8.1	7.8	6.2	31.7	1.8	113.5	127.7	12.9	4.6	121.7	53.0	22.2	97.4	72.5
146	46.8	40.6	10.4	7.5	11.6	18.1	19.9	18.9	2.3	6.9	7.8	6.6	35.7	1.0	113.0	131.6	16.4	6.4	122.3	50.8	19.8	97.2	71.7

Reproduced with permission of the copyright owner. Further reproduction prohibited without permission.

	16	17	18	19	20	21	22	23	24	25	26	27	28	29	30	31	32	33	34	35	36	37	38
	UMA XWD	AFA CHT	PFA CHT	RAM SHT	I2PA LW	P3PA LW	M1P ALW	M3P ALW	I2PA LD	P3PA LD	M1P ALD	M3P ALD	PAL LGT	PAL THK	KRO GAG	ENL OAG	SLO POC	FAC CNV	FAC SIZ	PFN ALO	ORBI HT	CRL GTH	NCL GTH
147	48.1	42.9	11.9	10.5	12.1	18.5	20.9	19.9	2.4	7.7	8.1	7.5	32.8	0.9	113.4	128.3	11.6	5.1	124.4	50.5	24.2	98.8	73.4
148	42.8	29.0	8.9	8.1	11.2	19.1	19.3	17.4	2.8	7.3	7.1	6.1	29.9	0.7	114.4	119.5	9.4	-0.2	104.7	33.7	18.0	86.7	70.0
149	42.6	32.2	10.2	8.3	11.2	19.1	19.8	18.1	2.3	6.7	6.4	4.7	31.9	0.5	114.4	124.8	12.3	1.7	112.3	45.5	18.4	91.4	69.7
150	46.1	34.7	10.6	10.7	9.4	18.3	19.8	18.7	2.0	6.8	7.6	6.9	31.0	0.5	111.9	118.5	5.7	-4.4	111.0	33.6	20.1	90.5	71.5
151	43.9	31.6	7.8	6.5	11.4	18.1	19.0	15.8	1.5	5.2	5.6	4.0	30.0	0.4	113.2	119.5	8.0	8.8	107.1	41.6	19.7	85.0	68.5
152	45.0	31.5	9.4	11.2	10.4	17.9	18.2	16.7	2.6	6.8	6.9	5.6	27.4	0.2	108.4	118.3	6.3	3.0	109.8	34.0	20.7	83.4	70.4
153	43.1	34.0	9.7	10.1	10.7	17.9	18.0	17.6	1.9	7.3	6.7	5.0	29.7	0.4	108.5	121.6	9.5	6.8	107.4	42.5	19.3	88.5	71.1
154	43.4	31.6	7.3	6.9	11.1	17.4	18.4	16.5	2.6	6.8	6.9	4.4	27.0	0.0	103.9	121.4	16.3	5.8	104.9	32.0	18.7	84.2	69.2
155	45.0	44.8	10.3	9.8	11.1	15.7	18.2	16.7	2.2	6.8	6.8	5.6	36.6	2.3	119.7	131.4	9.8	3.2	119.6	46.0	23.2	101.5	74.6
156	47.7	35.7	11.0	7.0	9.2	16.9	18.8	17.3	1.7	7.3	6.9	5.7	29.8	0.8	103.3	124.1	18.3	2.9	115.3	40.3	22.9	89.9	73.4
157	47.7	34.8	12.6	13.6	12.2	19.6	19.8	19.7	2.4	8.7	8.8	7.5	31.4	0.4	111.7	121.9	8.7	2.3	120.3	44.0	21.3	94.6	74.1
158	53.5	56.2	14.2	15.7	13.9	21.6	23.7	22.3	2.6	8.2	8.2	7.8	51.2	3.7	120.7	136.9	12.1	5.2	158.3	66.5	21.4	124.9	89.3
159	49.5	50.1	13.9	10.2	11.0	18.6	20.0	20.8	1.8	6.9	7.1	6.5	42.5	1.3	117.4	134.5	18.3	3.9	138.2	50.3	24.7	109.8	80.2
160	46.8	47.2	17.6	12.4	10.3	20.2	21.0	21.2	2.0	8.3	8.8	7.6	46.2	2.2	121.6	135.4	16.8	6.3	144.6	56.6	25.2	112.5	79.0
161	54.9	54.9	13.5	6.8	14.0	21.8	24.4	20.3	2.5	7.9	8.6	5.7	50.8	2.9	120.5	134.8	20.9	7.2	153.4	68.9	22.9	126.6	89.6
162	57.1	55.4	19.9	20.5	14.3	22.9	23.8	25.9	2.7	10.8	11.0	8.6	57.0	3.0	122.6	140.3	11.4	12.9	171.8	66.1	28.1	134.0	88.9
163	56.8	59.2	17.1	17.0	15.0	23.9	25.8	26.4	3.0	8.3	9.3	8.8	52.5	4.1	119.9	136.9	13.8	10.5	167.6	65.6	23.4	126.5	85.7
164	55.7	55.0	18.9	18.7	14.9	23.5	26.0	24.4	2.1	9.7	9.8	7.7	54.8	1.9	123.9	136.5	10.6	8.9	166.4	62.0	23.9	129.0	90.1
165	54.6	61.9	15.8	10.1	13.4	22.6	24.6	22.3	2.2	7.5	7.7	6.2	55.3	3.9	119.0	139.8	19.1	6.2	164.6	63.2	25.5	128.5	85.2
166	54.0	60.4	12.2	9.1	13.0	21.3	23.3	23.8	2.3	7.7	7.4	5.5	47.9	2.3	118.2	137.1	19.6	5.0	153.6	68.5	24.5	121.3	84.3
167	48.9	49.4	13.1	10.4	12.3	18.1	20.5	17.4	2.5	6.0	6.2	4.5	44.6	1.8	121.3	135.7	13.2	7.3	142.7	57.4	22.9	112.8	81.5
168	44.9	48.6	12.5	8.3	11.7	16.4	18.8	17.3	2.7	6.2	5.7	5.0	41.5	4.0	115.9	137.3	18.1	2.4	129.5	57.0	20.6	101.8	74.7
169	44.1	43.4	10.2	6.9	11.4	16.3	18.4	15.9	3.0	6.3	6.3	4.4	36.5	1.2	115.5	133.8	15.7	3.9	119.3	57.0	20.1	95.8	74.2
170	44.3	41.9	14.5	15.0	9.8	16.4	17.5	18.0	2.6	4.9	5.4	5.1	38.3	1.3	121.7	130.8	6.1	0.7	122.0	61.1	19.8	97.2	72.8
171	40.6	37.4	10.8	11.2	9.9	15.0	16.9	16.4	2.0	4.7	4.7	4.3	31.6	1.3	116.1	126.3	8.4	6.2	112.0	45.5	19.1	90.1	70.7
172	43.9	36.4	11.5	7.9	10.6	14.4	16.5	14.3	2.0	4.8	4.7	4.2	33.8	1.9	116.0	128.1	13.0	5.4	112.7	49.8	18.4	89.7	70.6
173	44.3	40.5	13.3	13.1	8.6	15.2	17.8	17.3	2.3	6.9	7.5	6.2	35.9	0.4	119.9	127.7	6.5	3.2	119.1	55.3	21.5	94.8	71.8
174	43.2	40.7	10.4	9.2	10.8	15.5	16.3	14.0	2.2	5.5	4.8	4.2	35.5	2.4	119.0	130.4	12.9	-0.2	112.5	51.5	20.3	90.3	67.9
175	44.2	45.9	14.8	12.7	11.4	16.6	18.8	18.3	2.4	6.7	6.8	5.7	37.9	0.3	119.2	132.8	10.0	6.6	125.9	58.1	21.8	99.6	71.2
176	44.0	45.7	12.8	11.2	11.1	17.4	19.9	19.7	2.8	6.7	6.6	6.2	38.7	1.4	119.2	134.6	14.1	3.2	127.2	54.3	21.4	102.9	75.5
177	42.6	39.3	13.5	12.0	11.6	18.3	18.3	18.3	2.4	5.7	5.6	6.1	37.5	0.8	120.4	128.7	10.0	2.7	118.3	53.0	18.5	97.7	75.1
178	51.3	48.8	17.3	14.2	10.5	17.5	21.6	21.9	2.6	6.4	6.0	4.9	43.1	2.9	116.9	129.8	10.5	5.7	140.2	54.8	22.9	110.3	83.4
179	51.3	46.2	14.9	12.6	8.1	16.8	18.5	16.8	1.5	5.5	5.5	5.6	43.0	2.5	118.0	130.8	12.9	6.8	135.9	54.5	23.3	106.6	80.3
180	49.6	48.4	14.6	11.6	10.7	18.3	20.4	17.2	3.6	6.5	7.4	5.2	39.6	1.4	109.8	132.0	16.1	11.3	137.4	55.8	22.8	103.1	82.4
181	48.5	42.9	15.0	14.9	10.5	17.5	18.4	16.5	2.6	6.2	6.2	5.6	37.4	3.3	113.5	126.6	9.0	6.7	128.3	52.8	23.3	100.6	78.9
182	46.7	44.6	12.8	15.1	10.0	15.4	19.0	17.8	2.8	5.7	6.1	5.8	36.3	2.2	116.0	127.0	8.2	5.4	123.5	51.2	19.9	98.7	74.5

Reproduced with permission of the copyright owner. Further reproduction prohibited without permission.

	16	17	18	19	20	21	22	23	24	25	26	27	28	29	30	31	32	33	34	35	36	37	38
	UMA XWD	AFA CHT	PFA CHT	RAM SHT	I2PA LW	P3PA LW	M1P ALW	M3P ALW	I2PA LD	P3PA LD	M1P ALD	M3P ALD	PAL LGT	PAL THK	KRO GAG	ENL OAG	SLO POC	FAC CNV	FAC SIZ	PPN ALO	ORBI HT	CRL GTH	NCL GTH
183	50.4	45.2	12.1	11.7	10.9	17.3	18.3	17.8	3.8	6.5	7.0	6.7	36.4	2.0	111.7	127.4	14.0	5.1	127.1	56.5	21.3	97.3	75.3
184	49.4	43.1	12.0	11.1	9.8	17.9	17.5	15.2	1.8	5.1	5.9	4.4	38.1	1.7	111.8	128.5	14.9	6.6	127.9	46.1	21.3	97.1	75.5
185	45.3	43.7	12.9	11.3	9.1	15.2	16.5	16.8	2.4	3.8	4.0	4.2	38.5	2.6	113.8	130.2	13.3	3.7	122.9	60.6	21.8	97.7	75.3
186	49.9	48.8	12.7	9.7	10.8	16.7	19.7	16.9	2.9	7.7	6.9	5.0	39.2	2.4	112.0	130.2	17.8	6.5	130.8	54.9	21.7	101.3	79.5
187	49.6	46.5	14.5	13.4	10.7	18.4	20.2	20.5	1.9	5.7	6.0	6.4	41.2	1.4	117.8	132.6	11.1	7.8	134.2	58.7	23.8	104.9	77.6
188	65.3	99.7	27.6	22.4	19.4	27.4	28.2	24.0	3.4	8.3	10.5	9.0	78.5	3.3	121.9	143.9	20.3	5.7	240.2	73.6	24.9	181.2	110.5
189	60.4	82.1	21.4	12.7	18.1	25.0	25.3	20.4	3.4	8.0	8.0	5.3	69.4	3.3	119.2	141.8	21.6	5.0	204.6	73.4	23.9	158.7	106.1
190	63.6	93.8	30.3	19.3	16.4	23.9	25.5	24.1	3.8	7.5	8.1	7.7	72.8	3.5	118.4	140.8	22.1	-0.9	225.1	67.9	26.3	169.5	108.7
191	61.9	93.8	24.4	17.3	18.3	24.7	26.9	25.8	1.6	7.7	9.6	8.3	73.4	4.1	122.5	144.1	21.0	3.3	226.5	65.8	24.2	174.7	106.9
192	60.1	78.0	23.3	23.7	15.3	23.4	23.5	23.6	2.5	7.7	6.5	7.1	68.6	3.9	131.0	140.5	11.0	-1.0	200.6	66.1	21.1	152.2	92.1
193	59.9	87.6	22.0	11.0	18.2	26.4	26.8	23.1	6.5	9.4	9.1	7.3	69.6	1.5	120.6	145.0	25.5	4.4	215.4	71.0	24.1	161.2	99.7
194	61.3	94.5	28.5	20.7	18.7	25.3	26.4	25.9	4.0	9.1	10.4	6.9	74.6	5.1	119.0	141.9	21.6	-1.5	229.3	71.1	23.9	170.5	105.6
195	48.8	51.1	16.4	16.9	14.1	21.0	22.5	20.7	2.9	7.7	7.1	7.5	45.9	2.1	118.2	132.8	11.8	5.1	143.8	50.5	18.7	117.3	83.1
196	52.0	51.7	17.4	18.6	13.8	19.9	21.0	19.2	2.6	7.8	7.8	6.7	48.2	2.4	117.9	131.5	12.2	6.7	147.8	50.4	23.0	120.0	86.0
197	48.0	48.8	14.7	16.9	14.4	18.8	20.3	19.3	2.1	6.7	7.3	7.3	41.7	1.3	118.7	129.0	9.0	3.7	133.2	48.6	21.5	110.5	82.3
198	50.0	49.6	14.0	15.3	13.7	19.7	20.5	17.2	2.5	5.7	6.1	6.0	41.2	1.3	118.6	129.6	8.1	2.4	138.7	43.9	23.5	113.1	83.3
199	50.2	51.2	15.9	14.9	14.1	20.0	20.4	20.2	2.0	6.9	6.9	7.0	44.6	1.4	117.7	132.2	14.7	6.6	142.1	49.7	23.0	114.1	83.0
200	50.4	45.6	11.3	12.4	13.3	18.5	20.2	17.9	2.2	5.3	6.8	5.9	41.5	1.8	118.5	130.8	13.3	3.2	133.8	40.3	21.7	110.0	80.1
201	50.9	53.1	15.9	16.3	14.2	20.5	22.0	20.6	2.1	7.2	7.6	7.7	47.6	2.0	114.7	130.0	12.9	6.7	146.8	44.4	22.6	117.5	86.2
202	49.1	53.5	18.0	15.5	14.7	21.1	21.1	19.1	1.7	7.8	7.2	6.7	46.4	1.6	121.8	133.0	11.1	4.7	145.7	46.5	23.0	125.2	89.2
203	51.5	49.5	16.3	19.6	15.3	21.7	22.5	20.7	1.4	5.4	6.1	6.8	45.3	2.4	122.3	131.2	4.8	4.9	142.4	45.2	22.1	117.8	83.9
204	48.8	47.7	14.9	18.2	13.5	21.2	21.6	19.9	2.2	6.6	6.6	6.6	43.3	2.0	119.9	129.2	9.7	3.6	136.0	43.6	21.1	112.8	81.6
205	54.6	41.7	10.1	11.6	11.6	19.5	19.2	18.0	1.3	6.5	7.3	5.6	43.4	2.8	119.0	135.5	8.6	1.0	133.0	32.3	21.8	106.4	75.2
206	55.5	43.1	11.3	15.8	10.5	20.0	20.7	19.8	1.8	5.7	8.0	8.4	47.3	2.9	122.2	128.9	2.5	-1.1	135.5	32.7	22.4	106.8	73.1
207	54.9	44.2	10.9	16.5	10.5	20.2	20.5	17.2	1.1	5.2	8.9	8.6	48.7	1.9	123.9	129.9	1.6	-2.1	137.8	38.7	22.9	115.0	79.0
208	53.5	39.2	11.2	14.8	8.5	21.8	22.6	19.9	0.6	4.7	7.6	6.9	44.6	1.0	119.8	131.9	4.1	-2.6	133.4	32.4	21.3	107.5	77.2
209	55.3	47.3	13.3	15.4	11.2	19.3	21.2	19.7	1.4	5.2	8.1	7.8	48.1	3.6	121.2	132.8	2.4	-0.8	140.5	27.4	22.3	111.2	77.2
210	50.9	41.9	10.3	12.3	10.2	20.7	22.0	18.1	1.4	6.3	8.4	6.6	46.7	2.3	121.7	130.4	7.8	-2.1	135.2	29.9	21.3	107.4	76.3
211	49.6	38.0	10.2	15.3	9.5	18.6	20.0	17.5	1.2	4.8	6.4	5.3	43.7	3.5	122.2	129.0	2.5	-0.2	127.5	31.8	19.6	106.0	75.9
212	49.9	42.6	11.8	9.1	10.1	18.1	19.6	16.5	1.1	4.3	6.1	3.3	45.6	3.4	121.8	137.2	14.0	0.9	129.5	36.4	19.9	106.9	73.1
213	56.1	42.3	10.2	13.4	10.1	19.4	20.3	18.2	1.2	6.4	7.5	7.1	44.9	2.9	119.7	131.6	5.1	0.7	134.3	28.5	21.7	111.9	80.1
214	57.0	45.1	11.2	15.3	11.9	22.9	23.2	21.2	1.0	5.5	8.6	7.8	48.9	3.3	117.8	131.7	5.7	-0.6	144.8	35.0	22.1	116.1	82.8
215	46.8	36.1	11.1	7.3	10.4	17.6	19.5	15.9	1.2	3.8	6.0	4.6	36.9	1.1	118.9	131.8	10.8	-0.4	120.3	42.3	20.7	100.0	75.9
216	51.3	40.3	13.9	12.6	8.9	18.6	19.8	17.4	1.9	4.4	5.3	4.5	39.3	2.7	116.6	129.0	6.0	-0.5	127.8	33.2	21.6	103.6	78.1
217	52.7	39.4	11.2	7.8	9.3	18.3	20.1	15.1	0.7	3.9	5.8	4.9	36.8	1.6	113.1	130.0	9.0	6.1	124.1	36.0	22.4	98.3	77.0
218	50.1	38.6	12.0	8.7	9.3	17.6	19.0	15.9	1.3	3.6	5.0	3.2	36.3	2.4	118.7	131.0	8.8	-1.6	122.2	31.7	23.8	96.7	72.0

Reproduced with permission of the copyright owner. Further reproduction prohibited without permission.

	16	17	18	19	20	21	22	23	24	25	26	27	28	29	30	31	32	33	34	35	36	37	38
	UMA XWD	AFA CHT	PFA CHT	RAM SHT	I2PA LW	P3PA LW	M1P ALW	M3P ALW	I2PA LD	P3PA LD	M1P ALD	M3P ALD	PAL LGT	PAL THK	KRO GAG	ENL OAG	SLO POC	FAC CNV	FAC SIZ	PPN ALO	ORBI HT	CRL GTH	NCL GTH
219	52.2	40.8	13.6	10.4	9.0	16.2	17.4	14.6	1.4	4.5	6.0	5.6	39.0	3.9	111.9	129.7	9.2	-0.3	127.8	40.8	21.2	100.9	76.9
220	53.8	39.1	14.4	10.7	9.0	18.2	20.7	17.3	1.2	4.3	6.6	5.3	39.8	2.5	120.2	129.2	3.2	2.5	130.5	40.7	22.8	107.0	83.5
221	54.2	40.2	14.9	12.7	9.6	19.9	19.4	14.6	1.4	5.2	6.4	6.0	40.1	2.7	117.7	128.1	4.9	-0.6	130.9	36.1	21.8	102.4	76.5
222	51.4	34.2	12.3	10.6	9.9	19.0	18.8	16.2	1.3	4.2	5.4	5.7	38.0	2.2	120.6	128.0	4.3	-0.9	123.1	37.9	21.2	99.0	73.7
223	53.2	39.1	15.0	13.8	9.9	18.9	21.3	18.2	1.1	5.0	7.8	7.0	41.4	1.8	119.5	129.3	3.4	-4.3	131.8	31.6	22.4	107.1	81.9
224	52.6	42.6	16.5	10.1	9.1	16.7	19.2	16.1	1.1	4.0	6.6	6.1	40.0	4.8	114.1	131.2	10.6	2.5	133.4	38.5	22.1	108.1	82.0
225	54.0	44.7	15.0	8.9	11.1	19.5	20.9	17.2	2.5	4.3	5.8	5.6	36.8	3.9	114.2	133.7	15.1	1.2	135.8	43.8	23.1	109.4	81.2
226	53.8	43.7	16.5	12.6	10.6	16.7	19.6	16.8	2.6	4.2	6.2	6.4	38.3	3.9	114.8	128.7	8.9	3.2	136.1	45.5	22.8	108.9	84.6
227	48.9	44.8	13.7	11.1	12.0	18.9	20.5	17.5	2.4	4.0	5.5	5.1	35.6	3.7	114.7	132.0	14.4	-0.3	134.5	52.7	22.6	104.2	78.3
228	52.2	44.1	13.5	9.0	11.1	17.5	20.2	18.6	2.2	5.1	6.0	5.8	35.0	3.4	113.4	129.5	17.1	2.6	134.2	42.6	22.7	106.7	80.3
229	49.8	43.2	14.0	11.3	10.5	20.0	21.9	18.1	2.9	4.4	5.1	6.1	34.0	4.0	112.7	130.7	15.6	0.0	134.5	45.9	22.0	105.4	78.8
230	49.8	41.0	10.4	10.5	11.1	18.6	18.7	16.4	2.9	4.6	4.8	4.4	35.8	2.9	114.3	131.8	12.8	2.3	129.5	38.6	22.7	106.5	82.0
231	52.2	44.5	15.0	13.1	11.8	19.8	20.5	16.7	2.3	4.7	5.7	6.2	39.1	4.4	114.6	129.9	11.4	0.5	138.2	42.8	22.4	111.3	85.7
232	50.9	39.7	15.9	17.8	10.0	18.8	21.6	19.9	1.9	3.8	4.3	5.5	36.3	3.2	120.3	126.6	2.9	3.1	133.2	46.6	23.0	108.3	83.7
233	51.4	42.9	15.3	15.0	11.3	19.5	20.6	19.2	3.0	5.9	6.5	6.4	35.8	2.1	116.6	128.1	7.9	1.9	133.0	43.4	22.5	110.0	86.3
234	53.8	33.6	10.8	6.7	8.6	17.3	17.6	16.0	1.4	6.9	7.0	6.1	28.7	1.1	105.5	122.3	13.2	-1.5	118.1	20.0	24.8	92.5	76.3
235	56.5	32.2	10.3	7.3	9.0	18.8	20.5	18.2	1.3	5.7	6.4	5.8	29.7	2.0	109.5	121.3	10.8	-4.9	120.8	21.0	23.9	97.4	78.3
236	55.1	30.4	10.4	10.4	9.3	16.7	18.6	17.1	1.3	5.4	6.8	5.7	28.9	1.9	107.5	116.1	5.6	-2.3	119.3	21.5	23.8	90.7	75.6
237	55.6	29.7	10.9	10.8	9.1	17.7	20.4	17.6	1.8	4.4	6.1	5.5	28.8	2.4	109.4	115.6	2.9	-5.3	118.4	15.9	24.2	90.3	75.8
238	55.2	27.3	11.1	10.7	8.5	16.7	18.0	16.4	1.6	4.6	5.6	5.1	26.2	1.2	106.0	114.2	2.0	-4.2	114.3	19.4	23.2	89.5	74.4
239	52.5	26.7	9.8	11.4	8.8	18.0	18.6	16.5	1.8	5.0	6.4	4.8	28.4	2.8	112.7	117.7	3.7	-3.2	115.7	19.2	23.9	87.5	70.3
240	52.2	27.6	10.2	9.1	9.1	17.3	19.7	17.3	1.6	5.0	6.1	5.3	29.1	2.2	108.1	117.8	7.3	0.1	113.8	16.8	22.2	87.7	72.9
241	52.5	27.2	9.2	9.6	9.7	16.4	18.5	16.8	1.8	4.8	5.4	4.0	27.7	1.9	106.5	117.3	7.3	-1.6	114.8	22.6	22.1	87.3	72.1
242	52.7	29.8	11.9	10.4	8.4	15.2	17.8	16.5	1.6	4.2	5.7	4.9	27.8	2.1	105.0	116.7	7.9	1.3	116.2	25.9	22.8	90.1	74.8
243	52.5	28.7	9.0	7.6	8.4	16.7	18.3	17.1	1.9	5.1	6.4	4.4	26.0	1.3	102.4	116.3	8.1	-0.5	111.7	19.9	24.0	86.0	74.5
244	59.0	37.0	14.3	16.4	9.9	19.4	20.7	18.2	1.2	4.7	5.9	6.3	39.1	1.0	112.3	122.1	0.6	1.6	131.9	38.9	21.2	102.5	82.4
245	47.2	31.8	8.2	9.1	8.4	16.9	19.9	18.0	1.4	4.5	6.0	5.0	33.9	0.5	119.2	127.2	6.5	0.1	112.7	28.0	21.3	90.1	70.5
246	50.7	32.1	11.1	10.8	9.3	18.9	22.1	19.5	2.2	4.9	5.8	4.8	36.7	1.0	118.3	127.2	7.0	-1.4	121.5	30.6	21.0	97.9	77.0
247	50.1	32.0	8.5	10.7	8.5	16.0	20.3	18.4	1.1	3.8	6.2	6.1	32.8	0.5	116.2	128.1	5.0	-2.1	115.1	28.9	21.5	91.8	73.1
248	50.1	35.6	11.0	7.2	9.2	17.7	20.9	18.4	1.5	4.7	5.9	4.8	35.5	1.8	113.2	126.7	12.2	1.2	119.4	30.7	22.2	94.1	75.0
249	48.0	28.8	8.1	8.7	9.0	16.1	18.5	17.4	1.4	3.2	4.8	4.1	30.2	0.2	115.0	120.5	4.7	0.1	108.6	27.0	21.4	86.3	70.0
250	50.3	33.4	9.2	10.4	9.1	17.7	20.6	18.2	1.6	4.4	6.7	6.0	34.7	0.3	118.9	128.7	5.5	-3.7	116.2	25.6	24.0	93.6	70.7
251	48.8	31.7	7.9	10.2	8.7	15.6	18.8	17.9	2.1	3.8	4.9	5.6	33.2	0.3	117.6	128.0	4.9	0.1	110.8	26.4	23.2	91.7	73.1
252	48.7	32.1	8.9	8.2	8.4	16.7	18.9	18.1	1.2	3.6	5.7	4.5	35.4	0.3	120.2	127.6	7.6	-3.4	113.3	27.1	22.4	91.7	70.2
253	50.4	37.2	12.5	14.2	9.8	16.7	20.3	19.6	1.3	3.9	5.6	5.7	34.6	0.2	116.2	125.1	2.8	-2.1	123.1	34.1	23.2	101.1	80.5
254	51.4	36.9	11.6	16.8	8.8	17.6	20.8	21.7	1.6	4.9	6.4	6.7	34.5	0.1	117.9	126.1	1.0	-1.2	125.0	26.4	23.7	98.9	77.8

Reproduced with permission of the copyright owner. Further reproduction prohibited without permission.

	16	17	18	19	20	21	22	23	24	25	26	27	28	29	30	31	32	33	34	35	36	37	38
	UMA XWD	AFA CHT	PFA CHT	RAM SHT	I2PA LW	P3PA LW	M1P ALW	M3P ALW	I2PA LD	P3PA LD	M1P ALD	M3P ALD	PAL LGT	PAL THK	KRO GAG	ENL OAG	SLO POC	FAC CNV	FAC SIZ	PPN ALO	ORBI HT	CRL GTH	NCL GTH
255	58.3	33.5	13.8	14.3	11.8	19.8	20.0	21.5	0.7	5.1	7.4	7.2	42.0	0.5	126.6	118.5	0.8	-0.4	131.4	35.5	23.7	108.1	82.6
256	57.1	33.3	14.5	16.3	11.7	17.6	18.5	21.3	1.1	5.0	6.4	6.0	38.1	1.1	122.4	121.9	1.0	7.3	128.4	38.7	23.5	104.3	81.8
257	57.1	31.6	14.3	14.9	12.1	19.7	20.7	21.5	1.5	4.2	5.6	5.5	39.8	0.1	126.3	120.8	1.2	2.7	128.3	34.8	23.2	107.2	85.5
258	64.5	40.4	20.0	20.2	15.2	24.5	25.3	23.0	1.5	4.1	7.1	7.8	53.1	0.2	124.2	125.7	1.0	1.4	162.3	34.2	22.8	125.9	95.9
259	61.4	45.0	17.7	20.0	12.8	21.0	21.8	21.1	1.4	3.9	6.7	7.2	54.5	0.8	122.1	127.0	1.6	-0.3	159.0	30.7	25.9	124.7	91.9
260	62.0	47.0	21.1	18.9	15.4	23.0	24.6	24.9	1.6	6.2	8.8	8.8	57.2	1.1	125.0	128.9	1.9	0.7	167.1	38.2	25.2	131.2	96.3
261	55.6	41.4	19.2	19.2	13.1	21.1	22.8	21.8	1.1	4.6	8.1	8.6	51.6	2.1	121.0	123.2	1.2	1.5	153.0	38.8	24.3	121.8	91.9
262	66.3	43.5	20.2	18.0	13.7	22.6	24.0	24.8	1.8	4.9	7.3	8.2	55.7	0.4	123.9	128.7	2.8	1.9	162.1	36.6	24.7	131.0	97.8
263	55.6	41.4	19.2	19.2	13.1	21.1	22.8	21.8	1.1	4.6	8.1	8.6	51.6	2.1	121.0	123.2	1.2	1.5	153.0	38.8	24.3	121.8	91.9
264	60.1	43.6	15.5	15.1	14.1	21.2	22.9	22.1	2.0	5.7	7.4	7.1	54.9	0.2	122.9	129.0	4.5	1.9	156.3	26.6	25.7	125.3	92.9
265	55.3	40.4	15.7	12.9	12.5	22.5	25.4	22.0	1.7	4.1	6.0	6.3	48.7	2.6	119.6	125.9	8.3	-3.4	149.1	31.4	22.4	118.6	88.4
266	55.1	39.2	16.5	15.7	12.5	21.1	23.5	22.3	1.6	5.0	8.2	7.3	48.0	1.4	120.8	127.9	5.8	-3.0	148.6	25.6	22.8	117.4	89.8
267	65.4	42.3	20.9	21.5	13.5	24.3	26.0	23.8	1.5	5.7	9.1	8.7	54.5	0.5	117.9	124.8	4.7	1.6	166.0	34.3	23.8	127.1	95.5
268	75.5	92.4	52.9	51.9	26.0	36.0	35.9	32.3	2.1	10.0	13.3	12.5	72.1	3.1	137.8	125.3	5.6	-7.7	249.4	34.2	38.8	190.0	113.5
269	80.3	97.0	50.5	42.3	28.0	42.3	40.1	36.4	2.7	16.1	18.0	15.8	76.4	3.2	127.8	125.5	5.2	-10.4	260.4	21.9	38.7	192.1	124.6
270	72.6	94.6	51.5	39.9	23.1	34.0	32.5	30.8	1.1	11.3	12.7	13.1	77.3	5.0	129.6	136.7	7.7	-4.2	249.0	41.4	37.8	194.3	118.5
271	95.9	98.6	47.2	57.0	26.4	36.0	35.4	34.9	3.9	13.5	18.9	19.1	91.8	2.4	123.3	129.1	1.4	-2.8	287.0	46.4	40.0	228.0	153.6
272	97.1	92.1	55.8	54.7	22.3	32.9	36.0	29.3	4.7	10.3	16.0	14.0	85.8	1.3	117.6	126.9	2.2	-4.4	270.1	48.2	40.5	211.7	144.4
273	101.4	101.2	59.0	60.6	23.2	36.3	36.3	37.5	3.2	8.9	15.8	17.1	80.9	1.1	116.2	123.4	1.5	-10.3	282.6	34.5	40.1	217.9	151.8
274	96.7	92.1	53.2	54.0	25.4	35.5	33.5	28.4	3.3	7.1	14.9	16.5	83.4	1.7	125.2	126.7	1.6	-2.9	273.4	49.8	40.9	213.2	142.9
275	99.3	94.0	55.2	58.5	25.9	34.2	34.8	36.4	5.0	10.7	18.4	16.9	86.1	0.7	122.9	127.2	1.4	-0.8	289.4	47.3	37.7	239.0	167.6
276	111.7	96.9	45.9	61.9	25.5	37.2	36.6	38.7	3.0	10.4	16.9	21.2	89.2	1.1	122.4	128.8	1.4	5.1	299.9	44.9	41.0	241.4	169.1
277	97.5	91.3	55.6	57.8	23.4	29.4	30.4	29.8	5.5	10.0	14.2	16.2	83.7	0.2	115.7	125.9	1.7	-2.5	279.0	51.6	40.5	214.6	147.5
278	98.3	94.3	49.4	68.2	23.1	36.3	31.1	28.9	2.4	7.3	11.6	13.9	92.4	1.5	126.3	128.1	7.3	-5.9	279.0	49.8	36.5	224.2	150.1
279	99.8	94.6	56.4	59.3	19.9	34.6	36.6	38.2	2.7	15.3	16.6	17.9	88.0	1.7	119.3	123.4	1.6	-6.2	291.0	50.8	38.9	234.8	162.3
280	99.2	64.3	37.4	38.1	15.0	30.4	35.3	41.3	4.2	9.1	13.4	13.0	52.1	2.6	97.5	102.4	1.1	7.0	215.8	27.7	37.5	200.0	185.5
281	97.7	67.8	39.5	34.7	18.1	33.6	37.3	38.7	4.4	10.4	12.8	10.9	54.7	0.3	107.7	111.3	7.8	3.2	222.3	31.1	35.4	200.1	170.5
282	97.8	66.6	39.0	30.7	16.5	31.8	37.7	37.0	3.9	13.3	15.3	12.4	57.4	2.4	103.4	104.9	8.1	6.0	219.6	33.5	37.6	197.6	169.9
283	93.1	60.2	37.4	26.7	14.0	29.3	35.6	38.1	2.2	8.1	10.4	6.9	51.4	2.3	97.5	105.9	14.3	7.3	209.7	26.2	31.2	191.3	171.9
284	97.3	63.8	37.5	29.1	14.5	28.2	36.1	41.7	4.1	11.3	14.5	12.8	47.5	0.7	93.6	105.8	13.8	4.8	213.6	26.5	32.2	193.7	172.6
285	95.9	67.3	40.9	37.0	17.3	29.1	35.7	37.8	3.7	6.7	10.0	9.7	52.0	3.3	99.1	106.1	5.1	5.5	220.3	22.8	33.3	200.3	173.5
286	99.8	63.4	42.1	37.3	16.4	30.9	38.2	38.2	3.7	9.1	12.3	8.1	55.6	1.2	101.3	98.3	4.8	-0.3	224.2	27.5	36.7	213.2	190.4
287	85.7	70.1	45.9	33.4	15.0	26.9	33.2	37.6	4.4	12.5	13.4	14.2	52.1	4.6	95.4	106.0	15.0	12.3	223.7	33.8	34.0	203.0	189.1
288	96.0	66.8	37.6	30.8	15.7	30.1	40.2	44.1	0.9	5.3	9.6	10.9	53.6	3.6	104.1	110.2	9.7	9.5	221.9	37.4	34.7	204.4	173.6
289	92.5	76.7	41.0	32.0	16.5	29.2	36.0	36.6	3.6	10.6	14.6	12.6	58.3	1.7	102.1	113.5	15.4	7.1	230.5	33.1	36.9	204.1	177.0
290	71.7	57.5	23.5	16.2	18.1	26.9	25.8	22.8	2.1	7.5	10.3	7.4	52.1	1.6	118.9	128.4	16.5	-6.8	181.3	28.7	30.9	145.8	112.6

Reproduced with permission of the copyright owner. Further reproduction prohibited without permission.

	16	17	18	19	20	21	22	23	24	25	26	27	28	29	30	31	32	33	34	35	36	37	38
	UMA XWD	AFA CHT	PFA CHT	RAM SHT	I2PA LW	P3PA LW	M1P ALW	M3P ALW	I2PA LD	P3PA LD	M1P ALD	M3P ALD	PAL LGT	PAL THK	KRO GAG	ENL OAG	SLO POC	FAC CNV	FAC SIZ	PPN ALO	ORBI HT	CRL GTH	NCL GTH
291	80.7	81.3	38.1	29.9	23.1	39.2	40.1	36.2	0.1	8.1	13.5	14.2	73.6	4.1	120.4	130.6	10.8	-4.7	228.7	34.3	34.0	195.0	136.7
292	79.3	79.5	35.0	36.8	25.6	33.8	34.9	27.9	3.8	8.9	10.6	9.4	64.6	7.9	122.8	127.7	2.1	-8.3	217.6	22.9	33.5	176.6	125.6
293	87.4	87.1	42.5	27.3	24.8	42.3	39.7	37.0	0.9	8.6	12.4	12.1	77.4	2.2	125.4	131.8	10.1	-9.3	242.5	24.2	36.7	198.3	139.8
294	92.1	77.5	37.4	32.4	22.6	41.0	39.5	41.7	3.8	12.0	15.0	13.6	72.9	3.6	126.8	130.7	4.6	-5.3	235.5	25.1	39.2	187.3	129.7
295	85.7	81.4	40.2	36.1	23.4	35.2	34.5	33.9	2.1	7.6	13.7	16.5	68.5	2.8	115.1	121.6	6.0	-7.7	230.5	24.3	36.0	172.3	130.6
296	85.1	81.9	37.9	38.6	24.0	41.2	38.0	35.5	2.5	9.1	13.4	13.2	72.6	1.8	119.5	125.6	4.3	-10.3	232.4	20.2	34.7	187.6	137.3
297	82.1	81.1	43.2	39.2	23.4	40.8	40.4	36.4	2.6	7.9	12.5	13.7	78.4	4.5	123.6	126.7	3.4	-3.9	238.5	32.3	32.5	188.7	129.9
298	84.6	79.4	42.7	36.8	26.2	37.1	35.7	30.8	2.5	10.4	15.2	14.2	73.0	1.6	120.9	124.9	8.1	-4.9	234.8	30.5	35.7	182.7	134.9
299	87.9	84.1	40.2	35.4	22.7	33.9	32.5	31.4	1.8	8.7	14.1	13.0	71.8	2.5	125.4	127.8	2.7	-6.4	228.8	20.5	39.1	185.4	127.7
300	87.3	90.8	42.5	25.9	21.4	33.4	34.0	35.2	2.2	8.2	13.2	10.2	67.9	1.8	114.4	130.7	16.1	-3.0	239.0	34.9	34.6	174.8	127.4

Reproduced with permission of the copyright owner. Further reproduction prohibited without permission.

	39	40	41	42	43	44	45	46	47	48	49	50	51	52	53	54	55	56	57	58	59	60	61
	BCLG TH	BIPO RB	SKC NTR	CRBT HK	OFB VOL	OFB ARE	ORBS CR	ORB TC1	ORB TC2	ORB A12	IORB DS	BFPU I1	BFPU I2	BFPU P3	BFPU P4	BFPU M1	BFPU M2	BFPU M3	ANT BFM	PSTB RM	RELB FM	MAX BFM	APM ASS
1	59.4	48.8	342.4	1.6	446.7	62.4	24.7	29.5	64.1	86.5	11.0	26.0	27.0	34.5	38.1	42.4	39.9	35.0	26.5	38.0	69.7	34.7	41.8
2	60.6	48.7	349.1	2.0	283.0	58.8	21.9	31.0	65.7	83.3	10.8	26.2	26.7	34.7	38.1	43.7	43.7	37.3	26.5	39.5	67.0	35.8	32.6
3	61.5	48.3	341.9	1.4	212.2	41.2	25.8	30.8	64.1	85.1	9.6	27.2	27.6	35.8	39.1	44.2	42.8	38.1	27.4	40.0	68.6	36.4	37.0
4	58.8	46.7	335.4	1.5	346.9	57.2	23.8	28.2	66.0	85.8	10.5	25.5	26.7	34.1	37.1	41.7	38.8	35.8	26.1	37.5	69.6	34.2	36.8
5	59.4	44.3	332.9	1.5	314.7	58.7	26.9	28.9	65.6	85.5	10.3	26.5	27.1	35.2	38.5	43.6	40.9	35.7	26.8	38.8	69.1	35.4	36.4
6	63.8	46.5	346.7	1.4	338.7	61.7	26.4	29.3	65.9	84.8	11.1	28.7	29.5	38.4	41.6	47.1	42.5	38.0	29.1	41.5	70.1	38.0	39.5
7	57.3	46.1	330.3	2.2	215.6	19.8	23.1	33.9	68.1	78.0	7.9	24.2	25.1	31.9	35.5	39.4	39.5	34.7	24.6	36.2	68.1	32.9	37.0
8	60.7	48.4	349.6	3.3	314.6	53.5	24.9	28.8	65.9	85.3	10.2	27.6	28.1	36.7	39.8	44.5	43.1	38.6	27.9	40.5	68.8	36.9	43.3
9	60.6	49.7	339.2	1.2	332.4	53.9	27.4	29.4	63.4	87.1	11.5	26.5	27.3	36.0	39.7	44.5	39.8	36.3	26.9	39.2	68.5	35.7	36.2
10	61.8	46.7	345.8	2.0	198.9	29.7	23.3	29.1	63.0	87.9	8.2	27.2	27.6	35.7	39.1	43.8	40.9	37.0	27.4	39.3	69.7	35.9	33.1
11	63.6	53.1	348.6	3.0	432.7	74.1	20.9	19.4	77.5	83.1	13.8	26.6	28.1	34.9	37.1	35.5	32.1	29.8	27.3	33.9	80.7	32.0	41.3
12	59.5	49.8	333.4	1.4	240.4	57.4	20.4	13.3	75.2	91.5	10.4	23.1	24.1	30.7	32.9	34.4	31.1	28.4	23.6	31.5	75.0	29.2	39.1
13	61.9	53.8	344.0	1.4	394.9	50.1	21.8	14.8	79.2	86.1	10.8	25.5	26.8	34.2	36.9	38.8	35.8	32.6	26.2	35.7	73.4	32.9	44.1
14	58.3	49.5	325.5	1.9	174.1	39.2	23.1	15.5	82.6	81.9	8.5	23.1	24.4	32.0	34.9	37.0	33.6	34.0	23.7	34.3	69.2	31.3	44.6
15	59.8	52.9	349.2	2.9	368.6	53.1	20.5	14.6	73.8	91.5	11.7	26.2	27.6	35.5	37.8	36.0	33.4	31.5	26.9	34.9	77.3	32.6	36.7
16	55.7	44.2	306.2	1.2	266.5	54.7	22.0	17.4	80.6	82.0	11.2	19.2	20.3	26.8	29.2	31.4	27.1	24.6	19.7	27.8	70.9	25.5	37.2
17	59.0	47.5	319.2	1.9	305.0	46.5	20.3	17.5	72.1	90.5	11.0	23.3	23.8	30.7	33.4	36.1	31.4	28.7	23.5	32.1	73.3	29.6	36.1
18	64.2	52.0	359.9	3.1	428.9	91.8	21.9	14.1	83.4	82.5	13.6	25.8	26.8	35.2	37.7	36.7	34.0	31.9	26.3	35.1	74.9	32.6	36.1
19	62.6	51.4	351.5	2.4	183.1	37.0	19.6	20.2	74.9	84.9	8.2	26.8	28.3	36.2	38.9	39.1	35.9	33.7	27.5	36.8	74.9	34.1	42.1
20	60.6	48.6	341.2	2.2	231.0	43.8	19.7	12.0	81.9	86.1	10.4	22.0	22.9	29.8	31.8	35.0	32.6	30.1	22.5	31.9	70.5	29.2	29.7
21	62.5	51.9	341.1	2.0	162.3	51.2	18.9	21.7	79.3	79.0	6.6	25.6	26.3	34.0	36.2	38.0	34.7	31.5	25.9	34.9	74.4	32.3	41.3
22	64.2	50.2	342.1	1.6	135.6	39.3	20.5	21.4	72.3	86.3	6.1	27.5	28.7	36.2	39.3	41.7	37.7	34.7	28.1	37.9	74.0	35.1	42.4
23	60.5	49.8	341.1	1.4	89.6	39.4	18.9	24.1	72.9	82.9	5.6	26.1	27.5	35.1	38.2	37.9	34.6	32.3	26.8	35.6	75.2	33.1	36.3
24	60.5	52.4	338.3	2.3	118.0	50.8	20.4	23.5	72.4	84.2	8.1	27.9	28.7	36.9	39.6	40.1	36.9	34.5	28.3	37.6	75.3	34.9	43.9
25	58.5	50.1	329.1	1.4	139.4	36.6	21.9	23.5	76.5	80.1	6.2	25.3	26.1	33.8	36.1	37.9	34.8	32.6	25.7	35.1	73.2	32.4	40.0
26	57.4	50.3	329.6	1.8	264.9	50.1	20.3	20.7	72.7	86.6	8.6	25.9	26.7	33.9	36.3	38.4	35.5	33.0	26.3	35.4	74.3	32.8	43.9
27	62.2	52.0	339.4	1.5	221.8	37.6	21.2	23.7	74.8	81.5	7.5	24.6	25.3	32.2	34.9	38.8	36.9	33.7	25.0	35.3	70.7	32.3	36.9
28	60.2	50.5	323.1	1.3	174.4	45.3	18.5	21.6	75.6	82.9	6.2	22.8	24.1	30.9	33.6	35.3	31.9	29.4	23.5	32.2	72.9	29.7	39.9
29	63.5	50.2	342.1	1.3	141.3	42.9	22.5	21.2	78.9	80.0	7.2	24.4	25.5	33.1	35.8	39.9	35.6	32.8	25.0	35.4	70.4	32.4	41.1
30	59.9	49.0	331.5	1.8	139.9	48.6	20.4	22.6	79.3	78.2	8.0	23.7	24.6	32.2	35.0	37.4	33.7	30.9	24.1	33.8	71.3	31.1	43.7
31	63.3	53.9	363.4	1.8	171.5	57.7	19.1	26.4	73.2	80.4	11.3	25.5	26.1	32.7	36.0	40.5	38.5	35.4	25.8	36.6	70.5	33.5	45.1
32	51.4	44.6	265.4	1.3	84.3	11.3	20.4	27.1	71.6	81.3	4.1	18.3	19.0	28.3	31.0	34.2	31.9	28.0	18.6	30.7	60.8	27.2	42.7
33	50.0	44.6	273.5	1.3	128.9	15.9	21.8	24.1	71.0	84.9	6.3	19.2	20.4	29.2	32.2	31.1	28.4	25.9	19.8	29.4	67.6	26.6	40.4
34	51.3	43.9	267.4	2.6	145.7	21.2	21.1	25.9	75.2	78.8	4.8	18.0	19.1	27.5	30.1	31.4	28.3	25.4	18.5	28.5	65.0	25.7	43.8
35	47.3	45.4	262.0	1.5	199.5	28.7	23.0	25.6	70.9	83.5	6.6	15.3	16.3	22.9	25.3	27.0	24.4	22.4	15.8	24.4	64.9	21.9	41.7
36	51.3	42.3	274.2	1.9	113.9	18.1	19.1	23.4	73.0	83.6	5.3	18.2	19.2	28.2	30.9	30.4	28.3	26.5	18.7	28.9	64.8	26.0	44.9
37	52.2	44.7	272.0	2.1	176.2	16.4	19.4	24.8	69.8	85.3	5.1	20.0	21.2	29.4	32.1	34.6	31.2	28.1	20.6	31.1	66.3	28.1	43.7

Reproduced with permission of the copyright owner. Further reproduction prohibited without permission.

	39	40	41	42	43	44	45	46	47	48	49	50	51	52	53	54	55	56	57	58	59	60	61
	BCLG TH	BIPO RB	SKC NTR	CRBT HK	OFB VOL	OFB ARE	ORBS CR	ORB TC1	ORB TC2	ORB A12	IORB DS	BFPU I1	BFPU I2	BFPU P3	BFPU P4	BFPU M1	BFPU M2	BFPU M3	ANT BFM	PSTB RM	RELB FM	MAX BFM	APM ASS
38	48.8	40.9	255.6	1.7	139.1	12.4	21.0	25.5	74.1	80.4	4.8	18.0	19.0	26.0	28.9	30.2	27.6	25.6	18.5	27.7	66.9	25.0	42.0
39	48.2	44.3	256.0	1.6	80.2	11.4	20.4	26.4	73.0	80.6	4.2	15.6	16.5	23.3	25.8	28.6	25.2	22.8	16.1	25.1	63.9	22.5	41.9
40	48.1	42.5	256.3	1.7	106.9	10.9	18.4	23.6	73.2	83.3	3.8	16.2	16.4	23.2	25.1	28.3	27.5	24.4	16.3	25.7	63.6	23.0	42.1
41	48.8	40.9	260.5	1.9	204.9	18.6	19.8	25.1	68.8	86.2	5.6	17.1	18.1	25.3	27.6	30.6	31.3	27.7	17.6	28.5	61.8	25.4	42.8
42	46.3	39.9	247.9	1.1	90.3	16.6	19.2	23.9	69.3	86.8	6.8	16.0	17.1	22.8	24.8	26.2	23.9	21.1	16.5	23.7	69.6	21.7	44.5
43	46.8	37.7	245.2	1.6	74.2	17.0	17.9	24.4	74.4	81.2	6.3	15.0	15.8	20.8	22.8	23.8	21.8	20.6	15.4	21.9	70.0	20.1	46.0
44	44.6	38.0	237.8	1.3	64.4	12.6	18.3	22.3	74.9	82.9	4.7	13.3	14.1	19.2	21.3	23.9	22.9	20.6	13.7	21.6	63.5	19.3	39.6
45	44.4	37.4	236.9	1.1	118.8	11.8	15.5	24.6	70.2	85.2	5.9	16.9	18.0	23.8	25.8	28.3	26.6	24.0	17.4	25.7	67.9	23.3	45.6
46	43.4	35.4	233.5	1.3	66.7	6.2	16.9	24.4	67.0	88.6	4.7	17.0	18.0	26.0	26.1	28.9	28.3	25.5	17.5	27.0	64.8	24.3	37.5
47	43.4	36.2	229.4	1.0	68.5	11.6	17.3	21.0	73.6	85.4	4.8	13.6	14.5	19.4	21.4	24.0	23.6	21.4	14.0	22.0	63.9	19.7	43.8
48	45.8	39.3	247.1	1.3	72.5	12.6	17.2	21.4	74.4	84.2	6.8	15.6	16.5	22.2	23.9	26.3	24.0	21.7	16.1	23.6	68.0	21.5	44.6
49	45.9	39.4	248.6	1.6	65.4	18.7	17.6	22.4	75.8	81.8	6.7	16.4	17.3	23.6	25.5	28.0	25.7	22.6	16.8	25.1	67.1	22.7	42.0
50	45.9	37.5	241.7	2.0	49.7	14.4	18.1	21.0	73.6	85.4	5.4	15.5	16.4	22.1	23.8	24.5	22.4	20.6	16.0	22.7	70.5	20.8	47.6
51	43.6	37.2	237.0	1.1	86.4	15.4	21.0	23.9	66.6	89.4	6.2	15.2	16.1	21.1	22.8	25.2	26.5	24.2	15.7	24.0	65.5	21.6	42.3
52	50.1	41.8	267.1	1.9	95.0	20.2	20.2	24.2	66.1	89.7	7.1	16.1	17.4	23.3	25.0	27.4	24.7	22.3	16.8	24.5	68.3	22.3	47.0
53	53.2	40.6	271.4	2.2	151.2	15.1	17.2	25.5	68.7	85.9	6.2	18.1	19.2	25.7	27.6	30.4	28.1	25.7	18.7	27.5	67.9	25.0	44.9
54	49.9	40.8	266.7	1.9	110.8	16.5	21.9	23.2	70.5	86.3	7.2	18.1	19.1	26.7	28.8	29.9	27.0	24.5	18.6	27.4	68.0	24.9	40.4
55	46.5	40.0	249.7	1.8	62.6	17.7	22.4	24.1	72.2	83.7	6.2	16.0	17.0	22.9	25.2	27.7	25.4	23.1	16.5	24.9	66.2	22.5	42.1
56	44.6	34.4	214.4	2.0	82.0	10.8	22.2	22.9	70.5	86.6	6.8	12.8	13.7	16.9	18.2	19.5	17.4	15.8	13.3	17.5	75.5	16.3	50.6
57	40.7	31.2	201.3	1.7	75.5	11.9	20.9	24.9	71.0	84.1	5.1	12.7	13.4	16.3	17.9	19.7	18.0	16.8	13.1	17.8	73.5	16.4	47.8
58	39.1	30.6	201.3	1.1	65.7	14.3	20.8	22.5	66.6	90.9	5.7	15.3	15.9	20.4	22.0	22.7	20.4	18.8	15.6	20.9	74.8	19.4	48.8
59	39.5	30.8	213.3	1.3	113.7	20.8	18.9	26.4	62.9	91.1	6.0	14.3	15.4	19.2	20.7	21.5	19.7	18.6	14.9	19.9	74.7	18.5	49.6
60	42.8	33.7	215.2	1.6	60.1	11.6	18.0	24.2	69.1	86.7	5.2	16.1	17.2	21.2	22.7	24.9	23.1	21.2	16.6	22.6	73.5	20.9	47.2
61	41.5	30.9	204.6	1.0	50.2	11.7	20.6	23.1	67.7	89.2	5.6	15.9	16.7	20.7	22.3	23.5	21.3	19.7	16.3	21.5	75.7	20.0	46.9
62	40.7	30.5	196.5	1.1	43.1	12.9	21.1	22.8	68.1	89.1	4.5	14.4	15.2	18.8	20.4	22.3	21.1	19.3	14.8	20.4	72.6	18.8	46.9
63	36.6	29.3	183.7	1.1	89.2	13.4	20.0	24.4	72.8	82.8	4.9	10.0	10.6	13.0	14.3	16.0	15.6	13.9	10.3	14.6	71.0	13.4	46.6
64	41.2	30.6	198.0	2.1	79.6	14.6	21.0	24.1	69.4	86.5	5.1	11.6	12.5	16.0	17.2	19.1	17.1	15.6	12.1	17.0	70.9	15.6	41.9
65	40.5	32.1	204.8	0.6	121.5	20.9	21.7	23.3	76.7	79.9	6.7	12.6	13.5	16.7	18.3	20.3	18.5	17.1	13.1	18.2	71.8	16.7	48.5
66	54.8	43.9	285.8	2.0	152.1	26.8	18.6	23.0	74.9	82.1	5.9	20.4	21.1	28.7	31.1	32.3	29.6	27.2	20.8	29.8	69.8	27.2	35.1
67	50.2	39.9	275.7	1.5	154.0	18.6	22.2	15.5	82.2	82.3	5.0	19.3	20.0	26.9	29.5	32.7	29.4	26.3	19.6	29.0	67.8	26.3	39.1
68	51.6	43.9	285.3	1.9	173.6	27.9	20.5	18.3	83.2	78.6	5.2	20.0	21.0	27.9	30.6	34.6	32.2	29.4	20.5	30.9	66.3	28.0	38.3
69	50.8	42.5	279.7	1.0	162.2	22.8	21.1	21.7	79.4	78.9	4.9	16.6	17.2	23.5	26.0	29.6	29.2	25.9	16.9	26.8	63.1	24.0	36.4
70	49.1	42.3	280.7	1.2	107.8	25.8	23.1	20.8	76.0	83.3	4.8	20.2	20.7	28.2	30.5	34.3	31.9	28.7	20.5	30.7	66.6	27.8	34.7
71	50.0	42.6	273.2	0.9	167.2	22.8	17.7	17.4	80.9	81.8	5.8	18.3	19.0	26.3	29.3	32.1	28.4	25.9	18.7	28.4	65.7	25.6	37.4
72	54.8	46.2	287.4	1.0	100.9	16.4	21.8	21.3	80.1	78.7	4.2	21.4	22.2	30.1	33.2	34.3	31.0	28.3	21.8	31.4	69.6	28.6	37.2
73	51.2	43.3	285.5	1.4	128.9	18.6	23.0	17.8	78.0	84.3	4.5	19.9	20.9	29.4	32.0	35.9	31.9	29.1	20.4	31.6	64.4	28.4	38.5
74	50.3	39.7	274.9	0.7	160.9	23.7	21.9	18.6	79.4	82.0	5.1	18.8	19.5	27.6	31.1	33.6	29.4	27.0	19.2	29.7	64.5	26.7	39.2

Reproduced with permission of the copyright owner. Further reproduction prohibited without permission.

	39	40	41	42	43	44	45	46	47	48	49	50	51	52	53	54	55	56	57	58	59	60	61
	BCLG TH	BIPO RB	SKC NTR	CRBT HK	OFB VOL	OFB ARE	ORBS CR	ORB TC1	ORB TC2	ORB A12	IORB DS	BFPU I1	BFPU I2	BFPU P3	BFPU P4	BFPU M1	BFPU M2	BFPU M3	ANT BFM	PSTB RM	RELB FM	MAX BFM	APM ASS
75	53.1	43.8	292.3	1.5	240.7	24.2	21.6	17.4	78.8	83.9	5.6	20.4	21.3	29.0	32.1	36.3	32.1	28.5	20.9	31.6	66.0	28.6	38.4
76	53.5	48.1	294.4	1.4	129.5	20.6	18.4	14.5	82.9	82.6	6.4	18.0	18.8	25.9	28.2	31.4	32.3	28.1	18.4	29.2	63.1	26.1	42.5
77	52.5	47.0	285.2	1.5	203.3	21.8	20.1	16.5	82.8	80.7	6.1	17.6	18.3	24.9	27.3	30.7	31.3	27.3	18.0	28.3	63.5	25.4	41.2
78	53.4	47.1	290.9	1.7	161.8	23.5	18.7	15.7	82.6	81.7	6.5	20.0	21.0	28.5	31.5	35.1	32.3	29.6	20.5	31.4	65.3	28.3	41.0
79	55.8	48.0	302.2	2.5	248.5	32.3	17.5	17.8	78.1	84.2	7.0	20.1	20.8	28.3	31.2	34.9	32.1	28.8	20.5	31.1	65.9	28.0	39.5
80	52.6	46.2	291.0	2.6	190.7	21.4	19.6	12.7	86.9	80.4	7.8	17.9	18.5	25.2	27.8	31.0	30.0	26.6	18.2	28.1	64.8	25.3	44.1
81	57.8	47.7	301.0	1.3	185.6	28.5	18.3	16.5	80.5	83.0	6.3	20.9	21.7	28.7	31.3	34.9	32.4	29.7	21.3	31.4	67.8	28.5	45.0
82	58.7	49.3	307.7	1.7	149.4	25.9	17.7	19.1	78.1	82.8	6.5	20.6	21.5	29.4	32.1	36.1	35.2	31.8	21.0	32.9	63.8	29.5	45.8
83	53.4	48.5	292.6	2.1	297.8	26.1	17.9	13.8	85.4	80.8	6.5	17.3	18.2	24.7	26.9	30.3	29.7	25.9	17.8	27.5	64.7	24.7	42.4
84	52.3	43.5	282.8	1.5	132.2	26.0	19.7	15.5	86.7	77.8	6.5	18.8	19.8	26.6	29.3	33.1	30.5	27.6	19.3	29.4	65.7	26.5	46.5
85	52.0	44.2	284.3	1.6	165.7	26.9	17.7	16.6	79.5	84.0	6.4	20.3	21.1	29.0	31.7	34.9	34.1	31.1	20.7	32.2	64.4	28.9	41.3
86	33.4	29.8	189.7	1.5	58.2	8.4	17.9	16.6	77.3	86.2	3.0	11.5	12.2	16.2	17.6	17.1	15.3	14.4	11.8	16.1	73.6	14.9	38.3
87	32.2	28.7	187.0	1.6	71.1	10.0	22.1	20.4	77.3	82.3	3.5	11.1	11.6	15.8	17.4	17.0	15.2	14.1	11.4	15.9	71.6	14.6	40.9
88	34.0	28.9	186.3	1.4	41.8	8.5	19.2	18.7	78.6	82.8	3.1	11.9	12.3	16.5	18.0	18.3	16.3	15.1	12.1	16.9	71.8	15.5	40.0
89	32.2	26.7	177.0	0.6	40.5	8.0	18.2	19.2	80.4	80.4	2.6	10.3	10.8	14.5	15.7	15.8	14.2	13.1	10.5	14.7	71.9	13.5	39.9
90	32.0	26.7	179.8	1.1	38.3	9.1	19.8	19.3	77.3	83.4	3.3	10.3	10.7	14.3	15.7	16.6	15.1	14.1	10.5	15.2	69.2	13.8	39.9
91	34.5	29.3	191.2	0.8	79.3	13.0	19.1	17.3	76.1	86.6	3.9	14.0	14.8	19.5	20.6	20.5	18.5	17.2	14.4	19.3	74.8	17.9	43.7
92	34.5	29.4	189.7	1.1	73.1	6.5	18.7	17.0	81.7	81.3	3.6	10.4	10.9	14.1	15.6	16.6	14.7	13.4	10.7	14.9	71.8	13.7	44.0
93	35.1	28.1	185.1	1.2	35.0	7.2	17.8	18.9	78.0	83.0	3.0	11.9	12.5	16.7	18.3	18.7	17.0	15.4	12.2	17.2	70.9	15.8	40.7
94	34.3	28.2	187.2	1.4	75.3	7.5	16.4	15.8	81.7	82.5	3.4	11.0	11.6	15.6	17.1	16.4	14.9	14.2	11.3	15.6	72.2	14.4	45.7
95	33.6	28.5	185.3	0.7	57.9	12.0	16.9	16.8	73.9	89.3	3.7	11.8	12.3	16.3	17.7	17.9	15.8	14.6	12.1	16.4	73.3	15.2	49.6
96	42.3	31.0	207.9	0.9	155.6	25.0	26.4	27.5	61.8	90.7	5.7	12.2	12.9	16.6	18.0	19.1	17.6	16.5	12.5	17.6	71.4	16.1	45.2
97	38.1	30.2	198.4	1.0	102.7	19.7	25.7	34.3	60.1	85.6	4.5	9.3	10.0	13.0	14.4	15.8	15.9	14.3	9.6	14.7	65.7	13.2	39.5
98	35.5	29.3	189.9	0.8	98.8	15.0	23.9	25.3	60.7	94.1	4.7	8.2	8.7	10.9	11.8	13.4	12.4	11.3	8.4	12.0	70.5	11.0	47.1
99	40.4	31.4	210.7	0.9	166.4	23.3	28.4	26.4	61.6	92.0	5.9	11.4	12.2	15.9	17.0	18.5	17.1	15.7	11.8	16.8	70.3	15.4	44.3
100	40.3	32.1	200.5	1.3	104.9	13.7	27.6	29.0	61.9	89.1	5.0	11.0	11.8	14.9	16.2	17.2	15.5	14.2	11.4	15.6	73.0	14.4	52.2
101	37.4	30.9	197.3	1.0	96.7	14.9	24.9	25.6	63.2	91.3	4.9	8.5	9.2	11.8	13.0	15.3	14.0	12.7	8.9	13.4	66.4	12.1	37.0
102	41.0	31.3	207.8	1.2	138.3	17.5	27.3	29.3	63.2	87.5	5.9	10.5	11.1	13.8	15.0	16.5	16.5	15.0	10.8	15.4	70.4	14.1	46.9
103	38.3	31.8	204.4	1.1	121.9	20.0	27.4	29.1	61.2	89.7	4.9	10.6	11.3	14.2	15.4	17.1	17.4	15.6	10.9	16.0	68.6	14.5	48.8
104	39.1	29.8	196.4	1.4	89.2	13.1	25.7	23.3	63.5	93.2	4.6	10.1	10.7	14.3	15.6	16.6	14.9	14.0	10.4	15.1	69.0	13.7	46.5
105	36.8	30.0	197.4	0.8	108.7	13.3	30.6	30.1	56.9	93.0	4.4	9.2	9.8	12.6	13.7	15.5	14.6	13.2	9.5	13.9	68.3	12.7	44.1
106	32.6	25.5	162.0	1.7	94.1	11.3	26.0	14.3	79.7	86.0	6.6	12.9	13.9	19.1	18.2	16.2	15.1	29.1	13.4	19.6	68.5	17.8	38.7
107	24.3	18.1	114.8	1.4	19.3	6.8	27.0	11.5	86.2	82.4	4.4	7.7	8.1	9.9	10.7	11.2	9.3	8.6	7.9	9.9	79.8	9.4	52.2
108	25.4	17.7	114.5	1.7	16.8	5.8	27.3	14.1	85.6	80.3	4.5	7.0	7.4	9.3	10.0	9.7	8.4	7.7	7.2	9.0	80.1	8.5	44.2
109	22.2	17.7	109.2	0.6	13.4	5.1	27.6	7.5	86.1	86.4	4.6	5.4	5.8	7.3	7.7	7.8	6.8	6.4	5.6	7.2	78.0	6.7	42.1
110	23.9	18.3	113.6	1.1	11.2	6.0	27.1	6.3	87.0	86.8	4.6	6.5	6.9	8.1	8.9	9.7	8.6	7.6	6.7	8.6	77.6	8.0	43.5

Reproduced with permission of the copyright owner. Further reproduction prohibited without permission.

	39	40	41	42	43	44	45	46	47	48	49	50	51	52	53	54	55	56	57	58	59	60	61
	BCLG TH	BIPO RB	SKC NTR	CRBT HK	OFB VOL	OFB ARE	ORBS CR	ORB TC1	ORB TC2	ORB A12	IORB DS	BFPU I1	BFPU I2	BFPU P3	BFPU P4	BFPU M1	BFPU M2	BFPU M3	ANT BFM	PSTB RM	RELB FM	MAX BFM	APM ASS
111	23.6	18.3	110.5	1.3	16.9	7.5	27.8	14.5	88.4	77.1	4.1	6.7	7.2	8.7	9.6	10.0	8.5	7.6	6.9	8.9	77.9	8.3	32.6
112	25.0	17.9	117.6	0.6	7.6	8.4	28.7	15.7	83.3	81.0	4.5	7.4	7.8	9.6	10.4	9.8	8.6	8.0	7.6	9.3	82.2	8.8	43.4
113	22.5	17.3	111.8	0.9	11.6	6.0	27.0	8.9	81.4	89.7	3.7	6.4	6.8	8.2	9.0	9.2	8.2	7.5	6.6	8.4	77.8	7.9	31.1
114	23.7	17.9	113.8	1.1	28.3	8.5	24.8	12.7	80.9	86.4	4.4	6.5	6.9	8.6	9.1	9.1	8.4	7.5	6.7	8.5	78.9	8.0	38.8
115	24.1	18.1	116.5	1.2	16.3	5.7	31.1	18.6	74.7	86.7	3.3	7.3	7.5	9.4	9.9	10.4	8.8	8.1	7.4	9.3	79.4	8.8	42.2
116	25.0	19.1	118.2	1.5	26.2	6.5	27.8	13.9	83.3	82.8	4.6	6.9	7.0	8.9	9.5	10.2	8.9	7.9	6.9	9.1	76.6	8.5	43.9
117	34.5	29.4	189.7	1.1	73.1	6.5	18.7	17.0	81.7	81.3	3.6	10.4	10.9	14.1	15.6	16.6	14.7	13.4	10.7	14.9	71.8	13.7	44.0
118	53.8	52.6	293.8	2.1	147.8	16.1	20.9	16.3	84.6	79.1	5.5	17.4	18.2	23.7	25.2	28.4	29.3	26.5	17.8	26.6	66.9	24.1	38.3
119	51.6	50.2	289.5	1.7	106.0	19.6	22.0	17.7	81.3	80.9	5.2	15.0	16.0	20.6	22.4	25.2	27.3	23.8	15.5	23.8	64.9	21.5	37.2
120	53.2	51.4	300.9	1.4	172.6	18.2	20.9	17.8	85.6	76.6	4.9	17.1	18.1	24.5	26.3	29.3	30.4	26.3	17.6	27.4	64.4	24.6	35.2
121	52.4	47.0	286.9	3.1	109.5	22.3	20.6	18.8	75.6	85.6	5.4	16.3	17.2	21.7	23.6	26.8	30.9	27.2	16.7	26.0	64.3	23.4	40.9
122	55.2	49.7	297.4	1.8	96.7	20.0	17.4	20.9	82.3	76.8	4.7	16.5	17.4	22.5	24.9	28.0	29.4	25.1	16.9	26.0	65.1	23.4	40.2
123	55.5	50.3	311.4	2.0	174.6	28.2	19.3	19.1	85.2	75.7	5.0	17.9	19.0	24.0	26.2	29.7	31.0	27.2	18.4	27.6	66.7	25.0	37.1
124	55.9	53.8	318.8	1.2	203.3	21.0	19.4	18.2	79.7	82.1	4.7	17.6	18.3	23.2	25.2	28.4	29.3	26.7	17.9	26.6	67.5	24.1	33.4
125	48.8	44.8	270.0	1.5	92.1	12.6	23.5	20.0	78.2	81.8	3.8	16.0	16.8	21.0	22.6	25.4	27.4	23.2	16.4	23.9	68.6	21.8	34.5
126	52.2	48.8	295.6	1.5	197.0	19.6	21.4	16.0	85.7	78.3	6.1	15.5	16.3	21.5	23.8	26.6	28.7	25.7	15.9	25.3	62.9	22.6	38.9
127	52.0	47.7	278.8	1.9	138.1	14.5	19.7	18.5	80.9	80.5	4.8	14.8	15.7	20.1	21.9	24.6	29.5	25.2	15.3	24.2	62.9	21.7	36.7
128	53.1	50.4	303.4	1.3	94.1	12.8	20.8	22.0	70.5	87.5	4.5	17.3	18.3	23.4	25.9	28.8	31.5	27.3	17.8	27.4	65.1	24.6	29.6
129	57.4	54.5	315.3	0.9	135.6	20.1	21.7	17.0	78.3	84.7	5.8	17.2	18.5	24.1	26.6	29.8	34.9	30.3	17.8	29.1	61.1	25.9	32.2
130	58.5	52.8	320.4	2.0	173.4	25.2	17.1	25.2	76.4	78.4	5.5	21.2	22.1	28.3	30.8	34.6	36.1	31.3	21.7	32.2	67.2	29.2	36.2
131	57.6	55.2	316.3	0.9	196.4	21.8	21.6	19.8	80.7	79.5	5.3	19.6	20.7	26.5	28.8	32.5	34.6	29.8	20.1	30.4	66.1	27.5	31.6
132	59.0	56.7	327.4	1.9	127.3	16.3	21.1	24.6	75.8	79.6	4.6	21.0	22.5	28.2	30.8	34.7	37.4	33.4	21.7	32.9	66.0	29.7	34.4
133	55.1	50.0	311.9	2.3	129.0	18.5	19.1	24.1	65.5	90.4	6.0	19.4	20.6	26.5	28.9	32.6	33.5	29.2	20.0	30.1	66.4	27.2	27.4
134	60.7	58.1	326.8	1.9	111.7	18.2	15.9	17.9	81.4	80.7	3.9	20.7	22.0	27.6	30.3	33.6	36.5	31.6	21.3	31.9	66.9	28.9	29.3
135	54.7	51.3	307.1	1.2	71.1	21.3	19.4	27.5	71.1	81.4	4.2	19.3	20.1	25.0	27.1	30.7	29.8	26.3	19.7	27.8	70.8	25.5	33.0
136	55.5	54.5	325.3	2.2	291.5	45.7	21.7	26.4	65.5	88.1	6.4	20.7	22.1	27.4	29.6	33.0	35.8	31.6	21.4	31.5	68.0	28.6	35.8
137	54.1	56.2	305.3	14.8	183.5	19.4	21.4	17.3	76.5	86.3	6.9	18.3	19.5	24.9	27.1	30.5	33.9	29.4	18.9	29.1	64.8	26.2	35.0
138	57.1	55.0	321.6	1.4	133.8	17.2	23.1	18.0	74.2	87.8	6.4	21.0	22.3	27.4	30.1	33.4	35.0	31.0	21.7	31.4	69.1	28.6	36.4
139	54.3	51.9	308.2	1.9	253.4	26.6	21.7	24.9	69.9	85.2	5.3	17.9	19.0	24.3	26.4	30.2	31.4	27.5	18.4	27.9	66.0	25.2	34.0
140	57.3	54.0	327.1	1.4	112.4	14.3	22.5	21.1	74.2	84.8	5.6	20.3	21.4	27.8	30.2	33.7	36.3	33.8	20.9	32.4	64.5	29.1	32.5
141	58.5	52.7	323.1	1.9	273.1	24.9	18.3	19.8	74.9	85.3	5.7	22.1	24.0	30.3	33.0	36.8	36.1	32.2	23.0	33.7	68.4	30.6	31.8
142	56.5	52.8	319.1	1.4	143.6	22.4	21.9	21.5	73.1	85.4	5.5	19.2	20.2	25.7	27.6	31.1	33.4	29.6	19.7	29.5	66.8	26.7	36.0
143	56.0	54.0	321.2	2.0	144.8	18.2	20.3	19.3	72.6	88.1	5.7	19.2	20.2	25.5	27.1	30.6	33.5	29.7	19.7	29.3	67.2	26.5	36.6
144	55.3	53.9	306.0	1.5	162.4	28.3	21.3	24.3	70.8	84.9	5.6	17.8	19.0	24.6	26.7	30.4	30.2	26.5	18.4	27.7	66.5	25.0	33.8
145	57.2	55.8	319.5	1.6	154.3	23.0	21.1	19.0	74.9	86.2	6.7	20.1	21.2	27.1	29.3	32.9	32.1	28.9	20.7	30.1	68.7	27.4	36.0
146	56.4	53.2	314.2	1.1	226.4	26.2	19.2	16.6	76.3	87.1	6.2	18.5	19.8	25.3	27.8	31.3	33.5	28.9	19.1	29.4	65.2	26.4	34.2

Reproduced with permission of the copyright owner. Further reproduction prohibited without permission.

	39	40	41	42	43	44	45	46	47	48	49	50	51	52	53	54	55	56	57	58	59	60	61
	BCLG TH	BIPO RB	SKC NTR	CRBT HK	OFB VOL	OFB ARE	ORBS CR	ORB TC1	ORB TC2	ORB A12	IORB DS	BFPU I1	BFPU I2	BFPU P3	BFPU P4	BFPU M1	BFPU M2	BFPU M3	ANT BFM	PSTB RM	RELB FM	MAX BFM	APM ASS
147	59.8	56.1	323.3	1.3	162.4	26.4	20.6	21.4	72.4	86.2	5.7	18.8	19.8	25.6	28.0	31.4	32.0	28.2	19.3	29.0	66.5	26.3	31.8
148	53.5	46.8	280.3	2.1	103.0	16.1	18.4	18.5	76.0	85.5	5.0	16.6	17.9	22.7	25.1	28.7	30.4	27.1	17.2	26.8	64.3	24.1	37.1
149	51.7	47.7	293.0	1.8	132.8	12.1	20.1	18.8	73.8	87.4	4.1	16.8	17.8	22.6	24.8	27.8	30.6	27.4	17.3	26.6	65.0	24.0	38.4
150	53.1	51.5	295.4	2.3	103.9	13.4	20.6	19.0	81.8	79.2	4.1	18.3	19.3	23.8	26.0	29.4	31.0	27.2	18.8	27.5	68.3	25.0	36.7
151	52.3	48.1	278.1	1.8	125.1	21.5	19.9	23.0	73.9	83.1	4.6	16.5	17.8	22.1	24.5	28.1	31.0	26.3	17.2	26.4	65.0	23.8	40.0
152	52.5	49.3	283.4	1.3	126.0	18.0	22.8	24.2	78.3	77.5	5.0	17.9	18.8	24.2	26.2	29.4	30.9	27.0	18.3	27.5	66.6	24.9	35.6
153	53.9	48.1	284.5	1.1	176.6	31.2	19.6	19.9	78.2	81.9	5.8	18.9	20.2	24.3	26.2	29.4	30.6	26.6	19.5	27.4	71.2	25.2	38.0
154	51.5	47.3	277.5	1.5	121.8	17.2	19.0	15.5	73.5	91.0	5.5	17.3	18.3	22.3	24.6	27.8	31.6	26.7	17.8	26.6	66.9	24.1	40.8
155	55.2	55.1	318.3	1.2	87.9	18.6	20.2	20.1	70.1	89.7	4.9	19.8	21.0	26.1	28.7	32.5	36.6	30.5	20.4	30.9	66.1	27.9	35.0
156	52.7	52.5	293.3	1.8	205.8	21.9	22.0	17.8	84.0	78.2	5.9	17.9	18.7	23.7	25.8	28.9	32.9	28.8	18.3	28.0	65.4	25.2	33.8
157	53.7	52.7	307.7	2.2	192.3	23.1	21.6	17.6	79.9	82.5	5.6	19.0	19.5	25.0	27.3	30.7	31.7	28.0	19.2	28.5	67.3	25.9	35.7
158	62.8	65.9	389.1	2.0	227.9	26.5	20.9	20.0	76.8	83.2	6.1	23.4	24.5	29.7	32.3	36.3	39.0	35.8	24.0	34.6	69.2	31.6	27.4
159	56.5	55.5	352.8	2.7	166.9	16.9	21.8	17.6	78.0	84.4	5.2	23.6	24.7	30.1	31.9	35.6	41.4	35.7	24.2	34.9	69.2	31.8	27.6
160	55.1	59.9	362.0	1.7	122.5	16.9	18.2	20.5	72.6	86.9	4.2	23.7	24.4	29.9	31.9	35.6	38.6	34.1	24.1	34.0	70.7	31.2	27.5
161	61.1	67.1	389.7	1.5	170.2	12.6	21.4	17.0	79.7	83.3	5.3	23.8	24.9	31.4	34.0	38.4	46.2	40.6	24.3	38.1	63.9	34.2	27.3
162	61.4	64.4	416.2	2.1	220.4	30.2	25.4	19.5	79.5	81.1	7.0	29.9	31.4	39.0	42.1	47.0	44.9	39.7	30.7	42.5	72.1	39.1	29.3
163	63.3	70.5	407.5	1.8	316.3	25.2	22.9	22.1	73.8	84.1	7.2	25.2	26.2	32.4	35.4	39.3	41.9	37.7	25.7	37.3	68.8	34.0	26.7
164	58.8	69.8	405.2	1.6	347.4	23.5	23.9	17.7	80.9	81.4	6.5	25.4	26.5	33.2	36.0	40.7	44.0	40.8	26.0	38.9	66.7	35.2	26.2
165	64.3	62.7	398.7	3.0	273.6	17.3	23.1	19.8	76.3	83.9	5.5	22.7	23.8	29.9	32.9	36.8	39.6	35.7	23.3	35.0	66.6	31.6	28.2
166	61.5	60.6	374.5	0.9	228.1	20.1	23.3	23.2	76.0	80.7	4.7	19.5	20.5	26.7	29.0	32.6	34.7	30.4	20.0	30.7	65.2	27.6	30.8
167	59.9	64.1	361.4	1.8	150.4	23.6	21.9	21.5	73.0	85.5	6.1	22.7	23.6	29.4	31.8	36.4	41.1	37.0	23.2	35.1	65.9	31.7	31.4
168	53.9	56.4	326.3	2.2	135.9	12.0	21.7	20.0	81.0	79.0	3.6	18.6	19.6	24.5	26.9	30.1	33.5	29.3	19.1	28.9	66.3	26.1	27.2
169	54.1	50.6	305.2	1.8	99.2	15.5	24.1	22.1	83.4	74.5	4.6	17.5	18.4	22.6	25.0	28.3	34.3	29.7	17.9	28.0	64.1	25.1	30.3
170	51.2	51.0	309.4	2.0	116.3	16.4	21.5	19.2	80.8	80.0	4.7	18.4	19.5	24.2	26.4	29.6	35.2	32.9	18.9	29.7	63.8	26.6	31.7
171	50.4	49.0	290.3	1.2	83.5	12.3	19.9	21.7	81.3	77.0	4.2	17.9	18.8	23.4	25.5	28.8	31.3	26.9	18.3	27.2	67.5	24.7	38.2
172	51.6	48.7	287.9	0.9	147.7	18.1	25.8	19.1	86.9	74.0	5.0	15.8	16.6	21.4	23.3	26.4	32.0	26.9	16.2	26.0	62.1	23.2	31.0
173	52.1	50.9	305.6	1.0	127.5	23.5	23.9	23.3	85.9	70.9	4.6	20.2	21.2	26.1	28.1	31.7	36.2	31.6	20.7	30.7	67.2	27.9	32.3
174	51.0	45.4	288.6	1.6	93.8	17.7	23.3	21.6	77.2	81.2	3.8	14.0	14.6	18.0	20.0	22.7	26.9	23.8	14.3	22.3	64.3	20.0	31.6
175	54.5	50.5	315.6	1.3	99.8	12.6	21.0	26.3	75.4	78.3	4.5	18.3	19.5	24.4	26.6	29.8	33.0	29.8	18.9	28.7	65.8	25.9	31.7
176	53.9	55.2	326.6	1.6	138.8	17.0	22.1	20.8	79.7	79.5	5.0	20.4	21.3	25.9	27.7	31.3	32.9	29.6	20.8	29.5	70.7	27.0	35.9
177	51.7	52.7	307.7	1.6	93.0	15.3	19.4	23.2	78.0	78.8	3.3	18.4	19.7	24.2	26.4	30.3	31.8	28.7	19.0	28.3	67.3	25.6	28.6
178	59.0	57.7	358.2	2.5	147.3	26.4	22.5	16.4	77.1	86.5	5.9	23.5	24.8	29.5	32.1	36.3	42.4	36.8	24.1	35.4	68.1	32.2	31.1
179	58.7	54.3	342.1	1.8	102.0	15.9	26.3	18.9	78.3	82.9	6.1	21.3	22.4	27.0	30.0	33.3	39.5	35.4	21.9	33.0	66.2	29.8	38.7
180	58.9	55.2	343.0	2.5	165.5	21.2	24.3	18.8	78.4	82.7	5.5	19.0	19.7	23.6	25.8	29.3	34.8	33.5	19.3	29.4	65.8	26.5	39.5
181	56.1	52.9	332.2	1.4	195.2	29.5	23.2	17.1	79.9	83.1	5.9	20.6	21.4	26.2	28.4	32.4	38.6	34.1	21.0	32.0	65.8	28.8	35.6
182	53.8	53.4	319.3	2.9	106.6	19.5	21.9	18.9	80.6	80.5	5.3	19.5	20.3	25.1	27.4	30.5	36.1	33.7	19.9	30.5	65.3	27.5	32.0

Reproduced with permission of the copyright owner. Further reproduction prohibited without permission.

	39	40	41	42	43	44	45	46	47	48	49	50	51	52	53	54	55	56	57	58	59	60	61
	BCLG TH	BIPO RB	SKC NTR	CRBT HK	OFB VOL	OFB ARE	ORBS CR	ORB TC1	ORB TC2	ORB A12	IORB DS	BFPU I1	BFPU I2	BFPU P3	BFPU P4	BFPU M1	BFPU M2	BFPU M3	ANT BFM	PSTB RM	RELB FM	MAX BFM	APM ASS
183	55.5	57.5	326.0	1.9	165.4	30.6	27.2	18.0	80.6	81.4	6.5	20.4	21.2	25.4	27.8	31.7	37.0	31.6	20.8	30.7	67.9	27.9	37.6
184	56.6	55.1	324.7	1.6	202.2	31.5	25.7	17.9	77.8	84.2	6.0	18.4	19.3	23.0	25.3	29.1	35.6	36.1	18.9	29.8	63.3	26.7	28.5
185	54.9	49.0	321.6	2.2	136.2	13.9	20.4	14.1	81.0	84.8	4.6	21.3	22.4	27.3	29.7	33.4	39.4	33.5	21.8	32.7	66.9	29.6	34.1
186	58.3	55.3	332.9	1.4	140.7	23.8	23.8	20.8	76.3	82.9	5.6	18.4	19.4	23.3	25.1	28.6	35.0	31.7	18.9	28.8	65.7	25.9	35.8
187	57.3	55.9	341.0	1.8	230.9	23.2	22.3	20.2	83.4	76.5	6.2	20.1	21.1	24.7	27.0	30.4	35.1	31.5	20.6	29.7	69.3	27.1	34.5
188	78.0	82.2	559.9	2.4	293.8	33.2	20.5	13.5	89.5	77.0	6.5	30.5	31.8	38.2	41.0	46.2	54.1	45.7	31.2	45.0	69.3	41.1	27.0
189	74.7	69.6	486.1	3.0	321.5	25.4	19.6	15.7	93.1	71.2	5.7	23.4	24.6	30.1	33.5	38.0	45.1	38.5	24.0	37.1	64.8	33.3	37.5
190	74.7	76.5	524.4	2.0	358.3	21.3	21.5	9.6	92.7	77.8	5.8	29.3	29.9	37.0	40.2	44.6	52.3	45.1	29.6	43.9	67.5	39.8	30.2
191	74.6	79.4	529.5	2.5	455.2	33.7	21.0	18.3	88.4	73.4	7.0	27.5	28.9	36.6	39.5	43.9	50.5	42.5	28.2	42.6	66.2	38.5	29.6
192	66.0	71.6	475.2	2.5	262.4	16.3	21.2	17.4	88.0	74.6	6.1	25.7	26.6	33.0	35.9	39.7	48.0	43.5	26.2	40.0	65.4	36.1	33.7
193	70.8	77.3	500.1	2.3	428.0	20.2	21.8	12.3	85.5	82.2	6.2	26.4	28.3	34.0	37.3	42.9	52.5	46.0	27.4	42.5	64.3	38.2	29.5
194	77.2	76.9	527.3	2.5	752.2	28.2	22.1	11.4	100.7	68.0	7.3	24.7	25.9	32.9	35.4	39.6	47.4	41.5	25.3	39.4	64.2	35.3	29.6
195	62.1	63.3	371.7	1.7	210.5	26.3	21.7	18.0	81.1	80.8	4.7	25.1	26.7	34.2	37.1	41.4	45.6	39.5	25.9	39.6	65.5	35.7	37.1
196	64.9	62.9	376.7	1.2	137.9	14.6	19.4	20.0	81.5	78.5	4.6	24.7	27.0	35.2	37.8	42.4	48.8	40.9	25.8	41.0	63.0	36.7	37.8
197	60.3	59.4	347.7	1.8	126.8	20.2	17.8	16.5	76.4	87.1	4.4	19.9	21.5	27.9	30.5	34.1	36.8	30.7	20.7	32.0	64.7	28.8	38.3
198	62.1	59.1	357.4	1.8	192.6	16.1	22.8	22.0	75.1	83.0	4.0	20.2	21.8	28.4	30.7	35.0	38.7	33.1	21.0	33.2	63.2	29.7	37.3
199	60.9	60.7	361.2	1.4	229.8	28.1	19.8	17.2	73.2	89.6	5.9	20.1	21.6	27.1	29.5	32.9	38.9	33.9	20.8	32.5	64.2	29.1	39.8
200	60.7	59.6	345.4	1.4	119.1	18.2	23.0	19.6	76.6	83.9	4.0	17.1	18.6	24.1	26.8	30.3	36.2	29.3	17.9	29.3	60.9	26.1	36.7
201	64.9	63.3	372.6	1.5	115.5	18.1	21.0	15.4	79.3	85.4	3.6	21.2	22.6	29.7	32.7	36.5	43.2	38.2	21.9	36.0	60.7	32.0	35.6
202	65.8	67.4	383.8	2.2	141.8	19.3	18.6	15.2	80.1	84.6	5.5	25.4	26.9	34.6	37.1	41.3	45.4	40.0	26.1	39.7	65.9	35.8	37.0
203	61.8	62.5	368.3	1.7	151.2	20.4	23.4	17.8	72.3	89.8	5.9	23.1	24.8	33.2	36.2	39.8	45.9	40.8	23.9	39.2	61.1	34.8	34.7
204	59.5	61.4	355.9	2.8	147.4	19.5	20.4	18.6	73.6	87.8	5.2	21.7	23.5	29.4	32.4	36.2	42.7	37.4	22.6	35.6	63.6	31.9	34.1
205	64.1	56.7	350.1	1.1	168.0	36.4	23.7	20.4	74.8	84.8	11.0	22.9	23.4	29.4	32.0	36.0	40.9	35.1	23.2	34.7	66.7	31.4	32.2
206	64.1	58.6	359.2	1.9	115.9	57.1	20.6	20.7	82.6	76.7	11.3	22.9	23.9	29.8	33.0	37.3	44.3	39.1	23.4	36.7	63.7	32.9	39.0
207	71.3	60.8	375.1	1.3	128.0	57.2	21.9	20.0	79.0	81.0	10.3	29.0	29.8	37.0	40.1	43.9	48.4	44.0	29.4	42.7	69.0	38.9	33.3
208	65.3	55.9	354.8	1.3	174.3	49.0	22.7	20.9	79.3	79.8	10.5	24.3	25.2	31.1	34.0	38.0	40.2	35.8	24.7	35.8	69.1	32.7	36.7
209	66.7	62.4	368.2	1.5	151.0	56.3	19.6	18.7	79.6	81.7	10.8	26.3	26.8	34.3	37.3	41.5	46.1	40.3	26.6	39.9	66.6	36.1	30.8
210	64.9	56.5	355.2	1.5	176.2	40.3	20.1	21.3	74.2	84.6	9.9	19.2	20.4	25.9	28.1	31.7	37.5	33.6	19.8	31.3	63.1	28.0	31.1
211	62.7	56.3	345.3	1.0	78.1	42.7	20.7	18.0	74.3	87.7	9.2	19.7	20.9	26.1	28.9	32.4	37.4	32.8	20.3	31.5	64.5	28.3	32.5
212	59.6	57.6	342.0	1.5	80.2	25.7	19.1	16.6	79.1	84.2	7.9	19.5	20.8	26.2	29.4	33.6	40.6	35.9	20.2	33.1	60.8	29.4	31.4
213	67.0	60.1	362.6	1.2	80.5	44.0	21.3	19.5	81.3	79.2	10.9	25.1	25.9	32.5	35.5	39.5	43.9	38.5	25.5	38.0	67.1	34.4	33.8
214	70.6	61.9	384.0	1.4	224.5	54.5	21.0	18.1	86.2	75.7	11.1	27.1	28.5	34.9	37.8	42.0	48.0	41.0	27.8	40.7	68.3	37.1	35.9
215	57.8	57.5	324.9	1.6	259.7	51.5	22.6	19.7	77.5	82.8	8.8	21.1	22.2	27.3	30.1	34.6	40.8	33.6	21.6	33.3	65.0	30.0	25.6
216	58.7	56.2	339.1	1.8	360.7	68.1	23.5	16.8	76.2	87.0	11.1	24.3	25.4	31.0	33.9	37.9	44.7	41.3	24.8	37.7	65.8	34.1	31.9
217	58.7	55.2	326.1	1.3	185.6	57.6	26.2	17.8	76.9	85.3	10.9	22.1	23.4	28.9	31.9	35.8	43.7	36.8	22.8	35.4	64.2	31.8	35.9
218	56.6	55.5	317.3	1.5	327.3	46.7	26.1	19.6	73.9	86.5	8.7	19.3	20.8	25.8	28.4	32.7	40.6	32.6	20.0	32.0	62.6	28.6	33.0

Reproduced with permission of the copyright owner. Further reproduction prohibited without permission.

	39	40	41	42	43	44	45	46	47	48	49	50	51	52	53	54	55	56	57	58	59	60	61
	BCLG TH	BIPO RB	SKC NTR	CRBT HK	OFB VOL	OFB ARE	ORBS CR	ORB TC1	ORB TC2	ORB A12	IORB DS	BFPU I1	BFPU I2	BFPU P3	BFPU P4	BFPU M1	BFPU M2	BFPU M3	ANT BFM	PSTB RM	RELB FM	MAX BFM	APM ASS
219	61.1	59.9	335.1	1.8	298.8	62.4	25.6	19.6	77.7	82.8	10.7	20.0	20.9	26.1	28.6	33.0	39.9	38.8	20.5	33.3	61.5	29.6	31.6
220	62.4	57.6	349.0	1.8	293.6	68.7	25.6	19.8	80.2	80.0	11.1	23.2	24.5	31.0	33.5	37.7	45.8	41.2	23.8	37.8	63.0	33.8	29.8
221	61.7	55.7	343.5	2.3	387.5	70.8	25.2	19.6	82.0	78.4	12.1	23.4	24.4	30.9	33.4	37.7	44.7	42.3	23.9	37.8	63.3	33.8	38.4
222	61.5	56.3	336.7	1.8	175.9	33.8	22.9	17.8	81.1	81.1	8.4	21.5	22.8	28.6	31.5	35.3	38.9	34.1	22.1	33.7	65.8	30.4	35.0
223	63.6	57.0	353.5	1.9	279.4	42.9	22.0	13.8	79.7	86.4	10.5	26.1	27.7	35.1	37.5	42.2	50.1	45.4	26.9	42.1	63.9	37.7	25.4
224	63	59.1	353.7	2.2	267.0	44.3	24.0	16.5	84.2	79.3	9.8	25.2	26.4	32.3	35.3	39.2	47.0	41.9	25.8	39.1	65.9	35.3	36.4
225	61.4	58.2	357.7	2.5	472.1	47.5	24.1	18.9	82.2	78.9	8.7	23.0	24.2	28.4	31.1	35.5	40.2	34.8	23.6	34.0	69.3	31.0	35.8
226	61.5	58.5	360.0	2.3	147.6	25.2	23.2	22.1	86.2	71.8	7.4	24.7	25.4	30.8	33.5	37.4	42.7	37.1	25.0	36.3	69.0	33.1	35.6
227	60.4	55.9	349.0	1.1	192.0	29.6	20.7	21.6	79.9	78.5	6.7	22.8	24.2	28.4	31.0	35.5	43.2	36.7	23.5	35.0	67.3	31.7	30.6
228	61.4	58.0	354.3	1.5	259.8	32.0	21.7	19.9	82.0	78.1	8.0	23.1	24.2	28.8	31.9	36.1	42.3	36.4	23.6	35.1	67.3	31.8	26.8
229	59.5	53.6	350.1	1.7	398.6	44.9	20.3	21.8	84.4	73.7	6.7	21.2	22.1	26.5	29.2	33.3	40.2	35.1	21.6	32.9	65.8	29.7	26.6
230	60.4	57.6	343.3	2.0	164.4	27.3	20.3	18.2	84.5	77.4	5.9	18.0	18.7	23.2	26.0	30.1	37.5	33.8	18.4	30.1	61.0	26.8	37.4
231	62.2	59.0	360.4	1.8	196.3	37.9	22.5	18.0	86.6	75.5	7.4	20.9	22.0	27.0	29.4	33.0	39.9	35.5	21.4	32.9	65.0	29.7	35.4
232	61.4	57.6	360.5	1.6	215.0	40.1	20.1	19.0	81.2	79.8	8.3	24.0	24.6	29.0	31.8	35.1	38.6	34.6	24.3	33.8	72.0	31.1	30.0
233	61.1	57.2	356.2	2.2	235.2	34.6	22.9	19.8	87.0	73.3	7.3	24.6	25.5	30.1	32.7	36.1	40.4	35.3	25.0	34.9	71.6	32.1	41.1
234	58.7	54.6	318.9	1.3	151.9	42.2	20.9	13.2	76.7	90.2	7.9	26.9	28.2	34.2	37.6	41.9	46.7	38.9	27.6	39.9	69.1	36.4	37.3
235	59.8	55.8	325.3	1.4	344.8	29.7	21.5	15.0	78.0	87.0	7.7	26.3	27.9	33.2	36.3	41.4	41.4	35.4	27.1	37.6	72.1	34.6	36.1
236	60.8	57.9	324.1	1.5	151.9	22.1	19.1	14.7	78.8	86.5	7.5	27.6	29.2	35.0	37.8	43.0	51.2	42.9	28.4	42.0	67.6	38.1	38.4
237	59.3	54.3	316.9	1.8	171.5	25.3	20.3	18.8	79.5	81.7	8.3	24.6	25.7	31.4	33.9	38.3	42.0	35.5	25.1	36.2	69.3	33.1	33.2
238	58.8	57.4	315.6	1.8	92.7	24.0	23.6	18.1	79.7	82.2	7.7	26.1	27.5	33.4	36.5	40.5	41.7	34.5	26.8	37.3	71.8	34.3	40.4
239	57.6	52.4	310.9	1.4	212.2	29.4	21.7	18.5	75.6	86.0	7.1	25.4	26.4	32.5	35.7	40.2	44.0	37.8	25.9	38.0	68.1	34.6	37.1
240	56.1	53.8	305.5	1.8	114.0	24.7	22.4	13.8	78.0	88.2	6.8	25.7	26.7	32.3	35.4	40.0	43.1	37.4	26.2	37.6	69.6	34.4	39.3
241	57.6	53.7	309.2	1.5	93.5	32.3	21.2	16.8	76.2	86.9	7.2	25.7	27.2	32.8	35.8	40.5	43.2	37.4	26.5	38.0	69.7	34.7	41.1
242	57.7	56.6	316.0	2.0	170.6	15.0	19.2	11.7	79.5	88.8	6.5	26.7	27.4	32.7	35.6	40.2	46.6	37.8	27.1	38.6	70.1	35.3	38.8
243	58.2	52.6	304.2	1.1	257.7	31.9	21.1	16.1	79.4	84.6	6.0	23.7	24.6	29.4	31.8	36.6	40.6	33.8	24.2	34.4	70.1	31.5	43.2
244	65.1	59.2	350.7	2.2	191.1	49.5	25.2	17.1	91.8	71.1	10.5	24.1	25.0	30.4	33.2	37.3	44.2	40.8	24.6	37.2	66.1	33.6	37.0
245	54.5	54.6	305.2	1.1	237.0	21.0	21.8	20.2	77.2	82.6	8.0	18.9	19.6	24.0	25.9	29.0	33.5	32.8	19.2	29.0	66.3	26.2	42.4
246	60.1	57.4	328.1	1.9	309.5	35.0	21.9	21.2	78.8	80.0	10.5	21.7	22.9	28.0	30.0	33.6	39.7	36.7	22.3	33.6	66.5	30.4	43.1
247	58.4	53.9	317.9	1.7	186.5	16.5	23.8	21.0	77.3	81.7	8.1	23.7	24.4	29.2	31.9	35.4	41.6	39.4	24.1	35.5	67.9	32.2	42.6
248	59.2	56.7	324.0	1.5	213.9	32.7	22.3	19.9	78.3	81.9	9.8	23.5	24.2	29.4	31.7	35.8	42.1	39.5	23.8	35.7	66.7	32.3	45.9
249	54.0	53.6	295.0	1.2	157.0	28.1	23.7	23.0	76.8	80.2	8.6	18.7	19.7	23.8	26.5	29.8	35.9	32.7	19.2	29.7	64.5	26.7	42.1
250	56.0	55.3	315.0	1.7	165.0	22.2	22.0	18.9	73.2	87.9	8.1	21.3	22.5	27.1	29.5	33.0	39.3	37.2	21.9	33.2	65.9	30.0	41.9
251	54.2	53.2	307.2	1.6	130.7	18.8	23.5	23.5	74.7	81.8	7.4	22.4	22.8	27.7	30.0	33.3	38.8	35.6	22.6	33.1	68.3	30.1	47.5
252	55.2	52.2	310.9	1.3	200.6	23.8	23.8	21.0	73.8	85.2	8.3	20.5	21.3	25.5	28.0	31.4	37.4	34.2	20.9	31.3	66.6	28.3	41.7
253	62.2	58.7	339.2	1.7	243.7	24.1	20.5	19.8	75.2	84.9	9.3	24.7	25.5	31.2	34.2	38.4	39.0	33.8	25.1	35.3	71.1	32.4	42.6
254	60.6	57.6	336.9	1.7	206.0	27.2	21.2	24.6	75.9	79.5	9.8	23.1	24.3	29.3	31.8	35.4	40.1	35.3	23.7	34.4	68.9	31.3	39.9

Reproduced with permission of the copyright owner. Further reproduction prohibited without permission.

	39	40	41	42	43	44	45	46	47	48	49	50	51	52	53	54	55	56	57	58	59	60	61
	BCLG TH	BIPO RB	SKC NTR	CRBT HK	OFBV OL	OFB ARE	ORBS CR	ORB TC1	ORB TC2	ORB A12	IORB DS	BFPU I1	BFPU I2	BFPU P3	BFPU P4	BFPU M1	BFPU M2	BFPU M3	ANT BFM	PSTB RM	RELB FM	MAX BFM	APM ASS
255	61.1	64.6	346.3	1.8	92.8	62.5	18.7	20.4	82.0	77.7	12.1	25.0	25.8	33.7	36.8	40.7	38.9	35.1	25.4	37.0	68.6	33.7	33.9
256	59.8	62.5	334.9	1.5	249.3	82.3	20.7	21.3	84.7	74.0	11.9	22.0	22.7	29.0	31.2	34.6	34.3	31.5	22.3	32.1	69.5	29.3	34.6
257	62.0	66.7	342.7	1.3	164.2	72.7	21.2	23.7	85.7	70.6	11.7	23.5	24.7	31.7	34.3	36.9	34.1	31.3	24.1	33.7	71.7	30.9	33.9
258	78.2	70.1	417.8	2.1	290.5	119.4	17.9	14.4	80.5	85.2	16.2	29.9	30.4	38.8	42.0	47.4	52.8	47.7	30.1	45.7	65.9	41.3	32.8
259	77.3	69.8	414.4	2.2	452.7	86.0	15.0	20.7	79.2	80.1	13.2	29.4	30.1	38.3	41.6	46.2	52.0	47.0	29.7	45.0	66.1	40.7	38.4
260	81.5	77.4	427.1	1.9	193.8	115.8	14.7	16.6	89.7	73.7	14.0	29.5	30.4	39.3	42.4	47.4	52.8	46.2	29.9	45.6	65.6	41.1	38.9
261	76.1	66.9	403.4	2.0	656.2	92.2	17.9	16.3	88.2	75.5	11.8	25.3	26.2	33.7	37.0	42.1	44.8	40.6	25.7	39.6	64.9	35.7	35.2
262	79.4	68.6	419.4	2.2	714.4	95.1	20.1	16.3	88.3	75.5	12.7	28.0	28.8	36.7	40.6	45.8	49.9	44.4	28.4	43.5	65.3	39.2	39.6
263	76.1	66.9	403.4	2.0	656.2	92.2	17.9	16.3	88.2	75.5	11.8	25.3	26.2	33.7	37.0	42.1	44.8	40.6	25.7	39.6	64.9	35.7	35.2
264	75.1	72.5	408.5	1.7	334.5	88.5	15.6	20.4	82.8	76.8	12.8	32.7	34.0	43.8	48.2	52.8	58.5	50.2	33.4	50.7	65.8	45.8	26.9
265	71	69.2	390.5	2.5	247.5	78.0	17.6	17.0	86.6	76.5	11.0	23.0	24.0	30.8	34.0	38.3	40.8	37.3	23.5	36.2	64.8	32.6	31.4
266	71.0	67.8	387.2	2.1	368.2	52.9	18.5	16.5	84.0	79.5	11.9	28.5	29.2	36.1	39.6	44.6	44.9	40.2	28.8	41.1	70.2	37.6	28.4
267	77.2	73.9	425.4	1.4	411.2	126.7	17.4	12.0	90.5	77.4	14.5	34.1	35.1	44.0	48.4	53.3	55.3	49.2	34.6	50.0	69.2	45.6	38.4
268	86.6	98.7	626.2	2.2	122.8	22.9	13.0	27.0	65.6	87.5	8.3	41.7	43.7	54.7	59.9	66.2	68.3	60.6	42.7	61.9	68.9	56.4	39.7
269	94.7	101.5	642.3	1.8	1574.9	115.4	15.4	23.6	76.6	79.9	12.2	47.5	50.0	62.5	68.1	76.1	71.9	65.0	48.8	68.8	71.0	63.0	33.7
270	90.1	104.7	631.2	13.3	586.6	35.4	13.3	23.2	71.4	85.4	8.4	43.7	44.4	53.9	58.9	65.7	71.8	62.1	44.1	62.5	70.5	57.2	30.9
271	115.6	122.7	714.0	4.6	1922.0	115.2	13.4	18.3	85.7	76.0	15.5	40.4	41.3	53.6	59.5	68.3	83.0	69.1	40.9	66.7	61.3	59.3	38.7
272	106.9	116.1	677.6	2.4	1045.4	163.4	14.4	18.3	87.6	74.2	18.4	36.8	37.7	47.6	52.6	59.7	74.4	67.7	37.2	60.4	61.7	53.8	40.9
273	118.1	120.4	692.1	4.3	694.1	127.6	20.4	23.5	84.4	72.1	16.6	34.4	36.3	45.5	50.7	58.5	72.7	60.8	35.4	57.6	61.3	51.3	31.6
274	105.5	109.8	664.4	2.9	1035.5	160.8	19.0	22.8	81.2	76.0	19.2	28.0	28.7	37.9	42.6	49.8	63.3	54.7	28.4	49.7	57.1	43.6	34.0
275	117.2	119.2	733.6	3.9	3046.6	284.3	18.9	18.6	82.4	79.0	22.0	46.9	48.8	60.2	66.4	74.6	83.7	74.0	47.9	71.8	66.7	64.9	39.1
276	113.1	130.3	746.5	4.6	4563.2	251.6	19.2	14.8	82.7	82.5	25.0	40.0	41.0	50.5	55.6	63.4	75.1	76.0	40.5	64.1	63.2	57.4	35.5
277	113.7	109.6	677.9	5.6	3127.0	118.1	15.8	20.4	85.0	74.7	18.7	38.5	39.7	50.5	57.4	67.3	75.5	65.6	39.1	63.3	61.8	56.4	41.6
278	113.7	112.4	705.9	4.7	1763.2	192.6	16.3	22.7	82.1	75.2	20.3	44.5	45.1	54.7	60.6	69.9	84.9	80.5	44.8	70.1	63.8	62.9	38.7
279	114.1	116.7	717.2	6.3	2981.3	115.5	16.0	20.5	79.8	79.7	16.8	37.2	38.2	47.7	53.5	60.1	73.2	68.5	37.7	60.6	62.3	54.1	36.8
280	96.5	98.8	619.0	3.3	659.9	233.7	22.7	8.6	92.2	79.2	23.8	32.2	33.0	34.8	40.7	45.6	53.3	49.6	32.6	44.8	72.8	41.3	43.9
281	92.8	96.0	620.7	3.7	203.7	337.0	20.6	10.1	87.9	82.0	23.5	38.5	39.8	46.6	50.4	56.2	56.5	50.0	39.2	51.9	75.4	48.3	43.5
282	100.1	95.3	619.2	2.9	854.3	160.5	17.6	8.2	94.4	77.4	20.2	35.5	36.9	43.5	47.6	53.4	57.5	51.6	36.2	50.7	71.4	46.6	42.9
283	96.3	97.0	598.8	3.9	318.1	198.7	21.7	5.9	95.4	78.7	21.0	32.8	34.9	40.6	44.3	49.8	49.8	45.6	33.8	46.0	73.6	42.5	40.6
284	93.7	92.2	603.5	2.6	672.1	220.3	19.5	2.9	93.2	84.0	21.5	34.0	34.9	40.3	43.8	49.0	49.7	44.6	34.5	45.5	75.8	42.3	46.0
285	96.8	96.4	619.4	3.6	1145.6	203.6	20.3	10.5	90.6	78.9	24.1	38.2	39.2	45.8	50.2	56.1	59.9	50.7	38.7	52.5	73.6	48.6	44.8
286	101.5	99.7	646.5	3.0	1254.9	304.6	19.5	7.4	93.8	78.8	23.4	36.3	37.9	44.5	48.4	54.4	63.7	53.4	37.1	52.9	70.2	48.4	45.1
287	96.7	96.0	620.5	4.3	880.7	241.4	17.3	4.4	93.7	81.9	18.9	30.5	31.8	38.3	40.9	46.6	46.6	40.8	31.1	42.7	73.0	39.4	38.6
288	94.6	108.6	622.6	3.6	485.0	238.3	17.8	5.7	86.0	88.3	23.1	39.6	40.6	47.4	50.1	56.4	59.2	52.3	40.1	53.1	75.6	49.4	46.2
289	95.9	107.4	631.1	4.0	150.3	144.3	16.7	7.8	87.0	85.2	20.5	33.8	35.0	40.6	44.3	50.4	54.8	49.2	34.4	47.9	71.9	44.0	39.7

Reproduced with permission of the copyright owner. Further reproduction prohibited without permission.

	39	40	41	42	43	44	45	46	47	48	49	50	51	52	53	54	55	56	57	58	59	60	61
	BCLG TH	BIPO RB	SKC NTR	CRBT HK	OFBV OL	OFB ARE	ORBS CR	ORB TC1	ORB TC2	ORB A12	IORB DS	BIPU I1	BIPU I2	BIPU P3	BIPU P4	BIPU M1	BIPU M2	BIPU M3	ANT BFM	PSTB RM	RELB FM	MAX BFM	APM ASS
290	76.4	87.4	477.6	2.6	843.2	99.3	11.5	19.7	77.5	82.8	8.9	27.7	29.4	38.2	42.1	47.9	49.2	43.5	28.5	44.2	64.6	39.7	37.0
291	95.0	102.9	597.3	3.2	750.9	105.8	13.7	17.2	82.3	80.5	17.5	39.5	40.7	52.2	56.3	59.1	56.3	52.7	40.1	55.3	72.5	51.0	34.1
292	86.8	96.2	555.0	4.4	405.4	99.7	17.2	15.3	83.4	81.3	15.3	32.8	34.8	44.8	48.7	54.9	55.4	50.8	33.8	50.9	66.4	46.0	40.1
293	96.8	106.8	614.6	3.3	441.7	112.4	18.5	20.4	80.6	79.0	19.5	39.4	41.0	54.1	58.5	60.3	57.5	53.6	40.2	56.8	70.8	52.1	31.6
294	96.4	104.5	600.7	2.9	1163.2	93.2	21.9	24.6	83.9	71.5	15.0	39.9	41.6	53.6	58.1	64.7	67.8	64.5	40.8	61.7	66.0	55.7	35.6
295	98.5	107.4	578.7	2.6	354.4	126.2	16.9	16.1	85.7	78.2	17.5	37.1	38.4	49.1	54.1	61.7	61.8	54.2	37.7	56.2	67.2	50.9	41.1
296	98.7	101.1	599.6	3.5	999.4	108.6	17.8	22.4	85.0	72.6	18.2	41.6	43.1	56.7	61.7	69.5	68.7	62.3	42.3	63.8	66.4	57.7	40.0
297	100.7	106.8	621.9	3.2	1820.1	88.3	14.5	18.2	80.8	81.0	17.8	43.4	44.1	56.3	61.7	67.5	68.2	63.8	43.7	63.5	68.9	57.8	37.6
298	91.7	99.2	589.2	3.2	1070.6	169.1	18.7	20.5	84.5	75.0	17.9	33.9	35.0	45.7	50.5	56.8	59.6	52.0	34.5	52.9	65.1	47.7	38.8
299	92.4	105.6	582.7	5.0	680.8	134.7	17.8	23.6	75.9	80.5	15.8	37.7	38.7	48.5	52.9	58.4	58.2	52.4	38.2	54.1	70.6	49.5	37.6
300	94.6	105.2	590.5	4.3	1347.9	131.1	17.3	17.5	81.0	81.6	19.5	39.9	41.4	51.0	55.5	61.3	56.8	51.1	40.6	55.2	73.7	51.0	37.2

Reproduced with permission of the copyright owner. Further reproduction prohibited without permission.

	62	63	64	65	66	67	68	69	70	71	72	73	74	75	76	77	78	79	80	81	82	83	84
	APTE MP	LEV ADV	TEM PMM	CFOR CE	RMM EFF	APF MAG	SLOP FM	APO CND	CBFL EX	ENL WCP	ENL WOB	ENL OBO	SLPC PF	SLPC PO	SLPO BF	SLPO BO	MCF LGT	ACFL GT	FMA GSZ	CEPH ID	CANI NE	DSK WGT	BRNS IZ
1	26.3	62.8	38.0	67.5	81.5	18.4	33.3	16.6	176.5	79.0	112.6	76.7	41.9	30.1	75.4	63.6	43.4	22.6	104.3	82.3	55.1	51.22	50
2	23.3	61.9	39.3	70.7	85.0	17.7	32.7	14.0	175.3	87.1	98.1	54.6	52.4	40.0	63.3	50.9	41.9	23.8	124.6	78.2	103.9	49.01	55
3	23.1	60.5	40.7	73.1	91.5	20.7	36.4	17.6	179.1	93.7	101.6	68.5	51.5	48.9	59.4	56.8	39.5	24.0	129.7	72.8	85.2	48.55	53
4	27.1	60.2	38.6	69.1	89.0	18.0	33.9	16.3	178.5	85.7	105.5	83.1	49.3	39.4	69.2	59.2	41.6	23.1	136.7	77.3	55.5	45.26	50
5	24.0	63.1	38.4	69.2	90.9	19.5	33.0	18.4	179.2	92.7	111.0	85.9	54.1	47.6	72.4	65.9	39.1	25.7	125.8	74.9	63.7	49.97	45
6	25.2	63.4	41.6	74.3	87.6	15.8	40.2	12.7	178.3	75.0	94.9	70.9	38.0	29.2	57.8	49.1	44.2	21.6	106.6	78.1	67.3	48.65	51
7	22.8	58.9	36.6	66.9	85.6	20.5	31.3	19.0	171.4	103.1	113.7	61.0	62.1	52.5	72.7	63.1	41.0	23.7	124.8	80.6	56.8	44.14	49
8	31.1	59.6	42.5	74.7	90.6	23.7	35.9	22.7	179.3	95.5	91.5	71.0	56.3	48.8	52.3	44.8	38.7	21.9	144.8	80.7	84.1	43.67	59
9	21.9	62.5	38.9	71.5	94.8	16.4	44.0	13.0	176.3	96.7	98.5	73.4	57.3	52.5	59.1	54.3	42.1	22.9	145.9	80.6	91.2	41.10	55
10	24.1	61.2	39.0	71.6	94.5	15.1	48.1	9.8	176.2	104.9	105.4	74.0	67.9	61.8	68.4	62.3	41.9	23.8	125.6	77.9	80.1	41.03	50
11	30.2	70.4	32.6	57.3	96.3	27.9	24.3	25.6	166.9	92.8	108.0	80.0	31.6	41.9	46.8	57.2	35.4	21.1	158.8	74.8	47.9	45.38	98
12	27.6	66.9	31.9	53.8	92.2	29.0	22.0	26.6	170.1	90.4	93.9	79.4	27.8	39.0	31.3	42.5	31.7	25.4	167.8	76.0	48.1	43.27	103
13	26.8	66.6	35.3	60.3	88.4	26.8	21.0	25.3	165.1	84.8	95.2	67.7	23.8	29.8	34.1	40.2	32.1	25.2	166.7	75.8	56.6	52.59	107
14	16.9	66.8	31.0	57.3	77.8	27.3	19.1	27.1	165.0	87.0	115.7	89.2	25.3	32.2	54.1	60.9	35.0	23.2	150.3	75.1	56.0	44.08	101
15	18.9	68.0	32.9	61.4	88.1	29.1	20.1	26.8	166.7	82.2	109.8	85.9	25.4	35.2	53.0	62.8	33.3	22.7	228.1	74.2	35.3	51.09	95
16	28.8	68.6	28.3	47.6	94.2	26.7	18.5	23.8	172.5	91.1	107.8	78.8	26.3	38.3	42.9	55.0	31.4	25.0	134.6	81.1	40.5	37.55	87
17	21.6	67.4	31.0	54.8	86.0	27.9	18.0	27.2	175.0	84.8	114.3	88.9	24.7	30.0	54.2	59.5	33.5	23.2	158.4	76.2	32.2	40.66	89
18	16.7	68.5	32.7	60.3	82.4	25.4	23.4	23.8	163.6	94.4	106.8	88.3	32.3	43.8	44.7	56.2	33.4	25.2	178.2	74.7	49.3	68.04	111
19	22.0	67.4	34.6	62.9	86.3	24.1	23.5	20.1	173.4	84.3	105.0	81.6	27.4	38.2	48.1	58.9	36.1	23.1	162.7	75.6	52.0	54.92	103
20	21.3	63.8	29.9	54.8	93.3	24.6	19.2	22.8	166.8	82.4	125.2	89.6	16.9	33.1	59.8	75.9	32.7	23.8	219.9	75.2	75.8	45.36	107
21	27.3	65.1	33.9	61.6	87.7	21.5	30.6	18.0	177.0	96.2	94.9	78.3	36.1	37.6	34.8	36.4	37.9	23.6	147.1	83.4	52.9	47.97	105
22	23.6	67.0	35.1	64.5	84.0	21.4	29.7	18.2	177.3	85.1	96.9	87.3	27.8	32.0	39.6	43.8	40.7	21.3	160.5	80.3	51.5	48.31	103
23	24.9	67.6	35.1	62.4	87.7	24.9	27.2	24.3	177.4	84.8	89.1	75.8	26.3	29.3	30.7	33.7	40.7	20.5	216.2	76.9	61.7	51.15	100
24	21.5	65.5	35.8	66.0	80.7	20.3	29.0	18.1	177.1	86.2	92.5	81.8	29.8	29.7	36.1	36.1	46.0	18.9	149.0	80.4	66.0	39.75	92
25	27.0	64.7	34.9	62.2	86.9	22.8	25.3	20.9	179.1	76.8	87.0	90.0	20.4	23.7	30.6	33.9	39.4	21.8	174.6	83.7	49.9	38.50	84
26	19.5	64.4	33.9	62.4	78.7	22.0	24.4	21.4	167.1	84.5	100.6	87.0	28.9	29.6	44.9	45.6	38.0	22.2	165.6	84.8	53.8	38.93	82
27	28.1	62.9	35.5	61.7	90.7	21.7	32.7	18.7	173.4	83.3	96.5	80.3	25.6	30.4	38.7	43.5	38.7	22.8	193.0	80.5	58.0	35.19	89
28	28.8	66.7	32.4	56.1	90.7	22.4	31.7	22.5	172.1	84.5	91.9	84.1	23.9	32.0	31.3	39.4	37.5	22.2	177.2	82.1	38.7	44.78	95
29	31.6	64.4	36.0	62.0	95.3	21.3	27.1	18.6	174.4	90.6	94.7	83.8	30.1	36.6	34.1	40.7	36.9	24.2	173.6	82.0	54.8	40.26	98
30	27.2	66.4	34.5	58.5	87.7	21.5	29.6	19.2	170.8	93.7	96.3	80.0	35.8	43.7	38.4	46.3	38.3	23.7	165.5	84.8	52.9	41.64	91
31	32.7	60.3	39.5	67.1	90.9	18.4	26.9	17.8	179.4	93.7	103.4	47.2	40.7	45.3	50.4	55.0	42.0	21.3	193.7	86.6	62.8	61.85	112
32	18.4	66.3	28.3	52.0	84.4	26.1	21.2	22.7	175.9	81.9	92.1	72.1	23.7	31.3	33.9	41.6	35.3	24.3	115.3	79.4	126.8	19.27	50
33	18.5	72.3	26.8	48.9	84.8	25.8	21.6	24.7	175.6	85.9	96.2	73.4	27.0	39.0	37.3	49.4	35.5	25.2	120.3	81.0	122.5	27.15	55
34	29.2	70.0	26.2	48.6	90.0	24.9	24.8	22.3	175.6	86.9	112.2	89.4	23.1	32.2	48.4	57.6	37.1	23.8	133.0	82.5	98.4	24.40	64
35	20.3	68.3	22.8	41.7	94.0	27.7	20.7	25.1	178.9	89.5	116.1	87.3	26.7	40.8	53.3	67.4	38.2	21.3	129.5	83.5	107.1	22.51	58
36	21.8	69.5	27.6	49.4	83.9	22.7	28.5	19.4	178.2	90.5	98.6	86.8	31.3	41.7	39.5	49.8	38.6	24.7	120.2	84.0	104.1	22.30	55
37	18.5	69.0	27.5	51.4	82.8	26.2	25.9	23.8	173.2	79.1	101.6	80.1	18.1	27.4	40.6	49.9	35.3	23.7	123.0	77.4	93.1	25.26	59

Reproduced with permission of the copyright owner. Further reproduction prohibited without permission.

	62	63	64	65	66	67	68	69	70	71	72	73	74	75	76	77	78	79	80	81	82	83	84
	APTE MP	LEV ADV	TEM PMM	CFOR CE	RMM EFF	APF MAG	SLOP FM	APO CND	CBFL EX	ENL WCP	ENL WOB	ENL OBO	SLPC PF	SLPC PO	SLPO BF	SLPO BO	MCF LGT	ACFL GT	FMA GSZ	CEPH ID	CANI NE	DSK WGT	BRNS IZ
38	24.5	68.0	25.5	46.9	89.0	22.6	23.4	21.5	179.2	85.3	105.4	74.4	22.1	34.0	42.2	54.2	39.2	22.5	109.4	83.1	71.5	22.13	49
39	26.1	67.0	23.8	42.6	91.8	26.8	22.8	23.7	178.3	84.3	110.4	87.4	23.2	31.4	49.3	57.6	36.7	23.6	97.6	80.5	75.3	21.50	57
40	29.1	64.3	24.3	44.0	86.3	25.3	30.0	22.4	179.7	84.7	108.4	72.1	20.4	28.8	44.0	52.5	35.5	23.3	117.8	84.8	66.3	23.27	54
41	19.3	63.2	26.2	48.5	85.1	27.2	22.9	23.2	178.5	83.7	100.8	66.9	22.2	31.6	39.3	48.8	36.9	23.7	115.4	80.9	55.4	22.27	47
42	24.4	69.5	23.7	40.1	92.3	29.0	21.3	26.9	176.2	92.7	120.9	65.3	38.4	51.9	66.6	80.2	38.0	20.3	86.7	77.3	38.6	15.22	31
43	29.0	67.7	22.8	37.1	96.3	26.0	20.3	25.5	173.4	104.0	112.1	43.6	45.5	61.8	53.6	69.9	40.2	20.6	87.9	81.0	28.5	14.81	33
44	24.6	63.5	22.7	37.6	90.2	27.7	22.0	26.3	176.5	93.8	108.7	65.6	35.9	48.5	50.7	63.4	36.7	21.9	93.3	84.0	33.9	15.15	35
45	20.6	64.1	24.7	44.2	84.5	25.0	25.2	24.6	179.6	92.6	125.4	66.3	33.9	44.2	66.7	77.0	38.5	22.4	107.8	81.1	38.3	14.20	31
46	19.9	64.0	25.0	45.1	89.5	26.3	24.2	25.3	161.0	80.6	127.8	63.2	28.2	39.6	75.4	86.8	36.9	21.5	83.1	80.0	31.6	13.57	26
47	14.1	63.5	21.0	37.8	80.8	27.6	9.3	27.5	171.6	89.3	99.8	47.8	28.5	41.1	39.0	51.6	38.2	21.9	79.5	85.6	18.1	14.69	34
48	23.2	66.4	22.8	39.9	86.4	27.2	12.2	26.8	161.9	101.7	107.8	62.0	46.6	56.4	52.7	62.5	35.5	24.1	84.7	79.8	69.2	17.56	34
49	23.7	67.5	23.6	41.5	89.4	27.6	21.2	26.2	170.1	99.0	104.0	57.0	43.2	56.1	48.2	61.1	37.6	21.7	82.6	79.5	46.0	16.55	33
50	17.1	67.8	21.6	38.7	81.5	25.1	21.9	23.0	175.3	96.8	102.7	54.4	37.5	53.8	43.4	59.7	40.0	21.6	76.6	81.4	41.3	17.56	31
51	16.5	60.9	23.4	41.4	89.0	26.4	30.5	22.6	173.2	102.1	115.0	70.3	48.8	61.7	61.8	74.7	35.0	24.2	74.9	83.8	38.3	14.85	27
52	19.1	67.2	25.3	41.9	89.0	22.2	20.2	19.9	176.8	95.9	95.7	63.3	45.2	53.1	44.9	52.8	35.6	24.0	94.3	82.8	76.1	24.17	44
53	24.7	64.6	27.3	47.0	83.0	22.7	34.1	18.7	177.8	89.9	105.0	61.2	39.1	46.3	54.2	61.4	38.4	20.5	90.0	79.6	45.1	24.36	35
54	12.2	68.2	26.5	46.7	76.5	24.2	22.8	20.8	175.0	101.2	109.8	68.3	49.0	57.6	57.6	66.2	39.5	22.0	85.1	79.7	56.4	24.76	38
55	13.6	65.1	23.8	43.0	80.0	25.3	23.6	23.4	178.8	93.3	106.0	64.6	39.3	50.3	52.0	62.9	35.4	22.0	77.4	85.5	51.4	19.44	41
56	24.1	65.6	18.6	30.1	92.5	24.2	16.0	24.0	173.9	96.8	117.5	57.9	48.4	47.0	69.0	67.6	39.0	19.4	45.8	87.6	7.4	11.23	17
57	26.5	62.6	19.9	31.5	95.3	25.5	22.1	25.4	179.2	92.3	119.7	60.2	40.5	48.4	68.0	75.9	35.3	21.7	46.3	79.5	8.4	9.71	16
58	13.7	67.4	19.2	36.3	66.1	27.4	17.3	27.4	179.0	95.2	106.7	68.4	44.9	46.8	56.5	58.3	36.1	19.0	54.6	81.5	7.0	7.85	16
59	16.5	63.8	20.4	35.8	80.4	28.1	26.5	25.8	177.4	83.5	111.1	81.6	38.3	39.3	66.0	67.0	32.6	20.3	57.3	80.5	10.5	11.10	17
60	16.8	63.5	21.0	39.3	80.4	24.8	18.4	23.9	177.1	83.4	105.2	71.2	29.7	33.1	51.5	55.0	33.2	22.2	62.7	80.4	7.3	12.81	18
61	15.2	66.3	20.5	37.5	80.6	24.2	34.0	21.9	175.8	92.8	113.4	56.8	44.4	44.1	65.0	64.6	38.8	17.5	47.8	86.7	7.5	10.06	16
62	7.0	62.5	18.8	35.7	66.4	27.2	2.3	25.8	173.3	93.3	102.1	59.6	41.8	45.3	50.6	54.0	32.9	19.4	28.5	81.5	8.0	8.16	16
63	18.7	60.8	15.3	26.2	92.3	30.8	13.2	31.9	172.5	89.5	112.3	71.7	29.3	42.8	52.1	65.6	28.2	22.6	51.9	74.1	3.0	6.43	15
64	14.4	63.2	16.5	30.1	82.1	25.9	22.9	24.0	175.3	95.5	116.2	51.0	47.3	52.3	68.1	73.0	30.0	20.9	47.5	81.0	9.5	10.10	17
65	20.2	62.6	18.4	32.4	85.4	27.1	19.9	27.3	174.4	87.0	118.9	61.4	38.0	40.7	69.9	72.6	33.9	19.2	43.9	86.3	7.8	9.71	16
66	19.2	67.7	29.2	52.3	81.8	29.1	19.7	27.0	173.8	92.8	99.1	86.8	31.6	43.1	37.9	49.3	36.6	22.4	95.8	77.3	60.4	33.15	71
67	22.9	65.7	29.4	50.5	86.2	30.4	18.7	29.3	163.6	95.5	106.6	79.5	29.0	47.4	40.1	58.4	38.3	20.2	124.3	83.5	54.5	27.39	63
68	24.5	64.0	31.1	54.0	84.2	29.1	20.4	27.2	170.6	93.3	100.9	81.7	32.3	44.7	39.8	52.3	37.6	19.5	119.0	83.1	66.3	27.91	63
69	26.9	62.0	27.2	47.7	93.0	35.0	20.2	34.1	178.3	79.1	107.5	88.6	12.8	28.7	41.2	57.1	32.3	19.7	122.3	74.5	61.0	28.25	64
70	22.4	64.8	29.0	53.0	84.3	28.2	17.8	27.0	161.3	86.8	98.1	87.5	22.9	35.7	34.2	47.0	39.1	20.5	154.9	77.4	54.9	26.00	66
71	22.1	66.2	28.1	49.7	84.5	29.8	21.1	27.7	158.8	86.0	98.3	73.2	20.5	34.7	32.8	46.9	35.4	23.1	125.2	79.0	64.4	26.60	63
72	22.4	69.4	30.8	54.6	85.2	24.5	17.3	23.8	170.5	88.7	102.0	80.7	22.4	34.0	35.7	47.3	40.2	23.3	165.7	82.0	55.1	26.70	69
73	24.0	66.3	30.1	54.8	79.9	29.3	19.6	28.4	173.5	84.3	101.1	87.9	22.6	31.7	39.4	48.5	34.3	23.1	151.3	78.5	66.1	30.32	70
74	22.3	67.9	29.3	51.9	82.9	28.7	18.2	26.6	166.9	81.7	110.1	81.4	17.8	31.7	46.2	60.1	34.6	23.0	127.2	76.4	60.8	29.76	65

Reproduced with permission of the copyright owner. Further reproduction prohibited without permission.

	62	63	64	65	66	67	68	69	70	71	72	73	74	75	76	77	78	79	80	81	82	83	84
	APTE MP	LEV ADV	TEM PMM	CFOR CE	RMM EFF	APF MAG	SLOP FM	APO CND	CBFL EX	ENL WCP	ENL WOB	ENL OBO	SLPC PF	SLPC PO	SLPO BF	SLPO BO	MCF LGT	ACFL GT	FMA GSZ	CEPH ID	CANI NE	DSK WGT	BRNS IZ
75	23.7	66.7	31.4	54.5	85.2	27.5	18.0	25.9	168.6	77.3	100.3	87.7	12.0	24.3	35.0	47.3	38.0	23.5	128.2	81.7	71.5	31.67	70
76	18.0	61.9	30.5	50.8	78.3	30.4	18.3	30.6	159.9	92.3	107.5	73.6	29.1	40.9	44.2	56.1	34.9	22.7	172.9	80.4	59.7	24.39	74
77	17.2	61.1	28.5	50.2	73.1	27.4	14.1	28.2	163.6	76.9	109.1	74.4	18.0	28.7	50.2	60.9	38.4	20.5	153.7	80.8	70.2	23.45	60
78	16.3	64.5	29.6	54.4	72.0	28.1	11.4	28.5	171.3	93.4	123.4	77.9	32.4	42.5	62.4	72.5	37.2	21.7	150.3	77.9	64.0	21.36	64
79	19.1	64.5	31.1	54.5	76.7	27.1	18.4	27.4	174.8	82.6	103.7	89.2	18.1	28.4	39.2	49.4	34.9	24.1	159.4	78.0	68.0	35.48	76
80	15.5	62.9	27.5	49.2	72.6	29.7	15.0	30.8	164.2	93.4	108.5	75.4	28.8	44.0	43.9	59.1	38.7	20.7	154.4	79.8	77.7	32.18	71
81	24.6	65.3	31.8	53.4	76.9	24.0	20.7	24.1	174.6	89.2	109.0	85.2	24.4	39.5	44.2	59.3	39.3	22.7	161.9	81.5	64.7	30.07	73
82	15.2	62.4	32.9	57.9	76.5	28.7	22.8	28.6	170.6	88.0	105.8	72.2	30.0	40.2	47.8	58.0	36.1	22.0	164.7	76.4	80.3	34.07	69
83	16.4	62.6	27.6	48.4	78.0	32.0	17.5	30.4	167.0	88.3	102.8	73.4	22.4	39.2	36.9	53.7	38.5	18.7	159.5	79.1	56.4	29.16	78
84	15.2	63.6	29.1	52.0	70.9	29.6	19.5	31.6	176.9	88.7	103.8	72.2	24.9	37.9	40.0	53.1	34.3	24.0	153.2	74.5	62.6	26.88	69
85	13.7	62.4	30.1	55.9	68.4	28.8	19.0	29.2	173.8	92.2	101.6	75.5	30.0	44.2	39.4	53.6	36.9	23.1	130.5	75.5	54.9	24.23	58
86	22.1	69.7	17.1	28.1	80.4	40.2	8.3	39.9	164.4	90.1	108.7	69.8	20.7	32.3	39.3	50.9	25.9	21.3	69.7	74.6	17.4	8.31	27
87	25.4	69.9	16.9	27.7	79.8	37.8	11.0	38.2	162.4	91.8	103.8	77.2	22.4	32.0	34.4	44.0	25.6	23.6	65.1	74.9	18.4	8.88	24
88	16.7	67.9	16.9	29.4	77.3	38.1	5.5	38.2	171.0	92.1	101.5	62.3	21.1	34.5	30.6	43.9	25.3	22.3	62.3	72.2	11.2	8.40	24
89	30.0	67.9	16.3	25.6	82.3	35.1	13.3	35.9	164.0	98.4	114.6	78.4	23.7	38.1	39.9	54.2	27.7	24.7	62.3	75.1	8.8	7.61	23
90	25.2	65.8	16.9	26.7	85.3	41.5	10.9	41.7	164.7	93.4	101.0	67.0	18.3	34.4	25.9	42.0	24.1	24.4	58.2	72.6	8.0	7.89	29
91	18.5	69.2	19.5	33.0	76.8	38.3	16.7	37.1	167.7	89.1	100.7	75.8	18.3	28.5	30.0	40.2	29.0	22.1	57.3	70.6	7.0	8.71	25
92	26.5	67.8	16.8	25.6	76.0	40.9	17.2	41.3	166.1	87.0	110.2	67.4	13.8	25.5	37.0	48.7	23.5	23.9	61.8	75.2	6.3	8.29	32
93	19.3	68.0	18.0	29.7	77.0	34.1	20.8	33.8	173.4	88.0	101.4	70.1	17.7	27.9	31.0	41.2	29.4	23.2	56.0	76.6	8.6	7.85	24
94	19.6	70.0	17.8	27.7	71.8	38.3	13.3	37.3	164.9	87.3	109.8	71.5	12.4	27.4	35.0	50.0	27.8	24.2	71.6	73.7	9.8	7.66	27
95	24.6	68.1	18.3	28.5	75.6	36.1	11.8	35.3	175.7	90.6	101.9	55.2	22.5	34.5	33.7	45.8	25.3	25.0	60.5	76.2	9.2	6.63	24
96	11.6	63.1	17.6	31.3	74.3	25.4	25.0	25.3	166.5	88.4	113.9	56.0	37.5	42.5	63.0	67.9	29.8	23.6	63.0	80.0	8.7	7.74	17
97	13.6	58.6	15.0	26.9	80.0	30.6	12.9	29.0	176.8	96.3	117.3	60.6	45.4	47.9	66.4	68.9	28.3	26.5	76.5	74.9	14.4	5.98	16
98	19.9	61.9	14.1	21.7	87.1	35.6	9.5	36.7	164.7	93.3	112.3	49.7	39.9	46.3	59.0	65.3	27.7	22.6	65.8	75.7	2.7	5.38	16
99	16.0	63.9	16.9	29.5	81.5	30.0	12.7	28.7	169.8	85.7	124.1	58.3	35.0	40.0	73.3	78.3	29.9	24.3	79.9	79.3	14.5	7.65	17
100	10.7	66.0	15.4	26.9	72.2	27.2	13.8	29.2	170.4	89.2	127.7	60.6	33.9	36.5	72.4	75.0	30.8	22.7	77.9	80.8	6.3	7.08	18
101	15.0	62.3	14.4	24.5	81.3	33.2	14.5	31.4	167.0	89.6	113.4	52.2	31.5	36.4	55.4	60.2	25.4	26.5	76.6	76.9	2.7	6.51	18
102	27.0	60.7	17.0	27.1	85.8	30.9	27.4	30.8	166.6	89.3	125.1	55.5	38.4	39.7	74.3	75.6	27.9	23.0	92.4	79.1	6.7	8.62	18
103	5.6	61.3	16.0	27.9	68.7	30.6	10.9	29.1	172.1	90.6	122.5	53.5	37.3	42.1	69.2	73.9	29.3	23.3	78.0	78.7	11.7	7.39	15
104	21.2	65.2	16.3	27.0	85.0	32.9	19.6	31.4	170.5	85.4	129.5	64.7	33.0	40.3	77.0	84.3	28.5	23.1	52.8	83.0	8.5	6.98	14
105	12.9	62.1	14.9	24.9	82.7	33.2	17.4	31.4	168.2	89.9	117.3	54.6	37.9	45.5	65.3	72.9	28.4	21.1	76.9	76.9	10.4	6.34	14
106	14.3	79.6	16.3	29.1	71.4	29.1	35.5	27.0	167.3	95.4	120.1	60.2	37.6	44.2	62.4	69.0	33.6	23.0	62.0	76.6	11.7	5.11	10
107	31.0	71.0	11.4	16.6	79.3	30.9	29.7	28.7	162.8	102.9	113.4	40.3	37.8	43.2	48.4	53.7	35.2	19.1	29.1	83.2	2.2	1.61	4
108	29.3	72.5	10.0	15.1	75.5	25.5	31.0	25.9	173.4	108.7	113.3	60.6	42.9	49.1	47.4	53.6	35.6	22.5	19.4	79.0	2.2	1.34	4
109	34.3	67.4	8.7	12.4	83.0	31.0	15.9	30.6	178.6	103.4	117.4	54.9	40.7	49.6	54.7	63.6	29.9	23.5	21.6	77.8	1.6	1.22	3
110	34.2	67.7	9.7	14.3	78.1	30.4	26.1	31.3	177.9	101.1	92.2	54.1	39.3	47.3	30.4	38.4	31.4	20.6	23.2	83.3	1.5	1.55	4

Reproduced with permission of the copyright owner. Further reproduction prohibited without permission.

	62	63	64	65	66	67	68	69	70	71	72	73	74	75	76	77	78	79	80	81	82	83	84
	APTE MP	LEV ADV	TEM PMM	CFOR CE	RMM EFF	APF MAG	SLOP FM	APO CND	CBFL EX	ENL WCP	ENL WOB	ENL OBO	SLPC PF	SLPC PO	SLPO BF	SLPO BO	MCF LGT	ACFL GT	FMA GS2	CEPH ID	CANI NE	DSK WGT	BRNS IZ
111	30.1	69.5	9.9	14.8	87.0	31.3	22.1	30.7	164.4	98.3	113.3	57.8	33.8	44.9	48.7	59.9	30.8	22.1	23.8	78.4	2.4	1.26	3
112	34.7	72.2	10.9	15.6	85.9	25.7	28.1	25.3	147.6	116.8	115.0	28.5	51.9	61.1	50.0	59.2	36.9	22.6	28.2	82.4	2.3	1.94	4
113	24.6	67.6	9.2	14.6	83.9	31.9	12.0	33.1	177.2	103.3	115.0	49.5	39.9	52.8	51.5	64.4	32.1	21.7	24.8	77.2	1.8	1.22	3
114	21.2	69.6	9.5	14.7	77.7	32.5	19.5	33.9	177.5	98.3	102.7	69.6	37.3	46.2	41.6	50.6	32.1	20.1	33.0	79.2	1.9	1.25	3
115	31.4	69.3	10.4	15.4	79.2	28.6	25.7	28.3	153.4	106.8	118.4	45.9	48.4	54.7	59.9	66.2	33.4	20.3	29.4	82.5	1.5	1.61	3
116	33.6	68.5	10.7	15.0	80.0	28.3	23.5	27.3	178.3	115.6	114.5	58.0	53.1	59.4	52.0	58.3	36.2	21.3	23.5	81.0	1.6	1.66	4
117	26.5	67.8	16.8	25.6	76.0	40.9	17.2	41.3	166.1	87.0	110.2	67.4	13.8	25.5	37.0	48.7	23.5	23.9	61.8	75.2	6.3	5.64	11
118	25.8	57.7	30.8	49.2	85.6	27.9	19.6	26.3	162.7	89.2	93.7	83.6	29.4	40.6	33.8	45.0	36.5	26.1	120.5	88.0	51.9	31.10	55
119	27.4	57.3	27.4	44.0	85.5	30.2	13.4	28.9	178.2	95.2	95.9	73.9	39.0	48.3	39.7	49.1	32.1	25.7	157.2	86.6	54.5	19.32	60
120	30.3	59.9	29.8	49.0	86.4	22.8	19.9	23.9	162.5	83.9	87.8	89.4	27.1	36.4	31.1	40.4	36.2	29.2	134.5	84.6	122.2	28.00	57
121	33.5	55.1	30.1	48.6	91.3	28.6	18.1	27.9	149.2	94.3	94.1	80.9	38.1	47.7	38.0	47.6	32.6	29.1	122.0	82.9	55.6	28.55	40
122	30.5	58.4	30.9	47.9	81.9	24.6	24.5	23.9	168.0	82.7	82.4	86.4	26.5	32.3	26.2	32.0	35.0	27.6	141.7	84.0	53.1	29.58	61
123	29.8	58.6	31.1	50.7	90.6	29.8	16.6	28.5	165.6	84.9	89.2	89.6	24.3	38.7	28.7	43.0	35.9	27.5	129.5	81.5	87.2	39.80	73
124	31.7	58.0	30.6	49.0	88.5	32.8	15.5	32.9	172.1	88.9	93.5	79.1	27.6	40.0	32.2	44.6	37.4	22.4	175.9	83.1	95.0	38.30	76
125	27.2	57.2	26.9	44.5	86.8	29.4	26.3	29.8	152.5	90.6	91.2	85.1	29.8	37.8	30.4	38.4	33.4	27.7	142.0	80.7	35.6	18.00	45
126	30.5	57.3	30.0	46.5	89.5	29.6	15.8	29.4	164.7	90.6	89.6	88.4	33.1	44.2	32.1	43.2	34.7	25.8	141.0	83.9	60.1	27.91	67
127	29.3	55.0	27.3	44.7	88.1	29.7	23.3	28.8	149.3	90.3	92.8	78.3	26.5	40.0	29.0	42.5	30.9	27.6	135.9	81.2	56.7	33.15	55
128	26.8	57.7	30.3	49.9	96.1	28.1	9.0	27.1	176.2	94.2	85.8	63.2	35.2	50.0	26.9	41.6	37.7	22.3	126.3	83.7	71.9	31.08	59
129	19.1	55.0	30.9	54.2	86.8	28.1	24.5	27.2	175.5	93.9	90.0	86.4	36.5	48.5	32.6	44.6	38.4	21.7	141.4	86.5	65.3	41.38	67
130	24.7	58.6	34.1	59.1	92.2	26.8	15.2	25.6	178.3	93.2	103.1	75.7	35.3	49.9	45.1	59.8	37.3	22.1	153.5	83.6	61.8	38.56	70
131	40.0	59.7	33.2	54.4	100.0	27.2	24.6	27.0	173.2	93.8	95.4	76.5	34.0	47.6	35.6	49.1	37.5	22.4	140.2	87.1	81.0	35.97	67
132	32.8	57.3	37.0	60.6	92.9	27.7	16.7	28.0	179.1	92.7	90.7	74.1	34.6	43.1	32.6	41.2	39.3	21.0	162.6	82.7	83.0	35.79	64
133	37.3	59.6	33.3	54.6	104.6	26.5	22.7	26.9	169.5	96.9	101.5	85.4	45.0	57.1	49.6	61.7	34.7	23.1	145.4	83.8	70.4	31.67	56
134	31.2	58.3	34.4	57.6	96.1	27.2	23.9	26.1	177.3	94.5	96.8	74.0	34.9	48.3	37.2	50.6	37.9	24.4	109.4	87.6	58.8	40.91	74
135	39.2	61.5	31.3	49.9	100.8	26.0	26.2	25.3	176.3	101.8	104.0	75.8	42.8	55.4	44.9	57.6	40.2	21.7	106.9	89.4	49.2	25.41	54
136	26.5	56.9	35.1	58.0	94.4	27.8	17.2	28.0	173.5	91.6	106.4	78.4	37.0	48.6	51.8	63.5	44.0	20.5	162.2	91.6	80.1	37.32	65
137	29.7	59.3	30.6	51.4	87.8	17.9	24.0	19.4	146.2	90.8	92.2	72.7	31.6	42.2	33.0	43.5	47.5	20.2	157.9	97.0	84.6	35.42	68
138	30.5	59.1	34.3	56.5	92.4	29.1	18.2	26.3	172.0	90.2	89.2	87.6	35.5	42.8	34.5	41.8	38.0	23.7	132.7	83.3	56.4	35.85	61
139	32.4	59.9	31.2	50.5	97.6	26.9	20.8	25.4	175.2	78.3	109.4	89.3	22.9	37.8	54.1	68.9	37.0	24.2	133.0	87.6	52.7	36.48	57
140	21.5	58.0	32.6	58.1	86.3	30.0	14.0	29.4	172.5	92.0	93.5	89.2	35.1	46.1	36.5	47.5	37.0	23.9	140.2	82.0	78.1	34.33	70
141	29.7	61.7	33.7	59.7	91.8	28.7	12.9	26.6	170.5	77.3	96.5	79.3	17.3	30.6	36.5	49.7	37.8	25.5	132.1	78.8	55.2	40.85	66
142	28.9	58.8	32.9	52.9	84.3	28.1	14.5	27.8	169.1	86.1	108.4	87.0	29.3	35.1	51.6	57.4	40.7	21.7	163.7	88.4	73.0	31.55	72
143	25.2	56.6	31.2	54.1	91.2	28.5	18.2	28.1	168.3	89.5	110.2	86.0	29.0	43.2	49.7	63.9	37.7	24.4	124.7	86.5	58.5	44.16	64
144	29.6	60.0	31.1	50.6	91.2	24.9	21.3	23.1	172.4	82.4	88.8	87.7	29.0	35.1	35.4	41.5	37.0	26.2	140.6	87.3	58.9	26.70	61
145	29.3	61.8	31.4	53.2	92.1	27.0	24.4	24.6	178.2	94.6	106.4	77.7	35.0	47.8	46.7	59.6	40.6	20.6	160.0	88.9	75.4	30.71	67
146	27.4	59.6	31.9	52.4	95.9	26.2	22.7	25.1	165.2	84.6	111.3	85.7	22.9	39.2	49.6	65.9	38.5	26.8	150.8	83.9	50.9	31.84	63

Reproduced with permission of the copyright owner. Further reproduction prohibited without permission.

	62	63	64	65	66	67	68	69	70	71	72	73	74	75	76	77	78	79	80	81	82	83	84
	APTE MP	LEV ADV	TEM PMM	CFOR CE	RMM EFF	APF MAG	SLOP FM	APO CND	CBFL EX	ENL WCP	ENL WOB	ENL OBO	SLPC PF	SLPC PO	SLPO BF	SLPO BO	MCF LGT	ACFL GT	FMA GSZ	CEPH ID	CANI NE	DSK WGT	BRNS IZ
147	36.4	59.3	32.8	52.9	95.8	23.7	19.9	21.9	174.7	86.4	95.2	81.3	28.3	39.9	37.2	48.7	38.3	23.1	149.6	89.8	54.7	33.53	70
148	16.7	58.1	27.0	49.5	76.6	25.1	23.6	23.3	164.0	80.6	95.2	88.8	19.7	28.9	34.3	43.5	34.8	25.4	144.7	82.1	42.8	29.21	60
149	25.9	56.3	28.8	49.3	84.8	27.2	19.5	26.3	162.1	91.5	93.2	76.9	29.2	41.5	30.9	43.2	34.0	25.8	141.8	82.5	49.5	29.01	59
150	21.4	60.2	28.0	48.9	74.9	28.5	20.3	26.9	174.5	77.9	93.3	85.2	14.8	20.5	30.2	36.0	36.5	24.1	133.0	84.9	54.9	30.88	65
151	25.3	56.7	28.5	49.6	86.2	26.7	16.1	23.8	166.0	84.5	90.2	64.8	21.0	29.0	26.8	34.8	35.6	25.7	112.3	82.1	54.4	29.30	63
152	29.6	57.9	29.6	50.7	82.3	29.7	21.9	28.3	163.8	93.9	98.4	80.9	28.2	34.5	32.6	38.9	35.1	24.1	126.4	83.6	42.6	25.80	64
153	28.8	59.6	29.1	49.3	82.3	27.3	24.5	25.9	171.4	85.2	92.0	76.8	20.3	29.8	27.1	36.7	35.5	22.9	141.0	80.5	42.2	26.67	62
154	32.4	57.0	30.5	48.8	89.2	28.7	29.4	28.2	162.2	91.6	99.2	78.0	21.6	37.9	29.3	45.5	31.6	24.7	143.4	81.4	41.9	25.57	60
155	35.2	58.1	35.1	55.8	98.4	28.6	16.6	28.4	178.8	88.5	92.3	70.1	32.2	41.9	35.9	45.7	38.1	21.1	160.3	83.8	78.1	32.69	67
156	27.9	56.9	29.3	50.8	92.9	32.1	15.9	30.4	170.5	91.9	99.7	65.1	23.2	41.5	31.0	49.3	34.0	20.7	118.9	84.7	34.5	32.64	61
157	25.9	60.5	30.0	50.8	83.0	31.1	20.2	28.0	166.8	86.9	104.4	89.7	26.1	34.8	43.5	52.2	36.8	22.2	128.4	89.8	46.7	36.37	65
158	34.0	56.3	37.7	64.5	104.1	32.6	15.5	34.8	158.8	91.5	101.2	89.7	38.7	50.8	48.4	60.5	42.0	20.7	198.5	82.1	81.4	72.58	101
159	31.6	56.1	37.5	63.5	103.5	31.3	14.7	33.1	167.1	84.9	101.8	86.6	27.1	45.4	43.9	62.2	41.4	21.4	186.4	85.2	64.1	52.61	82
160	29.8	57.1	35.9	62.3	102.7	28.8	14.6	30.3	151.3	81.1	103.8	81.3	24.8	41.6	47.4	64.3	44.0	19.2	159.2	85.8	65.6	55.01	75
161	32.1	53.9	41.5	71.1	108.5	31.7	15.8	35.3	165.4	80.6	101.6	83.4	23.0	43.9	44.1	65.0	39.3	21.3	193.0	83.0	115.8	72.44	106
162	29.4	64.1	45.0	73.4	99.9	35.5	10.6	37.1	157.0	93.0	97.4	81.7	38.2	49.6	42.7	54.1	41.0	17.9	195.0	90.0	59.1	68.54	109
163	28.9	56.9	41.0	69.1	102.4	27.5	26.6	27.3	159.3	96.3	91.0	77.2	39.5	53.3	34.2	48.0	41.4	23.0	191.6	91.4	79.5	84.85	100
164	33.0	55.7	41.8	73.1	106.2	34.8	7.9	36.3	149.4	89.9	87.6	89.1	36.4	47.0	34.0	44.6	37.5	21.7	176.6	87.8	90.9	83.01	101
165	29.5	56.0	40.4	65.8	103.5	30.9	19.4	29.6	165.1	89.6	93.8	70.4	34.4	53.5	38.6	57.7	41.1	19.3	214.0	85.0	119.4	83.71	98
166	34.5	58.1	36.1	56.1	106.7	33.0	21.0	34.8	167.0	85.7	111.8	78.1	26.7	46.3	52.7	72.3	42.0	21.0	181.2	82.4	77.4	58.37	103
167	34.2	55.2	38.6	66.0	102.3	30.4	16.3	32.9	160.2	76.8	99.8	81.1	22.3	35.5	45.3	58.5	39.3	22.2	161.2	85.8	68.9	57.28	93
168	30.7	55.7	32.7	54.1	98.8	29.6	10.8	29.8	167.2	89.3	91.3	76.0	32.4	50.5	34.4	52.5	39.5	23.3	162.3	84.7	60.2	48.18	68
169	28.7	53.8	30.4	52.6	96.8	28.0	14.2	30.2	170.0	103.0	90.5	82.4	44.9	60.6	32.3	48.0	42.1	23.3	135.3	84.0	57.1	33.36	62
170	32.9	52.6	33.7	56.3	92.3	29.3	14.3	32.6	171.7	87.3	88.8	87.4	33.6	39.7	35.2	41.3	38.8	23.3	155.3	87.7	37.6	35.56	59
171	28.0	57.1	29.6	50.5	88.1	29.2	7.7	30.9	175.3	75.3	98.5	84.8	17.5	25.9	40.7	49.1	42.4	20.3	142.6	84.5	39.8	32.55	55
172	32.2	54.4	28.2	48.6	96.6	26.3	22.5	27.7	167.5	80.6	89.5	89.1	21.5	34.4	30.4	43.3	39.3	23.7	148.8	81.2	47.3	25.57	57
173	32.0	55.7	33.5	56.8	92.9	30.3	11.0	32.9	164.1	95.1	100.4	76.1	40.3	46.8	45.7	52.2	41.9	21.2	153.3	84.5	34.8	25.69	57
174	25.7	53.3	25.8	42.5	93.2	28.0	21.5	31.9	168.4	84.4	94.6	86.2	27.7	40.6	37.9	50.8	37.7	23.2	129.9	83.2	48.1	30.65	54
175	25.3	55.6	31.0	53.5	92.6	29.4	17.4	30.7	179.4	92.7	104.5	80.3	38.6	48.6	50.5	60.5	46.2	18.3	149.8	85.6	46.2	32.17	63
176	31.9	56.5	34.0	55.4	99.0	30.3	17.4	33.2	172.3	86.6	97.9	76.8	32.6	46.6	43.9	58.0	42.3	18.7	153.5	87.4	49.4	34.57	67
177	29.6	57.5	30.0	52.7	88.9	32.0	12.8	34.5	165.1	83.1	114.8	72.8	27.2	37.3	58.9	68.9	40.2	20.2	141.8	82.9	51.8	35.13	62
178	35.4	55.0	39.8	65.9	97.3	33.7	6.9	33.5	159.4	87.1	97.0	75.7	30.3	40.8	40.2	50.7	37.5	21.3	156.7	79.6	51.8	48.86	89
179	27.4	54.0	37.7	61.6	91.8	29.7	12.6	29.6	161.5	85.8	95.1	73.8	29.8	42.7	39.1	52.0	37.6	23.2	153.1	81.3	40.9	40.22	70
180	31.9	51.3	36.4	57.0	94.9	37.4	13.5	37.1	157.8	91.4	99.4	86.3	29.8	45.8	37.7	53.8	34.1	21.3	184.3	78.7	50.4	42.98	80
181	31.1	53.5	36.6	60.7	92.0	31.2	13.7	30.0	158.6	92.7	108.5	80.8	31.3	40.3	47.2	56.2	38.5	21.6	159.4	84.9	38.5	48.10	88
182	25.6	52.3	33.8	58.3	86.8	32.3	17.8	28.6	173.0	84.6	97.2	78.9	24.6	32.8	37.3	45.5	38.8	22.0	152.0	84.6	55.5	37.12	71

Reproduced with permission of the copyright owner. Further reproduction prohibited without permission.

	62	63	64	65	66	67	68	69	70	71	72	73	74	75	76	77	78	79	80	81	82	83	84
	APTE MP	LEV ADV	TEM PMM	CFOR CE	RMM EFF	APF MAG	SLOP FM	APO CND	CBFL EX	ENL WCP	ENL WOB	ENL OBO	SLPC PF	SLPC PO	SLPO BF	SLPO BO	MCF LGT	ACFL GT	FMA GSZ	CEPH ID	CANI NE	DSKW GT	BRN SIZ
183	30.5	55.5	33.8	57.1	97.8	31.1	14.3	33.0	164.5	82.1	91.8	71.6	20.2	34.3	29.9	43.9	40.3	19.6	184.2	89.0	37.5	45.43	78
184	32.0	49.9	34.0	58.3	98.9	29.9	21.8	30.7	166.9	82.5	88.7	73.8	20.0	34.9	26.2	41.1	34.7	24.6	147.4	83.2	38.3	47.20	74
185	31.4	56.1	34.9	59.4	98.3	31.5	8.2	29.8	162.6	88.2	99.7	89.0	28.3	41.5	39.8	53.1	39.0	22.8	106.0	81.7	51.4	44.11	63
186	32.1	52.1	34.7	55.0	98.1	32.1	17.3	30.2	166.9	82.2	98.4	77.1	20.2	38.0	36.4	54.2	39.2	23.0	184.9	83.0	52.6	49.90	81
187	32.7	53.9	36.6	56.4	95.1	28.6	14.5	29.2	165.2	89.3	100.1	75.9	33.9	45.1	44.7	55.8	37.5	22.2	179.4	86.5	45.3	41.76	73
188	31.9	55.8	50.9	82.7	108.7	30.4	23.5	28.4	161.9	84.1	90.1	89.2	29.1	49.4	35.2	55.5	44.1	18.3	384.0	86.1	275.5	184.37	187
189	30.6	53.7	48.4	70.8	109.8	33.7	15.8	32.2	158.1	84.1	94.5	77.7	27.0	48.6	37.5	59.0	37.7	22.1	313.6	80.1	140.3	135.82	175
190	22.1	56.2	47.3	79.4	101.1	31.8	20.2	30.1	154.5	78.1	89.6	84.5	18.8	40.9	30.3	52.4	41.9	20.5	385.9	84.8	129.1	150.31	199
191	28.8	57.5	50.8	76.3	102.1	28.6	16.0	27.9	166.4	92.2	83.9	88.2	36.9	58.0	28.6	49.6	42.3	20.1	353.7	85.8	204.4	176.94	169
192	19.1	52.3	47.2	75.8	91.3	28.3	16.2	26.1	152.0	72.0	73.2	75.5	25.1	36.1	26.3	37.3	39.2	22.9	254.4	90.4	119.6	107.10	120
193	26.2	52.8	50.8	81.3	109.2	32.3	17.2	30.9	149.6	81.5	82.0	87.3	24.8	50.3	25.4	50.9	39.0	21.3	281.5	89.7	201.4	142.13	161
194	23.8	53.8	45.8	73.5	100.1	27.4	17.7	26.0	159.6	88.7	98.9	88.2	31.6	53.1	41.8	63.4	41.3	21.4	332.1	84.5	193.0	163.64	158
195	38.1	58.8	44.1	70.3	99.2	27.2	24.1	26.5	168.1	81.0	90.0	87.3	24.5	36.3	33.5	45.3	42.1	21.9	197.7	87.7	62.1	59.43	90
196	27.4	58.3	44.2	72.7	95.4	24.8	22.0	25.7	170.8	79.9	93.5	85.1	23.6	35.8	37.1	49.3	42.3	23.6	235.3	81.5	59.7	62.81	90
197	33.5	59.2	37.1	57.6	95.0	28.9	14.7	28.3	173.2	82.8	87.8	87.4	25.8	34.8	30.7	39.7	36.4	22.5	233.5	81.0	69.5	52.70	94
198	32.5	58.0	39.0	60.4	95.2	28.0	17.4	30.5	170.1	88.9	85.0	78.7	33.5	41.6	29.6	37.7	37.8	22.5	237.2	81.1	77.4	50.49	97
199	33.5	56.4	37.4	58.4	102.8	30.4	22.8	29.6	166.6	96.1	95.1	78.2	39.1	53.8	38.0	52.7	37.1	22.0	285.6	81.7	65.9	57.66	90
200	37.7	56.6	36.0	53.6	99.6	27.2	22.4	26.5	167.6	88.4	89.8	81.5	31.3	44.6	32.7	45.9	39.2	21.7	225.3	85.9	52.7	51.50	88
201	32.0	56.0	40.1	65.1	95.2	25.9	17.3	25.7	165.9	93.2	92.7	80.8	32.7	45.6	32.2	45.1	42.4	21.0	227.4	81.4	64.8	58.75	104
202	31.1	60.5	42.3	68.2	98.1	29.0	25.7	28.8	174.1	89.8	90.8	80.2	36.5	47.6	37.5	48.6	41.6	20.6	228.9	83.8	54.6	66.76	101
203	26.9	57.9	39.8	68.8	90.1	29.4	21.4	28.2	167.2	92.5	94.4	80.0	40.4	45.2	42.3	47.1	36.2	20.8	249.0	84.2	52.8	60.66	93
204	28.2	57.3	38.7	63.2	101.5	30.0	17.6	28.9	176.6	88.7	86.7	88.5	32.7	42.3	30.7	40.3	39.3	20.6	237.5	84.4	56.4	45.26	92
205	32.4	57.6	39.9	62.6	96.0	19.2	28.8	16.0	175.9	93.2	98.7	87.5	40.3	48.9	45.9	54.5	39.8	27.0	133.6	89.6	188.8	54.15	62
206	30.1	55.4	40.7	67.3	89.0	15.3	29.9	10.5	178.6	94.9	91.5	59.5	43.9	46.4	40.5	43.0	43.8	27.2	183.2	93.3	243.6	58.84	77
207	28.4	60.1	42.5	73.1	92.9	13.5	39.5	8.5	179.3	83.0	89.9	71.0	33.8	35.4	40.7	42.3	42.5	27.1	175.5	84.3	286.2	55.95	80
208	32.8	58.2	41.2	65.2	93.5	17.9	38.5	14.7	174.8	86.0	97.3	73.2	34.9	39.1	46.3	50.4	43.8	25.4	190.7	85.9	226.7	55.27	72
209	27.5	58.2	42.3	71.2	93.5	18.1	29.3	15.4	178.6	95.9	100.4	58.1	46.9	49.3	51.4	53.7	43.0	26.6	157.8	93.4	213.8	56.12	69
210	38.7	55.0	38.1	57.6	100.4	16.3	27.5	14.3	175.4	95.5	96.8	59.8	43.1	50.8	44.4	52.2	40.9	28.0	213.3	86.3	162.5	53.64	83
211	30.4	56.7	36.6	57.1	92.8	16.3	23.4	14.1	169.5	76.5	86.3	47.3	24.8	27.3	34.5	37.0	41.6	28.2	176.1	88.7	188.8	51.63	71
212	31.7	54.8	37.0	61.4	104.1	20.9	27.8	17.9	169.1	81.0	97.5	87.5	27.2	41.2	43.7	57.6	38.4	25.6	178.6	90.1	222.1	53.00	67
213	30.0	58.8	40.5	67.1	94.7	21.2	28.3	19.0	177.2	94.4	87.1	56.7	41.8	46.9	34.6	39.6	40.7	26.6	175.2	84.8	189.9	59.28	79
214	36.8	59.7	45.9	70.4	93.1	17.1	24.1	14.1	170.2	93.0	102.2	63.8	40.0	45.7	49.1	54.8	42.9	27.3	198.2	86.2	188.0	58.86	88
215	33.3	57.1	38.0	60.5	98.4	30.1	19.5	28.4	158.0	100.3	100.5	75.6	44.7	55.5	44.9	55.7	37.3	24.9	188.0	84.4	78.6	38.08	78
216	38.0	55.2	41.9	68.7	97.1	29.3	14.5	32.1	166.3	90.9	100.3	89.4	35.8	41.8	45.2	51.2	39.3	23.2	202.2	87.2	63.7	47.50	77
217	32.8	55.3	39.2	64.8	91.8	28.9	19.8	27.2	161.6	89.7	99.0	85.6	31.1	40.2	40.5	49.5	38.8	24.8	212.6	84.3	50.6	43.23	74
218	32.4	55.0	36.7	59.5	96.6	24.0	21.4	24.3	170.8	89.1	100.7	80.0	34.3	43.1	45.9	54.7	39.0	27.8	168.0	90.2	93.6	34.38	63

Reproduced with permission of the copyright owner. Further reproduction prohibited without permission.

	62	63	64	65	66	67	68	69	70	71	72	73	74	75	76	77	78	79	80	81	82	83	84
	APTE MP	LEV ADV	TEM PMM	CFOR CE	RMM EFF	APF MAG	SLOP FM	APO CND	CBFL EX	ENL WCP	ENL WOB	ENL OBO	SLPC PF	SLPC PO	SLPO BF	SLPO BO	MCF LGT	ACFL GT	FMA GSZ	CEPH ID	CANI NE	DSK WGT	BRNS IZ
219	40.5	52.4	38.5	62.9	98.8	26.6	17.4	25.9	164.7	96.7	89.5	60.0	37.6	46.8	30.4	39.6	38.6	26.6	187.7	90.8	70.8	46.47	83
220	36.6	53.4	42.3	70.6	95.1	27.8	17.0	28.1	168.0	89.9	94.8	75.5	38.3	41.5	43.2	46.4	42.2	21.6	205.9	80.1	74.3	46.71	83
221	43.6	55.1	43.2	68.4	98.4	19.4	16.5	19.4	168.1	78.5	90.6	85.9	22.5	27.4	34.6	39.6	41.8	29.8	173.4	87.8	89.6	50.21	65
222	34.8	57.2	39.0	61.6	93.0	19.9	22.3	20.5	163.8	81.8	105.7	67.6	28.8	33.1	52.7	57.0	45.2	25.9	191.3	91.5	86.0	46.18	68
223	33.9	56.0	45.0	75.5	95.5	24.7	23.3	26.3	156.7	88.5	95.3	89.4	36.4	39.8	43.2	46.6	41.5	25.6	210.8	86.1	88.1	45.51	71
224	35.5	56.1	41.6	69.9	97.1	26.2	20.6	23.3	158.8	88.0	91.3	63.6	29.2	39.8	32.4	43.1	39.0	25.1	203.7	85.1	84.2	53.39	87
225	45.2	56.9	40.2	62.4	103.3	25.6	19.6	24.6	162.9	86.9	117.3	87.3	26.6	41.7	57.0	72.1	38.4	23.3	206.9	85.0	100.6	42.02	80
226	33.6	56.6	41.1	66.1	94.8	27.2	20.1	27.4	159.9	83.8	102.2	81.4	24.1	33.0	42.5	51.4	38.7	23.2	222.4	82.4	53.1	42.05	85
227	34.7	53.9	39.8	65.9	101.1	22.8	19.8	22.2	161.1	89.2	103.6	76.6	29.2	43.6	43.6	58.0	39.2	23.6	204.7	85.3	81.2	47.82	80
228	33.5	56.3	39.3	64.1	105.8	25.3	21.2	23.4	160.1	88.7	113.4	76.1	24.2	41.2	48.8	65.9	35.9	24.0	229.8	82.0	66.9	42.92	92
229	38.4	53.2	38.1	62.5	99.9	26.1	23.8	24.2	152.9	74.0	108.5	79.6	10.7	26.3	45.2	60.8	38.0	22.0	168.3	87.4	59.6	43.24	91
230	37.0	52.5	35.4	57.3	96.4	27.2	22.7	26.3	160.6	81.3	93.2	85.2	19.0	31.8	30.9	43.7	34.9	22.0	243.9	83.7	87.2	42.92	94
231	32.9	54.3	38.3	60.8	96.4	29.0	19.2	27.5	153.2	87.5	100.9	78.1	26.9	38.3	40.3	51.6	35.3	21.7	187.5	81.5	86.5	52.45	93
232	38.7	57.1	37.2	61.5	97.9	24.7	20.2	25.9	158.1	88.2	91.2	75.9	33.4	36.3	36.5	39.4	35.2	22.8	250.4	79.5	46.1	42.53	85
233	31.7	58.2	38.1	62.0	95.5	28.8	15.3	27.2	160.5	90.3	95.8	82.7	32.4	40.3	37.9	45.8	37.4	22.8	239.3	78.5	55.7	41.62	87
234	32.8	59.7	40.3	70.3	95.9	30.7	19.9	29.8	161.0	84.5	106.1	81.5	21.1	34.3	42.7	55.9	33.0	26.4	147.0	84.2	57.3	39.88	75
235	26.2	62.1	37.8	66.7	91.9	29.9	15.2	28.7	156.5	85.0	109.1	84.7	24.3	35.1	48.4	59.2	30.9	28.3	156.7	79.5	92.3	39.40	79
236	24.9	57.0	42.2	75.4	83.1	28.2	21.1	27.5	157.8	91.2	108.6	89.7	27.9	33.6	45.4	51.0	34.4	28.1	134.1	84.5	74.3	40.76	76
237	32.3	59.9	36.6	64.0	92.6	28.6	20.1	29.5	158.6	85.3	102.4	87.5	24.3	27.2	41.5	44.3	32.0	28.3	148.7	79.6	63.2	41.53	81
238	34.4	63.3	38.3	64.0	90.4	26.9	16.1	26.1	152.8	90.8	95.9	76.6	26.7	28.7	31.8	33.8	35.6	29.7	130.3	81.7	53.3	40.07	77
239	23.4	59.7	37.7	67.4	84.2	27.7	20.8	25.6	158.4	81.9	106.5	88.2	24.6	28.3	49.2	52.9	34.2	28.6	139.6	84.4	75.1	36.44	64
240	23.5	59.2	37.1	67.6	83.5	29.3	14.2	28.4	157.5	87.9	97.6	71.7	25.8	33.2	35.5	42.8	34.4	25.9	141.0	80.5	52.7	35.04	69
241	25.3	58.7	38.9	68.9	86.3	27.0	19.0	25.8	157.0	88.3	96.7	70.9	26.2	33.5	34.6	41.9	33.4	29.6	152.5	82.5	62.8	41.43	70
242	22.7	59.0	38.1	68.1	83.9	31.5	19.0	31.6	161.1	87.2	110.3	84.8	22.6	30.5	45.8	53.7	31.9	27.0	159.5	80.2	62.9	37.56	77
243	39.1	59.2	37.2	61.8	92.0	30.2	9.9	29.5	155.5	89.9	97.0	75.8	24.1	32.2	31.2	39.3	30.2	29.4	151.7	78.0	49.7	38.05	78
244	27.4	54.9	39.0	68.0	90.1	25.9	17.1	23.2	160.8	90.1	99.4	86.3	31.5	32.2	40.8	41.5	39.3	28.7	180.1	88.6	49.9	37.71	85
245	33.4	53.7	33.9	54.0	92.4	21.9	19.6	21.2	163.5	79.7	97.6	82.8	22.8	29.3	40.7	47.2	38.3	29.1	137.9	87.7	82.4	38.94	57
246	26.5	53.8	37.1	62.5	85.2	26.6	27.2	26.1	162.1	95.1	88.6	80.6	40.9	47.9	34.5	41.5	34.9	26.9	160.2	81.7	50.8	45.40	64
247	29.5	54.1	39.8	65.4	87.7	23.2	27.1	21.1	165.5	81.9	97.2	85.0	26.2	31.1	41.4	46.4	37.7	26.8	153.6	85.7	45.9	41.24	63
248	23.9	55.8	37.8	64.1	89.4	22.5	23.5	22.3	166.3	89.9	102.6	80.6	30.3	42.5	43.0	55.2	38.6	26.5	161.4	83.7	55.8	45.71	61
249	29.4	53.2	32.9	56.0	88.9	23.6	18.6	22.7	163.7	89.6	95.2	76.0	28.6	33.3	34.2	38.9	37.7	27.5	162.0	86.4	52.0	33.30	65
250	27.3	53.4	37.4	61.8	87.8	23.4	31.0	23.6	164.2	87.0	98.1	74.7	30.7	36.2	41.8	47.3	35.8	27.6	211.1	87.5	73.1	40.62	64
251	28.3	54.6	36.3	61.1	87.3	26.1	19.3	27.6	174.3	85.3	95.1	85.3	29.4	34.2	39.1	44.0	36.8	23.5	210.2	82.0	49.1	32.42	58
252	31.5	53.1	37.8	59.2	91.3	22.8	19.6	22.3	167.0	94.5	99.4	88.0	39.5	47.1	44.3	52.0	38.4	26.5	156.4	82.1	75.6	38.18	59
253	30.0	60.3	37.7	63.7	88.9	23.5	18.3	24.8	168.0	86.8	109.5	86.3	32.2	35.0	54.8	57.6	38.8	23.2	219.0	87.6	112.1	51.07	74
254	35.5	56.5	37.5	62.7	94.5	23.9	16.7	24.6	168.0	85.4	115.2	89.9	33.7	32.9	63.5	62.7	39.6	23.5	200.9	87.4	94.6	53.35	65

Reproduced with permission of the copyright owner. Further reproduction prohibited without permission.

	62	63	64	65	66	67	68	69	70	71	72	73	74	75	76	77	78	79	80	81	82	83	84
	APTE MP	LEV ADV	TEM PMM	CFOR CE	RMM EFF	APF MAG	SLOP FM	APO CND	CBFL EX	ENL WCP	ENL WOB	ENL OBO	SLPC PF	SLPC PO	SLPO BF	SLPO BO	MCF LGT	ACFL GT	FMA GSZ	CEPH ID	CANI NE	DSK WGT	BRNS IZ
255	22.4	62.3	34.9	65.5	72.9	25.0	26.6	23.8	166.3	89.7	91.9	78.0	35.5	34.7	37.6	36.9	29.8	27.4	188.4	85.8	155.8	55.29	113
256	31.4	60.9	32.8	56.9	73.9	24.9	21.7	24.3	165.3	92.2	95.4	85.6	37.4	36.4	40.6	39.6	27.9	27.3	223.5	79.3	113.4	33.58	98
257	24.2	63.2	33.4	59.7	68.1	25.6	18.7	25.9	162.3	86.0	88.6	69.1	32.2	31.0	34.8	33.6	26.6	27.2	249.6	84.1	152.5	45.26	119
258	26.4	53.9	50.1	87.9	76.5	18.5	36.9	17.5	169.4	88.3	81.4	65.1	36.7	37.7	29.9	30.9	32.2	29.2	235.3	80.7	188.2	80.82	130
259	30.6	55.7	48.8	83.0	76.5	16.7	33.8	13.8	179.4	90.6	106.2	87.6	37.5	39.1	53.0	54.6	36.1	27.2	263.4	83.0	235.3	72.66	138
260	25.7	57.5	46.8	82.4	74.4	18.2	41.2	15.4	175.3	90.5	96.7	60.7	41.9	43.8	48.1	50.0	31.4	30.2	269.4	84.8	252.3	80.09	144
261	28.3	56.1	43.3	75.2	73.1	19.3	32.6	15.8	176.1	80.4	95.9	64.2	25.2	26.4	40.6	41.8	32.3	28.2	216.6	81.1	276.9	83.87	140
262	25.4	56.1	48.7	81.6	74.1	20.4	29.9	17.0	174.9	93.6	105.1	76.5	44.1	46.9	55.6	58.5	31.8	29.6	263.0	79.0	253.6	72.53	125
263	28.3	56.1	43.3	75.2	73.1	19.3	32.6	15.8	176.1	80.4	95.9	64.2	25.2	26.4	40.6	41.8	32.3	28.2	216.6	81.1	276.9	73.04	118
264	26.1	57.1	49.8	92.6	85.1	18.6	29.2	17.5	176.2	82.6	98.2	66.5	30.4	34.9	46.0	50.5	32.1	26.5	260.0	83.6	168.5	77.45	142
265	24.7	53.9	40.7	71.2	78.5	17.4	38.2	17.0	177.6	88.7	92.0	66.2	30.3	38.6	33.6	42.0	35.7	25.7	267.2	92.0	264.8	75.00	135
266	29.0	58.5	42.5	76.2	87.7	20.8	30.3	19.6	168.3	89.0	104.8	77.6	35.0	40.8	50.8	56.6	32.9	27.2	245.3	80.1	182.5	75.00	107
267	26.4	58.6	50.5	91.0	75.4	13.8	36.7	13,8	179.6	86.2	86.7	74.9	28.3	33.0	28.8	33.5	34.7	30.8	232.9	85.9	249.3	66.84	126
268	38.7	60.4	64.9	109.6	95.6	24.6	32.2	19.0	171.0	94.9	124.6	84.3	51.6	46.1	81.4	75.8	32.8	22.7	801.7	94.4	495.5	337.20	320
269	38.4	61.4	70.7	124.1	99.9	28.1	27.9	23.1	167.4	85.2	84.5	82.4	31.3	36.5	30.6	35.8	31.9	22.5	809.2	87.9	589.0	341.00	478
270	39.2	60.1	63.9	109.3	104.5	22.6	27.8	27.7	179.2	87.4	86.5	81.3	40.8	48.5	39.9	47.6	33.7	18.5	685.1	91.1	372.1	333.26	352
271	27.0	54.4	75.3	125.6	84.2	23.5	31.3	20.4	158.1	87.3	82.0	79.8	37.8	39.2	32.5	33.9	30.2	22.6	735.8	90.6	434.1	516.39	433
272	33.9	48.6	75.5	122.8	87.1	27.8	18.6	26.3	173.3	86.8	77.0	79.1	33.4	35.7	23.6	25.9	30.5	24.2	512.7	87.5	723.5	450.42	400
273	25.4	51.5	67.1	113.5	84.4	23.6	22.1	22.8	172.1	95.5	64.4	73.0	42.3	40.9	11.3	9.9	31.8	26.1	630.5	92.0	573.7	490.73	447
274	21.7	49.2	58.8	101.3	86.5	21.6	26.5	20.2	168.4	88.2	97.4	69.1	38.6	37.1	47.8	46.3	37.6	20.8	651.4	87.8	559.1	444.50	362
275	32.4	55.3	80.6	134.7	85.8	18.7	26.4	18.0	167.2	83.7	88.1	90.0	34.3	32.9	38.7	37.3	36.9	22.6	931.5	83.0	531.4	472.13	442
276	32.3	51.3	76.0	123.7	86.2	24.4	32.1	23.7	178.7	84.6	104.3	81.3	32.6	31.3	52.3	51.0	33.9	20.4	956.3	92.8	365.0	672.22	494
277	35.1	55.8	74.2	120.6	86.0	20.6	22.9	20.0	168.7	93.2	91.0	84.1	37.9	39.6	35.7	37.4	36.4	21.1	638.2	87.7	481.5	376.24	384
278	35.1	51.0	82.8	137.2	82.7	21.0	24.7	18.8	175.0	86.2	86.0	73.8	38.9	31.6	38.7	31.5	28.8	27.3	625.1	84.5	574.8	469.08	405
279	29.1	48.8	75.4	123.1	86.7	21.0	26.8	19.5	160.9	98.5	89.8	89.3	46.6	45.7	37.8	36.9	31.8	26.7	800.8	90.0	441.5	525.86	435
280	43.3	53.4	51.6	85.4	82.1	46.6	14.4	51.9	128.5	102.4	116.0	67.7	20.6	21.3	34.2	34.8	24.3	21.8	718.0	73.0	55.7	702.42	1264
281	37.6	59.5	56.4	94.6	89.3	43.9	7.9	47.7	143.0	84.1	87.0	46.7	10.8	18.6	13.7	21.5	26.0	19.6	808.9	79.0	105.7	400.35	1075
282	37.8	56.3	56.3	94.9	85.4	37.7	7.2	41.9	142.8	94.5	101.0	85.7	13.9	22.0	20.4	28.5	23.5	27.0	719.1	76.3	100.1	480.58	1223
283	43.2	58.3	51.3	85.4	94.6	43.1	7.1	45.6	134.6	96.9	104.9	82.5	13.6	28.0	21.6	35.9	25.3	21.8	649.2	81.1	87.9	530.42	1247
284	37.2	57.8	53.6	84.7	87.6	44.7	9.4	48.2	128.8	89.5	107.2	63.2	4.5	18.3	22.2	36.0	25.4	20.9	766.2	75.3	84.8	510.49	1168
285	39.3	58.0	57.2	96.7	81.4	42.0	3.6	45.2	136.1	95.2	118.0	57.2	12.8	17.9	35.6	40.7	26.0	22.6	805.1	74.5	87.7	560.25	1169
286	34.4	56.0	58.3	97.1	86.5	44.7	0.8	50.7	131.7	92.5	98.7	93.0	11.8	16.6	18.0	22.8	22.8	21.6	832.1	76.7	122.4	757.97	1400
287	40.4	59.0	48.8	79.0	92.6	48.2	5.1	53.4	129.8	87.4	97.3	62.7	4.5	19.5	14.4	29.4	22.4	19.7	899.1	74.1	123.0	657.70	1547
288	35.0	58.0	58.5	97.2	89.8	43.3	3.2	48.9	130.3	93.1	97.9	81.2	16.0	25.7	20.8	30.6	24.5	19.4	819.0	82.7	71.4	630.64	1260
289	35.5	56.7	53.1	88.9	94.5	45.0	6.2	51.0	124.4	92.9	92.0	90.0	15.4	30.8	14.6	29.9	22.8	24.2	926.5	78.3	143.7	517.83	1243

Reproduced with permission of the copyright owner. Further reproduction prohibited without permission.

	62	63	64	65	66	67	68	69	70	71	72	73	74	75	76	77	78	79	80	81	82	83	84
	APTE MP	LEV ADV	TEM PMM	CFOR CE	RMM EFF	APF MAG	SLOP FM	APO CND	CBFL EX	ENL WCP	ENL WOB	ENL OBO	SLPC PF	SLPC PO	SLPO BF	SLPO BO	MCF LGT	ACFL GT	FMA GSZ	CEPH ID	CANI NE	DSK WGT	BRNS IZ
290	32.7	60.0	47.9	79.8	103.2	29.9	6.1	30.9	139.0	86.6	98.5	72.1	25.3	41.8	37.2	53.7	30.5	21.3	392.7	89.1	199.8	190.55	291
291	30.5	63.3	60.2	98.1	92.2	28.9	20.4	28.4	151.3	89.5	83.4	60.6	33.0	43.8	26.9	37.7	30.8	22.3	540.6	86.1	329.9	325.51	390
292	25.9	59.9	54.8	91.6	84.2	31.9	17.2	29.3	153.0	86.6	85.0	84.5	32.3	34.4	30.7	32.8	35.9	19.3	393.3	91.3	315.8	302.92	343
293	31.5	63.5	62.2	101.4	94.2	28.5	14.6	28.4	155.1	88.5	92.2	82.7	36.8	46.9	40.5	50.6	32.4	22.9	683.9	88.1	462.2	364.95	410
294	28.1	59.0	64.1	109.7	94.2	21.7	27.6	18.1	162.4	82.4	77.0	86.1	31.6	36.2	26.3	30.8	33.5	23.5	564.8	92.7	331.8	296.13	345
295	32.3	60.8	61.0	101.5	83.4	23.8	24.3	22.4	170.0	94.1	94.8	42.2	33.9	39.9	34.6	40.7	34.7	23.7	449.9	92.3	338.4	340.08	358
296	29.6	60.8	67.9	114.3	86.0	28.1	22.8	27.7	165.9	90.7	86.4	77.9	33.4	37.7	29.1	33.4	32.9	24.3	556.7	85.9	428.4	365.70	436
297	35.1	59.1	68.3	114.1	90.2	18.5	22.8	16.3	150.0	84.1	88.7	75.0	28.4	31.7	32.9	36.3	30.4	27.2	652.6	90.4	576.0	353.65	397
298	31.7	57.9	60.4	98.1	87.3	26.7	15.2	26.7	161.3	89.9	74.8	74.8	31.5	39.6	16.3	24.5	31.9	23.4	507.5	86.8	521.4	319.22	360
299	34.0	60.0	61.3	97.3	88.7	26.0	14.1	27.6	156.3	85.1	82.8	80.5	32.9	35.6	30.6	33.4	32.3	21.7	553.0	94.5	312.5	297.96	387
300	39.4	63.5	60.8	96.5	98.0	22.5	17.3	22.0	159.6	93.9	97.9	64.5	35.1	51.2	39.1	55.2	34.6	22.4	613.8	93.8	329.5	232.09	365

Reproduced with permission of the copyright owner. Further reproduction prohibited without permission.

Appendix F. Deviations after GLS super-imposition of the three landmarks common to endocranial-radiographic and ectocranial configurations (in mm).

Genus	Species	AMNH #	Prosthion	Bregma	Lambda
Alouatta	*palliata*	128109	0.003	0.040	0.037
Alouatta	*palliata*	141852	0.012	0.019	0.007
Alouatta	*palliata*	17230	0.008	0.017	0.026
Alouatta	*palliata*	17231	0.007	0.002	0.009
Alouatta	*palliata*	17236	0.008	0.018	0.026
Alouatta	*palliata*	17250	0.000	0.005	0.005
Alouatta	*palliata*	176641	0.007	0.080	0.072
Alouatta	*palliata*	18935	0.076	0.023	0.053
Alouatta	*palliata*	62828	0.007	0.041	0.034
Alouatta	*palliata*	66707	0.003	0.072	0.069
Ateles	*geoffroyi*	123280	0.020	0.027	0.007
Ateles	*geoffroyi*	139829	0.012	0.074	0.086
Ateles	*geoffroyi*	141980	0.009	0.030	0.040
Ateles	*geoffroyi*	141981	0.043	0.008	0.052
Ateles	*geoffroyi*	176644	0.027	0.001	0.027
Ateles	*geoffroyi*	176646	0.008	0.054	0.062
Ateles	*geoffroyi*	176647	0.035	0.041	0.077
Ateles	*geoffroyi*	24172	0.005	0.027	0.022
Ateles	*geoffroyi*	24173	0.018	0.065	0.082
Ateles	*geoffroyi*	24176	0.010	0.050	0.040
Lagothrix	*lagothrica*	67697	0.009	0.051	0.042
Lagothrix	*lagothrica*	71768	0.013	0.025	0.038
Lagothrix	*lagothrica*	71776	0.007	0.002	0.005
Lagothrix	*lagothrica*	71779	0.031	0.145	0.176
Lagothrix	*lagothrica*	73555	0.003	0.076	0.079
Lagothrix	*lagothrica*	73556	0.001	0.016	0.017
Lagothrix	*lagothrica*	75291	0.015	0.008	0.007
Lagothrix	*lagothrica*	76393	0.011	0.103	0.114
Lagothrix	*lagothrica*	76395	0.010	0.007	0.018
Lagothrix	*lagothrica*	76396	0.005	0.094	0.098
Brachyteles	*arachnoides*	80405	0.009	0.018	0.028
Chiropotes	*satanas*	94118	0.023	0.097	0.120
Chiropotes	*satanas*	94120	0.018	0.077	0.095
Chiropotes	*satanas*	94122	0.067	0.044	0.111
Chiropotes	*satanas*	94125	0.019	0.094	0.113
Chiropotes	*satanas*	94129	0.054	0.021	0.075
Chiropotes	*satanas*	94130	0.071	0.047	0.117
Chiropotes	*satanas*	95867	0.020	0.048	0.069
Chiropotes	*satanas*	96339	0.015	0.020	0.035
Chiropotes	*satanas*	96340	0.001	0.062	0.063
Chiropotes	*satanas*	96344	0.040	0.020	0.059
Pithecia	*pithecia*	36321	0.008	0.016	0.025
Pithecia	*pithecia*	36322	0.004	0.113	0.118
Pithecia	*pithecia*	42417	0.009	0.001	0.010
Pithecia	*pithecia*	42743	0.024	0.011	0.035
Pithecia	*pithecia*	48123	0.016	0.030	0.015
Pithecia	*pithecia*	48400	0.013	0.001	0.012
Pithecia	*pithecia*	79383	0.016	0.012	0.028
Pithecia	*pithecia*	79384	0.006	0.086	0.080
Pithecia	*pithecia*	94132	0.006	0.086	0.080
Pithecia	*pithecia*	94133	0.002	0.099	0.098
Pithecia	*monachus*	230798	0.009	0.029	0.020
Pithecia	*monachus*	239854	0.001	0.017	0.018
Pithecia	*monachus*	77822	0.007	0.074	0.080
Pithecia	*monachus*	98399	0.011	0.050	0.038
Callicebus	*cupreus*	174286	0.013	0.037	0.024
Callicebus	*cupreus*	72141	0.036	0.056	0.020
Callicebus	*cupreus*	75994	0.018	0.039	0.057
Callicebus	*cupreus*	76419	0.003	0.001	0.004
Callicebus	*cupreus*	76422	0.017	0.043	0.060
Callicebus	*cupreus*	98320	0.006	0.053	0.046
Callicebus	*cupreus*	98370	0.020	0.057	0.037
Callicebus	*cupreus*	98381	0.005	0.058	0.052
Callicebus	*cupreus*	98385	0.014	0.111	0.098
Callicebus	*cupreus*	98389	0.007	0.024	0.017
Cebus	*apella*	133593	0.014	0.034	0.020
Cebus	*apella*	133626	0.001	0.040	0.041
Cebus	*apella*	133631	0.017	0.025	0.009
Cebus	*apella*	133635	0.003	0.009	0.005
Cebus	*apella*	133736	0.009	0.031	0.040
Cebus	*apella*	133864	0.008	0.002	0.005
Cebus	*apella*	136375	0.011	0.051	0.062
Cebus	*apella*	136383	0.015	0.017	0.002
Cebus	*apella*	136384	0.006	0.036	0.041
Cebus	*apella*	136386	0.027	0.089	0.062
Cebus	*capucinus*	128119	0.018	0.104	0.122
Cebus	*capucinus*	128120	0.009	0.084	0.093
Cebus	*capucinus*	128145	0.010	0.027	0.017
Cebus	*capucinus*	137993	0.026	0.094	0.121
Cebus	*capucinus*	176630	0.000	0.079	0.079
Cebus	*capucinus*	19220	0.008	0.045	0.036
Cebus	*capucinus*	24429	0.002	0.002	0.000
Cebus	*capucinus*	28493	0.016	0.038	0.022
Cebus	*capucinus*	29610	0.000	0.075	0.076
Cebus	*capucinus*	29620	0.002	0.054	0.056
Saimiri	*sciureus*	26992	0.016	0.016	0.001
Saimiri	*sciureus*	26997	0.024	0.029	0.005
Saimiri	*sciureus*	27002	0.023	0.050	0.027

Reproduced with permission of the copyright owner. Further reproduction prohibited without permission.

Genus	Species	AMNH #	Prosthion	Bregma	Lambda
Saimiri	*sciureus*	37468	0.006	0.028	0.023
Saimiri	*sciureus*	64096	0.040	0.012	0.051
Saimiri	*sciureus*	76871	0.015	0.014	0.000
Saimiri	*sciureus*	80442	0.016	0.019	0.003
Saimiri	*sciureus*	80443	0.003	0.053	0.050
Saimiri	*sciureus*	94205	0.047	0.051	0.098
Saimiri	*sciureus*	94210	0.007	0.041	0.047
Aotus	*trivirgatus*	187963	0.007	0.018	0.011
Aotus	*trivirgatus*	76915	0.010	0.076	0.066
Aotus	*trivirgatus*	76919	0.018	0.031	0.049
Aotus	*trivirgatus*	78587	0.008	0.019	0.027
Aotus	*trivirgatus*	93078	0.039	0.008	0.031
Aotus	*trivirgatus*	67692	0.013	0.033	0.046
Aotus	*trivirgatus*	72058	0.018	0.022	0.004
Aotus	*trivirgatus*	72061	0.013	0.047	0.034
Aotus	*trivirgatus*	72063	0.041	0.045	0.004
Aotus	*trivirgatus*	73417	0.020	0.023	0.043
Saguinus	*oedipus*	32702	0.029	0.101	0.072
Callithrix	*pygmaea*	239606	0.076	0.084	0.007
Callithrix	*pygmaea*	44365	0.033	0.077	0.109
Callithrix	*pygmaea*	72036	0.020	0.027	0.007
Callithrix	*pygmaea*	72037	0.049	0.035	0.014
Callithrix	*pygmaea*	73751	0.075	0.071	0.004
Callithrix	*pygmaea*	74056	0.031	0.006	0.037
Callithrix	*pygmaea*	74362	0.022	0.062	0.040
Callithrix	*pygmaea*	74365	0.063	0.079	0.015
Callithrix	*pygmaea*	74369	0.030	0.086	0.056
Callithrix	*pygmaea*	76328	0.028	0.107	0.080
Callimico	*geoldii*	183290	0.074	0.026	0.100
Chlorocebus	*aethiops*	116268	0.029	0.048	0.019
Chlorocebus	*aethiops*	161104	0.041	0.025	0.016
Chlorocebus	*aethiops*	161107	0.022	0.162	0.140
Chlorocebus	*aethiops*	27706	0.043	0.152	0.108
Chlorocebus	*aethiops*	34716	0.016	0.018	0.034
Chlorocebus	*aethiops*	52475	0.014	0.058	0.044
Chlorocebus	*aethiops*	52479	0.013	0.023	0.036
Chlorocebus	*aethiops*	54231	0.018	0.003	0.022
Chlorocebus	*aethiops*	80789	0.010	0.084	0.093
Chlorocebus	*aethiops*	83924	0.031	0.047	0.016
Cercopithecus	*neglectus*	52414	0.038	0.044	0.007
Cercopithecus	*neglectus*	52416	0.004	0.013	0.017
Cercopithecus	*neglectus*	52424	0.002	0.077	0.079
Cercopithecus	*neglectus*	52425	0.001	0.036	0.037
Cercopithecus	*neglectus*	52428	0.009	0.054	0.045
Cercopithecus	*neglectus*	52441	0.016	0.122	0.105
Cercopithecus	*neglectus*	55008	0.016	0.051	0.035
Cercopithecus	*neglectus*	86854	0.001	0.069	0.070

Genus	Species	AMNH #	Prosthion	Bregma	Lambda
Cercopithecus	*neglectus*	200761	0.002	0.038	0.036
Cercopithecus	*neglectus*	189380	0.057	0.019	0.013
Cercopithecus	*mitis*	52350	0.008	0.057	0.065
Cercopithecus	*mitis*	52356	0.003	0.072	0.070
Cercopithecus	*mitis*	52357	0.019	0.047	0.028
Cercopithecus	*mitis*	52358	0.008	0.055	0.047
Cercopithecus	*mitis*	52363	0.030	0.011	0.019
Cercopithecus	*mitis*	52366	0.023	0.093	0.116
Cercopithecus	*mitis*	52372	0.010	0.030	0.039
Cercopithecus	*mitis*	52377	0.027	0.016	0.043
Cercopithecus	*mitis*	52382	0.019	0.014	0.005
Cercopithecus	*mitis*	52406	0.010	0.042	0.032
Cercopithecus	*ascanius*	51020	0.001	0.015	0.014
Cercopithecus	*ascanius*	52531	0.005	0.027	0.022
Cercopithecus	*ascanius*	52551	0.008	0.073	0.065
Cercopithecus	*ascanius*	52557	0.006	0.025	0.031
Cercopithecus	*ascanius*	52566	0.002	0.038	0.037
Cercopithecus	*ascanius*	55021	0.007	0.025	0.032
Cercopithecus	*ascanius*	55027	0.000	0.032	0.032
Cercopithecus	*ascanius*	55030	0.007	0.000	0.007
Cercopithecus	*ascanius*	55033	0.018	0.048	0.066
Cercopithecus	*ascanius*	55068	0.002	0.036	0.034
Macaca	*nemestrina*	102202	0.018	0.072	0.054
Macaca	*nemestrina*	103398	0.040	0.169	0.129
Macaca	*nemestrina*	103399	0.007	0.014	0.021
Macaca	*nemestrina*	103728	0.017	0.059	0.042
Macaca	*nemestrina*	106050	0.017	0.042	0.025
Macaca	*nemestrina*	106559	0.008	0.009	0.001
Macaca	*nemestrina*	106562	0.023	0.014	0.009
Macaca	*nemestrina*	11091	0.017	0.087	0.070
Macaca	*nemestrina*	57111	0.008	0.002	0.006
Macaca	*nemestrina*	83434	0.035	0.049	0.014
Macaca	*fascicularis*	102764	0.059	0.030	0.029
Macaca	*fascicularis*	103652	0.003	0.116	0.113
Macaca	*fascicularis*	103654	0.036	0.072	0.037
Macaca	*fascicularis*	103655	0.006	0.022	0.028
Macaca	*fascicularis*	103657	0.004	0.000	0.004
Macaca	*fascicularis*	103660	0.014	0.003	0.011
Macaca	*fascicularis*	103663	0.013	0.047	0.034
Macaca	*fascicularis*	107094	0.021	0.008	0.012
Macaca	*fascicularis*	107095	0.009	0.010	0.001
Macaca	*fascicularis*	107096	0.024	0.103	0.079
Macaca	*mulatta*	112732	0.030	0.056	0.026
Macaca	*mulatta*	112740	0.003	0.017	0.014
Macaca	*mulatta*	112971	0.033	0.134	0.167
Macaca	*mulatta*	112972	0.026	0.047	0.021
Macaca	*mulatta*	163612	0.014	0.049	0.035

Reproduced with permission of the copyright owner. Further reproduction prohibited without permission.

Genus	Species	AMNH #	Prosthion	Bregma	Lambda
Macaca	*mulatta*	27573	0.046	0.002	0.048
Macaca	*mulatta*	27574	0.002	0.034	0.032
Macaca	*mulatta*	54679	0.014	0.013	0.002
Macaca	*mulatta*	59987	0.018	0.002	0.021
Macaca	*mulatta*	60038	0.018	0.147	0.129
Papio	*hamadryus*	52668	0.001	0.045	0.043
Papio	*hamadryus*	89361	0.025	0.043	0.069
Papio	*hamadryus*	216250	0.004	0.003	0.001
Papio	*hamadryus*	82097	0.004	0.029	0.025
Papio	*hamadryus*	161115	0.012	0.060	0.048
Papio	*hamadryus*	52674	0.003	0.046	0.043
Papio	*hamadryus*	169141	0.002	0.027	0.029
Lophocebus	*albigena*	52581	0.029	0.009	0.020
Lophocebus	*albigena*	52589	0.001	0.011	0.010
Lophocebus	*albigena*	52600	0.019	0.073	0.054
Lophocebus	*albigena*	52606	0.031	0.002	0.033
Lophocebus	*albigena*	52607	0.010	0.033	0.043
Lophocebus	*albigena*	52613	0.014	0.013	0.002
Lophocebus	*albigena*	52620	0.058	0.005	0.063
Lophocebus	*albigena*	52621	0.060	0.075	0.015
Lophocebus	*albigena*	52624	0.039	0.010	0.049
Lophocebus	*albigena*	52625	0.043	0.150	0.108
Colobus	*polykomos*	52221	0.010	0.074	0.084
Colobus	*polykomos*	52225	0.009	0.066	0.056
Colobus	*polykomos*	52226	0.007	0.030	0.037
Colobus	*polykomos*	52228	0.015	0.135	0.120
Colobus	*polykomos*	52241	0.009	0.010	0.002
Colobus	*polykomos*	52245	0.002	0.062	0.060
Colobus	*polykomos*	52249	0.007	0.030	0.023
Colobus	*polykomos*	52213	0.004	0.060	0.056
Colobus	*polykomos*	52223	0.023	0.001	0.022
Colobus	*polykomos*	52238	0.006	0.011	0.017
Procolobus	*pennantii*	52263	0.016	0.046	0.030
Procolobus	*pennantii*	52267	0.000	0.087	0.087
Procolobus	*pennantii*	52273	0.027	0.055	0.082
Procolobus	*pennantii*	52275	0.042	0.025	0.017
Procolobus	*pennantii*	52280	0.008	0.102	0.094
Procolobus	*pennantii*	52283	0.050	0.004	0.054
Procolobus	*pennantii*	52301	0.005	0.133	0.138
Procolobus	*pennantii*	52305	0.060	0.055	0.115
Procolobus	*pennantii*	52310	0.001	0.066	0.064
Procolobus	*pennantii*	52257	0.032	0.003	0.035
Nasalis	*larvatus*	103460	0.014	0.089	0.074
Nasalis	*larvatus*	103464	0.035	0.101	0.067
Nasalis	*larvatus*	103465	0.012	0.020	0.008
Nasalis	*larvatus*	103466	0.002	0.040	0.038
Nasalis	*larvatus*	103467	0.009	0.004	0.005

Genus	Species	AMNH #	Prosthion	Bregma	Lambda
Nasalis	*larvatus*	103668	0.002	0.035	0.033
Nasalis	*larvatus*	103669	0.020	0.074	0.094
Nasalis	*larvatus*	106033	0.012	0.014	0.026
Nasalis	*larvatus*	106034	0.010	0.080	0.070
Presbytis	*melalophos*	102744	0.002	0.041	0.039
Presbytis	*melalophos*	102746	0.019	0.044	0.063
Presbytis	*melalophos*	102751	0.001	0.008	0.007
Presbytis	*melalophos*	102752	0.016	0.025	0.009
Presbytis	*melalophos*	102760	0.014	0.035	0.049
Presbytis	*melalophos*	102762	0.006	0.017	0.022
Presbytis	*melalophos*	102882	0.007	0.001	0.006
Presbytis	*melalophos*	102884	0.008	0.012	0.004
Presbytis	*melalophos*	102886	0.041	0.007	0.048
Presbytis	*melalophos*	102890	0.006	0.062	0.068
Semnopithecus	*entellus*	163082	0.019	0.012	0.030
Semnopithecus	*cristata*	102730	0.015	0.016	0.031
Semnopithecus	*cristata*	102733	0.020	0.003	0.023
Semnopithecus	*cristata*	102736	0.018	0.046	0.027
Semnopithecus	*cristata*	102743	0.002	0.047	0.049
Semnopithecus	*cristata*	106042	0.004	0.046	0.042
Semnopithecus	*cristata*	106587	0.020	0.026	0.005
Semnopithecus	*cristata*	106588	0.024	0.083	0.059
Semnopithecus	*cristata*	106674	0.018	0.060	0.042
Semnopithecus	*cristata*	107570	0.025	0.080	0.054
Semnopithecus	*cristata*	107571	0.025	0.084	0.059
Hylobates	*lar*	208985	0.012	0.021	0.009
Hylobates	*lar*	31593	0.003	0.006	0.003
Hylobates	*lar*	54659	0.001	0.075	0.076
Hylobates	*syndactylus*	102186	0.006	0.064	0.058
Hylobates	*syndactylus*	102188	0.011	0.002	0.009
Hylobates	*syndactylus*	102190	0.012	0.003	0.009
Hylobates	*syndactylus*	102195	0.008	0.001	0.007
Hylobates	*syndactylus*	102196	0.030	0.075	0.045
Hylobates	*syndactylus*	102463	0.008	0.001	0.007
Hylobates	*syndactylus*	102721	0.010	0.016	0.006
Hylobates	*syndactylus*	102727	0.002	0.125	0.127
Hylobates	*syndactylus*	106582	0.023	0.059	0.036
Hylobates	*syndactylus*	106583	0.038	0.246	0.208
Pongo	*pygmaeus*	200900	0.020	0.092	0.073
Pongo	*pygmaeus*	201811	0.006	0.060	0.053
Pongo	*pygmaeus*	200898	0.147	0.137	0.122
Gorilla	*gorilla*	1472	0.016	0.007	0.022
Gorilla	*gorilla*	167330	0.010	0.029	0.019
Gorilla	*gorilla*	167337	0.006	0.126	0.120
Gorilla	*gorilla*	167339	0.014	0.100	0.114
Gorilla	*gorilla*	167340	0.011	0.020	0.031
Gorilla	*gorilla*	214108	0.020	0.008	0.012

Reproduced with permission of the copyright owner. Further reproduction prohibited without permission.

Genus	Species	AMNH #	Prosthion	Bregma	Lambda
Gorilla	*gorilla*	54327	0.026	0.092	0.066
Gorilla	*gorilla*	54356	0.057	0.096	0.040
Gorilla	*gorilla*	81652	0.027	0.031	0.004
Homo	*sapiens*	998452	0.036	0.010	0.026
Homo	*sapiens*	2385	0.005	0.314	0.319
Homo	*sapiens*	2396	0.015	0.184	0.199
Homo	*sapiens*	2462	0.006	0.061	0.056
Homo	*sapiens*	2793	0.020	0.037	0.017
Homo	*sapiens*	3281	0.053	0.004	0.058
Homo	*sapiens*	3449	0.031	0.030	0.060
Homo	*sapiens*	4927	0.039	0.067	0.106
Homo	*sapiens*	5281	0.015	0.103	0.088
Homo	*sapiens*	642	0.075	0.142	0.217
Pan	*paniscus*	86857	0.009	0.042	0.051
Pan	*troglodytes*	167343	0.015	0.074	0.059
Pan	*troglodytes*	167345	0.021	0.061	0.040
Pan	*troglodytes*	174860	0.001	0.066	0.067
Pan	*troglodytes*	201469	0.014	0.015	0.001
Pan	*troglodytes*	89351	0.016	0.028	0.012
Pan	*troglodytes*	89354	0.008	0.020	0.012
Pan	*troglodytes*	89355	0.001	0.067	0.066
Pan	*troglodytes*	90191	0.002	0.065	0.063
Pan	*troglodytes*	90292	0.005	0.094	0.090
Pan	*troglodytes*	90293	0.002	0.035	0.035

Reproduced with permission of the copyright owner. Further reproduction prohibited without permission.

Bibliography

Adams CD; Meikle MC; Norwick KW; Turpin DL (1972) Dentofacial remodelling produced by intermaxillary forces in *Macaca mulatta*. *Archives of Oral Biology*. 17:1519-1535.

Adams LM; Moore WJ (1975) Biomechanical appraisal of some skeletal features associated with head balance and posture in the Hominoidea. *Acta Anatomica*. 92:580-594.

Ahlgren J (1966) Mechanism of mastication. *Acta Odont. Scand.* 24: Supl.44,109

Aiello L; Dean C (1990) An Intoduction to Human Evolutionary Anatomy. Academic Press: San Diego.

Alberch P (1983) Morphological variation in the neotropical salamander genus *Bolitoglossa*. *Evolution*. 37:906-919.

Alberch P (1990) Natural selection and developmental constraints: external versus internal determinants of order in nature. *Primate Life History and Evolution*. DeRousseau CJ (ed.) Wiley-Liss Inc.: New York. pp. 15-35.

Alberch P; Gale EA (1983) Size dependence during development of the amphibian foot. Colchicine-induced digital loss and reduction. *J. Embryol. Exp. Morphol.* 76:177-197.

Alberch P; Gale EA (1985) A developmental analysis of an evolutionary trend: Digital reduction in amphibians. *Evolution*. 39:8-23.

Alberch P; Gould SJ; Oster FG; Wake DB (1979) Size and shape in ontogeny and phylogeny. *Paleobiology*. 5:296-317.

Albercht GH et al. (1979)

Albrecht GH (1978) The craniofacial morphology of the Sulawesi macaques: multivariate approaches to biological problems. *Contrib. Primatol.*. 13:1-151.

Alexandridis C; Caputo AA; Thanos CE (1985) Distribution of stresses in the human skull. *J Oral Rehab*. 12(6):499-507.

Ameghino F (1909) Le *Diprothomo platensis*. *Anales del Museo nacional de Buenos Aires*. 19:107-209.

Anderson JC; Gerbing DW (1988) Structural equation modeling in practice: a review and recommended two-step approach. *Psychological Bulletin*. 103:411-423.

Andrews P; Martin L (1987) Cladistic relationships of extant and fossil hominoids. *Journal of Human Evolution*. 16:101-118.

Andrews P; Martin L (1991) Hominoid dietary evolution. *Philos Trans R Soc Lond B Biol Sci* 334(1270):199-209.

Reproduced with permission of the copyright owner. Further reproduction prohibited without permission.

Anselin L (1982) A note on small sample properties of estimatorsin a first-order spatial autoregressive model. *Environment and Planning.* 14:1023-1030.

Anthony R (1928) Introduction à l'étude expérimentale de la morphogénie. Bull. et Mém. Soc. d'Anthrop., paris V. Sér., 4:119-145.

Anton H (1984) *Calculus with Analytic Geometry. Second Edition.* John Wiley & Sons. New York.

Aristotle (1910) *Historia animalium* (tr. D'Arcy W. Thompson) Clarendon Press, Oxford.

Aristotle (1937) *De Partibus Animalium* (tr. Arthur L. Peck). Loeb: London.

Aristotle (1943) *De Generatione Animalium* (tr. Arthur L. Peck). Loeb: London.

Ashton EH; Zuckerman S (1952) Age changes in the position of the occipital condyles in the chimpanzee and gorilla. *American Journal of Physical Anthropology.* 10:227-288.

Ashton EH; Zuckerman S (1956) Age changes in the position of the foramen magnum in hominoids. *American Journal of Physical Anthropology.* 315-325.

Atchley WR (1993) Genetic and developmental aspects of variability in the mammalian mandible. *The Skull. Volume 1. Development.* Hanken J & Hall BK, eds., University of Chicago Press: Chicago. pp. 207-247.

Atchley WR; Hall BK (1991) A model for development and evolution of complex morphological structures. *Biol. Rev. Cambr. Phil. Soc.* 66(2):101-157.

Avis V (1959) The relation of the temporal muscle to the form of the coronoid process. *American Journal of Physical Anthropology.* 17:99-104.

Avis V (1961) The significance of the angle of the mandible: an experimental and comparative study. *American Journal of Physical Anthropology.* 19:55-61.

Baba M; Darga L; Goodman M (1980) Biochemical evidence of the phylogeny of Anthropoidea. In: *Evolutionary Biology of the New World Monkeys and Continental Drift.* Ciochon RL; Chiarelli AB (eds.). Plenum: New York.pp. 423-443.

Bailey DW (1985) Genes that affect morphogenesis of the murine mandible. *Journal of Heredity.* 77:17-25.

Baker LW (1941) The influence of the formative dental organs on the growth of the bones of the face. *American Journal of Orthodontics.* 27:489-506.

Baker RR; Parker PH (1979) The evolution of bird colouration. *Philosophical Transactions of the Royal Society of London.* Ser. B, 287:63-130.

Baldwin JD; Baldwin JI (1981) The squirrel mondys, genus *Saimiri.* In: *Ecology and Behavior of Neotropical Primates, Vol. 1.* Coimbra-Filho AF; Mittermeier RA (eds.). Academia Brasileira de Ciências: Rio de Janeiro. pp. 277-330.

Barth M (1919) Ueber die funktionalle struktur des oberkiefer apparates bei neuwelfaffen. *Anatomische Hefte.* 34:189-206.

Reproduced with permission of the copyright owner. Further reproduction prohibited without permission.

Barton RA, Purvis A, Harvey PH (1995) Evolutionary radiation of visual and olfactory brain systems in primates, bats and insectivores. *Philos Trans R Soc Lond B Biol Sci.* 348(1326):381-392.

Bass WM (1971) *Human Osteology: A Laboratory and Field Manual of the Human Skeleton.* Missouri Archaeological Society: Columbia, Missouri.

Baume LJ (1961) Principles of cephalofacial development revealed by experimental biology. *American Journal of Orthodontics.* 47:881-901.

Baume LJ (1968) Patterns of cephalofacial growth and development. A comparative study of the basicranial growth centers in rat and man. *Internatinal Dental Journal.* 18:489-513.

Bee J; Thorogood P (1980) The role of tissue interactions in the skeletogenic differentiation of avian neural crest cells. *Developmental Biology.* 78:47-62.

Beecher RM; Corruccini RS (1981) Effects of dietary consistency on craniofacial and occlusal development in the rat. *Angle Orthod.* 51(1):61-69.2.

Beecher RM; Corruccini RS; Freeman M (1983) Craniofacial correlates of dietary consistency in a nonhuman primate. *J. Craniofac. Genet. Dev. Biol.* 3:193-202.

Bell G (1989) A comparative method. *The American Naturalist.* 133(4):553-571.

Bell RHV (1971) Agrazing ecosystem in the Serengeti. *Scientific American.* 225(1):86-93.

Belsley DA (1990) *Conditioning Diagnostics: Collinearity and Weak Data in Regression.* Wiley: New York.

Belsley DA; Kuh E; Welsch RE (1980) *Regression Diagnostics: Identifying Influential Data and Sources of Collinearity.* Wiley: New York.

Bennett EL; Davies AG (1994) The ecology of Asian colobines. In: *Colobine Monkeys: Their Behaviour and Evolution.* Davies G; Oates JF (eds.). Cambridge University Press: Cambridge, UK. pp. 129-172.

Bentler PM (1990) Comparative fit indexes in structural models. *Psychological Bulletin.* 107:238-246.

Bentler PM; Bonett DG (1980) Significance tests and goodness-of-fit in the analysis of covariance structures. *Psychological Bulletin.* 88:588-606.

Bentler PM; Chou CP (1987) Proactical issues in structural modeling. *Sociological Methods & Research.* 16:78-117.

Beresford WA (1993) Cranial skeletal tissues: diversity and evolutionary trends. *The Skull. Volume 2. Patterns of Structural and Systematic Diversity.* Hanken J & Hall BK, eds., University of Chicago Press: Chicago. pp. 69-130.

Biegert J (1957) Der formwandel der primaten schadels und seine beziehungen zur ontogenetischen (Entwicklung und den phylogenetischen spezialisationes der kopforgane). *Gegnbrs. Morphol. Jhb.* 98:77-199.

Reproduced with permission of the copyright owner. Further reproduction prohibited without permission.

Biegert J (1963) The evaluation of characters of the skull, hands, and feet for primate taxonomy. *Classification and Human Evolution*. Washburn L (ed.). Aldine: Chicago.

Biewener AA (1989) Scaling body support in mammals: limb posture and muscle mechanics. Science. 245:45-48.

Biewener AA; Swartz SM; Bertram JEA (1986) Bone modeling during growth: dynamic strain equilibrium in the chick tibiotarsus. Calcified Tissue International. 39:390-395.

Bilsborough A; Wood BA (1988) Cranial morphometry of early hominids: facial region. *American Journal of Physical Anthropology*. 76:61-86.

Björk A (1955) Cranial base development. *Amer. J. Orthodont*. 41:198-225.

Björk A (1972) The role of genetic and local environmental factors in normal and abnormal morphogenesis. *Acta Morphologica Neerlando-Scandinavica*. 10:49-58.

Blackith RE; Reyment RA (1971) *Multivariate Morphometrics*. Academic Press: London.

Bluntschli H (1926) Ruckwirkunge des Kieferapparatus auf den Gesamtschadel. *Z. Zahnartzte Orthoped.* 18:57-59.

Bock RD (Ed.) (1989) *Multilevel Analysis of Educational Data*. Academic Press: New York.

Bock WJ (1973) Philosophical foundations of classical evolutionary classification. *Systematic Zoology*. 22:375-392.

Bock WJ (1988) The nature of explanations in morphology. *American Zoologist*. 28:205-215.

Bock WJ; von Wahlert G (1963) Two evolutionary theories-a discussion. *British Journal for the Philosophy of Science*. 14:140-146.

Bolk L (1909) On the position and displacement of the foramen magnum in the primates. *Kon. Akad. van Wet. Amst*. 12:362-377.

Bolk L (1910) On the slope of the foramen magnum in primates. *Kon. Akad. van Wet. Amst*. 12:525-534.

Bolk L (1915) Über Lagerung, Verschiebung und Neigung des foramen magnum am Schädel der Primaten. *Ztschr. Morph. Anthrop*. 17:611-692.

Bolk L (1926) *Das Problem der Menschwerdung*. Jena.

Bollen KA (1989) *Structural Equations with Latent Variables*. John Wiley & Sons: New York.

Bollen KA (1990) Overall fit in covariance structure models: twotypes of sample size effects. *Psychological Bulletin*. 107:256-259.

Bookstein FL (1978) The measurement of biological shape and shape change. *Lecture Notes in Biomathematics. No. 24*. Springer-Verlag: New York.

Reproduced with permission of the copyright owner. Further reproduction prohibited without permission.

Bookstein FL (1992) *Morphometric Tools for Landmark Data: Geometry and Biology.* Cambridge University Press: New York.

Bookstein FL; Chernoff B; Elder R; Humphries J; Smith G; Strauss R (1985) *Morphometrics in Evolutionary Biology.* Academy of Natural Sciences of Philadelphia: Philadelphia. Special Pub. 15.

Boomsma A (1982) The robustness of LISREL against small sample sizes in factor analysis models. *Systems Under Indirect Observation: Causality, Structure, Prediction (Part I).* Jöreskog KG; Wold H (eds.). North-Holland: Amsterdam.

Boomsma A (1983) *On the Robustness of LISREL (Maximum Likelihood Estimation) Against Small Sample Size and Non-normality.* Sociometric Research Foundation: Amsterdam.

Boomsma A (1986) On the use of bootstrap and jackknife in covariance structure analysis. *Compstat.* 1986:205-210.

Bouvier M; Hylander WL (1981) Effect of bone strain on cortical bone structure in macaques (*Macaca mulatta*). *Journal of Morphology.* 167:1-12.

Bouvier M; Hylander WL (1982) The effect of dietary consistency on morphology of the mandibular condylar cartilage in young macaques (*Macaca mulatta*). In: *Factors and Mechanisms Influencing Bone Growth.* Dixon DA; Sarnat BG (eds.) Alan R. Liss: New York 569-579.

Bouvier M; Hylander WL (1996) The mechanical or metabolic function of secondary osteonal bone in the monkey *Macaca fascicularis. Archives of Oral Biology.* 41(10):941-950.

Bouvier M; Zimny ML (1987) Effect of mechanical loads on surface morphology of the condylar cartilage of the mandible in rats. *Acta Anatomica.* 129:293-300.

Boyd RL; Gibbs CH; Mahan PE; Richmond AF; Laskin JL (1990) Temporomandibular joint forces measured at the condyle of *Macaca arctoides. American Jour Orthod Dentofacial Orthop.* 97(6):472-479.

Boyd TG; Castelli WA; Hvelke DF (1967) Removal of the temporalis muscle from its origin: effects on the size and shape of the coronoid process. *Journal of Dental Research.* 46:997-1001.

Brandt A (1898) Das hirngewicht und die zahl der peripherischen nervenfasern in ihrer beziehung zur körpergrösse. *Biol. Centralbl.* 18:475-488.

Bravo LA; Nielsen IL; Miller AJ (1989) Changes in facial morphology in Macaca mulatta: a cephalometric study from 1.5 to 5 years of age. *American Journal of Dentofacial Orthopedics.* 96(1):26-35.

Bromage TG (1980) A brief review of cartilage and controlling factors in chondrocranial morphogenesis. *Acta Morphol Neerl Scand.* 18(4):317-322.

Bromage TG (1986) A comparative scanning electron microscope study of facial growth and remodeling in early hominids. Ph.D. Dissertation. University of Toronto.

Reproduced with permission of the copyright owner. Further reproduction prohibited without permission.

Bromage TG (1992) Microstructural organization and biomechanics of the macaque circumorbital region. In: *Structure, Function and Evolution of Teeth*. Smith P; Tchernov E (eds.). Freund: London. pp. 257-272.

Bromage TG; Smolyar I; Doty SB; McMahon JM; Holtz E (1997) Circadian growth rate variability of lamellar bone in rats exposed to microgravity. *Gravitational and Space Biology Bulletin*. 11(1):39.

Brooks DR; McLennan DA (1991) *Phylogeny, Ecology, and Behavior: a Research Program in Comparative Biology*. University of Chicago Press: Chicago.

Brown MB; Forsythe AB (1974) Robust tests for equality of variances. *Journal of the American Statistical Association*. 69:364-367.

Browne MW (1982) Covariance Structures. *Topics in Multivariate Analyses*. Hawkins, DM (ed.) Cambridge University Press: New York.

Browne MW (1984) Asymptotically distribution-free methods for the analysis of covariance structures. *British Journal of Mathematical and Statistical Psychology*. 37:62-83.

Brullé M; Hugueny M (1845) Expériences sur le développement des os dans les mammifères et les oiseaux, faites au moyen de l'alimentation par la garance. *Ann. Sci. Nat. Zool*. 4:283-357.

Bryk AS; Raudenbush SW (1992) *Hierarchical Linear Models: Applications and Data Analysis Methods*. Sage: Thousand Oaks, CA.

Buchanan DB; Mittermeier RA; van Roosmalen MGM (1981) The saki monkey, genus *Pithecia*. In: *Ecology and Behavior of Neotropical Priamtes. Vol. 1*. Coimbra-Filho AF; Mittermeier RA (eds.). Academia Brasileira de Ciências: Rio de Janeiro. pp. 391-418.

Buchman SR; Bartlett SP; Wornom IL; Whitaker (1994) The role of pressure on regulation of craniofacial bone growth. *J Craniofac Surg*. 5(1):2-10.

Buckland-Wright JC (1978) Bone structure and the pattern of force transmission in the cat skull (*Felis catus*). *J. Morphology*. 155:35-62

Burnaby TP (1966) Growth-invariant discriminant functions and generalized distances. *Biometrics*. 22:96-110.

Burstein L (1978) Assessing differences between grouped and individual-level regression coefficients. *Sociological Methods and Research*. 7:5-28.

Butow KW (1990) Craniofacial growth disturbance after skull base and associated suture synostoses in the newborn chacma baboon: a preliminary report. Cleft Palate Journal. 27(3):241-251.

Butynski TM (1990) Guenon birth seasons and correlaes with rainfall and food. In: *A Primate Radiation: Evolutionary Biology of the African Guenons*. Gautier-Hion A; Bourlière F; Gautier JP; Kingdon J (eds.). Cambridge University Press: Cambridge. pp. 284-322.

Reproduced with permission of the copyright owner. Further reproduction prohibited without permission.

Byrd KE; Swindler DR (1980) Palatal growth in *Macaca nemestrina*. *Primates*. 21(2):253-261.

Cachel S (1984) Growth and allometry in primate masticatory muscles. *Archives of Oral Biology*. 29:287-293.

Caldecott JO (1986) *An Ecological and Behavioral Study of the Pig-tailed Macaque*. Karger: Basel.

Calder WA (1984) *Size, Function, and Life History*. Harvard University Press: Cambridge, MA.

Camin J; Sokal R (1965) A method for deducing branching sequences in phylogeny. *Evolution*. 19:311-326.

Camper P (1782) Natuurkundiege Verhandelingen over den Orang Outang; en eenige andere Aapsoorten over den Rhinoceros met den Dubbelen Horen; en over het Rendier. Amsterdam (cited in Schultz, 1955)

Carlson DS; Schneiderman ED (1983) Cephalometric analysis of adaptations after lengthening of the masseter muscle in adult rhesus monkeys, *Macaca mulatta*. *Arch Oral Biol*. 28(7):627-637.

Cartmill M (1972) Arboreal adaptations and the origin of the order Primates. *The Functional and Evolutionary Biology of the Primates*. Tuttle RH (ed.). Aldine-Atherton: Chicago. 97-122.

Cartmill M (1974) Rethinking primate origins. *Science*. 184:436-443.

Chapman C (1987) Flexibility in diets of three species of Cost Rican primates. *Folia Primatologica*. 49:90-105.

Cheng MZ; Zaman G; Rawlinson SC; Pitsillides AA; Suswillo RF; Lanyon LE (1997) Enhancement by sex hormones of the osteoregulatory effects of mechanical loading and prostaglandins in explants of rat ulnae. *J Bone Miner Res* 12(9):1424-1430

Cheverud J; Dow MM; Leutenegger W (1985) The quantitative assessment of phylogenetic constraints in comparative analyses: sexual dimorphism in body weight among primates. *Evolution*. 39(6):1335-1351.

Cheverud JM; Richtsmeier JT (1986) Finite-element scaling applied to sexual dimorphism in rhesus macaque (*Macaca mulatta*) facial growth. *Systematic Zoology*. 35(3):381-399.

Chibon P (1966) Analyse expérimentale de la régionalisation et des capacités morphogénétiques de la crête neural chez l'Amphibien Urodèle *Pleurodeles waltlii* Michah. *Memoires de la Societe Zoologique de France*. 36:1-107.

Chibon P (1970) Capacité de régulation des excédents dans la crête neurale d'Amphibien. *J. Embryol. Experim. Morphol.* 24:479-496.

Chuang SY (1995) The relationship between masticatory function and craniofacial morphology. *Kao Hsiung I Hsueh Ko Hsueh Tsa Chih*. 11(8):458-69

Reproduced with permission of the copyright owner. Further reproduction prohibited without permission.

Ciochon RL; Nisbett RA; Corruccini RS (1997) Dietary consistency and craniofacial development related to masticatory function in minipigs. *J Craniofac Genet Dev Biol.* 17(2):96-102.

Clark AG (1987) Genetic correlations: the quantitative genetics of evolutionary constraints. *Genetic Constraints on Adaptive Evolution.* Loeschcke V (ed.) Springer-Verlag: Berlin.pp. 25-46.

Cliff AD; Ord JK (1973) *Spatial Autocorrelation.* Pion: London.

Clutton-Brock TH (1975) Feeding behavior of red colobus and black and white colobus in East Africa. *Folia Primatologica.* 23:165-207.

Clutton-Brock TH; Harvey PH (1977a) Primate ecology and social organization. *Journal of Zoology.* 183:1-39.

Clutton-Brock TH; Harvey PH (1977b) Species differences in feeding and ranging behaviour in primates. In: *Primate Ecology.* Clutton-Brock TH (ed.). Academic Press: New York.

Clutton-Brock TH; Harvey PH (1984) Comparative approaches to investigating adaptation. *Behavioral Ecology: An Evolutionary Approach. 2nd Ed.* Krebs J; Davies N. (eds.). Sinauer: New York.pp. 7-29.

Cochard LR (1985) Ontogenetic allometry of the skull and dentition of rhesus monkey (*Macaca mulatta*). In: *Size and Scaling in Primate Biology.* Jungers WL (ed.). Plenum Press: New York. 231-255.

Cochran WG (1957) Analysis of covariance: its nature and uses. *Biometrics.* 13:261-281.

Cock AG (1966) Genetical aspects of metrical growth and form in animals. *Quart. Rev. Biol.* 29:103-137.

Cody RP; Smith JK (1997) *Applied Statistics and the SAS Programming Language. Fourth Edition.* Prentice Hall: Saddle River, NJ.

Cohen J (1988) *Power Analysis for the Social Sciences.* Lawrence Erlbaum: New York.

Cole TM III (1992) Postnatal heterochrony of the masticatory apparatus in Cebus apella and Cebus albifrons. *Journal of Human Evolution.* 23:253-282.

Collins ET (1951) cited in GN209O76:129/134: Hylander (1977):

Conover WJ; Johnson ME; Johnson MM (1981) A comparative study of tests for homogeneity of variances. *Technometrics.* 23:351-361.

Conroy GC (1990) *Primate Evolution.* WW Norton & Company: New York.

Cope ED (1888) The mechanical origin of the dentition of the Rodentia. *American Naturalist.* 22:3-11.

Copi IM (1982) *Introduction to Logic. Sixth Edition.* MacMillan Publishing Co.: New York.

Reproduced with permission of the copyright owner. Further reproduction prohibited without permission.

Copray JCVM (1986) Growth of the nasal septal cartilage of the rat in vitro. *Journal of Anatomy*. 144:99-111.

Cords M (1987) Forest guenons and patas monkeys: male-male competition in one-male groups. In: *Primate Societies*. Smuts BB; Cheney DL; Seyfarth RM; Wrangham RW University of Chicago Press: Chicago. pp. 98-111.

Corner BD; Lele S; Richtsmeier JT (1992) Measuring precision of three-dimensional landmark data. *Journal of Quantitative Anthropology*. 3(4):347-359.

Corruccini RS; Beecher RM (1982) Occlusal variation related to soft diet in a nonhuman primate. *Science*. 218:74-76.

Corruccini RS; Henderson AM (1978) Multivariate dental allometry in primates. *American Journal of Physical Anthropology*. 48(2): 203-208.

Coulombre AJ; Coulombre JL; Mehta H (1962) The skeleton of the eye. I. Conjunctival papillae and scleral ossicles. *Developmental Biology*. 5:382-401.

Couly G (1976) La statique osseuse de la face. *Revue de Stomatologie*. 77:420-426.

Cowley DE; Atchley WR (1992) Quantitative genetic models for development, epigenetic selection, and phenotypic evolution. *Evolution*. 46:495-518.

Cramer DL (1977) Craniofacial morphology of *Pan paniscus*. A morphometric and evolutionary appraisal. *Contributions to Primatology. Vol. 10*. Szalay FS (ed.). S. Karger: Basel. pp. 1-64.

Crockett CM; Eisenberg JF (1987) Howlers: variations in groups size and demography. In: *Primate Societies*. Smuts BB; Cheney DL; Seyfarth RM; Wrangham RW; Struhsaker T (eds.). University of Chicago Press: Chicago. pp. 54-68.

Cronin JE; Cann R; Sarich VM (1980) Molecular evolution and systematics of the genus Macaca. In: *The Macaques: Studies in Ecology, Behavior and Evolution*. Lindburg DG (ed.). Van Nostrand-Reinhold: New York. pp. 31-51.

Cronin JE; Sarich (1976) ?

Cudeck R; Henly SJ (1991) Model selection in covariance structures analysis and the "problem" of sample size: a clarification. *Psychological Bulletin*. 109:512-519.

Curtin SH; Chivers DJ (1978) Leaf-eating primates of peninsular Malaysia: the siamang and the dusky leaf-monkey. *The Ecology of Arboreal Folivores*. Montgomery GG (ed.). Smithsonian Institution Press: Washington, DC., pp. 441-464.

Dabelow A (1929) Über Korrelationen in der phylogenetischen Entwicklung der Schädelform. I Die Beziehungen zwischen Rumpf und Schädelform. *Morphol. Jahrb.* 63:1-49.

Dabelow A (1931) Über Korrelationen in der phylogenetischen Entwicklung der Schädelform. II. Beziehungen zwischen Gehirn und Schadelbasisform bei den Mammaliern.. *Morphol. Jahrb.* 67:84-133.

Reproduced with permission of the copyright owner. Further reproduction prohibited without permission.

Daegling DJ; Hylander WL (1997) Occlusal forces and mandibular bone strain: is the primate jaw "overdesigned"? *Journal of Human Evolution*. 33(6):705-717.

Darwin C (1844) Charles Darwin's Notebooks, 1836-1844*: Geology, Transmutation of Species, Metaphysical Enquires*. Barrett, P. H., Gautrey, S. H. Kohn, D. and Smith, S. (transcribed and edited) Cornell University Press: Ithaca. Reprint 1987.

Darwin C (1859) *On the Origin of Species*. New American Library: New York. Reprint 1958.

Darwin C (1860) Charles Darwin to Asa Gray. *The Life and Letters of Charles Darwin. Volume II*. Francis Darwin (ed.) D. appleton and Company: New York. pp. 130-131.

Darwin C; Wallace A (1859) On the tendency of species to form varieties; and on the perpetuation of varieties and species by natural means of selection. *J. Proceedings of the Linnaen Society (Zool.)*. 3:45-62.

Davidson EH (1976) *Gene Activity in Early Development*. 2nd. ed. Academic Press: New York.

Davies AG; Bennett EL; Waterman PG (1988) Food selection by two south-east Asian colobine monkeys (*Presbytis rubicunda* and *Presbytis melalophos*) in relation to plant chemistry. *Biological Journal of the Linnean Society*. 34:33-56.

de Beer GR (1930) *Embryology and Evolution*. Clarendon Press: Oxford.

de Beer GR (1937) *The Development of the Vertebrate Skull*. The University of Chicago Press: Chicago. Reprint 1985.

de Beer GR (1940) *Embryos and Ancestors*. Clarendon Press: Oxford.

de Beer GR (1948) Embryology and the evolution of man. Robert Broom Commemorative Volume. du Toit A (ed.) *Special Publication of the Royal Society of South Africa*.

de Beer GR (1958a) *Embryos and Ancestors*. Clarendon Press: Oxford.

de Beer GR (1958b) Darwin and embryology. *A Century of Darwin*. Barnett SA (ed.) Harvard University Press: Cambridge, Mass. Reprint 1959.

Dean D (1986) Covariation between craniofacial form and chewing. M.A. Thesis. Columbia University.

Dean MC; Wood BA (1982) Basicranial anatomy of Plio-Pleistocene hominids from East and South Africa. *American Journal of Physical Anthropology*. 59:157-174.

Dean MC; Wood BA (1984) Phylogeny, neoteny and growth of the cranial base in hominoids. *Folia Primatologica*. 43(2-3):157-180.

Dechow PC; Carlson DS (1990) Occlusal force and craniofacial biomechanics during growth in rhesus monkeys. *American Journal of Physical Anthropology*. 83:219-238.

Reproduced with permission of the copyright owner. Further reproduction prohibited without permission.

Delson E (1980) Fossil macaques, phyletic relatinships and a scenario of deployment. In: *The Macaques: Studies in Ecology, Behavior and Evolution.* Lindburg DG (ed.) Van Nostrand-Reinhold: New York. pp. 10-30.

Delson E (1992) Evolution of Old World monkeys. *The Cambridge Encyclopedia of Human Evolution.* Jones S; Martin R; Pilbeam D (eds.). Cambridge University Press: Cambridge, UK.pp. 217-222.

Delson E (1994) Evolutionary history of the colobine monkeys in paleoenvironmental perspective. In: *Colobine Monkeys: Their Behaviour and Evolution.* Davies G; Oates JF (eds.). Cambridge University Press: Cambridge, UK.pp.11-44.

Demes B (1985) Biomechanics of the primate skull base. *Advances in Anatomy, Embryology and Cell Biology.* 94:1-59.

Demes B (1987) Another look at an old face: biomechanics of the neandertal facial skeleton reconsidered. *Journal of Human Evolution.* 16:297-303.

Demes B; Creel N (1988) Bite force, diet, and cranial morphology of fossil hominids. *Journal of Human Evolution.* 17:657-670.

Dessem D (1989) Interactions between jaw-muscle recruitment and jaw-joint forces in *Canis familiaris. Journal of Anatomy.* 164:101-121.

Diewert VM, Wang KY, Tait B (1993) A morphometric analysis of cell densities in facial prominences of the rhesus monkey embryo during primary palate formation. *J Craniofac Genet Dev Biol* 13(4):236-49

Diewert VM; Lozanoff S; Choy V (1993) Computer reconstructions of human embryoic craniofacial morphology showing changes in relations between the face and brain during primary palate formation. *J Craniofac Genet Dev Biol* 13(3):193-201

Dillon WR; Goldstein M (1984) *Multivariate Analysis. Methods and Applications.* John Wiley & Sons: New York.

Ding L; Velicer WF; Harlow LL (1995) Effects of estimation methods, number of indicators per factor, and imporper solutions on structural equation modeling fit indices. *Structural Equation Modeling.* 2:119-143.

Disotell TR; Honeycutt RL; Ruvolo M (1992) Mitochondrial DNA phylogeny of the Old World monkey tribe Papionini. *Mol. Biol. Evol.* 9:1-13.

Doran D (1993) Sex differences in adult chimpanzee positional behavior: the influence of body size on locomotion and posture. *American Journal of Physical Anthropology.* 91:99-115.

Doran D (1996) Comparative positional behavior of the African apes. *Great Ape Societies.* McGrew W; Marchant L; Nishida T (eds.). Cambridge University Press: Cambridge. Chpt. 16.

Doran D (1997) Ontogeny of locomotion in mountain gorillas and chimpanzees. *Human Evolution.* 32:323-344.

Reproduced with permission of the copyright owner. Further reproduction prohibited without permission.

Dorenbos J (1972) In vivo cerebral implantation of the anterior and posterior halves of the spheno-occipital synchondrosis in rats. *Archives of Oral Biology*. 17:1067-1072.

Droschl H (1975) The effect of heavy orthopedic forces on the maxilla in the growing *Saimiri sciureus* (squirrel monkey). *Am. J. Orthod.* 63:449-461.

DuBrul EL (1950) Posture, locomotion and the skull in *Lagomorpha. American Journal of Anatomy*. 87:277-313.

DuBrul EL (1962) The general phenomenon of bipedalism. *American Zoologist*. 2:205-208.

DuBrul EL (1964) Evolution of the temporomandibular joint. In: *The Temporomandibular Joint, 2nd Edition*. Sarnat BG (ed.). Charles C.Thomas: Springfield, Ill.

DuBrul EL (1965) Skull of the lion marmoset *Leontideus rosalia* Linneaus: a study in biomechanical adaptation. *American Journal ofPhysical Anthropology*. 23(3):261-276.

DuBrul EL (1977) Early hominid feeding mechanisms. *Amer. J. Phys. Anthropol.* 47(2):305-320.

DuBrul EL (1979) Origin and adaptations of the hominid jaw joint. In: *The Temporomandibular Joint, 3rd Edition*. Sarnat BG; Laskin DM (eds.). Thomas: Springfield, IL., pp. 5-35.

DuBrul EL; Laskin DM (1961) Preadaptive potentialities of the mammalian skull: an experiment in growth and form. *American Journal of Anatomy*. 109:117-132.

DuBrul EL; Sicher H (1954) *The Adaptive Chin*. Charles C. Thomas: Springfield. Ill.

Dullemeijer P (1972) Explanation in morphology. *Acta Biotheoretica*. 21:260-273.

Dullemeijer P (1974) *Concepts and Approaches in Animal Morphology*. Van Gorcum & Company: Netherlands.

Dullemeijer P (1980) Functional morphology and evolutionary biology. *Acta Biotheoretica*. 29:151-250.

Dullemeijer P (1985) Diversity of functional morphological explanation. *Acta Biotheoretica*. 34:111-124.

Dumont ER (1997) Cranial shape in fruit, nectar, and exudate feeders: implications for interpreting the fossil record. *American Journal of Physical Anthropology*. 102(2):187-202

Dunbar DC; Badam CL (1998) Development of posture and locomotion in free-ranging primates. *Neurosci Biobehav Rev*. 22(4):541-546.

Duncan OD (1975) *Introduction to Structural Equation Models*. Academic Press: New York.

Reproduced with permission of the copyright owner. Further reproduction prohibited without permission.

Dunham AE; Miles DB (1985) Patterns of covariation in life history traits of squamate reptiles: the effects of size and phylogeny reconsidered. *American Naturalist.* 126:231-257.

Dunnett CW (1980) Pairwise multiple comparisons in the homogeneous variance, unequal sample size case. *Journal of the American Statistical Association.* 75:789-795.

Duterloo HS; Enlow DH (1970) A comparative study of cranial growth in *Homo* and *Macaca*. *American Journal of Anatomy.* 127:357-367.

Dutrillaux G (1979) Chromosomal evolution in primates: tentativephylogeny from *Microcebus murinus* (Prosimian) to Man. *Human Genetics.* 48:251-314.

Edwards SV; Kot M (1995) Comparative methods at the species level: geographic variation in morphology and group size in grey-crowned bablers (Pomatostomus temporalis). *Evolution.* 49(6):1134-1146.

Eisenberg JF (1989) Order Primates. In: *The Northern Neotropics: Panama, Colombia, Venezuela, Guyana, Suriname, French Guiana. Mammals of the Neotropics.* Unviersity of Chicago Press: Chicago.pp. 233-261.

Eisthen HL (1997) Evolution of vertebrate olfactory systems. *Brain Behav Evol.* 50(4):222-33

Eldredge N (1989) *Macroevolutionary Dynamics. Species, Niches, and Adaptive Peaks.* McGraw-Hill: New York.

Eliason SR (1993) *Maximum Likelihood Estimation: Logic and Practice.* Sage: Thousand Oaks, CA.

Ellies DL; Langille RM; Martin CC; Akimenko MA; Ekker M (1997) Specific craniofacial cartilage dysmorphogenesis coincides with a los of dlx gene expression in retinoic acid-treated zebrafish embryos. *Mech Dev.* 61:23-36.

Emerson SB; Bramble DM (1993) Scaling, Allometry, and Skull Design. *The Skull. Vol. 3. Functional and Evolutionary Mechanisms.* Hanken J & Hall BK, eds., University of Chicago Press: Chicago. pp. 384-421.

Endo B (1965) Distribution of stress and strain produced in the human facial skeleton by the masticatory force. *J. Anthrop. Soc. Nippon.* 73:123-136.

Endo B (1966) Experimental studies on the mechanical significance of the form of the human facial skeleton. *Journal of the Faculty of Science.* Tokyo. Section 5. 3(1):1-106.

Endo B (1970) Structure of the human facial skeleton from the viewpoint of statics. *Proceedings of the 19th Japan National Congress for Applied Mechanics, 1969.* 8-14.

Endo B (1973) Stress analysis on the facial skeleton of Gorilla by means of wire strain gauge method. *Primates.* 14(1):37-46.

Enlow DH (1963) *Principles of Bone Remodeling.* Charles C Thomas: Springfield, IL.

Reproduced with permission of the copyright owner. Further reproduction prohibited without permission.

Enlow DH (1966) A comparative study of facial growth in *Homo* and *Macaca*. *American Journal of Physical Anthropology*. 24:293-307.

Enlow DH (1975) *Handbook of Facial Growth*. W.B. Saunders: Philadelphia.

Enlow DH (1986) Structural and functional "balance" during craniofacial growth. *Orthodontics: State of the Art, Essence of the Science*. Graber LW (ed.). C.V. Mosby: St. Louis.

Enlow DH (1990) *Facial Growth. 3rd Edition*. W.B. Saunders: Philadelphia.

Enlow DH; Azuma M (1975) Functional growth boundaries in the human and mammalian face. In: *Morphogenesis and Malformations of the Face and Brain*. Langman J, ed. The National Foundation: New York. 217-230.

Enlow DH; Bang S (1965) Growth and remodeling of the human maxilla.

Enlow DH; Hunter WS (1968) The growth of the face in relation to the cranial base. *European Orthod. Society, Congress Rep*. 44:321-335.

Enlow DH; Kuroda T; Lewis AB (1971) Intrinsic craniofacial compensations. *Angle Orthod*. 41:271-285.

Enlow DH; McNamara JA (1973) The neurocranial basis for facial form and pattern. *Angle Orthod*. 43:256.

Epple C; Alveario MC; Katz Y (1982) The role of chemical communication in aggressive behavior and its gonadal control in the tamarin (*Saguinus fuscicollis*). In: *Primate Communication*. Snowdon CT; Brown CH; Petersen MR (eds.). Cambridge University Press: Cambridge. pp. 279-302.

Epple C; Belcher AM; Küderling I (1993) Making sense out of scents: species differences in scent glands, scent-marking behaviour, and scent-mark composition in the Callitrichidae. In: *Marmosets and Tamarins: Systematics, Behaviour, Ecology*. Rylands AB (ed.). Oxford University Press. pp. 123-151.

Erhardson S; Sheikholeslam A; Forsberg CM; Lockowandt P (1993) Vertical forces developed by the jaw elevator muscles during unilateral maximal clenching and their distribution on teeth and condyles. *Swedish Dental Journal*. 17:23-24.

Estrada A (1984) Resource use by howler monkeys (*Aloutta palliata*). *International Journal of Primatology*. 5(2):105-131.

Fadiman C (1985) *The Little, Brown Book of Anecdotes*. Brown: New York.

Fanghänel J (1972) The influence of statics on the maxillo-mandibular apparatus. In: *Morphology of the Maxillo-Mandibular Apparatus*. Schumacher GH (ed.) Thieme: Leipzig. pp. 59-64.

Feistner ATC (1991) Scent marking in mandrills, *Mandrillus sphinx*. *Folia Primatologica*. 57:42-47.

Reproduced with permission of the copyright owner. Further reproduction prohibited without permission.

Felsenstein J (1985) Phylogenies and the comparative method. *American Naturalist.* 125:1-15.

Felts WJL (1961) In vivo implantation as a technique in skeletal biology. International *Review of Cytology.* 12:243-302.

Ferrario VF; Sforza C (1994) Biomechanical model of the human mandible in unilateral clench: distribution of temporomandibular joint reaction forces between working and balancing sides. *J Prosthet Dent* 72(2):169-176.

Fields HW Jr.; Metzner L; Garol JD; Kokick VG (1978) The craniofacial skeleton in anencephalic human fetuses. I. Cranial floor. *Teratology.* 17:57-66.

Fleagle JG (1977) Locomotion behavior and muscular anatomy of sympatric Malaysian leaf-monkeys (*Presbytis obscura* and *Presbytis melalophos*). *American Journal of Physical Anthropology.* 46(2):297-308.

Fleagle JG (1978) Locomotion, posture, and habitat utilization in two sympatric Malaysian leaf-monkeys (*Presbytis obscura* and *Presbytis melalophos*). *The Ecology of Arboreal Folivores.* Montgomery GG (ed.). Smithsonian Institution Press: Washington, DC., pp. 243-253.

Fleagle JG (1988) *Primate Adaptation and Evolution.* Academic Press, Inc.: New York.

Fleagle JG; Rosenberger AL (1983) Cranial morphology of the earliest anthropoids. *Morphologie, Evolutive, Morphogenese du Crane et Origine de l'Homme.* Sakka M (ed.). Centre Nat. de la Recherche de Scientifique: Paris. pp. 141-153.

Fooden J (1969) Taxonomy and evolution of the monkeys of Celebes (Primates: Cercopithecidae). *Bibliotheca Primatologica.* Vol. 10. Karger, S. (ed.).

Fooden J (1980) Classification and distribution of living macaques (Macaca Lacepede, 1799). *The Macaques: Studies in Ecology, Behavior, and Evolution.* Lindburg DG (ed.). Van Nostrand Reinhold: New York.

Ford EHR (1958) Growth of the human cranial base. *Am. J. Orthodont.* 44:498-506.

Ford SM (1986) Systematics of the New World Monkeys. In: *Comparative Primate Biology. Volume 1.* Erwin and Swindler (eds.). Alan R. Liss, Inc: New York. pp. 73-135.

Ford SM (1994) Evolution of sexual dimorphism in body weight in platyrrhines. *American Journal of Primatology.* 34:221-244.

Forster A (1927) La lame criblée de l'ethmoïde. *Arch. Anat. Histol. Embryol.* 7:81-131.

Franceschi S; Favero A; Parpinel M; Giacosa A; La Vecchia C (1998) Italian study on colorectal cancer with emphasis on influence of cereals. *Eur J Cancer Prev.* Suppl 2:S19-23

Freedman L (1962) Growth of muzzle length relative to calvaria length in Papio. *Growth.* 26:117-128.

Reproduced with permission of the copyright owner. Further reproduction prohibited without permission.

Freese CH: Oppenheimer JR (1981) The capuchin monkey, genus *Cebus*. In: *Ecology and Behavior of Neotropical Primates, Vol 1*. Coimbra-Filho AF; Mittermeier RA (eds.). Academia Brasileira de Ciências: Rio de Janeiro. pp. 331-390.

Frisancho AR (1981) *Human Adaptation. A Functional Interpretation*. The University of Michigan Press: Ann Arbor.

Frost HM (1987) The mechanostat: a proposed pathogenic mechanism of osteoporoses and the bone mass effects of mechanical and nonmechanical agents. *Bone and Mineral*. 2:73-85.

Galileo Galilei (1638) *Discourses and Mathematical Demonstrations on Two New Sciences Pertaining to Mechanics and Local Motion*. (English translation: S. Drake, University of Wisconsin Press: Madison, 1974).

Galton F (1886) Regression towards mediocrity in hereditary stature. *Journal of the Anthropological Institute*. 15:246-263.

Garol JD; Fields HW Jr; Metener L; Kokick VG (1978) The craniofacial skeleton in anencephalic human fetuses. II. Calvarium. *Teratology*. 17:67-74.

Garstang W (1922) The theory of recapitulation: a critical restatement of the biogenetic law. *J. Linn. Soc. Zool*. 35:81-101.

Garstang W (1928) The morphology of the Tunicata, and its bearings on the phylogeny of the Chordata. *Quart. J. Microscop*. Sci. 72:51-187.

Gartlan JS; Brain CK (1968) Ecology and social variability in *Cercopithecus aethiops* and *C. mitis*. In: *Primates. Studies in Adaptation and Variability*. Jay PC (ed.). Holt, Rinehart, and Winston: New York, pp. 253-292.

Gautier-Hion A (1988) The diet and dietary habits of forest guenons. In: *A Prmate Radiation: Evolutionary Biology of the African Guenons*. Gautier-Hion A; Bourliere F; Gautier JP; Kingdon J. Cambridge University Press: Cambridge.pp. 257-283.

Gebo DL; Chapman CA (1995) Positional behavior in five sympatric Old World monkeys. *American Journal of Physical Anthropology*. 97(1):49-76.

Gibson AR; Baker AJ; Moeed A (1984) Morphometric variation in introduced populations of the common Myna (*Acridotheres tristis*): an application of the jackknife to principal components analysis. *Systematic Zoology*. 33(4):408-421.

Gilbert SF (1988) *Developmental Biology. 2nd Edition*. Sinauer Associates: Sunderland, Mass.

Giles E (1956) Cranial allometry in the great apes. *Human Biology*. 28:43-58.

Gingerich PD (1979) The human mandible: lever, link, or both? *American Journal of Physical Anthropology*. 51(1):135-137

Gingerich PD (1984) Primate evolution: evidence from the fossil record, comparative morphology, and molecular biology. *Yearbook of Physical Anthropology*. 27:57-72.

Reproduced with permission of the copyright owner. Further reproduction prohibited without permission.

Gingerich PD; Smith BH; Rosenberg K (1982) Allometric scaling in the dentition of primates and predictions of body weight from tooth size in fossils. *American Journal of Physical Anthropology*. 58:81-100.

Gittleman JL (1981) The phylogeny of parental care in fishes. *Animal Behavior*. 29:936-941.

Gittleman JL; Kot M (1990) Adaptation: statistics and a null model for estimating phylogenetic effects. *Systematic Zoology*. 39:227-241.

Gittleman JL; Luh H-K (1992) On comparing comparative methods. *Annual Review of Systematics*. 23:383-404.

Glasstone S (1971) Differentiation of the mouse embryonic mandible and squamomandibular joint in organ culture. *Archives of Oral Biology*.16:723-729.

Goldfoot DA (1982) Multiple channels of sexual communication in rhesus monkeys: role of olfactory cues. In: *Primate Communication*. Snowdon CT; Brown CH; Petersen MR (eds.). Cambridge University Press: Cambridge. pp. 413-428.

Goldsmith TH (1991) *The Biological Roots of Human Nature. Forging Links Between Evolution and Behavior*. Oxford University Press: New York.

Goodall J (1996) *The Chimpanzees of Gombe: Patterns of Behavior*. Belknap Press of Harvard University Press: Cambridge.

Goodman M; Bailey WJ; Hayasaka K; Stanhope MJ; Slightom J; Czelusniak J (1994) Molecular evidence on primate phylogeny from DNA sequences. *Am J Phys Anthropol*. 94(1):3-24.

Goodman M; Moore GW (1971) Immunodiffusion systematics of the Primates. I. The Catarrhini. *Systematic Zoology*. 20:19-62.

Goodman M; Romero-Herrera AE; Dene H; Czelusniak J; Tashian RE (1982) Amino acid sequence evidence on the phylogeny of primates and other eutherians. In: *Macromolecular Sequences in Systematics and Evolutionary Biology*. Goodman M (ed.). Plenum: New York.pp. 115-191.

Goodman M; Tagle DA; Fitch DHA; Bailey W; Czelusniak J; Koop BF; Benson P; Slightom JL (1990) Primate evolution at the DNA level and a classification of hominoids. *Journal of Molecular Evolution*. 30:260-266.

Gorke O (1904) Beitrag zur funktionellen gestaltung des schadels bei den anthropomorphen und menschen durch untersuchung mit roent genstrahlen. *Arch Anthropol*. 1:91-108.

Goss AN; White J; Townsend GC (1983) Craniofacial growth in young marmosets (*Callithrix jacchus*). *Laboratory Animal*. 17(4):303-306.

Gottlieb G (1991) Experiential Canalization of Behavioral Development: Theory. *Developmental Psychology*. 27:4-13.

Gould SJ (1966) Allometry and size in ontogeny and phylogeny. *Biological Review*. 41:587-640.

Reproduced with permission of the copyright owner. Further reproduction prohibited without permission.

Gould SJ (1971) Geometric similarity in allometric growth: a contribution to the problem of scaling in the evolution of size. *American Naturalist*. 105:113-136.

Gould SJ (1977) *Ontogeny and Phylogeny*. Belknap Press: Cambridge.

Gould SJ (1981) The evolutionary biology of constraint. *Daedalus*. 109:39-52.

Gould SJ; Vrba ES (1982) Exaptation: a missing term in the science of form. *Paleobiology*. 8:4-15.

Graening J; Nibbelink WH (1975) *Geometry*. Charles E. Merrill Publishing Co.: Columbus, OH.

Grafen A (1989) The phylogenetic regression. *Philosophical Transactions of the Royal Society, London*. Ser. B 326:119-157.

Gray R (1992) *Death of the Gene: Developmental Systems*. Holt, Rinehart and Winston: New York.

Greaves WS (1973) The inference of jaw motion from tooth wear facets. *Journal of Paleontology*. 47(5):1000-1001.

Greaves WS (1978) The jaw lever system in ungulates: a new model. *Journal of Zoology, London*. 184:271-285.

Griffiths PE; Gray RD (1994) Developmental systems and evolutionary explanation. *Journal of Philosophy*. 91: 277-304

Groves CP (1978) Phylogenetic and population systematics of the mangabeys (Primates: Cercopithecoidea). *Primates*. 19:1-34.

Groves CP (1993) Order Primates. In: *Mammalian Species of the World. A Taxonomic and Geographic Reference. 2nd. Ed. Wilson* DE; Reader EM (eds.). Smithsonian Institution Press: Washington, DC. pp. 243-277.

Grubbs FE (1969) Procedures for detecting outlying observations in samples. *Technometrics*. 11:1-21.

Grüneberg H (1975) How do genes affect the skeleton? *New Approaches to the Evolution of Abnormal Embryonic Development*. Neuberg D & Merker HJ, eds. Georg Thieme: Stuttgart, pp. 354-359.

Guelinckx P; Dechow PC; Vanrusselt R; Carlson DS (1986) Adaptations in the temporalis muscles of rabbits after masseter muscle removal. *Journal of Dental Research*. 65(11):1294-1299.

Haeckel E (1866) *Generelle Morphologie der Organismen*. Georg Reimer: Berlin.

Hahn R (1971) *The Anatomy of a Scientific Institution. The Paris Academy of Sciences, 1666-1803*. University of California Press: Berkeley, CA.

Reproduced with permission of the copyright owner. Further reproduction prohibited without permission.

Hailman JP (1982) Ontogeny: toward a general theoretical framework for ethology. *Perspectives in Ethology, 5: Ontogeny*. Bateson PPG; Klopfer PH (Eds.). Plenum: New York. pp. 133-189.

Hall BK (1978) *Developmental and Cellular Skeletal Biology*. Academic Press: New York.

Hall BK (1980) Tissue interactions and the initiation of osteogenesis and chondrogenesis in the neural creast-derived mandibular skeleton of the embryonic mouse as seen in isolated murine tissues and in recombinatinos of murine and avian tissues. *Journal of Embryology and Experimental Morphology*. 58:251-264.

Hall BK (1982) The role of tissue interactions in the growth of bone. *Factors and Mechanisms Influencing Bone Growth*. Dixon AS; Sarnat BG (eds.) A.R. Liss: New York. pp. 205-215.

Hall BK; Hanken J (1993) Bibliography of skull development, 1937-89. *The Skull. Volume 1. Development*. The University of Chicago Press: Chicago.

Hall BK; Hörstadius S (1988) *The Neural Crest*. Oxford University Press: Oxford.

Hamberger V (1984) Hilde Mangold, co-discoverer of the organizer. *J. Hist. Biol.* 17:1-11.

Hanken J; Hall BK (eds.) (1993) *The Skull. Volumes 1-3*. Development. The University of Chicago Press: Chicago.

Hannan MT; Burstein L (1974) Estimation from grouped observations. *American Sociological Review*. 39:374-392.

Hanson NR (1958) *Patterns of Discovery: An Inquiry into the Conceptual Foundations of Science*. Cambridge University Press: New York.

Happel R (1988) Seed-eating by West African cercopithecines, with reference to the possible evolution of bilophodont molars. *American Journal of Physical Anthropology*. 75(3):303-327.

Harada ML, Schneider H, Schneider MP, Sampaio I, Czelusniak J, Goodman M (1995) DNA evidence on the phylogenetic systematics of New World monkeys: support for the sister-grouping of *Cebus* and *Saimiri* from two unlinked nuclear genes. *Mol Phylogenet Evol*. 4(3):331-49

Harding RSO (1981) An order of omnivores: nonhuman primate diets in the wild. In: *Omnivorous Primates*. Harding RSO; Teleki G (eds). Columbia University Press: New York. 191-214.

Harrington J (1979) Olfactory communication in *Lemur fulvus*. In: *Prosimian Biology*. Martin RD; Doyle GA; Walker AC (eds.). University of Pittsburgh Press: Pittsburgh. pp. 331-346.

Harrison ML; Tardif SD (1994) Social implications of gumnivory in marmosets. *American Journal of Physical Anthropology*. 95(4):399-408.

Reproduced with permission of the copyright owner. Further reproduction prohibited without permission.

Hartley HO; Rao JNK (1967) Maximum likelihood estimation for the mixed analysis of variance model. *Biometrika*. 54:383-385.

Harvey PH; Clutton-Brock TH (1985) Life history variation in primates. *Evolution*. 39(3):559-581.

Harvey PH; Mace GM (1982) Comparisons between taxa and adaptive trends. In: *Current Problems in Sociobiology*. King's College Sociobiology Group (eds.) Cambridge University Press: Cambridge, UK., pp. 343-361.

Harvey PH; Pagel M (1991) *The Comparative Method in Evolutionary Biology*. Oxford University Press: Oxford.

Hatcher L (1994) *A Step-by-Step Approach to Using the SAS System for Factor Analysis and Structural Equation Modeling*. SAS Inc.: Cary, NC.

Hecht JT; Horton WA; Reid CS; Pyeritz RE; Charkraborty R (1989) Growth of the foramen magnum in achondroplasia. *American Journal of Medical Genetics*. 32(4):528-535.

Hecker P (1926) Le region ptérique osseuse chez l'homme et les simiens. *Arch. d'Anat, d'Hist. et de l'Embr*. 6:283-320.

Heinrichs C; Colli M; Yanovski JA; Laue L; Gerstl NA; Kramer AD; Uyeda JA; Baron J (1997) Effects of fasting on the growth plate: systemic and local mechanisms. *Endocrinology*. 138(12):5359-5365.

Heise DR (1975) *Causal Analysis*. Wiley: New York.

Helms JA; Kim CH; Hu D; Minkoff R; Thaller C; Eichele G (1997) Sonic hedgehog participates in craniofacial morphogenesis and is down-regulated by teratogenic does of retinoic acid. *Developmental Biology*. 187(1):25-35.

Hemple CG (1962) Deductive-nomological vs. statistical explanation. *Minnesota Studies in the Philosophy of Science III*. Feigle H & Maxwell G (eds.) pp. 98-169.

Hendricksen RP; McNamara JA; Carson DS; Yellich GM (1982) Changes in the gonial region induced by alterations of muscle length. *J. Oral Maxillofac. Surg*. 40:570-577.

Herring SW (1976) The dynamics of mastication in pigs. *Archs Oral Biol*. 21:473-480.

Herring SW (1993) Epigenetic and functional influences on skull growth. *The Skull. Vol. 1. Development*. Hanken J & Hall BK, eds., University of Chicago Press: Chicago. pp. 153-206.

Herring SW; Lakars TC (1981) Craniofacial development in the absence of muscle contraction. *J. Craniofac. Genet. Dev. Biol*. 1:341-357.

Herring SW; Mucci RJ (1991) In vivo strain in cranial sutures: the zygomatic arch. *Journal of Morphology*. 207:225-239.

Hershkovitz P (1977) *Living New World Monkeys (Platyrrhini)*. University of Chicago Press: Chicago.

Reproduced with permission of the copyright owner. Further reproduction prohibited without permission.

Hertwig WAO (1881) *Die Coelomtheorie.* Jena.

Hiiemae KM (1978) Mammalian mastication: a review of the activity of the jaw muscles and the movements they produce in chewing. In: *Development, Function and Evolution of Teeth.* Butler PM; Joysey KA (eds.). Academic Press: New York. 359-397

Hiiemae KM; Crompton AW (1971) A cinefluorographic study of feeding in the American opossum, Didelphis marsupialis. *Dental Morphology and Evolution.* Dahlberg, A. A. (ed.). University of Chicago Press: Chicago. pp. 299-334.

Hill RE; Jones PF; Rees AR; Sime CM Justice MJ Copelend NG; Jenkins NA; Graham E; Davidson DR (1989) A new family of mouse homeo box-containing genes: molecular structure, chromosomal location, and developmental expression of Hox-7.1. *Genes and Development.* 3:26-37.

Hoaglin DC (1992) Diagnostics. in *Perspectives on Contemporary Statistics.* Hoaglin DC; Moore DS (eds.). Mathematical Association of America: Washington, DC. pp. 123-144.

Hoaglin DC; Welsch RE (1978) The hat matrix in regression and ANOVA. *The American Statistician.* 32:17-22.

Hofer H (1952) Der gestaltwandel des schädels der säugetiere und Vogel, mit besonderer berüucksichtigung der knickungstypen und der schädelbasis. *Anatomischer Anzeiger.* 99:102-113.

Hohl TH (1983) Masticatory muscle transposition in primates: effects on craniofacial growth. *Journal of Maxillo-Facial Surgery.* 11:149-156.

Holloway RL (1999) Hominid brain volume. *Science.* 283:34-35.

Horn JL (1965) A rationale and test for the number of factors in factor analysis. *Psychometrika.* 30:179.

Horovitz I, Zardoya R, Meyer A (1998) Platyrrhine systematics: a simultaneous analysis of molecular and morphological data. *American Journal of Physical Anthropology.* 106(3):261-81.

Horowitz SL; Shapiro HH (1955) Modification of skull and jaw architecture following removal of the masseter muscle in the rat. *American Journal of Physical Anthropology.* 13:301-308.

Howells W (1959) *Mankind in the Making. The Story of Human Evolution.* Doubleday & Company, Inc.: New York.

Howship J (1815) Experiments and observations in order to ascertain the means employed by the animal economy in the formation of bone. *Med.-Chir. Trans. (Lond.)* 6:1-33

Huang L; Solursh M; Sandra M (1996) The role of transforming growth factor alpha in rat craniofacial development and chondrogenesis. *Journal of Anatomy.* 189(1):73-86.

Huber (1902)

Reproduced with permission of the copyright owner. Further reproduction prohibited without permission.

Huey RB (1987) Phylogeny, history, and the comparative method. In: *New Directions in Ecological Physiology*. Feder ME; Bennett AF; Burggren W; Huey RB (eds.). Cambridge University Press: Cambridge, U.K. pp. 76-98.

Hugot JP (1998) Phylogeny of neotropical monkeys: the interplay of morphological, molecular, and parasitological data. *Mol Phylogenet Evol.* 9(3):408-13

Huitema BE (1980) *The Analysis of Covariance and Alternatives*. Wile: New York.

Humphrey T (1971) Development of oral and facial motor mechanisms in human fetuses and their relation to craniofacial growth. *Journal of Dental Research*. 50:1428-1441.

Humphries JM; Bookstein FL; Chernoff B; Smith GR; Elder RL; Poss SG (1981) Multivariate discrimination by shape in relation to size. *Systematic Zoology*. 30:291-308.

Hutten EH (1962) *The Origins of Science: An Inquiry into the Foundations of Western Thought*. Allen and Unwin: London.

Huxley J (1932) *Problems of Relative Growth*. MacVeagh: London.

Huxley TH (1863) *Evidence as to Man's Place in Nature*. Williams and Norgate: London.

Huxley TH (1867) On two widely contrasted forms of the human cranium. *Journal of Anatomy and Pysiology, London*. 1:60-77.

Huxley TH (1896) *Darwiniana*. D. Appleton and Company: New York.

Huxley TH (1896) *Man's Place in Nature, and Other Anthropological Essays*. D. Appleton and Company: New York.

Hylander WL (1975) The adaptive significance of Eskimo craniofacial morphology. *Oro-facial Growth and Development*. Dahlberg, A. A. and Graber, T. (eds.). Mouton:

Hylander WL (1975) The human mandible: lever or link? *American Journal of Physical Anthropology*. 43:227-242.

Hylander WL (1979) An experimental analysis of temporomandibular joint reaction force in macaques. *American Journal of Physical Anthropology*. 51(3):433-456.

Hylander WL (1986) In vivo bone strain as an indicator of masticatory bite force in *Macaca fascicularis*. *Arch. Oral Biol.* 31:149-157.

Hylander WL; Johnson KR (1997) In vivo bone strain patterns in the zygomatic arch of macaques and the significance of thes patterns for functional interpretations of craniofacial form. *American Journal of Physical Anthropology*. 102(2):203-232.

Hylander WL; Johnson KR; Crompton AW (1987) Loading patterns and jaw movements during mastication in *Macaca fascicularis*: a bone-strain, electromyographic, and cineradiographic analysis. *American Journal of Physical Anthropology*. 72(3):287-314.

Reproduced with permission of the copyright owner. Further reproduction prohibited without permission.

Hylander WL; Johnson KR; Crompton AW (1992) Muscle force recruitment and biomechanical modeling: an analysis of masseter muscle function during mastication in *Macaca fascicularis*. *American Journal of Physical Anthropology*. 88(3):365-387.

Hylander WL; Picq PG; Johnson KR (1991) Masticatory-stress hypotheses and the supraorbital region of primates. *American Journal of Physical Anthropology*. 86(1):1-36.

Ichikawa M; Konishi S (1995) Application of the bootstrap methods in factor analysis. *Psychometrika*. 60:77-93.

Ikeda J; Wanatable T (1966) Morphological studies of *Macaca fuscata*. III. Craniometry. *Primates*. 7:271-288.

Ingervall B; Bitsanis E (1987) A pilot study of the effect of masticatory muscle training on facial growth in long-face children. *European Journal of Orthodontics*. 9:15-23.

Iwasaki K (1989) Dynamic responses in adult and infant monkey craniums during occlusion and mastication. *J Osaka Dent Univ*. 23(2):77-97.

Jackson GW; Kokich VG; Shapiro PA (1979) Experimental and postexperimental response to anteriorly directed extraoral force in young *Macaca nemestrina*. *American Journal of Orthodontics*. 75(3):318-333.

Janis CM (1990) Correlation of cranial and dental variables with dietary preferences in mammals: a comparison of macropodoids and ungulates *Mem Queensl Mus*. 28(1):349-366.

Jarman P (1974) The social organization of antelope in relation to their ecology. *Behaviour*. 48:215-267.

Johnson DR (1986) *The Genetics of the Skeleton*. Clarendon Press: Oxford.

Johnson SE; Shapiro LJ (1998) Positional behavior and vertebral morphology in atelines and cebines. *American Journal of Physical Anthropology*. 105(3):333-354.

Johnston MC; Bronsky PT (1995) Prenatal craniofacial development: new insights on normal and abnormal mechanisms. *Crit Rev Oral Biol Med*. 6(4):368-422.

Jolicoeur P (1963) The multivariate generalization of the allometry equation. *Biometrics*. 19:497-499.

Jolly A (1972) *The Evolution of Primate Behavior*. MacMillan: New York.

Jolly CJ (1970) The seed-eaters: A new model of hominid differentiation based on a baboon analogy. *Man*. 5:5-26

Jones FW (1916) *Arboreal Man*. E. Arnold: London.

Jöreskog KG; Sörbom D (1989) *LISREL 7. User's Reference Guide*. Scientific Software Inc.: Mooresville, IN.

Jöreskog KG; Sörbom D (1993) *LISREL 8. Structural Equation Modeling with the SIMPLIS Command Language*. Lawrence Erlbaum Associates: Hillsdate, NJ.

Reproduced with permission of the copyright owner. Further reproduction prohibited without permission.

Judd CM; McClelland GH (1989) *Data Analysis: A Model-Comparison Approach.* Harcourt Brace Jovanovich: San Diege, CA.

Jungers WL (1985) Body size and scaling of limb proportions in primates. in *Size and Scaling in Primate Biology.* Jungers WL (ed) Plenum Press: New York.

Jungers WL; Cole MS (1992) Relative growth and shape of the locomotor skeleton in lesser apes. *Journal of Human Evolution.* 23:93-105.

Jungers WL; Falsetti AB; Wall CE (1995) Shape, relative size, and size-adjustments in morphometrics. *American Journal of Physical Anthropology.* Suppl 21:137-161.

Kakudo Y; Amano N (1968) Strain in the rabbit and dog maxillomandibular bones during biting and mastication. *J. Dent. Res.* 47:496.

Kao KR; Elinson (1988) The entire mesodermal mantle behaves as Spemans's organizer in dorsoanterior enhanced *Xenopus laevis* embryos. *Developmental Biology.* 127:64-77.

Katsaros C; Kiliaridis S; Berg R (1994) Functional influence on sutural growth. A morphometric study in the anterior facial skeleton of the growing rat. *European Journal of Orthodontics.* 16(5):353-360.

Kay RF (1976) The functional adaptations of primate molar teeth. *American Journal of Physical Anthropology.* 43:195-216.

Kay RF (1977) The evolution of molar occlusion in the cercopithecidae and early catarrhines. *American Journal of Physical Anthropology.* 46:327-352.

Kay RF (1984) On the use of anatomical features to infer foraging behavior in extinct primates. In: *Adaptations for Foraging in Non-human Primates.* Rodman PS; Cant JGH (eds.). Columbia University Press: New York.

Kay RF; Hiiemae KM (1974) Jaw movement and tooth use in recent and fossil primates. *American Journal of Physical Anthropology.* 40(2):227-256.

Kean MR; Houghton P (1982) The Polynesian head: growth and form. *Journal of Anatomy.* 135:423-435.

Kiliaridis S (1986) Masticatory muscle function and craniofacial morphology, an experimental study in the growing rat fed a soft diet. *Swed. Dent. J.* Suppl. 36:

Kiliaridis S (1995) Masticatory muscle influence on craniofacial growth. *Acta Odontol Scand.* 53(3):196-202.

Kiliaridis S, Bresin A, Holm J, Strid KG (1996) Effects of masticatory muscle function on bone mass in the mandible of the growing rat. *Acta Anatmica.* 155(3):200-205

Kiliaridis S, Kjellberg H, Wenneberg B, Engstrom C (1993) The relationship between maximal bite force, bite force endurance, and facial morphology during growth. A cross-sectional study. *Acta Odontol Scand.* 51(5):323-31.

Reproduced with permission of the copyright owner. Further reproduction prohibited without permission.

King AH; Schneiderman ED (1993) Differential growth among components of the palate in rhesus monkeys (Macaca mulatta). *Cleft Palate Craniofac J.* 30(3):302-308.

Kingdon J (1974) Primates. In: *East African Mammals: An Atlas of Evolution in Africa. Vol. 1.* University of Chicago Press: Chicago.pp. 99-328.

Kinzey WG (1974) Ceboid models for the evolution of hominoid dentition. *Journal of Human Evolution.* 3(3):193-204.

Kinzey WG (1981) The titi monkey, genus *Callicebus*. In: *Ecology and Behavior of Neotropical Primates.*, Vol. 1. Coimbra-Filho AF; Mittermeier RA (eds.). Academia Brasileira de Ciências: Rio de Janeiro. pp. 240-276.

Kinzey WG (1992) Dietary and dental adaptations in the Pitheciinae. *American Journal of Physical Anthropology.* 88:499-514.

Kinzey WG; Norconk MA (1993) Physical and chemical properties of fruit and seeds eaten by *Pithecia* and *Chiropotes* in Surinam and Venezuela. *International Journal of Primatology.* 14(2):207-227.

Kjaer I (1991) The midline craniofacial skeleton in holoprosencephalic fetuses. *J. Med Genet.* 28(12):846-855.

Kjaer I (1995) Human prenatal craniofacial development related to brain development under normal and pathologic conditions. *Acta Odontol Scand.* 53(3):135-143.

Kjaer I (1998) Neuro-osteology. *Crit Rev Oral Biol Med.* 9(2):224-244.

Koolstra JH; van Eijden TM; Weijs WA; Naeije M (1988) A three-dimensional mathematical model of the human masticatory system predicting maximum possible bite forces. *Journal of Biomechanics.* 21(7):563-576.

Koop BF; Tagle DA; Goodman M; Slightom JL (1989) A molecular view of primate phylogeny and important systematic and evolutionary questions. *Mol. Biol. Evol.* 6:580-612.

Kramer CY (1956) Extension of multiple range tests to groups means with unequal numbers of replications. *Biometrics.* 12:307-310.

Kreft I; De Leeuw J; Aiken LS (1995) The effect of different forms of centering in hierarchical linear models. *Multivariate Behavioral Research.* 30:1-21.

Krogman WM (1931) Studies in growth changes in the skull and face of anthropoids: IV. Growth changes in the skull and face of the chimpanzee. *American Journal of Anatomy.* 46:325-342.

Krogman WM (1931) Studies in growth changes in the skull and face of anthropoids. V. Growth changes in the skull and face of the orangutan. *American Journal of Anatomy.* 47:343-365.

Krogman WM (1974) Craniofacial growth and development: an appraisal. *Yearbook of Physical Anthropology.* 18:31-64.

Reproduced with permission of the copyright owner. Further reproduction prohibited without permission.

Kruskall W (1988) Miracles and statistics: the casual assumption of independence. *Journal of the American Statistical Association*. 83:929-940.

Kummer B (1952) Untersuchungen über die schädelbasisform bei mensch und primaten. *Anatomischer Anzeiger*. 99:122-126.

Kurland JA; Pearson JD (1986) Ecological significance of hypometabolism in nonhuman primates: allometry, adaptation, and deviant diets. *American Journal of Physical Anthropology*. 71(4):445-457.

Lande R (1980) The genetic covariance between characters maintained by pleiotropic mutations. *Genetics*. 94:203-215.

Lande R (1986) *Paleobiology*. 12:343-

Langbein LI; Lichtman AJ (1978) *Ecological Inference*. Sage: Thousand Oaks, CA.

Lange B (1924) Über Rassenunterschiede an der Regio pterica beim Menschen. *Anat. Anz.* 58:353-374.

Langille RM; Hall BK (1993) Pattern formation and the neural crest. *The Skull. Volume 1. Development*. Hanken J; Hall BK (eds.) The University of Chicago Press: Chicago.77-111.

Lanyon LE (1996) Using functional loading to influence bone mass and architecture: objectives, mechanisms, and relationship with estrogen of the mechanically adaptive proccess in bone. *Bone*. 18(1):37S-43S.

Laplace (1787) Théorie de Jupiter et de Saturne. *Mémoires de l'Académie Royale des Sciences de Paris*. Cited in Stigler, 1986.

Latham RA (1966) Observations on the growth of the cranial base in the human skul. *Journal of Anatomy*. 100:435.

Latham RA (1972) The sella point and postnatal growth of the cranial base. *American Journal of Orthodontics*. 61:156-162.

Latif A (1957) An electromyographic study of the temporal muscle in normal persons during selected positions and movements of the mandible. *American Journal of Orthodontics*. 43:577-591.

Lauder GV (1982) Historical biology and the problem of design. *Journal of Theoretical Biology*. 97:57-67.

Lawes MJ; Henzi SP; Perrin MR (1990) Diet and feeding behaviour of samango monkeys (*Cercopithecus mitis labiatus*) in Ngoye Forest, South Africa. *Folia Primatologica*. 54:57-69.

Reproduced with permission of the copyright owner. Further reproduction prohibited without permission.

Le Gros Clark WE (1950) New paleontological evidence bearing on the evolution of the Hominoidea. *Quarterly J. Geol. Soc. Lond.* 105:225-264.

Le Gros Clark WE (1959) *The Antecedents of Man: an Introduction to the Evolution of the Primates*. University Press: Edinburgh.

LeDouarin NM; Dupin E; Ziller C (1994) Genetic and epigenetic control in neural crest development. *Curr Opin Genet Dev.* 4(5):685-695.

Leutenegger W; Masterson TJ (1989) The ontogeny of sexual dimorphism in the cranium of bornean orang-utans (*Pongo pygmaeus pygmaeus*): 2. Allometry and heterochrony. *Z. Morph. Anthrop.* 78(1):15-24.

Lewontin R (1968) The concept of evolution. *IESS.* 5:202-210.

Lewontin R (1969) The bases of conflict in biological explanation. *J. Hist. Biol.* 2:35-45.

Li CC (1975) *Path Analysis. A Primer.* Boxwood Press: Pacific Grove, CA.

Loireau JN; Gautier-Hion A (1988) Olfactory marking behavior in guenons and its implications. In: *A Primate Radiation: Evolutionary Biology of the African Guenons.* Gautier-Hion A; Bourlière F; Gautier JP; Kingdon J (eds.). Cambridge University Press: Cambridge. pp. 246-254.

Longford NT (1993) *Random Coefficient Models.* Clarendon Press: Oxford.

Luboga SA; Wood BA (1990) Position and orientation of the foramen magnum in higher primates. *American Journal of Physical Anthropology.* 81(1):67-76.

Lucas PW (1981) An analysis of canine size and jaw shape in some Old and New World non-human primates. *Journal of Zoology.* 195(4):437-448.

Luschei ES; Goodwin GM (1974) Patterns of mandibular movement and jaw muscle activity during mastication in the monkey. *Journal of Neurophysiology.* 37:954-966.

Lush JL (1949) Heritability of quantitative characters in farm animals. *Hereditas.* Supl.356-375.

Lynch M (1991) Methods for the analysis of comparative data in evolutionary biology. *Evolution.* 45(5):1065-1080.

Madeira MC, Watanabe IS, De Oliveira JA, Matheus MT (1976) Facial skeletal changes following unilateral resection of the masseter muscle and zygomatic arch in juvenile and adult monkeys. *Rev Fac Odontol Aracatuba.* 5(1-2):93-107.

Maeda N; Wu CI; Bliska J; Reneke J (1988) Molecular evolution of intergenic DAN in higher primates: pattern of DNA changes, molecular clock, and evolution of repetitive sequences. *Mol. Biol. Evol.* 5:1-20.

Mahner M; Bunge M (1997) *Foundations of Biophilosophy.* Springer: Berlin.

Reproduced with permission of the copyright owner. Further reproduction prohibited without permission.

Manson JD (1968) *A Comparative Study of the Postnatal Growth of the Mandible*. Henry Kempton: London.

Mansour RM; Reynik RJ (1975) In vivo occlusal forces and moments: I. Forces measured in terminal hinge position. *Journal of Dental Research*. 54:114-120.

Marcoulides GA; Schumacker RE (eds.) (1996) *Advanced Structural Equation Modeling. Issues and Techniques*. Lawrence Erlbaum: Mahwah, NJ.

Marcus LF (1990) Traditional morphometrics. *Proceedings of the Michigan Morphometrics Workshop*. Rohlf FJ; Bookstein FL (eds.). University of Michigan Museum of Zoology: Ann Arbor. pp. 77-122.

Marcus LF; Corti M; Loy A; Naylor GJP; Slice DE (eds.) (1996) *Advances in Morphometrics*. Plenum Press: New York.

Marks L; Teng S; Artun J; Herring S (1997) Reaction strains on the condylar neck during mastication and maximum muscle stimulation in different condylar positions: an experimental study in the miniature pig. *Journal of Dental Research*. 76(7):1412-1420.

Marsh HW; Balla JR; Hau KT (1996) An evaluation of incremental fit indices: a clarification of mathematical and empirical properties. *Advanced Structural Equation Modeling: Issues and Techniques*. Marcoulides GA; Schumacker RE (eds.) Lawrence Erlbaum Associates: Mahwah, NJ. pp. 315-354.

Marsh HW; Balla JR; McDonald RP (1988) Goodness-of-fit indexes in confirmatory factor analysis: the effect of sample size. *Psychological Bulletin*. 103:391-410.

Martin RD (1979) Phylogentic aspects of prosimian behavior. *The Study of Prosimian Behavior*. Doyle A; Martin R (eds.). Academic Press: New York. pp.45-77.

Martin RD (1982) Allometric approaches to the evolution of the primate nervous system. In: *Primate Brain Evolution: Methods and Concepts*. Armstrong E; Falk D (eds.). Plenum Press: New York. pp. 39-56.

Martins EP (1996) Phylogenies, spatial autoregression, and the comprative method: a computer simulation test. *Evolution*. 50(5):1750-1765.

Martins EP; Garland T Jr. (1991) Phylogenetic analyses of the correlated evolution of continuous characters: a simulation study. *Evolution*. 45:534-557.

Mason WA (1968) Use of space by callicebus groups. In: *Primates. Studies in adaptation and Variability*. Jay PC (ed.). Holt, Rinehart, and Winston: New York, pp. 200-216.

Masters AV; Falk D; Gage TB (1991) Effects of age and gender on the location and orientation of the foramen magnum in rhesus macaques *Macaca-mulatta*. *American Journal of Physical Anthropology*. 86(1):75-80.

Maynard Smith J; Burian R; Kauffman S; Alberch P; Campbell J; Goodwin B; Lande R; Raup D; Wolpert L (1985) Developmental constraints and evolution. *Quarterly Review of Biology*. 60(3):265-287.

Reproduced with permission of the copyright owner. Further reproduction prohibited without permission.

Maynard Smith J; Savage RJG (1959) The mechanics of mammalian jaws. *Sci. Rev.* 40:289-301.

Mayr E (1961) Cause and effect in biology. *Science.* 134:1501-1506.

Mayr E (1970) *Populations, Species, and Evolution: An Abridgment of Animal Species and Evolution.* Belknap Press of Harvard University Press: Cambridge, MA.

Mayr E (1982) *The Growth of Biological Thought. Diversity, Evolution and Inheritance.* Harvard University Press: Cambridge, Mass.

Mayr E (1983) How to carry out the adaptationist program? *American Naturalist.* 121:324-334.

Mayr E (1991) *One Long Argument: Charles Darwin and the Genesis of Modern Evolutionary Thought.* Harvard University Press: Cambridge, Mass.

McArdle JJ; Goldsmith HH (1990) Some alternative structural equation models for multivariate biometric analyses. *Behavior Genetics.* 20(5):569-508.

McArdle JJ; Hamagami F (1996) Multilevel models from a multiple group structure equation perspective. In: *Advanced Structural Equation Modeling. Issues and Techniques.* Marcoulides GA; Schumacker RE (eds.). Lawrence Erlbaum Associates: Mahwah, NJ.

McDevitt WE (1989) *Functional Anatomy of the Masticatory System.* Wright: London.

McGraw WS (1998) Comparative locomotion and habitat use of six monkeys in Tai Forest, Ivory Coast. *American Journal of Physical Anthropology.* 105(4):493-510.

McKenzie AEE (1967) *The Major Achievements of Science. Volume 1.* Cambridge University Press: Cambridge, England.

McKinney (1988) *Journal of Human Evolution.* 23:

McMahon JM (1994) Developmental constraints on priamte craniofacial morphology: the effects of ethmoid orientation on "facial projection." *American Journal of Physical Anthropology.* Suppl. 18:145-146.

McMahon JM; Boyde A; Bromage TG (1995) Pattern of collagen fiber orientation in the ovine calcaneal shaft and its relation to locomotor-induced strain. *The Anatomical Record.* 242:147-158.

McMahon TA (1975) Allometry and biomechanics: limb bones in adult ungulates. *American Naturalist.* 109:547-563.

Melsen B; Melsen F (1980) The cranial base in anencephaly and microcephaly studied histologically. *Teratology.* 22:271-277.

Michael RP; Keverne EB (1968) Pheromones in the communication of sexual status in primates. *Nature.* 218:746-749.

Reproduced with permission of the copyright owner. Further reproduction prohibited without permission.

Michejda M (1971) Ontogenetic changes in the cranial base in *Macaca mulatta*: histological study. *Proceedings of the Third International Congress of Primatology*, vol. 1, Taxonomy, Anatomy, Reproduction. Biegert J; Leutenegger W (eds.). S. Karger: Basel. 215-222.

Michejda M (1975) Ontogenetic growth changes of the skull base in four genera of nonhuman primates. *Acta Anatomica*. 91:110-117.

Michejda M; Lamey D (1971) Flexion and metric age changes of the cranial base in Macaca mulatta: I. Infant and juveniles. *Folia Primatologica*. 14:84-94.

Miller SC; Miller MA; Omura TH (1988) Dietary lactose improves endochondral growth and bone development and mineralization in rats fed a vitamin D-deficient diet. *Journal of Nutrition*. 118(1):72-77.

Milton K (1984) Habitat, diet, and activity patterns of free ranging woolly spider moiney (*Brachyteles arachnoides* E. Geoffroy 1806). *International Journal of Primatology*. 5(5):491-514.

Milton S (1986) A sample size formula for multiple regression studies. *The Public Opinion Quarterly*. 50:112-118.

Mollison T (1926) Uber die Kopfform des Mikrokephalen Mesek. *Z. Morphol. Anthrop.* 25:109-128.

Montagu MFA (1960) *A Handbook of Anthropometry*. Charles C. Thomas: Springfield, IL.

Moore AW (1949) Head growth of the macaque monkey. *American Journal of Orthodontics*. 35:654-671.

Moore RN (1978) A cephalometric and histologic study of the cranial base in foetal monkeys, *Macaca nemestrina*. *Archives of Oral Biology*. 23:57-67.

Moore WJ (1965) Masticatory function and skull growth. *J. Zool.* 146:123-131.

Moore WJ (1967) Muscular function and skull growth in the laboratory rat (*Rattus norvegicus*). *J. Zool.* 152:287-296.

Moore WJ (1973) An experimental study of functional components of growth in the rat mandible. *Acta Anatomica*. 85:378-385.

Moore WJ (1981a) *The Mammalian Skull*. Cambridge University Press: Cambridge.

Moore WJ (1981b) Facial growth in primates with special reference to the Hominoidea. *Symp. Zool. Soc. Lond.* 46:37-62.

Moore WJ; Adams LM; Lavelle CLB (1973) Head posture in the hominoidea. *Journal of the Zoological Society, London*. 169:409-416.

Morales JC, Melnick DJ (1998) Phylogenetic relationships of the macaques (Cercopithecidae: *Macaca*), as revealed by high resolution restriction site mapping of mitochondrial ribosomal genes. *Journal of Human Evolution*. 34(1):1-23

Reproduced with permission of the copyright owner. Further reproduction prohibited without permission.

Mosimann JE (1970) Size allometry: size and shape variables with characterizations of the log-normal and gamma distributions. *Journal of the American Statistical Association*. 56:930-945.

Mosimann JE (1975) Statistical problems of size and shape. I. Biological applications and basic theorems. In: *Statistical Distributions in Scientific Work 2*. Patil GP; Kotz S; Ord K (eds.) D Reidel: Dordecht, Holland. pp. 187-217.

Mosimann JE; James FC (1979) New statistical methods for allometry with applications to Florida re-winged blackbirds. *Evolution*. 23:444-459.

Moskalewski S; Osiecka A; Hyc A; Malejczyk J (1989) Difference in shape of bone formed by isolated calvarial and scapular osteoblasts transplanted under various conditions. *Folia Histochemica et Cytobiologica*. 27:25-34.

Moss ML (1958) Rotations of the cranial components in the growing rat and their experimental alteration. *Acta Anat*. 32:65-86.

Moss ML (1958) The pathogenesis of artificial cranial deformation. *American Journal of Physical Anthropology*. 16:269-285.

Moss ML (1961) Rotation of the otic capsule in bipedal rats. *American Journal of Physical Anthropology*. 19:301-307.

Moss ML (1962) The functional matrix. *Vistas of Orthodontics*. Kraus BS; Riedel RA (eds.) Lea & Febiger: Philadelphia.

Moss ML (1968) The primacy of functional matrices in orofacial growth. *Dental Practitioner*. 19:65-73.

Moss ML (1973) A functional cranial analysis of primate craniofacial growth. *Symposia 4th Int. Congr. Primatol*. 3:191-208.

Moss ML (1976) Experimental alteration of basi-synchondrosal cartilage growth in rat and mouse. In *Development of the Basicranium*. Bosma JF (ed.), U.S. Department of Health, Education, and Welfare:Bethesda, Md., pp. 541-575.

Moss ML (1997a) The functional matrix hypothesis revisited. 1. The role of mechanotransduction. *Am J Orthod Dentofacial Orthop*. 112(1):8-11.

Moss ML (1997b) The functional matrix hypothesis revisited. 2. The role of an osseous connected cellular network. *Am J Orthod Dentofacial Orthop*. 112(2):221-226.

Moss ML (1997c) The functional matrix hypothesis revisited. 3. The genomic thesis. *Am J Orthod Dentofacial Orthop*. 112(3):338-342.

Moss ML (1997d) The functional matrix hypothesis revisited. 4. The epigenetic antithesis and the resolving synthesis. *Am J Orthod Dentofacial Orthop*. 112(4):410-417.

Moss ML; Greenberg SN (1955) Postnatal growth of the human skull base. *Angle Orthodont*. 25:77-84.

Reproduced with permission of the copyright owner. Further reproduction prohibited without permission.

Moss ML; Meehan M (1970) Functional cranial analysis of the coronoid process in the rat. *Acta Anatomica*. 77:11-24.

Mulaik SA; James LR; Alstine JV; Bennett N; Lind S; Stilwell CD (1989) Evaluation of goodness-of-fit indices for structural equation models. *Psychological Bulletin*. 105:430-445.

Müller H; Punt-van Manen JA (1982) Maxillo-facial deformities in patients with dystropic myotonica and the anaesthetic implications. *Journal of Maxill-Facial Surgery*. 10:224-228.

Murphy M; Bartlett PF (1993) Molecular regulation of neural crest development. *Molecular Neurobiology*. 7(2):111-135.

Murray PDF (1936) *Bones*. Cambridge University Press: Cambridge. Reprint 1985.

Murray PDF; Drachman DB (1969) The role of movement in the development of joints and related structures: the head and neck in thechick embryo. *Journal of Embryology and Experimental Morphology*. 22:349-371.

Muthén BO (1987) Response to Freedman's critique of path analysis: improve credibility by better methodological training. *Journal of Educational Statistics*. 12:178-184.

Muthén BO (1994) Multilevel covariance structure analysis. *Sociological Methods and Research*. 22(3):376-398.

Nagel E (1961) *The Structure of Science*. Barcourt, Brace & World: New York.

Nagel E (1965) Types of causal explanation in science. *Cause and Effect*. Lerner D (ed.) Free Press: New York.11-26.

Nanda R; Baume RM; Tanne K; Sugawara J (1987) Longitudinal study of craniofacial growth in *Macaca fascicularis*. *American Journal of Physical Anthropology*. 73:215-225.

Napier JR; Napier PH (1967) *A Handbook of Living Primates*. Academic Press: New York.

Negus (1958)

Neville MK; Glander KE; Braza F; Rylands AB (1988) The howling monkeys, genus *Alouatta*. In: *Ecology and Behavior of Neotropical Priamtes. Vol. 2*. Mittermeier RA; Rylands AB; Coimbra-Filho AF; de Fonseca GAB (eds.). World Wildlife Fund: Washington DC. pp. 349-453.

Newton I (1686) *Principia*. Reprint. University of California Press: Los Angeles. 1934.

Nicholas JS (1930) *Journal of Experimental Zoology*. 55:1-14.

Nielsen IL; Bravo LA; Miller AJ (1989) Normal maxillary and mandibular growth and dentoalveolar development in *Macaca mulatta*. A longitudinal cephalometric study from 2 to 5 years of age. *Am J Orthod Dentofacial Orthop*. 96(5):405-415.

Reproduced with permission of the copyright owner. Further reproduction prohibited without permission.

Nishimura A; de Fonseca GAB; Mittermeier RA; Young AL; Strier KB; Valle CMC (1988) The muriqui monkey, genus *Brachyteles*. In: *Ecology and Behavior of Neotropical Priamtes. Vol. 2*. Mittermeier RA; Rylands AB; Coimbra-Filho AF; de Fonseca GAB (eds.). World Wildlife Fund: Washington DC. pp. 577-610.

Noden DM (1978) The control of avian cephalic neural crest cytodifferentiation. I. Skeletal and connective tissues. *Developmental Biology*. 67:296-312.

Noden DM (1982) Patterns and organization of craniofacial skeletogenic and mygenic mesenchyme: a perspective. *Factors and Mechanisms Influencing Bone Growth*. Dixon DA; Sarnat BG (eds.) Alan R. Liss: New York 167-203.

Noden DM (1983) The role of the neural crest in patterning of avian cranial skeletal, connective, and muscle tissue. *Developmental Biology*. 96:296-312.

Nowak RM (1991) Primates. In: *Walker's Mammals of the World 5th Ed.* Johns Hopkins University Press: Baltimore. pp. 400-514.

Nowak RM; Paradiso JL (1983) *Walker's Mammals of the World*. Johns Hopkins University Press: Baltimore.

Nozawa K; Shotake T; Ohkura Y; Tanabe Y (1977) Genetic variations within and between species of Asian macaques. *Jpn. Journal of Genetics*. 52:15-30.

Ord K (1975) Estimation methods for models of spatial interaction. *J. Amer. Stat. Assoc.* 70:120-126.

Orton J (1878) *Comparative Zoology. Structural and Systematic*. Harper & Brothers: New York.

Osborn JW (1987) Relationship between the mandibular condyle and the occlusal plane during hominid evolution: some of its effects on jaw mechanics. *American Journal of Physical Anthropology*. 73(2):193-207

Osborn JW (1995) Biomechanical implications of lateral pterygoid contributino to biting and jaw opening in humans. *Archive of Oral Biology*. 40(12):1099-1108.

Oster GF; Shubin N; Murray JD; Alberch P (1988) Evolution and morphogenetic rules: the shape of the vertebrate limb in ontogeny and phylogeny. *Evolution*. 42:862-884.

Oyama S (1985) *The Ontogeny of Information*. Cambridge University Press: Cambridge.

Oyen OJ (1984) Palatal growth in baboons (*Papio cynocephalus anubis*). *Primates*. 25(3):337-351.

Oyen OJ; Melugin MB; Indresano AT (1996) Strain gauge analysis of the frontozygomatic region of the zygomatic complex. *J. Oral Maxillofac Surg.* 54(9):1092-1095.

Oyen OJ; Tsay TP (1991) A biomechanical analysis of craniofacial form and bite force. *Am J Orthod Dentofacial Orthop*. 99(4):298-309.

Reproduced with permission of the copyright owner. Further reproduction prohibited without permission.

Oyen OJ; Walker AC; Rice RW (1979) Craniofacial growth in olive baboons (*Papio cynocephalus anubis*): browridge formation. *Growth*. 43:174-187.

Pagel MD (1992) A method for the analysis of comparative data. *Journal of Theoretical Biology*. 156:431-442.

Pagel MD; Harvey PH (1988) Recent developments in the analysis of comparative data. *Quarterly Review of Biology*. 63(4):413-440.

Pai AC (1965) Developmental genetics of a lethal mutation, muscular dysgenesis (mdg), in the mouse. I. Genetic analysis and grossmorphology. *Developmental Biology*. 11:82-92.

Passingham RE (1975) Changes in the size and organisation of the brain in man and his ancestors. *Brain Behav Evol*. 11(2):73-90.

Pastorini J, Forstner MR, Martin RD, Melnick DJ (1998) A reexamination of the phylogenetic position of *Callimico* (primates) incorporating new mitochondrial DNA sequence data. *Journal of Molecular Evolution*. 47(1):32-41

Pearson K (1956) *Karl Pearson's Early Statistical Papers*. Cambridge University Press: Cambridge.

Pedhazur EJ (1997) *Multiple Regression in Behavioral Research. Explanation and Prediction. Third Edition*. Harcourt Brace: New York.

Peres C (1994) Diet and feeding ecology of gray woolly monkey (*Lagothrix lagotricha cana*) in central Amazonia: comparison with other atelines. International Journal of Primatology. 15(3):333-372.

Picq PG; Hylander WL (1989) Endo's stress analysis of the primate skull and the functional significance of the supraorbital region. *American Journal of Physical Anthropology*. 79(3):393-398.

Pirinen S (1995) Endocrine regulation of craniofacial growth. *Acta Odontol Scand*. 53(3):179-185.

Pirinen S, Majurin A, Lenko HL, Koski K (1994) Craniofacial features in patients with deficient and excessive growth hormone. *J Craniofac Genet Dev Biol* 14(3):144-52

Plomin R; DeFries JC; McClearn GE (1980) *Behavior Genetics*. A Primer. W.H. Freeman and Co.: San Francisco.

Poirier FE; Stini WA; Wreden KB (1990) *In Search of Ourselves: An Introduction to Physical Anthropology*. Rentice Hall: Englewood Cliffs, NJ.

Pook AG; Pook G (1981) A field study of the socio-ecology of the Goeldi's monkey, *Callimico goeldii*, in northern Bolivia. *Folia Primatologica*. 35:288-317.

Popper KR (1957) *The Poverty of Historicism*. Beacon Press: Boston.

Popper KR (1959) *The Logic of Scientific Discovery*. Basic Books: New York.

Reproduced with permission of the copyright owner. Further reproduction prohibited without permission.

Porter CA; Sampaio I; Schneider H; Schneider MPC; Czelusniak J; Goodman (1995) Evidence on primate phylogeny from e-globin gene sequences and flanking regions. *Journal of Molecular Evolution*. 40:30-55.

Pratt LW (1943) Experimental masseterectomy in the laboratory rat. *J. Mammal*. 24:204-211.

Presley R (1993) Preconception of adult structural pattern in the analysis of the developing skull. *The Skull. Volume 1. Development*. Hanken J; Hall BK (eds). University of Chicago Press: Chicago. pp. 347-377.

Preuschoft H; Demes B; Meyer M; Bar HF (1986) The biomechanical principles realised in the upper jaw of long-snouted primates. *Primate Evolution*. Else and Lee. (eds.). 249-264.

Pruim GJ; de Jongh HJ; ten Bosch JJ (1980) EMG-activity and static loading of the mandible. *Journal of Biomechanics*.

Pucciarelli HM; Dressino V; Niveiro MH (1990) Changes in skull components of the squirrel monkey evoked by growth and nutrition: an experimental study. *Am J Phys Anthropol*. 81(4):535-543.

Purvis A; Gittleman JL; Luh HK (1994) Truth or consequences: effects of phylogenetic accuracy on two comparative methods. *Journal of Theoretical Biology*. 167:293-300.

Raadsheer MC; Kiliaridis S; van Eijden TM; van Ginkel FC; Prahl-Anderson B (1996) Masseter muscle thickness in growing individuals and its relation to facial morphology. *Arch Oral Biol*. 41(4):323-332.

Radinsky L (1967) Relative brain size: a new measure. *Science*. 155:836-838.

Radinsky L (1975) Primate brain evolution. *American Scientist*. 63:656-663.

Radinsky LB (1981) Evolution of skull shape in carnivores. I. Representative modern carnivores. *Biological Journal of the Linnean Society*. 15:369-388.

Raemaekers J (1979) Ecology of sympatric gibbons. *Folia Primatologica*. 31:227-245.

Rak Y (1983) The Australopithecine Face. Academic Press: New York.

Rak Y (1986) The Neanderthal: a new look at an old face. *Journal of Human Evolution*. 15:151-164.

Ramirez M (1988) The woolly monkeys, genus *Lagothirx*. In: *Ecology and Behavior of Neotropical Priamtes. Vol. 2*. Mittermeier RA; Rylands AB; Coimbra-Filho AF; de Fonseca GAB (eds.). World Wildlife Fund: Washington DC. pp. 539-575.

Ravin AW (1965) *The Evolution of Genetics*. Academic Press: New York.

Ravosa MJ (1988) Browridge development in cercopithecidae: a test of two models *American Journal of Physical Anthropology*. 76(4):535-556.

Ravosa MJ; Shea BT (1994) Pattern in craniofacial biology: evidence from the Old World monkeys (Cercopithecidae). *International Journal of Primatology*. 15(6):801-821.

Reproduced with permission of the copyright owner. Further reproduction prohibited without permission.

Raykov T; Widaman KF (1995) Issues in applied structural equation modeling research. *Structural Equation Modeling*. 2(4):289-318.

Reddi AH; Cunningham NS (1993) Initiation and promotion of bone differentiation by bone morphogenetic proteins. *Journal of Bone and Mineral Research*. Suppl 2:S399-S502.

Richard AF (1985) *Primates in Nature*. W. H. Freeman and Company: New York.

Richard AF; Goldstein SJ; Dewar RE (1989) Weed macaques: the evolutionary implications of macaque feeding ecology. *International Journal of Primatology*. 10(6):569-591.

Richman JM; Diewert VM (1988) The fate of Meckel's cartilage chondrocytes in ocular culture. *Developmental Biology*. 129:48-60.

Richter W (1920) Der obergesichtsschadel des menschen als gebissturm, ein statisches kunstwerk. *Arch Dtsch Monatsschr Zahnheilkd*. 38(2):49-68.

Ridley M (1983) *The Explanation of Organic Diversity. The Comparative Method and Adaptations of Mating*. Clarendon: Oxford.

Rieppel O (1987) The development of the trigeminal jaw adductor musculature and associated skull elements in the lizard *Podarcis sicula*. *Journal of Zoology, London*. 212:131-150.

Riesenfeld A (1975) Endocrine control of skeletal robusticity. *Acta Anat*. 91(4):481-499

Ringqvist M (1973) Isometric bite force and its relation to dimensions of the facial skeleton. *Acta Odontol Scand*. 31(1):35-42.

Riska B (1986) Some models for development, growth and morphometric correlation. *Evolution*. 40:1303-1311.

Robb RC (1935) A study of mutations in evolution. I. Evolution in the equive skull. II. Ontogeny in the equine slull. *J. Genetics*. 31:39-52.

Roberts D; Tattersall I (1974) Skull form and the mechanics of mandibular elevation in mammals. *Amer. Mus. Novit*. 2536:1-9.

Roberts KH; Burstein L (eds.). (1980) *Issues in Aggregation*. Jossey-Bass: San Francisco.

Roberts RC (1967) Some concepts and methods in quantitative genetics. *Behavior-genetic Analysis*. Hirsch J (ed.). McGraw-Hill: NewYork.pp. 214-257.

Robinson JG; Wright PC; Kinzey WG (1987) Monogamous cebids and their relatives intergroup call and spacing. In: *Primate Societies*. Smuts BB; Cheney DL; Seyfarth RM; Wrangham RW (eds.). University of Chicago. Press: Chicago. pp. 44-53.

Robinson JT (1954) The genera and species of the Australopithecinae. *American Journal of Physical Anthropology*. 12:181-200.

Reproduced with permission of the copyright owner. Further reproduction prohibited without permission.

Robinson WS (1950) Ecological correlations and the behavior of individuals. *American Sociological Review*. 15:351-357.

Rodman PS (1979) Skeletal differentiation of *Macaca fascicularis* and *Macaca nemestrina* in relation to arboreal and terrestrial quadrupedalism. *American Journal of Physical Anthropology*. 51:51-62.

Rohlf FJ; Bookstein FL (1987) A comment on shearing as a method for "size correction." *Systematic Zoology*. 36:356-367.

Rohlf FJ; Chang WS; Sokal RR; Kim J (1990) Accuracy of estimate phylogenies: effects of tree topology and evolutionary model. *Evolution*. 44:1671-1684.

Rohlf FJ; Slice D (1990) Extensions of the procrustes method for the optimal superimposition of landmarks. *Systematic Zoology*. 39:40-59.

Romer AS; Parsons TS (1985) *The Vertebrate Body. Sixth Edition*. Saunders College Publishing: New York.

Roonwal ML; Mohnot SM (1977) *Primates of South Asia: Ecology, Sociology, and Behavior*. Harvard University Press: Cambridge.

Rose MD (1974) Postural adaptations in New and Old World Monkeys. In: *Primate Locomotion*. Jenkins FA (ed.). Academic Press: New York. 210-222.

Rose MD (1978) Feeding and associated positional behavior of black and white colobus monkeys (*Colobus guereza*). *The Ecology of Arboreal Folivores*. Montgomery GG (ed.). Smithsonian Institution Press: Washington, DC., pp. 253-264.

Rosenberger AL (1981) Systematics: the higher taxa. In: *Ecology and Behavior of Neotropical Primates*. (Coimbra-Filho AF; Mitermeier RA, eds) Academia Brasiliera de Ciencias: Rio de Janeiro.

Rosenberger AL (1984) Fossil New World monkeys dispute the molecular clock. *Journal of Human Evolution*. 13:737-742.

Rosenberger AL (1992) Evolution of feeding niches in New World monkeys. *American Journal of Physical Anthropology*. 88(4):525-62

Ross CF; Ravosa MJ (1993) Basicranial flexion, relative brain size, and facial kyphosis in nonhuman primates. *American Journal of Physical Anthropology*. 91(3):305-324.

Roux W (1881) *Der Kampf der Theile im Organismus*. Engelmann: Leipzig.

Rowe N (1996) *The Pictorial Guide to the Living Primates*. Pogonias Press: East Hamptom, NY.

Rubin CT; Lanyon LE (1985) Regulation of bone mass by mechanical strain magnitude. *Calcified Tissue International*. 37:411-417.

Rubin CT; Lanyon LE (1987) Osteoregulatory nature of mechanical stimuli: function as a determinant for adaptive remodeling in bone. *Journal of Orthopaedic Research*. 5:300-310.

Reproduced with permission of the copyright owner. Further reproduction prohibited without permission.

Rubin CT; McLeod KJ (1994) Promotion of bony ingrowth by frequency-specific, low-amplitude mechanical strain. *Clin Orthop.* 298:165-74

Ruf S; Pancherz H; Kirschbaum M (1994) Facial morphology and the size and activity of the masseter muscle. *Fortschr Kieferorthop.* 55(5):219-227.

Russell B (1929) *Mysticism and Logic.* Allen and Unwin: London.

Russell ES (1916) *Form and Function.* The University of Chicago Press: Chicago. Reprint 1982.

Saijo S; Sugimura T (1993) Dynamic response of the adult monkey maxilla to occlusal forces. *J Osaka Dent Univ.* 27(1):1-22.

Saitou N (1991) Reconstruction of molecular phylogeny of extant hominoids from DNA sequence data. *American Journal of Physical Anthropology.* 84(1):75-87.

Sakka M (1984) Cranial morphology and masticatory adaptations. *Food Acquisition and Processing in Primates.* Chivers DJ; Wood BA; Bilsborough A (eds.) Plenum Press: New York. pp.415-427

Sall J; Lehman A (1996) *JMP Start Statistics. A Guide to Statistical and Data Analysis Using JMP and JMP IN Software.* Duxbury Press: New York.

Sara M (1996) A "sensitive" cell system. Its role in a new evolutionary paradigm. *Rev Biol.* 89(1):139-156.

Sarich VM; Cronin JE (1976) Molecular systematics of the primates. In: *Molecular Anthropology.* Goodman M; Tashian RE (eds.). Plenum: New York. pp. 141-170.

Sarich VM; Cronin JE (1980) South American mammal molecular systematics, evolutionary clocks, and continental drift. In: *Evolutionary Biology of the New World Monkeys and Continental Drift.* Ciochon RL; Chiarelli AB (eds.). Plenum: New York. pp. 399-421.

Sarnat BG (1973) The monkey facial skeleton after postnatal surgical experimentation. *Symposia of the Fourth International Congress of Primatology. Vol. 3: Craniofacial Biology of Primates.* Zingeser MR (ed.) Karger: Basel. 209-226.

SAS Inc. (1990) *SAS/STAT User's Guide. Volume 1. Version 6. First Edition.* SAS Institute Inc.: Cary, NC.

SAS Inc. (1990) *SAS/STAT User's Guide. Volume 2. Version 6. Fourth Edition.* SAS Institute Inc.: Cary, NC.

SAS Inc. (1992) *SAS Procedures Guide. Version 6. Third Edition.* SAS Institute Inc.: Cary, NC.

SAS Inc. (1993) *SAS/STAT User's Guide. Volume 1. Version 6. Fourth Edition.* SAS Institute Inc.: Cary, NC.

SAS Institute Inc. (1990) *SAS Procedures Guide, Version 6, Third Edition.* SAS Inc.: Cary, NC.

Reproduced with permission of the copyright owner. Further reproduction prohibited without permission.

SAS Institute Inc. (1997) *SAS/STAT Software: Changes and Enhancements through Release 6.12.* SAS Inc.: Cary, NC.

Sasaki K; Hannam AG; Wood WW (1989) Relationships between the size, position, and angulation of human jaw muscles and unilateral first molar bite force. *Journal of Dental Research.* 68(3):499-503.

Savara BS (1965) A method for measuring facial bone growth in three dimensions. 245-255.

Savostin-Asling I, Nakaiye R, Asling CW (1980) Roentgen cephalometric studies on skull development in rats. III. Gigantism versus acromegaly: age differences in response to prolonged growth hormone administration. *Anat Rec.* 196(1):9-21.

Schaefer SA; Lauder GV (1986) Historical transformation of functional design: evolutionary morphology of feeding mechanisms of loricarioid catfishes. *Systematic Zoology.* 35:489-508.

Scharloo W (1987) Constraints in selection response. *Genetic Constraints on Adaptive Evolution.* Loeschcke V (ed.) Springer-Verlag: Berlin.pp. 125-150.

Schmidt-Nielsen K (1984) *Scaling. Why Is Animal Size So Important?* Cambridge University Press: Cambridge.

Schneck GH (1985) Untersuchungen zum ontogenetischen Formwandel der Schädelbasis bei *Hylobates. Z. Morph. Anthrop.* 76:37-48.

Schultz AH (1926) Variations in man and their evolutionary significance. *American Naturalist.* 60:297-323.

Schultz AH (1940) The size of the orbit and the size of the eye in primates. American *Journal of Physical Anthropology.* 26:389-408.

Schultz AH (1942) Conditions for balancing the head in primates. *American Journal of Physical Anthropology.* 29:483-497.

Schultz AH (1955) The position of the occipital condyles and of the face relative to the skull base in primates. *American Journal of Physical Anthropology.* 13:97-120.

Schultz AH (1962) Metric age changes and sex differences in primate skulls. *Z. Für Morph. Anthrop.* 52:239-255.

Schumacher GH; Ivánkievicz D; Fanghänel J (1979) The role of function in the formation of the skull. *Acta Morphologica Academiae Scientiarum Hungaricae.* 27:53-56.

Schumacker RE; Lomax RG (1996) *A Beginner's Guide to Structural Equation Modeling.* Lawrence Erlbaum Associates: Mahwah, NJ.

Schwartz GT; Conroy GC (1996) Cross-sectional geometric properties of the *Otavipithecus* mandible. *American Journal of Physical Anthropology.* 99(4):613-23

Scott JH (1954) The growth of the human face. *Proceedings of the Royal Society of Medicine.* 47:91-100.

Reproduced with permission of the copyright owner. Further reproduction prohibited without permission.

Scott JH (1958) The cranial base. *American Journal of Physical Anthropology*. 16:319-348.

Scott JH (1959) Further studies on the growth of the human face. *Proceedings of the Royal Society of Medicine*. 47:91-100.

Senyurek MS (1938) Cranial equilibrium index. *American Journal of Physical Anthropology*. 24:23-41.

Shea BT (1983) Allometry and heterochrony in the African apes. *American Journal of Physical Anthropology*. 62:275-289.

Shea BT (1983) Size and diet in the evolution of African ape craniodental form. *Folia Primatologia*. 40:32-68.

Shea BT (1985) Bivariate and multivariate growth allometry: statistical and biological considerations. *Journal of Zoology, London*. 206(3):367-390.

Shoshani J; Groves CP; Simons EL; Gunnell GF (1996) Primate phylogeny. morphological vs molecular results. *Molecular Phylogenetics and Evolution*. 5(1):102-154.

Sibley CG (1992) DNA-DNA hybridization in the study of primate evolution. *The Cambridge Encyclopedia of Human Evolution*. Jones S; Martin R; Pilbeam D (eds.). Cambridge University Press: Cambridge, U.K.pp. 313-315.

Sicher H; DuBrul EL (1975) *Oral Anatomy*. C.V. Mosby: St. Louis.

Sicher H; Tandler J (1928) Anatomie für Zahnärzte. Berlin.

Siebert JR; Kokich VG; Beckwith JB; Cohen MM Jr; Lemire RJ (1981) The facial features of holoprosencephaly in anencephalic human specimens. II. Craniofacial anatomy. *Teratology*. 23(3):305-315.

Siebert JR; Kokich VG; Warkany J; Lemire RJ (1987) Atelencephalic microcephaly: craniofacial anatomy and morphologic comparisons with holoprosencephaly and anencephaly. *Teratology*. 36(3):279-285.

Siegel S; Castellan NJ (1988) *Nonparametric Statistics*. McGraw-Hill: New York.

Sirianni JE; Newell-Morris L (1980) Craniofacial growth of fetal Macaca nemestrina: a cephalometric roentgenographic study. *American Journal of Physical Anthropology*. 53(3):407-421.

Sirianni JE; Van Ness AL (1978) Postnatal growth of the cranial base in *Macaca nemestrina*. *American Journal of Physical Anthropology*. 49(3):329-340.

Slice D (1994) *Generalized rotational fitting of n-dimensional landmark data*. Reference Manual.

Slice DE; Bookstein FL; Marcus LF; Rohlf FJ (1996) A glossary for geometric morphometrics. In: *Advances in Morphometrics*. Marcus LF; Corti M; Loy A; Naylor GJP; Slice DE (eds.). Plenum Press: New York.

Reproduced with permission of the copyright owner. Further reproduction prohibited without permission.

Smith G (1912) The origin of man. *Smithson. Inst. Annu. Rep.* 1912:553-572.

Smith KK (1993) The form of the feeding apparatus in terrestrial vertebrates: studies of adaptation and contraint. *The Skull. Volume 3. Functional and Evolutionary Mechanisms.* Hanken J; Hall BK (eds.). The University of Chicago Press: Chicago.pp. 150-196.

Smith KK; Redford KH (1990) The anatomy and function of the feeding apparatus in two armadillos (Dasypodidae): anatomy is not destiny. *Journal of Zoology*, London. 222:27-47.

Smith RJ (1984) Allometric scaling in comparative biology: problems of concept and method. *American Journal of Physiology.* 246:R152-R160.

Smith RJ (1984) The plan of the human face: a test of three general concepts. *American Journal of Orthodontics.* 85:103-108..

Smith RJ, German RZ, Jungers WL (1986) Variability of biological similarity criteria. *J Theor Biol.* 118(3):287-293.

Sober E (1984) *The Nature of Selection: Evolutionary Theory in Philosophical Focus.* MIT Press: Cambridge, Mass.

Sober E (1988) *Reconstructing the Past. Parsimony, Evolution, and Inference.* The MIT Press: Cambridge, Mass.

Soini P (1993) The ecology of the pygmy marmoset, *Cebuella pygmaea*: some comparisons with two sympatric tamarins. In: *Marmosets and Tamarins: Systematics, Behaviour, Ecology.* Rylands AB (ed.). Oxford University Press: Oxford.pp. 257-261.

Sokal RR; Rohlf FJ (1981) *Biometry.* W.H. Freeman: San Francisco

Sokal RR; Rohlf FJ (1995) *Biometry. the Principles and Practice of Statistics in Biological Research. Third Edition.* W.H. Freeman: San Francisco.

Solow B (1966)

Solow B (1966) The pattern of craniofacial associations: A morphological and methodological correlation and factor analysis study on young male adults. *Acta Odontol. Scand.* 24(Suppl. 46).

Solow B; Tallgren A (1976) Head posture and craniofacial morphology. *American Journal of Physical Anthropology.* 44:417-436.

Sörbom D (1989) Model modification. *Psychometrika.* 54:371-384.

Southard TE; Southard KA; Stiles RN (1990) Factors influencing the anterior component of occlusal force. *Biomechanics.* 23(12):1199-1207.

Southgate DA (1991) Nature and variability of human food consumption. *Philosophical Transactions of the Royal Society of London.* 334:281-288.

Reproduced with permission of the copyright owner. Further reproduction prohibited without permission.

Spatz WB (1970) Binokulares sehen und kipfgestaltung: ein beitrag zum problem des gestaltwandels des schädels der primaten, insbesondere der Lorisidae. *Anat.* 75:489-520.

Spemann H (1902) *Arch. Entw. Mech.* 15:448.

Spemann H (1918) Über die determination der ersten organanlagen des amphibienembryo. *Wilhelm Roux Arch. Entwicklungsmech. Org.* 43:448-555.

Spemann H (1938) *Embryonic Development and Induction.* Yale University Press: New Haven.

Spemann H; Mangold H (1924) Induction of embryonic primordia by implantation of organizers from a different species. *Foundations of Experimental Embryology.* Willier BH; Oppenheimer JM, eds., Hafner: New York, pp. 144-184.

Spencer H (1864) *Principles of Biology. Part 2.*

Spencer MA (1998) Force production in the primate masticatory system: electromyographic tests of biomechanical hypotheses. *Journal of Human Evolution.* 34(1):25-54.

Spencer MA; Demes B (1993) Biomechanical analysis of masticatory system configuration in Neandertals and Inuits. *American Journal of Physical Anthropology.* 91(1):1-20.

Spyropoulos MN (1977) The morphogenetic relationship of the temporal muscle to the coronoid process in human embryos and fetuses. *American Journal of Anatomy.* 150:395-410.

Stadtmüller F (1936) Kranium und Visceralskelett der Stegocephalen und Amphibien. In: Hanbuch der Vergleichenden Anatommie der Wirbeltiere. (Bolk L; Göppert E; Kallius E; Lubosch W, eds.) Urban & Schwarzenberg: Berlin.

Starck D (1954) Morphologische untersuchungen am kopf der säugetiere, besonders der prosimier, ein beitrag zum problem des formwandels des Säugerschädels. *Z. Wiss Zool.* 157:169-219.

Stearns S (1984) The effects of size and phylogeny on patterns of covariation in the life-history traits of lizards and snakes. *American Naturalist.* 123:56-72.

Steinitz E (1906) *Arch. EntwMech.* 20:537-.

Stephan H; Frahm H; Baron G (1981) New and revised data on volumes of brain structures in insectivores and primates. *Folia primatologica.* 35:1-29.

Stewart GW (1987) Collinearity and least squares regression. *Statistical Science.* 2:68-100.

Stewart RM; Gerhart JC (1990) The anterior extent of dorsal development of the *Xenopus* embryonic axis depends on the quantity of organizer in the late blastula. *Development.* 109:363-372.

Reproduced with permission of the copyright owner. Further reproduction prohibited without permission.

Stigler SM (1986) *The History of Statistics. The Measurement of Uncertainty Before 1900.* The Belknap Press of Harvard University Press: Cambridge, MA.

Stolzenberg RM; Land KC (1983) Causal modeling in survey research. In: *Handbook of Survey Research.* Rossi PH; Wright JD; Anderson AB (Eds.). Academic Press: New York.613-675.

Stone LS (1930) *J. Exp. Zool.* 55:193-207.

Strasser E; Delson E (1987) Cladistic analysis of cercopithecid relationships. *Journal of Human Evolution.* 16:81-99.

Strier KB (1992) Atelinae adaptations: behavioral strategies and ecological constraints. *American Journal of Physical Anthropology.* 88(4):515-524.

Struhsaker TT (1975) *The Red Colobus.* University of Chicago Press: Chicago.

Struhsaker TT; Oates JF (1975) Comparison of the behavior and ecology of red colobus and black-and-white colobus in Uganda: a summary. In: *Socioecology and Psychology of Primates.* Tuttle RH (ed.) Mouton: The Hague. pp. 103-124.

Studer T (1901) Die prähistorischen Hunde in ihrer Beziehung zu den gegenwärtig lebenden Rassen. *Mém. Soc. Paléont. Suisse,* Vol. 28:1-138.

Suzuki A; Thies RS; Yamaji N; Song JJ; Wozney JM; Murakami K; Ueno N (1994) A truncated bone morphogenetic protein receptor affects dorsal-ventral patterning in the early *Xenopus* embryo. *Proc Natl Acad Sci USA.* 91(22):10255-10259.

Swindler DR; Sirianni JE (1973) Palatal growth rates in *Macaca nemestrina* and *Papio cynocephalus. American Journal of Physical Anthropology.* 38:83-92.

Swindler DR; Sirianni JE; Tarrant LH (1973) A longitudinal study of cephalofacial growth in *Papio cynocephalus* and *Macaca nemestrina* from three months to three years. *Symposia of the Fourth International Congress of Primatology. Vol. 3: Craniofacial Biology of Primates.* Zingeser MR (ed.) Karger: Basel. 227-240.

Szalay FS; Bock WJ (1991) Evolutionary theory and systematics: relationships between process and patterns. *Z. zool. Syst. Evolut.-forsch.* 29:1-39.

Szalay FS; Delson E (1979) *Evolutionary History of the Primates.* Academic Press: New York.

Teixeira LA, Madeira MC, Martins AA (1990) Transposition of masseter muscle insertion and its influence on anatomical musculo-skeletal changes in the adult rabbit. *Rev Odontol UNESP* 19(1):13-20

Thomas RDK; Reif WE (1993) The skeleton space: a finite set of organic designs. *Evolution.* 47(2):341-360.

Thomason JJ; Russell AP (1986) Mechanical factors in the evolution of the mammalian secondary palate: a theoretical analysis. *J. Morphol.* 189:199-213.

Reproduced with permission of the copyright owner. Further reproduction prohibited without permission.

Thompson D'AW (1917) *On Growth and Form*. Abridged and edited by JT Bonner. Cambridge University Press: Cambridge. [1961 edition, reprinted 1994]

Thomson A; Buxton LHD (1923) Man's nasal index in relation to certain climatic conditions. *Journal of the Royal Anthropological Institute*. 53:92-122.

Thomson KS (1988) *Morphogenesis and Evolution*.

Thorogood P (1988) The developmental specification of the vertebrate skull. *Development*. 103 (suppl.):141-153.

Thorogood P (1993) Differentiation and morphogenesis of cranial skeletal tissues. *The Skull. Volume 1. Development*. Hanken J & Hall BK, eds., University of Chicago Press: Chicago. pp. 112-152.

Throckmorton GS; Dechow PC (1994) In vitro strain measurement in the condylar process of the human mandible. *Archives of Oral Biology*. 39(10):853-867.

Throckmorton GS; Groshan GJ; Boyd SB (1990) Muscle activity patterns and control of temporomandibular joint loads. *J Prosthet Dent*. 63(6):685-695.

Tonneyck-Müller I (1976) Das Wachstum von Augen und Augenhölen beim Höhnerembryo. IX. Die Entwicklung der Augen-und Schädelanlage bei Embryonen von 3-9 Tagen mit künstlich erzeugterdoppelseitiger Mikrophthalmie. *Acta morphologica neerlando-acandinavica*. 14:139-164.

Topinard P (1891) La transformation du crane animal en crane humain. *L'Anthropologie*. 2:649-675.

Tukey JW (1954) Causation, regression, and path analysis. In: *Statistics and Mathematics in Biology*. Kempthorne O; Bancroft TA; Gowen JW; Lush JD (Eds.). Iowa State College Press: Ames, IA. pp. 35-66.

Turnbull WD (1970) Mammalian masticatory apparatus. *Fieldiana Geol*. 18:147-356.

Turner ME; Stevens CD (1959) The regression analysis of causal paths. *Biometrics*. 15:236-258.

Tutin CD; Fernandex M; Rogers ME; Williamson EA; McGrew WC (1991) Foraging profiles of sympatric lowland gorillas and chimpanzees in the Lope Reserve Gabon. *Philosophical Transactions of the Royal Society of London*. 334:179-185.

Tyler MS; Hall BK (1977) Epithelial influences on skeletogenesis in the mandible of the embryonic chick. *Anatomical Record*. 188:229-240.

van der Klaauw CJ (1946) Cerebral skull and facial skull: a contribution to the knowledge of skull structure. *Arch. Neerl. Zool*. 9:16-37.

van der Klaauw CJ (1948) Size and position of the functional components of the skull: a contribution to the knowledge of the architecture of the skull, based on data in the literature. *Arch. Neerl. Zool*. 9:16-

Reproduced with permission of the copyright owner. Further reproduction prohibited without permission.

van der Klaauw CJ (1952) Size and position of the functional components of the skull. *Arch. Neerl. Zool.* 9:1-559.

van Eijden TMGJ (1991) Three-dimensional analyses of human bite-force magnitude and moment. *Arch Oral Biol.* 36:535-539.

van Limborgh J (1982) Factors controlling skeletal morphogenesis. *Factors and Mechanisms Influencing Bone Growth.* Dixon DA; Sarnat BG (eds.) Alan R. Liss: New York 1-17.

van Roosmalen MGM; Klein LL (1988) The spider monkey, genus *Ateles*. In: *Ecology and Behavior of Neotropical Priamtes. Vol. 2.* Mittermeier RA; Rylands AB; Coimbra-Filho AF; de Fonseca GAB (eds.). World Wildlife Fund: Washington DC. pp. 455-538.

van Roosmalen MGM; Mittermeire RA; Milton K (1981) The bearded sakis, genus *Chiropotes*. In: *Ecology and Behavior of Neotropical Priamtes. Vol. 1.* Coimbra-Filho AF; Mittermeier RA (eds.). Academia Brasileira de Ciências: Reo de Janeiro. pp. 419-442.

van Spronsen PH; Weijs WA; Valk J; Prahl-Andersen B; van Ginkel FC (1991) Relationships between jaw muscle cross-sections and craniofacial morphology in normal adults, studied with magnetic resonance imaging. *European Journal of Orthodontics.* 13(5):351-361.

Varrela J (1991) Genetic and epigenetic regulation of craniofacial development. *Proc Finn Dent Soc.* 87(2):239-244.

Vilmann H; Juhl M; Kirkeby S (1985) Bone-muscle interactions in the muscular dystropic mouse. *European Journal of Orthodontics.* 7:185-192.

Vinyard CJ; Ravosa MJ (1998) Ontogeny, function, and scaling of the mandibular symphysis in papionin primates. *Journal of Morphology.* 235(2):157-175.

Vogel C (1968) The phylogenetical evaluation of some characters and some morphological trends in the evolution of the skull in catarrhine primates. *Taxonomy and Phylogeny of Old World Primates with References to the Origin of Man.* Chiarelli AB (ed.) Rosenberg and Sellier: Torino. 21-55.

Vogt C (1867) Über die microcephalen oder affenmenschen. *Arch. F. Anthrop.* 2:129-284.

von Koenigswald GHR (1966) *The Evolution of Man.* The University of Michigan Press: Ann Arbor.

Wagner G (1949) Die Bedeutung der Neuralleiste für die kipfgestaltung der Amphibienlarven. *Revue suisse de zoologie.* 56:519-620.

Wagner GP (1989) The biological homology concept. *Annual Review of Ecology and Systematics.* 20:51-69.

Wagner K (1929) Recente Hunderassen. Eine osteologische Untersuchung. *Skrifter Norske Videnskaps Akademi Oslo. I. Mat.-Nat.* Kl. 9:157.

Reproduced with permission of the copyright owner. Further reproduction prohibited without permission.

Walker BE; Quarles J (1976) Palate development in mouse foetuses after tongue removal. *Archives of Oral Biology*. 21:405-412.

Wallace RA (1973) *The Ecology and Evolution of Animal Behavior*. Goodyear Publishing Company: Pacific Palisades, CA.

Ward SC, Molnar S (1980) Experimental stress analysis of topographic diversity in early hominid gnathic morphology. American Journal of Physical Anthropology. 53(3):383-95.

Ward SC; Sussman RW (1979) Correlates between locomotor anatomy and behavior in two sympatric species of lemur. *American Journal of Physical Anthropology*. 50:575-590.

Washburn S (1947) The relation of the temporal muscle to the form of the skull. *The Anatomical Record*. 99:239-248.

Washburn SL; Detwiler SR (1943) An experiment bearing on the problems of physical anthropology. *American Journal of Physical Anthropology*. 1:171-190.

Watt DG; Williams CH (1951) The effects of the physical consistency of food on the growth and development of the mandible and maxilla of the rat. *American Journal of Orthodontics*. 37:895-928.

Waugh LM (1937) Dental observations among Eskimos. *J. Dent. Res*. 16:355-356.

Wayne RK; Benveniste RE; Janczewski DN; O'Brien SJ (1989) Molecular and biochemical evolution of the Carnivora. In: *Carnivore Behavior, Ecology, and Evolution*. Gittleman JL (ed.). Cornell University Press: Ithaca, NY.pp. 465-494.

Weidenreich F (1924) Die sonderform des menschenschadels als anpassung an den aufrechten Gang. *Z Morphol Anthropol*. 24:157-189.

Weidenreich F (1924) Über die pneumastischen nebenräume des kopfes. Ein beitrag zur kenntnis des bauprinzips de Knochen, des schädels und des köpers. *Zeit. Für Anatomie und Entwicklungsgeschichte*. 72:55-93.

Weidenreich F (1934) Das Menschenkinn und seine Entstehung. *Ergebn. Anat. Entwicklungsgesch*. 31:1-124.

Weidenreich F (1941) The brain and its role in the phylogenetic transformation of the human skull. *Transactions of the American Philosophical Society*. 31(5):321-442.

Weidenreich F (1947) Generic, specific, and subspecific characters in human evolution. *American Journal of Physical Anthropology*. 31:413.

Weijs WA (1980) Biomechanical models and the analysis of form: a study of the mammalian masticatory apparatus. *Am. Zool*. 20:707-719.

Werdelin L (1986) Comparison of skull shape in marsupial and placental carnivores. *Australian Journal of Zoology*. 34:109-117.

Reproduced with permission of the copyright owner. Further reproduction prohibited without permission.

Wilcox (1998) How many discoveries have been lost by ignoring modern statistical methods? *American Psychologist*. 53:300-314.

Williams PL; Warwick R (1980) *Gray's Anatomy. 36th British Edition*. WB Saunders: Philadelphia.

Woelfel JB; Hickey JC; Stacy RW; Rinear LL (1960) Electromyographic analysis of jaw movements. *J. Pros. Dent.* 10:688-697.

Wolf E, Rapp K, Wanke R, Hermanns W, Pirchner F, von Butler-Wemken I, Brem G (1991) Growth characteristics of metallothionein-human growth hormone transgenic mice as compared to mice selected for high eight-week body weight and unselected controls. II. Skeleton. *Growth Dev Aging*. 55(4):237-48

Wolff J (1892) *Das Gesetz der Transformation der Knochen*. (The Law of Bone Remodeling) Trans. by P. Maquet. Springer-Verlag: Berlin. Reprint 1986.

Wood B (1991) *Koobi Fora Fesearch Project Volume 4: Hominid Cranial Remains*. Oxford University Press: New York.Alberch P (1983) Morphological variation in the neotropical salamander genus Bolitoglossa. *Evolution*. 37:906-919.

Wright PC (1994) The behavior and ecology of the owl monkey. In: *Aotus: The Owl Monkey*. Baer J; Weller RE; Kakoma I (eds.). Academic Press: New York. pp. 97-112.

Wright S (1934) The method of path coefficients. *Annals of Mathematical Statistics*. 5:161-215.

Wright S (1960) Path coefficients and path regressions: alternative or complementary comcepts? *Biometrics*. 16:189-202.

Wright S (1968) *Evolution and genetics of populatoins I. Genetic and biometric foundations*. University of Chicago Press: Chicago.

Wylie WL; Elsasser WA (1948) Undistorted vertical projections of the head from lateral and posteroanterior roentgenograms. *Amer. J. Roentgenol.* 60:414-417.

Yamamoto S (1996) The effects of food consistency on maxillary growth in rats. *European Journal of Orthodontics*. 18(6):601-615.

Yeager CP (1989) Feeding ecology of the proboscis monkey (*Nasalis larvatus*) *International Journal of Primatology*. 10(6):497-529.

Yung YF; Bentler PM (1994) Bootstrap-corrected ADF test statistics in covariance structure analysis. *British Journal of Mathematical and Statistical Psychology*. 47:63-84.

Zahrowski JJ; Turley PK (1992) Force magnitude effects upon osteoprogenitor cells during premaxillary expansion in rats. *Angle Orthod.* 62(3):197-202.

Zeller AC (1987) Communication by sight and smell. In: *Primate Societies*. Smuts BB; Cheney DL; Seyfarth RM; Wrangham RW; Struhsaker T (eds.). University of Chicago Press: Chicago. pp. 433-439

Reproduced with permission of the copyright owner. Further reproduction prohibited without permission.

Zingeser MR (1972) Occlusofacial morphological integration (*Homo sapiens, Alouatta caraya, Cebus capucinus*). *Symposia of the Fourth International Congress of Primatology. Vol. 3: Craniofacial Biology of Primates*. Zingeser MR (ed.) Karger: Basel. 241-257.

Reproduced with permission of the copyright owner. Further reproduction prohibited without permission.